

Lecture Notes in Mechanical Engineering

Kripa Shanker
Ravi Shankar
Rahul Sindhvani *Editors*

Advances in Industrial and Production Engineering

Select Proceedings of FLAME 2018

 Springer

Lecture Notes in Mechanical Engineering

Lecture Notes in Mechanical Engineering (LNME) publishes the latest developments in Mechanical Engineering—quickly, informally and with high quality. Original research reported in proceedings and post-proceedings represents the core of LNME. Volumes published in LNME embrace all aspects, subfields and new challenges of mechanical engineering. Topics in the series include:

- Engineering Design
- Machinery and Machine Elements
- Mechanical Structures and Stress Analysis
- Engine Technology
- Aerospace Technology and Astronautics
- Nanotechnology and Microengineering
- Control, Robotics, Mechatronics
- Theoretical and Applied Mechanics
- Dynamical Systems, Control
- Fluid Mechanics
- Engineering Thermodynamics, Heat and Mass Transfer
- Precision Engineering, Instrumentation, Measurement
- Materials Engineering
- Tribology and Surface Technology

To submit a proposal or request further information, please contact the appropriate Springer Editor:

Li Shen at li.shen@springer.com (China)

Dr. Akash Chakraborty at akash.chakraborty@springernature.com (India)

Dr. Leontina Di Cecco at Leontina.dicecco@springer.com (all other Countries)

Please check the Springer Tracts in Mechanical Engineering at <http://www.springer.com/series/11693> if you are interested in monographs, textbooks or edited books.

To submit a proposal, please contact Leontina.dicecco@springer.com and Li.shen@springer.com.

Indexed by SCOPUS. The books of the series are submitted for indexing to Web of Science.

More information about this series at <http://www.springer.com/series/11236>

Kripa Shanker · Ravi Shankar ·
Rahul Sindhwani
Editors

Advances in Industrial and Production Engineering

Select Proceedings of FLAME 2018

 Springer

Editors

Kripa Shanker
Industrial and Management Engineering
Department
Indian Institute of Technology Kanpur
Kanpur, Uttar Pradesh, India

Ravi Shankar
Department of Management Studies
Indian Institute of Technology Delhi
New Delhi, Delhi, India

Rahul Sindhwani
Department of Mechanical Engineering
Amity University
Noida, Uttar Pradesh, India

ISSN 2195-4356 ISSN 2195-4364 (electronic)
Lecture Notes in Mechanical Engineering
ISBN 978-981-13-6411-2 ISBN 978-981-13-6412-9 (eBook)
<https://doi.org/10.1007/978-981-13-6412-9>

Library of Congress Control Number: 2019930371

© Springer Nature Singapore Pte Ltd. 2019

This work is subject to copyright. All rights are reserved by the Publisher, whether the whole or part of the material is concerned, specifically the rights of translation, reprinting, reuse of illustrations, recitation, broadcasting, reproduction on microfilms or in any other physical way, and transmission or information storage and retrieval, electronic adaptation, computer software, or by similar or dissimilar methodology now known or hereafter developed.

The use of general descriptive names, registered names, trademarks, service marks, etc. in this publication does not imply, even in the absence of a specific statement, that such names are exempt from the relevant protective laws and regulations and therefore free for general use.

The publisher, the authors and the editors are safe to assume that the advice and information in this book are believed to be true and accurate at the date of publication. Neither the publisher nor the authors or the editors give a warranty, express or implied, with respect to the material contained herein or for any errors or omissions that may have been made. The publisher remains neutral with regard to jurisdictional claims in published maps and institutional affiliations.

This Springer imprint is published by the registered company Springer Nature Singapore Pte Ltd. The registered company address is: 152 Beach Road, #21-01/04 Gateway East, Singapore 189721, Singapore

Preface

This book brings together the collection of cutting-edge research articles on industrial and production engineering from the First International Conference on Future Learning Aspects for Mechanical Engineering (FLAME), which was organized by Amity University, Noida, Uttar Pradesh, India, from October 3 to 5, 2018.

The primary mission of this conference was to lay a platform that brings together academicians, scientists, and researchers across the globe to share their scientific ideas and vision in the areas of thermal, design, industrial, production, and interdisciplinary areas of mechanical engineering. FLAME 2018 played a key role to set up a bridge between academia and industry.

The conference hosted almost 550 participants to exchange scientific ideas. During 3 days of the conference, researchers from academics and industries presented the most recent cutting-edge discoveries, went through various scientific brainstorming sessions, and exchanged ideas on practical socioeconomic problems. This conference also provided a scope to establish a network for joint collaboration between academia and industry. Major emphasis was focused on the recent developments and innovations in various fields of mechanical engineering through plenary lectures.

This book covers the industrial and production engineering areas such as sustainable manufacturing systems, decision sciences, logistics and supply chain management, operations management, computer-aided engineering, rapid prototyping, manufacturing management and automation, metrology, manufacturing process optimization, machining and machine tools, casting, welding, and forming. This book caters to the industrial and production engineering aspects, will mainly serve as a reference guide for researchers and practitioners, and is expected to foster better communication and closer cooperation between academia and industry partners.

We would like to acknowledge all the participants who have contributed to this volume. We also deeply express our gratitude for the generous support provided by Amity University, Noida; Science Engineering and Research Board (SERB), an enterprise of Department of Science and Technology (DST), Government of India; Siemens; ISME; and Begell House. We also thank the publishers and every staff

of the department and institute who have directly or indirectly helped to accomplish this goal. Finally, we would also like to express our gratitude to Respected Founder President, Amity University, Dr. Ashok K. Chauhan, for providing all kinds of support, and this book is not complete without his blessings.

In spite of sincere care, there might be typos and there is always space for improvement. We would appreciate any suggestions from the reader for further improvements to this book.

Noida, India
New Delhi, India
Kanpur, India
January 2019

Dr. Rahul Sindhvani
Prof. (Dr.) Ravi Shankar
Prof. (Dr.) Kripa Shanker

Contents

Enhanced Fluorescence-Based Detection of Vibrio Cells Over Nanoporous Silica Substrate	1
Geeta Bhatt, Rishi Kant and Shantanu Bhattacharya	
Wear Analysis of Al-5083 Alloy Reinforced with Chromium Oxide Filler on Air Jet Erosion Test Rig	11
Amit Kumar, Shiv Ranjan Kumar and Anand Prakash	
Statistical Analysis of Surface Roughness Using RSM in Hard Turning of AISI 4340 Steel with Ceramic Tool	17
Asutosh Panda, Sudhansu Ranjan Das and Debabrata Dhupal	
A Current Review of Supply Chain Performance Measurement Systems	27
Shubham Tripathi and Manish Gupta	
Development of Hybrid Forms of Abrasive Flow Machining Process: A Review	41
Anant Bhardwaj, Parvesh Ali, R. S. Walia, Qasim Murtaza and S. M. Pandey	
Analysis of Green Supply Chain Management Enablers in FMCG Sector Using Integrated ISM and MICMAC Approach	69
Prabhakar Vivek and Jha Sanjay Kumar	
Deformation Behavior of Semi-solid Forged A356–5TiB₂ Nano-In Situ Composites	77
Sahini Deepak Kumar, Ananya Chattee, Sanjay Kumar Jha, Nirnanjan Kumar Singh and Animesh Mandal	
Study of MRR and TWR in Electric Discharge Machining of AISI D2 Tool Steel	85
Himanshu Payal, Satish Kumar Sharma, Aakash, Ashish kumar, Avinash kumar and Himanshu	

Optimization of Quality and Productivity of Wire EDM by Using L₉ Orthogonal Array	93
Shailesh Kumar Dewangan, Prakash Kumar and Sanjay Kumar Jha	
Numerical Simulation of Hot Isostatic Pressing Process Utilized During Sintering of Tool Inserts	101
Akshay Chandras and Chandrakant Sonawane	
Development of Hydrophobic Coating with Polymer–Metal Oxide Nano-composites	117
Jaya Verma, Vishakha Baghel, Basant Singh Sikarwar, Arpita Bhattacharya and D. K. Avasthi	
Recent Developments in Fabrication of Super-Hydrophobic Surfaces: A Review	127
Deepak Kumar Sharma, Vishakha Baghel, Ranjit Kumar, D. K. Avasthi and Basant Singh Sikarwar	
Conceptual Analysis of Reliability Aspect for Various Process Industries: A Critical Review	141
Gaurav Sharma and Puran Chandra Tewari	
Estimation of Hardness During Heat Treatment of EN8 and C25 Steels	149
Sachin V. Bagali, Maruti, N. R. Abhaya Simha, M. P. Sushanth, T. S. Prasanna Kumar and V. Krishna	
Service Quality in Indian SMEs: Developing a Dual Directional Scale at Supplier–Manufacturer Dyad	161
Surjit Kumar Gandhi, Anish Sachdeva and Ajay Gupta	
Parametric Investigation into Alumina Nanopowder Mixed EDM of Inconel 825 Alloy Using RSM	175
Deepti Ranjan Sahu, Amit Kumar, Biplob Kumar Roy and Amitava Mandal	
Eco-design Approaches for Developing Eco-friendly Products: A Review	185
Prashant Kumar Singh and Prabir Sarkar	
Plumbene: A New 2D-Material Resembling Graphene	193
D. K. Das and S. K. Singh	
Study the Wear Behaviour of Al5083-7% B₄C Composite Fabricated by Stir Casting Technique	199
Ram Singh, Malik Shadab, Ram Naresh Rai, Chiranjit Bhowmik and Shankar Swarup Das	

Study of Machining Performance in EDM Through Response Surface Methodology	207
Raghav Rajneesh, Singh Subhash, R. S. Mulik and Pal Kaushik	
Friction Stir Welding of Thermoplastic Composites	221
Sudhir Kumar, Tanmoy Medhi and Barnik Saha Roy	
Numerical Simulation of Temperature Distribution in Laser Welding of AISI 316	237
Pramod Kumar and Amar Nath Sinha	
A Framework for Flexible Job Shop Scheduling Problem Using Simulation-Based Cuckoo Search Optimization	247
Rakesh Kumar Phanden, Zuzana Palková and Rahul Sindhvani	
An Experimental Study to Evaluate the Warpage and Cracking Issues in Fused Deposition Modeling	263
A. Suhas, Rohit Rajpal, K. V. Gangadharan and U. Pruthviraj	
Optimization of Electrical Discharge Coating of WS₂ and Cu Powder Mixture Deposited Through Green Compact Electrode	273
Rashi Tyagi, Kshitij Pandey, Shalini Mohanty, Shakti Kumar, Alok Kumar Das and Amitava Mandal	
Optimization by AHP-ARAS of EDM Process Parameters on Machining AA7050-10%B₄C Composite	285
Arvind Kumar, Sayed Abou Iltaf Hussain and Ram Naresh Rai	
Supply Chain Issues and Challenges for Cement Industries of India: A Case Study	297
Ankur Taak and Ravinder Kumar	
Powder Metallurgy Processing and Mechanical Characterization of Iron-Based Composite Reinforced with Alumina and Zirconium Diboride	303
Bhupendra Prakash Sharma, G. S. Rao and Umesh Kumar Vates	
Challenges for Effective and Efficient Supply Chain Management for Fast Moving Electrical Goods (FMEG): A Case Study	309
Ravinder Kumar and Ankur Taak	
Investigation of Titanium as Thin Film Deposited Material Thereon Effect on Mechanical Properties	315
Gaurav Gupta and R. K. Tyagi	
Modeling the Metrics of Human Resource, Time, and Asset Level Barriers in the Implementation of Lean Manufacturing Using an Analytical Network Process Approach	325
Bhupendra Prakash Sharma, A. Chauhan, H. Singh, Umesh Kumar Vates and G. S. Rao	

Feature Extraction and Recognition Information System for Manufacturing Prismatic Part	339
Vinod V. Rampur and Sachhidanand Reur	
Fabrication and Characterization of Al₂O₃-TiC-Reinforced Aluminum Matrix Composites	349
Anbesh Jamwal, Umesh Kumar Vates, Pallav Gupta, Ankur Aggarwal and Bhupendra Prakash Sharma	
Optimization of Critical Parameters of EDD Steel in Die Cavity Manufacturing	357
Naveen Anand Daniel, Nirmal Kumar Singh, Umesh Kumar Vates, Bhupendra Prakash Sharma and Sivaraos Subramanian	
A Theoretical Analysis for Prioritization of Lean Strategies: A Survey of Indian Manufacturing Industries	365
Virender Chahal and M. S. Narwal	
A Systematic Review: Effect of TIG and A-TIG Welding on Austenitic Stainless Steel	375
Himanshu Garg, Karan Sehgal, Rahul Lamba and Gianender Kajal	
Evaluation of Key Challenges to Industry 4.0 in Indian Context: A DEMATEL Approach	387
Ankur Aggarwal, Sumit Gupta and Manish Kumar Ojha	
AHP Based Model for Evaluation of Sustainable Manufacturing Enablers in Indian Manufacturing Companies	397
Abhishek Singh, Zareef Askary, Sumit Gupta, Ashwini Kumar Sharma and Priyank Shrivastava	
Informal Investigation of Fourth-Party and Third-Party Logistics Service Providers in Terms of Indian Context: An AHP Approach	405
Nishant Gautam, Manish Kumar Ojha, Pritam Swain, Ankur Aggarwal and Anbesh Jamwal	
An Image-Based Approach of Generating Automatic Toolpath for Profile Milling	415
Vishal Agrawal, Avinash Kumar, Narendra Kumar and Prashant K. Jain	
Experimental Investigation of Forming Forces in Single Point Incremental Forming	423
Ajay Kumar, Vishal Gulati and Parveen Kumar	
Solid Waste Management Through Plasma Arc Gasification in Delhi: A Step Towards Swachh Bharat	431
Monika Singh, Rishabh Arora, Anubhav Ojha, Durgesh Sharma and Sumit Gupta	

Analysis and Optimization of Surface Integrity Characteristics of EDMed Work Surface Inconel 718 Super-Alloy Using Grey-Based Taguchi Method	441
Md. Ghaus Ali, Rahul, Dipraj Banik, Akshansh Yadav, B. C. Rautara and Ashok Kumar Sahoo	
Framework the Food Supply Chain Network in the Present Indian Scenario	449
Bhavya Nidhi Vats, Anuj Gupta and Ganesh Sharma	
A Comprehensive Review on Jute Fiber Reinforced Composites	459
Ekta Gogna, Ramanuj Kumar, Anurag, Ashok Kumar Sahoo and Amlana Panda	
Analysis of Lean Manufacturing Implementation in SMEs: A “SS” Technique	469
Shyam Sunder Sharma, D. D. Shukla and Bhupendra Prakash Sharma	
Performance and Combustion Characteristics of Thumba and Argemone as Dual Fuel Blends in a DICl Engine: An Experimental Approach	477
Shahid Qayoom and Sumit Kanchan	
Biogeographical and Variable Neighborhood Search Algorithm for Optimization of Flexible Job Shop Scheduling	489
Rakesh Kumar Phanden and João Carlos E. Ferreira	
A Study on the Effect of Varying Revolution Pitch for Different Tool Design: Friction Stir Welding of AA 6061-T6	505
Abhijit Banik, John Deb Barma, Ram Singh and S. C. Saha	
Analysing Attributes of Food Supply Chain Management: A Comparative Study	515
Mohd Sufiyan, Abid Haleem, Shahbaz Khan and Mohd Imran Khan	
Optimization of Electric Discharge Machining Process Parameters for H13 Steel by Using Taguchi Method	525
Mahendra M. Ghayatadak and Amar S. Bhandare	
Machining Performance Optimization During Electro Discharge Machining on Titanium (Grade 4): Application of Satisfaction Function and Distance-Based Approach	535
Dipraj Banik, Rahul, Gitimaya Kar, Biswajit Debnath, B. C. Routara, Ashok Kumar Sahoo and Dhiraj Kochar	
Self-Healing Al 6061 Alloy Reinforced with Low Melting Point Alloys	543
Nitin Kumar Gupta, G. D. Thakre and Manoj Kumar	

A Novel Approach in Developing Aluminum Hybrid Green Metal Matrix Composite Material Using Waste Eggshells, Cow Dung Ash, Snail Shell Ash and Boron Carbide as Reinforcements	551
Soutrik Bose, Anand Pandey, Ashmik Mondal and Pritam Mondal	
Detection of Punch Wear in Stamping Process Using Acoustic Emission	563
Tushar Y. Badgajar, Rahul N. Chandore and Vijay P. Wani	
Sustainable Machining Using Hybrid Nanofluids Under Minimum Quantity Lubrication (MQL)	573
Anjali Gupta, Rajesh Kumar, Harmesh Kumar and Harry Garg	
A Review on Different Dielectric Fluids and Machining of Si_3N_4 and Al_2O_3 Composites via EDM	585
Kanav Bhatia, Ankit Singla, Anirudh Sharma, Shailesh Singh Sengar and Ashish Selokar	
Mechanical Behavior of Powder Metallurgy Processed $\text{Al} + \text{ZrB}_2 + \text{Al}_2\text{O}_3$ Metal Matrix Composites	597
Bhupendra Prakash Sharma, D. Akhil, M. Junaid, Umesh Kumar Vates and G. S. Rao	
Reliability Analysis of Sheet Manufacturing Unit of a Steel Industry	605
Munish Mehta, Jujhar Singh and Manpreet Singh	
Modeling the Metrics of MRB, TRB, and ORB in the Implementation of Green Agile Manufacturing Strategies: An ANP Approach	629
Bhupendra Prakash Sharma, K. Ranade, Ankit Singh, Umesh Kumar Vates and G. S. Rao	
Agile System in Health Care: Literature Review	643
Rahul Sindhvani, Punj Lata Singh, Devendra Kumar Prajapati, Aamir Iqbal, Rakesh Kumar Phanden and Vasdev Malhotra	
Evaluation of Common Barriers to the Combined Lean-Green-Agile Manufacturing System by Two-Way Assessment Method	653
Punj Lata Singh, Rahul Sindhvani, Naresh Kumar Dua, Anbesh Jamwal, Ankur Aggarwal, Aamir Iqbal and Nishant Gautam	
Simulation for Effective Shop-Floor Decision Making: A Case Study	673
Durgesh Sharma	
Modeling and Analysis of Factors Influencing Agility in Healthcare Organizations: An ISM Approach	683
Rahul Sindhvani, Punj Lata Singh, Aamir Iqbal, Devender Kumar Prajapati and Varinder Kumar Mittal	

An Empirical Study of Performance Improvement in Product Delivery System Through Six Sigma DMAIC Approach	697
Rajak Anup Kumar, Kumar Nilesh, Nayak Yogesh Kumar and Peesapati V. V. Rajagopal	
A Critical Review on Friction Stir Welding of Dissimilar Aluminium Alloys	707
Munna Singh Dahiya, Vikas Kumar and Shubham Verma	
Microstructure, Economic, and Emission Evaluation of Castings Produced from Biodiesel-fired Self-designed Rotary Furnace	721
Purshottam Kumar and Rohit Sharma	
Study of Sliding Wear Behavior of Alumina Oxide Filled Fiber Composite Using Design of Experiment	735
Bhanu Pratap, R. K. Gupta and Bhuvnesh Bhardwaj	
Role of Acoustic Softening Effects in Ultrasonic Spot Welded Dissimilar Materials	743
Mantra Prasad Satpathy, Susanta Kumar Sahoo and Diptikanta Das	
Agility Evaluation in the Rolling Industry: A Case Study	753
Rahul Sindhvani, Punj Lata Singh, Raj Chopra, Karan Sharma, Apratim Basu, Devendra Kumar Prajapati and Vasdev Malhotra	
Weld Strength Analysis of Ultrasonic Polymer Welding Using Adaptive Neuro-Fuzzy Inference System	771
T. Chinnadurai, S. Saravanan, M. Karthigai Pandian, N. Prabakaran and J. Dhanaselvam	
Mechanical Properties of Flax Fiber Reinforced Composites Manufactured Using Hand Layup and Compression Molding—A Comparison	781
Vishnu Prasad, C. V. Muhammed Hunize, R. I. Abhiraj, M. A. Jospeh, K. Sekar and Mubarak Ali	
Design and Development of an Online Process Measurement System for Zero Defect Production	791
Joseph John Valiaveetil, Saurabh Singh, Akshat Jain, AkshayUpadhyaya and Sumit Gupta	
Performance Study of Gas-Assisted Electric Discharge Machining on Carbon–Chromium Die Steel	801
Nishant K. Singh, Rakesh Prasad, Dilip Johari and Yashvir Singh	
Effects of Welding Parameters in Friction Stir Welding of Stainless Steel and Aluminum	815
Pankul Goel, A. W. Mohd, Nidhi Sharma, A. N. Siddiquee and Zahid A. Khan	

Case Study of Critical Success Factors Affecting Knowledge Management in Small- and Medium-Sized Enterprises in Developing State: Steel Sector	825
Agrawal Animesh and Suraj Kumar Mukti	
Optimization of FSW Process Parameters During Joining of Al to Cu Using Taguchi-Based GA	833
Nidhi Sharma, Pankul Goel, M. A. Wahid, Zahid. A. Khan and Arshad Noor Siddiquee	
Analyzing Success Factors of Small and Medium Enterprises (SMEs): A Study in Indian Context	843
Sachin Meshram and A. M. Rawani	
A Brief Review on Different Lubricants Used in MQL Process During Hard Turning	853
Hemant Tiwari, Ramanuj Kumar, Amlana Panda, Ashok Kumar Sahoo and Soumikh Roy	
Applicability of Lean Six Sigma in Hospitals	861
Vimal Kumar Deshmukh, Suraj Kumar Mukti and Animesh Agrawal	

About the Editors

Dr. Kripa Shanker is the former Vice-Chancellor of Uttar Pradesh Technical University, Lucknow, and former Deputy Director of Indian Institute of Technology, Kanpur. He obtained his M.S and Ph.D. in Operations Research and Industrial Engineering from Cornell University, USA. His main areas of teaching and research include production and operations management, supply chain management, quantitative and statistical decision models, computer integrated and flexible manufacturing systems, cellular manufacturing, and simulation. He has published more than a hundred papers in international journals and conference proceedings and has organized several education courses for engineering college teachers and engineers and managers from the industry. He is a Fellow and Life Member of several organizations such as Indian National Academy Engineering, Institution of Engineers (India), Indian Institution of Industrial Engineering, and Indian Society for Technical Education.

Dr. Ravi Shankar is the “Amar S. Gupta Chair Professor of Decision Science” in the Department of Management Studies (DMS), Indian Institute of Technology, Delhi, India. His areas of interest include decision sciences, business analytics, and big data, operations and supply chain management, project management, total quality management and six sigma, sustainable freight transportation, strategic technology management, telecom system planning and design, and knowledge management. He has published more than 300 research papers in reputed journals and co-authored 3 text books. Besides having a highly productive academic career of over 30 years, he has undertaken several international teaching assignments and research-driven collaborations.

Dr. Rahul Sindhwani is an Assistant Professor in the Department of Mechanical Engineering, Amity School of Engineering and Technology, Amity University, Noida, Uttar Pradesh, India. His research interests are in the area of industrial and production engineering, especially in lean, green and agile manufacturing systems, quantitative and statistical decision models. He has published several research articles in international peer-reviewed journals.

Enhanced Fluorescence-Based Detection of *Vibrio* Cells Over Nanoporous Silica Substrate



Geeta Bhatt , Rishi Kant  and Shantanu Bhattacharya 

Abstract The food and waterborne pathogens threaten the human health through porous borders that require immediate detection in real time. The present work reports the development of a nanoporous silica-based platform for the rapid detection of *Vibrio* cells. The nanoporous thin film has been developed over silicon substrate utilizing PMSSQ (polymethylsilsesquioxane, $(\text{CH}_3\text{SiO}_{1.5})_n$) and PPG (polypropylene glycol, $\text{CH}((\text{CH}_3\text{CH}_2\text{O})_n)$) combination in PGMEA (propylene glycol methyl ether acetate) solvent as provided earlier by Gangopadhyay et al. (Nanotechnology 20, 2009 [1]). The PPG acts as a porogen and evaporates on heat treatment giving a porous structure and assembles the PMSSQ nanoparticles. The films were characterized through FTIR, EDAX, and SEM microscopy, and it was found out that the functional groups like OH, CH_3 , Si- CH_3 , Si-O, and Si-O-Si were present abundantly in the porous structure, which can be further modified for its application in biology. An aliquot of 2.5 μl *Vibrio* cell solution was immobilized (over nanoporous silica film) to study its fluorescence intensity under an epifluorescence microscope. *Vibrio* (*Vibrio harveyi* (ATCC[®] 700106[™])) cells possess self-fluorescing effects with bleaching characteristics. The fluorescence images (with the progression of time) are acquired and processed through Image J (courtesy NIH), and relative fluorescence of the cells are calculated as a function of time. A 1.7 times increase in the overall fluorescence intensity level is recorded in the presence of the porous silica layer as compared to uncoated silicon substrate showing immobilization capabilities of these films.

Keywords *Vibrio harveyi* cells · Nanoporous · Silica · Fluorescence · Detection

1 Introduction

Vibrio is a gram-negative microorganism, which is generally found in water bodies like coastal or marine environment. Some strains of *Vibrio* are recorded as pathogenic

G. Bhatt · R. Kant · S. Bhattacharya (✉)
Department of Mechanical Engineering, Indian Institute of Technology Kanpur, Kanpur 208016,
Uttar Pradesh, India
e-mail: bhattacs@iitk.ac.in

[1, 2], which may make their detection complicated, but depending on its pathogenicity level (i.e., severity to cause illness and subsequent death), it is very important that a strategy may be developed to sensitively detect the presence of *Vibrio* cells in a convenient manner. The *vibrio* cells may be detected through hybridization [3], through fluorescence detection or other molecular techniques like polymerase chain reaction (PCR). PCR, in any event, is a technique which serves as an industry gold standard as regards the molecular identification of many biological entities, and in this case too, PCR process has emerged as a prominent tool for the specific detection of the *tdh* and *trh* genes in *Vibrio parahaemolyticus* [4]. PCR has also been heavily deployed for detecting *Vibrio* via detection of the *Vibrio vulnificus* DNA, the DNA which is present in culturable or non-culturable strains of *Vibrio* [5]. The different genes of *Vibrio parahaemolyticus* like *tl*, *tdh*, and *trh* are also detected by multiplex PCR to up to a high sensitivity level of 10–100 CFU per 10 g of tissue extracted [6], which has been further extended to optimizing the multiplex PCR process using DNA microarray, etc. [7]. This integration has been carried out to further enhance the accuracy of detection. Multiplex PCR has also been extended to simultaneous detection of five pathogenic species through PCR with primers designed through comparative genomics scheme [8].

Further TaqMan techniques have been developed for the detection of *Vibrio* molecularly [9]. Even though the conventional PCR methods are highly sensitive and efficient, these methods require rigorous post-processing of samples through a variety of staining techniques like gel electrophoresis and subsequent optical absorption of the electrophoresed species, which is cumbersome. Keeping this in mind, the conventional PCR has transcended to the qPCR (real-time PCR) domain where we are enabled to directly quantitate the progress of the PCR reaction by recording the overall fluorescence level of a specific/nonspecific intercalating fluorescent dye or dye pair. Further, many more fluorescence assisted techniques can be utilized for making detection quantifiable. In this context, *Vibrio* cells have been subjected to detection through quorum sensing [10] and other fluorescence-based sensing. Fluorescence-based sensing is combined with solid-phase cytometry [11] and antibody-based detection [12] to very accurately detect the presence of *Vibrio*. Quantum dots [13] are utilized well to detect the *Vibrio* cells.

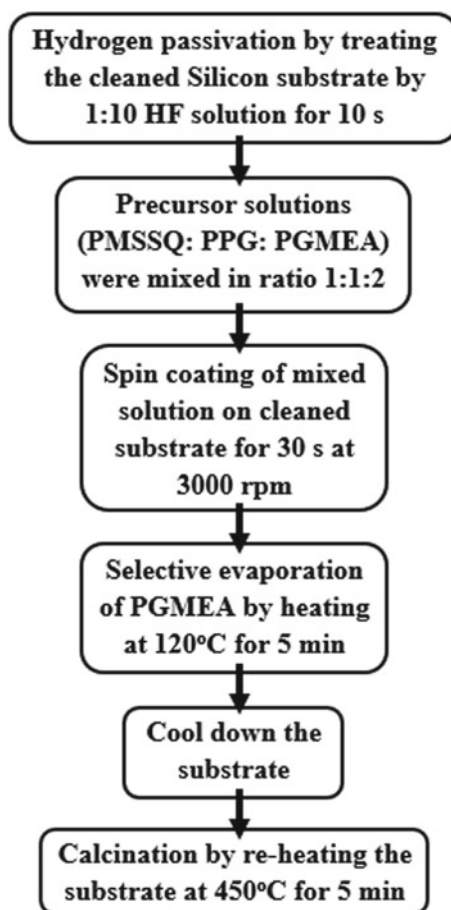
Most of the detection schemes that are devised using microsystems approaches are carried out over silicon substrates as it is accepted as very well-evolved micro-electronic material. Hence, the substrate is of utmost importance, which can further add sensitivity to the detection. The modification of substrate where such modification may cause an enhancement in the overall level of the fluorescence signal is always prudent for a sensitive detection. Such strategies of substrate modification to cause signal enhancement have not been proposed earlier to increase the sensitivity level. The current work aims at such a modification by coating through a film which is known for its bio-friendly properties [14], leads to a rise in the signal level of the fluorescence coming out of the *Vibrio* strains (*Vibrio harveyi* (ATCC® 700106™)).

2 Materials and Methods

2.1 Nanoporous Silica Layer

Nanoporous substrates add the benefit of providing a larger surface area to volume ratio for facilitating binding of target species through nanopores. Pore size can be chosen from tens of micrometer to nanometer size depending on whether we are working with whole cell or a single nucleic acid. In this study, the pore size is chosen compatible with whole cell analysis. Thin nanoporous silica layer (refractive index: 1.14) is prepared by conventional porogen method on silicon substrate. The precursors used for growing silica layer are PMSSQ, PPG (molecular weight: 20,000 g/mol), and PGMEA (molecular weight: 90.1 g/mol). Among these precursors, PMSSQ, PPG, and PGMEA act as matrix, porogen, and solvent, respectively. The flowchart for the

Fig. 1 Flowchart to fabricate porous silica structure



fabrication of nanoporous silica is demonstrated in Fig. 1. Hydrogen-passivated (HF denotes hydrofluoric acid) and washed silicon substrate is spin-coated with a 1:1:2 solution of PMSSQ: PPG: PGMEA (mixed through ultrasonication). The spin-coated samples are baked at 120 °C for removing the solvent and facilitating cross-linking between PMSSQ and PPG. This step is followed by cooling the sample to room temperature and then again re-heating the cooled sample to ≈ 450 °C, which helps in evaporation of PPG as the temperature of the substrate passes 200 °C. This way, selective and consecutive evaporation of PGMEA and then PPG generates enthalpy interaction between the particles and results in self-assembled porous structure.

The film is characterized through FESEM microscopy, FTIR and EDAX spectroscopy. The SEM images (Fig. 2a and b) show that there is a uniform porous structure (open pores) in the film with circular silica particles connected to each other. The figure shows that the particle sizes of 2–4 μm are obtained with pore size varying between few nanometers and micrometer. The FTIR analysis shows various peaks showing the presence of functional groups like OH, CH₃, Si–H, Si–CH₃, and Si–O–Si (Fig. 2c) in the developed film. The EDAX analysis (Fig. 2d) confirms the presence of Si and O in the film.

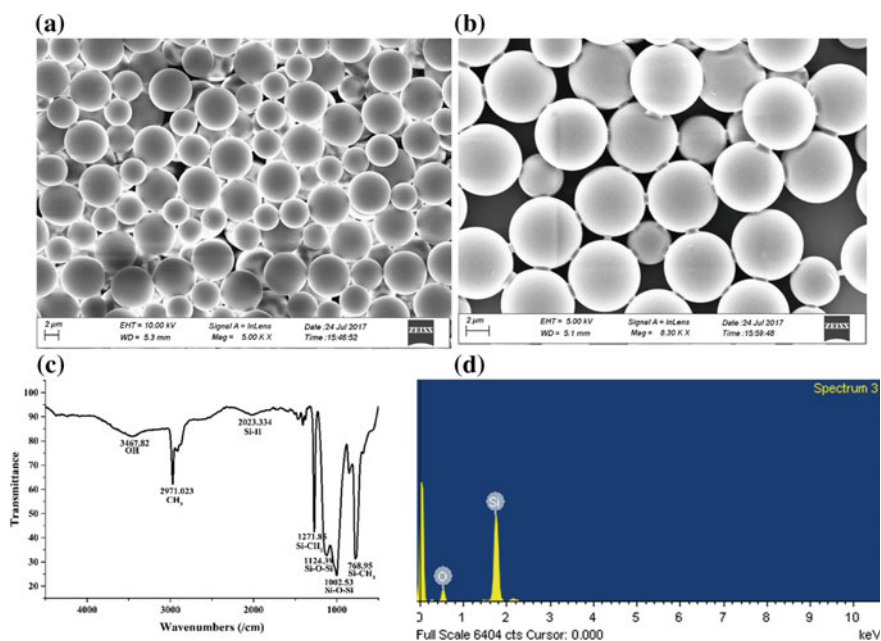


Fig. 2 Analysis of nanoporous silica film. **a, b** FESEM images of the nanoporous silica layer at different magnifications; **c** FTIR image of nanoporous silica layer; **d** EDAX of grown silica layer

2.2 *Vibrio harveyi* (ATCC® 700106™) Cells

The cell culture is bought in freeze-dried condition from M/S ATCC, USA, which is stored at 2–8 °C. The cells are thawed and extracted using ATCC® 2034 (autoinducer bioassay medium) medium at 30 °C in aerobic condition by incubating for 24 h (concentration: 10⁸ CFU/ml). The grown strain emits bioluminescence, and the expression of light is not a function of cell density. These cells are categorized under biosafety level 1 and hence are safe to work within the normal laboratory environment. The experiments are carried out on fully grown cells.

3 Results and Discussion

The various fluorescence-based detection schemes like qPCR deploy silicon as the base substrate [15]. So it becomes an important aspect to study the substrate characteristics as well. In this study, the effect of fabricated porous silica structure on the silicon substrate is observed for biosensing of cells through fluorescence route. The cells are immobilized on the two substrates (silicon substrate and the grown porous silica on silicon substrate), and a detailed comparison is done to analyze the effect of porous silica film on the fluorescence intensity measurements. Since *V. harveyi* cells are self-fluorescence illuminating (bioluminescence) cells with fluorescence quenching effect, these cells tend to lose their fluorescence as the time progresses (with every captured frame). An aliquot of 2.5 µl *Vibrio* cell solution is poured onto the porous silica-developed structure on the silicon substrate. Corresponding fluorescence is observed through images captured via an epifluorescence microscope (Nikon ECLIPSE 80i) (with a light of wavelength ≈ 520 nm). The fluorescence images are captured at a time gap of 5 s. The corresponding captured images are processed through ImageJ software (source: NIH), and relative fluorescence is calculated by evaluating the gray value of the image, which keeps decreasing with the decrease in the fluorescence level.

All the parameters are kept constant for the comparative study like aliquot amount, observation area, and the magnification (10×). Figures 3 and 4 show the fluorescence images at different time intervals, i.e., (a) at 5 s, (b) 45 s, (c) 85 s, and (d) 125 s, for the silicon substrate and silica-coated silicon substrate, respectively. The individual image comprises of fluorescence image clubbed with the analyzed gray value plot of that image (obtained from ImageJ). From the gray value plots, the maximum value is fetched for the analysis. When both sets of images are compared, it is seen that the images from silica-coated silicon substrate are of higher gray values than those on the normal silicon substrate. The maximum fluorescence intensity observed in case of a silicon substrate is 53 RFU (at $t = 5$ s, first capture instance), while it is 88 RFU for the silica-coated substrate which reduces down to 40 RFU and 68 RFU in case of the silicon substrate and coated silica substrate, respectively.

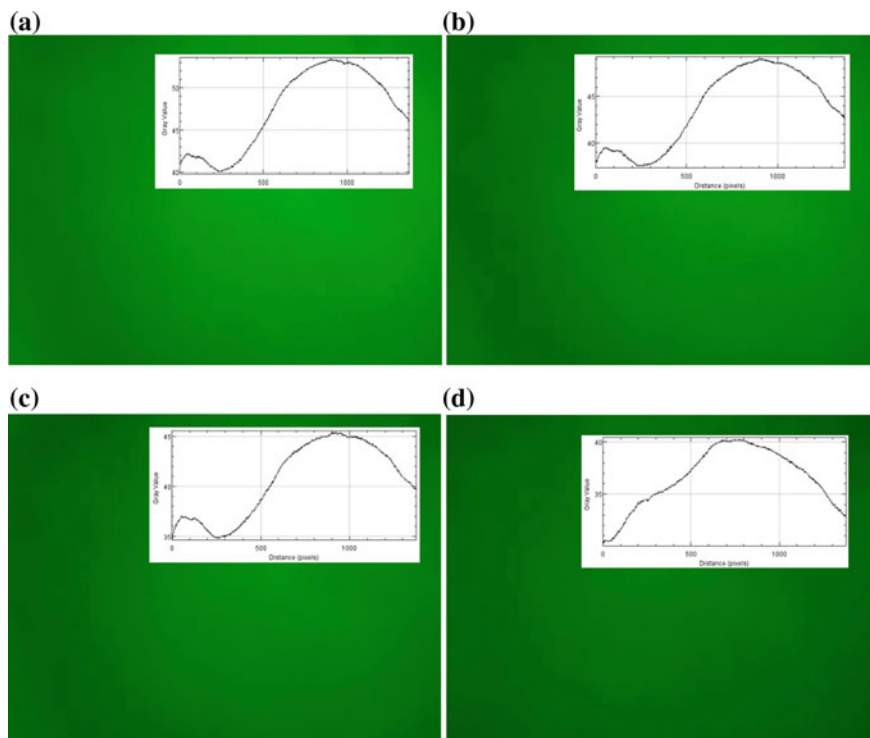


Fig. 3 Capture frames showing different fluorescence intensities at different instances and corresponding intensity plot for *Vibrio* cells over bare silicon substrate **a** at 5 s; **b** at 45 s; **c** at 85 s; **d** at 125 s

As observed through the images, the *Vibrio* cells on nanoporous silica film emit light with higher fluorescence intensity in comparison to the *Vibrio* cells on plan substrate. In case of a silicon substrate, there are possibilities of light scattering which is emitted from the cells as it contains non-confined region. In a comparison of this, the nanoporous silica provides dispersed pores (confined region of nm size) throughout the film which are responsible for reducing the light scattering during visualization of these cells over the film. The nanopores developed on silica film restrict the scattering of the light from the film which finally adds light intensity so that the detection of *Vibrio* cells with low concentration could be possible.

Figure 5 shows the overall fluorescence intensity plot for both the substrates, plotted at different time instances from 5 to 125 s. It shows the trend of fluorescence intensity which decreases with every frame. From the plot, it can be concluded that almost 70% enhancement in fluorescence intensity has been observed by depositing a thin silica layer. This way, the deposited silica layer has offered a better platform for carrying out the more sensitive detection, while helping as a supporting tool for major detection techniques.

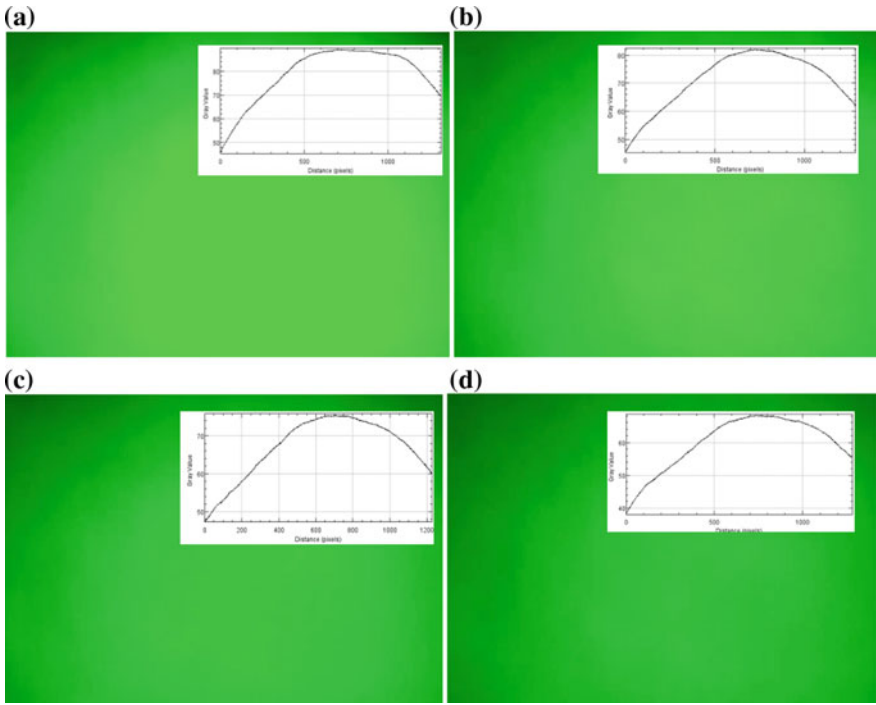
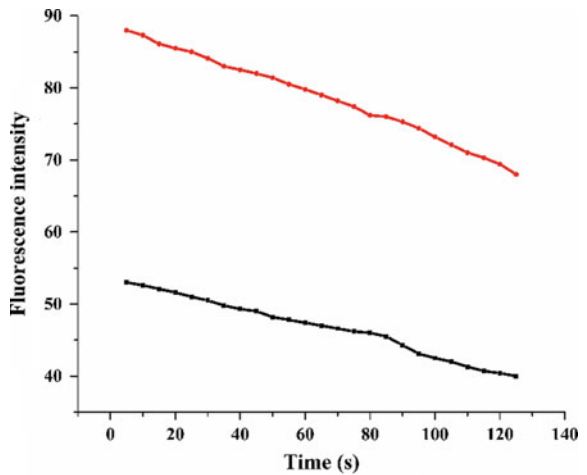


Fig. 4 Capture frames showing different fluorescence intensities at different instances and corresponding intensity plot for Vibrio cells over silica-coated silicon substrate **a** at 5 s; **b** at 45 s; **c** at 85 s; **d** at 125 s

Fig. 5 Fluorescence intensity plot for **—■—**silicon substrate and **—●—**silica-grown silicon substrate



4 Conclusions

This study includes the development of nanoporous silica film for biosensing application. The experimental analysis has been performed for quantifying the fluorescence intensity on bare silicon and nanoporous silica film. It is found that the nanoporous silica film is suitable for carrying out fluorescence measurement on bio-samples as it provides confined regions in the form of nanopores. So, it adds a new perspective to the visualization of cells in the detection scheme of cells/pathogens. As the fabricated platform is well capable of performing next-level processing, like channel formation, it helps as a precursor for the sensitive detection.

References

1. Korampally V, Yun M, Rajagopalan T, Dasgupta PK, Gangopadhyay K, Gangopadhyay S (2009) Entropy driven spontaneous formation of highly porous films from polymer-nanoparticle composites. *Nanotechnology* 20
2. West PA (1989) The human pathogenic vibrios—a public health update with environmental perspectives. *Epidemiol Infect* 103:1
3. Da-Silva E, Barthelmebs L, Baudart J (2017) Development of a PCR-free DNA-based assay for the specific detection of *Vibrio* species in environmental samples by targeting the 16S rRNA. *Environ Sci Pollut Res* 24:5690–5700
4. Tada J, Ohashi T, Nishimura N, Shirasaki Y, Ozaki H, Fukushima S, Takano J, Nishibuchi M, Takeda Y (1992) Detection of the thermostable direct hemolysin gene (tdh) and the thermostable direct hemolysin-related hemolysin gene (trh) of *Vibrio parahaemolyticus* by polymerase chain reaction. *Mol Cell Probes* 6:477–487
5. Brauns LA, Hudson MC, Oliver JD (1991) Use of the polymerase chain reaction in detection of culturable and nonculturable *Vibrio vulnificus* cells. *Appl Environ Microbiol* 57:2651–2655
6. Bej AK, Patterson DP, Brasher CW, Vickery MCL, Jones DD, Kaysner CA (1999) Detection of total and hemolysin-producing *Vibrio parahaemolyticus* in shellfish using multiplex PCR amplification of tl, tdh and trh. *J Microbiol Methods* 36:215–225
7. Panicker G, Call DR, Krug MJ, Bej AK (2004) Detection of pathogenic *Vibrio* spp. in shellfish by using multiplex PCR and DNA microarrays. *Appl Environ Microbiol* 70:7436–7444
8. Kim H-J, Ryu J-O, Lee S-Y, Kim E-S, Kim H-Y (2015) Multiplex PCR for detection of the *Vibrio* genus and five pathogenic *Vibrio* species with primer sets designed using comparative genomics. *BMC Microbiol* 15:239
9. Lyon WJ (2001) TaqMan PCR for detection of *Vibrio cholerae* O1, O139, non-O1, and non-O139 in pure cultures, raw oysters, and synthetic seawater†. *Appl Environ Microbiol* 67:4685–4693
10. Lenz DH, Mok KC, Lilley BN, Kulkarni RV, Wingreen NS, Bassler BL (2004) The small RNA chaperone Hfq and multiple small RNAs control quorum sensing in *Vibrio harveyi* and *Vibrio cholerae*. *Cell* 118:69–82
11. Schauer S, Sommer R, Farnleitner AH, Kirschner AKT (2012) Rapid and sensitive quantification of *Vibrio cholerae* and *Vibrio mimicus* cells in water samples by use of catalyzed reporter deposition fluorescence in situ hybridization combined with solid-phase cytometry. *Appl Environ Microbiol* 78:7369–7375
12. Huq A, Colwell RR, Rahman R, Ali A, Chowdhury MAR, Parveen S, Sack DA, Russek-Cohen E (1990) Detection of *Vibrio cholerae* O1 in the aquatic environment by fluorescent-monoclonal antibody and culture methods. *Appl Environ Microbiol* 56:2370–2373

13. Arshad E, Anas A, Asok A, Jasmin C, Pai SS, Bright Singh IS, Mohandas A, Biju V (2016) Fluorescence detection of the pathogenic bacteria *Vibrio harveyi* in solution and animal cells using semiconductor quantum dots. RSC Adv. 6:15686–15693
14. Sayuti M, Sarhan AAD, Salem F (2014) Novel uses of SiO₂ nano-lubrication system in hard turning process of hardened steel AISI4140 for less tool wear, surface roughness and oil consumption. J Clean Prod 67:265–276
15. Nayak M, Singh D, Singh H, Kant R, Gupta A, Pandey SS, Mandal S, Ramanathan G, Bhattacharya S (2013) Integrated sorting, concentration and real time PCR based detection system for sensitive detection of microorganisms. Sci Rep 3:3266

Wear Analysis of Al-5083 Alloy Reinforced with Chromium Oxide Filler on Air Jet Erosion Test Rig



Amit Kumar, Shiv Ranjan Kumar and Anand Prakash

Abstract Due to the operational requirement in a dusty environment, there is a strong need of research and development for the selection of metal matrix composites to reduce and control wear. In this regard, effects of various parameters on the wear rate have been studied to find the best formulation of material and the best design of machine elements. Hence, in this work, a series of preliminary experiments have been conducted as per Taguchi Orthogonal Array Methodology to investigate erosive wear behavior of Al-5083 metal matrix composites reinforced with chromium oxide filler. Analysis of variance (ANOVA) has been performed on the measured data. The findings of the result indicated that for this metal matrix, impingement angle and filler content indicated the most significant factors followed by impact velocity for minimization of erosion rate of all the particulate-filled composites.

Keywords Erosive wear · Al-5083 · Chromium oxide · Taguchi Orthogonal Array

1 Introduction

In most of the cases, the reason behind the damage, failure, and inefficient working of various machine parts, steam turbine blades, pipelines, etc., is solid particle erosion. The wear in target materials occurs as the result of impact by irregular particles at different speeds. As a result of striking of a jet of erosive particles, wear of material results in the decrease in service life of the material. Therefore, a number of materials especially alloy and composite have been developed and tested for erosive wear behavior. It was reported that the addition of filler improved the mechanical and wear properties of alloy and composite [1–5]. In this regard, Prasad et al. [6] studied the slurry wear behavior of zinc–aluminum alloys (Zn 59.8%, Al 37.5%, Cu 2.5%, and Mg 0.2%) with and without the addition of silicon content by the sample rotation method over a range of sliding speeds and distances. The slurry was made of 40% sand particles of 212–300 μm size suspended in an electrolyte. The electrolyte was

A. Kumar (✉) · S. R. Kumar · A. Prakash
Mechanical Engineering Department, JECRC University, Jaipur, India
e-mail: amitkumarjecrcu@gmail.com

© Springer Nature Singapore Pte Ltd. 2019
K. Shanker et al. (eds.), *Advances in Industrial and Production Engineering*, Lecture Notes in Mechanical Engineering, https://doi.org/10.1007/978-981-13-6412-9_2

prepared by mixing 5 ml concentrated sulfuric acid and 4 g sodium chloride in 10 l of water. It was concluded that initially, the wear rate was increased with sliding distance, later attained maximum wear, and then decreased. However, wear increased with increasing the sliding speed irrespective of the alloy composition. Further, it was reported that the addition of silicon decreased the wear rate of zinc–aluminum alloy material. Flynn et al. [7] reported that the erosive wear decreased with the increase in toughness and strain energy of the material. Das et al. [8] fabricated LM13 alloy and LM13–SiC composites to study the erosion–corrosion wear of aluminum alloy composites. They observed that an increase in speed resulted in the decrease in mass loss irrespective of the material. This was due to the fact that at higher speed, the sand particles slide over the surface without any wear. Recco et al. [9] reviewed the surface treatment processes for improving the erosion resistance of an AISI 304 stainless steel. Six kinds of sample conditions were tested in slurry composed of distilled water and SiC particles. The erosive wear test was conducted on a test rig for 6 h with jet velocity of 8.0 m/s and normal angle of incidence. The results showed that the wear rate of AISI 304 stainless steel was reduced by 1.5 times in high temperature gas nitriding and reduced by 2 times in low temperature pulsed plasma nitriding. Disale et al. [10] conducted experiments in a pot tester to investigate the effect of particle size on erosion wear of aluminum alloy 6063 (AA 6063). Slurry consisted of 37.5–655 μm was used at 3 m/s velocity for 20 wt% concentration of solids at 30°–90° angle of impact. It was concluded that the material removal from erosion changed to three-body abrasion. Due to three-body abrasion, the wear due to smaller-sized particles was little higher compared to that of bigger-sized particles.

Factor et al. [11] evaluated the erosion wear using solid particles SiC in He gas of Wc-17Co and $\text{Cr}_3\text{C}_2 + 25\text{NiCr}$ coatings on steel alloy. They evaluated that coating decreased the erosion wear rate. At an angle of 90°, Wc-17Co showed the better result but at low impact angles, $\text{Cr}_3\text{C}_2 + 25\text{NiCr}$ was better. On the other hand, Harsha et al. [12] explained the erosion mechanism in which they worked on aluminum, brass, and copper as non-ferrous and stainless steel and cast iron as ferrous material. The impact parameters such as erodent size, erodent shape, impingement angle, impact velocity, and erodent feed rate were taken. They performed erosion test on air jet erosion test for experimental analysis and Taguchi method for theoretical calculation. After performing various experiments, they obtained mechanical and wear properties such as tensile strength, hardness, erosion rate, and modulus of elasticity as the final output.

Hence, the aim of this work was to fabricate Al-5083 metal matrix composites reinforced with chromium oxide and study the effect of various parameters that influence the erosive performance of materials.

2 Experimental Procedure

2.1 Materials and Sample Preparation

Aluminum-5083 and chromium trioxide (Cr_2O_3) were procured from the local market in Jaipur, India. Aluminum-5083 (390 g) in powder form was put in burnout furnace machine in which temperature was controlled by PID controller furnace and heated up to the melting point of Al-5083 which was 570°C . The filler was added to the molten Al-5083 in different composition (2, 3, and 4 wt%) in different graphite crucibles and stirred to mix the filler homogeneously. Then, it was poured it into the mold to give it perfect shape. Then, the material was allowed to cool by air cooling. The homogenization process was done on prepared sample in which we put our sample in the furnace at 420°C for 55 min.

2.2 Air Jet Erosion Test

The erosive wear test was performed on air jet erosion test rig, DUCOM, Bangalore, India. The experiments were performed as per the standard ASTM G76 international test procedure. The parameters were taken in such a way to simulate erosive situations. Impact velocity, impingement angle, and filler content were varied to find the best condition for minimum erosive wear.

2.3 Design of Experiment (DOE)

Taguchi orthogonal design of experiment was used to examine the effect of more than one variable and their interactions on the output of the process. S/N ratio was calculated in DOE to obtain an improved solution. The following equation is used to find out the S/N ratio:

$$\frac{S}{N} = 10 \log \left[\frac{1}{n} \sum_{i=1}^n y_i^2 \right] \quad (1)$$

where n is the number of tests and y_i is the value of experimental result of the i th test. The characteristics of S/N ratio have been categorized into three classes, i.e., smaller-the-better, larger-the-better, and nominal-the-better. For obtaining optimal and improved performance, smaller-the-better characteristic has been selected for erosion wear. Table 1 indicates the factors selected for experimental analysis using Taguchi method. The array chosen in this study was L_{16} orthogonal array design which has 16 rows corresponding to the number of variables selected.

Table 1 List of factors and levels in Taguchi Orthogonal Array

Factor	Type	Level	Value	Unit
Impact velocity	Fixed	3	20, 25, 30	m/s
Impingement angle	Fixed	3	30, 60, 90	°
Filler content	Fixed	3	2, 3, 4	wt%

3 Results and Discussion

3.1 Erosive Wear Analysis Using Taguchi Orthogonal Array

In design of experiment, the main application of Taguchi method was to find the best combination of parameters for minimum wear rate of Al-5083 alloy reinforced with chromium oxide filler. The experiments were performed, and results were presented in Table 2. In Table 2, the eighth column was *S/N* ratio of the wear rate of the Al-5083 alloy. The overall mean for the *S/N* ratio of the specific wear rate was found to be 64.36 db for the Al-5083 alloy reinforced with chromium oxide filler. The analysis was performed using the software Minitab 16 to analyze the wear rate of Al-5083 alloy reinforced with chromium oxide filler. The analysis based on *S/N* ratio was depicted in Fig. 1.

Figure 1 indicated the analysis related to *S/N* (signal-to-noise) ratio and revealed that the factor combination of A3, B3, and C2 gives minimum erosion rate for the prepared sample of the metal matrix composite. Therefore, wear rate of Al-5083 alloy reinforced with chromium oxide filler was minimum at the impact velocity of 30 m/s, impingement angle of 90°, and filler content of 3 wt%.

Table 2 Experimental design using L₉ orthogonal array

Impact velocity (m/s)	Impingement angle (°)	Filler content (wt%)	Initial weight (g)	Final weight (g)	Erosion loss (g)	Specific wear (g/min)	<i>S/N</i>
20	30	2	14.574	14.566	0.008	0.0008	61.9382
20	60	3	14.441	14.436	0.005	0.0005	66.0206
20	90	4	15.271	15.265	0.006	0.0006	64.4370
25	30	3	14.145	14.139	0.006	0.0006	64.4370
25	60	4	15.487	15.481	0.006	0.0006	64.4370
25	90	2	15.830	15.824	0.006	0.0006	64.4370
30	30	4	16.015	16.008	0.007	0.0007	63.0980
30	60	2	15.482	15.476	0.006	0.0006	64.4370
30	90	3	14.555	14.550	0.005	0.0005	66.0206

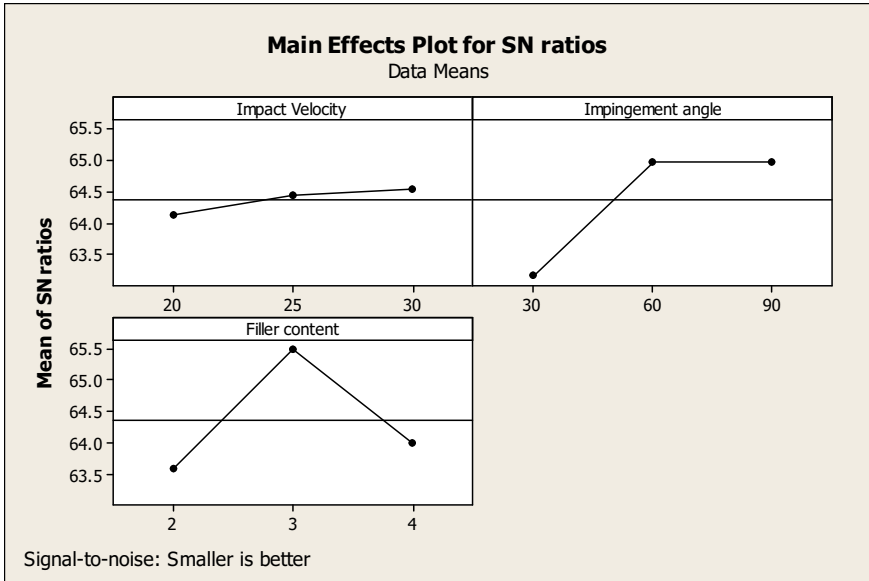


Fig. 1 Analysis related to S/N ratio

3.2 ANOVA

Analysis of variance (ANOVA) was used to investigate the influence of various input parameters like impact velocity, impingement angle, and erodent discharge on the basis of experimental results. By ANOVA, we determined the percentage contribution of that particular variable and its dominance over other factors. Table 3 presented ANOVA results for erosion rate for Al-5083 metal matrix composites reinforced with chromium oxide.

The percentage contribution of impingement angle, filler content, and impact velocity was 0.037, 0.040, and 0.5, respectively. Out of these factors, impingement

Table 3 Analysis of variance for SNRA1 versus impact velocity, impingement angle, and filler content

Source	DF	Seg SS	Adj SS	Adj MS	F	P
Impact velocity	2	0.2492	0.2492	0.1246	1.00	0.500
Impingement angle	2	6.5313	6.5313	3.2657	26.21	0.037
Filler content	2	5.9728	5.9728	2.9864	23.97	0.040
Error	2	0.2492	0.2492	0.1246		
Total	8	13.0024				

angle and filler content indicated the most significant factor followed by impact velocity.

4 Conclusions

Al-5083 metal matrix composites with ceramic fillers Cr_2O_3 were successfully fabricated. The experiments were performed as per Taguchi Orthogonal Array. The significant factors affecting the erosion rate have been identified by applying ANOVA. Impingement angle and filler content indicated the most significant factors followed by impact velocity for minimization of erosion rate of all the particulate-filled composites. The addition of particulate filler Cr_2O_3 in metal matrix composites improves their erosion wear resistance.

References

1. Hutchings IM, Deuchar DWT (2012) Erosion of unfilled elastomers by solid particle impact. *J Mater Sci* 22:4071–4076
2. Besztercey G, Karger-Kocsis J, Szaplónczay P (2012) Solid particle erosion of electrically insulating silicon and EPDM rubber compounds. *Polym Bull* 42:717–724
3. Arnold JC, Hutchings IM (2011) Erosive wear of rubber by solid particles at normal incidence. *Wear* 161:213–221
4. Zahavi J, Schmitt GF (2009) Solid particle erosion of polymeric coatings. *Wear* 71:191–210
5. Barkoula NM, Karger-Kocsis J (2008) Review processes and influencing parameters of the solid particle erosion of polymers and their composites. *J Mater Sci* 37:3807–3820
6. Prasad BK, Modi OP, Jha AK, Patwardhan AK (2007) Effects of some material and experimental variables on the slurry wear characteristics of zinc aluminium alloy. *ASM Int* (2007)
7. O' Flynn DJ, Bingley MS, Bradley MSA, Burnett AJ (2008) A model to predict the solid particle erosion rate of metals and its assessment using heat-treated steels. *Wear* 248:162–177
8. Das S, Sarswati YS, Mondal DP (2008) Erosive corrosive wear of aluminium alloy composites; influence of composition and speed. *Wear* 261:180–190
9. Recco AAC, Lopez D, Bevilacqua AF, Silva FD, Tschiptschin AP (2009) Improvement of the slurry erosion resistance of an austenitic stainless steel with combinations of surface treatments nitriding and TiN coating. *Surf Coat Technol* 202:993–997
10. Desale GR, Gandhi BK, Jain SC (2009) Particle size effects on the slurry erosion of aluminium alloy (AA 6063). *Wear* 266:1066–1071
11. Factor M, Roman I (2007) Micro-hardness as a simple means of estimating relative wear resistance of carbide thermal spray coatings. *J Therm Spray Technol*, 482–495
12. Harsha AP, Thakre AA (2007) Investigation on solid particle erosion behaviour of polyether imide and its composites. *Wear* 262:807–818

Statistical Analysis of Surface Roughness Using RSM in Hard Turning of AISI 4340 Steel with Ceramic Tool



Asutosh Panda, Sudhansu Ranjan Das and Debabrata Dhupal

Abstract The present study concerns the modeling and optimization of surface roughness in dry hard turning of high-strength low-alloy (HSLA) grade AISI 4340 steel (49 HRC) with coated ceramic tool. For parametric study, the turning operations have been established according to Taguchi L_{27} orthogonal array consisting of an experimental design matrix 3 levels and 3 principal turning parameters (factors) such as, cutting speed, axial feed, and depth of cut. Analysis of sixteen set experimental data with ANOVA showed that axial feed and speed are the most significant controlled cutting parameters for hard turning operation, if the improvement of the machined surface finish is considered. Thereafter, statistical regression model based on response surface methodology has been proposed for correlation of cutting parameters with machined workpiece surface roughness. Finally, optimal cutting conditions with the aim to minimize the surface roughness via desirability function approach of RSM are proposed.

Keywords Hard turning · AISI 4340 steel · Ceramic tool · OA · ANOVA · RSM

1 Introduction

Nowadays in metal cutting-based manufacturing industries, dry hard turning is widely used in machining of hardened steel because of its low cost, high machining efficiency and green environmental protection, and surface finish of hard turned components has greater influence on functionality of product concerning tribological behavior, fatigue strength, and wear as well as corrosion resistance. The cutting mechanism of dry hard turning is different from that of traditional turning because of multi-field coupling effect in machining process. Thus, the above-cited advantages of hard turning (HT) can only be obtained with appropriate selection of process parameters, cutting tool materials and geometry, and cutting environment. A number

A. Panda · S. R. Das (✉) · D. Dhupal
Department of Production Engineering, VSS University of Technology, Burla
768018, India
e-mail: das.sudhansu83@gmail.com

© Springer Nature Singapore Pte Ltd. 2019
K. Shanker et al. (eds.), *Advances in Industrial and Production Engineering*, Lecture Notes in Mechanical Engineering, https://doi.org/10.1007/978-981-13-6412-9_3

of investigative studies have been carried out for the assessment of various process variables (cutting parameters, tool geometry, workpiece hardness, and environmental conditions) using the statistical approach via analysis of variance (ANOVA) [1–4]. Similarly, researchers have focused on modeling as well as optimization in order to predict and control the result for minimizing surface roughness of various hardened steel materials (AISI D2, D3, D6, 1015, 1045, 4140, 4340, 52100, H11, and H13) during HT process using response surface methodology [5–7], which allowed to enrich the saving cost and time. However, relatively few investigations as well as lack of systematic studies have been executed concerning process modeling and parametric optimization for surface roughness, which is need to be explored for practical improvement in productiveness by hard turning as it is categorical worthy and beneficial for machining industries point of view to achieve their goal. Thus, the present research is focused on parametric study (assessment), process modeling, and optimization of surface roughness during turning hardened HSLA steel (49 HRC) with PVD–TiN coated Al_2O_3 –TiCN mixed ceramic tool using Taguchi's OA, analysis of variance, response surface methodology, and desirability function approach.

2 Experimental Procedure

Cylindrical specimens (diameter and length of 90 mm and 220 mm, respectively) made of AISI 4340 steel were turned on a high precision and accuracy CNC lathe (make: Batliboi ltd., model: SPRINT 16TC), having 7.5 kW power capacity and spindle speed varies from 50 to 5000 rpm. High-strength low-alloy (HSLA) grade AISI 4340 steel (49 HRC) was chosen in the experiment because of its hardenability and wide application. For experimentation, PVD coated ceramic with TiN layer, designated as ISO grade CNGA120408 AB2010, having negative rake angle 60, nose radius of 0.8 mm, and approach angle of 950 is used for finish hard turning employing design of experiments. The coated ceramic insert was rigidly held on a ISO-designated tool holder of PCLNL2525M12. The measurements of machined surface for each cutting conditions were acquired from Mitutoyo (Surftest SJ210) roughness tester. The arithmetic mean surface roughness (R_a) was taken at different three positions on the cylindrical surface of test specimen and its mean is taken as final average surface roughness value. Statistical Minitab 16 software has been used for optimization, modeling, normality plot, and surface plot. The schematic view of experimental work and methodology proposed in the current study is presented in Fig. 1.

To accomplish the objective of proposed research work, depth of cut, axial feed, and cutting speed are taken as major process variables with an attempt to analyze surface roughness as the only technological response parameter. The different cutting parameters and their values are shown in Table 1. The levels of the parameters were selected based on the recommendation of tool's manufacturer (TaeguTec). Taguchi's orthogonal array (OA) has been established as balanced approach for design of experiments which ensures the all levels of all factors equally and assures accuracy of

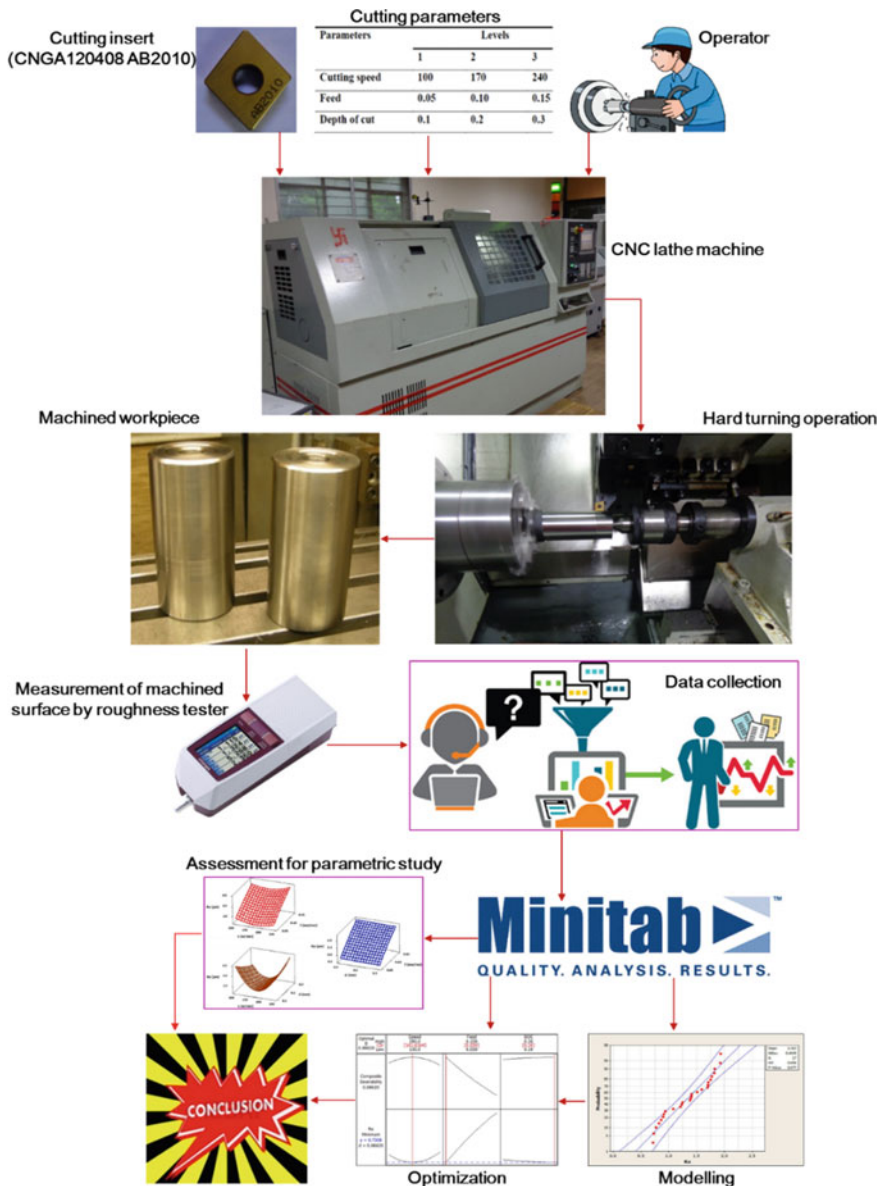


Fig. 1 Schematic of experimental setup and methodology presented

Table 1 Parameters and levels

Parameters	Levels		
	1	2	3
Cutting speed, v (m/min)	100	170	240
Feed, f (mm/rev)	0.05	0.10	0.15
Depth of cut, d (mm)	0.1	0.2	0.3

the statistical model. Hence, employing the selected controllable parameters (three) and levels (three), a well sequential design layout was established based on L27 OA in order to perform the dry longitudinal turning operation (Table 2).

3 Results and Discussion

3.1 Analysis of Surface Roughness

Experimental results by Taguchi OA are analyzed by employing analysis of variance which involves statistical treatment to access the significance as well as determines the percentage of contribution of each process variables (v , f , d) against a stated level of confidence (here, 95%) on the response under consideration (here, surface roughness Ra). Here, P -value indicates the influence of the factor on Ra as: significant if $P \leq 0.05$, and insignificant if $P > 0.05$. The ratio of factor-mean-square to the error-mean-square called Fisher's ratio (F) determines significant parameter affecting quality characteristic comparing the F -test value of the parameter with the standard F -table value at the 0.05 significance level. ANOVA for surface roughness has been illustrated in Table 3. From the analysis, it is illustrated that feed is the most effective variable, revealing significant contribution (80.05%) on surface roughness (Ra) as its P -value is under 0.05 and over F -value (4.46). The next parameter based on F -value is the cutting speed with 27.54 for Ra and its contribution on Ra is 13.56%. The depth of cut (d) does not have any noticeable effect on Ra (0.76% only). Also, the interaction of cutting variables like cutting speed-feed ($v*f$), feed-depth of cut ($f*d$), and cutting speed-depth of cut ($v*d$) do not exhibit any statistical imprint on the observed surface roughness. Respectively, their contributions are (0.96, 1.47, and 1.23% to Ra) and the error associated with the ANOVA is 1.97% for Ra.

Three dimension (3D) effect plots for surface roughness Ra is shown in Fig. 2. It was found that with increase in feed, Ra increased resulting degradation of surface finish predominantly (see, Fig. 2a). This phenomenon may be attributed to the following reasons: (1) neglecting the effect of BUE formation and tool flank wear [1], (2) increase in axial feed leads to increase in thrust force which in turn induces vibration followed by heat generation [8], and (3) as feed increases, the plowing action becomes predominant thereby forming deeper and broader helicoid furrows on machined surface due to insert's nose profile and workpiece-tool movements [9].

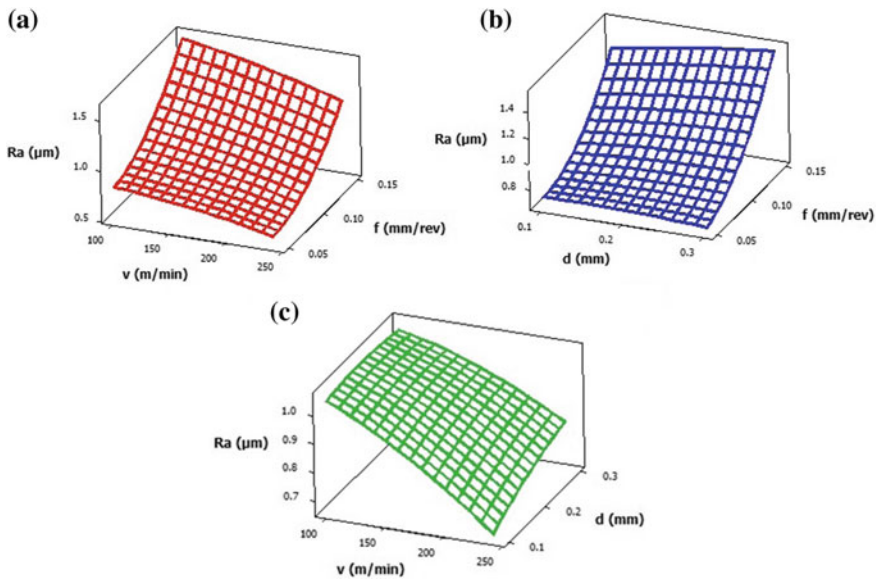
Table 2 Experimental design and results

Test no.	Coded values			Actual settings			Surface roughness Ra (μm)
	v	f	d	v (m/min)	f (mm/rev)	d (mm)	
1	1	1	1	100	0.05	0.1	0.854
2	1	1	2	100	0.05	0.2	0.643
3	1	1	3	100	0.05	0.3	0.843
4	1	2	1	100	0.1	0.1	0.951
5	1	2	2	100	0.1	0.2	1.188
6	1	2	3	100	0.1	0.3	1.073
7	1	3	1	100	0.15	0.1	1.569
8	1	3	2	100	0.15	0.2	1.620
9	1	3	3	100	0.15	0.3	1.596
10	2	1	1	170	0.05	0.1	0.829
11	2	1	2	170	0.05	0.2	0.762
12	2	1	3	170	0.05	0.3	0.629
13	2	2	1	170	0.1	0.1	0.914
14	2	2	2	170	0.1	0.2	0.955
15	2	2	3	170	0.1	0.3	0.928
16	2	3	1	170	0.15	0.1	1.361
17	2	3	2	170	0.15	0.2	1.382
18	2	3	3	170	0.15	0.3	1.463
19	3	1	1	240	0.05	0.1	0.516
20	3	1	2	240	0.05	0.2	0.631
21	3	1	3	240	0.05	0.3	0.573
22	3	2	1	240	0.1	0.1	0.629
23	3	2	2	240	0.1	0.2	0.705
24	3	2	3	240	0.1	0.3	0.788
25	3	3	1	240	0.15	0.1	1.071
26	3	3	2	240	0.15	0.2	1.267
27	3	3	3	240	0.15	0.3	1.427

It is also observed that the surface roughness decreases as cutting speed increases (refer, Fig. 2c). This can be attributed to intense elastic deformation and squeezing effect within workpiece-tool junction area at slower cutting speeds as compared to higher speeds, reported by Tang et al. [10]. Another possible explanation is that the heat dispersed by chip is much lesser than that absorbed by the turned surface at low cutting speed which is manifested as higher surface roughness Ra. Aouici et al. [11] also obtained similar results. As the cutting speed rises, the tool chip contact duration decreases thereby subsiding the BUE resulting improvement in surface finish,

Table 3 Analysis of variance (ANOVA) for surface roughness criteria (Ra)

Source	DOF	Seq SS	Adj SS	Adj MS	<i>F</i>	<i>P</i> -value	<i>C</i> (%)
<i>v</i> (cutting speed)	2	0.41872	0.41872	0.20936	27.54	<0.000	13.56
<i>f</i> (feed)	2	2.47242	2.47242	1.23621	162.63	<0.000	80.05
<i>d</i> (depth of cut)	2	0.02335	0.02335	0.01167	1.54	0.273	0.76
<i>v</i> * <i>f</i>	4	0.02960	0.02960	0.00740	0.97	0.473	0.96
<i>v</i> * <i>d</i>	4	0.04558	0.04558	0.01139	1.50	0.290	1.47
<i>f</i> * <i>d</i>	4	0.03812	0.03812	0.00953	1.25	0.363	1.23
Error	8	0.06081	0.06081	0.00760			1.97
Total	26	3.08859					100

**Fig. 2** Surface plots of surface roughness, Ra

in accordance with the previous study [2]. The depth of cut is not very sensitive to influence the surface roughness of turned surfaces; nevertheless, Ra increases slightly with increase in depth of cut (Fig. 2b) for harder material mainly due to chatter, as revealed by Naigade et al. [12].

3.2 Prediction of Optimal Performance

From the ANOVA analysis (Table 3), two cutting parameters (feed and speed) were found significant and obtained the lowest surface roughness at feed of 0.05 mm/rev

(level-1) and cutting speed of 240 m/min (level 3). Optimal performance of Ra when two most significant factors are at their best level, i.e., at $f_1 v_3$ level, then

$$\begin{aligned} \mu_{Ra} &= \bar{f}_1 + \bar{v}_3 - \bar{T}_{Ra} = (0.6978 + 0.8452) - 1.006 \\ &= 0.537 \mu\text{m} \quad (\bar{T}_{Ra} = 1.006 \text{ from Table 2}) \end{aligned}$$

Confidence interval (CI) for surface roughness (Ra) is calculated with the help of following equation

$$CI = \sqrt{\frac{F_{95\%;(1, DF_{error})} \times V_e}{\eta_{eff}}} \tag{1}$$

where

$$\eta_{eff} = \frac{\text{Number of trials}}{1 + \text{degrees of freedom corresponding to that level}} = \frac{27}{1 + 2 + 2} = 5.4$$

$$F_{95\%;(1, 8)} = 5.32 \quad \text{and} \quad V_e = 0.0076 \quad (\text{from Table 3})$$

$$\text{Hence, } CI_{Ra} = \sqrt{\frac{5.32 \times 0.0076}{5.4}} = 0.086 \mu\text{m}$$

The best optimal range of Ra is predicted as, $[\mu_{Ra} - CI_{Ra}] \leq \mu_{Ra} \leq [\mu_{Ra} + CI_{Ra}]$ i.e. $0.451 \leq \mu_{Ra} \leq 0.623 \mu\text{m}$.

3.3 Empirical Modeling for Surface Roughness

Empirical modeling can be described as compilation of mathematical function and statistical approach for the analysis and modeling of numeric problems which are connected with design of experiments as well as least square error fitting. The output responses are resolved by various input parameters and the major objective is to obtain the relation between the output response (here, Ra) and the input variables (here, v, f, d) studied. Predictive mathematical model for response, Ra is expressed using regression analysis named response surface methodology (RSM) with uncoded unit at 95% confidence level taking into consideration of L27 orthogonal array experimental result data set. From the surface roughness model Eq. (2), it is noticed that coefficient of determinations (experimental and adjusted) are $R^2 = 96.4\%$ and $R^2(\text{adj}) = 94.5\%$, respectively.

$$\begin{aligned} Ra &= 1.1259 - 0.9467d - 5.6443f - 0.0003v - 1.6222d^2 + 61.6444f^2 - 0.000v^2 \\ &\quad + 10.6500f * d + 0.0052v * d - 0.0095v * f \end{aligned} \tag{2}$$

The R^2 value is very close to unity, which ensures the excellence of fit for the model with greater statistical significance. Additionally, normal probability plot has

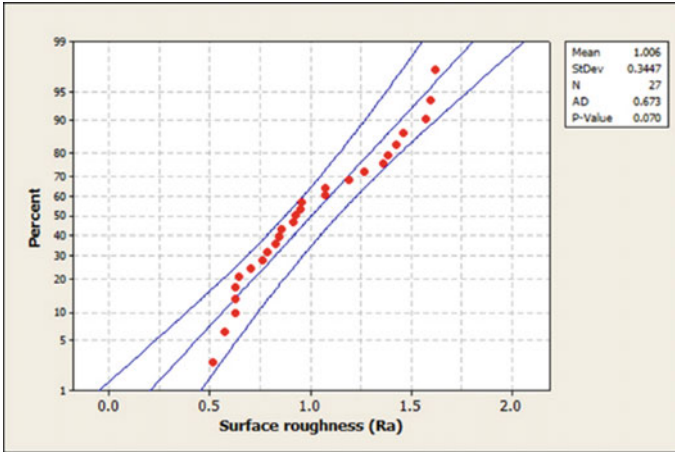


Fig. 3 Normal probability plot for Ra

been displayed for surface roughness as shown in Fig. 3, which ensures that the residuals distributed fairly approach to a straight line indicating the errors are dispersed normality that implies to good correlation between measured and predicted values. With *P*-value (0.07) complimented by Anderson-Darling test is over significance level value (0.05), which confirms the adequacy of model due to favorable reception of null-hypothesis.

4 Optimization of Surface Roughness Using RSM

In this study, with the goal to minimize the surface roughness, desirability function analysis of RSM is utilized for response optimization which is basically employed to determine the best parametric arrangement for single and multi-objective optimizations. This optimization unit looks for a combination of parameter levels that concurrently fulfill the necessities placed on each and every one of the responses, and parameter trying to set up the suitable model. Performance of the optimization procedure adopted is given by composite desirability index through gradient algorithm. It is the weighted geometric average of individual desirability indices for different responses in the range 0–1. If the value of desirability lies nearer to zero, the response would be absolutely rejected. On the other hand, if its value approaches unity, the response would be acknowledged. Optimum cutting speed, axial feed, and doc during hard turning of AISI 4340 steel obtained using RSM technique (see, Fig. 4) are 240 m/min, 0.0556 mm/rev, and 0.10 mm, respectively, for corresponding estimated minimum surface roughness (Ra) 0.5451 μm , is approaching good predictive ability as the percentage of error about 4.8% when it is compared with the experimental value (refer, Table 4).

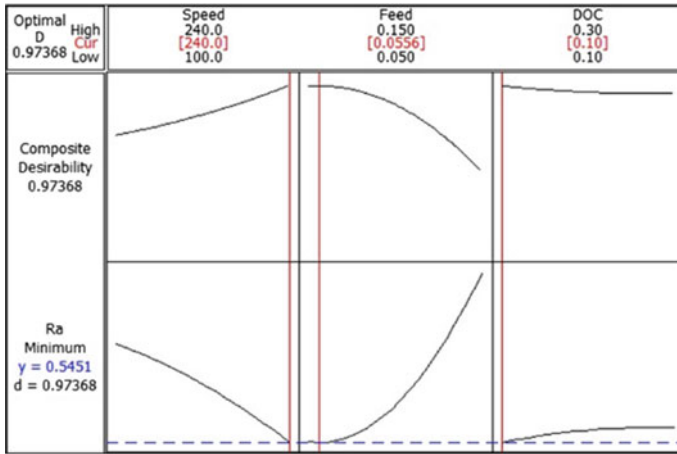


Fig. 4 Optimization plot for Ra

Table 4 Summary of confirmation experiments and comparison of results

Optimal control parameters			Surface roughness, Ra (μm)		Error (%)
V	f	d	Predicted	Experimental	
240 m/min	0.0556 mm/rev	0.1 mm	0.545 μm	0.52 μm	4.8

5 Conclusions

Based on experimental findings, modeling, and optimization in finish dry hard turning (FDHT) of HSLA steel utilizing PVD–TiN coated mixed (Al_2O_3 –TiCN) ceramic tool, machined surface quality of HSLA steel with coated ceramic insert produced roughness within 1.6 μ and can be comparable with cylindrical grinding. Surface roughness was highly emulated by the feed (Ra: 80.05%) followed by the cutting speed (Ra: 13.56%), which well agrees with ANOVA results. Increase in feed the surface roughness increases, but the opposite is seen with cutting speed. The predicted optimal range of surface roughness criteria (Ra) at 95% CI level is $0.451 \leq \mu_{\text{Ra}} \leq 0.623 \mu\text{m}$. Empirical model developed for response such as surface roughness has R^2 value close to unity. This ensures the excellence of fit for the model with greater statistical significance. The normal probability plots ensures that the residuals distributed fairly near to a straight line indicating that the errors are dispersed in normality and implying that the sources associated with the model are significant. Anderson–Darling test for model show adequate, as P -value is more than 0.05 at 95% confidence level.

References

1. Das SR, Panda A, Dhupal D (2017) Analysis of surface roughness in hard turning with coated ceramic inserts: cutting parameters effects, prediction model, cutting conditions optimization and cost analysis. *Ciência e Técnica Vitivinícola: Sci Technol J* 32:127–154
2. Bensouilah H, Aouici H, Meddour I, Yallese MA (2016) Performance of coated and uncoated mixed ceramic tools in hard turning process. *Measurement* 82:1–18
3. Das SR, Kumar A, Dhupal D (2016) Experimental investigation on cutting force and surface roughness in machining of hardened AISI 52100 steel using CBN tool. *Int J Mach Mach Mater* 18:501–521
4. Panda A, Das SR, Dhupal D Surface roughness analysis for economic feasibility study of coated ceramic tool in hard turning operation. *Process Integr Optim Sustain*. <https://doi.org/10.1007/s41660-017-0019-9>
5. Nouioua M, Yallese MA, Khettabi R, Belhadi S, Bouhalais ML, Girardin F (2017) Investigation of the performance of the MQL, dry, and wet turning by response surface methodology (RSM) and artificial neural network (ANN). *Int J Adv Manuf Technol* 93:2485–2504
6. Mia M, Dhar NR Prediction and optimization by using SVR, RSM and GA in hard turning of tempered AISI 1060 steel under effective cooling condition. *Neural Comput Appl*. <https://doi.org/10.1007/s00521-017-3192-4>
7. Das SR, Panda A, Dhupal D (2017) Experimental investigation of surface roughness, flank wear, chip morphology and cost estimation during machining of hardened AISI 4340 steel with coated carbide insert. *Mech Adv Mater Mod Processes* 3:1–14
8. Suresh R, Basavarajappa S, Samuel GL (2012) Some studies on hard turning of AISI 4340 steel using multilayer coated carbide tool. *Measurement* 45:1872–1884
9. Khellaf A, Aouici H, Smaiah S, Boutabba S, Yallese MA, Elbah M (2016) Comparative assessment of two ceramic cutting tools on surface roughness in hard turning of AISI H11 steel: including 2D and 3D surface topography. *Int J Adv Manuf Technol* 89:333–354
10. Tang L, Gao C, Huang J (2015) Experimental investigation of surface integrity in finish dry hard turning of hardened tool steel at different hardness levels. *Int J Adv Manuf Technol* 77:1655–1669
11. Aouici H, Yallese MA, Chaoui K (2012) Analysis of surface roughness and cutting force components in hard turning with CBN tool: prediction model and cutting conditions optimization. *Measurement* 45:344–353
12. Naigade DM, Patil DK, Sadaiah M (2013) Some investigations in hard turning of AISI 4340 alloy steel in different cutting environments by CBN insert. *Int J Mach Mach Mater* 14:165–193

A Current Review of Supply Chain Performance Measurement Systems



Shubham Tripathi and Manish Gupta

Abstract A supply chain is the network of entities (individual or organisation) who work together to fulfil customer demands efficiently with maximum profits without compromising quality of product or service. Traditionally, supply chains were assessed based on financial measures but increasing competition and changing scenarios. Supply chains today are assessed based on various non-financial parameters such as customer satisfaction, sustainability and resilience. Performance measurement quantifies the extent up to which a supply chain is achieving its perceived objectives based on performance indicators. With diverse sectors of industry and varying goals of different supply chains, the performance indicators vary as well. The paper intends to provide a critical review on supply chain performance measurement literature by compiling key performance indicators for various sectors to understand the diversity and complication of performance measurement systems.

Keywords Supply chain · Performance measurement · KPI · Supply chain performance

1 Introduction

A supply chain is the network of organisations that are involved, through upstream and downstream linkages, in the different processes and activities that produce value in the form of products and services delivered to the ultimate consumer [1]. With the onset of global economy, there has been immense increase in competition and global uncertainties, and organisations need to improve continuously to stay in market [2]. As pointed by Kaplan, ‘We cannot improve what we cannot measure’ [3], productivity measurement and improvement go hand in hand. Performance measurement is the process of quantifying action. This quantification is basically the indicator of an organisation’s efficiency. Prior to 1980s, efficiency and success of organisations

S. Tripathi (✉) · M. Gupta
Department of Mechanical Engineering, Motilal Nehru National Institute of
Technology Allahabad, Allahabad, India
e-mail: shubs0508@gmail.com

were measured by number or financial figures (return on investment, return on assets, sales volume, cost margin, etc.) which often gave a limited and misleading picture of the organisational performance. Measures involving both financial and non-financial aspects of performance are being researched since 1990s as the changing global scenario required improvement of features like customer satisfaction, quality of product, reliability and service; hence, the need of measuring performance based on multi-dimensional criteria increased. Performance measurement matrix [4], performance pyramid system [5], results and determinants framework [6], the balance scorecard [3, 7] and performance prism [8–10] are some actively adopted classical performance measurement frameworks given between 1989 and 2001 to give modified performance measurement frameworks specific to different industries and applications. The current performance measurement systems require quantification of numerous subjective factors which can be cost drivers or attributes for efficiency and customer satisfaction. Keegan et al. pointed out that performance measures must be derived from company vision which ultimately leads to strategy [4]. A lack of understanding of benefits of performance measurement is a major challenge to performance measurement systems in supply chain [11].

Performance measurement in supply chain is still a fruitful area of research [12]. Section 2 presents the review methodology and categorisation of articles based on journal, year of publication, geographical distribution and approach of study. Section 3 encompasses the various research themes in supply chain performance measurement. Section 4 presents tabulation of frequently used key performance indicators (KPIs) for various sectors. In Sect. 5, discussion and conclusion from the literature review are presented.

2 Review Methodology

There have been a limited number of literature reviews performed in supply chain performance measurement which can be referred from Refs. [12–21], some focusing on sustainability and others on overall supply chain. Google Scholar database was used to first identify the research papers for the review which were then downloaded with the help of ISI Web of Science, Scopus and website of various journals. There were 320 articles which had the phrase ‘supply chain performance measurement’ in their title for the time period of 2010–2017. Out of the 320 articles, the papers that have been published in renowned journals or special editions for proceedings of international conferences in English language and have already been cited by other scholars were taken up for review. Among the papers refined through selection criteria, the 84 papers accessible into the institute library have been reviewed (Fig. 1).

The topic being multidisciplinary, papers can be located in intersection of supply chain, performance measurement, business process measurement, operations management, industrial engineering, benchmarking, computer science and IT, and hence, journals concerned with varied topics serve as outlet for SCPM literature. Table 1 presents the journal-wise distribution of articles published.

Table 1 Journal-wise distribution

S. no.	Journal title	No. of publications
1	International Journal of Productivity and Performance Management	8
2	Benchmarking: An International Journal	7
3	Supply Chain Management: An International Journal	7
4	Computers and Industrial Engineering	6
5	International Journal of Logistics Systems and Management	6
6	International Journal of Production Research	5
7	Industrial Management and Data Systems	3
8	International Journal of Business Performance and Supply Chain Modelling	3
9	Production Planning and Control: The Management of Operations	3
10	International Journal of Business Performance Management,	2
11	International Journal of Production Economics	2
12	Journal of Cleaner Production	2
13	Journal of Humanitarian Logistics and Supply Chain Management	2
14	Baltic Journal of Management	1
15	Business Process Management Journal	1
16	Computers in Industry	1
17	Expert Systems with Applications	1
18	Facilities	1
19	International Journal of Agile Systems and Management	1
20	International Journal of Applied Decision Sciences	1
21	International Journal of Business Excellence	1
22	International Journal of Intelligent Enterprise	1
23	International Journal of Intercultural Information Management	1
24	International Journal of Procurement Management	1
25	International Journal of Product Development	1
26	International Journal of Services and Operations Management	1
27	International Journal of Value Chain Management	1
28	International Journal of Operations and Production Management	1
29	Journal of Business and Industrial Marketing	1
30	Journal of Computational Science	1
31	Journal of Rural Studies	1
32	Sustainable Production and Consumption	1
33	Miscellaneous Conferences	9
	Total	84

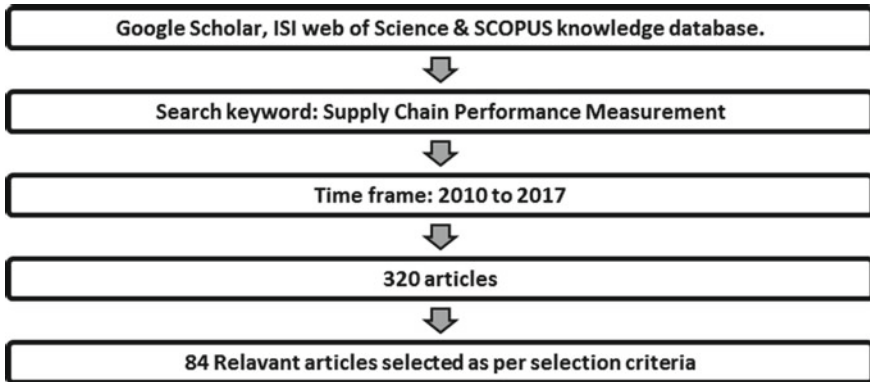


Fig. 1 Flowchart of review methodology

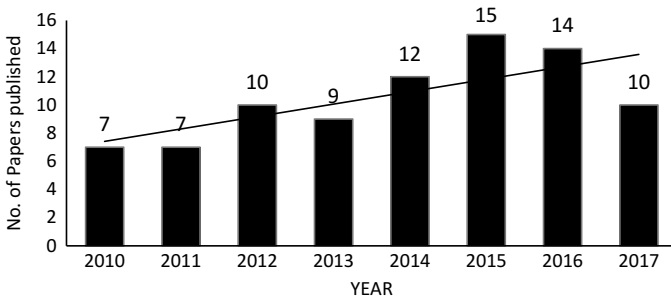


Fig. 2 Year-wise distribution of papers

There has been consistent increase in a number of articles over the years in supply chain performance measurement literature as concluded from graph (Fig. 2). A trend shift towards researches involving dynamic modelling and soft computing techniques like fuzzy, AHP, multiobjective decision making and IoT has been observed in SCPM literature.

Asia and Europe lead in the researches in SCPM (Fig. 3) with a total of 84% of researches done in this region. Contribution of India is about 24% with research comprising of case studies and surveys to understand the barriers of performance measurement in supply chain [22, 23] categorisation and interaction among KPIs [24, 25], green supply chain performance measurement [26–28], various frameworks for supply chain performance measurement [29–37] and literature reviews [13, 16, 28, 37].

Numerous researchers have presented their model or framework (Fig. 4) based either on case study, survey or literature review, but none of these models have been generalised, universally testified or widely accepted. There is a lack of benchmark in supply chain performance measurement studies. The reported frameworks were generally validated using case studies in food, automobile, textile, service industry

Fig. 3 Geographical distribution

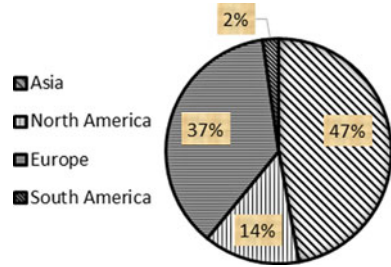
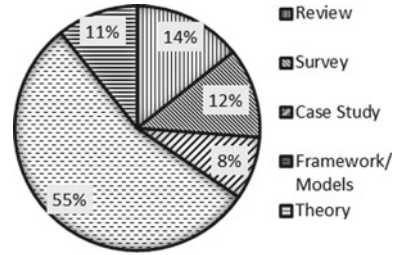


Fig. 4 Approach-wise distribution



and theoretical studies focused on interrelationships among various KPIs or the barriers to implementation of performance measurement systems in supply chain [38–40] and complexity in the supply chain performance measurement [41].

3 Basic Characteristics and Contributions

The papers included in the review can be categorised into subgroups according to their common themes:

- Sustainability or green supply chain performance measurement.
- Performance measurement using dynamic modelling or advanced computing techniques.
- Study of KPI and their effects on supply chain performance.
- Frameworks and case studies for supply chain performance measurement.

3.1 Sustainability or Green Supply Chain Performance Measurement

Over the years, a number of researches have been done towards making the supply chain green and sustainable. Along the efforts of sustainable supply chain, researchers developed key performance measures (Table 2) as it improves integration of

Table 2 Performance metrics

S. no.	KPI	Reference
1	Accuracy	[61, 83, 84]
2	Asset management	[30, 48, 70, 79]
3	Customer satisfaction	[12, 16, 24, 32, 53, 61, 66, 78, 75, 79, 84, 85]
4	Efficiency	[29, 62, 75, 86]
5	Employee development	[27, 53, 75]
6	Environment-friendly	[12, 27, 54, 53, 75, 79, 85]
7	Financial	[12, 23, 61, 78, 84, 87]
8	Flexibility	[12, 16, 23, 29, 30–32, 48, 53, 58, 62, 63, 70, 85, 86]
9	Forecast	[40, 79]
10	Free from error	[31, 48, 53, 76, 78]
11	Innovation	[12, 16, 23, 29, 31, 58, 62, 85, 88]
12	Internal process	[12, 84]
13	Inventory	[40, 63, 66, 73, 79, 84]
14	Lead time	[12, 24, 31, 32, 63, 66, 75, 76, 78, 83–85]
15	Management commitment	[27, 53, 54]
16	Material procurement performance	[73, 79]
17	No delay in treatment	[76]
18	Orders received	[52, 78, 79]
19	Overall equipment effectiveness	[73]
20	Process productivity	[76]
21	Product availability	[40, 75, 83]
22	Product features	[53]
23	Production/process cost	[66, 73, 76]
24	Profitability	[24, 73, 85]
25	Pure technical efficiency	[69]
26	Quality	[24, 61, 62, 78]
27	Recycling efficiency	[53]
28	Reliability	[12, 13, 30–32, 48, 70, 76, 89]
29	Research and development cost	[27, 31, 58, 73, 78, 88]
30	Research efficiency	[69]
31	Resource utilisation	[40, 58, 61, 86]
32	Responsiveness	[12, 16, 24, 29, 31, 48, 62, 70, 75, 83, 89]
33	Reverse logistics costs	[40, 52]

(continued)

Table 2 (continued)

S. no.	KPI	Reference
34	Service quality	[23, 32, 58, 78, 86]
35	Supplier	[78, 29, 67]
36	Supply chain integration and collaboration	[12, 29, 89, 87, 90]
37	Supply chain management cost	[63, 78]
38	Teaching efficiency	[69]
39	Total faults	[40, 52]
40	Total returns	[52, 78]

sustainability in supply chain [42–50]. KPIs to incorporate green practices in sustainable development and performance measurement were reported by case studies [16, 34, 51–55] and literature review [28].

3.2 Performance Measurement Using Dynamic Modelling or Advanced Computing Techniques

A number of decision-making techniques like fuzzy [15, 25, 30, 31, 34, 35, 56–60], MULTIMOORA [35], analytical hierarchy process (AHP) [15, 30, 32, 34, 50, 58, 61–63, 60], structural equation modelling (SEM) [33, 64, 65], imperative structural modelling (ISM) [22, 66], MICMAC [22, 25], data envelopment analysis (DEA) [15, 57, 67–69], Internet of things (IoT) [70, 71], multicriteria decision making (MCDM) [31, 45], grey-based neighbourhood set theory [45], multiagent system (MAS) [72], virtual gap measurement (VGM) [73], TOPSIS [31] and multiobjective optimisation (MOO) [74] are being used.

3.3 Study of KPI and Their Effects on Supply Chain Performance and Issues in SCPMS

Researchers have studied the effect of performance metrics on supply chain [74, 75] and their interdependence among each other [25] and prioritisation of KPIs [66] with methods like DEMATEL [45, 76] to examine the causal relationships among performance groups and among performance aspects within each group. The causal relationships are then used to determine weights of performance aspects applying modified ANP. The critical attributes and complexity of food supply chain with a huge number of KPIs have been researched quite thoroughly [41]. Barriers to implementation of SCPMS [22, 38–40] like complexity of supply chains, collaboration among

supply chain partners, involvement of multiple tiers and improper understanding or implementation of performance measures are identified.

3.4 Frameworks and Case Studies for Supply Chain Performance Measurement

Among the literature reviewed, 55% are models or frameworks generally validated through case studies in various sectors as automobile [25, 27, 33, 42, 66, 77], hospital [76], bank [68], manufacturing [24, 73], education [69], reverse supply chain [39, 59], food supply chain [36, 50, 60, 62, 64, 71, 78], plastic [34], small-scale enterprise [79], retail [24, 29], textile [31, 32], construction [63] and pharmaceutical [80].

4 Performance Metrics Identified

The various performance metrics in supply chain are generally categorised based on

- Qualitative and quantitative
- Supply chain operations reference (SCOR) model [81] which focuses on four basic supply chain processes: (i) plan; (ii) source; (iii) make; (iv) deliver
- Their strategic, operational or tactical focus [82]
- What they measure

The measurement metrics used by researchers have been tabulated in Table 2 and can be utilised as per sector and requirement.

5 Conclusion and Discussion

Supply chain performance measurement is a multidisciplinary topic and is being researched with various perspectives of supply chain. Most of the studies evaluate more than one performance dimension and are based on multicriteria decision-making techniques. Fuzzy, AHP and DEA are the most commonly used techniques. Fuzzy set theory is the dominant approach to deal with uncertainty. Most studies have reported real case applications and do not include a validation procedure, and hence, there are no standard frameworks generalised. The metrics studied vary with sectors, industry, context and perspective. Automation of the performance measurement processes can improve the benefits for system, but implementation of the automation framework has not been researched thoroughly. A number of key performance indicators used in various sectors are identified and indicates the diversity of metrics among which customer satisfaction, flexibility, innovation, lead time, reliability and

responsiveness are the most referred metrics. Choosing a suitable performance metric for measurement is as important as the performance measurement system, and these metrics must be driven from an organisations strategy.

References

1. Christopher M (1992) Logistics and supply chain management. Pitman Publishing, London
2. Mentzer JT, Keebler JS, Nix NW, Smith CD, Zacharia ZG (2001) Defining supply chain management. *J Bus Logist* 22:1–25
3. Kaplan RS, Norton DP (1992) The balanced scorecard—measures that drive performance. *Harv Bus Rev* 71–79
4. Keegan DP, Robert G, Charles R (1989) Are your performance measures obsolete? *Manag Account Res* 12:45
5. Lynch RL, Cross KF (1991) Measure up! The essential guide to measuring business performance. Mandarin, London
6. Brignall TJ, Fitzgerald L, Johnston R, Silvestro R (1991) Performance measurement in service businesses. *Manag Account* 69:34
7. Kaplan RS, Norton DP (2001) Transforming the balanced scorecard from performance measurement to strategic management: part II. *Am Account Assoc* 15:147–160
8. Neely A, Mills J, Platts K, Richards H, Gregory M, Bourne M, Kennerley M (2000) Performance measurement system design: developing and testing a process-based approach
9. Neely A, Gregory M, Platts K, Neely A, Gregory M, Platts K (2002) A literature review and research agenda
10. Neely A (2004) The performance measurement revolution: why now and what next ?
11. Gupta M, Narain R (2012) Investigation into barriers to adoption of e-procurement and measures of performance. *Int J Procure Manag* 5:567–607
12. Balfaqih H, Saibani N, Al-nory MT (2016) Review of supply chain performance measurement systems: 1998–2015. *Comput Ind* 82:135–150
13. Gopal PRC, Thakkar J (2012) A review on supply chain performance measures and metrics: 2000–2011. *Int J Product Perform Manag* 61:518–547. <https://doi.org/10.1108/17410401211232957>
14. Maestrini V, Caniato F (2016) Supply chain performance measurement systems: a systematic review and research agenda. *Intern J Prod Econ*. <https://doi.org/10.1016/j.ijpe.2016.11.005>
15. Lima-junior RF, Carpinetti LCR (2017) Quantitative models for supply chain performance evaluation: a literature review. *Comput Ind Eng*. <https://doi.org/10.1016/j.cie.2017.09.022>
16. Bulsara HP, Qureshi MN, Patel H (2014) Supply chain performance measurement—an exploratory study. *Int J Logist Syst Manag* 18:231–249
17. Akyuz GA, Erkan TE (2010) Supply chain performance measurement: a literature review. *Int J Prod Res* 48:5137–5155. <https://doi.org/10.1080/00207540903089536>
18. Haene CD, Verlinde S, Macharis C (2015) Measuring while moving (humanitarian supply chain performance measurement—status of research and current practice). *J Humanit Logist Supply Chain Manag* 5:146–161. <https://doi.org/10.1108/JHLSCM-04-2013-0016>
19. Beske-janssen P, Johnson MP, Schaltegger S (2015) 20 years of performance measurement in sustainable supply chain management—what has been achieved? *Supply Chain Manag An Int J* 20:664–680. <https://doi.org/10.1108/SCM-06-2015-0216>
20. Abidi H, De Leeuw S, Klumpp M (2014) Humanitarian supply chain performance management: a systematic literature review. *Supply Chain Manag An Int J* 19:593–608. <https://doi.org/10.1108/SCM-09-2013-0349>
21. Estampe D, Lamouri S, Paris J, Brahim-djelloul S (2013) A framework for analysing supply chain performance evaluation models. *Intern J Prod Econ* 142:247–258. <https://doi.org/10.1016/j.ijpe.2010.11.024>

22. Katiyar R, Barua MK (2014) Modelling the barriers of supply chain performance measurement in the Indian automotive industries. *Int J Intercult Inf Manag* 4:51–66
23. Ramaa A, Subramanya KN, Rangaswamy TM (2013) Performance measurement system of supply chain—an empirical study. *Int J Bus Perform Supply Chain Model* 5:343–360
24. Sillanpää I (2015) Empirical study of measuring supply chain performance. *Benchmark Int J* 22:290–308. <https://doi.org/10.1108/BIJ-01-2013-0009>
25. Katiyar, Barua M, Meena P (2015) Modelling the measures of supply chain performance in the Indian automotive industry. *Benchmark Int J* 22:665–696. <https://doi.org/10.1108/BIJ-09-2014-0091>
26. Bulsara HP, Qureshi MN (2016) Green supply chain performance measurement: an exploratory study. *Int J Logist Syst Manag* 23:476–498
27. Das D (2017) Development and validation of a scale for measuring sustainable supply chain management practices and performance. *J Clean Prod.* <https://doi.org/10.1016/j.jclepro.2017.07.006>
28. Mishra D, Gunasekaran A, Papadopoulos T, Hazen B (2017) Green supply chain performance measures: a review and bibliometric analysis. *Sustain Prod Consum.* <https://doi.org/10.1016/j.spc.2017.01.003>
29. Gawankar S, Kamble S, Raut R (2016) Development, measurement and validation of supply chain performance measurement (SCPM) scale in Indian retail sector. *Benchmark Int J* 23:25–60. <https://doi.org/10.1108/BIJ-06-2013-0068>
30. Jothimani D, Samarah S (2014) Supply chain performance measurement for third party logistics. *Benchmark Int J* 21:944–963. <https://doi.org/10.1108/BIJ-09-2012-0064>
31. Chithambaranathan P, Subramanian N, Subramanian P (2015) An innovative framework for performance analysis of members of supply chains. *Benchmark Int J* 22:309–334. <https://doi.org/10.1108/bij-11-2012-0081>
32. Charkha PG, Jaju SB (2014) Designing innovative framework for supply chain performance measurement in textile industry. *Int J Logist Syst Manag* 18:216–230
33. Dhona NC, Kamble SS (2016) Development and validation of an integrated supply chain operational performance model for Indian automobile industry. *Int J Procure Manag* 9
34. Golghate CD, Pawar MS (2013) Measurement and analysis of the plastic films green supply chain performance. *Int J Intell Enterp* 2
35. Sahu A, Datta S, Mahapatra S (2014) Use of IVFNs and MULTIMOORA method for supply chain performance measurement, benchmarking and decision-making: an empirical study. *Int J Bus Excell* 7:237–280
36. Joshi R, Banwet DK, Shankar R, Gandhi J (2012) Performance improvement of cold chain in an emerging economy. *Prod Plan Control Manag Oper* 23:817–836. <https://doi.org/10.1080/09537287.2011.642187>
37. Tewari S, Misra M (2013) Developing supply chain evaluation framework through performance assessment approach. *Int J Bus Perform Supply Chain Model* 5:28–45
38. Tarasewicz R (2016) Integrated approach to supply chain performance measurement—results of the study on Polish market. *Transp Res Procedia* 14:1433–1442. <https://doi.org/10.1016/j.trpro.2016.05.216>
39. Butzer S, Schötz S, Petroschke M, Steinhilper R (2017) Development of a performance measurement system for international reverse supply chains. *Procedia CIRP* 61:251–256. <https://doi.org/10.1016/j.procir.2016.11.264>
40. Papakiriakopoulos D, Pramatarı K (2010) Collaborative performance measurement in supply chain. *Ind Manag Data Syst* 110:1297–1318. <https://doi.org/10.1108/02635571011087400>
41. Kirwan J, Maye D, Brunori G (2017) Acknowledging complexity in food supply chains when assessing their performance and sustainability. *J Rural Stud* 52:21–32. <https://doi.org/10.1016/j.jrurstud.2017.03.008>
42. Mara UT, Alam S (2011) Performance measurement for sustainable supply chain in automotive industry: a conceptual framework. *Int J Value Chain Manag* 5:232–250
43. Santiteerakul S, Sekhari A, Bouras A, Sopadang A (2015) Sustainability performance measurement framework for supply chain management. *Int J Prod Dev* 20:221–238

44. Fritz MMC, Baumgartner RJ, Sch J (2016) Toward supply chain-wide sustainability assessment: a conceptual framework and an aggregation method to assess supply chain performance. *J Clean Prod* 1–14. <https://doi.org/10.1016/j.jclepro.2016.04.035>
45. Uysal F (2012) An integrated model for sustainable performance measurement in supply chain. *Procedia Soc Behav Sci* 62:689–694. <https://doi.org/10.1016/j.sbspro.2012.09.117>
46. Bai C (2012) Evaluating ecological sustainable performance measures for supply chain management. *Supply Chain Manag An Int J* 17:78–92. <https://doi.org/10.1108/13598541211212221>
47. Taticchi P, Tonelli F, Pasqualino R, Taticchi P (2013) Performance measurement of sustainable supply chains: a literature review and a research agenda. *Int J Product Perform Manag Perform* 62:782–804. <https://doi.org/10.1108/IJPPM-03-2013-0037>
48. Tajbakhsh T, Hassini H (2015) Performance measurement of sustainable supply chains: a review and research questions. *Int J Product Perform Manag* 64:744–783. <https://doi.org/10.1108/IJPPM-03-2013-0056>
49. Liebetruht T (2017) Sustainability in performance measurement and management systems for supply chains. *Procedia Eng* 192:539–544. <https://doi.org/10.1016/j.proeng.2017.06.093>
50. Yakovleva N, Sarkis J, Sloan T (2012) Sustainable benchmarking of supply chains: the case of the food industry. *Int J Prod Res* 50:1297–1317. <https://doi.org/10.1080/00207543.2011.571926>
51. Carvalho H, Azevedo SG (2010) Supply chain performance management: lean and green paradigms. *Int J Bus Perform Supply Chain Model* 2:304–333
52. Mondragon AEC, Lalwani C, Mondragon CEC, Mondragon AEC, Lalwani C (2014) Measures for auditing performance and integration in closed-loop supply chains. *Supply Chain Manag An Int J* 16:43–56. <https://doi.org/10.1108/135985411111103494>
53. Kafa N, Hani Y, Mhamedi AEL (2013) Sustainability performance measurement for green supply chain management. In: *Proceedings of the volumes IFAC*. <https://doi.org/10.3182/20130911-3-br-3021.00050>
54. Kumar P, Cheffi W (2013) Green supply chain performance measurement using the analytic hierarchy process: a comparative analysis of manufacturing organisations. *Prod Plan Control* 24:702–720
55. Ferreira LMDF, Silva C, Azevedo SG, Silva C (2016) An environmental balanced scorecard for supply chain performance measurement (Env_BSC_4_SCPM). *Benchmark Int J* 23:1398–1422. <https://doi.org/10.1108/BIJ-08-2013-0087>
56. Zaman K, Ahsan A (2014) Lean supply chain performance measurement. *Int J Product Perform Manag* 63:588–612. <https://doi.org/10.1108/IJPPM-05-2013-0092>
57. Damghani K, Fard M, Abtahi A (2012) A fuzzy two-stage DEA approach for performance measurement: real case of agility performance in dairy supply chains. *Int J Appl Decis Sci* 5:293–317
58. Cho DW, Lee YH, Ahn SH, Hwang MK (2012) A framework for measuring the performance of service supply chain management. *Comput Ind Eng* 62:801–818. <https://doi.org/10.1016/j.cie.2011.11.014>
59. Yang J (2010) On the construction and implementation methods for performance measurement of reverse supply chain. In: *2010 seventh international conference on Fuzzy Systems and Knowledge Discovery (FSKD 2010)*, pp 899–903
60. Pungchompoo S, Sopadang A (2010) A supply chain performance measurement improved with integrated methods FDSM, MOO and DEA part I: a conceptual of performance measurement framework in Thailand: frozen shrimp chains. In: *Proceedings of the 2010 IEEE IEEM*, pp 235–239
61. Santos TF, Leite MS (2016) Performance measurement system in supply chain management: application in the service sector. *Int J Serv Oper Manag* 23:298–315
62. Pungchompoo S, Sopadang A (2015) Confirmation and evaluation of performance measurement model for the Thai frozen shrimp chain. *Bus Process Manag J* 21:837–856. <https://doi.org/10.1108/BPMJ-06-2014-0053>

63. Wibowo MA, Nur M (2015) The analysis of supply chain performance measurement at construction project. *Procedia Eng* 125:25–31. <https://doi.org/10.1016/j.proeng.2015.11.005>
64. Chiadamrong N, Sophonsaritsook P (2015) Relationships between supply chain capabilities, competitive advantage and business performance: an exploratory study of the food industry in Thailand. *Int J Logist Syst Manag* 20:447–479
65. Kusriani E, Subagyo Masruroh N (2016) A new approach to design supply chain key performance indicator for actors and regulator: a case study in innovative product in Indonesia. *Int J Bus Perform Manag* 17:1–29
66. Azevedo S, Carvalho H, Machado VC (2013) Using interpretive structural modelling to identify and rank performance measures: an application in the automotive. *Balt J Manag* 8:208–230. <https://doi.org/10.1108/17465261311310027>
67. Bai C, Sarkis J, Bai C, Sarkis J (2014) Determining and applying sustainable supplier key performance indicators. *Supply Chain Manag An Int J* 19:275–291. <https://doi.org/10.1108/SCM-12-2013-0441>
68. Wang C (2017) Performance evaluation of heterogeneous bank supply chain systems from the perspective of measurement and decomposition. *Comput Ind Eng*. <https://doi.org/10.1016/j.cie.2017.05.028>
69. Jauhar SK, Pant M, Nagar AK (2016) Sustainable educational supply chain performance measurement through DEA and differential evolution: a case on Indian HEI. *J Comput Sci*. <https://doi.org/10.1016/j.jocs.2016.10.007>
70. Rezaei M, Shirazi M, Karimi B (2017) IoT-based framework for performance measurement. *Ind Manag Data Syst* 117:688–712. <https://doi.org/10.1108/IMDS-08-2016-0331>
71. Dweekat AJ, Hwang G, Park J (2017) A supply chain performance measurement approach using the internet of things: toward more practical SCPMS. *Ind Manag Data Syst* 117:267–286. <https://doi.org/10.1108/imds-03-2016-0096>
72. Teimoury E, Fathain M, Chambar I (2013) Automation of the supply chain performance measurement based on multi-agent system. *Int J Agil Syst Manag* 6:25–42
73. Liu FF, Liu Y (2017) A methodology to assess the supply chain performance based on virtual-gap measures. *Comput Ind Eng*. <https://doi.org/10.1016/j.cie.2017.06.010>
74. Laihonon H, Pekkola S (2016) Impacts of using a performance measurement system in supply chain management: a case study. *Int J Prod Res*. <https://doi.org/10.1080/00207543.2016.1181810>
75. Piotrowicz W, Cuthbertson R (2015) Performance measurement and metrics in supply chains: an exploratory study. *Int J Product Perform Manag* 64:1068–1091. <https://doi.org/10.1108/IJPPM-04-2014-0064>
76. Supeekit T, Somboonwiwat T, Kritchanchai D (2016) DEMATEL-modified ANP to evaluate internal hospital supply chain performance. *Comput Ind Eng*. <https://doi.org/10.1016/j.cie.2016.07.019>
77. Cuthbertson R, Piotrowicz W (2011) Performance measurement systems in supply chains. *Int J Product Perform Manag* 60:583–602. <https://doi.org/10.1108/17410401111150760>
78. Bigliardi B, Bottani E (2010) Performance measurement in the food supply chain: a balanced scorecard approach. *Facilities* 28:249–260. <https://doi.org/10.1108/02632771011031493>
79. Banomyong R, Supatn N, Banomyong R (2011) Developing a supply chain performance tool for SMEs in Thailand. *Supply Chain Manag An Int J* 16:20–31. <https://doi.org/10.1108/13598541111103476>
80. Lauras M (2011) A business process oriented method to design supply chain performance measurement systems Jacques Lamothe and Hervé Pingaud. *Int J Bus Perform Manag* 12:354–376
81. Stewart G (1997) Supply-chain operations reference model (SCOR): the first framework for integrated supply-chain. *Logist Inf Manag Supply-Chain* 10:62–67
82. Gunasekaran A, Patel C, Tirtiroglu E (2001) Performance measures and metrics in a supply chain environment. *Int J Oper Prod Manag* 21:71–87
83. Panjehfouladgaran H, Yusuf R (2016) Fuzzy performance measurement for supply chain management in Malaysian rubber glove manufacturer. *Int J Logist Syst Manag* 24:178–199

84. Pettersson AI, Anders S (2011) Performance measurements in supply chains within Swedish industry. *Int J Logist Syst Manag* 9:69–88
85. André A, Callado C, Jack L (2015) Balanced scorecard metrics and specific supply chain roles. *Int J Product Perform Manag* 64:288–300. <https://doi.org/10.1108/IJPPM-05-2014-0071>
86. Haavisto I, Goentzel J (2015) Measuring humanitarian supply chain performance in a multi-goal context. *J Humanit Logist Supply Chain Manag* 5:300–324. <https://doi.org/10.1108/JHLSCM-07-2015-0028>
87. Whitten GD, Jr KWG, Zelbst PJ, Whitten GD (2012) Triple-A supply chain performance. *Int J Oper Prod Manag* 32:28–48. <https://doi.org/10.1108/01443571211195727>
88. Chan FTS, Nayak A, Raj R, Chong AY, Manoj T (2014) An innovative supply chain performance measurement system incorporating research and development (R & D) and marketing policy. *Comput Ind Eng* 69:64–70. <https://doi.org/10.1016/j.cie.2013.12.015>
89. Santarelli G, Abidi H, Klumpp M, Regattieri A (2015) Humanitarian supply chains and performance measurement schemes in practice. *Int J Product Perform Manag* 64:784–810. <https://doi.org/10.1108/IJPPM-11-2013-0185>
90. Ramanathan U (2014) Performance of supply chain collaboration—a simulation study. *Expert Syst Appl* 41:210–220. <https://doi.org/10.1016/j.eswa.2013.07.022>

Development of Hybrid Forms of Abrasive Flow Machining Process: A Review



Anant Bhardwaj, Parvesh Ali, R. S. Walia, Qasim Murtaza and S. M. Pandey

Abstract In the present era, the demand of products with better surface finish and quality has improved drastically which promoted the industries to make their products with better functional performance and sustainability in the market. Due to low productivity of abrasive flow machining (AFM), there is a need to develop an efficient process which will inculcate a better surface finish and good quality. Hence, it is required to identify various hybrids of abrasive flow machining which involve the development of new process having high material removal, optimum surface finish and better type of fixturing during the finishing operation. This paper describes various hybrid forms of abrasive flow machining developed so far for productivity enhancement and involved parameters with their working principle.

Keywords Nano-finishing · Hybridization · Material removal

Nomenclature

AFM	Abrasive flow machining
CFG	Centrifugal force generated
UAAFAM	Ultrasonic-assisted AFM
EC ² A ² FM	Electrochemical and centrifugal force-assisted AFM
FMAB	Flexible magnetic brush
MAF	Magnetic abrasive finishing
MFP	Magnetic float polishing
MRF	Magnetic rheological finishing
DBG-AFM	Drill bit-guided AFM
CFAAFM	Centrifugal force AFM

A. Bhardwaj · P. Ali (✉) · R. S. Walia · Q. Murtaza · S. M. Pandey
Mechanical Department, Delhi Technological University, Delhi, India
e-mail: parvesh1133@gmail.com

© Springer Nature Singapore Pte Ltd. 2019
K. Shanker et al. (eds.), *Advances in Industrial and Production Engineering*, Lecture Notes in Mechanical Engineering, https://doi.org/10.1007/978-981-13-6412-9_5

1 Introduction

In the present scenario, there is a larger demand of the components with better functionality and geometrical conformity, so this develops a huge competition in the market regarding the quality characteristics of the product which are more economical and thus the need to use such a process which can produce good-quality product easily increases. Conventional process cannot be used for this because it is slow and also there is a difficulty during the machining of complex cavities. Surface finishing has a crucial role in the functional performance of the product. Abrasive flow machining is a non-conventional process used for the nano-finishing of the complex cavities which cannot be achieved by the other conventional processes [1]. It uses a non-Newtonian media which passes through the restrictive path and provides finishing. This media is a combination of polymer, gel and abrasives. When the media passes through the restrictive path with a high-pressure, abrasive cutting edges will abrade the work surface and provides better finished surface. It provides finishing in the range of $0.05\ \mu\text{m}$ [2]. This process is very fast and consumes about 10% of the finishing time required by using other conventional techniques [3].

On the basis of working and configuration, AFM process has three categories (one-way AFM [4], two-way AFM [5] and orbital AFM [2]). One-way AFM is simple in operation and controls the temperature of media in a better manner. One-way AFM process is simpler, but better process control can be obtained in two-way AFM process. The disadvantage of this process is that its material removal is very less. So, various hybridizations are used to improve the system efficiency and to minimize the disadvantages.

Gupta and Chahal [6] found experimentally that voltage contributes 45.35% in the material removal during finishing using electrochemical-aided AFM process. Tzeng et al. [7] studied about self-modulating abrasive medium on finished micro-channel formed by wire EDM. The author stated that micro-channel formed by EDM has a recast layer with blowholes which affected the quality of micro-channel. The result also showed that coarse abrasive particle with greater concentration gives higher velocity and improves the surface finish of workpiece. Tzeng et al. [8] used a sample of stainless steel (SUS304) containing micro-slit of width of 0.23 ± 0.02 . The results showed that the optimum parameter of micro-slits along with AFM is $150\ \mu\text{m}$ size of abrasive particle, 50% concentration, 6.7 MPa extrusion pressure and 30 min machining time. Wan et al. [9] studied the variation of slip line velocity and wall shear stress against extrusion pressure at different values of extrusion pressure 6, 12 MPa for two different elliptical cross sections. They concluded that if the variation is low in the cross section then zero-order methodology was used and when there is change in the cross-sectional frits, order chronology is taken.

Jain and Jain [10] had prepared a simulation model to calculate the dynamic abrasive particles, involving in nano-finishing process, and found that grain density improved with increasing abrasive mesh size. Gorona et al. [11] presented a model to calculate forces developed on a single grain during material removal and also calculated the axial, radial forces involved in cutting. They concluded that these

forces have a significant effect on the material deformation. Kenda et al. [12] had analysed the parameters for the responses as surface roughness and residual stresses on the electrically discharged pre-machined hardened tool steel AISI D2 and stated that its surface integrity was improved using abrasive flow machining process.

Jain et al. [13] observed that larger value of extrusion pressure reduces with the surface roughness. Rhoades [14] has reported that media flow rate has negligible effect on the material removal. AFM process cannot be used for larger surface irregularities as during the finishing process it removes material uniformly from all surfaces. So, larger imperfections cannot be corrected [15]. The experimental results showed that using centrifugal force inside the media flow path requires reduced amount of cycles for removing the same amount of material in comparison with conventional abrasive flow machining process [16]. When centrifugal force is added in the conventional abrasive flow machining process, dynamic abrasive grains in the media are improved [17]. CFAAFM produces better surface finishing in comparison with simple AFM process after specific number of cycles [17]. Sushil et al. [18] finished Al/SiC MMCs using abrasive flow machining and optimized the parameter for better results. The results showed that extrusion pressure and material of workpiece have a significant role in the material removal. Mali and Manna [19] optimized the cutting conditions during the finishing of Al/15 wt% SiC MMC and stated that mesh size of abrasive particle is the most significant parameter in the material removal. Chen and Cheng [20] made a model to identify the behaviour of the flowing media in different passageways using CFD-ACE software and reported that helical passageways performed better than the polygonal passageways. Marzban and Hemmati [21] developed abrasive flow rotary machining process by using artificial neural network (ANN). The author observed from the experiment that using spin motion along with the rotating workpiece gives better MRR. Mohammadian et al. [22] explained that chemical-abrasive flow machining can reduce the R_a value by about 45% in the SLM-built IN 625 components. Venkatesh et al. [23] used ultrasonic-assisted abrasive flow finishing for bevel gears and found that abrasive particles in UAAFMM remove the asperity peaks of the work surface at a higher velocity in comparison with the conventional AFM. Uhlmann [24] used a pragmatic modelling approach in AFM process for complex shaped automotive parts and observed that the flow velocity and shear rate increase the cutting rate but decrease the abrasive holding capacity. Seifu et al. [25] reported that the velocity of the media is maximum at the centre, surface quality got worse up to 20% and material removal reduces up to 30% during finishing.

2 Development of Hybrid Abrasive Flow Machining

From the literature, it was reported that the material removal of AFM process is less. So, various researchers have hybridized this process with other non-conventional techniques to improve the material removal. Various hybrid forms of AFM are discussed below.

2.1 Magnetic Force-Assisted AFM Process

The concept was coined by Singh and Shan in 2002 [26]. The authors stated that when magnetic field was applied along the full length of the workpiece, material removal and surface finish improved drastically [26]. This process requires less number of cycle for higher material removal. The researchers also observed the significant improvement in the process when brass was used as the workpiece material with higher magnetic flux density and low flow rate of medium.

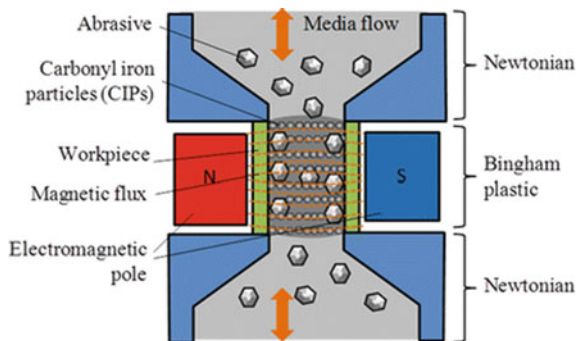
This process uses magnetic abrasive particles (ferromagnetic particles sintered with abrasives). When magnetic field is applied around the workpiece, then normal magnetic force causes abrasive to penetration inside the work surface. Maximum material removal was obtained at 0.4 T, after 0.6 T the material removal was decreased, and also the applied magnetic field retains ferromagnetic abrasive particles in the gap to improve the contact region [26] (Fig. 1).

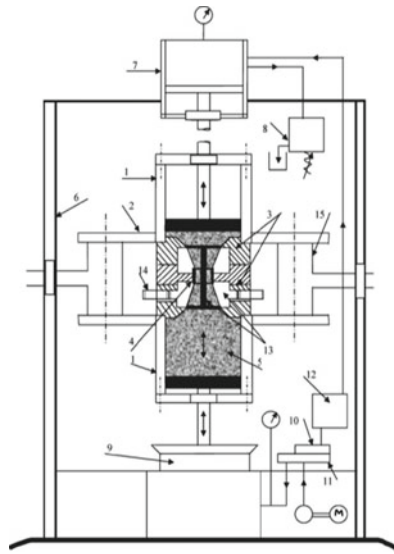
2.2 Centrifugal Force-Assisted AFM

The concept was developed by Walia et al. in 2006 [28]. In this arrangement, researchers rotated different shapes of rods at the centre of media flow path for finishing of workpiece. The abrasive laden media was rotated with the help of centrifugal force-generating (CFG) rod by the action of centrifugal force which increased intensity of abrasive particle action over the workpiece. The process can be described as shown in Fig. 2. The key point of the process is that the direction of centrifugal force on abrasive particle is normal to the axis of workpiece [29]. Erosion process is responsible for material removal due to the contact of the abrasive particle with the work surface [30].

$$\begin{aligned} \text{Surface area of abrasives contacting inner work surface} &= \pi [D^2 - (D - 2d)^2] / 4 \\ &= \pi (Dd - d^2) \end{aligned} \quad (1)$$

Fig. 1 Magnetic force-assisted AFM process [27]





- | | | | | |
|------------------------------|------------------------|------------------------|------------------------------|--|
| 1-Cylinder containing media, | 4- Work piece, | 7- Auxiliary cylinder, | 10- Direction control valve, | 13- Centrifugal force generating rod assembly, |
| 2- Flange, | 5-Non-Newtonian Media, | 8- Relief valve, | 11 & 12- Manifold blocks, | 14- Intermediate gear, |
| 3- Fixture, | 6- Hydraulic press, | 9- Piston, | | 15- Eye bolt |

Fig. 2 Centrifugal force-assisted AFM process [31]

2.3 Ultrasonic AFM

Ultrasonic AFM was developed by Sharma et al. [32]. In this process, high-frequency and low-amplitude ultrasonic vibrations are provided to the workpiece perpendicular to the media flow direction. The frequency used is in the range of 5–20 kHz, and amplitude varies from 10 to 50 μm. This process uses piezo actuator and special fixture arrangement to provide vibration. Relative velocity of abrasives is increased due to ultrasonic vibration which hits the piece asperities [33]. Active grain density increases as the velocity of the workpiece is greater than the velocity of the abrasive particles. This arrangement can result in better cutting conditions and provides more depth of penetrations which improves material removal and surface finish. Workpiece vibrates at high frequency and experiences additional radial forces along with AFM process in ultrasonic AFM (Fig. 3).

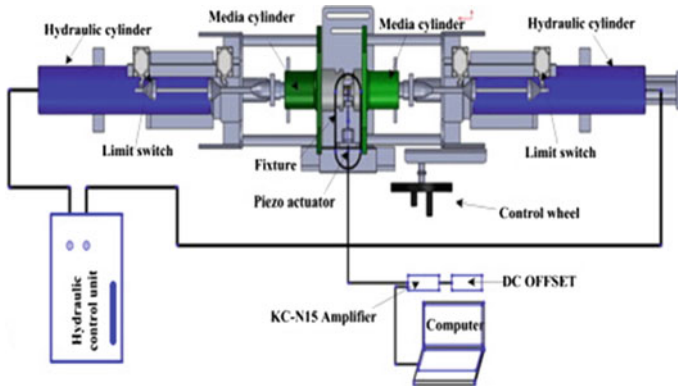


Fig. 3 Ultrasonic-assisted AFM process [34]

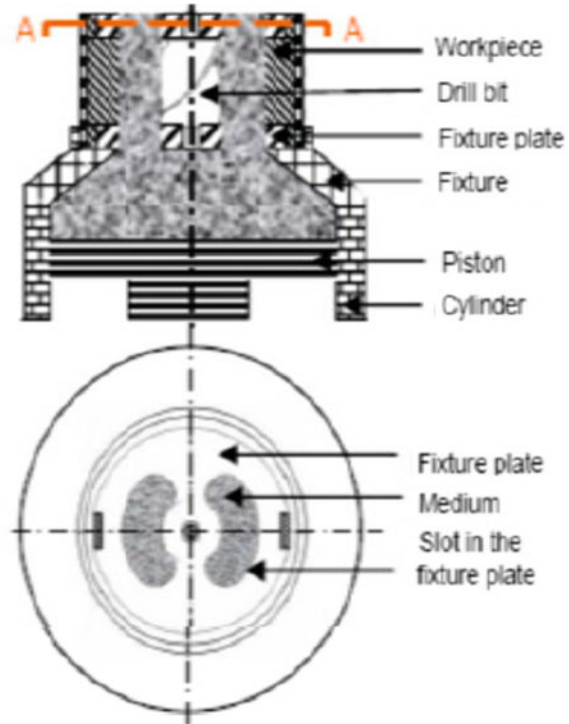
2.4 Drill Bit-Guided AFM

This method was developed by Sankar et al. in 2009 [35]. It is called drill bit-guided AFM as it has drill bit placed in the media flow path that results in better finishing rate and material removal. The media slug flows along a helical passage which creates random mixing of abrasive particles in the medium. This reshuffling of abrasive particles at outer region leads to interaction of more number of active grains with work surface. DBG-AFF has high finishing rate in comparison with simple AFM. The results showed that the material removal is directly proportional to the drill diameter [35]. As the drill diameter decreases, material removal also decreases. This machine uses circular fixture plate which restricts the flow of media in a cylindrical region. Abrasive particles have shortest contact length due to which material removal is not good, but in drill bit-guided AFM process fixture plate used is of twin slots that assist aligning drill bit along the finishing zone. The abrasive and work surface contact lengths become curved due to intermixing of media. This results in shearing of more number of peaks which increases material removal (Fig. 4).

2.5 Rotational AFM

This process was developed by Sankar et al. in 2010 [36]. The process is similar to CFAAFM, the only difference being that instead of the use of a rod to generate the centrifugal force; the workpiece itself is rotated using a suitable set-up explained in Fig. 5. The material removal for the rotational AFM is more as the rotation of workpiece along with the extrusion pressure on the medium increases the contact length between the work surface and the abrasive particles. It has five main components which are machine structure, rotational set-up, tooling, hydraulic power pack and medium [37]. The experimental results showed that the rotational AFM can produce

Fig. 4 Cross-sectional front view of tooling in DBG-AFF process [35]



44% more smoothness and 81.8% more material removal in comparison with AFF process.

2.6 Electrochemical-Assisted AFM

This process was developed by Dabrowski in 2011, for the fine finishing of flat surfaces [38, 39] and for cylindrical surface [40]. The name given to AFM with electrochemical machining process is electrochemical-assisted abrasive flow machining (ECA²FM). The process involves dissolution of anodic workpiece in the form of atoms. The application of ECM is in micro-scale batteries or nanoscale machining methods. The process of continuous improvement in micro scale parts, such as medical implants, micro scale batteries and fuel cells, more attempts are being made to use ECM for micromachining. Experimentally, it has found that the surface becomes rough due to more material electrolyte dissolution, resulting in deep scratches on surface. At 10 V, 87.43% improvement in R_a was obtained for brass material [40]. The workpiece with R_a value of 4.02 μm leads to final R_a of 0.49 μm (Fig. 6).

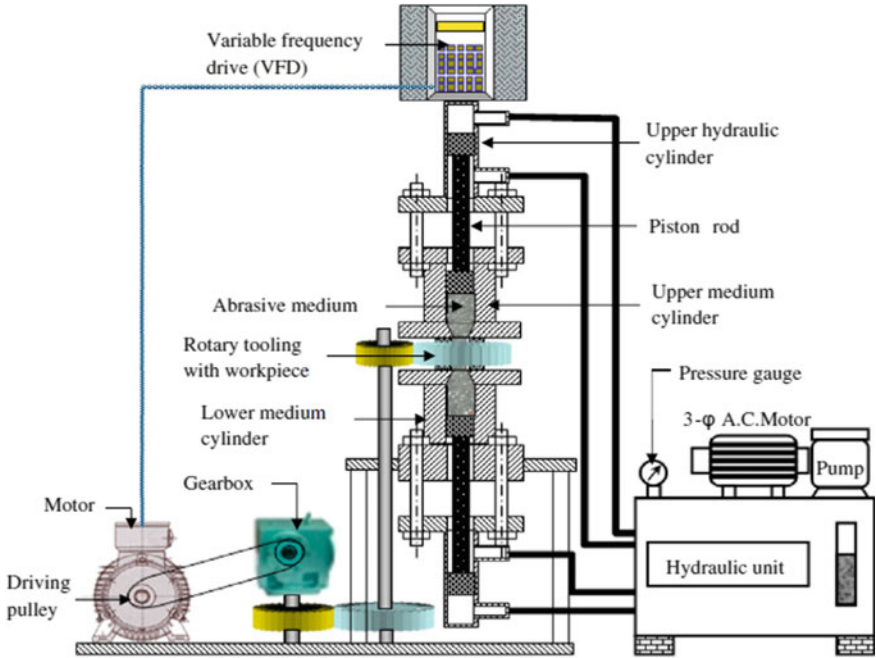


Fig. 5 Rotational AFM set-up [36]

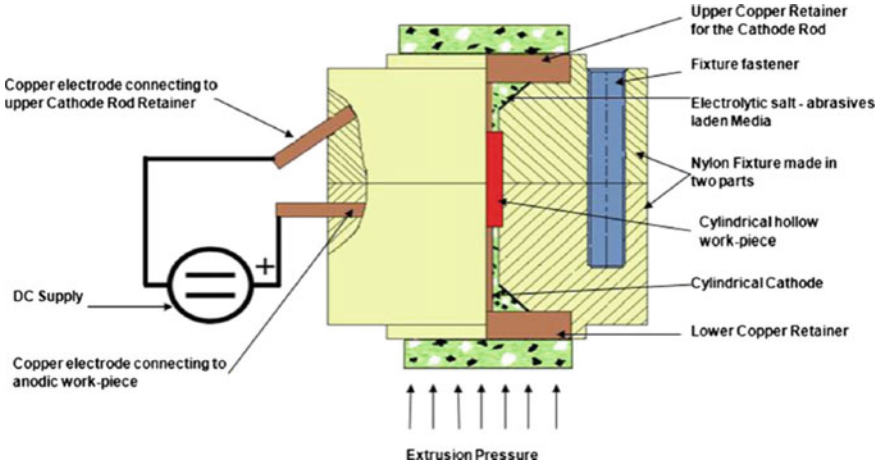


Fig. 6 Model of electrochemical-assisted AFM [41]

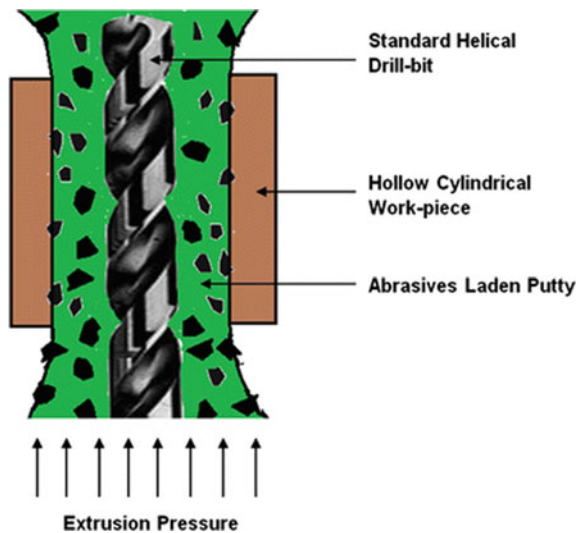
2.7 Helical AFM

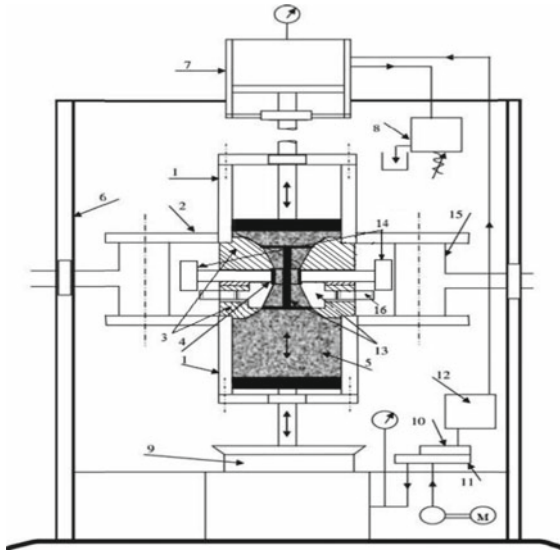
This hybridization of abrasive flow machining includes the combined effects of axial, radial and centrifugal force which is produced by the helical profile in the media flow path. Brar et al. [42] introduced helical abrasive flow machining in 2012 and stated that helical AFM process improves the R_a up to 2 μm . The experimental set-up includes drill bit having a helical profile co-axially with workpiece. The abrasive media was forced to flow in space provided between the workpiece and the profile which corresponds to increase in dynamic abrasive grains. The experimental observation showed that extrusion helical profile contributes to 78.89% and number of cycle is contributing to 6.70% in the material removal. Walia et al. [43, 44] rotated different shaped rods and drill bit in the media flow path and found 10 to 2.35 times improvement in material removal; also, it was observed that helical AFM showed 2.66 times improvement in material removal in comparison with the simple AFM process (Fig. 7).

2.8 Centrifugal–Magnetic Force-Assisted AFM

This process was developed by Singh et al. in 2015 [45]. The fixture consists of three parts which includes different shaped CFG rods for the application of centrifugal force with required arrangements for providing magnetic field. The adjustment is so made that the magnetic field is applied to the full length of workpiece. When DC supply is given to the workpiece, magnetic field is produced on the work surface

Fig. 7 Model of helical AFM [44]





- | | | | |
|-------------------------------|--------------------------|--------------------------------|--|
| 1- Media Cylinder, | 5- Non -Newtonian Media, | 9- Piston, | 13-Centrifugal force generating rod setup, |
| 2- Flange, | 6- Hydraulic press, | 10- Directional control valve, | 14- Electro-magnet, |
| 3- Work piece holding device, | 7- Auxiliary cylinder, | 11 & 12- Manifold blocks, | 15- Eye bolt, |
| 4-Test- piece, | 8- Relief valve, | | 16-Intermediate gear |

Fig. 8 Centrifugal–magnetic force-assisted AFM [45]

that attracts the abrasive particles towards its inner surface, thus resulting in more material removal. The range of magnetic force developed is 0–0.6 T with 60 rpm of CFG rod. Taguchi utility method was used for optimization, and maximum utility function was obtained at 0.3 T magnetic field [45] (Fig. 8).

2.9 Hybrid Electrochemical and Centrifugal Force-Assisted Abrasive Flow Machining

This process was developed by Vaishya et al. in 2015 [46]. This process clubs electrochemical process and CFAAFM process. This process uses nylon fixture which is made up of three parts consisting of CFG rod within it. It is held by retainer and fasteners. Extrusion pressure is kept low up to 6 N/mm² to prevent damaging of thin component. Power supply was taken in the range of 0–30 V. The polymeric media was made by adding KI to produce the ECM effect. EC²A²FM set-up is shown in Fig. 9. Clubbing of rotating CFG rod and the ECM process reduces 70–80% of the

Table 1 Comparison of hybrid forms of abrasive flow machining

Authors and title of papers	Research work	Parameters	Results
Tzeng et al. [7], 2007	Wire EDM was used to fabricate a complex micro-channel	Abrasive particle size, abrasive particle concentration in the media, machining time and extrusion pressure of media	Surface roughness of media using coarse abrasive particle is less in comparison with media with fine abrasive particle
Tzeng et al. [8], 2007	Use of ANOVA method to optimize parameters in finishing of micro-slit (SUS304) using AFM	Size of abrasive particle, abrasive concentration, machining time and extrusion pressure of media	Tool marks were visible at higher value of extrusion pressure. The surface finish was better at 50% concentration and 30 min machining time
Wan et al. [9], 2014	Plotting of variation of slip line velocity and wall shear stress against different extrusion pressures for two different cross sections. Introduction of zero-order and first-order methodology for the variation of cross sections		If the variation in cross section is less, then zero-order methodology can be used. When there is significant change in the cross section then first-order methodology can be used
Venkatesh et al. [34], 2015	A three-dimensional model was developed to simulate the UAAFMM process	Pressure of media, fluid velocity profile, temperature distributions	Change in vibration amplitude significantly affects the wall shear stress
Fu et al. [47], 2016	Three different types of drill bits were used and optimized	Media pressure, amount of cycle, type of rod	MRR increases with three start bit types for CI
Uhlmann et al. [48], 2016	AFM process was used to polish blisk blade surfaces		A new fixture with guide blocks is proposed. In the absence of guide blocks, roughness of straight blade surface decreases
Seifu et al. [25], 2016	Application of abrasive flow machining for intersecting holes, fuel rails and feed lines with high aspect ratios. Relation between edge rounding and abrasive media temperature	Abrasive-to-media ratio, abrasive grain size, number of cycles	Flow velocity and shear rates improve the cutting rate but also reduce the grain holding capability. Results hold good for the machining of ceramics materials

(continued)

Table 1 (continued)

Authors and title of papers	Research work	Parameters	Results
Mohammadian et al. [22], 2018	Combination of chemical and abrasive flow polishing on interior surface of tabular IN625 designed for aerospace industry	Flow of abrasive particle suspended in water. Flow of chemical solution without abrasive. The flow of abrasive particle suspended in chemical solutions	Reduction in the R_a value by about 45% for a built orientation of 15° and by 20% for a built orientation of 135° . In combined chemical-abrasive flow action, the polishing time reduces from 3 to 1 h for a given R_a improvement from $17.4 \mu\text{m}$ (as-built) to $14.2 \mu\text{m}$
Wang et al. [49], 2014	Use of different types of helical cores using variable parameters to finish circular holes		Helical passageway performs better than circular passageways in reducing RIR
Chen and Cheng [20], 2014	Presented a model for studying motion of media in different passageways using CFD-ACE software		Strain rate deviation decreases from 72 to 40% on using helical passageway in comparison with square passageway. Uniformity of the polygon holes was improved by helical passageway
Venkatesh et al. [23], 2015	Ultrasonic variant of AFM was used on the bevel gears. CFD technique was used for the simulation	Ultrasonic frequency, media pressure, time, media flow rate	Surface roughness was improved. The peaks were scratched at the higher velocity, thus enhancing the efficiency of the process
Sushil et al. [18], 2015	SiC composite material was machined. Microstructure analysis was performed using SEM and XRD	Amount of cycles, extrusion pressure, percentage of oil in the media, concentration of abrasive	Extrusion pressure was the most significant parameter for MR. SEM results showed surface defects were removed by using AFM process

(continued)

Table 1 (continued)

Authors and title of papers	Research work	Parameters	Results
Mali and Manna [19], 2010	AFM process was used to finish conventionally machined cylindrical surface of Al/15 wt per cent step MMC workpiece	Abrasive mess size, amount of cycle, media pressure, abrasive concentration, viscosity of media	Abrasive particle size was the significant parameter for MR
Marzban and Hemmati [21], 2017	Stirring and rotation of workpiece. Comparison between ANN and AFM	Speed, pressure, initial roughness, concentration, time	Stirring was done instead of reciprocation for optimum utilization of abrasive media. Rotation of workpiece with the spin motion increases MR
Walia et al. [30], 2008	Determination of surface morphology, surface micro-hardness	Media pressure, abrasive size, media flow rate, concentration of abrasive (by weight), polymer-to-gel ratio (by weight), amount of cycles	CFG rod increased productivity. CFAAFM does not affect the surface micro-layer
Walia et al. [31], 2006	Introduction of rotating CFG rod for performance improvement. FEM analysis on non-Newtonian visco-elastic fluid		CFG rod increased productivity. Resultant pressure was maximum at inlet and minimum at outlet. Velocity was maximum near the CFG rod
Brar et al. [44], 2013	Helical abrasive flow machining was proposed	Helical drill bit, number of cycle, extrusion pressure, media flow rate	Result showed MR improved 2.5 times the MR obtained in the general process. Drill bit contributed to 89.74% in MR
Jain et al. [50], 1999	Prediction of radial stresses on workpiece surface. Model for material removal	Size of abrasive particles, extrusion pressure, workpiece hardness, size of workpiece	Velocity increases with piston pressure. Piston pressure increases with reduction ratio. Normal stress on the work surface increases with reduction ratio

(continued)

Table 1 (continued)

Authors and title of papers	Research work	Parameters	Results
Petri et al. [51], 1998	Neuristic search algorithms which avoid extrapolation of neural network. Validation with various test pieces		Proposed model is effective. Model can also be used for predicting alternative parameters in the absence of certain type of media
Brar et al. [52], 2011	Taguchi method used for optimization Design was based on L ₉ OA array Selection of optimum parameter based on S/N ratio	Abrasive-to-media ratio, extrusion pressure, amount of cycles	Abrasive-to-media ratio shows highest contribution to MR
Singh and Shan [26], 2002	Introduction of magnetic field around the workpiece	Magnetic flux density (T) Amount of cycle Flow volume of media	Surface roughness decreases with high magnetic flux density but MR increases
Jain and Jain [53], 2000	A backpropagation neural network was used	Abrasive mesh size = 100–240 Abrasive conc. = 33–45% Piston velocity = 40–85 cm/min	Optimization process can be performed on observation of experimental information
Jain and Jain [10], 2004	Simulation model for active grain density determination and correlation with experimental results	Abrasive type = silicon carbide Work hardness = 2177 MPa Media cylinder diameter = 80 mm	Abrasive grain density increases with abrasive mesh size. Abrasive grain density increases with concentration of abrasive particles
Gorona et al. [11], 2006	Presented a theoretical model for calculation of forces on single abrasive grain	Workpiece material—mild steel Abrasive = SiC Abrasive grain mesh size = 80–220 Medium velocity = 0.098–1.94 mm/s Pressure = 0.4–0.8 kg/mm ² Initial roughness = 0.7–0.9 μm	AFM results showed that axial force and radial force significantly affect material deformation

(continued)

Table 1 (continued)

Authors and title of papers	Research work	Parameters	Results
Wang and Weng [54], 2007	Development of cost-effective abrasive media for enhancement of R_a in WEDM surface	Medium = P-Silicone, A-Silicone Workpiece = mild steel (SKD 11) Abrasive = SiC (24–330 mesh) Abrasive conc. = 33–71% Hydraulic pressure = 500 Psi Abrasive weight = 600 g	At high concentration media, surface roughness was minimum according to the experimental result
Wang and Lee [55], 2009	Development of abrasive media with silicone gel for ensuring mixing of ferromagnetic particles and abrasives	Workpiece = SKD-11 SiC mesh = 2000–8000 SiC weight = 5–10 g SG weight = 5–15 g Current = 1–3 A	Silicone gel does not stick to work surface due to its semi-solid nature and deformable properties; besides due to its flexible nature, it wraps around the workpiece. An excellent surface roughness reduction was achieved with high mesh of SiC or SG (it decreased from 0.25 to 0.042 μm in 30 min by 800 mesh SiC)
Kar et al. [56], 2009	Development of a visco-elastic carrier-based media characterized through rheological properties for fine finishing in AFM	Abrasive = SiC Abrasive mesh size = 80–1200 Processing oil = naphthenic oil Workpiece = aluminium, EN8	Use of mixture of butyl rubber, silicon carbide, naphthenic oil as media showed better performance in comparison with natural rubber-based media
Walia et al. [17], 2009	A CFG rod is used in the media flow path to generate centrifugal force	CFG rod speed = 0–70 rpm Extrusion pressure = 20–34 bar No. of cycles = 3 Abrasive = Al_2O_3 Grit size = 100–250 μm	CFAAFM gives better surface finish compared to conventional AFM after a certain number of cycles

(continued)

Table 1 (continued)

Authors and title of papers	Research work	Parameters	Results
Kenda et al. [12], 2011	Effects of the process parameters on surface roughness and residual stresses	Media viscosity = 2650 Pa-s Abrasive mesh size = 80 Machining time = 0.5 h	High tensile stresses in the work surface were generated by EDM. A high compressive stress was observed, and the surface integrity was improved with the application of AFM
Bin et al. [57], 2012	Development of new nozzle abrasive flow machining tool		The control system improved the needle flow coefficient to 38% and controlled the flow variation within $\pm 1\%$ range
Bähre et al. [58], 2012	The goal was to improve surface quality and reduce stress concentrations at bore intersections	Medium: EM24640 Abrasive: Al_2O_3 Size: 300–600 μm	The machined AISI 4140 workpieces significantly improve surface values R_a and R_z after 15 cycles. Greater surface finish is achieved by higher piston pressure. Linear relationship of axial force with passage length and piston pressure
Uhlmann et al. [59], 2013	Modelling of abrasive-laden media in AFM	Abrasive mass fraction: 33–67% Abrasive: silicon carbide Size: 185 μm dia.	The model was applicable to every AFM media having a different viscosity, grain size, mass fraction
Yang and Sha [60], 2014	A predictive model was developed with RBF neural network	Abrasive size: 25 μm Abrasive concentration: 0.1 Processing pressure: 4 MPa	The RBF neural network having high nonlinear approach is useful in relating processing effect and the input parameters

(continued)

Table 1 (continued)

Authors and title of papers	Research work	Parameters	Results
Kenda et al. [61], 2014	Energy consumption analysis was done to compare AFM and novel upgraded AFM with movable mandrel, i.e. AFMmm	Media viscosity: 2650 Pa-s Abrasive mesh: 80 Abrasive conc.: 57% Abrasive material: boron carbide	Using AFMmm, fatigue life of plastic gears prolonged for 125%. AFMmm generated cambered shape with maximum convexity of 5 μm ; besides, finished surface
Swat et al. [62], 2014	An optimized process control is proposed by combining different levels of piston pressure in one machining procedure	Highly viscous EM24640 medium density: 1.9 g/cm ² Abrasive: Al ₂ O ₃ Grain size: 300–600 μm	AFM machining with 40 bar piston pressure leads to lower surface roughness. Less pressure increases the machining time per cycle
Sooraj and Radhakrishnan [63], 2014	Response surface methodology was applied to investigate the effect of axial pressure, grain size of elastic abrasives on surface finish	Workpiece: hardened steel 440C 58HRC Abrasive grain size: 10–250 Axial pressure: 1–5 bar	Axial pressure with a magnitude of 0.38 MPa and cutting velocity with a magnitude of 12 m/min gave optimum processing condition with abrasive grain size of 23 μm
Chen and Cheng [20], 2014	Analytical model was developed to understand the abrasive media motion in different passageways using CFD-ACE software	Abrasive: SiC Mesh size: 100 Weight %: 50	Performance of helical passageway is better than polygon passageway after 5 cycles of polishing
Ibrahim et al. [64], 2014	L-18 mixed orthogonal array was used. Optimization of process parameters	Workpiece: Al alloy Abrasive conc.: 25% Grain size: 355 μm Extrusion pressure: 8 MPa Number of cycle: 40	The optimum condition for maximum material removal is 140 mm stroke, 8 MPa pressure, 40 cycles, 25% abrasive concentration and 355 μm grain size. The optimum condition for minimum surface roughness is 40 mm stroke, 8 MPa pressure, 40 cycles, 75% abrasive concentration and 355 μm grain size

(continued)

Table 1 (continued)

Authors and title of papers	Research work	Parameters	Results
Kenda et al. [65], 2014	Polishing of gear tool using AFM	Workpiece: AISI H11 Abrasive: SiC Mesh size: 80 Polishing time: 240 s	The marks of pre-machining process of WEDM were completely removed, after AFM
Jang et al. [66], 2010	Hard materials like glassy carbon (GC) are polished using MR fluids	Permanent magnet = neodymium-iron alloy (Nd-Fe) Flux density = 0.1–0.2 T MR fluid = DI water-based suspension of CI particles (42%) Dia. of particles = 0.5–2 μm Electrolyte = NaOH (pH 12.4) Voltage = 1 V	This process increased the MRR and surface finish
Paul and Hiremath [67], 2013	Study of process parameters of ECDM on MRR for borosilicate glass. As MRR is nonlinear, RSM is used for process parameter optimization	Voltage = 50–70 V Electrolytic concentration (% wt.) = 20–30	Optimum value obtained was 60 V, 30% electrolyte concentration. MRR increases with electrolytic concentration. TWR decreases with increase in concentration
Brar et al. [40], 2012	Two processes ECM and AFM are combined. Taguchi method of optimization was used	Voltage = 0–15 V Salt molal concentration = 0.75–1.25 M Dia. of cathode rod = 3.3–5.2 mm Pressure = 3–7 MPa Abrasive grain size = 100–200 mesh	ECA ² FM process requires less extrusion cycles. The optimal MR was 18.02 mg

(continued)

Table 1 (continued)

Authors and title of papers	Research work	Parameters	Results
Vaishya et al. [46], 2015	A study was undertaken to explore the novel way of integrating abrasive flow machining with electrochemical machining, and the effect of parameters like voltage, RPM, salt molal concentration on surface roughness and material removal was studied	Voltage: 0–25 V Molal concentration: 0.75–1.25 Rotational speed: 0–50 RPM	With the help of rotating CFG rod, surface finish obtained was in the range of 0.7–0.8 μm. Enhancement in material removal was obtained by high pressure
Singh and Shan [26], 2002	Magnetic field was applied along the full length of workpiece. Material removal and R_a value were improved by applying magnetic field in the AFM process	Fixture = nylon Ferromagnetic particles (40%) Abrasives = 45% Al_2O_3 , 15% Si_2O_3 Poke and yoke material = M.S. (0.25% Si) Coil = copper wire (dia. 1.21 mm) Turns = 1500 Flux density = 0.9 T	The slope of the curve shows that the material removal is more as compared to R_a by using magnetic field in the finishing process. Reduced amount of cycle is required for same MR
Singh et al. [68], 2013	The paper reported the mixed factorial design experimental study to understand the MR and wear behaviour	Extrusion pressure = 15 bar Media flow rate = 450 cm ³ /min Abrasive conc. = 1.5:1 (by wt.) Abrasive = Al_2O_3 (355 μm)	Magnetic-assisted AFM increased MR for non-ferromagnetic workpieces. The surface roughness of aluminium was not much improved by magnetic field as compared to brass
Jayswal et al. [69], 2005	The paper deals with investigation of MAF process. Use of FEM for the evaluation of magnetic field distribution on work surface	Magnetic flux = 0.8 T No. of turns = 3000 Workpiece = SUS304 stainless steel Hardness = 5.5 GPa Abrasive = Al_2O_3 (dia. 5 μm) Iron particles = 70%	Due to the edge effect, normal magnetic force is higher near the edge of magnetic pole

(continued)

Table 1 (continued)

Authors and title of papers	Research work	Parameters	Results
El-Taweel [70], 2008	In the paper, combination of electrochemical turning (ECT) and magnetic abrasive finishing (MAF) was used that improved MRR and Ra	Tool = brass Voltage = 8–24 V Electrolytic pressure = 0.4 MPa Electrolyte = 20% Na ₂ NO ₃ Magnetic abrasives = Al ₂ O ₃ (1.5 μm) + steel (150 μm)	Surface quality is less than 0.15 μm
Das et al. [71], 2008	Calculation of normal force on the application of magnetic field in AFM	Abrasives = SiC (800 mesh) Visco-plastic base medium = 20 wt% AP3 grease and 80 wt% paraffin	Current results in reduction in surface roughness
Yamaguchi et al. [72], 2012	Uncoated carbide tool surfaces were finished using MAF process	Steel grits: 700 μm dia., 0.3–0.5 g Iron particles: 44–105 μm Lubricant: barrelling compound	Experiments showed that for films with $t > 40$ nm the ratio of DC to optical conductivity was 13, which lead to sheet transmittance and resistance as 80% and 110 Ω, respectively
Amineh et al. [73], 2013	MAF process was used to remove the recast layer produced by WECDM	Voltage: 110 V Pulse off time: 35 μs Servo: 30 V Magnetic abrasive powder: carbon steel grit Mesh size: 60–120 Lubricant: SAE 40 oil 90.1 ml	MAF process removed the recast layer produced by WEDM without any micro-crack
Lee et al. [74], 2013	Enhanced the polishing efficiency of magnetic abrasive finishing (MAF) by providing vibration	Weight of steel particles: 1–2 g SiC: 1–3 g Machining fluid: 1–3 g SiC particle mesh size: 1000 (18 μm)–8000 (1 μm) Steel grit: 50 (0.3 mm)–120 (0.125 mm)	Two-dimensional VAMAF helped in increasing polishing efficiency and surface quality. Dense intersecting machining paths were formed that contributed to better precision

(continued)

Table 1 (continued)

Authors and title of papers	Research work	Parameters	Results
Judal and Yadava [75], 2014	Distribution of magnetic field between magnetic poles is calculated using FEM techniques	Current to electromagnet = 0.5–2.5 T Electrolytic current = 0.5–2.5 T Electrolyte = 20% dilute Na ₂ NO ₃ No. of turns = 2000 Unbounded magnetic abrasives Ferromagnetic particles = steel grit (180 μm) Abrasives = SiC (10 μm) Magnetic flux = 0.85 T	Developed magnetic field causes the normal and tangential cutting forces at the edge of magnetic poles
Mishra et al. [76], 2014	Transient thermal analysis of workpiece was done to predict temperature rise due to magnetic flux	Current in coil: 0.45–0.91 A Number of turns: 480 Volume ratio of iron: 43–70	Magnetic flux density was found to be 0.10–0.223 T for the coil current in the range of 0.45–0.91 A. The maximum rise in temperature occurred at 450 rpm rotation of electromagnet and 0.23 T magnetic flux
Das et al. [77], 2015	Calculation of stress developed during polishing using 2D computational fluid dynamics		The value of axial force is higher than the reaction force. Simulation model confirms that abrasive grains cut the roughness peak along the straight-line path
Walia et al. [15], 2008	Developed a mathematical model for calculation of dynamically active abrasive particle in AFM and centrifugal force-assisted AFM	Extrusion pressure = 40 bar Flow rate of media = 215 cm ³ /min Abrasive particle size = 150 μm Abrasive-to-media conc. = 50% (by wt.)	The amount of dynamically active grains in the media increases due to centrifugal effect

(continued)

Table 1 (continued)

Authors and title of papers	Research work	Parameters	Results
Sankar et al. [37], 2009	Experimental study on R-AFF was conducted	Workpiece = Al alloy, Al alloy/SiC (10%), Al alloy/SiC (15%) Medium = low molecular weight soft styrene butadiene polymer (SBP) + processing oil = hydrocarbon oil Abrasives = SiC (220 mesh size) Abrasives = 66.67 wt% Processing oil = 2.5–17.5 wt%	Fort-four percentage improvement in roughness and 82% more MR are produced by R-AFM compared to AFM. Rotating workpiece results in the existence of tangential force which assists axial and radial forces; hence, resultant force shears the workpiece surface peaks easily
Sankar et al. [35], 2009	In the paper, the concept of medium rotation has been introduced to achieve high MR and better finishing	Workpiece = AISI 1040, AISI 4340	The abrasive traverse path is larger in DBG-AFF than that in AFF, which results in higher finishing rate
Das et al. [78], 2012	The study showed that combination of magnet and rotational speed contributed to improvement in surface roughness	Magnetic flux = 0.2 T MRP fluid = mixture of CIP of CS grade (diameter = 18 μ m) + SiC abrasives with base medium of paraffin oil (48 vol.%) + AP3 grease (12 vol.%) Hydraulic pressure = 32.5–42.5 bar	Atomic force and SEM images show cross-hatch marks which results in increase of oil retention capabilities. The efficiency of R-MRAFF process is more than the MRAFF in terms of surface roughness
Uhlmann [24], 2009	Developed a model for ceramic materials	Advanced ceramic materials	Modelling result shows improvement in the response
Wang et al. [79], 2009	Determines polishing methods for complex holes		Used a silicone gel which would not stick to the workpiece during AFM
Walia et al. [80], 2006	Introduction of centrifugal force-generating (CFG) rod inside the work passage to improve material removal	Shape and rotational speed of CFG rod Extrusion pressure Abrasive grit size Number of process cycle	Seventy to eighty percentage increase in MR. Shapes of CFG showed decreasing order of CFG spline, square, rectangle, triangle

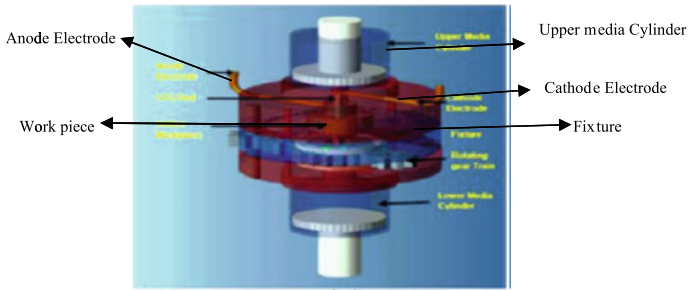


Fig. 9 EC²A²FM set-up [46]

machining time and is operated at low extrusion pressure. The result also showed that surface finish obtained was in the range of 0.5–0.6 R_a [46].

Table 1 shows various developments in abrasive flow machining which is explained.

3 Conclusion

AFM process is an emerging technique which is capable of providing surface finish up to nano-level and replaces the conventional manufacturing processes. AFM provides an appropriate method to produce mirror-like surface finish in hard to reach surface. Many researchers have done a lot of work in AFM, but still there is gap for the development of more hybrid AFM processes to enhance the material removal and surface finish with lesser time and cost. The major limitation of AFM is low MR, which can be rectified by developing various hybrids of AFM. There is a scope of further research in the variants, hybrids and in the abrasive media to make the process efficient and cost effective that result in achieving high material removal and better surface finish.

References

1. Ali P, Dhull S, Walia RS, Murtaza Q, Tyagi M (2017) Hybrid abrasive flow machining for nano finishing—a review. *Mater Today Proc* 4:7208–7218
2. Sankar MR, Ramkumar J, Jain VK (2008) Abrasive flow machining (AFM): an overview. In: INDO-US WORKSHOP on smart machine tools, intelligent machining systems and multi-scale manufacturing, Dec 2008
3. Singh S (2002) Studies in metal finishing with magnetically assisted abrasive flow machining. PhD thesis, IIT Roorkee
4. Rhoades LJ, Kohut TA, Nokovich NP, Yanda DW (1994) Unidirectional abrasive flow machining. US patent number 5,367,833, 29 Nov 1994

5. Rhoades LJ, Kohut TA (1991) Reversible unidirectional AFM. US patent number 5,070,652, 10 Dec 1991
6. Gupta R, Chahal B (2015) Investigation and optimization of process parameters in electro-chemical aid abrasive flow machining. *Int J Sci Eng Res* 6(2), Feb 2015
7. Tzeng HJ, Yan B-H, Hsu RT, Lin YC (2007) Self-modulating abrasive medium and its application to abrasive flow machining for finishing micro channel surfaces. *Int J Adv Manuf Technol* 32:1163–1169
8. Tzeng H-J, Yan B-H, Hsu R-T, Lin Y-C (2007) Finishing effect of abrasive flow machining on micro silt fabricated by wired EDM. *Int J Adv Manuf Technol* 34:649–656
9. Wan S, Ang YJ, Sato T, Lim GC (2014) Process modelling and CFD simulation of two-way abrasive flow machining. *Int J Adv Manuf Technol* 71:1077–1086
10. Jain RK, Jain VK (2004) Stochastic simulation of active grain density in abrasive flow machining. *J Mater Process Technol* 152:17–22
11. Gorona VK, Jain VK, Lal GK (2006) Forces prediction during material deformation in abrasive flow machining. *Wear* 260:128–139
12. Kenda J, Pusavec F, Kermouche G, Kopac J (2011) Surface integrity in abrasive flow machining of hardened tool steel AISI D2. 1st CIRP conference on surface integrity. *Procedia Eng* 19:172–177
13. Jain RK, Jain VK, Kalra PK (1999) Modelling of abrasive flow machining process: a neutral network approach. *Wear* 231:242–248
14. Rhoades LJ (1985) Abrasive flow machining and its use. In: *Proceedings of non-traditional machining conference*, Cincinnati, OH, pp 111–120
15. Walia RS, Shan HS, Kumar PK (2008) Determining dynamically active abrasive particles in the media used in centrifugal force assisted abrasive flow machining process. *Int J Adv Manuf Technol* 38:1157–1164
16. Fang L, Zhao J, Sun K, Zheng D, Ma D (2009) Temperature as sensitive monitor for efficiency of work in abrasive flow machining. *Wear* 266:678–687
17. Walia RS, Shan HS, Kumar PK (2009) Enhancing AFM process productivity through improved fixturing. *Int J Adv Manuf Technol* 44:700–709
18. Sushil M, Vinod K, Harmesh K (2015) Experimental investigation and optimization of process parameters of Al/SiC MMCs finished by abrasive flow machining. *Mater Manuf Processes* 30(7):902–911
19. Mali HS, Manna A (2010) Optimum selection of abrasive flow machining conditions during fine finishing of Al/15 wt% SiC-MMC using Taguchi method. *Int J Adv Manuf Technol* 50:1013–1024
20. Chen KY, Cheng KC (2014) A study of helical passageways applied to polygon holes in abrasive flow machining. *Int J Adv Manuf Technol* 74:781–790
21. Marzban MA, Hemmati SJ (2017) Modelling of abrasive flow rotary machining process by artificial neural network. *Int J Adv Manuf Technol* 89:125–132
22. Mohammadian N, Turenne S, Brailovski V (2018) Surface finish control of additively-manufactured Inconel 625 components using combined chemical-abrasive flow polishing. *J Mater Process Technol* 252:728–738
23. Venkatesh G, Sharma AK, Kumar P (2015) On ultrasonic assisted abrasive flow finishing of bevel gears. *Int J Mach Tools Manuf* 89:29–38
24. Uhlmann E (2009) Modelling the AFM process on advanced ceramic materials. *J Mater Process Technol* 209(20):6062–6066
25. Seifu Y, Kumar SS, Hiremath SS (2016) Modeling and simulation: machining of mild steel using indigenously developed abrasive flow machine. *Global colloquium in recent advancement and effectual researches in engineering, science and technology (RAEREST 2016)*. *Procedia Technol* 25:1312–1319
26. Singh S, Shan HS (2002) Development of magneto abrasive flow machining process. *Int J Mach Tools Manuf* 42:953–959
27. Sato T, Yeo SH, Zarepour H (2014) Loose abrasive machining. In: *Handbook of manufacturing engineering and technology*, pp 1051–1088

28. Walia RS, Shan HS, Kumar P (2006) Parametric optimization of centrifugal force-assisted abrasive flow machining (CFAAFM) by the Taguchi method. *J Mater Manuf Processes* 21(4)
29. Singh R, Walia RS (2012) Study the effects of centrifugal force on abrasive flow machining process. *Int J Res Mech Eng Technol* 2(1):34. ISSN: 2249-5762
30. Walia RS, Shan HS, Kumar P (2008) Morphology and integrity of surfaces finished by centrifugal force assisted abrasive flow machining. *Int J Adv Manuf Technol* 39(11–12):1171–1179
31. Walia RS, Shan HS, Kumar P (2006) Finite element analysis of media used in the centrifugal force assisted abrasive flow machining process. <https://doi.org/10.1243/09544054jem325>
32. Sharma AK, Kumar P, Rajesh S (2011) An improved ultrasonic abrasive flow machining. Patent number 3578/DEL/201, India
33. Rajesh S (2011) Some studies to enhance the capabilities of abrasive flow machining process. PhD dissertation, IIT Roorkee
34. Venkatesh G, Sharma AK, Singh N (2015) Simulation of media behaviour in vibration assisted abrasive flow machining. *Simul Model Pract Theory* 51:1–13
35. Sankar MR, Mondal S, Ramkumar J, Jain VK (2009) Experimental investigations and modelling of drill bit guided abrasive flow finishing (DBG-AFF) process. *Int J Adv Manuf Technol* 42(7–8):678–688
36. Sankar MK, Jain VK, Ramkumar J (2010) Rotational abrasive flow finishing process and its effects on finished surface. *Int J Mach Tools Manuf* 50(7):637–650
37. Sankar MR, Jain VK, Rajkumar J (2009) Experimental investigations into rotating workpiece abrasive flow finishing. *Wear* 267(1–4):43–51
38. Dabrowski L, Marciniak M, Wiczarek W, Zygmunt A (2006) Advancement of abrasive flow machining using an anodic solution. *J New Mater Electrochem Syst* 9:439–445
39. Dabrowski L, Marciniak M, Szweczyk T (2006) Analysis of abrasive flow machining with an electrochemical process aid. *Proc Inst Mech Eng* 220
40. Brar BS, Walia RS, Singh VP (2012) Electro chemical aid to abrasive flow machining process: harnessed for improved surface finishing. In: International conference on advancements and futuristic trends in mechanical and materials engineering
41. Brar BS, Walia RS, Singh VP (2015) Electrochemical aided abrasive flow machining process: a hybrid machining process. *Int J Adv Manuf Technol* 79:329–342
42. Brar BS, Walia RS, Singh VP, Sharma M (2012) Helical abrasive flow machining (HLX-AFM) process. *Int J Surf Eng Mater Technol* 2(2):48–52
43. Walia RS (2006) Development and investigations in centrifugal force assisted abrasive flow machining process. PhD thesis, IIT Roorkee
44. Barr BS, Walia RS, Singh VP, Sharma M (2013) A robust helical abrasive flow machining process (HLX-AFM). *J Inst Eng India Ser C* 94(1):21–29
45. Singh R, Walia RS, Suri NM (2015) Parametric optimization of centrifugal-magnetic force assisted abrasive flow machining process using utility concept. *Int J Res Eng Technol* 4(8):2321–2730
46. Vaishya R, Walia RS, Kalra P (2015) Design and development of hybrid electrochemical and centrifugal force assisted abrasive flow machining. 4th international conference on materials processing and characterization. *Mater Today Proc* 2:3327–3341
47. Fu Y, Wang X, Gao H, Wei H, Li S (2016) Blade surface uniformity of blisk finished by abrasive flow machining. *Int J Adv Manuf Technol* 84:1725–1735
48. Uhlmann E, Mihotovic V, Roßkamp S, Dethlefs A (2016) A pragmatic modelling approach in abrasive flow machining for complex shaped automotive components. 7th HPC 2016—CIRP conference on high performance cutting. *Procedia CIRP* 46:51–54
49. Wang AC, Cheng KC, Chen KY, Lin YC (2014) Enhancing the surface precision for the helical passageways in abrasive flow machining. *Mater Manuf Processes* 29:153–159
50. Jain RK, Jain VK, Dixit PM (1999) Modelling of material removal and surface finish in abrasive flow machining process. *Int J Mach Tools Manuf* 39:1903–1923
51. Petri KL, Billo RE, Bidanda B (1998) A neural network process model for abrasive flow machining operations. *J Manuf Syst* 17

52. Brar BS, Walia RS, Singh VP, Singh M (2011) Development of a robust abrasive flow machining process set up. *Int J Surf Eng Mater Technol* 1. ISSN: 2249-7250
53. Jain RK, Jain VK (2000) Optimum selection of machining conditions in abrasive flow machining using the neural network. *J Mater Process Technol* 108:62–67
54. Wang AC, Weng SC (2007) Developing the polymer abrasive gels in AFM process. *J Mater Process Technol* 192–193:486–490
55. Wang AC, Lee SJ (2009) Study the characteristics of magnetic finishing with gel abrasive. *Int J Mach Tools Manuf* 49(14):1063–1069
56. Kar KK, Ravikumar NL, Tailor PB, Ramkumar J, Sathiyamoorthy D (2009) Performance evaluation and rheological characterization of newly developed butyl rubber based media for abrasive flow machining process. *J Mater Process Technol* 209(4):2212–2221
57. Bin W, Wei C, Xia C (2012) A new type of nozzle AFM machine tool and control system research. INSPEC accession number: 12962727. <https://doi.org/10.1109/icma.2012.6285705>
58. Bähre D, Brünnel H, Swat M (2012) Investigation of one-way abrasive flow machining and in-process measurement of axial forces. *Procedia CIRP* 1:419–424
59. Uhlmann E, Dotis M, Schmiedel C (2013) Development of a material model for visco-elastic abrasive medium in abrasive flow machining. *Procedia CIRP* 8:351–356
60. Yang S, Sha L (2014) Study on processing effect prediction system of AFM for injector hole of twin flapper-nozzle valve. INSPEC accession number: 14855314. <https://doi.org/10.1109/es.2014.63>
61. Kenda J, Pušavec F, Kopac J (2014) Modelling and energy efficiency of abrasive flow machining on tooling industry case study. *Procedia CIRP* 13:13–18
62. Swat M, Brünnel H, Lyubenova N, Schmitt J, Diebels S, Bähre D (2014) Improved process control and model of axial forces of one-way abrasive flow machining. *Procedia CIRP* 14:19–24
63. Sooraj VS, Radhakrishnan V (2014) Fine finishing of internal surfaces using elastic abrasives. *Int J Mach Tools Manuf* 78:30–40
64. Ibrahim AF, Shather SK, Hamdan WK (2014) Studying abrasive flow machining conditions by using Taguchi method. *Eng Technol J* 32(4 Part (A))
65. Kenda J, Duhovnik J, Tavčar J, Kopač J (2014) Abrasive flow machining applied to plastic gear matrix polishing. *Int J Adv Manuf Technol* 71(1–4):141–151
66. Jang K-I, Seok J, Min B-K, Lee SJ (2010) An electro chemo mechanical polishing process using magnetorheological fluid. *Int J Mach Tools Manuf* 50(10):869–881
67. Paul L, Hiremath SS (2013) Response surface modelling of micro holes in electrochemical discharge machining process. *Procedia Eng* 64:1395–1404
68. Singh S, Shan HS, Kumar P (2013) Wear behaviour of materials in magnetically assisted abrasive flow machining. *J Mater Process Technol* 128(1–3):155–161
69. Jayswal SC, Jain VK, Dixit PM (2005) Modelling and simulation of magnetic abrasive finishing process. *Int J Adv Manuf Technol* 26(5–6):477–490
70. El-Taweel TA (2008) Modelling and analysis of hybrid electrochemical turning-magnetic abrasive finishing of 6061 Al/Al₂O₃ composit. *Int J Adv Manuf Technol* 37(7–8):705–714
71. Das VK, Jain VK, Ghoshdastida PS (2008) Analysis of magnetorheological abrasive flow finishing (MRAFF) process. *Int J Adv Manuf Technol* 38(56):613–621
72. Yamaguchi H, Srivastava AK, Tan MA, Riveros RE, Hashimoto F (2012) Magnetic abrasive finishing of cutting tools for machining of titanium alloys. *CIRP Ann* 61(1):311–314
73. Amineh SK, Tehrani AF, Mohammadi A (2013) Improving the surface quality in wire electrical discharge machined specimens by removing the recast layer using magnetic abrasive finishing method. *Int J Adv Manuf Technol* 66(9–12):1793–1803
74. Lee YH, Wu KL, Jhou JH, Tsai YH, Yan BH (2013) Two-dimensional vibration-assisted magnetic abrasive finishing of stainless steel SUS304. *Int J Adv Manuf Technol* 69(9–12):2723–2733
75. Judal KB, Yadava V (2014) Modelling and simulation of cylindrical electrochemical magnetic abrasive machining process. *Mach Sci Technol* 18:221–250
76. Mishra V, Goel H, Mulik RS, Pandey PM (2014) Determining work-brush interface temperature in magnetic abrasive finishing process. *J Manuf Process* 16(2):248–256

77. Das M, Jain VK, Ghoshdastidar PS (2015) A 2D CFD simulation of MR polishing medium in magnetic field-assisted finishing process using electromagnet. *Int J Adv Manuf Technol* 76(1–4):173–187
78. Das M, Jain VK, Ghoshdastidar PS (2012) Nano-finishing of flat workpieces using rotational–magnetorheological abrasive flow finishing (R-MRAFF) process. *Int J Adv Manuf Technol* 62(1–4):405–420
79. Wang A-C, Tsai L, Liang KZ, Liu C-H, Weng S-H (2009) Uniform surface polished method of complex holes in abrasive flow machining. *Trans Nonferr Met Soc China* 19:250–257
80. Walia RS, Shan HS, Kumar P (2006) Abrasive flow machining with additional centrifugal force applied to the media. *Mach Sci Technol* 10:341–354

Analysis of Green Supply Chain Management Enablers in FMCG Sector Using Integrated ISM and MICMAC Approach



Prabhakar Vivek and Jha Sanjay Kumar

Abstract The objective of this paper is to identify and model the relationship amongst various green supply chain management (GSCM) enablers encountered while implementing GSCM practices in fast-moving consumer goods (FMCG) industry. 11 key enablers were identified and Interpretive Structure Modelling (ISM) is used to construct a model describing mutual relationship amongst various enablers. Matriced' Impacts Croisés Multiplication Appliquée á un Classement (MICMAC) analysis is conducted to give results regarding driving and dependence power of enablers. The results of this study can be considered by the top management while formulating strategies for implementation of GSCM practices in their respective organization.

Keywords Interpretive structural modelling · MICMAC · Green supply chain management · GSCM enablers

1 Introduction

During present times, organizations need to adopt an environmentally conscious approach in their business framework to sustain themselves. Supply chain of an organization forms the backbone of a business, starting from extraction of material up till delivery of goods to customer and in the process, producing large amount of waste and harmfully affecting the environment [1].

GSCM involves implementing a greener approach in all supply chain actions starting from green purchasing up to retrieval of the recyclable scrap back to the organization [2]. The sudden focus towards GSCM implementation is driven due to increased profit value, higher market shares and customer goodwill it brings [3]. GSCM practices and implementation demands that the manufacturers, customer and suppliers work together so as to design an environmentally sound supply chain structure [4].

P. Vivek (✉) · J. Sanjay Kumar
Department of Production Engineering, Birla Institute of Technology, Mesra 835215, India
e-mail: prabhakarvivekrke@gmail.com

© Springer Nature Singapore Pte Ltd. 2019
K. Shanker et al. (eds.), *Advances in Industrial and Production Engineering*, Lecture Notes in Mechanical Engineering, https://doi.org/10.1007/978-981-13-6412-9_6

Diabat and Govindan [5] used ISM MICMAC analysis to rank barriers of GSCM, and it was established that government regulations and reverse logistics were amongst the chief barriers identified. Dube and Gawande [6] used a combination of ISM and Fuzzy MICMAC approach to model the enablers for GSCM implementation. Malviya et al. [7] used fuzzy ANP technique to identify the best strategy for sustainable supply chain implementation. Sari [8] combined VIKOR and AHP technique under fuzzy environment to develop a novel framework for GSCM implementation.

2 Problem Description

There are four firms selected for this study that are leading manufacturers of FMCG products in India. Five experts from academician and four from industry, working in the field of GSCM are selected to provide consultation and opinions on the importance of drivers identified in the study. After rigorous literature survey and comments from the expert panel, 11 drivers were selected for the study.

3 ISM Methodology and Model Development

ISM can be defined as a learning technique used to obtain a structure showcasing various indirect and direct relationships existing between different factors. The model developed using ISM can be used by an individual or a group to obtain a map of the complex interrelationship existing between various factors of a complex problem.

3.1 Structural Self-interaction Matrix

After extensive literature review, 11 most relevant enablers were identified for the study namely Government Rules and Regulations (GRR), Top Management Commitment (TMC), Reverse Logistics (RL), Financial Support (FS), Adoption of Cleaner Technology (ACT), Global Competitiveness (GC), Society and Public Pressure (SPP), Green Manufacturing (GM), Green Purchasing (GP), Supplier Involvement (SI) and Environmental Training (ET) and these enablers were further reevaluated by the expert panel consisting of four experts from academic and four from industry well versed with GSCM practices and their implementation in the FMCG industry. The same expert panel was asked to give comments on the interrelationship existing amongst the enablers so as to develop a contextual relationship matrix shown in Table 1. Following annotations have been used in the SSIM matrix to represent the various interrelationships amongst the enablers (i represents row and j represents column):

Table 1 Structural self-interaction matrix

			11	10	9	8	7	6	5	4	3	2
1	GRR	V	V	V	V	V	V	V	V	O	V	V
2	TMC	O	X	V	V	V	A	V	O	V	V	
3	RL	V	A	X	X	V	A	O	V	A		
4	FS	O	A	V	V	V	A	V	V			
5	ACT	V	A	X	X	V	O	V				
6	GC	O	O	A	A	A	O					
7	SPP	O	V	V	V	O						
8	GM	V	A	A	A							
9	GP	A	A									
10	SI	V										
11	ET	-										

- V GSCME *i* helps achieving GSCME *j*
- A GSCME *j* helps achieving *i*
- X GSCME *i* and *j* help achieving each other
- O GSCME *i* and *j* are not related.

3.2 Initial Reachability Matrix

SSIM obtained in the previous steps is further converted into binary matrix known as initial reachability matrix (Table 2). This is achieved by substituting the symbols V, A, X and O into 1 and 0, i.e. if enabler *i* effects *j*, input 1 and if it does not, input 0 in the corresponding column. After we have obtained initial reachability matrix, we check for its transitivity. After application of transitivity rule, the final matrix is obtained in Table 3.

3.3 Level Partitions

After obtaining the final matrix, antecedent set as well as reachability set for each enabler was found out. Reachability set included the enabler itself as well as other enablers it is helping to achieve also antecedent set included the enabler itself as well as other enablers which are helping to achieve the given enabler. After that, the intersection of these sets is identified for each enabler. Those enablers for which the intersection set and the reachability set are identical are placed at top level of the hierarchy. Top-level enablers do not help achieving any other enabler. After identifying the top-level enabler, they are eliminated for the further analysis hereby

Table 2 Reachability matrix

Enablers	TMC	RL	ECL	MD	IT	EPM	AS	SCI	RTC	FC	LNS	Driving power
TMC (1)	1	1	1	1a	1	1	1	1	1	1	1	11
RL(2)	0	1	1	1	1a	1	0	1	1	1	1a	9
ECL (3)	0	0	1	0	1	1a	0	1	1	0	1	6
MD (4)	0	0	1	1	1	1	0	1	1	0	0	6
IT (5)	0	0	1a	0	1	1	0	1	1	0	1	6
EPM (6)	0	0	0	0	0	1	0	0	0	0	0	1
AS (7)	0	1	1	1	1	1a	1	1a	1	1	1a	10
SCI (8)	0	0	0	0	1a	1	0	1	1a	0	1	5
RTC (9)	0	0	1	0	1	1	0	1	1	0	0	5
FC (10)	0	1	1a	1	1	1a	0	1	1	1	1	9
LNS (11)	0	0	1a	0	1	1a	0	1a	1	0	1	6
Dependence power	1	4	9	5	10	11	2	10	10	4	8	

Table 3 Final reachability matrix

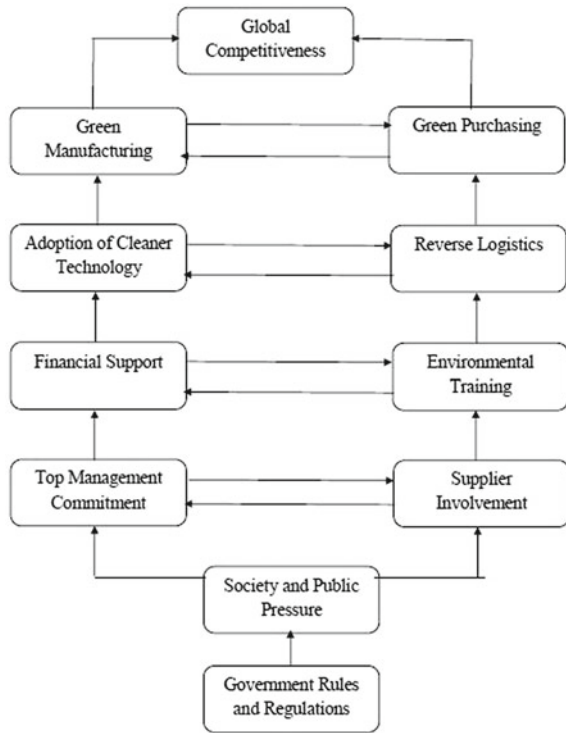
Enablers	Reachability set	Antecedent set	Intersection	Level
GRRs	1, 2, 3, 4, 5, 6, 7, 8, 9, 10, 11	1	1	I
TMC	2, 3, 4, 5, 6, 8, 9, 10	1, 2, 7, 10	2, 10	III
RL	3, 5, 6, 8, 9, 11	1, 2, 3, 4, 5, 7, 9, 10, 11	3, 5, 9, 11	V
FS	3, 4, 5, 6, 8, 9	1, 2, 3, 4, 5, 7, 8, 9, 10, 11	4	IV
GC	3, 5, 6, 8, 9, 11	1, 2, 3, 4, 5, 6, 7, 8, 9, 10, 11	3, 5, 9, 11	V
SPP	6	1, 2, 3, 4, 5, 6, 7, 8, 9, 10, 11	6	VII
ACT	2, 3, 4, 5, 6, 7, 8, 9, 10, 11	1, 7	7	II
GM	5, 6, 8, 9, 11	1, 2, 3, 4, 5, 7, 8, 9, 10, 11	5, 8, 9, 11	VI
GP	3, 5, 6, 8, 9	1, 2, 3, 4, 5, 7, 8, 9, 10, 11	3, 5, 8, 9	VI
SI	2, 3, 4, 5, 6, 8, 9, 10, 11	1, 2, 7, 10	2, 10	III
ECT	3, 5, 6, 8, 9, 11	1, 2, 3, 5, 7, 8, 10, 11	3, 5, 8, 11	IV

completing the first iteration shown in Table 3. Subsequent iterations were done after which final reachability matrix is obtained as shown in Table 3.

3.4 Building the ISM Mode

The final reachability matrix is then used to obtain the final structured model. The blocks in the final model indicate the enablers with the arrow from *i* to *j* indicating that enabler *i* lead to enabler *j*. For the final step, the transitivity associated with the model is removed to obtain the final ISM model shown in Fig. 1.

Fig. 1 Final ISM model



3.5 ISM Model Formulation for GSCM Drivers

The final ISM model developed is depicted in Fig. 1. ‘Global Competitiveness’ is the top-level enabler and ‘Government Rules and Regulations’ stands as the bottom level barrier in the final structure followed by ‘Society and Public Pressure’. The enablers at the bottom portion influence those at the upper portion of the model and hold greater significance. ISM model can be used to understand interrelationship amongst enablers and its result is further used as input for MICMAC analysis.

3.6 MICMAC Analysis

MICMAC analysis is conducted to identify the driving as well as dependence powers for the variables and is based upon the matrix multiplication properties. After doing the MICMAC analysis, the various enablers can be classified into four categories depending upon their driving and dependence power.

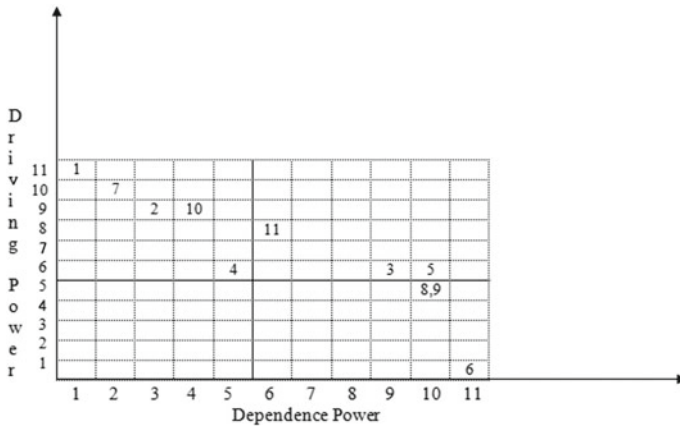


Fig. 2 Driving dependence power diagram and MICMAC analysis

From the results of Table 1, the driving and dependence power for various enablers are calculated which is further used to draw the driving dependence power diagram shown in Fig. 2.

4 Results and Discussions

Results from ISM model and MICMAC analysis dictate that GRR and SPP are the key enablers that drive GSCM implementation and if pursued will form the way for other enablers. GC forms the topmost level; thus, it is the weakest enabler. Management need not focus on GC because it will be taken care of by other enablers once they are pursued. TMC and SI are codependent and driven by societal pressure and are two of the key enablers for GSCM which in turn affect other enablers such as ET, FS and RL.

The MICMAC analysis revealed that RL (3), ACT (5) and ET (11) are Linkage Enabler which refers to enablers with high driving dependence power which implies that these enablers have high driving as well as dependence power. These enablers are most unstable in nature and can disrupt the whole model, hence, most vital to the system. Enablers GC (6), GM (8) and GP (9) namely are dependent enablers with strong dependence and weak driving power with no effect on the structure. SI (1), FS (2), SPP (4), GRR (7) and TMC (10) are the independent enablers with strong driving and weak dependence power. These enablers drive other enablers and hence play a key role in GSCM implementation. No enablers were found the occupy quadrant I, i.e., autonomous enablers category.

5 Conclusion and Future Scope

GSCM implementation can be a complex task, especially if a number of variables are involved with complex interrelationship existing amongst them. Therefore, it is imperative for a firm to identify which enablers are of the most vital importance and should be pursued first. Also the complex relationship amongst the enablers has to be adequately explained. For this purpose, an ISM model was developed after identifying the chief 11 enablers involved in GSCM implementation in FMCG sector using past literature research. The ISM model clearly showcases the various relationships and hierarchy of the enablers in a lucid and well-defined manner. It can be concluded that the enablers ‘Government Rules and Regulations’ and ‘Societal Public Pressure’ are the key enablers and form the bottommost level in ISM. Thus, these enablers should be approached first while implementing GSCM.

Further MICMAC analysis was conducted for the enablers obtained to classify enablers into four categories based on their driving and dependence power. The results of the analysis indicated that no autonomous enablers were identified for the study. Furthermore, three enablers fall in linkage category, five in independent and three in dependent enabler category.

The following study can be used for various managerial implications while implementing GSCM in existing supply chain of FMCG industry. Furthermore, it acts as a blueprint for future studies to be conducted in the FMCG sector regarding GSCM studies. Extension of the work can be further carried out by conducting Structural Equation Modelling (SEM), to validate the model. Hypothesis testing can also be carried out for validation purposes.

References

1. Beamon N (1999) Designing the green supply chain. *Logist Inf Manag* 12(4):332–342
2. Bhateja AK, Babbar R, Singh S, Sachdeva A (2012) Study of the critical factor finding’s regarding evaluation of green supply chain performance of indian scenario for manufacturing sector. *Int J Comput Manag* 15(1):74–80
3. Srivastava S (2007) Green supply-chain management: a state-of the-art literature review. *Int J Manag Rev*, 53–80
4. Zhu Q, Sarkis J (2006) An inter-sectoral comparison of green supply chain management in China: drivers and practices. *J Clean Product* 14(5):472–486
5. Diabat A, Govindan K (2011) An analysis of the drivers affecting the implementation of green supply chain management. *J Resour Conserv Recycl* 55(6):659–667
6. Dube A, Gawande R (2016) ISM-fuzzy MICMAC approach for analysis of GSCM enablers. *Int J Logist Syst Manag* 24(4):136–143
7. Malviya RK, Kant R, Dutta A (2018) Evaluation and selection of sustainable strategy for green supply chain management implementation. *Bus Strategy Environ* 27(4)
8. Sari K (2017) A novel multi-criteria decision framework for evaluating green supply chain management. *Comput Ind Eng* 105(3):338–347

Deformation Behavior of Semi-solid Forged A356–5TiB₂ Nano-In Situ Composites



Sahini Deepak Kumar, Ananya Chatttee, Sanjay Kumar Jha,
Niranjan Kumar Singh and Animesh Mandal

Abstract The research work investigates the application of semi-solid metal processing (SSMP) to predict the deformation behavior of semi-solid A356–5TiB₂ nano-in situ composites. The semi-solid forging of A356–5TiB₂ in situ composites was carried out in three steps. In the first step, cooling slope (CS) casting setup was developed to generate the non-dendritic feedstock of the composites for subsequent thixoforging. In the second step, differential thermal analysis was used to estimate the semi-solid temperature range in order to achieve partial remelting temperatures and solid fraction profiles of the composites. In the final step, the non-dendritic feedstock of the composites was thixoforged with different % reductions ranging from 30 to 50%. It is noted that the semi-solid A356–5TiB₂ nano-in situ composites with 40% deformation attained the ultimate tensile strength (UTS) of 318 MPa, in peak aged condition which is about 110.6% compared to gravity-cast alloy. This is attributed due to the presence of nano-TiB₂ particles in the semi-solid forged A356–5TiB₂ in situ composite, which clearly indicates the influence of semi-solid forging on the deformation behavior and tensile properties of composites.

Keywords Semi-solid forging · Thixoforging · A356 alloy · In situ · TiB₂ · Nano-composites

S. Deepak Kumar (✉) · A. Chatttee · S. K. Jha
Department of Production Engineering, Birla Institute of Technology Mesra, Ranchi 835215,
Jharkhand, India
e-mail: dks10@iitbbs.ac.in

N. K. Singh
Department of Forge Technology, National Institute of Foundry & Forge Technology (NIFFT),
Ranchi 834003, Jharkhand, India

A. Mandal
School of Minerals, Metallurgical and Materials Engineering, Indian Institute of Technology
Bhubaneswar, Bhubaneswar 751007, Odisha, India

1 Introduction

Lightweight metal matrix composites (MMCs) are considered as a potential material for automotive, aerospace, and other engineering applications [1]. The ductility of the matrices deteriorates with the addition of ceramic particles like SiC and Al₂O₃ due to their tendency to crack during mechanical loading and relatively high reinforcement concentration in the matrix. However, it is crucial to achieve a uniform distribution of nano-particles through the matrix and good bonding between the matrix and nano-particles in order to maximize composite mechanical properties [2, 3]. Deepak Kumar et al. [4] reported that TiB₂ is a promising candidate owing to its high strength, hardness, and ability to form a strong interfacial bond with Al matrix. Thus, such difficulties can be overcome by the addition of in situ formed TiB₂ particulates in the alloy [5].

Thixoforming is one of the routes of semi-solid metal processing (SSMP) [6]. This involves forming metallic alloys and composites in the semi-solid state. The key step in thixoforming is to generate a feedstock material having non-dendritic or nearly globular microstructure [7, 8]. In thixoforming, one of the emerging rheocasting processes for generation of non-dendritic feedstock is the cooling slope (CS) casting process [9, 10]. Thixoforming in the semi-solid state of commercial alloys and MMCs has received significant attention in recent years [11]. The tensile deformation behavior plays a vital role in deciding upon the suitability of a material for structural applications [12]. Among the various thixoforming routes, forging has substantial potential to generate sufficient plastic deformation and for the improvement of hardness and tensile properties [13]. Dodangeh et al. [14] have studied the plastic deformation behavior in multi-directional forgings for Al–Si alloys and suggested that severe strain can be imposed on rheoforged parts compared to conventional cast parts. Tahamtan et al. [15] investigated thixoforging properties of A356 alloy and reported the enhancement in mechanical properties of thixoforged alloys compared to rheo-cast and gravity-cast counter parts. Comparing the tensile properties of rheo-cast and gravity-cast parts with their corresponding thixoforged parts is of considerable interest. Based on the extensive literature survey suggests that, no information is available on the tensile deformation behavior of Al alloy-based nano-in situ composites subjected to thixoforming. Therefore, the present investigation is undertaken to study the tensile deformation behavior of thixoforged A356–5 wt% TiB₂ nano-in situ composites.

2 Materials and Methods

2.1 Fabrication of Nano-In Situ Composites

In the present work, a commercial A356 aluminum casting alloy which is widely used for semi-solid forming was used for the fabrication of nano-in situ TiB₂ composites.

TiB₂ particulates which were formed by in situ route were used as reinforcements for strengthening the Al-based alloy. The A356–5TiB₂ nano-in situ composite was fabricated by mixed salt route. At a reaction temperature of 800 °C, the halide salts, K₂TiF₆ and KBF₄, undergo an exothermic reaction with molten Al–7Si alloy and form titanium diboride (TiB₂) particles in the melt. The details of the synthesis of the nano-in situ composites have been described previously [3, 4].

2.2 Semi-solid Forging

The semi-solid forging was carried using an 80-ton hydraulic press (Flowmech Engineers Private Limited, India, Model No. HP-50) on both alloy and composite specimens. The load applied was 150 kg/cm² at a ram speed 20 mm/s. A schematic illustration of the thixoforging press is shown in Fig. 1a. The specimens were independently subjected between 30 and 50% forging. A silicone spray was used as a lubricant in order to reduce the friction between semi-solid billets and the dies. Further, the forming dies were preheated up to 200 °C to prevent the forged specimens from cooling. The heating process was monitored using K-type thermocouples to control the temperature fluctuation in the range of ±2 °C. Once the desired temperature was reached, and the thermocouple was extracted, the billet was thixoforged into the die. The thixoforged alloy and composite samples were sectioned in lateral, transverse, and longitudinal directions as illustrated in Fig. 1b. The gravity-cast alloys and composite specimens have been designated as gravity-cast alloy (GCA) and gravity-cast composite (GCC), respectively, while the thixoforged specimens were designated as thixoforged alloy (TFA) and thixoforged composite (TFC), respectively.

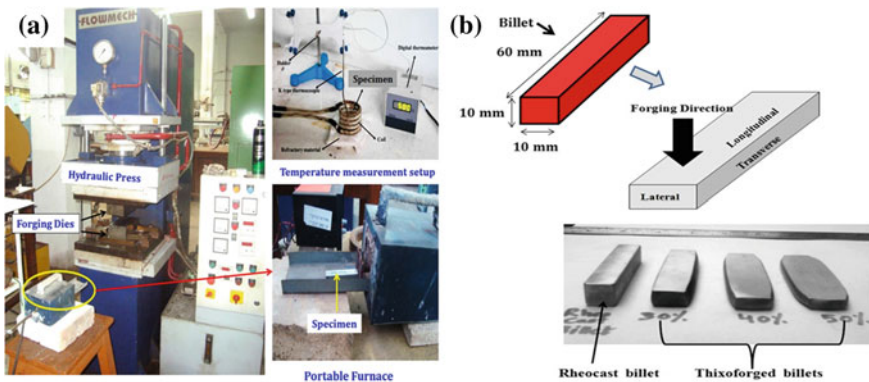


Fig. 1 a Thixoforging press and b thixoforged billets

2.3 *Microstructural Characterization and Mechanical Testing*

Microstructural analyses were performed by optical microscopy and scanning electron microscope (SEM, Model: 40, Carl-Zeiss SMT, Germany) fitted with EDX analysis. Vickers hardness (macro-) measurements were carried out at an indentation load of 5 kgf. For tensile testing, flat tensile specimens of 4×4 mm cross section and gauge length of 16 mm were machined from the alloy and composites and tested following ASTM E-8M standards.

3 Results and Discussion

3.1 *Microstructures of Semi-solid Forged Samples*

The morphologies of A356 alloy processed by conventional casting having a dendritic structure are shown in Fig. 2a, while that processed via semi-solid forging typically consists of mixture of rosettes and nearly spherical grains as shown in Fig. 2b. Moreover, in the thixoformed samples shown in Fig. 2b the Si particles are uniformly distributed as compared to gravity-cast alloy. The decrease in the size of Si particles is more significant in the thixoformed composite as shown in Fig. 2b. The spheroidized Si particles are evident, and this is due to thermal modification. This is quite evident from micrographs in Fig. 2c which reveals the nano-TiB₂ particles in the size range 0.1–0.5 μm which are distributed uniformly in the thixoforged composite along the grain boundaries of $\alpha\text{-Al}$. The EDX analysis shown in Fig. 2d confirms the presence of Ti and B atoms and its segregation to inter-dendritic regions of the semi-solid forged composite, and the corresponding EDX mapping of Al, Si, Ti, and B is presented in Fig. 3a–d. Thus, the minute TiB₂ particles refine the eutectic silicon and influence the tensile properties of thixoformed composites.

3.2 *Stress–Strain Behavior*

The typical true stress–true strain curves of gravity-cast alloy (GCA) and that of thixoforged alloys (TFA) and composites (TFC) are presented in Fig. 4. It can be seen from true stress–true strain curves that the yield strength and ultimate tensile strength increase in the order: gravity-cast samples < thixoforged alloy < thixoforged composite. The flow curves of thixoformed alloy and composites were found to be higher indicating that thixoforging process has a significant impact on flow behavior as compared to the gravity-cast counter parts. Further, the trend increased after the T6 treatment in the composites.

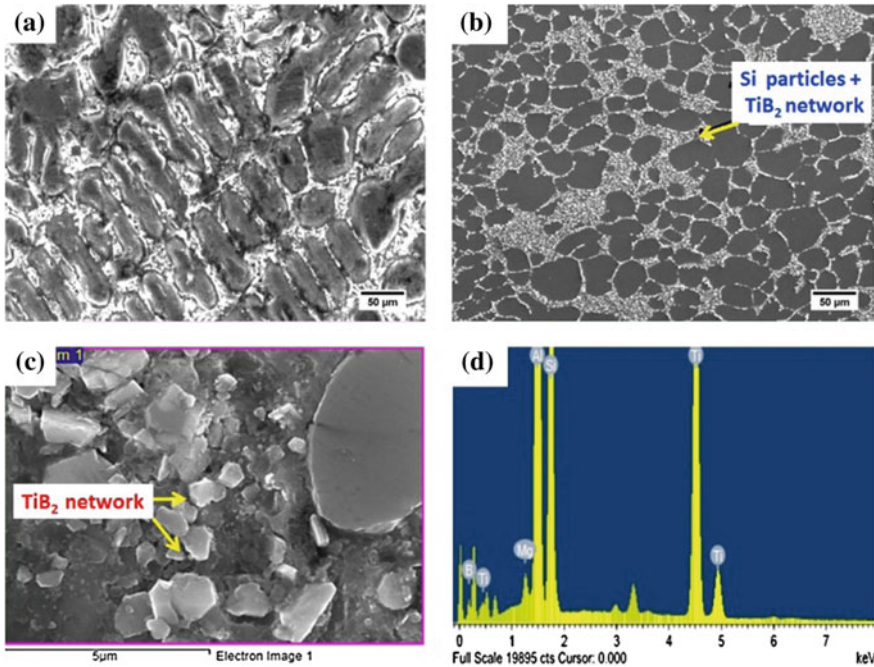


Fig. 2 FESEM micrographs of **a** gravity-cast alloy, **b** thixoforged composites (TFC), **c** nano-TiB₂ network in TFC, and **d** EDX analysis of bulk TFC

3.3 Tensile Properties

The tensile properties of the alloy and composites under study in gravity-cast and thixoforged conditions, before and after T6 treatment, are presented in Fig. 5.

From Fig. 5, it indicates that the tensile properties are significantly higher for the thixoforged alloys and composites compared to the gravity-cast counter parts. The % increase in yield strength and UTS for thixoforged alloy is found to be 43 and 36% higher, respectively, compared to the gravity-cast alloy. It is noted that the % elongation increased by 36.5% in the thixoforged alloy. This is attributed to plastic deformation caused during thixoforging which resulted in globular morphology of Si particles. The tensile properties steadily increased, with the addition of TiB₂ particles in the matrix. Moreover, the thixoforged composite (TFC) has shown a 40% increase in UTS compared to GCA and the % elongation of TFC is 12.73 which is 41% higher than the GCA. The thixoforged composite after T6 treatment has resulted in 110% increase in UTS compared to the GCA and at the same time maintaining the ductility values at 10.2. This can be attributed to combined effect of the thermal modification during T6 treatment and thixoforging which resulted in globular morphology of Si. In addition, the presence of nano-TiB₂ particles throughout the matrix causes grain refinement of α-Al.

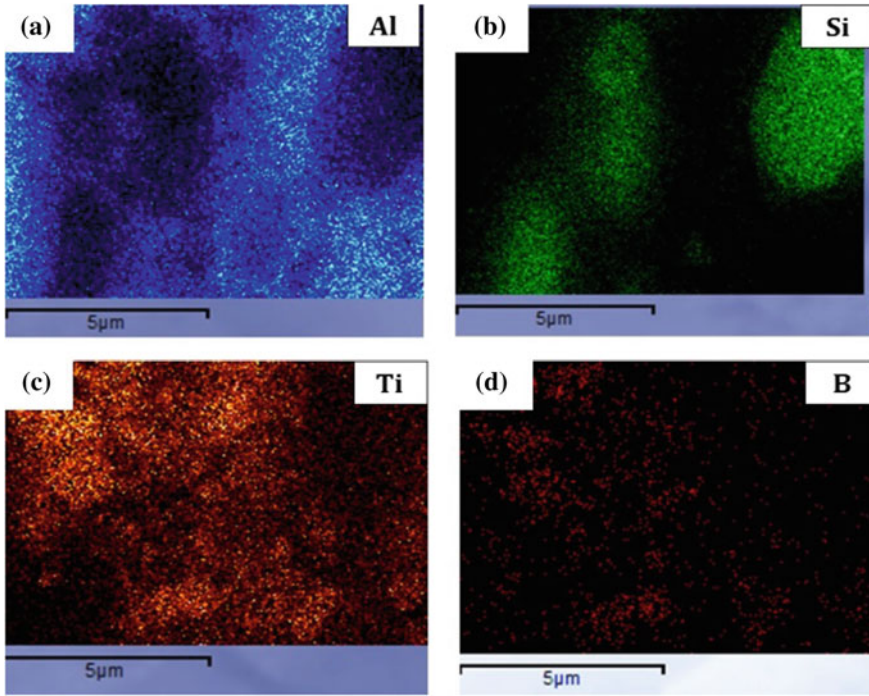


Fig. 3 EDS elemental mapping of semi-solid forged A356–5TiB2 in situ composite. **a** Al, **b** Si, **c** Ti, and **d** B

Fig. 4 True stress–strain curves of alloys and composites

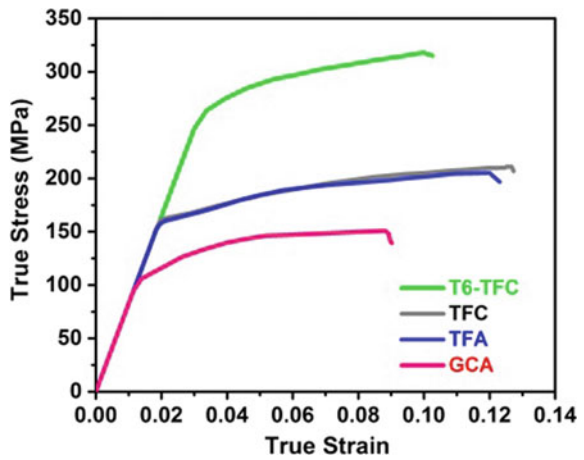
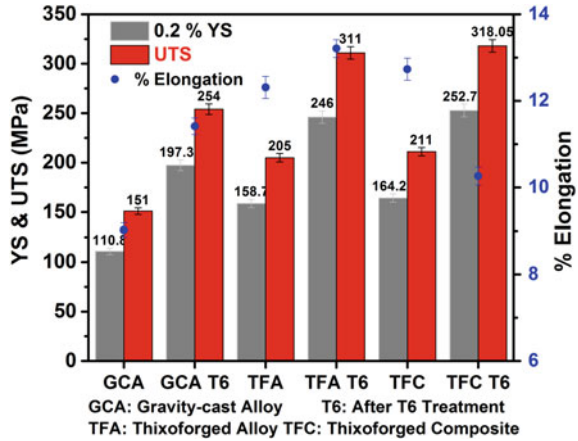


Fig. 5 Tensile properties of the alloys and composites



4 Conclusions

The present investigation deals with the tensile deformation behavior of semi-solid forged A356–5 wt% TiB₂ nano-in situ composite. The following conclusions can be summarized from the present study:

- The stress–strain curves of thixoformed alloy and composites were found to be higher indicating that thixoforging process has a significant impact on flow behavior as compared to gravity-cast counter parts.
- The yield strength and tensile strength of thixoformed alloy after T6 treatment increased to 121.6 and 106%, respectively, compared to gravity-cast alloy.
- The thixoformed composite attained the highest UTS of 318 MPa which is 110.6% higher than the gravity-cast alloy. This is attributed due to combined effect of T6 treatment and thixoforging which resulted in globular morphology of Si.
- The tensile strength of thixoformed composite is found to be significantly higher than of gravity-cast alloy due to the presence of nano-TiB₂ particles.

References

1. Surappa MK (2003) Aluminium matrix composites: challenges and opportunities. *Sadhana* 28(1–2):319–334
2. Chawla KK (2012) *Composite materials: science and engineering*, 3rd edn. Springer, New York
3. Kumar P, Kumar A, Racic V (2018) Modelling of longitudinal human walking force using self-sustained oscillator. *Int J Struct Stab Dyn* 18(6):1850080
4. Deepak Kumar S, Vundavilli PR, Mantry S, Mandal A, Chakraborty M (2014) A Taguchi optimization of cooling slope casting process parameters for production of semisolid A356 alloy and A356-5TiB₂ in-situ composite feedstock. *Procedia Mater Sci* 5:232–241
5. Deepak Kumar S, Mandal A, Chakraborty M (2015) On the age hardening behavior of thixoformed A356-5TiB₂ in-situ composite. *Mater Sci Eng A* 636(11):254–262

6. Fan Z (2002) Semisolid metal processing. *Int Mater Rev* 7(2):49–85
7. Pola A, Tocci M, Kapranos P (2018) Microstructure and properties of semi-solid aluminum alloys: a literature review. *Metals* 181(8):1–17
8. Haga T, Suzuki S (2001) Casting of aluminum alloy ingots for thixoforming using a cooling slope. *J Mater Process Technol* 118(1–3):169–172
9. Atkinson HV, Liu D (2008) Microstructural coarsening of semi-solid aluminium alloys. *Mater Sci Eng A* 496(1–2):439–446
10. Das P, Samanta SK, Chattopadhyay H, Dutta P (2012) Effect of pouring temperature on cooling slope casting of semi-solid Al-Si-Mg alloy. *Acta Metall Sin (Engl Lett)* 25(5):329–339
11. Mathew J, Mandal A, Deepak Kumar S, Bajpai S, Chakraborty M, West GD, Srirangam P (2017) Effect of semi-solid forging on microstructure and mechanical properties of in-situ cast Al-Cu-TiB₂ composites. *J Alloy Compd* 712:460–467
12. Fadavi Boostani A, Tahamtan S (2010) Effect of a novel thixoforming process on the microstructure and fracture behavior of A356 aluminum alloy. *Mater Des* 31(8):3769–3776
13. Mallapur DG, Rajendra Udupa K, Kori SA (2011) Studies on the influence of grain refining and modification on microstructure and mechanical properties of forged A356 alloy. *Mater Sci Eng A* 528:4747–4752
14. Dodangeh A, Kazeminezhad M, Aashuri H (2012) Severe plastic deformation of rheoforged aluminum alloy A356. *Mater Sci Eng A* 558:371–376
15. Tahamtan S, Golozar MA, Karimzadeh F, Niroumand B (2008) Microstructure and tensile properties of thixoformed A356 alloy. *Mater Charact* 59:223–228

Study of MRR and TWR in Electric Discharge Machining of AISI D2 Tool Steel



Himanshu Payal, Satish Kumar Sharma, Aakash, Ashish kumar, Avinash kumar and Himanshu

Abstract Owing to its mechanical and metallurgical properties, AISI D2 is extensively used as tool steel in die-making industry. Typical shapes and intricate die cavities along with its high hardness make conventional operations of machining unsuitable and uneconomical for machining of AISI D2 steel. Electrical discharge machining (EDM) is an appropriate process for machining of such high-strength tool steels. Therefore, this study was carried out to characterize and optimize the process parameters of die-sinking EDM for material removal rate (MRR) and tool wear rate (TWR) in machining of AISI D2 tool steel. Discharge current, gap voltage, pulse-on-time, and tool material were taken as process parameters. Taguchi's orthogonal array approach coupled with analysis of variance is applied to design the experiments and analyze the relationship between process parameters and process outcomes. Methodology developed in this study assists in adjusting machining parameters for desired outcomes. Moreover, the process parameters can be utilized to economically manufacture the quality die tools.

Keywords Electrical discharge machining (EDM) · Metal removal rate (MRR) · Tool wear rate (TWR) · Tool steel · Signal-to-noise ratio (S/N)

1 Introduction

Due to its excellent mechanical and metallurgical properties, D2 steel finds a wide application in highly stressed cutting and punching tools for thin sheets, profile rolls, drawing and deep drawing tools [1]. This steel finds difficulty in the machining stage

H. Payal (✉)

Department of Mechanical Engineering, Sharda University, Greater Noida 201310, India
e-mail: himanshupayal@rediffmail.com

S. K. Sharma

Department of Mechanical Engineering, Thapar Institute of Engineering and Technology, Patiala 147004, Punjab, India

Aakash · Ashish kumar · Avinash kumar · Himanshu

MPAE Division, Netaji Subhas Institute of Technology, New Delhi 110078, India

© Springer Nature Singapore Pte Ltd. 2019

K. Shanker et al. (eds.), *Advances in Industrial and Production Engineering*, Lecture Notes in Mechanical Engineering, https://doi.org/10.1007/978-981-13-6412-9_8

due to its high wear strength properties. In order to generate typical shapes and intricate cavities in this steel by conventional processes, it is a difficult task. Hence, EDM is one of the substitute methods to machine this alloy. EDM is one of the most popular non-conventional material removal processes for the manufacturing sectors like aerospace, automotive, nuclear, and medical and die-mold production. The EDM process is thermoelectric process in which material removal takes place by the erosion effect of recurring spark generated between workpiece and tool immersed in dielectric media. The recurring spark causes the ionization of dielectric medium. The process involves the temperature of around 8000–12000 °C which is generated by the discharge energy at the point of spark which is enough to melt and vaporize the material from the workpiece and tool electrode [2]. The main advantage of EDM process is that physical and metallurgical properties of workpiece do not hamper the machining due to non-contact between tool and workpiece.

EDM has become one of the widely established non-conventional processes in many manufacturing industries because of the specialty of maintaining high precision accuracy. A considerable amount of work has been done by various researchers in the past in order to improve the significant output performance measures like MRR, TWR, and surface roughness (SR). However, the full potential of this process is not explored completely because of the stochastic and conflicting nature of this process which involves different variables. The prediction ability of the MRR and TWR while machining D2 tool steel has been studied by various researchers. Prabhu and Vinayagam [3] studied the surface characteristics like SR, micro-cracks of D2 steel workpiece. They have used the properties of single-wall carbon nanotube which is mixed in the dielectric fluid for the analysis of performance measures. Singh et al. [4] did a review on the D2 steel material by considering various EDM parameters such as discharge current, pulse-on-time, pulse-off-time, gap voltage which directly affects the surface roughness. Again, Prabhu and Vinayagam [5] conducted an experimental investigation on EDM for D2 tool steel by taking copper as an electrode material. Jadhav et al. [6] studied the effects of discharge current, pulse-on-time, pulse-off-time on EDM process by taking D2 tool steel as an electrode material. Gupta et al. [7] did the optimization of the various responses such as MRR, TWR, and overcut (OC) by taking AISI D2 tool steel as workpiece. Shivade and Shinde [8] reported an experimental investigation on wire EDM for D3 tool steel. They have used Taguchi technique as single objective with GRA as multi-objective technique. Kansal et al. [9] studied the effects of adding silicon powder mix into the dielectric fluid, while doing EDM of tool steel and significant improvement in machining rate were observed after the addition of silicon powder.

However, enormous studies were carried out to enhance the machining ability of EDM process, and investigations exploring the process performance of die-sinking EDM of die steels with different electrode materials along with other process parameters are reported meagerly in the literature. Therefore, this experimental investigation is carried out with an objective to explore the effect of different electrode materials along with other process parameters of die-sinking EDM on the process performance in terms of MRR and TWR during machining of AISI D2 tool steel.

2 Experimentation

Mechanical properties and chemical composition of AISI D2 tool steel are shown in Tables 1 and 2, respectively. Experiments have been carried out on Elektra 5535 PS die-sinking EDM shown in which the Z-axis is servo controlled and X- and Y-axes are manually controlled (refer Fig. 1a). From the reported literature and trial experiments, process parameters are chosen as discharge current, gap voltage, pulse-on-time, and tool material. The working range of input parameters and the levels taken are shown in Table 3. For deciding the level, some exploratory experiments were conducted in the given range of input parameters. In this work, experiments have been designed according to Taguchi’s L₉ (3⁴) orthogonal array as shown in Table 4. The electrodes selected for this work are aluminum, copper, and brass, as shown in Fig. 1b. The diameter of all the electrodes is 12 mm. To attain the stable machining conditions, a study of 10 min or 0.5 mm depth of cut (whichever earlier) is taken during experimentations. The machined surfaces of the D2 tool steel using different electrode materials are shown in Fig. 2.

MRR/TWR is evaluated by measuring the loss in weight of the work-piece/electrode before machining and after machining divided by the density of workpiece/electrode into machining time. The initial and final weights of the work-piece are measured on electronic balance having a resolution of 0.0001 g. MRR and TWR are calculated by the following equation.

$$\text{MRR or TWR (mm}^3\text{/min)} = \frac{\text{Reduction in weight of work piece or electrode}}{\text{density of work piece or electrode } \left(\frac{\text{g}}{\text{mm}^3}\right) \times \text{machining time (min)}} \quad (1)$$

Table 1 Mechanical properties of D2 material

Rockwell hardness	56 HRC
Poisson’s ratio	0.20–0.30
Elastic modulus	190–210 GPa
Density	7.7 g/cm ³

Table 2 Chemical composition of D2 material

Elements	C	Cr	W
% Contribution	2–2.35	11–13	1.0
Elements	Mn	Mo	P
% Contribution	0.6	0.0	0.03
Elements	Si	S	V
% Contribution	0.6	0.03	1.1

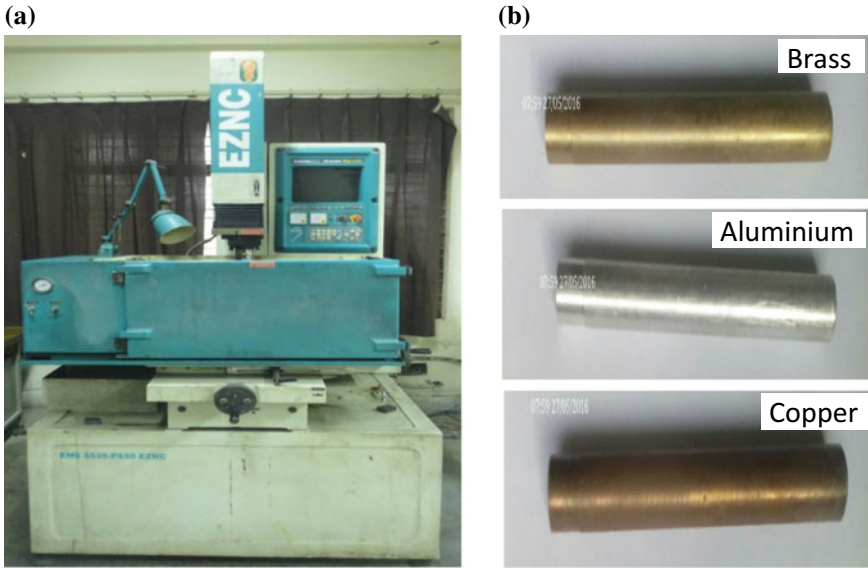


Fig. 1 a Setup for die-sinking EDM and b EDM electrodes of different materials

Table 3 Machining parameters and their levels

Input parameter	Symbol	Unit	Level 1	Level 2	Level 3
Discharge current	I_d	A	8	12	16
Gap voltage	V_g	V	40	50	60
Pulse-on-time	T_{on}	μs	50	75	100
Tool material	T_M	–	Aluminum	Copper	Brass

3 Results and Discussion

3.1 Material Removal Rate

Based on the ANOVA analysis of results, a significant relationship between process parameters and performance measures is observed. ANOVA results for MRR are shown in Table 5. Discharge current is found to be the most influential parameter having highest contribution (59.72%) followed by pulse-on-time (15.2%) on MRR value. It can be clearly seen in Fig. 3a that with increase in discharge current there is a significant increase in MRR value. This phenomenon is due to the fact that

Table 4 Designed experiments

Exp. no	I_d	V_g	T_{on}	T_M	MRR (mm ³ /min)	S/N	TWR (mm ³ /min)	S/N
1	1	1	1	1	3.36	3.24	1.45	3.66
2	1	2	2	2	4.76	6.09	0.157	30.96
3	1	3	3	3	3.39	3.15	2.18	0.79
4	2	1	2	3	5.04	6.30	2.75	-1.71
5	2	2	3	1	5.64	7.65	1.77	2.44
6	2	3	1	2	4.47	5.43	0.98	7.82
7	3	1	3	2	12.5	14.69	1.45	3.92
8	3	2	1	3	6.24	8.50	3.08	-2.55
9	3	3	2	1	7.13	9.55	2.30	0.18

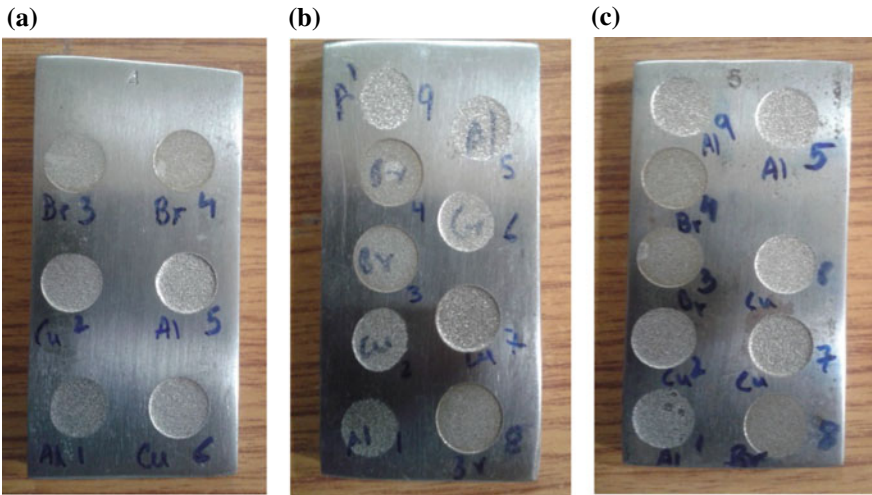


Fig. 2 Machined surfaces using electrode of **a** copper, **b** brass, **c** aluminum

increase in discharge current increases the spark energy between the electrode and the workpiece. High spark energy increases the temperature that ultimately leads to higher MRR. However, this effect leads to larger overcut and causes higher MRR. Hence, the influence and significance of discharge current are greater on MRR. Figure 3b depicts the graph of MRR vs pulse-on-time. The pulse-on-time basically indicates the duration of current flow allowed per cycle. Hence, the material removal mechanism is directly proportional to the amount of energy supplied during this period. Therefore, it is the second most influencing factor after discharge current in deciding MRR.

Table 5 Results of ANOVA analysis for MRR

Source	DF	SS	M.S	F	P	Percentage contribution
Discharge current (I_d)	2	37.39	18.7	4.45	0.065	59.72
Gap voltage (V_g)	2	6.29	3.14	0.33	0.728	10.04
Pulse-on-time (T_{on})	2	9.54	4.77	0.54	0.609	15.23
Tool material (T_M)	2	9.38	4.69	0.53	0.614	14.98
Total		1.738				

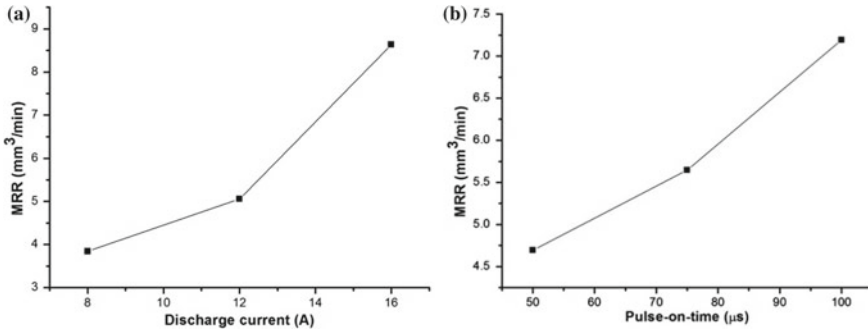


Fig. 3 a MRR versus discharge current and b MRR versus pulse-on-time for D2 material

3.2 Tool Wear Rate

Based on the results of ANOVA analysis listed in Table 6, it can be concluded that tool material is the most significant parameter to affect TWR having contribution to 66.2% followed by discharge current which has 18.8% contribution while deciding the TWR during operation. TWR in case of machining with Al electrode is highest among all electrode materials (refer Fig. 4a). Minimum values of TWR are observed while machining with brass electrode. This happens due to the fact that melting point of aluminum among the other two electrodes, i.e., brass and copper, is very much low. The other factor is that density of aluminum is also very low as compared to other electrode materials. In Fig. 4b, graph indicates that with increase in discharge current value there is an increase in TWR. This occurred because increased value of discharge current has produced high spark energy resulting in more material removal from the tool as well as from the workpiece.

Table 6 Results of ANOVA analysis for TWR

Source	DF	SS	M.S	F	P	Percentage contribution
Discharge peak current (I_d)	2	0.327	0.164	0.70	0.535	18.8
Gap voltage (V_g)	2	0.11	0.056	0.21	0.820	6.38
Pulse-on-time (T_{on})	2	0.141	0.070	0.26	0.776	8.11
Tool material (T_M)	2	1.158	0.579	6.00	0.037	66.62
Total		1.738				

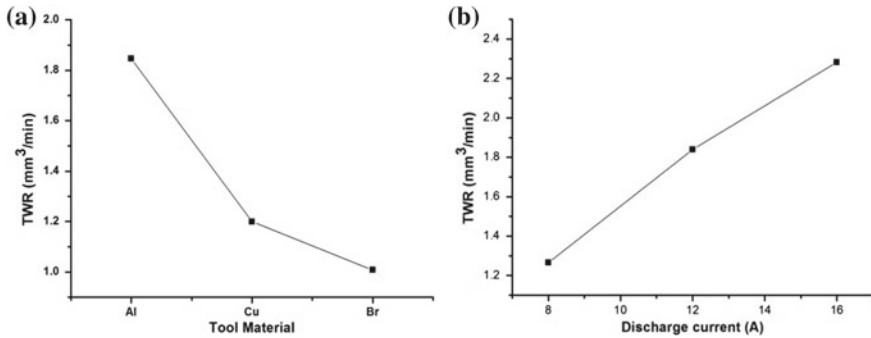


Fig. 4 a TWR vs tool material and b TWR vs discharge current during die-sinking EDM on AISI D2 steel

4 Conclusion

In this study, the parameter characterization of die-sinking EDM on D2 tool steel was done and their influence on MRR and TWR is analyzed. Pulse-on-time, discharge current, tool material, and gap voltage were taken as process parameters, and process performance was measured in terms of MRR and TWR. From the findings of this experimental investigation, valuable conclusions were drawn. In case of MRR, the most significant process parameter is discharge current followed by pulse-on-time during die-sinking EDM of AISI D2 steel. On the other hand, for TWR the tool material is the significant factor followed by discharge current. It was seen from the experiments that brass electrode material has shown the lowest TWR followed by copper. Therefore, results of this experimental investigation can be utilized by the die-manufacturing industry for desired outcome.

References

1. Miller SF et al (2004) Investigation of the spark cycle on material removal rate in wire electrical discharge machining of advanced materials. *Int J Mach Tools Manuf* 44(1):391–400

2. Payal H, Maheshwari S, Bharti PS (2016) Investigative study on metal removal rate and tool wear rate in electric discharge machining of H11 using different electrode material. In: 5th international symposium on fusion of science and technology, Jan 18–22
3. Prabhu S, Vinayagam BK (2010) Analysis of surface characteristics of AISI D2 tool steel material using electric discharge machining process with single wall carbon nano tubes. *Int J Eng Technol* 2(1)
4. Singh PK et al (2014) Variation in surface roughness of AISI D2 tool steel after machining on EDM (Electrical Discharge Machine): a review. *Int J Res Advent Technol* 2(4)
5. Prabhu S, Vinayagam BK (2012) Modelling the machining parameters of AISI D2 tool steel material with multi wall carbon nano tube in electrical discharge machining process using response surface methodology. *Int J Phys Sci* 7(2):297–305
6. Jadhav, Prasad A et al. (2014) Analysis and optimization of EDM process parameters for AISI D2 Steel. *Int J Adv Eng Res Stud* 3(1):46–48
7. Gupta S, Pandey H, Sen S (2016) Experimental investigation of machining parameters for EDM using D2 tool steel. *Int J Innov Sci Eng Technol* 3(6)
8. Shivade AS, Shinde DV (2014) Multi-objective optimization in WEDM of D3 tool steel using integrated approach of Taguchi method and Grey relational analysis. *Ind Eng Int* 10:149–162
9. Kansal HK, Singh S, Kumar P (2007) Effect of silicon powder mixed EDM on machining rate of AISI D2 die steel. *J Manuf Processes* 9(1)

Optimization of Quality and Productivity of Wire EDM by Using L₉ Orthogonal Array



Shailesh Kumar Dewangan, Prakash Kumar and Sanjay Kumar Jha

Abstract Quality and productivity are two essential facets developed in present competitive global market. In the present study, wire EDM process of AISI P20 tool steel optimized the quality as well as productivity simultaneously. MRR in the terms of productivity, this can be maximized and overcut in terms of quality that can be minimized. This study highlights AISI P20 tool steel of best combination of machining parameter setting with Taguchi design of experimental technique, of WIRE EDM. The selected input parameters are pulse-on time (T_{on}), wire feed (f) and pulse-off time (T_{off}). The objective of this paper is to achieve the maximum MRR and the minimum overcut. They used copper wire of 0.25 mm diameter as a tool, and dielectric fluid was used in distilled water,; L₉ orthogonal array based on Taguchi design has been used. These two responses (MRR and overcut) have been converted into signal quality characteristics for optimal process environment (optimum input parameters setting). Principal component analysis (PCA) combined with grey relational analysis (GRA) with Taguchi design of experiment techniques has been used to solve the problem.

Keywords L₉ orthogonal array · Principal component · Grey relational analysis · AISI P20 tool steel · Wire EDM

1 Introduction

In today's fastest development of machine-driven industry, the demands for alloy materials and other type of steel material they have good hardness and impact resistance are increasing. Nevertheless, some materials are challenging to be machined by conventional methods. Hence, non-conventional machining methods including ECM, electrical discharging machine and abrasive jet machining are applied to machine such as difficult-to-machine tools and materials. Moreover, it has been used in wide applications such as railways, bridges and suspension system [1–4].

S. K. Dewangan (✉) · P. Kumar · S. K. Jha
Department of Production Engineering, BIT Mesra, Ranchi 835215, India
e-mail: shaileshdewangan123@gmail.com

© Springer Nature Singapore Pte Ltd. 2019
K. Shanker et al. (eds.), *Advances in Industrial and Production Engineering*, Lecture Notes in Mechanical Engineering, https://doi.org/10.1007/978-981-13-6412-9_9

However, wire EDM is a continuous process in which electrode they can be made of thin brass or tungsten and copper with diameter 0.05–0.35 mm, which is capable of machining for very small corner radii [2]. The wire undergoes tension using a device so reducing the trend of producing inaccurate parts. During the process of wire EDM, the material is eroded from wire zone, and there is no contact between the tool (wire) and workpiece; it can be controlled by servo controller eliminating the mechanical stresses during machining.

Durairaj et al. [3] have described the multi-optimization techniques by grey relational analysis and optimized the machining parameters in wire EDM for SS304 material. The main objective is to optimize the kerf width and the best surface quality. Sreenivasa et al. [4] established the influence of various process parameters of wire EDM such as pulse-on time, pulse-off time, peak voltage, pulse current, wire speed and wire tension on the responses are material removal rate (MRR), surface roughness (Ra), width of cut, wire wear ratio and surface integrity factors. Saravanan et al. [5] used Titanium Grade 2 alloy for machining of wire EDM and also optimized the machining parameters with the help of Taguchi strategy. Ishfaq et al. [6] used stainless-clad steel for machining of wire EDM and also optimized machining parameters setting. Other researchers did wire EDM and EDM process for optimization of different machining parameters [7, 8].

In the available literature, a number of gaps have been perceived in machining of wire EDM. Most of the scholars have investigated influence of process parameters on the different response measures of wire EDM. Literature review exposes that the researchers have carried out most of the work on wire EDM developments, observing and controlling but partial work has been reported on optimization of process variables with multi-objective optimization. The effect of machining parameters on AISI P20 tool steel has not been fully explored using wire EDM with copper wire as electrode.

2 Experimentation

The present work conducted an Electronica MAXICUT 734 Wire Electric Discharge Machine, with the workpiece dimension of 10 mm × 1 mm square block, and copper wire tool material individual was used having 0.25 mm diameter. Distilled water is used as dielectric fluid to accomplish the experiment. Side flushing system is used for the sparking zone.

The total three machining parameters are selected as variables, and other factors are kept constant (such as dielectric fluid pressure, cutting speed, servo voltage, servo feed, wire speed, wire tension and cutting length). The factors have three levels along L_9 orthogonal array have been selected with Taguchi design that are presented in Table 1.

The calculation of material removal rate has been done by weight loss method with the help of electronic balance weight machine. This electronic balance weight machine has maximum capacity of 300 g, and accurateness is 0.1 mg. Overcut was

Table 1 Input parameters and their levels

Machining parameter	Symbol	Unit	Levels		
			1st	2nd	3rd
Pulse-on time	T_{on}	μs	112	118	124
Wire feed	F	mm/min	6	9	12
Pulse-off time	T_{off}	μs	20	30	40

measured by using Toolmaker microscope. The design of experiment with observed MRR and overcut value is shown in Table 2 (Fig. 1).

Table 2 Experimental observed value

Run No.	T_{on} (μs)	F (mm/min)	T_{off} (μs)	MRR (mm^3/min)	OC (mm)
1	112	6	20	2.3524	0.050
2	112	9	30	3.6990	0.060
3	112	12	40	4.1077	0.066
4	118	6	30	4.3135	0.040
5	118	9	40	5.7362	0.045
6	118	12	20	6.8456	0.048
7	124	6	40	7.0920	0.030
8	124	9	20	8.1400	0.036
9	124	12	30	8.8865	0.039

**Fig. 1** Wire electric discharge machining with tool and workpiece

3 Results and Discussion

In this section, the impact of process parameters on the responses like material removal rate and overcut of AISI P20 tool steel was described. And also discussed which parameters are most influencing factors for increasing the quality and productivity in the form of overcut and material removal rate.

3.1 Impact of Process Parameters of MRR and Overcut

The histogram plot for MRR versus input factors such as pulse-on time, wire feed and pulse-off time is shown in Fig. 2. According to this graph, pulse-on time has better impact on MRR as compared to pulse-off time and wire feed, in which MRR increases with increases on T_{on} . MRR representing the T_{on} is the most significant factor during machining of AISI P20 tool steel.

Figure 3 indicates the overcut (OC) against pulse-on time, wire feed and pulse-off time, respectively. When the T_{off} increases OC when T_{on} increases OC decreases, when F increases OC has slightly increases similarly, when T_{off} increases, OC increasing. This analysis clearly indicates that the factors T_{off} are directly

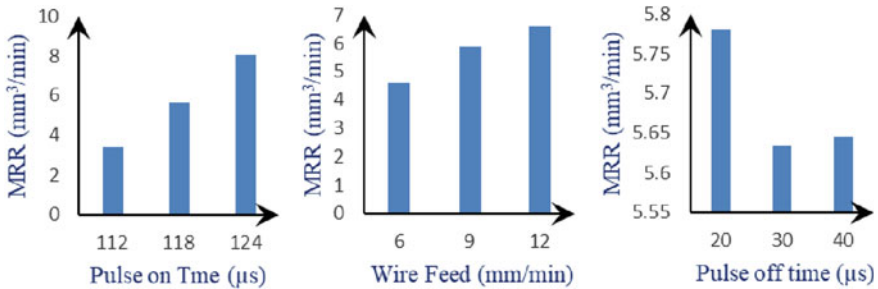


Fig. 2 Impact of process parameter versus MRR

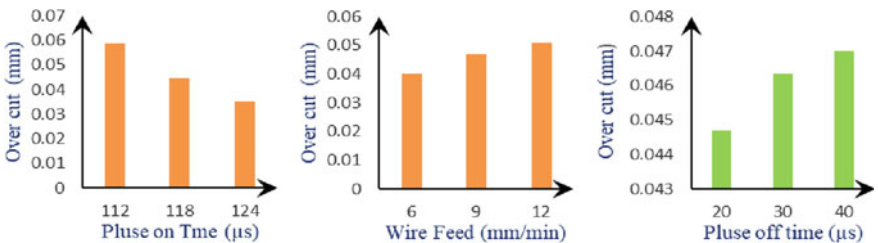


Fig. 3 Impact of process parameters versus OC

proportional to OC and the value of T_{on} is maximum influencing of OC, and also wire feed of copper wire tool is significant effect.

3.2 Multi-objective Optimization Using PCA-Based GRA Analysis

All the experimental values (Table 2) have been converted to the optimal quality performance index (OQPI). The OQPI value is obtained using hybrid multi objective optimization techniques that is PCA based grey relation analysis. Calculation of PCA-based GRA analysis the following stages is given below.

Converting the MRR and OC to S/N ratio.

Converted S/N ratio of MRR and OC is to find principal component scores (PCS).

Normalized principal component scores.

After normalized data finding GRC using principal component score.

Calculating optimal quality performance index (OQPI).

All experimental run to finding MRR and Overcut is higher-the-better and lower-the-better conditions has been chosen. The maximum value of MRR is 8.8865 mm³/min, and minimum value of overcut is 0.030 mm. In order to avoid complexity, in computing S/N ratio. The S/N ratio for MRR and OC is represented in Eqs. (1) and (2) correspondingly.

$$\eta_{ij} = -10 \log \left[\frac{1}{n} \sum_{i=1}^n y_i^{-2} \right] \tag{1}$$

$$\eta_{ij} = -10 \log \left[\frac{1}{n} \sum_{i=1}^n y_i^2 \right] \tag{2}$$

whereas η_{ij} represents the S/N ratios i th experiment and j th result (MRR and OC), and y_i is observe resulted value of MRR and OC. In this calculation for all nine experiments, n is kept as one because there is no repeated number of experiments. After calculating the S/N ratio, the second step is computing principal component score by using Eq. (3).

$$PCS_{il} = a_{l1}\eta_{i1} + a_{l2}\eta_{i2} + \dots + a_{lj}\eta_{ij} \tag{3}$$

whereas $a_{l1}^2 + a_{l2}^2 + \dots + a_{lj}^2 = 1$. The $a_{l1}, a_{l2} \dots a_{lj}$ are the elements of eigenvector. The calculated eigenvalue with respective eigenvector is represented in Table 3. Then the next step to normalizing all PCS data in this equation:

$$X_{il} = \frac{PCS_{il} - PCS_{il}^{\min}}{PCS_{il}^{\max} - PCS_{il}^{\min}} \tag{4}$$

Table 3 Eigenvalue and their correspondence matrix

Variable	Eigenvectors		Eigenvalue	Proportion
	PC1	PC2		
SN-MRR	0.707	-0.707	1.6202	0.81
SN-OC	0.707	0.707	0.3798	0.19

Table 4 Design of optimal quality performance index

Sr. No.	SN-MRR	SN-OC	PCS-1	PCS-2	GRC1	GRC2	OQPI
1	7.4302	26.0206	23.6497	13.1434	0.3333	1.0000	0.4600
2	11.3617	24.4370	25.3097	9.2442	0.3752	0.4597	0.3913
3	12.2720	23.6091	25.3680	8.0153	0.3769	0.3928	0.3799
4	12.6967	27.9588	28.7434	10.7903	0.5070	0.5851	0.5218
5	15.1726	26.9357	29.7706	8.3166	0.5665	0.4074	0.5363
6	16.7082	26.3752	30.4600	6.8345	0.6150	0.3447	0.5636
7	17.0154	30.4576	33.5634	9.5036	1.0000	0.4769	0.9006
8	18.2125	28.8739	33.2901	7.5376	0.9477	0.3718	0.8383
9	18.9746	28.1787	33.3374	6.5073	0.9564	0.3333	0.8380

whereas X_{il} is the normalized data with i th experiment expending l th principal component score. And PCS_{il} are normalized data. Eigenvalue and their correspondence matrix are given in Table 3.

After normalizing, then calculate the grey relational coefficient of normalized PCS data with the help of Eq. (5).

$$GRC_{ij} = \frac{\Delta_{\min} + \zeta \Delta_{\max}}{\Delta_{ij} + \zeta \Delta_{\max}} \tag{5}$$

whereas $\Delta_{ij} = |1 - X_{il}|$; in this equation GRC_{ij} of i th experiment using j th result (MRR and OC), Δ_{\max} and Δ_{\min} are the global maximum and global minimum values for corresponding values, correspondingly. The distinguishing coefficient (ζ) range is 0–1; this is clearly designated by Dewangan and Biswas [9]. In computing grey relation coefficient value for both response, then finding the optimal quality performance index by using Eq. (6).

$$OQPI = \frac{1}{n} \sum_{i=1}^n W_i \zeta_{ij} \tag{6}$$

whereas w_i is the proportion of variance that is associated with Table 3. The magnitude of OQPI replicates that optimal quality performance index value. That value is higher-the-better quality characteristics. In all the nine experimental runs the OQPI was calculated and is presented in Table 4.

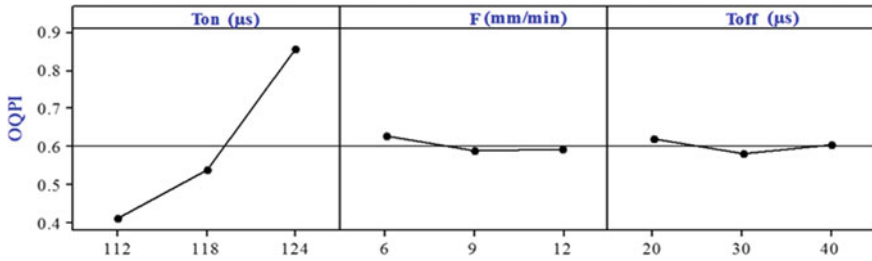


Fig. 4 Influence plots for OQPI

4 Exploration of OQPI

Optimal quality performance index value is higher-the-better quality characteristics means high value of OQPI (run no 7, value 0.9006) which represent better quality and productivity for this machining parameters setting. According to the graph (Fig. 4) of influence plot for OQPI to knowing the optimal setting of machining parameters that is T_{on} is 124 μs , F is 6 mm/min and T_{off} is 20 μs . which would simultaneously ensure better quality in terms of minimum value of overcut and better productivity in terms of maximum value for MRR.

5 Conclusions

Based on the above experimental examination, MRR representing the T_{on} is the essential factor during machining of AISI P20 tool steel, whereas the factor T_{off} is directly proportional to OC and the value of T_{on} is maximum influencing of OC.

The modern research work develops hybrid multi-response optimization technique using PCA-based grey relational analysis for simultaneously optimizing the MRR and OC in wire EDM. The optimal wire EDM parameter setting was found to be as follows: T_{on} is 124 μs , F is 6 mm/min, and T_{off} is 20 μs , which would simultaneously ensure better quality in terms of minimum value of overcut and better productivity in terms of maximum value for MRR.

References

1. Sharma SK, Kumar A (2018) Ride comfort of a higher speed rail vehicle using a magnetorheological suspension system. Proc Inst Mech Eng Part K J Multi-body Dyn 232(1):32–48
2. Sharma SK, Kumar A (2018) Disturbance rejection and force-tracking controller of nonlinear lateral vibrations in passenger rail vehicle using magnetorheological fluid damper. J Intell Mater Syst Struct 29(2):279–297

3. Durairaja M, Sudharsunb D, Swamynathanb N (2013) Analysis of process parameters in wire EDM with stainless steel using single objective Taguchi method and multi objective grey relational grade. *Int Conf Des Manuf* 64:868–877
4. Sreenivasa R, Venkaiah S (2013) Review on wire-cut EDM process. *Int J Adv Trends Comput Sci Eng* 2(6):12–17
5. Saravanana M, Vinoth Kumar AM, Kannan VN, Thangaiyah SS (2017) Optimization of process parameters during wire electrical discharge machining of Ti Gr 2 for improving corner accuracy. *Mater Today Proc* 4(2A):2105–2113
6. Ishfaq K, Mufti NA, Mughal MP, Saleem MQ, Ahmed N (2018) Investigation of wire electric discharge machining of stainless-clad steel for optimization of cutting speed. *Int J Adv Manuf Technol* 96(1–4):1429–1443
7. Dewangan S, Gangopadhyay S, Biswas CK (2015) Study of surface integrity and dimensional accuracy in EDM using Fuzzy TOPSIS and sensitivity analysis. *J Int Meas Confed* 63:364–376
8. Hewidy MS, El-Taweel TA, El MF (2005) Safty: modelling the machining parameters of wire electrical discharge machining of Inconel 601 using RSM. *J Mater Process Technol* 169:328–336
9. Dewangan S, Biswas CK (2013) Optimisation of machining parameters using grey relation analysis for EDM with impulse flushing. *Int J Mechatron Manuf Syst* 6(2):144–158

Numerical Simulation of Hot Isostatic Pressing Process Utilized During Sintering of Tool Inserts



Akshay Chandras  and Chandrakant Sonawane 

Abstract Sintering is a popular technique, where powder compacts are heated in a furnace to impart strength and integrity. Usually, sintering process is a one of the essential stage followed during powder metallurgy along with powder production and powder compaction. Sintering process is multistage and carried out in a partial vacuum with the controlled atmosphere to achieve required metallurgical properties. To make a product completely pore-free and dense, hot isostatic pressing (HIP), a secondary powder metallurgy operation is necessary. In hot isostatic pressing, argon gas is used as the pressure medium and isostatically applied to the sintered part with the pressure around 100 bar with a temperature range of 500–2000 °C. Although the hot isostatic pressing is a well-established technology, the understanding of local details like the internal gas flow and heat flux inside the furnace will help to improve the process itself as well as to reduce the rejection rate of the sintered inserts. In this paper, numerical simulation of hot isostatic pressing is presented. As the process involves unsteady flow through porous felt as well as graphite cylinders, transient analysis of argon flow inside the horizontal vacuum sintering furnace is simulated. The argon gas is passed into the furnace through an inlet at the mass flow rate of 300 L/h. The simulation is carried out for 1200 s with a time step of 0.01. Numerical results show the local temperature; pressure and flow conditions attained and eventually used for further process improvement particularly in the central zone of the furnace.

Keywords Sintering · Hot isostatic pressing · Inserts · Numerical simulation · Powder compacts · Porosity modeling

1 Introduction

Sintering is the process of consolidating loose aggregate of powder or a green compact of the desired composition under controlled conditions of temperature, pressure, and

A. Chandras · C. Sonawane (✉)
Symbiosis Institute of Technology, Symbiosis International (Deemed University),
Pune, Maharashtra, India
e-mail: chandrakant.sonawane@sitpune.edu.in

© Springer Nature Singapore Pte Ltd. 2019
K. Shanker et al. (eds.), *Advances in Industrial and Production Engineering*, Lecture Notes in Mechanical Engineering, https://doi.org/10.1007/978-981-13-6412-9_10

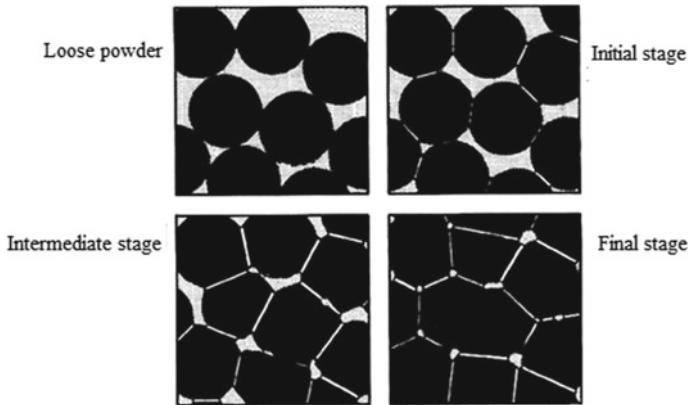


Fig. 1 Refinement of microstructural changes in powder compacts during sintering process

time. The process can be broken down into three stages which mainly contributes to the refinement of microstructural changes in powder compacts, refer Fig. 1. In the first stage, necks are formed at the contact points between the powder particles and irregularly shaped pores are interconnected to each other. Then during intermediate stage, neck growth occurs, and pore channels gain a cylindrical shape. In the final stage, pores become isolated and no longer interconnected. The porosity of sintered part does not change and remain even after sintering. It has been observed that these pores remained in sintered part, and these are the main cause of poor strength and density of the sintered part.

Hence, after sintering, it is recommended to apply hot isostatic pressing, in which isostatic pressure applied to the sintered product at elevated temperature simultaneously. The hot isostatic pressing cycle consists of two phases; in first phase, pressure is increased up to the peak value in certain time, and then during the second phase, the pressure inside the horizontal vacuum sintering furnace is maintained constant for some time. Temperature is high throughout these phases. Hot isostatic pressing consolidates the powders to higher densities and thus make sintered parts pore-free. Because of advantages of hot isostatic pressing, it is combined with sintering process, and the combined process is called as sinter-hot isostatic pressing.

Although the hot isostatic pressing is a well-established technology, the understanding of local details like the internal gas flow and heat flux inside the sintering furnace will help to improve the process itself as well as to reduce the rejection rate of the sintered inserts. Numbers of researchers have studied the hot isostatic pressing numerically. Manière et al. [1] carried simulation of sintering to predict the temperature distribution and densification of large size gears under various operating conditions. They developed the fluid dynamics thermo-mechanical model and concluded that homogeneity of the heating of large and complex samples depends on the duration of the heating and on the dimensions of the sample. Cheng et al. [2] proposed gaseous fuel segregation method which injects measured methane (in the

furnace) to improve the heat distribution imbalance to enhance the heat pattern and sinter strength. Fu et al. [3] used CFD modeling to find out the effects of several factors on blast furnace processing as well as to visualize and observe the processes occurring inside of blast furnace and generated a detailed numerical data.

Yuan et al. [4] studied the various furnace atmosphere which is suitable for sintering operation. Furnace atmosphere depends on the characteristics of the materials and the properties desired in the sintered product. They studied the flow of gas involved in sintering furnace process and found that a surface over which flow is continuous, more porosity was developed. They also concluded that, as separation distance between green compacts increases, the gas flow field is also found to be increased in between samples kept adjacent to each other. Al-Hazmi et al. [5] studied various parameters affecting mechanical properties and microstructure of sintered part. They had carried out both experimental and CFD simulation of sintering process. Their analysis shows that mechanical properties were enhanced with an increase in pressure and temperature, but it also highlighted that there was no significant effect on the microstructure of the sintered part material. Cai et al. [6] investigated the effect asynchronous and simultaneous loading on the surface qualities, microstructure, and mechanical properties of titanium alloy Ti6Al4V parts. The surface roughness of asynchronous load processed parts had lower value over simultaneous load processed parts.

Xu et al. [7] investigated the effect of pressure and temperature on microstructure, density, and mechanical properties of HIP'ed powder parts. They analyzed the parts, hipped at different operating conditions using response surface methodology and found that HIP'ing at 800 °C and 120 MPa can impart best tensile strength. But to eliminate metallurgical defects and to achieve better microstructure and mechanical properties, the optimized temperature range proposed was 900–940 °C and pressure over 100 MPa for holding time of 3 h. Janajreh et al. [8] carried out a numerical simulation of the water vapor flow in a full-scale flashing chamber of an operational MSF desalination plant. They had utilized Ergun's equation and empirical correlation of Svendsen to find pressure drop. Remigiusz et al. [9] studied the relationship between the porous material resistance coefficients and heat sink dimensions. They developed an approximation function that will allow the resistance coefficients to be calculated without the need of performing time-consuming calculations. They modeled heat sink as a simpler porous block to save computational time. Based on the results of the numerical analysis, they propose an approximation function for dimensions of the heat sink and resistance coefficients. Guhan et al. [10] used ANSYS CFX software to investigate gas flow analysis to optimize the geometry of existing exhaust system. Pressure drop and flow distribution were analyzed for the exhaust system.

From above review, it can be seen that numerical analysis mainly using ANSYS Fluent software is popular as well as powerful computational fluid dynamics (CFD) tool for simulating fluid flows and heat transfer for complex flow like hot isostatic pressing. Computational fluid dynamics (CFD) helps us to visualize the process occurring in a furnace to design better like hot isostatic pressing furnaces. Due to the intricate design and elevated temperature and pressure inside the sintering furnace,

where measuring equipment cannot be installed, hence use of CFD numerical tool is justified.

In this paper, numerical simulation of hot isostatic pressing is presented. The unsteady flow through the porous felt and graphite cylinders present inside the sintering furnace is simulated. Various operating pressure, as well as the temperature inside the furnace, is numerically predicted. The objective of this work is to model reliable CFD simulation of gas flow occurring in the HIP furnace and obtain intricate details occurring inside the furnace with possible visualization of minute local details.

2 Problem Under Consideration: Horizontal Vacuum Sintering Furnace

The problem under consideration is the sinter-hot isostatic pressing (sinter-HIP). This process is used to process powder metallurgical materials cemented carbides. To produce powder metallurgical parts, additives such as paraffin, PEG is added to powders and then the powder is pressed into near net shape before sintering.

In hot isostatic pressing, all the outlets are closed, and gas is pumped into the furnace. This causes pressure development in the furnace. Gas is passed for 20 min, and hence pressure rises to 90–100 bar (approx). Temperature is elevated to 1500 °C.

Additional steps of cooling the sintered parts in a sintering furnace and then transferring to a separate HIP furnace for heating and densification are eliminated. And hence two processes of sintering and HIP are combined which eliminated the need for a separate HIP furnace. This saved energy, labor cost, and material handling.

Figure 2 shows the horizontal vacuum sintering furnace, considered for simulation. The geometry is created in Siemens NX software. Horizontal vacuum sintering furnace consists of muffle, felt, heating coil assembly, and casing.

Muffle: Material of muffle is graphite. Argon passes through porous walls of muffle. Muffle covers the part to behipped, and hence ensures the clean environment is developed around parts.

Felt: It is a thermal shield which is made of a material which has low thermal conductivity and low specific heat. It permits rapid heating and cooling of furnaces which reduces cycle time.

Figure 3 shows the cross-section view of horizontal vacuum sintering furnace heating coil locations. These induction heaters generate the heat which is transferred to muffle heat zone by convection and radiation. Initially, up to 400 °C temperature, heat is transferred by means of convection but after 400 °C the heat is transferred majorly by radiation.

Figure 4 shows the charging system on which various products generally called as green parts carbide tool in the present case are placed. The charging system consists of racks and spacers. These are made of a material which shows increased strength at rising temperature and excellent resistance to embrittlement. Spacers are placed to

Fig. 2 A cross-sectional view of horizontal vacuum sintering furnace

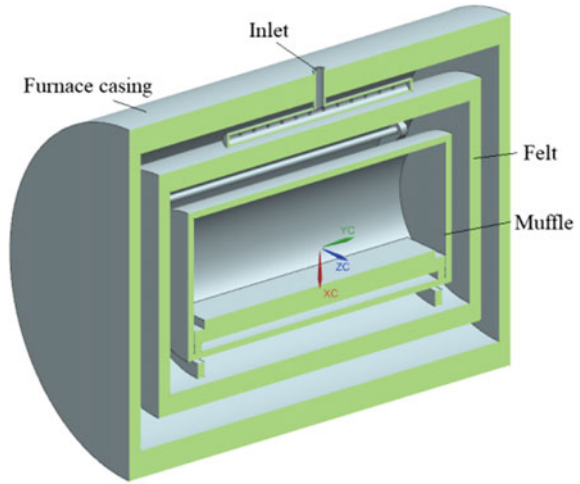
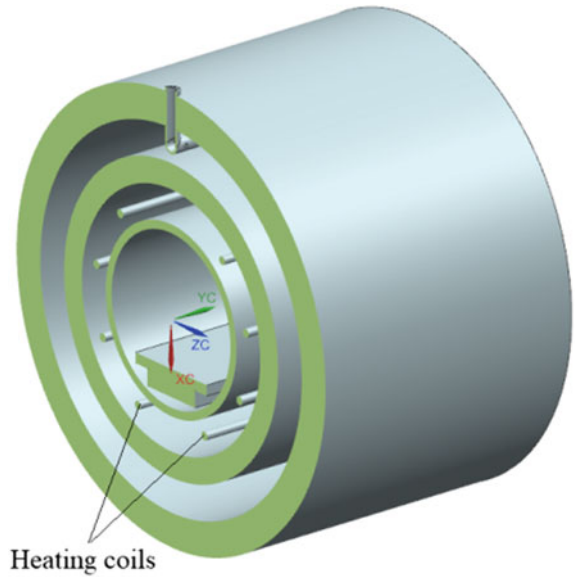


Fig. 3 Horizontal vacuum sintering furnace



maintain space between racks. Compacted parts which are also called as green parts are arranged on racks in a systematic manner, so gas passes over every green part. At a time, a number of small parts can be processed in one process cycle because of the charging system. Figure 5 shows the three-dimensional view of furnace loaded with green parts arranged on the charging system.

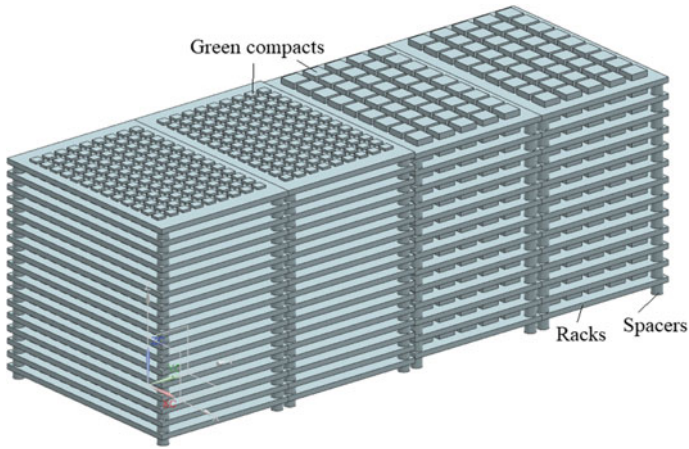
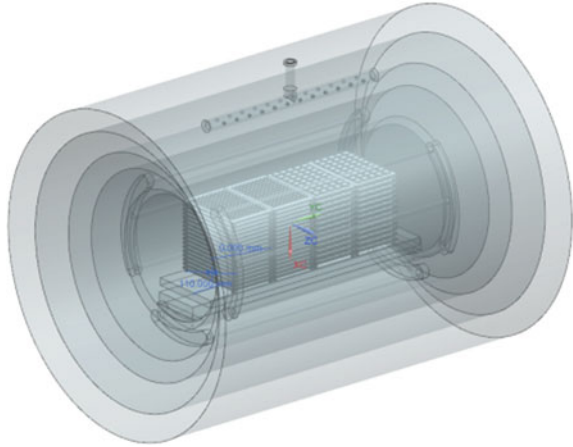


Fig. 4 Charging system

Fig. 5 Furnace loaded with green parts using the charging system



3 Numerical Method

Simulating by considering the three-dimensional model, as shown in Fig. 5, could become very complex and computationally expensive. So, it is being modeled in a 2D approach. Geometry is further simplified by removing solid domains as it will not have an impact on the flow. If solid domains are considered, a number of mesh elements increase, hence increasing computational time. Figure 6 shows the 2D geometry considered for current simulation.

Figure 7 shows the mesh generated using ANSYS Meshing software. The shared topology option is used, which allows continuous mesh generation across common regions where bodies touch each other. The structured mesh is generated at every

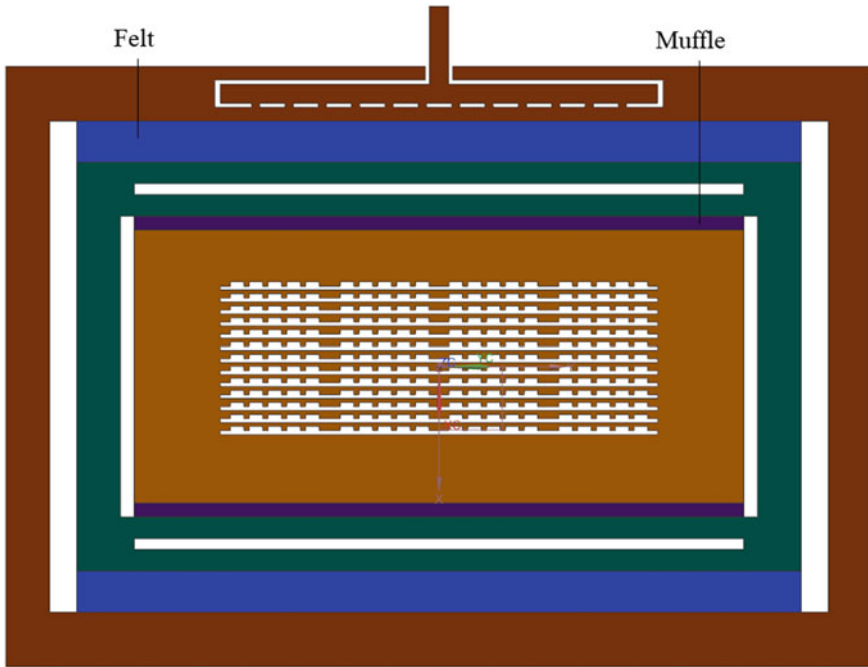


Fig. 6 two-dimensional geometry of horizontal vacuum sintering furnace

region of geometry. The mesh contains total 99,830 number of nodes with 91,949 number of quad mesh elements. The mesh has a maximum skewness of 0.2531 and minimum orthogonal quality of 0.9224. Hence, mesh is sufficient to capture all the physics of the sintering process. It is important to have fine mesh at critical regions such as inlet, gaps, and holes. Hence mesh is refined using a local mesh sizing option named as face sizing.

To simulate the hot isostatic pressing (HIP) process, gas (argon) is continuously passed into the furnace through the inlet. A compression phenomenon by argon gas is time-dependent for which the transient simulation is the appropriate approach. Effect of gravitational acceleration may impact the flow of gas, so it is considered during simulation. An arrangement of heating coils is asymmetric. Simulation is carried out considering two heating coils generate the heat.

For obtaining the numerical solution, pressure-velocity coupling: PISO is used with transient simulation conditions. For pressure, density as well as momentum equation discretization, second-order upwind method is adopted. For transient formulation, first order implicit time stepping is utilized. The flow inside the furnace is turbulent hence a realizable K -epsilon turbulent model is applied. The K -epsilon turbulent model has robustness, economy, and reasonable accuracy for a wide range of turbulent flows.

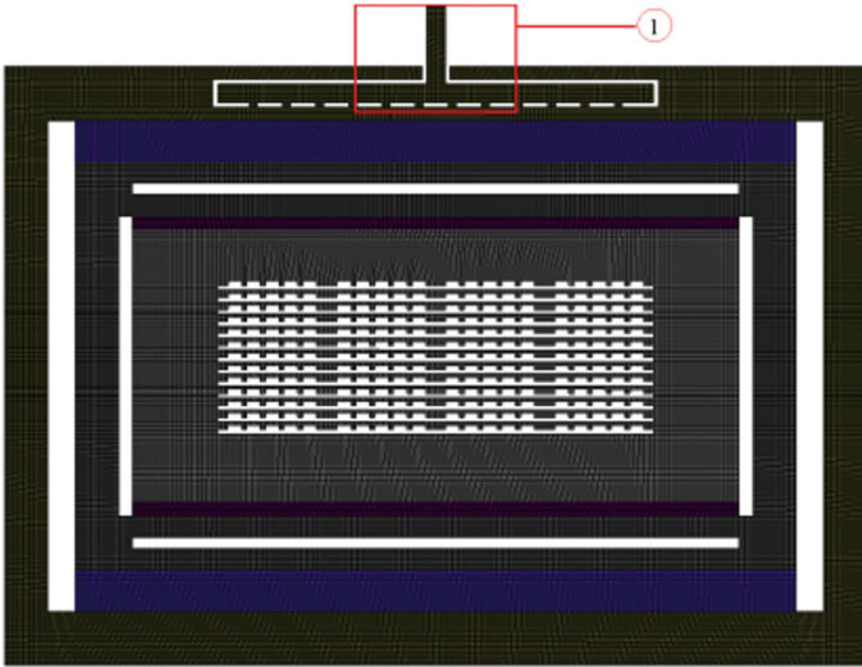


Fig. 7 Mesh generated for horizontal vacuum sintering furnace domain

During the HIP process, muffle and felt are closed using lids. Muffle (and felt) walls are porous in nature. So in cell-zone conditions, muffle walls are defined as a fluid domain. In Fluent, to define porous nature, two other inputs are required, i.e., viscous coefficient and inertia coefficient.

Defining viscous and inertia coefficients: Viscous and inertia coefficients are calculated from experimental pressure drop values. Experimental data in the form of pressure drop across porous media against the velocity of argon entering porous media is used to calculate the coefficients. Porous media are modeled by the combination of a momentum source term to the standard fluid flow equations. The source term is composed of two parts: a viscous loss and an inertial loss.

The source term is composed of two parts: a viscous loss and an inertial loss

$$S_i = -\left(\frac{\mu}{\alpha}v_i + C_2\frac{1}{2}\rho v v_i\right)$$

where α is the permeability and C_2 is the inertia resistance factor. μ is the viscosity of the fluid. Darcy's law for porous media: In laminar flows through porous media, the pressure drop is proportional to velocity. The constant C_2 can be zero.

$$\text{Pressure drop, } \nabla p = \frac{\mu}{\alpha}v_i \Delta n$$

where $\frac{1}{\alpha}$ is viscous coefficient, the v_i velocity component in the corresponding direction, and Δn is the thickness of the medium.

As discussed earlier, for calculating viscous coefficient, graph of experimental pressure drop across the porous region and experimental velocity of gas entering porous region is required. The experimental value of the pressure drop across muffle is 16 millibar. Velocity value of argon gas is not available hence it is derived from the general formula of mass flow rate. The value of the viscous coefficient for muffle: 57,399,103; viscous coefficient for felt: 18,759,526.3219.

As per as various boundary conditions are concerns: At a furnace, inlet mass flow rate of 300 L/h or 0.1161 kg/s is supplied. A mass flow inlet is used as it is more important to match a prescribed mass flow rate than to match the total pressure of the fluid. Walls formed at the boundaries of the porous domain are converted into the interior. Interior boundary conditions allow fluid to flow into the porous domain. Also, an ideal gas density model is used, where the value of operating density is kept zero. For heating coils: In 3D model, there are nine heating coils, but in 2D model, only two coils are considered, which has heat generation rate of 10 W/m³.

4 Results and Discussion

The unsteady simulation of hot isostatic pressing is carried for 20 min or 1200 s with a time step of 0.01. Hence, total numbers of time steps are 120,000 and it is allowed to carry maximum 20 iterations for each step. Care is taken that the residual for continuity, X and Y velocity, K and epsilon is dropped below 0.001 whereas for energy the residual drop below $10e^{-6}$ value.

Pressure distribution: Figs. 8 and 9 show the pressure distribution inside the sintering furnace at 900th and 1200th seconds time level. It is seen that argon gas is getting compressed at the bottom of the furnace during initial time level. In the simulation, it is observed that pressure drop across the top muffle wall is different from bottom muffle wall, i.e., pressure drop across the top muffle wall is 2.9 millibar; pressure drop across the bottom muffle wall is 4.6 millibar. This pressure drop values reduce over a time. At time 1200th second the pressure drop across top muffle wall: 1.5 millibar and pressure drop across bottom muffle wall: 4 millibar. In actual furnace apparatus, the pressure drop across muffle walls is 1.6–16 millibar. Hence, it can be seen that the mean simulation values are matching well with actual conditions.

Velocity distribution: Fig. 10 shows the velocity distribution across the furnace at 10th seconds time level. Figure 11 shows the enlarged view of velocity at inlet of the furnace. It is observed that gas is not flowing through all the holes of inlet manifold. It is observed that gas passing through the first adjacent hole is blocking the flow coming from next hole. Initially, the direction of gas passing through upper and lower felt is toward muffle. Means from upper felt, gas is flowing in downward direction, i.e., toward muffle and through lower felt, gas is flowing in upward direction, i.e., toward muffle.

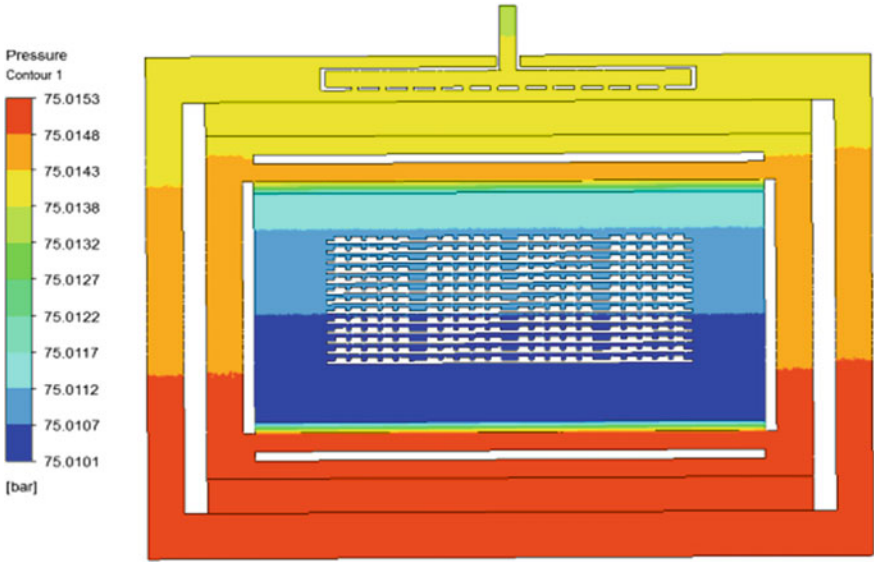


Fig. 8 Pressure at 900th seconds

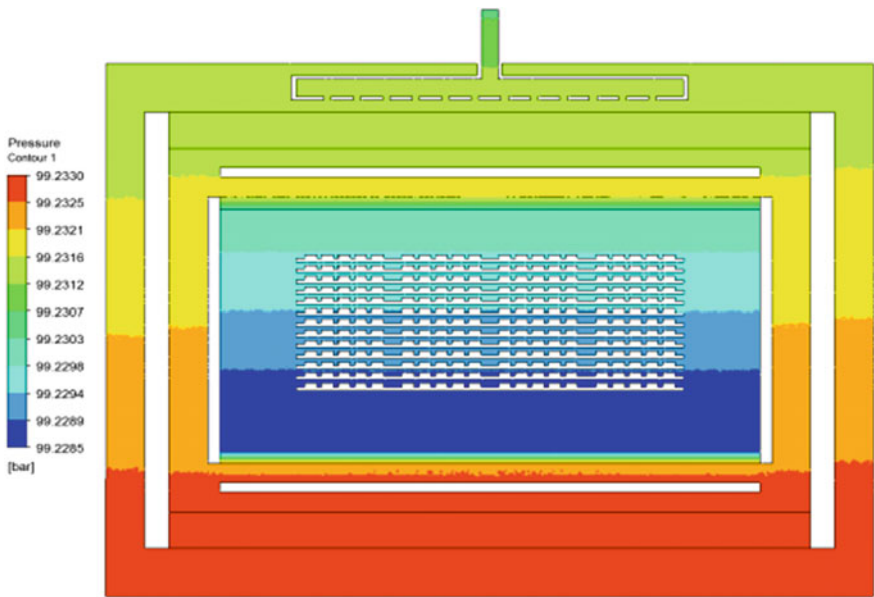


Fig. 9 Pressure at 1200th seconds

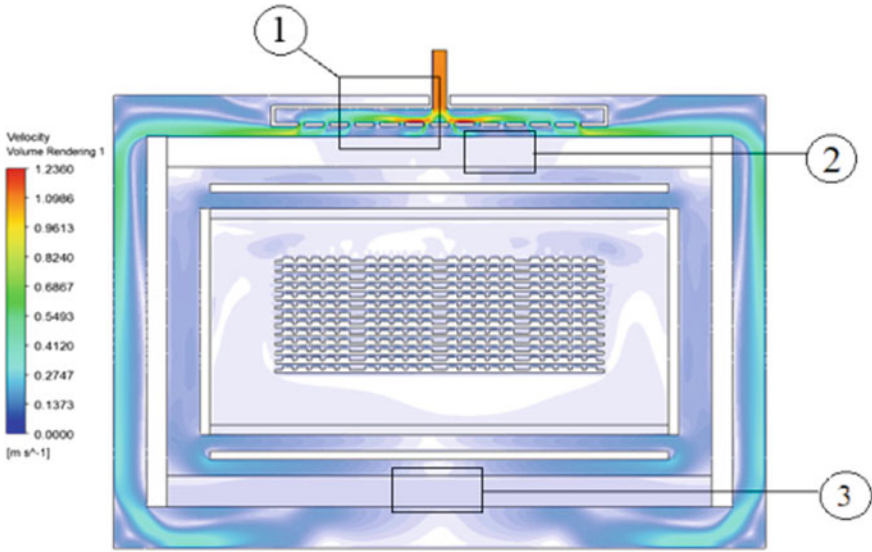


Fig. 10 Velocity rendering at 10th second

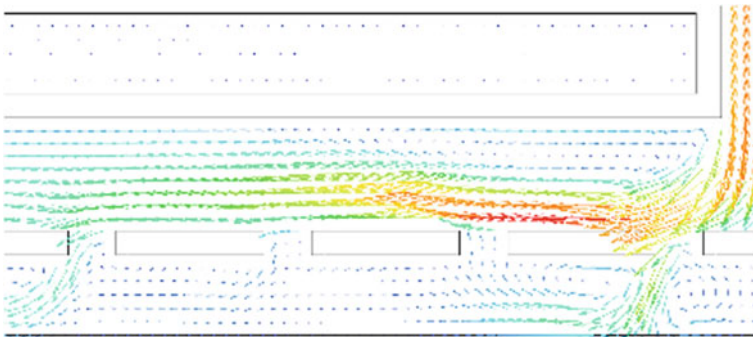


Fig. 11 Detailed view of 1

Figure 12 shows the velocity distribution after 30th second time level. After a 30th second, gas is filled in the space available inside the porous felt. Hence, it is coming out from top felt wall. Figure 13 shows the enlarged view of velocity and turbulence generated at charging system. It is seen that turbulence is generated inside the muffle. Change in gas velocity is observed near inserts and charging system as the gas flows through narrow area.

After 15 minutes of gas filling, turbulence is seen in the inlet manifold. Figure 14 shows the turbulence at inlet manifold. Back-flow phenomena are observed in the inlet manifold as the furnace is filled with gas. Table 1 shows the pressure developed inside the furnace at various time intervals.

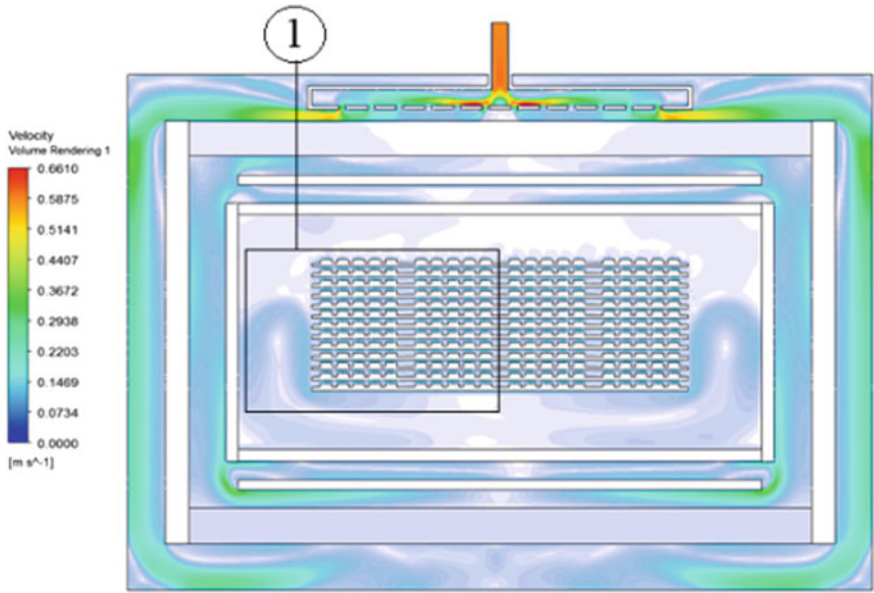


Fig. 12 Volume rendering of velocity at 30th second velocity

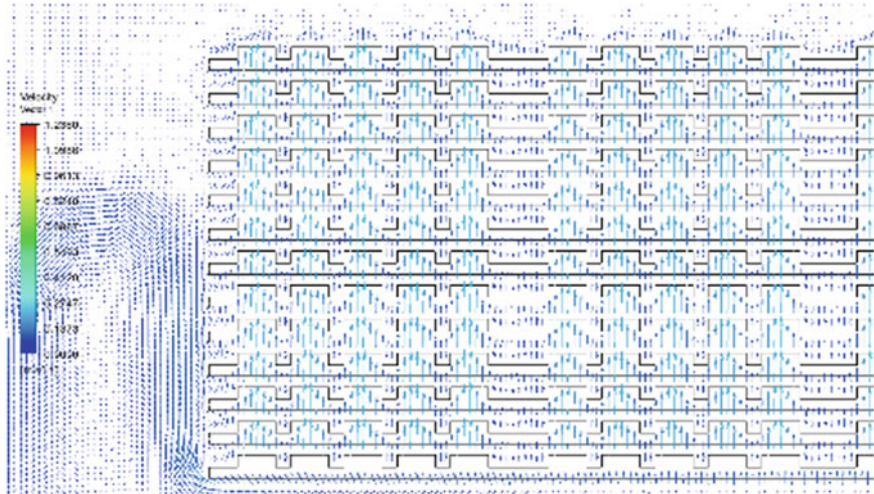


Fig. 13 Detailed view 1: velocity and turbulence at 30th second

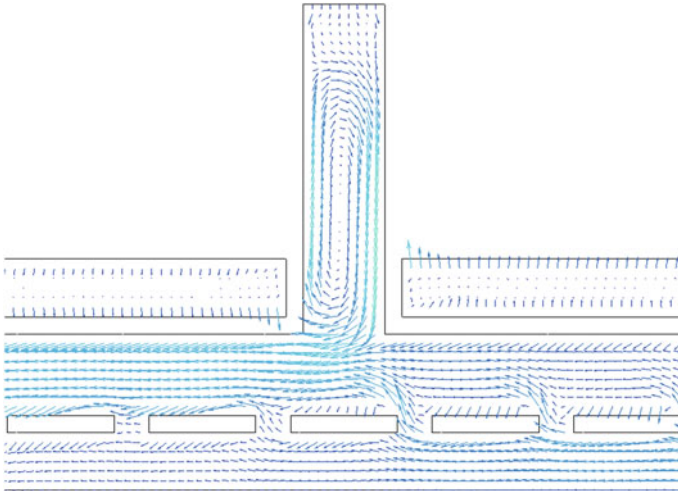


Fig. 14 Turbulence at the inlet manifold

Table 1 Pressure development inside the furnace

Time	Maximum pressure, P_{Max} (bar)	Pressure drop across top muffle wall, ΔP_{TM} (millibar)	Pressure drop across bottom muffle wall, ΔP_{BM} (millibar)
900th seconds	75.01	2.9	4.6
1200th seconds	99.2323	1.5	4

Temperature distribution: Fig. 15 shows the temperature distribution obtained at 1200th second time level. Elevated temperature value is detected inside the muffle. Heat is transferred to muffle region by convection until furnace reaches a 400 °C temperature. After that, the heat is transfer mainly by radiation. Highest temperature reached is 680 °C (953 K) which located at the central region of the charging system.

5 Conclusion

In this paper, numerical simulation of the hot isostatic pressing process carried out in the horizontal vacuum sintering furnace is presented. The unsteady simulations exactly mimic the actual hot isostatic pressing process for the 1200 s. The pressure, velocity, and temperature distribution are presented here. Due to the intricate conditions of high pressure and high temperature, it is not possible to have such minute details via experimentation, hence CFD simulations are justified as well as recommended.

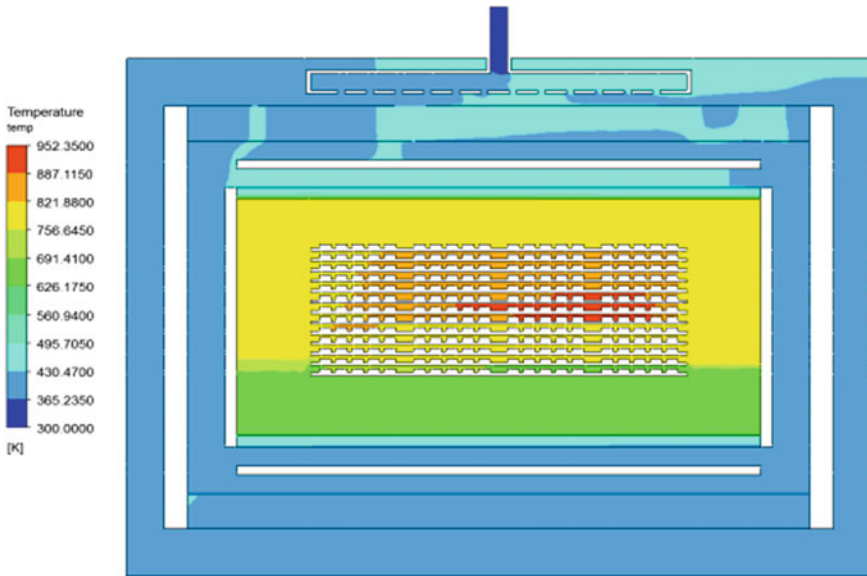


Fig. 15 Temperature distribution at 1200th seconds

From CFD simulation, it has been observed that, initially, argon gas is getting compressed at the bottom of the furnace. Then over a time whole furnace fills up with gas. After filling the space available inside the felt, gas comes out from the upper felt wall region. Eventually, the gas reaches near inlet manifold and blocks the path of flow. The pressure drop from the lower wall of the muffle is more than the upper wall, whereas, the simulated average pressure drop is matching closely with the actually measured one. The slight variation in pressure is because of the lack of more pressure point reading in actual practice. Also, it is worth to mention that, the gas once entered the muffle is not coming out of it and pressurizing the sintered compacts evenly. Rotational motion of gas is observed inside the muffle. The highest temperature of 680 °C is observed inside the charging system. Hence, we can charge the various sizes (small to large) of inserts according to this temperature distribution.

Acknowledgements This work has been carried out under the Kennametal Shared Services, Bangalore. Special thanks to Manoj Kulkarni, Ranjith Seenappa for their valuable guidance and suggestions.

References

1. Manière C, Zahrah T, Olevsky EA (2017) Fluid dynamics thermo-mechanical simulation of sintering: uniformity of temperature and density distributions. *Appl Therm Eng* 123:603–613

2. Cheng Z, Wang J, Wei S, Guo Z, Yang J, Wang Q (2017) Optimization of gaseous fuel injection for saving energy consumption and improving imbalance of heat distribution in iron ore sintering. *Appl Energ*
3. Fu D, Chen Y, Zhao Y, D'Alessio J, Ferron KJ, Zhou CQ (2014) CFD modeling of multiphase reacting flow in blast furnace shaft with layered burden. *Appl Therm Eng* 66:298–308
4. Yuan X, Aminossadati SM, Qian M (2016) Variation in pore distribution along sample length in sintered 7xxx aluminium alloy. *Trans Nonferrous Met Soc China* 26:2019–2028
5. Al-Hazmi FS, Al-Ghamdi AA, Bronstein LM, Memesh LS, Shokr FS, Hafez M (2017) The influence of sintering temperature on the structure, optical and magnetic properties of yttrium iron oxide YFeO₃ prepared via α -alanine-assisted combustion method. *Ceram Int* 43(11):8133–8138
6. Cai C, Song B, Xue P, Wei Q, Wu JM, Li W, Shi Y (2016) Effect of hot isostatic pressing procedure on performance of Ti6Al4V: surface qualities, microstructure and mechanical properties. *J Alloy Compd* 686:55–63
7. Xu L, Guo R, Bai C, Lei J, Yang R (2014) Effect of hot isostatic pressing conditions and cooling rate on microstructure and properties of Ti6Al4V alloy from atomized powder. *J Mater Sci Technol* 30(12):1289–1295
8. Janajreh A, Hasania H, Fath (2013) Numerical simulation of vapor flow and pressure drop across the demister of MSF desalination plant. *Energy Convers Manage* 65:793–800
9. Nowak R (2016) Estimation of viscous and inertial resistance coefficients for various heat sink configurations. *Procedia Eng* 157:122–130
10. Om Ariara Guhan CP, Arthanareeswaren G, Varadarajan KN (2015) CFD study on pressure drop and uniformity index of three cylinder LCV exhaust system. *Procedia Eng* 127:1211–1218

Development of Hydrophobic Coating with Polymer–Metal Oxide Nano-composites



Jaya Verma, Vishakha Baghel, Basant Singh Sikarwar, Arpita Bhattacharya and D. K. Avasthi

Abstract The hydrophobicity of the nano-coating developed with TiO_2 and $\text{SiO}_2\text{-TiO}_2$ nanoparticles in organic binder is investigated, where polyurethane was taken as model binder. Core SiO_2 nanoparticles have been synthesized using Stober method with average particle size of 92 nm. TiO_2 and nano-core@shell have been prepared using peptization process. Particle sizes were measured as 75 nm for TiO_2 and 144 nm for core-shell nanoparticles which were prepared using peptization process. In this process, hydrophobic titania was produced at 70 °C. Here, $\text{SiO}_2\text{-TiO}_2$ core-shell nanoparticle was synthesized because core silica improves the mechanical strength and shell TiO_2 on core silica provides the hydrophobicity of the coating surface. Characterization of these nanoparticles was performed by UV-vis spectrophotometer, dynamic light scattering (DLS), scanning electron microscopy (SEM), Fourier transform infrared spectroscopy (FTIR) and XRD. The coating formulations were developed with the aforementioned nanoparticles separately and concentration of nanoparticles was varied from 1 to 6 wt%. The best performance in terms of hydrophobicity was obtained with 4 wt% of the concentration of nanoparticles in polyurethane-coating system. In this work, prepared coatings were applied on glass substrate (20 × 20 × 10 mm) using a brush, dried in oven at 80 °C for 15 min, on drying, 100- μm -thick film was obtained. Static contact angle of water droplet on these dried films was measured and obtained as 129° for PU film-containing TiO_2 nanoparticle and 133.3° for PU film with $\text{SiO}_2\text{-TiO}_2$ core@shell nanoparticle.

Keywords $\text{SiO}_2\text{-TiO}_2$ core@shell nanoparticles · Polyurethane · Nano-coating · Goniometric measurement

J. Verma · A. Bhattacharya (✉) · D. K. Avasthi
Amity Institute of Nanotechnology, AUUP, 201303 Noida, India
e-mail: abhattacharya@amity.edu

V. Baghel · B. S. Sikarwar
Amity School of Engineering and Technology, AUUP, 201303 Noida, India

© Springer Nature Singapore Pte Ltd. 2019
K. Shanker et al. (eds.), *Advances in Industrial and Production Engineering*, Lecture Notes in Mechanical Engineering, https://doi.org/10.1007/978-981-13-6412-9_11

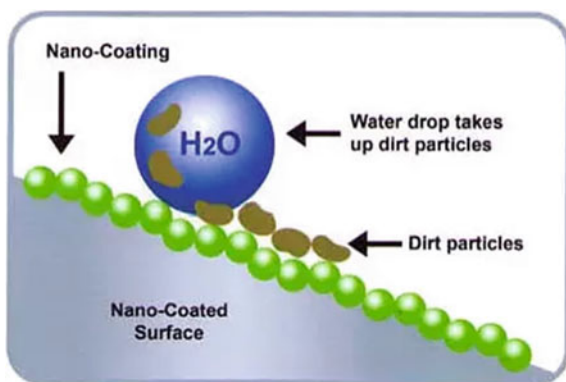
1 Introduction

TiO₂ is the promising material to use as a semiconductor having excellent photochemical stability with minimal effort. Well-dispersed nano-TiO₂ with very fine sizes is promising in numerous applications, for example, adsorbents, pigments, catalytic supports, paints, coating, floor covering, roofing material, cosmetics and automotive products [1–4]. In these cases, when the particle size is decreased enormously in nanoscale, because of the substantial surface-to-volume proportion, some novel optical properties can be enhanced [5]. It was typically discovered that distinctive courses frequently create diverse outcomes [6–8]. Along these lines, it is important to think in detail about the strategies which may affect nano-titania and its properties.

The property of self-cleaning has been outstanding with regards to shared impact between photocatalysis and hydrophobicity. The photocatalytic impact disintegrates natural substances that interact with the surface and keeps them away from building up. The hydrophobic property makes the cleaning more efficient when water moves over the surface. This gathers the clean particles, makes the surface simple and quick dry and counteracts unfortunate water streaking at first glance [9]. Nano-titania is a standout among the most broadly utilized materials in applications such as self-cleaning, because of its thermal stability and photocatalytic properties. [10–13]. By increasing the property of hydrophobicity and reducing the wettability characteristics of a surface, water can improve the cleanness of the surface because it depends on surface microstructure, surface chemical composition and surface geometry. Many researchers have worked upon to increase the hydrophobicity of thin nano-TiO₂ films. As shown in Fig. 1, the hydrophobicity can be improved in different types of polymeric coatings by adding nanoparticles in the formulations. [10, 12–18].

SiO₂–TiO₂ nanoparticles of core@shell structure have been set up to consolidate mechanical properties/hardness of silica nanoparticles and hydrophobicity of nano-TiO₂. Nanoparticles of core–shell constitute a novel class of materials with assortment of utilization in synthetically balancing out colloidal particles, catalysis, planning of bioconjugates [19]. These particles can be incorporated utilizing metals,

Fig. 1 Schematic diagram showing the self-cleaning phenomena on hydrophobic surface



semiconductors, protectors, metal oxides, composites, colors and even biomolecules as center or shell. A simple approach to get ready silica–titania core@shell materials is Stober strategy where the TiO_2 sol and SiO_2 sol can be arranged separately and blended to acquire nano-core@shell development [20, 21]; however, this technique does not give hydrophobic surface.

In this study, nano- TiO_2 and SiO_2 - TiO_2 nanoparticles of core@shell structure have been prepared by peptization method for the development of hydrophobic coating in polyurethane (PU) binder. Polyurethane (PU) coating system has several applications. Polyurethane coatings can make better product's appearance and increase its lifespan. PU adhesives provide another advantage of strong bonding and provide tighter seals. PU elastomers are lighter than metal; they can be molded into almost any shape. In addition, it offers superior stress recovery and provides resistant against environmental conditions.

2 Experimental Study

2.1 Materials

Titanium tetra-isopropoxide and tetraethyl orthosilicate were obtained from Sigma Aldrich Chemicals Pvt. Ltd, India. NH_4OH was acquired from Qualikems Fine Chemical Pvt. Ltd, India. Ethanol was acquired from Merck Limited, India. Nitric acid was purchased from Fisher Scientific (India). Polyurethane was obtained from Dalton Chemicals Pvt. Ltd (India).

Instruments The instruments used are as follows: UV 1800 Shimadzu UV spectrophotometer, Malvern instruments-Zetasizer Nano S-90, Shimadzu 8400 spectrophotometer, and Bruker D8 Focus XRD.

2.2 Methods

Preparation of SiO_2 nanoparticles through Stober process TEOS (8 ml) was utilized as a precursor for preparing nano-silica by blending this in 35 ml and 100 ml of DI water and ethanol, respectively. This mixture was stirred for 40 min and NH_4OH was included drop-wise in this solution for keeping up pH at 10 and after that kept for 1 d and centrifuged it at 8000 rpm for 10–15 min. Material was dried overnight at 100 °C in oven after centrifugation and calcinated at 650 °C for 2 h.

Synthesis of nano- TiO_2 through peptization process. In preparation of nano- TiO_2 by peptization process, 2 ml of TTIP was added to DI water (50 ml) under blending condition. White suspension was formed, after that coagulated titanium oxide was

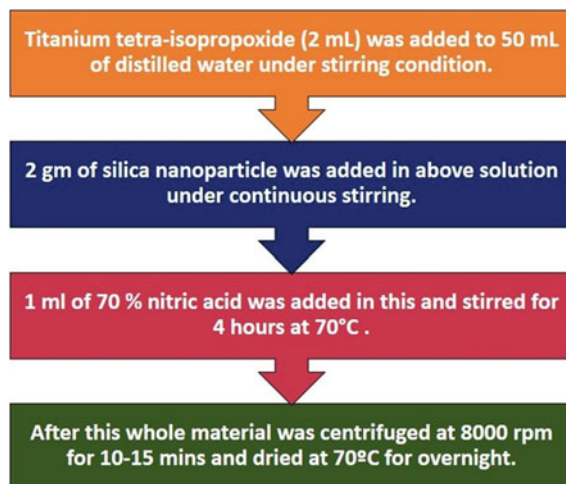
precipitated. Nitric acid (1 ml) was added to the titania gel. From that point onward, the precipitate was mixed for 4 h at 70 °C temperature. Following 4 h mixing, entire material was dried in oven at 70 °C for overnight.

Synthesis of nano-SiO₂-TiO₂ core-shell nanoparticles through peptization process. For the synthesis of SiO₂-TiO₂ nanoparticles, same methodology was taken as depicted in preparation of TiO₂ nanoparticle using peptization method in the presence of SiO₂ nanoparticle (2 gm) prepared through Stober method (Fig. 2).

Coating development and measurement of contact angle. Coating formulations were developed with SiO₂, TiO₂, and SiO₂-TiO₂ nanoparticles separately in PU binder system. In this coating formulation, different concentrations of nanoparticle were used from 1 to 6 wt%. These coatings were applied on a glass slide (20 × 20 × 10 mm) using paintbrush. After that, films were dried in oven for 15–20 min at 100 °C. The thickness of the dried film was measured around 100 μm. Goniometric measurements were carried out to measure the static contact angle of water droplet on these coated substrates using custom built-in goniometer.

Characterization. Particle size measurement was performed by Malvern instruments-Zetasizer Nano S-90 (DLS). UV-vis analysis was carried out through spectrophotometer (Shimadzu UV-1800). XRD analysis was performed by X-ray diffractometer (Bruker D8 Focus). Scanning electron microscopy of PU-based coatings on glass slide developed with SiO₂ and SiO₂-TiO₂ core-shell nanoparticles was analyzed by Zeiss scanning electron microscope and element identification of these samples was performed by Bruker EDX.

Fig. 2 Flow chart for SiO₂-TiO₂ core-shell nanoparticles preparation procedure



3 Results and Discussion

Average particle size of core–shell nanoparticles was measured as 144 nm on 92 nm of nano-silica. Results demonstrates that thin layer of TiO_2 (26 nm) was formulated on center material silica as shown in Fig. 3. UV-vis study was carried out in the wavelength range of 200–700 nm, and absorbance peak was obtained at 310 nm for both in TiO_2 and SiO_2 – TiO_2 nanoparticles. As appeared in Fig. 4, result confirms the thin covered layer of TiO_2 on center SiO_2 and furthermore development of nanoparticles of core–shell structure.

Figure 5 shows the XRD patterns of the prepared samples. Results confirm the nano SiO_2 – TiO_2 core-shell formation with one broad peak i.e. amorphous nature appeared at $2\theta = 15^\circ$ i.e. $(hkl = 100)$ for silica nanoparticles and other sharp peaks i.e. crystalline nature available at $2\theta = 25^\circ, 46^\circ, 55^\circ$ and $(hkl = 110, 211, 220)$ for titania nanoparticles with respect to individual XRD analysis of silica and titania nanoparticles.

Figure 6 shows the FTIR spectra of SiO_2 , TiO_2 , and SiO_2 @ TiO_2 core-shell nanoparticles. In the spectra of nano- SiO_2 , band obtained at 1070 cm^{-1} corresponds to asymmetric stretching vibration of Si–O–Si bond, whereas 3300 and 1640 cm^{-1} bands have appeared for H–O–H stretching and bending of absorbed water. Another peak obtained at 910 cm^{-1} corresponds to Si–OH bond. In case of SiO_2 – TiO_2 spectra, along with the peaks of nano-silica, a band at around 950 cm^{-1} was appeared for Si–O–Ti bond which supports a layer of TiO_2 formation on core SiO_2 . SEM and EDX studies were completed for created coatings in polyurethane (PU) with

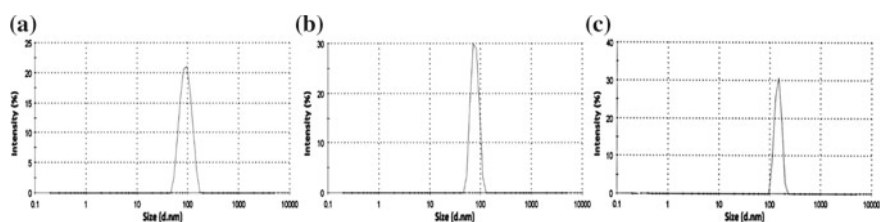


Fig. 3 DLS graph: **a** nano- SiO_2 , **b** nano- TiO_2 , **c** nano- SiO_2 – TiO_2 nanoparticles of core–shell structure

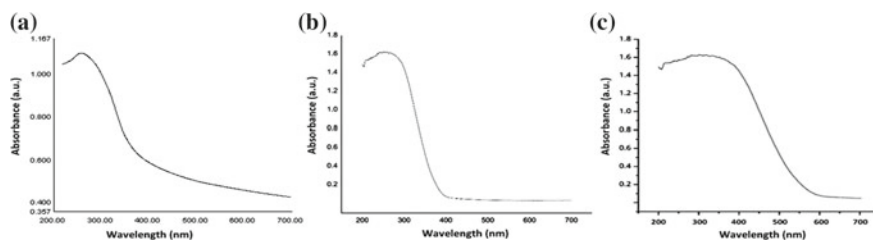


Fig. 4 UV-vis spectra: **a** nano- SiO_2 , **b** nano- TiO_2 , **c** nano- SiO_2 – TiO_2 nanoparticles of core–shell structure

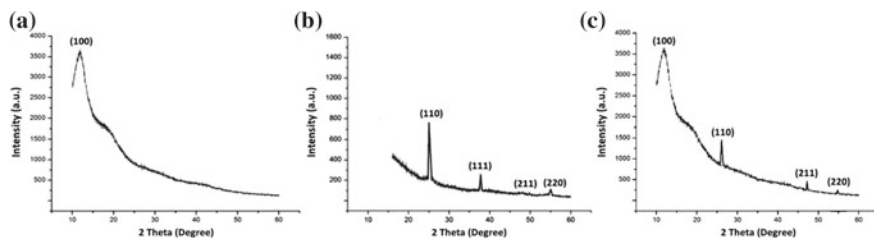


Fig. 5 XRD: **a** nano-SiO₂, **b** nano-TiO₂, **c** nano-SiO₂-TiO₂ nanoparticles of core-shell structure

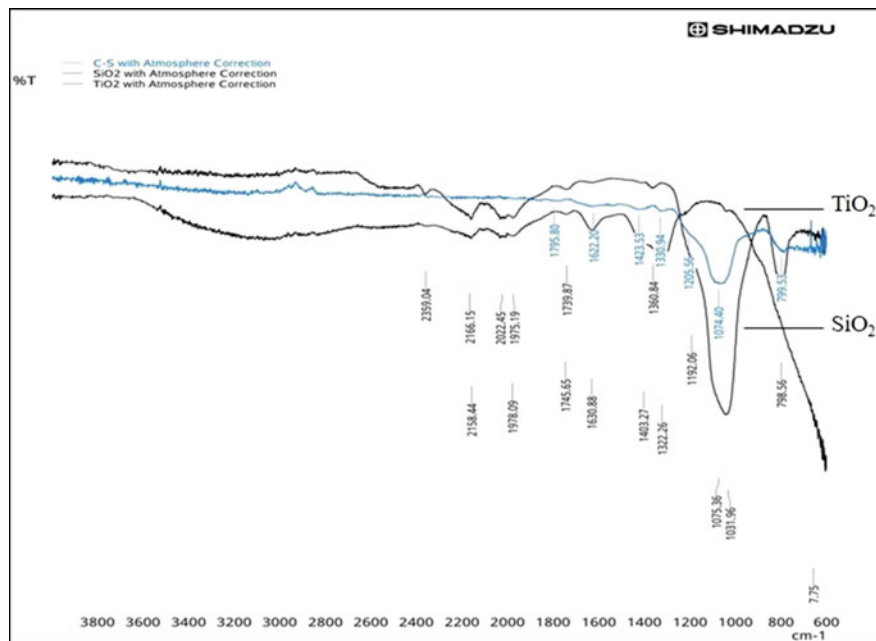


Fig. 6 Spectroscopy of SiO₂-TiO₂ nanoparticles of core-shell with individual SiO₂ and TiO₂ nanoparticles

SiO₂-TiO₂ nanoparticles at 20 kV and 500 \times magnification which are shown in Fig. 7. EDX investigations were done for elemental analysis in created coatings which is appeared in Fig. 7c.

Contact angle measurements were performed for coating system developed in PU on glass slide with SiO₂, TiO₂, and SiO₂-TiO₂ core-shell nanoparticles containing nanoparticle concentration of 1–6 wt%. Custom built-in goniometer was used to measure the contact angle of water droplet on these coated substrates. A 10 μ l DI water droplet was dispensed using micropipette on these coated substrates. High-resolution images of water droplet were captured using high-speed camera (Phantom LAB3a10), mounted with macrolens (Nikon AF-S VR). Further, these

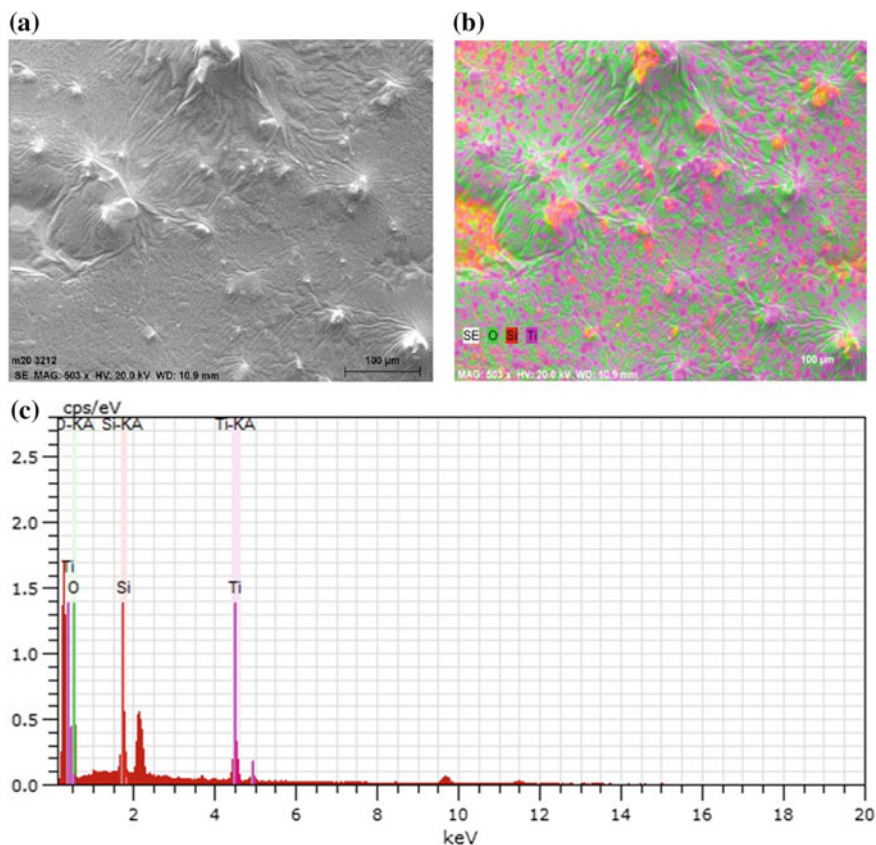


Fig. 7 a SEM analysis of SiO₂–TiO₂ core–shell in PU coating, b–c EDX of same coating formulation

high-resolution images were processed using commercially available ImageJ software and contact angle (θ), i.e., the angle between the solid–liquid interfaces was measured for various substrates as shown in Figs. 8 and 9. The goniometric measurement results show that the hydrophobicity improves from 80° to 133.3° for the coating materials and it was observed that surface exhibits superior hydrophobic properties at 4 wt% concentration of nanoparticles in PU. Polyurethane-coated surface developed with TiO₂ nanoparticle at 4 wt% concentration shows contact angle of 129° and the contact angle was measured as 133.3° on coating with silica–titania core–shell nanoparticle with same concentration of nanoparticle.

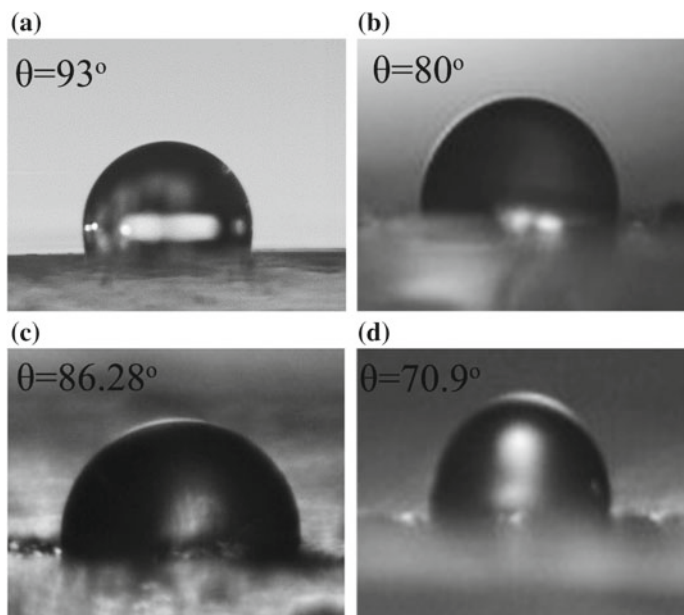


Fig. 8 High-resolution images on various coating substrates: **a** pure polyurethane coating, **b** polyurethane-coating system with SiO_2 nanoparticles 1 wt%, **c** polyurethane-coating system with SiO_2 nanoparticles 4 wt% **d** polyurethane-coating system with SiO_2 nanoparticles 6 wt%

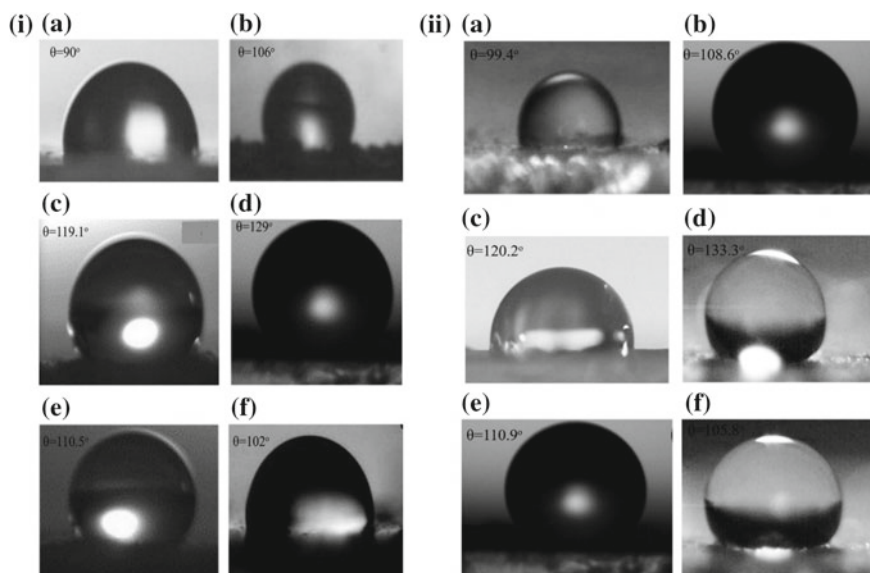


Fig. 9 Water droplet on polyurethane-coating system with (i) TiO_2 nanoparticles and (ii) SiO_2 - TiO_2 core-shell nanoparticles with **a** 1 wt%, **b** 2 wt%, **c** 3 wt%, **d** 4 wt%, **e** 5 wt%, and **f** 6 wt%

4 Conclusion

SiO₂, TiO₂, and SiO₂–TiO₂ core–shell nanoparticles were prepared successfully by Stober method and peptization method. Polyurethane-based coatings were developed with all prepared nanoparticles at various concentrations of nanoparticles from 1 to 6 wt%. Goniometric measurements were performed for all the polyurethane-based coatings. Results of the experimental study conclude that the coating surface formulated with SiO₂–TiO₂ core–shell nanoparticle in polyurethane (PU) at 4 wt% shows superior hydrophobic properties.

Acknowledgements One of the authors would like to acknowledge the financial support from Science and Engineering Research Board (SERB), DST Project No: ECR/2016/000020. We also thank IUAC Delhi and IIT Delhi for their help and support in characterizing the samples.

References

1. Williams DF (2008) The relationship between biomaterials and nanotechnology. *Biomaterials* 29:1737–1738
2. Tomkiewicz M (2000) Photocatalytic activity of mesoporous TiO₂. *Catal Today* 58:115
3. Ngoc TL, Van CN, Thi HD, Le HHT, Duy LP, Hung MD, Dinh LV, Van HL (2014) Optical properties of TiO₂ nanotube arrays fabricated by the electrochemical anodization method. *Adv Nat Sci: Nanosci Nanotechnol* 5:1.6
4. Rahman MM, Krishna KM, Soga T, Jimbo T, Umeno M (2009) Structure and photoluminescence properties of TiO₂ nanoparticles. *J Phys Chem Solids* 60:201
5. Pelizzetti E, Minero C (2010) Titanium in medicine. *Electrochim Acta* 38:47
6. Sahni S, Reddy SB, Murty BS (2012) Synthesis and characterization of nano TiO₂. *Mater Sci Eng A* 452–453:758
7. Pedro MÁ, Pawel KP (2010) Preparation and characterization of magnetic TiO₂ nanoparticles and their utilization for the degradation of emerging pollutants in water. *Appl Catal B: Environ* 100(1–2):338–345
8. Kolenko YV, Churagulov BR, Kunst M, Mazerolles L, Colbeau-justin C (2014) TiO₂ nanoparticles via microwave assisted method. *Appl Catal B: Environ* 54:51
9. Zhou W, Cao Q, Tang S (2016) Synthesis and characterization of nano TiO₂ via different methods. *Powder Technol* 168:32
10. Mudassar A, Hina I, Mumtaz HM, Ahsan N (2017) Surface coatings of TiO₂ Nanoparticles onto the designed fabrics for enhanced self-cleaning properties. *Coatings* 8(35):1–9
11. Adawiya J, Chafic TS (2017) Exploring potential environmental applications of TiO₂ nanoparticles. *Energy Procedia* 119:332–345
12. Shamsudin S, Ahmad M, Murakami M (2017) Hydrophobic rutile phase TiO₂ nanostructure and its properties for self-cleaning application. *AIP* 1883(1):20–30
13. Mo C, Zheng Y, Wang F, Mo Q (2015) A simple process for fabricating organic/TiO₂ super-hydrophobic and anti-corrosion coating. *Int J Electrochem Sci* 10:7380–7391
14. Yadav HM, Kim J-S, Pauer SH (2016) Developments in photocatalytic antibacterial activity of nano TiO₂. *Korean J Chem Eng* 33:7
15. Damchan J, Sikong L, Kooptarnond K, Niyomwas S (2008) Contact angle of glass substrate coated with TiO₂/SiO₂ thin films. *CMU J Nat Sci* 7:19–23
16. Liu Q, Wu X, Wang B, Liu Q (2002) Preparation and super-hydrophilic properties of TiO₂/SnO₂ composites thin films. *Mater Res Bull* 37:2255–2262

17. Ching-Lee H, Weng-Sing H (2006) Substrate effects on the oxygen gas sensing properties of SnO₂/TiO₂ thin films. *Appl Surf Sci* 253:889–897
18. Wahyuni S, Prasetya A (2017) Enhanced the hydrophobic surface and the photo-activity of TiO₂–SiO₂ composites. *Mater Sci Eng* 172:1–12
19. Hu J-L, Qian H-S, Li J-J, Hu Y, Li Z-Q, Yu S-H.: Synthesis of mesoporous SiO₂@TiO₂ core/shell nanospheres with enhanced photocatalytic properties (2015) 30(4):306–310
20. Greene D, Serrano-Garcia R, Govan J, Gun'ko YK (2014) Synthesis characterization and photocatalytic studies of cobalt ferrite-silica-titania nanocomposites. *Nanomaterials* 4:331–343
21. Ranjith KS, Nivedita LR, Sokan KA, Krishnamurthy S, Pandian R, Kamruddin M, Avasthi DK, Thangavelu R, Kumar R (2017) *Sci Rep* 7:3251

Recent Developments in Fabrication of Super-Hydrophobic Surfaces: A Review



Deepak Kumar Sharma, Vishakha Baghel, Ranjit Kumar, D. K. Avasthi and Basant Singh Sikarwar

Abstract Nature has many biological structures with water repellency phenomena depicting super-hydrophobicity which are observed in various plants, insects, and animals. The advancements in the broad area of biomimetics provide scope toward development and fabrication of nanotextured surfaces. With biological design, replicating adaptation and derivation from various natural environments which is referred to as “biomimetics.” Related to exceptional properties of super-hydrophobicity, researchers have recently developed and fabricated biomimetic nanotextured super-hydrophobic materials. Surface modification to prepare chemical and physical textured super-hydrophobic metallic surfaces with standard protocols so that repeatable and well-characterized surfaces can be obtained with a high contact angle, low contact angle hysteresis, bounce, and proper roll-off rate. A review-based approach is provided in this paper with developments in surface modification and fabrication of super-hydrophobic materials by various nanotextured processes.

Keywords Super-hydrophobic · Water repellence · Contact angle · Contact angle hysteresis · Nanotextured fabrication · Roll-off rate

Nomenclature

r	Surface roughness factor
f_1	Surface fraction of material 1
f_2	Surface fraction of material 2
θ_Y	Droplet contact angle in Young state
θ_w	Droplet contact angle in Wenzel state

D. K. Sharma (✉) · R. Kumar · D. K. Avasthi
Amity Institute of Nanotechnology, AUUP, Noida 201313,
Uttar Pradesh, India
e-mail: deepaksharmananotech@gmail.com

V. Baghel · B. S. Sikarwar
Department of Mechanical Engineering, AUUP, Noida,
Uttar Pradesh, India

θ_c	Droplet contact angle in Cassie state
θ	Contact angle
γ	Surface tension
SG	Properties at the solid–gas interface
SL	Properties at the solid–liquid interface
LG	Properties at the liquid–gas interface
WCA	Water contact angle

1 Introduction

In nature, there are many surfaces and materials with a wider area of interest for researchers having unique properties with distinct wettability governed by surface free energy and morphology [1]. However, surface hydrophobicity depending on surface texture is controlled by contact angle (CA) of liquid droplets on these surfaces described by Wenzel [2], Cassie and Baxter [3] states. Many biologically diverse plants and animals depict the properties of being hydrophobic in nature. In relevance to previous literature [4], lotus leaves in nature provides a self-cleaning and phenomenon of super-hydrophobicity termed as “lotus effect” governed by hierarchical roughness on their leaf surface. Thus, nature has inspired us to fabricate various biomimetic metallic surfaces with special wettability properties [5] important for widespread industrial applications. Physical and chemical textured metallic surfaces have both combinations of micro-nano surface roughness and chemical composition providing water repellency on impinging surfaces with bounce and proper rolling [6]. There have been two generic methods that can be used to modify the hydrophobicity of these metallic substrates. Firstly physical texturing alters the surface topography/roughness or its patterning and the second chemical texturing in terms of chemical grafting or adsorbing molecules which enhances the surface wetting characteristics. Recent research paper provides an overview for preparation and nanotexturing of super-hydrophobic metallic surfaces. Numerous methods for crafting super-hydrophobic surfaces have been dealt upon with techniques simple and cost-effective, however, involving multiple stepwise procedures and diverse conditions. Recently, various procedures for measurement of surface roughness and altering hydrophobicity have been studied for these metallic surfaces. In literatures previous methods of surface treatment such as electrochemical deposition, wet chemical reaction, casting method, immersion method, ion beam implantation and plasma coating has been reported for fabricating super-hydrophobic surfaces [7, 8].

As reported in the literature [9], altering the morphology of metallic surfaces by creating roughness in form of nano/microscale pillars, dimples, and channels are durable in the phase-change process. However, creating a nanoscale structured roughness on the surface is a difficult and expensive task [10]. This review focuses on recent developments in fabrication of super-hydrophobic metallic surfaces viable for water harvesting from the humid air via dew formation which is reliable solution for water shortage world wide [11, 12]. Wide area of this review is divided into

three different sections. First part provides a brief introduction of super-hydrophobic surfaces. The second part provides theoretical background and experimental synthesis significant to wettability of metallic surfaces. The third part provides complete overview and direct towards the fabrication of super-hydrophobic metallic surfaces.

2 Theory and Experimental Synthesis

This approach deals with quantifying the hydrophobicity of surfaces by the contact angle of a liquid drop on a flat homogenous surface where θ represents the contact angle and is represented by Young's equation for contact angle analysis as provided in the equation below.

$$\cos \theta_Y = \frac{\gamma_{sv} - \gamma_{sl}}{\gamma_{lv}} \quad (1)$$

where γ_{sv} , γ_{sl} , and γ_{lv} are the interfacial tensions of the solid–vapor, solid–liquid, and the liquid–vapor interface, respectively, in Fig. 1a.

In Wenzel state [2] the liquid drop fills the rough grooves on the surface shown in Fig. 1b, where the liquid drop forms a contact angle on the rough surface is given by θ_w and r represents surface roughness factor with the difference between states from solid to gas as well as solid to liquid.

$$\cos \theta_W = \frac{\gamma_{SG} - \gamma_{SL}}{\gamma_{LG}} = r \cos \theta_Y \quad (2)$$

In Cassie–Baxter state [3], the liquid drop sits on the vapor filled composite surface as provided in the equation below.

$$\begin{aligned} \cos \theta_C &= \phi_1 \cos \theta_{Y,1} + \phi_2 \cos \theta_{Y,2} \\ \cos \theta_C &= \phi_s \cos \theta + (1 - \phi_s) \cos 180^\circ = \phi_s \cos \theta - 1 + \phi_s \end{aligned} \quad (3)$$

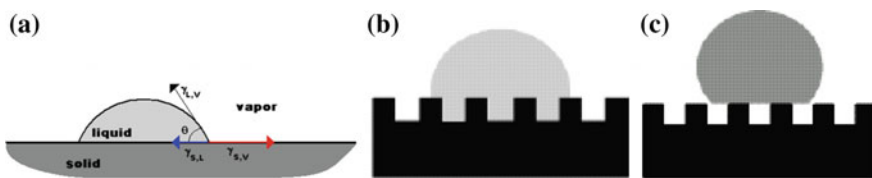


Fig. 1 a Contact angle and liquid droplet on the surface in Young's equation. b Liquid droplet on the surface in Wenzel's state. c The wetting behavior of a liquid droplet on the rough solid surface: Cassie's state

The Cassie–Baxter Eq. (3) can be elaborated in terms of the figure provided below which has contact angle, θ_c of two different phases which are phase 1 and phase 2.

In the preparation of super-hydrophobic surfaces, recently many physical and chemical texturing methods are reviewed. In relevance to these metallic surfaces, widespread use of aluminum and copper surfaces in industrial applications having a high thermal conductivity which is 6–7 times greater than that of stainless steel are used recently. It has been observed that the copper surface gets easily oxidized when exposed to moist environmental conditions and forms a nanoscale CuO layer [5] and aluminum oxide Al_2O_3 [6]. This inspires us to completely review these methods which will help us to evaluate surface morphology, roughness, and super-hydrophobicity in a much simple, acclaimed, and cost-effective manner for preparation of nanotextured super-hydrophobic metallic surfaces in terms of water potability and regeneration.

2.1 Physical and Chemical Texturing

The bare copper plates with 95% purity and 2 mm thickness are marked as having a dimension of 10×10 mm. The oxide layers are removed from plates by using #1000 and #6000 grid emery papers and surface finishing was done for 10 min with each grid emery paper. Cut ten pieces of 10×10 mm copper plates using a metal cutter or hand grinder machine which thus, induces surface roughness [5]. Similarly, bare aluminum plates with 95% purity and 1.5 mm thickness are marked having a dimension of 10×10 mm dimension. The oxide layer from plates are removed by using #800 and #1000 grid emery papers using sander machine and surface finishing was done for 10 min with each grid emery paper [6]. Physical texturing is an efficient process for removing surface imperfection. These metallic surfaces after physical texturing need to be chemical textured with microfabrication coating techniques to enhance the surface topography. Experiments described in the table below providing the various micro coating methods used for surface modification of metallic surfaces (Table 1).

2.1.1 Electrochemical Deposition

The surface preparation of copper surfaces by electrochemical deposition by Huang et al. [19] prepared various copper super-hydrophobic surfaces. Uniform cut and polished copper plates vertically immersed in the dilute concentration of ethanolic stearic acid applied with a voltage in terms of direct current. This turned the anodic copper surface super-hydrophobic after electric discharge is passed having WCA of 153° and contact angle hysteresis of 2° . The increment in water contact angle and the reduction in contact angle hysteresis at 3 hours can be described to the concurrence of the miniaturized scale nanostructured surface morphology and lower surface energy together diminishing the fondness of water toward the surface (Fig. 2).

Table 1 Micro coating methods available to modify the wettability of metallic surfaces

Texturing method	Chemical composition of the top of the surface	Reported wettability	Fabrication methods
Additive	Pure copper, aluminum		
	Oxide	Super-hydrophilic (10°–30°)	MAND process,
		NA	Anodization + Annealing
		Super-hydrophilic/Super-hydrophobic (0°–153°)	Heating in air/Annealing
		Super-hydrophilic (0°)	Alkali-assisted oxidation
		Super-hydrophilic–Super-hydrophobic W. (0°–140°)	Oxidation (NH ₄ OH)
	Hydroxide	NA	Anodization
	Silane	Super-hydrophobic C.B. (140°–160°)	Hydroxylation + FAS17
Fluorocarbon	Super-hydrophobic C.B. (170°)	Alkali-assisted Oxidation + Thiol [13] deposition (HDFT)	
Subtractive	Pure copper	Hydrophobic–Super-hydrophobic W. (90°–150°)	Chemical etching [14]
	Oxide		
	Hydroxide		
	Silane		
	Fluorocarbon	Super-hydrophobic C.B. (171°)	Etching + Thiol deposition (HDFT) [15]
Subtractive then Additive	Pure copper, aluminum, bronze		
	Oxide	Super-hydrophobic C.B. (160°)	Chemical Etching + Oxidation (NH ₄ OH)
	Hydroxide		
	Silane		
	Fluorocarbon		

(continued)

Table 1 (continued)

Texturing method	Chemical composition of the top of the surface	Reported wettability	Fabrication methods
None	Pure copper, aluminum,		
	Oxide	Super-hydrophilic (0° – 10°)/Super-hydrophobic WCA (90° – 160°)	POSS-Silica nanoparticles [16–18]
		Super-hydrophilic 0°	CuO, Al ₂ O ₃ deposition
	Hydroxide		
	Silane		
	Fluorocarbon	NA	<i>n</i> -Alkanethiol deposition

2.1.2 Wet Chemical Reaction

The copper wafer was etched by HNO₃ in the presence of cetyltrimethyl ammonium bromide (CTAB) by Pan et al. [20] and ultrasonicated. The increase in water contact angle with the increase in time of chemical etching with HNO₃ and CTAB with ultrasonication led to the formation of uniform nano-microstructures as shown in Fig. 3d on the surface of the copper wafer with water CA $155 \pm 2^\circ$ and sliding less than 5° .

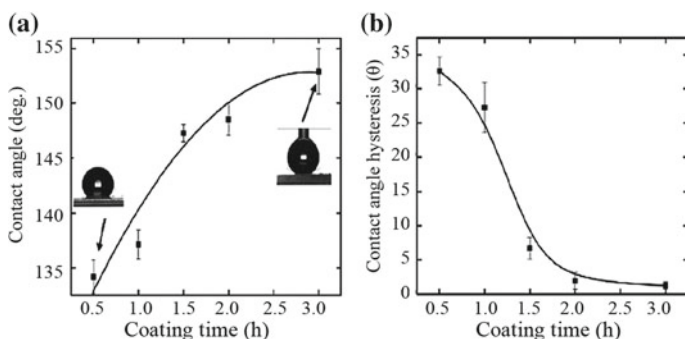


Fig. 2 **a** Plot showing time duration in terms of contact angle and **b** plot showing variation time versus contact angle hysteresis [19]

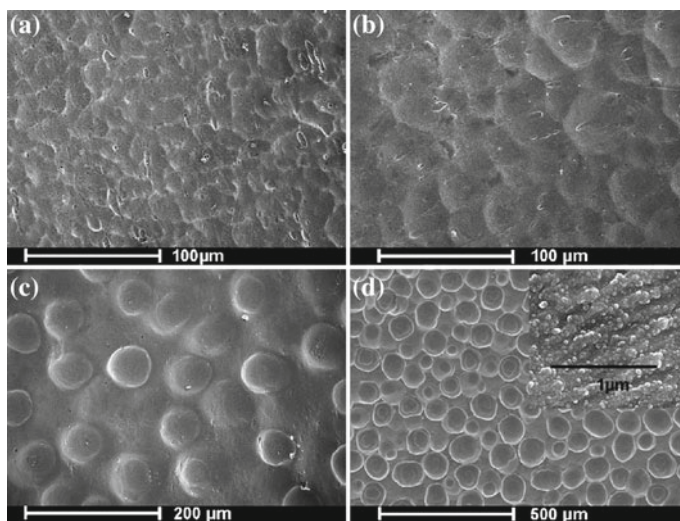


Fig. 3 Surface morphological images shown by SEM with etching duration of is 20 min [20]

2.1.3 Sol-gel Dip Coated

A originally modified alcosol is prepared with methyltrimethoxysilane (MTMS) by Parale et al. [21] used for the deposition on a different metal substrate. The coating sol has a molar ratio of MTMS: MeOH: H₂O constant at 1: 5.63: 1.58, respectively with PMMA 7 wt% and 0.5 M NH₄F as a catalyst where PMMA bonds with the CH₃ to achieve super-hydrophobicity with nanostructured silica network on the substrate surface which is responsible for gelation. These substrates annealed at 150 °C for 3 h led to the removal of residual solvent. The contact angle measurement showed an angle above 150° with the presence of super-hydrophobicity [21] (Fig. 4).

2.1.4 Immersion Coated

This experimental method is much less time consuming and requires reagents in an effective manner. As per the proposed work in this paper by Kong et al. [22], a novel approach for the fabrication of super-hydrophobic copper foil substrate is been reported with sliced crystalline preparation using a solution-immersion coating method with sodium hydroxide, cupric nitrate, and 1H,1H,2H,2H-perfluorodecyltriethoxysilane (FAS-17). Figure 5 shows scanning electron microscope images which provide an improved contact angle with fluorinated silane bonding with uniform micro-nanostructures and higher water contact angle.

In this work, Varshney et al. [23] have prepared super-hydrophobic coating self-cleaning for polished aluminum, Al surfaces. The Al surfaces were chemically etched in a mixture of HCl and HNO₃ and further, the samples were treated in lauric

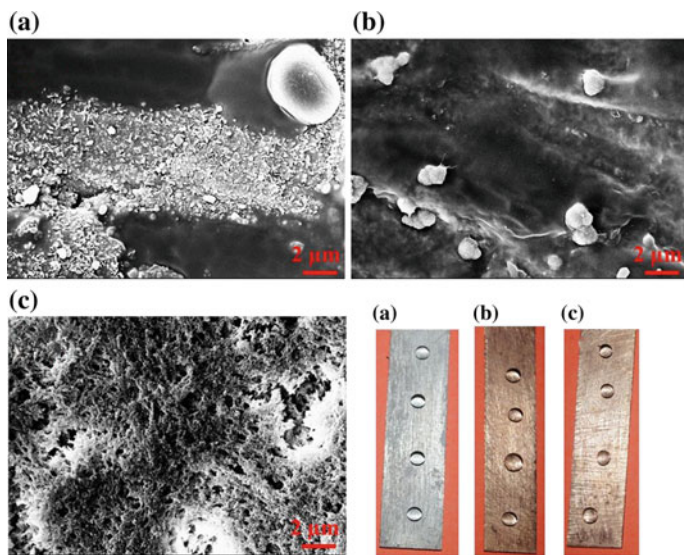


Fig. 4 FESEM image of the silica film prepared on **a** aluminum substrate, **b** bronze substrate, and **c** copper substrate. Images reprinted [21]

acid. Analysis showed morphological changes on surface properties of Al surfaces with super-hydrophobic Al substrate having micropits or microgrooves on the rough treated substrate and having WCA $170 \pm 3.9^\circ$ (Fig. 6).

2.1.5 Ion Irradiation/Implantation

In the field of material science, energetic ions play a vital role. Effect of ion beam implantation on the materials broadly depends on ion energy, fluence, and ion species. Surface modification in terms of hydrophobicity and super-hydrophobicity is available from ion implanters with low energy ions as per Avasthi [24] with a range up to few hundred keV. The ion beam implantation-based material modification has the interaction of the ion with material which is the deciding factor. As per Do et al. [25] aluminum alloy surfaces were irradiated by nitrogen and argon ions. Contact angle analysis, SEM, AFM, and X-ray diffraction were performed for surface characterization. The contact angle increased due to surface composition and surface roughness changes in terms of argon ion beam rather than nitrogen ion as shown in Fig. 7. The ion beam irradiation for synthesis and modification of nanomaterials with ions of different energies from few keV to hundreds of MeV always attracts the interests of material scientists as per Avasthi et al. [26]. Formation of metallic substrates with surface diffusion and ion beam sputtering as per Singh et al. [27]. Study of various low surface energy ion beam irradiation effects shows changes in surface

Fig. 5 SEM images of **a** Cu_2O and **b** slice-like Cu-OH crystalline bondings [23]

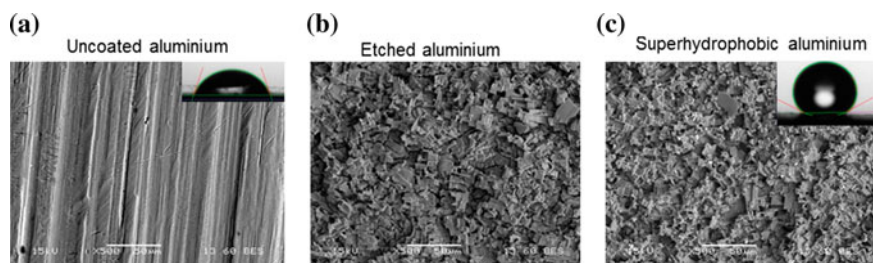
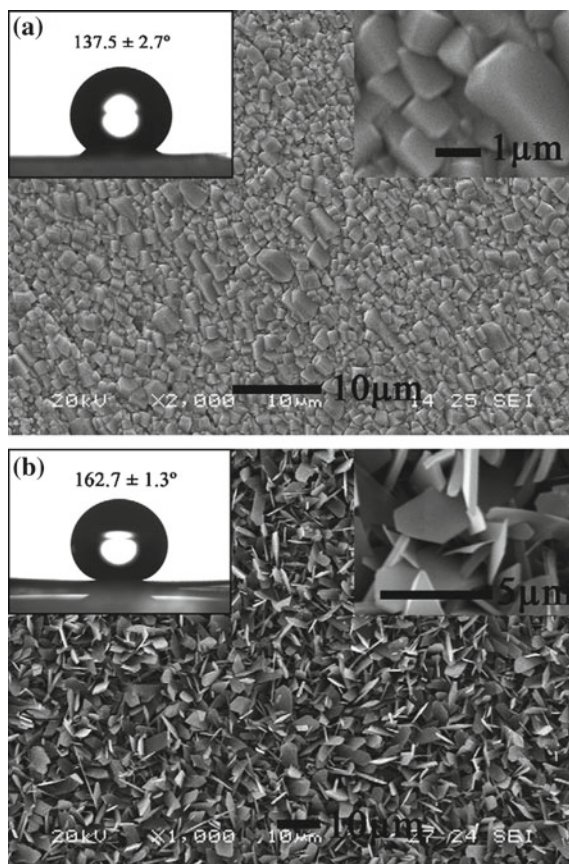


Fig. 6 SEM images of **a** bare Al, **b** chemically etched, and **c** super-hydrophobic Al surfaces [23]

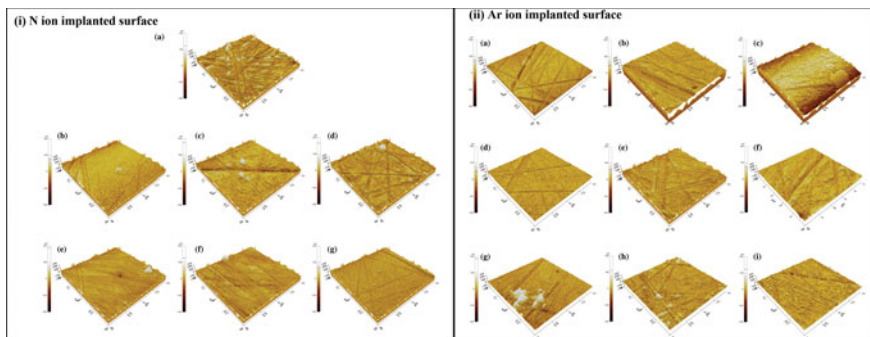


Fig. 7 Ion implanted AFM images of polished aluminum alloy surfaces (i) N ion implanted surface (ii) Ar ion implanted surface [25]

morphology of substrates with super-hydrophilic films altered to highly hydrophobic in nature [28, 29].

2.1.6 Plasma Coated

Plasma treatment generally deals with ionized gas constituting 99% of the universe. Plasma generation is initiated with large energy applied to a gas. The literature on the plasma etching for altering surface morphological is very limited. However, some of the international researcher communities have reported in their studies that the energy of plasma ion can be easily tuned to make surface nanopatterning which is generally provided by an electrical source. Plasma etching provides stability and longevity to chemically functionalized fluorinated copper surfaces exhibiting micro/nanoscale roughness [30, 31]. Plasma technology takes advantage of highly reactive plasma species to modify the functionality of various substrates. Recent enchantments in plasma treatment in terms of preparation of super-hydrophobic surfaces have acquired a recent area of innovation and interest as per Jafari et al. [32]. Low-temperature plasma is useful for surface etching and cleaning. It provides effective surface modification of the polystyrene (PS) substrate as per Dhayal et al. [33]. Design of 3D integrated circuits is a recent area of demand in the development of miniaturized electrical circuits, electronic components with its dependence on copper interconnections having wide area of demand as to avoid corrosion in these copper interconnections a super-hydrophobic coating was prepared by Vilaro et al. [32] and used plasma etching with functionalized fluorinated copper surfaces showed micro/nanoscale roughness with super-hydrophobic coating having WCA 163° and low contact angle hysteresis 1° (Fig. 8a, b).

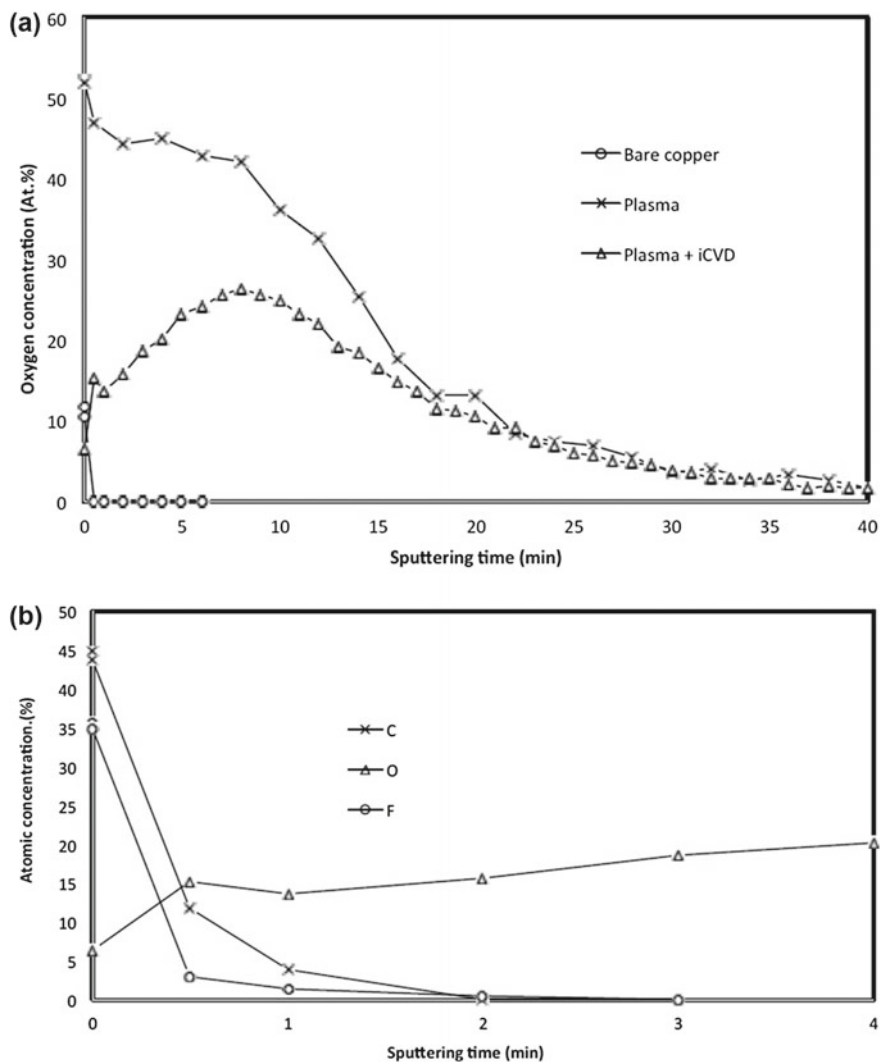


Fig. 8 **a** XPS depth profile using oxygen plasma for bare copper, plasma-etched copper, and coated plasma-etched copper **b** XPS depth profile using carbon, oxygen and fluorine signals for iCVD plasma-etched copper [32]

3 Conclusions and Outlook

The super-hydrophobic surfaces exhibit distinct properties which are biologically acclaimed in nature. This review paper deals with primary metal substrates, namely, copper, aluminum, and common heat transfer engineering materials. Surface modification of these metallic surfaces by chemical and physical texturing methods help us with various standard protocols providing well-characterized surfaces which are repeatable in nature. These surfaces due to its properties of super-hydrophobicity will alter wettability, in general, with the formation of special patterns of the right scale textured for water harvesting applications. Fabrication of super-hydrophobic surfaces requires a large extent of applications with a proper approach toward theoretical models with advanced stable surface fabrication and synthesis techniques in relationship to surface composition, structure, and durability of these super-hydrophobic surfaces. Further, large-scale cost-effective production and price incurred toward raw materials are also an area of concern. Development of super-hydrophobic self-cleaning surfaces has distinct importance in various applications like paints of boats with anti-biofouling properties, antennas, and windows with anti-sticking of snow, windshields of automobiles with self-cleaning properties, microfluidics, refining of metal surfaces, textiles with stain resistant properties, buildings with dust-free coatings, architectural anti-soiling coatings, etc. Hence, it provides a great area of research-oriented interest and challenge for material scientists to fabricate super-hydrophobic surfaces by nanotexturing processes in terms of permanent or semi-permanent super-hydrophobic surfaces with widespread commercial implementations.

Acknowledgements I am indebted to Mr. Mohit Bhandwal, Assistant Professor, Mechanical Engineering Department, Amity School of Engineering and Technology, Amity Center for Computational Fluid Dynamics, Science and Engineering Research Board (SERB), Department of Science and Technology (DST), Government of India (Project no: ECR/2016/000020) for contribution toward detail review of theoretical and numerical synthesis.

References

1. Barthlott W, Neinhuis C (1997) Purity of the sacred lotus, or escape from contamination in biological surfaces, vol 202. Springer Planata, pp 1–8
2. Wenzel R (1936) Resistance of solid surfaces to wetting by water. *Ind Eng Chem* 28(8):988–994
3. Cassie ABD, Baxter S (1944) Wettability of porous surfaces. *Trans Faraday Soc* 40:546–551
4. Bhushan B, Jung Y, Koch K (2009) Micro- nano and hierarchical structures for superhydrophobicity, self-cleaning and low adhesion. *Philos Trans R Soc A* 367:1631–1672
5. Liu K, Jiang L (2011) Metallic surfaces with special wettability. *Nanoscale* 3:825–838
6. Kim A, Lee C, Kim H, Kim J (2015) Simple approach to superhydrophobic nanostructured Al for practical anti-frosting application based on enhanced self-propelled jumping droplets. *ACS Appl Mater Interfaces*. <https://doi.org/10.1021/acsami.5b00292>
7. Yamada Y, Takahashi K, Ikuta T, Nishiyama T, Takata Y, Ma W, Takahara A (2015) Tuning surface wettability at the submicron-scale. *J Phys Chem*. <https://doi.org/10.1021/acs.jpcc.5b09019>

8. Stamatopoulous C, Schutzius MT, Koppl JC, Hayek N, Maitra T (2016) On the shedding of impaled droplets: the role of transient intervening layers. *Nat Sci Rep* 6(18875). <https://doi.org/10.1038/srep18875>
9. Li Y, Wang J, Kong Y, Zohu J, Wu J, Wang G, Bi H, Wu X (2016) Micro/Nano hierarchical peony-like Al doped ZnO superhydrophobic film: the guiding effect of (100) preferred seed layer. *Nat Sci Rep* 6(19187). <https://doi.org/10.1038/srep19187>
10. Schneider L, Laustsen M, Mandsberg N, Taboryski R (2016) The influence of structure heights and opening angles of micro- and nanocones on the macroscopic surface wetting properties. *Nat Sci Rep* 6(21400):1–9
11. Lee JH, Park K (2016) Development of hybrid surfaces with tunable wettability by selective surface modifications materials. *Materials* 9(136):1–12
12. Seo D, Lee J, Lee C, Nam Y (2016) The effects of surface wettability on the fog and dew moisture harvesting performance on tubular surface. *Nat Sci Rep* 6(24276):1–11
13. Ujjain S, Roy P, Kumar S, Singha S, Khare K (2016) Uniting superhydrophobic, superoleophobic and lubricant infused slippery behavior on copper oxide nano-structured substrates. *Nat Sci Rep* 6(35524):1–10
14. Ye L, Guan J, Li Z, Zaho J, Ye C, You J, Li Y (2017) Fabrication of superhydrophobic surfaces with controllable electrical conductivity and water-adhesion. *33(6):1368–1374*
15. Morrisette J, Mahapatra P, Ghosh A, Ganguly R, Megaridis C (2017) Rapid, self-driven liquid mixing on open-surface microfluidic platforms. *Nat Sci Rep* 7(1800):1–13
16. Mandsberg KN, Hansen O, Taboryski R (2017) Generation of micro-droplet arrays by dip-coating of biophilic surfaces; the dependence of entrained droplet volume on withdrawal velocity. *Nat Sci Rep* 7(12794). <https://doi.org/10.1038/s41598-017-12658-z>
17. Das P, Dhal S, Ghosh S, Chatterjee S, Rout SC, Ramgir N, Chatterjee S (2017) Superhydrophobic to hydrophilic transition of multi-walled carbon nanotubes induced by Na⁺ ion irradiation. *Elsevier Nucl Inst Methods Phys Res B* 413:31–36
18. Latthe S, Gaurav A, Maruti C, Vhatkar R (2012) Recent progress in preparation of superhydrophobic surfaces: a review. *J Surf Eng Mater Adv Technol* 2:76–94
19. Huang YH, Wu JT, Yang SY (2011) Direct fabricating patterns using stamping transfer process with PDMS mold of hydrophobic nanostructures on surface of micro-cavity. *Microelectron Eng* 88(6):849–854
20. Pan L, Dong H, Bi P (2010) Facile preparation of super-hydrophobic copper surface by HNO₃ etching technique with the assistance of CTAB and ultrasonication. *Appl Surf Sci* 257(5):1707–1711
21. Parale GV, Mahadik BD, Phadtare DV, Paisal AA, Park HH, Wategaonkar SB (2016) Dip coated superhydrophobic and anticorrosive silica coatings. *Int J Mater Sci Eng* 4(1):60–67
22. Kong XC, Yang G, Yu L, Zhang P (2008) Preparation and characterization of slice-like Cu₂(OH)₃NO₃ superhydrophobic structure on copper foil. *Appl Surf Sci* 254(22):7255–7258
23. Varshney P, Mohapatra SS, Kumar A (2017) Fabrication of mechanically stable superhydrophobic aluminium surface with excellent self-cleaning and anti-fogging properties. *Biomimetics* 2(2):1–12
24. Avasthi KD (2000) Some interesting aspects of swift heavy ions in materials science. *Curr Sci* 78(11):1297–1303
25. Do CS, Kim WK, Jeong HJ (2015) The variation of hydrophobicity of aluminium alloy by nitrogen and argon ion implantation. *Heat Mass Transf* 51:487–495
26. Avasthi KD, Pivin CJ (2011) Ion beam for synthesis and modification of nanostructures. *Curr Sci* 98(6):780–792
27. Singh BU, Agarwal CD, Khan AS, Tripathi A, Kumar Ajay, Choudhury KR, Panigrahi KB, Avasthi KD (2011) Creation of self-organized gold nanostructures by keV ion beam irradiation. *Radiat Eff Defects Solids* 166(8–9):553–557
28. Lakshmi SVBG, Avasthi KD (2016) Tuning of wettability of PANI-GNP composites using keV energy ions. *Elsevier Nucl Instr Methods Phys B* 379:152
29. Singh BU, Agarwal CD, Khan AS, Kumar M, Tripathi A, Singhal R, Panigrahi KB, Avasthi KD (2011) Engineering of hydrophilic and plasmonic properties of Ag thin film by atom beam irradiation. *Elsevier Appl Surf Sci* 258(4):1464–1469

30. Tendeore C, Tixier C, Tristant P, Desmaison J, Leprince P (2006) Atmospheric pressure plasmas: a review. *Spectrochim Acta Part B* 61(1):2–30
31. Jafari R, Asadollahi S, Farzaneh M (2013) Applications of plasma technology in development of superhydrophobic surfaces: a review. *Springer Plasma Chem Plasma Process* 33(1):177–200
32. Vilaro I, Yague LJ, Borros S (2016) Superhydrophobic copper surfaces with anti-corrosion properties fabricated by solventless CVD methods. *ACS Appl Mater Interfaces* 1–23. <https://doi.org/10.1021/acsami.6b12119>
33. Dhayal M, Awasthi K, Vijay KY, Avasthi KD (2006) Using fast atomic source and low-energy plasma ions for polymer surface modification. *Vacuum* 80(6):643–646
34. Grill A (1994) *Cold plasma in materials fabrication: from fundamentals to applications*. IEEE Press, New York

Conceptual Analysis of Reliability Aspect for Various Process Industries: A Critical Review



Gaurav Sharma  and Puran Chandra Tewari

Abstract The reliability field has gone through fruition development and burst through during previous four decades. The current paper reflects a historical outlook of momentous expansion and methodically spells out the contributions in reliability field since its commencement. The paper additionally looks into the significance and advancement of a range of numerical methods for the analysis of reliability, diagrammatical models, logical, and other reliability tools that had fashioned the appearance of reliability concept. Higher productivity and maximum profitability have nowadays become very essential for the processing industries to ensure their survival. To meet this challenge, all the systems and subsystems of these industries should have high reliability and availability. If the manufacturing systems are of improved quality and are having higher availability levels, this will definitely lead to enhancement of productivity and hence profitability. It has been realized that reliability and availability have great importance in all the processing industries and complex plants. Reliability concept is of great importance at design stage, development stage, procurement stage, operation stage, and maintenance stage. The study has been undertaken by many researchers for recognizing the performance behavior of systems in various process industries. A critical review has been conducted to present the brief overview of performance behavior and optimization of different systems related to various process industries. Lastly, the paper emphasizes the restrictions with on-hand methods for analysis of reliability and make out a small number of latent openings for more research.

Keywords Availability · Maintainability · Reliability · Performance evaluation

G. Sharma (✉) · P. C. Tewari
Department of Mechanical Engineering, N.I.T., Kurukshetra, Haryana, India
e-mail: reach4gaurav123@rediff.com

P. C. Tewari
e-mail: pctewari1@rediffmail.com

© Springer Nature Singapore Pte Ltd. 2019
K. Shanker et al. (eds.), *Advances in Industrial and Production Engineering*, Lecture Notes in Mechanical Engineering, https://doi.org/10.1007/978-981-13-6412-9_13

1 Introduction

For the improvement in quality as well as quantity of curriculum concerned with manufacturing segment, real focus is required on the operational management. Excellent performance based on qualitative and quantitative production is the key to success for a process plant or processing industry. However, due to poor design, use of wrong manufacturing techniques, and poor maintenance policies, these systems undergo random failures. It leads to loss of prestige and sometimes threat to national security also. Therefore, to survive in the global market, the quality of industrial systems must be good, operation wise as well as performance wise. This can only be achieved by maintaining these systems failure free for long durations. This will, in turn, provide higher system availability. Therefore, all the related activities must be well organized and coordinated so as to ensure optimum utilization of men, machine, material, and supporting resources. If the manufacturing systems are of improved quality and are having high availability level, this will definitely lead to enhancement of productivity.

During the last four decades, the concept of availability of systems has been developed. In late 1940s and early 1950s, reliability engineering appeared on the scene. Military aircraft manufacturing is one of the fields in which reliability engineering has been focused for several years. Transportation sector is one other area where the reliability found major success. The concept of reliability has also shown a significant impact in space programs. The observers also realized that the success rate of space launching projects is now increasing in a spectacular manner. Presently, it has become the concern for all those who are working in the industries. Availability concept has greater worth in modern industries. The role of reliability and availability is significant at all stages starting from design and development to operation, procurement, and maintenance.

The systems and subsystems of process industries are very large and complex generally. The arrangement of these systems/subsystems may be in the series or may be in parallel or a combination of these two is also possible. For the process plant to operate in most efficient and most economic manner, it becomes vital that all the systems/subsystems should run without failures for prolonged hours under the specified conditions of working in the industry. Therefore, in order to achieve the above, there should be proper and effective utilization of 5Ms (man, method, machine, material, money) in the process industries. A proper coordination and organization of all these resources are also required to develop optimum strategies to meet the production targets. It increases production volume and hence profitability of the industry concerned. This will lead to increase in production volumes and profitability of the industry in a noticeable manner.

2 Conceptual Analysis of Reliability Aspect

Ouhbi and Limnios [1] presented the reliability and availability analysis of a turbo-generator. They observed the set of data in a real situation of engineering. This data was provided by Electricite de France. They used this set of data and performed the modeling for the rotor using semi-Markov approach. This model was used further for reliability and availability estimation.

Khobare et al. [2] presented the analysis of reliability for microcomputer circuit modules and the control systems. These control systems are of great importance for safety purpose of nuclear power plants. They developed a model of fault tree for comparator system. The comparator system taken by them was programmable and integrated. They tried to establish the quantitative values of reliability for standardized hardware modules of microcomputer circuit and for C and I systems.

Yang et al. [3] applied genetic algorithm to the issue related to the reliability allocation for a typical water reactor under pressure. They stated that defining the real objective function is the basic problem for reliability allocation. They suggested that the cost involved for the improvement and/or degradation of the system must be included in the process of reliability allocation in order to optimize the system reliability.

Ni and Zhang [4] established a new method of analysis of fatigue reliability under two-stage loading. They used the probabilistic Miner's rule for carrying out this analysis. Large eight samples of testing data were used. Experimental verification was then done for two-stage cyclic loading, i.e., high–low and low–high.

Cizelj et al. [5] developed a Bayesian approach-based method that clearly contains linguistic and numerical information for the assessment of failure rate. Generic database was used to select prior distribution selected, while theory of fuzzy set was used for the assessment of likelihood. Fuzzy inference system was used to develop a model that shows the influence of operating conditions on failure rate of the components.

Arulmozhi et al. [6] provided a method of calculating the system reliability of K-out-of-N systems with the help of an expression and algorithm. They stated the expression provided by them was fast and easy to implement. The algorithm given was memory efficient, and the efficiency of computation can also be considerably improved by using this expression.

Ebrahimi [7] introduced a technique for the assessment of reliability of a system that mainly uses the failure rate data. They also emphasized on a process which evaluates reliability of the system having components that are highly reliable for which the collection of failure data is very difficult. Failure time as well as reliability of system can be expressed in terms of numerous explanatory variables using this method.

Ramirez-Marquez et al. [8] worked on a multi-state series–parallel having binary component from which different levels of multi-state performance can be attained. They proposed that there should be a proper supply of different levels of demand

during the operation period of the system. This will lead to multi-state character of that system, and also, new method of solution will provide different benefits.

Ramirez-Marquez et al. [9] used Monte Carlo simulation technique for the estimation of reliability of a network having multiple states. They dealt with the problem involving Multi-state-two-terminal reliability calculation. In their study, the issues concerned with the computing the reliability on the basis of minimal cut with multi-state vectors had been conferred.

AlSalamah et al. [10] dealt with reliability of the pumping station for cooling of sea water that pumps the water of sea to the refineries and petro-chemical industries in Kuwait country. In the insensitive operating environment and in the absence of other substitute sources of water, the higher value of reliability is essential for pumping system.

Levitin [11] suggested a method for evaluation of reliability and the performance parameters for systems having multiple states with exposed failures. It is a modification of the generalized reliability block diagram method. The proposed method allows the performance of complicated multi-state-series-parallel system having exposed failures that are to be achieved by applying a recursive approach which is a straightforward.

Lyonnet and Toscano [12] concluded that many reliability models are useful at the time of designing and these models are based on the analysis of lifetime data. But these are not of much use during the operational phases because the conditions at operational phases are changing constantly. These models are not prepared for estimation of reliability of systems under dynamic conditions of operations. So, they proposed a dynamic model for reliability that was able to consider the history of running process.

Khanduja et al. [13] discussed about the study of bleaching system of a paper industry. They studied the steady-state behavior of the bleaching system. Maintenance planning was the other area of their study on the same system. For this, a mathematical model was developed for the system using Markov birth-death technique and probabilistic approach. On this basis, they derived an expression for the steady-state availability. On the basis of available maintenance data, they explicate that how the availability of the system get affected with the performance of each working unit.

Kajal et al. [14] developed a decision support system for a butter oil unit of the dairy plant. The Markov process was applied to develop differential equation related to the transition diagram. The solution using normalizing conditions was made for expanding the expression for availability under steady state. The performance of butter oil unit can be measured in terms of this availability.

Kumar and Tewari [15] applied Markov birth-death process and developed a mathematical model for one of the systems of fertilizer plant. Using probabilistic approach, the differential equations connected with the transition diagram of CO₂ cooling system were developed. After doing the analysis of availability, they applied genetic algorithm technique to optimize the performance of CO₂ cooling system.

Garg and Sharma [16] worked on complex and repairable system of a process industry using uncertain data. Membership functions of reliability indices of this

system were determined by using a very new PSOBLT technique. Utilization of in-hand information and use of uncertain data were done in calculating the reliability indices. Providing the compressed search freedom for each reliability index was the major benefit of this technique.

Wang et al. [17] analyzed the reliability and availability of building cooling, heating and power system. The state-space method technique combined with probabilistic approach of Markov model was applied for analyzing the reliabilities. The reliability of all three energy forms involving heat, cool, and electric form was analyzed. The failure and repair rates, availability and mean time between failures were figured out and analyzed for both redundant and the non-redundant building cooling, heating, and power system.

Doostparast et al. [18] applied simulated annealing technique for developing a model for planning the maintenance, periodically. The model was developed for feeding unit in a sugar plant, and it was based on reliability. The purpose of this work was to reduce the overall maintenance cost to a minimum level. Further, they developed decision support system for the same system which was used for deciding the maintenance priority level of various subsystem of the feeding system.

Hou et al. [19] introduced the application of random set theory for assessment of availability of the systems. They suggested that pseudo-system observations can be directly constructed from the observations of components. They did not use the probabilities of failures by observing each component. Systems undergoing rare failures were selected for analysis of availability. Operations that were characterized in the framework of random set were applied for obtaining the upper bound, lower bound, and also the confidence intervals of the availability of the system. No assumption was done regarding previous distribution of failures of the components.

Sabouhi et al. [20] developed the model for reliability and analyzed the availability of combined cycle power plants. Firstly, they develop the reliability models for both the gas turbine and steam turbine power plants. By doing this, they get the input for evaluating the reliability of combined cycle power plants. After that, the sensitivity indices oriented with reliability were given for identifying the critical components of the plant in order to decide the strategies for maintenance which were efficient and effective. Steam turbine power plants were found to be comparatively more reliable than gas turbine power plants and combined cycle power plants.

Kumar and Tewari [21] presented the analysis of performance and its optimization for carbonated soft drink glass bottle filling system at a beverage plant by applying particle swarm optimization method. This system has mainly seven subsystems that are arranged in series arrangement. Exponential distribution was considered for the possible failures as well as repairs. Mathematical model was then made by using Markov approach (MA).

Kumar [22] proposed the simulated annealing technique for the redundancy optimisation of a power plant that was coal fired. They carried out a balanced integration of operational availability, thermal performance, and the cost analysis module of the power plant for achieving profitable funds investment in thermal power plant.

Wang et al. [23] proposed a novel model of reliability for a system having multiple states, with performance sharing. The multi-state system comprises N number

of multi-state units that are linked in series configuration. Every unit has random performance level and has a random demand as well. If the level of performance of any unit becomes more than its requirement, the excess performance can be passed on to its neighboring units via halfway transmitters. Every transmitter is having a random level of capacity, and only, a restricted value of performance transmission is possible. For evaluation of reliability value, an algorithm that works on the basis of universal generating function was developed through their work.

Panchal et al. [24] proposed a framework that was based on fuzzy methodology and was able to analyze the failure of a transmission unit of a commercial vehicle. Identification of critical components of system was done using risk priority number and through failure mode and effect analysis. The results were helpful in intelligent decision making of components that are risky.

3 Conclusions and Future Scope

In modern years, there is a great enhancement of automation and the necessity for better cost-effectiveness in the industries. This has drawn the attention of process industries toward the fact that the maintenance services are the integral part of the production system and these cannot be considered just as a supporting service. After the study of obtainable literature, it is clear that there is no stiff system that can be universally applied in the process industries for accommodating every condition related to maintenance. Therefore, design and development of a proper maintenance system must be done that will outfit the necessity of that particular industry. The analysis of behavior of the systems and maintenance planning in a scientific manner would be helpful for keeping the equipments/systems available for extended duration of time.

Proper application of reliability, availability as well as maintainability techniques can help to overcome most of the above-mentioned problems. Conducting an availability assessment of the system helps in optimizing the inherent performance of the system. The availability assessment identifies those components of the system which have maximum contribution to most of the downtimes. It also helps to determine the outcomes of design changes on the performance of the system in a cost-effective way. Continuous monitoring technique and proper maintenance planning of equipment/system in an industry by introducing precautionary measures and diagnosis methods are the various technologies or approaches which cope with these problems. Proper maintenance decisions also affect the reliability of industrial systems, their availability, lifespan, and lifecycle cost. These can all be quantified, predicted, and evaluated. An outlook of key developments and the role in the area of reliability presented in the present paper would definitely identify some latent openings for further research in the sector of reliability engineering.

References

1. Ouhbi B, Limnios N (1997) Reliability estimation of semi-markov systems: a case study. *Reliab Eng Syst Saf* 58:201–204. [https://doi.org/10.1016/S0951-8320\(97\)00070-7](https://doi.org/10.1016/S0951-8320(97)00070-7)
2. Khobare SK, Shrikhande SV, Chandra U, Govindarajan G (1998) Reliability analysis of microcomputer circuit modules and computer based control systems important to safety of nuclear power plants. *Reliab Eng Syst Saf* 59:253–258. [https://doi.org/10.1016/S0951-8320\(97\)00151-8](https://doi.org/10.1016/S0951-8320(97)00151-8)
3. Yang JE, Hwang MJ, Sung TY, Jin Y (1999) Application of genetic algorithm for reliability allocation in nuclear power plants. *Reliab Eng Syst Saf* 65:229–238. [https://doi.org/10.1016/S0951-8320\(98\)00103-3](https://doi.org/10.1016/S0951-8320(98)00103-3)
4. Ni K, Zhang S (2000) Fatigue reliability analysis under two-stage loading. *Reliab Eng Syst Saf* 68:153–158. [https://doi.org/10.1016/S0951-8320\(00\)00009-0](https://doi.org/10.1016/S0951-8320(00)00009-0)
5. Cizelj RJ, Mavko B, Kljenak I (2001) Component reliability assessment using quantitative and qualitative data. *Reliab Eng Syst Saf* 71:81–95. [https://doi.org/10.1016/S0951-8320\(00\)00073-9](https://doi.org/10.1016/S0951-8320(00)00073-9)
6. Arulmozhi GL (2002) Exact equation and an algorithm for reliability evaluation of K-out-of-N: G system. *Reliab Eng Syst Saf* 78:87–91
7. Ebrahimi NB (2003) Indirect assessment of system reliability. *IEEE Trans Reliab* 52(1):58–62. [https://doi.org/10.1016/S0951-8320\(02\)00046-7](https://doi.org/10.1016/S0951-8320(02)00046-7)
8. Ramirez-Marquez JE, Coit DW (2004) A heuristic for solving the redundancy allocation problem for multi-state series-parallel systems. *Reliab Eng Syst Saf* 83:341–349. <https://doi.org/10.1016/j.res.2003.10.010>
9. Ramirez-Marquez JE, Coit DW (2005) A monte-carlo simulation approach for approximating multi-state two-terminal reliability. *Reliab Eng Syst Saf* 87:253–264. <https://doi.org/10.1016/j.res.2004.05.002>
10. AlSalamah MJ, Shayan E, Savsar M (2006) Reliability analysis of cooling sea water pumping station. *Int J Qual & Reliab Manag* 23(6):670–695
11. Levitin G (2007) Block diagram method for analyzing multi-state systems with uncovered failures. *Reliab Eng Syst Saf* 92:727–734. <https://doi.org/10.1016/j.res.2006.02.009>
12. Lyonnet P, Toscano R (2008) On-line reliability prediction via dynamic failure rate model. *IEEE Trans Reliab* 57(3):452–457. <https://doi.org/10.1109/TR.2008.927808>
13. Khanduja R, Tewari PC, Kumar D (2009) Steady state behavior and maintenance planning of the bleaching system in a paper plant. *J Ind Eng Int* 7(12):39–44
14. Kajal S, Tewari PC, Kaushik D (2010) Decision support system for butter oil system of a dairy plant at NDRI. *IUP J Sci Technol* 6(1):63–71
15. Kumar S, Tewari PC (2011) Mathematical modeling and performance optimization of CO₂ cooling system of a fertilizer plant. *Int J Ind Eng Comput* 2(3):689–698. <https://doi.org/10.5267/j.ijec.2010.08.004>
16. Garg H, Sharma SP (2012) Stochastic behavior analysis of complex repairable industrial systems utilizing uncertain data. *ISA Trans* 51:752–762. <https://doi.org/10.1016/j.isatra.2012.06.012>
17. Wang JJ, Fu C, Yang K, Zhang X, Shi GH, Zhai J (2013) Reliability and availability analysis of redundant BHP system. *Int J Energy* 60:531–540. <https://doi.org/10.1016/j.energy.2013.09.018>
18. Doostparast M, Mohammad D, Kolahan F (2014) A reliability based approach to optimize preventive maintenance scheduling for coherent system. *Int J Reliab Syst Saf* 126:198–206. <https://doi.org/10.1016/j.res.2014.01.010>
19. Hou Y, Sallak M, Schon W (2015) Availability analysis of systems using random set theory. *IFAC-Pap Online* 4(21):1315–1320. <https://doi.org/10.1016/j.ifacol.2015.09.707>
20. Sabouhi H, Abbaspour A, Firuzabad M, Dehghanian P (2016) Reliability modeling and availability analysis of combined cycle power plants. *Electr Power Energy Syst* 79:108–119. <https://doi.org/10.1016/j.ijepes.2016.01.007>

21. Kumar P, Tewari PC (2017) Performance analysis and optimization for CSDGB filling system of a beverage plant using particle swarm optimization. *Int J Ind Eng Comput* 8(3):303–314. <https://doi.org/10.5267/ijiec.2017.1.002>
22. Kumar R (2017) Redundancy optimisation of a coal fired power plant using simulated annealing technique. *Int J Intell Enterp* 4(3):191–203. <https://doi.org/10.1504/IJIE.2017.087625>
23. Wang G, Duan F, Zhou Y (2018) Reliability evaluation of multi-state series systems with performance sharing. *Reliab Eng Syst Saf* 173(3):58–63. <https://doi.org/10.1016/j.res.2018.01.012>
24. Panchal D, Jamwal U, Srivastava P, Kamboj K, Sharma R (2018) Fuzzy methodology application for failure analysis of transmission system. *Int J Math Oper Res* 12(2):220–237. <https://doi.org/10.1504/IJMOR.2018.089678>

Estimation of Hardness During Heat Treatment of EN8 and C25 Steels



Sachin V. Bagali, Maruti, N. R. Abhaya Simha, M. P. Sushanth,
T. S. Prasanna Kumar and V. Krishna

Abstract The hardness of EN8 and C25 steels during Jominy-type end-quench test was numerically estimated. The cooling curve near the quenched end of the specimen was used to estimate the heat flux during quenching. Heat transfer in the specimen during quenching was modeled as a 2D axisymmetric heat conduction coupled with austenite decomposition. The relevant equations were solved inversely for the heat flux with cooling data as input. The microstructure distribution within the specimen was computed, and a hardness model was developed based on microstructure distribution. The measured hardness values were compared with the estimated hardness values. The predicted and experimentally determined hardness along the length of the specimen has been shown to be in good agreement within ± 3 HRC/HRB.

Keywords Hardness prediction of steels · Jominy end-quench test · Maynier's equation · Inverse heat conduction · Cooling curve · Heat flux

1 Introduction

Steel is a very widely used material in engineering that can be imparted with varying microstructures by varying heat treatment. Alternate solutions are required as traditional methods used to determine hardness of steels are usually time-consuming and are expensive to carry out in laboratories. The Jominy-type end quench is a test used to measure the hardness of steels. It involves heating the test specimen (26 mm diameter and 75 mm length) to its austenitizing temperature (above 850 °C) and end quenching the specimen with water which induces the formation of different microstructures. Hardness is measured along the length of the specimen at

S. V. Bagali · Maruti
Department of Mechanical Engineering, PES University, Bengaluru 560085, India

N. R. Abhaya Simha (✉) · M. P. Sushanth · T. S. Prasanna Kumar · V. Krishna
Process Modelling Research Lab (PMR Lab), Department of PG Studies,
Mechanical Engineering, PES University, Bengaluru 560085, India
e-mail: abhaysimha@pes.edu

determined locations. Hardness decreases as we move away from the quenched end due to the formation of different microstructures depending on the cooling rate.

Nunura et al. [1] presented a correlation between cooling rate, microstructure, and mechanical properties of Jominy end-quenched AISI 1045 steel; the experiment was mainly focused on heating and quenching the steel to different austenitizing temperatures. Mehmet Cakir and Abdullah Özsoy [2] investigated the correlation between the thermal properties and hardenability of Jominy bars quenched with air–water mixture for AISI 1050 steel. The results of water-quenched and water–air-quenched steels were compared at different pressures. Song et al. [3] worked on improving the nonlinear mathematical model for simulating Jominy end-quench curves. Narazaki et al. [4] used the inverse heat method for evaluating the heat transfer coefficient for the quench end and validated it with a simulated model. Taher Ghrib et al. [5] used photo-thermal detection to obtain a correlation between hardness and the determined thermal properties. The Jominy hardness profile by training an artificial neural network with 4000 examples was obtained by Vermeulen [6]. A relation between magnetic Barkhausen noise and hardness for Jominy quench tests was obtained at low excitation frequency range by Franco et al. [7]. Prasanna Kumar [8] worked on nonlinear inverse heat transfer, coupled with austenite phase transformation, microstructure development, and hardness estimation on mathematical models during quenching of plain carbon steels. A numerical study based on two-dimensional estimation of a convective heat transfer coefficient during Jominy end-quench test was carried out by Le Masson et al [9].

In this study, cylindrical specimens of C25 and EN8 were machined and thermocouples were fixed. Time–temperature data were captured with the help of data acquisition system during end quenching. The surface temperatures and heat-flux values of the specimens were estimated through inverse analysis using the temperature data as input. Also the volume fractions of the microstructure were computed using TmmFE [13]. Empirical formulas developed by Maynier et al. [16] along with rule of mixtures were modified to estimate hardness of specimen at different locations. The estimated hardness was compared with measured hardness and found to be within $\pm 3\text{HRC/HRB}$.

2 Experimental Method

2.1 Specimen Preparation

Cylindrical specimens of C25 and EN8 steels (chemical compositions mentioned in Table 1) of diameter 26 mm and length 75 mm were used. Four thermocouples were placed at specified locations as shown in Fig. 1. Bores of 1.3 mm were drilled at a depths of 17.5, 45, 65, and 71 mm to place the thermocouples. The first three thermocouples are placed at 8.5 mm and the fourth one at 7.5 mm measured radially from the center. The top end of the hole is drilled to 5 mm in diameter and 8 mm in

Table 1 Chemical composition of C25 and EN8

Steel	C	Si	Mn	Ni	Cr	Mo	Cu	V	B	N	S	P
C25	0.25	0.4	0.5	0	0	0	0	0	0	0	0.045	0.045
EN8	0.446	0.187	0.74	0	0	0	0	0	0	0	0.033	0.022

length and counterbored with the 3.3 mm diameter and 5 mm length to facilitate the use of collets to secure the position of thermocouples.

2.2 Experimental Setup

The apparatus consists of a tubular furnace to heat the specimen to its austenitizing temperature, a quenchant sump, a pump with a flow-regulating valve and a tank to maintain pressure head which feeds a nozzle to create a steady water jet as shown in Fig. 2.

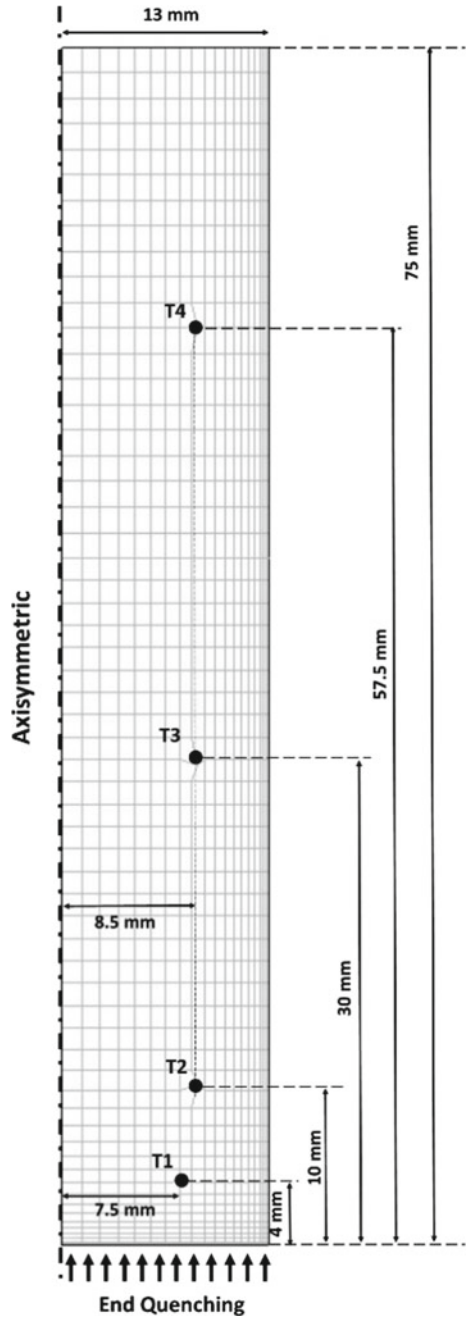
2.3 Experimental Procedure

The specimen is initially heated to its austenitizing temperature (850 °C) inside the furnace in an inert atmosphere maintained by supplying nitrogen gas at a positive pressure to avoid surface scaling. It is maintained at the same temperature for fifteen minutes to ensure soaking. The quench probe is then lowered to 1 in. above the nozzle which quenches the circular flat end of the specimen with a jet, which in this case is a water jet as shown in Fig. 3. Cooling curves are obtained at the specified thermocouple locations using the data acquisition (DAQ) system with a time interval of 0.5 s. After cooling, the specimen was cut at the thermocouple locations and the hardness was measured at multiple points along the cross sections of the specimen using Rockwell hardness tester.

3 Inverse Heat Conduction Model

The unknown heat-flux transients at the quenched surface of the probes were estimated from the measured temperature at selected interior points during quenching using an inverse method. The serial inverse heat conduction algorithm developed by Prasanna Kumar [10] was used to estimate the heat-flux components at the probe–quenchant interface. The algorithm is capable of computing the multiple heat fluxes in a serial manner as opposed to simultaneous estimation. The complete mathematical model and its implementation details of the serial inverse algorithm

Fig. 1 2D axisymmetric meshed model of the specimen



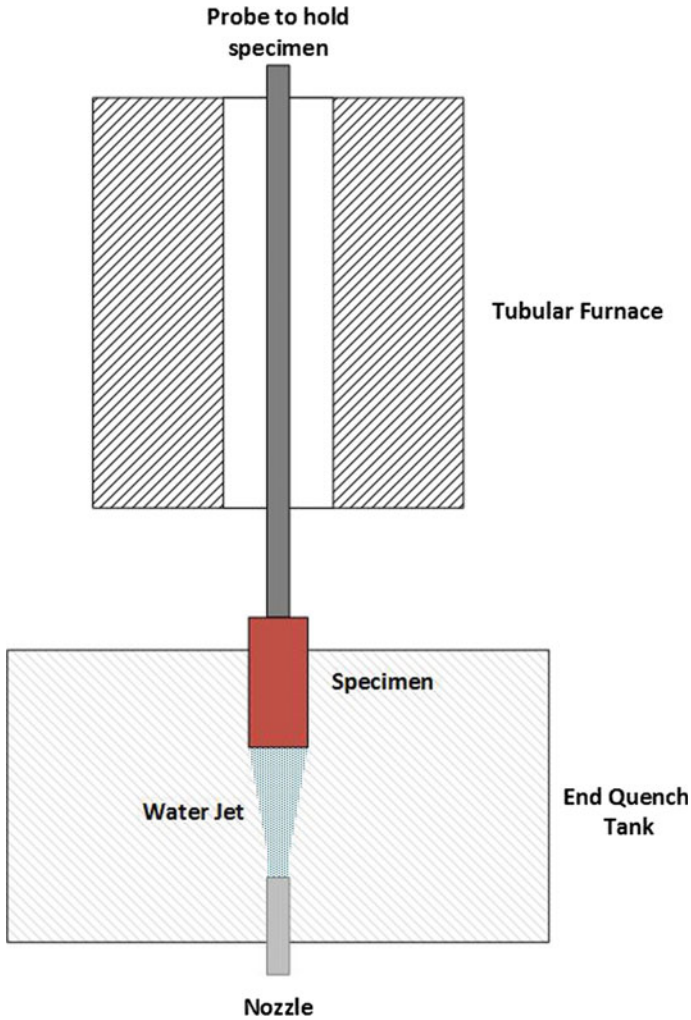


Fig. 2 Experimental setup

for heat-flux estimation in multiple segments have been discussed elsewhere [10–13] and is briefly summarized in this section in regard to the quenching problem. The equation that governs the 2D transient heat conduction within the solution domain in the (r, z) coordinate system can be expressed as follows:

$$\frac{\partial}{\partial r} \left(k \frac{\partial T(r, z, t)}{\partial r} \right) + \frac{\partial}{\partial z} \left(k \frac{\partial T(r, z, t)}{\partial z} \right) = \rho c \frac{\partial T(r, z, t)}{\partial t} \quad (1)$$

With the following initial condition:

Fig. 3 Photograph of end quenching



$$T(r, z) = T_{\text{soak}} \text{ at } t = 0$$

and the following boundary condition (unknown):

$$-k \left(\frac{\partial T}{\partial r} n_r + \frac{\partial T}{\partial z} n_z \right) = q(r, z, t)$$

The Eq. (1) with the unknown boundary condition at the bottom (Fig. 1) of the specimen was solved by FEM to obtain the converged heat-flux values at every time step. Simultaneously, austenite decomposition was modeled based on the temperature distribution at the end of each time steps. The InverseSolver module of TmmFE software [13] was used to solve the equation.

A cylindrical axisymmetric FE model was created and discretized using a mesh of 1200 elements (4-node quadratic) for a total of 1281 nodes. Convective heat flux of $100 \text{ W/m}^2\text{K}$ and radiative emissivity of 0.8 was assigned to the lateral boundaries. Figure 1 shows the finite element (FE) mesh of the specimen. Material properties data (density, thermal conductivity, specific heat, latent heat, and enthalpy) and time–temperature transformation (TTT) diagram data (as shown in Fig. 4) obtained from JMatPro software [15] for C25 and EN8 steels were assigned to the finite element model.

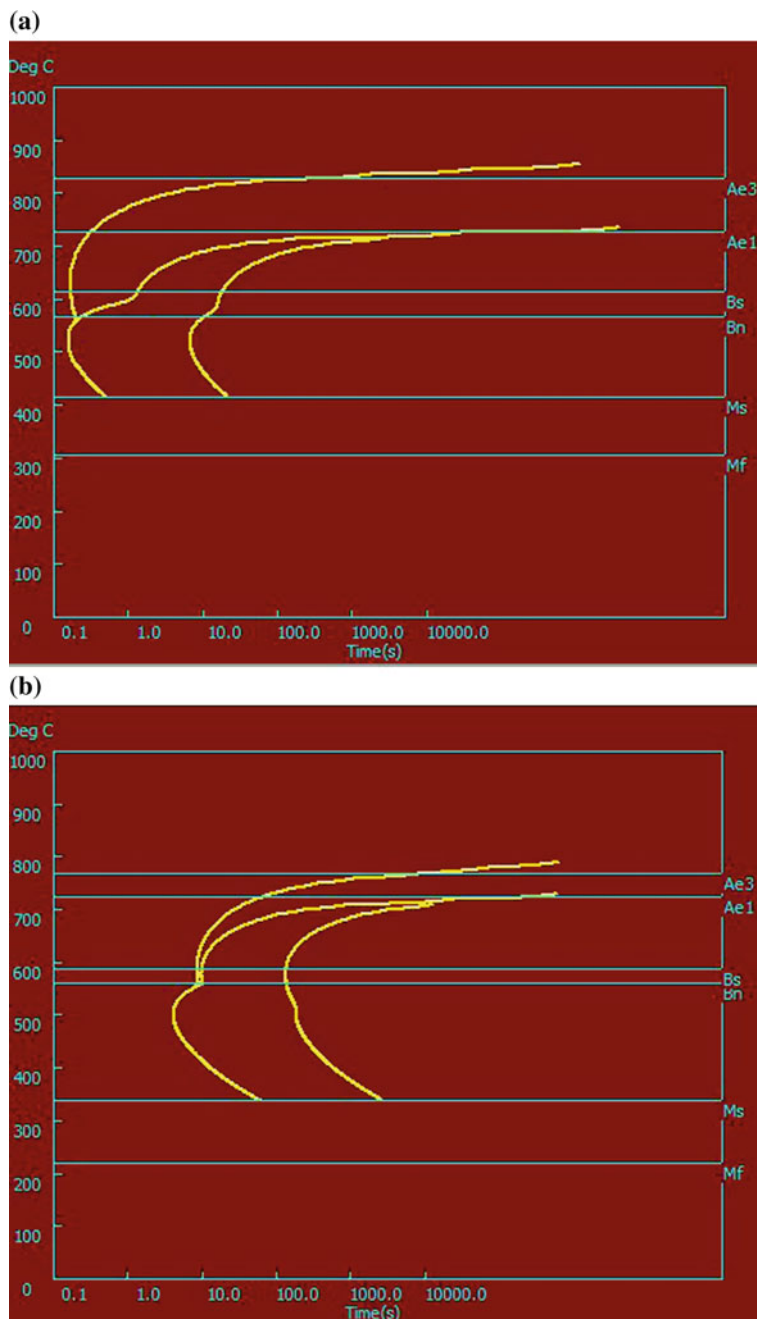


Fig. 4 TTT diagram a C25 and b EN8

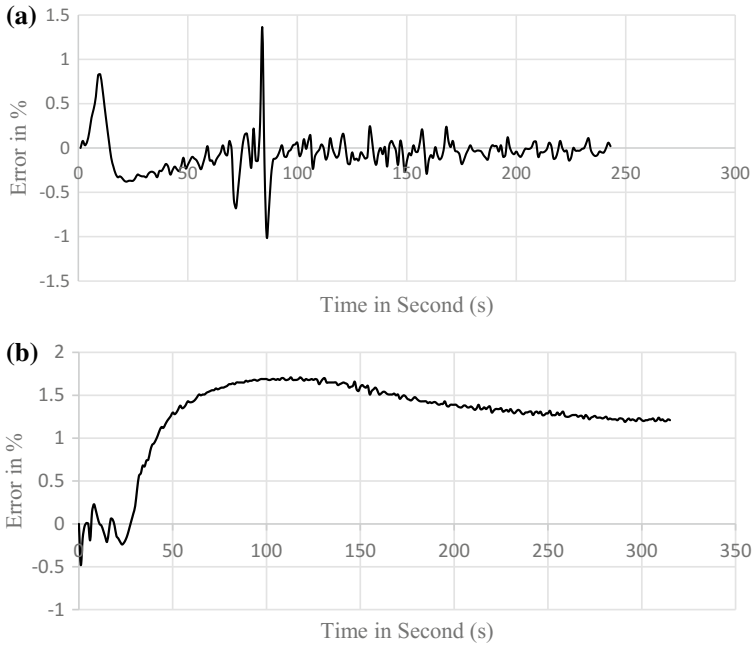


Fig. 5 Error in estimated and measured temperatures at TC1 **a** C25 and **b** EN8

4 Results and Discussion

4.1 Experimental Data

The temperatures were recorded at four thermocouple locations (T1, T2, T3, and T4). Cooling rates were seen to decrease from T1 to T4. The hardness was measured using the Rockwell hardness B-scale (HRB) for C25 steel and Rockwell hardness C-scale (HRC) for EN8 steel. The average hardness was calculated from readings across the cross section. The variation in error between the simulated and experimental cooling curves of C25 and EN8 as time progresses is found to be less than 2% as shown in Fig. 5.

4.2 Hardness Calculation

Using the Maynier equation (Eqs. 2, 3, and 4), hardness of different phase bands was calculated using the chemical composition of the steels (Table 1). Maynier's mixture rule [14] was modified as in Eq. (5) to determine the Vickers hardness at the said thermocouple locations.

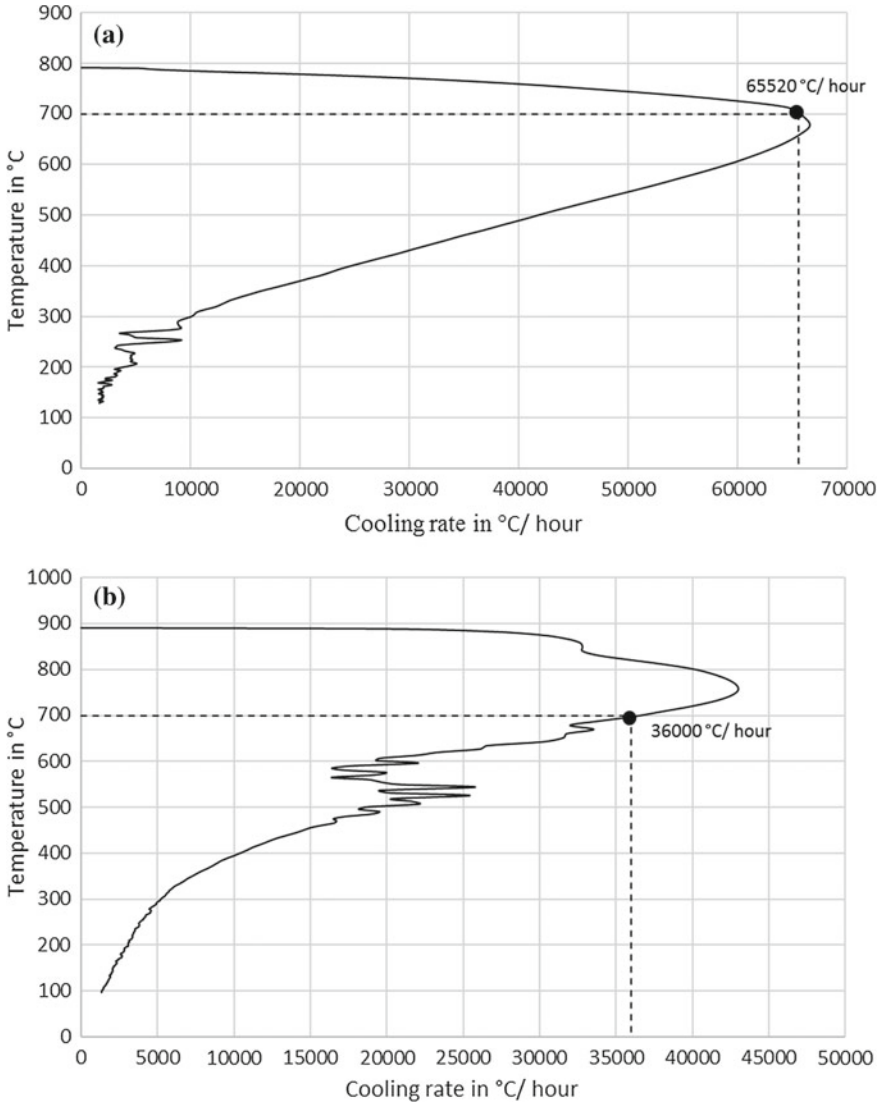


Fig. 6 Cooling rate curve versus temperature at 700 °C **a** C25 and **b** EN8

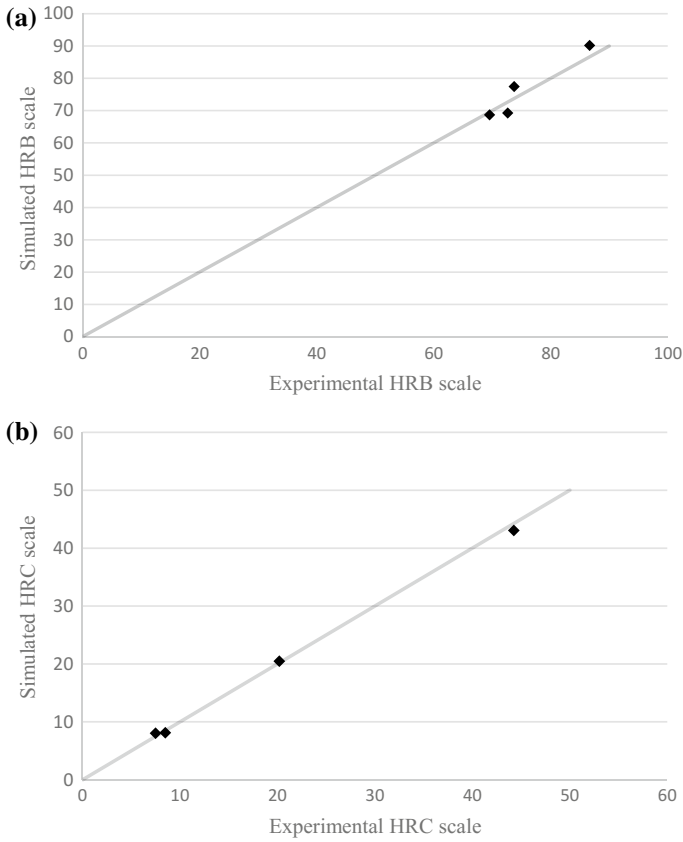


Fig. 7 Comparison of simulated and experimental hardness **a** C25 and **b** EN8

$$HV_m = 127 + 949C + 27Si + 11Mn + 8Ni + 16Cr + 21 \log (V_r) \quad (2)$$

$$HV_b = -323 + 185C + 330Si + 153Mn + 65Ni + 144Cr \\ + 191 Mo + (89 + 53C - 55Si - 22Mn \\ - 10Ni - 20Cr - 33Mo) \log (V_r) \quad (3)$$

$$HV_{f-p} = 42 + 223C + 53Si + 30Mn + 126Ni + 7Cr + 19Mo \\ + (10 - 19Si + 4Ni + 8Cr + 130V) \log (V_r) \quad (4)$$

$$HV = 0.95X_m * HV_m + 0.8X_b * HV_b + 0.9 * (X_f + X_p) * HV_{f-p} \quad (5)$$

where HV_m , HV_b , and HV_{f-p} are Vickers hardness values for martensite, bainite, and ferrite–pearlite mixture, respectively. X_m , X_b , X_f , and X_p are volume fractions of martensite, bainite, and ferrite and pearlite phases, respectively, predicted by

InverseSolver. V_r is the cooling rate at 700 °C per hour (V_r calculation at T3 location is shown in Fig. 6).

Vickers hardness values obtained from Eq. (5) were converted to the Rockwell hardness scale and compared with experimental results. Figure 7 shows the comparison of experimental hardness and predicted hardness of the C25 and EN8 steels.

5 Summary and Conclusion

In this paper, the hardness of C25 and EN8 steels was estimated during end quenching. A 2D axisymmetric heat conduction coupled with austenite decomposition model was used to obtain the volume fractions of microstructure distribution. Maynier's equation was modified to predict the hardness at specific locations and compared with experimental results which were found to be in good agreement.

Further analysis can be carried out by applying the modified Maynier equation obtained in this literature with other composition of steels and compared it with experimental results.

References

1. Nunura CRN, dos Santos CA, Spim JA (2015) Numerical—experimental correlation of microstructures, cooling rates and mechanical properties of AISI 1045 steel during the Jominy end-quench test. *Mater Des* 76:230–243
2. Mehmet Cakir F, Abdullah Özsoy S (2011) Investigation of correlation between thermal properties and hardenability of Jominy bars quenched with air-water mixture for AISI 1050 steel. *Mater Des* 32:3099–3105
3. Song Y-P, Liu G-Q, Liu S-X, Liu J-T, Feng C (2007) Improved nonlinear equation method for numerical prediction of jominy endquench curves. *J Iron Steel Res* 14(1):37–41
4. Narazaki M, Kogawara M, Shirayori A, Fuchizawa S (2003) Evaluation of heat transfer coefficient in jominy end-quench test. In: *Proceedings of the fourth international conference on quenching and the control of distortion*, pp 97–104
5. Taher Ghrib F, Fatah Bejaoui S, Abdelwahheb Hamdi S, Nouredine Yacoubi S (2008) Correlation between thermal properties and hardness of end-quench bars for C48, 42CrMo4 and 35NiCrMo16 steels. *Thermochim Acta* 473:86–91
6. Vermeulen WG, van der Wolk PJ, de Weijer AP, van der Zwaag S (1996) Prediction of jominy hardness profile of steels using artificial neural networks. *JMEPEG* 5:57–63
7. Franco FA, González MFR, de Campos MF, Padovese IR (2013) Relation between magnetic barkhausen noise and hardness for jominy quench tests in SAE 4140 and 6150 steels. *J Non-destruct Eval* 32:93–103
8. Prasanna Kumar TS (2012) Coupled analysis of surface heat flux, microstructure evolution, and hardness during immersion quenching of a medium carbon steel in plant conditions. *Mater Perform Charact* 1(1)
9. Le Masson P, Loulou T, Artioukhine E, Rogeon P, Carron D, Quemener J-J (2002) A numerical study for the estimation of a convective heat transfer coefficient during a metallurgical “Jominy end-quench” test. *Int J Therm Sci* 41:517–527
10. Prasanna Kumar TS (2004) A serial solution for the 2-D inverse heat conduction problem for estimating multiple heat flux components. *Numer Heat Transfer, Part B Fundam* 45(6):541–563

11. Prasanna Kumar TS, Kamath HC (2004) Estimation of multiple heat-flux components at the metal/mold interface in bar and plate aluminum alloy castings. *Metall Mater Trans* 35B: 575–585
12. Arunkumar S, Sreenivas Rao KV, Prasanna Kumar TS (2008) Spatial variation of heat flux at the metal–mold interface due to mold filling effects in gravity die-casting. *Int J Heat Mass Transf* 51(11–12): 2676–2685
13. TmmFE by TherMet Solutions Homepage, <http://www.thermetsolutions.com>, last accessed 2018/05/05
14. Li MV, Niebuhr DV, Meekisho LL, Atteridge DG (1998) A computation module for the prediction of steel hardenability. *Metall Mater Trans* 29B(3):661–672
15. JMatPro by SENTE Software, Homepage, <https://www.sentesoftware.co.uk>, last accessed 2018/05/05
16. Maynier P, Dollet J, Bastien P (1978) Hardenability concepts with applications to steels. In: Doane DV, Kirkaldy JS (eds) *AIME*, New York, NY, pp 518–544

Service Quality in Indian SMEs: Developing a Dual Directional Scale at Supplier–Manufacturer Dyad



Surjit Kumar Gandhi, Anish Sachdeva and Ajay Gupta

Abstract This paper investigates the role played by service quality at supplier–manufacturer dyad in small–medium manufacturing units and presents a model to establish that contribution of both the supplier and manufacturer towards service quality leads to satisfaction followed by loyalty. The research process for this study comprises a literature survey in conjunction with exploratory interviews with practitioners, and a structured interview schedule conducted with 120 respondents working in different small–medium manufacturing units in North India. SME has been employed for analysing the data thus collected. The paper has developed dual directional scales to evaluate service quality at supplier–manufacturer dyad and has also tested a set of four propositions. A model showing linkages of manufacturer (manufacturing unit’s) service quality with supplier unit’s service quality leading to satisfaction and loyalty is finally developed. The model is empirically tested and is found to be fit. This study would be of interest to SME managers particularly engaged in ‘purchase’ function and researchers working on inter-firm supply chains in such units. This study recommends forming strong collaborative relationships with suppliers to achieve a win-win situation.

Keywords Service quality · SMEs · Service quality factors · Supplier · EFA · CFA · SEM

1 Introduction

The fierce competition of today’s marketplace is forcing small- and medium-sized enterprises (SMEs) to reshape their strategies in order to curtail overall cost and

S. K. Gandhi (✉) · A. Sachdeva · A. Gupta
Department of IPE, Dr. B. R. Ambedkar NIT Jalandhar, Jalandhar, India
e-mail: skgandhi21@gmail.com

A. Sachdeva
e-mail: asachdeva@nitj.ac.in

A. Gupta
e-mail: guptaa@nitj.ac.in

© Springer Nature Singapore Pte Ltd. 2019

K. Shanker et al. (eds.), *Advances in Industrial and Production Engineering*, Lecture Notes in Mechanical Engineering, https://doi.org/10.1007/978-981-13-6412-9_15

cut down inefficiencies. Therefore, there is a growing recognition of building and nurturing relationships with supply chain partners for improvements in profitability, serviceability and reduced costs across the supply chain [1]. Purchasing is the ultimate goldmine for success for manufacturing enterprises. Because of the mutual benefits they offer, partnerships or strategic alliances between suppliers and manufacturers (i.e. buyers) have emerged as a popular business trend and are being looked upon as the wave of the future [2].

Managing suppliers is critical to adding value in the supply chain since this function has both internal and external customers [3]. Supplier (external) service quality, SSQ, implies the attitude and demeanour exhibited by staff of the supplier unit in fulfilling the requisitions made by manufacturing unit and what value they place upon continuing the relationship with the unit. On the other hand, manufacturer (internal) service quality, MSQ, implies how efficiently the purchase, inventory and store officials of manufacturing unit facilitate the functioning of its suppliers and what attitudes they hold towards the seller unit [4].

Supplier partnership deals with the long-term relationship between the manufacturing unit and its suppliers, and includes make/buy decisions and managing sourcing function. Small–medium manufacturing units prefer to have few reliable suppliers, and therefore tend to reduce the pool of suppliers, and many-a-times rely on a sole source. In an attempt to regain their competitiveness, these units should adopt the Japanese keiretsu system of manufacturers and suppliers working in lockstep [5]. For supply chain effectiveness, manufacturers and suppliers need to keep costs across the supply chain low so that they result in lower market prices and higher margins. This is akin to gainsharing arrangements wherein everyone who contributes to greater profitability is rewarded.

The inter-firm linkages between the suppliers and small–medium manufacturing units could relate to product, process, service and market, and through these linkages, it is expected that the suppliers will provide necessary support to SMEs and contribute to the process of creating appropriate technologies. In this backdrop, the present research work has been undertaken [6].

The major challenge for SMEs is to understand the role of each member in the supply chain and in the entire delivery system, and to focus upon the immediate customer in the chain to the ultimate customer. By delivering the superior value to ultimate consumers, the chain as a whole achieves the objective of *differential advantage*. This enhances the performance of the chain as a whole as well as delivers results to the individual members of the chain [7].

SME sector in India, once shielded by the government policies of reservation, quota and licence, etc., is facing a number of challenges to survive due to globalization [8]. In order to gain the competitive edge, such units should slowly make transition from their total offering as a manufacturer dealing with tangibles only and must include services, and finally, outgrow into relationship-based offerings [9]. Studies on Indian SMEs are largely confined to competitive priorities, manufacturing strategies, capacity building, and innovation trends. However, the ‘service dominance perspective’ that establishes the importance of intangible aspects such as service quality has been largely unexplored [10].

Researchers argue that service quality has a strong positive impact on customer satisfaction. A number of empirical studies indicate a positive influence of SQ on ‘customer loyalty’ too. Service quality is also linked to behavioural outcomes as word of mouth, complaint, recommending and switching [11–13].

In this paper, a focused review of literature was made to develop an instrument for conducting a questionnaire survey. Application of EFA, CFA and SEM brings out a model to answer these questions.

2 Literature Review

Collaboration is a set of management levers that enables cost savings through transfer of best practices, improves effectiveness of decision making through sharing of opinion, induces innovation through cross-pollination of ideas and enhances capacity of collective action [14]. Since much of the value addition occurs in the upstream stages (i.e. supply function) of the supply chain, manufacturers need to manage business-to-business relationships (B2B) with their suppliers. Coordination, collaboration, commitment, communication, trust, flexibility, dependence, joint engineering and information technology-based integration are possible if partners are contributing equal value [15]. To manage collaborative relationships, it is critical to measure performance on service quality scales. Feedbacks on customer requirements, capabilities of the manufacturing unit and its suppliers, and ongoing collaborations are vital as they reveal the inner working of collaborative processes [16].

Though the performance of supplier firms is quite a well-researched area in literature, empirical researches on the application of service quality determinants at supplier–manufacturer interface are nascent. Thus, there is a major scope for visualizing the attributes of supplier and manufacturer service quality, which also justifies need of developing a model to establish their linkages with satisfaction and loyalty. Various issues related to relationship management in supply chain with respect to the supply function are enlisted in Table 1.

Table 1 Relationship issues at the supplier–manufacturer dyad

Type	Bilateral
Characteristics	Strength, closeness, physical proximity
Dimensions	Coordination, collaboration, commitment, trust, communication, flexibility, dependence
Development	Strategic/operational alignment
Infrastructure	Partner selection intangible criteria, tangible criteria
Information exchange	Information systems, knowledge transfer

PZB in their pioneering work identified five components of service quality, viz. reliability, assurance, tangibles, empathy and responsiveness. These five dimensions used to evaluate service quality are called SERVQUAL dimensions [17]. Carr pointed a major weakness of SERVQUAL scale by arguing that it overlooks equity theory for selection of SQ determinants, though it is well established that SME suppliers as well as manufacturers do evaluate service by way of ‘fairness’ is often evaluated in business encounters [18]. The hybrid scale comprising FAIRSERV, in conjunction with SERVQUAL, is considered suitable for this study, since its outcome parameters are satisfaction and loyalty intentions. An interview schedule is structured on the basis of five determinants (RATER) of PZB’s SERVQUAL scale and draws one determinant, viz. ‘Systematic Fairness (F)’ from Carr’s FAIRSERV model. Thus, using features of both the existing scales, an attempt has been made to bring out a new metric, namely RATERF scale in this study.

3 Research Methodology

Figure 1 represents the sequence followed for determining factors of MSQ and SSQ, followed by establishing their linkages with satisfaction and loyalty.

The questionnaire was generated using with a focus on purchase–supply-related issues using newly constructed RATERF scale. The questionnaire was refined after focus group discussion with five managers working in different SMEs and three academicians with work published in similar areas.

The questionnaire thus emerged comprised four sections as follows:

- Section A comprises 21 items related to service quality offered by the manufacturer towards supplier (MSQ) and one question to directly obtain overall manufacturer service quality (OMSQ).
- Section B consists of 24 items related to service quality delivered by supplier (SSQ) and one question to directly obtain overall supplier service quality (OSSQ).
- Section C consists of *two* outcome variables, viz. *satisfaction* (mapped by two items) and *loyalty* (mapped by three items).
- Section D focuses on gathering the demographic information.

The data was collected from prospective SMEs engaged in one or other manufacturing activity, and having personal rapport with researchers. Prior to making personal visits for conduct of interview(s), respondent units were mailed cover letter along with questionnaire stating the objective of survey. The CEOs of units directed the researcher to important functionaries to collect the responses. Most of the responses were got filled-in through interview schedule manner where respondent was sitting with researcher at the time of filling the response sheet. However, in a few cases (14 nos.), after having a brief session with the researcher, the respondents required few days to fill the questionnaire and returned response sheet to the researcher during the subsequent visits. The objective of making personal visits to the units was to

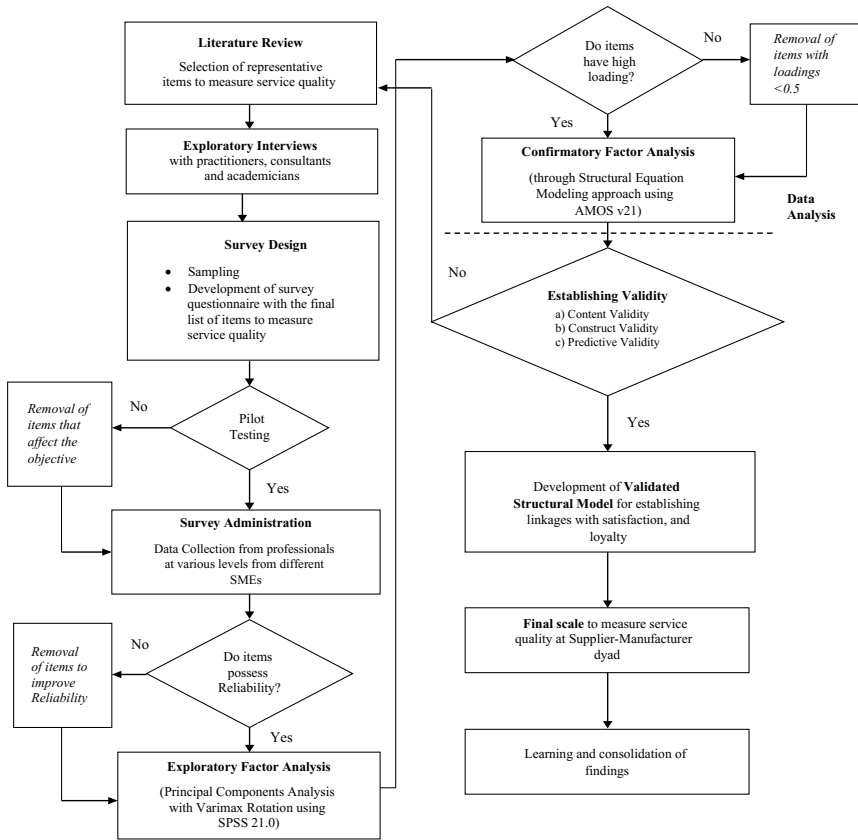


Fig. 1 Flow chart of research methodology adopted for measurement and modelling of service quality at supplier–manufacturer interface

increase the response rate besides getting quality information. This approach has been endorsed by several other researchers in contemporary studies [11–13].

The method of snowball sampling was used to execute this survey. The respondents were top executives of supplier firms working for small–medium manufacturing units located in North India. Respondents were asked to respond their opinions of SQ that was being offered to them (and delivered by them) by manufacturing units (supplier unit) on Likert scale ranging from 1 (Strongly disagree) to 5 (Strongly agree). The researcher visited 165 units in all but, however, was able to obtain responses from 120 units. The response rate (73%) is still considered quite satisfactory. Most of the respondents were top functionaries like proprietors themselves, managing directors, plant heads, works managers, general managers, sales managers, logistics in-charge, shift engineers, HoDs and sections heads, etc.

4 Data Analysis

Since the factors of the scale along with indicators of MSQ and SSQ are synthesized from similar works reported in the SQ literature, it is essential to check the scales for reliability, EFA and CFA.

4.1 Reliability Analysis

The reliability of both MSQ and SSQ scales was analysed using Cronbach's alpha coefficient using IBM SPSS v21, and the output is shown below in Table 2.

4.2 Exploratory Factor Analysis (EFA)

EFA is a multivariate statistical technique commonly used to explore the dimensionality of a measurement. The main objective of using EFA in this paper is to group the factors into various subgroups for making further analysis simpler. However, prior to that, Bartlett's test is used to assess the suitability of conducting factor analysis. To check whether the sample size is adequate or not, Kaiser–Meyer–Olkin (KMO) test of sample adequacy ($N = 120$, in this case) and significance value was performed. The value of KMO greater than 0.6 with the value for significance less than 0.005 indicates that data size is sufficient for grouping the various relevant factors. The result of Bartlett's test and the KMO value are depicted in Table 3.

The results being significant thus indicate the suitability for factor analysis. Application of EFA resulted in the extraction of five factors each for MSQ and SSQ scales, explaining 74.802 and 73.301% of the variance, respectively. Output of EFA obtained using SPSS v21 is presented in Tables 4 and 5.

Table 2 Reliability analysis of items in MSQ and SSQ scales

Service quality measurement	MSQ items ($n = 21$)	SSQ items ($n = 24$)
Value of α	0.926	0.897
Finding	Quite Good [19]	

Table 3 KMO and Bartlett's test of sphericity

Scale at manufacturer–supplier dyad		MSQ	SSQ
KMO measure for sampling adequacy		0.888	0.880
Bartlett's test of sphericity	Approx. chi-square	2101	2221
	df	210	231
	Sig.	0.000	0.000

Table 4 Communalities, factor structure and loadings for items of MSQ

S. No.	Factors and associated items	Communalities	Factor loadings
<i>Assurance</i>			
1.	Long-term collaborative relationship	0.859	0.879
2.	Purchase orders are timely and accurate	0.851	0.881
3.	Has modern and adequate physical facilities	0.851	0.882
4.	Possesses right tools and equipment	0.821	0.890
5.	Terms and conditions are fair with supplier	0.735	0.822
6.	Confidentiality in transactions	0.698	0.699
<i>Communication</i>			
7.	Honest in providing information/data	0.792	0.854
8.	Pays attention to suppliers' views	0.540	0.667
9.	Shares information related to inventory	0.647	0.756
10.	Inform changes in manufacturing schedule	0.760	0.833
11.	Prompt feedback about quality of products	0.816	0.853
12.	Have latest IT infrastructure	0.635	0.761
<i>Alignment</i>			
13.	Flexible approach in dealing with suppliers	0.693	0.736
14.	Shares company's future plans	0.819	0.820
15.	Equitable sharing of responsibilities	0.803	0.811
16.	Shares knowledge/training/innovation base	0.863	0.852
17.	Based at convenient location	0.865	0.869
<i>Responsiveness</i>			
18.	Willingness to share supplier problems	0.698	0.814
19.	Supplier's queries are solved promptly	0.604	0.735
20.	Respect and positive attitude for supplier	0.730	0.828
21.	Values convenience of suppliers	0.630	0.714

As shown in above Table 4, the extracted factors were named as: Assurance, Communication, Alignment and Responsiveness. All the items have significant communalities (more than 0.50) and significant factor loadings (more than 0.55) [19]. Internal reliability of the items of the various factors of the MSQ scale is also examined using the Cronbach alpha coefficient and ranges from 81.4 to 94.7% and hence is acceptable [20].

Likewise on the SSQ scale in Table 5, the five factors were named as: *Credibility*, *Relationship*, *Alignment*, *Understanding* and *Dependability*. All the items have significant communalities and factor loadings. The reliability score for each factor ranges from 83.6 to 95.1% and hence is acceptable.

Table 5 Communalities, factor structure and loadings for items of SSQ

S. No.	Factors and associated items	Communalities	Factor loadings
<i>Credibility</i>			
1.	Supplier has strong market reputation	0.859	0.879
2.	Supplier has financial strength	0.851	0.881
3.	Flexibility to change product design	0.851	0.882
4.	Has required knowledge/expertise/skills	0.821	0.890
5.	Competent and technically sound employees	0.735	0.822
6.	Supplier is innovative in operations	0.698	0.699
7.	Supplier has latest IT infrastructure		
<i>Relationship</i>			
8.	Long-term relationship with your unit	0.677	0.622
9.	Flexible terms and conditions	0.736	0.702
10.	Supplier has willingness to serve your unit	0.645	0.646
11.	Supplier's employees are polite and courteous	0.689	0.698
12.	Supplier is fair in dealings with your unit	0.720	0.700
13.	Terms and conditions with your unit are fair	0.763	0.686
<i>Alignment</i>			
14.	Right tools/equipment/technology	0.712	0.812
15.	Supplier has modern and certified facilities	0.775	0.859
16.	Supplier is easily approachable	0.695	0.815
17.	Quick solutions to failures/complaints	0.706	0.884
<i>Understanding</i>			
18.	Understands requirements of your unit	0.689	0.778
19.	Supplier values your convenience	0.726	0.827
20.	Shares work-related information	0.682	0.801
21.	Honest in providing information/access	0.646	0.753
<i>Dependability</i>			
22.	Right quality and quantity in right time	0.848	0.857
23.	Charges minimum price for supplies	0.812	0.849
24.	Maintains confidentiality in operations	0.766	0.836

4.3 Confirmatory Factor Analysis (CFA)

CFA is undertaken to further purify the scales for measuring MSQ and SSQ. CFA model is run using SPSS AMOS v21, for four individual factors describing MSQ scale and five factors describing SSQ scale, with respective items. Table 6 shows the key model fit indices for the individual factors.

Table 6 Key fit indices for measurement model of MSQ and SSQ scales

Factors	Cmin/df	GFI	NFI	CFI	RMSEA
Assurance	1.346	0.982	0.991	0.998	0.054
Communication	1.337	0.970	0.978	0.994	0.053
Alignment	0.760	0.990	0.994	1.000	0.000
Responsiveness	0.367	0.997	0.995	1.000	0.000
Credibility	0.496	0.987	0.994	1.000	0.000
Relationship	0.968	0.982	1.000	1.000	0.000
Alignment	3.232	0.974	0.972	0.980	0.037
Understanding	0.529	0.996	0.994	1.000	0.000
Dependability	–	1.000	1.000	1.000	–

Since all the GFI values are greater than 0.9, the validation of individual factors of CFA models is established [20].

4.3.1 CFA Matrix Purification for MSQ and SSQ Scales

For purification of MSQ scale, three iteration runs of CFA were performed to yield acceptable values of key GFIs. During this process, 5 items out of initial 21 items were deleted due to low explained variance. The five items were:

1. the manufacturing unit maintains confidentiality in transactions;
2. the unit possesses the latest information technology infrastructure;
3. the unit pays attention to suppliers' views in dealings;
4. the unit has equitable sharing of responsibilities with the supplier firm; and
5. the unit is based at convenient and approachable location.

Likewise during purification of SSQ scale, five iterations of CFA were undertaken and during this process, one dimension, viz. *Alignment*, completely disappeared. In total, 11 out of initial 24 items were removed owing to low variance. The deleted items were:

1. the supplier has financial strength
2. the supplier has required knowledge/expertise/skills
3. the supplier firm has latest infrastructure;
4. the supplier has willingness to serve your unit
5. the supplier is fair in dealings with your unit
6. terms and conditions with the unit are reasonable
7. the supplier uses right tools/equipment/technology
8. the supplier has modern and certified facilities
9. the supplier is easily approachable
10. the supplier has quick solutions to failures/complaints
11. the supplier maintains confidentiality in operations

5 Conceptual Model and Analysis

Since this study aims at examining the impact of (a) *Manufacturer service quality* on *Supplier service quality*, and (b) *Supplier service quality* on *Satisfaction*, and *Loyalty*, the conceptual structural model for this relationship is depicted in Fig. 2.

where

γ : Path Coefficient from MSQ \rightarrow SSQ

$\beta_1, \beta_2, \beta_3$: Path Coefficients from SSQ \rightarrow Satisfaction; Satisfaction \rightarrow Loyalty, SSQ \rightarrow Loyalty, respectively

$\zeta_1, \zeta_2, \zeta_3$: Residual error in measurement of SSQ, Satisfaction, and Loyalty

The following four testable hypotheses were formulated:

Proposition 1: *MSQ* is a source of *SSQ*.

Proposition 2: *Supplier service quality* is a source of *Satisfaction*.

Proposition 3: *Satisfaction* is a source of *Loyalty*.

Proposition 4: *Supplier service quality* is a source of *Loyalty*.

The hypotheses developed for testing these relationships are enumerated in Table 7.

Figure 3 depicts the pictorial representation of various path estimates of the model using AMOS v21.

Various path estimates among latent variables of the model are depicted in Table 8. The positive signs of the parameters represent that paths between the latent variables are in line with hypothesized relationships.

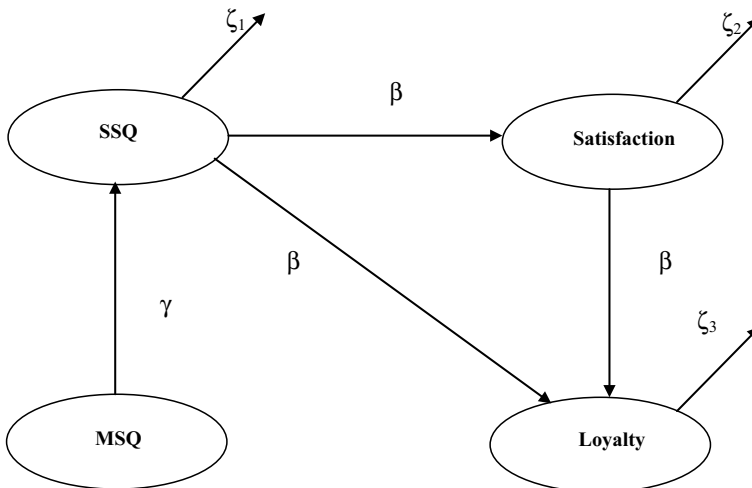


Fig. 2 Conceptual structural model

Table 7 Null and alternative hypotheses formulated for testing relationships

S. No.	Null hypothesis (H ₀)	Alternative hypothesis (H _a)
H ₁	H ₀ 1: Path coefficient γ is not significantly different from 0	H _a 1: <i>MSQ</i> is positively linked to <i>SSQ</i>
H ₂	H ₀ 2: Path coefficient β_1 is not significantly different from 0	H _a 2: <i>SSQ</i> is positively linked to <i>Satisfaction</i>
H ₃	H ₀ 3: Path coefficient β_2 is not significantly different from 0	H _a 3: <i>Satisfaction</i> from the <i>supplier</i> is positively linked to <i>Loyalty</i>
H ₄	H ₀ 4: Path coefficient β_3 is not significantly different from 0	H _a 4: <i>SSQ</i> is positively linked to <i>Loyalty</i>

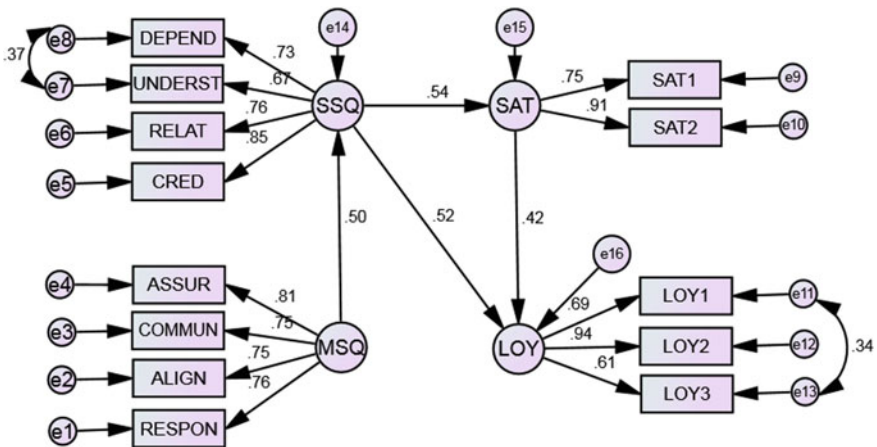


Fig. 3 Path estimates of the conceptual model

Table 8 Results for structural relationship in the model

Path	Estimate	t value*	Conclusion
MSQ to SSQ	0.50	4.241	Supported
SSQ to satisfaction	0.54	6.178	Supported
SSQ to loyalty	0.52	3.568	Supported
Satisfaction to loyalty	0.42	3.770	Supported

*-1.96 < t < 1.96 indicate that parameter is not significantly different from zero at 5% level of significance

6 Conclusions

The present study was intended to study (a) *Service quality* offered by the manufacturing unit (MSQ) towards facilitation of working of its supplier; (b) *Supplier service quality* (SSQ) delivered by supplier; and (c) the relationship of these constructs, i.e. MSQ and SSQ with *satisfaction* and *loyalty* measures. The attributes identified and propositions tested by this research can help practitioners and researchers in further appreciating the SQ issues relating to the purchase–supply function in manufacturing SMEs. This paper also comes out with a set of four hypotheses as enumerated in previous section at supplier–manufacturer interface. Some of the typical benefits of the proposed scales are as follows:

- i. The proposed structure fills the gaps that exist in the conceptualization of service quality issues related to purchasing and supply functions in small–medium enterprises of emerging economies like India. The study brings out useful determinants (four each) to measure both MSQ and SSQ. The mean scores obtained on individual questionnaire items call attention of managers to strengthen the weak areas.
- ii. The MSQ and SSQ scales thus developed can also be utilized as diagnostic tools which can be used as benchmarks to identify excellent/poor performance of different functions within a single buyer/supplier unit. Further improvements shown by the departments/subunits can be compared from period to period.
- iii. The study also derived linkages between *MSQ* and *SSQ* with *satisfaction* and *loyalty* based on structural equation modelling. Operations improve process and design quality, reduce waste, fine-tune internal processes and develop synchronized linkages with suppliers and distributors, and thereby achieve operational efficiencies. By way of cost reduction and increase in product and service reliability, these operational efficiencies improve the attractiveness of the products and services. In the market, improved service quality enhances satisfaction and loyalty of suppliers, and lures them away from competitors who are perceived low in service quality.
- iv. Thus, to achieve loyalty, it is vital for supply chain stakeholders to coordinate, synchronize and integrate their activities to produce desired outputs by incorporating service quality initiatives.

However, these findings can be extended to add distributor, retailer and end user's perspective. Traditionally, SQ-driven operations have been set aside by managers in such units with a wrong prejudice that transaction-specific opportunistic approach may work best for SMEs. In the supply of raw materials, the quality of service is a major factor in competition. This may be more relevant in the SME clusters where manufacturers produce intrinsically similar products [21]. This study demonstrates that high service quality is increasingly important as a tool which is used by the supplier towards their manufacturers. The service quality provided by the supplier and manufacturer to each other helps in establishing close relationships which are important in creating mutual commitment and understanding. Various empirical studies on the supply function demonstrate that satisfaction is derived from relationships

between the supplier and the manufacturer. The findings of this study are in line those of other scholars who report that satisfaction results from satisfaction with products and services and satisfaction with various facets of the manufacturing organization (i.e. manufacturers) such as financial or social aspects [22].

In order to compete globally, SME units need to benchmark themselves against quality standards and practices of small manufacturers in countries such as USA, the European Union and Japan. Nevertheless, in their quest for excellence, these units should evolve at a fast pace, and shift from rigid traditional structure to more responsive and customer-centric business models, replacing vertical business process with horizontal business processes so as to increase organizational and process flexibility, and sharing information with their stakeholders and coordinate processes leading to effective and timely decision making and responsiveness to customer needs.

In a nutshell, the honest sharing of operational information, integrating supply chain strategy, promptness in handling queries or failures, meeting deadlines, maintaining secrecy in dealings, flexibility in terms and conditions as per requirements, and preference for long-term collaborative relationship are few attributes that need to be incorporated at various supplier–manufacturer dyad of the supply chain.

At this point, it is essential to offer a caveat that some scholars have suggested that SME managers, instead of building relationships with suppliers, still adhere to practices such as competition between suppliers to drive down prices, and weeding out suppliers who do not provide competitive prices. In the case of logistics-based services, there is often a dichotomy in what manufacturers say that they consider as desirable (relationship with supplier), and what they actually practice (transaction-specific behaviour). However, this dichotomy has so far not been resolved in this study.

References

1. Kannan VR, Choon TK (2003) Attitudes of US and European managers to supplier selection and assessment and implications for business performance. *Benchmarking Int J* 10(5):472–489
2. Gupta TK, Singh V (2017) Measurement of service quality of automobile organization by artificial neural network. *Int J Manag Concepts Philos* 10(1):32–53
3. Seth N, Deshmukh SG, Vrat P (2006) SSQSC: a tool to measure supplier service quality in supply chain. *Prod Plan Control* 17(5):448–463
4. Prakash G (2014) QoS in the internal supply chain: the next lever of competitive advantage and organizational performance. *Prod Plan Control* 25(7):572–591
5. DeWitt T, Giunipero LC, Melton HL (2006) Clusters and supply chain management: the Amish experience. *Int J Phys Distrib Logist Manag* 36(4):289–308
6. Holl A (2008) Production subcontracting and location. *Reg Sci Urban Econ* 38(3):299–309
7. Benton WC, Maloni M (2005) The influence of power driven buyer/seller relationships on supply chain satisfaction. *J Oper Manag* 23(1):1–22
8. Saranga H (2009) The Indian auto component industry—estimation of operational efficiency and its determinants using DEA. *Eur J Oper Res* 196(2):707–718
9. Nix N (2001) *Customer service in supply chain management context*. Supply Chain Management, CA; Sage Publications, Beverly Hills

10. Lusch RF, Vargo SL, O'Brien M (2007) Competing through service: insights from service-dominant logic. *J Retail* 83(1):5–18
11. Izogo EE, Ogba IE (2015) Service quality, customer satisfaction and loyalty in automobile repair services sector. *Int J Qual Reliab Manag* 32(3):250–269
12. Yavas U, Benkenstein M, Stuhldreier U (2004) Relationships between service quality and behavioral outcomes: a study of private bank customers in Germany. *Int J Bank Mark* 22(2):144–157
13. Santouridis I, Trivellas P, Tsimonis G (2012) Using ES-QUAL to measure internet service quality of e-commerce web sites in Greece. *Int J Qual Serv Sci* 4(1):86–98
14. Hansen MT, Nohria N (2004) How to build collaborative advantage. *MIT Sloan Manag Rev* 46(1):22
15. Govindan K, Kannan D, Noorul Haq A (2010) Analyzing supplier development criteria for an automobile industry. *Ind Manag Data Syst* 110(1):43–62
16. Jagdev HS, Thoben KD (2001) Anatomy of enterprise collaborations. *Prod Plan Control* 12(5):437–451
17. Parasuraman A, Zeithaml VA, Berry LL (1988) SERVQUAL: a multiple-item scale for measuring consumer perception of service quality. *J Retail* 64(1):12
18. Carr CL (2007) The FAIRSERV model: consumer reactions to services based on a multidimensional evaluation of service fairness. *Decis Sci* 38(1):107–130
19. Nunnally JC, Bernstein IH (1978) Psychometric theory
20. Hair JF Jr, Black WC, Babin BJ, Anderson RE, Tatham RL (2010) SEM: an introduction. In: *Multivariate data analysis: a global perspective*, pp 629–686
21. Mohanty MK, Gahan P, Choudhury S (2014) Why most of the supplier development programs fail in discrete manufacturing—findings from selected Indian discrete manufacturing industries. *Int J Manag Sci Eng Manag* 9(3):201–211
22. Prakash G (2011) Service quality in supply chain: empirical evidence from Indian automotive industry. *Supply Chain Manag Int J* 16(5):362–378

Parametric Investigation into Alumina Nanopowder Mixed EDM of Inconel 825 Alloy Using RSM



Deepti Ranjan Sahu, Amit Kumar, Biplab Kumar Roy and Amitava Mandal

Abstract Nanopowder mixed electrical discharge machining (NPMEDM) is a recent development in the non-traditional machining process. In this process, addition of powder into dielectric increases the spark gap between the electrodes resulting in more number of low intense sparks. Therefore, both the material removal rate (MRR) and surface finish improve. The present work investigates the effect of Al_2O_3 nanopowder mixed EDM oil on various responses like MRR and surface roughness (SR). The Al_2O_3 nanopowder is mixed with EDM oil at a concentration of 0.5 g/L. Pulse duration (T_{on}), peak current (IP) and gap voltage (GV) are taken as the process parameters. The experiment is designed using response surface methodology (RSM), where two sets of experiments have been conducted using two different dielectric conditions (i.e. EDM oil and powder mixed in EDM oil). Analysis of variance (ANOVA) shows that all the three selected parameters are significant for MRR and SR. The study shows that there is considerable increase in MRR and reduction in SR after mixing Al_2O_3 nanopowder in EDM oil. Using field emission scanning electron microscope (FESEM), a detailed study on the surface integrity of the machined surface has been carried out. It has been found that NPMEDM reduced microcracks, microholes, uneven deposit and recast layer thickness of the machined surface to a great extent.

Keywords NPMEDM · RSM · FESEM · MRR · Surface texture

1 Introduction

Currently in many of the applications, superalloys or other materials are mostly used. Inconel 825 is such a nickel based superalloy. Even at very high temperature, it has very good mechanical and chemical properties. They have good resistance to corrosion and oxidation. Because of these properties, they find prominent application

D. R. Sahu (✉) · A. Kumar · B. K. Roy · A. Mandal
Department of Mechanical Engineering, Indian Institute of Technology (ISM),
Dhanbad, India
e-mail: deeptiranjansahoo@yahoo.in

in aerospace industries, food processing industries, chemical and nuclear industries, components of furnace, moulds and dies, heat-treated tools and die steels [1, 2]. But poor thermal conductivity, high hardness and work hardening behaviour are some of its properties that make machining of these materials a challenging job. In conventional machining process, particles of the Inconel 825 workpiece sample get adhered to the tool yielding poor quality surface. Also low rate of material removal, difficulty in generating complex profiles, rapid tool wear, tool life reduction due to heat generation during machining Inconel 825 are some other issues in conventional machining process [1, 2]. Hence, electrical discharge machining (EDM) being a non-contact type thermo-electric process is an alternate method of machining such materials. In this process, a very small gap is maintained between the workpiece and tool electrode while keeping both of them submerged in the dielectric fluid. Very high temperature is generated by the produced sparks which removes material by melting and vaporization [1, 3].

Powder mixed electrical discharge machining (PMEDM) is a variation of EDM process. By adding powder in the dielectric, the overall resistance of the dielectric gets reduced. Therefore, the spark takes place from a higher distance, thereby increasing the spark gap. Apart from this, mixing powder in dielectric helps in widening the spark channel and increasing the number of discharges. This in turn yields better surface finish and dimensional accuracy as compared to conventional EDM [4]. Erden and Bilgin [5] are credited for inception of the research work using powder mixed dielectric. Shalini et al. investigated the effect of low voltage-current, pulse duration, high voltage-current, flushing pressure and pulse off time on MRR, tool wear rate (TWR) and SR by adding Al_2O_3 nanopowder in EDM oil while machining Al-SiC MMC using copper tool on EDM. Box-behnken design was used for designing the experiment. The study revealed that addition of nanopowder increased the MRR and reduced the surface roughness [6]. Talla et al. analysed the effect of adding graphite powder in dielectric fluid while machining Inconel 625 on EDM. A reduction in crater size, crack density, microhardness, tensile stress and recast layer thickness has been observed [7]. Elsitı et al. mixed maghemite nanopowder in the dielectric while machining CoCrMo on micro-EDM for studying MRR, TWR, taper and over-cut and obtained satisfactory result [8]. Karunakaran et al. studied the influence of mixing nanopowders of 5 nm size in the dielectric fluid while machining Inconel 800 nickel based superalloy on EDM. Aluminium, silicon and multiwalled carbon nano tube powders were taken as the powder for NPMEDM. Considerable improvement in the responses was observed for all the powders but multiwalled carbon nano tube was found to be most effective [9]. Gopalakannan et al. while machining aluminium based metal matrix nanocomposite reinforced with nano sized SiC particles on EDM found that MRR became maximum at high value of pulse on time and peak current. Voltage was insignificant for TWR. With rise in pulse current, pulse on and pulse off time, TWR was found to increase. Surface roughness also increased with rise in pulse on time and pulse current [10]. Mohanty et al. in their study, found that for MRR and SR peak current and pulse on time were significant. High MRR was obtained at high values of pulse on time and peak current, and low surface roughness was obtained at low value of peak current and pulse on time. Accuracy and precision of the cut was

high at low values of pulse on time and peak current [11]. Jeykrishnan et al. studied the influence of various process parameters on surface roughness while machining Inconel 825 on EDM. The study revealed that for surface roughness current was the most influencing factor followed by pulse on time [12]. Amit et al. studied the influence of peak current, pulse on time and gap voltage on MRR and surface roughness by mixing Al_2O_3 nanopowder in deionized water while machining Inconel 825 using copper tool. Considerable increment in MRR and SR has been found in case of NPMEDM as compared to the conventional EDM. The pulse train captured by them confirmed low arcing in case of NPMEDM as compared to conventional EDM [13].

From past literatures, it has been seen that the various combinations of powder and dielectric fluid have different effects on the response parameters. Again depending upon the properties of the workpiece material, the responses may vary. In this regard, the powder mixed dielectric needs to be explored further. Hence, in the present study, a parametric study of machining Inconel 825 using Al_2O_3 nanopowder mixed EDM has been carried out.

2 Experimentation

For the current study, Inconel 825 is taken as the workpiece material and copper as the tool electrode. High electrical conductivity of tool electrode helps in yielding high MRR. Because of high electrical conductivity copper has been taken as the tool electrode. Al_2O_3 nanopowder mixed in EDM oil is taken as the dielectric fluid. Following Box–behnken approach of response surface method (RSM), an experiment can be designed with less number of trials. Hence, the experiment has been designed using Box–behnken approach. T_{on} , IP, GV are taken as the input parameters. The duty factor has been kept constant at 8. The bypass current, spark time and flushing pressure are also kept as constant. MRR, TWR and surface roughness are taken as the responses for the study.

Mathematically

$$MRR = \frac{W_i - W_f}{T_m} \quad (1)$$

$$TWR = \frac{T_i - T_f}{T_m} \quad (2)$$

where

T_f = Final weight of tool (mg),

T_i = Initial weight of tool (mg),

T_m = Machining time (minute),

W_f = Final weight of workpiece (mg),

W_i = Initial weight of workpiece (mg).



Fig. 1 Experimental set-up



Fig. 2 Workpiece and tool

The machining was carried out by using ZNC/EDM35 set-up of Sparkonix make. For determining the MRR, TWR the weight of workpiece and tool before and after machining has been measured by using weighing machine of sartorius make of model no. BSA4202S-CW which is significant up to 4 digit. Surface roughness has been measured by using surface roughness tester SJ-210 of mitutoyo make. For keeping the Al_2O_3 nanopowder in suspended condition and ensuring proper flushing at the machining zone, a submersible pump has been used. Surface texture has been studied using FESEM. In one set, 15 experiments have been carried out without mixing the powder followed by another set of experiments, in which 15 experiments were carried out by mixing Al_2O_3 nanopowder in the dielectric fluid. The experimental set-up image is presented in Fig. 1. Work piece and tool images are presented in Fig. 2.

3 Results and Discussion

From the pilot experiment, it has been noticed that there is not much variation in TWR for both conventional as well as NPMEDM. Even in some cases, the TWR value is zero. The values of process parameters and the responses for different trials are presented in Table 1.

Table 1 Observation table

Expt. No.	Input factors			Responses			
				Conventional EDM		Al ₂ O ₃ NPMEDM	
	IP (A)	T _{on} (Coded value)	GV (V)	MRR (mg/min)	SR (μm)	MRR (mg/min)	SR (μm)
1	2	10	30	8.13	2.14	9	2
2	8	10	30	60	3.66	66.36	3.1712
3	2	70	30	26	4.02	24	3.832
4	8	70	30	83	7.04	99	7.8
5	2	40	10	23	3.648	38	4.3
6	8	40	10	125	6.42	135	7.5794
7	2	40	50	18	3.51	24.67	3.3
8	8	40	50	90	4.914	90	7.1006
9	5	10	10	34	3.455	50	4.2188
10	5	70	10	70	6.1	80	7.5376
11	5	10	50	22	3.01	30	3.2
12	5	70	50	35	6.2	77	6.8182
13	5	40	30	108	5.56	130	6.198
14	5	40	30	105	5.202	132	6.203
15	5	40	30	102	5.59	135	6.001

3.1 Analysis of Variance

Analysis of variance has been conducted for MRR and SR in conventional EDM as well as NPMEDM. In case of conventional EDM for MRR, P value for IP, T_{on} and GV are 0.000, 0.030 and 0.034, respectively, indicating that all the considered input parameters are significant. IP is the most significant parameter for MRR. For SR, P value for IP, T_{on} and GV are 0.000, 0.000 and 0.047 indicating that all the input parameters are significant. IP and T_{on} are the most significant parameters for SR. Similarly in case of NPMEDM for MRR, P value for IP, T_{on} and GV are 0.000, 0.004 and 0.022, respectively, indicating that all the considered input parameters are significant. IP is the most significant parameter for MRR. For SR, P value for IP, T_{on} and GV are 0.000, 0.000 and 0.018 indicating that all the input parameters are significant. IP and T_{on} are the most significant parameters for SR.

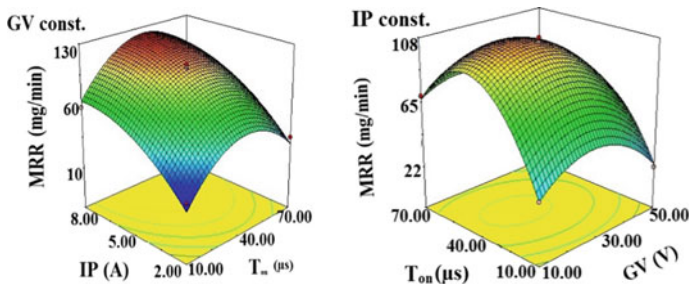


Fig. 3 Variation of MRR in conventional EDM

3.2 Variation of MRR

From Figs. 3 and 4, it is shown that both in conventional and Al_2O_3 NPMEDM, the observed trend of variation of MRR is similar. With the increase in pulse duration, initially MRR increases up to a certain value and then decreases. This may be because of the fact that with the increase in pulse duration availability of energy for melting and evaporation increases leading to higher MRR [4]. But with the rise in pulse duration the pulse off time is reducing accordingly, since the duty factor is held constant. So after a specific value of pulse on time, pulse off time may not be adequate for removal of the debris leading to reduction in MRR. With the rise in peak current in both conventional as well as NPMEDM, MRR has been found to increase first and then decrease. Increase in MRR is justified because as the peak current increases discharge energy also increases. But after, a specific value of peak current MRR was found to decrease. Process instability at very high value of peak current may be the reason behind this. The surface plot depicts that with the rise in gap voltage, MRR first increases then decreases. As the gap voltage increases, the spark gap increases. This makes the spark less intense causing a reduction in MRR. So reduction in MRR with increase in gap voltage is justified. But the initial increment in MRR with increase in gap voltage is unusual and may be due to the interaction effect between other process parameters.

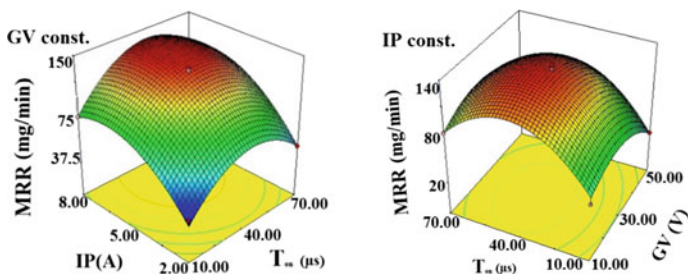


Fig. 4 Variation of MRR in Al_2O_3 NPMEDM

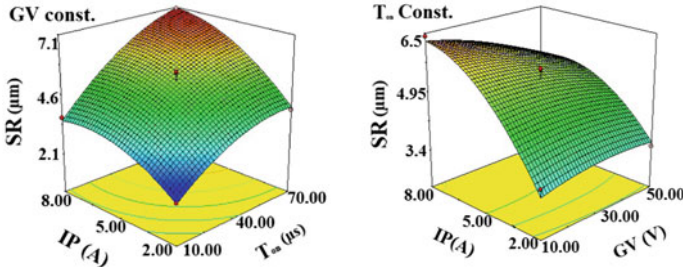


Fig. 5 Variation of SR in conventional EDM

3.3 Variation of SR

The surface plots shown in Figs. 5 and 6 depict that with rise in peak current as well as pulse duration, surface roughness increases. This is obvious because with the rise in peak current or pulse duration the available discharge energy also increases. This produces craters of larger size leading to higher surface roughness. But with increase in gap voltage, surface roughness has been found to decrease. This may be due to the fact that with rise in gap voltage the spark becomes less intense. So small and shallow craters are formed leading to a smoother surface with lower surface roughness [14].

MRR for NPMEDM in most of the trials is higher than that that of conventional EDM. Though in case of NPMEDM better SR was obtained, but in some trials SR in conventional EDM was better than that in NPMEDM. So to reach at a precise conclusion optimum machining conditions for MRR and SR were determined using response surface method. Confirmation tests were carried out at these optimum conditions. MRR and SR at the obtained optimum conditions are presented in Table 2.

From the optimum responses, it is clear that MRR obtained in case of NPMEDM is 18.6% higher than that of conventional EDM. SR in case of NPMEDM is 10.19% better than that in case of conventional EDM.

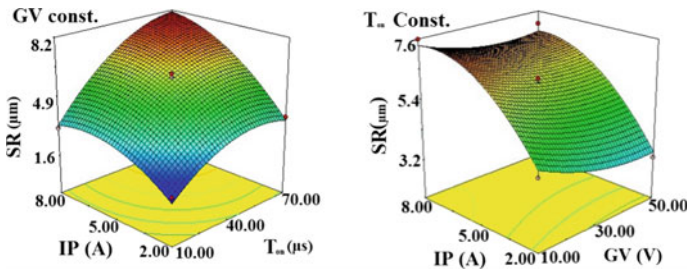


Fig. 6 Variation of SR in Al₂O₃ NPMEDM

Table 2 Responses at optimum condition

At optimum condition	IP (A)	T _{on} (Coded value)	GV (V)	MRR (obtained) (mg/min)	SR (obtained) (μm)
For MRR in conventional EDM	8	16	21	156	–
For MRR in Al ₂ O ₃ NPMEDM	7	14	24	185	–
For SR in conventional EDM	2	5	22	–	2.903
For SR in Al ₂ O ₃ NPMEDM	2	5	30	–	2.607

3.4 Study of Surface Texture

From the FESEM images (Fig. 7), it is evident that the recast layer formed in case of Al₂O₃ NPMEDM is thinner than that in case of conventional EDM. In conventional EDM because of low spark gap, the material melted is not cleared off the spark gap properly and gets deposited as the recast layer (RL). By addition of Al₂O₃ nanopowder, the spark gap increases. This makes the flushing more effective causing easy removal of debris. So, the materials which would have solidified forming the recast layer is cleared off the spark gap easily. Hence, very less amount of material gets deposited leading to a thinner recast layer as compared to conventional EDM.

From the FESEM images (Fig. 8), it is evident that the surface texture on the machined surface in case of Al₂O₃ NPMEDM is better than that in case of conventional EDM. This may be because of the fact that by addition of nanopowder in the

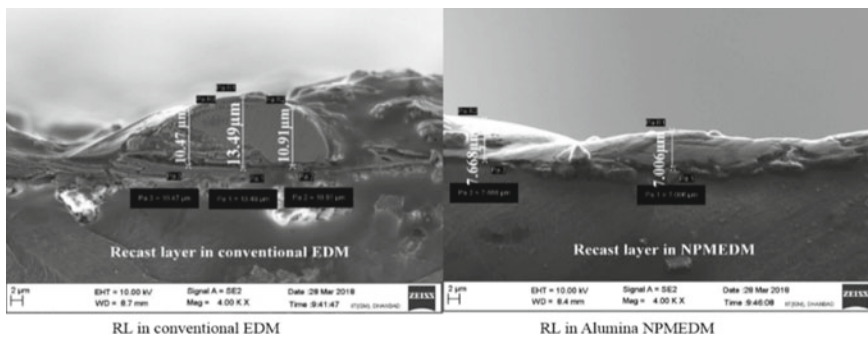


Fig. 7 FESEM image for recast layer thickness

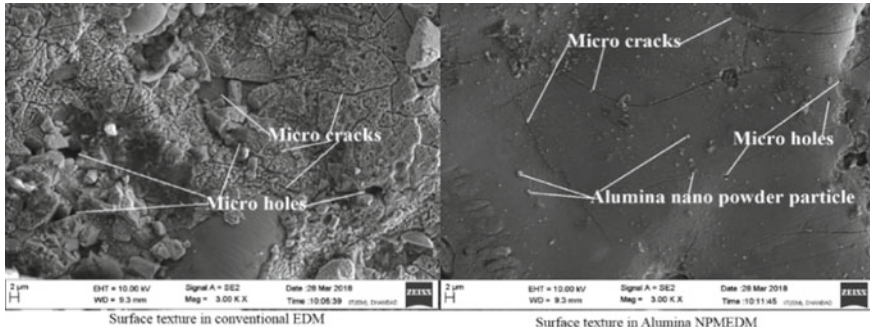


Fig. 8 FESEM image for surface texture

dielectric fluid the discharge gap increases. This makes the spark less intense which leads to formation of smaller craters, microcracks and microholes yielding a better machined surface.

4 Conclusion

From the comparative study conducted on conventional EDM and Al₂O₃ NPMEDM while machining Inconel 825, the following conclusions are drawn.

MRR in case of NPMEDM has been found to be 18.69% higher than that in case of conventional EDM at optimum condition.

Surface quality of the machined surface in case of NPMEDM is better than that in case of conventional EDM. SR in NPMEDM has been found to be 10.19% lower than that in case of conventional EDM. Reduction in recast layer thickness, microcracks and micropits confirms improvement in the surface texture of the machined surface in case of NPMEDM as compared to that in case of conventional EDM.

For MRR in conventional EDM as well as NPMEDM, IP has been found to be the most influencing parameter followed by T_{on}. For surface roughness in conventional EDM as well as NPMEDM, IP and T_{on} have been found to be equally significant.

Tool wear rate is not much affected in both conventional EDM as well as Al₂O₃ NPMEDM.

References

1. Rahul S, Datta BB, Biswal SS (2017) Mahapatra, electrical discharge machining of inconel 825 using cryogenically treated copper electrode: emphasis on surface integrity and metallurgical characteristics. *J Manuf Process* 26:188–202
2. Prabhu S, Vinayagam BK (2013) AFM nano analysis of inconel 825 with single wall carbon nano tube in die sinking EDM process using taguchi analysis. *Arab J Sci Eng* 38:1599–1613

3. Prabhu S, Vinayagam BK (2011) AFM surface investigation of Inconel 825 with multi wall carbon nano tube in electrical discharge machining process using Taguchi analysis. *Arch Civ Mech Eng* 11:149–170
4. Talla G, Gangopadhyay S, Biswas CK (2016) State of the art in powder-mixed electric discharge machining: a review. *J Eng Manuf* 1–16
5. Erden A, Bilgin S (1980) Role of impurities in electric discharge machining. In: 21st International Conference Machine Tool Design Research. Macmillan, London, pp 345–350
6. Mohanty S, Mishra A, Nanda BK, Routara BC (2017) Multi-objective parametric optimization of nano powder mixed electrical discharge machining of AlSiC_p using response surface methodology and particle swarm optimization. *Alexandria Eng J* 2–12
7. Talla G, Gangopadhyay S, Biswas CK (2016) Influence of graphite powder mixed EDM on the surface integrity characteristics of inconel 625. *Part Sci Technol* 6351
8. Nagwa Mejid E, Noordin MY, Idris A, Faraj Saed M (2017) Optimization of maghemite (γ -Fe₂O₃) nano- powder mixed micro-EDM of CoCrMo with multiple responses using gray relational analysis (GRA). *J Phys Conf Ser*
9. Karunakaran K, Chandrasekaran M (2017) Experimental investigation nano particles influence in NPMEDM to machine inconel 800 with electrolyte copper electrode. *Mater Sci Eng*
10. Gopalakannan S, Senthilvelan T (2013) Application of response surface method on machining of Al–SiC nano-composites. *Measurement* 46:2705–2715
11. Mohanty A, Talla G, Gangopadhyay S (2014) Experimental investigation and analysis of EDM characteristics of inconel 825. *Mater Manuf Process* 29:540–549
12. Janardhanan J, Vijaya Ramnath B, Sureshrajn G, Siva Bharath M, Hervin Savariraj X, Akilesh S (2016) Effects of die-sinking electro-discharge machining parameters on surface roughness in inconel 825 alloy. *Indian J Sci Technol* 9
13. Kumar A, Mandal A, Dixit AR, Das AK (2017) Performance evaluation of Al₂O₃ nano powder mixed dielectric for electric discharge machining of Inconel 825. *Mater Manuf Process* 1–10
14. Kumar A, Kumar S, Mandal A, Dixit AR (2017) Investigation of powder mixed EDM process parameters for machining Inconel alloy using response surface methodology. In: 7th international conference of materials processing and characterization. Elsevier, Hyderabad, pp 6183–6188

Eco-design Approaches for Developing Eco-friendly Products: A Review



Prashant Kumar Singh  and Prabir Sarkar 

Abstract Producing eco-friendly products has become the need of the present due to the alarming conditions of global warming issues and depletion of natural resources. These issues have forced the industries to adopt the eco-design strategies in their production processes. Eco-design approaches are used by the designers to deal with these issues not only in the development of eco-friendly products but also in the development of sustainable buildings, eco-industrial parks and services. Efficient integration of the eco-design approaches in product development is still under question due to the uncertainties involved in the eco-design methods. This study provides an insight into the various eco-design methods and tools available for developing eco-friendly products. Different challenges and barriers to the implementation of eco-design have also been reported in this study. Further, the uncertainties associated with the implementation of the eco-design methods are discussed.

Keywords Eco-design · Product development · Uncertainty · Product life cycle

1 Introduction

Depleting natural resources across the world and increasing global warming issues are the serious concerns for the governments and environmental agencies. Global Footprint Network estimated the ecological footprints for over 200 nations in 2013 and found that the rate at which natural resources are being utilized is 1.6 times more than the rate at which they are renewed. Eco-design is a concept that attempts to lead the world toward a sustainable future. This concept is assumed to be originated from an idea that was developed at the beginning of the 1970s. Meadows et al. [1] suggested in 1972 that the current behavior of global world will lead this world to an unavoidable situation and a collapse might occur within a century. They believed that this collapse would be caused mainly due to the depletion of natural resources. They also urged the designers to take responsibility and to play an active role in avoiding

P. K. Singh (✉) · P. Sarkar

Department of Mechanical Engineering, IIT Ropar, Rupnagar, Punjab, India

e-mail: pkstitrpr@gmail.com

© Springer Nature Singapore Pte Ltd. 2019

K. Shanker et al. (eds.), *Advances in Industrial and Production Engineering*, Lecture Notes in Mechanical Engineering, https://doi.org/10.1007/978-981-13-6412-9_17

this situation by using the concept of ecological and social design. In the 1980s, the industries and the research institutions were more focused and dedicated to discussing the concepts of low impact designs for achieving sustainable development. But in the 1990s, the eco-design started to draw the attention and gain support from society, researchers and governments across the world. In the meantime, several manuals were released by the institutes and some regulations by the governments. Central America became the first part of the world where the eco-design program was initiated and known as “Ecodiseño CentroAmerica.” Most of the countries of USA, Japan, Australia and Europe started the implementation of eco-design concepts in the last decade of twentieth century. However, these concepts were hardly implemented in the developing countries of Africa, Asia and Latin America. Therefore, some research activities and programs were organized in these countries by the Delft University of Technology as a part of Design for Sustainability programme [2].

The Biofore Company defines eco-design as “design and produce products responsibly to be safe and sustainable, and ensure that, whenever possible, the end of products’ life cycle is the birth of something new.” Eco-design considers the entire life cycle of a product from cradle to grave and tries to minimize the environmental impact caused by each phase of the product life cycle. These life cycle phases include extraction of raw material, production, distribution, use and end of life. The importance of the integration of eco-design principles has been realized by the researchers [3, 4] in the early stages of the product development process as most of the key decisions are made in these stages only. The cost of changing the design keeps on increasing as we move further during the product development. Therefore, it becomes crucial for the designers to take all the decisions related to design alteration during the initial phases of product development. These initial phases are the conceptual design and detailed design phases of the products. Karlsson and Luttropp [5] suggested a linguistic map that represents the economic and ecological aspects of eco-design, as shown in Fig. 1.

Various definitions of eco-design given by different researchers are listed in Table 1.

Fig. 1 Linguistic map of “eco-design” [5]

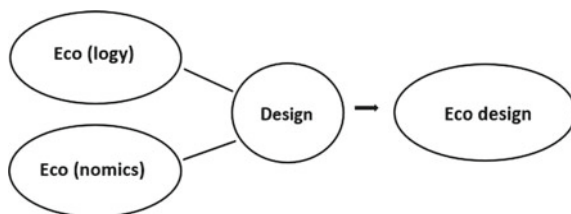


Table 1 Definitions of eco-design

Author	Definition	Ref.
Platcheck	“Eco-design is a holistic view in that, starting from the moment we know the environmental problems and its causes, we begin to influence the conception, the materials selection, the production, the use, the reuse, the recycling and final disposition of industrial products”	[6]
Bhamra	“Eco-design is understood to be the systematic integration of environmental considerations into the design process across the product life cycle, from cradle to grave”	[7]
Alonso	“Eco-design is an approach that integrates environmental criteria in the design of products and services, to get the reduction of environmental impacts they produce, taking into account all stages of their life cycle”	[8]
Borchardt et al.	“Eco-design is a set of Project practices oriented to the creation of eco-efficient products and processes”	[9]
Wimmer et al.	“Eco-design is how to integrate environmental considerations into product design and development”	[10]
Pigosso et al.	“Eco-design is a proactive approach of environmental management that aims to reduce the total environmental impact of products”	[11]
Plouffe et al.	“Eco-design means taking simultaneously into account the environmental impacts in the selection of raw materials, the manufacturing process, the storage and transportation phase, usage, and final disposal”	[12]
IHOBE	“Eco-design means that the environment is taken into account when making decisions during the product development process as an additional factor that traditionally has been taken into account”	[13]

2 Eco-design Methods/Tools

A significant number of eco-design methods and tools have been developed by the researchers and designers to be employed in industries to measure the environmental load of the products during its whole life cycle. Most commonly used eco-design methods with their different categories are given in Table 2.

Brezet and Van Hemel [3] suggested some eco-design strategies represented by seven spokes of a wheel which is known as the eco-design strategy wheel, as shown in Fig. 2. These strategies are associated with the different phases of the product life cycles and are classified at three levels of the products, viz., component level, structure level and system level. Eco-design strategy wheel is also termed as Life cycle Design Strategy (LiDS) wheel [14]. In Fig. 2, @ sign represents the concept of developing a new product. It always leads to a novel approach to providing services. One example is the elimination of the surface post by e-mail services.

Table 2 Eco-design methods/tools

Category	Method/tool	Description
Framework	Tool for environmentally sound product innovation (TESPI)	Guides business-related strategies to determine the features of greener products
	Sustainability assessment framework and tool (SAFT)	Provides cross-disciplinary evaluation to identify concerns from multiple criteria
Checklists and guidelines	Screening life cycle modeling (SLCM)	Evaluates the effects of promising product concepts by creating life cycle scenarios
	DfE matrix	Provides scores to a product to track the improvements in its life cycle impact
	MET-matrix (material, energy and toxicity)	Helps to identify the environmental load of the materials, energy and toxicity of products
Rating and ranking	ABC analysis	Provides ranking to the impacts caused by a product
	LiDS wheel	Lists out the strategies to reduce the impacts of a product life cycle
	Electronic product environmental assessment tool (EPEAT)	Rates the life cycle issues to suggest the design changes for eco-labeling
Software and expert system	Autodesk eco-materials advisor	Suggests the product design changes by considering the material properties
	Solid works sustainability package	Provides a measure of the impacts of the 3D model
	Eco-it	Identifies the parts of the products that cause the major impacts
Analytical	MIPS	Indicates the resource utilization by a product for providing per unit of a service
	The eco-design indicator tool	Builds the life cycle profile of a product for the measurement of its impact
	Trade-off modeling method Carnahan-Thurston	Evaluates the designer's estimates for different design alternatives of a product

(continued)

Table 2 (continued)

Category	Method/tool	Description
	Environmental design cost	Provides a way to reduce the cost of the products for better environmental design
Comparison	Philips fast five awareness	Compares various product concepts with a reference product to formulate strategies for reducing the environmental impact
	Econcept spiderweb	Choose the best design by comparing the severity of the impacts
	Morphological box	Facilitates the eco-idea generation for multiple design concepts

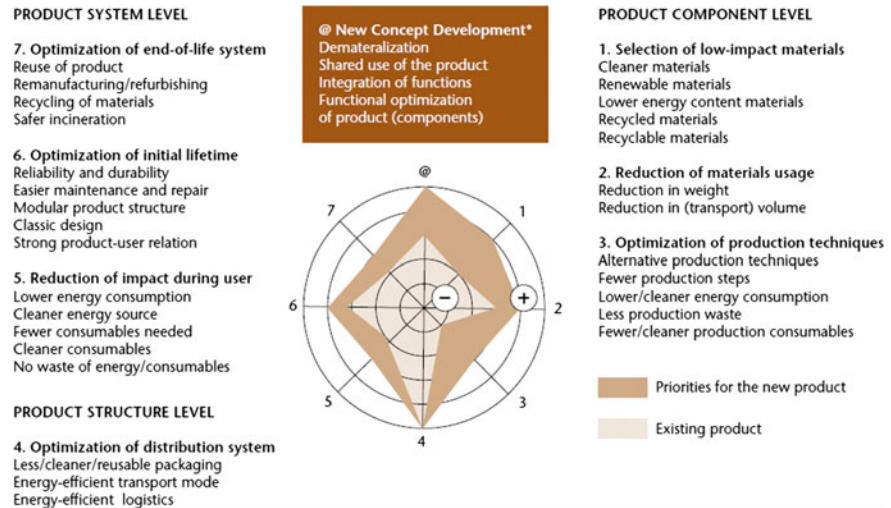


Fig. 2 Eco-design strategy wheel [3]

3 Barriers and Challenges in the Implementation of Eco-design Methods/Tools

There are some noticeable barriers and challenges which are associated with the eco-design tools and methods. These barriers are not only related to the structures of these tools but also to their implementation in the companies. These barriers can be summarized as follows:

- i. The specific knowledge required which is not only related to the usage of the tool but also to the awareness of the environmental issues so that the obtained results can be easily interpreted to propose the correct solutions [15].
- ii. Some tools require a significant amount of time and data for the assessment of the products [16].
- iii. In case of small- and medium-scale industries, there is a limitation of financial and personnel resources [17].
- iv. Most of the tools are not able to handle the trade-off situations required by the products and production processes [18].
- v. There is a significant difference between the academic methods and actual requirement of the industries and the designers [19].

Dekoninck et al. [20] identified and categorized the challenges that are faced by the companies during the implementation of eco-design approaches.

4 Uncertainties in Eco-design Methods

Uncertainties are associated with the different eco-design methods. The literature on eco-design suggests that most of the uncertainties occur during the life cycle assessment of the products. Huang et al. [21] proposed a model to measure the uncertainties in the manufacturing and post-use phases of product life cycle. This model facilitates the eco-friendly material selection for products. Yu et al. [22] observed that there is a significant difference between the predicted and estimated life cycle inventory (LCI) values of the products at the end of life phase. A novel method based on the sensitivity coefficients was developed and validated for analyzing the uncertainties in LCI data. Kota and Chakrabarti [23] proposed that the uncertainty in the development of a product can be categorized into three parts, viz., product structure, life cycle phases and data quality. They developed a method for estimating these uncertainties by the assessment of the mismatch between the required and available information about the life cycle of the product in each category. In some cases, there might be some uncertainty in the measurement of the CO₂ equivalent for electricity consumption using LCI database. It may happen because the technologies for producing electricity are improving continuously and require a frequent update in LCI database.

5 Conclusion

This study shows that although the researchers have proposed a significant number of eco-design approaches and tools, still companies are facing difficulties in the effective implementation of these methods. It happens as there are some barriers in the implementations of these methods. These barriers include specific knowledge about the tools, awareness of the environmental issues, time-consuming efforts and

limited financial and personnel resources in small- and medium-scale industries. Also, some uncertainties are associated with the product life cycles that make it difficult to predict the impacts during the initial design. Therefore, there is a need to modify the existing methods or develop new methods that are easy to implement with significant effectiveness.

References

1. Meadows DH, Meadows DL, Randers J, Behrens W (1972) Los límites del crecimiento: informe al Club de Roma sobre el predicamento de la Humanidad. Maite Zapiain Aizpuru
2. Carel Dihel J, Crul M, Bijma A (2001) Ecodesign in Central America, ecodesign methodology: product improvement tool (PIT). *J Sustain Prod Des* 1:197–205
3. Brezet H, Van Hemel C (1997) Eco-design, a promising approach to sustainable production and consumption. UNEP, Delft
4. Byggeth S, Hochschorner E (2006) Handling trade-offs in ecodesign tools for sustainable product development and procurement. *J Clean Prod* 14(15–16):1420–1430
5. Karlsson R, Luttrupp C (2006) Ecodesign: what's happening? An overview of the subject area of ecodesign and of the papers in this special issue. *J Clean Prod* 14:1291–1298
6. Platcheck ER, Schaeffer L, Kindlein W Jr, Candido LHA (2008) Methodology of ecodesign for the development of more sustainable electro-electronic equipment. *J Clean Prod* 16:75–86
7. Bhamra TA (2004) Ecodesign: the search for new strategies in product development. *Proc Inst Mech Eng B* 218:557–569
8. Alonso García M (2006) La Norma de ecodiseño UNE1503001, CONAMA, Congreso Nacional del Medio Ambiente, en Los retos del desarrollo sostenible en España, Madrid
9. Borchardt M, Wendt MH, Pereira GM, Sellitto MA (2011) Redesign of a component based on ecodesign practices: environmental impact and cost reduction achievements. *J Clean Prod* 19:49–57
10. Wimmer W, Züst R, Kun-Mo L (2004) Ecodesign implementation: a systematic guidance on integrating environmental considerations into product development. Alliance for global sustainability book series, vol 6. Springer, Berlin
11. Pigosso D, Zanette ET, Filho AG, Ometto AR, Rozenfeld H (2010) Ecodesign methods focused on remanufacturing. *J Clean Prod* 18:21–31
12. Plouffe S, Lanoie P, Berneman C, Vernier MF (2011) Economic benefits tied to eco-design. *J Clean Prod* 19(6–7):573–579
13. IHOBE (2011) Manual práctico de ecodiseño. Operativa de implantación en 7 pasos. Sociedad Pública de Gestión Ambiental. Gobierno Vasco. España
14. Wong YL (2009) An integrated environmental product assessment model on ecodesign for electrical products and electronic appliances. Ed. The Hong Kong Polytechnic University
15. Ritzen S (2000) Integrating environmental aspects into product development—proactive measures. Department of Machine Design. Royal Institute of Technology, Integrated Product Development Division, Stockholm, Sweden
16. Michelin F, Vallet F, Reyes T, Eynard B, Duong VL (2014) Integration of environmental criteria in the co-design process: case study of the client/supplier relationship in the French mechanical industry. In: International design conference—DESIGN 2014, pp 1591–1600
17. Hillary R (2004) Environmental management systems and the smaller enterprise. *J Clean Prod* 12:561–569
18. Rossi M, Germani M, Zamagni A (2016) Review of ecodesign methods and tools. Barriers and strategies for an effective implementation in industrial companies. *J Clean Prod* 129:361–373
19. Tukker A, Eder P, Charter M, Haag E, Vercalsteren A, Wiedmann T (2001) Eco-design: the state of implementation in Europe. *J Sustain Prod Des* 1:147–161

20. Dekoninck EA, Domingo L, O'Hare JA, Pigosso DC A, Reyes T, Troussier N (2016) Defining the challenges for ecodesign implementation in companies: development and consolidation of a framework. *J Clean Prod.* <https://doi.org/10.1016/j.jclepro.2016.06.045>
21. Huang H, Zhang L, Liu Z, Sutherland JW (2011) Multi-criteria decision making and uncertainty analysis for materials selection in environmentally conscious design. *Int J Adv Manuf Tech* 52(5–8):421–432
22. Yu X, Zhang H, Shu H, Zhao W, Yan T, Liu Y, Wang X (2017) A robust eco-design approach based on new sensitivity coefficients by considering the uncertainty of LCI. *J Adv Manuf Syst* 16(3):185–203
23. Kota S, Chakrabarti A (2010) A method for estimating the degree of uncertainty with respect to life cycle assessment during design. *J Mech Design* 132(9):1–9

Plumbene: A New 2D-Material Resembling Graphene



D. K. Das and S. K. Singh

Abstract Over two decades, two-dimensional materials attracted the attention of researchers due to their superior mechanical and thermal properties. Plumbene, the new two-dimensional material, is a single layer of lead atoms hexagonally arranged like honeycomb structure. It already has the application as a topological insulator. In this paper, we will compare between structure and properties of graphene, silicene, and plumbene for the application of plumbene in batteries, machine manufacturing, shipbuilding, etc.

Keywords Graphene · Silicene · Plumbene · Nanomaterials

1 Introduction

Due to unique properties, nanomaterials found immense applications in diverse fields. The causes of their unique properties are their unique structures. The only 2D nanomaterial, an allotrope of carbon, graphene is discovered by Andre Geim and Konstantin Novoselov in 2004 [1, 2]. It is hexagonally arranged sp^2 -hybridized carbon atom structure [3]. It is designated as the ‘mother’ [4] of all graphitic carbon materials by some researchers as it is essentially being the building block for graphite (stacked graphene sheets with C–C bond distance of 1.41 Å and interlayer distance 3.35 Å held together by strong van der Waals forces) and carbon nanotubes (effectively ‘rolled-up’ graphene sheets). Graphene has very good mechanical, electrical, and thermal transport properties for which it can be used in electronics industries. But the band gap in graphene is very less (Fig. 1).

Silicene is a single atomic layer of silicon (Si) resembling graphene in hexagonal honeycomb-like structure [5, 6]. Interatomic distance between two silicon atoms in silicene, distance between two atomic layers, and buckling heights are 3.82, 2.248, and 0.44 Å, respectively [7, 8]. Silicon atoms in silicene possess both sp^2 and sp^3

D. K. Das (✉) · S. K. Singh

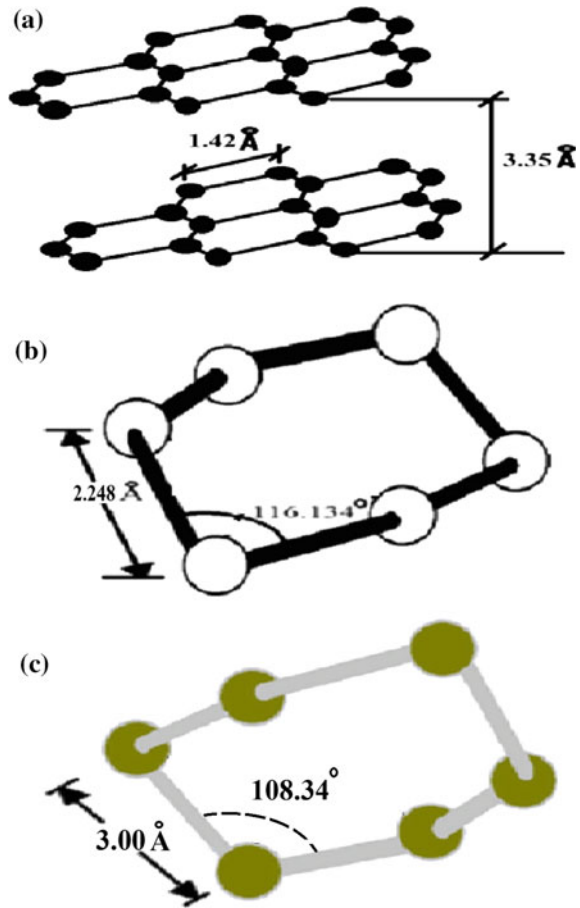
Department of Mechanical Engineering, Indian Institute of Technology (Indian School of Mines) Dhanbad, Dhanbad 826004, Jharkhand, India
e-mail: gourmetaidas@rocketmail.com

© Springer Nature Singapore Pte Ltd. 2019

K. Shanker et al. (eds.), *Advances in Industrial and Production Engineering*, Lecture Notes in Mechanical Engineering, https://doi.org/10.1007/978-981-13-6412-9_18

193

Fig. 1 **a** Crystalline structure of graphene. **b** Unit cell of silicene. **c** Unit cell of plumbene



hybridizations. Silicene due to enhanced transport properties than existing silicon is preferred for electronics industries. It also has band gap more than graphene.

Plumbene also possesses buckled honeycomb structure resembling graphene and silicene. The lattice constant of plumbene is 4.93 \AA , and the nearest neighbor atoms' Pb-Pb bond distance in plumbene is 3.00 \AA [9, 10]. The Pb-Pb bond angle in plumbene is 108.34° [9] which results in buckled structure of plumbene. π - π overlapping is also observed in plumbene-like graphene but weaker in nature than graphene due to longer bond length. Overlapping between σ and π orbitals in plumbene is enhanced due to its buckled configuration, and thus the system is stabilized [9]. Very high band gap is observed in plumbene and hence can be an ideal material for topological insulator. It can also have applications in batteries, machine manufacturing, shipbuilding, etc., where lead is used till now.

2 Comparison Between Properties of Graphene, Silicene, and Plumbene

High remarkable charge-carrier mobility of 2000–5000 cm²/V s is found in graphene [10]. Under optimal conditions, charge-carrier motilities in excess of 200,000 cm²/V s [11–13] are also reported for graphene. Due to this highly permitting electron transport property of graphene, it found applications in field effect transistors (FETs) which operate in very large frequencies of 100 GHz to terahertz range [14, 15]. Graphene has optical absorptive power of 2.3% [16] and a tremendously high optical transparency of up to 97.7% [17] for a monolayer. These properties of graphene found its potential applications in holographic data storage devices [18] and transparent electrodes in solar cells [19]. A high mechanical strength of Young’s modulus of 1 TPa [20], thermal conductivity of 5000 W/m K [21], and exceptionally large specific surface area of 2630 m² g⁻¹ [22] are also observed in graphene.

In modern electronics industries, silicene has potential applications such as light-emitting diodes (LEDs) and field effect transistors (FETs) [23]. Another advantage of silicene is its edges are not affected by oxygen [24]. Young’s modulus and Poisson’s ratio of silicene are 0.178 TPa and 0.34, respectively [25, 26]. Thermal conductivity of silicene is 9.4 W/m K [8].

High band gaps are observed in plumbene which claims its promising applications in topological phenomenon and high-temperature applications [27]. Few comparable properties between graphene, silicene, and plumbene are presented in Table 1.

3 Conclusion and Future Work Direction

In Table 1, it is observed that band gap in plumbene is much higher than existing other two-dimensional materials, graphene and silicene. Hence, they can have potential applications such as topological insulators and high-temperature operations. Structural configurations also result in advantageous unique properties of plumbene than graphene and silicene. Even it possesses superior properties than lead and can be applied for the application in batteries, machine manufacturing, shipbuilding, etc., where convectional lead is used till now. Plumbene can also have applications in

Table 1 Comparison of few properties between graphene, silicene, and plumbene

Elements	Mechanical properties	Thermal properties	Band gap
Graphene	1 TPa (Young’s modulus)	5000 W/m K	10 ⁻³ meV
Silicene	0.178 TPa (Young’s modulus) and 0.34 (Poisson’s ratio)	9.4 W/m K	Accessible
Plumbene	NA	NA	1.34 eV

nuclear plants for power generations, preparation of plumbene-reinforced nanocomposites, etc. Plumbene can have predicted applications where conductivity is the prime concern.

Mechanical and thermal properties of plumbene are not yet being reported. In our future, we will work on mechanical and thermal properties of plumbene and evaluate them.

References

1. Maity S, Ganguly M (2003) Elements of chemistry 1. Publishing Syndicate, Kolkata
2. Das DK, Sahoo S (2014) Monolayer, bilayer and trilayer graphene. *Phys Educ* 30(3), article 4, 1
3. Soldano C, Mahmood A, Dujardin E (2010) Production, properties and potential of graphene. *Carbon* 48:2127–2150
4. Xie H, Hu M, Bao H (2014) Thermal conductivity of silicene from first-principles. *Appl Phys Lett* 104:131906
5. Guzmán-Verri GG, Lew Yan Voon LC (2007) Electronic structure of silicon-based nanostructures. *Phys Rev B (Condens Matter Mater Phys)* 76:075131
6. Novoselov KS, Geim AK, Morozov SV, Jiang D, Zhang Y, Dubonos SV, Grigorieva IV, Firsov AA (2004) Electric field effect in atomically thin carbon films. *Science* 306(5696):666–669
7. Lew Yan Voon LC, Sandberg E, Aga RS, Farajian AA (2010) Hydrogen compounds of group-IV nanosheets. *Appl Phys Lett* 97:163114
8. Lew Yan Voon LC (2016) Silicene: structure, properties and applications. In: Spencer M, Morishita T (eds). Springer
9. Yu XL, Huang L, Wu J (2017) From a normal insulator to a topological insulator in plumbene. *Phys Rev B* 95:125113
10. Tsai W-F, Huang C-Y, Chang T-R, Lin H, Jeng H-T, Bansil A (2013) Gated silicene as a tunable source of nearly 100% spin-polarized electrons. *Nat Commun* 4(1500):1–6
11. Novoselov KS, Jiang D, Schedin F, Booth TJ, Khotkevich VV, Morozov SV, Geim AK (2005) Two-dimensional atomic crystals. *Proc Natl Acad Sci USA* 102(30):10451–10453
12. Bolotin KI, Sikes KJ, Jiang Z, Klima M, Fudenberg G, Hone J, Kim P, Stormer HL (2008) Ultrahigh electron mobility in suspended graphene. *Solid State Commun* 146(9–10):351–355
13. Bolotin KI, Sikes KJ, Hone J, Stormer HL (2008) Temperature-dependent transport in suspended graphene. *Phys Rev Lett* 101:096802
14. Lin YM, Dimitrakopoulos C, Jenkins KA, Farmer DB, Chiu HY, Grill A, Avouris P (2010) 100-GHz transistors from wafer-scale epitaxial graphene. *Science* 327:662
15. Zheng J, Wang L, Quhe R, Liu Q, Li H, Yu D, Mei W, Shi J, Gao Z, Lu J (2013) Sub-10 nm gate length graphene transistors: operating at terahertz frequencies with current saturation. *Sci Rep* 3(1314):1–9
16. Nair RR, Blake P, Grigorenko AN, Novoselov KS, Booth TJ, Stauber T, Peres NMR, Geim AK (2008) Fine structure constant defines visual transparency of graphene. *Science* 6:1308
17. Brownson DAC, Kampouris DK, Banks CE (2012) Graphene electrochemistry: fundamental concepts through to prominent applications. *Chem Soc Rev* 41(21):6944–6976
18. Li X, Zhang Q, Chen X, Gu M (2013) Giant refractive-index modulation by two-photon reduction of fluorescent graphene oxides for multimode optical recording. *Sci Rep* 3(2819):1–4
19. Kim KS, Zhao Y, Jang H, Lee SY, Kim JM, Kim KS, Ahn J, Kim P, Choi J, Hong BH (2009) Large-scale pattern growth of graphene films for stretchable transparent electrodes. *Nature* 457(7230):706–710
20. Lee C, Wei X, Kysar JW, Hone J (2008) Measurement of the elastic properties and intrinsic strength of monolayer graphene. *Science* 321(5887):385–388

21. Balandin AA, Ghosh S, Bao W, Calizo I, Teweldebrhan D, Miao F, Lau CN (2008) Superior thermal conductivity of single-layer graphene. *Nano Lett* 8(3):902–907
22. Zhu Y, Murali S, Cai W, Li X, Suk JW, Potts JR, Ruoff RS (2010) Graphene and graphene oxide: synthesis, properties, and applications. *Adv Mater* 22(35):3906–3924
23. Ni Z, Zhong H, Jiang X, Quhe R, Luo G, Wang Y, Ye M, Yang J, Shi J, Lu J (2014) Tunable band gap and doping type in silicene by surface adsorption: towards tunneling transistors. *Nanoscale* 6(13):7609–7618
24. Padova PD, Leandri C, Vizzini S, Quaresima C, Perfetti P, Olivieri B, Oughaddou H, Aufray B, Le Lay GL (2008) Burning match oxidation process of silicon nanowires screened at the atomic scale. *Nano Lett* 8(8):2299–2304
25. Liu G, Wu MS, Ouyang CY, Xu B (2012) Strain-induced semimetal-metal transition in silicene. *EPL (Europhys Lett)* 99(1):17010
26. Sahin HS, Cahangirov S, Topsakal M, Bekaroglu E, Akturk E, Senger RT, Ciraci S (2009) Monolayer honeycomb structures of group-IV elements and III-V binary compounds: first-principles calculations. *Phys Rev B* 80(15):155453
27. Zhao H, Zhang C, Ji W, Zhang R, Li S, Yan S, Zhang B, Li P, Wang P (2016) Unexpected giant-gap quantum spin hall insulator in chemically decorated plumbene monolayer. *Sci Rep* 6:20152

Study the Wear Behaviour of Al5083-7% B₄C Composite Fabricated by Stir Casting Technique



Ram Singh , Malik Shadab, Ram Naresh Rai, Chiranjit Bhowmik and Shankar Swarup Das

Abstract Aluminium composite significantly possesses better properties as compared to unreinforced aluminium alloy such as high specific strength and higher damping capacity. Metal matrix composite (MMC) is widely used in various industries because they are ductile in nature and light in weight. This paper presents an investigation of the dry sliding wear behaviour of the Al5083 composite produced by stir casting technique with 7%B₄C weight percentage and Al5083. Evaluation of wear rate was conducted by an advanced pin-on-disc tribotester at different loads (30, 40, and 50 N) and different sliding speed (134, 200, and 267 RPM). Then, the investigation from the result of scanning electron microscope (SEM) images of worn surfaces shows that the wear resistance of the Al5083 composite is higher than Al5083. It is found that the damages of the surfaces at low load are less than at high loads and also the damages of surfaces at low sliding distance are less than at high sliding distance. The volume loss increases as the load increases, and similarly at the same applied load, volume loss increases as the sliding distance increases.

Keywords Al5083 · MMC · B₄C

1 Introduction

Aluminium alloy is extensively used in the modern industries because of its less density, high corrosion resistance, and high stiffness, but its application is restricted due to poor wear resistance. In order to enhance the wear resistance of aluminium alloy, the ceramic hard particle is used as the reinforced material. The material obtained after adding of hard particle is known as aluminium composite. The wear resistance

R. Singh (✉) · M. Shadab · R. N. Rai
Department of Production Engineering, National Institute of
Technology Agartala, Agartala, India
e-mail: ramsingh650@gmail.com

C. Bhowmik · S. S. Das
Department of Mechanical Engineering, National Institute of
Technology Agartala, Agartala, India

and mechanical properties of the aluminium composite are higher than the aluminium matrix. Senthilkumar et al. [1] studied about the pure aluminium composite which is synthesised by stir casting technique and the effect of reinforcement particle of graphite and boron carbide where the wear test result shows that there is a reduction in coefficient of friction and frictional force for 5%B₄C. The wear rate decreases with the increases in B₄C percentage in a pure aluminium matrix. Aluminium alloy is broadly used in various sectors such as automobile, aviation, marine, and defence industries [2, 3]. Boron carbide is black in colour with metallic luster, and it is known as third hardest material after diamond and cubic boron nitride [4]. Gopal et al. [5] synthesized the Al6061 composite reinforced with B₄C at various weight percentages by stir casting method, and he analysed the hardness, tensile strength.

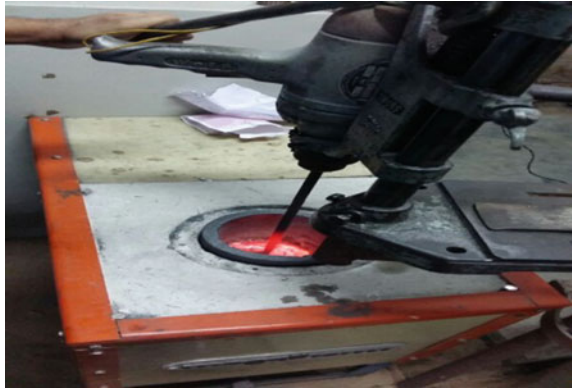
Magnesium and silica are the major elements of A356 and B₄C which are used as reinforced particle and the composite shows that wear rate and wear volume decrease as the weight percentage of hard particle increases [6]. Baradeswaran et al. [7] studied the effect of B₄C particle on Al7075 and found that the hardness, tensile strength, compression strength, flexural strength, and wear resistance of the composite increase with the increasing the volume fraction of hard particle. Harichandran et al. [8] investigated the effect of micro- and nanoparticle of B₄C on composite which is synthesized by stir and ultrasonic cavitation-assisted stir casting and found that the nanoparticles more than 6% lead to agglomeration and porosity into the casting and also decrease the strength and ductility of the casting. The wear resistance of nanoparticle composite is higher than the microparticle composite up to 8% of B₄C.

Al-Qutab et al. [9] investigated the wear and coefficient of friction of aluminium composite with alumina as a reinforcement particle of 10, 20, and 30%, and they found that wear rate decreases with the increases in reinforcement particle. Praba-garan et al. [10] studied the wear behaviour of Al6061, Al6061/B₄C metal matrix, and Al6061/B₄C/Gr hybrid composite which are higher than the Al6061/B₄C and Al6061 matrix.

In this paper, an attempt has been made to test the wear rate and coefficient of friction of the Al5083/7%B₄C at different loads and distances. Then, the morphology study of worn surfaces was done by thorough investigation of the images obtained from SEM.

2 Experimental Description

The material used for the preparation of the specimen is Al5083/7%B₄C composite which is prepared by stir casting technique. It was developed at 730 °C by an ex situ technique in an induction furnace (see Fig. 1), Al5083 of small pieces, 7%B₄C of 300 mesh size were used as raw materials. At first, Al5083 of small pieces was melted into a graphite crucible at a temperature of 650 °C, afterwards, B₄C was added with the speed of 1 gm/s into the molten melt at temperature of 650–700 °C, and by the help of graphite stirrer, the molten mixture was continuously stirred for 10 min.

Fig. 1 Induction furnace**Fig. 2** Wear testing set-up (pin-on-disc)

Subsequently, the liquid mixture was poured into the metallic mould for carrying out the specimen preparation for the wear test.

A dry sliding wear test was performed at room temperature using a pin-on-disc wear testing machine as shown in Fig. 2 (DUCOM wear friction monitor, model—TR20LE-M5). The specimen of 6 mm diameter of the length of 40 mm was used for the testing. For achieving the similar grade of surface roughness of each specimen, every sample would follow the same polishing procedure. The polishing process was performed in disc polisher machine with different grades of emery paper. The disc plate which was used as counter plate for sliding is made of EN31 material of hardness 62 HRC. Before starting the experiment, the disc must be polished with emery paper and, at last, cleaned with acetone to remove the foreign particles. The experiment was performed at a load (30, 40, and 50 N) and sliding distance of (1000, 2000, and 3000 m). After performing every experiment, the disc must be cleaned before every experiment. The EDS of worn surface confirms the presence of B₄C (see in Fig. 3).

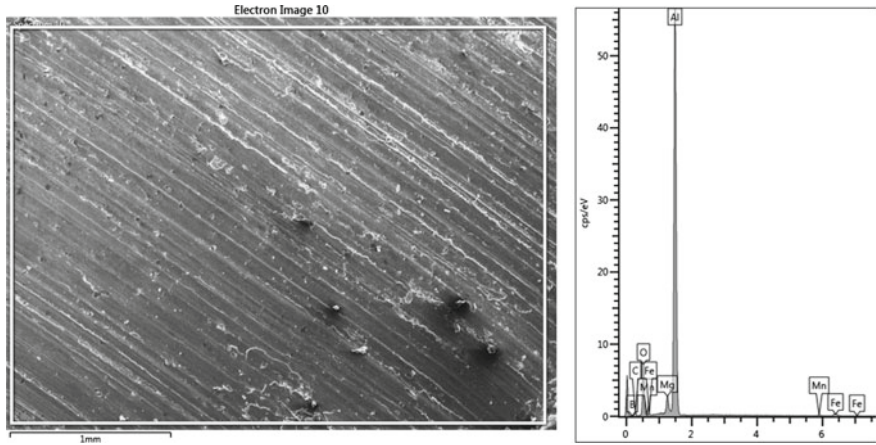


Fig. 3 Worn surface of composite and corresponding EDS analysis

3 Result and Discussion

3.1 Effect of Normal Load

The effect of applied load on the wear rate of Al5083/7%B₄C composite and Al5083 is shown in Fig. 4, and it is also shown in the graph that wear rate of the composite and Al5083 increases as the applied load increasing. This result follows Archard’s law of wear, which states that wear rate increases with an increase of applied load. As the applied load increases, the contact between the asperities of the tested pin and counter-surface of disc increases which leads the deformation of the soft asperities.

The volumetric losses of specimen in the form of wear debris go on increasing as the applied load increases, resulting in volumetric losses leading to more material loss.

$$\text{Volumetric loss (mm}^3\text{)} = \pi r^2 x l$$

whereas r is radius of pin in mm and l is change in length of pin in mm.

The wear resistance of composite decreases as the load increases. At low applied loads, few of the asperities may get deformed plastically or remain elastically attached. This plastically deformed material gets detach from the specimen and fills the valley of the specimen surface as well as disc. During the beginning of the load, the harder asperities of the counter surface may dig the soft surface of the specimen. This wear mechanism is known as abrasive wear.

The applied load affects the contact surface area between the specimen and its counter surface, which in turn affect the quantity of generated frictional heat. After 40 N load, the wear loss for both the material decreases with an increase in the load.

The wear losses are more stable and linear due to the generation of high frictional heat leading to the oxidation of specimen surface and strain hardening.

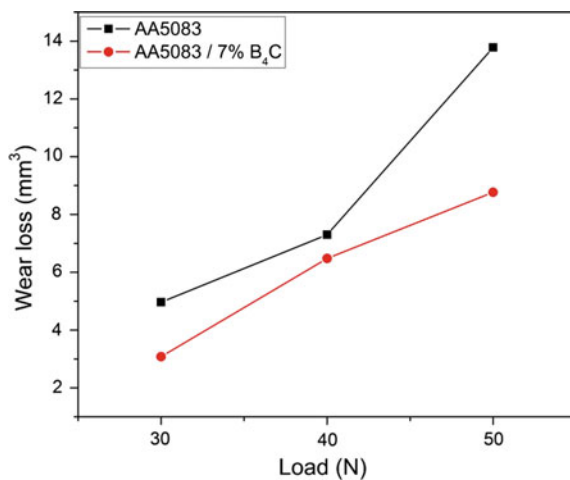
Figure 5 shows the SEM images of worn surface of casted Al5083/7%B₄C at a load of (30, 40, and 50 N), sliding speed of 134 RPM, and sliding duration are 45 min for the each and every applied load.

At low applied load, the worn surface of Al5083 shows more deeper and bigger groove on the worn surface. Small pits, adhesive wear, and micro-cutting were also seen into the surface. On the other hand, it is observed that the worn surface of composite shows smaller groove with lesser depth (presence of hard particle resist the wear mechanism) at same experimental conditions and craters are also seen into the worn surface. More debris are produced during sliding of specimen at low load this happen due to the breaking of soft asperities of the matrix. During the increase of load more frictional heat is generated and this causes the deformation of asperities. Initially craters are developed due to delamination and cracking of surface. At higher loads, the ploughing of hard particles takes place and this initiates the crack. The material removal rate is higher at higher loads because material removal takes place due to delamination as well as micro-cutting.

3.2 Effect of Sliding Distance

It is clear from Fig. 6 that wear losses increase with the increases of sliding distance. At the beginning of the sliding distance up to the first 3.5 km, the material removal is more gradually increases for both the material, but the material removal rate is high for the Al5083 as compared with the composite. The wear losses of the specimen due to sliding distance are related to the actual contact between the asperities of the

Fig. 4 Effect of applied load on wear losses



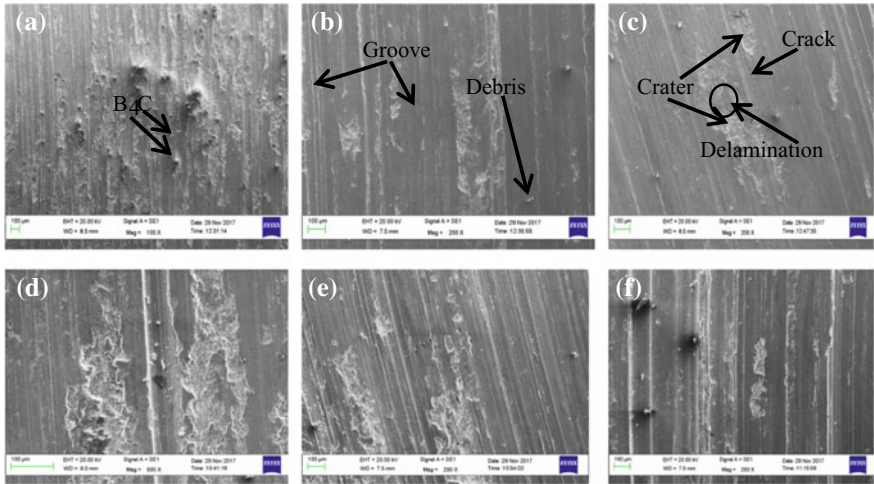
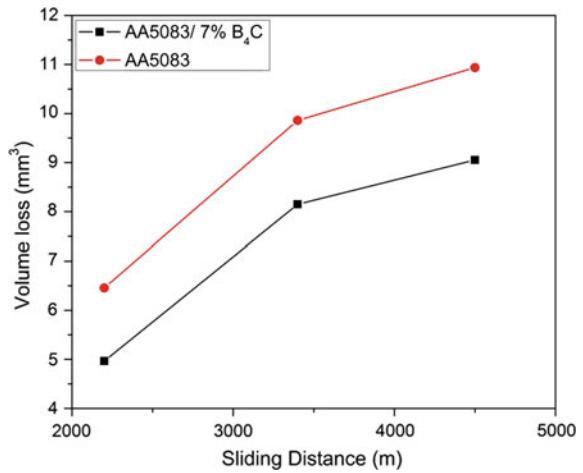


Fig. 5 SEM micrographs of worn surface at sliding speed of 134 RPM and load of 30, 40, 50 N is **a,b,c** for composite and **d,e,f** for Al5083, respectively

Fig. 6 Effect of sliding distance on wear losses



specimen and sliding surface of the disc, asperities of specimen could not resist the generated shear force, the asperities may get deformed and detached, and these are mainly happened due the cutting action of the hard asperities of the disc.

These deformed and detached materials fill the valleys of asperities. The loose debris which is present between the surface of specimen and disc during the sliding of the specimen is the combination of fractured part of the asperities as well as the hard particle of reinforcement which is pulled out during the sliding of specimen; this loose debris acts as an abrasive medium and increases the wear losses. This wear mechanism is known as abrasive wear.

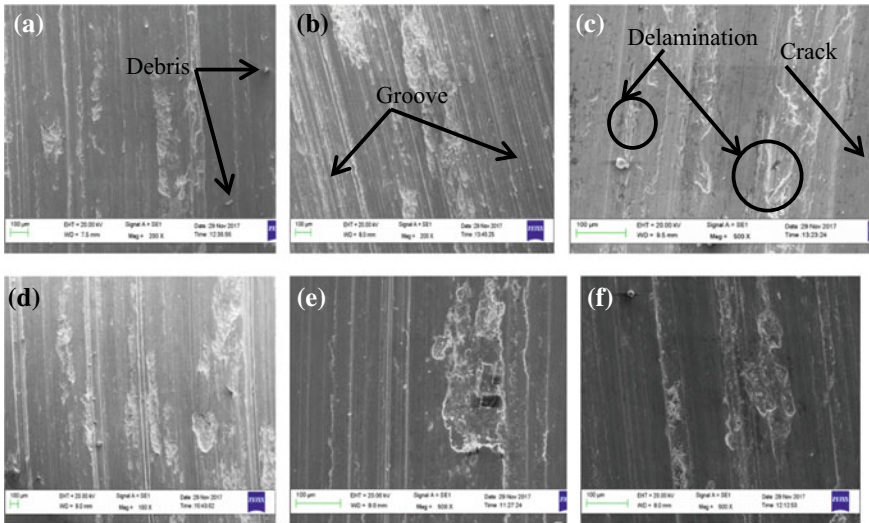


Fig. 7 SEM micrographs of worn surface at applied load 40 N and sliding distance of 2.2, 3.4, and 4.5 km are **a,b,c** for composite and **d,e,f** for Al5083, respectively

After 3.5 km sliding distance, the removal of material from the specimen is more linear. Because as the sliding distance increases, more frictional heat generated between the contact surface, and this leads the adhesion of loose debris into the disc which leads the stability and linearity into the wear losses.

Figure 7 shows the worn surface of casted Al5083/7%B₄C composite and Al5083 at 40 N load and sliding distance of 2.2, 3.5, and 4.5 km, respectively. Above SEM image shows the severity of worn. At lowest distance, the SEM images of Al5083 shows deeper and continuous groove and ploughing of surface, whereas the discontinuity in ditch and less deeper groove and ploughing are seen into the worn surface of Al5083 composite. The small craters and continuous groove are shown in SEM images of sliding distance 2.2 km. Whereas the SEM images of sliding distance of 3.5 and 4.5 km show deeper groove with deformed edges when compared with smaller sliding distance, severe delamination of the worn surface of specimen is clearly shown in the SEM images at higher sliding distance. The damages of surface are more in Al5083 when compared to Al5083 composite because the hard particle resists the wear of composite. At higher sliding distance, the generation of frictional heat is high, and this leads the plastically deformation of edges of groove and cracks are developed into the surfaces. The worn surfaces of both materials show the delamination of subsurfaces at higher sliding distance. It is clear from the SEM images that the abrasive and delamination wear are major at higher sliding distance.

4 Conclusions

The wear losses of the composite and Al5083 are increasing with the increases of sliding distance and normal load. The wear loss of composite and Al5083 is more gradually increasing as the sliding distance increasing up to 3.5 km (8.1489 and 9.8587 mm³, respectively) after that wear loss more uniform and stable (9.0536 and 10.9356 mm³, respectively) due to the adhesion of loose debris into the disc surface.

Whereas the wear losses of composite and Al5083 (6.48 and 7.2992 mm³, respectively) is increases more gradually as the load increases up to 40 N. After that, wear loss increases more linear and stable (8.77 and 13.7795 mm³, respectively) due to more frictional heat generated at higher load which lead the oxidation and strain hardening the specimen surface.

References

1. Senthilkumar N, Tamizharasan T, Anbarasan M (2014) Mechanical characterization and tribological behaviour of Al-Gr-B₄C metal matrix composite prepared by stir casting technique. *J Adv Eng Res* 1(1):48–59
2. Miller WS, Zhuang L, Bottema J, Wittebrood AJ, Smet PD, Haszler A, Vieregge A (2000) Recent development in aluminium alloys for the automotive industry. *Mater Sci Eng A* 280(1):37–49
3. Brown KR, Venie MS, Woods RA (1995) The increasing use of aluminium in automotive applications. *J Miner Met Mater Soc* 47(7):20–23
4. Thevenot F (1990) Boron carbide—a comprehensive review. *J Eur Ceram Soc* 6(4):205–225
5. Gopal KUB, Sreenivas RKV, Vasudeva B (2012) Effect of percentage reinforcement of B₄C on the tensile property of aluminium matrix composites. *Int J Mech Eng Rob Res* 1(3):290–295
6. Sridhar RKS, Bupesh RVK (2014) Effect of boron carbide particle in wear characteristic of cast aluminium A356 composite. *IOSR J Mech Civ Eng* 73–77
7. Baradeswaran A, Perumal AE (2013) Influence of B₄C on the tribological and mechanical properties of Al 7075–B₄C composites. *Compos B Eng* 54:146–152
8. Harichandran R, Selvakumar N (2015) Effect of nano/micro B₄C particles on the mechanical properties of aluminium metal matrix composites fabricated by ultrasonic cavitation assisted solidification process. *Arch Civ Mech Eng* 326:12
9. Al-Qutub AM, Allam IM, Samad M (2008) Wear and friction of Al-A1203 composites at various sliding speeds. *J Mater Sci* 43(17):5797–5803
10. Prabakaran S, Chandramohan G, Shanmugasundaram P (2014) Influence of graphite on the hardness and wear behavior of AA6061–B₄C composite. *Mater Technol* 48(5):661–667

Study of Machining Performance in EDM Through Response Surface Methodology



Raghav Rajneesh, Singh Subhash, R. S. Mulik and Pal Kaushik

Abstract Electric discharge machining (EDM) is thermal erosion advanced machining process which is capable of machining very hard conductive materials that cannot be machined by any other conventional machining processes. However, process parameters used in EDM have a wide range and for achieving efficient machining optimum selection of these parameters plays an important role. In the present study, discharge current (I), pulse on and pulse off time were taken as process variables in machining AISI 202 stainless steel using a copper alloy tool. This study aims to optimize electrode wear rate, material removal rate, as well as surface roughness of work-piece using response surface methodology (RSM) approach. The results obtained after experimental procedure were analyzed by analysis of variance (ANOVA) technique. Regression equation for the EWR, MRR, and Ra was also generated. This study also focuses on surface changes and crystalline changes that occur after EDM process by using different characterization techniques. Atomic force microscopy (AFM), scanning electron microscopy (SEM), and X-ray diffraction (XRD) techniques have been used for studying the changes on materials after machining process. Based on the experiment, it was found that discharge current and pulse on time significantly affect the machining performance. The optimized electrode wear rate and material removal rate obtained were having values 0.000155 mg/min and 0.048175 mg/min, respectively. This study can be helpful for selecting optimum process parameters in machining of 202 stainless steel to achieve efficient machining.

Keywords Response surface methodology (RSM) · Energy-dispersive X-ray spectroscopy (EDS) · Atomic force microscopy (AFM) · Scanning electron microscopy (SEM) · X-ray diffraction (XRD)

R. Rajneesh · R. S. Mulik · P. Kaushik (✉)
Department of Mechanical and Industrial Engineering, IIT
Roorkee, Roorkee 247667, UK, India
e-mail: pl_kshk@yahoo.co.in

S. Subhash
Department of Manufacturing Engineering, NIT Jamshedpur, Jamshedpur 831014,
Jharkhand, India

© Springer Nature Singapore Pte Ltd. 2019
K. Shanker et al. (eds.), *Advances in Industrial and Production Engineering*, Lecture
Notes in Mechanical Engineering, https://doi.org/10.1007/978-981-13-6412-9_20

1 Introduction

Due to the limitation of conventional machining processes of not able to machine hard materials need for advanced machining processes was there. Sparking between two electrically conducting materials erodes some material from both materials this fact was utilized for machining of metals and electric discharge machining was thus invented. Electric discharge machining (EDM) a non-conventional thermo-electric advanced manufacturing process in which the continuously occurring sparks between tool and workpiece submerged in a dielectric fluid removes material from both the electrodes [1]. Removal of material in EDM takes place due to the heat energy of sparks. The thermal energy produced is a result of electric energy applied in this process. Consequently, for an efficient machining operation, the electrical process parameter needs to be optimized [2]. There is a huge requirement of components made up of very hard and difficult to machine materials in automotive, aerospace, electronics, optics, medical devices, and communications industries, machining these materials by conventional method is not possible. EDM offers a better alternative to machine these materials. During EDM process, there is always a small gap present between tool and workpiece thus removing any possibilities of vibration or mechanical stresses [3]. The main use of EDM is to produce dies for extrusion and forging industries. Besides this precise machining and making very complicated shapes on some difficult to machine materials can be done easily by EDM. EDM can also be applied for machining heat treated materials, ceramics, composite materials, etc. [4].

Having a very wide range of applications and being used widely for manufacturing various parts, there are some problems related to EDM machining. As the sparking erodes material from both the electrodes so, the wear of the tool is a problem in this process. Simultaneously, the material removal rate is also less. Research is going on to optimize the machining process and to improve the performance of EDM process. Material and fabrication cost of tool is also important as the cost of product manufactured depends upon tool cost [5]. Commonly graphite or copper materials are used in making tool for EDM but due to the problem of tool wear rate and material removal research for developing tool materials having low tool wear is going on. Many tool materials have been developed and tested. Khanra et al. investigated the performance of a ZrB_2 -Cu as a tool material in EDM and found this material gives less tool wear as compared to pure copper tool [6]. Lopez-Esteban et al. tried electric discharge machining of ceramics and concluded that finishing ceramic materials into complex geometries with the tolerance required can be done easily by EDM process [7]. Kiyak and Cakir examined machining parameters on surface roughness in EDM of tool steel using pure copper tool and observed that surface roughness of tool and workpiece was influenced by pulse duration and current, by increasing them the roughness also gets increased [8]. Some authors developed ZrB_2 -CuNi tool for EDM and described its applications [9]. Review of electric discharge machining also shows that efforts are being made to lower the tool wear and increase material removal in EDM process [10]. Fonesca and Marafona studied the effect of deionization time on electric discharge machining performance and their study shows that

material removal rate and tool wear rate get affected by the time needed to deionize the dielectric [11]. Tang and Guo investigated parametric optimization of EDM on stainless steel workpiece and concluded that discharge current and pulse on time as influential parameters in machining process [12]. Tsai et al. studied Cr/Cu composite electrode performance and found an increase in material removal but poor surface finish is obtained when using this tool in negative polarity [13]. Lee and Tai described a relationship between EDM parameters and surface crack formation using full factorial design [14]. Statistical analysis of tool wear in EDM has also been done which shows that on time and current were having significant effect on electric discharge machining [15]. Haron et al. studied the copper and graphite electrode performance in EDM process and found copper as a better tool for machining tool steel [16]. Hu et al. investigated material removal rate and surface damage in EDM of ceramic material and according to them, melting and decomposition are the main material removal mechanisms in EDM process [17]. Muttamara et al. described electrode material effects on electric discharge machining of alumina [18].

From the literature review on EDM technology, we found that several efforts have been made to lower the tool wear rate and increase the productivity of electric discharge machining but not much work has been done in EDM of AISI 202 stainless steel using Cu–Cr–Zr as tool electrode. Also, the application of RSM methodology in the electric discharge machining of combination of these two materials has never been attempted. So, in this research work authors are trying to fill this gap by analyzing the effects of machining parameters in EDM of AISI 202 stainless steel and optimizing the machining performance through RSM model. Changes on materials after electric discharge machining have also been studied in this work.

2 Materials and Methods

2.1 Tool Material

Copper–chromium–zirconium (Cu–Cr–Zr) one of the copper alloys was used as tool electrode material in this investigation. EDS image of its composition is shown in Fig. 1a. Pure copper is soft and used for electrical purposes due to its high electrical conductivity in comparison with its mechanical properties. Addition of zirconium will add to its strength and increases its softening temperature to 300 °C and there will be no effect on the conductivity of copper. So, a study on this copper alloy has been done.

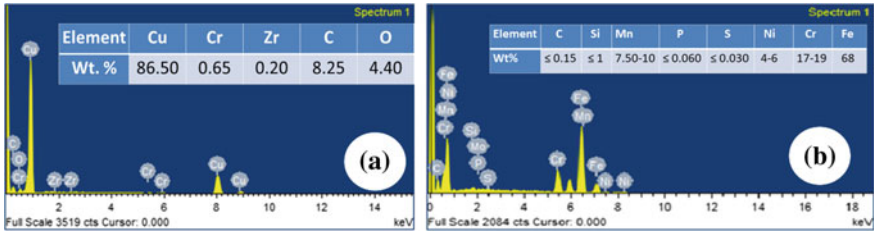


Fig. 1 EDS image and chemical of composition of tool and workpiece materials

2.2 Workpiece Material

Workpiece material used for the present study was AISI 202 stainless steel. The chemical composition and EDS analysis of the workpiece material are shown by Fig. 1b. Stainless steel has been selected for this work as there is huge demand of products manufactured by this material. Stainless steel is most important material used in industries mainly because of its corrosion resistant property which is due to high chromium content in it. Also due to its hygienic properties, it is used in making utensils, medical instruments, etc.

2.3 Design of Experiments

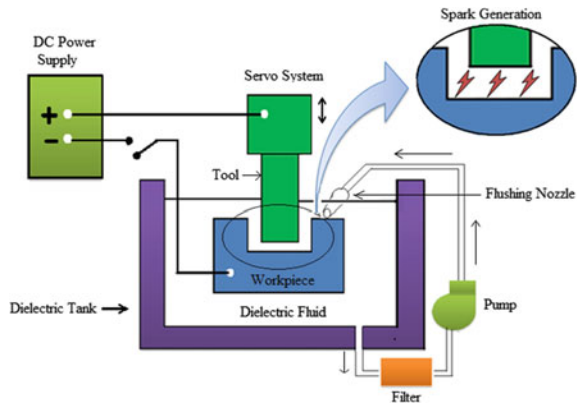
This paper used response surface methodology approach for designing the experiments. Collection of mathematical and statistical techniques used for modeling and analysis of problems are provided by RSM. This technique reduces the number of experiments without any reduction in accuracy [19]. A central composite design with 2^k factorial has been designed where k is the number of variables. RSM approach has been used to plan the experimentation, to analyze the results and to obtain a second-order polynomial regression equation for EWR, MRR and R_a [20]. The main objective of this approach is to analyze the relationship between the response of interest and the process parameters used in machining [21]. This methodology helps in understanding how the change in applied process parameters affects the response. Basic equation of response surface method is of the following form.

Where, Y is the response of our interest, e.g., MRR, EWR and R_a . X_i (1, 2 ... n) are the quantitative variables and $\beta_o, \beta_i, \beta_{ii}, \beta_{ij}$ are the second order regression coefficients. Table 1 gives the parameters used in the experiment, their units, symbols, and the coded levels.

Table 1 Level values of process parameters

Parameters	Unit	Symbol	Level		
			-1	0	1
Current	A	I	5	7	9
Pulse on time	μ s	T_{on}	55	65	75
Pulse off time	μ s	T_{off}	5	7	9

Fig. 2 Schematic view for the EDM machining operation



2.4 Experimental Procedure

During present investigation, Die sinking model electric discharge machining has been used. Polarity of tool electrode used was straight and commercial grade EDM oil as dielectric fluid for machining purpose has been used. Figure 2 shows the schematic view of EDM machining operation. The workpieces were prepared by first cutting them from stainless steel sheet and then grinding to make the both surface parallel and tool electrodes were prepared in the form of cylindrical shape of 7 mm diameter. As the number of parameters used is three so there are 20 numbers of experiments by RSM method. Before and after the machining operation, the weight of tool electrode and workpiece was taken and the time of machining was also noted so that further calculation can be done using this data.

3 Characterization

In this experimental investigation, we have characterizes the tool and workpiece surfaces with energy-dispersive X-ray spectroscopy (EDS), atomic force microscopy (AFM), scanning electron microscopy (SEM), optical surface profiler (OSP), and small angle X-Ray diffraction measurements (XRD), respectively.

4 Results and Discussion

All the data collected during the experimentation was used to calculate the values of tool wear rate and material removal rate. Surface roughness was measured by optical surface profilometer. Table 2 gives the design layout of experiments and all the calculated values of responses at different combination of process parameters.

After performing the experiments according to design of experiment, collecting all data and calculating the responses search for optimal values of process parameters has been done to achieve lowest electrode wear and surface roughness and highest material removal rate in this process. Table 3 gives the values of parameters in which optimum results were found.

Table 2 Design layout and experimental results

S. No.	Coded factors			Uncoded factors			Response variables		
	<i>X</i>	<i>Y</i>	<i>Z</i>	<i>I</i>	<i>T_{on}</i>	<i>T_{off}</i>	EWR (mg/min)	MRR (mg/min)	<i>R_a</i> (μm)
1	-1	1	1	5	75	9	0.000165	0.00155	1.92
2	0	-1	0	7	55	7	0.000204	0.01847	2.12
3	0	0	-1	7	65	5	0.000175	0.013095	2.14
4	-1	-1	-1	5	55	5	0.000163	0.00198	1.72
5	0	0	0	7	65	7	0.000179	0.012415	2.17
6	1	1	-1	9	75	5	0.000521	0.0342	3.33
7	0	1	0	7	75	7	0.000273	0.00669	2.03
8	-1	1	-1	5	75	5	0.000168	0.001495	1.71
9	0	0	0	7	65	7	0.000181	0.015095	2.19
10	1	0	0	9	65	7	0.000286	0.045095	3.12
11	0	0	0	7	65	7	0.000184	0.01382	2.21
12	-1	-1	1	5	55	9	0.000155	0.001205	1.87
13	1	1	1	9	75	9	0.000413	0.00264	3.61
14	0	0	0	7	65	7	0.000187	0.013985	2.25
15	1	-1	-1	9	55	5	0.000372	0.048175	2.50
16	0	0	1	7	65	9	0.000215	0.013375	2.53
17	0	0	0	7	65	7	0.000188	0.01385	2.33
18	-1	0	0	5	65	7	0.000162	0.001665	1.88
19	1	-1	1	9	55	9	0.000335	0.04203	2.72
20	0	0	0	7	65	7	0.000192	0.014535	2.41

Table 3 Optimal values of parameters obtained

Process parameters	Value obtained		
	EWR	MRR	R_a
Current (A)	5	9	5
Pulse on time (μ s)	65	75	75
Pulse off time (μ s)	7	9	5

4.1 Mathematical Modeling for Responses

Based on the basic response surface method equation effect of selected process parameters that were current, pulse on and pulse off time have been evaluated. The values of different constants in the basis equation have been evaluated using MINITAB 17 software. Regression equations in uncoded units for electrode wear rate, material removal rate, and surface roughness thus generated are shown below.

4.2 Analysis of Variance

The generated model is tested for its significance by analysis of variance (ANOVA). *F*-value and *P*-value have been obtained for EWR, MRR and R_a . If the associated *P*-value for the model is less than 0.05 (i.e., $\alpha = 0.05$) it means the model is statistically significant. The R^2 is used as a measure of the goodness of fit and can be defined as the ratio of variability explained by the model to the total variability in the actual data. The more R^2 approaches unity, the better model fits the experimental data. The value of 0.9509 was obtained for the R^2 which signifies that the model explains 95.09% of the variability of EWR, whereas the adjusted R^2 (adj) is 90.66%. The model explains 95.05% of the variability of MRR, whereas the adjusted R^2 (adj) is 90.60%. Again, the model has 96.68 and 93.63% of the variability of MRR for R^2 and adjusted R^2 (adj), respectively.

4.3 Parametric Influence of EDM on EWR

The effect of discharge current, pulse on and pulse off time on electrode wear rate is discussed here. 3-D surface plot has been plotted using Statistica software with the help of data used in during experimental work. Figure 3 shows influence of selected parameters on electrode wear rate. From the results for all values of pulse on time, if we increase discharge current then the electrode wear rate is also increasing the reason behind this may be as the current value increases the energy of spark gets increased and it erodes more material. It can be also noticed from Fig. 3a that for low values of current as pulse on time increases EWR is not increasing that much but for

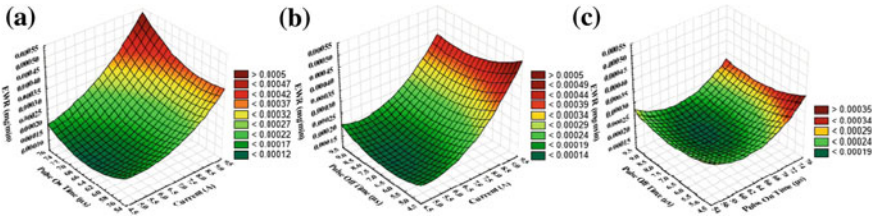


Fig. 3 a Surface graph showing influence of I and T_{on} on EWR. b Surface graph showing influence of I and T_{off} on EWR. c Surface graph showing influence of T_{on} and T_{off} on EWR

higher values of current EWR is increasing for increasing pulse on time. Figure 3b shows that EWR is not increasing for higher values of pulse off time at low current settings but as the current increases the EWR increases rapidly. On the other hand, EWR is seen decreasing a bit if pulse off time is increasing. Influence of pulse on and pulse off time is shown by Fig. 3c for low value of pulse off time as pulse on time increases EWR decreases but then it increases at higher values of pulse off time as by increasing machining duration more material get removed and flushing of that material takes place properly at high pulse off time.

4.4 Parametric Influence of EDM on MRR

From Fig. 4a–c, the influence of machining parameters on MRR can be studied. For all the values of pulse on and pulse off time as the current increase material removal rate increases slowly and then increases rapidly for high values of current due to increase in energy of spark generated. While a decrease in MRR can be noticed from these three graphs when pulse durations are increasing this is because when we increase the pulse duration the plasma channel gets expanded and thus reducing energy density of spark.

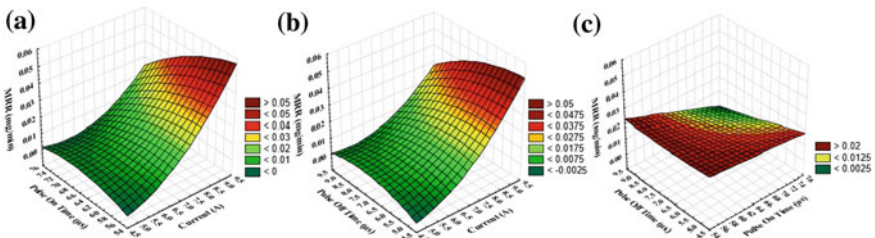


Fig. 4 a Surface graph showing influence of I and T_{on} on MRR. b Surface graph showing influence of I and T_{off} on MRR. c Surface graph showing influence of T_{on} and T_{off} on MRR

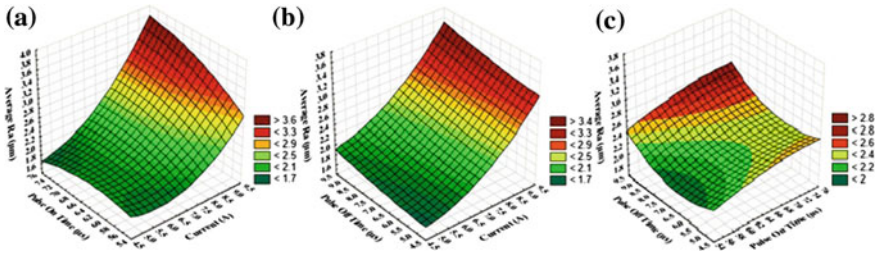


Fig. 5 a Surface graph showing influence of I and T_{on} on R_a . b Surface graph showing influence of I and T_{off} on R_a . c Surface graph showing influence of T_{on} and T_{off} on R_a

4.5 Parametric Influence of EDM on R_a

Figure 5a, b shows that for all values of pulse on time and pulse off time the surface roughness increases for increasing values of discharge current this may be because as the current increases it will produce a stronger spark making the crater oh higher depth on the work surface as a result the surface roughness increases. Surface roughness also increases for increasing pulse on time and pulse off time.

4.6 Scanning Electron Microscopic Study

Effects of machining on the surface of tool and workpiece material were investigated by doing scanning electron microscopic study. During the machining process, the temperature of spark is very high due to which the material melts but between the sparks when molten material is flushed away by the dielectric suddenly the temperature between tool and workpiece decreases. So, during the whole machining process, the surface of both the materials faces various changes. Figure 6a–c shows the SEM images of tool used at 5, 7, and 9 A, respectively. The SEM images of machined workpiece surfaces at optimum values of process parameters for all the three current settings are shown in Fig. 6d–f. This study shows that the surface after machining has changed it has recast layer, globules of debris, pores, microcracks, and craters because of high energy of sparks and subsequent quenching. Some microcracks can be observed on the machined surface which is formed due to increase in residual stresses, this increase in stresses is due to increase in non-homogeneities within white layer. The molten metal which does not get flushed away and re-solidifies forms this white layer.

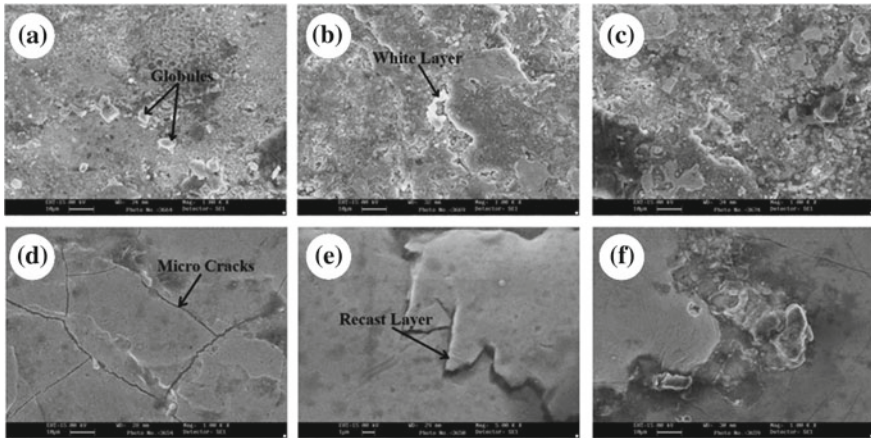


Fig. 6 SEM images of tool surface (a–c) and workpiece surface (d–f) after machining

4.7 Atomic Force Microscopic Study

AFM is one of the most widely used techniques for measuring, imaging, and manipulating the required information at nanoscale level. 3-D surface profiles of electrode and workpiece after electric discharge machining were taken. Surface roughness also depends on the hardness of material to a great extent. Figure 7a shows AFM image of tool that was used to machine at 5 A current and Fig. 7b, c shows AFM image of tool used at 7 and 9 A, respectively. These figures show that the machined surface of tool used at high current setting is rougher than the tool used at lower current settings because the roughness depends on discharge energy during machining. Figure 7d–f shows AFM images of machined workpiece at optimal parameters, these figures also show that roughness is increasing with increase in current. In this experiment, we used a different combination of all the three parameters and images of best the combination of parameters are shown here. It is observed that by optimizing these parameters.

4.8 X-ray Diffraction Study

X-ray diffraction study of the top layer of both tool and workpiece before and after the machining operation at three different current settings has been performed to study the changes the materials undergo after the machining process. Figure 8a shows XRD pattern of unmachined tool surface and Fig. 8b shows XRD patterns of tool used to machine at 5, 7, and 9 A. From these figures, we can see that tool material before machining has peaked with high intensity and as the current settings are increasing peaks intensity is also decreasing. During machining process, the surface

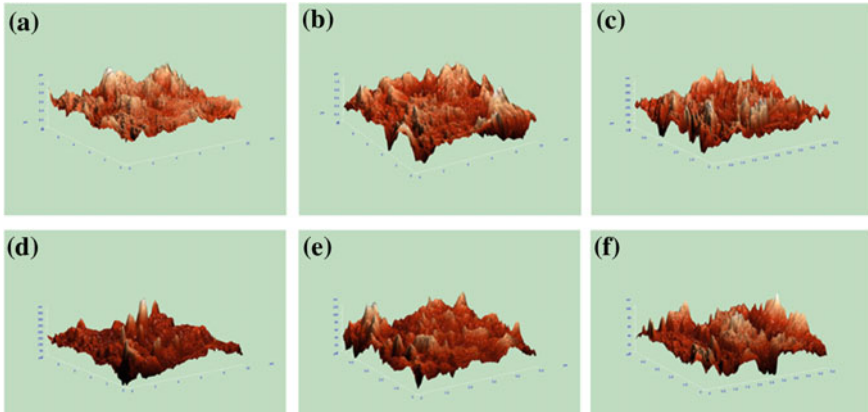


Fig. 7 AFM images of tool surface and workpiece surface after machining

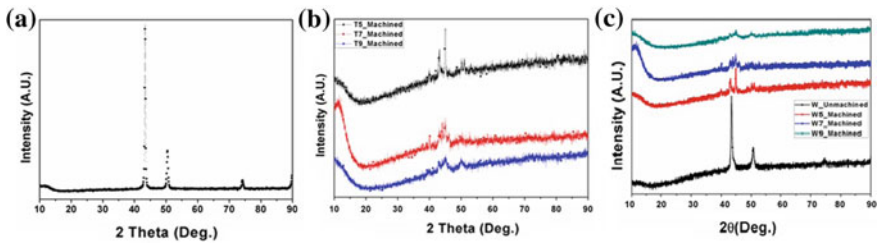


Fig. 8 a XRD patterns of tool before machining. b XRD pattern of tool after machining at different current. c XRD patterns of workpiece before and after machining

is subject to many physical processes and temperature changes because of this there are microstructural changes in the material its grain size changes and change of phases also takes place. As a result, change of intensities can be noticed in the XRD patterns as grain size is indirectly proportional to the lattice strain. Figure 8c shows XRD pattern of workpiece before and after machining at three different parameters settings. In this figure also, the intensity is decreasing as the current value increased. Slight shifting and broadening of peak can be observed, this may be because of a very high-temperature generation because of change in phases during machining operation.

5 Conclusion

In the present study, an attempt was made to investigate the effect of process parameters on EDM of AISI stainless steel 202 using a copper alloy tool and thus optimizing the parameters using the RSM approach. Following conclusions were drawn.

- Electrode wear rate (EWR), material removal rate (MRR) and surface roughness all are greatly influenced by discharge current in this process. Pulse on and pulse off time have a considerable effect on these responses.
- Response surface methodology has been to form mathematical models. Regression equation of these models was generated and the interactive effect of process parameters on machining performance can be seen by these equations.
- SEM and XRD studies show that the machined surface of workpiece and the tool surface both undergo some changes by this machining process. Because of the material removal mechanism, recast layer was formed on the surface. Due to many complex physical processes and high temperature changes occurring at the surface materials also undergo change in phases.

References

1. Rajmohan T, Prabhu R, Subbarao G, Palanikumar K (2012) Optimization of machining parameters in electrical discharge machining (EDM) of 304 stainless steel. *Procedia Eng* 38:1030–1036
2. Muthuramalingam T, Mohan B (2014) A review on influence of electrical process parameters in EDM process. *Arch Civil Mech Eng*
3. Marafona J, Catherien W (2000) A new method of optimizing material removal rate using EDM with copper-tungsten electrode. *Int J Mach Tool Manuf* 40:153–164
4. Ho KH, Newman ST (2003) State of the art electrical discharge machining (EDM). *Int J Mach Tool Manuf* 43:1287–1300
5. Li Li YS, Wong JYH, Fuh L (2001) EDM performance of TiC/copper-based sintered electrodes. *Mater Des* 22:669–678
6. Khanra AK, Sarkar BR, Bhattacharya B, Pathak LC, Godkhindi MM (2007) Performance of ZrB₂-Cu composite as an EDM electrode. *J Mater Process Technol* 183:122–126
7. Lopez-Esteban S, Gutierrez-Gonzalez CF, Mata-Osoro G, Pecharrroman C, Diaz LA, Torrecillas R, Moya JS (2010) Electrical discharge machining of ceramics/semiconductor/metal nanocomposites. *Scripta Mater* 63:219–222
8. Kiyak M, Cakir O (2007) Examination of machining parameters on surface roughness in EDM of tool steel. *J Mater Process Technol* 191:141–144
9. Czelusniak T, Amorim FL, Lohrengel A, Higa CF (2014) Development and application of copper-nickel zirconium diboride as EDM electrodes manufactured by selective laser sintering. *Int J Adv Manuf Technol*
10. Rajurkar KP, Sundaram MM, Malshe AP (2013) Review of electrochemical and electrodischarge machining. *Procedia CIRP* 6:13–26
11. Fonseca J, Marafona JD.: The effect of deionization time on the electric discharge machining performance. *Int J Adv Manuf Technol*
12. Tang L, Guo YF (2013) Electrical discharge precision machining parameters optimization investigation on S-03 special stainless steel. *Int J Adv Manuf Technol*
13. Tsai HC, Yan BH, Huang FY (2003) EDM performance of Cr/Cu-based composite electrode. *Int J Mach Tools Manuf* 43:245–252
14. Lee HT, Tai TY (2003) Relationship between EDM parameters and surface crack formation. *J Mater Process Technol* 142:676–683
15. Zarepour H, Fadaei Tehrani A, Karimi D, Amini S (2007) Statistical analysis on electrode wear in EDM of tool steel DIN 1.2714 used in forging dies. *J Mater Process Technol* 187–188:711–714
16. Haron CH, Ghani JA, Burhanuddin Y, Seong YK, Swee CY (2008) Copper and graphite electrode performance in electrical-discharge machining of XW42 tool steel. *J Mater Process Technol* 201:570–573

17. Hu CF, Zhou YC, Bao YW (2008) Material removal and surface damage in EDM of Ti_3Si_2 ceramic. *Ceram Int* 34:537–541
18. Muttamara A, Fukuzava Y, Mohri N, Tani T (2009) Effect of electrode material on electric discharge machining of alumina. *J Mater Process Technol* 209:2545–2552
19. Hewidy MS, Al-Tawel TA, El-Safty MF (2005) Modelling and machining parameters of wire electrical discharge machining of inconel 601 using RSM. *J Mater Process Technol* 169:328–336
20. Assarzadeh S, Ghoreishi M (2013) Statistical modeling and optimization of process parameters in electro-discharge machining of cobalt-bonded tungsten carbide composite. *Procedia CIRP* 6:463–468
21. Habib SS (2009) Study of parameters in electric discharge machining through response surface methodology approach. *Appl Math Model* 33:4397–4407

Friction Stir Welding of Thermoplastic Composites



Sudhir Kumar , Tanmoy Medhi and Barnik Saha Roy 

Abstract Polymer matrix composites (PMCs) are replacing traditional metals and unfilled polymers due to their superior properties such as excellent strength/stiffness-to-weight ratio with enhanced toughness and low cost. Friction stir welding (FSW) is a new addition for joining of plastics and it has many advantages when compared with traditional joining process. The aim of this work is to investigate the feasibility of glass-filled Nylon 6 composites by FSW. Glass-filled Nylon 6 composites were fabricated by an injection molding machine and joined by FSW process with H13 tool steel with cylindrical pin profile. In order to study the mechanical and morphological properties of FSWed sections of glass filled Nylon 6 composites, a full factorial design of experiment was employed using the factors like tool rotational speed (400, 500 and 600 rpm), tool traverse speed (0.2, 0.3 and 0.4 mm/s) and tool tilt angle (0°, 1° and 2°) having constant standoff distance 0.2 mm. Analysis of variance (ANOVA) was used to find out the significance of process parameters (tool rotational speed, tool traverse speed, and tool tilt angle) with the tensile strength, and percentage elongation. The optimized result was achieved at a tool rotational speed of 600 rpm, welding speed of 0.2 mm/s, and tilt angle of 2° with defect-free welds. It is observed that joining of glass-filled Nylon 6 composites is feasible one with proper selection of process parameters and tool rotational speed has a significant effect on weld strength followed by tool traverse speed and tool tilt angle.

Keywords Glass-filled Nylon · FSW · Mechanical properties

S. Kumar (✉) · T. Medhi · B. S. Roy
Department of Mechanical Engineering, National Institute of Technology,
Agartala 799 046, India
e-mail: sudhir007gec@gmail.com

B. S. Roy
e-mail: barnik.me@nita.ac.in

1 Introduction

Nylon is high-performance, semi-crystalline thermoplastics with a number of attractive chemical, physical, and mechanical properties. Glass-filled Nylon 6 finds application in a wide range of products that requires high-strength materials [1]. Recently, the non-conventional joining processes such as high-speed laser welding, hot tool welding, ultrasonic welding, friction welding, resistance welding, microwave welding, vibration welding, and induction welding were used to join plastics. The various polymer joining methods for thermoplastics are shown in Fig. 1 [2, 3]. The most commonly used for joining of polymers is friction-based joining methods [4]. Friction stir welding (FSW) is a non-melting welding technique for joining of thermoplastics which can be substituted for other welding processes effectively [5]. So, a research is required to find the influence of various welding parameters on joint strength. An overview of the various factors influencing the quality of FSW is shown in Fig. 2 [6].

Nylon requires a low tool rotational speed and tool traverse speed for joining by FSW due to its low-melt viscosity property [7, 8]. The frictional heat generated between shoulder and workpiece is reduced by standoff distance, i.e., the gap between tool shoulder and workpiece [9–11]. Thermoplastics have a low melting temperature, a low hardness, a low thermal conductivity, and a very short solidification time with

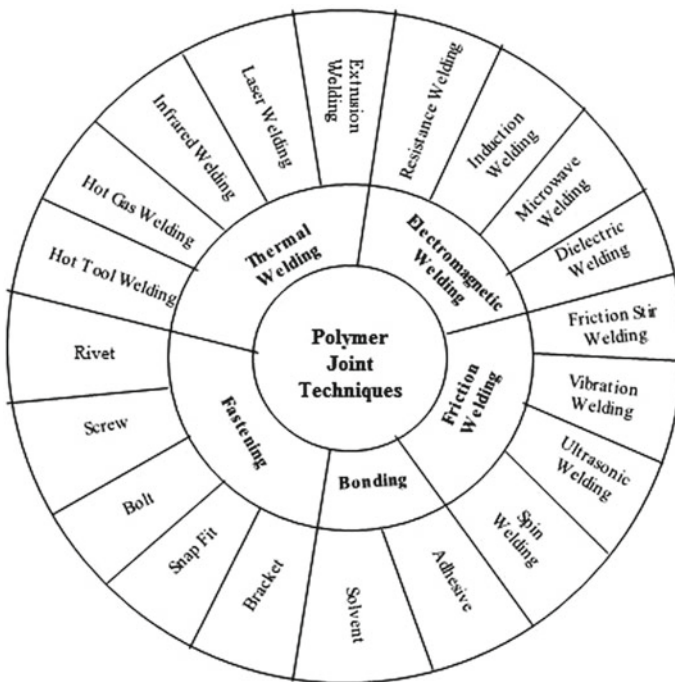


Fig. 1 Polymer joining techniques for thermoplastics

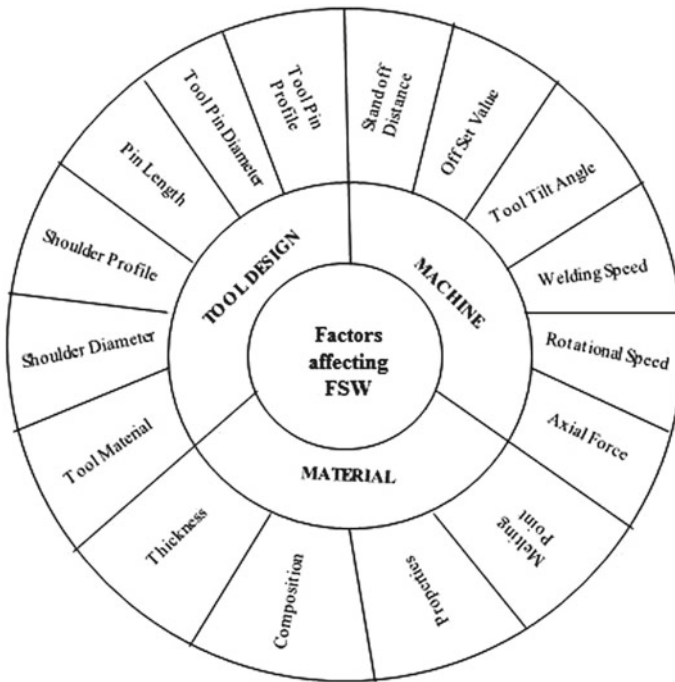


Fig. 2 Factors affecting friction stir welding

comparison to the metallic material. In case of FSW of polymer, the poor thermal conductivity creates nonuniform temperature distribution which restricts heat from advancing side to retreating side so mainly defects observed in retreating side [12, 13]. When using FSW to weld polymer materials, the main defects, such as pores, cracks, cavity, and voids, occurred in the retreating side. These defects could be minimized, even eliminated, by optimising process parameters [14]. The ultimate tensile strength of friction-stir-welded specimens at extreme low tool rotational speed was found low and defects, like crack, wormholes, or tunnel defects, observed in the retreating side due to less heat generation while at extreme high rotational speed, tensile strength was low due to more heating of tool and burns the materials [15, 16]. The ultimate tensile strength decreases to a minimum value as the tool traverse speed increases. This may be due to insufficient time duration for plasticization and proper mixing of materials. At extreme low tool traverse speed tensile strength was found low, nonuniform weld appearance was observed due to overheating in weld zone [16, 17]. The ultimate tensile strength of welded polymer increases with tool tilt angle increases up to a certain limit. [15].

From the previous works, it can be noted that there are few publications concerning FSW of polymer. The study of joining of glass-filled Nylon 6 by FSW is still to be explored. In this study, the feasibility of joining glass-filled Nylon 6 by

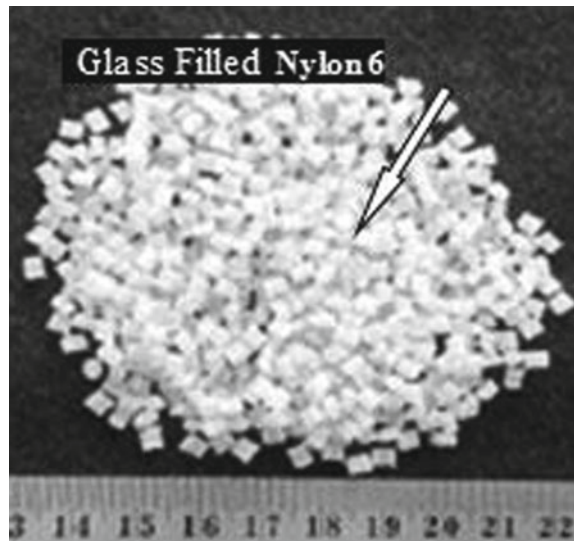
FSW is investigated for butt joint. In the present investigation, the primary methodology fabricates glass-filled Nylon 6 composites by using injection molding machine and joined by FSW process. The tensile strength, percentage elongation, and joint efficiency was carried out with three control factor such as tool rotational speed, tool traverse speed, and tool tilt angle; each has three levels using L'27 orthogonal arrays. Analysis of variance (ANOVA) was used to find out the significance of process parameters (tensile strength and percentage elongation) with the tool rotational speed, tool traverse speed, and tool tilt angle. Analyze the relationship between the morphological and mechanical property of the joints by using SEM.

2 Experimental Procedures

2.1 Materials

The raw materials used for injection molding are commercially available glass-filled Nylon 6 in the form of granules as shown in Fig. 3. Injection molding machine (Modern plastic and equipment's, Model-MPE-TLH-01) was used to fabricate the glass-filled Nylon 6 (30 wt%) composite specimens for joined by FSW process. The temperature is maintained at 240 °C for glass-filled Nylon 6, respectively. Sheet materials used in this work consisted of 130 mm × 80 mm × 5 mm (length, width, and thickness) glass-filled Nylon 6 composite sheets.

Fig. 3 Glass-filled Nylon 6 (granule form)



2.2 Welding Procedure

FSW process was performed on a 3T friction stir welding machine Model No. WS005E made in Hartford, Taiwan. A non-consumable rotating tool of cylindrical pin profile with a cylindrical shank was used. The FSW tool made of H13 tool steel with a shoulder diameter of 18 mm, pin diameter 6 mm, and pin length 4.8 mm was used in this study. The standoff distance between tool shoulder and top of the workpiece was taken 0.2 mm as shown in Fig. 4.

2.3 Process Parameters for FSW Processed Glass-Filled Nylon 6 Composites' Joints

In this study, a 3^3 full factorial design of experiment was conducted to explore the effects of processing parameters on the ultimate tensile strength and elongation of welded samples. An ANOVA method was performed in order to determine the significance of process parameters effects on weld strength [18]. After a large trial and error experiments, the acceptable ranges of tool rotational speed, tool traverse speed, and tool tilt angle were determined using weld appearance of the generated weld joint. Figures 5 and 6 show two defected fabricated samples beyond the ranges of selected parameters at high tool rotational speed and high traverse speed. The welding process parameters and their ranges used for the experiment are shown in Table 1.

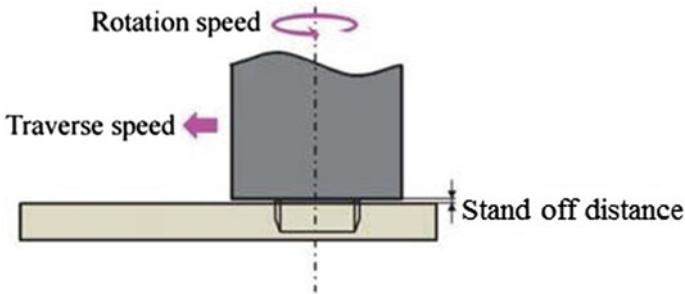


Fig. 4 Schematic diagram of standoff distance [9]



Fig. 5 Typical macrograph of weld crown at tool traverse speed of 0.6 mm/s, tool rotational speed of 600 rpm, and tilt angle of 2°



Fig. 6 Typical macrograph of weld crown at tool rotational speed of 1000 rpm, tool traverse speed 0.2 mm/s, and tilt angle of 2°

Table 1 FSW process parameters and their levels

Sl. No.	Welding parameters	Units	Level 1	Level 2	Level 3
1	Tool rotational speed	rpm	400	500	600
2	Tool traverse speed	mm/s	0.2	0.3	0.4
3	Tool tilt angle	°	0	1	2

2.4 Tensile Strength of FSW Processed Glass-Filled Nylon 6 Composites' Joints

The tensile test of the FSW of glass-filled Nylon 6 composites was carried out according to ASTM D638 at ambient temperature using a computerized tensometer at a strain rate of 0.5 mm/min and the constant gage length of 50 mm. The tensile strength of the base material glass-filled Nylon 6 composites was found about 86.01 MPa and the percent of elongation 13.68%, respectively.

3 Results and Discussion

FSW experimentation proposed to investigate the effect of processing parameters on the mechanical strength of the weld joint. The results of tensile tests based on proposed design welding process of welded samples are presented in Table 2. These results were statistically analyzed by Minitab Version 17 software and main effect diagram of each parameter's effect on weld strength was obtained. In the following sections, the obtained results were analyzed and the effects of each parameter on the weld strength were discussed. The main effect plots for ultimate tensile strength and elongation with respect to process parameters are shown in Figs. 7, 8, 9, 10, 11, and 12.

3.1 Effect of Tool Rotational Speed on the Ultimate Tensile Strength and Elongation

The effect of different tool rotational speed on the ultimate tensile strength and elongation of glass-filled Nylon 6 composites joints by FSW is shown in Figs. 7 and 8. Figure 7 shows that the ultimate tensile strength of glass-filled Nylon 6 composites increases to a maximum value as the tool rotational speed increases from 400 to 600 rpm in steps of 100 rpm. At low rotational speeds, the heat generated by the friction between the tool shoulder and the base material may be low. Under this condition, the material transportation from the advancing side of the tool to the retreating side of the tool may not occur sufficiently which end in the formation of joints with lower strength. Low tool rotational speed leads to defects like crack, wormholes, or tunnel defects observed in the retreating side due to less heat generation. In case of excess tool rotational speed, weld material burns and plasticized materials are expelled out from the weld area or stuck into the tool pin due to the lower melt viscosity, which results in lower tensile strength. The obtained results of ultimate tensile strength were also in correlation with the results [15, 16].

After the successful completion of tensile tests for all the welded samples, the fractured specimens were measured for the change in length to calculate the %

Table 2 Experimental results for tensile test

Ex. No.	Tool rotational speed (rpm)	Tool traverse speed (mm/s)	Tool tilt angle (°)	Ultimate tensile strength (MPa)	Joint efficiency (%)	Elongation (%)
1	400	0.2	0	14.87	17.29	4.12
2	400	0.2	1	15.98	18.57	4.42
3	400	0.2	2	18.96	22.04	4.76
4	400	0.3	0	14.02	16.30	3.23
5	400	0.3	1	15.89	18.47	3.44
6	400	0.3	2	17.29	20.10	3.78
7	400	0.4	0	13.10	15.23	2.73
8	400	0.4	1	13.16	15.30	2.92
9	400	0.4	2	15.43	17.93	3.33
10	500	0.2	0	24.39	28.36	6.14
11	500	0.2	1	25.74	29.93	6.32
12	500	0.2	2	31.13	36.19	6.62
13	500	0.3	0	20.76	24.14	5.08
14	500	0.3	1	23.35	27.15	5.25
15	500	0.3	2	26.41	30.70	5.56
16	500	0.4	0	17.38	20.21	4.54
17	500	0.4	1	17.53	20.38	4.71
18	500	0.4	2	19.13	22.24	5.01
19	600	0.2	0	29.63	34.45	7.02
20	600	0.2	1	31.79	36.97	7.16
21	600	0.2	2	36.51	42.45	7.35
22	600	0.3	0	24.29	28.24	5.87
23	600	0.3	1	25.72	29.91	6.02
24	600	0.3	2	28.63	33.28	6.27
25	600	0.4	0	18.03	20.96	5.33
26	600	0.4	1	18.53	21.54	5.37
27	600	0.4	2	20.60	23.95	5.64

elongation. The friction-stir-welded plate shows lower elongation in comparison to the base material for all the cases. This may be mainly attributed to the concentration of high plastic strain within the TMAZ. The plastic deformation concentrated at the transition zone between the weld nugget and base material. Figure 8 shows that elongation of glass-filled Nylon 6 composites increased with the increase of tool rotational speed. The obtained results of ultimate tensile strength were also in correlation with the results [16].

Fig. 7 Effect of tool rotational speed on the tensile strength

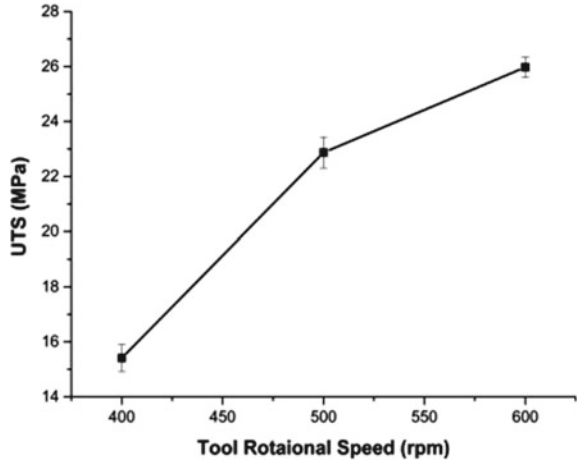
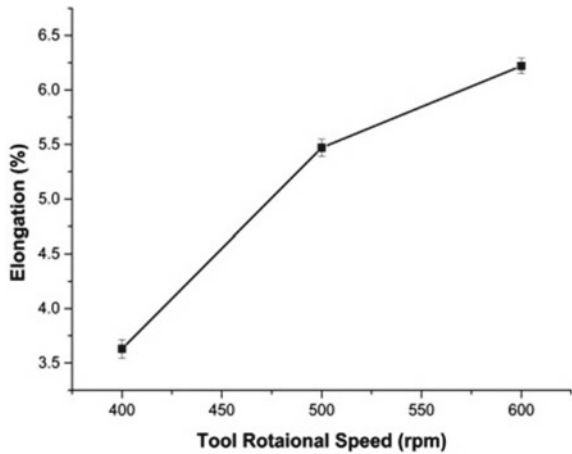


Fig. 8 Effect of tool rotational speed on the elongation



3.2 Effect of Tool Traverse Speed on Ultimate Tensile Strength and Elongation

The effect of different tool traverse speed on the ultimate tensile strength and elongation of glass-filled Nylon 6 composites joints by FSW is shown in Figs. 9 and 10. Figures 9 and 10 show that the ultimate tensile strength and elongation of glass-filled Nylon 6 composites decrease to a minimum value as the tool traverse speed increases from 0.2 to 0.4 mm/s. The tool traverse speed should be selected in such a way that there should be sufficient amount of duration for the joints to be consolidated. The tensile strength and elongation of friction-stir-welded specimens at high tool traverse speed were found low and defects observed in retreating side of weld appearance, and this may be due to not enough time to melt polymer, so weak mixing of material

Fig. 9 Effect of tool traverse speed on the tensile strength

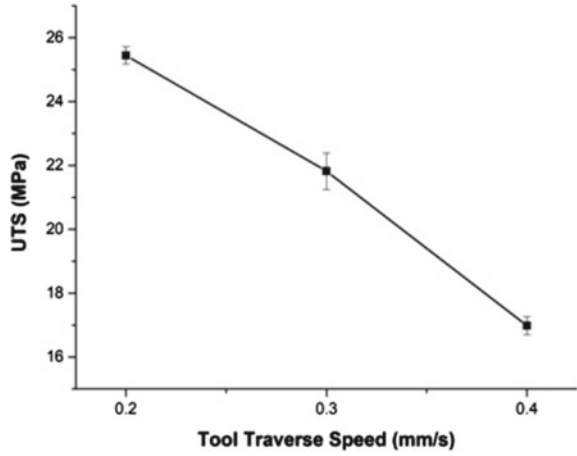
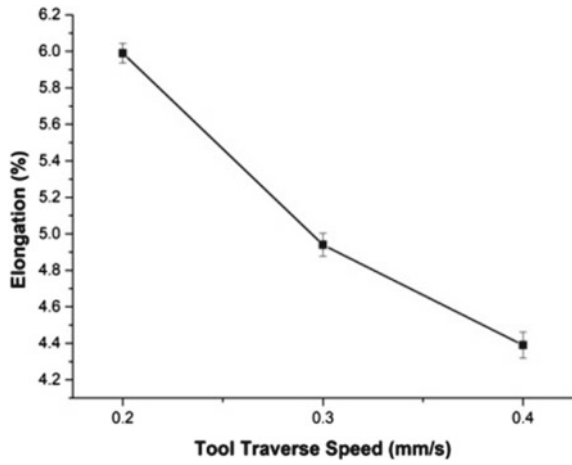


Fig. 10 Effect of tool traverse speed on the elongation



produce and low thermal conductivity of polymer heat generated non-uniformly as shown in Fig. 5. With lower values of tool traverse speed (less than 0.2 mm/s), tensile strength was found low and weld appearance observed non-uniform, and this may be due to overheating of weld zone. The obtained results of ultimate tensile strength were also in correlation with the results [15–17].

3.3 Effect of Tool Tilt Angle on Ultimate Tensile Strength and Elongation

The effect of different tool tilt angle on the ultimate tensile strength and elongation of glass-filled Nylon 6 composites joints by FSW is shown in Figs. 11 and 12. Figures 11 and 12 show that the ultimate tensile strength and elongation of glass-filled Nylon 6 composites increase to a maximum value as the tool tilt angle increases from 0 to 2° (in steps of 1°). This may be mainly attributed to the edge of shoulder creates an extra pressure and heat generation for proper mixing of weld material. The obtained results of ultimate tensile strength were also in correlation with the results [15].

Fig. 11 Effect of tool tilt angle on the tensile strength

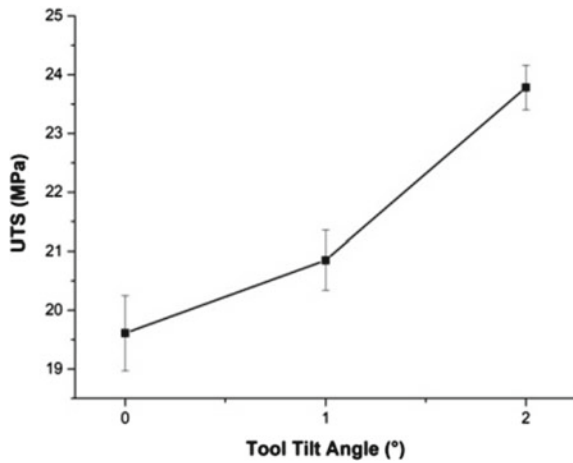
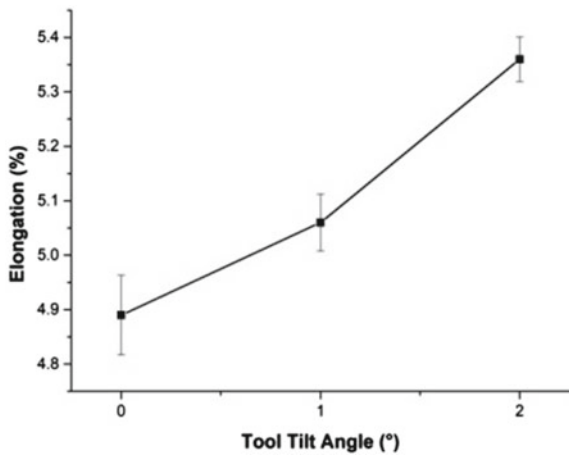


Fig. 12 Effect of tool tilt angle on the elongation



3.4 Analysis of Variance

On the basis of ANOVA, we observed that the contribution of tool rotational speed, tool traverse speed, and the tool tilt angles are 50.80%, 31.05%, and 7.92% respectively. For elongation, the tool rotational speed 71.15% has the most contribution on the output followed by tool traverse speed 26.27% and tool tilt angle 2.30%.

3.5 Microstructural Studies

The scanning electron microscopy was used to analyze the relation between the morphology and joint characteristics of glass-filled Nylon 6 composite. Typical macro- and microstructure of maximum tensile strength and elongation of glass-filled Nylon 6 composite are shown in Fig. 13a–d, (a) weld crown, (b) weld seam, (c) SEM microstructure of weld, and (d) fracture surface of weld. As Figs. 13 and 14 show the friction-stir-welded specimens with the highest ultimate tensile strength and elongation and lowest ultimate tensile strength and elongation, it is obvious in a samples with the optimized parameters highest ultimate tensile strength and elongation achieved at tool rotational speed of 600 rpm, tool traverse speed of 0.2 mm/s, and tilt angle of 2°, perfect surface quality with laminar flows uniform structure and free of defects such as crack, porosity, and cavity as shown in Fig. 13c. Typical macro- and microstructure of minimum tensile strength and elongation of glass-filled Nylon 6 composite are shown in Fig. 14a–d, (a) weld crown, (b) weld seam, (c) SEM microstructure of weld, and (d) fracture surface of weld. The lowest tensile strength and elongation at tool rotational speed 400 rpm, tool traverse speed 0.4 mm/s, and tool tilt angle 0°, a poor weld line with defects such as tunnel defects, crack, voids, and surface deflection was created as shown in Fig. 14c. Porous sites were found at the weld interface and discontinuity at the joint zone was observed due to improper flow of the molten layer. This has led to weakening of joints. The presence of glass fibers hindered diffusion of the polymer across the interface and lead to porous sites. The microstructure of welded samples illustrated that laminar flow and uniform structure resulted in high ultimate tensile strength and elongation while the presence of cracks and voids resulted in low ultimate tensile strength and elongation.

A critical examination of the fracture surfaces revealed that most of the samples with low UTS had an S-shape fracture surface, whereas some of the samples with high UTS values had ductile fracture surface with necking region. Figures 13d and 14d show the images of the fractured specimen. Scanning electron microscope (SEM) analysis was conducted for studying the fracture morphology of tensile specimens with low UTS and brittle failure as shown in Fig. 14d. For Fig. 13d with maximum UTS in weld joint, tiny cups and cone (dimple formation) were noticed all over the sample which is representative of ductile fracture. The fracture occurred near the boundary of TMAZ and NZ of advancing side of the welded joint for maximum UTS and elongation. However, the fracture occurred in NZ at the retreating side

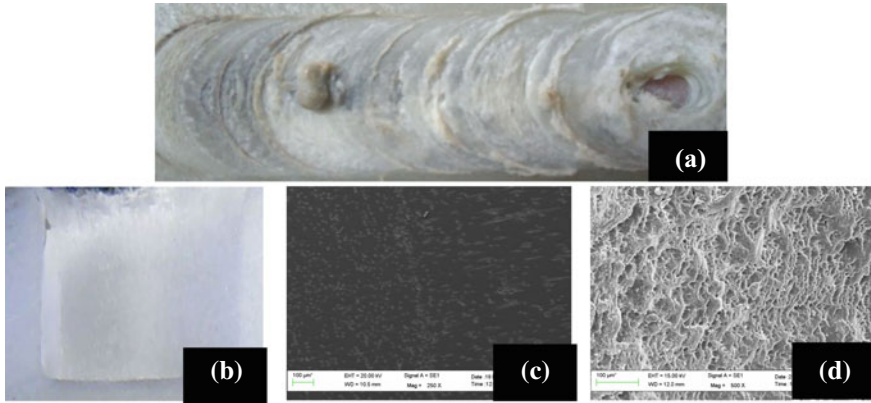


Fig. 13 Typical macro- and microstructure of maximum tensile strength and elongation: **a** weld crown, **b** weld seam, **c** SEM microstructure of weld, and **d** fracture surface of weld

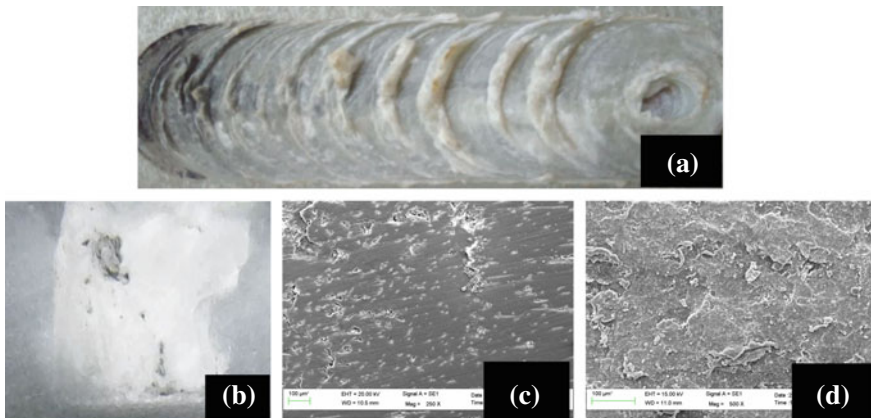


Fig. 14 Typical macro- and microstructure of minimum tensile strength and elongation: **a** weld crown, **b** weld seam, **c** SEM microstructure of weld, and **d** fracture surface of weld

for minimum UTS and elongation. However, tensile specimens of minimum weld tensile strength and elongation broke up at the retreating side. The joint efficiency for glass-filled Nylon 6 composites is shown in Table 2. Joint efficiency is calculated to compare parent material ultimate tensile strength. In the entire test that was carried on glass-filled Nylon 6 composites, the best parameter was at tool rotational speed 600 rpm, tool traverse speed 0.2 mm/s, and tool tilt angle 2° with no defect in welding zone. Tensile test result showed that it reached the value of 42.45% of the UTS compared to base material and joint efficiency was lowest (15.23%) at tool rotational speed 400 rpm, tool traverse speed 0.4 mm/s, and tool tilt angle 0°.

4 Conclusions

In this experimental study, FSW of glass-filled Nylon 6 composite carried out at varying tool rotational speed, tool traverse speed, and tool tilt angle, based on the results in presented above; the following major conclusions are drawn:

- The present work showed that successful fabrication of glass-filled Nylon 6 composites using injection molding machine.
- The study demonstrates that welding of glass-filled Nylon 6 is feasible and the optimized result was achieved at a tool rotational speed of 600 rpm, tool traverse speed of 0.2 mm/s, and tool tilt angle of 2° with defect-free welds.
- The tensile strength and percentage elongation of glass-filled Nylon 6 composites increase with an increase in tool rotational speed and tool tilt angle while the tensile strength and percentage elongation of glass-filled Nylon 6 composites decrease with increase tool traverse speed.
- Tensile specimens of FSWed joint of maximum weld tensile strength and elongation, fractures occurred in advancing side. However, the tensile specimens of minimum weld tensile strength and elongation broke up at the retreating side.
- The microstructure of welded samples illustrated that laminar flow and uniform structure resulted in high ultimate tensile strength and elongation while the presence of cracks and voids resulted in low ultimate tensile strength and elongation.

References

1. Panneerselvam K, Lenin K (2014) Joining of Nylon 6 plate by friction stir welding process using threaded pin profile. *Mater Des* 53:302–307
2. Troughton MJ (2008) *Handbook of plastics joining: a practical guide*. William Andrew
3. Jafrey DD, Panneerselvam K (2017) Study on tensile strength, impact strength and analytical model for heat generation in friction vibration joining of polymeric nanocomposite joints. *Polym Eng Sci* 57(5):495–504
4. Strand S (2003) Joining plastics-can friction stir welding compete? In: *Electrical insulation conference and electrical manufacturing & coil winding technology conference, proceedings*. IEEE, pp. 321–326
5. Thomas WM, Nicholas ED, Needham JC, Murch MG, Templesmith P, Dawes CJ (1994) GB patent application No. 9125978.8, Dec 1991
6. Grewell D, Benatar A (2007) *Welding of plastics: fundamentals and new developments*. *Int Polym Process* 22(1):43–60
7. Zafar A, Awang M, Khan SR (2017) Friction stir welding of polymers: an overview. In: *2nd international conference on mechanical, manufacturing and process plant engineering*, pp 19–36
8. Zafar A, Awang M, Khan SR, Emamian S (2016) Investigating friction stir welding on thick nylon 6 plates. *Weld J* 95
9. Inaniwa S, Kurabe Y, Miyashita Y, Hori H (2014) Application of friction stir welding for several plastic materials. In: *Proceedings of the 1st International Joint Symposium on Joining and Welding: Osaka, Japan, 6–8 Nov 2013*, p 137
10. Panneerselvam K, Lenin K (2013) Study on friction stir welding of nylon 6 plates. *Int J Concept Mech Civ Eng* 1(1):116–133

11. Zafar A, Awang M, Khan SR, Emamian S (2015) Effect of double shoulder tool rotational speed on thermo-physical characteristics of friction stir welded 16 mm thick Nylon6. *Appl Mech Mater* 799:251–255
12. Eslami S, Tavares PJ, Moreira PMGP (2017) Friction stir welding tooling for polymers: review and prospects. *Int J Adv Manuf Technol* 89(5–8):1677–1690
13. Mendes N, Loureiro A, Martins C, Neto P, Pires JN (2014) Effect of friction stir welding parameters on morphology and strength of acrylonitrile butadiene styrene plate welds. *Mater Des* 58:457–464
14. Huang Y, Meng X, Xie Y, Wan L, Lv Z, Cao J, Feng J (2018) Friction stir welding/processing of polymers and polymer matrix composites. *Compos A Appl Sci Manuf* 105:235–257
15. Sadeghian N, Givi MKB (2015) Experimental optimization of the mechanical properties of friction stir welded acrylonitrile butadiene styrene sheets. *Mater Des* 67:145–153
16. Youssif MS, Ei-Sayed MA, Khourshid AM (2016) Influence of critical process parameters on the quality of friction stir welded nylon 6. *Int Rev Mech Eng* 10:501–507
17. Panneerselvam K, Lenin K (2013) Optimizing the welding parameters of friction stir welding by using resultant force and defects for nylon 6 material. *Int J Mech Eng* 1(2):87–94
18. Kumar S, Panneerselvam K (2016) Optimization of friction and wear of nylon 6 and glass fiber reinforced (GFR) nylon 6 composites against 30 wt.% GFR nylon 6 disc. *J Adv Res Mater Sci* 19:14–32

Numerical Simulation of Temperature Distribution in Laser Welding of AISI 316



Pramod Kumar and Amar Nath Sinha

Abstract A numerical simulation of temperature distribution of laser welding of 316L austenitic stainless steel has been investigated in the present research. A three-dimensional Gaussian conical moving heat source has been implemented in the present numerical simulation. ANSYS with certain modifications has been used to account for thermomechanical analysis during laser welding. Temperature-dependent thermal physical properties of 316L austenitic stainless steel have been considered, which influence the temperature profile in the weldment. The temperature distribution was measured at different process parameters. The effect of laser welding process parameters such as average beam power, welding speed, and laser spot diameter on weld bead geometry has been studied. The temperature distribution obtained from the numerical results is in good agreement with the experimental results. The shape of the weld pool profile obtained through numerical simulation is in good agreement with the experimental results.

Keywords Laser welding · Numerical simulation · Temperature distribution · Heat source

1 Introduction

Laser welding process is a high-power density welding. It is a widely growing technology due to its smooth, precise, and effective operation. Numerical simulation method has been an evolution in this area because this technique can be used to describe the physical phenomena during complex welding processes and can also be used to optimize the laser welding process parameters. Laser welding is a non-conventional welding process of joining wide range similar and dissimilar materials. Laser welding has become an important area of research for many researchers over the last decade and has been working to predict the temperature profile and weld geometry during laser welding using analytical as well as numerical simulation method. Rosenthal has developed an analytical method for solving temperature distribution of the welded joint considering point, line, or plane heat source. Rosenthal

P. Kumar (✉) · A. N. Sinha
Department of Mechanical Engineering, National Institute of Technology, Patna, India
e-mail: pramod.me14@nitp.ac.in

© Springer Nature Singapore Pte Ltd. 2019
K. Shanker et al. (eds.), *Advances in Industrial and Production Engineering*, Lecture Notes in Mechanical Engineering, https://doi.org/10.1007/978-981-13-6412-9_22

solutions give accurate results for peak temperature less than 20% of the melting point [1]. Frewin and Scott have studied pulsed laser welding and developed three-dimensional finite element model of heat flow using a subroutine in ANSYS APDL [2]. Carmignani et al. [3] have investigated the residual stresses and strains in laser welding of austenitic stainless steel 304L sheet of 10 mm thickness with maximum laser beam power of 15 kW. Numerical simulation of temperature and stress field developed during laser welding has been measured as a function of welding speed using ABAQUS. Numerical simulation of laser beam welding process for keyhole formation with transient thermal analysis has been studied by Tsirkas et al. [4]. Sabbaghzadeh et al. [5] have studied the numerical simulation of pulsed laser welding with the help of two different methods such as finite element method and finite difference method for finding the temperature distribution and weld geometry. Balasubramanian et al. [6] have calculated the temperature profile and weld geometry (bead width and depth of penetration) using FEA code SYSWELD for different process parameters of laser welding and compared the results obtained with experimental. Bag et al. [7] studied the heat flow in laser spot welding with combined effect of adaptively defined volumetric heat source and surface heat flux. Capriccioli and Frosi have studied thermal and mechanical simulation of TIG and laser beam welding of INCONEL 625 and AISI 316 using birth and death technique in ANSYS software package [8]. They have simulated the fusion zone of INCONEL 625 and AISI 316 during TIG and laser welding compared their numerical results with experimental values. Belhadj et al. [9] have developed a three-dimensional FEM model to simulate the temperature distribution and the weld bead geometry of magnesium alloy in laser welding. Kim et al. [10] have studied the numerical simulation of pulsed laser welding of 304L using finite element code to optimize the welding conditions. Shanmugam et al. [11] have developed a FEM code using SYSWELD to evaluate the transient temperature distribution and weld bead geometry in T-joint laser welding of AISI 304L of 1.6-mm-thick sheet considering the material properties as temperature-dependent. Yilbas et al. [12] have studied the transient temperature profile and the residual stresses induced in the low carbon mild steel of thickness 2 mm by developing a finite element model using finite element code ANSYS. They have found that the temperature decreases first very rapidly and then gradually along the thickness of the material. Casalino et al. [13] presented a finite element model to predict the thermal aspect and weld bead shape in fiber laser welding of both similar (Ti6Al4V) and dissimilar (AA5754 aluminum alloy and T40 pure titanium sheet) materials. Chukkan et al. [14] investigated laser beam welding using three different sources.

The present investigation aims to study the effect of laser process parameters, namely average beam power, welding speed, and laser spot size on temperature distribution curve and weld geometry in laser welding of austenitic stainless steel 316L using finite element code ANSYS APDL for butt joint. Temperature-dependent thermal-physical properties such as density, thermal conductivity, and specific heat of 1.4-mm-thin sheet of 316L were considered for the analysis purpose. A three-dimensional Gaussian moving heat source with conical shape has been used in this numerical simulation.

2 Numerical Simulation

2.1 Heat Transfer Analysis

The basic governing equation of the three-dimensional heat conduction for transient temperature is given as in Eq. 1 [1].

$$\rho c \frac{\partial T}{\partial \tau} + v \rho c \frac{\partial T}{\partial y} = \frac{\partial}{\partial x} \left(K_x \frac{\partial T}{\partial x} \right) + \frac{\partial}{\partial y} \left(K_y \frac{\partial T}{\partial y} \right) + \frac{\partial}{\partial z} \left(K_z \frac{\partial T}{\partial z} \right) + Q(x, y, z) \quad (1)$$

It has been assumed that laser beam follows the Gaussian heat-source distribution of conical shape moving with velocity v along the y -axis. Figure 1 shows the schematic representation of laser welding system used in the present research work.

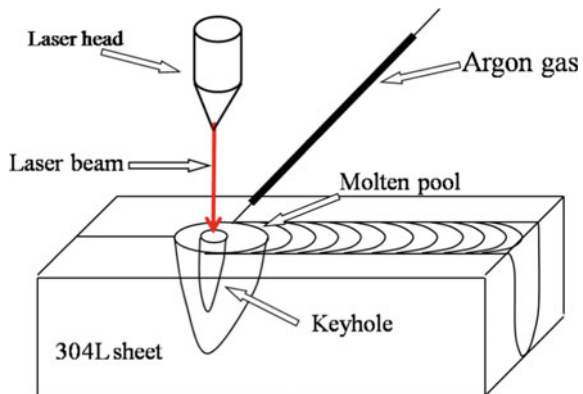
It has been found experimentally that 30.7% of the total power is lost and rest 69.3% power is absorbed by the workpiece in case of AISI 316L austenitic stainless steel. It is assumed that of 69.3% of total power, 17.3% power is absorbed on the top surface (Q_{surf}), and rest 52% power is distributed inside the material in conical shape ($Q_{keyhole}$). The distribution of heat on the top surface is given by Eq. 2.

$$Q(x, y) = \frac{3 Q_{surf}}{\pi R^2} e^{-\frac{3(x^2+(y-vx\tau)^2)}{R^2}} \quad (2)$$

where Q_{surf} is the heat power of the plane heat source (17.3%). It has been assumed the simulation of keyhole is a cone, the Gaussian distribution of heat flux is given as in Eq. 3.

$$Q(z) = \frac{2 Q_{keyhole}}{\pi r_o^2 H} e^{-\left(\frac{x^2+(y-vx\tau)^2}{r_o}\right)^2} (1 - z/H) \quad (3)$$

Fig. 1 Schematic representation of laser welding



The total heat input given to the model is the combination of both surface and volume heat-source models, which can be expressed as given by Eq. 4.

$$Q_v(r, z) = Q(x, y) + Q(z) \quad (4)$$

2.2 Finite Element Modeling

A three-dimensional transient analysis finite element model has been developed to simulate the laser welding process using commercial ANSYS APDL 17.2 software package. The finite element model used in the present simulation is designed for 50 mm × 25 mm × 1.4-mm-size sheet. The model developed is used to predict the temperature profile, molten pool shape and peak temperature and the effect of laser process parameters, namely average power, welding speed, and laser spot diameter. The geometry of the weld structure is modeled using two types of elements: three-dimensional volume elements with eight nodes (SOLID 70) and two-dimensional element with four nodes (PLANE 55). Very fine meshing of small-size element is done near weld line, and coarser mesh of increasing element size is done away from the weld line as shown in Fig. 2. In the present simulation, several trials have been done for obtaining optimum grid size with varying element size from 23,000 to 105,000. Mesh convergence test has been carried out and is found that the peak temperature becomes independent of mesh density after 78,750 elements. The element size near the weld line is 0.2 mm × 0.2 mm × 0.2 mm. There are total 82,530 nodes and 78,750 elements in full part of the model.

The heat flux is applied on the element faces for simulating the moving heat source. The moving heat source has been developed by using ANSYS APDL language subroutine. For simplifying the finite element model, some of the basic considerations have been made.

The following assumptions have been made in this model:

- (a) The initial temperature of workpiece is taken as 40 °C.

Fig. 2 Mesh of the geometry

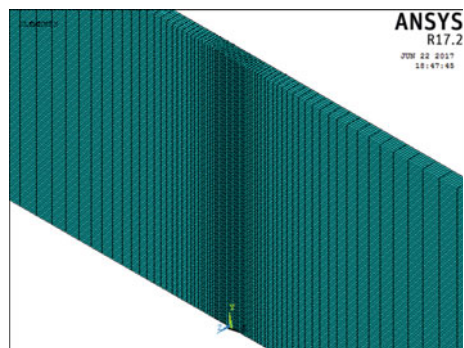


Table 1 Laser welding process parameters

Sl. No.	Beam power (W)	Welding speed (mm/s)	Spot diameter (mm)
1	125	3	0.60
2	225	3	0.60
3	325	3	0.60
4	425	3	0.60
5	125	5	0.60
6	225	5	0.60
7	325	5	0.60
8	425	5	0.60
9	425	5	0.75

- (b) Thermophysical properties of the material such as density, specific heat and thermal conductivity are considered as temperature-dependent [15].
- (c) Radiation and convection heat loss from the surfaces of the workpiece are taken into account.
- (d) Combined radiation and convection are considered by using lumped heat transfer coefficient [2].
- (e) The physical phenomenon like viscous force, buoyancy force, convective melt flow, and Marangoni effect are neglected.

The laser beam welding process parameters considered for the present numerical simulation of temperature distribution are given in Table 1.

3 Experimental Method

To validate the numerical simulation of temperature distribution of austenitic stainless steel of 1.4 mm thickness, Nd: YAG laser welding was performed on JK 600HP Nd: YAG Laser with a maximum average laser power of 600 W and wavelength of 1.06 μm . An argon gas with a flow rate of 6 L/min was used for shielding in the experiment. Four *K*-type thermocouples with the temperature range between -40 and 1250 $^{\circ}\text{C}$ were used for measuring the temperature distribution during laser welding at four different locations (X) away from the weld line (*a*) $X = 3$ mm, $X = 6$ mm and $X = -6$ mm and (*d*) $X = 9$ mm with $Y = 10$ mm and $Z = 1.2$ mm, fixed for all thermocouple positions. The temperature were recorded using Data Logger Thermometer Centre 309 attached with PC interface. Thermal-physical properties, namely thermal conductivity ($\text{W/m } ^{\circ}\text{C}$), density (kg/m^3), and specific heat ($\text{J/kg } ^{\circ}\text{C}$), are temperature-dependent which are illustrated in Table 2 [15]. The laser welding of 316L for validating the numerical simulation results was carried out at 425 W average beam power, 5 mm/s welding speed, and 0.75 mm laser spot diameter.

Table 2 Thermo-physical properties of AISI 316L stainless steel

Temperature (°C)	Density (kg/m ³)	Heat capacity (J/kg °C)	Thermal conductivity (W/m °C)
0	7885.8624	498.528	13.5368
150	7706.13641	518.682	15.8933
300	7476.15568	538.782	18.24983
450	7195.920211	558.882	20.60633
600	6865.4300	578.982	22.96283
750	6484.68506	599.082	25.31933
900	6053.685377	619.182	27.67583
1050	5572.430956	639.282	30.03233
1200	5040.921797	659.382	32.38883
1350	4459.1579	679.482	34.74533

4 Results and Discussion

The temperature distribution are numerically computed using finite element code ANYS APDL for varying average beam power, varying welding speed and laser spot diameter. A series of numerical simulations over the range of laser welding process parameters were performed as listed in Table 1. Figure 3 shows the transient temperature distribution of laser welding of 316L SS at constant welding speed (3 and 5 mm/s) and laser spot diameter of 0.60 mm and for varying average power (125–425 W) along the weld line. Figure 4 shows the effect of peak temperature distribution at constant welding speed (3 and 5 mm/s) and laser spot diameter of 0.60 mm and for varying average beam power away from the weld line. Figure 5a and b show the variation of peak temperature along the thickness at constant speed $V = 5$ mm/s and beam power $P = 425$ W at two different laser spot diameters of 0.60 and 0.75 mm, respectively.

Figure 6 shows the 3-D temperature field distribution at constant welding speed $V = 5$ mm/s, for varying average beam power (125–425 W). Figure 7 shows the effect of laser beam power and welding speed on weld bead geometry at constant laser spot size of 0.60 mm diameter. It has been observed that weld bead geometry profile changes with increasing average beam power and welding speed. It has been also found that at very high heat input (beam power/welding speed) the weld bead geometry changes nearly to H shaped. Temperature distribution results obtained numerically were validated through experimentally, measured with K -type thermocouple fixed at different positions. Figure 8 shows the comparison of numerical simulation temperature distribution results with K -type thermocouples at different positions (X) away from the weld line (a) $X = 3$ mm, $X = 6$ mm, and $X = 9$ mm and (b) $X = -6$ mm.

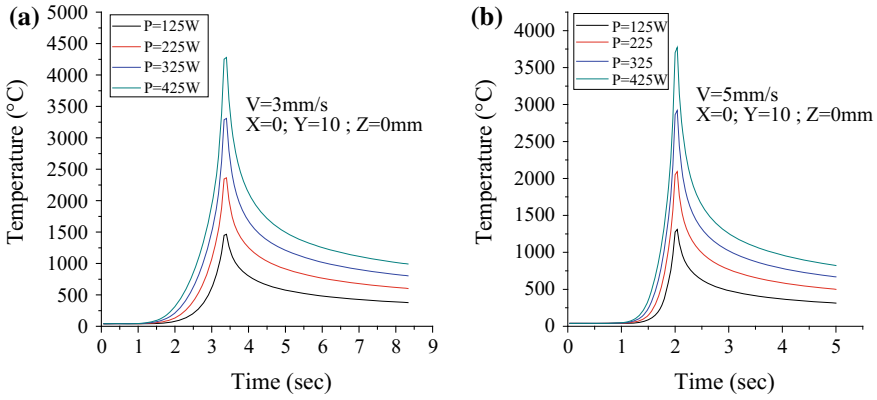


Fig. 3 Transient temperature distribution for varying average beam power at constant welding speed along the weld line. **a** $V = 3 \text{ mm/s}$ and **b** $V = 5 \text{ mm/s}$

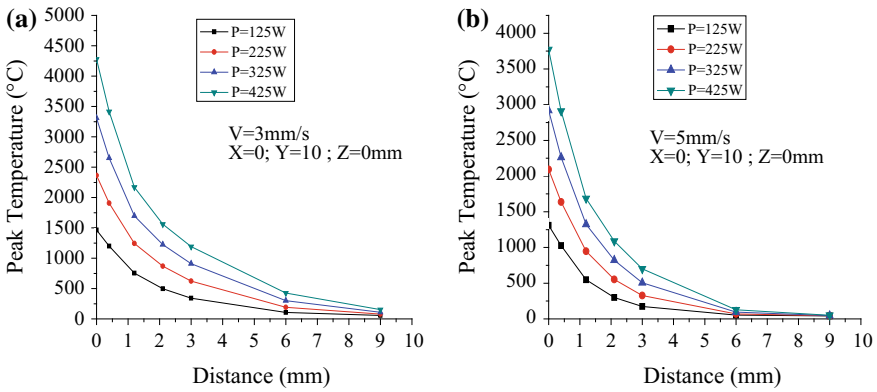


Fig. 4 Peak temperature distribution for varying average beam power at constant welding speed away from the weld line. **a** $V = 3 \text{ mm/s}$ and **b** $V = 5 \text{ mm/s}$

5 Conclusions

The laser welding process parameters such as beam power, welding speed and spot diameter and their effect on temperature profile, shape, and size of molten pool and bead geometry have been investigated. The numerical simulated results were validated with laser welding experimental value with good agreement. The following conclusions can be made from the above investigation:

- The peak temperature increases with increase in average power at constant welding speed.

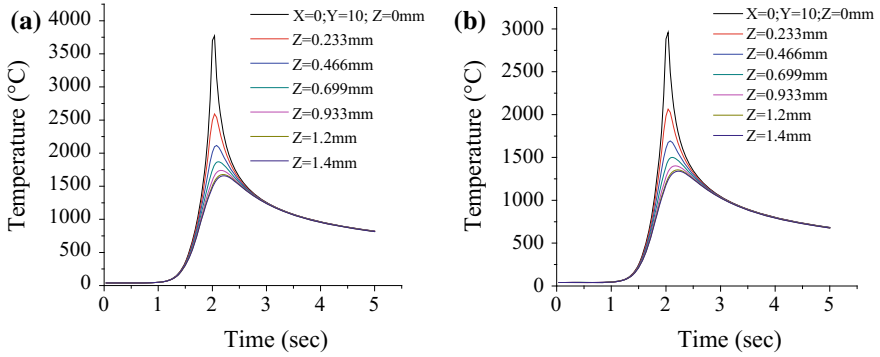


Fig. 5 Variation of peak temperature along the thickness at constant speed $V = 5$ mm/s and beam power $P = 425$ W at **a** laser spot diameter of 0.60 mm, **b** laser spot diameter of 0.75 mm

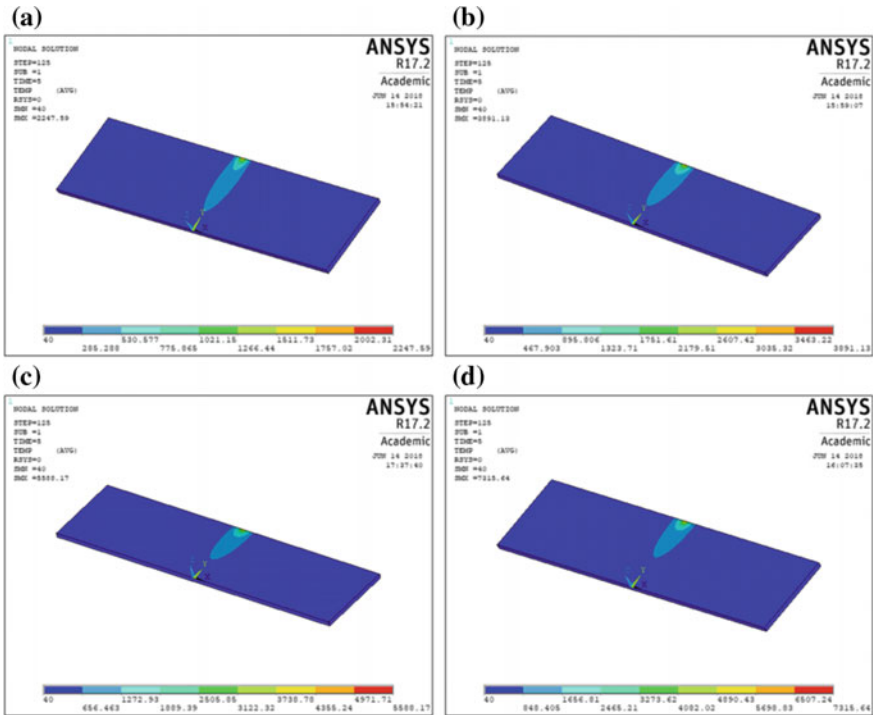


Fig. 6 3-D temperature field distribution at constant welding speed $V = 5$ mm/s, for varying average beam power. **a** $P = 125$ W, **b** $P = 225$ W, **c** $P = 325$ W, **d** $P = 425$ W

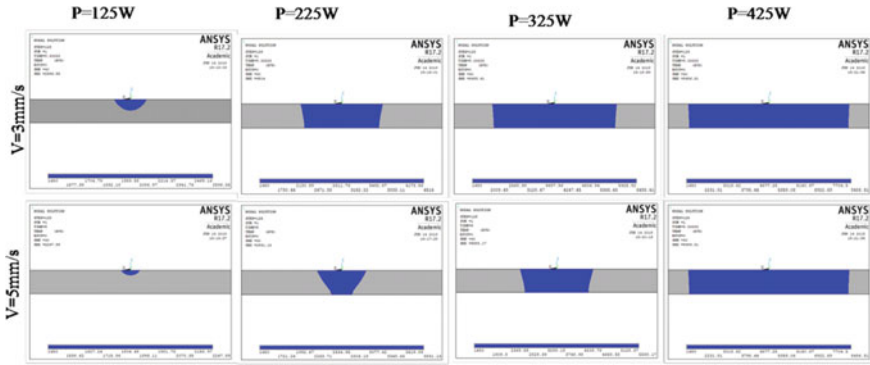


Fig. 7 Effect of laser power and welding speed on weld geometry at constant laser spot size of 0.60 mm diameter. **a** $V = 2$ mm/s, **b** $V = 3$ mm/s, and **c** $V = 5$ mm/s

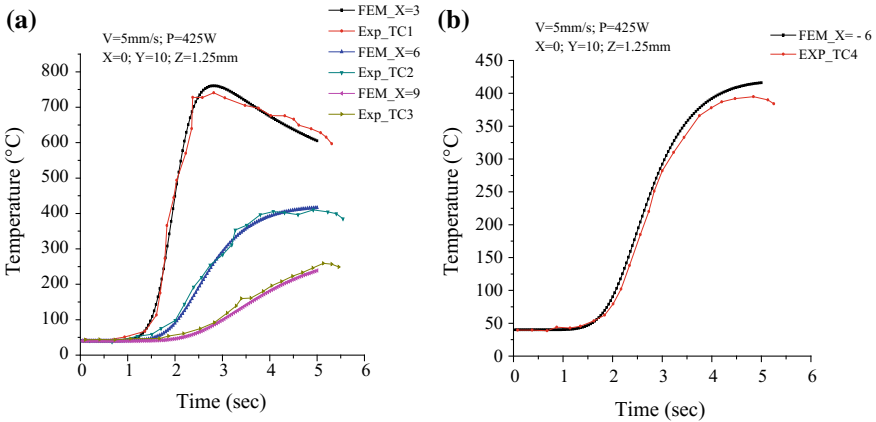


Fig. 8 Comparison of numerical simulation temperature distribution result with K -type thermocouples at different locations (X) away from the weld line. **a** $X = 3$ mm, $X = 6$ mm, and $X = 9$ mm and **b** $X = -6$ mm

- The maximum peak temperature measured along the weld line is 4278.91 °C at welding speed of 3 mm/s and average beam power of 425 W and minimum peak temperature is 1309 °C at welding speed of 5 mm/s and average power of 125 W.
- The peak temperature decreases as we move away from the weld line.
- The weld bead geometry becomes nearly H shaped at very high heat input.
- The peak temperature measured experimentally with all four K -type thermocouples with good agreement.

References

1. Rosenthal D (1946) The theory of moving sources of heat and its application of metal treatments. *Trans ASME* 68:849–866
2. Frewin MR, Scott D (1999) Finite element model of pulsed laser welding. *Weld J* 78:15–s
3. Carmignani C, Mares R, Toselli G (1999) Transient finite element analysis of deep penetration laser welding process in a single pass butt-welded thick steel plate. *Comput Methods Appl Mech Eng* 179(3):197–214
4. Tsirkas SA, Papanikos P, Kermandis T (2003) Numerical simulation of the laser welding process in butt-joint specimens. *J Mater Process Technol* 134(1):59–69
5. Sabbaghzadeh J, Azizi M, Torkamany MJ (2008) Numerical and experimental investigation of seam welding with a pulsed laser. *Opt Laser Technol* 40(2):289–296
6. Balasubramanian KR, Siva Shanmugam N, Buvanashakaran G, Sankaranarayana-samy K (2008) Numerical and experimental investigation of laser beam welding of AISI 304 stainless steel sheet. *Adv Prod Eng Manag* 3(2):93–105
7. Bag S, Trivedi A, De A (2009) Development of a finite element based heat transfer model for conduction mode laser spot welding process using an adaptive volumetric heat source. *Int J Therm Sci* 48(10):1923–1931
8. Capriccioli A, Frosi P (2009) Multipurpose ANSYS FE procedure for welding processes simulation. *Fusion Eng Des* 84(2):546–553
9. Belhadj A, Bessrou J, Masse JE, Bouhafis M, Barrallier L (2010) Finite element simulation of magnesium alloys laser beam welding. *J Mater Process Technol* 210(9):1131–1137
10. Kim K, Lee J, Cho H (2010) Analysis of pulsed Nd: YAG laser welding of AISI 304 steel. *J Mech Sci Technol* 24(11):2253–2259
11. Shanmugam NS, Buvanashakaran G, Sankaranarayananasamy K, Kumar SR (2010) A transient finite element simulation of the temperature and bead profiles of T-joint laser welds. *Mater Des* 31(9):4528–4542
12. Yilbas BS, Arif AFM, Aleem BA (2010) Laser welding of low carbon steel and thermal stress analysis. *Opt Laser Technol* 42(5):760–768
13. Casalino G, Mortello M, Contuzzi N, Minutolo FMC (2015) Finite element model for laser welding of titanium. *Procedia CIRP* 33:434–439
14. Chukkan JR, Vasudevan M, Muthukumaran S, Kumar RR, Chandrasekhar N (2015) Simulation of laser butt welding of AISI 316L stainless steel sheet using various heat sources and experimental validation. *J Mater Process Technol* 219:48–59
15. Kumar KS (2015) Numerical modeling and simulation of a butt joint welding of AISI 316L stainless steels using a pulsed laser beam. *Mater Today Proc* 2(4):2256–2266

A Framework for Flexible Job Shop Scheduling Problem Using Simulation-Based Cuckoo Search Optimization



Rakesh Kumar Phanden, Zuzana Palková and Rahul Sindhvani

Abstract Cuckoo search optimization (CSO) is an evolutionary, nature-inspired, swarm intelligence meta-heuristic algorithm, which is compatible to optimize non-polynomial combinatorial problems. It works based on the living style of cuckoos. They have obligatory brood parasitism conduct. Basically, the CSO adopted the process of egg emplacing and breeding of cuckoos. CSO algorithm begins with initial population as if genetic algorithm, particle swarm optimization and other evolutionary algorithms. Basically, the CSO works based on the cuckoos endeavor to survive amid nests and societies. Due to this struggle, several cuckoos or eggs or chicks demise and the lived cuckoos colonize toward healthier environment. So, the process of “egg laying and breeding” starts again. The survival exertion of cuckoos unites them to form a society which has similar fitness quality of each cuckoo. Hence, this algorithm has been well known to solve complicated optimization problems. Therefore, in the present work a novel approach, based on CSO algorithm, has been framed to handle the flexible job shop scheduling problem. This problem belongs to the typical class of production scheduling having various manufacturing flexibilities as if the real-world manufacturing environment. Simulation is preferred as to compare the mathematical formulation, because it imitates the performance near to a realistic system. Quality function of CSO algorithm has been planned to determine through ProModel[®] simulation software. The proposed algorithm handles multiple objectives such as makespan, mean flow time and mean tardiness.

Keywords Evolutionary algorithm · Optimization · Cuckoo search · Flexible job shop scheduling · Framework

R. K. Phanden (✉) · R. Sindhvani
Department of Mechanical Engineering, Amity University, Noida 201313, Uttar Pradesh, India
e-mail: rkphanden@amity.edu

R. Sindhvani
e-mail: rsindhvani@amity.edu

Z. Palková
Department of Electrical Engineering, Automation and Informatics, Technical Faculty, Slovak University of Agriculture, Nitra Tr. A. Hlinku 2, 949 76, Slovakia

1 Introduction

The manufacturing scheduling (also called as production scheduling and detailed scheduling) plays the cardinal role in manufacturing industries [1, 2]. A manufacturing system always needs to modify its production schedule regularly in order to satisfy the huge production orders, to reduce the cost of manufacturing, to adjust the changes in the availability of resources and to enhance the production efficiency. The scheduling problem has been categorized as per the shop configuration such as single machine shop, parallel machine shop, open shop, close shop, flow shop and job shop [2]. Among all shops, the job shop system has been known as a hardest class of production scheduling due to its realistic nature. So, the deep study of job shop manufacturing system yields important conclusions while solving a complicated system of real nature. The job shop possesses non-polynomial hard characteristic. It processes various jobs on a predefined number of machines, and each job has a predefined sequence of operation [3]. This shop becomes more complex by considering manufacturing flexibility. In fact, the flexibility is an important aspect for growth of manufacturing industries. Today's competitive market demands fast delivery of products without compromising quality and price. In addition, the industries must utilize the highly flexible machines, which are much capable to process a variety of jobs. Therefore, the job shop must be configured to accommodate the changeable schedules and flexible machines. This transformation of shop is called as flexible job shop scheduling problem [1–3]. It can be defined as “the job shop in which any job may be processed on any machine at any time for its operation.” This setup is called as total flexible job shop scheduling environment which is practically infeasible. Another approach is the consideration of half or partial flexibility (may be termed as random flexibility), in which a set of operation or an operation of any job may have processed on a set of machines or a machine, because every machine type has different level of manufacturing flexibility. This scenario is most adoptable and realistic in present systems of manufacturing. Basically, the flexible job shop scheduling problem can be divided into two subproblems, namely (a) allocation of machines to the operation (i.e., called as resource assignment task) and (b) the selection of sequence of operations of jobs. The flexible job shop scheduling problem has been solved for objectives, viz., makespan (maximum completion time of jobs), tardiness of jobs, mean flow time of jobs and many more. However, the maximum completion time of jobs (i.e., makespan) is the commonly used performance measure for scheduling problems [4]. Plentiful research has been reported in the literature to find optimized schedule for the flexible job shop manufacturing system, but there is no efficient algorithm available so far. Meta-heuristics have been evidenced as most suitable approaches to solve flexible job shop scheduling problem [4, 5].

Next section presents the literature on nature-inspired evolutionary algorithm for flexible job shop scheduling problem as well as the contribution to CSO algorithm. Subsequently, the problem formulation, methodology, experimentation setup and conclusion are presented.

2 Literature Review

2.1 *Nature-Inspired Evolutionary Algorithms*

Various engineering problems such as system design, electricity generation, transmissions and network operations, and wireless communication steering are dealt with optimization process in order to find the minimum or maximum value of their objective functions [1–5]. These optimization algorithms are tested and validated for their accuracy based on the convergence rate and computation time consumed in addition to the quality and precision of optimal solution [5, 6]. Various researchers across the world are developing these revolutionary optimization algorithms based on nature phenomena, termed as nature-inspired algorithms. Yang [7] proposed a novel meta-heuristics algorithm which works based on echolocation behavior of bats. In an organized space, the echolocation behaviors do not change due to the distance to background target, while in case of unorganized space background, the bat will react to the background targets. The boundary among these two spaces is distinct by the changes in echolocation behavior of bats. Yang has provided the formulation and implementation procedure, as well as compared the performance of bat algorithm with particle swarm optimization and genetic algorithm. A latest review on the particle swarm optimization (PSO) algorithm is given in [8]. It works on the social behavior of fish schooling or bird flocking. PSO was developed by Eberhart and Kennedy in 1995. Differential evolution (DE) algorithm was proposed by Storm and Prince in 1997. DE word based on population evolution has various operators such as selection, crossover and mutation. The ant colony optimization (ACO) was proposed by Marco Dorigo in 1992. It works on the principle of searching food by ants. Initially, ants walk randomly to find food and consequently return to colony while leaving pheromone traces behind. Finally, other ants follow the same path of pheromone traces. Similarly, the bee colony optimization (BCO) algorithm imitates the food scavenging way of swarms of honeybees. It was developed by Pham et al. [9]. Biogeography-based optimization (BBO) algorithm was proposed by Dan Simon in 2008. It works based on the process of evolution of new species and their emigration and/or immigration among islands. The complete review on each nature-inspired optimization algorithms is given by X.S. Yang in his book “Nature-Inspired Optimization Algorithms.”

2.2 *Flexible Job Shop Scheduling and Meta-heuristics*

The schedule (solution) of flexible job shop has been optimized using two methods, viz., in first method, it is separated in two subproblems: One is operation sequence problem, and another is assignment problem; in second method, it is solved as an integrated problem. In the former method, one problem is solved after another in a hierarchical way, which makes the problem simpler to deal by subdividing it into two

sections. Brandimarte [1] presented the classified way of solution, in which operation sequence problem and machine assignment problem are resolved separately by dispatching rules and tabu search method, respectively. Barnes and Chambers [2] also proposed hierarchical method to solve flexible job shop scheduling problem using tabu search method. Xia and Wu [10] proposed two nature-inspired algorithms, namely simulated annealing algorithm for machine assignment problem and particle swarm optimization algorithm for operation sequence problem for a multi-objective flexible job shop scheduling problem.

On the other side, numerous researchers have proposed integrated approaches to solve flexible job shop scheduling problem without subdivisions, which is a complex way but produces good results. Kacem et al. [11] developed two integrated approaches called “approach by localization” (AL) and “controlled genetic algorithm” (CGA) that works in successive stages. They have considered partial and total manufacturing flexibility as well as single and multi-objectives to solve two hypothetical job shop scheduling problems. In AL, they solve resource allocation problem and constructed an assignment model called “assignment schemata.” The CGA is controlled by “assignment schemata” model, and they applied genetic manipulations to enhance the quality of solution. Ho et al. [12] proposed a model named “LEarnable Genetic Architecture” (LEGA) in which the interaction amid machine learning and evolutionary algorithm (genetic algorithm) is established to solve the flexible job shop scheduling problem. They developed a “schemata learning module” which pulls the information from earlier generation to enhance the excellence of offspring. The initial population is generated through dispatching rules. Gao et al. [13] presented hybrid genetic algorithm having a local search method (called bottleneck shifting), which is capable to adjust the neighborhood structure dynamically. They solved the flexible job shop scheduling problem for minimum maximal machine workload, minimum total machine workload and makespan. Zhang et al. [14] proposed a hybrid “variable neighborhood genetic algorithm” (VNGA) to solve flexible job shop scheduling problem, in which the initial population for genetic algorithm is generated by variable neighborhood search algorithm to explore the local search space in depth. Similarly, in Zhang et al. [15], the genetic algorithm is initialized by a mix of different strategies, namely random selection, global selection and local selection to get the high-quality initial population, to accelerate the convergence speed of algorithm and to improve the quality of the final solution. They considered makespan performance measure to optimize the flexible job shop scheduling problem. Also, Wang et al. [16] have applied a combination of immune and entropy principle in genetic algorithm to maintain the diversity of population, to control the premature convergence of algorithm and to control the selection pressure on similar chromosomes during optimization of a multi-objective flexible job shop scheduling problem. They proposed the Pareto optimality to calculate fitness value of chromosomes. Rahmati and Zandieh [17] proposed an algorithm based on biogeography concept named “biogeography-based optimization” (BBO) algorithm, which follows the migration strategy of species. The evolving features of habitats due to the emigration and immigration process is used to find the optimal solution for flexible job shop scheduling problem. They considered critical workload and total workload of machine, as well

as makespan to measure the performance of BBO algorithm, and compared with the performance of genetic algorithm. Thammano and Phu-ang [18] proposed an “artificial bee colony” algorithm, in which initial population is generated through the harmony search algorithm and dispatching rules, to solve flexible job shop scheduling problem for makespan performance measure. Also, the local convergence is prevented through the simulated annealing algorithm and search space was explored by crossover operator. Nouri et al. [19] presented particle swarm optimization (PSO) algorithm to solve flexible job shop scheduling problem for minimization of maximum completion time of production from partial and full manufacturing flexibility viewpoint. In, Nouri et al. [20] extend the proposed algorithm for unforeseen situations, which is capable to make decision in real time. They used multi-agent-based platform to make the algorithm intelligent. Zhou et al. [21] proposed a combination of “cultural algorithm and particle swarm optimization” called CPSO, to optimize maximum completion time of flexible job shop scheduling problem. Wang et al. [22] proposed a “social spider algorithm” (SSA) to solve flexible job shop scheduling problem. Phanden [23] proposed a parallel hybrid approach of genetic algorithm and variable neighborhood search method based on multi-agent system. He used JADE platform to set up communication among initialization agent, processing agent and coordinating agent to find the optimal makespan for a job shop scheduling problem. Sadiq and Hussein [24] proposed a swarm intelligence-based heuristic called “artificial fish swarm algorithm” (AFSA) which imitates the behaviors of cluster of fish to solve flexible job shop scheduling problem. The performance of regular AFSA is enhanced through “variable neighborhood descent” (VND) scheme. Xu et al. [25] presented bat algorithm to solve dual flexible job shop scheduling problem having flexibility in process selection and machine selection.

Cuckoo search optimization (CSO) algorithm was developed by X. S. Yang and S. Deb in 2009. In 2011, Rajabioun [26] explored the CSO algorithm in depth. Initially, the cuckoo’s eggs emplacing process united with Levy flights come into existence to form the algorithm rather than the simple random isotropic walk. CSO is nature-inspired biomimicry optimization algorithm which works on the basis of brood reproductive scheme of cuckoo bird to enhance their inhabitants. Cuckoo is a brutal and cunning species among bird breed. They secretly emplace the eggs in the nest of other birds in order to spare themselves from nurturing tasks of growing the offspring. They are trained for the trickery art every time during their reproductive life span. In fact, they learned to copy the design and shade of the eggs of host birds to cover their eggs from being noticed by host birds. Also, the cuckoos steal the host eggs in order to arrange extra food and space for their chicks. The host birds and cuckoos are continuously confronted with arm race. The host birds keep learning the way to detect the fraud, and they either kick out the less matching eggs or abandon the nest. Also, the cuckoo’s expertise themselves for imitation skill, to make their eggs to looks identical with host eggs. The literature reveals that the CSO is more effective as compared to other nature-inspired meta-heuristic algorithms. De facto, other approaches such as DE, PSO, ACO and BCO are diverse cases of CSO algorithm. Therefore, the performance of CSO is promising as to compare with them. In terms of convergence rate, the CSO algorithm outperforms

DE optimization algorithm in order to attain optimal result. Also, the CSO algorithm performs computationally effectively as compared to PSO algorithm [27]. Thus, the CSO algorithm has fascinated scholars to solve complicated problems of their research interest.

Zheng and Zhou [28] presented a Gauss distribution-based cuckoo search (GCS) algorithm in order to eradicate the low convergence rate of original CSO algorithm. They revealed that GCS converges faster than original CSO, while testing on standard functions such as Rosenbrock, Griewank, Rastrigin, Ackley, Easom and Sphere. Chandrasekaran and Simon [29] proposed fuzzy integrated CSO algorithm for single and multiple objectives (i.e., fuel cost, reliability and emission level) of power system scheduling problem. Burnwal and Deb [30] proposed CSO algorithm for the flexible manufacturing system (FMS) scheduling problem to minimize the manufacturing delay penalty cost as well as to maximize the utilization of machines. They considered FMS having sixteen machines and forty-three jobs, and they found that CSO outperformed on GA and PSO. Zhou et al. [31] proposed a CSO algorithm with multiple strategies such as greedy transformation, swap and inversion, as well as walking one scheme in order to solve the graphics pixel problem. They considered a case study of coloring map of China and found that proposed algorithm outperformed the PSO algorithm in terms of less number of iterations and more corrections in the rate of coloring. Ong [32] proposed adoptive cuckoo search algorithm (ACSA) for unconstrained optimization problems. This algorithm can adjust the step size (α) perpetually during the computation. They concluded that ACSA is converging promptly with less number of iterations as compared to original CSO algorithm. Marichelvam et al. [33] proposed CSO algorithm for flow shop scheduling problem of furniture manufacturing company to minimize the makespan performance. Nguyena and Vo [34] presented CSO algorithm for scheduling of short-term hydrothermal system in order to optimize the cost of thermal generators. They modify the CSO to improve the searchability by constructing dual groups of eggs, in which one (upper) group holds eggs of low fitness value and another (abandoned) group embraces remaining eggs. In order to improve the search speed, two eggs of the upper group exchange the information regularly. Singh and Singh [35] proposed CSO algorithm having “as-sorted individual enhancement strategy” to solve job shop scheduling problem for makespan performance measure. Al-Obaidi and Hussein [36] proposed two improvements in the original CSO algorithm, viz., (i) best neighborhood generation and (ii) iterative Levy flights to solve the flexible job shop scheduling problem. They find that proposed algorithms performed better than original CSO algorithm.

2.3 Summary of the Literature Review

All in all, the literature review clearly reveals the following points; (i) CSO algorithm has been applied successfully to each domain of engineering since last decade. (ii) CSO algorithm is a promising nature-inspired approach that yields better results as compared to other evolutionary algorithms. (iii) Simulation-based CSO algorithm

has not been explored yet. (iv) CSO algorithm has not been studied in depth to solve flexible job shop scheduling problem. Thus, the present work presents a simulation-based CSO algorithm, to solve flexible job shop scheduling problem.

3 Problem Formulation

3.1 Problem Statement

The element of a flexible job shop scheduling is jobs, machines, flexibility, assumptions (constraints) and objectives as well as hypothesis.

$$\text{Job } (J) = J_1, J_2, J_3 \dots J_n$$

Here, (n) number of jobs to be scheduled and job (J_i) have predefined number of operations. O_{ij} is an operation of any job (J_i).

$$\text{Machine } (M) = M_1, M_2, M_3 \dots M_m$$

Here, (m) number of machines are available in a job shop and an individual machine can process only one operation at any point of time.

Manufacturing flexibility plays a vital role to enhance the production rate of a shop. Here, partial flexibility has been planned to configure a job shop. The concept of full flexibility is not realistic, because a machine cannot process each type of operation. In case of limited flexibility, an operation of a job can be executed on a predefined group of machines.

The value of fitness function (nest) is calculated using simulation software (ProModel[®]), and multiple performance measures such as makespan, mean tardiness and mean flow time are planned to optimize for considered flexible job shop scheduling problem.

3.2 Assumptions

The job shop is planned to configure in ProModel[®] simulation software. The real configuration of a job shop is extremely complicated which increases the modeling difficulties as well. So, to rationalize the modeling, the present work follows some assumptions in line with earlier research, as given below [4, 5, 10].

- Jobs and machines are independent entities and available at zero time.
- Operation time is known in advance.
- Production quantity and transportation time are also predetermined.

- Shortest processing time is used as a dispatching rule in simulation.
- First come first serve criterion is used for tie breaker in scheduling.
- One machine can process one job's operation at a time.
- Arrival and departure locations are considered for production order execution.
- Sequence of operation and manufacturing flexibility are known in advance.
- The infinite buffer capacity is considered in front of each processing station.
- Part preemption is forbidden.

3.3 Objectives

This paper proposed a framework of CSO algorithm to optimize the flexible job shop scheduling problem. It involves the following objectives to attain:

- (i) To apply the simulation function in the CSO algorithm, as the simulation yields better performance of an actual manufacturing system as compared to a mathematical function;
- (ii) To propose algorithm will be capable to solve the flexible job shop scheduling problem for the multiple objectives such as makespan, mean tardiness and mean flow time;
- (iii) To develop the model which is capable to handle any size of job shop having varying production orders;
- (iv) To access the performance of proposed design by comparing with the original CSO as well as with other nature-inspired algorithms such as GA and PSO.

4 Cuckoo Search Optimization (CSO) Algorithm

Figure 1 shows the working process of CSO algorithm presented by Rajabioun [26]. The opening of the CSO algorithm is similar to the other evolutionary algorithms in which initial population is generated randomly. Cuckoo delivers the eggs in the host bird nest, and owing to the similarity of eggs the infiltrated eggs of cuckoo avail the opportunity to develop by carrying of host birds. In order to make proper space in the nest, the host bird kills some of their own eggs due to the lack of uniqueness among eggs. So, the fitness quality (profit rate) of nest depends on the growth rate of eggs in that vicinity. If the rate of survival of eggs is increasing, it means the fitness of that locality is rising. Hence, when the strength of living eggs of cuckoos is increased in the vicinity, it shows that the CSO algorithm is approaching near to convergence (optimization).

The cuckoos are always in search of better vicinity to lay the eggs in order to enhance the rate of survival of their eggs. When the eggs are matured, they built a society and the habitats are formed within it. Then, the race of finding better habitats starts in the society. This fight leads to immigration of cuckoos to start living near the

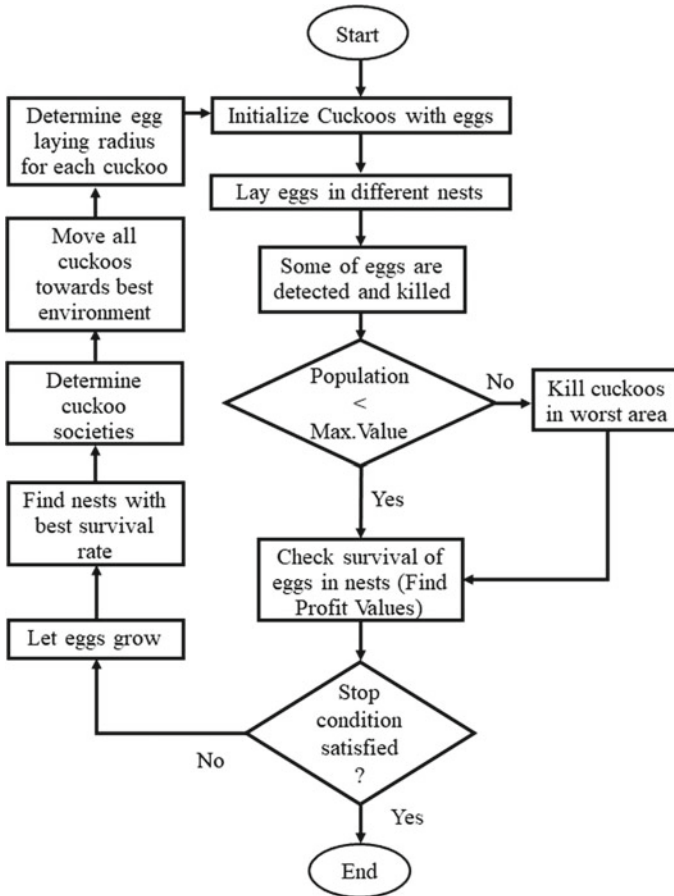


Fig. 1 Working procedure of cuckoos search [26]

beneficial habitats. Thus, a cuckoo is restricted to dual parameters: first, the counting (strength) of eggs, and second, distance traveled to get the beneficial habitat. These parameters calculate the “egg-laying radii,” i.e., laying of eggs randomly among the available nests within this area. Hence, the process accomplished in an iterative way until the good habitat is obtained and the population increases inside this area [26].

4.1 Generation of Initial Population and Process of Egg Laying

The variables of optimization problems are obligatory with formation of array. For instance, in genetic algorithm this arrangement is called as chromosome. In the

present algorithm, this array is named as habitat which comprises of $(1 \times \text{number of variables})$. That is, a habitat contains $x_1, x_2, x_3 \dots$ up to x_d . The CSO algorithm evaluates the profit function of a habitat $(x_1, x_2, x_3 \dots x_d)$, i.e., $\text{profit} = F(x)$, $x = (x_1, x_2, x_3 \dots x_d)$. It shows that the CSO algorithm maximizes the profit function, but in the present scheduling problem the objective function is to minimize the makespan performance of flexible job shop. Therefore, the maximization problem turned into minimization problem by considering the minus of cost [26].

The CSO algorithm is initialized by creating a matrix of size equal to the product of number of variables and size of population taken. Theoretically, the eggs are produced randomly in the habitats of inaugural cuckoos. A cuckoo delivers around 5–20 eggs. The eggs are preserved by each cuckoo according to this concept, as high and low limiting values during the iterative process of evolution. Moreover, the cuckoos deliver eggs inside a determined remoteness from their habitats. This distance is termed as “egg-laying radius” (ELR). Hence, ELR of each cuckoo is equal to the product of total number of eggs, eggs of current cuckoos as well as the difference of upper and lower limit of variables [26].

Cuckoos replace the eggs within the ELR in the nest of other birds. Once the laying process is completed, the host bird finds the eggs which are not resembling with her own eggs. These unlike eggs are thrown outside or killed by host bird. Normally, 10% of eggs are destroyed by the host bird which are considered as a smaller amount of profit values having very less or no possibility of growth. In addition, only one egg grows in one nest at a time, since after hatching process the chicks arise and host bird pushes her own eggs out of the nest to accommodate her three times larger body size as well as most of the food will be eaten by the cuckoo’s chicks. At the end, only cuckoo’s chick left in the nest [26].

4.2 *Immigration, Eradication and Convergence Process*

Once the cuckoos are matured enough and ready for egg laying, they leave the society and immigrate to healthier habitats in order to find the nests of host birds having similar eggs as well as to ensure the additional sources of food availability. Hence, the clusters of cuckoos are shaped in various zones. Every cluster strives to migrate toward the society having best profit value. This best society is considered as a goal which is to be attained by each cuckoo. To distinguish among various groups of cuckoos, the clustering method is adopted. A range of three to five cuckoos has been suggested for making a cluster. The “mean profit value” (MPV) is calculated for each cluster, and the maximum value of MPV is considered as goal group. Hence, the next habitat for immigrants (cuckoos) will be the best habitat of the goal group. In addition, all cuckoos may not fly toward best habitat of a goal group and they may deviate on any other ways. In other words, a cuckoo may fly “ xx ” amount of distance (in percentage) to the goal group and deviates with “ yy ” radians. Cuckoo search is explored through these parameters in every location. “ xx ” means a randomly generated and uniformly distributed number between 0 and 1. “ yy ” is a deviation from

goal habitat which is constrained between the angle of -30° and $+30^\circ$ to avoid the local convergence. The new habitats are stated after immigrating all cuckoos to the goal. After arriving, each cuckoo gives few eggs and further the ELR is calculated for individual cuckoo. Subsequently, the process of egg laying starts again [26].

Cuckoos are eradicated in poor habitats due to the limitation of food, predator killing and lack of suitable host's nest for emplacing eggs. De facto, the equilibrium of species (cuckoos) population always exists, therefore, a control number (say N) which is always sustained with the maximum value to bound the maximum number of live cuckoos. Hence, N number of cuckoos will survive that possesses good values of profit, while others will be dead. The process works in a repetitive manner, and subsequently, all cuckoos fly to a best habitat having full availability of food source as well as resemblance of eggs to the host birds. This best habitat has minimum loss of eggs and yields highest profit always. Hence, about 95% of cuckoos converge in this best habitat which accomplishes the CSO algorithm [26].

5 Simulation-Based CSO and Random Walk

Three compartments of CSO algorithm have been proposed by Yang and Deb [37], namely: (i) A set of solution is created by emplacing of cuckoos' eggs in randomly selected nest of host birds. Cuckoo delivers one egg at a time. (ii) The best solutions (i.e., the nests with good quality eggs) are carried forward in subsequent iterations of algorithm. (iii) The chances of discovering the foreigner eggs (i.e., cuckoos' eggs) by the host birds are varied either zero or one (i.e., either the host birds will destroy the eggs as well as nest or they move to another location to build new nests). The adopted methodology is called "simulation-based CSO algorithm" as shown in Fig. 2. The CSO philosophy presented by Yang and Deb [37] has been utilized in the present work.

Random walk strategy is divided into two categories, namely Lévy flights and Lévy walks. The concept of Lévy flights has been used in various engineering domains. It begins to express the photoconductivity of amorphous materials by physicists [38]. In Lévy flights, the span of a step is marked by the randomly selected direction with probability distribution. The new solution ($x^{(t+1)}$) to i th cuckoo is generated randomly using $\{x_i^{(t)} + \alpha \oplus \text{Lévy}(\beta)\}$ [37]. The step size ($\alpha > 0$) is decided as per the scale of problems. Generally, α is considered as 1. " \oplus " is considered for entry-wise multiplication factor. The step span is generated from Lévy distribution $\{\text{Lévy} \sim u = t^{-\beta} (1 < \beta \leq 3)\}$ at random with infinite variance value. The successive steps of a cuckoo embrace the evolution of random walk having power law distribution of a step span using her heavy trail control. So, the fresh nests are constructed at new locations by random walk and the fraction (p_a) of poor nests is abandoned.

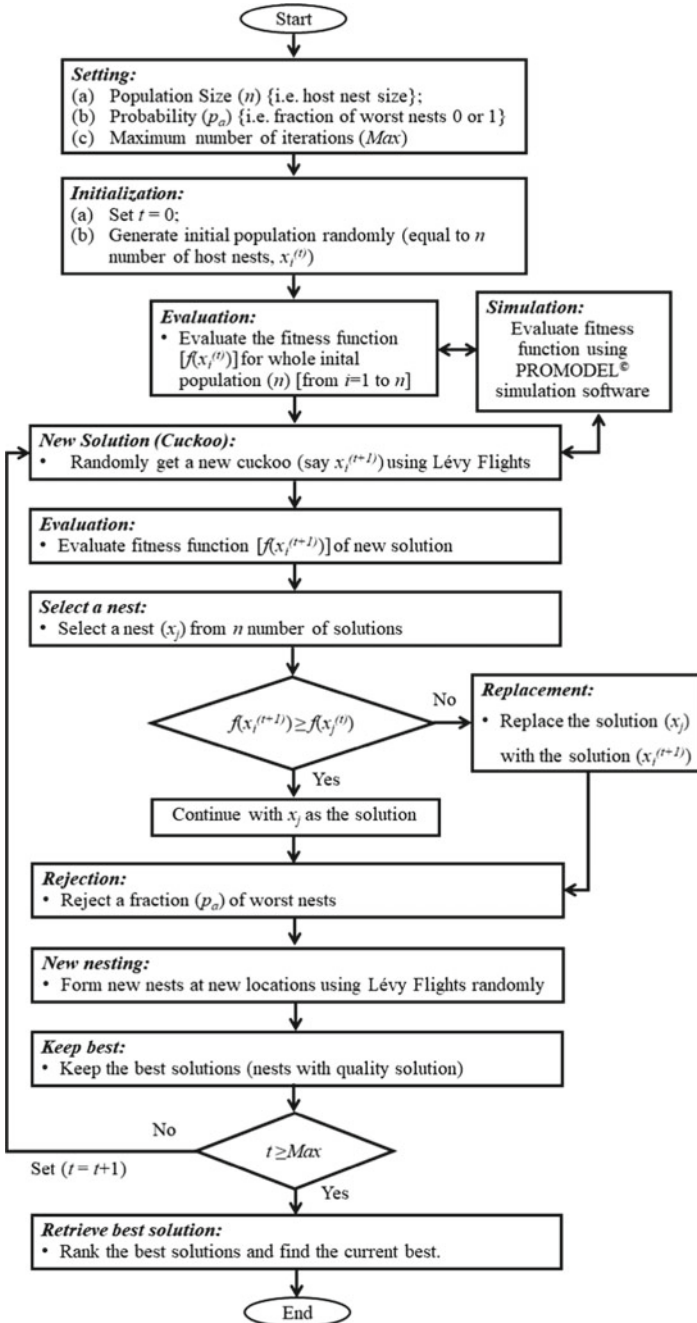


Fig. 2 Simulation-based CSO algorithm

6 Experimentation

Simulation-based CSO approach has been framed to solve flexible job shop scheduling problem as discussed in the previous section. The CSO algorithm has been updated to calculate the quality (profit) function of nests through the simulation software. The simulation is preferred as to compare with mathematical function because it is capable to model the system which resembles the real manufacturing system, and also it is suitable to deliver the performance of modeled system better than the conventional mathematical function of scheduling. Makespan, mean flow time and mean tardiness considered the performance measures for the considered flexible job shop manufacturing system.

It is planned to test the framed algorithm on the test bed problems of flexible job shop scheduling available in the literature. Various small-, medium- and large-size problems are given in the literature, viz., (i) a real production problem of size 10 machines and 8 jobs given in Wang et al. [39], (ii) a partial flexible job shop scheduling problem of 8 jobs and 8 machines given by Kacem et al. [11] and (iii) ten problem instances given by Brandimarte [1], in which number of job and machines are varied from 10 to 30 and 6 to 15, respectively. These benchmark problems have been solved by various researchers for different performance measures. Hence, the proposed algorithm will be compared with other revolution algorithms such as GA, PSO and ACO proposed by various researchers for makespan, mean tardiness and mean flow time criterions.

The flexible job shop systems will be modeled and configured in the ProModel[®] simulation software. A sample shop model is shown in Fig. 3. The production order is processed as follows. All orders will be received at in-location. Initially, the jobs will be loaded on machines or in the buffer/queue of machine according to the

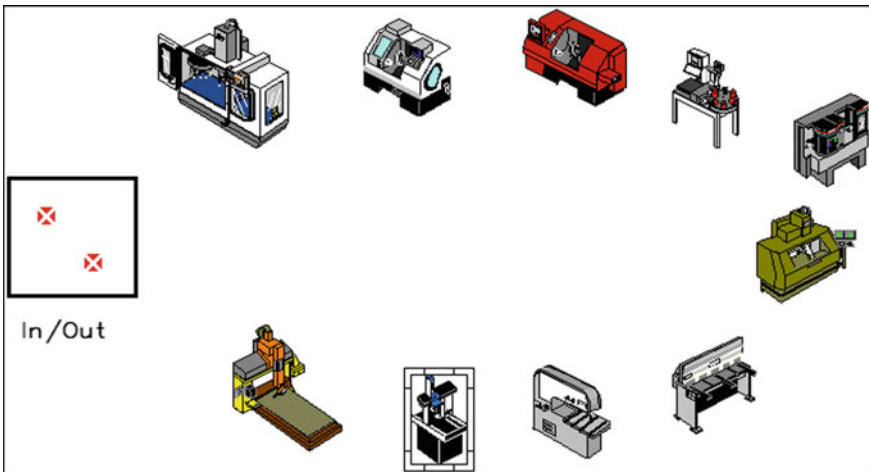
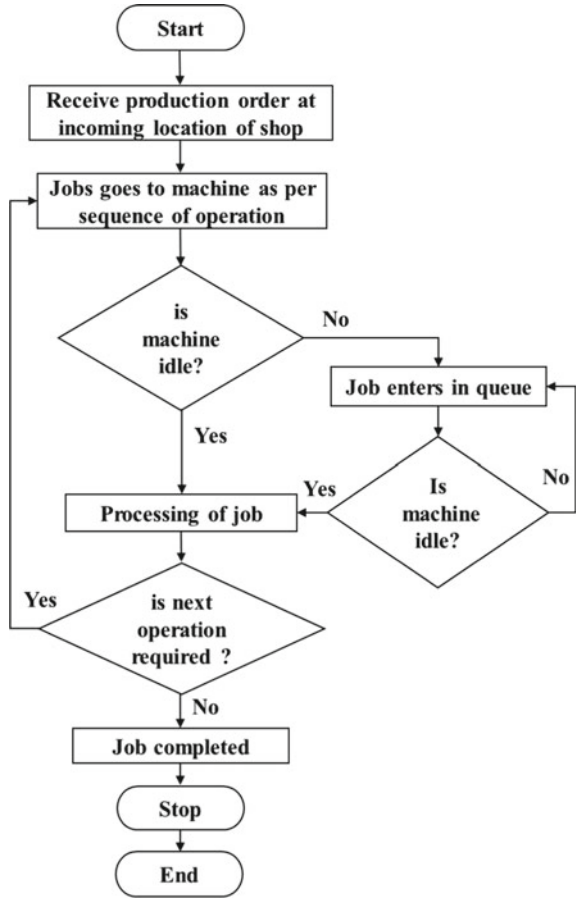


Fig. 3 A sample flexible job shop modeled in ProModel[®] simulation software

Fig. 4 Job flow pattern in a planned flexible job shop environment



operation sequence for the first process. Accordingly, the process will be executed if the machine is idle; otherwise, the job waits in the queue of machine. After completing first operation, the job will travel to next station according to the predefined operation sequence for the next operation. Thus, all jobs will move to different machines according to operation sequence. At the end, the finished product will exit the shop from out-location as shown in Fig. 4.

7 Conclusion

This paper presents a novel framework of simulation-based CSO algorithm for flexible job shop scheduling problem. CSO has been recognized as a promising evolutionary algorithm since its inception in 2009. The proposed framework is unique

and promising to yield the better performance as compared to other meta-heuristic approaches. This approach is framed to use the simulation software in order to simulate the flexible job shop manufacturing environment. It goes without saying that simulation function gives real configuration of a system rather than a mathematical function. The presented architecture will be capable to handle various performance measures such as makespan, mean flow time and mean tardiness as per the requirement of production manager. However, the development of algorithm is under process.

Acknowledgements We are very grateful to Prof. (Dr.) X. S. Yang for providing sample cuckoo search optimization algorithm code in the book “Nature-Inspired Optimization Algorithms.”

References

1. Brandimarte P (1993) Routing and scheduling in a flexible job shop by tabu search. *Annu Oper Res* 41:157–183
2. Barnes JW, Chambers JB (1996) Flexible job shop scheduling by tabu search. Graduate program in operations research and industrial engineering, University of Texas, Austin, Technical Report Series, ORP96-09
3. Pinedo ML (2012) Scheduling: theory, algorithms, and systems, 4th edn. Springer, Berlin
4. Phanden RK, Jain A, Verma R (2012) A genetic algorithm-based approach for flexible job shop scheduling. *Appl Mech Mater* 110–116(2012):3930–3937
5. Phanden RK, Jain A (2015) Assessing the impact of changing available multiple process plans of a job type on mean tardiness in job shop scheduling. *Int J Adv Manuf Technol* 2015(80):1521–1545
6. Palkova Zuzana (2010) Modeling the optimal capacity of an irrigation system using queuing theory. *Ann Warsaw Univ Life Sci SGGW Warsaw Univ Life Sci Press* 55(2010):5–11
7. Yang XS (2010) A new metaheuristic bat-inspired algorithm. In: Gonzalez JR, Pelta DA, Cruz C, Terrazas G, Krasnogor N (eds) Nature inspired cooperative strategies for optimization, vol 284. Springer, Berlin, pp 65–74
8. Rini DP, Shamsuddin SM, Yuhaziz SS (2011) Particle swarm optimization: technique, system and challenges. *Int J Comput Appl* 14(1):19–27
9. Pham DT, Ghanbarzadeh A, Koc E, Otri S, Rahim S, Zaidi M (2005) The Bees algorithm. Technical Note. Manufacturing Engineering Centre, Cardiff University, UK
10. Xia WJ, Wu ZM (2005) An effective hybrid optimization approach for multi-objective flexible job-shop scheduling problems. *Comp Ind Eng* 48(2):409–425
11. Kacem I, Hammadi S, Borne P (2002) Approach by localization multi-objective evolutionary optimization for flexible job-shops scheduling problems. *IEEE Trans Syst Man Cybern Part C Appl Rev* 32(1):1–13
12. Ho NB, Tay JCJ, Lai E (2007) An effective architecture for learning and evolving flexible job-shop schedules. *Eur J Oper Res* 179:316–333
13. Gao J, Gen M, Sun LY, Zhao XH (2007) A hybrid of genetic algorithm and bottleneck shifting for multiobjective flexible job shop scheduling problems. *Comput Ind Eng* 53(1):149–162
14. Zhang GH, Gao L, Li X, Li P (2008) Variable neighborhood genetic algorithm for the flexible job shop scheduling problems. In: Proceedings of Intelligent Robotics and Applications (ICIRA 08). LNCS Press, Oct 2008, pp 503–512
15. Zhang GH, Gao L, Shi Y (2011) An effective genetic algorithm for the flexible job-shop scheduling problem. *Experts Syst Appl* 38(4):3563–3573

16. Wang X, Gao L, Zhang G, Shao X (2010) A multi-objective genetic algorithm based on immune and entropy principle for flexible job-shop scheduling problem. *Int J Adv Manuf Technol* 51(5–8):757–767
17. Rahmati SHA, Zandieh M (2012) A new biogeography-based optimization (BBO) algorithm for the flexible job shop scheduling problem. *Int J Adv Manuf Technol* 2012(58):1115–1129
18. Thammano A, Phu-ang A (2013) A hybrid artificial bee colony algorithm with local search for flexible job-shop scheduling problem. *Procedia Comput Sci* 20:96–101
19. Nouiri M, Jemai A, Ammari AC, Bekrar A, Niar S (2013) An effective particle swarm optimization algorithm for flexible job-shop scheduling problem. In: *Proceedings of 2013 international conference on industrial engineering and systems management (IESM)*. IEEE, pp 1–6
20. Nouiri M, Bekrar A, Jemai A, Niar S, Ammari AC (2018) An effective and distributed particle swarm optimization algorithm for flexible job-shop scheduling problem. *J Intell Manuf* 29(3):603
21. Zhou W, Bu Y, Zhou Y (2014) Combining CA and PSO to solve flexible job shop scheduling problem. In: *The 26th Chinese control and decision conference (CCDC)*. IEEE, pp 1031–1036
22. Wang Y, Zhu LB, Wang J, Qiu J (2015) An improved social spider algorithm for the flexible job-shop scheduling problem. In: *International conference on estimation, detection and information fusion (ICEDIF)*. IEEE, pp 157–162
23. Phanden RK (2016) Multi agents approach for job shop scheduling problem using genetic algorithm and variable neighborhood search method. In: *Proceedings of the 20th world multi-conference on systemics, cybernetics and informatics*, pp 275–278
24. Sadiq AAT, Hussein SA (2017) An improved artificial fish swarm algorithm to solve flexible job shop. In: *Annual conference on new trends in information & communications technology applications*. IEEE
25. Xu H, Bao ZR, Zhang T (2017) Solving dual flexible job-shop scheduling problem using a Bat algorithm. *Adva Prod Eng Manag* 12(1):5–16. ISSN 1854-6250
26. Rajabioun R (2011) Cuckoo optimization algorithm. *Appl Soft Comput* 11(2011):5508–5518
27. Mareli M, Twala B (2017) An adaptive Cuckoo search algorithm for optimization. *Appl Comput Inf*. <http://dx.doi.org/10.1016/j.aci.2017.09.001>
28. Zheng H, Zhou Y (2012) A Novel Cuckoo search optimization algorithm base on gauss distribution. *J Comput Inf Syst* 8(10):4193–4200
29. Chandrasekaran K, Simon SP (2012) Multi-objective scheduling problem: hybrid approach using fuzzy assisted cuckoo search algorithm. *Swarm Evol Comput* 5:1–16
30. Burnwal S, Deb S (2013) Scheduling optimization of flexible manufacturing system using cuckoo search-based approach. *Int J Adv Manuf Technol* 64(5–8):951–959
31. Zhou Y, Zheng H, Luo Q, Wu J (2013) An improved Cuckoo search algorithm for solving Planar graph coloring problem. *Appl Math Inf Sci* 7(2):785–792
32. Ong P (2014) Adaptive Cuckoo search algorithm for unconstrained optimization. *Sci World J*
33. Marichelvam MK, Prabakaran T, Yang XS (2014) Improved cuckoo search algorithm for hybrid flow shop scheduling problems to minimize makespan. *Appl Soft Comput J* 19:93–101
34. Nguyen TT, Vo DN (2015) Modified cuckoo search algorithm for short-term hydrothermal scheduling. *Int J Electr Power Energy Syst* 65:271–281
35. Singh S, Singh KP (2015) Cuckoo search optimization for job shop scheduling problem. In: *Proceedings of fourth international conference on soft computing for problem solving advances in intelligent systems and computing*. Springer, Berlin, pp 99–111
36. Al-Obaidi ATS, Hussein SA (2016) Two improved Cuckoo search algorithms for solving the flexible job-shop scheduling problem. *Int J Percept Cogn Comput* 2(2):25–31
37. Yang XS, Deb S (2009) Cuckoo search via Levy flights. In: *World congress on nature & biologically inspired computing (NaBIC)*. IEEE Publications, pp 210–214
38. Fredriksson L (2009) A brief survey of Lévy walks with applications to probe diffusion. Diploma thesis for bachelor's degree in chemistry. Department of Chemistry, Karlstad University
39. Wang L, Cai J, Li M, Liu Z (2017) Flexible job shop scheduling problem using an improved ant colony optimization. *Sci Progr* 2017

An Experimental Study to Evaluate the Warpage and Cracking Issues in Fused Deposition Modeling



A. Suhas, Rohit Rajpal, K. V. Gangadharan and U. Pruthviraj

Abstract Research in 3D printing technology is growing immensely because of the advantage of manufacturing complex shapes in less time as compared to conventional manufacturing processes. However, warpage and cracking are the critical issues in fused deposition modeling technique which results in a reduction in the strength of the component. This paper aims to address the root causes for reducing the warpage and cracking in a 3D printed component. Fused-deposition-modeling-based 3D printer is used in this study to manufacture the samples. The behavior of warpage and cracking in the specimens are studied by altering bed temperature and extrusion width of the filament. The experimental results revealed that printing a component at 100 °C and 0.75 mm extrusion width led to minimum warpage and no crack condition.

Keywords Additive manufacturing · Fused deposition modeling · Warpage · Cracking

1 Introduction

3D printing is a layer-by-layer manufacturing process for building three-dimensional objects using a CAD model [1–4]. Among various types of 3D printing, fused deposition modeling (FDM) is one of the most popular and widely used methods for printing [5]. In this technique, the filament is made to pass through the heated nozzle which melts the material and deposits on the heated bed. Once the first layer is laid, the successive layer is laid on the top of it. The temperature between the layers helps to bind the layers by fusion. The advantage of using such technique is that it can manufacture any complex component in a short interval of time without much of the wastage.

Various steps involved in 3D printer are (a) Building a CAD model, (b) generating a.stl file (c) generating G-codes for the desired process parameter (d) printing a

A. Suhas (✉) · R. Rajpal · K. V. Gangadharan · U. Pruthviraj
SOLVE Lab, Centre for System Design, National Institute of Technology, Surathkal, Mangalore
575025, Karnataka, India
e-mail: suhasarampady@gmail.com

component [5–7]. Many commercial software are available to build a CAD model of the required dimensions. A mesh is created after finalizing the design in.stl format. Standard triangular language (.stl) is a file format widely accepted for building three-dimensional objects. This file is used to generate the coordinates for printing any 3D. During the printing, various process parameters need to be taken care to print a quality component [8, 9].

Layer thickness, heating temperature, the speed of printing are some of the parameters that play a prominent role while printing any 3D object. Gregorian recommended that build temperature and speed will affect the warp in the material due to heat dissipation in the ABS component. The effect of temperature is studied on ABS material and found that cracking initiates under tensile and impact loading at 120 °C. It was found that depositing the layers close to each other provides the better bonding strength to the overall component [10]. Tiganis et al. found that the parameter consideration of FDM process by using the gray Taguchi method and concluded that build orientation, the thickness of the layer, deposition angle, and width not only affect the build part but also affects in bonding and warpage of the specimen [5]. Nickel et al. studied the thermal stress and deposition pattern in layered manufacturing and found it produces minimum deflection for the beams in a raster pattern with its lines oriented 90 from its long axis it was also found that the plate structures with contour pattern deposited from outer side to inner side will have low and uniform deflections [6]. The number of layer increases, the temperature gradient will also be more toward the base of the build components [11, 12]. This results in good adhesion between the adjacent layers and strength of the ABS component increases. As the raster angle reduced, it increases the stress concentration along the deposition direction which results in a weaker bond. Similarly, as the raster thickens, it forms the adjacent layers of ABS strong. It was observed that as the component size increases the depositions to be laid also increases which increase the number of heating and cooling cycles, thereby increasing in stress accumulation within the component. The accumulated stress increases the chance of interlayer cracking, warps in the component and shrinkage and thus reduces the strength of the specimen. It was also seen that when no air gap between the successive raster, there will be an improvement in the diffusion; but, it decreases the heat dissipation, thereby weakens the bonding [13].

This paper aims to address the most significant issues of 3D printing, i.e., warpage and interlayer cracking. 100 mm × 100 mm × 20-mm-dimension specimen is chosen to understand the warpage and cracking occurring at various temperature profiles and extrusion width. The warpage is measured by a rack-and-pinion-based dial gauge, and it is transformed into angle from the bottom layer to compare the warpage of each specimen. Interlayer cracking is also studied by manual inspection. The possible reasons for occurrence of warpage and cracking are also discussed in detailed.

2 Methodology

In this study, FDM double extruder 3D printer of Stanley 3D Tech has been used with $300 \times 210 \times 160$ mm build platform. $100 \times 100 \times 20$ -mm rectangular ABS specimen is used, and analysis is carried out to understand warpage and cracking issues in the specimen at various bed temperatures and extrusion width. Following are the steps followed in this experimental study to understand the behavior of cracking and warpage:

- (a) Building the test specimen with various parameters,
- (b) Warpage measurement,
- (c) Crack diagnosis.

2.1 Building the Test Specimen with Different Parameters

In this study, the focus is laid on two printing parameters, i.e., bed temperature and extrusion width. It has to be noted that as the extrusion width decreases the mass of the component also decreases for the same infill percentage. This is because the gap between the fibers changes with the decrease in deposition width. In the present study, the mass of the specimens is maintained to be same to understand the warpage with a change in bed temperature and extrusion width. Fused deposition modeling is used to build the specimens. High-temperature resistant kapton tape was used at the surface of the heated bed on which the component was printed. It is to be noted that, to precisely study the effect of bed temperature in the specimen, the kapton tape was changed for each specimen. The parameters of printing such as speed of the printing, nozzle temperature, extrusion multiplier, and retraction were maintained to be constant. Table 1 depicts the values which were used while printing the components (Fig. 1).

Table 1 Depicting the fixed parameters used under the study

Printing parameter	Value
Speed of printing	30 mm/s
Pattern Shape	Rectilinear zig-zag
Extrusion multiplier	1
Nozzle temperature	260 °C
Support infill	0

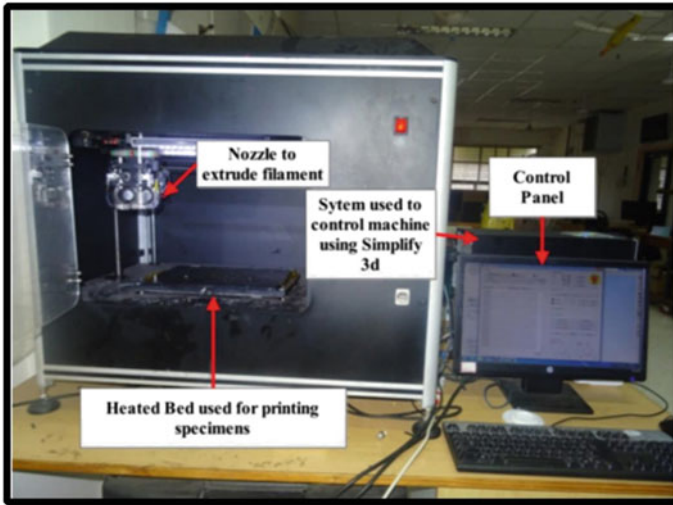


Fig. 1 Depicts the 3D printer used to build the specimens

2.2 Measurement of Warpage

After printing the specimen with various bed temperatures, the warpage was measured using a dial gauge as shown in Fig. 2. The plunger was settled at the center of the specimen, and it was translated toward each corner of the specimen to find the maximum deflection achieved. Using the sine rule of trigonometry, the warp angle was calculated to compare among the various specimens printed at different temperatures.

The angle of warp is measured and calculated using the sine rule of trigonometry. The warp angle was calculated to compare various specimens printed at different temperatures (Fig. 3).

Warp angle θ , from sine rule of trigonometry,

$$\theta = \tan^{-1} \frac{h}{l}$$

2.3 Analysis of Crack Initiation

The rectangular $100 \times 100 \times 20$ -mm ABS test specimens are considered for the analysis of crack initiation. The specimen is printed at various bed temperatures, and the possible conclusions are made to reduce them as much as possible. As the cracking was clearly visible after the completion of printing, the cracking is studied by inspection only. The still images of the printed specimens are captured through

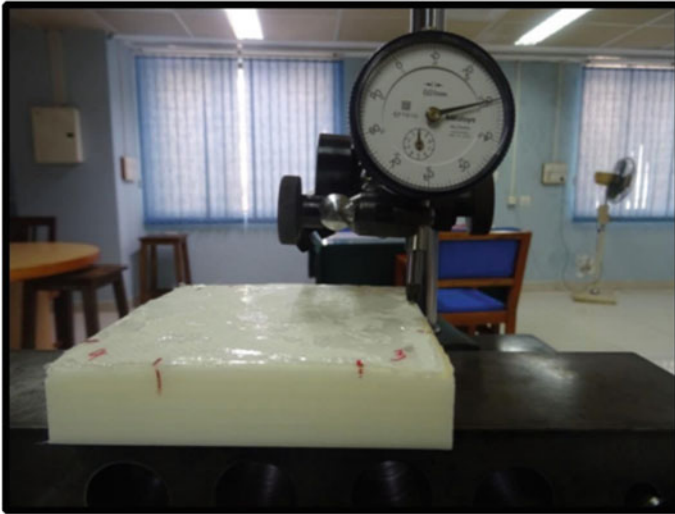


Fig. 2 Shows dial caliper gauge used to measure the linear displacement for measuring warpage

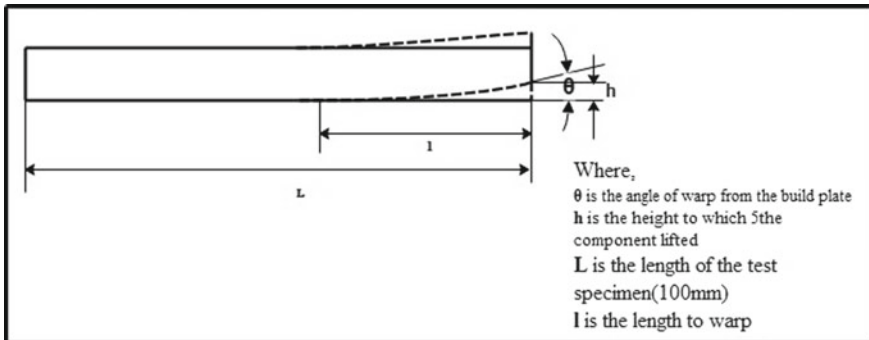


Fig. 3 Warp angle measurement

the camera from all the four faces. The captured images are observed for the different temperatures. By the inspection method, we could clearly note that the crack initiation reduces as the bed temperature increased.

3 Results and Discussion

The results obtained from the experimental study have been presented in this section to understand the warpage and cracking occurred in the printed specimen.

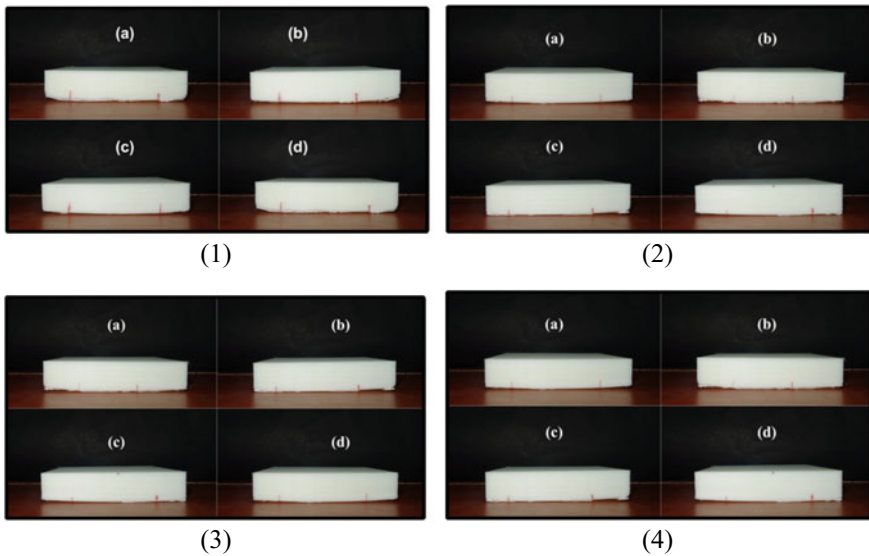


Fig. 4 (1–4) Depicting the warpage and cracking occurred at 1-mm extrusion width and 70, 80, 90, and 100 °C bed temperature

Figures 4(1–4) depict views of the test specimen to understand the warpage occurred at each face of the specimen. It is to be noted that the bed was calibrated before starting the printing of each specimen, and the gap between the nozzle tip and bed surface was maintained to be 100 μ . Three specimens of variable width (1, 0.75 and 0.5 mm) were used, each of which was printed at 5(70, 80, 90, 100, and 110 °C) different temperature profiles. Each of them is discussed in this section.

Figures 4(1–4) show the results obtained when the extrusion width was taken as 1 mm and the infill was maintained at 10%; it can be observed that as the temperature of the bed is increased there is a reduction in warpage is found.

From Fig. 4(1), it can be observed closely that the specimen is cracked almost from the center, whereas no other specimen is cracked at other temperature profiles. The possible reason of the component getting warped was because of insufficient bonding between the first layer and the kapton tape. There are two possible solutions to increase the bonding: (1) Speed of printing can be reduced so that more time of heating will be given to each layer for adhesion (2) more number of layers can be created at the bottom layer so that the overall resistance force for warpage can be increased. Reducing the printing speed will lead to an increase in printing time, whereas the latter method is much faster to print the component in a short time. Hence, the extrusion width is reduced to 0.5 mm so that the maximum bonding can be achieved with the bed.

In case of 0.5-mm extrusion width, two extreme temperature profiles are chosen to understand the warpage and cracking precisely. Figures 5(1–2) show the results obtained at 0.5-mm extrusion width at 70 and 100 °C. In this case, the infill was

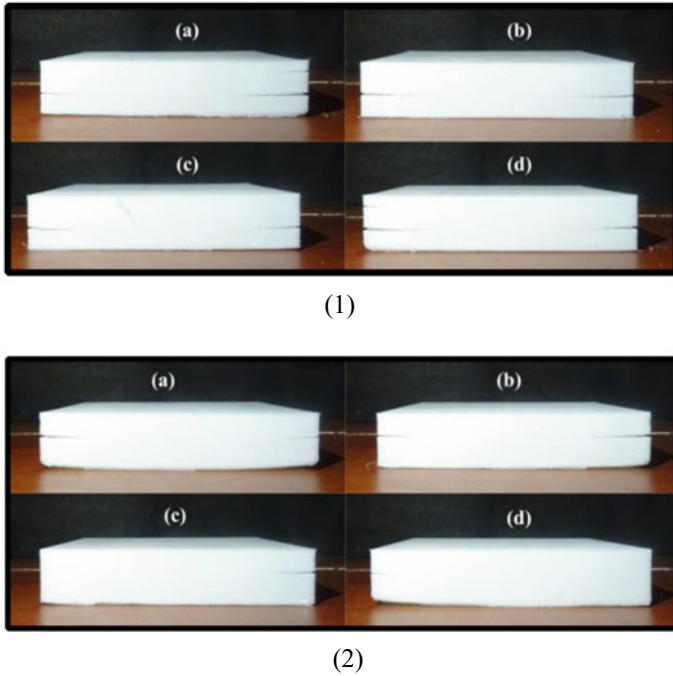


Fig. 5 (1–2) Depicting the warpage and cracking occurred at 0.5-mm extrusion width and 70 and 100 °C bed temperature

reduced to 5% to maintain the same mass. It can be observed that the warpage found in both the temperature profiles shows a reduction in warpage. But it can be seen from Figs. 5(1–2) that the cracking in these specimens has been increased which may be because of poor distribution of heat between the layers. It is to be noted that the number of fibers has been increased as the extrusion width is increased which in turn needs more heat to maintain the same bonding as 1-mm extrusion width. Hence, the study is taken further to check the warpage between two tested extrusion widths (0.5 and 1 mm), i.e., 0.75 mm. In this case, again two extreme temperature profiles are chosen for the study. Figures 6(1–2) show the obtained results at 0.75 extrusion width. Figures 6(1–2) clearly depict the reduction in warpage and cracking at higher temperature profile, whereas cracking at the lower temperature is still observed which infers not to print at the lower bed temperature for ABS polymer (Table 2).

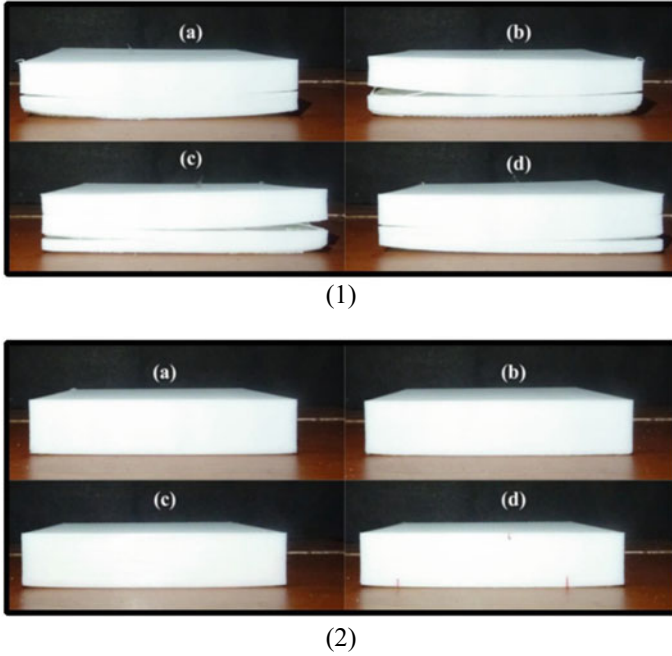


Fig. 6 (1–2) Depicting the warpage and cracking occurred at 0.75-mm extrusion width and 70 and 100 °C bed temperature

Table 2 Demonstrates the warpage in degrees at various extrusion widths and different bed temperature profiles

Extrusion width	Bed temperature	Angle of warpage (°)			
		a	b	c	d
1	70	5.94	3.65	4.01	3.70
	80	3.08	3.04	3.24	3.03
	90	2.38	4.06	1.34	2.43
	100	1.83	1.97	1.70	2.03
0.5	70	29.65	17.20	6.88	4.08
	100	2.64	3.09	5.88	5.01
0.75	70	4.02	7.54	8.20	7.10
	100	1.43	1.15	1.97	0.95

4 Conclusion

In this study, the two most common defects in 3D printed components, i.e., warpage and interlayer cracking are addressed. The specimen was printed at four constant bed temperatures (70, 80, 90, and 100) and three extrusion widths (0.5, 0.75, and 1 mm) to understand the occurrence of warpage and interlayer cracking between the layers.

Initially, four components were printed at 1-mm extrusion width to understand the warpage and cracking. Reduction in warpage and cracking was seen by raising the bed temperature from 70 to 100 °C, also the cracking was observed only at the lowest temperature, i.e., 70°. However, the results obtained were still not satisfactory and further measures were taken to print a warpage-free component. In this regard, the extrusion width was reduced to increase the surface contact of the bottom layer with the printing bed. Reduction in warpage was seen by reducing the extrusion width but due to increase in the adhesion between the bottom layer and printing bed, the removal component from the printing bed was not easy; hence, the extrusion width was increased to encounter this issue. Two extreme temperatures were chosen to print the component, i.e., 70° and 100° at 0.75-mm extrusion width, and the warpage was measured. Most satisfactory results were obtained at 0.75-mm extrusion width and 100 °C temperatures. In each extrusion width, the cracking was seen where the heat distribution was less and hence it was found that cracking can be reduced by increasing the bed temperature. There are following possible solutions which can be implemented to reduce warpage:

- Increasing the bed temperature to enhance the bonding between the bed and the fibers.
- Maintaining the bed layer thickness to be least enough so that the nozzle actually flattens the first layer in the bed while printing.
- It is also suggested to put glue after the completion of the first layer to make sure the bonding between the component and the bed is strong.
- The speed of printing should be as slow as possible to ensure that the bonding between each layer remains strong. 25–30 mm/s is the suggested speed at which FDM printers perform well.

References

1. Singh S, Ramakrishna S, Singh R (2017) Material issues in additive manufacturing: a review. *J Manuf Process* 25:185–200
2. Upadhyay M, Sivarupan T, El Mansori M (2017) 3D printing for rapid sand casting—a review. *J Manuf Process* 29:211–220
3. Bose S, Ke D, Sahasrabudhe H, Bandyopadhyay A (2018) Additive manufacturing of biomaterials *Prog. Mater Sci* 93:45–111
4. Dankar I, Haddarah A, Omar FEL, Sepulcre F, Pujolà M (2018) 3D printing technology: the new era for food customization and elaboration. *Trends Food Sci Technol* 75:231–242
5. Basavaraj CK, Vishwas M (2016) Studies on effect of fused deposition modelling process parameters on ultimate tensile strength and dimensional accuracy of nylon. In: *IOP conference series: materials science and engineering*, vol 149
6. Sood AK, Ohdar RK, Mahapatra SS (2010) Parametric appraisal of fused deposition modelling process using the grey Taguchi method. *Proc Inst Mech Eng Part B J Eng Manuf* 224:135–145
7. Zaldivar RJ, Witkin DB, McLouth T, Patel DN, Schmitt K, Nokes JP (2017) Influence of processing and orientation print effects on the mechanical and thermal behavior of 3D-printed ULTEM® 9085 material. *Addit Manuf* 13:71–80

8. Hashemi Sanatgar R, Campagne C, Nierstrasz V (2017) Investigation of the adhesion properties of direct 3D printing of polymers and nanocomposites on textiles: effect of FDM printing process parameters. *Appl Surf Sci* 403:551–563
9. Li L, Sun Q, Bellehumeur C, Gu P (2002) Composite modeling and analysis for fabrication of FDM prototypes with locally controlled properties. *J Manuf Process* 4:129–141
10. Tiganis BE, Burn LS (1999) The effects of heat aging on acrylonitrile-butadiene-styrene (Abs) blends durab. *Build Mater Compon* 8:912–922
11. Nickel AH, Barnett DM, Prinz FB (1999) Thermal stresses and deposition patterns in layered manufacturing. *Mater Sci Eng A* 317:1–9
12. Panda SK, Padhee S, Sood AK, Mahapatra SS (2009) Optimization of fused deposition modelling (FDM) process parameters using bacterial foraging technique. *Intell Inf Manage* 1:89–97
13. Sood AK, Ohdar RK, Mahapatra SS (2012) Experimental investigation and empirical modelling of FDM process for compressive strength improvement. *J Adv Res* 3:81–90

Optimization of Electrical Discharge Coating of WS₂ and Cu Powder Mixture Deposited Through Green Compact Electrode



Rashi Tyagi, Kshitij Pandey, Shalini Mohanty, Shakti Kumar,
Alok Kumar Das and Amitava Mandal

Abstract Electrical discharge coating (EDC) is performed to deposit the mixture of tungsten disulfide (WS₂) and copper (Cu) powder onto the mild steel surface for solid lubrication. The material deposition process takes place through green compact tool by using EDC setup inside the die-sink electrical discharge machine (EDM). The powder compact tool has been prepared in the hot mounting press for different values of powder mixing ratio, i.e., WS₂: Cu/40:60, WS₂: Cu/50:50, and WS₂: Cu/60:40. The coating material deposits due to series of chemical reactions between the tool and workpiece in the presence of hydrocarbon oil when reverse polarity has been used in die-sinking electrical discharge machine (EDM). Response surface methodology has been utilized for optimization by varying the molding press and machining input parameters such as mixing ratio, duty factor, and peak current. Reduction in micro-hardness value as a result of solid lubricant deposition has been revealed with the help of Vickers hardness testing machine. Field emission scanning electron microscope (FESEM) analysis has been performed to examine the presence of pores, voids, and gaps on the mild steel surface. X-ray diffraction study along with the energy-dispersive X-ray spectroscopy (EDX) results also confirms the presence of WS₂, W, S, Cu, and Cu₂S compounds in the coating. The effect of duty factor and peak current on different output parameters (mass transfer rate, tool wear rate, and micro-hardness) has been evaluated.

Keywords Solid lubricant · Coating · Micro-hardness · Peak current

1 Introduction

The process of surface modification has been used to improve the surface properties such as micro-hardness, wear resistance, and temperature resistance. by using various coating techniques [1]. The different coating techniques such as laser cladding,

R. Tyagi (✉) · K. Pandey · S. Mohanty · S. Kumar · A. K. Das · A. Mandal
Department of Mechanical Engineering, Indian Institute of Technology (Indian School of Mines)
Dhanbad, Dhanbad 826004, Jharkhand, India
e-mail: tyagirashi.bit@gmail.com

electro deposition, plasma spraying, electroless plating, physical vapor deposition, and chemical vapor deposition have many disadvantages. The requirement of high capital cost, high temperature, and vacuum restricts their use for few materials.

Electrical discharge coating (EDC) method has many benefits as compared to the other processes. EDC does not need sophisticated apparatus and high-temperature equipment and coating layer properties can be effectively controlled in EDC. EDC has been reported by researchers worldwide for its ability to improve the cutting performance and life of metal cutting tool, coating of rolling mill rolls [2], and alloying of machining parts [3]. Surface quality of aluminum alloy has also been improved through EDC process by mixing TiN in dielectric [4]. The experiments were conducted on EDC using green compact electrodes of Cu + W powder to deposit thick coating layer over plain carbon steel surface. The appropriate value of parameters (composition, sintering temperature, compaction pressure, peak current setting, pulse on-time, and duty factor) was evaluated by using Taguchi DOE analysis. Their results give the coating thickness of 3–785 μm , variation of MTR from 1 to 191 mg/min, and roughness value from 8 to 10 μm with improved micro-hardness (9.81–12.75 GPa) [5].

Solid lubrication has emerged as a needful process in high-temperature environment when the normal grease or lubricating oil cannot be used. Tungsten disulfide provides best lubricity being a solid lubricant with a friction coefficient of 0.07 to withstand high temperature in gear transmissions, manufacturing industries, agriculture, marine, and space vehicles. It can be effectively utilized in air for the temperature range from -270 to 650 $^{\circ}\text{C}$ and in vacuum of -188 to 1316 $^{\circ}\text{C}$ [6].

From the literature review, it can be said that limited work has been carried out on EDC process. There has been no work done on the optimization of solid lubricant coating of WS_2 and Cu powder using EDC process.

In the present research, electrical discharge coating has been deposited on the mild steel surface and the effect of peak current, and duty factor has been analyzed on the surface integrity, mass transfer rate (MTR), tool wear rate (TWR), and micro-hardness using response surface methodology (RSM).

2 Experimentation

The experimentation process has been started by preparing the green compact electrodes in hot mounting press at 130 $^{\circ}\text{C}$ sintering temperature for 10 min heating and 5 min cooling time. Initially, the powder has been mixed in a mortar for uniform mixing for one hour. As WS_2 is a semiconductor, a pure coating of WS_2 is not possible through EDM. Hence, copper has been mixed as a binder due to its excellent conductivity. The mixing ratio for WS_2 and Cu has been taken in such a way that the required green compact electrode with 15 mm diameter and 3 mm height has been formed which is connected with the conductive rod by using adhesive paste (Fig. 1a). The setup for EDC has been prepared inside the die-sinking EDM which consists of work clamping vice rest on a magnetic vice and tool electrode extension in a tool holder as

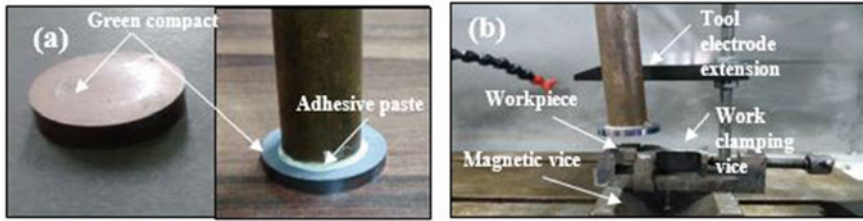


Fig. 1 a Green compact electrodes and tool extension; b set up for EDC

shown in Fig. 1b. The mild steel workpiece of dimension 10 mm × 10 mm × 3 mm has been taken for coating. The experiment starts by varying the duty factor and peak current by keeping the gap voltage 40 V, machining time 4 min, and pulse on-time 29 μs constant. EDC is one of the unfolding coating methods in which a coating layer is obtained due to chemical reaction between workpiece (connected to positive polarity) and tool (connected to negative polarity). When the voltage applied across the workpiece goes beyond the threshold value, the spark generates. The formation of these spark discharge results in high temperature across the electrodes. The high temperature between the electrodes causes the melting and evaporation of material. The chemical reaction between dielectric and electrodes causes the transfer of the material from green compact tool to the workpiece due to the weak bond between particles of powder. The mass transfer rate (MTR) and tool wear rate (TWR) are calculated by the formulas; $MTR = \text{weight of the workpiece after the experiment} - \text{weight of the workpiece before the experiment}$. $TWR = \text{weight of the tool before the experiment} - \text{weight of the tool after the experiment}$.

3 Results and Discussions

3.1 Response Surface Methodology

A Box–Behnken design of experiment (DOE) was employed with 3 levels and 3 variables with 15 runs. The effect of variable machining parameters on TWR, MRR, and Micro-hardness is analyzed. Response surface methodology (RSM) is carried out to establish the mathematical relation between independent variables and the dependent variables. Since, three process parameters and three responses are selected, a pilot number of experiments are carried out. By using RSM, total number of experiments can be deducted to some extent such that their interactions can be calculated easily. By the help of design of experiments (DOE) and regression study, a response can be achieved for independent input process parameters. In RSM, the independent parameters can be denoted quantitatively as given below:

$$y = f(x_1, x_2, x_3 \dots x_n) \pm \varepsilon \tag{1}$$

where y denotes desired response, f denotes response function, $x_1, x_2, x_3 \dots x_n$ denotes independent input variables, and ε denotes fitting error. The requisite surface obtained by plotting expected responses is known as response surface. The suitability of RSM is defined by the approximation of f . It can be attained by using second-order polynomial regression model, also known as quadratic model (Table 1). The quadratic model of f is as follows:

$$f = a_0 + \sum_{i=1}^n a_i x_i + \sum_{i=1}^n a_{ii} x_i^2 + \sum_{i < j}^n a_{ij} x_i x_j + \varepsilon \tag{2}$$

The final regression equation is as follows:

Tool Wear rate = $-14.87 - 0.210$ Peak current + 0.1174 Duty factor + 0.431 Mixing ratio + 0.0197 Peak current \times Peak current $- 0.000375$ Duty factor \times Duty factor $- 0.00233$ Mixing ratio \times Mixing ratio + 0.00069 Peak current \times Duty factor + 0.00025 Peak current \times Mixing ratio $- 0.001408$ Duty factor \times Mixing ratio.

Table 1 Experimental table for input parameters settings and their results

Experiment no.	Input parameters			Output parameters		
	Peak current (A)	Duty factor (%)	Mixing ratio (WS ₂ : Cu)	Tool wear rate (g/m)	Mass transfer rate (g/m)	Micro-hardness (at 0.2 kgf load)
1	10	60	60:40	3.48	0.385	46.83
2	10	60	40:60	1.40	0.926	59.12
3	7	30	40:60	-0.50	-0.200	78.95
4	10	90	50:50	2.49	0.260	68.15
5	4	60	60:40	2.86	0.829	63.57
6	4	30	50:50	1.70	0.220	90.44
7	10	30	50:50	2.40	0.260	60.14
8	7	30	60:40	2.89	0.320	75.12
9	4	60	40:60	0.81	0.145	61.06
10	7	90	40:60	1.20	0.100	73.29
11	7	60	50:50	2.19	0.255	65.96
12	7	90	60:40	2.90	0.250	72.64
13	4	90	50:50	1.54	0.190	77.05
14	7	60	50:50	2.18	0.245	64.85
15	7	60	50:50	2.21	0.259	66.42

Mass transfer rate = $-2.13 + 0.187 \text{ Peak current} + 0.0473 \text{ Duty factor} - 0.0015 \text{ Mixing ratio} + 0.02407 \text{ Peak current} \times \text{Peak current} - 0.000263 \text{ Duty factor} \times \text{Duty factor} + 0.001016 \text{ Mixing ratio} \times \text{Mixing ratio} + 0.000083 \text{ Peak current} \times \text{Duty factor} - 0.01021 \text{ Peak current} \times \text{Mixing ratio} - 0.000308 \text{ Duty factor} \times \text{Mixing ratio}$.

Micro hardness = $22.8 + 7.31 \text{ Peak current} - 2.309 \text{ Duty factor} + 4.05 \text{ Mixing ratio} - 0.509 \text{ Peak current} \times \text{Peak current} + 0.01420 \text{ Duty factor} \times \text{Duty factor} - 0.0352 \text{ Mixing ratio} \times \text{Mixing ratio} + 0.0594 \text{ Peak current} \times \text{Duty factor} - 0.1233 \text{ Peak current} \times \text{Mixing ratio} + 0.00265 \text{ Duty factor} \times \text{Mixing ratio}$.

3.2 Anova

The analysis of variance (ANOVA) for TWR, MTR, and Micro-hardness is shown by Tables 2, 3, 4. *F*-value helps to check the significance of values. The *P*-value denotes that the *F*-value probability is more than calculated because of noise. If *P*-value goes beyond 0.05, then the term is not significant and lacks fit which also denotes that the insignificant term is left away from the model and the model fits very well. It is shown in the table that *P*-values are significant since all the *P*-values are below 0.05. The coefficient of determination (*R*²) and Adj. *R*² for tool wear rate is found to be 96.27 and 89.29, respectively. Likewise, the coefficient of determination (*R*²) and Adj. *R*² for mass transfer rate are 95.15 and 86.41 and that of micro-hardness is found to be 96.05 and 88.94, respectively. Further, the normality test is performed by plotting the results. It can be observed from Figs. 2, 3 and 4 that the residuals are uniformly distributed as shown in normal distribution as the residues lie nearly same as that of normal probability plot. The experimental values are good in agreement with the predictive results for all the experiment performed in present work. Besides developing mathematical models, it is evident from the ANOVA results that for high proportion of WS₂ in mixing ratio (WS₂: Cu/50:50 and WS₂: Cu/60:40) as the peak current increases, tool wear rate and mass transfer rate increases. Moreover, for all the mixing ratios, micro-hardness decreases with increasing current but it decreases with duty factor up to a certain value (60%) and then again increases further. Also, the Vicker micro-hardness test revealed that the hardness of solid lubricant coating has been reduced (46.83HV_{0.2}–90.44HV_{0.2}) in comparison to mild steel (180HV_{0.2}) due to deposition of solid lubricant.

3.3 Microstructure and Chemical Composition Analysis

The morphology analysis has been carried out in FESEM (Model: Supra 55). The FESEM study of coating shows the top surface morphology at WS₂: Cu/50:50, peak current 7 A, and duty factor 60%. The uniform distribution of coating material with better microstructure at top surface and cross section without any voids and gap at 7 A peak current can be seen in Figs. 5 and 6. Some pores have been formed due to

Table 2 ANOVA table for tool wear rate

Source	DF	Adj SS	Adj MS	F-value	P-value
Model	9	13.4724	1.4969	13.97	0.005
<i>Linear</i>	3	11.9847	3.9949	37.27	0.001
Peak current	1	1.0224	1.0224	9.54	0.027
Duty factor	1	0.3362	0.3362	3.14	0.137
Mixing ratio	1	10.6261	10.6261	99.14	0.000
<i>Square</i>	3	0.7578	0.2526	2.36	0.188
Peak current × Peak current	1	0.1158	0.1158	1.08	0.346
Duty factor × Duty factor	1	0.4216	0.4216	3.93	0.104
Mixing ratio × Mixing ratio	1	0.2003	0.2003	1.87	0.230
<i>2-way interaction</i>	3	0.7299	0.2433	2.27	0.198
Peak current × Duty factor	1	0.0156	0.0156	0.15	0.718
Peak current × Mixing ratio	1	0.0002	0.0002	0.00	0.965
Duty factor × Mixing ratio	1	0.7140	0.7140	6.66	0.049
Error	5	0.5359	0.1072		
<i>Lack-of-fit</i>	3	0.5354	0.1785	764.93	0.001
<i>Pure error</i>	2	0.0005	0.0002		
Total	14	14.0083			

Table 3 ANOVA table for mass transfer rate

Source	DF	Adj SS	Adj MS	F-value	P-value
Model	9	0.97438	0.108264	10.89	0.009
<i>Linear</i>	3	0.11260	0.037532	3.78	0.093
Peak current	1	0.02498	0.024976	2.51	0.174
Duty factor	1	0.00500	0.005000	0.50	0.510
Mixing ratio	1	0.08262	0.082621	8.31	0.034
<i>Square</i>	3	0.45217	0.150725	15.16	0.006
Peak current × Peak current	1	0.17327	0.173267	17.43	0.009
Duty factor × Duty factor	1	0.20761	0.207612	20.88	0.006
Mixing ratio × Mixing ratio	1	0.03813	0.038133	3.84	0.108
<i>2-way interaction</i>	3	0.40961	0.136535	13.73	0.008
Peak current × Duty factor	1	0.00022	0.000225	0.02	0.886
Peak current × Mixing ratio	1	0.37516	0.375156	37.73	0.002
Duty factor × Mixing ratio	1	0.03423	0.034225	3.44	0.123
Error	5	0.04971	0.009942		
<i>Lack-of-fit</i>	3	0.04961	0.016536	318.00	0.003
<i>Pure error</i>	2	0.00010	0.000052		
Total	14	1.02409			

Table 4 ANOVA table for micro-hardness

Source	DF	Adj SS	Adj MS	F-value	P-value
Model	9	1419.50	157.722	13.50	0.005
<i>Linear</i>	3	467.03	155.676	13.33	0.008
Peak current	1	418.76	418.762	35.85	0.002
Duty factor	1	22.85	22.849	1.96	0.221
Mixing ratio	1	25.42	25.418	2.18	0.200
<i>Square</i>	3	780.69	260.232	22.28	0.003
Peak current × Peak current	1	77.34	77.339	6.62	0.050
Duty factor × Duty factor	1	602.90	602.901	51.62	0.001
Mixing ratio × Mixing ratio	1	45.79	45.793	3.92	0.105
<i>2-way interaction</i>	3	171.78	57.259	4.90	0.060
Peak current × Duty factor	1	114.49	114.490	9.80	0.026
Peak current × Mixing ratio	1	54.76	54.760	4.69	0.083
Duty factor × Mixing ratio	1	2.53	2.528	0.22	0.661
Error	5	58.40	11.680		
<i>Lack-of-fit</i>	3	57.10	19.032	29.22	0.033
<i>Pure error</i>	2	1.30	0.651		
Total	14	1477.90			

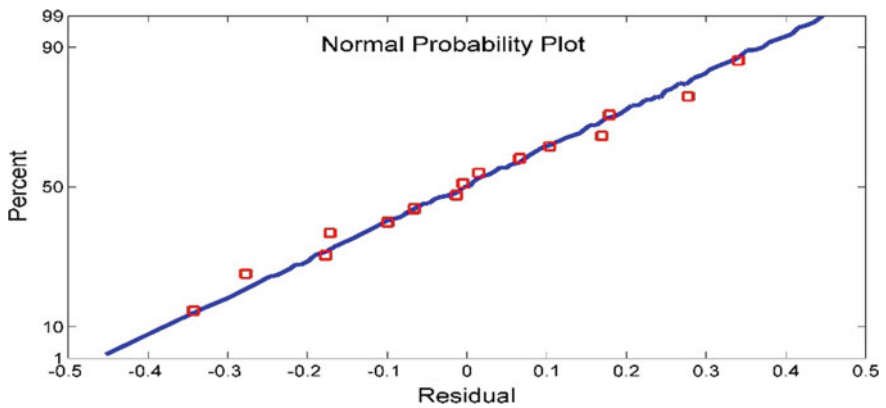


Fig. 2 Normal probability plot of residuals for TWR

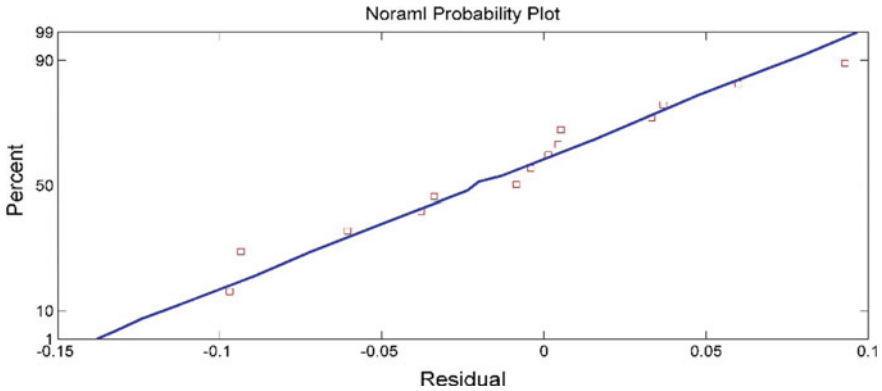


Fig. 3 Normal probability plot of residuals for MTR

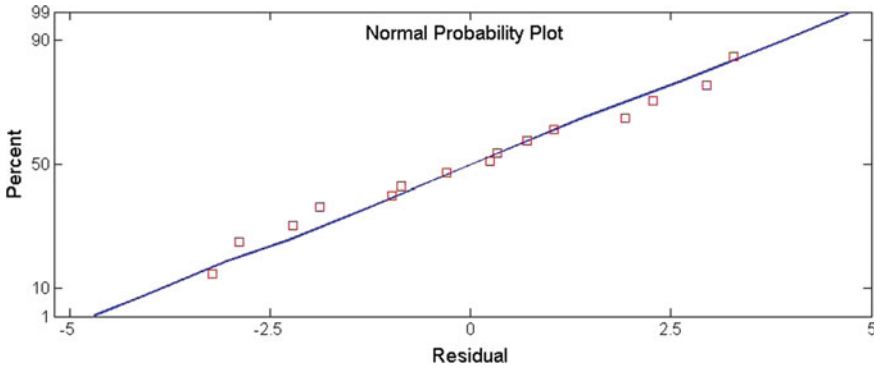


Fig. 4 Normal probability plot of residuals for micro-hardness

insufficient deposition of the coating material at low spark discharge. However, at 7 A peak current, the best morphology has been obtained with few pores formation.

Energy dispersive spectroscopy (EDS) study has been performed to check the existence of principal elements in coating such as W, S, and Cu. The cross-sectional EDS of the workpiece has been examined that proves the presence of W, S, Cu, Fe, and C peaks (Fig. 6a and b). Thus, EDS pattern supports the deposition of solid lubricant coating over the workpiece.

The X-ray diffraction test has been done to identify the elemental phase formed during the experiment. The XRD files were evaluated using X'Pert software for peaks identification. The angle of diffraction (2θ) was chosen from 10° and 40° . The XRD pattern detects the phases comprised of W, S, WS_2 , Cu, and Cu_2S elements' presence over the coated layer (Fig. 7). As the WS_2 proportion is more than the Cu, the large number of peaks of W and WS_2 is attained as compared to Cu. Thus, XRD results justify the outcome obtained from the EDS results.

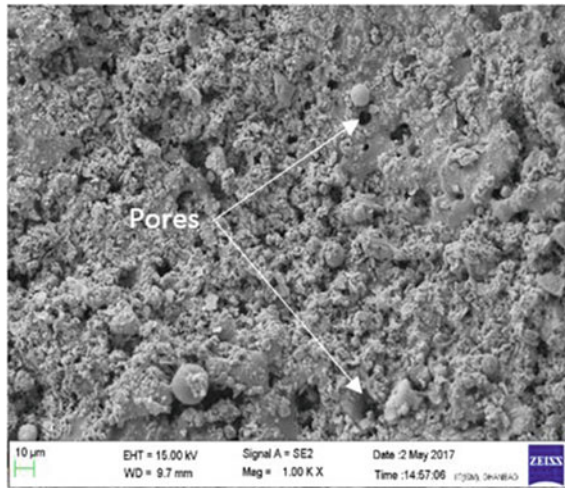


Fig. 5 FESEM image of coated samples for WS₂: Cu/50:50, 7 A peak current, and 60% duty factor

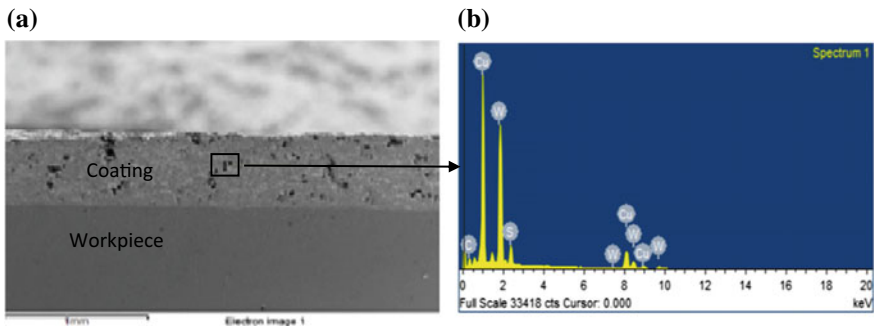


Fig. 6 **a** FESEM image of coating cross-sectional area and corresponding, **b** EDS analysis

4 Conclusions

EDC of WS₂ and Cu was successfully deposited onto the surface of mild steel. Following result has been obtained from this study:

- (1) Cu has been added as a binder because the pure coating of WS₂ is not possible as the powder is dry. However, different combination of powder such as Ti, brass, and Al can be used for future research trends in EDC. The solid lubricant coating could be employed for improving wear resistance of various components when oil and grease cannot be utilized at high temperature. Thus, EDC can be used to deposit the lubricant coating for tribology components as well as for coating of various cutting tools in machining.

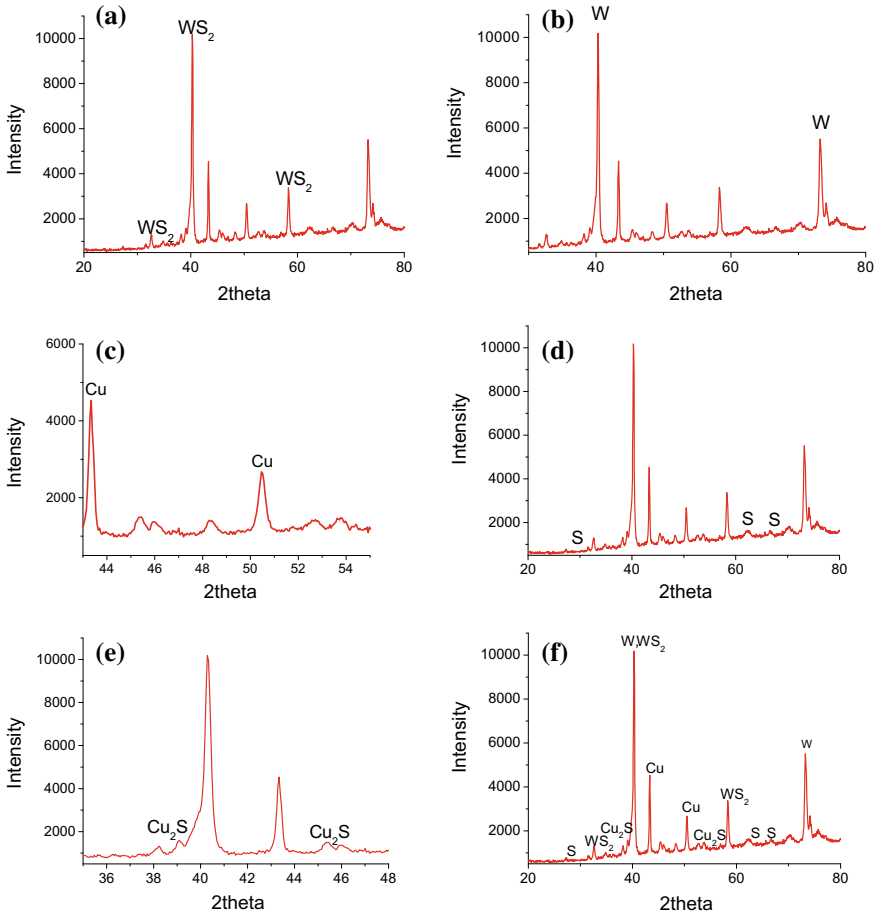


Fig. 7 XRD analysis of top surface of coating for WS₂: Cu/50:50, peak current 7 A, and duty factor 60%, for **a** WS₂, **b** W, **c** Cu, **d** S, **e** Cu₂S, and **f** combined plot for WS₂, W, Cu, S, and Cu₂S

- (2) The experimental values are good in agreement with the predictive results for all the experiment performed in present work. In addition to developing mathematical models, it can be seen from the ANOVA that when the peak current increases, TWR and MTR increases. The use of green compact tool shows significant material transfer rate and tool wear rate. Hence, by selecting the desired value of peak current, deposition rate can be controlled in EDC.
- (3) The micro-hardness of coating has been reduced to 46.83HV_{0.2} t 10 A peak current 60% duty factor and WS₂: Cu/60:40 in comparison to mild steel of 180HV_{0.2} that proves the deposition of solid lubricant material. Hence, solid lubricant EDC can be further used for tribological applications as the solid lubricant exhibit low coefficient of friction.

- (4) The better microstructure is obtained with 7 A peak current and 60% duty factor without any voids and gap formation. EDS analysis also confirms the deposition of solid lubricant coating by showing peaks of W, S, and Cu.

References

1. Simao J, Lee HG, Aspinwall DK, Dewes RC, Aspinwall EM (2003) Workpiece surface modification using electrical discharge machining. *Int J Mach Tools Manuf* 43:121–128. [https://doi.org/10.1016/S0890-6955\(02\)00187-6](https://doi.org/10.1016/S0890-6955(02)00187-6)
2. Elkoca O (2008) A study on the characteristics of electrical discharge textured skin pass mill work roll. *Surf Coat Technol* 202:2765–2774. <https://doi.org/10.1016/j.surfcoat.2007.10.004>
3. Gill AS, Kumar S (2015) Surface alloying of H11 die steel by tungsten using EDM process. *Int J Adv Manuf Technol* 78:1585–1593. <https://doi.org/10.1007/s00170-014-6743-1>
4. Chen HJ, Wu KL, Yan BH (2014) Characteristics of Al alloy surface after EDC with sintered Ti electrode and TiN powder additive. *Int J Adv Manuf Technol* 72:319–332. <https://doi.org/10.1007/s00170-014-5669-y>
5. Patowari PK, Saha P, Mishra PK (2011) Taguchi analysis of surface modification technique using W-Cu powder metallurgy sintered tools in EDM and characterization of the deposited layer. *Int J Adv Manuf Technol* 54:593–604. <https://doi.org/10.1007/s00170-010-2966-y>
6. Rapoport L, Fleischer N, Tenne R (2003) Fullerene-like WS₂ nanoparticles: superior lubricants for harsh conditions. *Adv Mater* 15:651–655. <https://doi.org/10.1002/adma.200301640>

Optimization by AHP-ARAS of EDM Process Parameters on Machining AA7050-10% B₄C Composite



Arvind Kumar, Sayed Abou Iltaf Hussain and Ram Naresh Rai

Abstract The present paper aims to develop AA7050/B₄C composite by stir casting method. The flux K₂TiF₆ has been used for proper incorporation of the B₄C particle in the molten matrix. The microstructures of the casted composite were analysed with FE-SEM. The microstructure shows the proper distribution of B₄C particle with the formation of encapsulating layers of Ti compounds around B₄C particles. Machining of AA7050/B₄C composite was done by the non-traditional machining process known as electro-discharge machine (EDM). Multi-criteria decision-making (MCDM) model of AHP-ARAS has been used to evaluate the optimal EDM process parameters for machining AA7050-B₄C composite. Taguchi L₉ orthogonal array was used to design the experiments. The process parameters selected for the experiments were pulse current (I_p), pulse on time (T_{on}), and pulse off time (T_{off}) for the responses like material removal rate (MRR), the surface roughness (R_a), and depth of cut (DC). The sensitivity analysis has been used to understand the consistency of the responses by interchanging the weights of the criterion. It has been observed that the process parameters of ninth experiment were the most effective among all selected alternatives. The sensitivity analysis confirmed that the proposed AHP-ARAS model was consistent and can be used to evaluate the performance of EDM process parameters.

Keywords MMC · Taguchi · EDM · MRR · MCDM · AHP-ARAS · Sensitivity analysis

A. Kumar (✉) · S. A. I. Hussain · R. N. Rai
Department of Production Engineering, NIT, Agartala, India
e-mail: arvja5@gmail.com

S. A. I. Hussain
e-mail: syedaboui8@gmail.com

R. N. Rai
e-mail: nareshray@yahoo.co.in

1 Introduction

Metal matrix composite (MMC) materials are very significant among all other monolithic or alloy materials due to its excellent mechanical properties like high strength to weight ratio, high stiffness, high hardness, and high wear resistance. These properties increase the utility of composite materials in automobiles and aerospace industries, especially in structural applications [1, 2]. Stir casting method is simple, economical, and best suited for mass productions irrespective of their shapes and sizes. The major challenges in developing MMC through stir casting technique are the wettability and uniform distribution of reinforcements as well as formations of unwanted inter-metallic phases [3]. Many researchers have used different techniques to overcome these challenges such as: Toptan et al. [4] have selected casting temperature as 850 °C, stirred at 500 rpm for five minutes with the application of K_2TiF_6 to get a homogeneous distribution of particles. Baradeswaran et al. [5] fabricated MMC with 5, 10, 15, 20 vol% of the B_4C particle by putting the mixture of B_4C and K_2TiF_6 within 4 min at 850 °C stirred at 500 rpm for 5 min. Prabu et al. [6] investigated the effect of stirring speed and stirring time on microstructure and other properties of metal matrix composite and found that lower speed and lower stirring time lead to particle clustering and particle-free region in the matrix. However, another most challenging aspect of metal matrix composite is its machinability. The poor machinability of metal matrix composites is mainly due to an increase in hardness, yield strength, and decrease in ductility [7]. The common flaws in machining of MMCs are de-boding of reinforcements, delamination, rapid tool wear due to ceramic particles [8, 9]. From the past research, it has been suggested that the nonconventional machining process especially electro-discharge machining is the most suitable for metal matrix composite materials because it works on thermo-electrical principle [10]. Hardness, yield strength, and ductility is not a constraint in EDM process as it is a non-contact type machining process; i.e., the harder workpiece can be machined by the softer tool [11]. Also there are numerous optimization techniques which have been used in literature to evaluate best machining parameters to get desired outputs such as: Assarzadeh et al. [12] found the optimum EDM parameters such as current (I), the period of pulses (T), and the source voltage (V) to get the responses like (MRR) and surface roughness (R_a) using ANN. Sidhu et al. [14] have performed the EDM operation on 30 vol.% SiC/A359 MMC and optimized the process parameters by two MCDM approach namely desirability function approach and lexicographic goal programming (LGP) approach. Peças et al. [15] have mixed the silicon powder in the dielectric and found that surface roughness values are reduced, the craters sizes reduced, and white layer thickness also reduced. Kumar et al. [16] Grey relation analysis has been used to optimize the performance characteristics of Al 6351-5 wt% SiC and 10 wt% boron carbide B_4C particles fabricated through stir casting method. Shukla et al. [17] have used firefly algorithm (FA) to optimize process parameters of electro-discharge machine.

From the literature survey, it is concluded that the development of metal matrix composite using Al 7050 alloy with boron carbide reinforcement and its

electro-discharge machining is very few. Therefore, present paper aims to develop AA7050-10%B₄C composite using stir casting technique and find the optimum process parameters such as pulse current (I_p), pulse on time (T_{on}), and pulse off time (T_{off}) to get best machining responses such as material removal rate, surface roughness, and depth of cut with the use of multi-criteria decision-making (MCDM) model of AHP-ARAS

2 Materials and Methods

Aluminium 7050 alloy (Zn—5.8, Mg—1.9, Cu—2.4, Si—0.031, Fe—0.095, Mn—0.022, Cr—0.006, and Al—balance) is used as matrix material for present experiment along with boron carbide as reinforcement and K₂TiF₆ flux to improve wettability of reinforcement into the molten matrix. 1.3 kg of matrix material was cleaned with acetone and placed in induction furnace, when the matrix material melted the preheated B₄C and K₂TiF₆—flux at about 400 °C for 2 h of amount 10 wt% of matrix was mixed at constant temperature of 900 °C during stirring duration of 5 min. 0.2 wt% of matrix material, hexachloroethane (degasser), was mixed in molten composite in order to remove unwanted hydrogen gas entrapped during stirring. After mixing, the molten composite at 900 °C was poured in steel mould preheated at 350 °C. The microstructure of AA7050-B₄C composite has been analysed using FE-SEM. Hardness was measured using Vickers hardness tester as per ASTM E 384 with the applied normal load of 2.5 kgf. Average of ten readings was taken as value of hardness. Electro-discharge machining has been done on spark EDM of make SPARKONIX F-25 (Fig. 1a). The casted composite material was cut in the size of 40 mm × 40 mm × 10 mm as shown in Fig. 2a. The copper rod of diameter 7 mm was used as tool electrode as shown in Fig. 2b. The responses of the EDM process parameters such as MRR were obtained by measuring the difference in weights of the specimen before and after experiment using an electronic balance of precision 0.001 divided by total machining time for one set of experiment. In the present experiment, the machining time was fixed for 6 min. The surface roughness of the specimen after experiment was measured using stylus-type 2D profilometer of make Taylor Hobson as shown in Fig. 1b with cut-off length (L) 0.8 mm and sample length (L) of 4.2 mm. The depth of cut as per machine reading has been recorded.

2.1 Design of Experiments

The experiments were designed using Taguchi L₉ orthogonal array (Table 1) to know the influence of process parameters such as pulse current, pulse on time, and pulse off time on electro-discharge machining performance in term of MRR, surface roughness, and depth of cut. The selection of process parameters was on the basis of several literature survey and trial run.

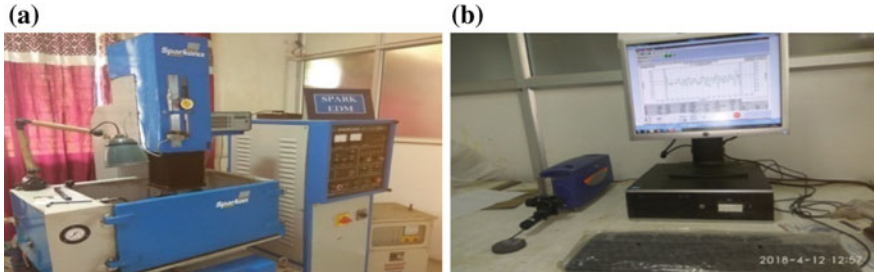


Fig. 1 a Spark electro-discharge system and machine and b 2D profilometer



Fig. 2 a Electro-discharge machined specimen and b copper rod as tool electrode

Table 1 Levels and factor for Taguchi L₉ orthogonal array

Parameters	Units	Levels
Pulse current (<i>I</i>)	A	10, 12, 14
Pulse on time (<i>T_{on}</i>)	μs	50, 100, 175
Pulse off time (<i>T_{off}</i>)	μs	30, 40, 75

2.2 Multi-Criteria Optimization Technique

2.2.1 The Additive Ratio Assessment (ARAS)

The additive ratio assessment (ARAS) was introduced in 2010 by Turskis and Zavadskas [18]. ARAS is a MCDM which evaluates the performance of selected alternatives as well as compares the scores of those selected alternatives with the ideal alternative [19]. It has been successfully applied in the fields of economics, transportation, technology, construction, and sustainable development [20]. The adopted algorithm for AHP-ARAS is as follows:

Step 1: Formation of the decision matrix (*D*): The decision matrix obtained by the experiment can be arranged into the matrix form where *Aⁱ* represent number of alternatives and *C^j* represent number of criteria.

$$C^1 \ C^2 \ C^3 \ \dots \ C^j$$

$$D = \begin{matrix} A^1 \\ A^2 \\ A^3 \\ \vdots \\ A^i \end{matrix} \begin{bmatrix} d_{11} & d_{12} & d_{13} & \cdots & d_{1j} \\ d_{21} & d_{22} & d_{23} & \cdots & d_{2j} \\ d_{31} & d_{32} & d_{33} & \cdots & d_{3j} \\ \vdots & \vdots & \vdots & \ddots & \vdots \\ d_{i1} & d_{i2} & \alpha_{i3} & \cdots & d_{ij} \end{bmatrix}$$

Step 2: Addition of the optimal C^n value in D : In this experiment MRR, DC is considered as benefit criteria and SR is considered as non-benefit criteria.

$$d_{0n} = \max_m(d_{mn}), \text{ for benefit criteria}$$

$$d_{0n} = \min_m(d_{mn}), \text{ for non-benefit criteria}$$

Step 3: Computation of normalized decision matrix (R).

Mostly, the criteria are a set of objects with different dimensions. The prime motive of making the data comparable is only achieved by reducing it into dimensionless weighted values. This process is called normalization, and the resultant matrix obtained from the decision matrix is called normalized decision matrix (R).

$$[r]_{(i \times j)} = \begin{cases} \frac{(d_{mn})}{\sum_{m=1}^i(d_{mn})}, & \text{for benefit criteria} \\ \frac{(1/d_{mn})}{\sum_{m=1}^i(1/d_{mn})}, & \text{for non-benefit criteria} \end{cases} \quad (n = 1, 2, 3, \dots, j)$$

Step 4: Creation of weighted normalized decision matrix (W).

In step 4, the weight of the criteria is multiplied with the normalized value of the data. It is done in order for the criteria to influence the output of the problem.

$$\varphi_{mn} = \omega^m \times r_{mn}$$

ω^m is the weights of the responses which is being evaluated through AHP and the relative weights are shown in table

MRR	SR	DC
0.722127	0.1916	0.086272

Step 5: Calculation of the optimality function (S^m).

$$S^m = \sum_{n=1}^j(\varphi_{mn}), \quad (m = 0, 1, 2, \dots, i)$$

Optimality function is the sum of all the weighted normalized value of an alternative for the different criteria.

Stage 6: Figure out the degree of utility K^m for each of the alternatives.

$$K^m = \frac{S^m}{S^i}$$

where K^m is the weightage of the alternatives and S^i is the Max value of all alternatives.

3 Results and Discussion

3.1 Microstructure and Hardness

Microstructure of the casted AA7050-10 (wt) % B4C metal matrix composite shows that the boron carbide particles are fairly distributed with proper incorporation as shown in Fig. 3. Some particles clustering as well as particle-free regions are seen in the microstructure. The B4C particles are surrounded by Ti compounds due to the application of K2TiF6 flux. Figure 4 shows the microstructure of EDM surface, and some cracks were identified that may be due to increase in pulse energy. Also, some spherical deposits were also seen, and this may be due to poor flushing which could not expel the machining debris from the machined surface. The hardness value of the composite recorded as 132 HV.

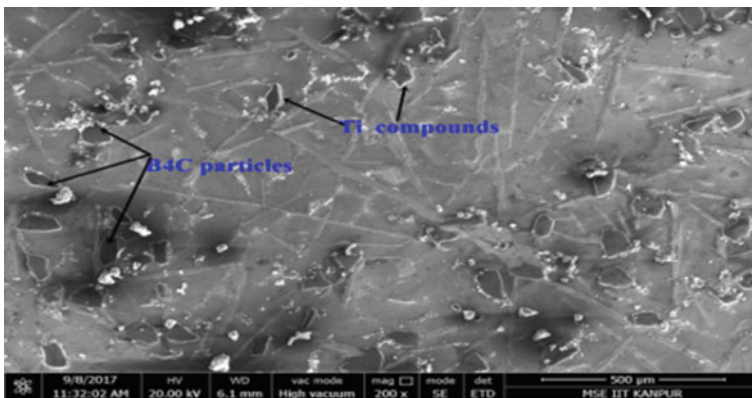


Fig. 3 Microstructure of composite

3.2 Impact of Process Parameters

Electro-discharge machining is thermo-electric process of machining the work material. Pulse energy has great influence on the machining performance. The metal removal rate and depth of cut increases with increase in pulse current, the number of spark increases which intern removes more materials (Fig. 4). On the other hand, if pulse current increases, the surface roughness of workpiece increases. When the pulse current increases, it creates bigger size crates and which intern increases surface roughness (Fig. 4) [8, 13]. Depth of cut in EDM process increases with increase in pulse energy (Fig. 5), although depth of cut and surface roughness are influenced by pulse off time, as the low pulse off time is unable to remove the melted debris from the machining surface and the debris gets re-solidify in the machining area which

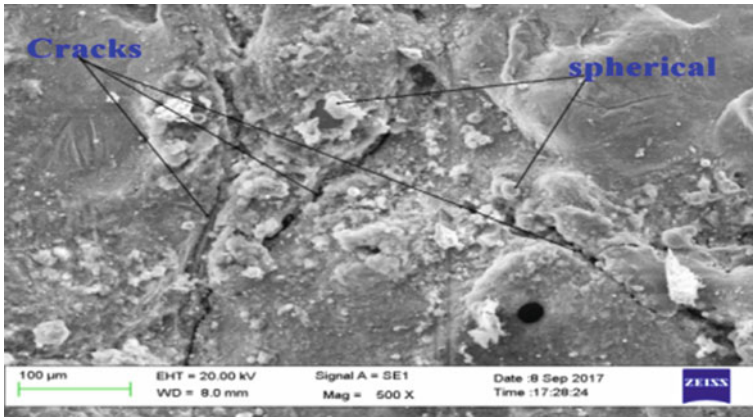


Fig. 4 EDM surface

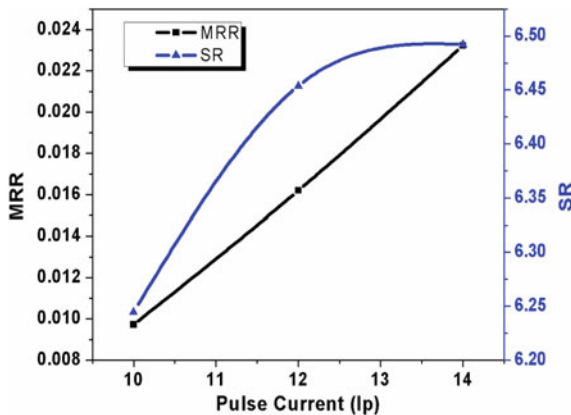
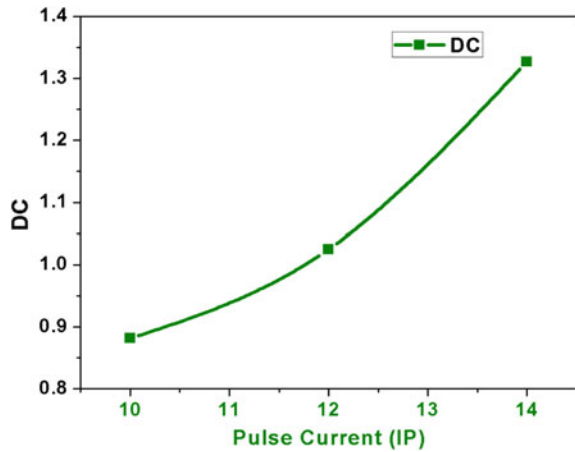


Fig. 5 MRRVs I_p and SR versus I_p

Fig. 6 DC versus I_p 

are called recast layers, eventually increases the surface roughness and decreases the actual depth of cut [21] (Fig. 6).

3.3 Ranks of the Alternatives

By following the steps of AHP-ARAS algorithm, the ranks of the selected alternatives were evaluated and listed in Table 2. The alternatives having higher value of weightage were considered as most effective alternative and those having least weightage was considered as worst alternative. From the experiment, it was noticed that run number 9 was ranked first with 96.07% weightage and run number 1 is ranked last with 24.69% weightage.

3.4 Sensitivity Analysis

The sensitivity analysis of the proposed AHP-ARAS, MCDM model was done by interchanging the weights of the criteria, and subsequently, the ranks of the alternatives were obtained. In the present experiment, four possible combinations were proposed namely C1, C2, C3, and C4. C1 was made by interchanging the weights of MRR with weight of surface roughness, C2 was made by interchanging the weight of MRR with depth of cut, C3 was made by interchanging the weight of surface roughness and depth of cut, and C4 was made without interchanging the weights. The ranks of all combinations are listed in Table 3. Experiment number 9 has been ranked first, and experiment number 1 has been ranked last in three combinations out of four (Fig. 7). All other alternatives are moreover the same; hence from sensitivity

Table 2 Results of the experiments

Ex. No	MRR	SR	DC	Normalized matrix			Weighted normalized matrix			Optimality function	Weightage	Ranks
0				0.1658	0.1231	0.1285	0.1197	0.0236	0.0111	0.1544	100.00	
1	0.00316	6.0419	0.77	0.0179	0.1004	0.0692	0.0129	0.0192	0.0060	0.0381	24.69	9
2	0.0085	6.368	0.81	0.0481	0.0952	0.0728	0.0347	0.0182	0.0063	0.0593	38.39	7
3	0.0175	6.3238	1.065	0.0990	0.0959	0.0957	0.0715	0.0184	0.0083	0.0981	63.57	5
4	0.0075	9.2063	1.07	0.0424	0.0659	0.0961	0.0306	0.0126	0.0083	0.0516	33.40	8
5	0.02	5.2258	0.91	0.1131	0.1161	0.0818	0.0817	0.0222	0.0071	0.1110	71.91	4
6	0.0211	4.9292	1.095	0.1194	0.1231	0.0984	0.0862	0.0236	0.0085	0.1183	76.62	3
7	0.0158	6.3231	1.175	0.0894	0.0959	0.1056	0.0645	0.0184	0.0091	0.0920	59.62	6
8	0.0246	6.5221	1.375	0.1392	0.0930	0.1235	0.1005	0.0178	0.0107	0.1290	83.55	2
9	0.0293	6.6317	1.43	0.1658	0.0915	0.1285	0.1197	0.0175	0.0111	0.1483	96.08	1

Table 3 Sensitivity analysis

C1	C2	C3	C4
9	8	9	9
7	7	8	7
5	5	5	5
8	9	7	8
4	2	6	4
3	1	3	3
6	6	4	6
2	4	2	2
1	3	1	1

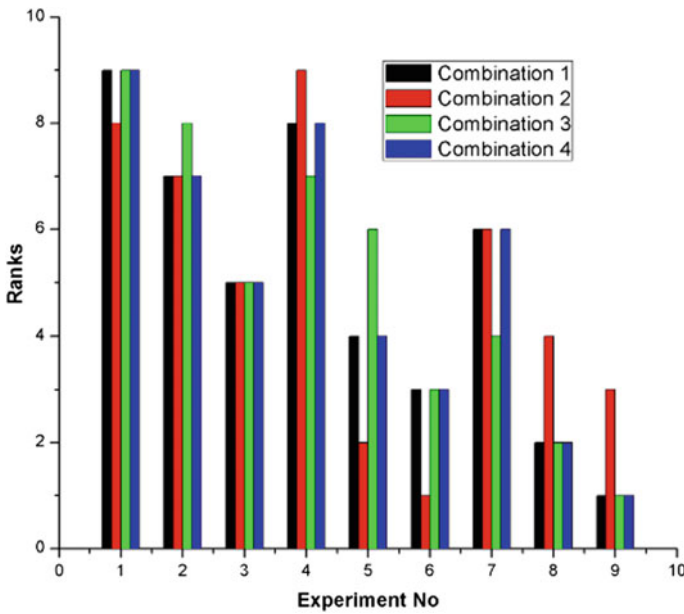


Fig. 7 Sensitivity analysis

analysis, it was concluded that the proposed MCDM model was consistent. Therefore, proposed ARAS model can be used for finding the optimum process parameters for electro-discharge machining of AA7050-10 (wt) % B₄C MMC.

4 Conclusion

AA7050/B4C metal matrixes' composite has been developed successfully by stir casting technique with the use of flux K_2TiF_6 and degasser (hexachloroethane). From the experiment, the following conclusions were drawn:

1. Microstructure shows the fair distribution of B4C particle with encapsulating layers of Ti compounds at particle–matrix interface.
2. Hardness of the composite material was recorded as 132 HV.
3. Ranks of the alternatives are obtained by AHP-ARAS, MCDM method.
4. From ARAS model, it is found that experiment number 9 is ranked first followed by experiment number 2 and 6 and experiment number 1 is ranked last.
5. I_p 14 (A), T_{on} 175 (μs), and T_{off} 40 (μs) were the best process parameter, and the responses obtained from this input parameters were MRR 0.0293 (g/min), surface roughness 6.6317 (μm), and depth of cut 1.43 (mm).
6. Sensitivity analysis of the proposed model suggests that the AHP-ARAS, MCDM model is consistent and can be used to obtain the best process parameters of electro-discharge machine.

References

1. Raj R, Thakur DG (2016) Qualitative and quantitative assessment of microstructure in Al-B₄C metal matrix composite processed by modified stir casting technique. Arch Civ Mech Eng 16(4):949–960
2. Poovazhagan L, Kalaichelvan K, Sornakumar T (2016) Processing and performance characteristics of aluminum-nano boron carbide metal matrix nanocomposites. Mater Manuf Processes 31(10):1275–1285
3. Kalaiselvan K, Murugan N, Parameswaran S (2011) Production and characterization of AA6061–B₄C stir cast composite. Mater Des 32(7):4004–4009
4. Toptan F, Kilicarslan A, Karaaslan A, Cigdem M, Kerti I (2010) Processing and microstructural characterisation of AA1070 and AA6063 matrix B₄Cp reinforced composites. Mater Des 31:S87–S91
5. Baradeswaran A, Perumal AE (2013) Influence of B₄C on the tribological and mechanical properties of Al7075–B₄C composites. Compos B Eng 54:146–152
6. Prabu SB, Karunamoorthy L, Kathiresan S, Mohan B (2006) Influence of stirring speed and stirring time on distribution of particles in cast metal matrix composite. J Mater Process Technol 171(2):268–273
7. Rengasamy NV, Rajkumar M, Senthil Kumaran S (2016) An analysis of mechanical properties and optimization of EDM process parameters of Al 4032 alloy reinforced with ZrB₂ and TiB₂ in-situ composites. J Alloy Compd 662:325–338
8. Gok A (2015) A new approach to minimization of the surface roughness and cutting force via fuzzy TOPSIS, multi-objective grey design and RSA. Measurement 70:100–109
9. Saha P, Tarafdar D, Pal SK, Saha P, Srivastava AK, Das K (2009) Modeling of wire electro-discharge machining of TiC/Fe in situ metal matrix composite using normalized RBFN with enhanced k-means clustering technique. Int J Adv Manuf Technol 43(1–2):107–116
10. Hassan EI-H (2005) Advanced machining processes. McGraw-Hill, pp 36–37
11. Jameson EC (2001) Electrical discharge machining. Society of Manufacturing Engineers

12. Assarzadeh S, Ghoreishi M (2008) Neural-network-based modeling and optimization of the electro-discharge machining process. *Int J Adv Manuf Technol* 39(5):488–500
13. Gopalakannan S, Senthilvelan T (2013) A parametric study of electrical discharge machining process parameters on machining of cast Al/B₄C metal matrix nanocomposites. *Proc Inst Mech Eng Part B: J Eng Manuf* 227(7):993–1004
14. Sidhu SS, Yazdani M (2018) Comparative analysis of MCDM techniques for EDM of SiC/A359 composite. *Arab J Sci Eng* 43(3):1093–1102
15. Peças P, Henriques E (2008) Effect of the powder concentration and dielectric flow in the surface morphology in electrical discharge machining with powder-mixed dielectric (PMD-EDM). *Int J Adv Manuf Technol* 37(11):1120–1132
16. Kumar SS, Uthayakumar M, Kumaran ST, Parameswaran P, Mohandas E (2014) Electrical discharge machining of Al (6351)-5%SiC-10%B₄C hybrid composite: a grey relational approach. *Model Simul Eng* 24
17. Shukla R, Singh D (2017) Selection of parameters for advanced machining processes using firefly algorithm. *Eng Sci Technol, Int J* 20(1):212–221
18. Zavadskas EK, Turskis Z (2010) A new additive ratio assessment (ARAS) method in multicriteria decision-making. *Ukio Technologinis ir Ekonominis Vystymas* 16(2):159–172
19. Özbek A, Erol E (2017) Ranking of factoring companies in accordance with ARAS and COPRAS methods. *Int J Acad Res Account, Financ Manag Sci* 7(2):105–116
20. Nguyen H-T, Siti Zawiah MD, Yusoff N, Achmad PR, Hideki A (2016) An integrated MCDM model for conveyor equipment evaluation and selection in an FMC based on a fuzzy AHP and fuzzy ARAS in the presence of vagueness. *PLoS one* 11(4):e0153222
21. Gopalakannan S (2012) Ph.D. Thesis, Pondicherry Engineering College, Pondicherry, India

Supply Chain Issues and Challenges for Cement Industries of India: A Case Study



Ankur Taak and Ravinder Kumar

Abstract Supply chain management (SCM) has become very important element for modern industry success. SCM integrates the all inbound and outbound activities of a company. Cement industries are the core manufacturing sectors affecting the growth of modern India. The cement industries in India are facing different challenges in modern time of competition. After GST implementation in India, cement industries face many issues and challenges. Supply chain of cement industries has transformed a lot. In this paper, authors have discussed the supply chain issues and challenges of cement industries in India and the impact of GST (Goods and Service Tax) have also been discussed. Old supply chain, modified supply chain, and critical factors like warehousing eliminations and effect on sale of cement are discussed. Authors have studied the supply chain issues and challenges in Indian cement industries in this research paper. SAP–LAP methodology has been applied for case study. Different factors which play a role in current scenario for Indian cement industries have been studied. Different issues and challenges having influence on performance of case organization have been discussed. Reduction in logistics and transportation cost, reduction in time of delivery and reduction in production cost are few main benefits for Indian cement industries in post GST scenario.

Keywords Supply chain management · Cement industry · SAP–LAP · India

1 Introduction

Cement is the most consumable building material after water in the construction industry all over the globe. It is an irreplaceable ingredient for construction. Cement is a mixed product of limestone, shell clay, and iron. In India, there are various cement industries like Ambuja Cements, ACC Cement, etc. Portland is the common type of cement used worldwide these days. As India is a developing country, there is a huge demand for cement in construction and infrastructure areas. On the other hand,

A. Taak · R. Kumar (✉)

Department of Mechanical Engineering, Amity University, Noida 201301, India
e-mail: ravinderkumar.ap@gmail.com

© Springer Nature Singapore Pte Ltd. 2019

K. Shanker et al. (eds.), *Advances in Industrial and Production Engineering*, Lecture Notes in Mechanical Engineering, https://doi.org/10.1007/978-981-13-6412-9_27

297

there are a number of challenges too for Indian cement Industries, i.e., productivity improvement, reduction in production cost, environmental friendly production, and improvement in distribution channel. Noche and Elhasia [1] observed that globalization brings opportunities and challenges to cement industries. Sahu and Sharma [2] studied SCM practices of Indian cement industries. A number of innovative projects and schemes are being run to manage operations in these industries. Jangra [3] stated that major demand for cement in India is from the housing sector. Indian government focused on infrastructure development in 12th five years plan (2012–2017).

2 Methodology

In this research paper, SAP–LAP methodology is adopted for finding out the issues and challenges in XYZ Ltd. There are primary and secondary data that are used to analyze the case study. Primary data is collected by interview of head of supply chain management in case organization for different departments i.e., procurement, sales, R&D, etc. supplier is evaluated on the basis of on-time delivery with right quantity in case organization. Secondary data is learning action on the identified factor which is analyzed by face-to-face interview. Current methodology is very efficient for case studies in cement sector or any other manufacturing sector.

3 Literature Review

Shukla et al. [4] observed that customization of the logistics networks, technical data handling and storage cost are some of the limitations in profit of SC. Busse et al. [5] characterized the topic of sustainability in global supply chain. Gupta et al. [6] stressed on policy formation at government and organizational level which can help in improving sustainability both in design and management of supply chain. Amrina et al. [7] proposed fuzzy criteria for sustainable manufacturing evaluation in cement industry. Compos et al. [8] observed that involvement of all partners of SC can improve the innovation potential in sustainable manufacturing.

3.1 General Issues

Being the second largest producer, India cement industry gives jobs to million peoples. This industry invites investors from local and global market. As a developing economy, India has lot of demand for cement.

Demonetization in India (2016) raised many financial challenges for cement industry such as fall in demand. Many infrastructure projects were stopped. Different government projects focused on infra help in raising demand. Implementation

of GST (Goods and Service Tax) in India also affected the cement industries and its supply chain management. Mahender et al. [9] observed that the cement industry has reduction in expenses after GST. Indian cement sector can take advantages of after GST scenario by concentrating on economical and supply chain management issues by reducing unwanted warehousing.

3.2 Inbound Coordination Issues

In the case association inbound, coordination issues are supply chain cooperation, inviting and handling quotation for raw material, process planning, supplier collection and assessment benchmarks, and customer order and market demand data flow in supply chain management. Case association faces the issues in operation planning. They requisite to make flexibility in supply chain controlling collaboration in supply chain managing. Vertical and horizontal collaboration helps the case organization in process planning. To solve issues of customers, there is need to organize frequent meeting of dealers, distributors and key customers by case organization. Suppliers should be rated and categorized on the basis of their performance.

3.3 Outbound Coordination Issues

Outbound coordination deals with all activities related to the delivery of finished products to customer. Major issues arise after GST in India is change in tax slab related to transport and logistics. Case organization finds it difficult to handle the transportation issues from manufacturing plant to warehouse and retailers. It was very difficult to track the delivery vehicles, and delivery gets delayed by days. To solve this issue, case organization has hired a private player (3PL) for transportation services.

There are some factors are identified which are affected by the GST.

Sale: In post-GST scenario, new tax slab of 28% have affected sale of cement. But in long run the tax reduction on raw materials of cement can help in reduction of cement and sales will improve with time.

Tax collection: In pre GST scenario, most of Indian cement distributors or retailers were not paying sale and Income taxes. There were difference in sale records on-papers and off-papers. In post GST scenario tax collection pattern have changed and impacted sales of cement.

Logistics cost: In post-GST scenario, procedure of paying taxes at entry point of every state has been simplified. New simplified procedure of paying taxes have saved transportation time and costs.

Transport: Before the GST transporters need to be go through out the different check points (Tolls) to reach at warehouses. Due to different taxations in India cement manufacturer are need to make warehouses in different states. But due to GST warehouses are wiped and reduce in tax on transport transportation is easy. Now company need to cement bags to direct distributor of consumer.

Warehouses: In post GST scenario, Supply chain of Indian cement industries have wiped out warehouses. This step has resulted in saving of many charges of warehouses and transportation. In pre-GST scenario cement companies have to maintain warehouses to avoid different taxations rates in different states. Lot of transportation delay was there due to different checkpoints in different states.

Time of delivery: Warehouses and complex transportations cause more time of delivery. GST effects the time of delivery which is reduced because of the elimination of warehouses and easy transport.

Raw material cost: The previous scenario of tax rate on raw material such as limestone, Cole and other cement concretes was high but now it effected by GST this cause into reduction of cost of raw material.

Production cost: One of major contributor in cost of cement is raw material. In post GST scenario change in tax slab of raw materials have reduced its production cost.

Mode of payment: Most of traders, retailers, distributes in cement supply chain were using cash as mode of payment in pre-GST scenario. But in post-GST scenario all payments modes changed to cheque or online payment. Even the payment to workers, staff members were supposed to be online or by cheque.

GST Slab: In post GST scenario rate of tax revised on cement to 28%. This have affected the sale of cement in current trends. In pre GST tax on cement was 24%.

Awareness about GST software: All members of cement supply chain need to learn about new GST tax calculation softwares and different methods of online banking.

Distributors: In pre-GST scenario, members of cement supply chain were not following procedures of filing sale taxes. In post-GST scenario paying tax as per new GST slab have made mandatory for all members of cement supply chain.

3.4 Supply Chain Model

See Fig. 1.

4 Conclusion and Remarks

According to the research findings, cement industry lacks supply chain management. Purpose of this study is to identify the issues and challenges of supply chain

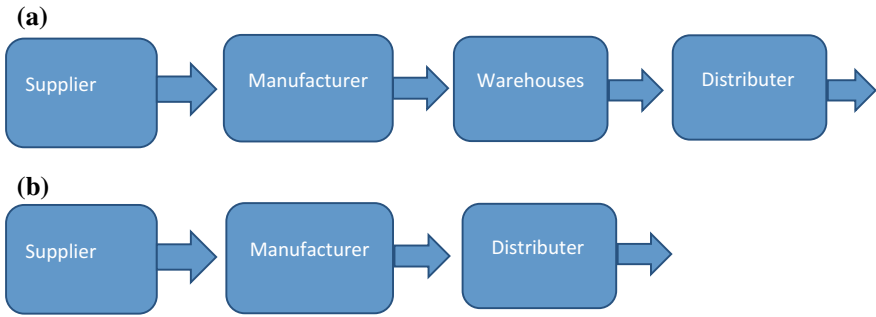


Fig. 1 **a** Supply chain of cement organizations before suggested modifications in India. **b** Supply chain of cement organizations after suggested modifications in India

management in Indian cement industries. Today's cement industries are facing financial problem so more investors are required to invest in this sector. Since cement is a commodity for which after sale services are not required but challenges like competitive pricing and barriers in distribution channel force the cement companies to rethink about their supply chain strategies. Due to 28% GST rate on cement sector, different infrastructure projects got affected. But after working on SCM issues (elimination of warehouses and multiple taxes) in cement sectors its overall cost got reduced. Apart from these, cement sector have option to think about for further investment and improvement in supply chain strategies. A modified supply chain model is given for better understanding supply chain model in cement industries.

References

1. Noche B, Elhasia T (2013) Approach to innovative supply chain strategies in cement industry: analysis and model simulation. In: 2nd international conference on leadership, technology and innovation management. *Procedia Soc Behav Sci* 75:359–369
2. Sharma DG, Sahu GK (2014) Quality in supply chain: a case study of Indian cement industry. *Research gate* V.75.28
3. Jangra A (2014) The back bone of Indian infrastructure. *Int J Sci Res Publ* 4(9):1–5
4. Shukla P, Sharma L (2015) Improvement of logistics and supply chain management in cement industry: a literature review. *Int J Eng Innov Technol* 4(10):104–113
5. Busse C, Schleper MC, Niu M, Wegner S (2016) Supplier development for sustainability: contextual barriers in global supply chains. *Int J Phys Distrib Logist Manag* 46(5):442–468
6. Gupta S, Palsule Desai OD (2011) Sustainable supply chain management: review and research opportunities. *IIMB Manag Rev* 23:234–245
7. Amrina E, Chintia R, Vilsil AL (2016) A fuzzy multi criteria approach for sustainable manufacturing evaluation in cement industry. In: 13th global conference on sustainable manufacturing—decoupling growth from resource use. *Procedia CIRP* 40:619–624

8. Campos JK, Straube F, Wutke S, Cardoso PA (2017) Creating value by sustainable manufacturing and supply chain management practices—a cross-country comparison, 1 Jan 2017. *Procedia Manuf* 8:686–690
9. Mahender P (2017) GST effect on manufacturing industry—India. *Int J Manag Stud Res* 5(1):28–30

Powder Metallurgy Processing and Mechanical Characterization of Iron-Based Composite Reinforced with Alumina and Zirconium Diboride



Bhupendra Prakash Sharma, G. S. Rao and Umesh Kumar Vates

Abstract In the present manufacturing scenario, iron-based metal matrix composites are the key requirement for heavy vehicle and structural applications. But, due to the problem of rapid oxidation during the development of iron-based composites, this field is only limited up to few research level. In the present research work, an easy formation of iron-based metal matrix composite materials are proposed through powder metallurgy process with different mass fractions of zirconium diboride and alumina reinforcement such as 5% Al_2O_3 –10% ZrB_2 , 5% Al_2O_3 –5% ZrB_2 , and 10% Al_2O_3 –10% ZrB_2 , all in the form of atomized particles. Further, microstructural readings on cross section as well as surface of the bar and hardness measurements were attained and investigated. Improved hardness and tensile strength are noted from newly developed performs.

Keywords Composite · Powder metallurgy · Mechanical properties · Microstructural readings

1 Introduction

It is a great challenge to develop proposed metal matrix nanocomposite material having adequate strength and hardness for heavy vehicle application, specifically in chassis which contributes maximum weight fraction as an individual component of any vehicle. Many researchers are striving to develop the metal matrix nanocomposites by using the most suitable fabrication methodology as powder metallurgy (PM) stir casting techniques and techniques [1]. The ferrous-based PM-processed structural parts have already been taken over by the automotive and off-highway vehicle applications due to the fulfillment of desired characteristics of materials from PM process. It is clear that alloy steels are suitable material for various applications such as power plants, aircraft, marine industries, and bearing manufacturing units [2].

B. P. Sharma (✉) · G. S. Rao · U. K. Vates
Department of Mechanical Engineering, Amity University, Noida,
Uttar Pradesh, India
e-mail: bpsharma@amity.edu

The limiting factors in the development of PM-processed specimen are pressing and sintering process. Without any doubt, the tensile strength, hardness, etc., are the most significant factors that depend on production methodology. In the sintered products, generally crack propagates during impact because of available pores act as stress developer [3, 4]. Therefore, fabrication and study of the mechanical behavior of such products under these loads are very important.

Few researches have already reported that strength of PM-processed metal matrix nanocomposite will be improved for the same size of components. A reinforcement of iron carbide, alumina, zirconium diboride, molybdenum carbide, and tungsten carbide also gives the better stiffness in the PM-processed components [5, 6]. It has been given in the literature that tensile, impact, and fatigue characteristics of sintered part are greatly influenced by temperature at which sintering is being conducted and time allowed [7]. The micromechanism of fracture is highly influenced by the matrix [8, 9]. Characteristics of high density sintered material (Fe–4.0Ni–1.5Cu–0.5Mo–0.5C) have already been studied by Moon [10]. It has been reported that the material characteristics vary with temperature and pressure at sintering. Trivedi et al. [11] and Rahimiana et al. [12] evaluated the sintering temperature particle size and sintering time on alloys. In addition, at low particle size, the hardness, yield strength, compressive strength, and elongation to fracture were higher, as compared to coarse particles size of alumina. Archarya [13] studied that the hardness value of iron aluminum by varying composition of iron (0, 10, 20, 25, 30, 35, 40 wt%) increases with Fe content; the best result has been obtained at 40% weight fraction of Fe particles (60% Al). Maximum hardness = 76.90 VHN.

Thus, the present investigation is aimed to improve the strength, stiffness, and desired mechanical properties by using sintered powder metallurgy process in alumina–zirconium diboride nanoparticles reinforcement in Fe matrix through change in its microstructure. Therefore, the strength of the powder metallurgy component such as tensile strength, impact strength, and yield strength is in the range of 66–86% of theoretical value. Hence, a challenge for researchers as improvement in desired mechanical properties of material for the heavy vehicle application may be achieved by applying innovative ways of fabrication methodology of the best suitable contribution of selected particles. XRD and SEM analysis will be done on fabricated Fe–Al₂O₃–ZrB₂ nanocomposites to estimate the improvements in their present characteristics than presently used chassis materials.

It is also a great challenge to adapt the suitable drilling process for newly developed hard, stiff, and high strength nanocomposite (Fe–Al₂O₃–ZrB₂) material. The drilling will be a very important process to create fine holes for chassis assembly in heavy-duty vehicle application which is not possible from conventional drilling process. The low-pressure water jet-assisted laser beam drilling has to be employed for the drilling of Fe–Al₂O₃–ZrB₂ because the present machining process is applicable for hard semiconductor and insulator, whereas many more unconventional machining techniques are reported only for hard and electrically conductive materials. Therefore, the provision of low-pressure water jet assistance may be incorporated with laser beam for proper material removal from semiconducting performs through adequate flushing of the generated debris. Laser power, pulse width, pulse frequency,

drilling speed, pulse duration, assisted water pressure, standoff distance (SOD), nozzle diameter, focal length, etc., are some important controllable process parameters that may be considered in LBD process. The important process measures which could be considered as hole taper, hole circularity, material removal rate (MRR), surface finish, HAZ, recast layer, aspect ratio and spatter formation, etc. [14, 15].

It is evident that mass of the chassis or parts may be further reduced by introducing such Fe-based metal matrix composite. PM technique is also important which need to be adopted for fabrication of such newly proposed nanocomposite which improves the hardness and the tensile strength as well.

2 Material and Design

Uniformly mixed compositions of metal matrix nanocomposite were compacted up to 1 MN using a suitable die-set assembly on a 7 MN capacity hydraulic press. Compacted performs were manually coated with the paste of concentrated acetone-alumina mixture to save with oxidation during sintering process. After drying at 300 °C for 2 h in a muffle furnace, sintering operation was carried out in an electric furnace at the temperature of 1200 °C for a holding period of 1 h. Cylindrical compacted performs having 22 mm of diameters were fabricated using PM technique. Hardness and tensile strength were tested in the strength of material lab at Amity University, Noida. Standard ASTM guidelines were followed to conduct the aforesaid mechanical testing.

The above specimens were prepared using compacting of the constituent powders in the appropriate die-punch arrangement having 22 mm of diameters. Powders of the entire constituent were weighted separately and mixed well. It is heated at 300 °C for 2 h to dry and then compressed by applying 1 MN force for compacting. All the specimens were sintered at 1200 °C for 1 h. Figure 1 shows the different compositions of the elements which have been fabricated under the same pressure of powder metallurgy process. In this experiment, three specimen 5% Al₂O₃-5% ZrB₂, 5% Al₂O₃-10% ZrB₂, 10% Al₂O₃-10% ZrB₂ with Fe have been fabricated using nanoparticles of ZrB₂. Nanoparticle of one component is being used to fill the intermolecular spacing which provides the more bond strength.

Microstructure of the 10% Al₂O₃-10% ZrB₂ with Fe composite is shown in Fig. 2. It is evident that the nano particles of ZrB₂ filling the intermolecular spacing to make the material comparatively very hard.

Figure 3 shows the influence and percentage contribution of Al₂O₃-ZrB₂ in Fe on the hardness of the plain matrix alloy and produced composites. It has been noticed that hardness increases with the increase in ZrB₂ along with Al₂O₃ particles, and it is significantly higher than the hardness of the plain Fe as given in specimen number '0'. It is evident that hardness of 5% Al₂O₃-5% ZrB₂ newly composite is greater than the 99.2% pure Fe powder processed through PM as trial 1. Similarly, trial 2 and trial 3 have been performed on 5% Al₂O₃-10% ZrB₂ and 10% Al₂O₃-10% ZrB₂,

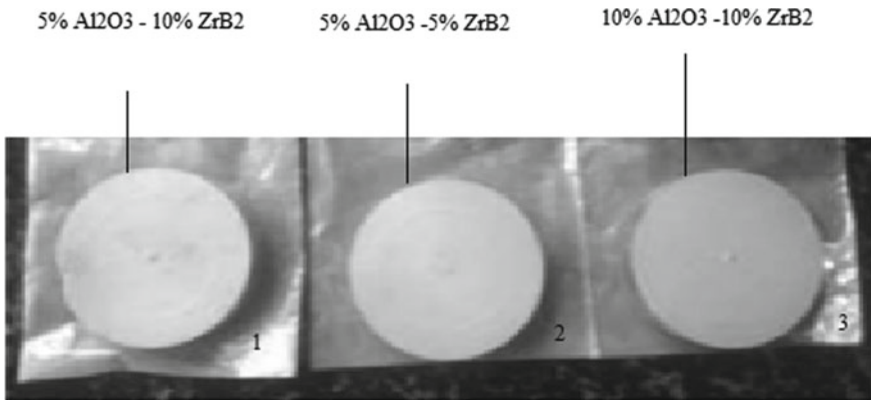


Fig. 1 Different compositions of Al_2O_3 and ZrB_2 in Fe

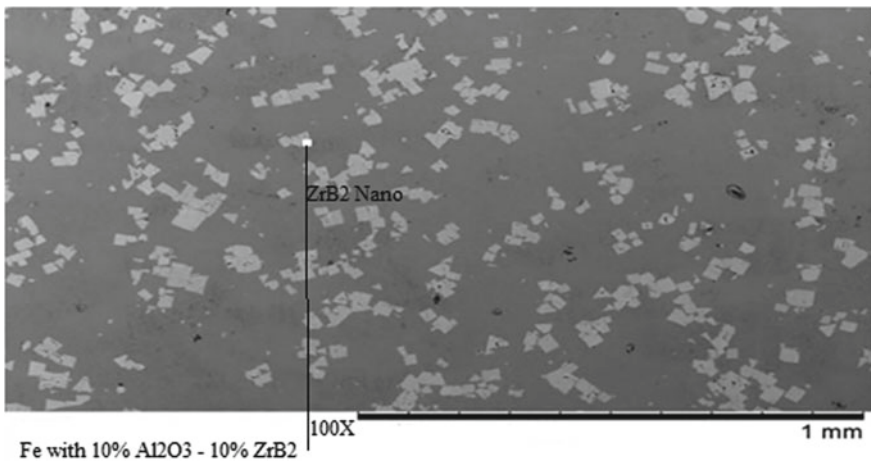


Fig. 2 Microstructure of powdered metallurgy Fe with 10% Al_2O_3 -10% ZrB_2

respectively, for the estimation of hardness. It is cleared that hardness of the present composite 10% Al_2O_3 -10% ZrB_2 is highest as trial 3.

The influence and percentage contribution of Al_2O_3 - ZrB_2 in Fe on the tensile strength is reported in Fig. 4. It has been noticed that tensile strength increases with the increase in the percentage of ZrB_2 along with Al_2O_3 particles, and it is significantly higher than the tensile strength of the plain Fe as given in specimen number '0'. It is evident that the tensile strength of 5% Al_2O_3 -5% ZrB_2 reinforced newly formed composite material is greater than that of the 99.2% pure Fe powder processed through PM as in trial 1. Similarly, trial 2 and trial 3 have been performed on 5% Al_2O_3 -10% ZrB_2 and 10% Al_2O_3 -10% ZrB_2 respectively for the estimation of tensile strength. It is cleared that hardness of the present composite 10% Al_2O_3 -10% ZrB_2 is highest as trial 3.

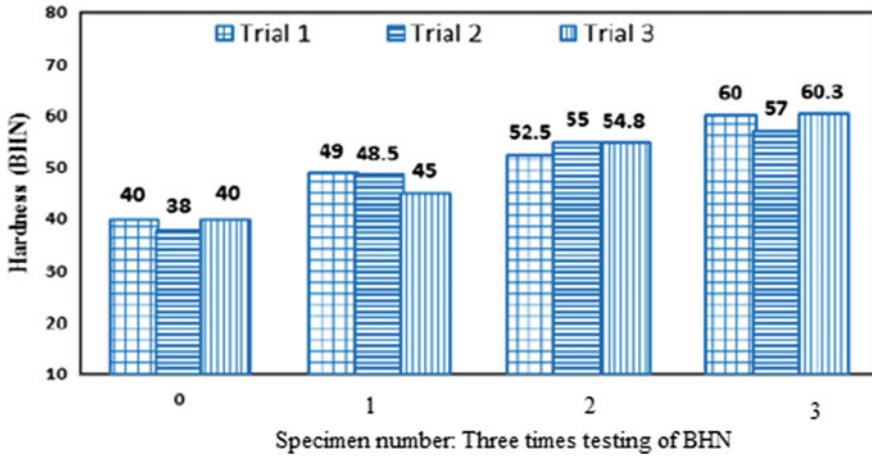


Fig. 3 Hardness of powdered metallurgy-processed specimen

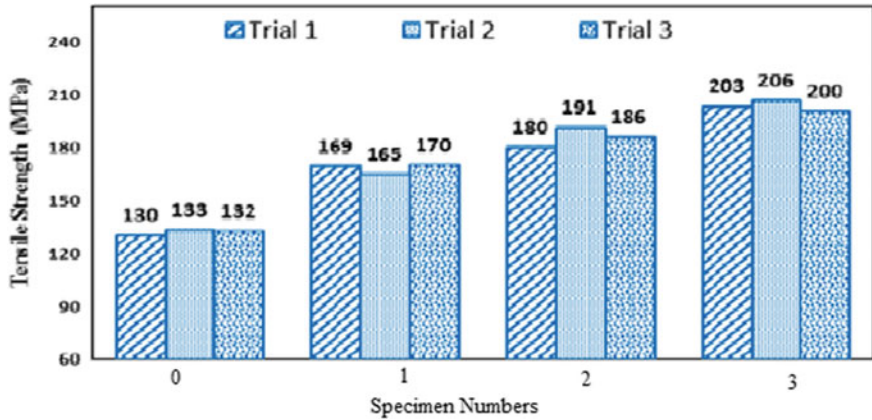


Fig. 4 Tensile strength of powdered metallurgy-processed specimen

3 Conclusion

Powder metallurgy has been found the most appropriate method for fabrication of nanometal matrix composite of such hardest material. As per the ASTM standard, the specimens were fabricated to conduct the hardness and tensile strength test. 10% Al_2O_3 -10% ZrB_2 with Fe is the best suitable combination to give the highest tensile strength as well as the high hardness among the four specimens. It is also evident that volume of the third specimen is comparatively low compared to others. It may be suggested that such newly developed metal matrix composite may be used for heavy vehicles application, which can wear more loads with compact in size.

References

1. Abouelmagd G (2004) Hot deformation and wear resistance of P/M aluminium metal matrix composites. *J Mater Process Technol* 155:1395–401
2. James WB, West GT (2002) Powder metal technologies and application. In: ASM hand-book. ASM International, USA
3. Narayan S, Rajeshkannan A (2010) Densification behavior informing of sintered iron-0.35% carbon powder metallurgy preform during cold upsetting. *Mater Des* 32:1008–1013
4. Shanmugasundaram D, Chandramouli R (2009) Tensile and impact behavior of sinter-forged Cr, Ni and Mo alloyed powder metallurgy steels. *Mater Des* 30:344–49
5. Danninger H, Jangg G, Weiss B, Stickler R (1993) Microstructure and mechanical properties of sintered iron. Part II: experimental study. *Powder Metall Int* 25:170–223
6. Danninger H, Jangg G, Weiss B, Stickler R (1993) Microstructure and mechanical properties of sintered iron. Part I: basic considerations and review of literature. *Powder Metall Int* 25:11–17
7. D'Armas H, Llanes L, Penafiel J, Bas J, Anglada M (2000) Tempering effects on the tensile response and fatigue life behavior of a sinter hardened steel. *Mater Sci Eng A* 277:291–296
8. Straffelini G, Molinari A, Danninger H (1992) Impact notch toughness of high strength porous steels. *Mater Sci Eng A* 272:300–309
9. Butuc MC, Gracio JJ, Rocha BA (2006) An experimental and theoretical analysis on the application of stress-based forming limit criterion. *Int J Mech Sci* 48:414–429
10. Moon JR (2002) Toughness and growth of fatigue cracks in P/M steels. *Powder Metall Prog* 2:63–80
11. Trivedi S, Mehta Y, Chandra K, Mishra PS (2010) Effect of chromium on the mechanical properties of powder-processed Fe–0.45 wt.% P alloys. *J Mater Process Technol* 210:85–90
12. Rahimiana M, Ehsania N, Parvin N, Baharvandic H (2009) The effect of particle size, sintering temperature and sintering time on the properties of Al–Al₂O₃ composites, made by powder metallurgy. *J Mater Process Technol* 209:5387–5393
13. Acharya A (2017) Fabrication and evaluation of various properties of iron-aluminium metal based composites. *IJSRD Int J Sci Res Dev* 5(3)
14. Hwang SS, Vasiliev AL, Pature NP (2007) Improved processing and oxidation-resistance of ZrB₂ ultra-high temperature ceramics containing SiC nano dispersoids. *Mater Sci Eng* 464:216–24
15. Telle R, Sigl LS, Takagi K (2000) Boride-based hard materials. In: Riedel R (ed) *Handbook of ceramic hard materials*. Wiley-VCH 2, Weinheim, Germany, pp 802–945

Challenges for Effective and Efficient Supply Chain Management for Fast Moving Electrical Goods (FMEG): A Case Study



Ravinder Kumar and Ankur Taak

Abstract Fast Moving Electrical Goods (FMEG) industries are among the most dynamic industry these days. Short product life cycle, intricate supply chain, unpredictable demand, tight profit margins are major challenges for FMEG industries. Scarcity of raw material, unpredictable delay in transportation from foreign suppliers, non-availability of affordable skilled labor, changing customer demand have completely transformed the electric goods industries. Increasing demand for good-quality low-cost products is giving abundant opportunities of growth to FMEG industries if they manage issues and challenges of supply chain management (SCM). In this research paper, authors have studied the issues and challenges of FMEG supply chain using situation actor process–learning action performance (SAP–LAP) methodology. Authors have observed that Indian FMEG are facing challenges like supply chain collaboration (outsourcing of non-core operations, vertically integrating core competencies), retail integration, supply risk management (natural, terrorism, demand and supply), supply chain planning (demand-driven supply chains), reverse logistic, sustainability, and green supply chain and digital supply chain.

Keywords Supply chain management · Fast Moving Electrical Goods · Opportunities and challenges

1 Introduction

Fast moving electrical goods industry is a dynamic industry in global competition. Fast moving electrical goods have large application in commercial and residential places. Life cycle of FMEG products is very short, and for existence FMEG industries need to continuously focus on innovation and design change. To reduce fluctuation in demand, these industries need to continuously study consumer behavior in relation to communication, entertainment, lifestyle, and change in organizing their lives. Fast moving electrical goods industry is the backbone of any country to grow in national

R. Kumar (✉) · A. Taak
Department of Mechanical & Automation, Amity University, Noida 201303, India
e-mail: ravinderkumar.ap@gmail.com

© Springer Nature Singapore Pte Ltd. 2019
K. Shanker et al. (eds.), *Advances in Industrial and Production Engineering*, Lecture Notes in Mechanical Engineering, https://doi.org/10.1007/978-981-13-6412-9_29

economics. FMEG industries are facing many challenges and issues in managing the supply chain network. These industries need strategic planning while handling key issues of SCM. Birhanu et al. [1] observed that supply chain strategies can help in improving competitiveness of industries. Supply chain strategy is used to show competitiveness and position in the market against the competitor.

2 Literature Review

International supply chain develops multifaceted due to fast growth of number of vigorous interaction which must be handled. FMEG industries are categorized by short product life cycle, discerned product, and nonlinearly in engineering process. These industries are also facing a volatile market due to unpredicted demand of customers. Al-Shboul et al. [2] discussed the seven dimensions (strategic supplier partnership, level of data allocation, consumer facility administration, internal lean practices, deferment, and total quality management) of supply chain management (SCM) practices. SCM practices have a positive effect on supply chain performance. Bala and Kumar [3] developed a framework of growth and flexibility in the supply chains. Battezzati and Mangnani [4] analyzed the supply chain of FMEG and the durables goods in Italy and discussed the manufacturing postponement and general lack of scale economic methods. Cunningham and Dale [5] investigated the effect of delivery performance of suppliers on the company's own delivery assurance and reputation. Forgionne and Guo [6] observed that information sharing between supply chain members improves performance of supply chain. Gorane and Kant [7] observed that organization can gain the keenness by rising the efficiency of manufacturing operations and fulfilling the changing need of customer and employees.

3 Methodology

Case study has been prepared by collecting data from primary and secondary sources. Primary data information has been collected, mainly through face-to-face interview with supply chain management department manager in case organization which is located at NCR of Delhi. Secondary data has been developed from the literature review of published resource and Web site of organization. As requested by the company, to maintain the confidentiality of information the name of the company is not revealed in this research paper. Aim of this research paper is to find out the challenges for effective and efficient supply chain management for Fast Moving Electrical Goods using sap-lap methodology. These interfaces are situation (S), actors (A), process (P). The situation represents the present condition and environment of a case organization. LAP is devised in three components. Learning issues represent from (L), action recommended (A), and estimated enhancement in performance in (P). The purposed model not only discussed the challenges in SCM of FMEG industry

but also examined how to deal with the challenges and flexible supply chain management.

4 Profile for Case Organization

XYZ Ltd. one of the leading Fast Moving Electrical Goods corporations in India was established in 1983. The case organization earned all these 28 years to acquire a distinctive identity for its brand as well as company name. Case organization is located in NCR of Delhi. The firm has product ranging from home and kitchen appliances, lighting from domestic, LED lights, switchgears, commercial and industrial application, fans, domestic circuit protection switchgear, home cables and wires, orientation motor, and capacitor among others. Case organization owns some of the most prestigious Indian brands like Havells, LLOYD, Crabtree, Standard Electric, and Promtest. XYZ Ltd. has 23 represented offices with over 6000 specialists in over 50 countries. In India, the company has 11 manufacturing plants located in Haridwar, Baddi, Noida, Faridabad, Bengaluru, and Ghaziabad. The plant located at city Ghaziabad is established in 2009 and have 250 employees with total area covered of 120,000 square feet. The plant is state of the art of low-voltage power capacitor. Manufacturing products are industrial switchgear—ACBs, MCCB, load bank, capacitor CFL component. The company has different plants with different manufacturing units at different locations in NCR of Delhi. The following are driven factors for case organization to become one of the largest companies in the world.

- Ecosphere's better quality
- Good supply chain network
- Delivery on time with right quantity
- Industrial innovation
- High professionalism
- Solution provides capability
- Exceedingly inspired and knowledgeable and innovated manpower
- Supports of mobile service provider
- Brilliant training in maintenance
- Give huge offers to customers
- Replacement of product
- Good relationship with all the members of supply chain management and customers.

4.1 Inbound Coordination Issues

These days, FMEG industry is most dynamic and fast growing. To maintain the delivery of right quantity, at right time requires efficient supply chain management.

The superiority of products depends on quality of raw material. Suppliers supply raw material as per the order placed by case organization. Implementation of supply chain management is always challenging. Coordination issues of SCM are divided into inbound coordination issues and outbound coordination issues. The inbound coordination issues deal with handling quotations for raw material, supplier selection and evaluation parameters, customer orders, preparation according to market demand and data sharing. Complete procurement operations are called inbound logistics. All orders are based on demand of customers and market scenario.

4.2 Outbound Coordination Issues

In outbound synchronization, altered activities correlated with customer/buyer demand are matched. There are different activities involved in outbound coordination such as order management finished good inventory, production at low economic order quantity, forecasting and replacement, risk management, wrapping and handling and conveyance.

5 Conclusion Remarks

Today's fast moving electrical goods (FMEG) industry is facing many challenges in their supply chain management. In this research paper, challenging factors are identified on the basis of the literature review which is shown above. SAP-LAP methodology is adopted to study the challenges of SCM, by personnel interview of different department heads of case organization. Due to fast-changing global market, supply chain becomes complex and need of flexibility of supply chain arises. Short product life cycle, intricate supply chain, unpredictable demand, tight profit margins are major challenges for FMEG industries. Scarcity of raw material, unpredictable delay in transportation from foreign suppliers, non-availability of affordable skilled labor, changing customers' demand have completely transformed the fast moving electrical goods industry. Customer demands for good-quality, cost-effective products give abundant opportunities for fast growth of FMEG industries.

- Case organization needs to form inventory management policy.
- Less use of modern IT and communication tools has high impact on supply chain management in case organization.
- Case organization evaluates the suppliers on the basis of parameters like worth and delivery of quality products, but some other parameters like distribution lead time, ability to serve in alternative, ability to produce in small batch size should be involved and supply rating/evaluation matrix should be designed.
- Government policies have high impact on FMEG industry.

This work helps in guiding the FMEG industries and will solve various issues coming while developing new supply chain strategies.

References

1. Birhanu D, Lanka K, Rao Neelakanterwara A (2014) A survey of classification in supply chain strategies. In: 12th global congress on manufacturing and management. *Procedia Eng* 97:2289–2297
2. Al-Shboul MD, Barber KD, Garza-Reyes JA, Kumar V, Abdi MR (2017) The effect of supply chain management practices on supply chain and manufacturing firms' performance. *J Manuf Technol Manag* 28(5):577–609
3. Bala M, Kumar D (1933) Supply chain performance attributes for the fast moving consumer goods industry. *Adv Logist Syst* 1
4. Basttezzati L, Magnani R (2000) Supply chains for FMCG and industrial products in Italy: practices and the advantages of postponement. *Int J Phys Distrib Logist Manag* 30(5):413–424
5. Chunningham MT, Dale BG (1983) The effects of supplier delivery reliability on company delivery assurance. *Int J Oper Prod Manag* 3(1):50–62
6. Forgionne G, Guo Z (2009) Internal supply chain coordination in the electric utility industry. *Int J Oper Prod Manag* 196(1):614–627
7. Gorane S, Kant R (2016) Supply chain practice—an implementation status in Indian manufacturing organization. *Benchmarking Int J* 23(5):1–53

Investigation of Titanium as Thin Film Deposited Material Thereon Effect on Mechanical Properties



Gaurav Gupta and R. K. Tyagi

Abstract In this article state of art of research on thin film deposition and their interaction with bulk material, along with morphological changes and their behaviour under different loading conditions are analysed, and hence, performances are reviewed. Researchers have put significant efforts to predict changes in structural property and their influences on performances of these coatings. These coatings can exhibit adaptive and chameleon kind attributes. The physical and structural properties of the element used for coating had relationship between amorphisation, chemical structure, chemical properties and thus altering performance of coated sample. Here, we selected mechanical properties as an indicator of performance measure. Material's microstructure, elastic modulus, hardness, roughness, lattice parameters, etc. as a function of the deposition might be examined by SEM, TEM, XRD, EDS, AFM, etc. and analysed by tribological applications, nanomechanical measurements, nanoindentation, wear behaviour and microabrasion. For tribological applications of materials; hardness and elastic modulus plays a significant role and mechanical properties of coated thin films is measured by nanoindentation, nanomechanical measurements. Here, a critical examination and review of theoretical and experimental frameworks are presented for better understanding of mechanical properties and metallurgical characteristics.

Keywords Thin film · Nanocoating · Mechanical property · Wear property · PVD · CVD

1 Introduction

With the advent of newer material, newer technologies and methods, enhanced life cycle of continuous mating and load-bearing parts, a greater emphasis in recent years have been on thin film development henceforth in its characterization investigating into material and surface properties especially at nanoscale.

G. Gupta (✉) · R. K. Tyagi

Mechanical Engineering Department, Amity University Uttar Pradesh, Noida, Uttar Pradesh, India
e-mail: 15.gaurav@gmail.com

© Springer Nature Singapore Pte Ltd. 2019

K. Shanker et al. (eds.), *Advances in Industrial and Production Engineering*, Lecture Notes in Mechanical Engineering, https://doi.org/10.1007/978-981-13-6412-9_30

315

There exists few studies in last decade representing facts on wear, mechanical properties and coefficient of friction at different environment (such as temperature and corrosion), for which a critical examination and review of theoretical and experimental frameworks are presented for better understanding of mechanical properties and metallurgical characteristics. Thin films deposited by various techniques such as PVD, CVD exhibits excellent potential to suit variety of technically challenging environments.

Different coating techniques find its usefulness in vast applications which can be broadly categorized as per their functionality such as mechanical, electrical, optical, chemical, medical, decorative, etc. [1]. Various deposition techniques are employed these days such as physical vapour deposition consisting evaporation and sputtering techniques and chemical vapour deposition consisting of thermal growth and polymerization techniques.

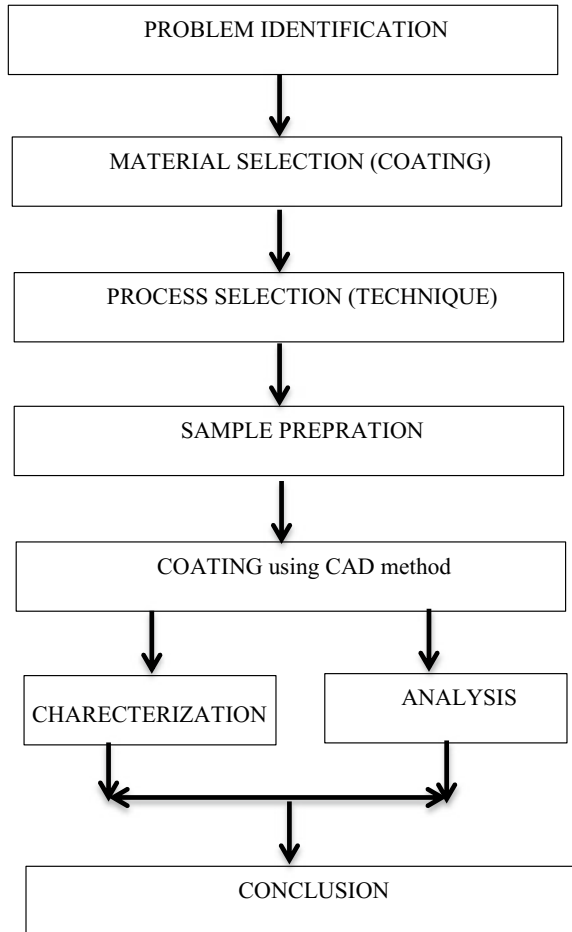
Coatings specially in the form of nanoparticles are finding its place in our day-to-day life in all range of products from food to all kind of FMCG products around 1600+ products are recognized as products infused with some sort of nanocoatings [2] thus this is an emerging science finding attention from all disciplines be it people from physics, chemistry, biology, material scientists, medical professionals and space industry [3, 4]. A more in-depth knowledge of nanotechnology and nanomachining along with techniques of smoothing is required for better understanding of friction and wear [5]. Variety of materials are used in numerous fields among that titanium, silicon and zinc are the most extensively used nanomaterials also in the form of thin film coatings commercially used at mass level. Among these Ti is most versatile material employed for numerous mechanical applications due to its properties but has certain limitation hence oxides, nitrides and some alloying elements are infused to overcome the problem. Ti and its nitrides in combination of constituting elements such as Al, Si and Cr present fair performance under the influence of extreme conditions [6–9]. Lot of efforts are made to produce Ti-based thin film which is adaptive in nature such as self-healing, antibacterial properties along with other properties such as antifogging [10, 11].

Due to limitations of manufacturing specially subtractive asperity present at the surface of tool, die, mating parts, moving parts acts as a wedge sliding on a surface hence increases friction henceforth wear and effect other mechanical properties [12]. To overcome this PVD and CVD techniques of coatings are employed which produces better results than obtained by conventional methods by forming layers of small grain sizes which essentially consist of usually two phases amorphous and monocrystalline phase.

2 Methodology

Based on problem and literature, survey selection of material to be deposited is taken and further the technique for coating is selected which shall fulfil the requirement. Here, basically vacuum coating processes are analysed which is further classified

Fig. 1 Work process flow for thin film coatings



broadly as physical vapour deposition (PVD) and chemical vapour deposition (CVD) which are further characterized as evaporation, sputtering and polymerization, thermal growth techniques. Figure 1 shows sequence of work process flow adopted by researchers to enhance properties as desired by thin film surface coatings.

2.1 Titanium Coating

For industrial applications, titanium coatings are intensively investigated and analysed which are formed in the form of single layer or multilayer which due to its good mechanical and wear resistance properties makes it a suitable candidate for providing

coating over cutting tools and mating parts but Ti oxidizes rapidly at higher temperatures for which combination materials are employed to counteract shortcomings [12, 13].

2.2 Morphology of Coatings

Scanning Electron Microscopy (SEM)

Solids surface imagined by using electron beam in the form of primary and secondary electrons where a beam of electrons known as primary electrons are directed towards sample which on interacting get scattered are some are sent back in the form of secondary electrons which are utilized to imagine surface of solid. Bonding between substrate and coating materials can also be analysed by SEM image Fig. 2. Gross et al. [14] had grown Ti films on a low-temperature growth environment on a stainless steel substrate where in the presence of nitrogen highly polycrystalline films are obtained, it is of significance that morphology of films obtained under varying process parameters remains same. Heterogeneous size of grains is present. Ti film shows gap among clusters of cauliflower-like structure which is found similar to what was stated by other researchers with an average particle size of 200 nm [15].

Demas et al. deposited TiN, TiAlN and CrN on steel substrate to determine thin film hardness, elastic modulus, surface morphology and effect of these on nanomechanical properties. Which shows the presence of unreactive Ti macro particles, in the morphology of a coated substrate. With the significant reduction in surface roughness of coated substrate from 124 nm RMS to 60 nm RMS [16].

Atomic Force Microscopy (AFM)

Surface roughness is lower during coating process/during thin film growth. AFM measurements Fig. 3 are performed using a cantilever—whose material is nonconductive or conductive with a fixed arm length and arm width usually in μm with some fixed spring constant having round tip at an angle and radius operating under some resonance prefixed frequency. AFM had major limitation of repeatability [17].

Georgiadis et al. [18] obtained films on H13 hot work steel where a common microstructure is visible where a dense microstructure in the form of microcolumns in perpendicular direction is found with increase in nitriding processes time it is found as increase in thickness of diffusion layer. AFM image indicates waviness of surface texture which is associated with roughness it is noted that lower values of sputter coated thin films this roughness is usually moderated due to reduction in grain size, though deposition time may affect coarseness of grain. Fu et al. showed that deposition of TiN on TiNi does not changes surface morphology roughness value obtained around 40 nm with average grain size of 300–400 nm with presence of oxide layer and carbon diffusion layer of 20 and 5 nm, respectively [19].

X-Ray Diffraction (XRD)

Zhang et al. [15] show a preferred orientation (0 0 2) in pure Ti film which also

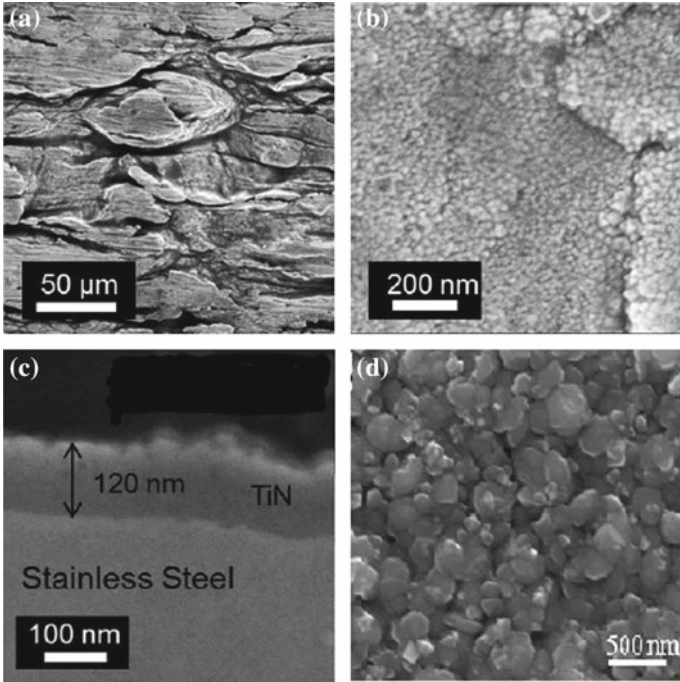
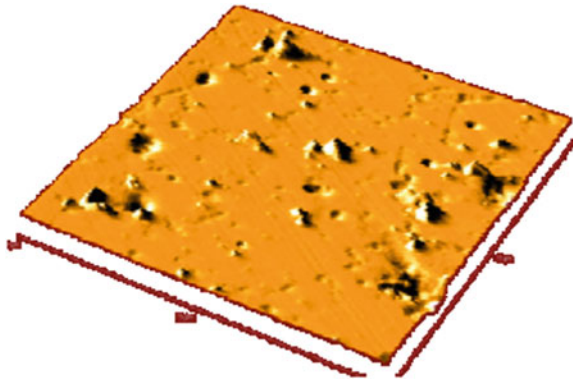


Fig. 2 SEM view of a Ti sample observed at a different magnification

Fig. 3 Three dimensional AFM images showing surface roughness of sample



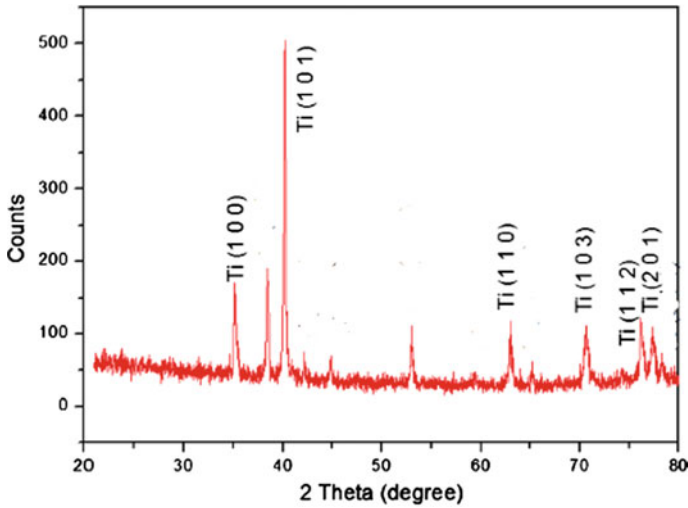


Fig. 4 XRD pattern of the TiN coated sample

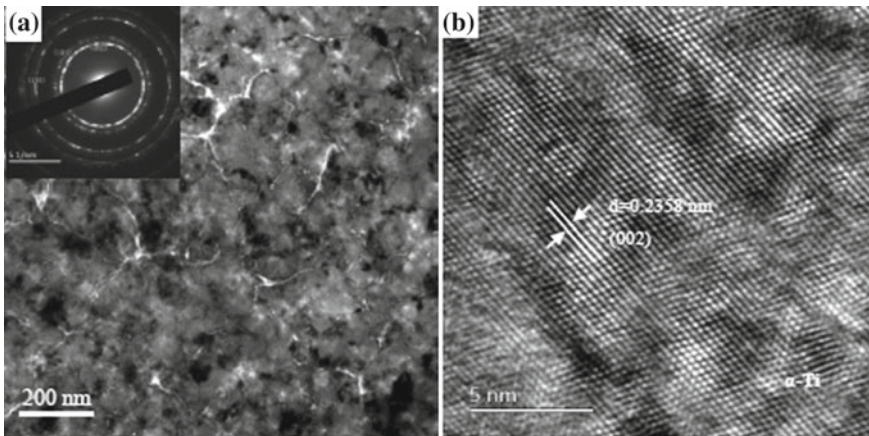


Fig. 5 TEM morphology of Ti coated sample

exhibited hexagonal closed packed (hcp) structure as is obvious from Fig. 4. Rebholz et al. [20] observed that α lattice with increase in carbon content expands there are deformation and expansion of lattice as is suggested by peak position and intensity changes in α (1 0 0).

XRD pattern of the Ti-6Al-4V-2B₄C coated AISI 1040 steel [21] coatings does not show any peak oxide in XRD whereas wider peaks is due to orientation, randomness and size of particles present at nanoscale exhibiting peak at 35.1°, 40.25°, 62.87°, 71°, 77° with orientation (1 0 0), (1 0 1), (1 1 0), (1 0 3), (1 1 2) also suggesting absence of intermetallic layer. Fu et al. [19] observed a gradual phase change

from martensite to austenite during XRD analysis at gradual elevated temperatures; at room temperature, it is dominated by presence of martensite.

Transmission Electron Microscopy (TEM)

TEM images (Fig. 5) confirm reported studies by others where clear crystallinity with equiax grain is present in pure Ti film. α and β polycrystalline structure are present in thin film [15].

Increased presence of carbon during sputtering process enhances densification of coated material [22]. Formation of coatings which are at nanolevel had shown significant improvement in mechanical properties [23, 24].

3 Conclusion

Above study presents utility of thin film deposition of titanium on a suitable bulk material using some suitable technique introduces significant changes which can be controlled as per desire. For achieving desired results, deposition parameters play an important role. The deposition parameters of layer to be deposited have significant effect on structural morphology and therefore reflected while measuring mechanical properties such as hardness, surface roughness, elasticity, etc. which is an interactive result of structure and composition of topmost layer affecting behaviour during tribological test, corrosion test, etc.

Deposited thin film has shown a significant increase in hardness and elastic modulus up to 6.8 and 77 GPa, respectively.

SEM images have confirmed presence of heterogeneous grain forming a polycrystalline layer in presence of nitrogen with significant reduction in surface roughness of coated substrate 124–60 nm RMS but also had shown gap among clusters.

AFM image indicates roughness value with presence of oxide layer up to 20 nm and carbon diffusion layer 5 nm with average grain size of 300–400 nm. Waviness associated with roughness is prominently noted.

Profile studies signify thin layer residing on top of substrate present up to few nanometres. This thin film on the top significantly improves load bearing, wear and friction resistance.

XRD shows any peak oxide in XRD whereas wider peaks is due to orientation, randomness and size of particles present at nanoscale exhibiting peak at 35.1° , 40.25° , 62.87° , 71° , 77° with orientation (1 0 0), (1 0 1), (1 1 0), (1 0 3), (1 1 2) also suggesting absence of intermetallic layer.

To have enhanced properties, most importantly mechanical, electrical and magnetic, it is very much necessary to have selection of a controlled process by virtue of which lattice structure, grain size, crystallographic orientation and shape can be controlled.

References

1. Bunshah RF (1994) Handbook of deposition technologies for films and coatings: science, technology and applications, 2nd edn. Noyes Publications, Park Ridge, N.J.
2. Vance ME, Kuiken T, Vejerano EP, McGinnis SP, Hochella MF Jr, Rejeski D, Hull MS (2015) Nanotechnology in the real world: redeveloping the nanomaterial consumer products inventory. Beilstein J Nanotechnol 6:1769–1780. <https://doi.org/10.3762/bjnano.6.181>. eCollection (2015)
3. Saini R, Saini S, Sharma S (2010) Nanotechnology: the future medicine. J Cutan Aesthetic Surg 3(1):32–33. <https://doi.org/10.4103/0974-2077.63301>
4. Suc TG, Umarjee DM, Prakash S, Bunshah RF (1991) Surf Coat Technol 13:199
5. Zhang L, Tanaka H (1997) Towards a deeper understanding of wear and friction on the atomic scale—a molecular dynamics analysis. Wear 211(1):44–53. [https://doi.org/10.1016/S0043-1648\(97\)00073-2](https://doi.org/10.1016/S0043-1648(97)00073-2)
6. Fox-Rabinovich GS, Endrino JL, Beake BD, Kovalev AI, Veldhuis SC, Ning L, Fontaine F, Gray A (2006) Impact of annealing on microstructure, properties and cutting performance of an AlTiN coating. Surf Coat Technol 201(6):3524–3529. <https://doi.org/10.1016/j.surfcoat.2006.08.075>
7. Birol Y, Yuksel B (2012) Performance of gas nitrided and AlTiN coated AISI H13 hot work tool steel in aluminium extrusion. Surf Coat Technol 207:461–466. <https://doi.org/10.1016/j.surfcoat.2012.07.051>
8. Ribeiro E, Rebouta L, Carvalho S, Vaz F, Fuentes GG, Rodriguez R, Zazpe M, Alves E, Goudeau P, Rivière JP (2004) Characterization of hard DC-sputtered Si-based TiN coatings: the effect of composition and ion bombardment. Surf Coat Technol 188–189:351–357. <https://doi.org/10.1016/j.surfcoat.2004.08.020>
9. Endrino JL, Fox-Rabinovich GS, Gey C (2006) Hard AlTiN, AlCrN PVD coatings for machining of austenitic stainless steel. Surf Coat Technol 200(24):6840–6845. <https://doi.org/10.1016/j.surfcoat.2005.10.030>
10. Herman JM, Disdier J, Pichat P (1984) Chem Phys Lett 108:618
11. Asahi R, Morikawa T, Ohawaki T, Aoki K, Taga Y (2001) Science 293:269
12. Torrance AA, Galligan J, Liraut G (1997) A model of the friction of a smooth hard surface sliding over a softer one. Wear 212(2):213–220. [https://doi.org/10.1016/S0043-1648\(97\)00150-6](https://doi.org/10.1016/S0043-1648(97)00150-6)
13. Bhushan B (2011) Nanotribology and nanomechanics, 3rd edn, vol I, II. Springer, Heidelberg, Germany
14. Grosso S, Latu-Romain L, Berthomé G, Renou G, Le Coz T, Mantel M (2017) Titanium and titanium nitride thin films grown by dc reactive magnetron sputtering physical vapor deposition in a continuous mode on stainless steel wires: chemical, morphological and structural investigations. Surf Coat Technol 324. <https://doi.org/10.1016/j.surfcoat.2017.05.089>
15. Zhang F, Li C, Yan M, He J, Yang Y, Yin F (2017) Microstructure and nanomechanical properties of co-deposited Ti-Cr films prepared by magnetron sputtering. Surf Coat Technol 325. <https://doi.org/10.1016/j.surfcoat.2017.07.005>
16. Demas N, Lorenzo-Martin C, Ajayi O, Erck R, Shareef I (2016) Measurement of thin-film coating hardness in the presence of contamination and roughness: implications for tribology. Metall Mater Trans A 47A. <https://doi.org/10.1007/s11661-016-3342-9>
17. Alam S, Ifan M, Soomro BD, Shahid M, Zeeshan M (2013) Optimization of loading factor of nanocomposite coatings deposited by physical vapor deposition. In: 6th vacuum and surface sciences conference of Asia and Australia (VASSCAA-6). J Phys Conf Ser 439:012016. <https://doi.org/10.1088/1742-6596/439/1/012016>
18. Georgiadis A, Fuentes GG, Almandoz E, Medrano A, Fernandez Palacio J, Miguel A (2017) Characterisation of cathodic arc evaporated CrTiAlN coatings: tribological response at room temperature and at 400 °C. Mater Chem Phys 190. <https://doi.org/10.1016/j.matchemphys.2017.01.021>

19. Fu YQ, Du H, Zhang S (2003) Deposition of TiN layer on TiNi thin films to improve surface properties. *Surf Coat Technol* 167:129–136. [https://doi.org/10.1016/s0257-8972\(02\)00898-8](https://doi.org/10.1016/s0257-8972(02)00898-8)
20. Rebolz C, Schneider JM, Leyland A, Matthews A (1999) Wear behaviour of carbon-containing tungsten coatings prepared by reactive magnetron sputtering. *Surf Coat Technol* 112(1–3):85–90. [https://doi.org/10.1016/S0257-8972\(98\)00786-5](https://doi.org/10.1016/S0257-8972(98)00786-5)
21. Selvakumar N, Malkiya Rasalin Prince R (2017) Microstructure, surface topography and sliding wear behaviour of titanium based coating on AISI 1040 steel by magnetron sputtering. *Arch Civ Mech Eng* 17(2):281–292. <https://doi.org/10.1016/j.acme.10.005> (2016)
22. Roy M (ed) (2013) *Surface engineering for enhanced performance against wear*. Springer, Vienna, Austria
23. Veprek S, Argon AS (2002) Towards the understanding of mechanical properties of super- and ultrahard nanocomposites. *J Vac Sci Technol B* 20(2):650–664. <https://doi.org/10.1116/1.1459722>
24. Patscheider J (2003) Nanocomposite hard coatings for wear protection. *MRS Bull* 28(3):180–183. <https://doi.org/10.1557/mrs2003.59>

Modeling the Metrics of Human Resource, Time, and Asset Level Barriers in the Implementation of Lean Manufacturing Using an Analytical Network Process Approach



Bhupendra Prakash Sharma, A. Chauhan, H. Singh, Umesh Kumar Vates and G. S. Rao

Abstract A philosophy, that describes an integration of advanced tools and techniques into the production layout of any industry for optimizing human resources, time, assets, and hence overall productivity, termed as ‘lean’ in the manufacturing or business environment. In present scenario, it is a verdict that effective manufacturing environment is not fulfilled the gap between entrepreneurship and organizational demand which remains competition for further improvements in product quality under barriers. The responses appear evident that concerns are always trying to reduce wastes in operations in order to become more profitable. Therefore, an attempt has been made for implementing lean practices in organization which need commitment toward tremendous learning experience against identification and recognition of critical barriers such as human resource level barriers (HLBs), time level barriers (TLBs), and asset level barriers (ALBs) which affect implementation process due to individual/employee/group level, waste time in production, infrastructures, facilities, and equipment, respectively. Main aim of research is to measure the effectiveness of HLBs, TLBs, and ALBs using an analytical network process (ANP) framework. It is suggested that ALBs are the most critical category which impacts 43.26%, trailed by HLBs, i.e., 35.17% and lastly TLBs, i.e., 21.55% directly on implementation. Key findings of this research may strengthen the top managements and decision makers in identification and recognition of category of hindrances during implementation of lean manufacturing on their shop floor. Also it helps them to derive suitable strategies to overcome identified barriers before implementation of lean practices.

B. P. Sharma (✉) · A. Chauhan · H. Singh · U. K. Vates · G. S. Rao
Department of Mechanical Engineering, Amity University, Noida, Uttar Pradesh, India
e-mail: bpsharma@amity.edu

© Springer Nature Singapore Pte Ltd. 2019
K. Shanker et al. (eds.), *Advances in Industrial and Production Engineering*, Lecture Notes in Mechanical Engineering, https://doi.org/10.1007/978-981-13-6412-9_31

Keywords Lean manufacturing · Human resource level barriers · Time level barriers · Asset level barriers · Analytical network process

1 Introduction

With preceding scenario, it is a verdict to explore such a manufacturing environment to remain in the competition. The responses appear evident that concerns are always trying to reduce wastes on working shop floor to become more productive [1]. Lean manufacturing (LM) bring up to a process of manufacturing improvements with the intention of maximizing production flow through eliminating waste which is based on the vital goal of Toyota production system (TPS). Few manufacturing sectors appreciate the standing of practicing lean techniques. However, some of those have applied the same with indispensable acquaintances and demonstrated tools to achieve the lean environment in their business units [2]. LM includes value stream to embrace all the processes and operations to transform raw materials into actionable goods and services, counting non-value-adding activities and necessary non-value-adding activities. Management of the value stream is a managerial tool for planning a production process concerning actual initiatives of LM techniques through systematic data synthesis and analysis [2]. It is a verified process for planning the improvements which allow companies to develop lean practices [3].

Manufacturing sectors are continually striving to upsurge productivity of their units. Their goal is to fulfill the customer's demand enabling with exact product, quality, features, quantity, and value within stipulated time [2]. The main idea is to find out the factors enhancing elimination of excess material movements, redundant inventory and production, waiting and delays, bottlenecks, over processing, excess worker motion, and the need for rework and corrections. Manufacturing process flow steps must be examined to determine that whether it is adding or not adding value to the product. If it is not adding value, the process should be deputized to outsourcing company or some other alternatives in order to focus the worker on value-added acts of its core units of the business. Intensifying challenges in the present global competition have driven many manufacturing sectors to adopt new manufacturing management strategies in order to enhance its efficiency and competitiveness. Manufacturing sectors have taken LM system as a widely acceptable and adaptable practice across countries and industries [4].

Therefore, the aim of this research is to further discuss the issues related to LM implementation in the manufacturing sectors. The investigation focuses on the identification and recognition of critical barriers such as HLBs, TLBs, and ALBs during LM implementation process. At present, the LM objectives and strategies are not incorporated in the business strategy due to lacking in metrics and identification of barriers during the implementation process. Thus, it is necessary to identify and measure the effectiveness of categories of these barriers. Barriers are categorized into three domains such as human resource, time, and asset level due to their equal effect on implementation process in the manufacturing sectors. In Table 1, the comparison

Table 1 Comparison of HLBs, TLBs, and ALBs during LM practice [2, 3, 6]

Sl. No.	Distinguishing attributes	HLBs	TLBs	ALBs
1.	Decisions and appropriate action	Awareness gap	Awareness gap	Awareness gap
2.	Quality of instructions	Medium	High	High
3.	Remediation or feedback	Less accurate	Less accurate	Less accurate
4.	Enhancement of latest tools and techniques	Increase reluctance	Increase reluctance	Increase reluctance
5.	Autonomy	Reduce teamwork	Reduce teamwork	Reduce teamwork
6.	Creative chaos	Reduce innovation	Reduce innovation	Reduce innovation
7.	Redundancy	Reduce complimentary skill development	Reduce complimentary skill development	Reduce complimentary skill development
8.	Requisite variety of trust	Reduce interaction	Reduce interaction	Reduce interaction
9.	Flexibility	Unpleasant working	Bounded working	Bounded working
10.	Lacking with innovative ideas	Update learning	Update learning	Update learning

among HLBs, TLBs, and ALBs has been done as per identified attributes. The main significance of this research is to evaluate differences between HLBs, TLBs, and ALBs in the form of percentage effectiveness for the ease of decision maker to identify the most effective category of LM implementation barriers to overcome them prioritywise. Therefore, an ANP model framework is presented for modeling the effect of HLBs, TLBs, and ALBs on the basis of interdependent variables. The framework provides support to the top management in analyzing the variables affecting decision making, flexibility, innovation, and competitiveness. Using an ANP approach in the context of LM Implementation, an influence of various dimensions of barriers can be evaluated. It also explicitly considers the influence of determinants on one another. Since dimensions and determinants of LM implementation barriers have systematic characteristics, they have been integrated into to one model as shown in Fig. 1. These systematic relationships represent the true linkages and interdependencies of these various determinants [5] (Table 2).

ANP FRAMEWORK FOR LEAN ENTERPRISE

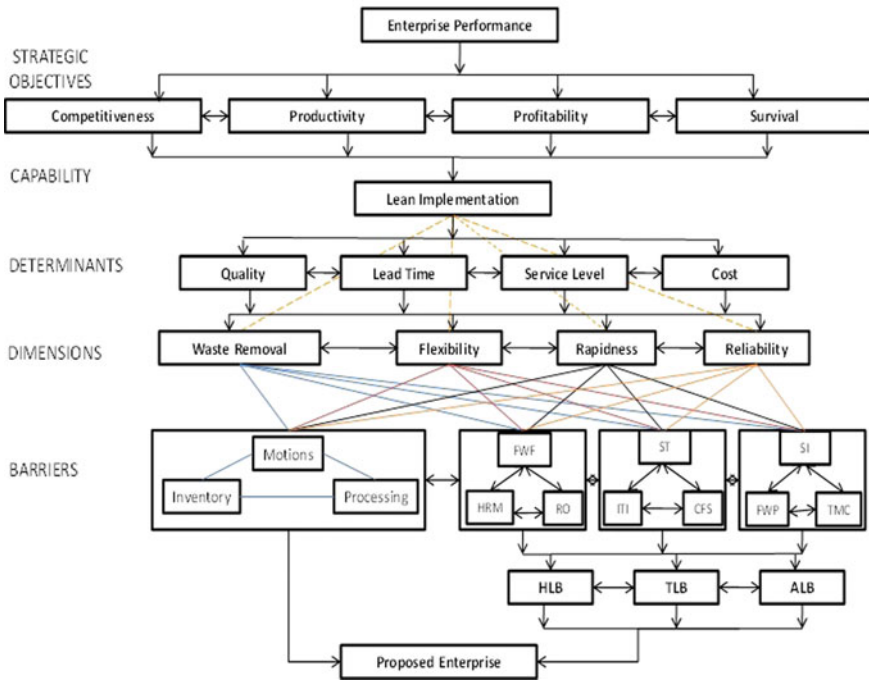


Fig. 1 ANP-based model for modeling the metrics of HLBs, TLBs, and ALBs during LM practice

Table 2 Abbreviation key

FWF	Flexible workforce	SI	Supplier involvement
HRM	Human resource management	FWP	Flexible workplace
RO	Resource optimization	TMC	Top management commitment
ST	Sharing resources and technology	ORB	Operator-related barriers
ITI	Information technology integration	TRB	Technology-related barriers
CFS	Customer feedback system	MRB	Management-related barriers

2 Impact of LM Implementation Barriers: A Review of Literature

Amid the changing procedure, different methodological troubles are associated with the procedure. The troubles are the hindrances to fruitful execution of lean manufacturing. To expel these hindrances, it initially needs to learn about the squanders that prompt these boundaries as follows:

1. Overproduction: Producing in overabundance or too early brings about poor stream of merchandise and data and causes abundance of stock [7].
2. Defects: Frequent and various mistakes in printed material and quality issues in the item or material outcomes in scrap or revamp and corrupted conveyance execution.
3. Unnecessary stock: Excessive capacity and deferral of data or items, brings about surfeit stock and costs, which prompts poor client benefit.
4. Inappropriate processing: Doing the work processes using wrong systems, procedures or set of tools often, when a much simpler approach might turn out to be more effective.
5. Excessive transportation: Extra movement of operators, goods, and information results in wastage of time and cost [8].
6. Waiting: Long periods of inactivity of goods, operators, machines, and information result in poor flow and long lead times.
7. Unnecessary motion: Poor space utilization or workplace organization results in poor ergonomics (e.g., frequently lost items and excessive stretching or bending).
8. Underutilization of employee: Unused skills and creativity of employees to improve the processes and practices refer to wastage of available knowledge, experience or skill of the workforce not using them in the proper department and by not exploiting their skills usefully. This can be due to poor hiring techniques by the management [9–11].

After identifying and examining these wastes, companies have moved further and accomplished in abolishing them. Now, the barriers which have to be abolished in order to attain lean environment in a company have been identified by performing a literature review and brain storming session from academia and experts from the industry.

3 Effectiveness Measurement of LM Barriers Paradigm: Research Methodology

3.1 *Pairwise Comparison and Consistency Check*

In view of the match insightful examination, Prof. Saaty has proposed the ANP procedure as an apparatus for multi-criteria basic leadership. In light of the audit of

Table 3 Matrix of pairwise comparison for the calculation of important weights and consistency [12–15]

Variables	Variable '1' (V ₁)	Variable '2' (V ₂)	Variable 'n' (V _n)	$M = \sqrt[n]{V_1 V_2 \dots V_n}$	Priority weights $W = \frac{M}{\sum M}$	$X = [A] \times [W]$	Eigenvalue $\lambda = \frac{[A] \times [W]}{W}$
V ₁	1	r	r'	M ₁	W ₁	X ₁	$\lambda_1 = X_1/W_1$
V ₂	1/r	1	r''	M ₂	W ₁	X ₂	$\lambda_2 = X_2/W_2$
V _n	1/r'	1/r''	1	M _n	W _n	X _n	$\lambda_n = X_n/W_n$
Matrix of pairwise comparison [A]; Here, 1/9 < r, r' ... r'' < 9 is based on a judgment				$\sum M = M_1 + M_2 + \dots + M_n$	Normalized matrix [W]		Maximum eigenvalue $\lambda_{max} = \sum \lambda/n$

Table 4 RI values for matrices used after pairwise comparisons [16]

n	2.0	3.0	4.0	5.0	6.0	7.0	8.0	9.0	10.0	
RI	00	0.5245	0.8815	0.1086	0.2479	0.3417	0.4056	0.4499	0.4854	
n	11.0	12.0	13.0	14.0	15.0	16.0	17.0	18.0	19.0	
RI	0.5141	0.5365	0.5551	0.5713	0.5838	0.5978	0.6086	0.6181	0.6265	
n	20.0	21.0	22.0	23.0	24.0	25.0	26.0	27.0	28.0	29.0
RI	0.6341	0.6409	0.647	0.6526	0.6577	0.6624	0.6667	0.6706	0.6743	0.6777
n	30.0	31.0	32.0	33.0	34.0	35.0	36.0	37.0	38.0	39.0
RI	0.6809	0.6839	0.6867	0.6893	0.6917	0.694	0.6962	0.6982	0.7002	0.702

the writing, a typical pair-wise comparisons have been created for combine savvy correlation as shown in Table 3.

Consistency Index (CI): where λ_{max} = maximum eigenvalue and n = the size of matrix of pairwise comparison.

Consistency Ratio (CR) = CI/RI [15] (Table 4).

3.2 Evaluation of the Framework Based on ANP

Structuring the metrics of HLBs, TLBs, and ALBs to evaluate the impact with the help of the steps of ANP approach is mentioned below (Tables 5, 6, 7, and 8).

Similarly, all pairwise comparison was conducted and incorporated to form supermatrices, and after their convergence to normalize the priority weights, overall impact of HLBs, TLBs, and ALBs was calculated followed by total desirability indices as per following tables (Tables 9, 10, and 11).

Table 5 Pairwise comparison of determinant w.r.t. productivity (CR = 0.0264)

	Cost	Lead time	Service level	Quality	<i>M</i>	<i>W</i>	<i>X</i>	Λ
Cost	1	0.263	0.269	4.041	0.731	0.306	1.237	4.042
LT Time	4.666	1	2.666	3.4	2.55	0.356	1.45	4.07
SL	4.333	0.722	1	4.75	1.963	0.285	1.137	3.989
Quality	2.777	1.8	1.428	1	1.634	0.366	1.404	3.836
	Pairwise comparison matrix [A]				6.878	<i>C</i>		

Table 6 Pairwise comparison of the dimensions w.r.t. quality/productivity (CR = 0.08961)

	Waste removal	Flexibility	Rapidness	Reliability	<i>M</i>	<i>W</i>	<i>X</i>	Λ
WR	1	5	3.277	1.114	2.066	0.288	1.158	4.020
Flexibility	0.205	1	1.436	3.083	0.976	0.371	1.49	4.016
Rapidness	1.703	4.416	1	0.888	1.607	0.395	1.674	4.237
Reliability	4.111	1.483	2.833	1	2.038	0.364	2.465	4.042
	[A]				6.68	<i>P_{j cos t}</i>		4.07

Table 7 Comparison of the barriers under waste removal w.r.t. quality/productivity (CR = 0.070)

	Inventory	Processing	Waiting	<i>M</i>	<i>W</i>	<i>X</i>	Λ
Inventory	1	0.33	2	0.87	0.18	0.55	3.055
Processing	3	1	5	2.46	0.51	1.53	3
Waiting	0.5	0.2	1	0.46	0.12	0.38	3.166
	[A]			3.79			3.073

Table 8 Comparison of barriers under waste removal w.r.t. inventory for quality (CI = 0)

	Processing	Waiting	<i>M</i>	<i>W</i>	<i>X</i>	Λ
Processing	1	6	2.4	0.85	1.96	1.98
Waiting	0.16	1	0.4	0.12	0.28	2
	[A]		2.8			

The estimation has been improved, and the situation adds up to the attractive quality records of all options as for determinant quality as appeared in Table 12. Meade and Sarkishas built up a relationship for the count of TDI as given [17]:

$$D_{ia} = \sum_{j=1}^j \sum_{k=1}^{kja} P_{ja} A_{kja}^D A_{kja}^I S_{ikja}$$

This step assesses the normalized values of Effectiveness Weighted Index of LM Implementation Barriers (EWILMBs) for effectiveness (HLBs, TLBs, and ALBs) [17] (Table 13).

Table 9 Supermatrix of interdependency of barriers w.r.t. quality

	Inventory	Processing	Waiting	FWF	HRM	RO	ST	ITI	CFS	SI	FWP	TMC
Inventory	0.00	0.75	0.16									
Processing	0.85	0.00	0.82									
Waiting	0.12	0.24	0.00									
FWF				0.00	0.75	0.87						
HRM				0.20	0.00	0.12						
RO				0.80	0.24	0.00						
ST							0.00	0.33	0.85			
ITI							0.75	0.00	0.14			
CFS							0.24	0.66	0.00			
SI										0.00	0.24	0.80
FWP										0.16	0.00	0.20
TMC										0.82	0.75	0.00

Table 10 Supermatrix of interdependency of barriers w.r.t. quality after convergence at power of 71

Cost	Inventory	Processing	Waiting	FWF	FWP	HRM	RO	SI	ITI	CF	TMC	ST
Inventory	0.10	0.10	0.10									
Processing	0.12	0.12	0.12									
Waiting	0.04	0.04	0.04									
FWF				0.31	0.31	0.31						
FWP				0.10	0.10	0.10						
HRM				0.27	0.27	0.27						
RO							0.18	0.18	0.18			
SI							0.16	0.16	0.16			
ITI							0.15	0.15	0.15			
CF										0.20	0.20	0.20
TMC										0.08	0.08	0.08
ST										0.23	0.23	0.23

Table 11 HLBs, TLBs, and ALBs on quality w.r.t. inventory (CR = 0.06)

	HLBs	TLBs	ALBs	M	W
HLBs	1.00	7	3	2.75	6.72
TLBs	0.14	1.00	0.33	0.35	0.08
ALBs	0.33	3	1.00	0.99	0.24
	[A]			4.09	

$$EWILMB_i = \sum_a D_{ia} C_a$$

4 Conclusion

In the present research, the adequacy of three classes of LM execution obstructions has been assessed by utilizing the ANP structure created. This system coordinates and depends on the different determinants, measurements, and obstructions and their connections. According to assessment, the asset level-related boundaries have the most extreme impact on LM execution trailed by human resource level and technology level obstructions. The outcome demonstrates that the asset value of any industry is most important factor for LM execution in the designing ventures. These discoveries likewise recommend that the enterprises can enhance their costs, service level, lead time, and quality through fruitful LM practices by dealing with these boundaries as per their effect. According to the outcome acquired by proposed ANP framework, it has been found that the ALBs have a maximum level of adequacy, i.e., 43.26% trailed by HLBs, i.e., 35.17% and TLBs, i.e., 21.55%. During evaluation of proposed model, values of consistency ratio for all the combine correlations differ from 0 to 0.09. The proposed model framework shows that effective examination was done to evaluate the effect of variety in the supposition of experts. This demonstration fills in as a rule to the directors for settling on a vital choice to accomplish the objectives of LM technique. It likewise causes the building ventures to stay aggressive in the business globalization. These findings recommend that LM is a proper system for enhancing their costs, service level, lead time, and quality of the building ventures and thus to accomplish fitting efficiency.

Table 12 TDI of alternatives w.r.t. quality

Dimensions	P_{ja}	Barriers	A_{kja}^D	A_{kja}^I	S_{ikja}				$P_{ja}A_{kja}^D A_{kja}^I S_{ikja}$		
					S1 (HLBs)	S2 (TLBs)	S3 (ALBs)	HLBs	TLBs	ALBs	
Waste removal	0.450	Inventory	0.44	0.10	6.72	0.08	0.24	0.1241	0.0015	0.0046	
	0.450	Processing	0.58	0.12	0.74	0.09	0.16	0.023	0.002	0.005	
	0.450	Waiting	0.42	0.04	0.07	0.67	0.25	0.0052	0.005	0.0018	
Flexibility	0.367	FWF	0.40	0.31	0.65	0.07	0.27	0.029	0.0031	0.0122	
	0.367	HRM	0.20	0.10	0.66	0.10	0.22	0.004	0.00073	0.0016	
	0.367	RO	0.39	0.27	0.08	0.71	0.21	0.0030	0.027	0.0081	
Rapidness	0.298	ST	0.19	0.18	0.11	0.77	0.36	0.0011	0.0078	0.0036	
	0.298	ITI	0.45	0.16	0.11	0.77	0.36	0.0023	0.016	0.0077	
	0.298	CFS	0.34	0.15	0.67	0.08	0.24	0.010	0.0012	0.0036	
Reliability	0.357	SI	0.53	0.20	0.74	0.07	0.18	0.0280	0.0026	0.0068	
	0.357	FWP	0.15	0.08	0.18	0.07	0.74	0.00007	0.00029	0.0031	
	0.357	TMC	0.30	0.23	0.18	0.07	0.74	0.0044	0.0017	0.018	
TDI of choices for determinant cost $D_{iLDM} = \sum_{j=1}^j \sum_{k=1}^{kja} P_{ja}A_{kja}^D A_{kja}^I S_{ikja}$											
								0.2341	0.0689	0.0764	

Table 13 EWILMB of HLBs, TLBs, and ALBs

Determinants	Cost	Service level	Lead time	Quality	Evaluated priority weights	
Weights (Ca)	0.5622	0.2857	0.1103	0.0418	Normalized values	
Alternatives (D_{ia})						% Impact
HLBs	0.0351	0.047	0.0474	0.2341	0.06541	35.17
TLBs	0.0351	0.0363	0.0294	0.0689	0.04008	21.55
ALBs	0.07671	0.0693	0.1032	0.0764	0.08046	43.26
Total					0.18595	

References

1. Stratton R, Warburton RDH (2003) The strategic integration of agile and lean supply. *Int J Prod Econ* 14(1):21–25
2. Goldman S, Nagel R, Preiss K (1995) *Agile competitors and virtual organizations*. Van Nostrand Reinhold, New York
3. Nagel R, Dove R (1991) *21st century manufacturing enterprise strategy: an industry led view of agile manufacturing*, vols I, II. Iococca Institute, Lehigh University
4. Gupta S, Herrmann JW, Lam G, Minis I (1997) Automated high level process planning to aid design for agile manufacturing. In: *IERC proceedings, 6th annual industrial engineering research conference*, Norcross, GA, USA, pp 1–19
5. Womack JP, Jones DT (2003) *Lean thinking: banish waste and create wealth in your corporation*, 2nd edn. Free Press, New York
6. Sindhvani R, Malhotra V (2016) Modelling the attributes affecting design and implementation of agile manufacturing system. *Int J Process Manag Benchmarking* 6(2):216–234
7. Sindhvani R, Malhotra V (2016) Modelling and analysis of agile manufacturing system by ISM and MICMAC analysis. *Int J Syst Assur Eng Manag* 8(2):253–263
8. Sindhvani R, Malhotra V (2013) Overview and drivers of agile manufacturing system: a review. *Int J Mark Technol* 3(12):144–154
9. Mittal VK, Sangwan KS (2014) Prioritizing barriers to green manufacturing: environmental. *Social Econ Perspect Elsevier Procedia CIRP* 17:559–564
10. Sangwan KS, Mittal VK (2015) A bibliometric analysis of green manufacturing and similar frameworks. *Manag Environ Qual Int J* 26(4):566–587
11. Singh MD, Shankar R, Narain R, Kumar A (2006) Survey of knowledge management practices in Indian manufacturing industries. *Int J Knowl Manag* 10(6):110–128
12. Saaty TL (2007) Time dependent decision-making; dynamic priorities in the AHP/ANP: generalizing from points to functions and from real to complex variables. *Math Comput Model* 46(7–8):860–891
13. Mittal VK, Sindhvani R, Kapur PK (2016) Two-way assessment of barriers to lean-green manufacturing system: insights from India. *Int J Syst Assur Eng Manag* 7(4):400–407
14. Singh MD, Kant R (2009) Selected knowledge management implementation issues: a sectorial analysis. *Int J Innov Learn* 6(5):550–567
15. Sharma BP, Singh MD (2014) Modeling the metrics of individual, organizational and technological knowledge sharing barriers: an analytical network process approach. *Int J Knowl Manag* 10(1):43–57
16. Alonso JA, Lamata MT (2006) Consistency in the analytic hierarchy process: a new approach. *Int J Uncertainty Fuzziness Knowl Based Syst* 14(4):445–459
17. Meade LM, Sarkis J (1999) Analyzing organizational project alternatives for agile manufacturing processes: an analytical network approach. *Int J Prod Res* 37:241–261

Feature Extraction and Recognition Information System for Manufacturing Prismatic Part



Vinod V. Rampur and Sachhidanand Reur

Abstract Feature extraction and recognition information systems are now widely located as a foundation for formulating an automated process planning system. Many methods have been reported in the kinds of literature, but a few of them acquired a status of generic methodology. In this research work explains the concept of automatic feature recognition system using CAD model neutral file in the format of ISO 10303 Standard for Exchange of Product model data (STEP) AP-214 to identify the hole feature of the CAD model. The geometrical information of the part design is analyzed by a feature recognition procedure that is created specifically to extract the features from the 3D CAD model based on geometric reasoning approach. Finally, a sample application description for a workpiece is presented for demonstration purposes.

Keywords STEP AP-214 · CAD · CAPP · CAM · Features · B-rep

1 Introduction

Automation of production activities for achieving manufacturing flexibility is becoming a major significant issue for manufacturing industries, as it leads to an improvement in production efficiency. The utilization of computer integrated manufacturing (CIM) approach is considered as a most doable approach to achieve efficiency. In such undertakings, computer-aided systems collaborate with a fused method to manage all through the product life cycle of a given part. As needs are the fundamental combination between CAD with CAPP and after that CAPP with CAM is perceived as the key zone of core interest. The integration of CAD and CAM through CAPP is

V. V. Rampur (✉)
Department of Mechanical Engineering, PESITM, Shivamogga,
Karnataka, India
e-mail: vinod.rampur@pestrust.edu.in

S. Reur
Department of Industrial and Production Engineering, PDACE, Kalburgi,
Karnataka, India
e-mail: sr.chidul@gmail.com

viewed as the key and significant issue as for the acknowledgment of CIM, and this is anticipated that would satisfy the need of present manufacturing enterprises for add up to automation of larger part its exercises. This integration procedure, CAPP frames a fundamental connection between CAD and CAM. Each automated system is expected to support on a specific and separate stage of the entire product life cycle of a given product, mainly design and manufacturing and for these issues of integration are normally not focussed during the development process of individual systems [1, 2].

CAPP is being regarded as the use of computers for assisting the process planner (human) for performing the various functions of process planning. The component information put away in the database of CAD system, created amid the design and modeling procedure directly flow to CAPP system and after that, from CAPP system to a given CAM system, for consistent integration of systems identified with CAD and CAPP and afterward CAPP and CAM. It implies, in real life manufacturing condition, there is dependably a need to oversee data exchange between the CAD stage and other computer-aided systems for different applications, which for all intents and purposes considered being troublesome, claiming each computer-aided system work with its own internal data model called proprietary data format. To determine this, the data flow issue ought to be tended to by means of considering a common file format which the distinctive CAD systems can read and process effortlessly. By utilizing direct translators at first between systems of a CAD with CAPP, at that point between CAPP with CAM the data can be exchanged. But the problem with this approach is, each unique computer-aided system requires an alternate interpreter, so there will be a huge number of translators required to deal with all computer-aided system in the world. A neutral file may be considered as the file which is having a format such that the format is totally independent of any given or specific system known as standards and has the capability to act as an 'agent' to connect two different and dissimilar computer systems which normally cannot be communicated with one another because of the data format incompatibility [3].

A neutral file format is generally considered as the file format which is 'acceptable' as well as consistent within a given industry or a group of industries and the format may differ from other industry and, they may set different format standards. A survey shows that most of the industries are employing a neutral format for achieving the necessary integration of their manufacturing systems. In this paper, ISO standard STEP, AP-214 is suggested as being the standard neutral file format, because it is accepted universally as the standard for transformation programs available for proprietary CAD packages, especially for automotive parts.

Initially, CAPP system development activities were supported by work related to generating DXF file of parts from its CAD representation. Fruitful efforts resulted in the direction of automation of feature recognition for both primitive as well as interacting features, machining planning, setup planning and generation of CNC codes. In a major research activity, successful efforts resulted in the development of a CAPP system by employing STEP AP-203 neutral file. However, in the present-day modern manufacturing organizations, STEP neutral file AP-214 is being recognized as most commonly accepted/employed file by latest CAD systems. On this background of

earlier works, the current work is carried out and a user-friendly CAPP system has been developed by employing AP-214 neutral file [4].

2 Product Data Flow Issue for Integrating CAD/CAPP/CAM

Computers are using more and more in all the domains of an organization, in the particular product development process. Data exchange and sharing are the main agenda for many businesses. The rise of such global efforts has created the need for sharing information among vendors involved in multi-disciplinary projects.

Individual CAD systems and many systems have their own format for categorizing and writing data, this makes difficult for organizations to communicate product model data without translation. To address interoperability problems encountered in the exchange of digital information, for this reason, international standard STEP is designed. STEP is a standard for exchanging the digital information of 3D CAD models and various technical information in CAD software [5].

The flow of product model data which is generated in computer-aided manufacturing is grouped into three categories. The first approach is single-system standards, in this, every supplier and borrower are using the same format to translate the product information, it increases the interoperability and reduces software cost for an organization because here only one software package is required.

In the second approach, the custom translators between the systems, in this the supplier and borrower use different CAD systems that are best for translating the information related to the particular product. These translators are directly converting the data files from one format to other required formats so that the users can access each other's data. By using custom translators, which maximize the interoperability between different CAD packages.

The third approach is to transfer the product data, in this utilization of neutral file format to exchange the information between different CAD packages. For this STEP, the proprietary data format is used to transfer the data from one software package to the other package. Each industry can purchase any software package that most efficiently manages and controls the flow of information between intra-organization or inter-department within the same industry. When the industry conducts intra-organization or inter-department exchange, first translate the data into a neutral file format that is accessible to all software application. By utilizing a neutral data, file format maximizes the interoperability across the organization but software development cost increases because the translating system is incorporated within the software.

3 Significance of Features for CAD/CAM Integration

The methods used for part modeling to provide product data as the input for the CAPP systems are, one is feature-based design and other CAD models of the part. Owing to the major limitations of feature-based design, it has not found wide application and most of the research works have used CAD models as the major input for generating process planning automatically. From the viewpoint of manufacturing, the biggest drawback of CAD systems is that the information made available in a CAD model is in the form of the modeling primitives, like faces, edges, and vertices.

These primitives have been widely interpreted as low-level information elements and cannot be directly used in downstream applications such as process planning, because, this description contrasts view of the component from an engineer's point of view since it is expressed in terms manufacturing features which are treated as functionally important regions. Manufacturing features such as slots, steps, and pockets are generally regarded as high-level information elements that are directly relevant in automated process planning. Hence, it is necessary to first develop a method of retrieving useful details of the given part through the characteristics of manufacturing features from a given CAD model. In this regard, feature extraction is being recognized as the necessary bridge between CAD and given CAPP system [6–8].

3.1 *Method of Extraction and Formatting of Data from STEP File*

When CAD systems are employed, then the machines will be depending directly on product-related information for producing the given product. Therefore, extraction of correct information about the product from CAD data becomes an important key issue. The data extracted from the CAD models will be used for feature recognition, machining planning, planning process, time scheduling, producing products, etc. All the information which is extracted from CAD data will be stored in a structured database. The major issue of this research is the extraction of CAD part model data from its STEP neutral file to generate the product-related information which in turn can be used for downstream activities of CAPP mainly for feature recognition, machining planning, and for NC code generation [9–12].

3.2 *Database for Storing Extracted Data from STEP File*

The CAD model data extracted from the neutral file STEP is stored in two database tables: one consists of B-rep data, and other constructive solid geometry data about the features are stored in a structured database which is designed specifically for this function (Table 1).

Table 1 Description of B-rep data

Name	Description
AF	ADVANCED_FACE—stores id of ADVANCED_FACE entity
FOB	FACE_OUTER_BOUND—stores the id of FACE_OUTER_BOUND entity
FB	FACE_BOUND—stores the id of FACE_BOUND entity
PL	PLANE—stores id of PLANE entity
EL	EDGE_LOOP—stores id of EDGE_LOOP entity
ELI	Edge_Loop_Id—stores number of id in the EDGE_LOOP entity

3.3 Feature Recognition from Neutral File

In common terms in CAPP systems, the function concerned with feature recognition is expected to serve the purpose of converting the design features into manufacturing features. For this, both geometrical and topological data of the part design will be utilized. The main purpose of such transition is to identify the size of the machinable volume, tool approach direction, and number of passes required for a machining operation. Feature recognition is getting an element show from a given geometric model. It can be performed either intelligently by the client, or naturally by the product. Automatic feature recognition is an important tool to integrate CAD/CAPP/CAM systems seamlessly.

The integration of automated manufacturing resources in the workshop floor is similarly hard to generate the required process plans, because of a lack of required data communication interface among CAD/CAM and CAPP system. At this stage, feature extraction and recognition play a merry role in manufacturing system from developed drawings [13, 14].

4 Implementation of Feature Extraction Process for Automotive Part

A unique method that captures the modeling method for the component is used to serve as an input to the CAPP module. Hence, the 3D modeling software makes for a major part in providing feature information. In the present work, procedures are developed for recognition of primitive features which are defined in the STEP neutral file like, boss, pocket, hole, slot, and protrusion, and interacted features with orthogonal, inclined and curved surfaces, which are resulted from the combination of primitive features (Fig. 1).

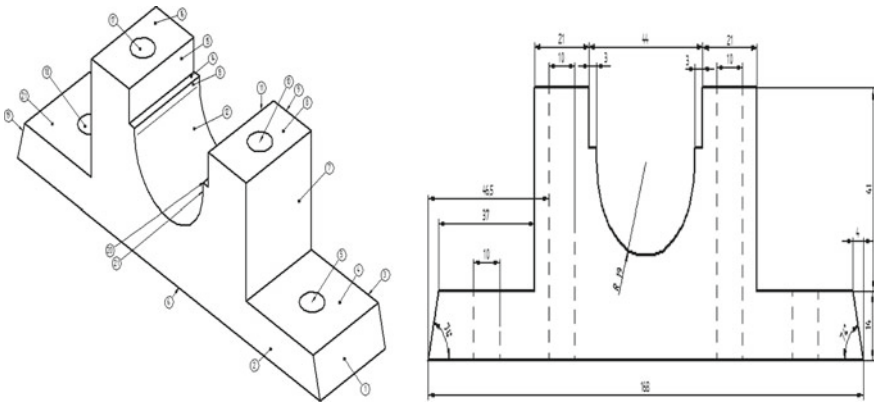


Fig. 1 Boundary representation structure

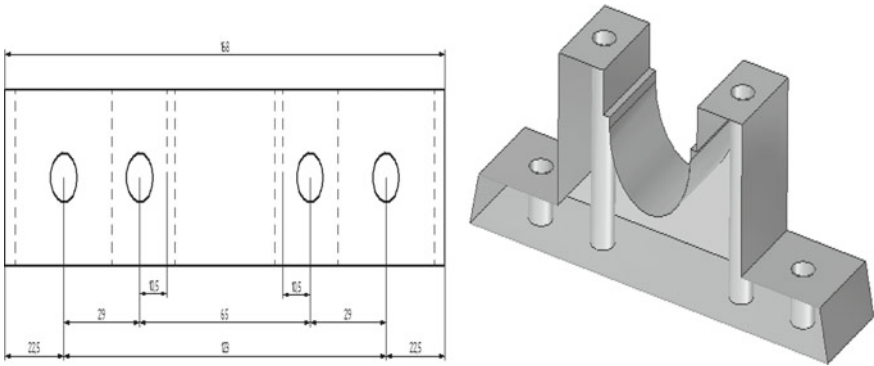


Fig. 2 Hole features on the given part

4.1 Extraction of Hole Feature

A hole is a type of machining feature that is the removal of a cylindrical volume from a part. Each hole is either a counter-borehole, countersunk hole or a round hole. The hole may be positioned at its bottom with the Z-axis in the direction out of the hole or at a position at the top of the hole with the Z-axis in the direction into the part. The hole features of the CAD part model are to be recognized from a neutral file STEP AP-214 of the part model. The required algorithm or procedure is developed for a given part as shown in Fig. 2.


```

#84 = ADVANCED_FACE (" , (#1173, #174), #175, .F.);
#173 = FACE_OUTER_BOUND (" , #258, .T.);
#258 = EDGE_LOOP (" , (#453));
#453 = ORIENTED_EDGE (" , *, *, #485, .F.);
#485 = EDGE_CURVE (" , #574, #574, #575, .T.);
#574 = VERTEX_POINT (" , #700);
#700 = CARTESIAN_POINT (" , (-56.50000000000000, 0.0000000000000000,
0.0000000000000000));
#574 = VERTEX_POINT (" , #700);
#700 = CARTESIAN_POINT (" , (-56.50000000000000, 0.0000000000000000,
0.0000000000000000));
#575 = CIRCLE (" , #701, 5.000000000000000);
#701 = AXIS2_PLACEMENT_3D(" , #847, #848, #849);
#847 = CARTESIAN_POINT (" , (-61.50000000000000, 0.0000000000000000,
0.0000000000000000));
#848 = DIRECTION (" , (0.0000000000000000, 0.0000000000000000,
1.0000000000000000));
#849 = DIRECTION (" , (1.0000000000000000, 0.0000000000000000,
0.0000000000000000));

```

In the above STEP line, the round hole feature is formed by extruding or lofting circular closed profile along a linear path. The circular closed profile and linear path are represented by two entities = AXIS2_PLACEMENT_3D and CARTESIAN_POINT. To identify and extract the data of machining feature round hole from STEP file, the following procedure is developed,

Step-1: Search the STEP file for the occurrence of the round hole entity using the key word #575 = CIRCLE (" ,); defined in the STEP file. The result of the search is shown below, #575 = CIRCLE (" , #701, 5.000000000000000).

Step-2: Next search for the Cartesian point, which defines the location of the feature in the CARTESIAN_POINT part model by using the key word as CARTESIAN_POINT (), which is an entity, the result of the search is shown below.

#847 = CARTESIAN_POINT (" , (-61.50000000000000, 0.0000000000000000, 0.0000000000000000)); From the above STEP line extract the parameters of the Cartesian point entity, which represent x , y , and z coordinates of the location point.

Step-3: Next search for the entities which define the orientation of the feature in the part model through DIRECTION () entities. Use the name of the entity as the key word for search, and the result of the search is shown below,

```

#848 = DIRECTION (" , (0.0, 0.0, 1.0));
#849 = DIRECTION (" , (1.0, 0.0, 0.0)).

```

The above procedure developed can be used to recognize other round hole features present in the part model and the above procedure which is implemented in the software recognizes all the round hole features. The data extracted from the above steps are stored in the database (Tables 2 and 3).

Table 2 Database table for ROUND_HOLE machining feature

AF	LM	CPX	CPY	CPZ	D1X	D2X	D1Z	D2X	D2Y	D2Z	Radius
#46	CIRCLE	-5	-18	40	0	1	0	1	0	0	5
#64	CIRCLE	5	18	40	0	1	0	1	0	0	5
#72	CIRCLE	61	-2	14	-1	0	1	0	1	0	5
#54	CIRCLE	-62	0	14	1	0	1	0	-1	0	5
#52	CIRCLE	-62	0	0	0	0	1	1	0	0	5
		61	-2	0	0	0	1	1	0	0	5
		33	0	0	0	0	1	1	0	0	5
		-33	0	0	0	0	1	1	0	0	5
#76	CIRCLE	33	0	55	0	0	1	1	0	0	5
#70	CIRCLE	5	18	40	0	1	0	1	0	0	19
		-5	-18	40	0	1	0	1	0	0	19
#84	CIRCLE	-62	0	0	0	0	1	1	0	0	5
		-62	0	14	1	-1	0	0	-1	0	5
#86	CIRCLE	62	-2	0	0	0	1	1	0	0	5
		62	-2	14	1	-1	0	0	1	0	5
#50	CIRCLE	33	0	0	0	0	1	1	0	0	5
		33	0	55	0	0	1	1	0	0	5
#88	CIRCLE	-33	0	0	0	0	1	1	0	0	5
		-33	0	55	0	0	1	1	0	0	5

Table 3 Hole machining feature details

	Key dimensions		Feature drawing
HOLE_1	Radius	05 mm	
	Hole depth (distance)	14 mm	
	Bottom condition	Through	
	Location Cartesian point		
HOLE_2	Radius	05 mm	
	Hole depth (distance)	55 mm	
	Bottom condition	Through	
	Location Cartesian point		
HOLE_3	Radius	05 mm	
	Hole depth (distance)	55 mm	
	Bottom condition	Through	
	Location Cartesian point		
HOLE_4	Radius	05 mm	
	Hole depth (distance)	14 mm	
	Bottom condition	Through	
	Location Cartesian point		

5 Conclusions

STEP is the major viable strategy which gives a prevailing support for CAD/CAPP/CAM integration. The incorporated resources of STEP give whole detail data of product information, for the worldwide product data technique for integration, this strategy is the root for that. The integration of CAD with CAPP systems will incredibly enhance the productivity of the manufacturing industry. Also, the change of incorporated STEP-based CAD/CAPP systems will be exceptionally valuable to the manufacturing designing authorities working in simultaneous building condition. In this present work, a model of the feature recognition system is prepared for the combination of manufacturing parts and activities parts by using STEP AP-214 as an input neutral file. The prescribed technique works in a 3D solid model which gives it a capacity to use by the present manufacturing innovation.

Acknowledgements The primary author would like to express special thanks to my Management and Principal of PES Institute of Technology and Management, Shivamogga, Karnataka, India for the kind consolation and support provided. I express my earnest and sincere thanks to my guide Dr. Sachhidanand Reur for the energy and motivation. His insight helped me to learn numerous new things. His precious recommendations and steady support have helped me all through for the fulfillment of my dissertation work. The second author would like to express special thanks to their Management and Principal of PDACE, Gulbarga, Karnataka, India for the kind consolation and support.

References

1. Altिंग L, Zhang HC (1989) Computer aided process planning: the state-of-the-art survey. *Int J Prod Res* 27(4):553–585
2. Adejuyigbe SB (2010) Manufacturing and computer aided engineering: a panacea for wealth creation. Inaugural Lecture Series, No. 27. Federal University of Agriculture, Abeokuta, Nigeria, Delivered at 13th Jan, 2010. pp 14–21
3. Jabri A, El barkany A, El Khalfi A (2013) Process planning—new process plans for agile manufacturing. *IJETT* 04(02):92–101
4. Markus A, Vancza J, Horvath M (1997) Process planning by retrieval and adaptation. *Comput Ind* 33(1):47–60
5. Sadaiah M et al (2002) A generative computer-aided process planning system for prismatic components. *Int J Adv Manuf Technol* 20(10):709–719
6. Hwang JS, Miller WA (1997) Using mixed-type reasoning in computer-aided process planning for feature interactions. *J Intell Manuf* 8(4):297–306
7. Lee HC, Jhee WC, Park HS (2007) Generative CAPP through projective feature recognition. *Comput Ind Eng* 53(2):241–246
8. Khoshnevis B, Sormaz DN, Park JY (1999) An integrated process planning system using feature reasoning and space search-based optimization. *IIE Trans Inst Ind Eng* 31(7):597–616
9. Abdughafour AB, Al-Bassam MA (2012) Automatic features recognition of symmetrical shapes. *Eng Tech J* 30(12)
10. Babic B, Nestic N, Miljkovic Z (2008) A review of automated feature recognition with rule-based pattern recognition. *Comput Ind* 59(4):321–337
11. Xu X, Hinduja S (1997) Determination of finishing features in 2½D components. *Proc Inst Mech Eng Part B J Eng Manuf* 211(2):125–142
12. Xu X, Hinduja S (1998) Recognition of rough machining features in 2½D components. *CAD Comput Aided Des* 30(7):503–516
13. Sridharan N, Shah JJ (2004) Recognition of multi axis milling features—Part I: topological and geometric characteristics. *J Comput Inf Sci Eng* 4(3):242–250
14. Woo Y et al (2005) A hybrid feature recognizer for machining process planning systems. *CIRP Ann Manuf Technol* 54(1):397–400

Fabrication and Characterization of Al₂O₃–TiC-Reinforced Aluminum Matrix Composites



Anbesh Jamwal, Umesh Kumar Vates, Pallav Gupta, Ankur Aggarwal and Bhupendra Prakash Sharma

Abstract With a wide range of applications, aluminum matrix composites (AMCs) play an important role in many of the engineering applications and industries, i.e., automobile and aerospace. AMCs are the composites having aluminum as matrix and ceramics or some other metals as reinforcement. The aim of the present study is to develop the Al₂O₃–TiC-reinforced AMCs and study the effect of reinforcements on the mechanical properties. In the present case, the Al₂O₃–TiC content is varying in composition of (0, 5, 10, 15, and 20 wt%) in aluminum matrix, fabricated by stir casting technique. It is found that reinforced AMCs show the better mechanical properties as compared to unreinforced AMCs. Various properties which were improved include tensile strength, hardness, and wear resistance. It is expected that the present composite will be useful for developing lightweight aerospace components.

Keywords Aluminum matrix composites · Stir casting · Mechanical properties

1 Introduction

With the rapid change in manufacturing scenario, materials play an important role. Materials are deep-seated in our life at the present time [1]. Our manufacturing system, daily needs, communication, and transportation all the segments depend upon the materials [2]. The material is simply a form of the matter [1]. Materials are being used in many applications, but with a change in time and human needs, new materials are being developed [3]. With the change in manufacturing scenario and human needs, a new form of materials is developed with better properties [4–6]. In the past few decades, composite materials gain more popularity because of the better properties and wide applicability. Composites materials are advanced forms of materials in which reinforcement is dispersed into the matrix either in the continuous phase or discontinuous phase [7, 8]. Composites are widely used in cutting tools these days, seal rings, bearing parts, and variety of engine parts where high temperature is

A. Jamwal · U. K. Vates · P. Gupta · A. Aggarwal · B. P. Sharma (✉)
Department of Mechanical Engineering, Amity University, Noida 201301, Uttar Pradesh, India
e-mail: bpsharma@amity.edu

© Springer Nature Singapore Pte Ltd. 2019
K. Shanker et al. (eds.), *Advances in Industrial and Production Engineering*, Lecture Notes in Mechanical Engineering, https://doi.org/10.1007/978-981-13-6412-9_33

349

required [9]. In the twenty-first century, the development of aluminum metal matrix composite is one of the major research areas for the development of lightweight materials because of their wide range of applicability in automobile industries and aircraft applications [10–12]. Aluminum metal matrix composites are composites in which aluminum is reinforced with other metals, organic compounds, or ceramics [13, 14]. These composites are prepared by dispersing the reinforcement (i.e., metal or ceramic) in the aluminum matrix [15]. The reinforcement in aluminum matrix composites (AMCs) could be in form of particulates, continuous or discontinuous fibers, and whiskers depending upon the industrial application [16]. Al-MMC can be categorized into four types on the basis of reinforcements, i.e., particle-reinforced AMC [17], continuous fiber-reinforced AMC [18], short fiber or whiskers-reinforced AMC [19] and monofilament-reinforced AMC [20]. It is found in some studies that reinforcement should be non-reactive and stable in given working temperature [21, 22]. The major advantage of using aluminum metal matrix composites is reduced density [23], greater strength [24], thermal stability [25], improved damping properties [26], improved abrasion [27], as well as wear resistance [28]. In order to provide better material properties like tensile strength, hardness, and wear resistance, SiC, B₄C, and Al₂O₃ ceramics are used as reinforcements [24, 29, 30]. A lot of research has been done on the improvement of aluminum metal matrix composites. AMCs can be manufactured by stir casting [31], infiltration [32], squeeze casting [33], powder metallurgy [34–36], and semisolid processing [37] techniques. Over the years, aluminum metal matrix composites were synthesized and characterized and used in many engineering applications for the better combination of properties. With a wide range of applicability in the transport system, Al-MMC provides low fuel consumption and less noise as compared to other materials [38]. The aim of the present study is to observe the effect of TiC and Al₂O₃ reinforcements addition in the aluminum metal matrix composites on the tensile strength, hardness, and wear resistance.

2 Experimental Procedure

2.1 Materials

Aluminum-1100 alloy was used as a base material or matrix material, and Alumina-TiC particles were added as reinforcement in powder form to metal. Al-1100 is an aluminum-based alloy with minimum 99% of aluminum. It is most heavy alloy in the 1100 series. The chemical composition of Al-1100 alloy is shown in Table 1.

Table 1 Composition of Al-1100 alloy used as matrix

Element	Aluminum	Copper	Iron	Manganese	Silicon	Zinc	Residual
%	99–99.5%	0.05–0.20%	0.95% max	0.05% max	0.95% max	0.1% max	0.15% max

Table 2 Composition of Al₂O₃-TiC reinforcement in Al matrix

Sample	Composition
AMC001	100% Al
AMC002	95% Al and 2.5% Al ₂ O ₃ - 2.5% TiC
AMC003	90% Al and 5% Al ₂ O ₃ -5% TiC
AMC004	85% Al and 7.5% Al ₂ O ₃ -7.5% TiC
AMC005	80% Al and 10% Al ₂ O ₃ -10% TiC

2.2 Preparation of Composites

Al₂O₃-TiC-reinforced composites were prepared by stir casting process. Five composites were prepared with the different compositions of reinforcement. The composition of Al₂O₃-TiC is shown in Table 2.

The experiment was done on a controlled furnace having the maximum temperature up to 1200 °C. Al-1100 ingots were melted in the furnace up to 950 °C for 30 min, and then, melted aluminum was stirred for 3 min at 400 rpm. Heat-treated Al₂O₃ particles were added to the furnace through the funnel at 950 °C and heated at 1070 °C for 20 min. The mixture was again stirred at 1070 °C for 5 min. TiC particles were added in the furnace at 1070 °C with the help of funnel and then heated up to 1150 °C for 30 min. Before pouring into the mold, the mixture was again stirred, and finally, the melt was poured and allowed to solidify under room temperature. The mold was covered from upper side with the help of a sheet to avoid the casting defects.

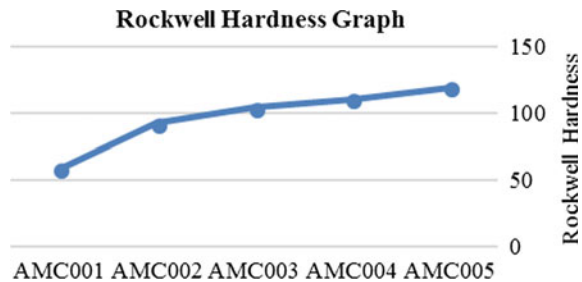
3 Results and Discussion

3.1 Hardness

The hardness number is indicated by the instrument by applying a minor load of 10 kg and a major load of 90 kg. Hardness for the different samples is shown in Table 3. It is found in the experiments that hardness number increases with increase in the % of reinforcements in AMCs. For pure Al sample without any reinforcements, hardness number is 58.4 HRB. It is found that hardness was more in reinforced AMCs than unreinforced AMC. Specimen AMC002 with 2.5% TiC-2.5% Al₂O₃ shows the Rockwell hardness value of 92 HB. It is found that increase in the ratio of

Table 3 Rockwell hardness of different samples

Sample	Composition	Rockwell hardness
AMC001	100% Al	58.4 HRB
AMC002	95% Al and 2.5% Al ₂ O ₃ -2.5% TiC	92 HRB
AMC003	90% Al and 5% Al ₂ O ₃ -5% TiC	104 HRB
AMC004	85% Al and 7.5% Al ₂ O ₃ -7.5% TiC	110 HRB
AMC005	80% Al and 10% Al ₂ O ₃ -10% TiC	119 HRB

Fig. 1 Rockwell hardness of different samples

reinforcements increases the hardness. In the composites, reinforcement particles act as strengthening agents which help in creating the stronger bond between the particles. It is found that stronger bond between the particles improves the mechanical properties of the material. The presence of well bonded and harder TiC–Al₂O₃ particles in the Al matrix increases the hardness of specimens by preventing the movement of dislocations. The specimens with 15 and 20% reinforcements exhibit the higher hardness values.

Table 3 shows that the addition of Al₂O₃–TiC reinforcement in Al matrix enhances the hardness of composites. The graph (Fig. 1) shows that there is an increase in the hardness with increase in wt% of reinforcement.

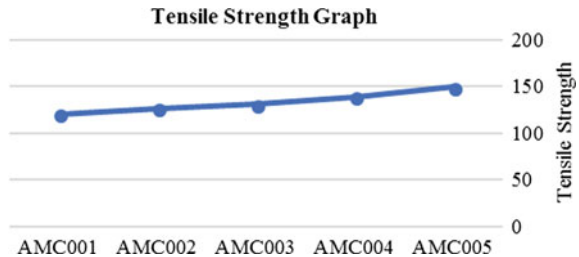
3.2 Tensile Strength

Tensile strength for different samples is shown in Table 3. It is found in the experiments that tensile strength is more in reinforced AMCs than the unreinforced Al composite. Tensile strength increases with increase in the wt% of Al₂O₃–TiC reinforcements in AMCs. It is found that the strong interfacial bonding between the TiC–Al₂O₃ and Al matrix increases the tensile strength of the material. In the AMCs, there is an increase in the tensile strength due to the transfer of applied load to strongly bonded TiC–Al₂O₃ reinforcements in the Al matrix. Lower the reinforcement in the

Table 4 Tensile strength of different samples

Sample	Composition	Tensile Strength (MPa)
AMC001	100% Al	120.4
AMC002	95% Al and 2.5% Al ₂ O ₃ -2.5% TiC	126.5
AMC003	90% Al and 5% Al ₂ O ₃ -5 % TiC	130.7
AMC004	85% Al and 7.5% Al ₂ O ₃ -7.5% TiC	139
AMC005	80% Al and 10% Al ₂ O ₃ -10% TiC	149.3

Fig. 2 Tensile strength graph of different samples



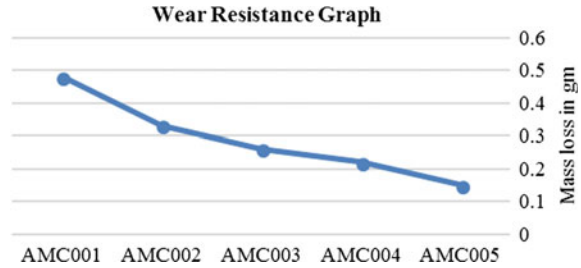
AMCs gives the lower tensile strength. Specimen AMC001 with pure Al shows the minimum tensile strength of 84.6 MPa. With increase of the reinforcement ratio in the Al matrix, the 15% and 20% reinforcements show the maximum tensile strength of 116 and 129.3 MPa, respectively.

Table 4 shows that addition of Al₂O₃-TiC reinforcement in Al matrix enhances the tensile strength of AMCs. The graph (Fig. 2) shows that there is an increase in the tensile strength with increase in wt% of reinforcement.

3.3 Wear Resistance

Wear behavior of the Al₂O₃-TiC-reinforced AMCs is obtained by wear test. Wear resistance of the material is the property of a material which resists the material loss by some mechanical actions. The wear test was performed at 300 rpm grinding speed for a fixed time of 4 min. A constant load of 10 N was applied to the sample. In the experiment, it is found that the mass loss in the unreinforced AMCs is greater than the reinforced AMCs. The Presence of TiC particles enhance greater wear resistance to the Al matrix. This is because of the pure Al matrix is worn out first from the surface of the specimen during the wear test and then leaving the TiC-Al₂O₃ particles on the surface. These exposed TiC-Al₂O₃ particles protect the Al matrix from further wear. It is also found that sliding distance is the most influencing parameter which affects

Fig. 3 Wear resistance at different samples with mass loss



the wear rate of AMCs than the applied load and sliding speed. With the increase in the wt% of reinforcements in the AMCs, there is an increase in the wear resistance also. Maximum wear resistance is obtained at 20 wt% of reinforcements. The graph (Fig. 3) shows the mass loss in grams when the wear test is conducted on the samples.

4 Conclusion

In this experimental study, AMCs were prepared with varying Al_2O_3 –TiC content by using stir casting fabrication process. Hardness, tensile strength, and wear resistance of composites were studied. Based on the experimental results, the following conclusions can be stated:

- Addition of Al_2O_3 and TiC particles in the Al matrix increases the hardness of the AMCs. Maximum hardness is obtained at 20 wt% of reinforcements in the Al matrix.
- Tensile strength is maximum in the reinforced AMCs than the unreinforced AMCs. With the increase in the wt% of reinforcements tensile strength increases, 20 wt% of reinforcement in the AMCs shows the maximum tensile strength.
- Addition of TiC particles in the AMCs increases the wear resistance of the composites. It was found that the maximum wear resistance of the AMCs resulted at 20 wt% of reinforcements.

It is found that addition of TiC particles with the alumina particles shows maximum tensile strength, hardness, and wear resistance than the unreinforced aluminum.

References

1. Callister WD, Rethwisch DG (2011) Materials science and engineering, vol 5. Wiley, NY
2. Kaczmar JW, Pietrzak K, Włosiński W (2000) The production and application of metal matrix composite materials. *J Mater Process Technol* 106(1):58–67
3. Hull D, Clyne TW (1996) An introduction to composite materials. Cambridge University Press, Cambridge

4. Jeon CH, Jeong YH, Seo JJ, Tien HN, Hong ST, Yum YJ, ... Lee KJ (2014) Material properties of graphene/aluminum metal matrix composites fabricated by friction stir processing. *Int J Precis Eng Manuf* 15(6):1235–1239
5. Ramnath BV, Elanchezian C, Annamalai RM, Aravind S, Atreya TSA, Vignesh V, Subramanian C (2014) Aluminium metal matrix composites—a review. *Rev Adv Mater Sci* 38(5)
6. Pramanik A (2014) Developments in the non-traditional machining of particle reinforced metal matrix composites. *Int J Mach Tools Manuf* 86:44–61
7. Jha P, Gupta P, Kumar D, Parkash O (2014) Synthesis and characterization of Fe-ZrO₂ metal matrix composites. *J Compos Mater* 48(17):2107–2115
8. Chou TW, Kelly A, Okura A (1985) Fibre-reinforced metal-matrix composites. *Composites* 16(3):187–206
9. Mallick PK (2007) *Fiber-reinforced composites: materials, manufacturing, and design*. CRC Press
10. Rawal SP (2001) Metal-matrix composites for space applications. *JOM* 53(4):14–17
11. Miracle DB (2005) Metal matrix composites—from science to technological significance. *Compos Sci Technol* 65(15):2526–2540
12. Gupta P, Kumar D, Quraishi MA, Parkash O (2016) Metal matrix nanocomposites and their application in corrosion control. In: *Advances in nanomaterials*. Springer India, pp 231–246
13. Youssef Y, El-Sayed M (2016) Effect of reinforcement particle size and weight fraction on the mechanical properties of SiC particle reinforced Al metal matrix composites. *Int Rev Mech Eng* 10(4)
14. Kumar UKAV (2017) Method of stir casting of aluminum metal matrix composites: a review. *Mater Today Proc* 4(2):1140–1146
15. Reddy AP, Krishna PV, Rao RN, Murthy NV (2017) Silicon carbide reinforced aluminium metal matrix nano composites—a review. *Mater Today Proc* 4(2):3959–3971
16. Shirvanimoghaddam K, Khayyam H, Abdizadeh H, Akbari MK, Pakseresh AH, Abdi F, Naebe M (2016) Effect of B₄C, TiB₂ and ZrSiO₄ ceramic particles on mechanical properties of aluminium matrix composites: experimental investigation and predictive modelling. *Ceram Int* 42(5):6206–6220
17. Lloyd DJ (1994) Particle reinforced aluminium and magnesium matrix composites. *Int Mater Rev* 39(1):1–23
18. Surappa MK (2003) Aluminium matrix composites: challenges and opportunities. *Sadhana* 28(1):319–334
19. Miyajima T, Iwai Y (2003) Effects of reinforcements on sliding wear behavior of aluminum matrix composites. *Wear* 255(1):606–616
20. Srivatsan TS, Ibrahim IA, Mohamed FA, Lavernia EJ (1991) Processing techniques for particulate-reinforced metal aluminium matrix composites. *J Mater Sci* 26(22):5965–5978
21. Dong Q, Chen LQ, Zhao MJ, Bi J (2004) Synthesis of TiCp reinforced magnesium matrix composites by in situ reactive infiltration process. *Mater Lett* 58(6):920–926
22. Lindroos VK, Talvitie MJ (1995) Recent advances in metal matrix composites. *J Mater Process Technol* 53(1–2):273–284
23. Torralba JM, Da Costa CE, Velasco F (2003) P/M aluminum matrix composites: an overview. *J Mater Process Technol* 133(1):203–206
24. Kang YC, Chan SLI (2004) Tensile properties of nanometric Al₂O₃ particulate-reinforced aluminum matrix composites. *Mater Chem Phys* 85(2):438–443
25. Molina JM, Rhême M, Carron J, Weber L (2008) Thermal conductivity of aluminum matrix composites reinforced with mixtures of diamond and SiC particles. *Scripta Mater* 58(5):393–396
26. Lavernia EJ, Perez RJ, Zhang J (1995) Damping behavior of discontinuously reinforced ai alloy metal-matrix composites. *Metall Mater Trans A* 26(11):2803–2818
27. Bhansali KJ, Mehrabian R (1982) Abrasive wear of aluminum-matrix composites. *JOM* 34(9):30–34
28. Mazahery A, Shabani MO (2012) Study on microstructure and abrasive wear behavior of sintered Al matrix composites. *Ceram Int* 38(5):4263–4269

29. Kerti I, Toptan F (2008) Microstructural variations in cast B₄C-reinforced aluminium matrix composites (AMCs). *Mater Lett* 62(8):1215–1218
30. Song MS, Zhang MX, Zhang SG, Huang B, Li JG (2008) In situ fabrication of TiC particulates locally reinforced aluminum matrix composites by self-propagating reaction during casting. *Mater Sci Eng, A* 473(1):166–171
31. Hashim J, Looney L, Hashmi MSJ (1999) Metal matrix composites: production by the stir casting method. *J Mater Process Technol* 92:1–7
32. Aghajanian MK, Rocazella MA, Burke JT, Keck SD (1991) The fabrication of metal matrix composites by a pressureless infiltration technique. *J Mater Sci* 26(2):447–454
33. Zhang Q, Chen G, Wu G, Xiu Z, Luan B (2003) Property characteristics of a AlNp/Al composite fabricated by squeeze casting technology. *Mater Lett* 57(8):1453–1458
34. Rack HJ (1988) Fabrication of high performance powder-metallurgy aluminum matrix composites. *Mater Manuf Process* 3(3):327–358
35. Guo MT, Tsao CY (2000) Tribological behavior of self-lubricating aluminium/SiC/graphite hybrid composites synthesized by the semi-solid powder-densification method. *Compos Sci Technol* 60(1):65–74
36. Gupta P, Kumar D, Quraishi MA, Parkash O (2013) Corrosion behavior of Al₂O₃ reinforced Fe metal matrix nanocomposites produced by powder metallurgy technique. *Adv Sci Eng Med* 5(4):366–370
37. Gupta P, Kumar D, Parkash O, Jha AK (2014) “Sintering and hardness behavior of Fe-Al₂O₃ metal matrix nanocomposites (MMNCs)” prepared by Powder Metallurgy. *J Compos*, 1–10
38. Eliasson J, Sandström R (1995) Applications of aluminium matrix composites. In: *Key engineering materials*, vol 104. Trans Tech Publications, pp 3–36

Optimization of Critical Parameters of EDD Steel in Die Cavity Manufacturing



Naveen Anand Daniel, Nirmal Kumar Singh, Umesh Kumar Vates, Bhupendra Prakash Sharma and Sivaraos Subramanian

Abstract Incremental sheet forming (ISF) process is identified as a potential and economically viable process for sheet metal forming for the low volume production. The process is to prove a very flexible and can be carried out on a computer numerical control (CNC) milling machine, robots, or on machines which are specially designed for ISF applications. In present work, the effort has been made to investigate the behavior of Extra Deep Drawing (EDD) steel in ISF process. The state of stresses and strains in incremental forming of VWACF and VWAPF parts have been studied through finite element simulations. The thickness distribution of these parts has been measured experimentally and compared with the results of finite element simulations (FES) using Ansys software. The changes in microstructure and microhardness are being detected due to incremental deformations which have also been studied through optical microscopic analysis and micro-Vickers hardness tester. It has been again verified by performing the experiments.

Keywords SIF · CATIA · FES

N. A. Daniel (✉) · N. K. Singh
IIT (ISM), Dhanbad, India
e-mail: nadaniel@amity.edu

N. K. Singh
e-mail: nks_221@yahoo.co.in

U. K. Vates · B. P. Sharma
Amity University, Noida 201313, Uttar Pradesh, India
e-mail: ukvates@amity.edu

B. P. Sharma
e-mail: bpsharma@amity.edu

S. Subramanian
UTeM, Melaka, Malaysia
e-mail: sivarao@utem.edu.my

1 Introduction

Incremental sheet forming (ISF) is a computer integrated forming technology based on layered manufacturing principles to produce the desired product in three dimensional. Suitable fixture is being provided during the ISF process. The geometry of the part has been manufactured as model given in CAD software. CAD models are being developed generally from cloud data collected using laser scanning in case of complex part geometries. CAM software is used to develop the model and to generate the profile tool path. The tool path is having a number of contours with certain spacing between them. Spacing between two consecutive contours is known as step depth. The blank is deformed into the required shape of the product incrementally in ISF using hemispherical headed forming tool. ISF processes are broadly classified into two specific categories: (a) symmetric and (b) asymmetric incremental sheet forming (AISF). SIFS process can be normally divided into shear spinning and normal spinning. AISF is also split into two types, single point incremental forming (SPIF) and two point incremental forming (TPIF) as per the available literature. It has been analyzed the form accuracy of parts produced in incremental forming using explicit finite element simulations [1]. They found very good correlation between experimental and simulation results [2, 3]. Researchers have simulated SPIF process on quadrangular pyramid using finite element code DYNA 3D [4]. The PAM-STAMP has to simulate the thickness distribution in incremental forming [5]. Researchers have studied effects on constitutive laws in predicting tool force in incremental forming of conical parts [6]. It has been analyzed the shape distortions and spring back problems in incremental forming through numerical simulations [7]. Many of the researchers have incorporated the fracture of used model to predict the simulated data in incremental forming of cone and funnel shapes [8, 9]. Studied is reported to know the strain behavior of materials during incremental forming process through digital image processing technique and FE simulations [10]. It has already been investigated the effect of process parameters on distribution of stresses, strains, and thickness in incremental forming through experimental and FE studies [11].

In the present SPIF process, sheet is formed by using hemispherical punch only without any counter tools. The major advantage of incremental forming is the automated process using robotic programming and simple tooling, which gives required quality. It has been observed that formability of material in ISF is quit better than the conventional deep drawing and stamping processes. This present ISF process can be applied for magnesium, aluminum, steel, and titanium alloys. The processes have ability and potential applications in low volume production, rapid prototyping, biomedical and automotive industries.

2 Experimental Setup

ISF experiments have been carried out on Bridgeport Hardinge 3-axis CNC milling machine on EDD steel. Suitable fixture and jigs are also applied to provide hold and adequate support of the blank and robotic controlled cylindrical tool having hemispherical head. The tool is made up of EN31 die steel, which applied in present investigation. A fine grit abrasive paper and lapping paste are used to improve the surface finish of the tool face and to reduce the friction exert between the tool and the forming sheet. EDD steel sheet having $250\text{ mm} \times 250\text{ mm} \times 1\text{ mm}$ size is being used as blank in order to make different parts during ISF. SAE-40 is applied to minimize the friction, temperature, and wear between the blank and the tool surface. All the experiments are performed with the tool having 10 mm diameter, feed rate of 700 mm/min and 0.2 mm depth in every step. The diagram of the process and experimental setup is shown in Fig. 1.

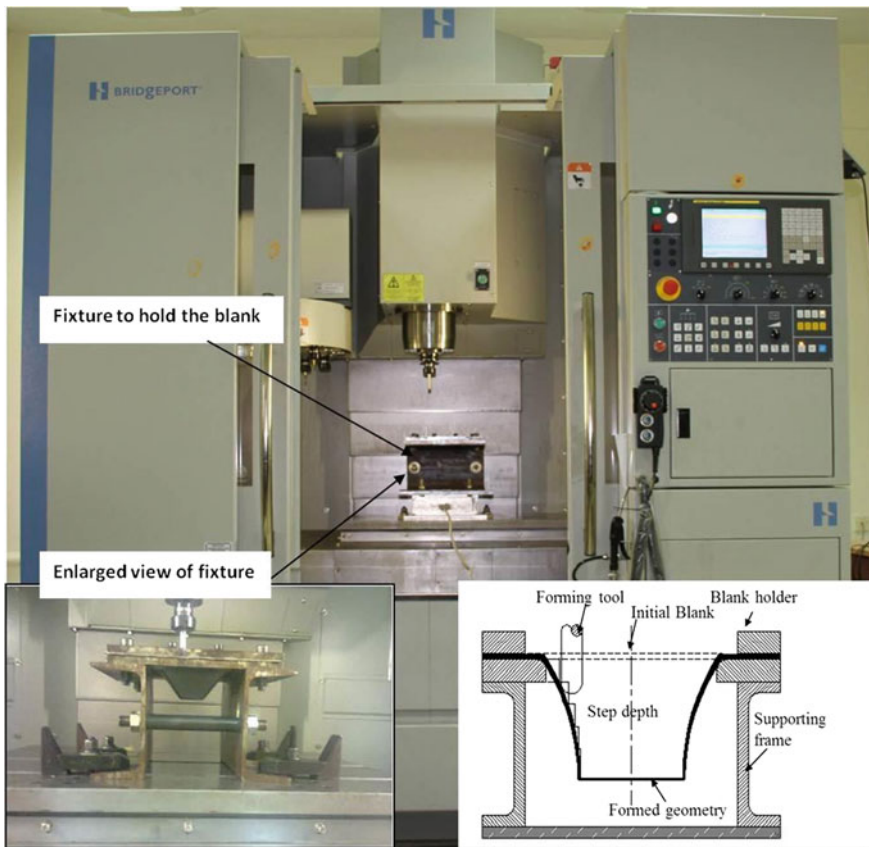


Fig. 1 Single point incremental metal forming

3 Result and Discussion

Thickness distributions along the depth have been studied from the middle so that the thickness could be measured with at every section. In order to increase thickness, the marking of the points is done for every constant distance from the upper portion to the bottom portion of the part using Vernier Height Gauge (VHG). Digital pointed anvil micrometer (DPAM) is used to measure the thickness at every point which instruments having value of least count 0.001 mm. In case of VWACF, the wall angle changes due to thickness changes continuously with the adequate depth. Hence, the theoretical thickness (t_p) and the wall angle (θ_p) corresponding to each marked point (p) is calculated.

It is evident from the applied Fig. 2 that an excellent correlation observed between measured and simulation value of results, which have been compared the correlation between measured value of thickness and analytical thickness distribution for all the used geometries. Depending on the statistical parameters, it is verdict that the accuracy of simulation model is quite higher than analytical model in thickness prediction. Contour plots of thickness distribution and numerical simulations are shown in Fig. 2.

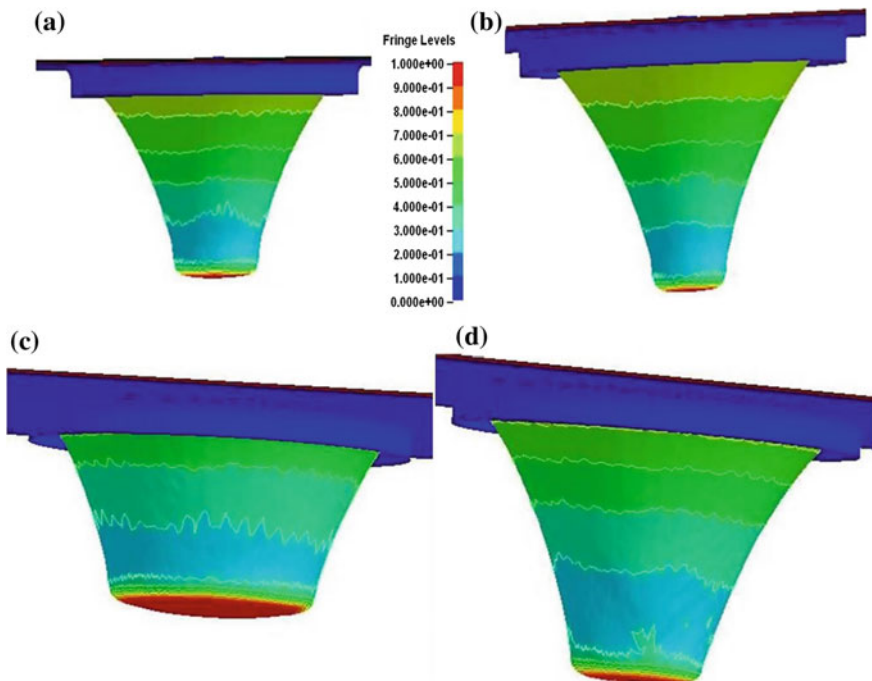


Fig. 2 Contour plots of thickness distribution

The optimal value of formable wall angles is calculated as 75.25° for average thickness of 0.256 mm EDD steel sheet. Maximum variation in thinning angle is 4.6° for different geometries of object. As per the report of researchers there is the deviation found in sheet. Transition point is used to measure the thinning and its characteristics. Circular, elliptical, and exponential generatrices are being considered as very good choices as benchmark parts for wall angle prediction during ISF. Very less variation is observed in wall angle after reaching a particular depth in parabolic generatrix. Varying wall angle of conical frustums are found generally more than the parts with constant wall angle to. It is due to larger force acting in case of constant wall angle product which compared with varying wall angle objects. Incremental sheet formed part has analyzed to detect the fracture surface using SEM photographs. In order to carry out fractographical study of formed product, a standard fracture specimen size is required.

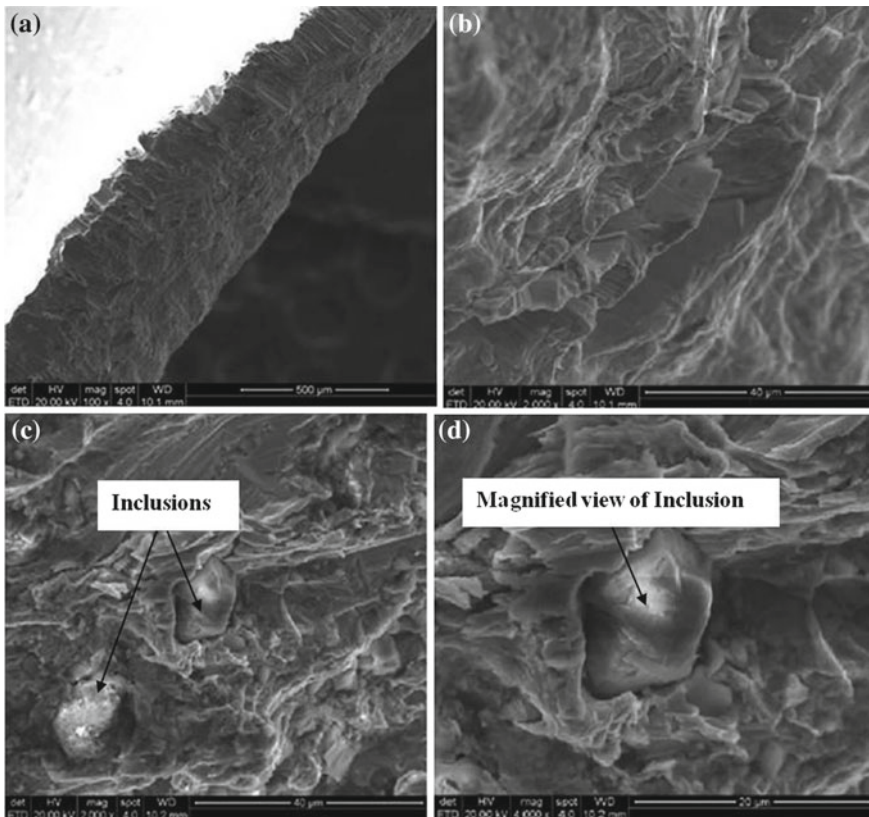


Fig. 3 SEM photograph on fracture point

Inhomogeneous plastic deformation is the main reason for occurrence of cleavage cracks in fracture zone. SEM result revealed that the ductile fracture as Gurson, J-C, and Lamatire models may be used to model which fractures in ISF as given in Fig. 3.

The focus of this work is on investigating thickness distribution, formability, microstructural changes, and distribution of strain in EDD steel in SPIF process using (VWA) pyramidal frustums. The exponential curve segments like circular, parabolic, and elliptic are required for design. The (VWA) pyramidal frustums have been used to minimize the number of experiments which required in evaluation of maximum wall angle compared with conventional and constant wall angle pyramidal frustum. Fracture depth, thickness distribution, and depth for maximum wall angle have been measured with different generatrices. The most optimal formable wall angles have been found as $73^\circ \pm 3^\circ$. Thickness distribution is observed from numerical simulations by LS-Dyna software and result compared with experimental data. Experimental and simulated numerical results revealed the very good correlation between them. Distribution of strains from numerical simulations revealed that faces of the pyramid are under plane strain condition, while the corners are stretching toward biaxial position. The microstructural study is also carried out which revealed that there is a refinement of grain appears after incremental forming of the sheet.

4 Conclusion

A single pass single point negative incremental forming process has been investigated in present work for the estimation of the thinning limit of EDD steel sheet and the maximum wall angle. Various parts (having different wall angle throughout the depth) have been formed till the fracture occurred. Numerical simulation has been performed and obtains the exact walls thickness distribution using LS-Dyna. It is also compared with experimental data which found very close. Thickness distributions obtained from numerical simulations are found more appropriate than the theoretical model. Theoretical model has been found too much poor in predicting variable thickness in formed region, whereas the finite element model is one of the unique tools to predict the thickness in bending and stretching regions. A very good correlation coefficient has been observed like 0.99 which reveals the model adequacy is fit. It is evident that wall angle and thinning are obtained as 75.25° and 0.256 mm, respectively. Maximum variation in wall angle with different generatrix curves has been found as 4.60.

References

1. Ambrogio (2005) Sheet thinning prediction in single point incremental forming. *Adv Mat Res* 6–8:479–486

2. Yamashita M, Mizusawa N, Hojo M, Yabu T (2008) Extensive apoptosis and abnormal morphogenesis in procaspase-3 transgenic zebrafish during development. *J Exp Biol* 211(Pt 12):1874–1881
3. Ceretti (2004) Further experimental investigations and fem model development in sheet incremental forming. *Adv Mat Res* 6–8:501–508
4. Desjardins CA, Perfectti F, Bartos JD, Enders LS, Werren JH (2010) The genetic basis of interspecies host preference differences in the model parasitoid *Nasonia*. *Heredity* 104:270–277
5. Shim MS, Park JJ (2001) The formability of aluminum sheet in incremental forming. *J Mat Process Tech* 113(1–3):654–658. [http://dx.doi.org/10.1016/S0924-0136\(01\)00679-3](http://dx.doi.org/10.1016/S0924-0136(01)00679-3)
6. Hussain G, Gao L, Dar NU (2007) An experimental study on some formability evaluation methods in negative incremental forming. *J Mat Process Tech* 186(1–3):45–53. <http://dx.doi.org/10.1016/j.jmatprotec.2006.12.005>
7. Jackson KP, Allwood JM, Landert M (2008) Incremental forming of sandwich panels. *J Mat Process Tech* 204(1–3):290–303. <http://dx.doi.org/10.1016/j.jmatprotec.2007.11.117>
8. Arfa H, Bahloul R, BelHadjSalah H (2013) Finite element modelling and experimental investigation of single point incremental forming process of aluminum sheets: influence of process parameters on punch force monitoring and on mechanical and geometrical quality of parts. *Int J Material Form* 6(4):483–510. <http://dx.doi.org/10.1007/s12289-012-1101>
9. Jeswiet J, Hagan E, Szekeres A (2002) Forming parameters for incremental forming of aluminium alloy sheet Metal. *Proc Inst Mech Eng [B]: J Eng Manuf* 216(10):1367–1371. <http://dx.doi.org/10.1243/095440502320405458>
10. Ziran X, Gao L, Hussain G, Cui Z (2010) The performance of flat end and hemispherical end tools in singlepoint incremental forming. *Int J Adv Manuf Tech* 46(9–12):1113–1118. <http://dx.doi.org/10.1007/s00170-009-2179-4>
11. Kim YH, Park JJ (2002) Effect of process parameters on formability in incremental forming of sheet metal. *J Mat Process Tech* 130–131:42–46. [http://dx.doi.org/10.1016/S0924-0136\(02\)00788-4](http://dx.doi.org/10.1016/S0924-0136(02)00788-4)

A Theoretical Analysis for Prioritization of Lean Strategies: A Survey of Indian Manufacturing Industries



Virender Chahal and M. S. Narwal

Abstract The purpose of this paper is to discover the lean strategies prioritization in Indian manufacturing industries. It also aims to select the best strategy for industries. It also helps to improve the performance of implemented lean strategies. This research provides a ranking of implemented lean strategies with grey relational analysis (GRA). Evaluating data were collected from seven different industrial experts in terms of four lean performance criteria such as cost, time, quality and flexibility. Here, fuzzy five Likert scale weighted methods are used which are integrated into the GRA with respect to weight the lean performance criteria. This study provides the priority of lean strategies based on selected criteria using the GRA method which is very effective, and the result will help decision-makers to recognize the best strategy in Indian manufacturing industries. To make results more effective, data were collected from 11 different manufacturing industries which will help in future and criteria can be more for a better result. Moreover, as an interesting proposal, the fuzzy linguistic environment may be further incorporated into the practical as per GRA results. In distinction to preceding research, it sets apart for priority based on the scores of GRA with performance criteria. Furthermore, there is very less work available in the literature with GRA for prioritization.

Keywords Grey systems · Indian manufacturing industries · Prioritization · Lean strategies · Grey relational analysis

1 Introduction and Literature Review

In today scenario, lean manufacturing (LM) is not a new word in the manufacturing sector. Every growing industry is focusing to implement of LM because of innovative

V. Chahal (✉) · M. S. Narwal

Department of Mechanical Engineering, Deenbandhu Chhotu Ram University of Science and Technology, Sonapat, Haryana, India
e-mail: vchahal68@gmail.com

M. S. Narwal

e-mail: narwalmohi@rediffmail.com

© Springer Nature Singapore Pte Ltd. 2019

K. Shanker et al. (eds.), *Advances in Industrial and Production Engineering*, Lecture Notes in Mechanical Engineering, https://doi.org/10.1007/978-981-13-6412-9_35

strategies for better quality and best customer satisfaction [1]. It has been approved by entire worldwide for implementation in many industrial sectors, i.e. automobiles, fabrication, manufacturing and public sectors, for minimization of wastes. So it can be said that LM is not only used for manufacturing industries, but also used all over. LM is a mixture of different lean strategies which are 5'S, JIT TQM, TPM, lean training, kaizen, lean thinking, Kan-Ban, zero defect concept, VSM, Six Sigma, etc. [2]. LM delivers superior accuracy and improved productivity with high customer satisfaction with strategies like VSM [3].

After World War II, in Toyota motor company, Eiji Toyoda and Taiichi Ohno find out a way for better quality that was "Toyota Production System" and today is known as "lean system (LS)". LS provide sets of maintenance for higher quality with fewer breakdowns [4]. According to [5], kaizen implementation with lean provides high quality in the industry. Here, industrial wastes can consider the activity such as value-added activity, nonvalue-added activity and necessary nonvalue-added activity. Wastes are unwanted in the industry as well as outside industry that can be eliminated, but it is also so difficult to eliminate. Kaizen is an effective strategy with continuous change for higher quality and better productivity. JIT is a pull system which prevents extra financially like excessive inventory and pressure on the industry. According to [6], lean is the successive agent to improve business scenario in current manufacturing era.

1.1 Research Need and Motivation

Here, question arises that which lean strategy is more effective in Indian manufacturing field. The Indian manufacturing sector is the fastest rising sector around the world. The manufacturing sector is the major pillar of the entire economic development of the country [7]. The manufacturing industries have been implemented LM and their strategies, but they do not know that which strategy is more effective. From last few years, Indian manufacturing industries are focusing on a best way to improve quality with minimum cost and best customer satisfaction, and this research will help them to identify [8]. If industries will know their prioritization with lean strategies, the industry quality will be high with good customer satisfaction. So it is very important to know lean strategies effectiveness as per their prioritization after the successful implementation of LM [9]. A successful implementation only can be possible if we have identified the system strong and weak points to improve [10].

1.2 Research Questions

To understand lean manufacturing concept
 To study lean strategies
 To explore the status of lean strategies by industrial experts
 Prioritization of studied lean strategies

1.3 Research objective

Selection of LS
 Selection of LS performance criteria
 Select the prioritization method
 Prioritization of LS based on selected LS performance criteria

There are so many techniques for prioritization for lean strategies, but grey relation analysis (GRA) is one of the most suitable methods for it [11]. After studying the literature, it is found that the GRA approach is a latent key for prioritization. GRA approach is used for multi-objective optimization which is practical on the calculated response results to select most preferred lean strategy in Indian manufacturing industry [12]. Response results are collected from different lean industrial experts from different industries with help of a well-designed questionnaire.

2 Methodology

This paper's result to prioritization of lean strategies which are 5'S, JIT, TPM, TQM and lean training. These selected lean strategies are selected by literature review. These are more dominating as compared to other lean strategies. This prioritization is based on GRA theory, and required data have been collected from seven industrial experts which have good implementation knowledge about LM. These lean strategies will be rated with help of fuzzy Likert scale five with identified their LM selection criteria's: cost, time, quality and flexibility. All required data will be collected with a well-oriented questionnaire. The linguistic response will be converted into fuzzy numbers and then rated with GRA.

2.1 Data Analysis

After prepare questionnaire, it is sent to different industrial experts to find the priority for the industry as per selected lean strategy selection criteria. Different seven expert's

data have been collected and got the average effect by the well-statistical tool to find the overall result. The responses have been arranged and shown in Table 1.

Selection scale for cost and time is as follows: extremely high—5, very high—4, high—3, low—2, very low—1 (lower the better).

Selection scale for quality and flexibility is as follows: extremely high—1, very high—2, high—3, low—4, very low—5 (higher the better).

Table 1 Combined response of industrial experts

Experts	Lean strategies →	5'S	JIT	TPM	TQM	Lean training
	Lean criteria ↓					
1	Cost	High	High	Very high	Low	High
	Time	High	Low	High	Low	High
	Quality	Very low	Very low	Very low	Low	Very low
	Flexibility	Very low	Low	High	High	Very low
2	Cost	High	High	Very high	Very low	Low
	Time	Very high	Low	High	Low	Low
	Quality	Low	Very low	Low	Low	Low
	Flexibility	Very low	Low	High	High	Very low
3	Cost	High	Very high	High	Low	High
	Time	High	Low	High	Low	High
	Quality	Very low	Very low	Very low	Low	Very low
	Flexibility	Very low	Low	High	High	Very low
4	Cost	High	High	High	Low	High
	Time	Very high	Low	High	Low	High
	Quality	Very low	Low	Very low	Low	Low
	Flexibility	Very low	Low	High	High	Very low
5	Cost	High	High	High	Low	High
	Time	High	Low	High	Low	High
	Quality	Very low	Very low	Low	Low	Very low
	Flexibility	Very low	Low	High	High	Very low
6	Cost	High	Very high	Very high	Low	High
	Time	High	Low	High	Low	High
	Quality	Very low	Low	Low	Low	Very low
	Flexibility	Low	Low	High	High	Very low
7	Cost	High	High	Very high	Low	High
	Time	High	Low	High	Low	High
	Quality	Very low	Very low	Very low	Low	Very low
	Flexibility	Low	Very low	Very high	High	Low

After arranging, the linguistic response result has been converted into the mathematical form shown in Table 2.

Every expert has a different opinion about the selection and prioritization of lean strategies. So it needs to make a common decision of all experts to prioritization lean strategies which is shown in Table 3. It can be solved with an average of all industrial expert response to make average response result.

Table 2 Mathematical value response

Experts	Lean criteria	5'S	JIT	TPM	TQM	Lean training
1	Cost	3	3	4	1	3
	Time	3	1	3	1	3
	Quality	2	2	2	1	2
	Flexibility	2	1	3	3	2
2	Cost	3	3	4	2	1
	Time	4	1	3	1	1
	Quality	1	2	1	1	1
	Flexibility	2	1	3	3	2
3	Cost	3	4	3	1	3
	Time	3	1	3	1	3
	Quality	2	2	2	1	2
	Flexibility	2	1	3	3	2
4	Cost	3	3	3	1	3
	Time	4	1	3	1	3
	Quality	2	1	2	1	1
	Flexibility	2	1	3	3	2
5	Cost	3	3	3	1	3
	Time	3	1	3	1	3
	Quality	2	2	1	1	2
	Flexibility	2	1	3	3	2
6	Cost	3	4	4	1	3
	Time	3	1	3	1	3
	Quality	2	1	1	1	2
	Flexibility	1	1	3	3	2
7	Cost	3	3	4	1	3
	Time	3	1	3	1	3
	Quality	2	2	2	1	2
	Flexibility	1	2	4	3	1

Table 3 Average response result for all experts

Lean strategies	Cost	Time	Quality	Flexibility
5'S	3	3.29	1.86	1.71
JIT	3.29	1	1.71	1.14
TPM	3.57	3	1.57	3.14
TQM	1.14	1	1	3
Lean training	2.71	2.71	1.71	1.86

After making an average response, next step into implement GRA for best result individual for all lean strategies select criteria's which are cost, time, quality and flexibility (Tables 4, 5, 6 and 7).

Table 4 GRA analysis for cost

Lean strategies	Average of all experts responses	Normalized value	Deviation	GRC
5'S	3	0.235	0.765	0.395
JIT	3.29	0.115	0.885	0.361
TPM	3.57	0.000	1.000	0.333
TQM	1.14	1.000	0.000	1.000
Lean training	2.71	0.354	0.646	0.436

Table 5 GRA analysis for time

Lean strategies	Average of all experts responses	Normalized value	Deviation	GRC
5'S	3.29	0.000	1.000	0.333
JIT	1	1.000	0.000	1.000
TPM	3	0.127	0.873	0.364
TQM	1	1.000	0.000	1.000
Lean training	2.71	0.253	0.747	0.401

Table 6 GRA analysis for quality

Lean strategies	Average of all experts responses	Normalized value	Deviation	GRC
5'S	1.86	0	1.000	0.333
JIT	1.71	0.174	0.826	0.377
TPM	1.57	0.337	0.663	0.430
TQM	1	1	0.000	1.000
Lean training	1.71	0.174	0.826	0.377

Table 7 GRA analysis for flexibility

Lean strategies	Average of all experts responses	Normalized value	Deviation	GRC
5'S	1.71	0.715	0.285	0.637
JIT	1.14	1	0.000	1.000
TPM	3.14	0	1.000	0.333
TQM	3	0.07	0.930	0.350
Lean training	1.86	0.64	0.360	0.581

Table 8 Weight for lean strategy selection criteria by experts

Selection criteria for lean strategies	Experts weight notation	Industrial experts weight for selection criteria
Cost	Wc	0.50
Time	Wt	0.25
Quality	Wq	0.15
Flexibility	Wf	0.10

Similarly, weight shown in Table 8 is the average given by the different industrial experts, and it can vary as per the industry implementation, where industrial weight can be varied according to industries which implement LS.

2.2 Method to Apply GRA

Normalize the collected data shown in Tables 4, 5, 6 and 7.

After normalizing, all data will be between 0 and 1.

$$x_1^*(t) = \frac{\max_i(t) - x_{1i}(t)}{\max_i(t) - \min_i(t)} \tag{1}$$

Identify deviation value with normalized data shown in Tables 4, 5, 6 and 7.

$$Dx_1(t) = 1 - x_1^*(t) \tag{2}$$

Computation of grey relational coefficients (GRCs) is noted with $\xi(t)$, and normally value is taken as 0.5.

Computation of grey relational grade (GRG) is shown in Table 9.

Table 9 Calculation of grey relational grade (GRG)

Lean strategies	GRC ξ (t) (cost)	GRC ξ (t) (time)	GRC ξ (t) (quality)	GRC ξ (t) (flexibility)	GRG	%	Rank order
5'S	0.395	0.333	0.333	0.637	0.395	14.60	4th
JIT	0.361	1.000	0.377	1.000	0.587	21.69	2nd
TPM	0.333	0.364	0.430	0.333	0.356	13.16	5th
TQM	1.000	1.000	1.000	0.350	0.935	34.55	1st
Lean training	0.436	0.401	0.377	0.581	0.433	16.00	3rd
Total GRG					2.706		

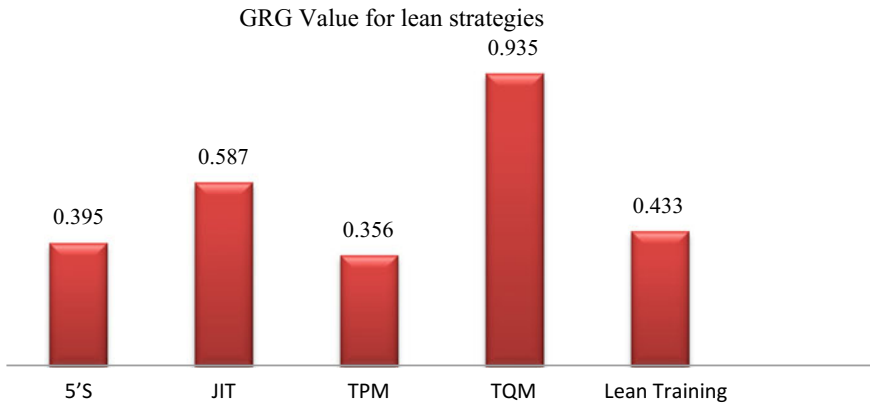


Fig. 1 Chart 1—GRG value for lean strategies

GRC will be the multiple of all GRC values with their related weight given by experts and then the summation of all, i.e.

$$GRG \text{ for } 5'S = GRC(\text{cost}) * Wc + GRC(\text{time}) * Wt + GRC(\text{quality}) * Wq + GRC(\text{flexibility}) * Wf = 0.395 \tag{3}$$

Similarly, GRG results for other lean strategies are shown in Table 9 (Fig. 1).

3 Results and Conclusion

After the complete study, it is found that GRA theory is very precise and effective to reflect the well-maintained prioritization of implemented lean strategies. As per the industrial present competitive behaviour, lean strategies must be prioritization

and GRA theory has very effective results. As result shown in Chart 1, it is clear that TQM is more dominating for manufacturing industry. JIT is in second position, and lean training is at number third. The whole study is based on survey analysis of different industries that know and implemented lean manufacturing. 5'S, JIT, TPM, TQM and lean training are the most useful and implemented strategies for manufacturing industries, so these are considered. After GRC identification, a sole result comes out about lean strategies, but the next thing which will affect is related weight. This weight will be given by industry. For further study, individual industry can be analysed to find its relative priority. Also, we can consider different lean strategies and different other industries for better results.

Future researcher can consider remaining lean strategies and can consider more industries to make research more precise and accurate in present Indian scenario.

References

1. Eswaremoorthi M, Kathiresan GR, Prasad PSS, Mohanram PV (2011) A survey on lean practices in Indian machine tool industries. *Int J Adv Manuf Technol* 52(9–12):1091–1101
2. Sundar R, Balaji AN, Kumar RS (2014) A review on lean manufacturing implementation techniques. *Procedia Eng* 97:1875–1885
3. Seth D, Gupta V (2005) Application of value stream mapping for lean operations and cycle time reduction: an Indian case study. *Prod Plan Control* 16(1):44–59
4. Chan HK, Yin S, Chan FT (2010) Implementing just-in-time philosophy to reverse logistics systems: a review. *Int J Prod Res* 48(21):6293–6313
5. García-Alcaraz JL, Oropesa-Vento M, Maldonado-Macías AA (2017) Kaizen and lean manufacturing. In: *Kaizen planning, implementing and controlling*. Springer, Cham, pp 1–21
6. Nordin N, Belal HM (2017) Change agent system in lean manufacturing implementation for business sustainability. *Int J Supply Chain Manage* 6(3):271–278
7. Thomas T, Sherman SR, Sawhney RS (2018) Application of lean manufacturing principles to improve a conceptual 238Pu supply process. *J Manuf Syst* 46:1–12
8. Tuli P, Shankar R (2015) Collaborative and lean new product development approach: a case study in the automotive product design. *Int J Prod Res* 53(8):2457–2471
9. Amin MA, Karim MA (2013) A time-based quantitative approach for selecting lean strategies for manufacturing organizations. *Int J Prod Res* 51(4):1146–1167
10. Viagi AF, Panizzolo R, Biazzo S (2017) Enablers and constraints in implementing lean manufacturing: evidence from Brazilian SMEs. *J Lean Syst* 2(3):64–86
11. Siddiquee AN, Khan ZA, Mallick Z (2010) Grey relational analysis coupled with principal component analysis for optimisation design of the process parameters in in-feed centreless cylindrical grinding. *Int J Adv Manuf Technol* 46(9–12):983–992
12. Mehat NM, Kamaruddin S, Othman AR (2014) Hybrid integration of Taguchi parametric design, grey relational analysis, and principal component analysis optimization for plastic gear production. *Chin J Eng*

A Systematic Review: Effect of TIG and A-TIG Welding on Austenitic Stainless Steel



Himanshu Garg , Karan Sehgal , Rahul Lamba 
and Gianender Kajal 

Abstract Austenitic stainless steel (ASS) plays an important role in fabrication and manufacturing of products due to its good mechanical properties and easy weldability mostly for all types of welding. In fabrication, there are numerous welding techniques available for ASS such as gas metal arc welding, tungsten inert gas (TIG) welding, electroslag welding, submerge arc welding, electron beam, thermite welding. TIG welding is the most common operation use for joining of two similar or dissimilar metals with heating or applying the pressure by using the filler material. TIG welding technique is used in several industries like automobile, aerospace, marine, etc. due to its quick and precise process. This paper systematically reviewed the TIG and A-TIG welding processes of ASS which included several recent experimental activities. In TIG welding, the inputs such as voltage, current, filler materials and shielding gasses, the type of flux and passes ultimately affect its output weld quality. In addition, a comparison has been provided for parameters of TIG and A-TIG welding process and their weld outcomes such as microstructure, mechanical, penetration depth, and weld bead quality. A-TIG has better hardness and mechanical properties than TIG welding.

Keywords TIG · Hardness · Tensile strength · Penetration depth · Weld joint

1 Introduction

In TIG welding process, inconsumable tungsten electrode is used to produce weld joint. The electrode and weld region is shielded by an inert gas. In this process, an electric arc is produced between a tungsten electrode and the base metal. The arc region is protected by an inert gas or a mixture of gases (Fig. 1). Shielding gas plays a very much significance role in TIG welding process. Shielding gas is selected on the basis of chemical–metallurgical process between the weld region and the gas that is used in TIG welding process [1]. Stainless steel (SS), aluminum, magnesium,

H. Garg (✉) · K. Sehgal · R. Lamba · G. Kajal
Manav Rachna University, Faridabad, Haryana, India
e-mail: garg.himanshu950@gmail.com

© Springer Nature Singapore Pte Ltd. 2019
K. Shanker et al. (eds.), *Advances in Industrial and Production Engineering*, Lecture Notes in Mechanical Engineering, https://doi.org/10.1007/978-981-13-6412-9_36

copper, and many other nonferrous metals, which are difficult to weld, are welded using this process. Efficiency of electric arc and weld region is greatly affected by the density of the shielding gas. Gases like CO_2 and argon (Ar) are having highest density and therefore they are most effective in TIG welding process as a shielding gas [2]. Welding process also has a great impact on microstructure, mechanical properties, and corrosion behavior of welded specimen. In fusion welding processes, there is a great challenge of metallurgical problems like precipitation of phases of weld metal, problem of hot cracking, and loss of metal due to vaporization and they are very common. TIG welding is the most suitable welding method for welding of SS due to its various advantages like ability to weld complex geometries with varying dimension, cleanliness relative to other welding process, and also it is an economical process for joining of two metals due to low setup cost [3]. In TIG welding process, the most important technique is the use of activating flux. In the 1960s, Paton Electric Welding Institute introduced the concept of A-TIG. The depth of penetration increases with A-TIG welding process. Mixture of inorganic material in a volatile medium forms activating flux [4]. Kuo et al. reported that the joints were clean and smooth without flux compared to those joints which are prepared by using flux in TIG welding. Kuo et al. reported that TIG welding joint formed without the use of flux are clean and smooth as compared to the welding joint formed with flux. Formation of slag is less in SiO_2 as compared to the slag produced by the fluxes CaO , Fe_2O_3 , and Cr_2O_3 . TIG welds without flux shows a wide and shallow structure as compared with fluxes such as Fe_2O_3 , Cr_2O_3 , and SiO_2 which gives a narrow and deep structure [5]. Without flux wide and shallowness observed due to less deposition and penetration rate ultimately, it gives the low productivity [6]. The flux powder has different compositions which are very important in increasing the depth of penetration in A-TIG welding process [6].

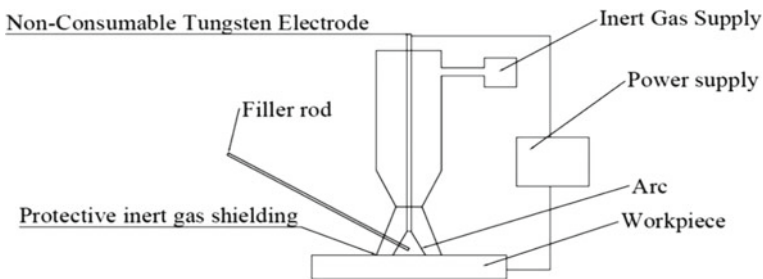


Fig. 1 Schematic diagram of TIG welding

2 Literature Review

Kurt and Samur [1] investigated the microstructure evaluation and mechanical properties of 304 SS welded by TIG welding process by using 308 SS rod as filler metal. It was found that ultimate tensile strength 1800 MPa, yield strength 75 MPa, breaking strength 150 MPa, and percentage elongation were 25% of welded joints. Also it was found that hardness of weld metal, base metal, and heat-affected zone (HAZ) was 233, 321, and 201 HV, respectively. HAZ has low hardness due to coarser grain size in comparison with weld metal. They use optical microscopy (OM) and stereo microscopy (SM) techniques for studying the microstructure of base metal, HAZ, and weld metal. Chromium carbide precipitation and dendrite structure were found in weld metal. Austenite, lathy, and skeletal delta ferrite is observed.

Durgutlu [2] presented a paper in which they studied the effect of H₂ in Ar as shielding gas for TIG welding of 316L SS. In this experiment, pure Ar, 1.5% H₂-Ar, and 5% H₂-Ar are the input parameters and they found that the highest tensile strength was obtained for weld under the shielding gas 1.5% H₂-Ar combination. When H₂ content is increased, the mean grain size in weld metal increased. Also, its width and weld penetration depth got increased. The grain characteristics are found to be more effective in a mixture of 5% H₂-Ar. The hardness of weld metal was lower than HAZ and base metal for all shielding gasses combinations.

Mirshekari et al. [3] has studied the effect on microstructure and hardness of single, multipass gas tungsten arc welding of 304L SS. They identify the presence of austenite and δ ferrite phase. At some point of the solidification process, primary δ ferrite solidifies within the fusion area, transformation of δ to gamma takes place, and complete phase transformation does not occur due to very fast cooling rate. In the weld zone, this results in the occurrence of primary δ ferrite, as it is beneficiary for the problem of hot cracking. It is observed that the δ ferrite are lathy and skeletal were formed in the austenite matrix. Different types of ferrite transformation occur due to different cooling rates in multipass welding. The value of hardness increases as the number of passes in the weld joint increases. Figure 2 shows the two specimens: (a) single pass and (b) multipass. Maximum value of hardness and HAZ was observed in multipass due to the high δ ferrite content and finer grain size in the HAZ by increasing the number of passes.

Nayee and Badheka [4] investigated the effect of activating flux on mechanical and metallurgical properties of dissimilar activated flux Tungsten inert gas welds: predicted the effect of current, welding speed, joint gap and electrode diameter on weld dimension of 6 mm between the carbon steel (CS) and SS. The activated TIG welding process is performed by using three different types of oxide fluxes TiO₂, ZnO and MnO₂. It was found out in activating flux that TiO₂ and ZnO are effective for activated flux TIG welding between CS and SS. Higher depth width ratio was achieved under the use of TiO₂ and ZnO flux as compared to normal TIG welding. Lower angular distortion was found under TiO₂ flux as compared to normal TIG welding. Activated TIG welded joint has better mechanical properties and joint elongation than normal TIG welded joints.

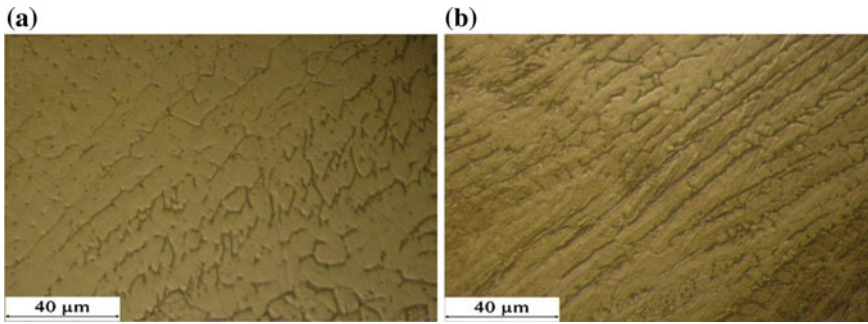


Fig. 2 Optical micrograph of weld region for: **a** single pass; **b** multipass of specimen [3]

Kuo et al. [5] observed the angular distortion, weld morphology, appearance of the surface of different metals like mild steel and 316 SS with and without the use of activated flux. The density of the flux powder which got coated found to be 5–6 mg/cm². It is observed that without using the flux the surface was smooth and clean but with the use of flux like Fe₂O₃, Cr₂O₃, and CaO caused huge amount of slag on the surface; but by using SiO₂, the formation of slag was very less. The angular distortion of TIG welding without flux is very high but still less than the plate thickness but with the use of SiO₂ flux the angular distortion decreases. TIG welding without using flux creates void in metal G3131 mild steel and by using flux like Fe₂O₃, Cr₂O₃, and CaO creates cracks in weld bead of 316 SS, but by the use of SiO₂ flux there is no void or cracks in any of the metal.

Tseng and Hsu [6] investigated the effect of new activating flux on A-TIG welding and investigated the influence of oxide-based activating flux and carrier solvent composite on welding angular distortion, surface appearance, ferrite content, and geometric shape of 316L SS. The flux powder containing sulfide, fluoride, oxide mixed with ethanol and methanol achieved good spread ability. The current range for investigation is taken and the maximum penetration of SS was obtained for activating flux. It was found that the arc pressure increases with an increase in current and in result TIG welding conjunction increases. High arc current increases the penetration capability of welding arc and ferrite content in 316L SS. Higher heat input results in slower cooling rate and that promotes δ ferrite phase transformation into austenite phase SS.

Kumar and Shahi [7] investigated the effect of heat input on microstructure and mechanical properties of TIG welding on 304 SS weld joints. They investigated the heat effect process by taking three heat input levels: low heat (2.563 kJ/mm), medium heat (2.784 kJ/mm), and high heat (3.017 kJ/mm) in TIG. It was found that the ultimate tensile strength at low-heat input was higher than medium- and high-heat inputs. The dendrite size in the fusion zone is smaller in low-heat input joints. With increase in heat input, the HAZ and fusion zone and coarsening of grain increases with an increase in heat input.

Vasantharaja et al. [8] investigated the effect of welding process on microstructure, distortion, and residual stresses in 316 LN SS which is joined by TIG welding and activated TIG welding. It was found that the activated TIG welding process showed lowest peak tensile residual stress, minimum distortion in geometry, and also lower ferrite content. Activated TIG and normal TIG weld joints show lower angular distortion values, while Y grooved joint shows maximum angular distortion values due to non-uniform distribution of residual stresses in top and bottom sides. Y grooved joint exhibited lower peak tensile residual stress on the A-TIG side and higher peak tensile residual stress on the TIG side.

Liu et al. [9] has studied the TIG and A-TIG welding processes on 304 SS. A-TIG welding increases the depth penetration up to 200–300% in one pass with better mechanical properties and refined microstructure. In A-TIG, the acetone is used on the surface of the material to remove the contamination and flux is blend with acetone in a proper amount to make it a thick liquid and applied on metal's surface. It was found that weld penetration in A-TIG welding turns to be 8 mm in comparison with TIG welding which was limited to only 3 mm, and this is due to flux molecule which gets dissociated by the heat generated from the arc and enough capable of collecting the electrons in peripheral region that moves forward to the constricting effect which induced and increased the temperature and pressure to get the deep weld penetration but it was also observed that active elements on the surface like O_2 and sulfur change the direction of fluid flow because the weld pool surface contains the surface tension gradients. The microstructure of A-TIG welding is having higher delta ferrite content in comparison with conventional TIG welding because of higher heat generated in A-TIG welding and also due to the rapid solidification causing meta-stable phase. A-TIG welding has a higher heat input and rapid cooling rate so the delta ferrite content is higher that ensures higher mechanical strength. The flux does not penetrate the weld metal and does not bring any considerable change in the weld metal composition chemically. Microhardness of A-TIG is higher in comparison with conventional TIG welding. The elongation and the tensile strength of A-TIG welding is much higher in comparison with conventional TIG welding due to higher delta ferrite content and also because of absence of inclusion. The bending test concluded that there was no crack or defect with single length more than 3 mm on the welded joint surface.

Choudhary and Duhan [10] observed that the use of different activated fluxes on SS 304 will have different effects on TIG welding. By using A-TIG, the number of passes got reduced without flux. If Ar is used with fluxes like $CaCl_2$, $PbCl_2$, and $LiCl$, then it can give depth penetration up to 100% and with MnO_2 it gives 80%. They observed that using $SiCO_2$ flux will have depth penetration up to 86%. If SiO_2 mixes with TiO_2 in 80 and 20% ratio, then the depth penetration increases around 400%. SiO_2 increases the depth penetration and also weld depth-to-width ratio. The MnO_2 gave the depth penetration up to 4.2 mm and width up to 2.8 mm, but Fe_2O_3 increased the depth penetration 1.2–3.8 mm and width decreased which is about 5.2–3 mm. The value of D/W is maximum in MnO_2 which is 1.50, and it is maximum in comparison with other fluxes. The MnO_2 gives the highest tensile strength of 640.32 MPa and ductility of 39.20 from convectional TIG of strength 605.32 MPa and ductility of 37.90. While using Fe_2O_3 , the tensile strength was

observed to be of 632.7 and ductility of 38.92. The ultimate tensile of ZnO and $MgCl_2$ were observed to be 628.15 and 618.5 MPa and elongation were 38.18 and 37.98%, respectively. TIG welding with activated flux ensures with narrow and deep morphology but without activated it have wide and shallow morphology.

Tseng and Hsien [11] observed that there are a large number of effects of mixing of N_2 with Ar during the welding of 316L SS in the morphology and microstructure of the weld. N_2 was added because it acted as an austenite stabilizer instead of nickel. Tungsten alloy electrode passes the heat from weld current to arc very easily because tungsten electrode has a very temperature resistance property and the choosing of this can improve the arc stability and weld quality. It was found that mixing of nitrogen up to excess amount lead to electrode deterioration that causes the arc instability during welding process with electrode of 2.4 mm. To obtain the stable arc, the electrode must be of 3.2 mm with the mixture of N_2 and Ar_2 to sustain the proper amount of arc heat. It was concluded that by increasing the amount of nitrogen in Ar would increase the arc voltage. The reason behind this is high thermal conductivity in nitrogen in comparison with Ar which further increases the power generated in arc and weld current. It was observed that using excess amount of nitrogen more than 10% in Ar increases the porosity because nitrogen content reaches the solubility limit in SS weld metal. It was observed that there was rapidly reduction in ferrite content of SS weld metal because of nitrogen get dissolved in austenite and is a strong austenite stabilizer. Hardness of 316L SS increases by increasing the amount of nitrogen in argon as shielding gas. Moslemi et al. [12] observed that MMA welding with gas is higher in productivity and quality of weld bead. They have used the TIG welding in which non-consumable electrode is used for the joining of thin material in manufacturing industries. Some processes like precipitation and solidification can cause changes in microstructure. Some other changes such as current can also cause change in mechanical properties. They concluded that if the value of the current increases, then the depth and width of weld pool also get increases. Some factors which get increased are peak temperature, heating rate, and cooling rate, and due to that there is a decrease in temperature gradient which causes an increase in crystallization to form a free dendrite crystal. The fine shape and size of the grains is because of unfinished recrystallization and rapid cooling rate as well as over heating degree of metal with constant speed leads to decrease in temperature gradient. It was observed that there is some sigma phase, carbide phase, and hot cracking on the diffusion welding joint. The sigma phase increased by increasing the arc current but the carbide phase and hot cracking get decreased. The sigma phase is occurred at 600–900 °C. It was found that at 100 A of value of current the value of tensile strength is high. Because of certain defects like hot cracking porosity and shrinkage that cause the fracture on the surface of the metal affects the tensile strength of the metallic samples. It was also observed that at 100 A the highest hardness value could be found. It was declared that as the value of diameter of indention increases the hardness decreases correspondingly.

Das Neves et al. [13] observed that sintered SS products are used for filtration in the petrochemical as well as food-processing industries. Powder form of SS is used for making sintered. It was observed that heat transfer changes by changing the thermal conductivity and the thermal expansion coefficient causing dimensional

changes. In their experiment, sintered plates and pipes were brought out for welding with and without weld metal. So they observed that using weld metal with sintered SS, the weld was totally filled and bead joint was uniformly leveled between the base metal surface and the weld. Weld penetration was totally through the plate with very less stress concentration. Weld penetration was high with high current value and slow welding speed which ultimately resulted in extreme HAZ which lowered the corrosion resistance. The resistance to rupture of welded joint is higher in welded joint with weld metal than without weld metal because of absence of discontinue in welded joint. Higher welding current leads to deep penetration and more weld width, but an increase in welding speed decreases the penetration and width. Longer arc increases the weld width and decreases the penetration. The occurrence of pores in weld width leads to reduction in mechanical properties which happens without weld metal. Weld metal addition will lead to reduction in corrosive properties. The weld zone with weld metal had higher cooling rate than without weld metal.

Tathgir et al. [14] observed the use of TiO₂ as flux in different graded materials like AISI 1020, 304, 316, Duplex 2205 steels. They observed that by using TiO₂ as flux, there was complete depth penetration of the plate but with the use of Ar and 5% of H₂ as shielding gas. This similar effect was found to be in AISI 316 steel also. The maximum depth penetration was observed to be in AISI 304. At 140 A current, the depth penetration in duplex SS is more than 100%. The H₂ gas which is added in shielding gas increases the welding speed and heat during welding. Microhardness was found to be more in AISI 304 and AISI 316 when there is no flux applied on the steels. The toughness gets increases in all the materials because of broken ferrite contents in smaller units (Table 1).

Table 1 Summary of major outcomes for various TIG and A-TIG welding process

Ref	Materials	Type of welding	Parameters	Outcomes
[1]	SS 304	TIG	308 SS filler wire	Coarse-grained structure in HAZ occurred, HAZ shows a dendrite structure. The tensile strength, yield strength, and elongation are 1800, 75 MPa, and 25%, respectively

(continued)

Table 1 (continued)

Ref	Materials	Type of welding	Parameters	Outcomes
[2]	SS 316L	TIG	H ₂ in Ar Gas [0% H ₂ , 1.5% H ₂ and 5% H ₂]	Higher tensile strength for 1.5% H-Ar. Penetration depth and weld bead width increases with increasing H ₂ content
[3]	SS 304L	TIG	308 SS filler metal Multipass TIG	The microstructure of the welds was dendritic which is δ -ferrite. For three pass specimens maximum value of hardness is achieved
[4]	Carbon steel and SS	A-TIG	TiO ₂ , ZnO and MnO ₂ as flux	TiO ₂ and ZnO are effective fluxes for A-TIG. Highest D/W ratio reported under TiO ₂ and ZnO fluxes than other. Lowest angular distortion in TiO ₂ flux
[5]	JIS G3131 mild steel and 316 SS	A-TIG	SiO ₂ as a flux	No void, no cracks, less slag, decrease in angular distortion, deep and narrow morphology
[6]	SS 316L	A-TIG	Current level 125–225 A	The depth of penetration increases with an increase in weld current. A-TIG produced lower angular distortion

(continued)

Table 1 (continued)

Ref	Materials	Type of welding	Parameters	Outcomes
[7]	SS 304	TIG	Low heat (2.563 kJ/mm), medium heat (2.784 kJ/mm), and high heat (3.017 kJ/mm)	Coarsening of grain increases with an increase in heat input. Dendrite size in the fusion zone is smaller in low heat, maximum tensile strength and ductility possessed by the weld joints made using low-heat input
[8]	SS 316LN	TIG, A-TIG	Square butt, double V-groove and Y grooved joint	Smaller grain size, higher ferrite content, and higher tensile residual stress values are obtained when double-sided TIG welding is used. Y grooved joint exhibited maximum angular distortion values
[9]	SS 304	A-TIG	Using oxides	Deep weld penetration and microhardness as well as tensile strength also increases
[10]	SS 304	A-TIG	Activated flux in different compositions	Increases the depth of penetration, deep and narrow morphology, and high tensile strength
[11]	SS 316L	TIG	Ar-N ₂ mixed gas for shielding purpose	Increases the arc current and increases the hardness

(continued)

Table 1 (continued)

Ref	Materials	Type of welding	Parameters	Outcomes
[12]	SS 316	TIG	Increases the welding current	Increase in depth and width of weld pool and increase in tensile strength and hardness
[13]	Sintered SS 316 L	TIG	Sintered material is used	Lower the corrosion resistance and resistance to rupture
[14]	AISI 1020, SS 304, SS 316, 2205 steels	A-TIG	Use of TiO ₂ as flux and addition of H ₂ in shielding gas	Microhardness, penetration and toughness increases

3 Conclusion

Considering the wide range of welding applications, TIG and A-TIG weld behavior of base and filler of various SS is extensively studied. In the present review, weld characteristics of SS in TIG and A-TIG with various parameters, their microstructure, mechanical properties, and comparison between both weld processes are comprehensively discussed. It was found that weld penetration in A-TIG welding is higher in comparison with conventional TIG welding which will vary the properties of welding. It was found that use of different fluxes changes the results of depth penetration and depth-to-width ratio. Weld penetration increases with an increase in the arc current, SiO₂ or TiO₂ as a flux, H₂ in Ar as a shielding gas. The higher hardness values of weldment are reported when Ar is employed with H₂ or N₂ as a shielding gas. The optimized values of tensile strength were obtained in A-TIG when the welding was carried out in multipass mode, MnO₂ used as a flux, Ar and H₂ as a shielding gas, heat input was low, and arc current was around 100 Amp. Dendrite structure was found in TIG welding of SS in which dendrite size increases as heat input, peak temperature, and cooling rate increases. δ ferrite was found in weld zone as welding is done in multipass mode and the content of δ ferrite increases when welded joint is produced in the absence of flux. During solidification, complete transformation of δ ferrite into gamma and austenitic phases is not completed due to faster cooling rate. δ ferrite content is increased as heat input increases in A-TIG. Grain size increases as the content of H₂, heat input, and cooling rate increases. The surface finish is more in A-TIG as compared to conventional TIG welding process.

Acknowledgements Authors would like to express our sincere gratitude to Dr. Ashish Selokar, Accendere KMS-CL Educate Ltd., New Delhi, India, for their valuable comments that led to substantial improvements on an earlier version of this manuscript.

References

1. Kurt Hİ, Samur R (2013) Study on microstructure, tensile test and hardness 304 stainless steel jointed by TIG welding. *Int J Sci Technol* 2:163–168
2. Durgutlu A (2004) Experimental investigation of the effect of hydrogen in argon as a shielding gas on TIG welding of austenitic stainless steel. *Mater Des* 25:19–23
3. Mirshekari GR, Tavakoli E, Atapour M, Sadeghian B (2014) Microstructure and corrosion behavior of multipass gas tungsten arc welded 304L stainless steel. *Mater Des* 55:905–911
4. Nayee SG, Badheka VJ (2014) Effect of oxide-based fluxes on mechanical and metallurgical properties of dissimilar activating flux assisted-tungsten inert gas welds. *J Manuf Process* 16:137–143
5. Kuo CH, Tseng KH, Chou CP (2011) Effect of activated TIG flux on performance of dissimilar welds between mild steel and stainless steel. *Key Eng Mater* 479:74–80
6. Tseng K, Hsu C (2011) Performance of activated TIG process in austenitic stainless steel welds. *J Mater Process Technol* 211:503–512
7. Kumar S, Shahi AS (2011) Effect of heat input on the microstructure and mechanical properties of gas tungsten arc welded AISI 304 stainless steel joints. *Mater Des* 32:3617–3623
8. Vasantharaja P, Vasudevan M, Palanichamy P (2015) Effect of welding processes on the residual stress and distortion in type 316LN stainless steel weld joints. *J Manuf Process* 19:187–193
9. Liu G-H, Liu M-H, Yi Y-Y et al (2015) Activated flux tungsten inert gas welding of 8 mm-thick AISI 304 austenitic stainless steel. *J Cent South Univ* 22:800–805
10. Choudhary S, Duhan R (2015) Effect of activated flux on properties of SS 304 using TIG welding. *Int J Eng* 28:290–295
11. Tseng KH, Hsien KC (2011) Effect of Ar-N₂ mixed gas on morphology and microstructure of type 316L stainless steel TIG weld metal. *Adv Mater Res* 295–297:1919–1924
12. Moslemi N, Redzuan N, Ahmad N, Hor TN (2015) Effect of current on characteristic for 316 stainless steel welded joint including microstructure and mechanical properties. *Procedia CIRP* 26:560–564
13. Das Neves MDM, Barbosa LP, Da Silva LCE, Correa OV, Costa I (2010) TIG welding of sintered AISI 316 L stainless steel. *Mater Sci Forum* 660–661:454–459
14. Tathgir S, Bhattacharya A, Bera TK (2015) Influence of current and shielding gas in TiO₂ flux activated tig welding on different graded steels. *Mater Manuf Process* 30:1115–1123

Evaluation of Key Challenges to Industry 4.0 in Indian Context: A DEMATEL Approach



Ankur Aggarwal, Sumit Gupta and Manish Kumar Ojha

Abstract The rapid development of information technology, analytics, computing capacity and hardware has led to increasing affinity towards the concept of Industry 4.0. Industry 4.0 uses cyber-physical systems (CPS), Industrial Internet of Things (IIoT) and cloud data sharing to develop intelligent manufacturing systems. The Indian industries under the patronage of national and local government initiatives like Make in India and Digital India are looking forwards to adopting best in class manufacturing infrastructure to support the changing industrial environment and utilize the immense opportunities ahead. For this purpose, Industry 4.0 will play a vital role in achieving manufacturing competitiveness. This paper is an attempt to evaluate the key challenges of Industry 4.0 in the Indian context. A decision-making trial and evaluation laboratory (DEMATEL) approach is used to establish relations between the key challenges.

Keywords Industry 4.0 · India · Challenges · DEMATEL · CPS · IIoT

1 Introduction

With the ever-changing economic scenario, India is again in the spotlight. It has been an IT stronghold of the world and now its manufacturing sector is on its way to another revolution labelled as ‘Industry 4.0’ [1]. Industry 4.0 is a highly efficient system of interconnected digital entities that work in coordination to help make intelligent decisions [2]. It majorly utilizes cyber-physical systems, information technology and smart devices. It can help transform Indian traditional plants into smart factories that can increase business gains. Decentralized control and self-learning are important factors [3]. Intelligent components are characterized by their ability to self-understand, communicate and implement information at every stage of the system. Decentralization of control aids by making the transition smoother with varying market demands. Customer requirements have also changed. This puts immense

A. Aggarwal (✉) · S. Gupta · M. K. Ojha
Department of Mechanical Engineering, Amity University, Noida, Uttar Pradesh, India
e-mail: ankuragg92@gmail.com

© Springer Nature Singapore Pte Ltd. 2019
K. Shanker et al. (eds.), *Advances in Industrial and Production Engineering*, Lecture Notes in Mechanical Engineering, https://doi.org/10.1007/978-981-13-6412-9_37

pressure on the industry to keep modifying their business models to stabilize competition. Majorly in India, a gap is seen between the application level and the factory level. Industry 4.0 can help bridge this gap.

Indian government has come up with initiatives like Green Energy Corridors, Make in India, Digital India and Skill India that aim to promote the use of renewable energy sources, in-house manufacturing, digitalization of industries by advanced technologies and training and education. According to IBEF, India has set a high target of achieving a 25% contribution from manufacturing sector of its gross domestic product (GDP) by the year 2025 [4]. This can be realized by adopting practices of Industry 4.0. In order to adopt Industry 4.0, the readiness of the industries must be checked. The manufacturing sector may face significant challenges in this process. This paper provides a summary of the key challenges that are/may be faced by industries.

The outline of the paper is: The research background of Industry 4.0, its components and key challenges are discussed in Sect. 2. Section 3 shows the application of DEMATEL approach on the case industry selected for research. After this, discussion of results is presented in Sect. 4 followed by concluding remarks in Sect. 5.

2 Research Background

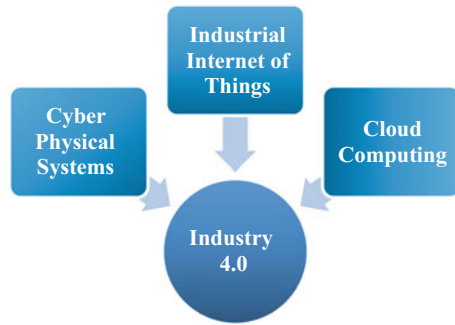
2.1 Industry 4.0

Industry 4.0 was first seen as part of a German project. It can be defined as the application of computing and IT technologies to enhance the connectivity of the various sections of the industry. This connectivity enables integration between the elements of the entire supply chain, i.e. machinery, workers, suppliers and end customers. Industry 4.0 makes it possible to collect and examines the technical details from the machines to make the processes faster, flexible and efficient. This will lead to increase in industrial output and productivity. Industry 4.0 promotes collaboration among different plants of the company irrespective of the location. This is achieved by communication devices that are focussed on factors like reliability and longevity. Industry 4.0 creates a highly flexible and intelligent factory known as ‘Smart Factory’ [5]. For this, it has core components that enable its realization and sustenance.

2.2 Core Components of Industry 4.0

The main components of Industry 4.0 are cyber-physical systems (CPS), Industrial Internet of Things (IIoT) and cloud computing. Figure 1 shows the core components of Industry 4.0.

Fig. 1 Core components of Industry 4.0



Cyber-Physical Systems (CPS). CPS is a system that is driven by computer algorithms which have been integrated with Internet and its users. It combines the software (cyber components) and hardware (physical components) to generate an intense link [6]. CPS aims to ensure deep connectivity and real-time data collection between the physical entities of the factory. It also enables the analysis of the data to help make intelligent decisions [7]. A simple CPS comprises a control unit which actuates the physical components interacting with the real world and sensors that detect and process the data [8]. In order to reach the stature of Industry 4.0, there needs to be a specific approach, which is addressed by CPS by making the processes self-managed and autonomous.

Industrial Internet of Things (IIoT). IIoT is a literal upgrade of the Internet of Things (IoT), as in when IoT is applied to industries. IoT is the larger out of the two which aims at harnessing the power of Internet connectivity to improve business functions [9]. IIoT focusses on stronger requirements of manufacturing namely longevity of operation and safety of personnel [10]. IIoT utilizes machine learning to capture and communicate data [11]. This data can help identify issues sooner and practise better process control. It also provides better insight into the operational parameters of the industry, which leads to transformation of processes [12]. This accelerates productivity, thereby improving profits, which is thought behind Industry 4.0.

Cloud Computing. Cloud computing is an enabler of Industry 4.0. It offers storage and memory through the Internet as a service to the user. As buying physical storages is expensive, companies have switched to cloud computing. It offers high performance at lower cost. Cloud storage stores the communication between the machines as well as between machines and personnel. Cloud computing provides its users with an IT platform and resources for all needs. It relies on sharing of information both within and outside the organization. This helps organizations run their business faster and meet the demands of the market and customers at the earliest [13]. This nature of cloud computing makes it important for application of Industry 4.0.

2.3 Key Challenges to Industry 4.0

In order to adopt the Industry 4.0 in Indian industries, the major roadblocks to its implementation need to be identified. The following six key challenges have been found out from the extensive literature review and discussion with academicians.

Management Commitment (C1). Any major organizational change has to pass through the management, and the management's willingness is important [14]. Industry 4.0 brings a major change and is required to be backed up by the management. The major challenge in India is the lack of leadership as any change comes from the top down in an industry [1]. The leaders must be committed to the goal of Industry 4.0. They must be willing to re-analyse their organizational structure and maintain an enthusiastic work atmosphere in order to drive this industrial revolution.

High Investment and Future Viability (C2). Industry 4.0 brings with it high implementation cost. This high cost is attributed to machinery and equipment, training of personnel and consultancy services. For Indian industries, that is dominated by a large percentage of small-scale industries, this transformation may come at a cost of their market value [15]. Moreover, new entrants may acquaint themselves with industry models and threaten the existence of the prevalent players. As Industry 4.0 can both be a complicated and calculated risk, this change has uncertain future benefits and absence of benchmarking tools to evaluate accurate business gains.

Employee Fear and Resistance (C3). The pillars of any industry are its employees. The employees need to be provided with advanced training and education. As Industry 4.0 is computer oriented and relies on high reliability and accuracy, the unskilled workers stand at the risk of losing their jobs [16]. India has always faced issues with availability of skilled workers, labour unions and their management. The workers may be reluctant to be a part of such an organizational change [17]. The workers are not only required to improvise technical skills but also analytical decision making, in order to extensively use the new technologies.

Technical Fit and Integration of CPS (C4). The concept of Industry 4.0 revolves around CPS. The development of CPS in accordance with the existing facilities is a tedious job. It not only requires monetary support but dependence on external services. Indian Industries have been practising conservative ways for long enough. This makes generation and verification of a CPS model complicated. In order to benefit from Industry 4.0, the organizations must have proper methods of data collection and computation. This will require new visualizations and development of mathematical models and algorithms.

IT Security Concerns (C5). As IIoT involves interconnection of everything in an industry, it brings the risk of cybersecurity. The overall connectivity implies the use of more computers which will be burdensome to handle and control [18]. Any glitch in IT systems can be a setback for the organization. Moreover, a cyberattack can

be devastating as it may cause a mark on the reputation of the company [19]. With increasing digitization of the assets, the security of the IT infrastructure is utmost important for the organization.

Lack of Government Support and Legal Issues (C6). The Indian government has come up in favour of Industry 4.0, but it lacks aggressiveness and supporting policies. It needs to promote the development of networking agencies that can help promote adoption of IIoT in industries. With the onset of new technologies, the government must promote cross-border trades to enhance technology sharing. On the other hand, strict laws regarding privacy protection must be enforced to avoid wrong handling of data. Legal regulations and compliances in regard to labour and safety management must be redesigned to aid adoption of Industry 4.0.

3 Application of DEMATEL and Case Example

This section discusses the DEMATEL approach and its application. For the analysis of the relationships between the key challenges, we have used decision-making trial and evaluation laboratory (DEMATEL) approach [20]. This technique was evolved by Battelle Memorial Institute, Geneva and is a structuring tool used to find out the cause and effect relationship among different factors. Other than finding out how the factors are connected; it also indicates the influence of the factors on the main system. The case example is a major automobile company with its strong presence in India. The study was subjected to its manufacturing facility in Delhi—NCR area. The respondents consisted of senior-level managers, production of charges, line managers and workers. The inputs were received in the form of pairwise comparisons (Table 1) between the identified challenges by brainstorming. The following are the steps of DEMATEL approach:

Table 1 Average (direct relation) matrix A

	C1	C2	C3	C4	C5	C6
C1	0	1.8	1.4	2.6	0.8	0.2
C2	3.5	0	2.2	3.2	1.7	0.6
C3	2.3	0.4	0	1.3	0.2	1.5
C4	3.4	2.3	2.1	0	2.6	0.4
C5	3.1	2.4	0.8	2.5	0	0.3
C6	3.7	2.8	2.3	1.6	2	0

3.1 Define Challenges and Evaluation Scale

The challenges have been described in Sect. 2. A total of six challenges are considered. The evaluation scale has numeric values ranging from ‘0’ to ‘4’, i.e. from low to high degree of influence/interrelation among the challenges.

3.2 Construct the Average (Direct Relation) Matrix

The responses have been obtained to form the inputs of the average matrix. The respondents have rated the influence of one challenge ‘i’ on another challenge ‘j’ based on the evaluation scale and filled a matrix of pairwise comparisons [21]. Let A [i × j] be the average matrix and k be the total respondents. The a_{ij} values of matrix A have been obtained by averaging the responses a_{ijk} of the k respondents for each comparison. Table 1 shows the average matrix A.

3.3 Calculate the Normalized Matrix B

Let B be the normalized matrix of the average matrix A. Calculate factor λ by using Eq. 1 which is as follows:

$$\lambda = \frac{1}{\text{Max}_{1 \leq i \leq n} \left(\sum_{j=1}^n a_{ij} \right)} \tag{1}$$

Matrix B as shown in Table 2 is calculated by using Eq. 2, i.e. multiplying matrix A by a factor λ,

$$B = A\lambda \tag{2}$$

Table 2 Normalized matrix B

	C1	C2	C3	C4	C5	C6
C1	0	0.15	0.11	0.21	0.06	0.02
C2	0.28	0	0.18	0.26	0.14	0.05
C3	0.19	0.03	0	0.10	0.02	0.12
C4	0.27	0.19	0.17	0	0.21	0.03
C5	0.25	0.19	0.06	0.20	0	0.02
C6	0.30	0.23	0.19	0.13	0.16	0

Table 3 Total relation matrix *C*

	C1	C2	C3	C4	C5	C6
C1	0.41	0.39	0.35	0.50	0.27	0.11
C2	0.84	0.39	0.52	0.70	0.43	0.18
C3	0.50	0.26	0.21	0.36	0.19	0.18
C4	0.81	0.53	0.50	0.47	0.47	0.16
C5	0.73	0.50	0.38	0.60	0.27	0.13
C6	0.93	0.63	0.57	0.66	0.48	0.15

3.4 Construct the Total-Relation Matrix *C*

The normalized matrix *B* can be transformed to total-relation matrix *C* as shown in Table 3 by using the Eq. 3,

$$C = B(I - B)^{-1} \tag{3}$$

where *I* = Identity Matrix.

3.5 Calculate the Challenge’s Degree of Influence

The degree of influence of the challenges is attributed to the degree of prominence and degree of cause and effect. The values *D* and *E* are calculated by the Eqs. 4 and 5,

$$D = [d_{ij}]_{n \times 1} = \left[\sum_{j=1}^n c_{ij} \right]_{n \times 1} \tag{4}$$

$$E = [e_{ij}]_{1 \times n} = \left[\sum_{i=1}^n c_{ij} \right]_{1 \times n} \tag{5}$$

The prominence or correlation with others is given by (*D* + *E*) and cause/effect is given by (*D* – *E*) as shown in Table 4.

3.6 Construct the Cause–Effect and Prominence Graph

The prominence and cause/effect are shown in Figs. 2 and 3, respectively. They have been developed from values obtained in Table 4.

Table 4 Prominence and cause/effect values

	<i>D</i>	<i>E</i>	<i>D + E</i>	<i>D - E</i>
C1	2.02	4.22	6.24	-2.19
C2	3.06	2.70	5.76	0.36
C3	1.70	2.53	4.22	-0.83
C4	2.94	3.29	6.23	-0.35
C5	2.62	2.11	4.72	0.51
C6	3.41	0.90	4.31	2.51

Fig. 2 Prominence graph

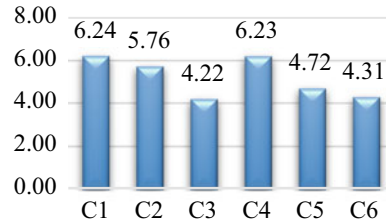
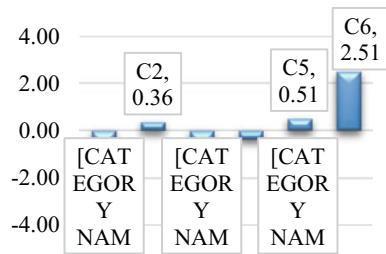


Fig. 3 Cause-effect graph



4 Results and Discussion

Table 4 shows the *D + E* and *D - E* values for the challenges. *D + E* signifies the prominence or the extent of correlation with other challenges. In other words, to what degree the challenges influence each other. The challenge, management commitment (C1) has the highest prominence value of 6.24 followed by technical fit and integration of CPS (C4) with a value of 6.23. This shows that C1 and C4 have the most correlation or influence on the other challenges. On the other hand, challenge employee fear and resistance (C3) has the lowest prominence value of 4.22, showing its low influence on the other challenges as well as on the system. Therefore, prominence of C1 and C4 is quite high signifying that commitment of management and the technical feasibility of the CPS have a high impact on the behaviour and influence of other barriers. *D - E* shows the values of cause and effect for the challenges. If (*D - E*) is greater than zero (0), the challenge is categorized as a cause challenge while if (*D - E*) is less than zero (0), the challenge is an effective challenge. From the values, high investment and future viability (C2), IT security concerns (C5) and lack of government support

and legal issues (C6) are the cause challenges, while management commitment (C1), employee fear and resistance (C3) and technical fit and integration of CPS (C4) are effect challenges. The challenge C6 has the highest positive value of 2.51, making it the primary cause challenge, while C1 has the highest negative value of -2.19 making it the most effected challenge. The cause challenges like C2, C5 and C6 indirectly results in the effect challenges or barriers like C1, C3 and C4. The cause challenges are considered the major obstacles to the implementation of Industry 4.0.

5 Conclusion

The paper has presented the key challenges to the adoption of Industry 4.0 in the Indian subcontinent. Six key challenges have identified that influence and can act as barriers to Industry 4.0. For the same, a case industry was selected to analyse the effect of these challenges by using DEMATEL approach.

Management commitment was found out to be the most prominent and influencing challenge for the industry. The guidance and direction of management are utmost important to bring any organizational change. It influences the decisions and actions of all the components in the industrial environment. Integration of CPS can almost equally affect the adoption of Industry 4.0. As CPS requires advanced technologies involving sensors, etc., its utilization is a complicated and difficult task. High monetary investment and lack of commercial analysis of the components of Industry 4.0 also creates a dilemma. The support of the government and its policies is the major challenge that affects other challenges. The Indian government has come up with new initiatives like Make in India, etc., but in order to acquire the benefits of Industry 4.0, it must develop a modelling and framework approach. The government must also develop consultancies in collaboration with top research institutes that can guide the industries. Also, ease of policies like import of foreign technologies, etc., can motivate the industrial management, to take a step forward in the direction of Industry 4.0.

Further, research can be amplified by analysing the above challenges in the context of other industries like machine tool and chemical. Also, a fuzzy-DEMATEL or grey-DEMATEL, a hybrid approach can be utilized to better incorporate the uncertainties that arise during response collection.

References

1. Bosch India Blog. <http://blog.boschindia.com/iot/industry-4-0-digitisation-of-manufacturing/>
2. Global Innovation & Technology Alliance (GITA). <https://www.gita.org.in/Attachments/Reports/India%E2%80%99s%20Readiness%20for%20Industry%204.0.pdf>
3. Srivastava SK (2016) Industry 4.0. Lucknow: BHU Engineer's Alumni
4. India Brand Equity Foundation. <https://www.ibef.org/>
5. Wikipedia. https://en.wikipedia.org/wiki/Industry_4.0

6. Wikipedia. https://en.wikipedia.org/wiki/Cyber-physical_system
7. Lee J, Bagheri B, Kao HA (2015) A cyber-physical systems architecture for industry 4.0-based manufacturing systems. *Manuf Lett* 3:18–23
8. Jazdi N (2014, May) Cyber physical systems in the context of industry 4.0. In: IEEE international conference on automation, quality and testing, robotics, 2014, pp 1–4
9. Roblek V, Meško M, Krapež A (2016) A complex view of industry 4.0. *SAGE Open* 6(2), 2158244016653987
10. Serpanos D, Wolf M (2018) industrial internet of things. In: *Internet-of-Things (IoT) systems*. Springer, Cham, pp 37–54
11. TechTarget Network. <http://internetofthingsagenda.techtarget.com/definition/Industrial-Internet-of-Things-IIoT>
12. Gilchrist A (2016) *Industry 4.0: the industrial internet of things*. Apress
13. Wikipedia. https://en.wikipedia.org/wiki/Cloud_computing
14. IIoT World. <http://iiot-world.com/connected-industry/nine-challenges-of-industry-4-0/>
15. Cleverism. <https://www.cleverism.com/industry-4-0/>
16. TRG International. <http://blog.trginternational.com/industry-4.0-the-fourth-industrial-revolution-opportunities-and-challenges>
17. Market Mogul. <https://themarketmogul.com/industry-4-0-challenges/>
18. Security Matters. <https://www.secmatters.com/blog/3-challenges-of-industry-4.0-and-how-to-address-them>
19. IoT Indian Mag. <https://www.iotindiamag.com/2017/06/industry-4-0-shaped-india-challenges-developments/>
20. Mangla S, Kumar P, Barua MK (2014) An evaluation of attribute for improving the green supply chain performance via DEMATEL method. *Int J Mech Eng Robot Res* 1(1):30–35
21. Tsai SB (2018) Using the DEMATEL model to explore the job satisfaction of research and development professionals in China's photovoltaic cell industry. *Renew Sustain Energy Rev* 81:62–68

AHP Based Model for Evaluation of Sustainable Manufacturing Enablers in Indian Manufacturing Companies



Abhishek Singh, Zareef Askary, Sumit Gupta, Ashwini Kumar Sharma and Priyank Shrivastava

Abstract In the present scenario, the success of an industry depends on its sustainable manufacturing performance where competitiveness is followed by superior performance. To remain competitive in the market, the manufacturing companies need to evaluate their performance through the manufacturing sustainability. This paper presents an AHP-based model for enablers of sustainable manufacturing evaluation in Indian manufacturing companies. A hierarchy structure is established based on the proposed key enablers of sustainable. The company's score is calculated to assess sustainability in manufacturing against the enablers and the companies rank is determined based on their scores.

Keywords AHP · Rank and weight · Sustainable manufacturing

1 Introduction

Since we depend on natural resources especially conventional ones and the process that we follow are also conventional, therefore wastage and environmental pollution are inevitable. Therefore, we need some alternative techniques for manufacturing of products.

Sustainable manufacturing plays a vital role in many areas of production. This is because sustainable manufacturing focuses upon three major areas along with the manufacturing of products, they are economic, social and environmental. But, the adoption of this technique is a very hard-core task for any organisation as they lag the knowledge of enablers and barriers of sustainable manufacturing [1].

A. Singh · Z. Askary · S. Gupta (✉) · P. Shrivastava
Department of Mechanical Engineering, Amity School of Engineering and Technology, Amity University,
Noida 201313, UP, India
e-mail: sumitgupta2007@gmail.com

A. K. Sharma
Kaziranga University, Jorhat 785006, Assam, India

Sustainable Manufacturing (SM):

SM may be defined as manufacturing of products in such a way that it reduces the harmful impacts on society and environment along with total utilization of resources and with minimum money expenditure. Also, it gives attention towards the conservation of conventional resources for the sake of future generations [2].

2 Literature Review

After reviewing several papers, it is clear that the gaps of the research in this field are in the area of key enablers. This is a new field so the research done here is lacking the necessary amount of literature. Although some papers have highlighted the enablers but it does not provide a clear view of the enablers.

SM gives priority to the improvement of materials' handling and waste management with optimum use of energy, hence creating the products that are environmental friendly [3]. SM has potential to handle the raw material optimally, by producing new product using present technology and rational behaviour of community [4]. SM covers problems related environmental issues, green manufacturing, product life cycle, and advance manufacturing services and processes [5]. SM gives priority to environmental, economic and social sustainability as crucial enablers for sustainable manufacturing [6]. SM focuses to minimize the manufacturing processes in order to achieve the best production efficiency for organizations [7]. The authors have highlighted about how sustainable machining process design is an important in factor in implementation of SM and for this designing more investments have to be made [8]. The authors highlighted about the use of alternative fuel than coal in cement industry, as burning of fossil fuels is hazardous and the use of alternative fuel will decrease the burden of waste disposal [9]. SM has become an important part in the business. The researchers have suggested that more importance must be given to product life cycle, reducing recycling, redesigning, remanufacturing and recover as these are very important features of SM [10, 11].

3 Problem Novelty

Even though there have been lots of researches done on sustainable manufacturing, yet there are very small amount of studies have actually integrated sustainability as a part of manufacturing process.

The purpose of this research is to:

- Identify the enablers for sustainable manufacturing.
- Assess these enablers of sustainable manufacturing using AHP technique.

4 Methodology

The enablers are identified through the brainstorming with industry professional and experts. Enablers are denoted as E1, E2, E3 ... E10, and the alternatives are represented as A1, A2, A3 and A4. The alternatives are industries from different four sectors viz. automobile, machinery, electrical and electronics and process sectors. The different enablers are shown in Table 1. The ranking of enablers is done using mean values and if they are same then the ranking is done on the basis of standard deviation.

4.1 Analytical Hierarchy Process (AHP)

The analytic hierarchy process (AHP) is a structured approach for arranging and analysing tough decisions in a hierarchy using mathematics and psychology. It was developed by Thomas L. Saaty in the 1970s.

The AHP helps in making decisions by finding best suits their goal and their understanding of the problem. It makes a thorough and reasonable framework for structuring a decision problem. This technique first breaks the problem into a hierarchy of easier comprehended sub-problems and then their evaluation is done individually. These each elements hierarchy are related to each other which are then evaluated cautiously and then estimated.

Table 1 List of enablers

S. no.	Name of enabler	Mean	SD	Rank
E1	Practices in organization for reduction of energy, raw material or any other natural resource	4.15	0.813	1
E2	Investment in innovation and technology	4.15	0.894	2
E3	Improve company image through green manufacturing products	4.1	0.852	3
E4	Organizational belief of long-term benefits through sustainability	4.0	0.795	4
E5	Availability of supporting infrastructure for environmentally friendly manufacturing	3.95	0.887	5
E6	Social cultural responsibilities towards green products	3.85	0.813	6
E7	Organization concerned about health and safety issues	3.85	0.852	7
E8	Organization rules, regulations and laws for better environmental practices	3.85	0.894	8
E9	Government promotions and regulations	3.8	0.768	9
E10	Disposal of waste	3.8	0.951	10

When the hierarchy is built, the decision makers methodically evaluates all the elements of the different each hierarchy by comparing the elements with each other by seeing how much one factor puts impact on the other factor. The decision makers used appropriate facts along with their own understanding and discussion with others, makes decision for which factor causes more impact on other.

5 Problem Analysis

Implementation of AHP:

The alternatives are compared with each other and rankings are given. Then normalized weightage and global weightage are calculated and the best decision is found out.

- Table 2 compares E1 enabler with each alternative and priority is given.
- Table 3 compares E2 enabler with each alternative and priority is given.
- Table 4 compares E3 enabler with each alternative and priority is given.
- Table 5 compares E4 enabler with each alternative and priority is given.
- Table 6 compares E5 enabler with each alternative and priority is given.
- Table 7 compares E6 enabler with each alternative and priority is given.
- Table 8 compares E7 enabler with each alternative and priority is given.
- Table 9 compares E8 enabler with each alternative and priority is given.
- Table 10 compares E9 enabler with each alternative and priority is given.
- Table 11 compares E10 enabler with each alternative and priority is given.
- Table 12 compares all the alternatives with each alternative and priority is given.

Table 2 Alternatives comparison for E1

A1	1	5	1	7
A2	0.2	1	0.2	3
A3	1	5	1	7
A4	0.142857	0.333333	0.142857	1

Table 3 Alternatives comparison for E2

A1	1	3	1	1
A2	0.333333	1	0.333333	0.333333
A3	1	3	1	1
A4	1	3	1	1

Table 4 Alternatives comparison for E3

A1	1	5	1	9
A2	0.2	1	0.2	5
A3	1	5	1	9
A4	0.111111	0.2	0.111111	1

Table 5 Alternatives comparison for E4

A1	1	3	3	5
A2	0.333333	1	1	3
A3	0.333333	1	1	1
A4	0.2	0.333333	1	1

Table 6 Alternatives comparison for E5

A1	1	1	3	9
A2	1	1	3	9
A3	0.333333	0.333333	1	7
A4	0.111111	0.111111	0.142857	1

Table 7 Alternatives comparison for E6

A1	1	3	0.333333	0.333333
A2	0.333333	1	0.2	0.2
A3	3	5	1	1
A4	3	5	1	1

Table 8 Alternatives comparison for E7

A1	1	3	1	5
A2	0.333333	1	0.333333	3
A3	1	3	1	5
A4	0.2	0.333333	0.2	1

Table 9 Alternatives comparison for E8

A1	1	1	0.333333	1
A2	1	1	0.333333	1
A3	3	3	1	3
A4	1	1	0.333333	1

Table 10 Alternatives comparison for E9

A1	1	3	1	7
A2	0.333333	1	0.333333	5
A3	1	3	1	7
A4	0.142857	0.2	0.142857	1

Table 11 Alternatives comparison for E10

A1	1	3	3	9
A2	0.333333	1	1	8
A3	0.333333	1	1	8
A4	0.111111	0.125	0.125	1

Table 12 Comparison matrix of alternatives

Level	Weight	A1	A2	A3	A4
E1	0.258729	0.422511	0.104383	0.422511	0.050596
E2	0.258729	0.3	0.1	0.3	0.3
E3	0.162806	0.424415	0.113806	0.424415	0.037364
E4	0.104373	0.5255	0.209803	0.157849	0.106849
E5	0.071966	0.397736	0.397736	0.168165	0.036364
E6	0.033308	0.152354	0.067924	0.389861	0.389861
E7	0.033308	0.389861	0.152354	0.389861	0.067924
E8	0.033308	0.166667	0.166667	0.5	0.166667
E9	0.021736	0.39502	0.162656	0.39502	0.047304
E10	0.021736	0.525517	0.219121	0.219121	0.036241

Table 13 Comparison of industries with weight and rank

S. no.	Alternative	Weight	Rank
1	A1	0.383124	1
2	A2	0.143116	3
3	A3	0.340583	2
4	A4	0.133177	4

After applying AHP, it can be seen that A1 is best ranked so that it can become more sustainable (Table 13).

Table 14 shows that A1 has ranked 1 and it means that it adopts SM more than the other industries.

6 Result and Conclusion

On the basis of key enablers of sustainable manufacturing in Indian industries, a structured hierarchy was constructed and company’s score is determined by calculations to assess sustainable manufacturing with respect to the enablers and the industries were ranked on the basis of this score. This research may help to industries

Table 14 Results

Alternatives	Rank
A1	1
A2	3
A3	2
A4	4

to take proper decisions for achieving sustainability in manufacturing. However, it is not necessary to undertake all these enablers individually and other different barriers at one time, but it will be very much helpful in identifying on other enablers and barriers. There is a scope in future for doing this type of case study in other different industries using other MCDM techniques.

References

1. Bhanot N, Rao PV, Deshmukh SG (2015) Enablers and barriers of sustainable manufacturing: results from a survey of researchers and industry professionals. *Procedia CIRP* 29:562–567
2. Magee L, Scerri A, James P, Thom JA, Padgham L, Hickmott S, Cahill F (2013) Reframing social sustainability reporting: towards an engaged approach. *Environ Dev Sustain* 15(1):225–243
3. Gunasekaran A, Spalanzani A (2011) Sustainability of manufacturing and services: investigation for research and applications. *Int J Prod Econ* 140(1):35–47
4. Garetti M, Taisch M (2012) Sustainable manufacturing: trends and research challenges. *Prod Plan Control Manag Oper* 23(2–3):83–104
5. Rosen MA, Kishawy HA (2012) Sustainable manufacturing and design: concepts, practices and needs. *Sustainability* 4(12):154–174
6. Vinodh S, Joy D (2012) Structural equation modeling of sustainable manufacturing practices. *Clean Technol Environ Policy* 14(1):79–84
7. Nordin N, Ashari H, Rajemi MF (2014) A case study of sustainable manufacturing practices. *J Adv Manage Sci* 2(1):12–16
8. Gupta S, Dangayach GS, Singh AK, Rao PN (2016) A pilot study of sustainable machining process design in Indian process industry. In: *CAD/CAM, robotics and factories of the future*. Springer, New Delhi, pp 379–385
9. Gupta S, Dangayach GS (2015) Sustainable waste management: a case from Indian cement industry. *Braz J Oper Prod Manage* 12(2):270–279
10. Gupta S, Dangayach GS, Singh AK (2015) Key determinants of sustainable product design and manufacturing. *Procedia CIRP* 26:99–102
11. Meena ML, Jain R, Kumar P, Gupta S, Dangayach GS (2018) Process improvement in an Indian automotive part manufacturing company: a case study. *Int J Prod Qual Manage* 23(4):524–551

Informal Investigation of Fourth-Party and Third-Party Logistics Service Providers in Terms of Indian Context: An AHP Approach



Nishant Gautam, Manish Kumar Ojha, Pritam Swain, Ankur Aggarwal and Anbesh Jamwal

Abstract This research is based on the investigation of logistics service providers (LSPs) in terms of their activities and role in providing boons to the primary industries and to the customer terminus. This study also reports about the futuristic ambit of “collaboration of outsourced partners, their substructure, manoeuvring to gain manpower, integration of LSPs”. The goal of this paper is to understand the leeway of betterment of Indian industries with the maximum utilization of LSPs, present in the current market. Alliances of LSPs will contribute to maintaining the competence strength of Indian industries in the global market. To achieve the best results and the benefit of above-mentioned points, this research work has found out three major criteria and their sub-criteria with the help of the literature study and with the support of survey amongst the experts and analytical hierarchy process (AHP) technique, and output has been achieved. AHP tool helps in decision-making and validation of priorities between different factors.

Keywords LSPs · Survey · AHP · Criteria · Sub-criteria

1 Introduction

Today’s competitive market craves a clear view so that companies can withstand the competition. When we talk about the competition, logistics service providers (LSPs) play an exigent role to maintain the value of primary companies in the market. Manufacturing companies can focus on the production of product and enhancement of the quality of product, and they do not need to foresee about the logistics part, as there are several LSPs in the market. LSPs can be of different types, amongst which third-party LSPs (3PLs) and fourth-party LSPs (4PLs) are in the mainstream

N. Gautam · M. K. Ojha (✉) · A. Aggarwal · A. Jamwal
Department of Mechanical Engineering, Amity University, Noida, Uttar Pradesh, India
e-mail: mkojha@amity.edu

P. Swain
Department of Computer Science and Engineering, Amity University, Noida,
Uttar Pradesh, India

nowadays. 3PL handles the logistics division of manufacturing or primary companies. They include storing and shipping, and some of the 3PLs helve the entire supply chain. On the other hand, 4PL provides the total supply chain solution to the primary company. 4PL companies operate several 3PL companies. Major difference between 3PL and 4PL companies is that 3PL companies work in a single way whereas 4PL holds multiple works in the supply chain. In general, we can say that 3PLs are good for small and medium enterprise and 4PLs for big enterprises as 4PL will cost more than 3PL, so if small companies opt for 4PL, there are chances that they can be at “no profit/no loss” or “loss” region. Because of extremely high competitiveness, ever-altering latest worldwide economy, companies cannot withstand slowness. Any of the logistics company should be smart enough to accustom to the vicissitude which assuredly occurs.

The newfangled logistics company requires agility and flexibility. Obdurate and unpliant companies generally are not able to vying with other companies. It is hard to foresee alterations in the rialto or in the firm; company should be patulous to those alterations and must revert to. Flaccidity of format and orderliness will be exceptive in the upcoming, predictable forthcoming. Working on criteria for deciding the best service provider is a good way to get the targets, but the difficulty grows with the increment of criteria and their sub-criteria [1, 2]. Here, the role of AHP comes into play. In this research analysis, main criteria and sub-criteria of aforesaid, in the context of user firms and LSPs, are defined, a survey has been done amongst the experts of this field, data has been collected accordingly, and with the help of this data, AHP technique has been applied and result has been concluded.

2 Literature Review

LSPs are those helping hands which are growing as an important part for any user firm. With the help of LSPs, primary companies can focus on the overall quality of the product by having a great production system and the rest of the work is the headache of LSPs. Fu and Zhang [3] stated that for the accomplishment of all the major tasks and for the management of information inside a plexus of actors, there is a necessity of a common information sharing dais. Xiu [4] explained that one major work of a fourth-party logistics is its act in applying the skills needed by purchasers and transit providers (third-party logistics), carriers (second-party logistics) and manufacturers along their personal logistics facilities (first-party logistics) to have needed services, technological connectedness and encouragement of mutual effort. Cheng and Tang [5] stated that the efficiency of trade potential to impact the entire supply chain with enhanced route technique of running the concentration to detail positions the groundwork for an accord of improved packaging pattern with whole supply chain groups with producer of the lot. Prakash and Deshmukh [6] described that plane integration generates when some unlinked or contending firms at the equal level of the supply chain and generating the same kind of products or dissimilar elements of a sole product make a unified alliance to share variety of resources such as warehouse

capacity or manufacturing potential. Such kind of integration or teamwork may defeat financial obstacles to retail and boon society by decreasing the quantity of trucks on the roadway and hence stenosis and discharge of carbon dioxide [7].

In terms of business, logistics industries play a very important role as a support as well as relief for manufacturing industries. In developed countries of western part of the world, logistics are no longer a saleable enterprise, the performing task, primarily from the extrinsic logistics services of proficient institutions, that is, 3PL (third-party logistics) provider in obtainment [8, 9]. However, there are still some manufacturing industries who handle the logistics activities and their management by themselves but most of the industries began to opt for third-party logistics to addendum their own performance [10]. Various leading international manufacturing firms outsource their logistics tasks and also form a key alliance with the 3PL (third-party logistics) companies. Decrement of expenditure for logistics activities and optimized in-house and foreign resources is achieved with the help of prudent and efficient third-party logistics activities. It also enables the firms to hold good position the this era of global competitiveness by enriching more value added services at the identical time [11, 12]. Shao and Chen [13] described that in the integration of resources available in logistics, fourth-party logistics (4PL) have made extraordinary efforts, which in turn commanded the output result of the third-party logistics (3PL). Li et al. [14] stated that the concept of fourth-party logistics in supply chain management strengthen the framework of supply chain by removing various barriers in the field of logistics such as flow of material, flow of information and transportation related issues. It also helps the enterprises to design and plan the supply chain effectively. Many researches have been done on logistics service providers, and following those studies, motive of this research work is to find out the importance of several criteria and sub-criteria of the formers. By comparing them, with the help of AHP (analytical hierarchy process) technique, ranking to those criteria and their sub-criteria is given, with the help of which industries can focus on them on the required priority basis.

3 Research Methodology

For any order of acquisition measures, AHP methodology can be utilized because of its pliable nature [15]. AHP is an organized technique for shaping and examining complicated decisions, depended on psychology and calculation. It was developed in the year 1970 by Thomas L. Saaty. This technique involves the reflection of engaging of human mind's abilities for the determination of best possible solution to a complicated decision problem. Till now, this technique has been broadly used in fields like atmosphere, use of land and militaristic power [16–18]. In the technique of analytic hierarchy process, a decision difficulty is disintegrated into the form of a hierarchy. In terms of logistics, disintegrating a user firm's preference problem includes the arranging of a hierarchy in the context of the complete objective, i.e. decision to set the priority of importance amongst different criteria and their sub-criteria related to logistics. The basic step in this research format is the identification

of criteria linked to logistics that influence the user firms directly. The literature review that has been done in this research work has generated the list of some important criteria in the context of logistics. After that, a discussion has been made amongst the experts of logistic companies and finally based on the literature review and expert advice, and three major criteria with their sub-criteria have been selected which are illustrated in the next section.

4 Data Collection

Basic data has been collected through a survey amongst experts by the use of questionnaires. The questionnaire was detached in four sections. The opening section needed the respondents to create pairwise comparisons of three different criteria, the second section comprised of pairwise comparison of three sub-criteria under first criteria, third section involved the pairwise comparison of three sub-criteria of second criteria, and the fourth section included the pairwise comparison of three sub-criteria under third criteria. The five-point scale was used to rate these comparisons (Fig. 1).

In this survey, overall 24 questionnaires were asked to the experts, having a reaction rate of 91.3%. Out of the total response, 65.2% of experts provided the exact data needed for the further analysis of the data through AHP technique.

5 Analytical Hierarchy Process (AHP) Methodology

In AHP calculations, spaciousness of usability of LSPs (C1) has priority vector (PV) value of 0.2255; declaration forming method (C2) has 0.6738 priority vector value,

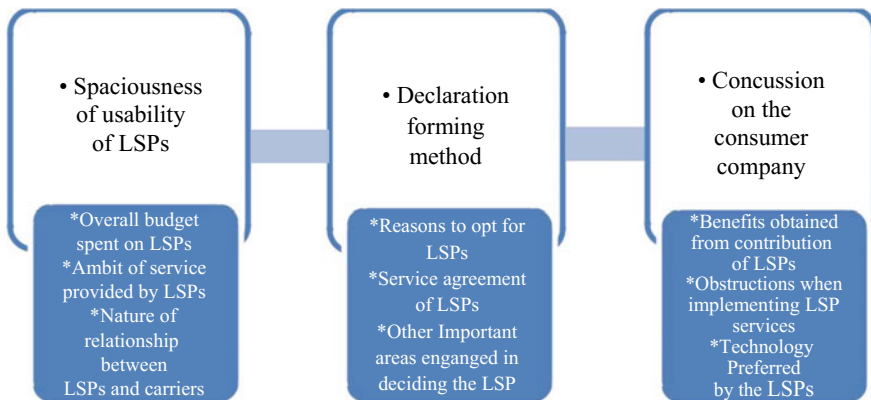


Fig. 1 Decision hierarchy showing three dissimilar criteria with their sub-criteria

and concussion on the consumer company (C3) has PV value of 0.1006. CR value of influencing power of C1, C2 and C3 upon each other has 0.0733. Similarly, PV values of overall budget spent on LSPs (S1), ambit of service provided by LSPs (S2) and nature of relationship between LSPs and carriers (S3) are 0.5815, 0.1094 and 0.3089, respectively. Consistency ratio (CR) value of influencing power of S1, S2 and S3 upon each other is 0.0024. PV values of reasons to opt for LSPs (S4), service agreement of LSPs (S5) and other important areas engaged in deciding the LSP (S6) are 0.1396, 0.5278 and 0.3325, respectively. CR value of influencing power of S4, S5 and S6 is 0.0459. In a similar way, PV values of S7, S8 and S9 are 0.1396, 0.3325 and 0.5278. CR value in this case is 0.0459.

In further calculations, values of normalized weights and their sums for criteria and sub-criteria are found in Tables 2, 3, 4 and 5.

Global weights with the percentage of normalized weights of all the sub-criteria are given in Table 6.

6 Result and Discussion

In AHP technique applied above, the first part includes the list of criteria and their sub-criteria in relative sections of the former in Table 1, which further divided into the separate calculations of priority vector (PV) and consistency ratio (CR) values. As mentioned in the previous section, the calculated value of CR for each case has found to be less than 0.10 that means all the calculated values for each of the criteria and sub-criteria are accurate. In Table 2, sum of pointers of influencing power of criteria C1, C2 and C3 towards C1 is calculated, i.e. a columnwise addition. In a similar way, sum of pointers of influencing power of all the three criteria towards C2 and C3 is calculated. After this, normalized weights and their sum have been calculated for C1, C2 and C3. Similarly, calculations have been done for S1, S2 and S3 in Table 3; S4, S5 and S6 in Table 4; and S7, S8 and S9 in Table 5. The sum of normalized weights is 3 in each table, which was required for the proceeding to the further calculations. Hence, in Table 6, global weights for each of the sub-criteria have been calculated to get the final values of normalized weights of each sub-criterion. Now, values of normalized weights have been converted into percentage form. So that, the rank has been given to each of the sub-criteria according to their weightage as shown in Table 6. Service agreement of LSPs (S5) has got rank 1 with the maximum weightage of 34.8955%, and following it, other important areas engaged in deciding the LSP (S6) and overall budget spent on LSPs (S1) achieved rank 2 and rank 3, respectively. Benefits obtained from contribution of LSPs (S7) have got the lowest rank with least weightage value, i.e. 1.4700%.

Table 1 Sub-criteria and criteria relation

Sub-criteria no. (S)	Sub-criteria name	Criteria no. (C)	Criteria name
S1	Overall budget spent on LSPs	C1	Spaciousness of usability of LSPs
S2	Ambit of service provided by LSPs	C1	Spaciousness of usability of LSPs
S3	Nature of relationship between LSPs and carriers	C1	Spaciousness of usability of LSPs
S4	Reasons to opt for LSPs	C2	Declaration forming method
S5	Service agreement of LSPs	C2	Declaration forming method
S6	Other important areas engaged in deciding the LSP	C2	Declaration forming method
S7	Benefits obtained from contribution of LSPs	C3	Concussion on the consumer company
S8	Obstructions when implementing LSP services	C3	Concussion on the consumer company
S9	Technology preferred by the LSPs	C3	Concussion on the consumer company

Table 2 Weights for criteria

Normalized weights							
	C1	C2	C3	C1	C2	C3	Weight
C1	1.0000	0.2500	3.0000	0.1875	0.1724	0.3333	0.6932
C2	4.0000	1.0000	5.0000	0.7500	0.6897	0.5556	1.9952
C3	0.3333	0.2000	1.0000	0.0625	0.1379	0.1111	0.3115
Sum	5.3333	1.4500	9.0000				3.0000

Table 3 Weights for sub-criteria under C1

Normalized weights							
	S1	S2	S3	S1	S2	S3	Weight
S1	1.0000	5.0000	2.0000	0.5882	0.5556	0.6000	1.7438
S2	0.2000	1.0000	0.3333	0.1176	0.1111	0.1000	0.3287
S3	0.5000	3.0000	1.0000	0.2941	0.3333	0.3000	0.9275
Sum	1.7000	9.0000	3.3333				3.0000

Table 4 Weights for sub-criteria under C2

Normalized weights							
	S4	S5	S6	S4	S5	S6	Weight
S4	1.0000	0.3333	0.3333	0.1429	0.1818	0.0999	0.4246
S5	3.0000	1.0000	2.0000	0.4286	0.5455	0.6000	1.5741
S6	3.0000	0.5000	1.0000	0.4286	0.2727	0.3000	1.0013
Sum	7.0000	1.8333	3.3333				3.0000

Table 5 Weights for sub-criteria under C3

Normalized weights							
	S7	S8	S9	S7	S8	S9	Weight
S7	1.0000	0.3333	0.3333	0.1429	0.1000	0.1818	0.4247
S8	3.0000	1.0000	0.5000	0.4286	0.3000	0.2727	1.0013
S9	3.0000	2.0000	1.0000	0.4286	0.6000	0.5455	1.5741
Sum	7.0000	3.3333	1.8333				3.0000

7 Conclusion

As discussed above, the sub-criteria which have got the highest weightage are service agreement of LSPs (S5) that means user firms should mainly focus on this sub-criterion while taking any decisions regarding logistics service providers. That is, user firms should do a deep analysis of service agreement of LSPs, so that it can prove to be a literal beneficiary step to hand over the part of your work to any LSP. Following S5, other important areas engaged in deciding the LSP (S6) and overall budget spent on LSPs (S1) have got second and third highest weightage, respectively. Hence, after S5, user firms should also strongly focus on S6 and S1, as there should be a proper list of each and every functional factor related to decision for any LSP and also the budget spent on LSP should be justifiable. The lowest weightage is of benefits obtained from contribution of LSPs (S7) that means companies should be least bothered about the same because while taking attention towards the sub-criteria with heavy weightages, S7 will already be at the peak level; i.e. benefits are directly linked to S5, S6 and other sub-criteria with weightage %, respectively. Hence, improve the sub-criteria with heavy weightages, and it will automatically result in improving the sub-criteria with lower weightages.

Table 6 Global weights

Sub-criteria	Name	Global weights	Normalized weights	%	Rank
S1	Overall budget spent on LSPs	1.2089	0.1343	13.4320	3
S2	Ambit of service provided by LSPs	0.2280	0.0253	2.5333	8
S3	Nature of relationship between LSPs and carriers	0.6430	0.0714	7.1439	5
S4	Reasons to opt for LSPs	0.8471	0.0941	9.4121	4
S5	Service agreement of LSPs	3.1406	0.3490	34.8955	1
S6	Other important areas engaged in deciding the LSP	1.9979	0.2220	22.1986	2
S7	Benefits obtained from contribution of LSPs	0.1323	0.0147	1.4700	9
S8	Obstructions when implementing LSP services	0.3119	0.0347	3.4660	7
S9	Technology Preferred by the LSPs	0.4904	0.0545	5.4487	6
Sum		9.0000	1.0000	100	

References

1. Simchi-Levi D, Kaminsky P, Simchi-Levi E (2000). *Designing and managing the supply chain*. Singapore: Irwin McGraw-Hill
2. Lynch CF (2000). *Logistics outsourcing: a management guide*. Illinois, USA: Council of Logistics Management publications
3. Fu D, Zhang W (2011) Integrating virtual logistics with the fourth party logistics. In: International conference on management and service science 2011 (MASS), Wuhan, China, pp. 1568–1570
4. Xiu X (2010) Study of collaborative information systems of 4PL based on Internet. In: Proceedings of the second international conference on modeling, simulation and visualization (WMSVM 2010). Sanya, China, pp. 206–209
5. Cheng JH, Tang CH (2014) Interorganizational cooperation and supply chain performance in the context of third party logistics services. *Asia Pac Manage Rev* 19(4):375–390
6. Prakash A, Deshmukh SG (2010) Horizontal collaboration in flexible supply chains: a simulation study. *J Stud Manuf* 1(1):54–58
7. McKinnon A, Edwards J (2010) Opportunities for improving vehicle utilization
8. Elten B, Timothy D (2010) Investigating the influence of velocity performance on satisfaction with third party logistics service. *Ind Mark Manage* 39:640–649
9. Beasley D (1993) A sequential niche technique for multimodal function optimization. *Evol Comput* 3:101–125
10. Jiang X (2011) A multi objective particle swarm optimization algorithm based on fuzzy learning subgroup. *Comput Appl Res* 12:4492–4494
11. Mitra B (2008) Key success factors, performance metrics, and globalization issues in the third-party logistics (3PL) industry: a survey of North American service providers. *Supply Chain Forum: Int J* 9(1):42–54
12. Li L, Zhu K (2011) An improved fuzzy C-means algorithm based on genetic algorithm and particle swarm optimization algorithm. *J Syst Manage* 6:728–733
13. Shao JG, Chen Q (2011) The advantages and development strategies of the fourth party logistics in China. In: 2nd international conference on engineering and business management, pp. 923–928
14. Li W, Wu MY, Mei Q (2012). The research of supply chain based on fourth party logistics optimization. In: International conference on building materials and structural engineering, pp. 393–397
15. Rangone A (1996) An analytical hierarchy process framework for comparing the overall performance of manufacturing departments. *Int J Oper Prod Manage* 16:104–119
16. Akbulak, Cengiz (2009) Application of analytical hierarchy process and geographic information systems in land-use suitability evaluation: a case study of Dümrek village (Çanakkale, Turkey). *Int J Sustain Dev World Ecol* 16(4):286–294
17. Dinh LC, Duc TT (2011). The integration of GIS and Fuzzy AHP for land suitability analysis. In: Proceedings of the second science and technology conference, Ho Chi Minh National University, 12 p
18. Setiawan A, Sedyono E, Moekoe DAL (2014). Application of AHP method in determining priorities of conversion of unusedland to food land in Minahasa Tenggara. *Int J Comput Appl* 89(8):0975–8887

An Image-Based Approach of Generating Automatic Toolpath for Profile Milling



Vishal Agrawal, Avinash Kumar, Narendra Kumar and Prashant K. Jain

Abstract This paper presents a novel approach for generating machining toolpath for milling operation directly from the given drawing image of the desired 2D profile. An image processing algorithm is implemented using python environment in which coordinates of the 2D profile are extracted to generate toolpath. The graphical user interface is also developed to ease the controlling and changing of machining-related parameters. The developed algorithm has been validated by simulating the generated toolpath using ‘CNC Simulator Pro software.’ The obtained results show that the developed algorithm is capable of generating a toolpath for any given 2D profiles.

Keywords Image processing · Computer-aided design and manufacturing · CNC machining · Profile milling · Drawing · Toolpath

1 Introduction

Advancement in computer-aided manufacturing (CAM) has played a vital role in the development and optimization of manufacturing processes [1–5]. CAM has reduced the total processing time and also improves the accuracy of the machining process resulting in round-the-clock production in industries. Generally, all the CAM processes are controlled by a set of coded instructions also known as computer numerical control (CNC) [6–9]. One of the widely used CNC operations in manufacturing industry is milling. It is used to perform drilling and cutting operations in which a cutting tool is used to remove materials from the feedstock [10]. The tool can be changed according to the required operation. Milling machine consists of rotating spindle, worktable, drive system, feedback system, and control unit. A cylindrical cutting tool is attached to a rotating chuck which is driven by a motor drive, and power is transmitted through a belt drive or gears or it is directly connected to the spindle. Most of the functions required to complete the milling operation can be controlled

V. Agrawal · A. Kumar · N. Kumar (✉) · P. K. Jain
PDPM Indian Institute of Information Technology, Design and Manufacturing,
Jabalpur, MP, India
e-mail: narendra.iiitdm@gmail.com

by the numeric codes which increases the ease of the operator to control and monitor the process. Other CNC controlled operations are laser engraving, electrochemical machining, electro-discharge machining, sketching, drawing, etc.

International Standard Organization (ISO) code set is a globally accepted coding system for current CNC operations. There can be a slight variation of codes depending on the type of machine controller. The code consists of several blocks which depends on the complexity of the workpiece profile. Each block consists of letters with some numbers associated with it. G, N, M, R, T, F, X, Y, Z are the letters used which have a well-defined function to control and perform the required operation [11]. G-code is the preparatory code which is to prepare the CNC operation such as selecting the feed type and giving movement commands. N-code indicates the block number in the code, and M-code is the miscellaneous code used to switch on or switch off the coolant, spindle rotation, etc. X, Y, and Z codes specify the position of the cutting tool, F-code sets up the feed rate value, T command is used to select the desired tool stored in a tool turret for the operation, and R code is used to define the radius of the circular interpolation in milling or retraction length during drilling or lathe operation.

CNC codes can be written manually or generated automatically using several available open-source or proprietary softwares. It requires CAD model of the desired workpiece in a specific format such as STL, DXF, STEP, and IGES [12]. There are certain cases where users have only the drawings of workpiece profile; in this situation, user has to prepare a CAD model to generate CNC code from different softwares. The generation of CNC code directly from the CAD drawings is more advantageous for the user as can save the efforts and processing time. Therefore, a platform needs to be developed to generate CNC codes directly from the available drawing which can reduce time and cost associated with the proprietary CAD/CAM softwares.

In the present paper, a novel approach has been proposed to overcome the aforementioned issues so that the CNC code can be generated directly from the part drawing by considering the top view of the required profile. Part drawing is used as the input in an image format which can be taken from a smartphone, a camera, or a computer-generated drawing file. It significantly reduces the total processing time to generate CNC code eliminating the requirement of a skilled CAD modeler for this purpose. The proposed approach has been implemented using Python environment which is an open-source software. It consumes very less space in the operating system than both the CAD/CAM softwares available for the same operation. A graphical user interface (GUI) is also developed which facilitates the user to enter other required parameters such as feed type, speed, feed, and depth of cut.

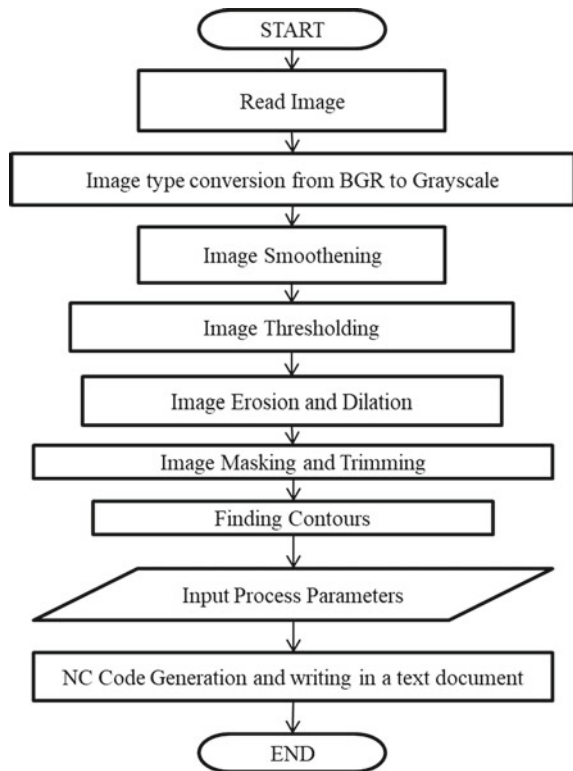
2 Proposed Approach

2.1 NC Code Generation Algorithm and Implementation

The current study deals with CNC code generation directly from an image of the given profile. Complete methodology of the current study is represented by a flowchart shown in Fig. 1, and CNC code generation algorithm is presented in Fig. 2. Generally, three image types RGB, gray scale, and binary are used for processing and analyzing an image. An RGB image type is given as input to the program which is read by the Python environment in BGR format followed by its conversion into a grayscale image. Every image contains some or high amount of noise due to the presence of high-frequency image components. High noise level produces irregular curve profile which generates inaccurate coordinates.

Gaussian blur is used to reduce the noise and smoothen the image for a smooth and regular curve profile. Image segmentation is performed using threshold method which converts the grayscale image into a binary image at a particular defined threshold value. Generally, an engineering drawing file also contains outer boundary and

Fig. 1 Methodology flowchart



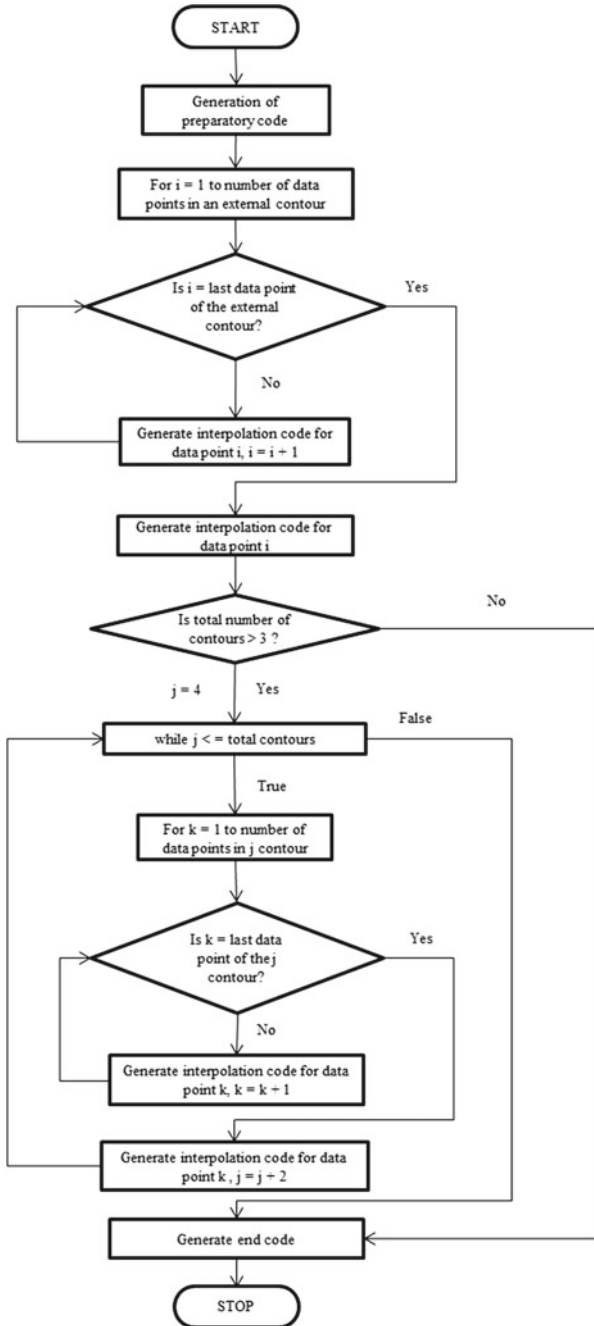


Fig. 2 CNC code generation algorithm

text information which is not a part of the profile, and it is removed for further processing. Image undergoes subsequent erosion, and dilation is performed to combine the boundary and text information. It is followed by image masking to keep the region of interest, i.e., the workpiece profile, and remove the combined boundary and text information. Having obtained the region of interest, profile/contour of the workpiece for milling is now detected.

CV_RETR_TREE function is used to obtain contours in a hierarchical order which helps in differentiating contours for internal and external milling. CHAIN_APPROX_SIMPLE function is used to store the contour points in a matrix form. It compresses the horizontal, vertical, and diagonal segments and stores only the endpoints removing the redundant data points of a contour. For nonlinear curves, the data points are stored such that it is a collection of many line segments. Anti-aliasing is done to smoothen the curves and remove the stair step like lines present in the profile.

NC code generation is performed in three steps. First, the preparatory codes are generated followed by the generation of interpolation codes and required end codes for the machining operation. Preparatory codes are the set of codes which sets up the process parameters for the machining operation such as feed type, feed rate, tool rpm, tool length compensation, tool radius compensation, and coolant on/off. Interpolation codes are the set of codes which generates the toolpath for the machining operation. Interpolation codes for the external milling profile are generated followed by the interpolation codes of the internal milling profile if present. Hierarchical storage of contours makes it simple for detecting whether the contour is an external or internal mill profile. Alternative contours are skipped because every individual polygon creates two contours. The last section of the code is generated to reset the initial preparatory parameter changes made in the machine for the machining operation. The generated NC code is directly exported to a text document. Currently, further work is being carried out to optimize the dimension of the image profile created to match the exact dimension of the workpiece for geometrically accurate NC code generation of the profile.

2.2 GUI Development

The algorithm for generation of NC code is implemented using a graphical user interface (GUI) developed in Python environment version 3.6.2. The input required by this GUI is a computer-generated engineering drawing file in .png or .jpeg image format containing the profile for the milling operation. The other required inputs by this GUI are the process parameters such as tool feed type, tool feed value, tool rotating speed, tool diameter, and workpiece thickness. The developed GUI has a provision to save the generated NC code and process parameters in the separate text document. GUI is very easy to understand and operate.

3 Validation

A solid model with uniform thickness is modeled in a CAD modeling software. Its computer-generated drawing file is obtained in an image format. An image is given as input in GUI, which undergoes several sequential image processing operations such as grayscale conversion of a BGR image, Gaussian blur, erosion, and dilation followed by the masking operation of the image. Finally, contours of the milling profile are generated and displayed in the output image window of the GUI as shown in Fig. 3 which can be saved for future references. Process parameters along with the workpiece thickness, code name, and tool number are entered in the parameter section of the GUI shown for generating the CNC code. The generated CNC code gets displayed in the NC code section shown in the GUI. The CNC code along with the process parameters can be saved separately in a different text document. The workpiece dimensions can also be seen by going through the 'Image with Scale' option in the toolbar. The generated NC code was tested in a CNC Simulator Pro software whose result is shown in Fig. 4. It can be seen that the milling profile obtained from the generated NC code is the same as the workpiece profile.

Further, the developed algorithm was tested for more complex profiles, as shown in Fig. 5. The NC code for the considered shapes was generated and tested through simulation. The obtained simulated profiles are presented in Fig. 5. It can be seen that the developed algorithm is self-capable to deal with 2D images having linear and curvy contours along the edges.

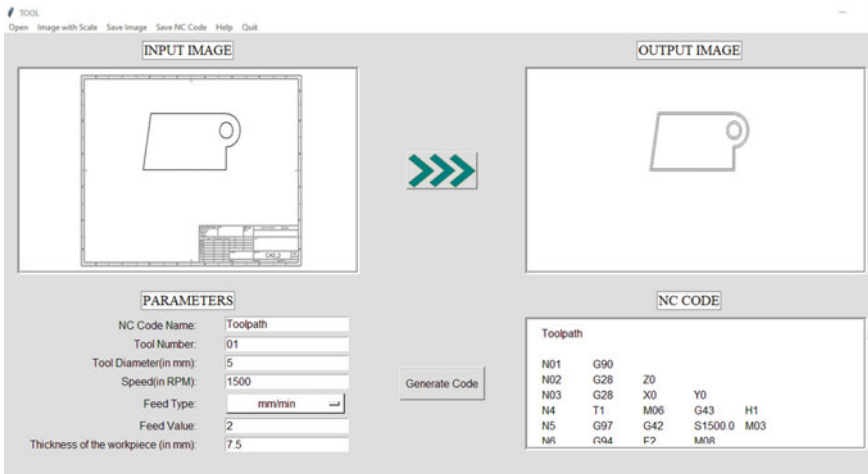


Fig. 3 Developed GUI for toolpath generation

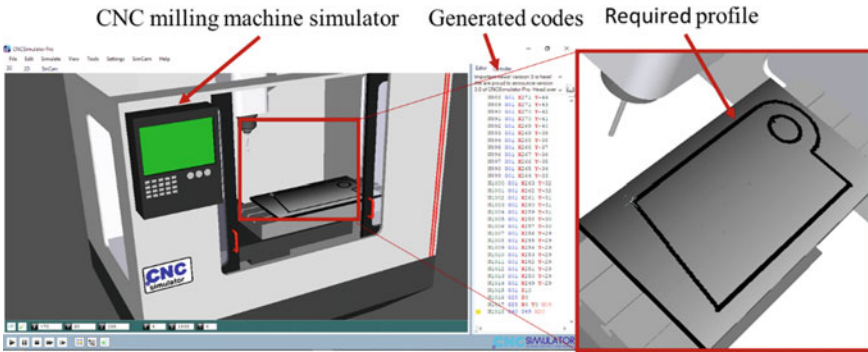


Fig. 4 Simulated workpiece profile in CNC Simulator Pro

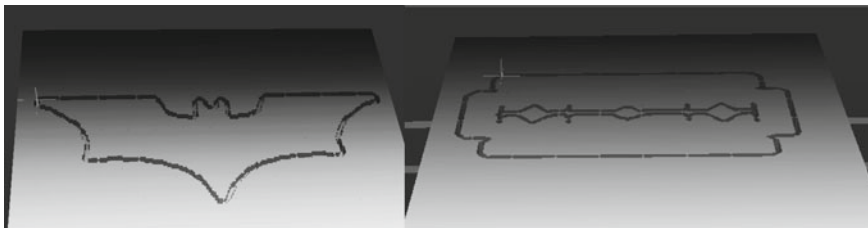


Fig. 5 Complex profiles simulated in CNC Simulator Pro

4 Conclusion

An image-based approach for generating NC code for milling operation has been successfully presented and implemented. An engineering drawing image was used as an input whose data points of the profile were extracted. The toolpath for profile milling operation was successfully generated for the workpiece containing uniform thickness. A simple graphical user interface was also developed to make the program user-friendly. Feasibility of the generated toolpath was tested through simulation using CNC simulator software. The obtained results from simulation showed that the proposed approach is capable of producing the machining toolpath for profile milling. Based on the above discussion, the proposed approach can be used in profile milling, laser engraving, laser cutting, electrochemical machining, electro-discharge machining, and drawing operations. In the future, the current work can be extended to the workpieces having a variable profile thickness.

References

1. Altintas Y, Tulsyan S (2015) Prediction of part machining cycle times via virtual CNC. *CIRP Ann Manuf Technol* 64:361–364
2. Kumar N, Jain PK, Tandon P, Pandey PM (2018) Additive manufacturing of flexible electrically conductive polymer composites via CNC-assisted fused layer modeling process. *J Braz Soc Mech Sci Eng* 40:175
3. Taufik M, Jain PK (2016) CNC-assisted selective melting for improved surface finish of FDM parts. *Virtual Phys Prototype* 11:319–341
4. Kumar N, Jain PK, Tandon P, Pandey PM (2018) Extrusion-based additive manufacturing process for producing flexible parts. *J Braz Soc Mech Sci Eng* 40:143
5. Kumar N, Shaikh S, Jain PK, Tandon P (2015) Effect of fractal curve based toolpath on part strength in fused deposition modelling. *Int J Rapid Manuf* 5:186–198
6. Kumar N, Jain PK, Tandon P, Pandey PM (2018) Experimental investigations on suitability of polypropylene (PP) and ethylene vinyl acetate (EVA) in additive manufacturing. *Mater Today Proc* 5:4118–4127
7. Shaikh S, Kumar N, Jain PK, Tandon P (2016) Hilbert curve based toolpath for FDM process. In: *CAD/CAM, robotics and factories future*. Springer, India, pp. 751–759
8. Kumar N, Jain PK, Tandon P, Pandey PM (2018) 3D printing of flexible parts using EVA material. *Mater Phys Mech* 37:124–132
9. Kumar N, Jain PK, Tandon P, Pandey PM (2019) Toolpath generation for additive manufacturing using CNC milling machine. In: Kumar LJ (ed) *3D printing and additive manufacturing technologies*. Springer, Singapore, pp 73–82
10. My CA, Bohez ELJ (2016) New algorithm to minimise kinematic tool path errors around 5-axis machining singular points. *Int J Prod Res* 54:5965–5975
11. Borangiu T, Dogar A, Dumitrache A (2007) Automatic generation of 3D machining surfaces with tool compensation from graylevel image models. *IFAC*
12. Nassehi A, Essink W, Barclay J (2015) Evolutionary algorithms for generation and optimization of tool paths. *CIRP Ann Manuf Technol* 64:455–458

Experimental Investigation of Forming Forces in Single Point Incremental Forming



Ajay Kumar, Vishal Gulati and Parveen Kumar

Abstract Single point incremental forming (SPIF) has been confirmed as a quiet economical process for rapid prototyping and batch-type production. It exempts complex and expensive tooling as required in the conventional sheet metal-forming processes. Investigation of forming forces becomes important for selecting the appropriate hardware and optimal process parameters in order to assure the perfection and precision of any process. Moreover, SPIF applicability can be ensured on the industrial scale when appropriate guidelines are highlighted regarding a relation between the input parameters and forming forces induced in the process. This paper investigates the influence of tool diameter, tool shape, and wall angle on the maximum axial forming forces on aluminum alloy (AA2024-O) sheets. Forming forces were recorded using a dynamometer and data logger system equipped with Microscada software. Tool shape has been proved a significant factor which affects the forming forces greatly. Combination of higher wall angle and flat-end tool with the lower side radius resulted in the fracture of components at a lower depth.

Keywords SPIF · Forming force · Process parameters · AA-2024-O · Tool shape

1 Introduction

Sheet metal forming has been an important manufacturing process in several industrial sectors. In the engineering field, parts are generally made of sheet metal particularly through conventional forming methods such as stretch forming, deep drawing,

A. Kumar (✉)

K. R. Mangalam University, Gurugram 122103, Haryana, India
e-mail: ajay.kumar30886@gmail.com

A. Kumar · V. Gulati

Guru Jambheshwar University of Science & Technology, Hisar 125001,
Haryana, India

P. Kumar

Rawal Institute of Engineering & Technology, Faridabad 121004,
Haryana, India

© Springer Nature Singapore Pte Ltd. 2019

K. Shanker et al. (eds.), *Advances in Industrial and Production Engineering*, Lecture Notes in Mechanical Engineering, https://doi.org/10.1007/978-981-13-6412-9_41

shearing, blanking, and bending, etc. These conventional forming techniques are expensive and uneconomical for the batch-type production due to the involvement of pressing dies and punches [1]. Batch-type production can be accomplished at the economical level using single point incremental forming (SPIF) process [2]. SPIF is also beatified with smaller lead time and negligible tooling cost for producing prototypes and smaller batch size components [3].

SPIF is a truly die-less technique which can easily form the components for aerospace, medical, and automotive sectors. The designed shape of components can be formed using a simple spherical-headed tool layer by layer as shown in Fig. 1. This die-less process can be accomplished on a CNC milling machine in order to form the predetermined shape of components. Moreover, a smaller amount of energy is required during this technique due to the incremental nature of the process. Less forming force is required in order to produce the components using the SPIF process. Forming forces are responsible for the structural integrity of the workpiece [4]. Maximum forming forces which are required to form the components define the capacity of the hardware used in this process. Hence, investigation of the maximum forming forces becomes customary to guarantee the secure utilization of the forming machinery. Forming force is the force required to deform the sheet at the tool–sheet interface. In the literature, table-type dynamometer [5–11] has mostly been used which is mounted between the machine bed and SPIF fixture.

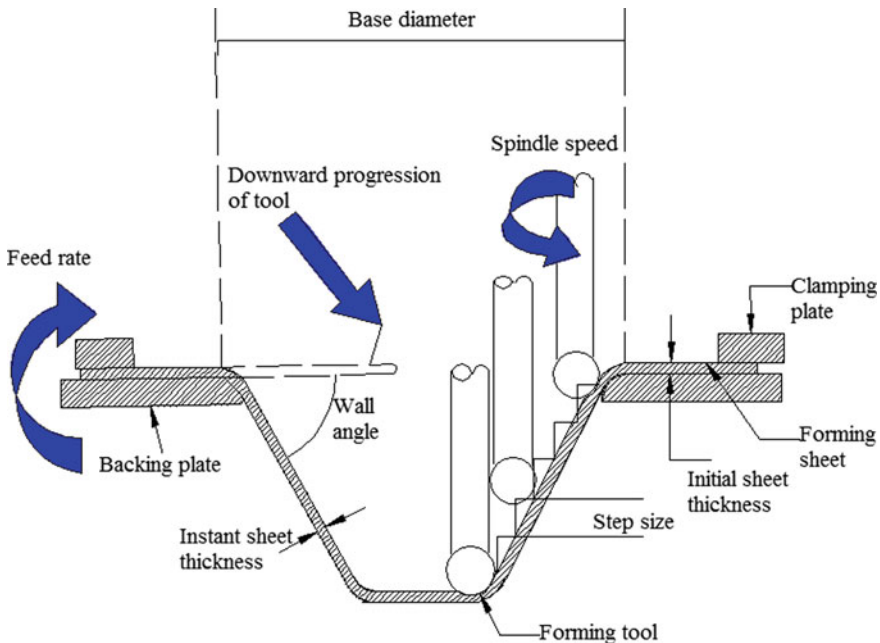


Fig. 1 Single point incremental forming

1.1 History of SPIF

Li et al. [5] deduced a model for predicting the forming forces based on the deformation analysis. The proposed model was validated by investigating the influence of different step sizes in order to produce the conical and pyramidal frustums by experimental tests on AA7075-O sheets. Results showed that the predicted and experimental results were found in good correlation. Liu et al. [11] investigated the impact of tool path strategies and wall angle on AA7075-O sheets. Results showed that the axial peak forces were found to be increased with the rise in wall angle. Bagudanch et al. [12] and Centeno et al. [13] performed experimental tests on PVC and AISI 304 stainless steel sheets, respectively. They found that the maximum axial forces increased with the rise in punch diameter. Petek et al. [14] also observed a similar trend of maximum axial forces. Oleksik et al. [15] investigated the effects of different tool diameters (12, 16, 20 mm) on forming forces during the SPIF process and elaborated the mathematical models. Results showed that the axial forming forces were much higher than those occurred in the x -direction. Fiorentino et al. [16] studied the influence of angular step sizes (2° , 4° , 6°) using the positive die on FePO4 deep drawing steel sheets. They found that the axial force was greater than that occurred in x -axis and y -axis. It has been revealed from the literature that the force component in the axial downward direction (F_z) of the forming tool is much more than the other two force components (F_x and F_y). Hence, determination of the axial force component becomes customary for the safe utilization of the hardware.

This work presents the investigation of input factors on axial peak forces on AA2024-O sheets. The impacts of tool shape, wall angle, and tool diameter have been investigated for conical frustums. Three different shapes of the forming tools have been investigated in this study. Table 1 and Fig. 2a represent the geometry of forming tools used in this study. Table 2 shows the input factors which are studied in this paper. Each input factor was investigated at three levels. Other input factors were taken constant as feed rate 1500 mm/min, wall angle 64° , tool diameter 11.60 mm, spindle speed 1000 rpm, sheet thickness 1.2 mm, and step size 0.5 mm. Castrol Alpha SP 320 was used for the lubricating purpose at the contact zone of tool and sheet.

2 Materials and Methods

2.1 Experimental Set up

A CNC milling machine has been used for experimental tests (Fig. 2b). Table 3 represents the chemical compositions of the AA2024-O aluminum alloy sheets. Conical frustums of 120 upper diameters have been designed for forming operation up to 70 mm forming depth. Lower diameters of conical frustums were controlled by wall angles.

Table 1 Geometrical details of forming tools

Tool diameter	Side radius of flat-end tool	Radius of hemispherical end tool	Symbol
T_D (mm)	r (mm)	R (mm)	
7.52	1.40	–	FlatEnd-R1
	2.00	–	FlatEnd-R2
	–	3.76	Hemispherical
11.60	1.98	–	FlatEnd-R1
	2.85	–	FlatEnd-R2
	–	5.80	Hemispherical
15.66	1.85	–	FlatEnd-R1
	3.76	–	FlatEnd-R2
	–	7.83	Hemispherical

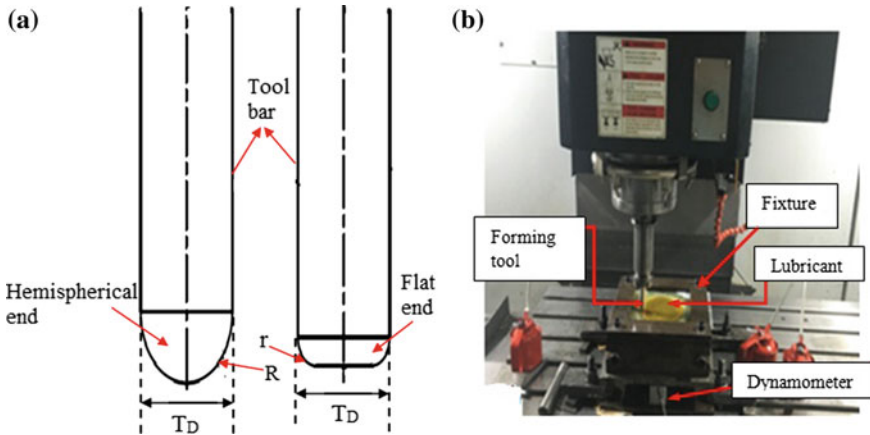


Fig. 2 Experimental set up

Table 2 Process parameters and their levels

Parameter	Level 1	Level 2	Level 3
Tool diameter (mm)	7.52	11.60	15.66
Tool shape	FlatEnd-R1	FlatEnd-R2	Hemispherical
Wall angle ($^\circ$)	60	64	68

Table 3 Chemical compositions of aluminum alloy used

Chemical composition (weight %)									
AA2024-O	Al	Cr	Cu	Fe	Mg	Mn	Si	Ti	Zn
	91.50	0.10	4.60	0.30	1.70	0.80	0.50	0.10	0.20

Table 4 Forming force test results with different process parameters

Forming force test results for tool diameter and tool shape				Forming force test results for wall angle and tool shape			
Sr. no	Tool diameter	Tool shape	Fz max	Sr. no	Wall angle	Tool shape	Fz max
1	7.52	FlatEnd-R1	938	10	60	FlatEnd-R1	1078
2	7.52	FlatEnd-R2	893	11	60	FlatEnd-R2	982
3	7.52	Hemispherical	805	12	60	Hemispherical	905
4	11.60	FlatEnd-R1	1208	13	64	FlatEnd-R1	1210
5	11.60	FlatEnd-R2	1086	14	64	FlatEnd-R2	1091
6	11.60	Hemispherical	997	15	64	Hemispherical	991
7	15.66	FlatEnd-R1	1463	16	68	FlatEnd-R1	1352
8	15.66	FlatEnd-R2	1371	17	68	FlatEnd-R2	1294
9	15.66	Hemispherical	1248	18	68	Hemispherical	1219

2.2 Methodology for Force Measurement

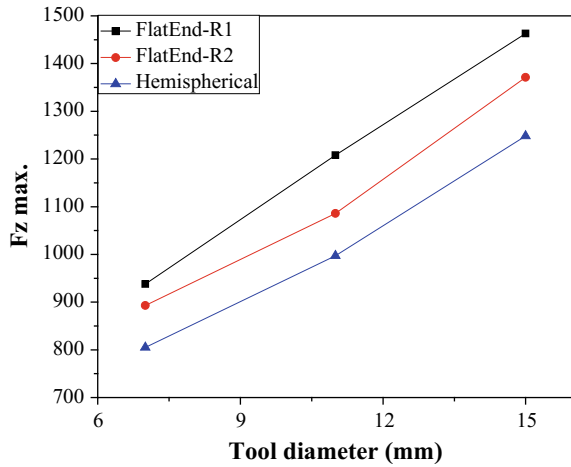
Forming forces in the axial direction (F_z) have been measured using a strain gauge-based dynamometer which was mounted below the fixture as shown in Fig. 2b. A data logger system equipped with Microscada software has been provided to the dynamometer in order to facilitate the processed force values in a PC-based environment. On the application of the load, the conducting material of strain gauge provides voltage as an output which is proportional to the elastic deformation. The analog signals of voltage received from strain gauge are required to convert into digital signals to display the real-time online observation of forming forces during operation. ADC 0808 analog to digital converter has been used in the data logger system for this purpose.

3 Results and Discussion

Experimental test results of different input factors on the forming forces are given in Table 4. Maximum axial forming forces (F_z max.) are taken into account for analysis.

Figure 3 shows the impacts of tool shape with the different tool diameters on the maximum axial forces. An increase in tool diameter resulted in the increment of forming forces. This is due to the fact that the larger contact zone occurs at the tool-sheet interface for larger tool diameter. Hence, more material is to be formed at that instant. Forming forces were found to be influenced significantly by changing the shape of the forming tool. Maximum axial forces were found to decrease with the increase in the side radius of the forming tool. This trend of decreasing force with the

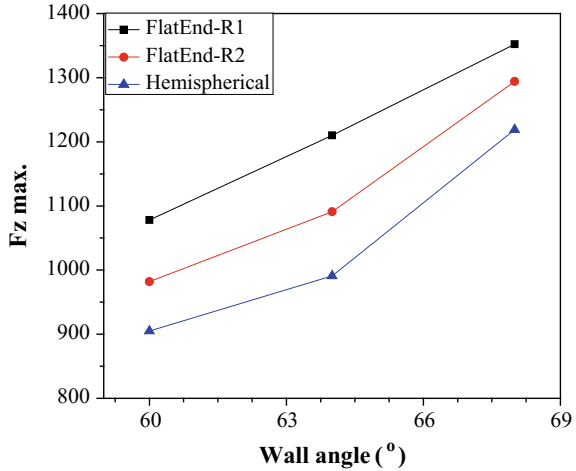
Fig. 3 Effects of tool diameter and tool shape on maximum axial forces



increase in the side radius was consistent for all levels of the tool diameter investigated in this study. When tool shape was changed from FlatEnd-R1 to Hemispherical end, maximum axial forces (F_z max) decreased approximately 14.17, 17.46, and 14.69% for 7.52, 11.60, and 15.66 mm tool diameters, respectively. Similarly, maximum axial forces were found to decrease by 35.88, 34.86, and 35.49% for FlatEnd-R1, FlatEnd-R2, and Hemispherical shape, respectively, when tool diameter was reduced from 15.66 to 7.52 mm.

Figure 4 shows the impacts of tool shape with the wall angles on maximum axial forces. Axial peak forces were found to increase with the increase in wall angle of conical parts. Moreover, sheet fracture was observed with 68° wall angle specimens for all shapes of the forming tools. This may be due to the fact that the higher wall angle results in excessive sheet-thinning according to sine law [17] which leads to an earlier fracture of the sheet material. In the case of the conical frustum of 64° wall angle, fracture occurred for FlatEnd-R1 and FlatEnd-R2 tool shapes. This can be due to the fact that the smaller radius of the tool increases penetration into the sheet and removes materials in the form of chips. Hence, a smaller radius of the tool-tip leads to cracking of the sheet material resulting in the lower forming depth. When tool shape was changed from FlatEnd-R1 to Hemispherical end, maximum axial forces (F_z max) decreased approximately 16.04, 18.10, and 9.83% for 60° , 64° , and 68° wall angles, respectively. Similarly, maximum axial forces were found to decrease by 20.26, 24.11, and 25.75% for FlatEnd-R1, FlatEnd-R2, and Hemispherical shape, respectively, when the wall angle was reduced from 68° to 60° .

Fig. 4 Effects of wall angle and tool shape on maximum axial forces



4 Conclusions

In this study, the axial forming forces have been investigated using the SPIF process on AA2024-O aluminum alloy sheets. For this purpose, the conical frustums of constant wall angle have been formed in order to investigate the impact of input factors. An increase in tool diameter resulted in the increment of the forming forces. Increasing side radius of flat-end tools resulted in the decrement of the forming forces. The shape of the tool has also been proved a significant factor during this process. Less forming forces are required to deform the sheet with the hemispherical end tools as compared to those required with the flat-end tools. Combination of flat-end tools having lower side radius and higher tool diameter requires higher forming forces in order to produce the components during the SPIF process. On the other hand, the hemispherical end tools with lower tool diameter resulted in lower forming forces required to produce the parts. Increase in wall angle led to an increase in the forming forces. Combination of higher wall angle and flat-end tool with lower side radius resulted in the fracture of components at a lower depth. Future work would focus on the analysis of thickness distribution and dimensional accuracy of the formed components which seeks importance and suitability in setting guidelines for the industrial application.

References

1. Kim YH, Park JJ (2002) Effect of process parameters on formability in incremental forming of sheet metal. *J Mater Process Technol* 130:42–46
2. Li P, He J, Liu Q, Yang M, Wang Q, Yuan Q, Li Y (2017) Evaluation of forming forces in ultrasonic incremental sheet metal forming. *Aerosp Sci Technol* 63:132–139

3. Wu SH, Reis A, Andrade Pires FM, Santos AD, Barata da Rocha A (2012) Study of tool trajectory in incremental forming. *Adv Mater Res* 472:1586–1591
4. Bagudanch I, Centeno G, Vallengano C, Garcia-Romeu ML (2013) Forming force in single point incremental forming under different bending conditions. *Procedia Eng* 63:354–360
5. Li Y, Daniel WJ, Liu Z, Lu H, Meehan PA (2015) Deformation mechanics and efficient force prediction in single point incremental forming. *J Mater Process Technol* 221:100–111
6. Azevedo NG, Farias JS, Bastos RP, Teixeira P, Davim JP, de Sousa RJA (2015) Lubrication aspects during single point incremental forming for steel and aluminum materials. *Int J Precision Eng Manuf* 16:589–595
7. Mohammadi A, Qin L, Vanhove H, Seefeldt M, Van Bael A, Dufloy JR (2016) Single point incremental forming of an aged AL–Cu–Mg alloy: influence of pre-heat treatment and warm forming. *J Mater Eng Perform* 25:2478–2488
8. Dufloy JR, Callebaut B, Verbert J, De Baerdemaeker H (2008) Improved SPIF performance through dynamic local heating. *Int J Mach Tools Manuf* 48:543–549
9. Al-Obaidi A, Kräusel V, Landgrebe D (2016) Hot single-point incremental forming assisted by induction heating. *Int J Adv Manuf Technol* 82:1163–1171
10. Asghar J, Reddy, N (2013) Importance of tool configuration in incremental sheet metal forming of difficult to form materials using electro-plasticity. In: *Proceedings of the World Congress on Engineering 2013*, vol 3, pp 1734–1738
11. Liu Z, Li Y, Meehan PA (2013) Experimental investigation of mechanical properties, formability and force measurement for AA7075-O aluminum alloy sheets formed by incremental forming. *Int J Precision Eng Manuf* 14:1891–1899
12. Bagudanch I, Garcia-Romeu ML, Centeno G, Elías-Zúñiga A, Ciurana J (2015) Forming force and temperature effects on single point incremental forming of polyvinylchloride. *J Mater Process Technol* 219:221–229
13. Centeno G, Bagudanch I, Martínez-Donaire AJ, Garcia-Romeu ML, Vallengano C (2014) Critical analysis of necking and fracture limit strains and forming forces in single-point incremental forming. *Mater Des* 63:20–29
14. Petek A, Kuzman K, Kopac J (2009) Deformations and forces analysis of single point incremental sheet metal forming. *Archives Mater Sci Eng* 35:35–42
15. Oleksik V, Pascu A, Gavrus A, Oleksik M (2010) Experimental studies regarding the single point incremental forming process. *Acad J Manuf Eng* 8:51–56
16. Fiorentino A, Ceretti E, Attanasio A, Mazzoni L, Giardini C (2009) Analysis of forces, accuracy and formability in positive die sheet incremental forming. *Int J Mater Form* 2:805–808
17. Jeswiet J, Micari F, Hirt G, Bramley A, Dufloy J, Allwood J (2005) Asymmetric single point incremental forming of sheet metal. *CIRP Annals Manuf Technol* 54:88–114

Solid Waste Management Through Plasma Arc Gasification in Delhi: A Step Towards Swachh Bharat



Monika Singh, Rishabh Arora, Anubhav Ojha, Durgesh Sharma and Sumit Gupta

Abstract Developing countries like India are facing a predicament scenario because of the solid waste and hence its management is becoming a critical issue. As urbanization is increasing, enhanced municipal solid waste and its unscientific handling are degrading the urban environment and causing health hazard. Various methods like landfilling (major source of methane (CH_4) emissions), incineration, composting have been used, but due to too slow operation, these processes have not fully satisfied the growing needs of the waste management. In this paper, we have shown that how CO_2 emissions can be prevented from a coal-fired thermal power plant in Delhi, if a better method, i.e., *plasma arc gasification (PAG) process* is used for waste management and power generation using the municipal solid waste generated in the city, which is the need of the hour. The plasma gasification process ensures close loop cycle, thereby reducing the pollutants from the air. We have done a complete analysis of waste generation and emission production, and it is concluded that by this approach we can reduce major pollutants causing global warming due to municipal solid waste. In the present work, we have calculated that technology based on CDM (Clean Development Mechanism) like plasma arc gasification is implemented large amount of carbon dioxide emission can be prevented in addition to power generation that could suffice the energy need of the city.

Keywords Municipality solid waste (MSW) · CO_2 emissions · Plasma arc gasification

M. Singh · R. Arora
Moradabad Institute of Technology, Moradabad, India

A. Ojha
Oil and Natural Gas Corporation Limited, Ahmedabad, India

D. Sharma (✉)
Raj Kumar Goel Institute of Technology, Ghaziabad, India
e-mail: durgeshrsharma@gmail.com

S. Gupta
Amity School of Engg and Tech, Amity University Uttar Pradesh, Noida, India

1 Introduction

Delhi is the most densely populated and urbanized city in India. It generates about 12,740 tonnes/day of municipal solid waste and not nearly half of it is processed daily for energy generation and a forecast of 18,000 metric tonnes per day by 2021 [1–4]. Proper disposal of MSW is the need of the hour as the city is flooded with various health diseases due to too much-polluted air the Citizen of Delhi breath in. The most common method used for waste management in Delhi is landfill which is discussed further in this work; this process mostly involves collecting the waste in dump site without proper technical treatment of the waste and without taking care of the evolving emissions to the soil air and water. There are three landfill sites in Delhi which contribute solid waste management [5]. In Delhi, five municipal authorities are responsible for municipal solid waste management.

Bhalswa Landfill (Established in 1994)

It receives 2700 tonnes of garbage per day [6]. The dump expired itself life in 2006 but is still in operation, the soaring mercury this year has drastically worsened the situation. According to the local inhabitants, there is a need of modern technology to manage the solid waste.

Ghazipur Landfill Site (Established in 1984)

This landfill produces of 12 MW (megawatt) of electricity using 2000 tonnes of garbage [7]. It receives 3000MT of waste every day. The landfill has already outlived its life by 15 years [8].

Timarpur Okhla Landfill Site (Established in 1996)

This landfill site processed 1300 tons of solid waste per day and supplied 16 MW of electricity to the grid [5].

All these landfills incinerate the waste for power generation. The limits in this landfill are so far exceeded and wastes are overflowing, [4]. Dumping from all kind of waste takes place from organic to inorganic. Piled up garbage has taken place of the shape of the hill. Fire keeps on burning due to the production of methane which is highly flammable and a potent greenhouse gas.

No safety measures are taken yet to prevent outbreak of fire in these landfills. Various other harmful effects from the landfill are the groundwater contamination by Leechate generated in the waste dump, surface water contamination by the runoff from waste dump, acidity of the surrounding soil, spreading of epidemic and infectious diseases to people living in nearby localities. And by going through various news articles from the past days, it is known that every time policies are to be set but nothing done practically to remove the sole cause of such diseases. There is an urgent need to enhance waste management process in India and strictly implementing policies and regulations or else it will become menace. While the burning waste in Delhi is legally banned but who cares?

Thermal treatment of solid waste can be accomplished by incineration. Incineration of Indian MSW is not suitable as the MSW has high organic constituents, moisture content, or inert content are present in the waste. A 300 TPD (tonnes per

day) capacity MSW incineration plant at Timarpur Delhi built in 1987 [9], the plant could not run for a long time due to unavailability of waste having required calorific value for incineration.

2 An Efficient and Alternative Approach to SWM (Plasma Arc Gasification)

Plasma gasification is one of the most recent and efficient methods for SWM. This method has been proposed by Ojha et al. [10]. It involves heating the waste to super high temperatures using plasma arc and treating the exhaust gases and employing synthesis gas to run the combined gas cycle or Rankine cycle for power generation, using the vitreous glassy slag for road building and construction purposes and harnessing toxic gasses like sulphur for laboratory and pharmaceutical purposes. Therefore, it ensuing zero emissions in the environment.

2.1 Plasma

It is considered as the fourth state of matter, it is a cloud of protons, neutrons, electrons charged particles, free radicals, where all electrons come close from their respective molecules and give plasma the ability to act as a whole rather than a bunch of atoms. It has properties of the fluid. It has high enthalpy. Plasma can be found in lightning, on the surface of the sun and in the outer space.

2.2 Plasma Arc Gasification Process [11]

Household waste like paper, card, glass, plastics of various kinds, metals (steel aluminium) and food waste, much of these are separated in different countries but in Delhi segregation is not done [12]. Other trash includes batteries toxic chemical wastes, medical wastes from hospitals, and some conventional forms of waste like waste from incinerators, recycling waste product or highly toxic bottom ash from incinerators that need to be disposed somehow. Plasma gasification claims all these waste. Plasma gasification proves to be one of the most efficient methods for treating all type of solid waste without segregating them.

The Plasma Arc Gasification waste management process:

1. The plasma gasification plant is a material recycling facility in which any metal can be recovered from residual waste. The residue obtained is first dried from the part of recovered heat from the plant to produce refuse-derived fuel (RDF).

2. The gasifier in the gas plasma process employs fluidized bed combustion gasifier. It transforms the organic waste into tar and char and **Syngas**. It does this by heating the RDF to high temperatures of around 800 °C in a highly controlled reduced oxygen environment [11].
3. Crude Syngas is now passed to a secondary plasma convertor. Heat from the plasma arc produced by high intensity current (approximately 60 V and 350 A) [10] with torch power in the range of 100 KW to 200 MW [13] at temp of about 7000 °C and the strong ultraviolet light of the plasma ensures complete damage of tar substances and the disintegration of char materials. Tar is the liquid dense flammable solid materials that can be sustained after combustion of carbonaceous materials.
4. Then the clean Syngas and the inorganic substance is now obtained in the ash carried from the gasifier being clotted into a product known as plasma rock. The plasma converter is able to sustain highly effective and energy-efficient damage of complex tar and char product.

Clean Syngas is then cooled and conditioned through wet and dry scrubbers before being used. Residual heat can also be used for combined heat and power mode within the process itself as well as for other users in the vicinity. Syngas can be piped away and burned to make energy or can be used to fuel the plasma arc torch. The scrubbing and cleaning of Syngas are necessary to dispose of some toxic gases (dioxins).

A long chain of carbon, hydrogen, and oxygen molecules breakdown at high temperature by plasma. These atoms favour the formation of carbon monoxide and H₂ molecules. This mixture rich in CO and H₂ molecules is called Syngas. To prevent the formation of dioxins, cooling is required and gas cleaning is done [14]. The cleaning includes removal of particulate matter sulphur compounds, chlorine compounds, nitrogen compounds, non-reacted hydrocarbons and heavy metals. These impurities can plug up reactors, root decay, poison downstream stimulant or prevent the plant being accord with environmental consents. Particulate matter (PM) in the Syngas stream is typically composed with ash, non-reacted carbon char and alkali compounds and condensed chlorine. Particulate matter can be removed using various dry and wet PM removal systems like water quench systems, cyclones and rotating particle separators, mesh-type filters, candle filters (ceramic or sintered metal), electrostatic precipitates (ESP). Tar removal process includes thermal cracking, partial oxidation, scrubbers, Wet Electrostatic Precipitates. Mercury removal process uses sulphur-impregnated activated carbon. Sulphur removal involves the removal of sulphur contaminants, i.e., H₂S or COS (carbonyl sulphide), and these are removed using solvent absorption process. Carbon dioxide (CO₂) is also removed during this process of absorption.

Using Rankine cycle or Brayton cycle, the heat from syngas is utilized for the production of electricity using a steam or gas turbine, respectively, [10] (Fig. 1).

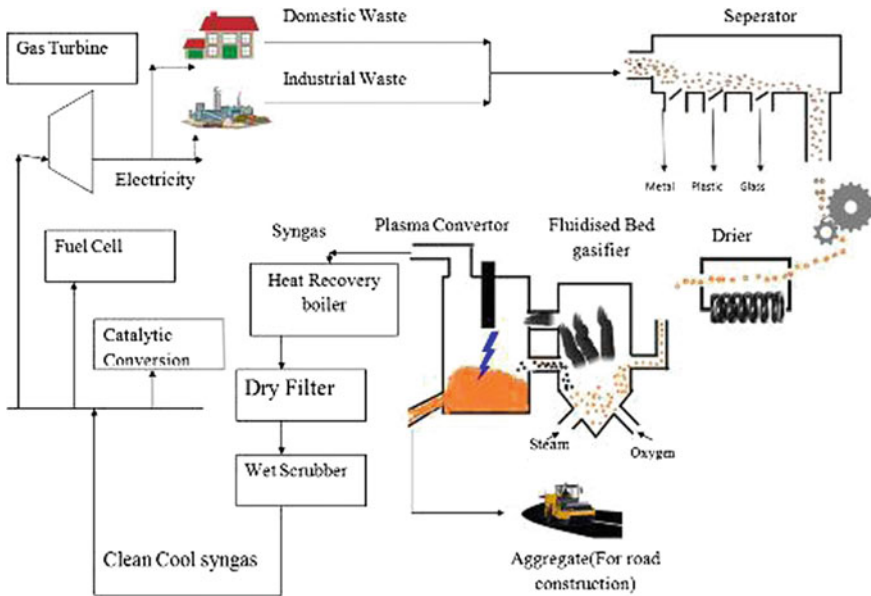


Fig. 1 Plasma arc gasification process chart

3 Survey of Municipal Solid Waste in Delhi

Municipal waste generation primarily depends upon economic activity. According to World Bank (1), study report with increase in economic activity waste generation increases. Today India is the fastest growing economy in the world estimating, with the average growth of around 7.5% in GDP per year, our economy will grow up to 5 times from present value in 2050. The graph below shows projected waste generation of Delhi.

According to a level of population based on the study done by University of Ontario [2] and per capita waste generation based on economic activity (Fig. 2).

3.1 Coal-Fired Thermal Power Plants in Delhi

There are three thermal power stations in Delhi which are as follows

1. Badarpur Coal Power Station
2. Indraprastha Coal Power Station
3. Rajghat Coal Power Station.

The Badarpur power station has installed capacity of 720 MW, and the coal source is Jharia coal fields, Dhanbad, Jharkhand, India [15].

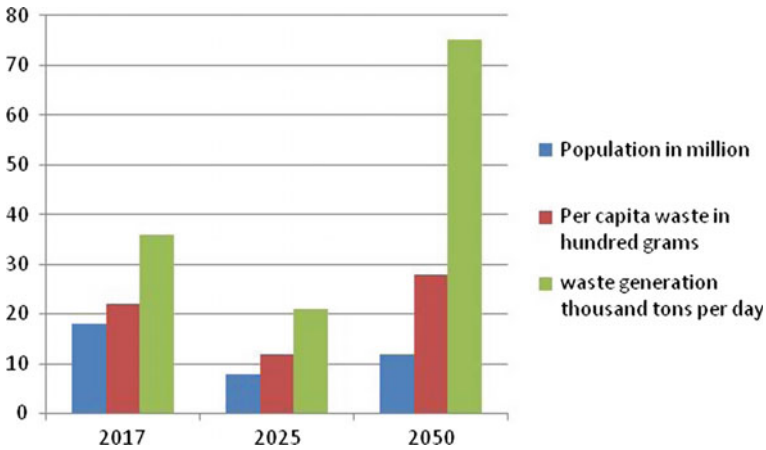


Fig. 2 Trend in MSW growth in Delhi

Table 1 Power generation in Badarpur power plant

Unit	Feed rate (in tonnes/day)	Capacity (in MW)
First	1664	100
Second	1692	100
Third	1640	100
Fourth	3193	210
Fifth	3036	210
Total	11,225	720

Capacity of power generation and feed rate of coal for each unit are as follows (Table 1).

The ultimate analysis of coal for Badarpur thermal power station is given as: Ash 46.56%, C 39.81%, H 3.35%, S 0.50%, N 0.78%, O 9% by mass [15].

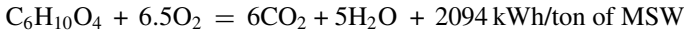
4 Calculation for Power Generation in a Plasma Arc Gasification Plant

The municipal solid waste (MSW) generated in Delhi is comprised of Compostable (54.42%), Recyclables (15.52%), C/N Ratio (34.87%), HCV (1802 kcal/kg), Moisture (49%) [16].

If the plant is going to be installed in Delhi then the HCV (high caloric value) of the MSW used is 1802 kcal/kg (as mentioned above).

$$\begin{aligned}
 \text{HCV} &= 1802 \times 4.184 \text{ kJ/kg} \\
 &= 7539.568 \text{ kJ/kg} \\
 &= 2094 \text{ kWh/ton of MSW}
 \end{aligned}$$

The organic fraction of waste can be represented as $\text{C}_6\text{H}_{10}\text{O}_4$, and the organic fraction is combustible and the inorganic one will constitute the remaining slag. Therefore, the overall combustion reaction is:



[17].

4.1 Finding Power Generated by Considering Data from InEnTec Process [17]

InEnTec's Plasma Enhanced Melter (PEM) System has its origins in many decades of work in the development of two different technologies—plasma technology and glass melter technology. By compounding these two technologies in a very unique way, InEnTec has built up an anarchistic concept that brings the eventual ability in transforming waste into salutary products, maximizing the potential for recycling. Syngas carries 90% of initial energy with 10% thermal losses in the gas reactor. This energy will be composed of 80% chemical energy and 20% thermal energy. We are considering only the chemical energy in our case. The calculation gives us gross energy per ton of MSW processed.

Therefore $90\% \times 80\%$ of 2094 = 1507.68 kWh/ton [17].

The thermal losses are measured experimentally are 400 kWh/ton of MSW processed. So net energy equals $1507.68 - 400 = 1107.68$ kWh/ton of MSW. Let gas turbine efficiency be 50%, hence, the net power obtained from gas turbine is $0.50 \times 1107.68 = 553.84$ kWh/ton of MSW.

The part of this energy is utilized for producing oxygen, (75k Wh/ton) and the plasma torch needs 180 KWh/ton of power, so the net energy that can be recovered from one ton of MSW to be:- $553.84 - 180 = 373.84$ kWh/ton of MSW. And for Delhi which generate nearly 12,740 tons of MSW per day, the power generation by plasma gasification plant will be equal to $373.84 \times 12,740 = 4,761,461.6$ kWh/day = 158.634 MW.

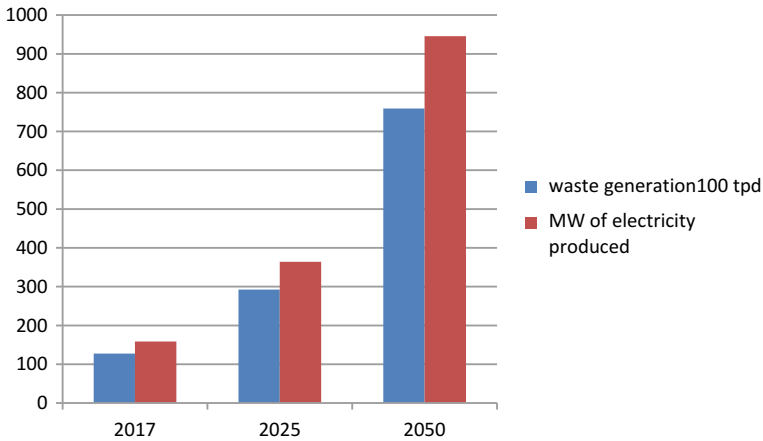


Fig. 3 Power generation

4.2 Estimation of Power Generation from Solid Waste Through Plasma Arc Gasification till 2050

We have shown the trend of waste generation in Delhi till 2050 in Fig 2 above we calculated the 1 ton of MSW would generate 298.84 KWh electricity. Combining the estimated future waste generation till 2050 with the calculation done in sec 5 about the estimated energy per ton of MSW, we can easily predict the potential of plasma arc gasification for energy generation till 2050. The graph given below clearly help to estimate that with the increase waste generation with the time energy generation will also increase. In 2017–18, estimated energy generated will be around 159 MW and it will increase to 950 MW in 2050 (Fig. 3).

5 Reduction in CO₂ from Atmosphere by Plasma Gasification Process

Today, the world is facing a horrendous problem of global warming due to unrestricted and unsustainable CO₂ emission level. Presently, 404 PPM CO₂ [17] in atmosphere and if the present trend of emission level through coal power is not arrested the problem of global warming unprecedented. In the section, we are giving estimated reduction in CO₂ level when the power is generated from PAG process then from coal-based power plant release about 1.2 kg of CO₂ per KWh of energy produced. PAG has emerged as Nobel Technology will drastically reduce. CO₂ emission to 0.2 kg/KWh energy produced. The graph below shows the level of CO₂ emission if the energy generated till 2050 in sec 7.2 would be produced by coal-based power

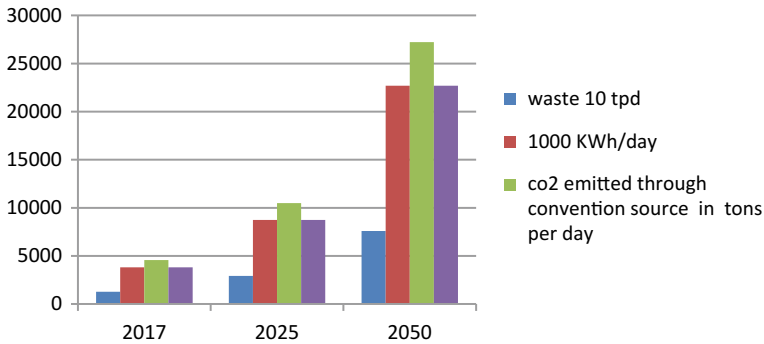


Fig. 4 CO₂ reduction

plant. The graph also shows the reduction in CO₂ emission if the energy would be generated by PAG of SWM (Fig. 4).

6 Conclusion

Today the world is at crossroads. If it is continued to keep up the things as they are of our present waste management and conventional power generation methods, the world will face existential threat due to environmental calamities. Every human being should pursue the goal of leaving this world a better place for our future generation. This paper is a humble attempt to suggest solid waste management through plasma arc gasification as alternative method in Delhi. The paper has shown that by opting to plasma arc gasification for solid waste management problem of finding land for landfilling of waste, health hazards due to open dumping of waste can be easily avoided. India is a growing economy and a responsible nation; it has been signed the Paris accord which personifies our commitment for sustainable development. It is required to be committed to reduce CO₂ emissions. Energy generation through plasma arc gasification will be a great leap forward in that direction.

References

1. World bank, waste generation. <http://siteresources.worldbank.org/INTURBANDEVELOPMENT/Resources/336387-1334852610766/Chap3.pdf>. Last Accessed May 21 2018
2. University of Ontario, Sustainability Today World's 200 largest city population predictions. <http://sites.uoit.ca/sustainabilitytoday/urban-and-energy-systems/Worlds-largest-cities/population-projections/city-population-2025.php>
3. <http://worldpopulationreview.com/world-cities/delhi-population/>. Last Accessed May 8 2018

4. Waste management is imperative in Delhi as the national capital inches closer to another Deonar–Firstpost. <https://www.firstpost.com/india/waste-management-is-imperative-in-delhi-as-the-national-capital-inches-closer-to-another-deonar-2697564.html>. Last Accessed May 10 2018
5. Ministry of Environment. <http://www.delhi.gov.in/wps/wcm/connect/environment/Environment/Home/Environmental+Issues/Waste+Management>
6. Delhi's 40-acre landfill site Bhalswa has been on fire for a week. <http://www.dailymail.co.uk/indiahome/article-3546535/Delhi-s-flaming-hell-40-acre-landfill-site-Bhalswa-fire-WEEK-thanks-42C-temperatures-leaving-locals-choking-putrid-black-smoke.html>. Last Accessed March 10 2018
7. <https://www.hindustantimes.com/delhi-news/municipal-corporation-inaugurates-india-s-largest-solid-waste-to-energy-plant-at-narela/story-dZuZaGLV3UFQPzU8vmSbyM.html>. Last Accessed on Nov 10 2017
8. <https://www.hindustantimes.com/delhi-news/it-looked-like-a-tsunami-witnesses-recount-garbage-avalanche-at-ghazipur-landfill-that-killed-2/story-fVIAOFISEDlw7LM7xawwbN.html>. Last Accessed on Nov 15 2017
9. Joshi R, Ahmed S (2016) Status and challenges of municipal solid waste management in India: a review. *Cogent Environ Sci* 2(1):1–18
10. Ojha A, Reuben FA, Sharma D (2012) Solid waste management in developing countries through plasma arc gasification: an alternative approach. *Elsevier APCBEE Procedia*, pp 193–198
11. <https://advancedplasmawater.com/solutions/process-overview/>. Last Accessed on April 09 2018
12. <https://www.explainthatstuff.com/plasma-arc-recycling.html>. Last Accessed on April 04 2018
13. Epaminondas Voutas, F (2016) Treatment and energy utilization of municipal and industrial solid waste with the plasma arc gasification technology. In: 4th international conference on sustainable solid waste management, National Technical University of Athens, Limassol Cyprus, pp. 1–31
14. Chandra A, Chandra HS (2004) Impact of Indian and imported coal on Indian thermal power plant. *J Sci Industrial Res* 152–162
15. Central Pollution Control board. http://cpcb.nic.in/uploads/hwmd/MSW_AnnualReport_2015-16.pdf. Last Accessed on Feb 04 2018
16. Ducharme C (2010) Technical and economic analysis of Plasma-assisted Waste-to-Energy processes. www.seas.columbia.edu. Columbia
17. <https://timesofindia.indiatimes.com/city/gurgaon/How-Surat-turned-clean-and-good-and-stayed-that-way/articleshow/7724287.cms>. Last Accessed on Feb 13 2018

Analysis and Optimization of Surface Integrity Characteristics of EDMed Work Surface Inconel 718 Super-Alloy Using Grey-Based Taguchi Method



Md. Ghaus Ali, Rahul, Dipraj Banik, Akshansh Yadav, B. C. Rautara and Ashok Kumar Sahoo

Abstract The aim of this research work is to find the optimum combination of input process parameters such as peak current (I_p), open voltage (V_g), pulse-on-time (T_{on}) and duty factor (τ) for machining of Inconel 718 on EDM. The output response parameters studied were metal removal rate (MRR), electrode wear rate (EWR) and surface roughness (R_a). L_{16} orthogonal array of input parameters was created as the design of experiments (DOEs) with the help of Minitab software. Grey relational analysis (GRA) method is used to get a single domain of multiple output response parameters. After that Taguchi optimization method was applied to find out the optimal parameter setting for higher MRR, lower TWR and lower R_a .

Keywords EDM · Inconel 718 super-alloy · Copper tool · GRA · Taguchi method

1 Introduction

Several machining processes involving the application of very intense local heat have come into use in recent years. In these processes, material is removed by erosion and evaporation at the surface of the work piece.

Mishra et al. [1] has presented the importance of EDM in today's industrial world. EDM is widely used as non-traditional machining process in manufacturing process. The advantages of EDM are as follows: EDM can be used effectively for machining of complex shapes, EDM machining process is independent of material's mechanical properties, and EDM machining can result in high accuracy. When both the tool and electrolyte are placed in a dielectric medium and a very high electric potential is applied, a high impulse electric spark is generated. The spark dissipates a huge amount of heat (8000–12,000 °C), resulting in melting of the work piece [2, 3]. Ezugwu et al. [4] has presented a typical problem as the cost of electrode becomes high during machining of Inconel 718 due to high EWR. It has become a crucial issue during machining of Inconel 718. Sudhakara et al. [5] has presented the

Md. Ghaus Ali · Rahul (✉) · D. Banik · A. Yadav · B. C. Rautara · A. K. Sahoo
KIIT (Deemed to Be University), Bhubaneswar, Odisha, India
e-mail: rahulkumar589@gmail.com

© Springer Nature Singapore Pte Ltd. 2019
K. Shanker et al. (eds.), *Advances in Industrial and Production Engineering*, Lecture Notes in Mechanical Engineering, https://doi.org/10.1007/978-981-13-6412-9_43

441

experimental investigation of machining of Inconel 718 on die-sink EDM. Various EDM parameters such as I_p , T_{on} , τ were taken during the machining of work piece. The output responses that were measured were metal removal rate and surface roughness. He showed the influence of I_p , T_{on} and τ on MRR, R_a and hardness. Ahamad and Lajis [6] in their work has analysed the electrode wear rate (EWR) of copper electrode during the machining of Inconel 718 by taking I_p and T_{on} high on EDM. They found that T_{on} is the most significant factor for TWR. Higher T_{on} can decrease TWR, but higher I_p can increase TWR. Rahul et al. [7] also conducted an experiment over the optimization of parameters on Inconel 601, Inconel 625, Inconel 718 and Inconel 825 super-alloys through electro-discharge machine based on 5-factor–4-level L_{16} orthogonal array and calculated the optimum results using the TOPSIS and Taguchi method for it. Rahul et al. [8] experimentally investigated machinability aspects of machining of Inconel 718 with copper tool. They conducted the research work based on L_{25} OA by taking various parameters such as V_g , I_p , T_{on} , τ and Flushing pressure F_p and various responses such as tool wear rate (TWR), surface roughness (R_a), surface crack density (SCD) and white layer thickness (WLT). Lin et al. [9] in his research work of optimizing EDM parameters used grey relational analysis in conjugation with fuzzy-based Taguchi method to find the optimum parameters.

In the present work, multilevel process parameter optimization of Inconel 718 super-alloy is done when machined with copper tool in EDM. Here, peak current, voltage, pulse-on-time and duty factor are taken as the variable parameters and MRR, TWR and R_a as machine responses.

2 Experimental Details and Data Collection

Inconel 718 super-alloy circular work piece having dimension (50 mm × 5 mm) has been used as work material. The snapshot of EDMed Inconel 718 is shown in Fig. 1. Copper (20 mm diameter) has been used as tool electrode (Fig. 2). Research work has been done on EDM (Model: ELEKTRA EMS 5535 Machine, Pune, India) set-up (Fig. 3). EDM oil 30 is used as dielectric fluid. The viscosity of EDM oil is 36 ssu at 38 °C. Work piece polarity has been chosen as positive. The design of experiment is taken as per 4-factor–4-level L_{16} orthogonal array (OA) given in Table 1. Here, peak current, voltage, pulse-on-time and duty factor are taken as the variable parameters each varied at four different levels. The duration of machining for every experiment was taken as 30 min. Various responses such as surface roughness (R_a), metal removal rate (MRR), electrode wear rate (EWR) have been measured for every experiment given in Table 2.

Fig. 1 EDMed Inconel

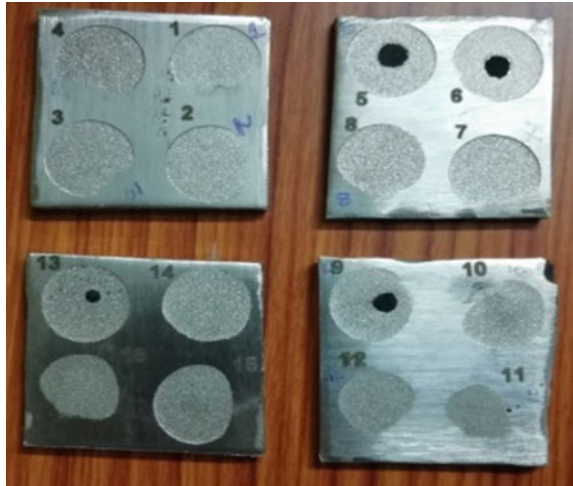


Fig. 2 Copper tool

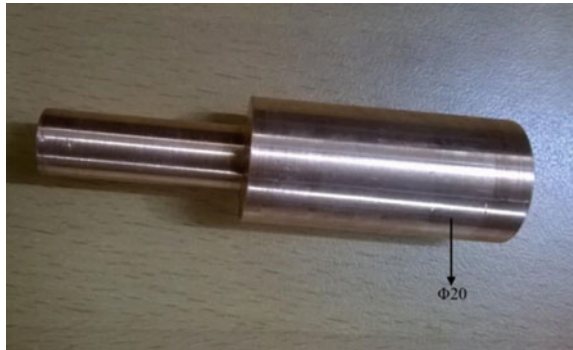


Table 1 Domain of experiments

Input parameters	Unit	Symbol	Levels of variation			
			1	2	3	4
Peak current (I_P)	A	A	8	10	12	14
Open voltage (V_g)	V	B	15	20	25	30
Pulse-on-time (T_{on})	μs	C	50	100	150	200
Duty factor (τ)	%	D	55	70	85	100

Fig. 3 EDM machine



Table 2 Design of experiments (DOEs): L₁₆ orthogonal array (collected data)

Exp. no.	Levels of parameters in coded form				Collected experimental data		
	A	B	C	D	MRR (mm ³ /min)	TWR (mm ³ /min)	SR (μm)
1	1	1	1	1	3.6621	0.0433	4.824
2	1	2	2	2	5.4932	0.0874	4.366
3	1	3	3	3	3.0518	0.1756	4.832
4	1	4	4	4	3.0518	0.1756	4.459
5	2	1	2	3	7.3242	0.0874	3.919
6	2	2	1	4	4.2725	0.1315	2.92
7	2	3	4	1	7.3242	0.1756	4.209
8	2	4	3	2	3.6621	0.2198	4.773
9	3	1	3	4	3.6621	0.0874	3.765
10	3	2	4	3	4.2725	0.0433	4.007
11	3	3	1	2	0.6104	0.0874	3.426
12	3	4	2	1	1.2207	0.1756	3.537
13	4	1	4	2	7.3242	0.0433	4.28
14	4	2	3	1	3.0518	0.0874	5.096
15	4	3	2	4	3.6621	0.1315	5.462
16	4	4	1	3	2.4414	0.1315	4.604

The output response parameters are explained below:

- MRR It is defined as the quantity of metal displaced from the job under a specific time. Unit was taken as mm³/min.
- TWR It is defined as the quantity of metal displaced from the tool under a specific time. Unit was taken as mm³/min.

3 Methodology

3.1 Grey Relational Analysis

In this analysis, the input parameters converted into normalized value in a scale range between 0 and 1. Since the response MRR is of larger-the-better type and TWR and R_a are of smaller-the-better type, then normalized value x_i^* for larger-the-better type, i.e. MRR, is expressed as:

$$x_i^* = \frac{x_i - x_{\max}}{x_{\max} - x_{\min}}$$

where i = experiment number, i.e. 1, 2, 3, 4, ..., 16, x_i^* = normalized value of MRR for i th experiment number, x_i = actual MRR value for the i th experiment number, x_{\min} = minimum actual value of MRR among all the 16 experiments done, and x_{\max} = maximum actual value of MRR among all the 16 experiments done. Normalized value $y_i^* = y_i - y_{\max} / y_{\min} - y_{\max}$ for “smaller-the-better” type, i.e. TWR and R_a , is expressed as:

where i = experiment number, i.e. 1, 2, 3, 4, ..., 16, y_i^* = normalized value of TWR or SR for i th experiment number, y_i = actual TWR or SR value for the i th experiment number y_{\min} = minimum actual value of TWR or SR among all the 16 experiments done, and y_{\max} = maximum actual value of TWR or SR among all the 16 experiments done.

Step I: Calculating deviation sequences (Δ) for the normalized data

After the normalization procedure, all performance values (MRR, TWR and R_a) will be scaled into [0, 1]. Deviation sequence aims to find the alternative whose normalized value is the closest to the reference value. Upon calculating the normalized value of MRR, TWR and SR for each experiment number, we calculate deviation sequences (quality loss function) with the help of normalized values of MRR, TWR and SR for each experiment number. Deviation sequence is denoted by Δ and mathematically calculated as:

$$\Delta_i = 1 - \text{Normalised Value of Response Parameters} \\ \text{(i.e. MRR, TWR and } R_a\text{) for } i\text{th experiment run.}$$

where i = experiment number, i.e. 1, 2, 3, ..., 16. Example: For $i = 1$, i.e. first experiment run, $\Delta_{MRR\ 1} = 1 - S_{MRR\ 1} = 1 - 0.4545 = 0.5455$

Step II: Determining grey relational coefficient (GRC) and grey relational grade (GRG)

The GRC is mathematically defined as follows:

$$GRC = \frac{\Delta_{\min} + \Gamma \Delta_{\max}}{\Delta_{ij} + \Gamma \Delta_{\max}}$$

where i = experiment number, j = refers to the response parameters, i.e. MRR, TWR and R_a , Δ_{\min} = minimum value of deviation sequence for j th response parameter among all the 16 experiments, Δ_{\max} = maximum value of deviation sequence for j th response parameter among all the 16 experiments, Γ = distinguishing factor (when all the response parameters are given the equal weightage, then usually its value is taken as 0.5). After finding GRC for each experiment run for every parameter, i.e. MRR, TWR and R_a , GRG was calculated for every experiment. GRG combines all the individual GRCs of parameters like MRR, TWR and R_a of a particular experiment run into one grade which can be compared with the other GRG of other experiment runs. GRG is mathematically found out by the relation given below:

$$GRG_i = (W_g \times GRC_{MRR_i}) + (W_g \times GRC_{TWR_i}) + (W_g \times GRC_{R_a_i})$$

where i = Experiment No., W_g = Weightage given to the response parameters = 0.33 (as $\Gamma = 0.5$).

Then, optimization of GRG function is done using Taguchi approach. As GRG is wished to be the maximum, so during signal-to-noise ratio calculation higher-the-better approach was used. The calculations of GRG and S/N ratio are given in Table 3.

4 Results and Conclusions

The machining responses obtained from the experiments were used to calculate S/N ratio plots, and the optimal parameter setting appears to be $A_2B_1C_4D_2$, i.e. $I_P = 10\text{ A}$, $V_g = 15\text{ V}$, $T_{on} = 200\ \mu\text{s}$ and $\tau = 66.67\%$.

The optimum process parameters found as $A_2B_1C_4D_2$ and the corresponding value found as -1.05155 are less than the corresponding values found in every experiment. Since the S/N ratio's need was higher-the-better, we found the highest corresponding value at the optimum setting showing the reliability of the Taguchi approach. The main effects plot for S/N ratios [$A_2B_1C_4D_2$] is shown in Fig. 4.

Table 3 Calculations

Exp. no.	MRR	TWR	R_a	Δ_{MRR}	Δ_{TWR}	Δ_{R_a}	GRC _{MRR}	GRC _{TWR}	GRG	S/N ratio	Predicted value
1	0.454	1.000	0.251	0.545	0.000	0.749	0.478	1.000	0.620	-4.152	
2	0.727	0.750	0.431	0.272	0.249	0.568	0.647	0.666	0.588	-4.612	
3	0.363	0.250	0.247	0.636	0.749	0.752	0.440	0.400	0.409	-7.765	
4	0.336	0.250	0.394	0.636	0.749	0.605	0.440	0.400	0.427	-7.391	
5	1.000	0.750	0.607	0.000	0.249	0.393	1.000	0.666	0.735	-2.674	-1.052
6	0.545	0.500	1.000	0.454	0.499	0.000	0.523	0.500	0.668	-3.504	
7	1.000	0.250	0.492	0.000	0.749	0.507	1.000	0.400	0.626	-4.068	
8	0.454	0.000	0.271	0.545	1.000	0.729	0.478	0.333	0.402	-7.915	
9	0.454	0.750	0.667	0.545	0.249	0.332	0.478	0.666	0.576	-4.791	
10	0.545	1.000	0.5724	0.4545	0.000	0.427	0.523	1.000	0.681	-3.337	
11	0.000	0.750	0.8009	1.0000	0.249	0.199	0.333	0.666	0.566	-4.943	
12	0.090	0.250	0.7573	0.9091	0.749	0.242	0.354	0.400	0.471	-6.539	
13	0.272	0.473	0.7916	0.0000	0.000	0.535	1.000	1.000	0.819	-1.734	
14	0.237	0.463	0.8301	0.6364	0.249	0.856	0.440	0.666	0.487	-6.249	
15	0.202	0.452	0.8686	0.5455	0.499	1.000	0.478	0.500	0.433	-7.270	
16	0.167	0.442	0.9072	0.7273	0.499	0.662	0.407	0.500	0.441	-7.111	

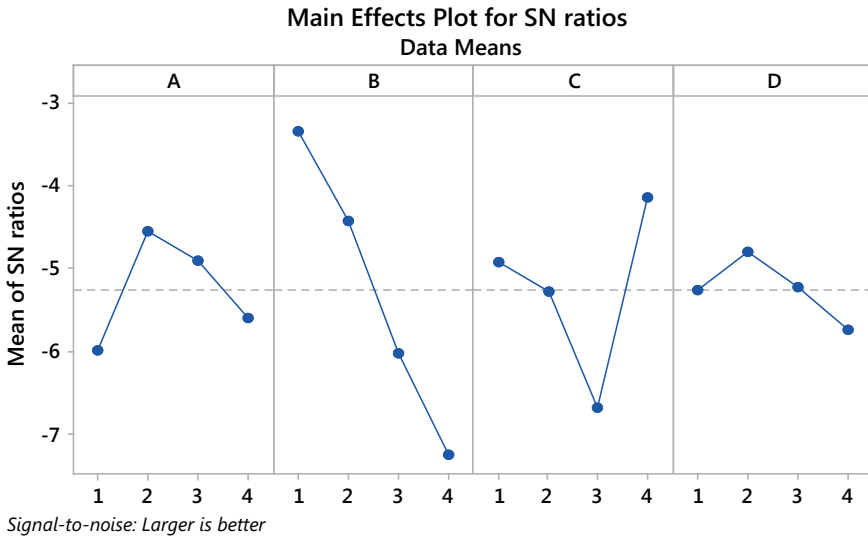


Fig. 4 Main effects plot for S/N ratios [A₂B₁C₄D₂]

References

- Mishra DN, Bhatia A, Rana V (2014) Study on EDM. *Int J Eng Sci* 3(2):24–35
- Muller F, Monaghan J (2000) Non-conventional machining of particle reinforced metal matrix composite. *Int J Mach Tools Manuf* 40(9):1351–1366
- Lau WS (2000) Unconventional machining of composite materials. *J Mater Process Technol* 48:199–205
- Ezugwu (2005) Key improvements in the machining of difficult to cut aerospace superalloys. *Int J Mach Tools Manuf* 45:1353–1367
- Sudhakara D, Venkataramana BN, Sreenivasulu B (2012) The experimental analysis of surface characteristics of inconel 718 using electrical discharge machining. *IJMERR* 1(3). ISSN: 2278-0149
- Ahmad S, Lajis MA (2014) Effect of higher peak current and pulse duration on EWR of copper electrode when electrical discharge machining (EDM) of inconel 718. *Adv Mat Res* 845:945–949
- Rahul, Abhishek K, Datta S, Biswal BB, Mahapatra SS (2017) Machining performance optimization for electro-discharge machining of inconel 601, 625, 718 and 825: an integrated optimization route combining satisfaction function, fuzzy inference system and Taguchi approach. *J Braz Soc Mech Sci Eng* 39(9):3499–3527
- Rahul, Datta S, Biswal BB, Mahapatra SS (2018) Optimization of electro-discharge machining responses of super alloy inconel 718: use of satisfaction function approach combined with Taguchi philosophy. *Mater Today Proc* 5(2):4376–4383
- Lin CL (2004) Use of the Taguchi method and grey relational analysis to optimize turning operations with multiple performance characteristics. *Mater Manuf Processes* 19(2):209–220. <https://doi.org/10.1081/amp-120029852>

Framework the Food Supply Chain Network in the Present Indian Scenario



Bhavya Nidhi Vats, Anuj Gupta and Ganesh Sharma

Abstract In India, agriculture sector always takes priority over the other leading areas as the maximum population is dependent on it for their bread and butter. It contributes the major proportion to the Indian economy and most significantly provides nutritional security to the country. Despite of all these facts, the issues like food security, post-harvest losses, and socioeconomic status of the farmers are the major challenges which create barriers to the development of the country. Recently, numerous studies have been found in the concern of food waste and losses along the supply chain. Even so, the 40% of the food is wasted in India according to a report of United Nations Development Programme. In this study, causes of food waste and losses along the supply chain network are identified and weighted based on the survey of previous literature. The aim of this study is to categorize the major causes as a superset and the minor causes as its subset and is represented through fishbone diagram for its clear vision. Secondly, the initiatives regarding the reduction in food waste are identified and prioritized using the weighted prioritization matrix approach. This study helps to give an idea about the most significant initiative that government should adopt at large scale in the context of reducing food waste and losses. It is concluded from the results that the linkages between farmers and industries require prior attention over the other initiatives to improve the efficiency and profitability of food supply chain.

Keywords Post-harvest losses · Fishbone diagram · Weighted prioritization matrix

1 Introduction

Food waste and losses are one of the major concern issues that dominate over the human society in the upcoming years. According to a report from the Food and

B. N. Vats (✉) · G. Sharma
Moradabad Institute of Technology, Moradabad, India
e-mail: vats.bhavya01@gmail.com

A. Gupta
G. L. Bajaj Institute of Technology and Management, Noida, India

© Springer Nature Singapore Pte Ltd. 2019
K. Shanker et al. (eds.), *Advances in Industrial and Production Engineering*, Lecture Notes in Mechanical Engineering, https://doi.org/10.1007/978-981-13-6412-9_44

Agriculture Organization (FAO) in 2011, one-third of the total worldwide food is wasted or ends up with losses per annum [1]. Wastage of food is the alarming issue as the population of the country increases rapidly by 2050. The goal is not just to focus on the reduction of food waste but also to address the cause of wastes or losses. Agriculture sector always takes priority over the other in spite of this fact, India ranks 63 among 88 countries in the Global Hunger Index [2].

Post-harvest losses are mainly those which are associated with the agriculture produce and take place after harvest and before human consumption. It includes the losses mainly spoilage in a food supply chain, by-products from the processing of agriculture produce (sugarcane bagasse from sugar), and the residues associated with the main crop type (wheat or rice husk). Post-consumer losses are those which are associated with the behavior and activities of the consumer regarding food consumption. According to a recent study by ASSOCHAM (2013), India's post-harvest fruits and vegetable losses is over Rs. 2 trillion annually, due to the lack of inadequate cold storage facilities and lack of proper food processing units [3]. Apart from this one example, there are so many other roadblocks in the different stages of food supply chain such as lack of proper transport medium, lack of loading and unloading facilities at the farm and marketplace, lack of packaging facilities, and lack of knowledge of advanced techniques that lead to the wastage [4]. Most of the post-harvest losses of agriculture produce and their residues are still simply dumped and undocumented which not only lead to the financial loss but impact on the environment badly. Lack of knowledge and awareness regarding the recoverable waste turns into the loss of economy. Waste generation in India is showing an increasing trend, if channelized properly will definitely enhance the development of the country. In India, 40% of the food production is wasted according to the report presented by the United Nations Development Programme [5]. It is indeed a matter of fact that poverty and hunger are the dominant issues, and the food never reaches to the needy. This shows the lack of management in the food life cycle, and there is a prerequisite need to improve it.

Now, we proceed with the discussions in the last recent years on the food supply chain management regarding the technological interventions and new strategies to avoid the post-harvest losses in the supply chain. In the study conducted by Beausang et al., the clear statement related to the term "food losses" and "food waste" has been defined. They stated that food loss generally occurs in the initial stages of FSC such as production or processing while the food waste is traced at every stage of the supply chain even after the consumer usage. They concluded that farmers play a vital role in reducing the food waste in the primary production stage [6]. Chegere analyzed different post-harvest handling practices in his study and their associated costs and benefits to the farmers. He found total 11.7% post-harvest loss to the maize farmers in which two-thirds mainly occurred during storage. He analyzed the economic feasibility of those post-harvest handling practices which is rarely seen in the research papers [7].

Muriana reviewed in his study that accidental events prompted the unavoidable food losses and wastage at each stage of the supply chain. Additionally, the author proposed new research topics in minimizing the food waste and loss by highlighting the parameters forecasting, innovative technologies for shelf life monitoring, redesign

of logistics SC models, pricing strategy, and risk analysis for managing the accidental events [8]. Kibler et al. proposed a conceptual model in which food waste affect the FEW nexuses in both the production and disposal stages [9]. Gardas et al. concluded his study by defining three significant factors which play a major role in post-harvest losses. These are lack of linkages between industry, Government and institutions, lack of technology and advanced technique in food procession, lack of linkage between farmers and processing unit [4].

The study conducted by Russell investigated the behavior of the consumers regarding the food waste using a comprehensive model of planned behavior, interpersonal behavior, and environmental behavior. The study involves the Questionnaires related to the food waste behavior, habits, and intentions to reduce food waste and self-reported food waste behavior. The result showed that participants intended to reduce their waste but contrary to these facts the food waste behavior is dominant over the mat higher level [10]. Food and Agriculture Organization (FAO) of the United Nations has carried out the study on the food losses in various areas of India between May and July 2016. The aim of this initiative is building capacities along the supply chain, use of innovative and new technologies, installation of local storage and distribution centers as well as raising general awareness about greater efficiency and sustainability [11].

Mukherjee et al. (2013) [12] highlighted the food supply chain issues of India in his study that despite having the second largest producer of grains feeding the safe, quality, and nutritious food to more than one billion people is a challenging task.

The study conducted by D. G. Mongale has examined the key issues in the food grain supply chain of bulk transportation between producing and consuming (deficit) states. The parameters such as operations and inventory holding cost of food grains at the surplus state silos, silo storage capacity, the demand for deficit states, and availability of food grains at surplus nodes are considered. With the objective to minimize the overall cost of bulk food grain shipment, operational and storage cost, the mixed inter-nonlinear programming model is formulated. The model involves the constraints of silo storage, vehicle capacity, seasonal procurement, vehicle preference, etc. [13].

Khera has defined the prominent issues such as wastage of resources through spoilage, leakage, and theft in the Indian food security system which is the primary cause of concern [14]. Related to his work, Biswal et al. investigated the impact of RFID adoption in the Indian food supply chain network. The comparison has been done with and without RFID for managing the inventory in terms of shrinkage and misplacement [15].

With the help of literature survey, the following objectives are designed to analyze the food supply chain management in the Indian context and proceed with the findings.

1. To identify and categorize the major causes as a superset and the sub-causes as its subset which is represented through the fishbone diagram for its clear vision

- 2. Secondly, the initiatives regarding the reduction in food waste are identified by the literature analysis and prioritized using the weighted prioritization matrix approach.

2 Finding Barrier from the Literature

In this section, the food supply chain has been analyzed through the previous recent literature survey. Figures 1 and 2 have shown the changes that occurred in the food supply chain with the increasing demand and urbanization. Earlier, the food supply chain possesses the straight path to fulfill the demand of the customer, as shown in Fig. 1. Due to which it takes more time to reach up to the individual customer and acquires the less variety. While in current scenario of the food supply chain, the farmer or processor has the opportunity to sell its product directly to their customers, as shown in Fig. 2. The Government of India has launched various schemes and e-mandis (market) for the ease of the farmers. Despite of having benefits, the current supply chain management also becomes intricate and complex due to the increasing trend of population and urbanization.

From the insights of the literature review, it is observed that at the initial stage of supply chain (pre-harvesting stage), there are so many barriers which may cause the food losses or wastes. Lack of forecasting results in the overproduction of the food items which will reduce the market rate and wastage of that product. Although farmers work hard for the production, they will not revert back the same results in terms of financial value. In the second stage of supply chain, major losses found



Fig. 1 Traditional supply chain network

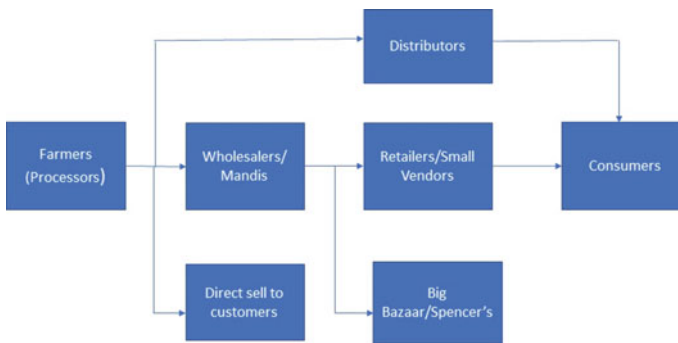


Fig. 2 Modern supply chain network

to be occurred due to the shortage of warehouses and cold storage facilities. In the year 2017, Madhya Pradesh Government has to suffer a loss of 785 crores due to the lack of ample storing facilities of onions. This large amount is consumed to dispose the onions at one-fifth of the actual cost through PDS and open market operations [16]. In the next stage of the supply chain, the losses incurred in protecting the food items, especially the perishable products like fruits and vegetables from the environmental impacts or in the logistics approach. Major losses are found due to the lack of suitable transport facilities, lack of temperature controlling environment during the transportation. It leads to the mechanical damage, early rotting which will end up with the unprocessed, unmarketable, and inconsumable food products. Last but not least, consumers are responsible for the food wastage in a major proportion. Food-consuming quality habits, lack of awareness and facilities regarding the proper disposal of food items lead not only the wastage of food but result in the environmental degradation.

3 Methodology

3.1 Qualitative Analysis

Qualitative analysis is the useful tool in research as it provides the opportunity to get open discussions and investigation of the complex issues. It does not impose any mathematical constraints to any practical situation for the deep analysis and understanding of the root cause of the problem. There are two qualitative techniques such as fishbone diagram (cause and effect diagram) and weighted prioritization approach implemented to the present study.

3.1.1 Fishbone Diagram (Cause and Effect Diagram)

A fishbone diagram, also known as cause and effect diagram, is a visualization tool for categorizing the potential causes of the problem in order to identify its root causes.

Dr. Kaoru Ishikawa, a Japanese Quality Control expert, is credited for inventing the fishbone diagram. This diagram is basically based on the brainstorming criteria that give varying causes according to their level of importance in a form of hierarchy. The design of the diagram is simply like a skeleton of a fish. These diagrams are generally worked from right to left, with each large bone (major cause) of the fish branching out to include smaller bones (sub-causes) containing vast detail about the problem.

Following major causes are considered for the study of present study to root cause of the food wastage:

3. Lack of standardized quality control
4. Lack of required storage facility

Table 1 Assign weight to the problem through literature analysis [17]

S. No.	Issues	Code	Ranking	Weightage
1.	Lack of standardized quality control	A	6	5
2.	Lack of refrigerated storage facilities	B	3	8
3.	Weak logistic approach	C	4	7
4.	Large number of intermediaries	D	1	10
5.	Lack of new harvesting techniques	E	2	9
6.	Overproduction	F	5	6

5. Weak logistics approach
6. Large number of intermediaries
7. Lack of new harvesting techniques
8. Overproduction

3.1.2 Weighted Prioritization Matrix

A prioritization matrix is a useful technique to identify which problems are the most significant to work on solving first. The matrix helps you rank problems or issues generated through brainstorming, using weighted criteria that are important to your study. In this paper, the major issues that play significant role in affecting the food waste and loss have been summarized and weighted (importance rating) according to the survey of previous literature report [17] as shown in Table 1.

4 Result and Discussion

4.1 Fishbone Diagram

This information is summarized by acquiring the knowledge from the previous literature related to the problem of food loss and waste. Hence, Fig. 3 gives the brief overview of the major causes and sub-causes that leads to the problem of food loss and wastes.

4.2 Weighted Prioritization Matrix

The importance rating (weightage) is given to the following issues which lies in the horizontal axis of the given Table 1. In the vertical axis, the initiatives or strategies are assigned for the respective issues. The number has been assigned in the blocks

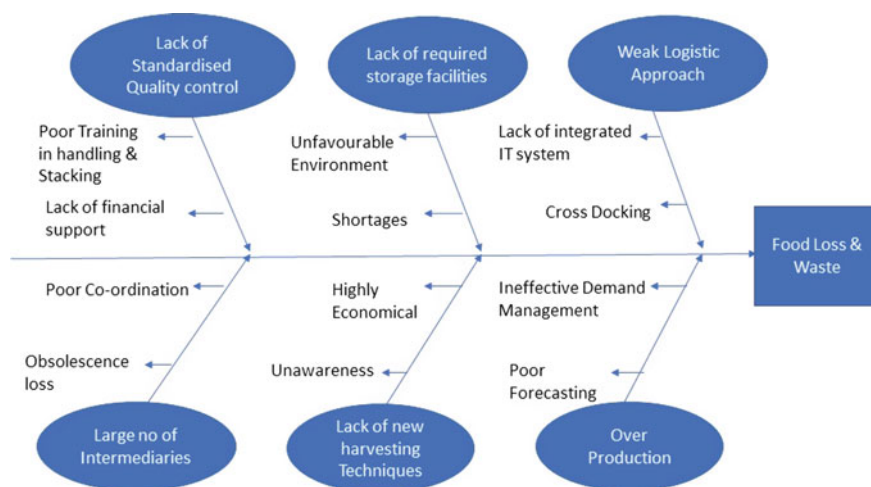


Fig. 3 Fishbone diagram

Table 2 Weighted prioritization matrix

Importance rating	5	8	7	10	9	6	
Strategy/initiatives	A	B	C	D	E	F	Total
New and innovative harvesting technologies	8	0	4	5	10	0	208
Linkage between farmers and industries	6	8	8	10	4	0	286
Forecasting techniques	2	0	4	5	0	10	148
Installation of local storage and distribution center	4	8	7	8	0	0	213
Optimal inventory management	6	7	4	5	0	9	220
Government laws regarding new policies, e.g., e-mandis	7	7	4	6	5	5	254
RFID adoption	5	3	7	3	5	2	191

in the manner how much each initiative related to that issue and then it is multiplied by the importance rating factor. The data has been compiled by doing the sum of all those results for getting the priority of each initiative which require maximum implementation for the profitable food supply chain (Table 2).

5 Conclusion

The food supply chain management is a prominent sector as it contributes in an economical aspect, provides employment and food security to our country. Despite of

the fact, there are so many challenges to prevent the food losses and wastes from the very initial stage to its final disposal. In this study, we investigated the past recent literature to understand the current scenario of food supply chain network and the major causes of food waste. It has been found that there are so many new techniques like RFID, various government schemes like e-mandis and improvisation in supply chain such as new pricing strategies are implemented to improve the performance of the food supply chain. Simultaneously, the complexity and intricacy in the supply chain network have also increased due to the growing demand in a less time. The study has been concluded by using qualitative techniques such as fish-bone diagram and weighted prioritization matrix approach. Surveys regarding new techniques, initiatives, and strategies have been summarized by undergoing the past recent literature.

It is found that “large number of intermediaries in a supply chain network” out of six major causes is assigned the highest weightage.

The initiative of government “to develop linkages between farmers and industries” needs priority over the other for the profitability of the food supply chain.

References

1. Raak N, Symmank C, Zahn S, Witzel JA, Rohm H (2017) Processing and Product related causes for food waste and implications for the food supply chain. *Waste Manage* 61:461–472
2. <http://thecsrjournal.in/food-wastage-in-india-a-serious-concern/>
3. Cardoen D, Joshi P, Diels L, Sarma PM, Pant D (2015) Agriculture biomass in India: Part 2. Post-harvest losses, cost and environmental impacts. *Resour Conserv Recycl* 101:143–153
4. Gardas BB, Raut RD, Narkhede B (2017) Modeling causal factors of post-harvesting losses in vegetable and fruit supply chain: an Indian perspective. *Renew Sustain Energy Rev* 80:1355–1371
5. thecsrjournal.in/food-wastage-in-india-a-serious-concern/
6. Beausang C, Hall C, Toma L (2017) Food waste and losses in primary production: qualitative insights from horticulture. *Resour Conserv Recycl* 126:177–185
7. Chegere MJ (2017) Post-harvest losses reduction by small-scale maize: economic studies. Department of Economics, School of Business, Economics and Law, University of Gothenburg
8. Muriana C (2017) A focus on the state of the art of food waste/losses issue and suggestions for future researches. *Waste Manage*
9. Kibler KM, Reinhart D, Hawkins C, Motlagh AM, Wright J (2018) Food waste and the food-energy-water nexus: a review of food waste management alternatives. *Waste Manage*
10. Russell SV, Young CW, Unsworth KL, Robinson C (2017) Bringing habits and emotions into food waste behavior. *Resour Conserv Recycl* 125:107–114
11. <http://www.fao.org/save-food/projects/study-fl-india/en/>
12. Mukherjee D, Bajaj H, Garg N, Abraham J (2013) Feeding a billion: role of the food processing industry
13. Mogale DG, Dolgui A, Kandhway R, Kumar SK, Tiwari MK (2017) A multi period inventory transportation model for tactical planning of food grain supply chain. *Comput Ind Eng*
14. Dreze J, Khera R Understanding leakages in the public distribution system. *Econ Polit. Weekly* 50(7):39
15. Biswal AK, Jenamani M, Kumar SK (2018) Warehouse efficiency improvement using RFID in humanitarian supply chain: Implications for Indian food security system. *Transp Res Part E* 109: 205–224

16. <http://www.krishijagran.com/news/low-cost-onion-storage/>
17. Balaji M, Arshinder K (2016) Modeling the causes of food wastage in Indian perishable food supply chain. *Resour Conserv Recycl* 114:153–167

A Comprehensive Review on Jute Fiber Reinforced Composites



Ekta Gogna, Ramanuj Kumar, Anurag, Ashok Kumar Sahoo
and Amlana Panda

Abstract Natural fiber composite is the novel materials in recent decades having a high strength to weight ratio and light in weight are widely used for structural and unstructured applications. Jute fiber is one of the most common biodegradable natural fibers which successfully replaced the synthetic fibers composite and also replaced glass fiber where the high strength is not obliged. Jute fiber composite has several attractive advantages over synthetic and glass fiber like as low processing cost, low density, stiffness easily available, excellent mechanical properties and low production energy required (2% of glass fiber). This advantage makes the jute a very attractive reinforced fiber for composites. This paper presented an overview on different fabrication techniques and the effects of the various factors on the mechanical properties of the jute fiber reinforced composite.

Keywords Jute fiber · Mechanical properties · Thermal properties · Wood

1 Introduction

Nowadays, the rapid deforestation due to high demand of wood make furniture's creates environmental issues to the society. A major portion of wood is used for making household products. However, there is need to search an alternatives of wood made products. Jute composite for replacement of wood could be a solution to the problem due to bounded matrix of high strength fibers. Jute fiber is biodegradable and eco-friendly product with improved properties such as dimensional stability, low cost, easily available and renewable. There are various applications of jute composites such as jute mat, thermoplastic composite, building and construction, fishing boats, and natural fiberboard are found. Composites are used for structural, thermal, electrical, environmental and other various applications. The natural fibers are preferred to the synthetic ones due to the abundance, biodegradable and renewable nature. By

E. Gogna · R. Kumar (✉) · Anurag · A. K. Sahoo · A. Panda
Kalinga Institute of Industrial Technology (Deemed to be University),
Bhubaneswar, Odisha, India
e-mail: ramanujkumar22@gmail.com

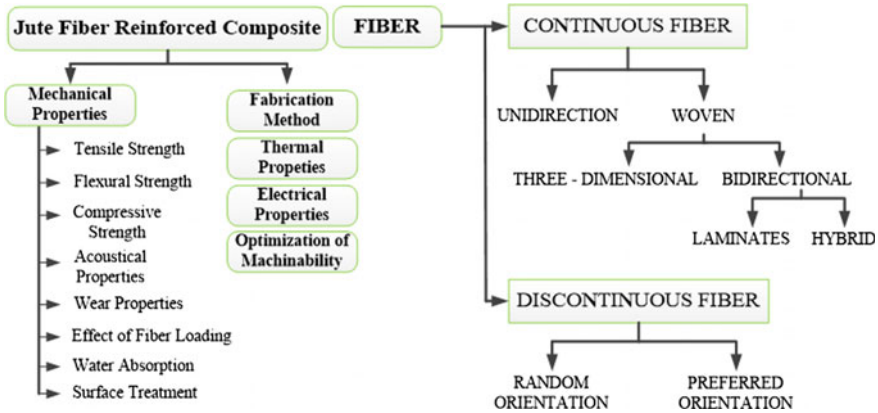


Fig. 1 Overview study of the jute fiber reinforced composite

implementation of innovation and advanced technologies, wood could be replaced by jute by enhancing the mechanical, thermal and electrical properties. Various researchers had worked on the jute composite and to investigate the mechanical properties of composite. Liu emphasized the influence of depositing the nano-SiO₂ particles on the properties and the microstructure of jute fibers [1]. Roy et al. explored the synergistic effect of nano-clay and jute fiber on the mechanical, dynamic mechanical and thermal properties of natural rubber composites which were reinforced by suitable hybrid fillers [2]. Boccardi et al. focused on using jute as reinforcement with varying matrices. The matrix used was polypropylene and poly-lactic and tests such as impact, cyclic and quasi-static bending were performed [3]. Jha studied the erosion and mechanical behavior of hybrid composite by fabricating it using hand lay-up technique [4]. The aspects of jute composite are displayed through Fig. 1.

2 Fabrication Technique of Composite

2.1 Hand Lay-Up Technique

By this technique, both natural and synthetic composites can be prepared. To avoid the mold to stick on the surface, releasing agent is sprayed and thin plastic sheets are used at the top and bottom. The reinforced fiber was woven in a mat form and a suitable resin with a hardener is poured over it and spread uniformly with a brush. Another layer of fiber was placed above the first and rolled to remove the excess of matrix. This process is repeated until the required thickness is achieved. Plastic sheet was placed on the top of the mold and pressure is applied. The mold was ready after keeping it for 24–72 h. Various researchers carried this technique to fabricate the composite.

The ceramic filler such as aluminum oxide fillers and silicon carbide filler effect on jute fiber which were illustrated and laminated and prepared by hand techniques and then tested by universal testing machine. The addition of fillers showed enhanced mechanical properties [5]. Effect of the epoxy on the fiber surface was used hand-lay technique for fabrication. Alkaline solution with different composition was used to prepare the composite specimen. Izod test under ASTM dimensions showed high impact strength when the solution of 0.5 M sodium hydroxide was soaked for 8 h [6]. Hand lay-up technique for fabricating jute fiber composite provided the improved laminated composites without sacrificing its performance [7].

2.2 Compressed Technique

This is a high pressure close molding process in which two equal metal molds hold the composite. The lower is fixed while the upper one is movable. The matrix and reinforcement are arranged in the mold and then compressed. The shape and size of the component determine the amount of heat and pressure required. The composite is compressed by adding jute fiber and aluminum and then the load applied varied from 2 to 15 weight percent. It was analyzed that the fusion of jute and aluminum increased the micro-hardness [8–10]. Compression technique used to prepare composite using jute fabric and biopol found the improved mechanical strength and adhesion phenomena was increased which provided the highest mechanical properties of biopol composite DG400G [11].

3 Mechanical Properties

3.1 Tensile Strength

Various researchers investigated the effect of the tensile strength under various loading condition by UTM and the impact testing of the materials and found that fiber composite material had improved mechanical properties [12, 13]. Tensile test and deflection temperature revealed that an adding of 40% weight of jute fiber to polypropylene increased the tensile strength by 19.7% noted [14]. Addition of jute into polymer epoxy gave increased properties but was inferior to glass reinforced in mechanical strength [15]. The mechanical properties of the jute-glass reinforced polypropylene-based composite with 30 weight percent fibers were better than the jute polypropylene-based composite whereas reinforced filler material enhanced the mechanical properties of composite up to a certain level [5, 16]. When using of plasma powers, the adhesion between the jute fiber and polyester matrix increased which enhanced the tensile strength and flexural strength [17]. Reinforced the jute fiber with paper laminated composite additional enhanced the tensile properties [18].

Composite of jute fabric and biopol by compression method enhanced the mechanical strength [10].

3.2 Flexural Strength

Flexural strength is the stress developed in the material before it yields in the flexural test. It represents the highest stress which is experienced when the materials yields. The impact of Charpy energy increased with the increased in volume of jute fraction [13, 19]. Solution of potassium permanganate of varying composition to soak the jute composite to increased flexural strength and examined the mechanical characteristics of jute fiber reinforced composite and found that voids were predominant influence factor for mechanical properties of jute fiber composite [20]. Hybrid jute performed better than the simple jute fiber composite in terms of flexural stiffness, tensile and compressive strength and moisture absorption and mechanical properties increased with rise in weight of TiO_2 from 0 to 6% [21, 22]. The hybrid paper composite offered better flexural properties than the pure paper composite [23]. Oxygen plasma-treated composite revealed the increased tensile strength and flexural strength which enhanced the mechanical properties of jute [24]. The jute–epoxy composite offered superior flexural and tensile properties as compare to the jute–polyester composite [25].

3.3 Compressive Strength

Compressive strength is the capability of the material to resist load. When the arrangement of the yarn in a direction of wrap was longitudinal and double layered with sawdust, then the most ideal and favorable characteristics were attained [26]. Mechanical properties of jute fiber composite decreased with increase of natural rubber [13]. Due to the poor adhesion between the fiber and matrix, the mechanical properties increase up to a precise level and then diminution [27]. A new jute material composite treated by hydroxyethyl acrylate enhanced the mechanical properties compared to untreated composites [28].

3.4 Acoustical Properties

Acoustical properties of the composite materials define the behavior of composites when it was subjected into sound waves medium. When the arrangement of the yarn in a direction of wrap was longitudinal and double layered with sawdust, then it showed the most ideal and favorable characteristics [29]. Jute fiber composite offered

better result as compare to the glass fiber composite also low-density jute indicated better performance as compare to high-density jute for absorption of sound [30].

3.5 Wear Properties

Wear represents the damage and loss of materials from composite surface and it was measured through abrasion test. Addition of fluorocarbon, hydrocarbon and fluorocarbon into the jute reinforced fiber composite enhanced the mechanical properties and when the fiber was placed normal to the direction of slide, the coefficient of friction with increment in applied load was reduced [29].

3.6 Effect of Fiber Loading

The fiber loading affected the mechanical properties of jute fiber composite and the presence of the holes in the composite was identified as an inspiring factor toward mechanical properties of the composite, also fiber loading and orientation arrangement affected the mechanical and electrical properties of matrix [20, 30].

3.7 Water Absorption

Ability of the water absorption of jute fiber composite affected its mechanical properties. Very less amount of water was absorbed in biopol when compared with jute composites. Due to the effect of fluorocarbon, hydrocarbon and hybrid fluorocarbon surface treatment the composite materials absorbed less amount of water which elevated the mechanical properties of jute fiber composites [29, 30]. Ability of water absorption was influenced by the size and flexural strength of composites [31]. The water absorption effect reduced the mechanical properties of recycled jute composite [32, 33].

3.8 Surface Treatment

Surface treatment was used to improve the overall performance of the composite. A two mm polymer film penetrated on the jute fiber which increased the mechanical properties of the composite [34]. Alkali, peroxide, permanganate and silicate treatment modified the surface of jute and enhanced the flexural and tensile properties [35].

4 Thermal Properties

The thermal conductivity of the material is the rate of heat transfer through it in steady state. The surface treatment (alkali) of the jute fiber enhanced the thermal conductivity of the composite [36]. At higher temperature, fracture toughness was improved with silane treatment but effects of treatment at lower temperature were insignificant. Also, the applied surface treatment affected the thermal properties of the composite [37, 38]. Addition of heat supplied improved the bond ability between the fiber and matrix materials [39, 40].

5 Electrical Properties

Study of electrical properties includes resistance, conductance and thermo-electricity behavior of jute composite. According to Ahmed et al., jute fiber and particles of copper are compressed through varying load for diffusion of copper in jute composites. It was examined that the fusion of jute and copper increased the electrical conductivity [5]. BCFA resin mixed with acrylic resin and catalyst in required proportions and compressed for Jute, jute-bamboo, glass, glass bamboo composite. The fiber loading and arrangement of fiber affected the electrical properties of matrix [34, 36].

6 Optimization of Machinability

Various optimization techniques (GRA, Taguchi, RSM, ANN, Fuzzy-logic, etc.) have been used to optimize the process variables. The drilling operation has been implemented to create holes on untreated and alkali-treated jute fiber composites and optimization based on GRA methodology has been accomplished. Aftermath found that the delamination failure increase with increment in feed rate and also ANOVA indicated that the effect of fiber treatment is insignificant factor to influencing the delamination of fabricated composite [41].

7 Conclusion

A comprehensive review has been made as follows:

- Jute fiber composite is better alternate of synthetic fibers composite due to low cost, low weight, easy availability, eco-friendly, biodegradable and high flexural strength of jute.
- Fabricating techniques with various sizes, orientation and weight segment of reinforced material highly influenced the mechanical behavior of composite.

- Various types of the surface treatment used by several researcher and achieved affirmative results to improve the mechanical strength of the composite.
- Moisture content influences the mechanical properties (bending and tensile) of the composite also flexural stress and shearing stress decline with grow in the immersion time.

Inadequate investigations on use of micro- /nano-sized reinforced material during fabrication jute composites have been found. Also, implementation of soft computing technique to judge the performance of jute composites in different mechanical tests was rare. However, it can be future of scope in jute composite fabrication works.

References

1. Liu X, Cui Y, Hao S, Chen H (2018) Influence of depositing nano-SiO₂ particles on the surface microstructure and properties of jute fibers via in situ synthesis. *Composites Part A* 109:368–375
2. Roy K, Debnath SC, Das A, Heinrich G, Potiyaraj P (2018) Exploring the synergistic effect of short jute fiber and nano clay on the mechanical, dynamic mechanical and thermal properties of natural rubber composites. *Poly Testing* 67:487–493
3. Boccardi S, Carlomagno GM, Meola C, Russo P (2018) The contribution of infrared thermography in the characterization of jute based composites. *Comp Struct* 190:119–126
4. Jha K, Samantaray BB, Tamrakar P (2018) A study on erosion and mechanical behavior of jute/e-glass hybrid composite. *Mater Today Proc* 5:5601–5607
5. Ahmed KS, Mallinatha V, Amith SJ (2011) Effect of ceramic fillers on mechanical properties of woven jute fabric reinforced epoxy composites. *J Reinf Plast Comp* 30(15):1315–1326
6. Bachtiar D, Sapuan SM, Hamdan MM. The influence of alkaline surface fibre treatment on the impact properties of sugar palm fibre-reinforced epoxy composites. *Polym Plast Technol Eng* 48(4):379–383. <https://doi.org/10.1080/03602550902725373>
7. Dobah Y, Bourchak M, Bezazi A, Belaadi A, Scarpa F (2016) Multi-axial mechanical characterization of jute fiber/polyester composite materials. *Composites Part B* 90:450–456
8. Biswas B, Chabri S, Mitra BC, Bandyopadhyay NR, Sinha A. Mechanical behaviour of aluminium dispersed unsaturated polyester/jute composites for structural applications. *J Inst Eng India Ser C*. <https://doi.org/10.1007/s40032-016-0329-7>
9. Biswas B, Chabri S, Mitra BC, Bandyopadhyay NR, Sinha A. Effect of copper/graphite addition on electrical conductivity and thermal insulation of unsaturated polyester/jute composites. *J Inst Eng India Ser D*. <https://doi.org/10.1007/s40033-015-0107-3>
10. Islam R, Islam T, Nigar F, Saha S, Tapash A, Sharmin N, Dey K, Mustafa AI, Khan RA, Khan MA, Zaman HU (2011) Fabrication and mechanical characterization of jute fabrics: reinforced polyvinyl chloride/polypropylene hybrid composites. *Int J Poly Mater* 60:576–590
11. Alam MK, Khan MA (2006) Comparative study of water absorption behavior in biopol and jute-reinforced biopol composite using neutron radiography technique. *J Reinf Plast Comp* 25(11):1179–1187
12. Zhong Z, Li M, Liao Z, Lu L. The impact of adhesive resin solution on carbon fibers cloth and jute-reinforced epoxy resin matrix composites. *J Text Inst* 107
13. Zaman HU, Khan MA, Khan RA (2011) Effect of ultraviolet radiation and potassium permanganate on the physico mechanical properties of jute polymer composites. *Polym Plast Technol Eng* 50:651–659
14. Nabila S, Juwono AJ, Roseno S (2017) Effect of weight fractions of jute fiber on tensile strength and deflection temperature of jute fiber/polypropylene composites. *Mater Sci Eng* 196:012029. <https://doi.org/10.1088/1757-899X/196/1/012029>

15. Raghavendra G, Ojha S, Acharya SK, Pal SK (2013) Jute fiber reinforced epoxy composites and comparison with the glass and neat epoxy composites. *J Compos Mater* 1–11
16. Dey K, Sharmin N, Khan RA, Nahar S, Parsons AJ, Rudd CD (2011) Effect of iron phosphate glass on the physico-mechanical properties of jute fabric-reinforced polypropylene-based composites. *J Therm Compos Mater* 24:695–711
17. Seki Y, Sarikanat M, Sever K, Erden S, Gulec HA (2010) Effect of the low and radio frequency oxygen plasma treatment of jute fiber on mechanical properties of jute fiber/polyester composite. *Fiber Polym* 11(8):1159–1164
18. Verma BB (2009) Continuous jute fibre reinforced laminated paper composite and reinforcement-fibre free paper laminate. *Bull Mater Sci* 32(6):589–595
19. Pereria AC, Monterio SN, de Assis FS, Margem FM, da Luz FS, Braga FO (2017) Charpy impact tenacity of epoxy matrix composites reinforced with aligned jute fibers. *J Mater Res Technol* 6(4):312–316
20. Mishra V, Biswas S (2013) Physical and mechanical properties of bi-directional jute fiber epoxy composites. *Procedia Eng.* 51:561–566
21. Deb A, Das S, Mache A, Laishram R (2017) A study on the mechanical behaviors of jute-polyester composites. *Proc Eng* 173:631–638
22. Seshanandan G, Ravindran D, Sornakumar T (2016) Mechanical properties of nano titanium oxide particles–hybrid jute-glass FRP composites. *Mater Today Proc* 3:1383–1388
23. Das S (2017) Mechanical properties of waste paper/jute fabric reinforced polyester resin matrix hybrid composites. *Carbohydr. polym:* 1–29
24. Karaduman Y, Gokcan D, Onal L (2012) Effect of enzymatic pretreatment on the mechanical properties of jute fiber-reinforced polyester composites. *J Comp Mater* 47(10):1293–1302
25. Gopinath A, Kumar S, Elayaperumal A (2014) Experimental investigations on mechanical properties of jute fiber reinforced composites with polyester and epoxy resin matrices. *Procedia Eng.* 97:2052–2063
26. Vignesh V, Balaji AJ, Karthikeyan MKV. Effect of wood sawdust filler on the mechanical properties of Indian mallow fiber yarn mat reinforced with polyester composites. *Int J Polym Anal Charact* 22(7):610–621
27. Gupta MK, Srivastava RK, Bisaria H (2015) Potential of jute fibre reinforced polymer composites: a review. *Int J Fibre Text Res* 5(3):30–38
28. Behera D, Bastia TK, Banthia AK (2011) Hydroxyethyl acrylate treated jute–esoa composite laminate: a new development for structural materials. *Int J Plast Technol* 15(1):86–92
29. Ali A, Shaker K, Nawab Y, Ashraf M, Basit A, Shaid S, Umair M. Impact of hydrophobic treatment of jute on moisture regain and mechanical properties of composite material. *J Reinf Plast Comp* 1–10. <https://doi.org/10.1177/0731684415610007>
30. Fatima S, Mohanty AR (2011) Acoustical and fire-retardant properties of jute composite materials. *Appl Acoust* 72:108–114
31. Thirmizir AMZ, Ishak MZ, Taib RM, Sudin R, Leong. Mechanical, water absorption and dimensional stability studies of kenaf bast fibre-filled poly(butylene succinate) composites. <https://doi.org/10.1080/03602559.2010.531871>
32. Osman EA, Vakhguelt A (2012) Kenaf/recycled jute natural fibers unsaturated polyester composites: water absorption/dimensional stability and mechanical properties. *Int J Comp Mater Sci Eng* 1(1):1–17
33. Aquino EMF, Sarmiento LPS, Oliveira W (2007) Moisture effect on degradation of jute/glass hybrid composites. *J Reinf Plast Comp* 26(2):219–233
34. Khan MA, Balo SK, Ali KMI (1999) Jute-reinforced urethane polymer composite under gamma radiation. *Polym Plast Technol Eng* 38(4):767–782
35. Goriparthi BK, Suman KNS, Rao NM (2012) Effect of fiber surface treatments on mechanical and abrasive wear performance of polylactide/jute composites. *Composites Part A* 43:1800–1808
36. Sudha S, Thilagavathi G. Analysis of electrical, thermal and compressive properties of alkali-treated jute fabric reinforced composites. <https://doi.org/10.1177/1528083717695840>

37. Basak R, Choudhury PL, Pandey KM (2018) Effect of temperature variation on surface treatment of short jute fiber-reinforced epoxy composites. *Mater Today Proc* 5:1271–1277
38. Samal S, Stuchlik M, Petrikova I (2017) Thermal behavior of flax and jute reinforced in matrix acrylic composite. *J Therm Anal Calorim*. <https://doi.org/10.1007/s10973-017-6662-0>
39. Pujari S, Ramakrishna A, Padal KTB. Investigations on thermal conductivities of jute and banana fiber reinforced epoxy composites. <https://doi.org/10.1007/s40033-015-0102-8>
40. Sever K (2010) The improvement of mechanical properties of jute fiber/LDPE composites by fiber surface treatment. *J Reinf Plast Comp* 29(13):1921–1929
41. Sridharan V, Muthukrishnan N (2013) Optimization of machinability of polyester/modified jute fabric composite using grey relational analysis (GRA). *Proc Eng* 64:1003–1012

Analysis of Lean Manufacturing Implementation in SMEs: A “5S” Technique



Shyam Sunder Sharma, D. D. Shukla and Bhupendra Prakash Sharma

Abstract The aim of this paper is to analyze the implementation of 5S technique on Indian SMEs to maximize efficiency in the workplace and to have the possibility of product diversification, higher quality, lower cost, reliable deliveries, etc. 5S is a basic tool of lean manufacturing system. It is a tool of classification, order, cleaning, standardization, and discipline. Findings of this research can be stated that the introduction of 5S technique for the improvement of SMEs in its process flow line, cost reduction, machine efficiency improvement, well-organized tools placement, shop floor cleanliness, and high-quality workplace are the identified key parameters to be optimized.

Keywords Lean manufacturing · Cost reduction · Production improvement

1 Introduction

5S is a continuous lean management improving tool, whose task is to create healthy, clean, and good working environment. 5S technique is considered a basic lean technique, as it establishes manufacturing stability and continuous improvement [1, 2]. In the 1980s, Japan was initially introduced the 5S technique in manufacturing sector. West countries and American countries' industries already used 5S technique in manufacturing sector and getting benefits in productivity, profit, and employees' behavior. So, Japanese industries also decide to getting benefit of 5S technique, and they also introduce 5S in manufacturing as well as in other sectors like hospitals and offices [3, 4]. The 5S improves the process efficiency and management performance [5]. 5S is the methodology from maintaining organization clean, effective,

S. S. Sharma (✉)

Department of Mechanical Engineering, Manipal University Jaipur, Jaipur, India
e-mail: shyamsunder.sharma@jaipur.manipal.edu

D. D. Shukla

Department of Mechanical Engineering, Amity University, Jaipur, India

B. P. Sharma

Department of Mechanical Engineering, Amity University, Noida, India

© Springer Nature Singapore Pte Ltd. 2019

K. Shanker et al. (eds.), *Advances in Industrial and Production Engineering*, Lecture Notes in Mechanical Engineering, https://doi.org/10.1007/978-981-13-6412-9_46

and systematic workplace. Due to this employees feels good working environment and it eliminates losses with failures and breaks, improve the quality of product and safety at workplace [6–8]. It is the technique to improve working environment derived from the Japanese words Seiri, Seiton, Seiso, Seiketsu, and Shitsuke. In English, the meaning is Selection, Systematization, Cleaning, Standardize, and Self-discipline [9]. This technique focuses to improve working environment, reduces industrial waste and non-value-adding activity, and improves quality and safety. 5S is literally five abbreviations of Japanese words with five initials of S.

1. **Selection:** Select the product on basis of “what is needed, when needed, what quantity is needed.” Remove all unnecessary items from the workplace; only selected items which are used in the running process are placed.
2. **Systematization:** Arrange all equipments in order and label the equipment and easily visible. The systematics will be ineffective if there are too many items that are stored in one workplace.
3. **Cleaning:** Remove all the unnecessary items and remove dirt/dust/waste. Workplace should be cleaned every day for improving comfort and reducing the risk of equipment failure.
4. **Standardization:** To set some rules to follow above three steps selection, systematization and cleaning which helps the employee to understand their task and try to achieve 5S method.
5. **Self-discipline:** In the concept of Kaizen, continuous improvement is required to compete in market. To improve self-discipline internal audits, bonus policies and checklist for various work station is applying.

5S technique was successfully implemented in manufacturing sector, offices, and health care sector. It is quality improvement lean tool to remove non-value-adding activities and increase the profit of the organization [10]. 5S increases environment performance and also reduces industrial waste in manufacturing industries. It promotes cleanness in stores of raw material and finished goods [11].

2 Phases of 5S Implementation Process

The successful implementation of 5S tool is the responsibility of company management and staff members. 5S must be implemented after the proper training, and employees must be aware about this technique. Teamwork is required for 5S implementation. Staff members and management decide the steps to follow 5S implementation. Divide the responsibilities between employees and make clear mission and vision of the company. Every employee tries to achieve these mission and vision. The duration of mission and vision should be 2–5 years. First we decide the objectives of 5S implementation.

- Remove the industrial waste
- Increase the quality of product

Fig. 1 Implementation of 5S method



- Decrease the unnecessary movement of part and operator
- Decrease the manufacturing cost
- Increase the security and safety
- Improve working environment

One of the most important elements of 5S implementation is habit of each employee from top level to bottom level. Each employee must follow the 5S rules and improve his/her habits in the company premises.

Second element is to assign responsibilities to each employee in different levels. Train all employees and motivate them to maintain 5S basic rules. 5S implementation method is shown in Fig. 1.

5S is implemented atleast two years period of time towards sustain. 5S implementation is usually classified into four phases. Responsibilities of different level employees are given in Table 1. Production head is responsible for setting the mission and vision of the company, and other employees can achieve these mission and vision. Same as shop floor head is responsible for the implementation of 5S. Shift incharge monitors the changes due to 5S implementation. Foreman and operators are responsible for training junior operators and maintaining the discipline.

- I. Preparatory phase
- II. Introductory phase
- III. Implementation phase
- IV. Maintenance phase

In Fig. 2, lean implementation flow chart is given. For full lean implementation, at least two-year time duration is required. After the implementation, it should be maintained for further time duration.

Table 1 5S responsibilities

Production dept. head	Company has set mission and vision, and these are to be achieved by introducing 5S
Shop floor manager	Responsible for 5S implementation
Shift incharge	Monitor employees in term of changes due to 5S
Foreman	Instruct the new employees about the functioning of system
Operator	Implement the instructions and maintain self-discipline

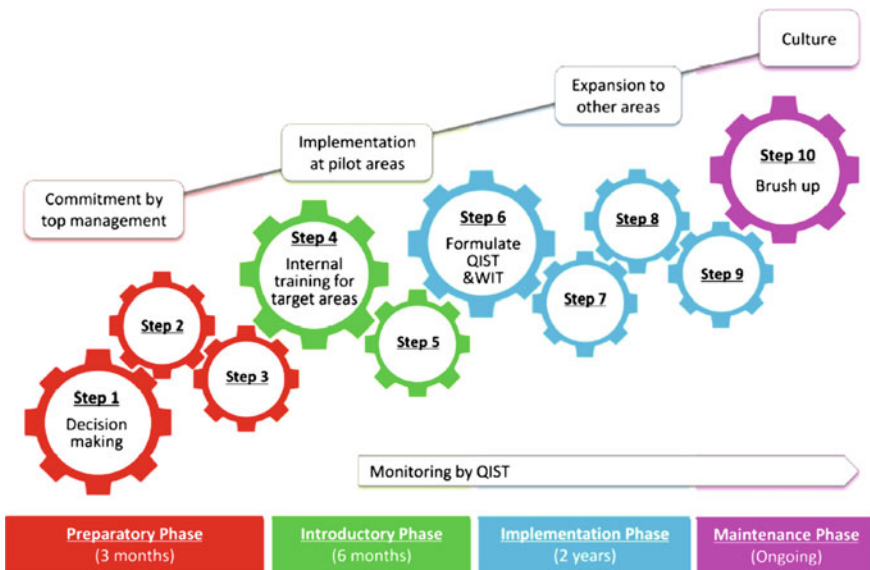


Fig. 2 5S implementation flow chart

In Fig. 3, raw material was placed on shop floor, and it was placed randomly; but after 5S is introduced, the raw material is separated according to its size and shape, and it was placed in racks, and in each rack naming is done according to its size. So it is very easy to identify the material according to its size.

In Fig. 4, it clearly shows that subassembly parts are placed in bins without nameplate. So it takes too much time to identify the correct subassembly parts. When 5S was implemented, all subassembly parts are properly arranged in bins and naming was done according to the part.

In Fig. 5, tools are placed haphazardly in rack and it is very difficult to find out the proper tool in very short time. To rectify this difficulty, 5S was introduced and tools are placed in proper manner, unwanted tools are removed from the rack, and proper name slip is placed in the tooling rack.



Fig. 3 Raw material was placed on floor, after 5S it was placed on racks with naming [12]



Fig. 4 Subassembly components are without nameplate, but after 5S naming was done [12]

In Fig. 6, we see that all scrap as well as finished goods are placed on the floor. So it takes so much time to separate them and some time by mistake scrap piece was mixed with the finished good or vice versa. After 5S was implemented, proper bins are placed for finished goods as well as raw materials. So it is very easy to identify raw material as well as finished goods.



Fig. 5 Tools were placed haphazardly but after 5S everything was placed in proper way with name slip [12]

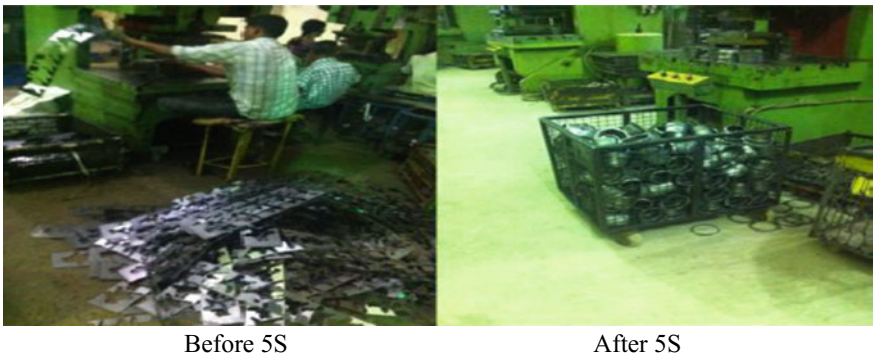


Fig. 6 Scrap was placed on floor, separate bin was provided for scrap and finished goods [12]

3 Methodology

5S technique means cleaning the workplace and arranging all tools in organized way in workplace. It was the first lean tool that was implemented by organizations. With the help of 5S technique, working condition of workers was improved and helped them to learn more to reduce the waste, reduce manufacturing time, and decrease work in process inventory.

5S implementation would result full utilization of workspace needed for existing operations. It also organized tools and work material by labeled and color coded.

5S methodology is a simple and universal approach that accepted by all over the world. It supported other manufacturing improvement tools like JIT, cellular manufacturing, TQM, Kanban and also played very vital role in better workplace to spend more time in shop floor.

What problems are avoided by 5S implementation?

- Reduce time wasted in searching parts and tools
- Reduce unneeded motion
- Save human energy
- Reduce defective work piece
- Machines that do not receive sufficient maintenance tend to break down and cause defect
- To avoid dirty work area
- Items are left in hazardous locations
- Dark, dirty disorganized workplace results to low the worker moral.

4 Results and Discussion

5S technique was implemented in Indian SMEs, and due to this technique, there is huge change in industries' profit and employee working. Now they start implementing more lean tools. Shop's floor looks more arranged, clean, well-organized, good working environment, and employees are self-motivated. Company put tag on each box and put signboard on specified locations. They are putting drums near to the machines where wastage is dumped. According to process tools are arranged and unwanted tools are separated. Company makes tool board where all tools are placed and easy to find out. 5S eliminates communication gap between management and employees. Now company shares each problem with the related department employees and gets best solution. Initially, company faces lots of problems in 5S implementation. Employees are not support due to misunderstanding and they fear about job loss.

5 Conclusion

The present paper aims to implement 5S in SMEs. It is very difficult to introduce 5S in SMEs because both management and labor are not supporting this technique. They think that there is huge investment in 5S implementation and there is production loss. One by one, 5S tool is introduced and after few months, management and employees have seen the result. The productivity of the company was improved; the working condition of workers also improved.

References

1. Maharjan S, Shyam K (2011) Implementing the 5S methodology for the graphic communications management
2. Cooper K, Keif MG, Macro KL (2007) Lean printing: pathway to success. Printing Industries Press
3. Hirano H (1995) 5 pillars of the visual workplace. Productivity press
4. Jackson TL (2009) 5S for healthcare. CRC Press
5. Filip FC, Marascu-Klein V (2015) The 5S lean method as a tool of industrial management performances. In: IOP conference series: materials science and engineering, vol 95, No. 1. IOP Publishing, p 012127
6. Michalska J, Szewieczek D (2007) The 5S methodology as a tool for improving the organization. *J Achiev Mater Manuf Eng* 24(2):211–214
7. Ho SK (1995) TQM: an integrated approach: implementing total quality through Japanese 5-S and ISO 9000. Kogan Page
8. Karkoszka T, Szewieczek D (2007) Risk of the processes in the aspect of quality, natural environment and occupational safety. *J Achiev Mater Manuf Eng* 20(1–2):539–542
9. Falkowski P, Kitowski P (2013) The 5S methodology as a tool for improving organization of production. *PhD Interdiscip J* 4:127–133
10. Kanamori S, Shibamura A, Jimba M (2016) Applicability of the 5S management method for quality improvement in health-care facilities: a review. *Trop Med Health* 44(1):21
11. Rojasra PM, Qureshi MN (2013) Performance improvement through 5S in small scale industry: a case study. *Int J Mod Eng Res* 3(3):1654–1660
12. Kakkar V, Dalal VS, Choraria V, Pareta AS, Bhatia A (2015) Implementation of 5S quality tool in manufacturing company: a case study. *Int J Sci Technol Res* 4(02):208–213

Performance and Combustion Characteristics of Thumba and Argemone as Dual Fuel Blends in a DIC Engine: An Experimental Approach



Shahid Qayoom and Sumit Kanchan

Abstract Dependence on import and concerns of continuous growth in the cost of imported fuels, because of insufficiency of petroleum resources, have created an essential need for investigators to start exploring and analyse the alternate resources of energy as a fuel for IC engines which can be generated from various easily available resources like vegetable oil, animal fats, waste cooking oil, etc. This is an experimental approach made to determine the performance and combustion characteristics of Thumba oil (*Citrullus colocynthis*) and Argemone Mexicana as dual biodiesel blends. The tests were conducted on a single-cylinder, four-stroke, direct injection, compression ignition engine. In this investigation, the analysis of various parameters like average cylinder pressure, net heat release rate (HRR), brake thermal efficiency (BTE) and mechanical efficiency was carried out by changing required operating conditions. The results obtained from the experimental investigation settle on a conclusion that average cylinder pressure for a heavier dual blend of biodiesel D60T20A20 (i.e. diesel 60%, Thumba 20%, Argemone 20% by vol) is greater than that of diesel fuel by 1.7%. The HRR for lighter dual blend D90T5A5 (i.e. diesel 90%, Thumba 5%, Argemone 5% by vol) is found to be 11.67% greater than that of diesel. Also, for almost every blend of Thumba and Argemone, there is a decline in BTE and mechanical efficiency than diesel.

Keywords Dual fuel biodiesel · Thumba oil (*Citrullus colocynthis*) · Argemone oil · Combustion · Performance · Diesel engine

S. Qayoom (✉)

B.S. Abdur Rahman Crescent Institute of Science and Technology, Vandalur,
Chennai, Tamil Nadu 600048, India
e-mail: qayoomshahid@gmail.com

S. Kanchan

Lovely Professional University, Phagwara 144411, India

© Springer Nature Singapore Pte Ltd. 2019

K. Shanker et al. (eds.), *Advances in Industrial and Production Engineering*, Lecture Notes in Mechanical Engineering, https://doi.org/10.1007/978-981-13-6412-9_47

477

1 Introduction

Increased attention towards environmental concerns originated by the contribution of pollution from the vehicle using diesel fuel. With continuous rise in vehicular emissions, different countries are taking stringent actions to control the pollution level into the environment. Several studies are made to formulate the feasible control methods and alternative fuels to find out appropriate solutions in order to reduce emission levels from automobiles. Also, rising demand and continuous depletion of petroleum resources caused the countries to initiate a research in the field of alternative fuels for reducing the dependency on import of petroleum-based fuels and sudden price hike. Therefore, it may be suggested to use biofuels as an alternative fuel for vehicles to provide a solution for alarming consequences [1]. Srithar et al. [2] revealed that biodiesel is an alternative fuel for petroleum-based fuels which is extracted from vegetable oils by means of transesterification process in the presence of a catalyst.

Thumba biodiesel (*Citrullus colocynthis*) mostly referred as Colocynth is categorized from a cucurbitaceous family [3]. In Hindi, mostly famous by the name of Indrayan and in English referred as Bitter Apple [4]. It is mostly found in desert areas of Africa and Asia due to its drought-resistant quality. In India, it is being found that Rajasthan and Gujarat are the two states, where this type of plant is cultivated mainly due to the presence of larger desert areas [5]. There are various qualities which enhance its cultivation economically because it does not require any special care or continuous requirement of irrigation. The plant requires six months to complete its growing cycle means it can be cultivated twice in a year. Currently, its oil is being mainly used for soap extraction [6]. Some researchers are considering it as most feasible than jatropha because of having fuel characteristics almost nearer to diesel. Further, some important characteristics of Thumba oil are grouped in Table 1, which stipulates that it can be fruitful for assisting rural economy.

Argemone Mexicana, on the other hand as a non-edible oil [8], is mostly found in wastelands or sandy soil and can be cultivated in poor-quality soil [9, 10]. Shukla et al. [8] revealed that total yield of oil is about 35%. Hence, it could be considered as a good source of alternative biodiesel. The advantage of using Argemone Mexicana

Table 1 Thumba plant characteristics [7]

S. No	Characteristics	Thumba plant
1	Plant type	Creepers
2	Soil type	Sandy soil
3	Crop cycle	180 days
4	Manure	No special requirement
5	Seeds colour	Brownish
6	Fruit size	7–10 cm
7	No. of fruits/plant	15–30 circular shaped

is its ease of production from infertile soil or an agricultural area which makes its production cost lesser than conventional diesel [11].

Presently, it has been discovered that straight vegetable oil cannot be directly used in the compression ignition engines due to various drawbacks like sticking of piston rings, carbon deposition, clogging of injectors. Hence, treatment of bio-oil from a method like transesterification process is considered as a preferred method to convert straight vegetable oil into refined quantity fatty acid methyl ester (FAME) or biodiesel [12].

Pal et al. [13] discovered the performance properties by comparing the effect of using Thumba biodiesel and *Jatropha* biodiesel on a four-cylinder, water-cooled, four-stroke diesel engine, by varying load parameter using Eddy current dynamometer. In this investigation, it was concluded that up to 2500 rpm, torque remains almost similar among all blends but beyond 2500 rpm, the torque output for Thumba biodiesel (TB10, TB20) becomes higher as compared to *jatropha* biodiesel (JB10, JB20) and diesel. It was further concluded that BSFC for both *jatropha* biodiesel and Thumba biodiesel is slower than diesel.

Also, Kumbhar et al. [14] performed an experiment to investigate the performance analysis by using Thumba oil blended with diesel on single-cylinder, four-stroke, variable compression ratio diesel engine in which it was calculated that BTE for TB10 (Thumba oil 10%, diesel 90%) at compression ratio of 18 showed significant increase in BTE, i.e. 36.31% as compared to diesel having 33.27%.

In another study [15], on a single-cylinder engine using blends of Thumba biodiesel (B20 and B40) with pure diesel, it was concluded that B40 is having higher BTE, i.e., 29.87% as compared to pure diesel 29.49%. Also, among the results B20 showed lower BSFC. Parida and Rout [16] carried out the experimental investigation on a single-cylinder variable compression ratio diesel engine using *Argemone Mexicana*-based biodiesel blend with diesel. The results showed that B40 (*Argemone* 40%, diesel 60%) blend indicates the higher peak pressure (57.4 bar) than B10 and pure diesel which is 57.1 and 54.4 bar, respectively, under the operating conditions with a compression ratio of 17.5 and loading condition of 8 kg.

The published data of various investigators reveals that India is a good producer of various non-edible oils like *Jatropha*, *Pongamia pinnata* (Karanja), *Argemone Mexicana*, etc. It has been estimated that by the year 2020, there will be about 20–22% of biofuel operated vehicles available on roads of India, Brazil, China and Europe. This estimated data enables India to research as much as possible in the cultivation of non-edible oils [19]. It can be noted that most of the investigation is carried out using single blended biodiesel with diesel and very few investigations were performed using dual biodiesel blends with diesel [17].

The objective of this investigation is to carry out the performance and combustion analysis of an engine using a dual biodiesel (a combination of two biodiesel blends with diesel fuels). The types of biodiesels used for this exertion are Thumba (*C. colocynthis*) and *Argemone Mexicana* which are blended with diesel to make a dual biodiesel fuel. The motive of this investigation is to find out the impact on performance and combustion characteristics of a DIC engine using Thumba and

Argemone Mexicana-based dual blends in comparison with diesel to find whether it is commercially feasible.

2 Materials and Methods

2.1 Biodiesel Production

In this study, the two vegetables named as Argemone Mexicana and Thumba are used for the investigation process because of their non-edible characteristics thereby having less effect on food security. Pure biofuels have higher viscosity due to which prolonged operation in engines creates various problems like clogging of fuel injectors, sticking of piston rings, higher engine deposition [18]. Viscosity levels are then lowered by transesterification process in order to bring the FAME to permissible limits [20, 21]. Transesterification process of raw Thumba vegetable oil showed free fatty acid value to be 4.4 mg KOH/g of sample, which suggests one-step transesterification process is required. A mixture of 1500 ml of oil with 390 ml of methanol and 10 grams of potassium hydroxide (KOH) is poured and stirred into the reactor and heated up to a temperature of 65 °C by means of hot water circulation. Later, the whole mixture is washed with water 5–10 times to eliminate heavy impurities like soap, glycerol, etc., and allowed to settle. Once settled and filtered, the fuel was heated to a temperature of 100–105 °C in a hot air oven and finally the pure Thumba biodiesel is extracted.

For Argemone, the measured fatty acid value is 12.27 mg KOH/g of sample for raw Argemone and requires two-step transesterification necessitating increased concentration of methanol two-step transesterification process because of higher acid content [22]. The biodiesel production process is summarized in Fig. 1. The properties of fuels measured for both the Thumba and Argemone biodiesels were summarized in Tables 2 and 3, respectively. It can be noted from the properties of biodiesels that their properties like density, specific gravity, calorific value and viscosity are almost similar to that of conventional diesel. Also, the viscosity of Argemone biodiesel is higher, i.e. 5.67 cSt as compared to Thumba biodiesel and diesel, i.e. 5.37 cSt and 2.80 cSt, respectively. Pramanik et al. [9] concluded that such high viscosity level for Argemone biodiesel is because of higher molecular weight like triglycerides. Also, properties like density, specific gravity, calorific value, flashpoint, fire point and viscosity for Argemone biodiesel are higher than Thumba biodiesel which justifies the Argemone can be used as a fuel to blend with Thumba oil which might result in enhancement of engine performance.

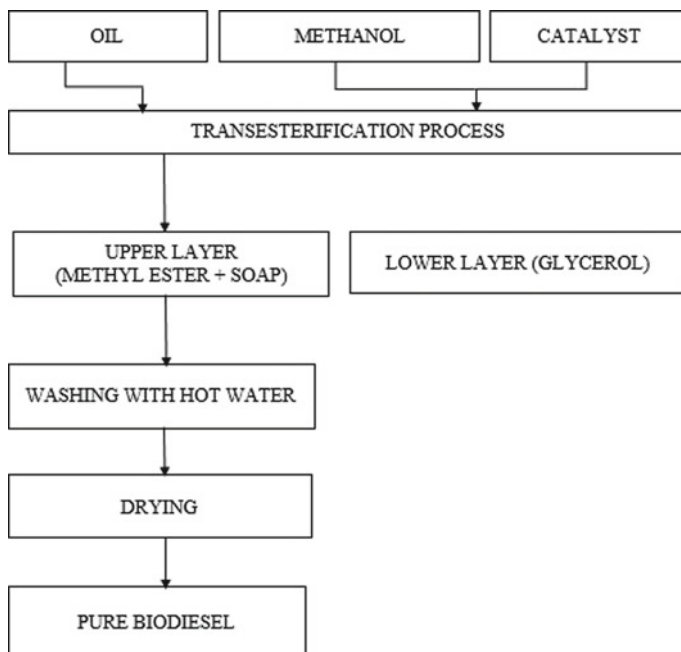


Fig. 1 Schematic representation indicating various steps during production of biodiesel from raw vegetable oils

Table 2 Thumba biodiesel properties

Properties	Thumba biodiesel	Diesel
Density @ 15 °C, g/cm ³	0.872	0.828
Specific gravity @ 20 °C	0.890	0.827
Calorific value, MJ/kg	38.1	42
Flash point, °C	191	68
Fire point, °C	201	72
Viscosity @ 40 °C, cSt	5.37	2.80

Table 3 Argemone biodiesel properties

Properties	Thumba biodiesel	Diesel
Density @ 15 °C, g/cm ³	0.913	0.828
Specific gravity @ 20°C	0.895	0.827
Calorific value, MJ/kg	39.1	42
Flash point, °C	205	68
Fire point, °C	217	72
Viscosity @ 40°C, cSt	5.67	2.80

2.2 Preparation of Biodiesel Blends

During the blend preparation process, the concentrations of both Thumba biodiesel and Argemone biodiesel were kept in a similar proportion with different diesel content. Different blends were prepared in order to find out the effect on various parameters of DIC I engine. The four blends which were prepared are D90T5A5, D80T10A10, D70T15A15 and D60T20A20, where 'D' represents diesel, 'T' represents Thumba and 'A' represents Argemone Mexicana.

3 Experimental Set-up

3.1 Engine and Instrumentation

The specifications of the engine used are listed in Table 4, and the schematic experimental set-up is shown in Fig. 2.

The test bench is equipped with coolant temperature control systems that are capable of maintaining the coolant temperature of 30–70 °C. The eddy current dynamometer was used to control the load on an engine using a load cell in a range of 0–15 kg. The fuel used in this study is the blend of Argemone, Thumba oil and diesel at variable proportions, which meets the limit of Bharat Stage IV Indian emission regulation norm. The lubricating oil of SAE 20W-40 viscosity grade was used for the test. The exhaust gas was collected at 0.4 m downstream of the exhaust valve with the help of exhaust gas analyser. The performance and combustion parameters can be accessed using a customized software supplied by Apex India Manufacturers.

Table 4 Engine specifications

Engine type	Diesel, four-stroke, single-cylinder, water-cooled, direct injection, in-line overhead valve
Suction type	Naturally aspirated
Bore * stroke	87.5 × 110 mm
Piston displacement	661 cc
Rated power	3.5 kW @ 1500 rpm
Injection timing	23° BTDC
Compression ratio	17.5:1

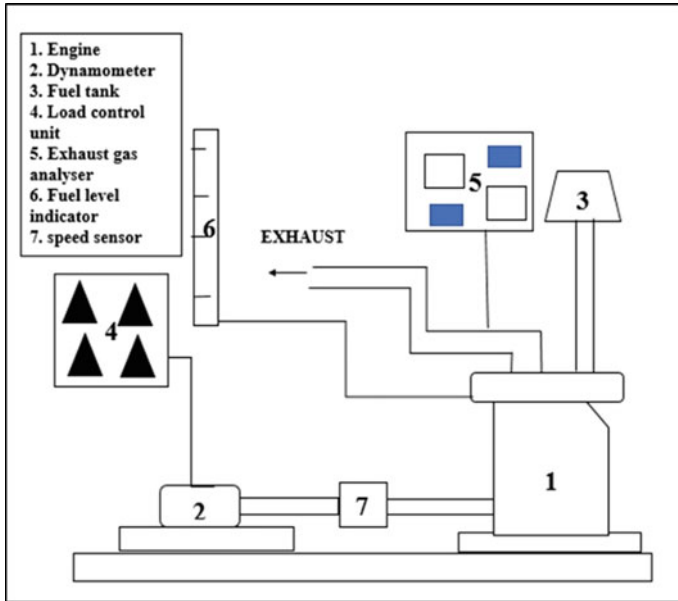


Fig. 2 Schematic diagram of experimental set-up

4 Results and Discussion

4.1 Combustion Characteristics

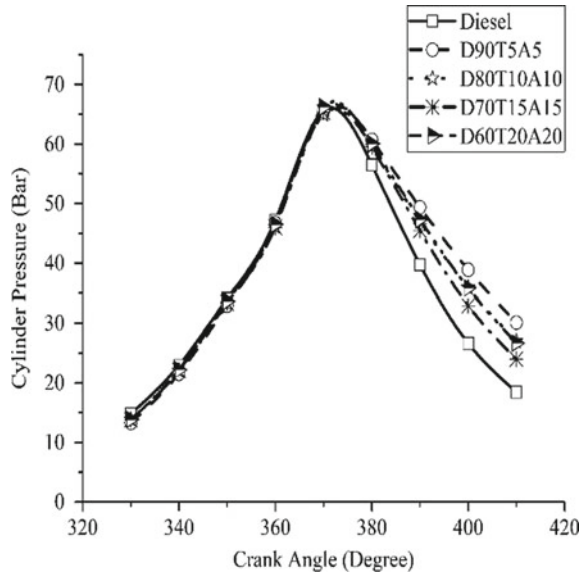
Cylinder Pressure

The variation in cylinder pressure vs. crank angle for various dual biodiesel blends is shown in Fig. 3. Cylinder pressure, in general, signifies the ability of the fuel to mix with air. It is observed from the results that the average pressure for almost all the dual biodiesel blends has higher cylinder pressure when compared to pure diesel. It is observed from the graph that maximum average cylinder pressure for the heavier blend D60T20A20 is greater than that of diesel fuel by 1.7%. This increase in cylinder pressure may perhaps be possible because biodiesels are having higher cetane numbers and density. Also, it might be due to shorter ignition delay which corresponds to earlier combustion.

Net Heat Release Rate

Heat release rate is being considered as the important parameter which indicates the rate at which the combustion takes place or which is used to investigate the combustion of diesel engines. From the graph shown in Fig. 4, it is indicated that the average maximum heat release rate for lighter dual blend D90T5A5 is 36 J/(°), which is 11.67% greater than diesel, i.e. 31.80 J/(°). The possible reason could be

Fig. 3 Variations in cylinder pressure with a crank angle for various fuel blends and diesel



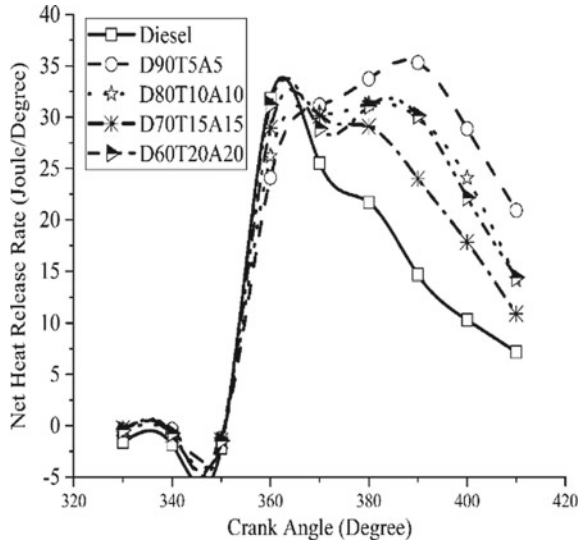
biodiesels are having higher oxygen content which corresponds to a rapid rate of combustion. The results from the graph further revealed that net heat release rate for higher blend D60T20A20 is 31.21 J/(°) which is almost similar to net heat release rate of diesel, i.e., 31.80 J/(°). The reason could be attributed to the fuel properties of D60T20A20 blend might be similar to that of diesel. Net heat release rate is also found to be in an increasing manner as compared to diesel after the crank angle 360° means after premixed stage of combustion. This indicates that in diffusion stage of combustion, almost all the biodiesel blends are showing increased heat release rate.

4.2 Performance Characteristics

Brake Thermal Efficiency

Brake thermal efficiency deals with the effective power developed in an engine by the application of fuel energy. Figure 5 indicates the change in BTE at different engine loads for diesel, D90T5A5, D80T10A10, D70T15A15 and D60T20A20. This was observed that at 6 kg load, the values of BTE were 20.66, 14.41, 14.93, 16.04 and 15.38% for diesel, D90T5A5, D80T10A10, D70T15A15 and D60T20A20, respectively. This concludes that diesel is having higher BTE as compared to other blends. This might be possible due to higher calorific value and lower viscosity of diesel than Thumba and Argemone biodiesels. For all the blends, BTE is increasing as the engine load increases. The reason could be because of less amount of heat loss and more power is developed (less amount of power is lost). For the maximum loading

Fig. 4 Variation in net heat release rate with a crank angle for various fuel blends and diesel



conditions, BTE value for heavier dual blend D60T20A20 is 23.20% which is higher than D90T5A5, D80T10A10 and D70T15A15 having BTE values like 22.22, 23.12 and 23.18%, respectively. This increment might be due to higher oxygen content and higher cetane number.

Mechanical Efficiency

Fig. 5 Variation in brake thermal efficiency with engine load for various fuel blends and diesel

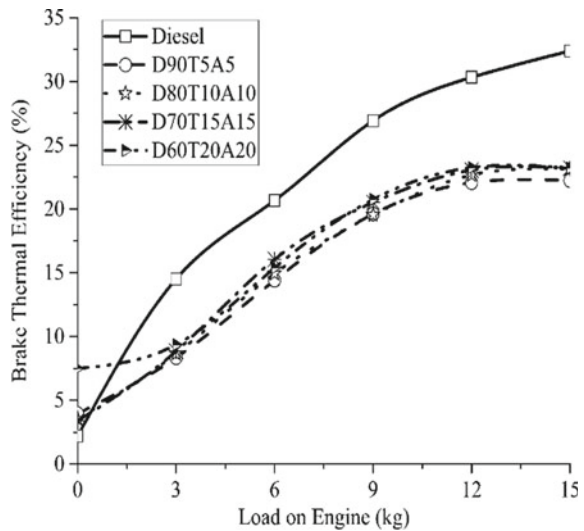
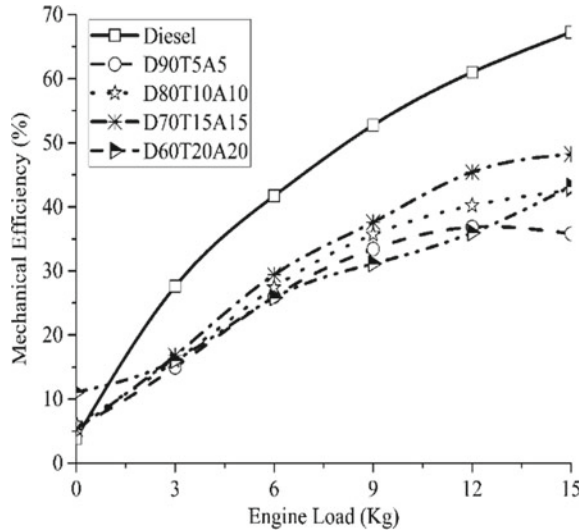


Fig. 6 Variation in mechanical efficiency with engine load for various fuel blends and diesel



The variation in mechanical efficiency with engine load for various fuel blends is shown in Fig. 6. Mechanical efficiency may be defined as a parameter which indicates the capability of an engine to convert total indicated power into useful power. The graph indicates that as the engine load is increased, mechanical efficiency increases accordingly. From the results obtained, diesel shows higher mechanical efficiency which is 67.27%. Mechanical efficiency for remaining blends is lower than diesel, whereas blend D70T15A15 is having higher mechanical efficiency, i.e. 48.23% when compared to other blends like D90T5A5, D80T10A10 and D60T20A20 having 35.81, 42.62 and 43.21%, respectively. The lower mechanical efficiency for all biodiesel blends might be due to their higher indicated power compared to diesel.

5 Conclusion

Based on the extensive studies following conclusions can be supported.

1. The fatty acid value for raw Argemone oil was higher, i.e. 12.27 mg KOH/g of sample compared to raw Thumba oil having 4.4 mg KOH/g of sample. Hence, two-step transesterification was used for reducing the viscosity level of Argemone oil.
2. Thumba and Argemone oils have properties like density, specific gravity, calorific value and viscosity that are almost similar to diesel.
3. It is evident from the study that almost all dual biodiesel blends are showing cylinder pressure higher than diesel in which maximum average cylinder pressure for the heavier blend D60T20A20 is greater by 1.7% than that of pure diesel.

4. It is evident from the study that the average maximum heat release rate for lighter dual blend, i.e. D90T5A5, is 36 J/(°) which is 11.67% greater than diesel having 31.80 J/(°) heat release rate. For heavier blend D60T20A20, the HRR is 31.21 J/(°) almost similar to diesel.
5. From the results, it is observed that at 6 kg of engine load, diesel is having higher BTE, i.e. 20.66% as compared to other dual biodiesel blends. Similarly, at maximum loading condition, heavier biodiesel blend like D60T20A20 is having 23.20% BTE which is higher than all other blends.
6. It is evident from the study that diesel is having a higher mechanical efficiency which is 62.27% compared to other dual biodiesel blends.

References

1. Sheehan J, Camobreco V, Duffield J, Shapouri H, Graboski M (1998) An overview of biodiesel and petroleum diesel life cycles. Department of Energy's National Renewable Energy Laboratory, U.S
2. Srithar K, Balasubramaniam KA, Pavendan V, Kumar BA (2014) Experimental investigations on mixing of two biodiesel blended with diesel as alternative fuel for diesel engines. J King Saud Univ Eng Sci
3. Herrari PA, Pattanashetti A, Hadagali B, Ghadge SS (2015) IJARIII 1(3):2395–4396
4. Pal A, Kachhwaha SS (2011) Biodiesel production of non-edible oils through ultrasound energy. Institute of Technology, Nirma University, Ahmedabad, pp 382–481
5. Jain NL, Soni SL, Poonia MP, Sharma D, Srivastava AK, Jain H (2017) Performance and emission characteristics of preheated and blended thumba vegetable oil in a compression ignition engine. Appl Thermal Eng 113:970–979
6. Karnwal N, Kumar N, Hasan M (2010) Production of biodiesel from thumba oil, optimization of process parameters. Iranica J Energy Environ 1:352–358
7. Mathur YB, Poonia MP, Jethoo AS (2011) Economics, formulation technique and properties of biodiesel: a review. Univ J Environ Res Technol 2:124–134
8. Shukla AK, Dixit AK, Singh RP (2003) Identification of argemone oil and its simple qualitative detection in mustard oil. Brassica 5:75–76
9. Pramanik P, Das P, Kim PJ (2012) Preparation of biofuel from argemone seed oil by an alternative cost-effective technique. Fuel 91:81–86
10. Sitha A, Kumar A, Mahla SK (2012) Utilization of argemone oil biodiesel in commercial DI CI engine, International journal of emerging technologies 3(2). ISSN 2249–3255:19–23
11. Singh D, Singh SP (2010) Low-cost production of the ester from the non-edible oil of Argemone Mexicana. Biomass Bioenergy 34:545–549
12. Agarwal AK, Dhar A (2013) Experimental investigations of performance, emissions and combustion characteristics of Karanja oil blends fuelled DI CI engine. Renew Energy 52:283–291
13. Pal A, Kachhwaha SS, Maji S, Babu MKG (2010) Thumba seed oil: a sustainable source of renewable energy for biodiesel production. J Sci Ind Res 69:384–389
14. Kumbhar SR, Dange HM (2014) Performance analysis of single cylinder diesel engine, using diesel blended with thumba oil. Int J Soft Comput Eng 4(4):2231–2307
15. Mishra B, Pal A, Sharma RB, Jain M (2015) Performance study of a diesel engine by using thumba oil (*Citrullus colocynthis*) biodiesel and its blends with diesel fuel and results. Int J Res Advent Technol 3(7)
16. Parida MK, Rout AK (2017) Combustion analysis of *Argemone mexicana* biodiesel blends. Energy Sour Part A Recovery Util Environ Eff 698–705. ISSN: 1556–7036

17. Prabhakar S, Annamalai K, Lalvani IJ (2012) Experimental study of using hybrid vegetable oil blends in a diesel engine. *J Sci Res* 6:12–5
18. Mofizur M, Atabani A, Masjuki H, Kalam M, Masum B (2013) A study on the effects promising edible and non-edible biodiesel feedstock on engine performance and emissions production: a comparative evaluation. *Renew Sustain Energy Rev* 23:391–404
19. Kumar A, Sharma S (2011) Potential non-edible oil resources as a biodiesel feedstock. *Indian Perspect Renew Sustain Energy Rev* 15:1791–1800
20. Sureshkumar K, Velraj R, Ganesan R (2008) Performance and exhaust emission characteristics of a CI engine fuelled with *Pongamia pinnata* methyl ester (PPME) and its blends with diesel. *Renew Energy* 33:2294–2302
21. Hussain A, Davies P (2010) Plants oils as fuel for compression ignition engine: a technical review and life cycle analysis. *Renew Energy* 35:1–13
22. Hifzur R, Prakash JC, Snehal J (2013) Performance of a diesel engine with blends of biodiesel (from a mixture of oils) and high-speed diesel. *Int J Energy Environ Eng*

Biogeographical and Variable Neighborhood Search Algorithm for Optimization of Flexible Job Shop Scheduling



Rakesh Kumar Phanden and João Carlos E. Ferreira

Abstract In the past two decades, numerous techniques have been proposed by researchers across the world to deal with combinatorial optimization problems. The majority of techniques are working on nature-inspired phenomena such as genetic seriatim of human beings, the way of ant colonizing, and the manners of fish and bees, etc. The biogeography is a nature-inspired population-based algorithm, which works on the concept of migration policy of animals. The working concept and definitions of biogeography are like the genetic algorithm, except the absence of reproduction phase in it. The migration operators have been designed to suit the current problem domain, and these have been used to solve the optimization problems. In the present work, biogeography algorithm has been used with variable neighborhood search method to enhance the local search during optimization of the flexible job shop scheduling problem. This hybrid approach is proposed to measure the makespan performance.

Keywords Biogeography algorithm · Variable neighborhood search method · Flexible job shop scheduling · Hybrid approach · Optimization

1 Introduction

The job shop scheduling problem is under the domain of production planning and control functions of a manufacturing system. If, the manufacturing flexibility considered on shop floor than, it is named as flexible job shop scheduling problem. In job shop scheduling problem, the jobs are processed with a fixed number of sequence of operations without considering alternative machine for any operation. However, aforementioned assumption is completely relaxed in case of flexible job shop scheduling problem and any job can visit any machine. This case is studied as

R. K. Phanden (✉)

Department of Mechanical Engineering, Amity University, Noida 201313, Uttar Pradesh, India
e-mail: rkphanden@amity.edu

J. C. E. Ferreira

The Federal University of Santa Catarina, Florianopolis, SC 88040-900, Brazil

© Springer Nature Singapore Pte Ltd. 2019

K. Shanker et al. (eds.), *Advances in Industrial and Production Engineering*, Lecture Notes in Mechanical Engineering, https://doi.org/10.1007/978-981-13-6412-9_48

full manufacturing flexibility, which is practically not possible. Consequently, partial flexibility is the realistic working environment for today's manufacturing systems, in which a set of operations of jobs are allowing to process on a set of machines. Hence, job shop scheduling is a classical problem and focus has been shifted to solve the flexible job shop scheduling problem. Moreover, the job shop scheduling is a non-polynomial hard problem; hence, the flexible job shop scheduling problem is also under the same class. In addition, the flexible job shop scheduling problem involves two complications first, assignment of a machine to an operation of a job or vice versa (i.e., assignment of resources) and secondly, the assignment of order of operations of various jobs on a machine (i.e., scheduling). So, the flexible job shop scheduling has been divided in two problems and termed as operation sequencing and machine assignment problem. This course of subdivision is called as hierarchical procedure to solve hard problems by dividing it into two sub-parts. Brandimarte [1] proposed this hierarchical process by means of dispatching rules to solve operation sequence and Tabu search method to solve the machine assignment problem. Barnes and Chambers [2] also applied TS method to solve the flexible jobs shop scheduling using hierarchical process. A multi-objective flexible job shop scheduling problem is solved by Xia and Wu [3]. They proposed particle swarm optimization and simulated annealing algorithm for machine assignment and operation sequence problem, respectively.

Many researchers have followed integrated process approach to solve both problems, concurrently. However, this approach is complex to solve but yields better results. Hurink et al. [4] applied Tabu search method to solve flexible job shop scheduling using integrated process. Chen et al. [5] developed genetic algorithm with a modified chromosome structure, having individual vectors for operation sequence and machine assignment functions to solve flexible job shop scheduling problem. Kacem et al. [6] developed an approach by localization to solve flexible job shop scheduling problem of single as well as multi-objectives. They constructed a model having genetic manipulations to enhance the results. Ho et al. [7] built an architecture of learnable genetic algorithm in which populations are generated using dispatching rules to solve flexible job shop scheduling problem. A hybrid genetic algorithm was proposed by Gao et al. [8] to optimize flexible job shop scheduling problem for multi-objectives. In, Zhang et al. [9, 10], variable neighborhood search and Tabu search methods are used to improve the local search with genetic algorithm and particle swarm optimization algorithm, respectively. Zhang et al. [11, 12] proposed an amalgamation of Tabu search method, variable neighborhood search, and genetic algorithm to solve multi-objective flexible job shop scheduling problem. Moreover, Zhang et al. [13] extended the same combination with a distinct design of generation of initial population for genetic algorithm. They compared the results with existing studies and found better results. Wang et al. [14] developed genetic algorithm having immune and entropy concepts to solve multi-objective flexible job shop scheduling problem.

The science of biogeography was stated by the findings of two renowned zoologists named Charles Darwin [15] and Alfred Wallace [16]. The optimization of engineering problems, which is based on biogeography concept is same as the genetic

algorithm and particle swarm optimization algorithm. Biogeography optimization algorithm is also motivated by the natural phenomenon based on relocation strategies of species to solve real-life complex engineering problems. A mathematical model of this algorithm was proposed by MacArthur and Wilson [17] in 1960. They initiated biogeography concept-based mathematical models as an important research topic to be explored in depth. These models show “how species migrate among different islands”, “how new species arise”, and “how species vanished”? In the literature, the island is considered as a habitat which is geographically secluded from other habitats. However, biogeographical algorithm is moved by natural occurrences, and it has few dissimilarities from genetic algorithm, particle swarm optimization, and ant colony optimization algorithms, such as (a) during evolution of every generation initial population is considered and the population is updated by migration strategy, (b) the value of fitness function is calculated through the rates of immigration and emigration to alter the population.

Simon [18] has introduced biogeographical algorithm, its concept, definitions, and phases to implement on engineering problems and shown good results. Hence, various researchers across the world have been used biogeographical algorithm for combinatorial optimization problems. Simon [19] has streamlined the biogeographical algorithm and presented evolution of population through probability theory. He illustrated that biogeographical algorithm with lower rate of mutation can perform better than genetic algorithm. Du et al. [20] implanted some typical characteristics of well-known optimization algorithms into biogeographical algorithm to enhance its performance. Ergezer et al. [21] proposed oppositional biogeographical algorithm in which the concept of “opposition-based learning” with migration rate of biogeographical algorithm was studied. They stated that among other “opposition-based learning” approaches, the proposed algorithm has maximum probability to attain the solution near to optimal value. Ma et al. [22] generalized the balance species count of biogeography concept and developed various migration models and found sinusoidal migration model performing better than others. A combination of mutation and crossover operators were presented by Ma and Simon [23]. They proposed a diverse biogeography algorithm to handle constrained driven problems. Various real-life combinatorial problems, viz. complex economic load dispatch optimization problems, satellite image cataloging problems, problems of retrieving groundwater opportunity, and production scheduling problem, have been solved by biogeography algorithm effectively [24].

This paper presents the combination of two algorithms, viz. biogeography, and variable neighborhood search to optimize the flexible job shop scheduling problem for makespan performance measure. The proposed hybrid approach utilizes the local search capability of neighborhood search method to generate the optimal solution. Also, the result of the proposed approach is compared with an existing study. A companion of the result is made among biogeography algorithm and proposed hybrid approach considering same parameter setting for makespan viewpoint.

Subsequent sections discuss the problem formulation of flexible job shops scheduling problem, adopted methodology which include the working of different operators, results and discussion, conclusions and future research directions.

2 Problem Statement

A flexible job shop scheduling problem can be defined as; “ m ” number of machine (M_i) are used to process “ n ” number of job (J_k) having a varied number of operations for a job (Ok_j).

where

$M_i \rightarrow i \in (1, 2, \dots, m)$

$J_k \rightarrow k \in (1, 2, \dots, n)$

$Ok_j \rightarrow j \in (1, 2, \dots, nk)$

nk —total number of operations for job J_k .

Pk_{ji} —processing time of operation j (Ok_j) on machine i for job J_k .

In addition, any operation (Ok_j) of an individual job (J_k) can be processed by one machine among the available alternative machines (M_{kj}) (i.e., each operation has a set of substitute machines to process a job). Hence, the flexible job shop problem has been divided into two segments; (i) selection of right machine for each operation and (ii) finding the order of operation on selected machine. The objective function may be to minimize the makespan value, minimize tardiness or mean flow time, etc. The assumptions are as follows;

- Each job must follow a fixed sequence of operation,
- All jobs have equal weightage in preference during waiting queue at every station,
- Jobs and machines are independent to each other and available at zero time,
- Transportation time of jobs is not considered among machines,
- Machine and job setup time are not considered,
- One machine can handle one job at a time.

3 Methodology

3.1 Biogeographical Algorithm

This algorithm is based on the theory of biogeography, which is a subclass of biology. Therefore, biogeographical algorithm works on natural phenomenon of circulation of species with respect to time and space. Moreover, this algorithm is similar to other population-based nature-inspired algorithms such as genetic algorithm, particle swarm optimization algorithm, and ant colony optimization algorithms to solve combinatorial optimization problems [18, 19]. In case of genetic algorithm, the capability of a chromosome (individual) is evaluated by the value of fitness function which depends on fertility of genes. Similarly, in case of geographical algorithm the habitat is named as individual and its capability is measured in term of “Habitat Fitness Index” (HF_index). Hence, habitats with high value of HF_index yield good result, while low value of HF_index gives poor result. Emigration is a leaving and immigration is an arriving phenomenon of species in the biogeographical algorithm. Hence,

the features travel from emigrating habitats to immigration habitats, i.e., from the habitats of high *HF_index* to the habitats of low *HF_index*. During the immigration development, low *HF_index* habitats acquire latest attributes and characters from low-value *HF_index* habitats. Thus, the result of an optimization problem is improved by the evolution process of immigration and emigration (i.e., migration operation). In the present problem of flexible job shop scheduling optimization, the objective is to maximize the *HF_index* value of habitats through the developmental process of biogeographical algorithm having emigration and immigration attributes of habitats.

Rahmati and Zandieh [25] presented the comparative details on definition, concept, and characteristics of biogeography algorithm versus genetic algorithm. The migration operator (emigration and immigration) and mutation operators are the key operators of biogeographical algorithm.

The algorithm is initialized through a procedural way. Initially, the population is arranged by generating sequence of operation at random from the available machines. Subsequently, only two machines are chosen against individual operation and lastly, the machines are chosen by generating the random numbers between 0 and 1. If the random number is greater than the value of 0.8, a machine having lengthier processing time is selected; else, a machine with smaller processing time is selected. This procedure is adopted from Wang et al. [14].

3.2 Encoding and Decoding Strategy

An individual is named as a habitat and the representation and working of this habitat are similar to an individual (chromosome) of the genetic algorithm. The present work utilized the dual vector strategy, in which the first vector is coded for the sequence of operations and the second is for the machine assignment to the operation from the available set of alternative machines. Both trajectories are integrated to yield a viable result (schedule) for a flexible job shop scheduling problem. In this coding scheme, the span of both trajectories is the same in length and varies with the total number of operations to process all job types. This strategy of two-vector habitat has been adopted from Wang et al. [14] and modified accordingly.

Table 1 shows the processing time (in minutes) for a sample flexible job shop scheduling problem of five machines and three jobs are considered to elaborate the coding and decoding scheme in detail. The seventh column in Table 1 illustrates the number of operations for each job type and the last column shows coding of operation, machine, and job. Herein, “-” indicates that the operation cannot be executed on a relevant machine. A, B, and C represent the job and “a, b, c, d, and e” represent machine.

For example, the first vector (*ca-eadc-dcb*) illustrating the assignment of machines to each operation of a job (i.e., first two variables for first job type (A), second four variables for second job type (B) and last three variables for job type (C) as per the sample problem. These variables are termed as “Suitability Index Variable”

Table 1 Sample problem of five machines and three jobs

Job	Machine					Operation number	Encoding (both vectors)
	<i>a</i>	<i>b</i>	<i>c</i>	<i>d</i>	<i>e</i>		
A	4	2	1	–	3	1st	$Op^1Aa; Op^1Ab; Op^1Ac; Op^1Ae$
	4	–	2	5	–	2nd	$Op^2Aa; Op^2Ac; Op^2Ad$
B	2	3	3	–	1	1st	$Op^1Ba; Op^1Bb; Op^1Bc; Op^1Be$
	1	3	–	3	–	2nd	$Op^2Ba; Op^2Bb; Op^2Bd$
	–	–	5	6	5	3rd	$Op^3Bc; Op^3Bd; Op^3Be$
	3	5	3	–	1	4th	$Op^4Ba; Op^4Bb; Op^4Bc; Op^4Be$
C	3	3	–	2	2	1st	$Op^1Ca; Op^1Cb; Op^1Cd; Op^1Ce$
	2	6	6	–	5	2nd	$Op^2Cb; Op^2Cc; Op^2Ce$
	6	4	4	–	–	3rd	$Op^3Ca; Op^3Cb; Op^3Cc$

(*S_index*). Hence, the second vector (i.e., operation sequence vector or scheduling vector) can be written as after assigning the corresponding machines as per *S_index*; (¹A; ¹B; ²B; ²A; ¹C; ³B; ²C; ⁴B; ³C). In decoding strategy, the habitat (individual) transfers to a feasible schedule (solution). As demonstrated by Rahmati and Zandieh [25], just for the sake of suitability, it has been assumed that operation *Okj* of an individual habitat can be redesignated as *Op*, the duration (processing time) of that operation can be represented as *D_Op* and the beginning time of the operation can be represented as *B_Op*. Thus, the completion time of each operation is *B_Op* + *Drops*. Moreover, it has been assumed that the start time of first job of each job type will be equal to zero (i.e., first operation’s starting time is zero). A schedule can be generated by following the *S_index* values of second vector (i.e., sequence of operations). In the present example, *Op¹Ac* is the first operation to be scheduled. It means first operation of job type “A” will be scheduled on machine “c” which is consuming 1 min. This is the first operation, so the start time will be zero. *Op¹Be* is the second operation to be scheduled as per the given vector. It is the first operation of job type “B” which uses machine “e” and consuming one minute of processing time. Again, this is the first operation of job type “B”; therefore, the starting time will be zero. *Op²Ba* is the third operation of vector and second operation of job type “B”, processing on machine “a” with 1 min. Here, the starting time of this operation will be calculated after the completion of the first operation of job type “B” which is processed on machine “e”. Hence, the decoding process will continue by following the sequence of operation from the second vector design. The decoded schedule of the present example is shown in Fig. 1.

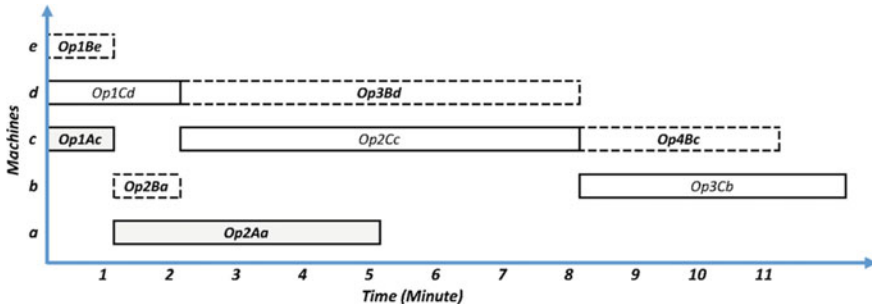


Fig. 1 Decoding of sample problem (Gantt Chart of active schedule)

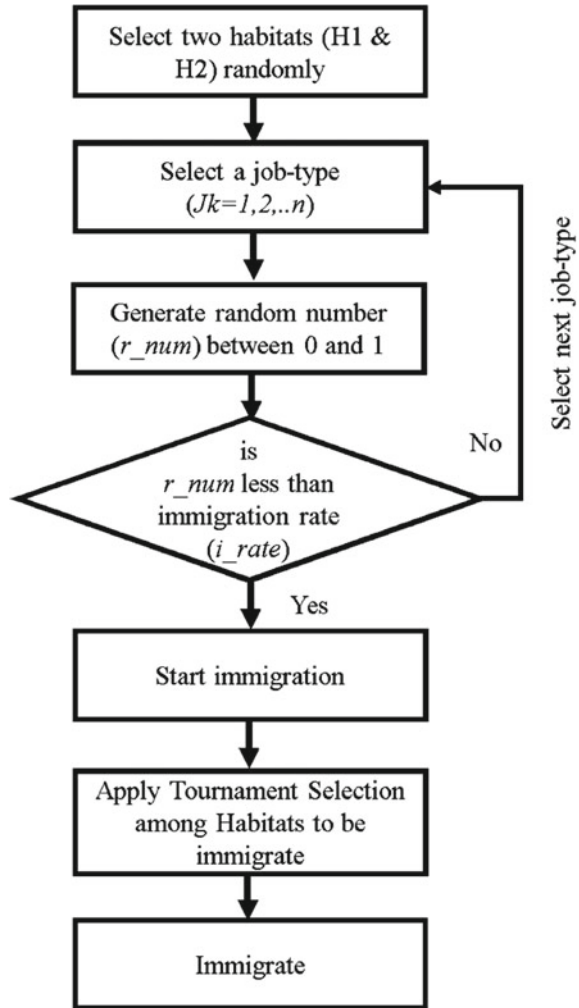
3.3 Selection Scheme

In biogeographical algorithm, the selection scheme is required during the migration and mutation operations. During migration operation, the tournament selection scheme is adopted with selection pressure (1.6) as suggested by Baker [26], while in mutation operation the selection is performed on the basis of mutation probability. This step is unique while comparing with other nature-inspired algorithms. Immigrants and emigrants are selected on the basis of their fitness function (*HF_index*) of habitats (solutions), which are termed as immigration rate (*i_rate*) and emigration rate (*e_rate*). Figure 2 shows the selection scheme designed to perform the immigration operation. In this scheme, habitats are taken under immigration process by comparing with the random number (*r_num*) and its immigration rate. Similarly, the selection scheme during emigration process also follows the philosophy of immigration process in series, as presented in Fig. 2. Moreover, the habitats undergo mutation operation on the basis of their *S_index* values and mutation probability.

3.4 Migration (Immigration and Emigration) Operator

Simon [18] has proposed a model to show the relationship among immigration and emigration balance in order to maintain the richness of species in a habitat through their *i_rate* and *e_rate*. He stated that whenever the number of species increases, *i_rate* and *e_rate* varies inversely proportional because, the distinctive attributes of a worthy solution having high *HF_index* value travels toward the deprived solution having low *HF_index* value. Hence, the migration operator is altering and sharing the attributes amid distinguished solutions. It works on the knowledge of migration phenomenon of biogeography, in which the species travels from one habitat to other in order to live with the worthy fellows (individuals). The immigration process yields solution (i.e., immigrated habitat) through the comparison of nominated *i_rate* with the immigrating habitat. Similarly, the emigration process also made the comparison

Fig. 2 Selection scheme adopted for immigration operation of biogeography algorithm



of chosen e_rate with emigrating habitat to validate the emigration of selected habitat. It shows that the chances of selection of emigration and immigration of a habitat are subjected to the taken rate of emigration and immigration.

During the migration process, the attributes of solutions are fine-tuned with respect to their value of S_index of solutions. The value of S_index represents the attribute of the solution, as if the values of genes in the chromosomes of genetic algorithm. The value of S_index performs as a variable to search better alternatives gene (or bit values in a habitat) during migration. Hence, the search space of biogeography algorithm is confined by the probable values of S_index in order to find the optimal or suboptimal solution. Ma et al. [24] present the further details on the calculation of e_rate and i_rate through an algorithm on liner migration function.

Original Habitat →	c	a	e	a	d	c	d	c	b
	Job-A		Job-B			Job-C			
Immigrating Habitat →	a	c	a	b	c	e	e	b	c
Emigrating Habitat →	b	a	a	d	e	a	d	c	c
After Crossover →	a	a	a	a	e	c	e	c	b

Fig. 3 Crossover operation for first vector (assignment of machines)

Original Habitat →	¹ A	¹ B	² B	² A	¹ C	³ B	² C	⁴ B	³ C
Immigrating Habitat →	¹ B	¹ C	² B	¹ A	² A	³ B	² C	³ C	⁴ B
Emigrating Habitat →	¹ A	¹ C	¹ B	² A	² C	² B	³ C	² B	⁴ B
After Crossover:									
Immigrating Habitat →	¹ B	¹ C	¹ B	¹ A	² A	² B	³ C	³ C	⁴ B
Emigrating Habitat →	¹ A	¹ C	² B	² A	² C	³ B	² C	² B	⁴ B
Random selection from immigrating or emigrating habitat:									
Selected Crossover →	¹ A	¹ C	² B	² A	² C	³ B	² C	² B	⁴ B
After Repairing →	¹ A	¹ C	¹ B	² A	² C	² B	³ C	³ B	⁴ B

Fig. 4 Crossover operation for second vector (operation sequence or scheduling vector)

After the choosing the migrating habitats, this operator works similar to the crossover operation of genetic algorithm. In the present work, a special crossover operation has been designed individually for first and second vector. Both vectors undertake crossover operation separately in sequence. Figure 3 presents the crossover operation for the first vector of machine assignment. After generation of immigrating and emigrating habitats, some specific variables (gene factor) are transferred in the original habitat. Two variables are selected randomly from each habitat and inserted in the original habitat at the corresponding positions as shown in Fig. 3. Here, the care should be taken for the availability of machine flexibility. Figure 4 presenting the crossover operation of the second vector of operation sequence. In this crossover, two pairs of variables are selected randomly and exchange among immigrating and emigrating habitats and one habitat is selected randomly from immigrating and emigrating habitat. In this crossover, repairing strategy is required to remove the illegal variables in the habitat as shown in Fig. 4.

3.5 Mutation

This operator amends the attributes of solutions in order to preserve the diversity of population based on selected probability. In biogeography algorithm, it works on the randomly chosen *S_index* variable values of a habitat on the bases of fixed mutation probability. Calculations on mutation probability (*m_pro*) and solution probability

Original Habitat →	c	a	e	a	d	c	d	c	b
	Job-A		Job-B			Job-C			
After Mutation →	c	a	d	a	d	c	e	c	b

Fig. 5 Mutation operation for first vector (assignment of machine)

Original Habitat →	¹ A	¹ B	² B	² A	¹ C	³ B	² C	⁴ B	³ C
After Mutation →	¹ A	¹ B	¹ B	² B	² A	¹ C	³ B	² C	⁴ B
After Repairing →	¹ A	¹ C	¹ B	² B	² A	² C	³ B	³ C	⁴ B

Fig. 6 Mutation operation for second vector (operation sequence or scheduling vector)

are given in Simon [18]. In the present work, both vectors of selected habitat undergo the mutation operation. In case of first vector (assignment of machine), two *S_index* variables are selected at random and exchange with each other while maintaining the legitimacy of available alternative machines as shown in Fig. 5. On the other hand, in the second vector (operation sequence vector), one *S_index* variable is chosen randomly within the habitat, and it is implanted just after the randomly selected operation as shown in Fig. 6. Moreover, this operation also needs repairing of vector in order to maintain the validity of sequence of operations. Figure 7 presents the framework of biogeography algorithm adopted in present work.

3.6 Variable Neighborhood Search (VNS)

It works on the philosophy of increasing the fitness of the current solution by a methodological way and continually altering the structures of neighborhood during the evolution of local search of solution space. Largely, every current local solution is dissimilar from their neighborhood vicinity [27–29]. The elementary procedure of this algorithm involves (a) formation of opening population, (b) finalize the neighborhood structure, (c) execute shaking operation, (d) execute local search procedure to find the good neighborhoods within the present space of solution, (e) compare the value of the current solution with previous solution to make the decision for further search or termination of algorithm.

In the present work, the variable neighborhood search method has been altered to fit in the biogeography algorithm. It involves the following steps.

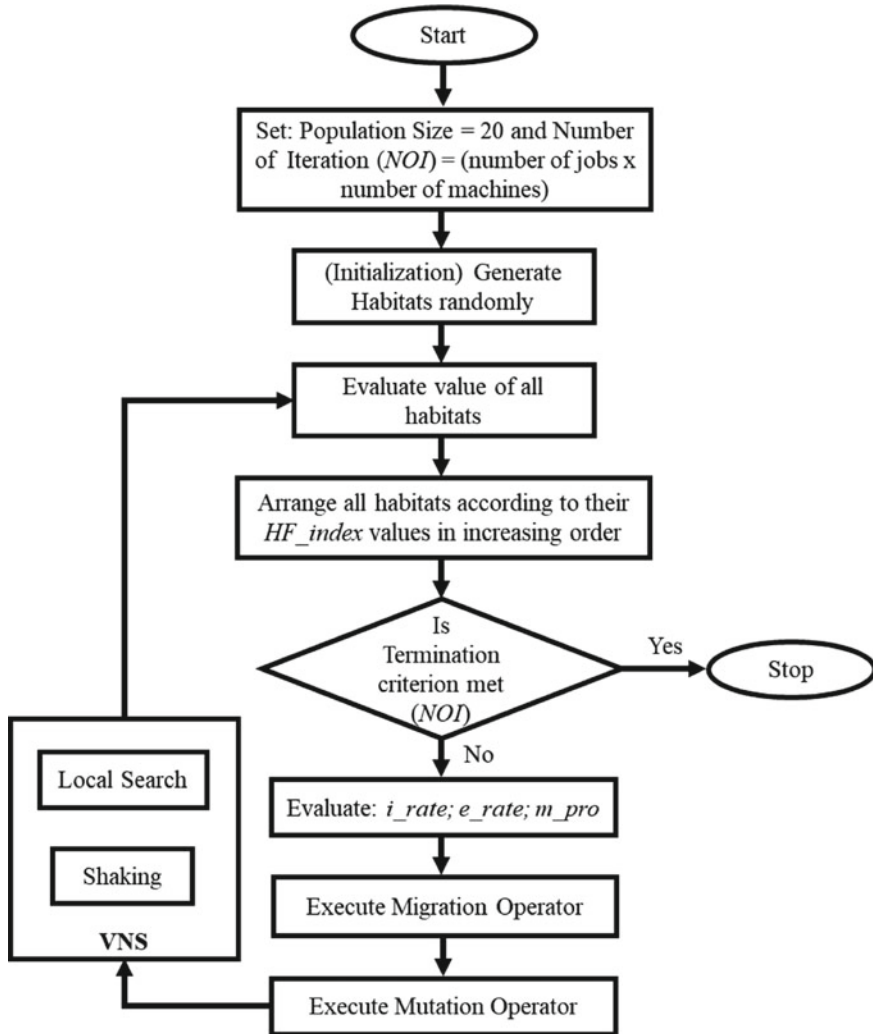


Fig. 7 Framework of biogeography and VNS algorithm adopted in the present work

3.7 Retrieve the Solution from Biogeography Algorithm

After applying the migration operator and mutation operator of biogeographical algorithm, a set of best solutions are transferred to process with variable neighborhood search operators. The habitat structure is decoded to suit the variable neighborhood search method.

3.8 Shaking Operation

All the retrieved habitats undertake shaking operation. During this process, each S_index variable exchanges to each other at random in all habitats for a fixed number of time.

3.9 Local Search Operation

This operator plays the cardinal role to search the improved solution in this algorithm. In order to skip the cycling situation, a neighborhood is selected randomly to explore for its feasibility to survive in the structure. In this step, all alternative machines are stabbed with the selected neighborhood habitat (structure) to find the most suitable and feasible fellow.

3.10 Termination Criterion

In this algorithm, the local search operator will decide the local termination of search. It works in iterative manner till the finding of a good neighbor. Figure 7 presents the framework of biogeography algorithm with variable neighborhood search method adopted in present work. Both algorithms work in series.

4 Results and Discussion

The proposed hybrid approach has been tested on a sample of three jobs and five machines flexible job shop scheduling problem as shown in Table 1. In the present work, the makespan performance measure is considered as an optimization objective. Moreover, the proposed approach has been compared with the existing problems solved by Kacem et al. [6]. The proposed methodology is coded in C++ programming language and executed on Intel® Core™ i5-4210U CPU @ 1.70 GHz on x64-based Window 10 platform.

Initially, the sample problem is solved through biogeographical algorithm alone with the same parameters as discussed in previous section. In which, module of VNS is disconnected and result of biogeography is considered as an optimal solution. Figure 8 presents the optimal schedule yield by biogeography algorithm having value of makespan is 9 min. Secondly, the same problem is optimized by the hybrid algorithm discussed above. Figure 9 shows the optimal solution obtained through the proposed approach having 8 min of makespan. Hence, the proposed approach improves 11.11% of makespan value for taken sample problem. It shows that the

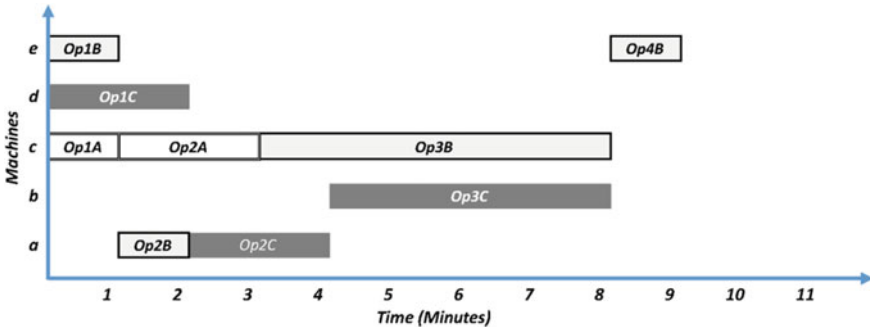


Fig. 8 Gantt chart of sample problem solved with biogeography algorithm (Makespan = 9)

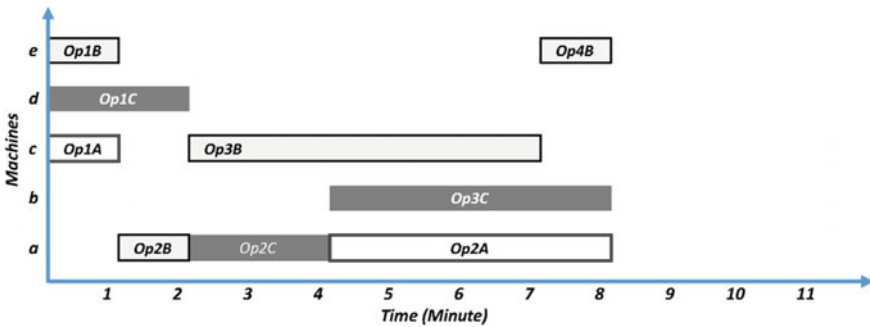


Fig. 9 Gantt chart of sample problem solved with biogeography and VNS algorithm (Makespan = 8)

proposed approach outperforms the biogeography algorithm. In the literature, only one study has been reported to optimize the flexible job shop scheduling using biogeography algorithm in which the authors concentrated on the comparison of the proposed algorithm with genetic algorithm with different performance measures and results of sample problem were not provided [25].

In order to compare the proposed approach with the existing studies, the various size of problems taken from Kacem et al. [6] as shown in column 1 (LHS) of Table 2. These problems are solved by Ho et al. [7] for makespan viewpoint. Hence, the results revealed that the proposed approach is effective enough to solve the varying size of problems.

5 Conclusion

Many techniques have been proposed by researchers across the world to deal with combinatorial optimization problems. Most of the techniques are working on

Table 2 Results comparison on test bed of Kacem et al. [6]

Problem size	Ho et al. [7]	Proposed approach
4 × 5	11	11
8 × 8	not given	14
10 × 10	7	7
10 × 15	12	12

Problems of full flexibility

nature-inspired phenomena such as genetic seriatim of human beings, the way of ant colonizing, and the manners of fish and bees, etc. The biogeography is a nature-inspired population-based algorithm, which works on the concept of migration policy of animals. The working concept and definitions of biogeography are like the genetic algorithm, except the absence of reproduction phase in it. This paper presents a hybrid approach of biogeography algorithm and variable neighborhood search method to solve the flexible job shop scheduling problem. The results revealed that variable neighborhood search helps biogeography algorithm to enhance the local search during optimization of makespan performance measure. Also, the results of the proposed approach validate the performance as good as “Learning and Evolving Genetic Algorithm” of Ho et al. [7] for varying size of problems. Moreover, the results proved that the addition of a local search method in biogeography algorithm makes the algorithm stronger. The present work can be extended in many directions such as apply the proposed approach to flow shop and open shop problems, considering other performance measures like workload content or optimum machine utilization, etc.

References

1. Brandimarte P (1993) Routing and scheduling in a flexible job shop by tabu search. *Ann Oper Res* 41(3):157–183
2. Barnes JW, Chambers JB (1996) Flexible job shop scheduling by tabu search. Graduate program in operations and industrial engineering. The University of Texas at Austin, Technical Report Series, ORP96-09
3. Xia W, Wu Z (2005) An effective hybrid optimization approach for multi-objective flexible job-shop scheduling problems. *Comput Ind Eng* 48(2):409–425
4. Hurink J, Jurisch B, Thole M (1994) Tabu search for the job-shop scheduling problem with multi-purpose machines. *Oper Res Spektrum* 15(4):205–215
5. Chen JC, Chen KH, Wu JJ, Chen CW (2008) A study of the flexible job shop scheduling problem with parallel machines and reentrant process. *Int J Adv Manuf Technol* 39(3–4):344–354
6. Kacem I, Hammadi S, Borne P (2002) Approach by localization multi-objective evolutionary optimization for flexible job-shops scheduling problems. *IEEE Trans Syst Man Cybern Part C Appl Rev* 32(1):1–13
7. Ho NB, Tay JC, Lai EMK (2007) An effective architecture for learning and evolving flexible job-shop schedules. *Eur J Oper Res* 179(2):316–333
8. Gao J, Gen M, Sun L, Zhao X (2007) A hybrid of genetic algorithm and bottleneck shifting for multiobjective flexible job shop scheduling problems. *Comput Ind Eng* 53(1):149–162

9. Zhang G, Gao L, Li X, Li P (2008) Variable neighborhood genetic algorithm for the flexible job shop scheduling problems. In: International conference on intelligent robotics and applications. LNCS, Oct 2008. Springer, Berlin, pp. 503–512
10. Zhang G, Shao X, Li P, Gao L (2009) An effective hybrid particle swarm optimization algorithm for multi-objective flexible job-shop scheduling problem. *Comput Ind Eng* 56(4):1309–1318
11. Zhang G, Gao L, Shi Y (2010) A genetic algorithm and tabu search for multi objective flexible job shop scheduling problems. In: 2010 International conference on computing, control and industrial engineering (CCIE), vol 1. IEEE, June 2010, pp 251–254
12. Zhang GH, Gao L, Shi Y (2010) A novel variable neighborhood genetic algorithm for multi-objective flexible job-shop scheduling problems. *Adv Mater Res* 118:369–373
13. Zhang G, Gao L, Shi Y (2011) An effective genetic algorithm for the flexible job-shop scheduling problem. *Expert Syst Appl* 38(4):3563–3573
14. Wang X, Gao L, Zhang C, Shao X (2010) A multi-objective genetic algorithm based on immune and entropy principle for flexible job-shop scheduling problem. *Int J Adv Manuf Technol* 51(5–8):757–767
15. Darwin C (1995) *The origin of species*. Gramercy, New York
16. Wallace A (2005) *The geographical distribution of animals (two volumes)*. Adamant Media Corporation, Boston
17. MacArthur R, Wilson E (1967) *The theory of biogeography*. Princeton University Press, Princeton
18. Simon D (2008) Biogeography-based optimization. *IEEE Trans Evol Comput* 12(6):702–713
19. Simon D (2011) A probabilistic analysis of a simplified biogeography-based optimization algorithm. *Evol Comput* 19(2):167–188
20. Du D, Simon D, Ergezer M (2009) Biogeography-based optimization combined with evolutionary strategy and immigration refusal. In: IEEE international conference on systems, man and cybernetics, 2009. SMC 2009. IEEE, Oct 2009, pp 997–1002
21. Ergezer M, Simon D, Du D (2009) Oppositional biogeography-based optimization. In: IEEE international conference on systems, man and cybernetics, 2009. SMC 2009. IEEE, Oct 2009, pp 1009–1014
22. Ma H, Ni S, Sun M (2009) Equilibrium species counts and migration model tradeoffs for biogeography-based optimization. In: Proceedings of the 48th IEEE conference on decision and control, 2009 held jointly with the 2009 28th Chinese control conference. CDC/CCC 2009. IEEE, Dec 2009, pp 3306–3310
23. Ma H, Simon D (2011) Blended biogeography-based optimization for constrained optimization. *Eng Appl Artif Intell* 24(3):517–525
24. Ma H, Simon D, Siarry P, Yang Z, Fei M (2017) Biogeography-based optimization: a 10-year review. *IEEE Trans Emerg Top Comput Intell* 1(5):391–407
25. Rahmati SHA, Zandieh M (2012) A new biogeography-based optimization (BBO) algorithm for the flexible job shop scheduling problem. *Int J Adv Manuf Technol* 58(9–12):1115–1129
26. Baker JE (1985) Adaptive selection methods for genetic algorithms. In: Proceedings of an international conference on genetic algorithms and their applications, July 1985, pp 101–111
27. Gao L, Li X, Wen X, Lu C, Wen F (2015) A hybrid algorithm based on a new neighborhood structure evaluation method for job shop scheduling problem. *Comput Ind Eng* 88:417–429
28. Phanden RK (2016) Multi agents approach for job shop scheduling problem using genetic algorithm and variable neighborhood search method. In: Proceedings of the 20th WMSCI, July 2016, pp 275–278
29. Feng Q, Liu S, Wu Q, Tang G, Zhang H, Chen H (2013) Modified biogeography-based optimization with local search mechanism. *J Appl Math*

A Study on the Effect of Varying Revolution Pitch for Different Tool Design: Friction Stir Welding of AA 6061-T6



Abhijit Banik , John Deb Barma, Ram Singh  and S. C. Saha

Abstract Friction stir welding (FSW) is a very promising joining process for joining of lightweight material. In this study, an attempt has been made to analyze the effect of different tool design for varying revolution pitch. Two different tool pin design namely square and cylindrical threaded is used for the purpose and revolution pitch has been varied in two levels. Spindle torque, downward vertical force (Z -force) and welding force (X -force) are considered in this study to analyze the effectiveness of tool pin design with revolution pitch. With varying revolution pitch, all these entities (spindle torque, Z -force and X -force) varied significantly whereas square tool exhibits higher amount torque and force. Comparatively improved tensile properties are achieved for square tool at lower revolution pitch. Microstructural analysis of the samples reveals finer grain structure is obtained at higher revolution pitch. With square tool, finer grains and dispersions are obtained.

Keywords Spindle torque · Force · Friction stir welding · AA 6061-T6

1 Introduction

Friction stir welding (FSW) is a solid-state joining process, invented in 1991 at ‘The Welding Institute’ (TWI) UK [1]. This process was invented specially for joining difficult to weld material like aluminum. From the very beginning, researchers from different fields have shown their interest to this process as it is a very complex process

A. Banik · J. D. Barma · S. C. Saha
Department of Mechanical Engineering, National Institute of Technology, Agartala, India
e-mail: jitnik_nita@yahoo.in

J. D. Barma
e-mail: debbarma_john@rediffmail.com

S. C. Saha
e-mail: subashchandrasaha@yahoo.in

R. Singh (✉)
Department of Production Engineering, National Institute of Technology, Agartala, India
e-mail: ramsingh650@gmail.com

© Springer Nature Singapore Pte Ltd. 2019

K. Shanker et al. (eds.), *Advances in Industrial and Production Engineering*, Lecture Notes in Mechanical Engineering, https://doi.org/10.1007/978-981-13-6412-9_49

and has the capacity to provide better welds in comparison with conventional fusion welding. A non-consumable rotating tool is plunged into the abutting surface of the plates and moves along the line to be joined, thus completing the joining process [2]. The final weld quality depends on combination of several process parameters like traverse speed, rotational speed, tilt angle, tool design, axial force etc. Tool design is one of the important parameters which facilitates better workpiece material deformation, improved material flow and heat generation [3–5]. Colegrove et al. [6] in their study of analytical estimation of amount of heat produced by tool pin concludes as high as 20% of the total generated heat is contributed by the tool pin. Zhao et al. studied the effect of pin geometry on bonding and mechanical properties in friction stir welded 2014 aluminum alloy for columnar and tapered pins both with and without threads. A difference in the material flow is observed for both the tool design. They concluded tapered pin with screw thread profile produced welds with minimum defects along with very fine grain and uniformly distributed precipitates [7]. Researchers also found a strong relation between different process forces with tool design attributed to the pin geometry [8, 9]. Elangovan et al. studied the effect of tool design variation on applied vertical load and final weld quality. They concluded application of moderate amount of vertical load produces defect-free welds for all tool design and square tool holds good welds for all vertical loads [10]. Trimble et al. had studied the effect of both tool shoulder and pin shape on AA 2024-T3 in terms of torque and forces, weld formation. They found as tool lift reduces, due to increased deformation and frictional heating beneath the shoulder, a scroll shoulder is capable of producing defect-free welds even at higher tool traverse speeds in comparison with a concave shoulder. They also identified triflute pin as the most effective shape for welding at high speeds due to its unique three flute helical ridge design which increases the amount of plastic deformation and stirring of the workpiece [11]. Yang et al. tried to establish monitoring prices with the help of computational algorithm for analysis of applied vertical loads for defect identification in the nugget [12]. Kumar et al. [13] stated an amount of welding and vertical forces has found when ultrasonic assisted friction stir welding is done. In the present investigation, it is attempted to understand the behavior of different tool design with respect to different revolution pitch. Understanding the behavior of different process parameter for FSW process always attracted the researchers, and it is evident from the above discussions. However, complex combination of process parameters and their behavior makes the analysis farther difficult. Tool rotational speed and traverse speed are two important parameters of FSW process. In this study, an attempt made to convert these two parameters into a effective one (revolution pitch). Thus, the complexity of understanding the process may be reduced to a certain extent.

2 Experimental Description

AA 6061-T6 plates with a 120 mm effective weld length in square butt configuration are considered for the study. The chemical composition and mechanical properties

Table 1 Base material properties, tool design and process parameters

Material	Chemical composition (wt%)						
AA 6061-T6	Mg	Mn	Cu	Cr	Si	Fe	Al
	1.20	0.15	0.2	0.04	0.60	0.75	Bal
<i>Mechanical properties</i>							
YS (MPa)	UTS (MPa)	Percentage elongation (%)			Hardness (HV0.1)		
310	276	18			107		
<i>Tool design</i>							
Tools used		Shoulder diameter		Pin diameter	Pin height		
Square, Cylindrical Threaded (mm)		18		6	5.6		
<i>Process parameter</i>							
Tool rotational speed (RPM)				900, 1300			
Tool traverse speed (mm/sec)				0.75, 1.75			
Tool tilt angle (°)				3°			
Revolution pitch (V/N)				0.08, 0.05			

are stated in Table 1. Two tool pin design namely square and cylindrical threaded (Fig. 1) made out of H13 tool steel is considered in this study. Detail tool geometry is mentioned in Table 1. Each tool is used for two welding with different revolution pitch. Tilt angle is kept constant at 3° throughout the experiment. A strain gauge-based load cell is used for measurement of spindle torque, vertical force (Z-force) and traverse force (X-force).

For microstructure analysis of the weldment, specimens are cut along the transverse to weld direction and polished in different grades of emery papers. Hifin diamond compound paste and hifin fluid with Selvyt cloth are used for final polishing.

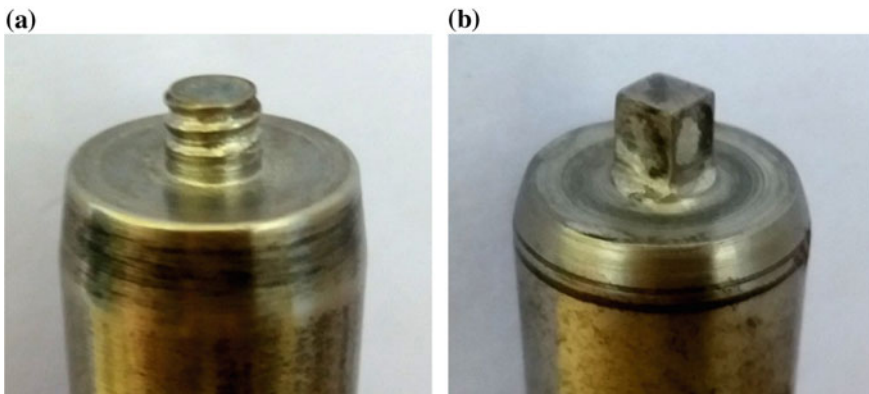


Fig. 1 Tools used in the experiment **a** cylindrical threaded tool, **b** square tool

Etching is conducted using Keller's reagent. Grain size analysis is conducted using light optical microscopy. Field emission scanning electron microscopy is used for second phase analysis. Tensile specimens are prepared by following ASTM E8 standard by taking specimen along the transverse to weld direction. All the tensile tests are conducted at 1 mm min^{-1} strain rate using INSTRON 8801 machine.

3 Result and Discussion

3.1 Torque and Force Analysis

Figure 2 represents the average spindle torque, Z-force and X-force, respectively, for both square and threaded cylinder. Spindle torque is the response of the material to be deformed to the rotation of the tool. Z-force is the downward vertical force applied by the tool shoulder to the workpiece and X-force is the resistance of the deformed material to the tool upon traversing. All these above stated parameters are very important in respect of effective deformation of material under consideration and weld formation. From the figure, it can be seen that with increase in revolution pitch (V/N) all these entities (spindle torque, Z-force and X-force) increases. It is because with increase in revolution pitch rotation of the tool for each unit length decreases. This leads to less heat generation due to less interaction time, as well as comparatively less deformation per unit length. As a result, the deformed material under tool becomes less viscous thus requirement of more torque arises. For the similar reason, the less viscous materials exhibit more resistance to flow while tool traverses thus X-force also increases. Whereas the increase encountered in Z-force is comparatively less for both tools. Since the experiments are conducted with constant plunge depth of tool to the workpiece hence the changes in upward vertical force (Z-force) is nominal though an increased vertical force will be required to consolidate the less viscous material under the shoulder behind the trailing side of the tool [2, 6]. It also can be observed that the entities under consideration (spindle torque, Z-force and X-force) are more for square tool compared to threaded cylinder tool. This behavior for this particular tool is attributed by the shape of the tool pin. The flat surface of the tool pin exhibits a cutting force along with the extrusion of the deformed material. Thus, the flat faces of square tool act as a bluff body causing more turbulence in material flow. Whereas due to the thread incorporated on cylindrical tool pin acts as a guiding path to the deformed material along the threads generating. This contributes to form more uniform and stable material flow [2, 3]. Thus, the requirement of torque, Z- and X-force reduces for cylindrical threaded tool.

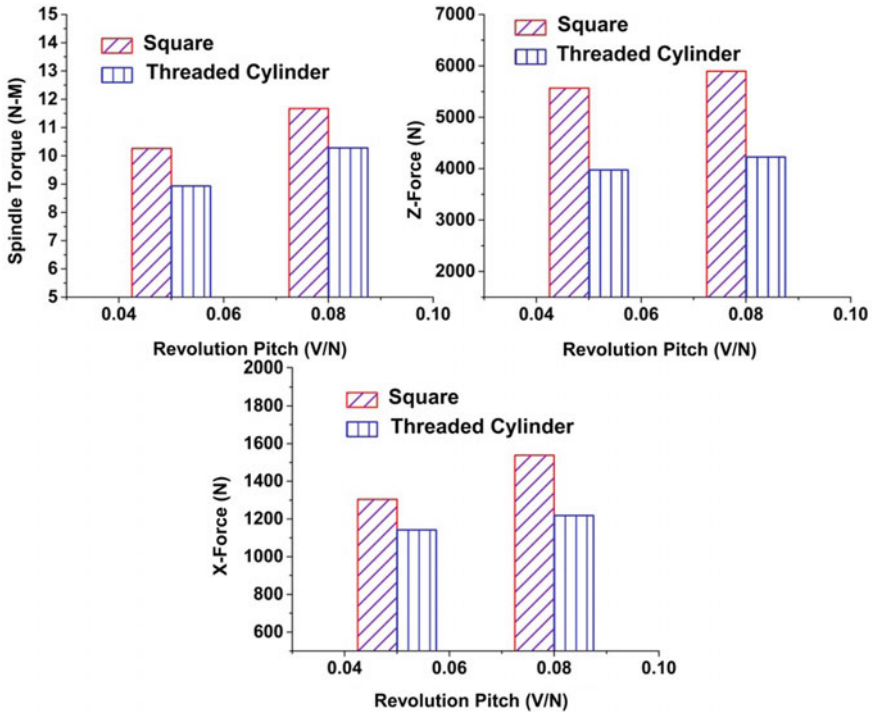


Fig. 2 Effect of revolution pitch for different tool design on spindle torque, Z-force, X-force

3.2 Grain Size Analysis and Scanning Electron Micrography

Figure 3 represents the variation of grain size with varying revolution pitch for both the tool. For aluminum alloys, the final grain size depends on two important factors considering the FSW process. One is the extent of material deformation and the amount of heat input and related thermal cycles which contributes to grain nucleation [2]. It can be seen that with increase in revolution pitch the grain diameter decreases for both the tool. It is due to the fact that with increase in revolution pitch the interaction time for unit length decreases causing less heat input and faster movement of the tool hence the heat source. This faster movement of the tool restricts the grain growth as nucleation time is reduced. Another observation is that with change in tool profile from square to cylindrical thread the grain diameter increases. The grain size obtained for square pin tool decreases due to increased stirring action incorporated pulsating stirring action by the flat face of the square pin tool.

Figure 4 represents the scanning electron micrograph of the nugget zone for all the welds. The black pits in the nugget zone are created due to the corrosive action of the etchant where secondary phase dispersions are present. From Fig. 4, it can be observed that more uniform distribution of particle occurs for the square tool due

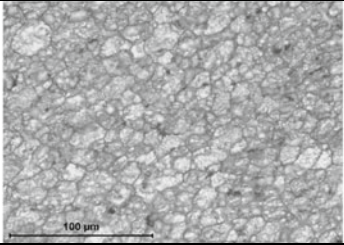
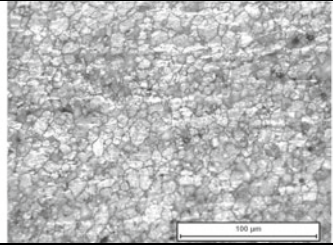
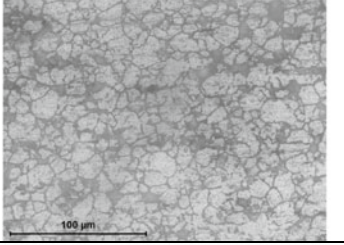
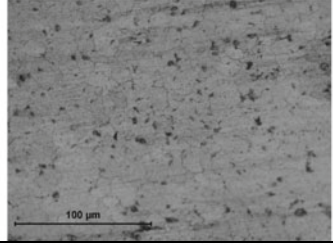
Tool type	Revolution pitch(V/N)	
	0.05	0.08
Square tool		
	12.03 μm	7.22 μm
Cylindrical Threadedtool		
	18.26 μm	10.27 μm

Fig. 3 Effect of revolution pitch for different tool design on nugget zone grain size

to increased pulsating action by the flat faced pin. It breaks the secondary particles more finely and distributes uniformly in the nugget zone. Whereas for cylindrical threaded tool the particle distribution is less uniform and coarser than square tool. At lower revolution pitch more uniform and dense particle distribution can be observed for both the tool.

3.3 Tensile Properties

Figure 5 represents the tensile properties of welded samples. All the tensile properties are evaluated at 1 mm sec^{-1} . It can be observed from the figure the tensile properties decreases with increase in revolution pitch. The ultimate tensile strength decreases from 204 and 184 MPa to 153 and 120 MPa for square and cylindrical threaded tool, respectively. The yield strength also decreases from 125 and 95.2 MPa to 113 and 80.506 MPa for square and cylindrical threaded tool, respectively. The reason of such decrease in tensile properties is due secondary phase distribution as discussed earlier (Fig. 4). The second phase dispersions are also more uniformly distributed at lower revolution pitch and become coarser with increase in revolution pitch. An important observation is though the grain size is less at increased revolution pitch but tensile strength is decreasing. A reason for such observation is may be as AA 6061-T6

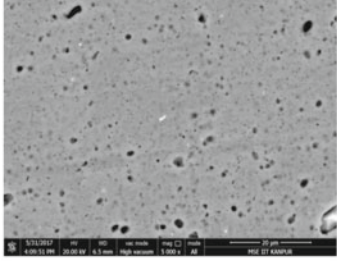
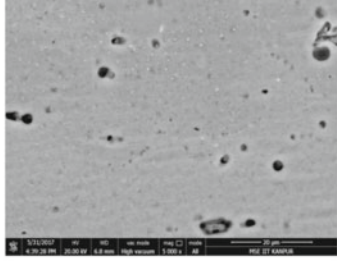
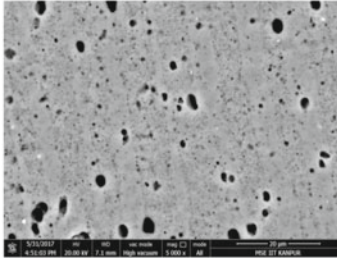
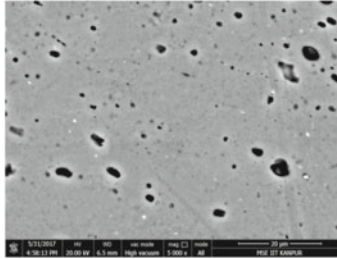
Tool type	Revolution pitch(V/N)	
	0.05	0.08
Square tool		
Cylindrical Threaded tool		

Fig. 4 Effect of revolution pitch for different tool design on nugget zone particle size and distribution

is a precipitate harden aluminum alloy the distribution of second phase particles affects the tensile property than the grain size. Square tool exhibits increased tensile properties for all cases. Increased spindle torque and Z-force also provides better deformation of stirred material for square tool. Increased pulsating stirring action of the material for square tool leads to finer grain, uniform and finer second phase distribution causing such observation.

4 Conclusions

In the present investigation, an attempt has been made to characterize the effects of tool shape in combination of tool pin profile variation and revolution pitch for FSW of 6 mm thick AA 6061-T6 plates. This was assessed through monitoring and analysis of the spindle torque and tool forces generated. It has been observed that the average spindle torque, Z-force and X-force increases with the increase in revolution pitch. Square pin tool exhibits increased amount of spindle torque, Z-force and X-force. With increase in revolution pitch, the grain size becomes finer. The second phase dispersions are more uniformly distributed and finer at lower revolution pitch. Square tool produces finer grains and second phase dispersions for

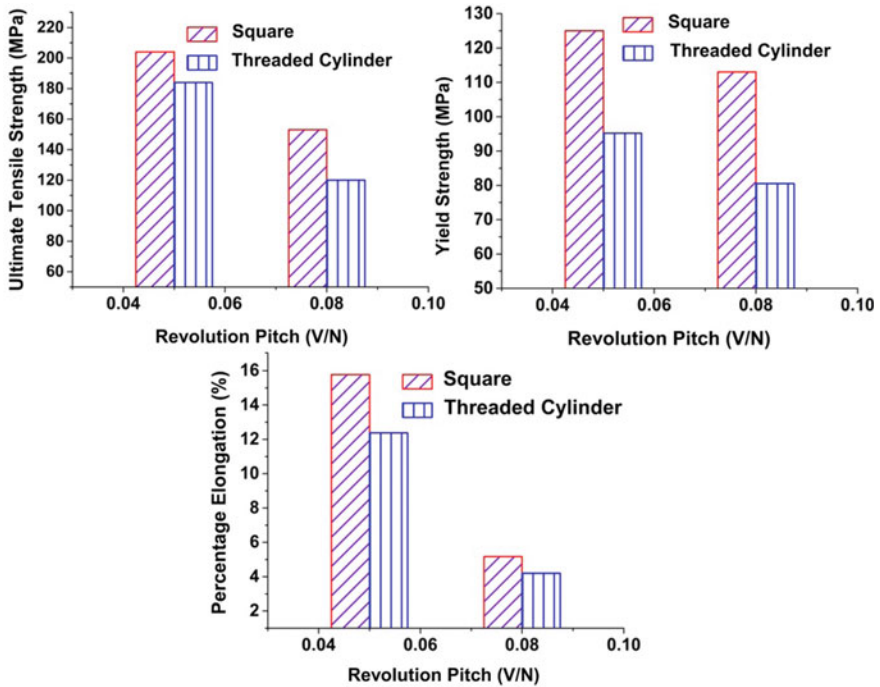


Fig. 5 Effect of revolution pitch for different tool design on different tensile properties

all welding conditions than cylindrical threaded tool. Tensile properties for square tool are more in comparison with cylindrical threaded tool. An increase in revolution pitch resulted in decrease of tensile properties for both the tool.

References

1. Thomas WM, Nicholas ED, Needham JC, Murch MG, Temple-Smith P, Dawes CJ (1991) International Patent Application PCT/GB92/02203 and GB Patent Application 9125978.8 [P]. UK Patent Office, London, 06/12/1991
2. Mishra RS, Ma ZY (2005) Friction stir welding and processing. *Mater Sci Eng: R*: Rep 50:1–78
3. Hattingh DG, Blignault C, VanNiekerc TI, James MN (2008) Characterization of the influences of FSW tool geometry on welding forces and weld tensile strength using an instrumented tool. *J Mater Process Technol* 203:46–57
4. Yang Q, Li X, Chen K, Shi YJ (2011) Effect of tool geometry and process condition on static strength of a magnesium friction stir lap linear weld. *Mater Sci Eng A* 528:2463–2478
5. Vijay SJ, Murugan N (2010) Influence of tool pin profile on the metallurgical and mechanical properties of friction stir welded Al-10 wt.% TiB₂ metal matrix composite. *Mater Des* 31:3585–3589
6. Colegrove P (2000) 3 Dimensional flow and thermal modelling of the friction stir welding process. In: 2nd international symposium on friction stir welding, Gothenburg, Sweden, TWI

7. Zhao YH, Lin SB, Wu L, Qu FX (2005) The influence of pin geometry on bonding and mechanical properties in friction stir weld 2014 Al alloy. *Mater Lett* 59(23):2948–2952
8. Arbogast WJ (2005) Using process forces as a statistical process control tool for friction stir welds. In: *Proceedings of the friction stir welding and processing III, TMS Annual Meeting, San Francisco, CA, USA*, pp 193–204
9. Banik A, Roy BS, Barma JD, Saha SC (2018) An experimental investigation of torque and force generation for varying tool tilt angles and their effects on microstructure and mechanical properties: friction stir welding of AA 6061-T6. *J Manuf Process* 31:395–404
10. Elangovan K, Balasubramanian V, Valliappan M (2008) Influences of tool pin profile and axial force on the formation of friction stir processing zone in AA6061 aluminium alloy. *Int J Adv Manuf Technol* 38:285–295
11. Trimble D, O'Donnell GE, Monaghan J (2014) Characterisation of tool shape and rotational speed for increased speed during friction stir welding of AA2024-T3. *Manuf Process*. <http://dx.doi.org/10.1016/j.jmapro.2014.08.007>
12. Yang Y, Kalya P, Landers R, Krishnamurthy K (2008) Automatic gap detection in friction stir butt welding operations. *Int J Mach Tool Manuf* 48:1161–1169
13. Kumar S (2016) Ultrasonic assisted friction stir processing of 6063 aluminum alloy. *Arch Civ Mech Eng* 16:473–484

Analysing Attributes of Food Supply Chain Management: A Comparative Study



Mohd Sufiyan, Abid Haleem , Shahbaz Khan  and Mohd Imran Khan 

Abstract With increasing human population and food variety, there is a challenge to provide quality and requisite food to people at the right time at the right place. Food supply chain management (FSCM) needs to analyse due to its complex nature. The objective of this paper is to review the food supply chain management (FSCM) and identify the significant attributes and further analyses them to differentiate from each other. The identified critical attributes of SCM are relationship and governance, coordination and integration, collaboration, agility, logistics, traceability, packaging, and waste management. We have distinguished the food supply chain (FSC) from other supply chains, because of the unique characteristics of the food products which pose a serious challenge. Based on the identified attributes, we have undertaken a comparative analysis of FSCM with non-food supply chain's management (Non-FSCM). The findings suggest towards the importance of traceability and packaging systems in FSC as compared to a Non-FSC.

Keywords Attributes · Comparison · Food supply chain management (FSCM) · Non-Food supply chain management (Non-FSCM) · Traceability systems

1 Introduction

Agriculture produce provides the raw material to many industries and is the primary input of the world economy. Technological, social, economic, industrial, legal, business and other factors have impacted the food sector and determine the food availability and its delivery to the final consumer, thus making the food supply chain (FSC) as a complex network. The companies must ensure that the food products reach to the end customers on time with maintained quality attributes [1]. Nowadays, more value or variety is being added to the food product as agro-industries are extracting the single product from many agro-materials, and this is increasing

M. Sufiyan · A. Haleem (✉) · S. Khan · M. I. Khan
Department of Mechanical Engineering, Faculty of Engineering and
Technology, Jamia Millia Islamia, New Delhi 110025, India
e-mail: ahaleem@jmi.ac.in

the number of suppliers for food manufacturers. The issues like perishability, shelf times, traceability, and seasonality make food supply chain management (FSCM) a complex problem. Moreover, a large amount of food waste is generated due to the perishable nature of food [2].

The FSC exhibits a unique set of characteristics that distinguished it from non-FSC by characteristics such as perishability, high product differentiation, seasonal behaviour, food quality and safety, environmental concern, need for specific attributes like traceability and visibility, specific transportation, storage conditions [3]. Agro-material is not available throughout the year, instead is available only limited time in a specific region. Thus, the processor needs to operate a flexible process to switch over to other agro-material when one is out of season. Agro-material is quite sensitive to changes in quality with time and temperature. Thus, there is a constraint on temperature maintained during storage and transportation, processing condition and the time for which a food product can be kept in inventory [4].

2 Literature Review

Many authors have defined FSC and underlined its significant echelons. Lakovou et al. [5] established agri-food supply chain as “a set of activities in a ‘farm-to-fork’ sequence which includes farming, processing/production, testing, packaging, warehousing, transportation, distribution, and marketing”.

2.1 Food Supply Chain Management

FSCM includes activities or operations from production, distribution, and consumption to manage the food quality and safety issues efficiently and effectively. According to Manning et al. [6], about one-third of the produced food has been abandoned or wasted yearly. Two-third of the food wastage is there at harvesting, shipping, and storage stages [7]. Perishable food (such as fruit and vegetables) was wasted by 492 million tons worldwide in 2011 due to weak management of FSC [8]. Therefore, it is necessary for us to manage FSC to save our food. Food quality, safety, and freshness concerns have made the FSC much complex. The supply chain complexities are significant in case of perishable products. Thus, there is a requirement of efficient packaging and temperature-controlled logistics to ensure the quality of perishable product along the supply chain. The functioning and performance of food chains are affected by the coordination modes and the kind of governance [9]. Due to highly variable or fluctuating nature of demand, FSC is required to be reliable and agile enough to respond to consumer demand and preferences to become a customer-focused and more responsive [10]. There should be appropriate collaboration among stakeholders to have focused on economic, environmental, social, organizational, marketing, food quality, and safety factors [7]. In FSCM, there is special requirements for food safety,

as well as a growing demand for food characterized by a specific identity (ethnicity, organic food, low carbon footprint, religious constraints, etc.), which calls for the implementation of an effective traceability system [11].

2.2 Non-food Supply Chain Management

SCM is a coordinated approach to perform all activities associated with goods and information flows from raw materials sourcing to product delivery to the end customers [11]. SCM should have collaboration among the stakeholders within a supply chain, which provides real-time analytical capabilities to produce planning solutions and executing tasks of the supply chain [12]. Khan et al. [13] suggest that to achieve competitive advantage, there should be partnerships among firms and mutually sharing information, risks, and rewards. Council of Logistics Management considers logistics as the subset of SCM. The organizational scope of SCM includes companies with supply chain orientation, information sharing, long-term relationships, inter-functional coordination, and integration of main processes [14].

3 Objectives of the Research

The principal objectives of this research are as follows:

- To identify the significant attributes of FSCM and Non-FSCM
- Undertake a comparative study of FSCM and Non-FSCM based on those attributes.

4 The Major Attributes of the Supply Chain Management as Identified Through the Review of the Literature

4.1 Relationship and Governance

For efficient information sharing, there is a need to manage relationships among the supply chain actors, and one has to choose the governance structure. Closer relationship and integrated governance structure may lead to greater information sharing [9]. The relationship is the way of intercommunication with each other among the firms [15, 16]. In Non-FSC, the relationship would be short term or long term depending on the amount and quality of the information to be shared, but in FSC, there are long-term relations between the chain partners. Governance drives the coordination mechanisms. Gereffi et al. [17] have classified the governance in five main typologies as a market, modular, relational, captive, and hierarchical (vertically

integrated). Food chains are having captive or hierarchical kind of governance. In captive governance, local firms have control over the other firms; moreover, switching to other partners is difficult and costly. Short food chains have hierarchic governance where managers/ headquarters have full power over the other chain partners.

4.2 Coordination and Integration

Integration can be horizontal integration (for example, different farmers integrates to form the corporation) or vertical integration (i.e., among the stakeholders from upstream to downstream) along the supply chain. Vertical integration in the FSC leads to greater coordination between food processors and farmers resulting in improved economic performance [18]. Bullwhip effect first discovered by Forrester was the result of uncoordinated approach in decision-making among the supply chain partners. Coordinated approach results in an interactive, joint decision-making process, where partners have a more direct influence on each other's decisions. The fundamental coordination mechanisms are standardization, mutual adjustment, and hierarchies. Standardization of output, process, and knowledge/skills is there in between separate, legally independent companies whereas hierarchical structures indicate either a high unilateral dependency or equity is shared. In FSC, to attain vertical integration, expensive and complicated coordination mechanisms are required, i.e., hierarchy or plan and coordination by the creation of lateral linkages. Fresh product supply chain is mostly bonded by a contract.

4.3 Collaboration Among Stakeholders

Active collaboration among stakeholders will result in joint decisions and activities. There should be teamwork effort indicating a high degree of joint implementation. Integration of resources (people, processes, and technology) is needed to have collaboration among stakeholders to achieve a common goal. Collaboration is more critical in FSC to achieve the common goals such as high product's value, flexible food production while integrating the environmental policy [19]. In FSC, one can implement both vertical and horizontal collaboration. Food companies are increasingly implementing collaborative planning forecasting and replenishment (CPFR) to enhance visibility [20].

4.4 Supply Chain Agility

Supply chain agility refers to the ability or quality of organizations in a network to quickly sense and respond to changes by reconfiguring their resources in

collaboration [21]. The performance of FSC gets influenced by natural disasters, technological accidents, infectious diseases, food safety incidents. FSC is comparatively more brittle (i.e., vulnerable to the risk of disease and volatility in commodity markets) than Non-FSC and thus need to be managed effectively and enhance its agility.

4.5 Logistic Management

Logistics is a critical part of SCM responsible for the efficient flow and storage of goods, services and related information from the point of origin to the point of consumption to meet customer's requirements [14, 22]. Food quality is mainly depending on time and environment condition such as temperature, humidity, and the presence of contaminants. Thus, the time for which the food product remains in the supply chain is crucial, which is mainly depends upon the mean of transportation. Thus, there is a necessity for temperature-controlled vehicles for transportation. The warehouse should have good refrigeration strategy and preservation conditions necessary for foods to increase their shelf life. For inventory management of food, the essential element is the use of real-time product quality information systems.

4.6 Traceability

In FSC, there is a requirement to monitor the composition and the position of each lot precisely along the chain; it uses traceability system for the precise monitoring along the supply chain [13]. A traceability system provides useful information during the product recall. The RFID-based traceability system is used for bulk products which allow online traceability of continuous flows. The sensors (e.g., temperature, humidity, etc.), are used for transmitting the measured data.

4.7 Packaging

Packaging is required to preserve the quality of products before reaching to end customer. Packaging is critical in food products as the food quality decreases continuously with time and change in environment. Nowadays, advanced concepts of active packaging and intelligent packaging are being used for safer and healthier food [23]. Active packaging includes moisture absorbers, antimicrobial packaging, carbon dioxide emitters, oxygen scavengers, and antioxidant packaging for extending the shelf life. Intelligent packaging monitors the condition of the packed food or the surrounding environment. Intelligent packaging effectively detects, senses, records, traces, or communicates information about the product's quality during the food chain [24].

4.8 Waste Management

In the Non-FSC, there can be product deletion at any point which will lead to waste output to the environment and needs to be adequately managed either through re-manufacturing or conversion to a new/existing product. Food spoils due to mismanagement of temperature during storage, harvesting or inefficient processing, or consumers throwing edible food. Local government could be a key player in reducing food wastes [25].

5 Comparison Between Food Supply Chain Management and Non-food Supply Chain Management

Eight major attributes of SCM undertake a comparison between FSCM and Non-FSCM (Table 1).

Table 1 Comparison between FSCM and Non-FSCM based on attributes

S No	Attributes	FSCM	Non-FSCM
1.	Relationship and governance	Long-term relations are required to have proper trust. Food chains are led by captive, relational or hierarchical governance having more formal administrative control	Relations could be short term or long term depending on the amount and quality of the information sharing. The governance structure is based more on price mechanisms
2.	Coordination and integration	Mostly vertically integrated with complex coordination mechanism, i.e., coordination by the creation of lateral linkages and hierarchy or plan	Low coordination is there among the chain partners. Coordination mechanism can be through standardization, mutual contracts or hierarchical depending on the integration level
3.	Collaboration among stakeholders	High collaboration is needed. Both vertical collaboration and horizontal collaboration are found to achieve the common goals of maintaining food quality and sustainability	Collaboration among stakeholders is comparatively low as there are not many quality and safety issues, but collaborative environment management is required to achieve sustainability

(continued)

Table 1 (continued)

S No	Attributes	FSCM	Non-FSCM
4.	Supply chain agility	FSC is agiler due to its brittle nature and high variable demand. Timely delivery of food product is essential	Comparatively supply chain is less agile since demand pattern is not as much variable as in the case of food
5.	Logistic management	Temperature-controlled means of transportation and warehouse are required. Controlled conditions used for the fruit to prolong its shelf life. Mostly air freight is used as transportation mean	There is no requirement of maintaining temperature and preservation conditions
6.	Traceability	Effective traceability is implemented which contains all the information regarding the food product such as origin, processing method, and ingredient to reduce the public health risks	Traceability is required only for the product identification
7.	Packaging	Packaging is critical, outstanding to the product's quality decay with reduced packaging. There is increased use of advanced packaging systems like active packaging and intelligent packaging	Packaging is essential only to control the product damage during the product movement along the supply chain
8.	Waste management	Need to implement advanced waste reduction techniques. Local governments are responsible for waste management	Non-FSC generates lesser waste than FSC. There should be re-manufacturing for waste management

6 Discussion

The food quality and safety issues and timely deliverance of food to the end customer require a coordinated approach and collaborative nature among the supply chain firms. Food companies are implementing collaborative planning forecasting and replenishment (CPFR) which provides visibility along the chain. FSCs are integrated vertically with the hybrid relationship. In FSCs, long-term relations are

required between chain partners to generate trust among them. FSC is agile due to higher variable demand, thus need to be very responsive. The perishable nature of the product due to temperature, humidity, and other environmental conditions are constraint to logistics management. Traceability issues are significant to respond to product recall at the time of food crisis. Efficient traceability system required to have proper product identity, properties, and other related data. Nowadays, advanced packaging systems are being used to have increased shelf life of the product. In FSC, more waste is generated compared to Non-FSC owing to perishable issues, which needs to be managed appropriately.

7 Conclusion

This paper identified eight significant attributes of FSCM and Non-FSCM. Based on these attributes, FSCM and Non-FSCM are compared. FSC is different from Non-FSC because of characteristics such as perishability, high product differentiation, seasonality, need for a particular attribute like traceability and visibility, temperature-controlled transportation and warehouses and changing product quality [26]. There is a need for high integration level, coordinated approach, collaboration among stakeholders, proper relationship and governance, good traceability system, advanced packaging, temperature-controlled logistics, and waste management in an efficient FSCM. The identified attributes can be used further for the quantitative/empirical studies.

References

1. Sitek P, Wikarek J, Nielsen P (2017) A constraint-driven approach to food supply chain management. *Ind Manag Data Syst* 117(9)
2. Yu M, Nagurney A (2012) Competitive food supply chain networks with application to fresh produce. *Eur J Oper Res* 224(2)
3. Van der Vorst JGAJ (2000) Effective food supply chains-generating, modeling and evaluating supply chain scenarios. Wageningen University, The Netherlands
4. Jonkman J, Bloemhof JM, van der Vorst JGAJ, van der Padt A (2016) Selecting food process designs from a supply chain perspective. *J Food Eng* 195
5. Iakovou E, Vlachos D, Achillas C, Anastasiadis F (2012) A methodological framework for the design of green supply chains for the agri-food sector. In: 2nd international conference on supply chains
6. Manning L, Baines R, Chadd S (2006) Quality assurance models in the food supply chain. *Br Food J* 108(2):91–104
7. Fritz M, Schiefer G (2008) Food chain management for sustainable food system development: a European research agenda. *Agribusiness* 24(4):440–452
8. Gustavsson J, Cederberg C, Sonesson U, van Otterdijk R, Meybeck A (2011) Global food losses and food waste. The Food and Agriculture Organization of the United Nations, Rome, Italy
9. Carbone A (2017) Food supply chains: coordination governance and other shaping forces. *Agric Food Econ* 5(3)

10. Dellino G, Laudadio T, Mari R, Mastronardi N, Meloni C (2018) A reliable decision support system for fresh food supply chain management. *Int J Prod Econ* 56(4)
11. Handfield RB, Ernest LN (1999) *Introduction to supply chain management*. Prentice-Hall, Upper Saddle River
12. Sahay BS, Gupta AK (2003) Development of software selection criteria for supply chain solutions. *Ind Manage Data Syst* 103(2):97–110
13. Khan S, Haleem A, Khan M, Abidi M, Al-Ahmari A (2018) Implementing traceability systems specific supply chain management (SCM) through critical success factors (CSFs). *Sustainability* 10(2):204
14. Mentzer JTT, Dewitt W, Keebler JS, Zacharia ZG (2001) Defining supply chain management. *J Bus Logist* 22:1–25
15. Cheng J-H (2011) Inter-organizational relationships and information sharing in supply chains. *Int J Inf Manage* 31(4):374–384
16. Khan MI, Haleem A (2018) Understanding “Halal” and “Halal certification & accreditation system: a Brief Review. *Saudi J Bus Manag Stud* 1(1):32–42
17. Gereffi G, Humphrey J, Sturgeon T (2005) The governance of global value chain. *Rev Int Polit Econ* 12(1):78–104
18. Carillo F, Caracciolo F, Cembalo L (2017) Do farms benefit of vertical coordination? Evidence from Italian durum wheat producers. *Agric Food Econ*
19. La Scalia G, Settanni L, Micale R, Enea M (2016) Predictive shelf life model based on RF technology for improving the management of food supply chain: a case study. *Int J RF Technol* 7(1):31–42
20. Blandon J, Henson S, Cranfield J (2009) Small-scale farmer participation in new agri-food supply chains: case of the supermarket supply chain for fruit and vegetables in Honduras. *J Int Dev* 21(7):971–984
21. Ismail HS, Sharifi H (2006) A balanced approach to building agile supply chains. *Int J Phys Distrib Logist Manag* 36(6)
22. Haleem A, Khan MI (2017) Towards successful adoption of Halal Logistics and its’ implications for the stakeholders. *Br Food J* 119(7)
23. Ghaani M, Cozzolino CA, Giulia C, Stefano F (2016) An overview of the intelligent packaging technologies in the food Sector. *Trends Food Sci Tech* 51
24. Yam KL, Takhistov PT, Miltz J (2005) Intelligent packaging: concepts and applications. *J Food Sci* 70:1–10
25. Kibler KM, Reinhart D, Hawkins C, Motlagh AM, Wright J (2018) Food waste and the food-energy-water nexus: a review of food waste management alternatives. *Waste Manage* 74
26. Tsolakis NK, Keramydas CA, Toka AK, Aidonis DA, Iakovou ET (2013) Agrifood supply chain management: a comprehensive hierarchical decision-making framework and a critical taxonomy. *Biosyst Eng* 120:47–64

Optimization of Electric Discharge Machining Process Parameters for H13 Steel by Using Taguchi Method



Mahendra M. Ghayatadak and Amar S. Bhandare

Abstract Electrical discharge machining (EDM) is the most versatile non-traditional machining process which is used for manufacturing geometrically complex and hard material that is extremely difficult to machine by conventional machining processes. As it is non-contact machining process, no or negligible amount of forces are acted on the workpiece so that it can machine any material irrespective of its hardness except non-conducting materials. In this investigation, the process parameters such as peak current, pulse on time, and gap voltage of EDM were experimentally optimized to obtain the optimum machining characteristics enumerated as material removal rate (MRR) and electrode wear rate (EWR) by using Taguchi technique for machining H13 steel. The obtained results were analyzed by using analysis of variance (ANOVA) to identify the significance of each process parameter on the machining characteristics of EDM. The analysis of Taguchi method reveals that pulse on time and peak current have significantly affected the material removal rate and electrode wear rate.

Keywords Analysis of variance · Electrical discharge machining · Optimization · Taguchi

1 Introduction

Electric discharge machining (EDM) is non-contact manufacturing process in which material removal takes place by a series of electrical sparks generated between tool and work materials with constant electric field, whereas both tool and work material are dipped into the dielectric fluid [1]. In this modern era of the world, as per the applications' demands, different new materials came into picture which are very difficult to machine by conventional manufacturing processes, as they possess properties like high strength, high hardness, and high temperature resistance. And that's why more and more efforts are taken by the researchers to perceive the different

M. M. Ghayatadak (✉) · A. S. Bhandare
Walchand College of Engineering, Sangli, India
e-mail: mahendraghayatadak98@gmail.com

© Springer Nature Singapore Pte Ltd. 2019
K. Shanker et al. (eds.), *Advances in Industrial and Production Engineering*, Lecture Notes in Mechanical Engineering, https://doi.org/10.1007/978-981-13-6412-9_51

525

non-conventional manufacturing process to machine this kind of work materials. In this aspect, Electro Discharge Machining (EDM) is one of the best alternatives in wide varieties of non-conventional machining processes for high-precision machining of all types of electrical conductive materials such as metals, metallic alloys, and even some ceramic materials of any hardness. The leading field of application of EDM is dies- and mold-manufacturing industries [2, 3].

EDM process is still considered as the expertise-demanding process as the sparking phenomenon of EDM process is difficult to correlate directly with machining characteristics of EDM. There is an ambiguity between the machining parameters such as peak current, pulse on time, pulse of time, voltage, duty factor and the thermal energy or discharge energy generated by a spark at the machining area, which is responsible for the machining characteristics of EDM like MRR, EWR, SR, and recast layer [4].

The process parameters can affect the various responses of the process like MRR, SR, TWR, recast layer, crater size, and corner deviation. So that close control over the setting of process parameters is must to achieve an economical and optimum machining. The process has to maximize the MRR and at the same time TWR, SR, etc. should be minimized. Shifting the current from low level to high level can significantly increase the MRR but it can also increase the SR and TWR [5].

For optimizing electrical discharge machining process parameters, researchers have been focusing on the use of different tools like analysis of variance (ANOVA), fuzzy logic, Gray relational analysis (GRA), response surface methodology (RSM), artificial neural networking (ANN) and genetic algorithm (GA) [6, 7].

Rather than focusing only on optimization of process parameters of EDM, a class of researchers are also emphasizing on the improvement of EDM process also called as hybrid EDM. It consists of different devices that aid the effective evacuation of debris particle from the machining gap which maintains optimum machining gap for stable and efficient sparking such as ultrasonic assisted EDM, rotary EDM, and magnetic-field-assisted EDM [8–10].

There is a need to identify the different process parameters and their impact on the response variables so as to achieve the optimized values of the different process parameters for getting optimum response variable of EDM process.

2 Experimental Details

2.1 *Experimental Setup and Procedure*

In this investigation, S50 CNC EDM machine was used for the experimentation. Considering the industrial application of EDM in dies- and mold-manufacturing industry, H13 steel plate is used as a workpiece, as it has high toughness and very good stability in heat treatment, and a copper rod of 6.35 mm diameter is considered

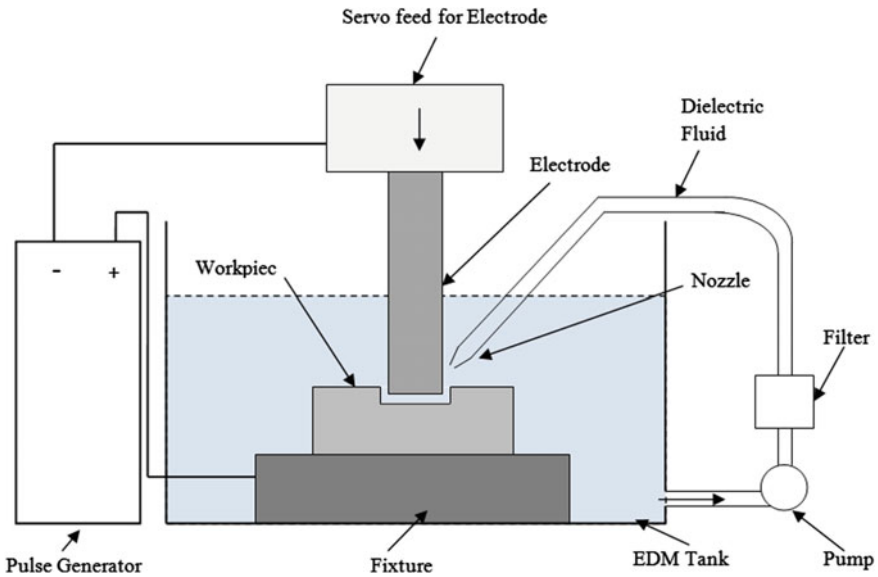


Fig. 1 Schematic of CNC EDM

Table 1 Composition of H13 steel

Element	Cr	Mo	Si	V	C	Ni	Cu	Mn
wt%	4.75–5.5	1.10–1.75	0.8–1.2	0.8–1.2	0.32–0.45	0.3	0.25	0.2–0.5

Table 2 Physical properties of copper electrode

Physical properties	Values
Thermal conductivity [W/mK]	380
Melting point [°C]	1081
Boiling temperature	2592
Specific heat [cal/g °C]	0.092
Specific gravity at 200 °C [g/cm ³]	8.81
Coefficient of thermal expansion [1/°C]	17×10^{-6}

an electrode. The schematic diagram of the experimental setup is shown in Fig. 1. It consists of workpiece and electrode separated by dielectric fluid such as kerosene.

Tables 1 and 2 represent the chemical composition of H13 steel and essential properties of copper electrode, respectively. Dimensions of the workpiece are $80 \times 180 \times 3.24$ mm. The surface of the workpiece and electrode was ground by 600 and 800 grit emery paper to ensure the flatness and surface quality of workpiece and electrode, before conducting the experimentation. Table 3 represents the experimental conditions of EDM which includes constant parameters like duty factor and dielectric fluid.

Table 3 Experimental conditions

Working conditions	Descriptions
Workpiece	H13 Steel (+)
Electrode	Copper (-)
Duty factor	0.3
Dielectric fluid	EDM oil
Machining strategy	Through hole drill

2.2 Process Parameters and Response Variables

Table 4 represents the factors with their levels. The factors or process parameters are peak current, pulse on time, and voltage, whereas the response variables or machining characteristics are MRR and EWR.

2.3 Material Removal Rate (MRR)

MRR is the most important variable in the EDM which decides its machining speed and that is why higher MRR is always appreciable. Equation (1) gives the derived formula to determine the MRR based on the volume of material removed and time required for the same. Here the volume of material removed was calculated by using top radius of hole (R), bottom radius of hole (r), and thickness of plate (h). R and r were calculated by a digital microscope (DinoLite).

$$\text{MRR} = \frac{\frac{\pi}{3} \times h \times (R^2 + r^2 + R \times r)}{t} \text{ mm}^3/\text{min} \quad (1)$$

2.4 Electrode Wear Rate (EWR)

As given by (2), EWR is nothing but the difference between the mass of electrode before (M_b) and mass of electrode after (M_a) machining per unit machining time (t). ρ indicates the density of copper.

Table 4 Process parameters and their levels

Factors	Level		
	1	2	3
Peak current (A)	12	16	20
Pulse on time (μs)	100	150	200
Voltage (V)	30	40	50

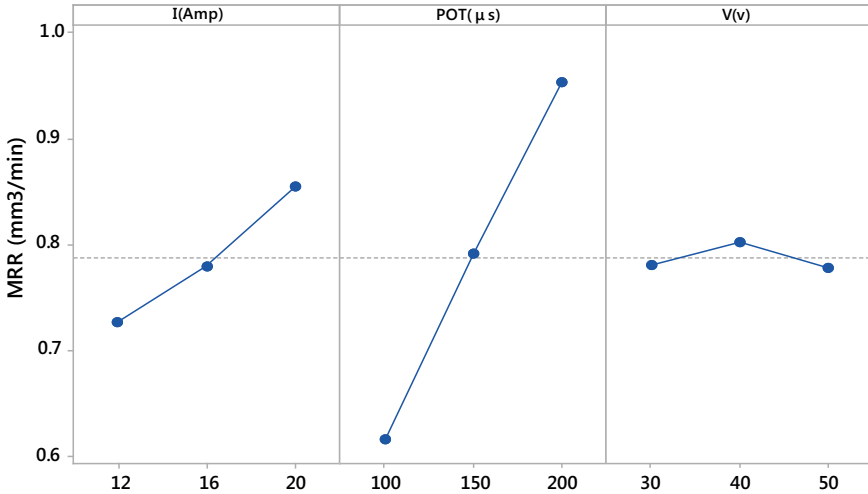


Fig. 2 Main effect plot for MRR

$$EWR = \frac{\frac{Mb - Ma}{\rho} \times 1000}{t} \text{ mm}^3/\text{min} \tag{2}$$

3 Experimental Results and Analysis

Taguchi design of L27 array was selected for experimentation with three factors, peak current, pulse on time, and voltage, with three levels. The basic reason behind using L27 array is to avoid the chance of error (variance) as compared to L9 array and to obtain interaction plots which are not possible in L9 array. Accordingly, 27 holes are drilled by copper electrode on H13 steel plate (workpiece). For optimization of process parameters with respect to their machining characteristics, Taguchi method was implemented. ANOVA of Minitab17 was implemented for analysis. Table 5 represents L27 array of Taguchi design for experimentation.

3.1 Analysis for Material Removal Rate

Table 5 indicates the results of EDM experimentation and on the basis of that analysis is done by using ANOVA.

ANOVA was used to investigate the significance of various process parameters affecting the response variable. F-test was carried out to understand the significance and rank of process parameters. Higher *F* value indicates the factor, and process parameter is highly significant in affecting the response variables. Table 6 represents

Table 5 L27 array of Taguchi design for experimentation

Sr. No.	I (Amp)	POT (μ s)	V (v)
1	12	100	30
2	12	100	40
3	12	100	50
4	12	150	30
5	12	150	40
6	12	150	50
7	12	200	30
8	12	200	40
9	12	200	50
10	16	100	30
11	16	100	40
12	16	100	50
13	16	150	30
14	16	150	40
15	16	150	50
16	16	200	30
17	16	200	40
18	16	200	50
19	20	100	30
20	20	100	40
21	20	100	50
22	20	150	30
23	20	150	40
24	20	150	50
25	20	200	30
26	20	200	40
27	20	200	50

Table 6 ANOVA results of MRR and EWR

Source	DF	MRR (mm ³ /min)			EWR (mm ³ /min)		
		F	P	Rank	F	P	Rank
I (Amp)	2	21.24	0.000	2	41.85	0.000	2
POT (μ s)	2	148.91	0.000	1	103.85	0.000	1
V (v)	2	0.92	0.417	3	5.91	0.010	3
Error	20						
Total	26						
		R-Sq = 94.48% R-Sq (adj) = 92.82%			R-Sq = 93.81% R-Sq (adj) = 91.96%		

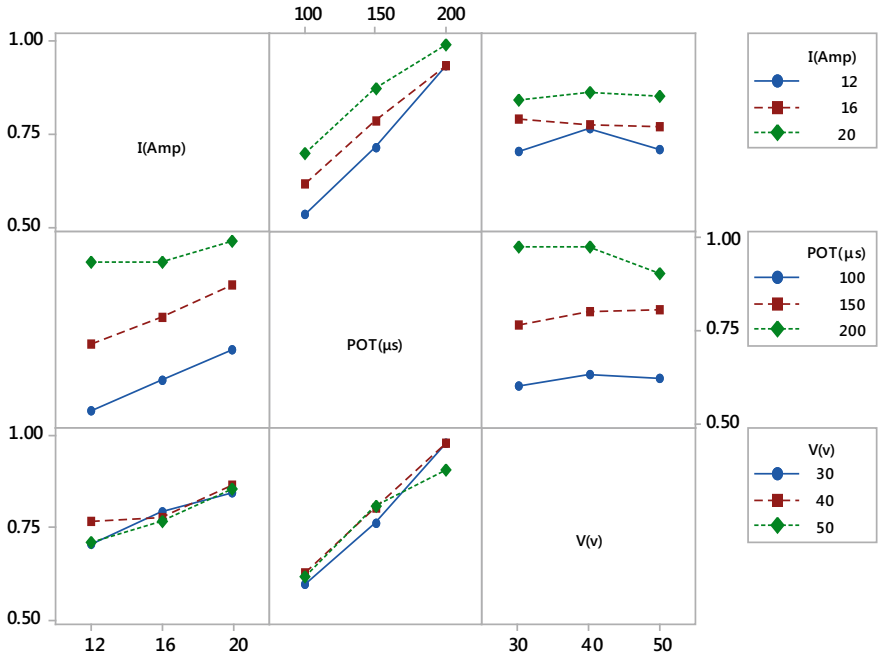


Fig. 3 Interaction plot for MRR

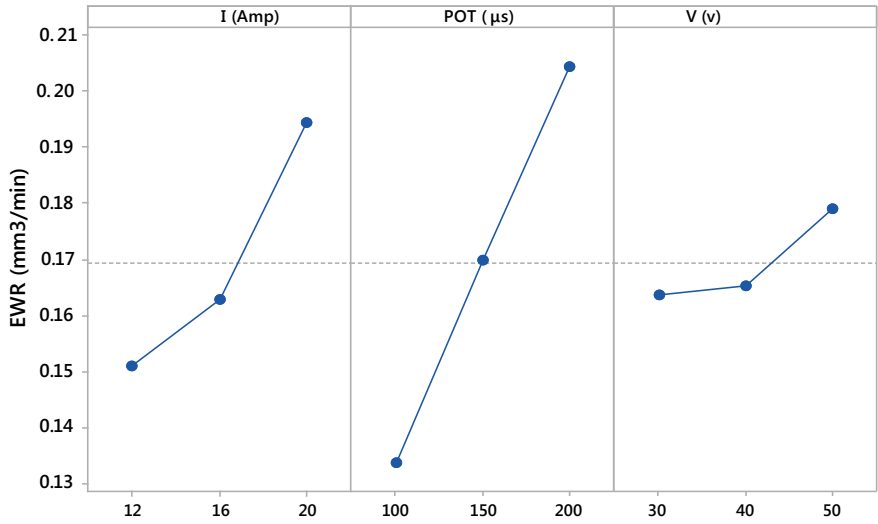


Fig. 4 Main effect plot for EWR

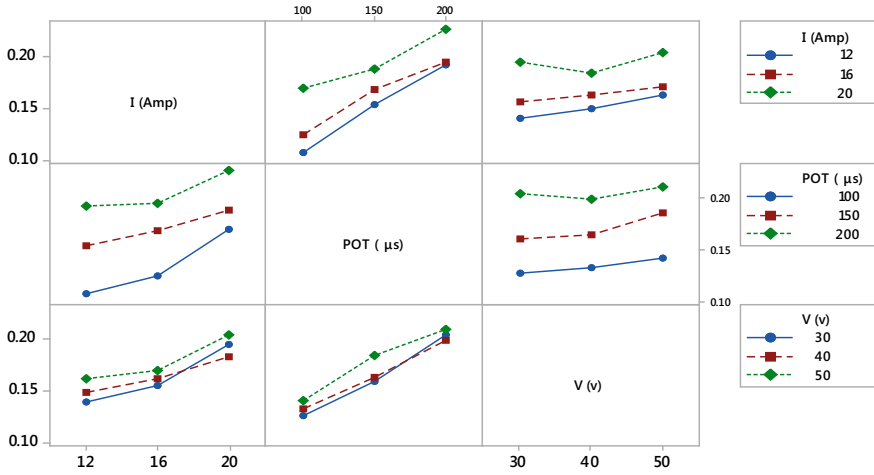


Fig. 5 Interaction plot for MRR

the ANOVA results for MRR and EWR of EDM experimentation. As in Table 6, pulse on time (POT) and current (I) are highest influencing parameters for both MRR and EWR, whereas the influence of voltage is negligible as compared to current and pulse on time. This is because, in general, MRR is the function of spark energy which depends on current, pulse on time, and voltage; so when the levels of these parameters increase, the spark energy increases resulting in an increment in MRR. Low values of gap voltage can give rise to an increase in MRR. However, application of very low values has arcing tendency. Also, higher values of gap voltage can result in relatively lower metal removal rates. So that middle value of voltage (40 V) gives best results which are represented in Fig. 2. In the case of electrode wear rate (EWR), as current, pulse on time, and voltage increase, spark energy in sparking zone also increases which results in an increment in EWR, and it is illustrated by Fig. 4. Interaction plots for both MRR and EWR are represented in Figs. 3 and 5, respectively.

For optimization of MRR, “larger is better” signal-to-noise ratio (SN ratio) is preferred. As given below, formula for “larger is better” SN ratio is illustrated in (3).

$$-10 \times \log_{10} \left\{ \frac{\text{sum}(\frac{1}{\bar{y}^2})}{n} \right\} \tag{3}$$

For optimization of EWR, “smaller is better” signal-to-noise ratio (SN ratio) is preferred, and that is illustrated in (4).

$$-10 \times \log_{10} \left\{ \frac{\text{sum}(Y^2)}{n} \right\} \tag{4}$$

4 Conclusion

An experimental study has been carried out to investigate the influence of various process parameters on machining characteristics of EDM for H13 steel with copper electrode by using Taguchi method. In this study, the influence of peak current, pulse on time, and voltage on MRR and EWR has been highlighted. Following observation can be drawn from this experimentation:

- MRR is the function of the discharge or spark energy which depends on pulse on time, peak current, and voltage.
- An ANOVA result indicates that the pulse on time and current have shown significant effect on both MRR and EWR, whereas voltage has shown least significant effect compared to other parameters.
- The optimal combination of process parameters and their levels for the maximization of MRR of the EDM process are A3B3C1 (Experiment No. 25) and for minimization of EWR are A1B1C1 (Experiment No. 1)
- Optimum MRR and EWR were observed as 1.03 mm³/min and 0.096 mm³/min, respectively.
- For both MRR and EWR, pulse on time, peak current, and voltage have ranks 1, 2, and 3, respectively.

Acknowledgements The authors wish to sincerely acknowledge financial support for Research Promotion Scheme by AICTE (Ref No: 8023/RID/RPS-114/2011-12) under which the procurement of equipment's and experimental work is performed.

References

1. Ho KH (2003) State of the art electrical discharge machining (EDM). *Int J Mach Tools Manuf* 43:1287–1300
2. Singha NK (2018) Electrical discharge drilling of D3 die steel using air assisted rotary tubular electrode. In: 7th international conference of materials processing and characterization. *Materials Today Proceeding*, pp 4392–4401
3. Verma V (2017) Process parameter optimization of die-sinking EDM on Titanium grade—V alloy (Ti6Al4 V) using full factorial design approach. In: 5th International conference of materials processing and characterization. *Materials Today Proceeding*, pp 1893–1899
4. Chandramouli S (2018) Experimental investigation of EDM process parameters in machining of 17–4 PH steel using Taguchi method. In: 7th international conference of materials processing and characterization. *Materials Today Proceeding*, pp 5058–5067
5. Dey A (2017) Optimization of electrical discharge machining process parameters for Al6061/cenosphere composite using grey-based hybrid approach. *Trans Nonferrous Met Soc China* 27:998–1010
6. Lina JL (2000) Optimization of the electrical discharge machining process based on the Taguchi method with fuzzy logics. *J Mater Process Technol* 102:48–55
7. Gangil M (2017) Review on modelling and optimization of electrical discharge machining process using modern Techniques. In: 5th international conference of materials processing and characterization. *Materials Today Proceeding*, pp 2048–2057

8. Uhlmann E (2016) Investigations on vibration-assisted EDM-machining of seal slots in high temperature resistant materials for turbine components – part II. In: 18th CIRP conference on electro physical and chemical machining (ISEM XVIII). Procedia CRIP, pp 334–339
9. Teimouri R (2012) Effects of magnetic field and rotary tool on EDM performance. *J Manuf Process* 14:316–322
10. Ghoreishi M (2002) A comparative experimental study of machining characteristics in vibratory, rotary and vibro-rotary electro-discharge machining. *J Mater Process Technol* 120:334–384

Machining Performance Optimization During Electro Discharge Machining on Titanium (Grade 4): Application of Satisfaction Function and Distance-Based Approach



Dipraj Banik, Rahul, Gitimaya Kar, Biswajit Debnath, B. C. Routara, Ashok Kumar Sahoo and Dhiraj Kochar

Abstract Titanium grade-4 (3.7065, R50700) is one of the most robust materials and finds its application in aerospace industry specially for making spacecraft, aircraft, missiles, naval ships, armor plating, etc. The main advantage of titanium is that it has a high strength, low-density results in less weight. It can withstand very high temperatures also. Machining of titanium was not an easy task, as it is a very hard material and it has poor thermal conductivity, higher pressure load, non-uniform chip thickness, etc. So we have chosen electro discharge machine (EDM) for the machining of titanium workpiece. Our aim was by taking peak current (I_p), pulse on time (T_{on}), and voltage gap (V_g) as input control parameters based on L_9 orthogonal array, to find optimum values of response parameters such as material removal rate (MRR), tool wear rate (TWR), and surface roughness (SR). In this research, work satisfaction function has been used to obtain the individual satisfaction values of the responses, and then these multi-responses have been converted into an equivalent single index. A distance measure has been computed next which basically determines the separation of each experimental setting (alternative) with respect to the ideal expectation (satisfaction). Finally, this distance function has been optimized (minimized) by Taguchi method.

Keywords Electro discharge machine · Titanium grade-4 · Copper tool · Satisfaction function · Taguchi method

1 Introduction: Background and Motivation

The development in the field of materials and their properties has reached a new peak in current time. These all modification proved as a challenge to current machining processes and lead to the arrival of advanced machining processes in the field of manufacturing technology. Titanium is a very useful material. The main advantage

D. Banik · Rahul (✉) · G. Kar · B. Debnath · B. C. Routara · A. K. Sahoo · D. Kochar
Kalinga Institute of Industrial Technology (Deemed to be University), Bhubaneswar, Odisha, India
e-mail: rahulkumar589@gmail.com

© Springer Nature Singapore Pte Ltd. 2019

K. Shanker et al. (eds.), *Advances in Industrial and Production Engineering*, Lecture Notes in Mechanical Engineering, https://doi.org/10.1007/978-981-13-6412-9_52

535

of titanium is that it has a high strength, low-density results in less weight. It can withstand very high temperatures also. It is used as alloying agent with many materials like molybdenum, aluminum iron, etc. They are widely used in aerospace industry specially for making spacecraft, aircraft, missiles, naval ships, armor plating; condensers of power plants use pipes made of titanium for their resistance to corrosion. It is a nontoxic metal, that's why it is used in medical operations also. Electro discharge machine is one of the most significant and remarkable technologies. Both the tool and electrolyte when placed in a dielectric medium and a very high electric potential are applied, a high impulse electric spark is generated. The spark dissipates a huge amount of heat (8000–12000 °C) as a result melts the workpiece. Then it vaporizes in the discharge column due to ionization and a flushing pressure imparted on the fluid by the pumped dielectric. The process consumes a lot of time so it is not an industrially suitable process.

Eminent researchers like Kao [1] have studied machining by EDM in detail and have conclusive evidence to prove their findings. Using Taguchi method, he has studied multiple performance relationships on Ti–6Al–4V alloy. He has then verified the most suitable parameters for getting lower tool wear, higher metal removal, and good surface finish through his confirmation experiment. An improvement of 15% in wear ratio, 12% in metal removal rate (MRR), and 19% in surface roughness (SR) was demonstrated. Jahrah et al. [2] from his investigation formulated the fact that tool wear was absent when AISI H13 tool steel was subjected to EDM machining at high peak current, high pulse on time, and low pulse off time using copper electrode. His other conclusion includes excellent surface finish at low peak current, pulse on time, and pulse of time and higher level of material removal at high I_p , moderate T_{on} , and low T_{off} . Both MRR and surface roughness were affected by I_p .

Chalisgaonkar and Kumar [3] during his experiment undertook development of multi-response optimization technique by customary utility method in association with concept of weight assessment. From the experiment, he found out that all the parameters taken in the experiment were statistically significant for the effect produced in overall utility index. Verma and Sahu [4] optimized the process parameters of a die sinking EDM using full factorial technique. He found out that MRR was directly proportional to applied current and voltage. Routara and Mishra [5] found various combinations of operation specifications are important in EDM to get increased metal removal rate and low electrode wear for EN-24 alloy steel. Signal to noise ratio and investigation of difference are used to interpret and understand the impact of input specifications on metal removal rate and tool wear rate.

Rahul et al. [6] in his experiment with Inconel 718 on EDM found that machining performances influenced by V_g mostly. He performed the investigation with the help of satisfaction function analysis. Rahul et al. [7] in his experiment with superalloy Inconel 718 on EDM, various responses such as MRR, EWR, Ra, etc took and found that I_p has most significance and P_{flush} has least significance.

In this present work, multilevel process parameter optimization of titanium grade-4 (3.7065, R50700) alloy is done when machined with copper tool in EDM. Here, peak current, voltage, and pulse on time are taken as the variable parameters and MRR, TWR, and R_a as machine responses.

2 Experimentation

Titanium grade-4 (3.7065, R50700) circular workpiece having diameter 15 mm has used as workpiece. The chemical properties (wt%) of titanium grade-4 are shown in Table 1. The snapshot of EDMed titanium grade-4 has been furnished in Fig. 1. Copper has been used as tool electrode (Fig. 2). The experiments have been carried out on EDM (Model: Smart ZNC, Electronica Machine Tools Ltd, Pune, India) setup (Fig. 3). 125 cc SAE-40 grade oil is used as dielectric fluid. The viscosity of EDM oil is 2.16 cs at 38 °C. Polarity of workpiece has been kept positive. Experiments have been carried out using three controllable process parameters (gap voltage, peak current, pulse on time) each varied at three different levels shown in Table 2. The design of experiment has been planned as per 3-factor-3-level L_9 orthogonal array (OA). The machining duration for each experimental run has been kept constant (30 min). The machining responses viz. roughness average (R_a), metal removal rate (MRR), and tool wear rate (TWR) have been measured for each experimental run. For all the experiments, flushing fluid pressure is taken as 8 kg/cm².

A brief explanation of the responses is given below.

2.1 Material Removal Rate (MRR)

It is defined as the quantity of metal displaced from the job under a specific time. Unit was taken as mm³/min.

$$\text{MRR} = \frac{(\text{weight before machining} - \text{weight after machining})}{\text{time taken}}$$

Table 1 Chemical composition of titanium grade-4 alloy

Elements	Carbon	Iron	Hydrogen	Nitrogen	Oxygen	Titanium
Weight %	0.1	0.5	0.015	0.05	0.335	99

Fig. 1 Titanium



Fig. 2 Copper tool



Fig. 3 EDM



Table 2 Machining control parameters

Parameters	Unit	Notation	Levels of variation		
			1	2	3
Peak current	I_p	A	19	21	23
Pulse on time	T_{on}	B	200	300	400
Gap voltage	V_g	C	55	65	75

2.2 Tool Wear Rate (TWR)

It is defined as the quantity of metal displaced from the tool under a specific time. Unit was taken as mm^3/min .

$$\text{TWR} = \frac{(\text{weight before machining} - \text{weight after machining})}{\text{time taken}}$$

2.3 Surface Roughness (R_a)

Comprising of irregularities on the surface that occur due to the mechanism of the material removal process. ‘Taylor Hobson Surface Finish Tester’ was used for surface roughness measurement. Unit was taken as μm . The values of MRR, TWR, and SR are shown with L_9 orthogonal array in Table 3.

Table 3 Design of experiment (L_9 OA) and collected experimental data

Sl. No	L_9 OA (DOE)			Experimental data		
	A	B	C	MRR ($\text{mm}^3 \text{min}^{-1}$)	TWR ($\text{mm}^3 \text{min}^{-1}$)	R_a (μm)
1	1	1	1	0.48120	0.07209	3.7866
2	1	2	2	0.51022	0.04299	4.3533
3	1	3	3	0.40975	0.15580	4.7866
4	2	1	2	1.05250	0.23002	4.7933
5	2	2	3	1.28450	3.55500	5.1466
6	2	3	1	1.36880	0.61040	6.0666
7	3	1	3	1.25120	0.22040	5.2266
8	3	2	1	1.70280	0.26400	6.9000
9	3	3	2	1.99895	0.053125	7.1000

3 Methodology

3.1 Satisfaction Function

Satisfaction function analysis (SFA) is one of the most widely used methods in industry. Martel and Aouni used the concept of the satisfaction functions as a strong tool to combine various quality characteristics simultaneously.

In this paper, satisfaction function approach is used to convert the experiment responses such as MRR, TWR, and SR to satisfaction values between 0 and 1, which does not contain their units. Then, the total distance from the ideal point (where the satisfaction value is 1) of all responses is calculated and used as a single criterion for comparison of all experiments. After getting all the nine distance functions, Taguchi approach is used to determine the optimal parameters in Minitab software.

$$D_T = \left[\sum_{i=1}^n (1 - s_i)^2 \right] \tag{1}$$

Figure 4a, b shows two cases of getting best satisfaction.

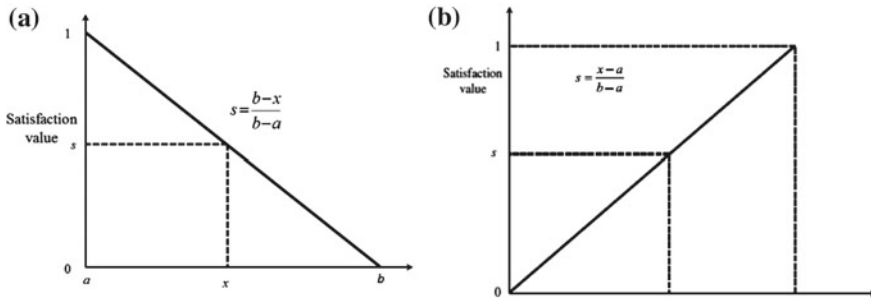


Fig. 4 **a** Characteristic graph where the lowest value gives the optimum satisfaction. **b** Characteristic graph where the highest value gives the optimum satisfaction

4 Data Analysis: Results and Discussions

In this paper, the aim is to find the optimum parameters where value of MRR is maximum and value of TWR and SR is minimum. When the TWR or SR is lowest, then it gives the optimum satisfaction, and when it is highest it provides zero satisfaction. Similarly, when the MRR is lowest, it gives zero satisfaction, and when it is highest, it gives the optimum satisfaction. Then optimisation of distance function is done using Taguchi approach. As D_T is wished to be lowest; so, lower-is-better (LB) characteristic is used for S/N ratio calculation shown in Table 4. The response table for means of D_T is shown in Table 5. The main effects plot for S/N ratios [$A_3 B_1 C_2$] is shown in Fig. 5.

Table 4 Computed satisfaction values

Serial no.	Satisfaction value			Total distance (D_T)	Corresponding S/N ratio (dB)	Predicted S/N ratio (dB)
	MRR (S_1)	EWR (S_2)	R_a (S_3)			
1	0.04	0.99	1.00	0.9550	0.3994	3.36170
2	0.06	1.00	0.82	0.9552	0.3979	
3	0.00	0.96	0.69	1.0450	-0.382	
4	0.40	0.94	0.69	0.6706	3.1699	
5	0.55	0.00	0.58	1.1707	-1.368	
6	0.60	0.83	0.31	0.8104	1.8254	
7	0.52	0.94	0.56	0.6424	3.2940	
8	0.81	0.93	0.06	0.9600	0.3544	
9	1.00	0.99	0.00	1.0000	-0.0009	

Table 5 Response table for means of D_T

Level	A	B	C
1	0.9851	0.7561	0.9085
2	0.8839	1.0286	0.8753
3	0.8675	0.9518	0.9527
Delta	0.1176	0.2726	0.0774
Rank	2	1	3

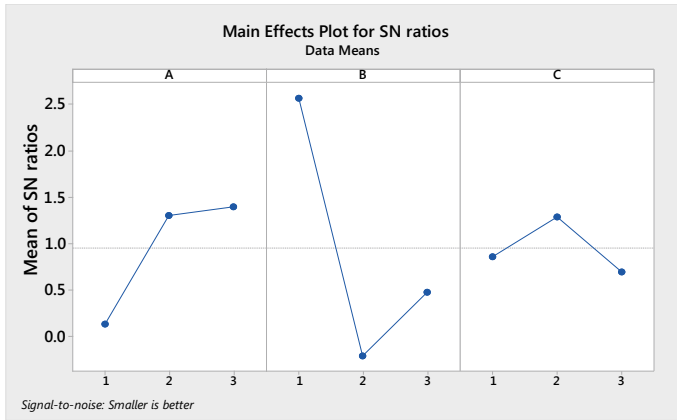


Fig. 5 Main effects plot for S/N ratios [$A_3 B_1 C_2$]

5 Conclusion

From the above research work, we concluded the points that are given below.

- The satisfaction function and distance-based approach (D_T) in combination with Taguchi approach used here to find a suitable combination of process parameters such as gap voltage, peak current, and pulse on time to increase MRR but to decrease TWR and SR simultaneously.
- The optimum process parameters found out as ($A_3 B_1 C_2$), i.e., $I_p = 23$ A, $T_{on} = 200 \mu\text{s}$, and $V_g = 65$ V.
- Mean response table (mean S/N ratio of D_T) indicates that pulse on time (T_{on}) has the highest significance on influencing the machining performances.

References

1. Kao JY (2010) Optimization of the EDM parameters on machining Ti-6Al-4V with multiple quality characteristics. *Int J Adv Manuf Technol* 47(2010):395-402
2. Jaharah AG, Liang CG, Wahid SZ (2008) Performance of copper electrode in EDM of AISI H13 harden steel. *Int J Mech Mater Des* 3(1):25-29

3. Chalisgaonkar R, Kumar J (2015) Multi response optimization and modelling of trim cut WEDM operation of commercially pure titanium (CPTi) considering multiple user's preferences. *Eng Sci Technol* 18:125–134
4. Verma V, Sahu R (2017) Process parameter optimization of die-sinking EDM on Titanium Grade-V alloy using full factorial design. *Mater Today Proc* 4:1893–1899
5. Routara BC, Mishra BP (2017) An experimental investigation and optimization in EDM of EN-24 alloy steel using Taguchi method and grey relational analysis. *Mater Today Proc* 4:7438–7447
6. Rahul, Datta S, Biswal BB, Mahapatra SS (2018) Optimization of electro-discharge machining responses of super alloy Inconel 718: use of satisfaction function approach combined with Taguchi philosophy. *Mater Today Proc* 5:4376–4383
7. Rahul, Srivastava A, Mishra DK, Chatterjee S, Datta S (2018) Multi-response optimization during electro-discharge machining of super alloy Inconel 718: application of PCA-TOPSIS. *Mater Today Proc* 5:4269–4276

Self-Healing Al 6061 Alloy Reinforced with Low Melting Point Alloys



Nitin Kumar Gupta , G. D. Thakre  and Manoj Kumar 

Abstract Self-healing materials can recover/repair damage automatically and autonomously with or without the external intervention. In recent times, many researchers have developed competitive technologies to achieve self-healing properties of materials. This paper presents a methodology to develop self-healing concept in metal matrix composite. Aluminium 6061 has been utilized as the base metal, and a low melting point metal filled into it to develop samples using the injection moulding method. Sand casting has also been used to cast the required sample of Al 6061. To demonstrate self-healing behaviour in the developed composite, an artificial crack developed in the sample using a lathe and drill machines. It has been observed that the low melting point alloy gets filled in the crack with heat. This shows the partially self-healing behaviour of composite. SEM and microstructural test has been performed to find out the topological and morphological characteristics of the matrix.

Keywords Self-healing · Al 6061 · Sand casting · Application of injection moulding · Low melting point alloys

1 Introduction

Self-healing can be defined as the ability of a material to heal (recover/repair) damages automatically and autonomously, that is, without any external intervention. Many common terms such as self-repairing, autonomic-healing, and autonomic-repairing are used to define the self-healing property in materials [1]. Self-healing materials prevent failure and extend the life of critical structure. Thus, the mechanism for self-healing can be divided into two categories: (i) extrinsic (ii) intrinsic healing. Self-healing means material can repair its damage partially or up to some extent [2].

N. K. Gupta (✉) · M. Kumar
DIT University, Dehradun, India
e-mail: nitin.gupta@dituniversity.edu.in

G. D. Thakre
CSIR-IIP, Dehradun, India

© Springer Nature Singapore Pte Ltd. 2019
K. Shanker et al. (eds.), *Advances in Industrial and Production Engineering*, Lecture Notes in Mechanical Engineering, https://doi.org/10.1007/978-981-13-6412-9_53

To understand the concept of self-healing materials, one can imagine the example of live plants and live skin. They all are susceptible to self-repair by triggering some form of chemicals from inside. Many researchers, scientists are trying to mimic this concept of the living organisms into the engineering materials, so that they may enhance the properties and utilization of the materials [3–6]. Engineering materials are mainly classified into three major categories' like plastics, ceramics and metals. Metals are one of the most important materials used in engineering application, which need improvements in terms of chemical as well as mechanical properties. There are many practical applications, where the concept of self-healing can improve mechanical properties and life of the materials like in structural, automobiles and aerospace and also application in deep-sea oil wells that operate under high pressure [4, 7, 8]. Self-healing materials are designed to mimic human skin, which can heal itself as needed. When these materials are cracked or damaged, a healing agent can be triggered to flow into the damaged area to heal the damage, much like a cut in human skin triggers blood flow to promote healing. It can be observed that engineering systems are becoming more sophisticated and taking on more of the characteristics of biological system [4, 9–12]. Now a day while designing any machine or materials the first question which is arising in the mind is? What will be the life of that material?

Many of the researchers around the globe are working on investigating the self-healing behaviour of composite. The composite has some specific properties like lightweight, chemical stability in any environment, load carrying capability and also it can sustain harsh environment. So, the importance of composite in engineering is very focused and specific. But exposed to harsh environment, sometimes unwanted load, temperature or stress easily lead to the formation of voids, cracks during the service life is very serious issues. So, to improve the life and usability of materials, a bio-mimic concept self-healing coined [13, 7].

The different types of materials such as plastics, polymers, ceramics and metal have their own self-healing mechanism [5, 14–18]. Metals are the most important materials available in all engineering materials. They exhibit very specific properties like high tensile strength, wear resistance, durability and compatible with very harsh environmental. But similar to polymer and ceramics, it also has problems like wear resistance, corrosive resistance, lack of mechanical properties, etc., which need more analysis to enhanced properties of materials for specific application [6, 18].

So, engineers and researcher are needed to analyse the healing mechanism from the nature. But all the mechanisms cannot be directly copied to develop new materials. To develop self-healing material, one needs to think beyond the limits of materials science.

2 Concept of Sample Design

Self-healing metal composite has been developed, for using Al6061 as base metal. In order to incorporate self-healing characteristics, a low melting point alloy of 60Pb–40Sn has been filled into the sample using injection moulding methods. Sample

Fig. 1 Hydraulic operated machine setup develops for filling material into the hole

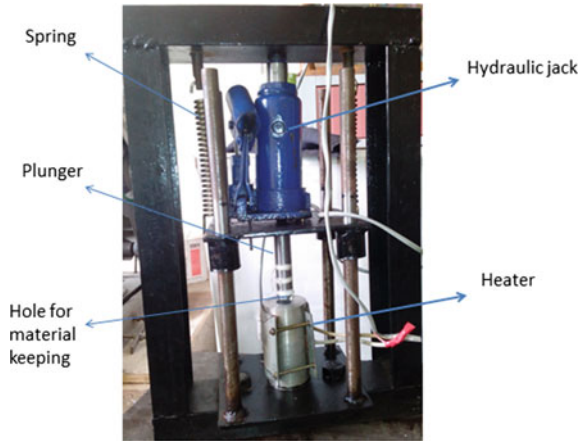
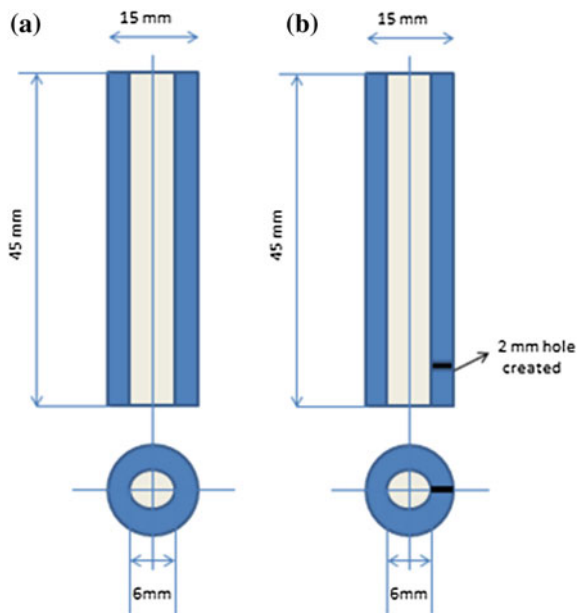


Fig. 2 Test sample of self-healing materials developed **a** without crack and **b** with artificial crack



of Al6061 has been developed through the sand casting process. Figure 1 shows the small injection moulding machine used for the said purpose.

Figure 2 shows the sample drawing for the said purpose. Different pattern has been developed to fabricate the samples, while filling low melting point alloys into the sample pressure injection moulding method has been utilized.

2.1 Sample Fabrication

The focus of present experimental work is to demonstrate the self-healing behaviour in cast Al6061 reinforcement with Pb40Sn solder materials. The solder material has a melting point of 238 °C. A cylinder of Al6061 was cast through the sand casting process. Thereafter 6 mm artificial hole was created using drill machine and then filled with solder material. Hydraulic operated pressure filling machine was used to fill the material into the hole. The sample was cut into 45 mm long and has 15 mm diameter to demonstrate the effect of gravity on flow of self-healing materials. The procedure adopted in [9] has been followed in the present study. The sample was kept in preheated fully temperature controlled furnace at 200–240 °C for 5–7 min. The sample was then held up for 20–25 min in preheated furnace. Then, the sample was allowed to slowly normalize in the furnace.

This has been observed from the above said procedure that the low melting point alloys have been partially filled the 2 mm hole under temperature. To investigate the internal flow of low melting point alloy into the artificially created 2 mm hole, the sample was cut into the piece at a point of 2 mm hole, in such a way that the flow of material due to gravity could be observed. Sectioned samples were polished and etched to investigate the microstructure. NaOH solution was used for etching.

Figure 3i shows the sample of Al6061 without filling of low melting point alloys and with low melting point alloys. Sample was put towards the gravity to show the flow of the low melting point alloy in 2 mm drill hole. Figure 3ii shows the artificial crack has been drilled through drill machine. Figure 3iii shows the damaged and healed self-healing composite, in that sample is kept towards the gravity into furnace for a period of 20–25 min and leaving the sample for cooling in furnace. It is observed that the 2 mm hole was healed through low melting point alloys.

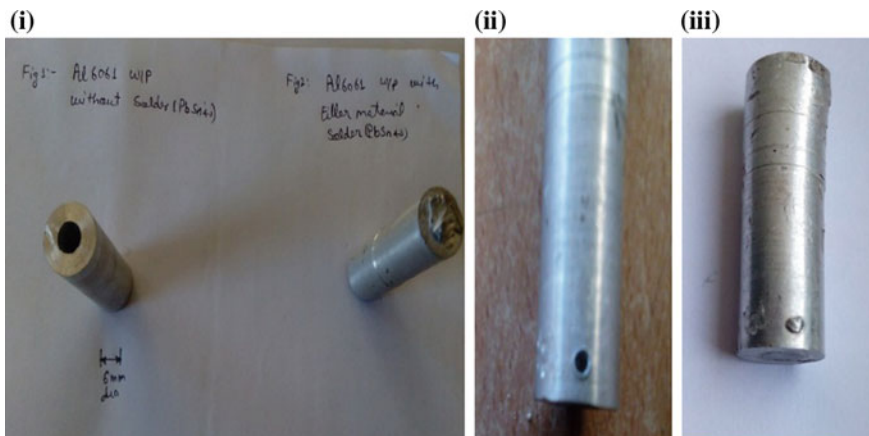


Fig. 3 i Sample cast Al6061 before filling and after filling (filling material 60Pb40Sn), ii 2 mm drilled into filled sample, iii partially healed cast Al 6061 materials

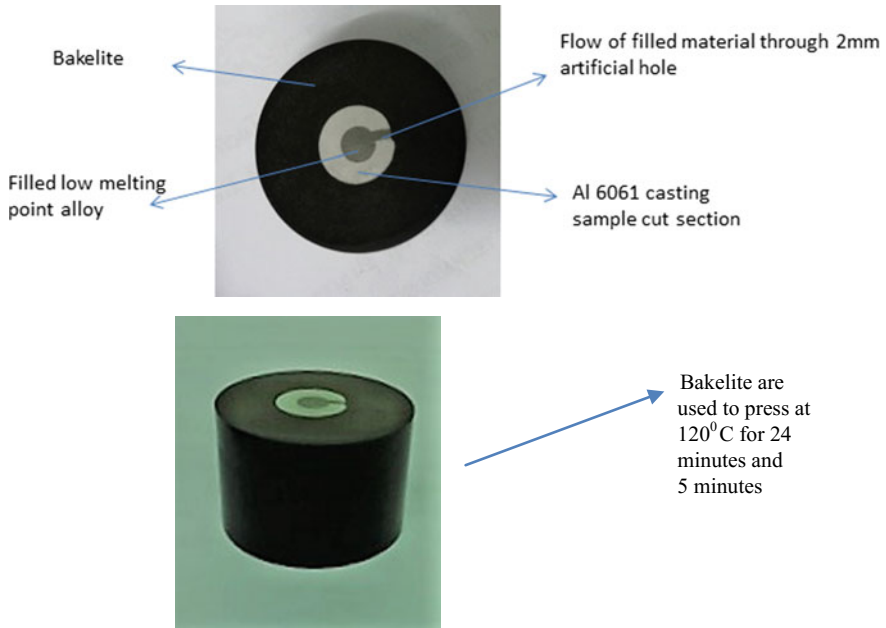


Fig. 4 Cut section of cast sample for microstructure analysis

Figure 4 shows the sample which has been developed through powder pressing machine into bakelite. Pressing of the sample done at 120°C for 24 and 5 min dwell time was also kept to be fixed, which helps to hold the sample of the various positions on the microscope.

3 Results and Discussion

To investigate the microstructure and internal flow behaviour of the self-healing materials, the developed sample was observed through a microscope. Figure 5 shows the magnified view of the low melting point alloy filled into Al 6061 and flow through a 2 mm hole under temperature. Gravity also plays an important role in it. Original sample was used in the further process of the microstructure investigation process.

Figure 6 shows the microstructure of the samples. The microstructure clearly shows that the healing of the low melting point alloys is more than 99.99% very low porosity is obtained through this process, thus very low melting points diffused and developed a good bond between the cast Al6061 and low melting point alloys. This type of process developed a barrier in the crack path in a matrix and improves the life of materials. But the point is to be noted that while filling the low melting point alloy, a void has appeared on the upper side of the solder area.

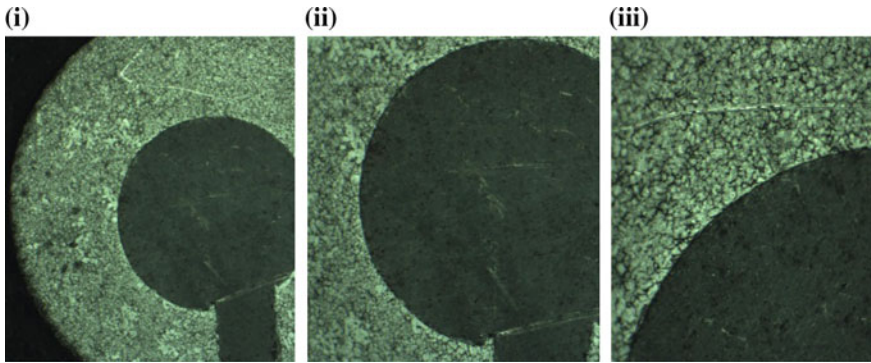


Fig. 5 Sample self-healing materials, i cut section-flow of material through hole, ii boundary layer of low melting point alloys and Al6061, iii boundary layer between low melting point and Al6061 at different magnification

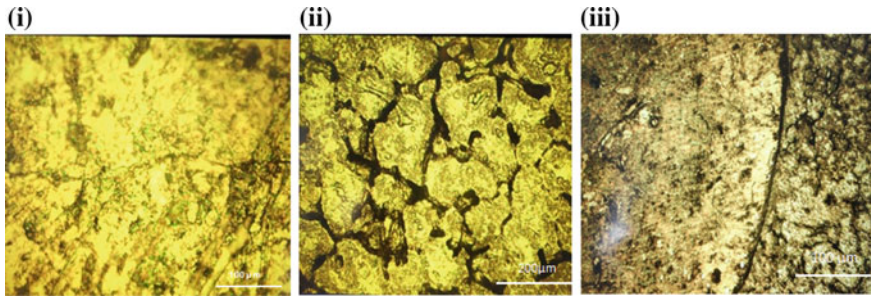


Fig. 6 Microstructure of the composite, i 100× magnification cold drawn Al6061, ii 200× cast Al6061 show brittleness, iii boundary layer where Al shows brittleness and solder material

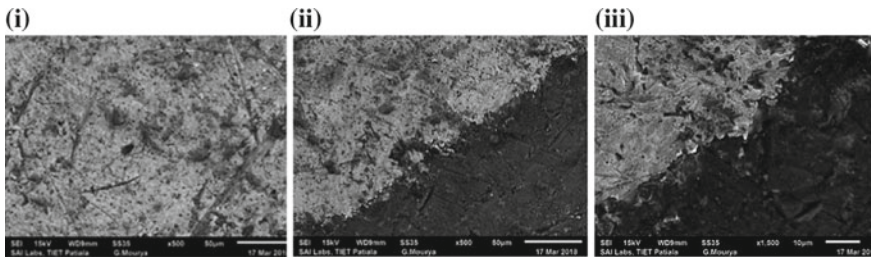


Fig. 7 SEM of the sample, i cast Al6061, ii heterogeneous nucleation between matrix and filler, iii boundary layer between Al6061 and low melting point alloy

SEM was employed to examine the surface and boundary condition of the prepared sample. Figure 7i shows the Al6061 and (ii) shows the boundary layer between Al6061 and low melting point alloy, as a low melting point alloy filled after casting and heterogeneous nucleation is formed. Figure 7iii shows the surface of low melting alloys and Al6061.

4 Conclusion

This experiment proves that by using a low melting point alloy 60Pb–40Sn, self-healing is possible. This type of mechanism will improve the life of the materials and improve some of the mechanical properties also. Gravity plays an important role to force the material into the lower cracks. In the rotating component centrifugal force through the material into crack, microstructure and SEM analysis shows the topology of developed sample. Cut sections of the sample clearly show the flow of low melting point alloy into the cavity under heat.

References

1. Ghosh SK (2008) Self-healing materials fundamentals, design strategies, and applications. ISBN: 978-3-527-31829-2, Dec 2008
2. Das R, Melchior C, Karumbaiah KM (2016) Self-healing composite for aerospace applications. In: Advanced composite materials for aerospace engineering, pp 333–364. <https://doi.org/10.1016/b978-0-08-100037-3.00011-0>
3. Gurumurthy BM, Shivaprakash MC (2016) Self-healing materials: a new era in material technology: a review. *Int J Appl Eng Res* 11(2):1373–1378. ISSN 0973-4562
4. Burgess SC Biomimetics—a review. *Proc Inst Mech Eng, Part H: J Eng Med* 223(8):919–939. <https://doi.org/10.1243/09544119JEIM561>
5. Alaneme KK, Bodurin MO (2016) Self-healing using metallic material systems—a review. 2352–9407/2016. <https://doi.org/10.1016/j.apmt.2016.11.002>
6. Martinez Lucci J, Amano RS (2009) Design and demonstration of self-healing behavior in a lead free solder alloy. In: 7th international energy conversion engineering conference 2–5 Aug 2009, Denver, Colorado AIAA2009-4514
7. Lumley R (2007) In: van der Zwaag S (ed) Self-healing materials: an alternative approach to 20 centuries of materials science, Springer series in materials science pp 219–254
8. Rohatgi PK, Afsanesh Dorri M, Schultz BF, Ferguson JB (2013) Synthesis and properties of metal matrix nano composites (MMNCS), syntactic foams, self-lubricating and self-healing metals. *The minerals, metals & materials society*, pp 1515–1524
9. Ferguson JB, Schultz BF, Rohatgi PK (2016) Self-healing metals and metal matrix composites. *JOM* 66(6). (The minerals, metals & materials society). <https://doi.org/10.1007/s11837-014-0912-4>
10. Nayak PR (1971) Random process model of rough surfaces. *Trans ASME J Basic Eng* 93:398–407
11. Lumley RN, Polmear IJ (2007) Advances in self-healing of metals. In: Proceeding of the first international conference on self-healing materials, Noordwijk aan Zee, The Netherlands, 18–20 Apr 2007

12. Guntur K, Amano RS, Lucci JM, Rohatgi PK (2009) Self-healing technology for compressor and turbine blades. In: Proceedings of ASME turbo expo 2009: power for land, sea and air GT 2009 Orlando, Florida, USA
13. Oladijo OP, Bodunrin MO, Sobiyi K, Maledi NB, Alaneme K Investigating the self-healing behavior of underaged and 60Sn-40Pb alloy reinforced aluminum hybrid composites. *Thin Solid Films*. <https://doi.org/10.1016/j.tsf.2016.08.071>
14. Martinez Lucci J, Amano RS, Rohtagi PK (2008) Self-healing in an aluminum alloy reinforced with microtubes. In: Proceeding of 3rd energy technology international conference ENIC2008
15. Wang Y, Pham DT, Zhang Z, Li J Sustainable self healing at ultra-low temperature in structural composites incorporating hollow vessels and heating elements. *Roy Soc Open Sci* 3:160488 www.rsos.royalsocietypublishing.org
16. Riefsnyder KL, Schulte K, Duke JC (1983) Long term failure behavior of composite materials, vol 813, pp 136–159. ASTM Special Technical Publications
17. Wool RP, O'Connor KM (1981) A theory of crack healing in polymers. *J Appl Phys* 52:5953–5963
18. Quemard L, Rebillat (2007) Self-healing mechanism of a SiC fiber reinforcement multi-layered ceramic matrix composite in high pressure steam environment. *J Eur Ceram Soc* 27(4):2085–2094, Dec 2007

A Novel Approach in Developing Aluminum Hybrid Green Metal Matrix Composite Material Using Waste Eggshells, Cow Dung Ash, Snail Shell Ash and Boron Carbide as Reinforcements



Soutrik Bose , Anand Pandey , Ashmik Mondal  and Pritam Mondal 

Abstract Global development of aluminum metal matrix composite (AMC) in research, industries and defense with reduced weight, enhanced strength and low cost leads to the establishment of a new hybrid green metal matrix composite using aluminum (Al) alloy as base material with silicon carbide (SiC) and reinforcing it with waste carbonized eggshells (WCE), cow dung ash (CDA), snail shell ash (SSA) and boron carbide (B_4C) by altering the different reinforcement weights using stir casting mechanism. Experimental results showed increased hardness, tensile strength and fatigue strength, while decrease in fracture toughness, ductility and corrosion rate which improved by heat treatment. The optimum values obtained were 7.5 wt% of WCE and SiC + SSA; preheat temperature of WCE and SiC was 300 °C and 500 °C, respectively. The stability and non-reactivity factors of the reinforcements were stringently considered at optimum temperature. Mono-ethylene glycol (MEG) in aqueous solution was used for experimenting different samples of AMC with varying proportion of SSA. The hardness of the Al alloy incremented to maximum when 7.5 wt% SiC + 7.5 wt% SSA was added and decremented when 10 wt% SiC + 10 wt% SSA was used as reinforcements. The results inferred that using WCE as reinforcement with the Al matrix gave better tribomechanical properties at a much cheaper rate than uncarbonized eggshells (ES) and SiC + SSA. The overall objective was to introduce a novel hybrid AMC by recycling and reutilizing wastes.

Keywords Hybrid green metal matrix composites · Corrosion rate · Waste carbonized eggshells · Wettability · Porosity

Nomenclature

A	Exposed area (cm^2)
CR	Corrosion rate
K	Constant

S. Bose (✉) · A. Pandey · A. Mondal · P. Mondal
MCKV Institute of Engineering, 243 G.T. Road (N), Liluah, Howrah 711204, West Bengal, India
e-mail: soutrikboseju@gmail.com

P	Percent porosity
t	Exposure time (h)
W	Weight loss (g)
ρ	Alloy density (g/cm^3)
ρ_{exp}	Experimental density
ρ_{theo}	Theoretical density
BHN	Brinell hardness number

1 Introduction

Different public sectors use AMC [1, 2] for their improved physical and mechanical properties. Recent improvement includes stir casting by Daoud et al. [3], powder metallurgy [4, 5], atomization through a spray nozzle and codeposition by Wu et al. [6], plasma spraying by Tiwari et al. [7], squeeze casting by Kim et al. [8] and compo-casting [1, 9]. In AMC, the ceramic reinforcements are generally Al_2O_3 , TiB_2 , TiO_2 , SiC , TiC , B_4C , etc. [1, 5]. In this paper, however, we have used uncarbonized eggshells (ES), waste carbonized eggshells (WCE), snail shell ash (SSA), silicon carbide (SiC) and boron carbide (B_4C) with varying weight fractions by stir casting at squeezed pressure and optimum controlled conditions which is a novel approach. The main objective of this research is to develop a novel hybrid AMC by recycling and reutilizing the hazardous wastes using liquid casting route for mass production at cheap rate.

Improper wettability is caused by the occurrence of oxide formation and adsorbed contaminants on the molten metal surface. Therefore, adding various coatings of magnesium or calcium and by heat treatment method leads to its improvements. Strong interfacial bonds are must criteria for improved wettability. Better tribomechanical characteristics are obtained with a higher percentage of WCE than ES by Hassan and Aigbodion [10] who researched about the microstructures of ES and WCE on aluminum with copper and magnesium on the particulate composites and obtained a huge decrement in the impact energy. Deep et al. [11] analyzed aluminum silicon carbide of different weight percentages and concluded that mechanical properties increased with increased weight fractions to an optimum level. But further addition of silicon carbide would result in wear and brittle fracture and was also expensive; therefore, hybrid material reinforcements would have to be introduced, which is another objective of this research. Solidification of AMC was characterized by Kayal et al. [12] by stir casting route. Jyothi and Bharath Kumar [13] concluded better performance of cow dung ash than rice husk ash with Al–5% Si alloy. Alaneme and Olubambi [14] obtained that the rate of corrosion increased with increase in volume percentage of ashes from rice husk. Emenike [15] obtained different corrosion characteristics of Al–Mg A535 alloy composites with fly ash and found enhanced corrosion rate with increasing content of fly ash. Al alloys are softer metals and vulnerable to erosion–corrosion [16, 17] in the cooling systems of automobiles, where ethylene glycol has been used as a coolant. But Shamim et al. [18] obtained hard

intermetallic phase consisting of Al_2Si , Mg_2Si , Al_3Ti and dispersed particles of CaO as he studied the microstructures and mechanical properties of Al–Si–Mg–Ti/eggshell particulate composites and concluded better characteristics than cow dung ash, rice husk ash or fly ash. Baradeswaran and Perumal [19] obtained hybrid AMC using $\text{Al7075}/\text{Al}_2\text{O}_3/5$ wt% graphite which proved to be effective in incorporating graphite for gaining wear reduction and coefficient of friction. But the limitation was of brittle failure on further increasing wt% of graphite which needs to be optimized. Therefore, Baradeswaran et al. [20] again investigated on mechanical behavior, modeling and optimization of wear parameters of B_4C and graphite reinforced aluminum hybrid composites and found superior results.

After studying the literature review, it was mandatory to develop a novel hybrid green AMC by obtaining superior physio-mechanical properties of Al matrix/eggshells green metal matrix composite with SiC , $\text{SiC} + \text{SSA}$, CDA and B_4C . A research was conducted to examine the feasibility to produce Al matrix/WCE composites by using stir casting process. Hence, the comparison of mechanical properties like hardness, tensile strength, fatigue strength, toughness, ductility and corrosion rate of Al matrix/WCE, Al matrix/ $\text{SiC} + \text{SSA}$, Al matrix/ SiC , Al matrix/ B_4C and Al matrix/ CDA is the prime concern of this research to develop the new green hybrid AMC.

2 Experimental Setup

2.1 Material Library

The chemical composition of the Al matrix is shown in Table 1. Table 2 contains 25 different samples with varying weight percentage of the reinforcements. Photographs of powdered ES, WCE and SEM morphology are shown in Fig. 1a–f.

2.2 Composite Development

Figures 2 and 3 depict the schematic experimental setup and squeeze casting in the universal testing machine (UTM). Heating the Al matrix to a temperature of 750°C , melting in a graphite crucible furnace and cooling to about 600°C were the steps followed where the reinforcements (initially preheated to 300°C for 30 min) were

Table 1 Chemical composition of the Al matrix

Element	Si	Fe	Cu	Mn	Mg	Zn	Ti	Ni	Cr	Al
wt%	0.5–0.9	0.5	3.9–5	0.4–1.2	0.2–0.8	0.25	0.2	0.1	0.1	Balance

Table 2 Different samples fabricated by varying the weight percentage of the reinforcements

Sample No.	SiC (wt%)	Eggshells (wt%)	Sample No.	SiC (wt%)	Eggshells (wt%)	Sample No.	SiC (wt%)	Eggshells (wt%)
S1	2.5	2.5	S10	5	12.5	S19	10	10
S2	2.5	5	S11	7.5	2.5	S20	10	12.5
S3	2.5	7.5	S12	7.5	5	S21	12.5	2.5
S4	2.5	10	S13	7.5	7.5	S22	12.5	5
S5	2.5	12.5	S14	7.5	10	S23	12.5	7.5
S6	5	2.5	S15	7.5	12.5	S24	12.5	10
S7	5	5	S16	10	2.5	S25	12.5	12.5
S8	5	7.5	S17	10	5			
S9	5	10	S18	10	7.5			

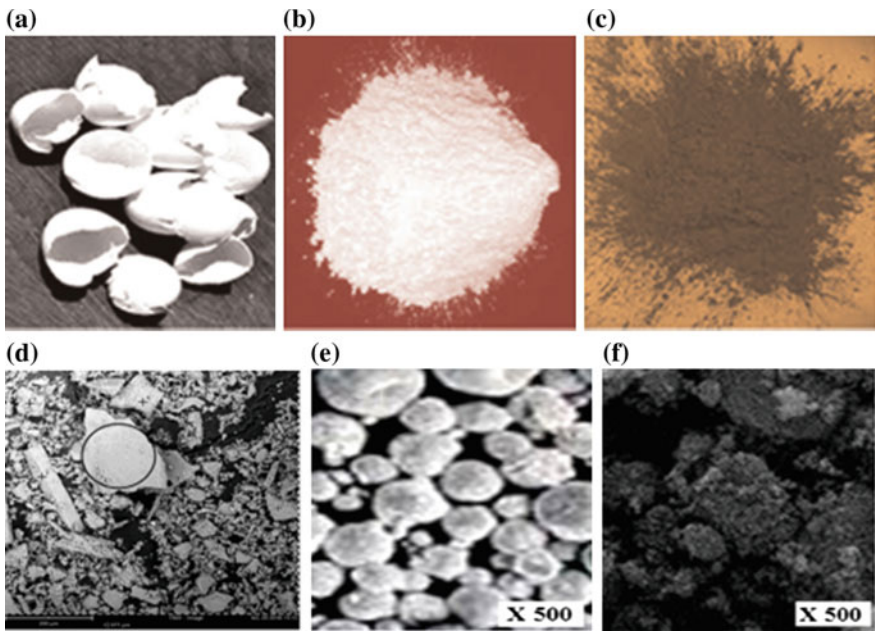


Fig. 1 Photograph of **a** eggshells, **b** ES powder, **c** WCE powder, **d** SEM morphology of SiC + SSA, **e** SEM morphology of ES, **f** SEM morphology of WCE

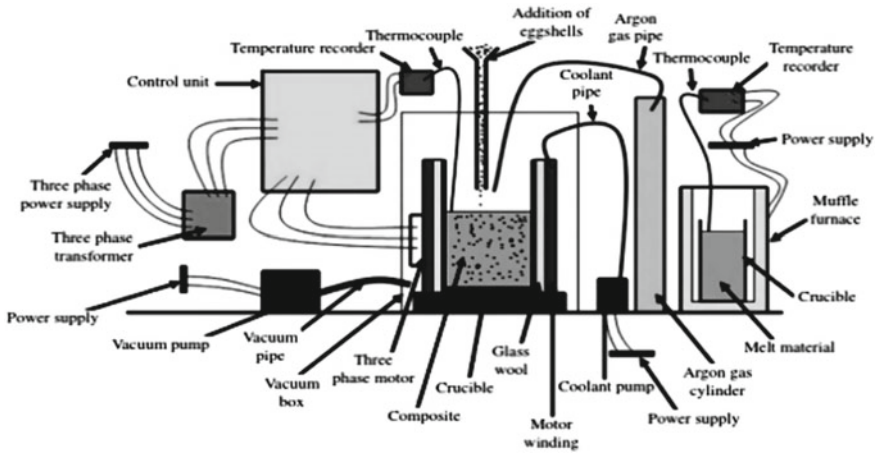
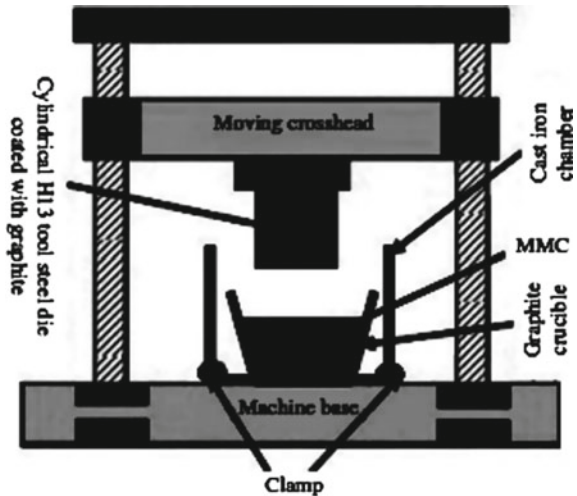


Fig. 2 Stir casting experimental setup

Fig. 3 Squeeze casting on UTM



added to eliminate dampness and to improve wettability and stirred manually for 5 min. The composite slurry was then superheated to 780 °C, and a mechanical stirrer was used to stir at a speed of 300 rpm for 10 min and a current of 12 A. The mixture varying the wt% (0, 2.5, 5, 7.5, 10, 12.5 and 15) of reinforcements before and after heat treatment was then solidified into the mold.

2.3 Porosity Analysis

Archimedes principle was used to determine the experimental densities of the composites. Material properties are highly influenced by porosity and compactness. Porosity is calculated as the incremental ratio of theoretical and experimental density of the composites as obtained by Dwivedi et al. [21].

$$P = 1 - \frac{\rho_{\text{exp}}}{\rho_{\text{theo}}} \times 100\% \quad (1)$$

2.4 Corrosion Test

The corrosion test of all fabricated AMC was engrossed in high alkaline bathtub for 120 h at room temperature in 3.5 wt% NaCl solution. Uniform corrosion was assumed throughout the composite surface and corrosion rate was calculated, where $K = 8.75 \times 10^4$, $A = 9 \text{ cm}^2$, $t = 120 \text{ h}$ as observed by Dwivedi et al. [21].

$$\text{CR} = \frac{W \times K}{\rho \times A \times t} \quad (2)$$

3 Results and Discussion

3.1 Evaluation of Mechanical Properties

In this research, the hardness of AMC increased up to 12.5 wt% of ES, and WCE particles 7.5 wt% of SiC + SSA with the Al matrix alloy. Hardness, when compared, reached to nearly 200 BHN with $\text{Al}_2\text{O}_3 + \text{Gr}$ by Mohanavel et al. [23], to 115 BHN when reinforced by B_4C by Kumar et al. [22], to 87.1 BHN when reinforced by SiC by Deep et al. [11] and to 68.2 BHN when reinforced by LM6/SiC by Kayal et al. [12] at 15 wt%. The hardness values increased from 60 BHN at 0 wt% to 101 BHN at 12.5 wt% for ES and 113 BHN at 12.5 wt% for WCE in this present experimental research. It was compared with Aribo et al. [17] which obtained as 61 BHN at 0 wt% to 110 BHN at 7.5 wt% of SiC + SSA; however, increase in wt% of SSA beyond 7.5 wt% resulted in decrease in hardness owing to a constant level. The increment was because of the existence of brittle phases of the eggshell particles in the Al alloy. Figure 4a represents a decrease in hardness beyond 12.5 wt% of reinforcements which might be due to the air entrapment indicating larger pore formation resulting in a decrease in the mechanical properties. However, when compared with results obtained by Jyothi and Bharath Kumar [13], hardness reached to a maximum about 64 BHN at 2.5 wt% on addition of CDA with the Al matrix and then decreased gradually. The

hardness of WCE and ES was improved to 118 and 112 BHN, respectively, after heat treatment.

Figure 4b indicates improvement in tensile strength up to 12.5 wt% in the Al alloy. Tensile strength improved from 185 MPa at 0 wt% to 252 and 270 MPa for ES and WCE, respectively, because uniform eggshell particles were distributed in the Al alloy matrix and then decreased due to weak particles–matrix interaction. This meager particle distribution reduced the particles–matrix interaction and resulted in decreased tensile strength. After the heat treatment, tensile strength of ES and WCE was further improved to 264 and 273 MPa due to strengthening, following a diminution in composite grain size. A high dislocation density was generated due to decrease in the residual stress. It is compared with that obtained by Mohanavel et al. [23] where increase in wt% of alumina (Al_2O_3) and graphite (Gr) increased the tensile strength up to 205 MPa and then decreased, but was lesser than ES and WCE at the same volume fraction and SiC reinforcements addition. Tensile strength increased with the increase in reinforcements to 167 MPa by Deep et al. [11], but with the addition of Al with B_4C by Kumar et al. [22] tensile strength increased to the maximum value of 153 MPa at 2.5 wt% and then decreased resulting in less ductility than with eggshell reinforcements.

Figure 4c, d illustrates the comparative analysis of mechanical properties for both ES and WCE of 25 samples on varying the different weight percentage of reinforcements. The toughness decreased with increase in the percent eggshell particles addition. The brittleness reduced the toughness and ductility of the composites, while using Al_2O_3 with Al matrix resulted in lowest toughness and thus, brittle failure. S3 proved to be the best sample (2.5 wt% of SiC + 7.5 wt% of ES/WCE) after comparing all the 25 samples where the optimum conditions were satisfied. The optimum value of tensile strength of ES is 274 MPa and of WCE is 295 MPa; fatigue strength of ES is 135 MPa and WCE is 151 MPa, where corrosion rate and porosity are the least.

3.2 Microstructural Analysis

Figure 5a, b displays the microstructures of Al matrix + 12.5 wt% ES and WCE, respectively, indicating a better behavior in terms of porosity of WCE reinforcements as it can react easily to atmosphere at high temperature resulting in good wettability. Figure 5c, d depicts the interfacial reaction layer of Al matrix + 12.5 wt% ES and WCE, respectively, which inferred excellent wettability of WCE.

3.3 Density and Porosity Analysis

Density of Al matrix/12.5 wt% WCE = $0.875 \times \text{density of Al matrix} + 0.125 \times \text{density of eggshell} = 0.875 \times 2.8 + 0.125 \times 2 = 2.7 \text{ g/cm}^3$ (rule of mixture). Figure 4e, f shows the percentage change in the density of composites and calculation

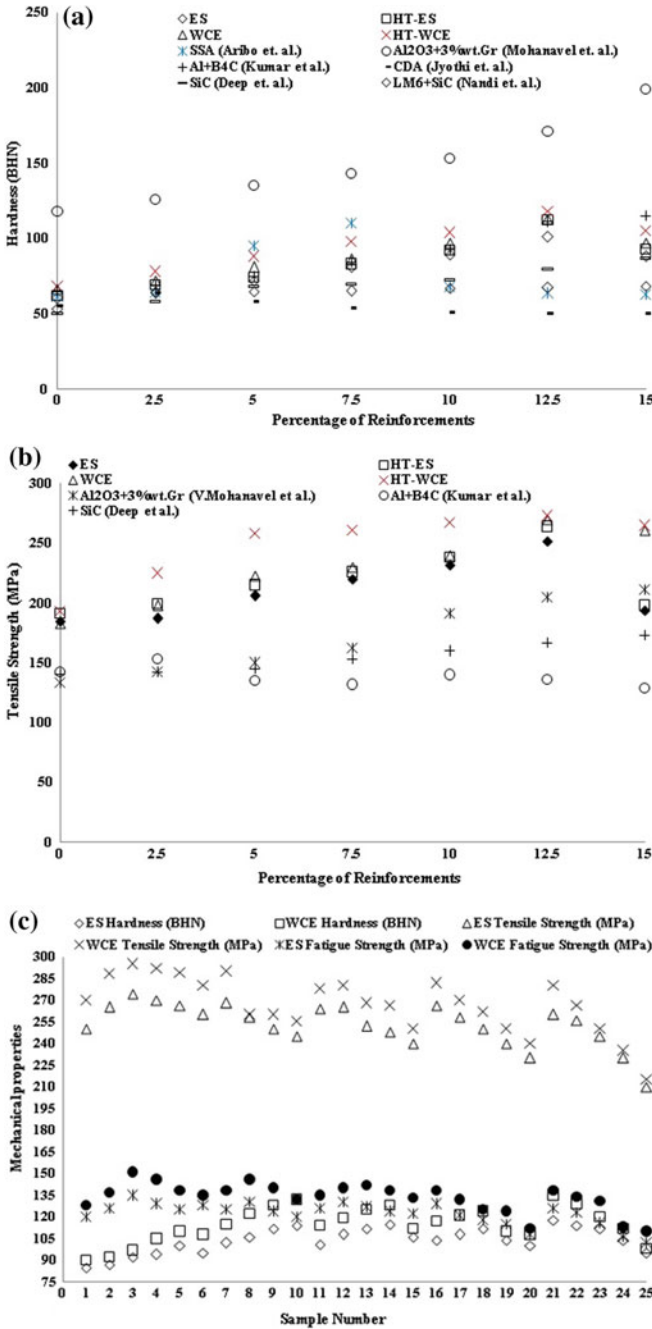


Fig. 4 Mechanical properties of Al matrix with percentage of reinforcements: **a** hardness, **b** tensile strength, **c** comparative analysis of hardness, tensile strength and fatigue strength, **d** toughness and corrosion rate, **e** porosity analysis, **f** % porosity, **g** corrosion rate

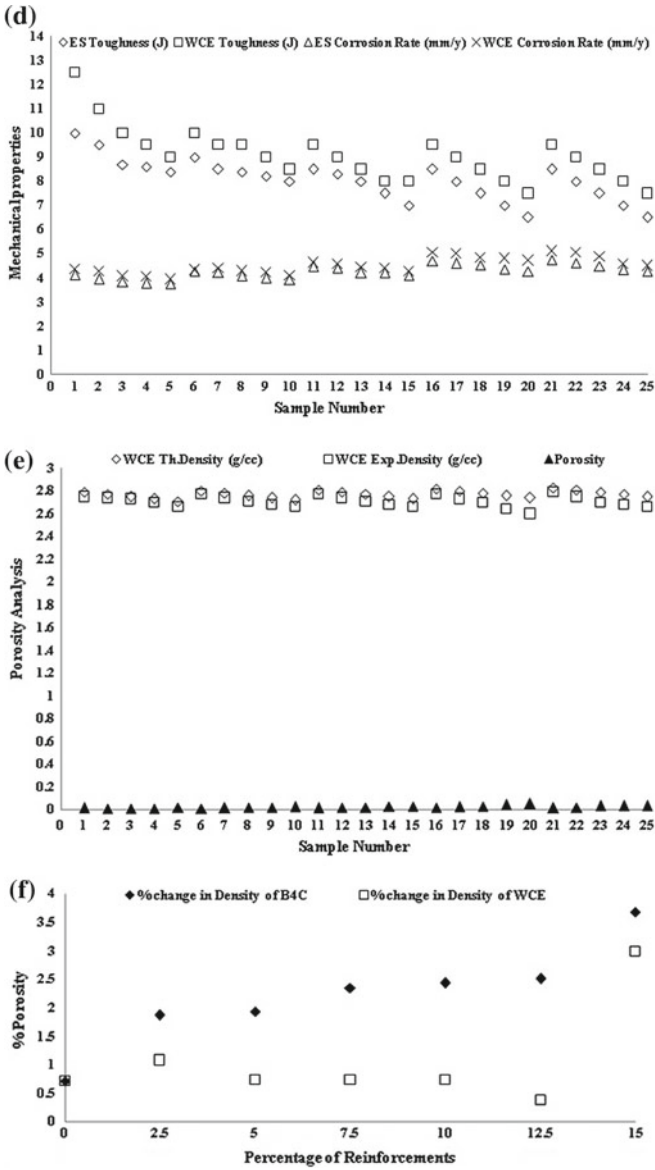


Fig. 4 (continued)

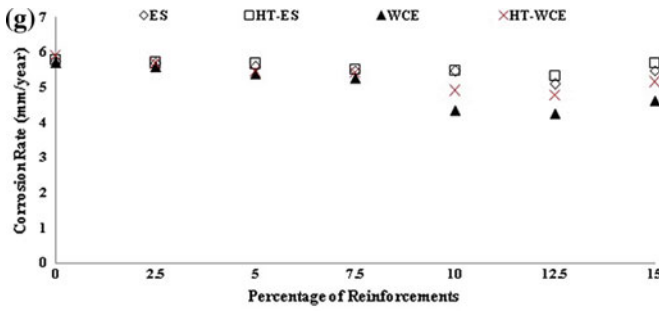


Fig. 4 (continued)

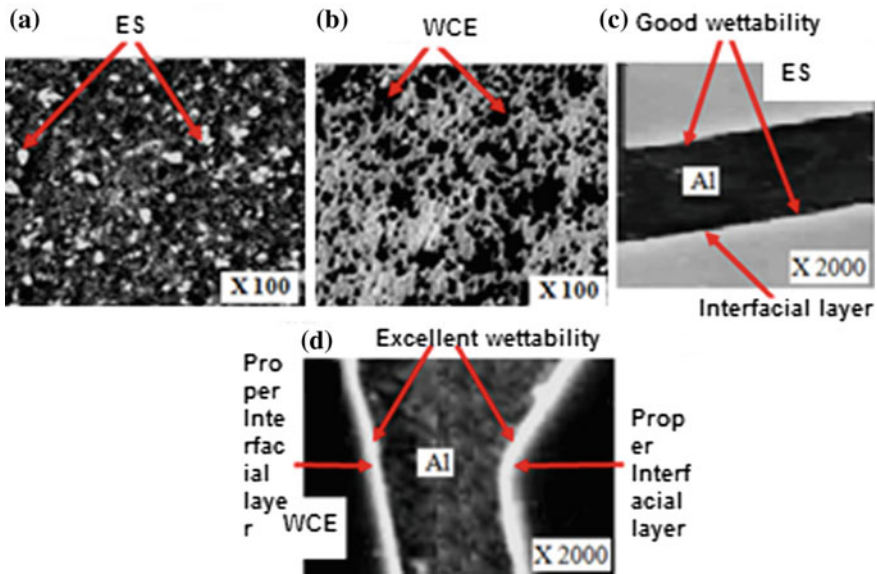


Fig. 5 Microstructure picture of a 12.5 wt% ES, b 12.5 wt% WCE and interfacial layer of c 12.5 wt% ES, d 12.5 wt% WCE

of porosity. Experimental density was obtained by Archimedes principle taking correct readings of mass and volume. Experimental density of composite = mass of composite/volume.

Porosity of Al matrix/12.5 wt% WCE (P) = $(1 - 2.69/2.70) \times 100 = 0.37\%$ which was found to be the best result on comparing with that of B_4C .

3.4 Corrosion Behavior

Corrosion rate and the weight of the Al alloy continuously decreased due to addition of ES and WCE powder as shown in Fig. 4g and were improved after the heat treatment process. The best result was obtained at 4.28 mm/year with WCE reinforcement at 12.5 wt%. Corrosion rate depends on several environmental factors like moisture content and the presence of other corrosive elements in the air, temperature gradient, physical and chemical stability. Less porous the composites were, lesser corrosion rate was obtained, so corrosion rate decreased till 12.5 wt% and again increased beyond 12.5 wt% because of the occurrence of certain degradation in matrix–reinforcement interfacial bonding, strength loss, weaker permeability and reduced stiffness in the hybrid matrix, thus resulting in structural instability.

4 Conclusion

Al matrix with different weight fractions of reinforcement particles like ES, WCE, SiC, SiC + SSA and B₄C was prepared using stir casting technique followed by squeeze pressure. Eggshell particles were adapted favorably for the fabrication of green Al matrix/eggshell particulate metal matrix composites as a reinforcement material, while SiC + SSA was favorable at much lower wt% and B₄C showed brittle failure at a higher reinforcement wt%, while when comparing with cow dung ash it was favorable at much lower wt%. The novel approach was to fabricate AMC with stir casting which is the easiest casting technique for mass production with fewer limitations. Precipitation kinetic was accelerated by adding B₄C particles but should be limited as brittle fracture can occur. Very few researchers fabricated AMC using SSA, so the new approach was to reutilize SSA and ES, WCE and to obtain the best experimental result. Hardness, tensile strength and fatigue strength were improved by addition of 12.5 wt% WCE, while toughness and ductility were reduced. Further, rising the wt% of reinforcements, mechanical properties (hardness, tensile strength and fatigue strength) kept on decreasing. The hardness values increased to 101 BHN at 12.5 wt% for ES and 113 BHN at 12.5 wt% for WCE, respectively. The hardness values decreased beyond 12.5 wt% on addition of eggshell particles for both WCE and ES giving optimum values. Minimum porosity was found to be 0.37% for Al matrix/12.5% carbonized eggshell particulate metal matrix composites which proved that reinforcing with WCE, Al resulted in a better composite material. Corrosion rate continuously decreased with the addition of eggshell particles in Al alloy and got improved after the heat treatment process. The mechanical properties and corrosion rate further increased, but the best result obtained was 4.28 mm/year with WCE reinforcement at 12.5 wt%.

References

1. Selvam JDR, Smart DSR, Dinaharan I (2013) Microstructure and some mechanical properties of fly ash particulate reinforced AA aluminum alloy composites prepared by compositing. *Mater Des* 49:28–34
2. Aribo S, Omotoyinbo JA, Folorunso DO (2011) High temperature mechanical properties of silicon carbide particulate reinforced cast aluminium alloy composite. *Leonardo Electron J Pract Technol* 18:9–16
3. Daoud A, Abou-Elkhair MT, Rohatgi P (2004) Wear and friction behavior of near eutectic Al–Si + ZrO₂ or WC particle composites. *Compos Sci Technol* 64:1029–1040
4. Prasad VVB, Prasad KS, Kurovillla AK, Pandey AB, Bhat BVR, Mahajan YR (1991) Composite strengthening in 6061 and Al-4Mg alloys. *J Mater Sci* 26:460–465
5. Marin E, Lekka M, Andreatta F, Fedrizzi I, Itskos G, Moutsatsou A, Koukouzas N, Kouloumbi N (2012) Electrochemical study of aluminum-fly ash composite obtained by powder metallurgy. *Mater Charact* 69:16–30
6. Wu Y, Lavemia E (1992) Prec. conference advancements in synthesis and processes. Society for advancement of material and process engineering, Toronto, M692
7. Tiwari R, Herman H, Sampath S, Gudmundsson B (1991) Plasma spray consolidation of high temperature composites. *Mater Sci Eng A* 144(1–2):127–133
8. Kim SW, Lee UJ, Han SW, Kim DK, Ogi K (2003) Heat treatment and wear characteristics of Al/SiCp composites fabricated by duplex process. *Compos Part B* 34:737–745
9. Amirkhanlou S, Rezaei MR, Niroumand B, Toroghinejad MR (2011) High-strength and highly-uniform composites produced by compositing and cold rolling processes. *Mater Des* 32:2085–2090
10. Hassan SB, Aigbodion VS (2015) Effects of eggshell on the microstructures and properties of Al-Cu-Mg/eggshell particulate composites. *J King Saud Univ Eng Sci* 27:49–56
11. Deep G, Idrisi AH, Siddiqui TU (2016) A new bio-filler for polypropylene composites. *Int J Innov Res Sci Eng Technol* 5:16720–16725
12. Kayal S, Behera R, Nandi T, Sutradhar G (2011) Solidification behavior of stir-cast Al alloy metal matrix composites. *Int J Appl Eng Res Dindigul* 2:350–359
13. Jyothi PN, Bharath Kumar BS (2015) Comparison of mechanical properties of Al-5%Si alloy reinforced with cow dung ash and rice husk ash. *Int J Latest Res Eng Technol* 1:55–58
14. Alaneme KK, Olubambi PA (2013) Corrosion and wear behavior of rice husk ash alumina reinforced Al–Mg–Si alloy matrix hybrid composites. *J Mater Res Technol* 2:188–194
15. Emenike RO (2008) Corrosion behaviour of fly ash reinforced aluminium magnesium alloy A535 composite. M.Sc. thesis, University of Saskatchewan, Canada
16. Prasad SD, Krishna RA (2011) Tribological properties of A356.2/RHA composite. *J Mater Sci Technol* 33:51–58
17. Aribo S, Barker R, Hu X, Neville A (2013) Erosion-corrosion behavior of lean duplex stainless steels in 3.5% NaCl solution. *Wear* 302:1602–1608
18. Shamim S, Singh H, Sasikumar C, Yadav DK (2017) Microstructures and mechanical properties of Al-Si-Mg-Ti/egg shell particulate composites. *Mater Today Proc* 4:2887–2892
19. Baradeswaran A, Perumal AE (2014) Study on mechanical and wear properties of Al 7075/Al₂O₃/graphite hybrid composites. *Compos Part B* 56:464–471
20. Baradeswaran A, Vettivel SC, Selvakumar N, Issac RF (2014) Experimental investigation on mechanical behaviour, modeling and optimization of wear parameters of B₄C and graphite reinforced aluminium hybrid composites. *Mater Des* 63:620–632
21. Dwivedi SP, Sharma S, Mishra RK (2016) Characterization of waste eggshells and CaCO₃ reinforced AA2014 green metal matrix composites: a green approach in the synthesis of composites. *Int J Precis Eng Manuf* 17:1383–1393
22. Kumar KCK, Raju TN, Laxmi YN (2017) Studies on Al6061-B₄C metal matrix composites fabricated by stir casting process. *SSRG Int J Mech Eng* 4:296–299
23. Mohanavel V, Rajan K, Senthil PV, Arul S (2017) Mechanical behaviour of hybrid composite (AA6351 + Al₂O₃ + Gr) fabricated by stir casting method. *Mater Today Proc* 4:3093–3101

Detection of Punch Wear in Stamping Process Using Acoustic Emission



Tushar Y. Badgujar , Rahul N. Chandore and Vijay P. Wani

Abstract Stamping process is widely used for the production of sheet metal components because of its high productivity and accuracy. The performance of stamping depends on the condition of punch and die. Variation in punch and die dimension has a significant influence on the product quality. The purpose of the present study is to identify the state of punch wear. In this paper, acoustic emission (AE) signals from the process utilized to identify the three different punch wear conditions. The recorded acoustic signals after filtering were processed using Hilbert–Huang Transform (HHT). Then, the instantaneous frequencies and amplitudes were obtained for the signal components. The Intrinsic Mode Functions (IMF) of the AE for the three punch condition were analyzed. With the increase in punch wear, the instantaneous amplitude of the signal increases while instantaneous frequency remains unaffected.

Keywords Punching process · Acoustic emission · HHT · EMD

1 Introduction

Punching is a stamping process. In this process, material removed by using a punch and die. The process parameters are first optimized for designed quality of output. Afterward, the quality of the product mostly depends on how well the optimized parameters are continued [1]. Tool wear directly affects the finish of products and causes the burr formation [2]. Hence, it becomes important to monitor the condition of the tool to have consistently good quality products [3, 4]. The offline tool condition monitoring requires halting of machine operation. Consequently, the offline tool condition monitoring process reduces the productivity. So nowadays online tool condition monitoring process is more preferred [5, 6].

T. Y. Badgujar (✉) · V. P. Wani
MET's Institute of Engineering, Nasik, India
e-mail: tybadgujar@gmail.com

T. Y. Badgujar · R. N. Chandore
Late G. N. Sapkal College of Engineering, Nasik, India

For punching process, the researchers have used vibration signal [7], acoustic emission [8], thermal imaging [9], strain signal [10], and lubricant analysis [11] to monitor the performing state of the process. Tushar et al. emphasised on condition monitoring for the performance study of the stamping process [12]. Out of all these, the acoustic signal capturing is considered most cost-effective [13]. Also, the punching process is based on shearing of material, and a significant amount of acoustic emission takes place at the time of operation [14, 15]. Hence in this study, AE of a stamping process utilized to monitor the condition of the punch [16].

Bassiuny et al. [10] used strain signal to monitor the stamping process. The strain signal captured by using strain sensor and the three different stamping conditions considered. The strain signals were analyzed by using HHT. Raja et al. [3] utilized acoustic emission to monitor the tool wear for the turning process. Sari et al. [2] used vibration signal and burr height to find the punch wear in the punching process, and it was noted that when burr height increases by 3.5% and the vibration signal rise by 15%. Jayakumar et al. [8] used the AE for online monitoring of blanking, forging, drawing, and grinding processes.

2 Objectives

- To study various signals considered significant by the researchers for condition monitor of the stamping process.
- Selection of cost-effective and easy to record signal.
- To collect AE of stamping process for the three different punch wear conditions.
- To analyze IMF concerning punch conditions.
- To compare instantaneous frequency and amplitude of the signal and identify the relation between punch wear, amplitude, and frequency.

3 Research Methodology

Following are the significant steps followed in the present research

- Three different punch conditions were identified.
- AE for punching process with new, partially worn, and severely worn punches was recorded using a microphone.
- Sound signals were decomposed into its IMFs using Empirical Mode Decomposition (EMD).
- Amplitude and frequency for each IMF were investigated using HHT.
- Marginal spectrum was constructed for the final analysis.
- Variation of instantaneous amplitude and frequency of the IMFs for a change in punch diameter was studied.

3.1 Hilbert–Huang Transform

HHT is widely used to decompose the nonstationary signal, and the acoustic signal is a nonstationary signal. HHT decomposes the acoustic multi-component signal into the mono-component signal. For the time signal $x(t)$, its HHT $y(t)$ is defined as:

$$y(t) = \frac{P}{\pi} \int_{-\infty}^{+\infty} \frac{x(\tau)}{t - \tau} d\tau \tag{1}$$

where P indicate Cauchy principal value. The HHT defines the convolution of the signal $x(t)$ with $1/t$. Therefore, HHT can recognize the local properties of $x(t)$. By using $x(t)$ and $y(t)$, we can get an analytical signal $z(t)$.

$$z(t) = x(t) + iy(t) = a(t)e^{i\varphi(t)} \tag{2}$$

$$a(t) = [x^2(t) + y^2(t)]^{1/2}, \quad \varphi(t) = \arctan(y(t)/x(t)) \tag{3}$$

where $a(t)$ represent the instantaneous amplitude of $x(t)$ and it indicate the variation of energy of $x(t)$ with respect to time, $\varphi(t)$ is an instantaneous phase of $x(t)$, $\omega(t)$ is instantaneous frequency.

$$\omega(t) = d\varphi(t)/d(t) \tag{4}$$

The recorded acoustic signal is a multi-component signal. To find the instantaneous frequency of the multi-component signal is reasonable tricky as compared to the mono-component signal. The multi-component signal decomposed into the mono-component signal using Empirical Mode Decomposition (EMD) method [17].

3.2 Empirical Mode Decomposition

The multi-component signals may have many similar modes of oscillation at a time. All oscillating modes are designated by an IMF. The IMF is defined in complete multi-component data set, the number of extrema must equal to some zero crossing, or at the most, it should vary by one. The shifting process is used to obtain IMF from given multi-component data set. First define all local maxima, subsequently, connect all local maxima by using cubic spline line, so the upper envelop get formed. Then, repeat the procedure for local minima to form lower envelop. Then, designate the mean between an upper and a lower envelope.

$$x(t) - m_1(t) = h_1(t) \tag{5}$$

To reduce the extracted signals from IMF, the shifting process is repeated many times.

$$h_1(t) - m_{11}(t) = h_{11}(t) \quad (6)$$

where $m_{11}(t)$ is the mean of upper and lower envelop $h_1(t)$. This process repeated k times.

$$h_{1(k-1)}(t) - m_{1k}(t) = h_{1k}(t) \quad (7)$$

Checking is done for zero crossing and extrema after every iteration. $c_1(t) = h_{1k}(t)$ designate the first IMF. The first IMF contains highest oscillation frequencies. The first IMF subtracted from original data, to find residue $r_1(t)$.

$$x(t) - c_1(t) = r_1(t) \quad (8)$$

The $r_1(t)$ has found from arbitrary signal $x(t)$, and this sifting process continued until the last mode was found.

$$x(t) = \sum_{j=1}^n C_j(t) + r_n(t) \quad (9)$$

3.3 Marginal Spectrum

Equation (2) is used to represent the instantaneous amplitude and frequency for IMF. Instantaneous amplitude is the height of time-frequency plane. The time-frequency distribution shown by HHT given as:

$$H(\omega, t) = \text{Re} \sum_{i=1}^n a_i(t) e^{j \int w_i(t) dt} \quad (10)$$

Moreover, the marginal spectrum is:

$$h(\omega) = \int_0^T H(\omega, t) dt \quad (11)$$

where T is total data length, ω is frequency and t is time.

4 Experimental Setup

For this study, punching process was performed on mechanical press of 30-ton capacity. The position of microphone was kept steady while recording the acoustic signal. The acoustic signal captured at three different conditions of the punch. The material and thickness of sheet and material of punch were kept constant during the experiment.

The detail of the experiment is given below:

Type of press	Mechanical
Punch diameter (mm)	8.00
Strokes per minute	60
Clearance (mm)	0.5
Sheet thickness (mm)	2.0
Sheet material	Cold rolled steel (CRC)
Material of punch	High-speed steel (HSS)
Die material	High carbon high chromium steel (HCHCR)
Microphone frequency response	50 Hz–44 kHz

Table 1 indicates punch conditions considered and to measure the punch wear, the punch cross-section was divided into eight sections.

Measurements of diameter and length of punch were taken at eight sections, and the average diameter and length were calculated. It was observed that with the use of punch, the diameter was increased and the length was slightly decreased.

4.1 Signal Recording and Processing

The acoustic signal was recorded using a D2202 microphone for various experimental conditions. Figure 1 shows the punch, and Fig. 2 shows the time domain signal for the new punch. Similarly, sound signals for all the conditions were recorded.

Table 1 Punch condition

Sr. no.	Punch type	Diameter (average) (mm)	Length (average) (mm)
1	New	8.00	89.380
2	Partially worn	8.02	89.354
3	Severely worn	8.04	89.315



Fig. 1 Punch

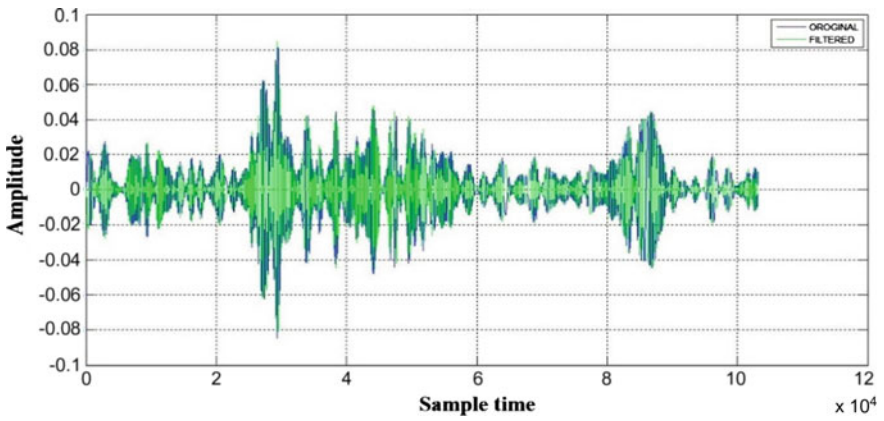


Fig. 2 The time domain acoustic signal for a new punch condition

The sound signals were first digitalized and processed using the MATLAB software. The time domain signal later was analyzed using HHT method.

4.2 Empirical Mode Decomposition of Signal

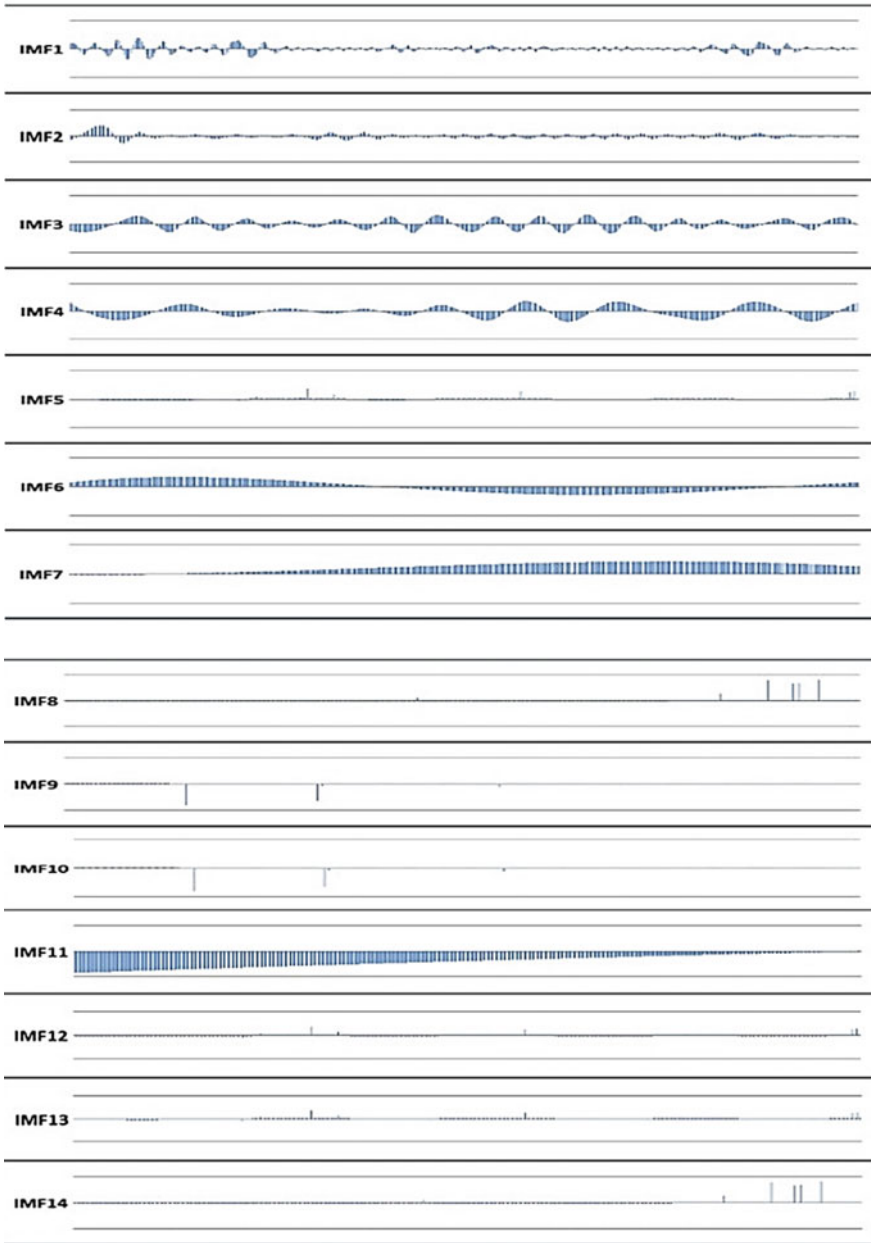


Fig. 3 Empirical modes of signal

4.3 Instantaneous Amplitude of IMF

Later, the comparison of instantaneous amplitudes of IMF of the new tool, partially worn tool and severely worn tool, was done.

5 Result and Discussion

Figure 2 shows the recorded sound signal of the new punch. In multi-component sound signals contain various data like sound emitted from the motor, bearing, the sound generated due to contact between the punch and the workpiece. Also, it contains external sound, the sound of other machining processes. First, the signals were filtered to reduce the noise. For the feature extraction, these multi-component signals were decomposed into several mono-component signals, IMFs, using EMD. Figure 3 shows 14 IMF for the new punch process signal. The HHT is then applied on IMFs to obtain instantaneous amplitudes and frequencies.

Figure 4 shows instantaneous amplitudes of IMFs for the new tool, partially worn tool and severely worn tool. It also shows the correlation between instantaneous amplitudes and tool wear, i.e., the amplitude is increasing as tool wear is developing. The amplitude value of 0.05, 0.4, and 0.9 was found for the new punch, partially worn punch, and severely worn punch, but frequency remains unaffected.

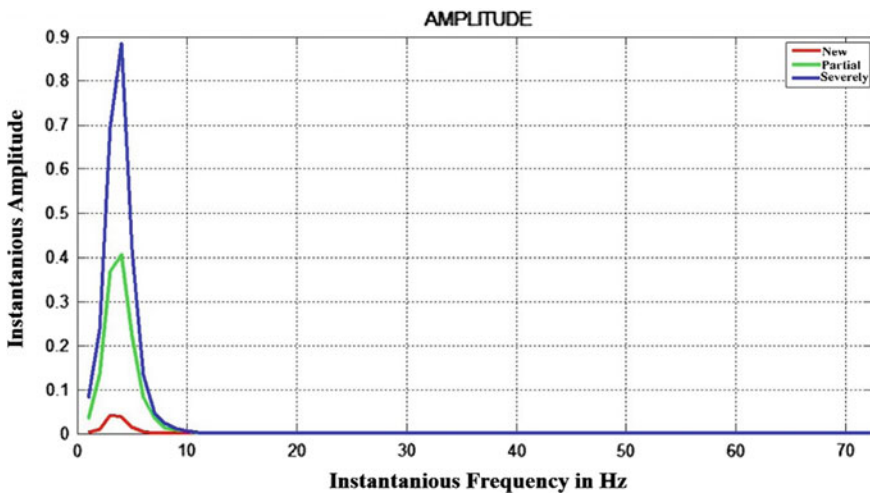


Fig. 4 Comparison of instantaneous amplitudes of new punch, partially worn, and severely worn punch condition

6 Conclusion

In this paper, the relationship between the punch wear and the variation in the amplitude IMFs of the punching operation AE signal studied for the punching process of CRC workpiece. Punching process emitted sound signal for three different punch conditions were considered and analyzed using Hilbert–Huang Transform (HHT). It was observed that the amplitude of some IMF components of the emitted sound signal increased with an increase in punch wear. The results of the study suggest that the HHT-based signal analysis can be used to punch wear monitoring.

References

1. Badgujar TY, Wani VP (2018) Stamping process parameter optimization with multiple regression analysis approach. *Mater Today Proc* 5(2):4498–4507
2. Sari DY, Wu T, Lin B (2017) Preliminary study for online monitoring during the punching process. *Int J Adv Manuf Technol* 88:2275–2276
3. Raja JE, Lim WS, Venkateshaiah C (2012) Emitted sound analysis for tool flank wear monitoring using hilbert huang transform. *Int J Comput Electr Eng* 4(2)
4. Roth JT, Djurdjanovic D, Yang X, Mears L, Kurfess T (2010) Quality and inspection of machining operations: tool condition monitoring. *J Manuf Sci Eng* 132:410151
5. Martin KF (1994) A review by discussion of condition monitoring and fault diagnosis in machine tools. *Int J Mach Tools* 34:527–551
6. Bogue R (2013) Sensors for condition monitoring: a review of technologies and applications. *Sens Rev* 33:295–299
7. Ge M, Zhang GC, Du R, Xu Y (2002) Feature extraction from energy distribution of stamping processes using wavelet transform. *J Vib Control* 8:1023–1032
8. Jayakumar T, Mukhopadhyay CK, Venugopal S, Mannan SL, Raj B (2005) A review of the application of acoustic emission techniques for monitoring forming and grinding processes. *J Mater Process Technol* 159:48–61
9. Ng Y-MH, Du R (2004) Reconstruction of 3D thermal distribution from infrared images. In: *Proceeding of the first international symposium on mechatronics*, pp 379–383
10. Li X, Bassiuny AM (2008) Transient dynamical analysis of strain signals in sheet metal stamping processes. *Int J Mach Tools Manuf* 48:576–588
11. Kim H, Sung JH, Sivakumar R, Altan T (2007) Evaluation of stamping lubricants using the deep drawing test. *Int J Mach Tools Manuf* 47:2120–2132
12. Badgujar TY, Wani VP (2019) Performance study of stamping process using condition monitoring: a review. In: Vasudevan H, Kottur V, Raina A (eds) *Proceedings of International Conference on Intelligent Manufacturing and Automation. Lecture Notes in Mechanical Engineering*. Springer, Singapore
13. Ubhayaratne I, Pereira MP, Xiang Y, Rolfe BF (2017) Audio signal analysis for tool wear monitoring in sheet metal stamping. *Mech Syst Signal Process* 85:809–826
14. Sharma SK, Kumar A (2017) Ride performance of a high speed rail vehicle using controlled semi active suspension system. *Smart Mater Struct* 26(5):55026. <https://doi.org/10.1088/1361-665X/aa68f7>
15. Sharma SK, Kumar A (2018) Disturbance rejection and force-tracking controller of nonlinear lateral vibrations in passenger rail vehicle using magnetorheological fluid damper. *J Intell Mater Syst Struct* 29(2):279–297. <https://doi.org/10.1177/1045389X17721051>

16. Hao S, Ramalingam S, Klamecki BE (2000) Acoustic emission monitoring of sheet metal forming: Characterization of the transducer, the work material and the process. *J Mater Process Technol* 101:124–136
17. Bassiuny AM, Li X, Du R (2007) Fault diagnosis of stamping process based on empirical mode decomposition and learning vector quantization. *Int J Mach Tools Manuf* 47:2298–2306

Sustainable Machining Using Hybrid Nanofluids Under Minimum Quantity Lubrication (MQL)



Anjali Gupta, Rajesh Kumar, Harmesh Kumar and Harry Garg

Abstract Over the last couple of decades, nanofluids have found tremendous scope as a potential heat transfer fluid. One prospective application is in sustainable machining method with minimum quantity lubrication (MQL). The use of a nanocutting fluid in machining under MQL conditions substantially reduces the amount of cutting fluid being used as compared to conventional methods. The overall performance of machining process also gets enhanced resulting in increased surface finish and reduced cutting temperature, tool wear, and cutting forces. Moreover, by replacing a nanocutting fluid with a hybrid nanocutting fluid, the performance of MQL is found to be further enhanced. A hybrid nanocutting fluid is composed by dispersing two or more nanoparticles of different materials in the conventional cutting fluid. This paper reviews the recent progress on the application of hybrid nanofluid in the machining process. Preparation methods and various thermophysical properties of hybrid nanofluids affecting the machining performance are also discussed.

Keywords Hybrid nanofluid · Machining · Minimum quantity lubrication (MQL)

1 Introduction

An extensive research has been observed in the last few decades in the field of nanofluids. Introduced by Choi [1], a nanofluid is a fluid that contains solid particles of the size usually less than 100 nm. It has been shown in many studies that dispersing nanosized solid particles in the commonly used coolants like water and oils enhances the thermal conductivity and the convective heat transfer coefficient of these fluids over the base fluids. This increase in heat transfer of the nanofluids is obvious as the thermal conductivity of solid particles is several hundred times higher than the conventional base fluids. Also, where microsized particles may cause clogging and

A. Gupta (✉) · R. Kumar · H. Kumar
U.I.E.T., Panjab University, Chandigarh, India
e-mail: anjali.uiet@gmail.com

H. Garg
CSIO, Chandigarh, India

© Springer Nature Singapore Pte Ltd. 2019
K. Shanker et al. (eds.), *Advances in Industrial and Production Engineering*, Lecture Notes in Mechanical Engineering, https://doi.org/10.1007/978-981-13-6412-9_56

the wear of the flow path, nanosized particles have an advantage of large surface to volume ratio and hence they result in large heat transfer enhancement of the base fluid. This promising thermal behavior of nanofluids has found its many engineering applications where cooling plays a important role in deciding the performance of products like electronic devices, vehicle engine cooling system, nuclear reactor, solar energy systems, etc [2]. It has been also established from studies that the addition of nanoparticles into the lubricating oils significantly improves its lubrication behavior. The enhancement of lubrication behavior of nanofluid is attributed to different mechanisms of nanoparticles such as rolling effect (act as ball bearings and convert the sliding friction into the rolling friction) filming effect (form a protective film of lubricant), mending effect (compensate for loss of material by depositing on distorted surfaces) and polishing effect (polish the rough surface by causing abrasion) [3, 4].

A recent application of nanofluids is in a machining process. In a machining process, a cutting fluid (CF) plays an important role where its primary functions are to lubricate and cool down the cutting zone. Dispersing metallic or non-metallic nanoparticles or nanofibers in a conventional CF is expected to improve the performance of a machining process by replacing a conventional CF with a nanocutting fluid (NCF). This happens due to the increased cooling ability as well as lubricating ability of a NCF, and both these properties substantially decide the performance of any machining operation. Furthermore, a hybrid nanofluid is an advancement of nanofluid. It contains the nanoparticles of more than one type. A significant improvement in the thermal conductivity of the hybrid nanofluid as compared to the base fluid and monoparticle-based nanofluids has been observed by many researchers. Hence, a notable heat transfer enhancement is expected using a hybrid nanofluid in comparison with the conventional fluid in the applications where high heat dissipation is desired.

Some literature in the recent past has discussed the advantages of using a hybrid nanofluid over single-particle-type nanofluid for a sustainable machining process. However, there are some issues reported with its use especially its preparation, cost, stability, the optimum number of nanoparticles and others. Therefore, in the present paper, an attempt has been made to thoroughly review the application of hybrid nanofluid as a potential heat transfer fluid in the sustainable machining process, discussing its preparation methods and its important thermo physical properties.

2 Hybrid Nanofluid

A hybrid nanofluid is the one which contains nanoparticles of different types. Synergistic effects allow the hybrid nanofluids to integrate advantages of constituent nanoparticles but avoid their disadvantages. This feature results in the enhanced properties of hybrid nanofluids compared to monoparticle-based nanofluids.

2.1 Preparation of Hybrid Nanofluid

Like nanofluids, hybrid nanofluids can also be prepared by either one-step or two-step method (Fig. 1). As nanoparticles tend to agglomerate due to strong van der Waal and cohesive forces, it is very important to ensure the stability of suspension so that it can be effectively used for the desired application. Zeta potential measurements of the prepared fluid indicate its stability. A stable solution with well-dispersed nanoparticles is obtained if the zeta potential value diverges away from iso-electric point (IEP). This is because the zeta potential values far from IEP result in strong repulsive forces and hence reduce agglomeration among the particles.

In one-step method, both the nanoparticle preparation and nanofluid preparation are carried out in single step. On the one hand, this method has an advantage of producing stable suspension with well-dispersed nanoparticles; on the other hand, this method is expensive and hence is suitable for small-scale production.

In two-step method, nanoparticles are produced in the first step and then suspended in the base oil in the second step. Hybrid nanofluid can be prepared by either dispersing of the individual constituent nanoparticles or by dispersing the synthesized nanocomposite in the base fluid. Different methods are used by various researchers to fabricate the hybrid nanocomposite. Agglomeration can be prevented by using

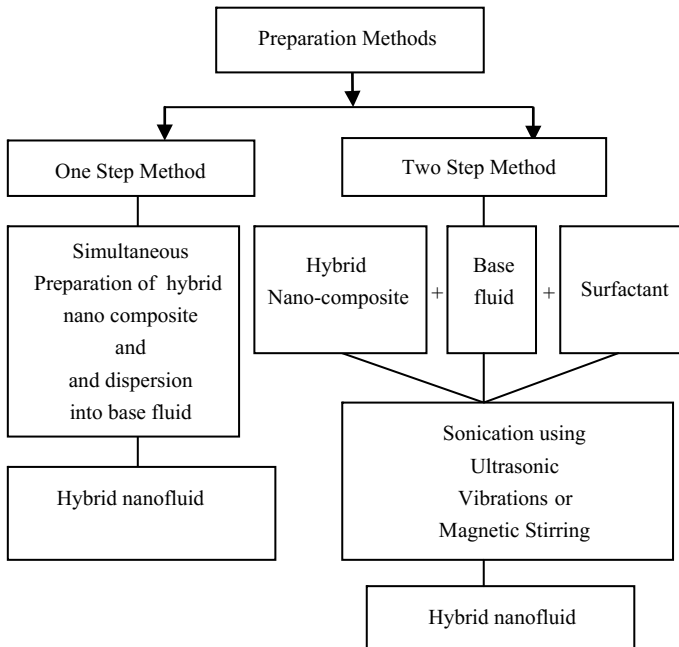


Fig. 1 Schematic diagram depicting the preparation of hybrid nanofluids

a suitable surfactant and by utilizing dispersing techniques like magnetic stirring, ultrasonic vibration, and high-pressure homogenization.

2.2 Thermophysical Properties of Nanofluids

The heat transfer performance of any system utilizing the hybrid nanofluid is determined by its various thermophysical properties like thermal conductivity, density, viscosity, specific heat, etc. The volume fraction of nanoparticles is a main factor which decides its thermophysical properties and can be estimated by using Eq. (1) [5]

$$\Phi = \frac{\left[\frac{m_{np}}{\rho_{np}} \right]}{\left[\frac{m_{np}}{\rho_{np}} + \frac{m_{bf}}{\rho_{bf}} \right]} \tag{1}$$

where m is mass and ρ is the density and subscripts np and bf represent nanoparticle and base fluid, respectively. Some of the other deciding factors are type, shape, size, and volume fraction of nanoparticles. Thermal conductivity is one of the most significant properties of hybrid nanofluids which decide its heat transfer behavior. Mixture rule can be applied to find thermal conductivity of hybrid nanofluid. According to the modified Maxwell model, hybrid nanofluid thermal conductivity can be calculated by Eq. (2) [5]

$$k_{hnf} = k_{bf} \left[\frac{\frac{\Phi_{np1}k_{np1} + \Phi_{np2}k_{np2}}{\Phi} + 2k_{bf} + 2(\Phi_{np1}k_{np1} + \Phi_{np2}k_{np2}) - 2\Phi k_{bf}}{\frac{\Phi_{np1}k_{np1} + \Phi_{np2}k_{np2}}{\Phi} + 2k_{bf} - 2(\Phi_{np1}k_{np1} + \Phi_{np2}k_{np2}) + \Phi k_{bf}} \right] \tag{2}$$

where Φ is the overall volume concentration of two different types of nanoparticles dispersed in hybrid nanofluid and is calculated as:

$$\Phi = \Phi_{np1} + \Phi_{np2} \tag{3}$$

k is thermal conductivity (W/m/k) and subscripts hnf and nf represent hybrid nanofluid and mononparticle nanofluid. Many studies have shown the significant augmentation in the thermal conductivity of the hybrid nanofluids over the base fluids. Table 1 presents the summary of the enhancement in the thermal conductivity of various hybrid nanofluids.

From the above section, it can be concluded that the thermal performance of hybrid nanofluid is largely improved over the base fluid due to significant improvement in thermal conductivity. The enhancement depends on type, size, and concentration of the nanoparticles. The increase in volume concentration of nanoparticles increases the thermal conductivity but affects the stability of the fluid. Thus, an optimum value

of the nanoparticles must be found out. For the same nanocomposite, the method of synthesis of nanomaterials may affect the thermal conductivity.

Table 1 Summary of thermal conductivity enhancement of hybrid nanofluids

Reference	Hybrid nanoparticles	Observations
Nine et al. [6]	Al ₂ O ₃ -MWCNT	Hybrid nanofluids showed higher thermal conductivity compared to monotype fluid Non-ground cylindrical-shaped MWCNT-based hybrid nanofluids gave better results as compared to ground spherical-shaped MWCNT-based fluids
Chen et al. [7]	Ag/MWCNT	The thermal conductivity enhancement of nanofluids containing nanocomposites of Ag/MWCNT was obtained higher than the nanofluid containing nanoparticles of MWCNT alone
Suresh et al. [8]	Al ₂ O ₃ /Cu	The thermal conductivity of the Al ₂ O ₃ -Cu/water hybrid nanofluids was obtained remarkably higher as compared to the base fluid water The thermal conductivity increased with increase in volume fractions from 0.1 to 2%
Baghbanzadeha et al. [9]	Silica and MWCNT	The maximum and the minimum enhancement in the thermal conductivity of the fluids was obtained with MWCNTs (23.3%) and silica nanospheres (8.8%), respectively, while the hybrid nanomaterial resulted in a in-between value Among the hybrid fluids, the fluid with higher percentage of MWCNT (50% silica nanosphere/50% MWCNT) showed more enhancement than the other hybrid fluid (80% silica nanosphere/20% MWCNT). Thermal conductivity increases with increase in concentration of nanomaterials

(continued)

Table 1 (continued)

Reference	Hybrid nanoparticles	Observations
Abbasi [10]	γ -Al ₂ O/MWCNTs	The thermal conductivity of the hybrid nanofluid is dependent on method of synthesis of nanomaterials
Madhesh et al. [11]	Cu/TiO ₂	The convective heat transfer coefficient, Nusselt number, overall heat transfer coefficient of hybrid nanofluid were enhanced by 52, 49, and 68%, respectively, for the volume concentration of up to 1.0%. This enhancement was attributed to improvement in effective thermal conductivity and diffusion kinetics of hybrid nanofluid which was said to be further due to the surface functionalized and highly crystalline nature of Cu-TiO ₂ hybrid nanocomposite
L. Syam Sundar et al. [12]	MWCNT/Fe ₃ O ₄	The thermal performance of composite-based hybrid nanofluids was stated to be superior as compared to monoparticle-based nanofluids. Also, as compared to the base fluid (distilled water), the Nusselt number of the hybrid nanofluid was enhanced by 9.35 and 20.62% (for 0.1% vol. concentration) and 14.81 and 31.10% (for 0.3% vol. concentration) for the Reynolds numbers of 3000 and 22,000, respectively
Nimmagadda Rajesh et al. [13]	Al ₂ O ₃ /Ag	It was observed that 3 vol.% concentration of hybrid nanofluid (0.6vol.% Al ₂ O ₃ + 2.4vol.%Ag) showed higher average convective heat transfer coefficient than that of nanofluids containing monoparticles of Al ₂ O ₃ and Ag

(continued)

Table 1 (continued)

Reference	Hybrid nanoparticles	Observations
Balla et al. [14]	Cu/CuO	For the same volume fraction, the maximum and minimum enhancement of the heat transfer coefficient over the base fluid (water) was obtained for Cu-based nanofluid and CuO-based nanofluid, respectively. Hybrid fluid containing Cu/CuO had in-between values

3 Minimum Quantity Lubrication in Machining (MQL)

A machining process is carried out by the shearing off the workpiece by a relatively harder tool. The fracture of the molecular bonds of the workpiece (at the primary shear zone) and the sliding friction at the tool–chip interface (at the secondary shear zone) results in a large amount of heat at the cutting zone (Fig. 2). These thermal conditions adversely affect tool life and the surface finish of the machined surface. Use of the cutting fluid (CF) provides the solution by not only cooling and lubricating the cutting zone but also washing away the chips and hence improving the surface finish. But along with these advantages, there are many problems associated with the use of the CF's use like serious occupational diseases caused to the workers, hazards to the environment, and high cost of maintenance. With the growing awareness in the society toward the environment and health concerns of the operators in the industry, the attempts have been made toward the reduction in the amount of CF being used. One solution has been suggested by many researchers is in terms of the method of delivering the CF by replacing the conventional flood lubrication (FL) method with minimum quantity lubrication(MQL) method.

3.1 Principle of MQL

The enormous reduction in the flow rate of CF in MQL (5–50 mL/h) compared to FL (order of 12,000 L/h) is the key feature of a MQL process. As shown in Fig. 3, CF is supplied usually in the form of droplets as an aerosol using compressed air in MQL unlike FL where large quantities of low pressure CF is supplied in a continuous stream. These droplets form a thin layer of CF in the cutting interface and hence reduce the friction and consequently the heat generated due to friction. The heat in the cutting zone finally vaporizes these droplets leaving the cutting tools and equipment dry and clean. As there is no residue left, the CF disposal problems also get away in MQL. Available literature shows that MQL has received a lot of attention

Fig. 2 Primary and secondary shear zones during machining operation

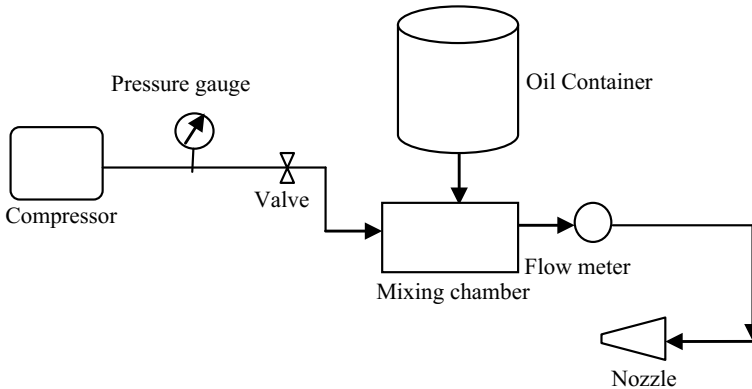
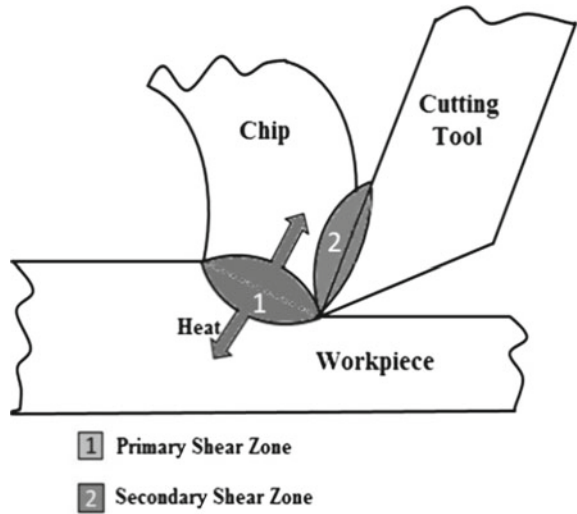


Fig. 3 Principle of working of MQL

in recent years due to its many advantages over FL technique. Latest studies have also pointed out that the use of MQL with nanofluids (NFMQL) further improves the cutting process significantly. The improvement is attributed to the better cooling and lubricating ability of the nanofluids.

3.2 Experimental Studies on MQL and NFMQL

To study the effect of different cutting parameters (feed, cutting speed, depth of cut) and different cooling conditions, dry cutting (DC), MQL, and FL, on surface

roughness during the turning of AISI 1050, Sarikaya and Gullu [15] found that feed rate and cooling condition were found to have maximum influence on surface roughness. Also, MQL was observed to perform better than other modes of application of CF. The effectiveness of MQL has been compared with FL for milling of steel by Kedare et al. [16] during the end milling of mild steel using uncoated HSS end mill cutter, in terms of surface roughness. Surface finish was found to be improved by 27% in MQL over FL. The improvements were attributed to the reduction in the cutting temperature in MQL over FL. MQL was found to be more effective than DC and FL for both continuous and interrupted orthogonal cutting during the turning of Ti-6Al-4V, carried out by Wang et al. [17]. Also, by replacing a CF with a nanocutting fluid (NCF), the effectiveness of MQL has been observed to be further increased. The NCF having nanoparticles of MoS₂ was used while carrying out grinding of hardened AISI 52100 steel by Molaie et al. [18]. nMoS₂ were added in two concentrations (2 wt% and 6 wt%) in two base oils (paraffin and soybean) to prepare NCFs for NFMQL cutting conditions. DC, FL (with water-based synthetic grinding fluid), and MQL (with paraffin and soybean-based oil) conditions were also used for comparative study. nMoS₂-based NCF resulted in the most effective machining with minimum grinding force. To investigate the effect of different lubrication conditions (DC, FL, MQL, and NFMQL), experimental investigation was carried out by Chatha et al. [19] during the drilling of Al 6063 alloy. The drilling experiments were continued until 200 holes. Thrust force and torque were measured after every 15 holes. The magnitudes of average drilling torques and thrust forces were found to be minimum for NFMQL followed by pure MQL and then FL conditions. Similar improved results for NFMQL were also obtained by Setti et al. [20] while performing the comparative study for different conditions such as DC, FL, MQL, and NFMQL (nAl₂O₃, nCuO-based NCF) during the CNC grinding of titanium alloy Ti-6Al-4V. nAl₂O₃-based NFMQL machining was found to be most effective with minimum value of coefficient of friction and most effective flushing of chips. Wang et al. [21] evaluated the lubrication properties of the wheel/workpiece interface while grinding a nickel-based alloy GH4169 under CFL, pure palm oil-based MQL, and NFMQL conditions. Different NCFs were prepared using nanoparticles of Al₂O₃, SiO₂, MoS₂, ND, CNTs, ZrO₂. Specific sliding grinding force, specific sliding grinding energy, and grinding ratio (G-ratio) were the various lubrication parameters used for evaluation of machining performance under different environments. The results predicted the best performance for NFMQL followed by palm oil-based MQL and then FL. The experimental study carried out by Huang et al. [22] also concluded that NFMQL with MWCNT (0.25% wt)-based NCF outperformed MQL conditions.

From the above discussion, it can be concluded that the machining carried out under MQL and NFMQL fulfills the requirement of three primary objectives of green manufacturing or sustainable manufacturing in the following ways:

Economical concerns—The amount of CF gets drastically reduced over conventional FL. Also, the cutting forces and hence the specific energy required for a machining process are reduced. The cost associated with tool also declines as tool wear is also found to be reduced.

Environmental concerns—In MQL as the CF is used up at once there is no disposal issue. Also, contrary to wet metal chips produced in FL which are treated like hazardous waste, whereas dry metal chips produced in MQL can be recycled.

Social concerns—The large reduction in the CF reduces health problems of the workers caused by the emissions of CF which may be breathed in or may come in contact with the skin of the operators.

4 Hybrid Nanofluid-Based MQL

From the discussion in the previous section, it may be concluded that effectiveness of MQL machining process increases by using a nanoparticle-based CF in a NFMQL process. Recently, the effect of dispersing mixed-type nanoparticles (instead of monotype) in the CF has been studied to investigate its effects on the machining performance. A hybrid nanocutting fluid (HyNCF) is composed by dispersing two or more nanoparticles of different materials in the conventional cutting fluid. In their experimental investigation, Zhang et al. [23] compared the performance of MoS₂/CNT HyNCF-based machining with pure nMoS₂ and pure CNT-based NCF machining while grinding Ni-based alloy. It was found that the combined MoS₂/CNT HyNCF-based machining yielded better results than grinding with single type of nanoparticle-based NCF in terms of lesser cutting force, lesser coefficient of friction, and lesser surface roughness. Due to physical encapsulation of CNTs by MoS₂ nanoparticles, MoS₂ nanoparticles could modify CNTs physically, improving their dispersion stability. The study carried out by Sharma et al. [24] established that the tribological properties of CF with hybrid nanoparticle Al₂O₃/GnP (graphene) are better (with lesser friction coefficient) than CF having nanoparticles of Al₂O₃ alone. With Al₂O₃/GnP HyNCF, the tool flank wear and nodal temperature were significantly reduced by 12.29 and 5.79%, respectively, as compared to CF having only Al₂O₃ NPs during turning of AISI 304 steel. Singh et al. [25] also obtained the enhanced performance of Al₂O₃/GnP HyNCF with reduction in the surface roughness by 20.28% and cutting force, thrust force, and feed force by 9.94, 17.38, and 7.25%, respectively, over NCF with nanoparticles of Al₂O₃ was obtained by while turning AISI 304 steel. The effect of mixed nanoparticle size ratio on the lubrication performance of MQL grinding has been investigated by Zhang et al. [26]. Different sizes (30, 50, and 70 nm) of Al₂O₃/SiC were used to prepare different HyNCFs. 30:70 was obtained as the optimized size ratio of the Al₂O₃/SiC mixed nanofluid.

5 Conclusion

The present study concludes that nanoparticle-enriched cutting fluid can perform better than the other commercially available cutting fluids. The improvements in the thermal performance under hybrid nanocutting fluid may be attributed to the trade-off

between the advantages and disadvantages of the individual particle and synergistic effect of nanomaterials. The study has shown that the HyNCF-based machining can perform better than the other available CFs. However, most of the studies have used the hybrid nanofluid obtained by mixing the nanoparticles of different types in fixed volumetric ratio. The optimization of mixing ratio may be further carried out to improve the performance of hybrid nanofluid-based machining. Moreover, much more work is needed to be carried out to investigate the influence of different operating parameters, such as nanoparticle shape, size, and their concentration on machining performance parameters. Also, optimization of different MQL operating parameters such as number of nozzles, nozzle orientation angle, flow rate, and air pressure can also be investigated.

References

1. Choi SUS, Eastman JA (1995) Enhancing thermal conductivity of fluids with nanoparticles. ASME Int Mech Eng Congr Expo 66(March):99–105. <https://doi.org/10.1115/1.1532008>
2. Sidik NAC, Yazid MNAWM, Mamat R (2015) A review on the application of nanofluids in vehicle engine cooling system. Int Commun Heat Mass Transf 68:85–90. <https://doi.org/10.1016/j.icheatmasstransfer.2015.08.017>
3. Peng DX, Kang Y, Hwang RM, Shyr SS, Chang YP (2009) Tribological properties of diamond and SiO nanoparticles added in paraffin. Tribol Int 42(6):911–917. <https://doi.org/10.1016/j.triboint.2008.12.015>
4. Mao C, Huang Y, Zhou X, Gan H, Zhang J, Zhou Z (2014) The tribological properties of nanofluid used in minimum quantity lubrication grinding. Int J Adv Manuf Technol 71(5–8):1221–1228. <https://doi.org/10.1007/s00170-013-5576-7>
5. Ranga Babu JA, Kumar KK, Srinivasa Rao S (2017) State-of-art review on hybrid nanofluids. Renew Sustain Energy Rev 77(September 2016):551–565. <https://doi.org/10.1016/j.rser.2017.04.040>
6. Nine MJ, Batmunkh M, Kim J-H, Chung H-S, Jeong H-M (2012) Investigation of Al₂O₃-MWCNTs hybrid dispersion in water and their thermal characterization. J Nanosci Nanotechnol 12(6):4553–4559. <https://doi.org/10.1166/jnn.2012.6193>
7. Chen L, Yu W, Xie H (2012) Enhanced thermal conductivity of nanofluids containing Ag/MWNT composites. Powder Technol 231:18–20. <https://doi.org/10.1016/j.powtec.2012.07.028>
8. Suresh S, Venkitaraj KP, Selvakumar P, Chandrasekar M (2012) Effect of Al₂O₃-Cu/water hybrid nanofluid in heat transfer. Exper Thermal Fluid Sci 38:54–60. <https://doi.org/10.1016/j.exptthermfluidsci.2011.11.007>
9. Baghbanzadeh M, Rashidi A, Rashtchian D, Lotfi R, Amrollahi A (2012) Synthesis of spherical silica/multiwall carbon nanotubes hybrid nanostructures and investigation of thermal conductivity of related nanofluids. Thermochem Acta 549:87–94. <https://doi.org/10.1016/j.tca.2012.09.006>
10. Abbasi SM, Rashidi A, Nemati A, Arzani K (2013) The effect of functionalisation method on the stability and the thermal conductivity of nanofluid hybrids of carbon nanotubes/gamma alumina. Ceramics Inter 39(4):3885–3891. <https://doi.org/10.1016/j.ceramint.2012.10.232>
11. Madhesh D, Parameshwaran R, Kalaiselvam S (2014) Experimental investigation on convective heat transfer and rheological characteristics of Cu-TiO₂ hybrid nanofluids. Exper Thermal Fluid Sci 52:104–115. <https://doi.org/10.1016/j.exptthermfluidsci.2013.08.026>
12. Sundar LS, Singh MK, Sousa ACM (2014) Enhanced heat transfer and friction factor of MWCNT-Fe₃O₄/water hybrid nanofluids. Int Commun Heat Mass Transf 52:73–83. <https://doi.org/10.1016/j.icheatmasstransfer.2014.01.012>

13. Nimmagadda R, Venkatasubbaiah K (2015) Conjugate heat transfer analysis of micro-channel using novel hybrid nanofluids ($\text{Al}_2\text{O}_3 + \text{Ag} / \text{Water}$). *European J Mech B/Fluids* 52:19–27. <https://doi.org/10.1016/j.euromechflu.2015.01.007>
14. Balla HH, Abdullah S, MohdFaizal W, Zulkifli R, Sopian K (2013) Numerical study of the enhancement of heat transfer for hybrid CuO-Cu nanofluids flowing in a circular pipe. *J Oleo Sci* 62(7):533–539. <https://doi.org/10.5650/jos.62.533>
15. Sarikaya M, Güllü A (2014) Taguchi design and response surface methodology based analysis of machining parameters in CNC turning under MQL. *J Cleaner Prod* 65:604–616. <https://doi.org/10.1016/j.jclepro.2013.08.040>
16. Kedare SB, Borse DR, Shahane PT (2014) Effect of minimum quantity lubrication (MQL) on surface roughness of mild steel of 15HRC on universal milling machine. *Proc Mater Sci* 6(Iempe):150–153. <https://doi.org/10.1016/j.mspro.2014.07.018>
17. Wang ZG, Rahman M, Wong YS, Neo KS, Sun J, Tan CH et al (2009) Study on orthogonal turning of titanium alloys with different coolant supply strategies. *Int J Adv Manuf Technol* 42(7–8):621–632. <https://doi.org/10.1007/s00170-008-1627-x>
18. Molaie MM, Akbari J, Movahhedy MR (2015) Ultrasonic assisted grinding process with minimum quantity lubrication using oil-based nanofluids. *J Cleaner Prod*, 212–222. Elsevier Ltd. <https://doi.org/10.1016/j.jclepro.2016.04.080>
19. Chatha SS, Pal A, Singh T (2016) Performance evaluation of aluminium 6063 drilling under the influence of nanofluid minimum quantity lubrication. *J Cleaner Prod* 137:537–545. <https://doi.org/10.1016/j.jclepro.2016.07.139>
20. Setti D, Sinha MK, Ghosh S, Venkateswara Rao P (2015) Performance evaluation of Ti-6Al-4V grinding using chip formation and coefficient of friction under the influence of nanofluids. *Int J Mach Tools Manuf* 88:237–248. <https://doi.org/10.1016/j.ijmactools.2014.10.005>
21. Wang Y, Li C, Zhang Y, Li B, Yang M, Zhang X et al (2016) Tribology international experimental evaluation of the lubrication properties of the wheel/workpiece interface in MQL grinding with different nano fluids. *Tribol Int* 99:198–210. <https://doi.org/10.1016/j.triboint.2016.03.023>
22. Huang WT, Liu WS, Wu DH (2016) Investigations into lubrication in grinding processes using MWCNTs nanofluids with ultrasonic-assisted dispersion. *J Cleaner Prod* 137:1553–1559. <https://doi.org/10.1016/j.jclepro.2016.06.038>
23. Zhang Y, Li C, Jia D, Li B, Wang Y, Yang M et al. (2016a) Journal of materials processing technology experimental study on the effect of nanoparticle concentration on the lubricating property of nanofluids for MQL grinding of Ni-based alloy. *J Mater Process Tech* 232:100–115. <https://doi.org/10.1016/j.jmatprotec.2016.01.031>
24. Sharma AK, Tiwari AK, Dixit AR, Singh RK, Singh M (2018) Novel uses of alumina/graphene hybrid nanoparticle additives for improved tribological properties of lubricant in turning operation. *Tribol Inter* 119(November 2017):99–111. <https://doi.org/10.1016/j.triboint.2017.10.036>
25. Singh RK, Sharma AK, Dixit AR, Tiwari AK, Pramanik A, Mandal A (2017) Performance evaluation of alumina-graphene hybrid nano-cutting fluid in hard turning. *J Cleaner Prod* 162:830–845. <https://doi.org/10.1016/j.jclepro.2017.06.104>
26. Zhang X, Li C, Zhang Y, Wang Y, Li B, Yang M, Zhang N et al (2016) Lubricating property of MQL grinding of $\text{Al}_2\text{O}_3/\text{SiC}$ mixed nanofluid with different particle sizes and microtopography analysis by cross-correlation. *Preci Eng* <https://doi.org/10.1016/j.precisioneng.2016.09.016>

A Review on Different Dielectric Fluids and Machining of Si_3N_4 and Al_2O_3 Composites via EDM



Kanav Bhatia , Ankit Singla , Anirudh Sharma ,
Shailesh Singh Sengar  and Ashish Selokar 

Abstract The limited efficiency and lack of feasibility of traditional manufacturing processes (TMPs) in ceramic industry restrict their applications in the machining of the ceramic materials having high hardness and brittleness. The use of unconventional methods of manufacturing overcomes the constraints of the conventional processes and therefore finds an enormous application in the industrial sector. The present study primarily focuses on the electrical discharge machining (EDM) of ceramic composites and reviews the different dielectric fluids that are being used in the modern machining, along with their effects on different EDM parameters like material removal rate (MRR), tool wear rate (TWR), surface roughness (SR), and surface hardness (SH) as well as the ability of EDM for machining the ceramic composites. It focuses on the main input parameters of EDM which influence the metal cutting procedure and discusses the machining of the ceramic materials like Al_2O_3 - and Si_3N_4 -based using EDM. The current study reveals that EDM is one of the best methods in machining the ceramic composites because of its high efficiency, high precision, and accuracy.

Keywords Electrical discharge machining · Material removal rate · Tool wear rate · Composite · Dielectric fluid · Surface roughness

1 Introduction

Manufacturing process is the process of transforming the raw materials into finished products that fulfill the needs of the consumers. Manufacturing sector is one of the vital contributors to a country's economy [1]. Traditional manufacturing processes (TMPs) involve the human-driven machines and require a direct contact of tool

K. Bhatia (✉) · A. Singla · A. Sharma · S. S. Sengar
Department of Mechanical Engineering, Faculty of Engineering and Technology,
Manav Rachna International Institute of Research and Studies, Faridabad,
Haryana, India
e-mail: Kanavbhatia1997@gmail.com

A. Selokar
Accendere Knowledge Management Services Pvt. Ltd., Chennai, India

with the material. They involve the direct interaction of mechanical energy with the workpiece, whereas the non-traditional processes depend upon the directed energy-based sources [2]. The latter uses advanced technology for the machining purposes, and there is no physical contact between the tool and the workpiece. Therefore, the wear and tear of the tool are nonexistent and the tool has a much longer life span. Machining by unconventional methods produces no noise pollution, and hence, they are less irritating, cause less health problems, and are more environment-friendly. The application of the non-traditional processes using tools like electric beam, laser beams, infrared beam, electric arc, and many more has made it possible to easily machine hard and brittle materials with high accuracy. EDM is the most widely used non-traditional concept of machining of removing the material by the thermal erosion process that occurs due to the series of electrical discharges occurring in the voltage gap between the tool and the “conductive” workpiece, which is filled with the dielectric fluid. As the result of discharge, the heat generated vaporizes the minute particles of the workpiece, which are flushed by the dielectric fluid. Materials like hardened and heat-treated steels, carbide, polycrystalline diamond, titanium, hot and cold rolled steels, copper, brass, and all other high temperature alloys as long as they conduct electricity. Several attempts have been made by the research scientists in order to find the most sustainable method of machining. Fifty percentage of research entries claim that EDM is one of the most widely applied machining processes and is at the top of sustainability list. About 31% of the studies are in support of laser beam machining as a sustainable process. Only 10% of the studies are concerned with the use of electrochemical machining (ECM) for machining purposes. The remaining 9% of the entries support the use of abrasive water jet cutting and photochemical machining [3]. Since EDM is a nearly non-contact process, it applies no cutting forces, and hence, there are no mechanical stresses and vibration problems, as a result of which burr-free edges are produced; therefore, it is used for machining of the engineering ceramic composites which requires high accuracy and excellent surface finish.

2 Dielectric Fluids

In EDM, dielectric fluid is one of the most important factors which influence the machining characteristics such as MRR, TWR, SR, and surface hardness. [4, 5]. As per the machining requirements, dielectric fluid is required to have the specific voltage and amperage characteristics [6]. It insulates the workpiece from the electrode [7] and cools both of them, and therefore, avoids high electrode wear. The fluid helps in the flushing of eroded metal particles from the area of erosion [8] and facilitates a stable and controlled spark gap ionization condition. The dielectric fluids are mainly of three types—(1) petroleum-based fluids, (2) synthetic fluids, and (3) vegetable-based fluids. The petroleum-based fluids are the most widely available and are 30% less expensive than the synthetic fluids but have the lowest life span. The synthetic fluids cost more but do not need replacing and cause less health problems than

the petroleum-based. The application of the vegetable-based dielectric fluids offer a cleaner, greener, and a safer way to improve the sustainability of the EDM process by increasing the environmental-friendliness [9].

In the year 1943, Russian researchers Lazarenko et al. discovered the utilization of erosive effect of electrical discharges in processing of metals. Initially, the ordinary air was used as the dielectric. Then, the products containing petroleum and products derived from Kristalol 60 (white spirit) were used.

Kibria et al. performed the experiment to explore the influence of the pure deionized water, kerosene, and boron carbide (B_4C) powder mixed in kerosene on the machining characteristics such as MRR, TWR, surface integrity, and overcut during the machining of titanium alloy (Ti-6Al-4V). The experiment results revealed that different dielectrics have varying influence on EDM characteristics. His study proved that the use of pure deionized water facilitates higher MRR and TWR as compared to kerosene. When BiC suspended dielectrics are used, better surface integrity is achieved, MRR is found to be increasing with deionized water, but TWR decreases with kerosene as dielectric [10, 11].

Yan et al. performed the experiments to analyze the influence of using Al or Si powder-mixed kerosene as dielectrics on EDM machining parameters using Ti-6Al-4V as the working material. The results revealed that kerosene added with either Al or SiC powder increases the material removal depth along with the SR. SiC produces a better material removal depth than Al added to the kerosene. The largest gap between the electrodes and the workpiece is generated with the use of Al powder added to the kerosene owing to its optimal conductivity and suspension [12].

Valaki et al. studied the use of *Jatropha curcas* oil as the dielectric fluid in EDM process. His investigations showed that use of *Jatropha* bio-diesel (BD) increases the MRR and production rate to a great extent [13]. It proved that lower SR is obtained with the use of *Jatropha* BD. It gives a very high quality of surface finish with an efficiency of 94.71%. The use of *Jatropha* BD increases SH which is desired to improve wear resistance of the surfaces for enhancing the life of dies, punches, and other tooling.

Shabgard et al. studied the carbon nanotubes (CNT) mixed with dielectric in the EDM process to elevate efficiency of Ti-6Al-4V alloy machining. His investigations proved that the use of CNTs makes the EDM process stable and MRR does not decrease with the rise in pulse duration. In the presence of the CNT powder, due to increase in machining gap distance, sparks can easily start and MRR increases [14]. In shorter pulse durations, TWR decreases [15]. With longer pulse of 48 A, the TWR of ordinary EDM is lesser than that of powder-mixed EDM. If the machining is unstable, the surface finish reduces. Otherwise, an excellent surface finish is achieved [16, 17]. The length and the size of the micro-cracks reduce with the use of CNT. Less stresses are developed with the use of CNT-added dielectrics [17, 18].

The use of urea solution as dielectric was investigated by Tsai et al., and his experiment indicated that the N_2 element decomposed from the dielectric containing urea migrates to the workpiece and forms a TiN layer, resulting in an excellent wear resistance of the machined surface after EDM [19] (Table 1).

Table 1 Comparison of various dielectric fluids used in EDM machining

Material used	Input parameters		Dielectric used	Output parameters		Major findings	
	Pulse time T_{on}	Current (A)		MRR	TWR		SR
Ti-6Al-4V	10	2	Pure deionized water	0.032 mg/min	0.006 mg/min	-	Because of quite larger debris size, the surface finish is not good. It results in the excellent and the most efficient machining process and forms lesser recast layer [10]
			Kerosene	0.004 mg/min	0.002 mg/Min	-	Although MRR is smaller, TWR is also considerably low. SR achieved is very high, but it is still better than that in deionized water [10]
			B ₄ C mixed DI water	0.04 mg/min	0.005 mg/min	-	MRR is increased linearly with increase in pulse duration at a constant peak current and requires higher machining time [10]
Ti-6Al-4V	10	0.1	Kerosene + Al powder	0.8 mm/min	10 mm/min	2.6	Kerosene with either Al powder added can increase the SR and material removal depth up to 2 times than in case of kerosene alone [12]
			Kerosene + SiC powder	1.0 mm/min	21 mm/min	2.7	SiC added to the kerosene can produce a better MRR. SiC interferes with the carbon nucleides adherence on the surface of the electrode while drifting within the dielectric fluid in the EDM process [12]
Pure Titanium	100	10	Urea solution	18 mg/min	3.7 mg/min	2.7	It proves that MRR and TWR increase with increasing peak current and MRR, TWR, and SR deteriorate with an increase in pulse duration. The surface exhibits excellent friction and wear characteristics [19]
P20 + plastic mold steel	50	9	Jatropha curcas oil	12.56 mm ³ /min	-	6.6	Higher production rates can be achieved. Current is the most determining parameter affecting MRR, while current and pulse on time are the most significant parameters for SR and SH [13]
Ti-6Al-4V	100	48	CNT-added dielectric	1.25 mm ³ /min	30%	6.7	Addition of CNT particles into dielectric decreases the length and the size of surface micro-cracks [14]

3 Machining of Silicon Nitride (Si_3N_4) via EDM

Si_3N_4 produced by direct nitridation of a compacted silicon powder, and because of the difficulty in complete reaction, it is hard to achieve a high component density. Machining of Si_3N_4 is very difficult due to its non-conducting nature and extreme mechanical properties. So as to machine Si_3N_4 via EDM, a conductive element or a compound is induced into its material matrix.

3.1 Si_3N_4 -TiN (Titanium Toughened Silicon Nitride)

Si_3N_4 -TiN which is extensively used in reinforced environments like heat exchangers and convoluted molds which find their applications in metal forming, wear opposing components, etc., is a high-performance composite ceramic comprised of about 50% TiN, 40% Si_3N_4 , and 5% other additives like Y_2O_3 and Al_2O_3 . It is known to have high MRR ranging from 100 to 110 μJ due to the addition of TiN which acts as a catalyst while its machining in EDM [21] (Table 2).

3.2 Optimization Techniques

Genichi Taguchi developed an analytical method called Taguchi method (TM) which helps in determining the machining parameters, like current (I), dielectric fluid pressure (DP), pulse on time (T_{on}), spark gap voltage (SV), and pulse off time (T_{off}) that have an intense impact on the machining characteristics like MRR, EWR, etc. TM is concerned with the design for the enhancement of high quality of finished products [25]. Famous Statistician and Evolutionary Biologist, Ronald Fisher, developed the analysis of variance method which provides the significance of the machining parameters for ceramic composite materials and gives the signal-to-noise ratio (S/N) data.

Kumar et al. investigated the mechanical properties, material removal rate, and tool wear rate in EDM machining process of Al 2618 alloy reinforced with Si_3N_4 , AlN, and ZrB_2 composites. They optimized the independent variables used in the study which are peak current, pulse on time (T_{on}), and pulse off time (T_{off}) and composite. They used L_{25} orthogonal array in their study to optimize the results for drilling operation of Al 2618 alloy reinforced with Si_3N_4 , AlN, and ZrB_2 composites, which has 25 rows and 4 columns. Further, they compared the various output parameters like MRR, TWR, and depth (D) from the results obtained from the optimized independent variables. The output results were obtained by reducing the MRR, TWR, and depth which were calculated with the help of mean and signal-to-noise ratio (S/N) [20].

Uhlmann et al. investigated the mechanical properties, material removal rate, and tool wear rate in EDM machining process of Si_3N_4 -TiN composite. They used

Table 2 Comparison of various experiments conducted for machining of Si₃N₄ via EDM

Base W/p material	Added material in material matrix	Dielectric fluid used	Input parameters		Pulse time T_{off} (μ s)	Output parameters			Major findings
			Pulse time T_{on} (μ s)			MRR	TWR	SR	
Si ₃ N ₄	Al 2618	Kerosene	6–8		4–8	0.656 g/min	0.0106 g/min	–	The addition of Al 2618 alloy decreases the MRR. With the increase in weight % of reinforcement, the MRR and TWR are reduced [20]
Si ₃ N ₄	TiN	1. H ₂ O 2. O ₂ 3. Ar	1.5 4.2 8.7		64.8 7.5 7.5	–	–	–	The MRR under oxygen as a dielectric fluid is equivalent to the MRR with liquid. But for air as dielectric fluid a lower MRR and a high EWR are detected [21]
Si ₃ N ₄	TiN	H ₂ O based emulsion	57		228	5.84 mm ³ /min	–	3.975 μ m	The use of molybdenum wire electrode leads to transfer of some tool electrode material to the w/p surface during machining. MRR is reduced with increase in the pulse off time [22]
Si ₃ N ₄	1. CNT 2. Graphene nanoplatelet (GNP)	Kerosene	3.0		1.0	–	–	–	The EWR and SR are better on the conductive materials than insulating materials. Better MRR is obtained on the insulating materials than the conductive materials In the CNT materials, the MRR is decreased with increasing electrical conductivity [23]
Si ₃ N ₄	TiN	Hydro carbon oil	7–10		1–4	0.011 mm ³ /min	5.4%	0.99/10.8	TWR increases with rising discharge energy. MRR, TWR, and SR are affected by the ceramic composition and the discharge energy [24]

optimization techniques for focusing on the identification of the main effects caused by the technologically relevant parameters for EDM machining with a pulsed relaxation generator. They used a cemented carbide electrode. They further selected the independent variables for EDM machining by methods of statistical design of experiments (DOE). They investigated the capacitance C_e , pulse on time (T_{on}), pulse off time (T_{off}), charging current (i_L), and open circuit voltage (\hat{u}_i) [21].

4 Machining of Al_2O_3 via EDM

Al_2O_3 is a ceramic material known to resist strong acid and alkali attack and possesses a strong interatomic bonding. As EDM uses electrical discharges for machining, it is the best method for operating ceramics. Some exceptional dielectric properties in DC at GHz frequencies are shown by Al_2O_3 , and these properties result in better machining of the ceramic by EDM.

5 Various Experiments on Machining of Al_2O_3 via EDM

An investigation was done by Liu et al., and the process parameters were observed in the EDM milling machine. ZnO/Al_2O_3 ceramic was selected as the workpiece with various Al_2O_3 contents. The MRR and EWR were calculated according to formulae [29] (Table 3).

A study was conducted by Fukuzawa et al. on the EDM of aluminum oxide using copper electrode and baked carbon layer as the assisting electrode. In this, the MRR decreased and the machining became unstable with increase in purity of alumina. Machining tests on sapphire, a single crystal of Al_2O_3 , observed different MRR along different machining directions. Micro-cracks were also observed on the EDMed surface which proves an increase in SR [30].

Liu et al. investigated machining of Al_2O_3 ceramic via EDM with the help of copper sheet electrode. Many factors like tool polarity and voltage rotational speed influenced the MRR and SR. Positive tool polarity and large pulse duration were responsible for large MRR, and smaller pulse duration was responsible for lower SR [31].

Ji et al. used a red copper for the tool electrode and were able to obtain single discharge crater volume 17.63 mm^3 . It was concluded that the primary MRR was spalling with melting and vaporization appears in the center. Studies assure that the knowledge of electrochemical discharge trepanning of Al_2O_3 also exists [32].

The discharge current and the pulse-in time also have satisfied on both the value of the EWR and SR EDM Operating Conditions for $Al_2O_3 + TiC$ Composite are explained in Table 4.

Patel et al. investigated the optimization of SR during the EDM of aluminum silicon alloy using the trust region method. They also studied surface integrity, surface

Table 3 Comparison of various experiments conducted for electrical discharge machining of Al₂O₃

Ceramic used	Al ₂ O ₃ %	Tool electrode used	Process parameters			Electrical resistivity (Ω cm)	Major findings
			MRR (mm ³ /min)	EWR %	SR		
Al ₂ O ₃	99.9	Cu tool electrode	–	–	–	10 ¹⁴	MRR is decreased, with increase in purity of Al ₂ O ₃ [30]
ZnO/Al ₂ O ₃	0	–	1.5	0.1	9.6	32,400	The MRR is increased with the decrease of electrical resistance.
	0.01		6	0.6	9.2	3410	
	0.05		9.86	1.05	6.98	2470	When the electrical resistivity decreases, the discharge channel is formed easily, and the electrode MRR increases; therefore, the EWR increases
	0.1		14.76	1.98	6	687	SR is also decreased with the decrease of electrical resistivity [31]
	0.5		23.68	2.2	5.5	15	
Al ₂ O ₃	–	Red Cu	–	–	–	–	Single discharge crater volume—17.63 mm ³ Sputtering appearance was observed on machined surface [29]

Table 4 Comparison of various experiments conducted for electrical discharge machining of Al_2O_3 with addition of SiC_w -TiC in material matrix

Researcher	Ceramic used	% of material	Dielectric fluid	Machine configuration	Major findings
Patel et al.	Al_2O_3 - SiC_w -TiC	Al_2O_3 (80%) TiC (11%) WC (9%)	Deionized water	Wire EDM (roughing condition)	Flexural strength degrades during machining [26]
Lauwers et al.	Al_2O_3 - SiC_w -TiC	–	Oil	Die-sinking EDM (medium and high energy input)	MRR is increased with increase in input energy [28]

characteristics, and the MRR. At low discharge energy, melting and spalling were found during the EDM process of the above-used ceramic component, whereas the oxidation of TiC and WC to TiO_2 and WO_3 also occurred repeatedly [27].

Lauwers et al. observed major material removal in EDM of Al_2O_3 - SiC_w -TiC. The operations were classified as melting, evaporation, spalling, and oxidation. The experiment was performed by conducting electric discharge and wire EDM experiment with the help of suitable dielectric [28].

6 Conclusion

1. Processing by using different dielectric fluid in EDM process is still at the experimental stage. With significant improvements in MRR, surface properties have been reported and the feasibility of the process is well established.
2. The literature review clearly shows that the non-traditional machining processes are far more advantageous than the age-old conventional machining processes. Here, we compare the outputs achieved in machining of Ti-6Al-4V via EDM under the use of different dielectric fluids.
3. EDM characteristics are widely influenced by the presence of different dielectric fluids. Most of the studies focus on the single dielectric fluid. However, a common observation has been made to compare the effects of different dielectric fluids. Finally, the use of *Jatropha curcas* oil proves to be far better than any other fluid due to its high feasibility and its ability to give the desired machining output parameters.
4. The development of high-performance advance ceramic composites like Si_3N_4 and Al_2O_3 has a variety of manufacturing challenges which generated the need for a more advanced machining method because of their unique physical and

chemical characteristics. Apart from economics, the process selection is based on the machined surface integrity. EDM, out of all the advanced machining processes, proves to be the most economical and sustainable process.

5. As Si_3N_4 (Silicon Nitride) is non-conducting in nature, in order for it to be machined by EDM, conductive elements or compounds are added into their material matrix.
6. And it has been seen that addition of TiN into Si_3N_4 matrix gives the best desired output parameters (MRR, TWR, SR). Machining of aluminum oxide (Al_2O_3) is also quite difficult because of its protective oxide layer, high mechanical properties, and low thermal conductivity.
7. Therefore, as in case of Si_3N_4 , additional compounds are added into its material matrix. And it has been investigated that the addition of TiC (11%) and WC (9%) corresponds to the best desired output parameters.
8. The study reviews that no stresses are generated in the work material during its machining using EDM, and thus, EDM can machine materials with high precision and accuracy. All the observations are still under further research.
9. However, EDM is not that widely used due to additional time and cost used for creating electrodes for ram/sinker EDM, high power consumption, and excessive tool wear occurrence during machining.

Acknowledgements The authors would like to express our sincere gratitude to Accendere KMS-CL Educate Ltd., New Delhi, for their valuable comments that led to substantial improvements on an earlier version of this manuscript.

References

1. Payal HS, Sethi BL (2003) Non-conventional machining processes as viable alternatives for production with specific reference to electrical discharge machining
2. Prasad K, Mahamani A, Sravani PS, Mounika K Electrical discharge machining of the composites—a literature review. *IJRET* 2321–7308
3. Gamage JR, DeSilva AKM (2015) Assessment of research needs for sustainability of unconventional machining processes. *Procedia CIRP* 26:385–390
4. Chakraborty S, Dey V, Ghosh SK (2015) A review on the use of dielectric fluids and their effects in electrical discharge machining characteristics. *Precis Eng* 40:1–6
5. Luo YF (1997) The dependence of interspace discharge transitivity upon the gap debris in precision electrodischarge machining. *J Mater Process Technol* 68:121–131
6. Mohri N, Saito N, Higashi M, Kinoshita N (1991) A new process of finish machining on free surface by EDM methods. *CIRP Ann Manuf Technol* 40:207–210
7. Boothroyd G, Winston AK (1989) Non-conventional machining processes. *Fundam Mach Mach Tools* 491
8. Zhang Y, Liu Y, Shen Y, Ji R, Li Z, Zheng C (2014) Investigation on the influence of the dielectrics on the material removal characteristics of EDM. *J Mater Process Technol* 214:1052–1061
9. Valaki JB, Rathod PP (2016) Assessment of operational feasibility of waste vegetable oil based bio-dielectric fluid for sustainable electric discharge machining (EDM). *Int J Adv Manuf Technol* 87:1509–1518

10. Lin YC, Yan BH, Chang YS (2000) Machining characteristics of titanium alloy (Ti-6Al-4V) using a combination process of EDM with USM. *J Mater Process Technol* 104:171-177
11. Ming QY, He LY (1995) Powder-suspension dielectric fluid for EDM. *J Mater Process Technol* 52:44-54
12. Kao JY, Tsao CC, Wang SS, Hsu CY (2010) Optimization of the EDM parameters on machining Ti-6Al-4V with multiple quality characteristics. *Int J Adv Manuf Technol* 47:395-402
13. Valaki JB, Rathod PP, Sankhavara CD (2016) Investigations on technical feasibility of *Jatropha curcas* oil based bio dielectric fluid for sustainable electric discharge machining (EDM). *J Manuf Processes* 22:151-160
14. Mai C, Hocheng H, Huang S (2012) Advantages of carbon nanotubes in electrical discharge machining. *Int J Adv Manuf Technol* 59:111-117
15. Shabgard M, Khosrozadeh B (2017) Investigation of carbon nanotube added dielectric on the surface characteristics and machining performance of Ti-6Al-4V alloy in EDM process. *J Manuf Processes* 25:212-219
16. Izman S, Ghodsiyeh D, Hamed T, Rosliza R, Rezazadeh M (2012) Effects of adding multiwalled carbon nanotube into dielectric when EDMing titanium alloy. In: *Advanced materials research*. Trans Tech Publications, pp 1445-1449
17. Guu YH, Mai CC, Hocheng H (2008) Applications of carbon nanotubes in nontraditional machining and microscopy. In: *Applications of carbon nanotubes*. Nova Science Publishers, Inc., pp 111-126
18. Khan AA, Ndaliman MB, Zain ZM, Jamaludin MF, Patthi U (2012) Surface modification using electric discharge machining (EDM) with powder addition. In: *Applied mechanics and materials*. Trans Tech Publications, pp 725-733
19. Kibria G, Sarkar BR, Pradhan BB, Bhattacharyya B (2010) Comparative study of different dielectrics for micro-EDM performance during microhole machining of Ti-6Al-4V alloy. *Int J Adv Manuf Technol* 48:557-570
20. Kumar NM, Kumaran SS, Kumaraswamidhas LA (2015) An investigation of mechanical properties and material removal rate, tool wear rate in EDM machining process of Al 2618 alloy reinforced with Si₃N₄, AlN and ZrB₂ composites. *J Alloy Compd* 650:318-327
21. Uhlmann E, Schimmelpfennig T-M, Perfilov I, Streckenbach J, Schweitzer L (2016) Comparative analysis of dry-EDM and conventional EDM for the manufacturing of micro holes in Si₃N₄-TiN. *Procedia CIRP* 42:173-178
22. Zhang C (2014) Effect of wire electrical discharge machining (WEDM) parameters on surface integrity of nanocomposite ceramics. *Ceram Int* 40:9657-9662
23. Hanaoka D, Fukuzawa Y, Ramirez C, Miranzo P, Osendi MI, Belmonte M (2013) Electrical discharge machining of ceramic/carbon nanostructure composites. *Procedia CIRP* 6:95-100
24. Schubert A, Zeidler H, Kühn R, Hackert-Oschätzchen M, Flemmig S, Treffkorn N (2016) Investigation of ablation behaviour in micro-EDM of nonconductive ceramic composites ATZ and Si₃N₄-TiN. *Procedia CIRP* 42:727-732
25. Nalbant M, Gökkaya H, Sur G (2007) Application of Taguchi method in the optimization of cutting parameters for surface roughness in turning. *Mater Des* 28:1379-1385
26. Patel KM, Pandey PM, Rao PV (2009) Surface integrity and material removal mechanisms associated with the EDM of Al₂O₃ ceramic composite. *Int J Refract Metal Hard Mater* 27:892-899
27. Patel KM, Pandey PM, Rao PV (2010) Optimisation of process parameters for multi-performance characteristics in EDM of Al₂O₃ ceramic composite. *Int J Adv Manuf Technol* 47:1137-1147
28. Pachaury Y, Tandon P (2017) An overview of electric discharge machining of ceramics and ceramic based composites. *J Manuf Processes* 25:369-390
29. Ji R, Liu Y, Diao R, Xu C, Li X, Cai B, Zhang Y (2014) Influence of electrical resistivity and machining parameters on electrical discharge machining performance of engineering ceramics. *Plos One* 9:e110775
30. Fukuzawa Y, Mohri N, Tani T, Muttamara A (2004) Electrical discharge machining properties of noble crystals. *J Mater Process Technol* 149:393-397

31. Liu YH, Li XP, Ji RJ, Yu LL, Zhang HF, Li QY (2008) Effect of technological parameter on the process performance for electric discharge milling of insulating Al_2O_3 ceramic. *J Mater Process Technol* 208:245–250
32. Ji R, Liu Y, Zhang Y, Zhang H, Li X, Dong X (2011) An experimental research on single discharge machining of insulating ceramics efficiently with high energy capacitor. *Sci China Technol Sci* 54:1537–1545

Mechanical Behavior of Powder Metallurgy Processed Al + ZrB₂ + Al₂O₃ Metal Matrix Composites



Bhupendra Prakash Sharma, D. Akhil, M. Junaid, Umesh Kumar Vates and G. S. Rao

Abstract Present investigation aimed to fabricate the aluminum-based metal matrix composites. Such composites play an important key role for heavy vehicle and structural applications. It can be used for lightweight and more stiff components of heavy vehicles. In the present research work, an easy formation of aluminum-based metal matrix composite materials are proposed through powder metallurgy process with different mass fractions of zirconium diboride and alumina reinforcement such as 3% Al₂O₃–7% ZrB₂, 3% Al₂O₃–5% ZrB₂, and 3% Al₂O₃–3% ZrB₂ all in the form of atomized particles. Further, microstructural readings on cross section as well as surface of the bar and hardness measurements were attained and investigated. Improved hardness as well as tensile strength is noted from newly developed performs.

Keywords Composite · Powder metallurgy · Mechanical properties · Microstructural readings

1 Introduction

It is the great challenge to develop proposed metal matrix nano-composite material having adequate strength and hardness for heavy vehicle application, specifically in chassis which contributes maximum weight fraction as an individual component of any vehicle. Many researchers are striving to develop the metal matrix nanocomposites by using most suitable fabrication methodology as powder metallurgy (PM) stir casting techniques and techniques [1]. The ferrous-based PM processed structural parts have already been taken over by the automotive and off-highway vehicle applications due to fulfillment of desire characteristics of materials from PM process. It is clear, that alloy steels are suitable material for various applications such as power plants, aircraft, marine industries, and bearing manufacturing units [2]. The limiting factors in the development of PM processed specimen is pressing and sintering

B. P. Sharma (✉) · D. Akhil · M. Junaid · U. K. Vates · G. S. Rao
Department of Mechanical Engineering, Amity University, Noida,
Uttar Pradesh, India
e-mail: bpsharma@amity.edu

process. Without any doubt, the tensile strength, hardness, etc., are the most significant factors that depend on production methodology. Sintered products are generally occurred crack during impact because of pores act as stress developer [3, 4]. Therefore, fabrication and study of the mechanical behavior of such products under these loads are very important.

Few researches have already reported that strength of PM processed metal matrix nanocomposite will be improved for the same size of components. A reinforcement of iron carbide, alumina, zirconium diboride, molybdenum carbide, and tungsten carbide also gives the better stiffness in the PM processed components [5, 6]. It has been given in literature that tensile, impact, and fatigue characteristics of sintered part are greatly influenced by temperature at which sintering is being conducted and time allowed [7]. The micro-mechanism of fracture is highly influenced by the matrix [8, 9]. Characteristics of high density sintered material (Fe—4.0Ni—1.5Cu—0.5Mo—0.5C) have already been studied by Moon [10]. It has been reported that the material characteristics vary with temperature and pressure at sintering Trivedi et al. [11] and Rahimiana et al. [12] have able to evaluate the sintering temperature particle size and sintering time on alloys. In addition, at low particle size, the hardness, yield strength, compressive strength, and elongation to fracture were higher, as compared to coarse particles size of alumina. Archarya [13] studied the hardness value of iron aluminum by varying composition of iron (0, 10, 20, 25, 30, 35, 40 wt%) increases with Fe content, the best result has been obtained at 40% weight fraction of Fe particles (60% Al). Maximum hardness = 76.90 VHN.

Thus, the present investigation is aimed to improve the strength, stiffness, and desire mechanical properties by using sintered powder metallurgy process in alumina–zirconium diboride nanoparticles reinforcement in Al matrix through change in its microstructure. Therefore, the strength of the powder metallurgy component such as tensile strength, impact strength, yield strength, etc., be in the range of 67–86% of theoretical value. Hence, a challenge for researchers as improvement in desire mechanical properties of material for the heavy vehicle application may be achieved by applying innovative ways of fabrication methodology of the best suitable contribution of selected particles. XRD and SEM analyses will be done on fabricated Al–Al₂O₃–ZrB₂ nanocomposites to estimate the improvements in their present characteristics than presently used chassis materials.

It is also the great challenge to adapt the suitable drilling process for newly developed hard, stiff, and high-strength nano-composite (Al–Al₂O₃–ZrB₂) material. The drilling will be very important process to create fine holes for chassis assembly in heavy duty vehicle application which is not possible from conventional drilling process. The low-pressure water jet assisted laser beam drilling has to be employed for the drilling of Al–Al₂O₃–ZrB₂ because the present machining process is applicable for hard semiconductor and insulator. Whereas many more unconventional machining techniques are reported only for hard and electrically conductive materials. Also, the provision of low-pressure water jet assistance will be incorporated with laser beam for proper material removal from semiconducting performs through adequate flushing of the generated debris. Laser power, pulse width, pulse frequency, drilling speed, pulse duration, assisted water pressure, standoff distance (SOD), nozzle diameter

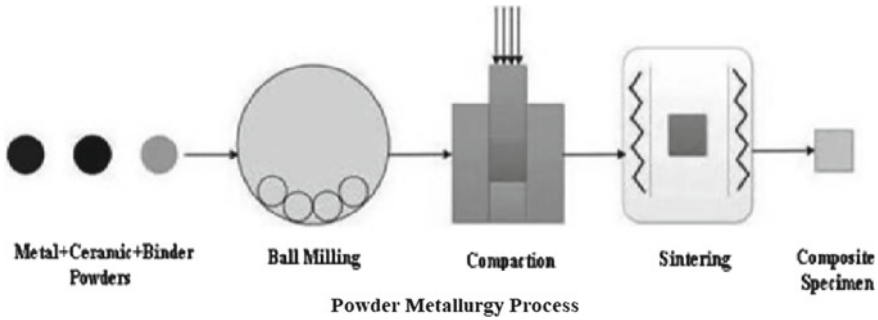


Fig. 1 Flow diagram of powder metallurgy process for Al–Al₂O₃–ZrB₂

and focal length, etc., are some important controllable process parameters that may be considered in LBD process. The important process measures which could be considered as hole taper, hole circularity, material removal rate (MRR), surface finish, HAZ, recast layer, aspect ratio and spatter formation, etc. [14, 15].

It is evident that mass of the chassis or parts may be further reduced by introducing such Al-based metal matrix composite. PM technique is also important which need to be adopted for fabrication of such newly proposed nanocomposite which able to improve the hardness and the tensile strength as well (Fig. 1).

2 Material and Design

Uniformly mixed compositions of metal matrix nanocomposite were compacted up to 1 MN using a suitable die set assembly on a 7 MN capacity hydraulic press. Compacted performs were manually coated with the paste of concentrated acetone–alumina mixture to save with oxidation during sintering process. After drying at 300 °C for 2 h in a muffle furnace, sintering operation was carried out in an electric furnace at the temperature of 800 °C for a holding period of 1 h. Cylindrical compacted performs having 22 MM of diameters were fabricated using PM technique. Hardness and tensile strength were tested in the strength of material lab at Amity University, Noida. Standard ASTM guidelines were followed to conduct the aforesaid mechanical testing. The schematic diagram of the used die and punch of D2 steel is given in Fig. 2.

The above specimens were prepared using compacting of the constituent powders in the appropriate die punch set having 22 MM of diameters. Powders of the entire constituent were weighted separately and mixed well. It is heated at 300 °C for 2 h to dry, then compressed by applying 1 MN force for compacting. All the specimens were sintered at 800 °C for 1 h. Figure 3 shows the different composition of the elements which has been fabricated under the same pressure of powder metallurgy process. In this experiment, three specimen 3% Al₂O₃–3% ZrB₂, 3% Al₂O₃–5%



Fig. 2 D2 die steel punch and die for compacting the powders



Fig. 3 Different composition of Al_2O_3 and ZrB_2 in Al

ZrB_2 , and 3% Al_2O_3 –7% ZrB_2 with Al have been fabricated using nanoparticles of ZrB_2 . Nanoparticle of one component is being used to fill the intermolecular spacing which provides the more bond strength.

Microstructure of the 3% Al_2O_3 –7% ZrB_2 with Al composite is being shown in Fig. 4. It is evident that the nanoparticles of ZrB_2 filling the intermolecular spacing and to make the material comparatively very hard. Sample 1, 2, 3, and 4 are showing the 3% Al_2O_3 –3% ZrB_2 , 3% Al_2O_3 –5% ZrB_2 , 3% Al_2O_3 –7% ZrB_2 , and pure aluminum, respectively, as given in Fig. 4.

Figure 5 is showing the influence and percentage contribution of Al_2O_3 – ZrB_2 in Al on the hardness of the plain matrix alloy and produced composites. It has been noticed that hardness increases with the increase in ZrB_2 along with Al_2O_3 particles

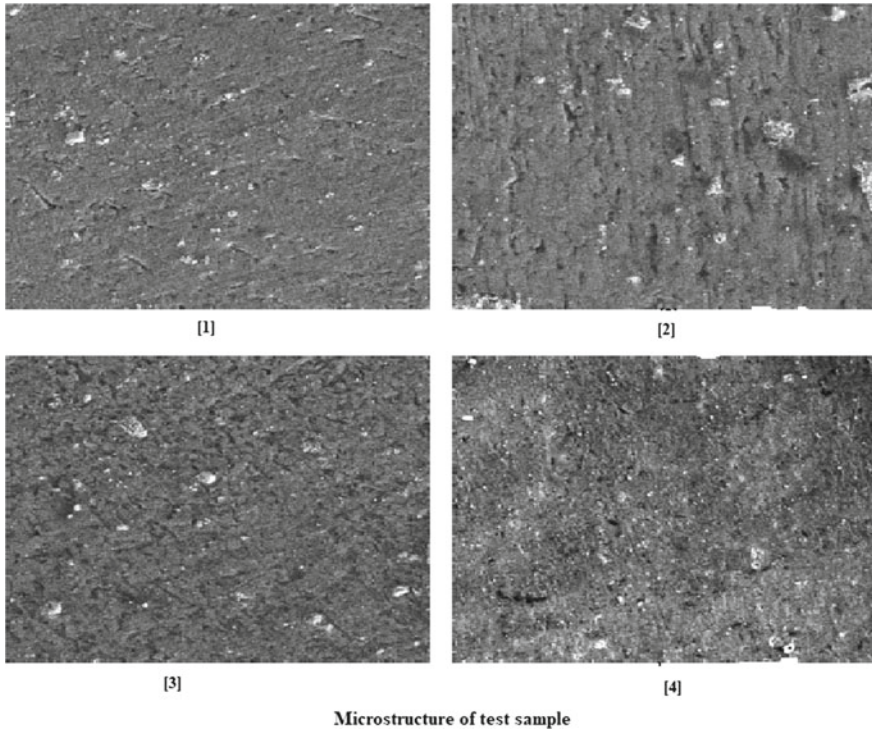


Fig. 4 Microstructure of the samples

and it is significantly higher than the hardness of the plain Al as given in specimen number '4'. It is evident that hardness of 3% Al_2O_3 -3% ZrB_2 newly composite is greater than the 99.2% pure Al powder processed through PM as trial 1. Similarly, trials 2 and 3 have been performed on 3% Al_2O_3 -5% ZrB_2 and 3% Al_2O_3 -7% ZrB_2 , respectively, for the estimation of hardness. It is cleared that hardness of the present composite 3% Al_2O_3 -7% ZrB_2 is highest as trial 3.

The influence and percentage contribution of Al_2O_3 - ZrB_2 in Fe on the tensile strength are being reported as Fig. 6. It has been noticed that tensile strength increases with the increase in percentage of ZrB_2 along with Al_2O_3 particles and it is significantly higher than the tensile strength of the plain Al as given in specimen number '4'. It is evident that tensile strength of 3% Al_2O_3 -3% ZrB_2 newly composite is greater than the 99.2% pure Al powder processed through PM as trial 1. Similarly, trials 2 and 3 have been performed on 3% Al_2O_3 -5% ZrB_2 and 3% Al_2O_3 -7% ZrB_2 , respectively, for the estimation of tensile strength. It is cleared that hardness of the present composite 3% Al_2O_3 -7% ZrB_2 is highest as trial 3 (Fig. 7).

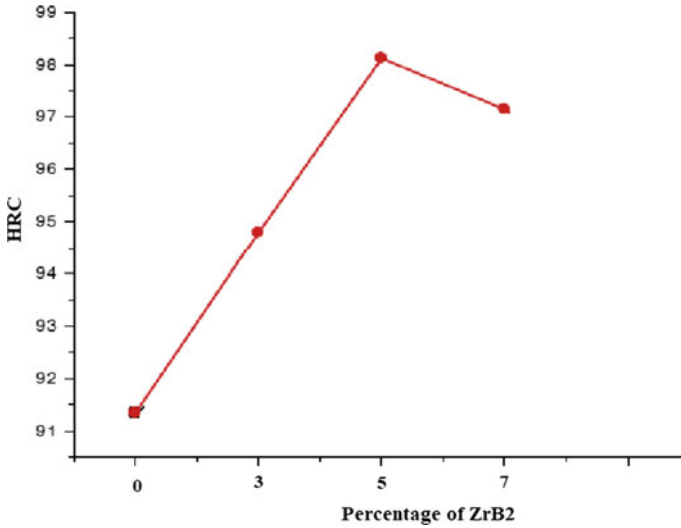


Fig. 5 Hardness of powdered metallurgies processed specimen

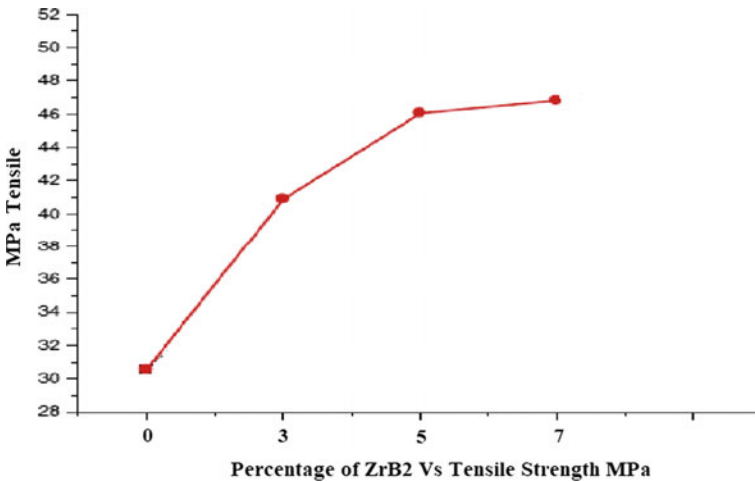


Fig. 6 Tensile strength of powdered metallurgies processed specimen

3 Conclusion

Powder metallurgy has been found the most appropriate method for fabrication of nano-metal matrix composite of such hardest material. As per the ASTM standard, the specimens were fabricated to conduct the hardness and tensile strength test. 3% Al_2O_3 -7% ZrB_2 with Al is the best suitable combination to give the highest tensile strength as well as the high hardness among the four specimens. It is also evident

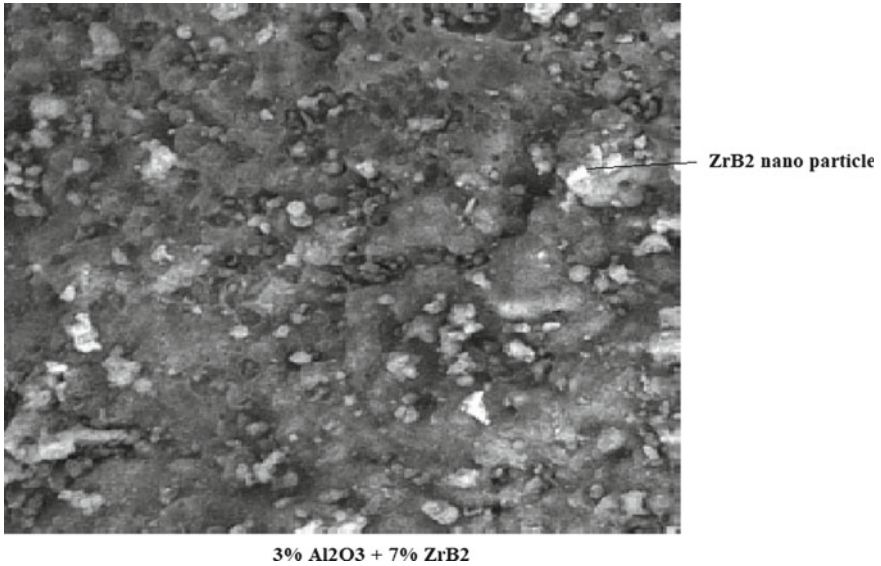


Fig. 7 Microstructure of powdered metallurgies processed specimen (3% Al_2O_3 –7% ZrB_2)

that volume of the third number specimen is comparatively low with compared to others. It may be suggested that such newly developed metal matrix composite may be used for heavy vehicles application, which can bear more loads with compact in size.

References

1. Abouelmagd G (2004) Hot deformation and wear resistance of P/M aluminium metal matrix composites. *J Mater Process Technol* 155:1395–1401
2. James WB, West GT (2002) Powder metal technologies and application. ASM hand-book. ASM International, USA
3. Narayan S, Rajeshkannan A (2010) Densification behavior informing of sintered iron-0.35% carbon powder metallurgy preform during cold upsetting. *Mater Des* 32:1008–1013
4. Shanmugasundaram D, Chandramouli R (2009) Tensile and impact behavior of sinter-forged Cr, Ni and Mo alloyed powder metallurgy steels. *Mater Des* 30:344–349
5. Danninger H, Jangg G, Weiss B, Stickler R (1993) Microstructure and mechanical properties of sintered iron Part II experimental study. *Powder Metall Int* 25:170–223
6. Danninger H, Jangg G, Weiss B, Stickler R (1993) Microstructure and mechanical properties of sintered iron Part I basic considerations and review of literature. *Powder Metall Int* 25:11–17
7. D'Armas H, Llanes L, Penafiel J, Bas J, Anglada M (2000) Tempering effects on the tensile response and fatigue life behavior of a sinter hardened steel. *Mater Sci Eng A* 277:291–296
8. Straffelini G, Molinari A, Danninger H (1992) Impact notch toughness of high strength porous steels. *Mater Sci Eng A* 272:300–309
9. Butuc MC, Gracio JJ, Rocha BA (2006) An experimental and theoretical analysis on the application of stress-based forming limit criterion. *Int J Mech Sci* 48:414–429

10. Moon JR (2002) Toughness and growth of fatigue cracks in P/M steels. *Powder Metall Prog* 2:63–80
11. Trivedi S, Mehta Y, Chandra K, Mishra PS (1993) Effect of chromium on the mechanical properties of powder-processed Fe-0.45 wt% P alloys. *J Mater Process Technol* 210:85–90
12. Rahimiana M, Ehsania N, Parvinb N, Baharvandic H (2009) The effect of particle size, sintering temperature and sintering time on the properties of Al-Al₂O₃ composites made by powder metallurgy. *J Mater Process Technol* 209:5387–5393
13. Acharya A (2017) Fabrication and evaluation of various properties of iron-aluminium metal based composites. *IJSRD Int J Sci Res Dev* 5(3)
14. Hwang SS, Vasiliev AL, Pature NP (2007) Improved processing and oxidation-resistance of ZrB₂ ultra-high temperature ceramics containing SiC nanodispersoids. *Mater Sci Eng* 464:216–224
15. Telle R, Sigl LS, Takagi K (2000) Boride-based hard materials. In: Riedel R (ed) *Handbook of ceramic hard materials*, vol 2. Wiley-VCH, Weinheim, pp 802–945

Reliability Analysis of Sheet Manufacturing Unit of a Steel Industry



Munish Mehta , Jujhar Singh  and Manpreet Singh 

Abstract This paper deals with reliability–availability–maintainability (RAM) of the sheet manufacturing system of a steel industry. The system comprises of various subsystems viz. conveyors, extractor, furnace, de-scaling unit, roughing mill, Steckel mill, down coiler, and strapping machine. State transition diagram has been developed which depicts various states (fully operational/reduced capacity/failed) of the system. Chapman–Kolmogorov differential equations have been developed from this diagram using mnemonic rule. Mathematical analysis has been carried out using supplementary variable technique. Repair rate has been varied whereas failure rate has been kept constant. Meantime between failure and transient state availability of the system has been calculated using Simpson’s 3/8 rule and Runge–Kutta fourth order method (using MATLAB), respectively. The conclusions drawn may be helpful to the plant management in enhancing system performance by taking accurate and timely maintenance decisions.

Keywords Steel industry · Supplementary variable technique · Runge–Kutta · MATLAB

1 Introduction

Reliability engineering is defined as an approach adopted by the industry to achieve optimum product performance. It deals with every area of corporate activity which can influence ultimate reliability of a product. Reliability engineering focuses on systematic study of failures of engineering components and systems during the specified time and under the specified operational and environmental conditions and their remedies thereof. It differs from traditional engineering approach in the sense that

M. Mehta (✉) · M. Singh

Department of Mechanical Engineering, Lovely Professional University, Phagwara, India
e-mail: munishmehta1@rediffmail.com

J. Singh

Department of Mechanical Engineering, I. K. Gujral Punjab Technical University,
Kapurthala, India

© Springer Nature Singapore Pte Ltd. 2019

K. Shanker et al. (eds.), *Advances in Industrial and Production Engineering*, Lecture Notes in Mechanical Engineering, https://doi.org/10.1007/978-981-13-6412-9_59

the latter deals with designing and manufacturing a product or a system with certain available inputs by applying known scientific principles and concepts. Achieving maximum efficiency and optimum performance are also taken care of in design and development of the products in traditional engineering. But, reliability engineering goes one step further. It designs a product for failure-free operation for predetermined mission time, understated operational and environmental conditions. It also deals with systematic analysis of product failures and tries to address the core issues.

Various researchers have done a lot of work in this area. Moustafa [1] presented Markov models to derive the transient reliability and the mean time between failures (MTBF) for repairable K-out-of-N: G systems subject to two failure modes. Limnios [2] presented a dependability analysis for semi-Markov systems with finite state space. Qamber [3] presented two different methods—LU decomposition and Runge–Kutta to calculate the steady-state probabilities and frequencies of two different engineering models. Biswas and Sarkar [4] used Fourier transformation technique to find the availability of a system maintained through several imperfect repairs before a replacement or a perfect repair. Dai and Jia [5] proposed some ways to improve the reliability of vertical machining center by analyzing its failure data. Avontuur and Werff [6] presented a method based on finite element equations for reliability analysis of mechanical and hydraulic systems. Zou et al. [7] proposed a method for reliability analysis of a vehicle body-door subsystem with respect to wind noise.

Ebrahimi [8] focused on a method that assesses the reliability of a system which has extremely high reliable components/systems, for which it is difficult to collect failure data. Rauzy [9] reported results of an experimental study on six iterative methods to compute the transient probabilities of large Markov models. Chen and Trivedi [10] built the semi-Markov decision process for the maintenance policy optimization of condition-based preventive maintenance problems. Samrout et al. [11] proposed a new method to minimize the preventive maintenance cost of series-parallel systems by developing a new method based on ant colony optimization technique. Hamada et al. [12] described the use of a discrete-event simulation model for determining the availability of industrial processes. Levitin [13] suggested a modification of the generalized reliability block diagram method for evaluating reliability and performance indices of multistate systems with uncovered failures. Dhillon and Shah [14] studied the combined effect of human error, common cause failure, redundancy, and maintenance policies on the performance of a system. Sachdeva et al. [15] presented an approach based on Petri Nets for studying the behavior of a real industrial system. Garg et al. [16] assessed the availability of crank-case manufacturing system using probability consideration and supplementary variable technique (SVT). Rodriguez and De Souza [17] presented a reliability-based analysis for calculating the critical tool life in machining processes.

Sinha [18] performed safety and reliability analysis of the brake-by-wire system of an automobile for functional safety of electrical/electronic systems in road vehicles. Levitin et al. [19] proposed a recursive and exact method for reliability evaluation of phased-mission systems. Doostparast et al. [20] considered the problem of reliability-based periodic preventive maintenance planning for systems with deteriorating components. Liu et al. [21] used universal generating function technique for

reliability analysis of lithium-ion battery pack in electric vehicles. Amann and Kadau [22] presented a modified Runge–Kutta algorithm which yields a conservative estimate of the crack size for fatigue crack growth even for large integration step sizes. Pakdaman et al. [23] solved fractional differential equations by using fundamental properties of artificial neural networks for function approximation.

This paper consists of 5 sections. Present section comprises of introduction and literature review. Section 2 consists of brief description of the system, various notations, and assumptions used in the analysis. In Sect. 3, mathematical modeling of the system has been carried out. Chapman–Kolmogorov differential equations of the system have been developed using SVT. The equations have also been developed keeping failure and repair rates constant. In Sect. 4, for analyzing the transient state availability, the differential equations have been solved using Runge–Kutta fourth order method with the help of MATLAB and the effects of various combinations of failure and repair rates of different subsystems on the sheet manufacturing system have been evaluated. MTBF has been calculated at the end of each row in Tables 1, 2, 3, 4, 5, 6, 7, 8, 9, 10 to give an insight into the maintenance time available. Section 5 consists of conclusion of the analysis done in previous section.

2 System Description, Notations, and Assumptions

Sheet manufacturing unit is an important part of the steel industry. The system takes in slab as input from the casting system and produces sheet coil of 5 mm thickness

Table 1 Effect of failure rate of furnace (α_1) on system availability

Time (days)	α_1				
	0.0014286	0.0073214	0.0132143	0.0191071	0.025
30	0.9667	0.9537	0.9273	0.8915	0.8496
60	0.9529	0.9215	0.8641	0.7945	0.7215
90	0.9470	0.9017	0.8245	0.7379	0.6535
120	0.9445	0.8898	0.8012	0.7068	0.6194
150	0.9434	0.8825	0.7875	0.6899	0.6024
180	0.9428	0.8781	0.7795	0.6805	0.5937
210	0.9426	0.8754	0.7747	0.6753	0.5892
240	0.9424	0.8737	0.7718	0.6724	0.5869
270	0.9423	0.8727	0.7701	0.6708	0.5857
300	0.9423	0.8720	0.7690	0.6698	0.5850
330	0.9423	0.8716	0.7684	0.6693	0.5847
360	0.9423	0.8713	0.7680	0.6690	0.5845
MTBF	341.30	321.71	291.47	260.50	232.50

Table 2 Effect of failure rate of roughing mill (α_2) on system availability

Time (days)	α_2				
	0.001	0.0015833	0.0021665	0.002750	0.0033333
30	0.9667	0.9559	0.9453	0.9348	0.9245
60	0.9529	0.9384	0.9243	0.9105	0.8970
90	0.9470	0.9313	0.9161	0.9013	0.8869
120	0.9445	0.9284	0.9128	0.8977	0.8830
150	0.9434	0.9271	0.9114	0.8962	0.8815
180	0.9428	0.9266	0.9108	0.8956	0.8809
210	0.9426	0.9263	0.9105	0.8953	0.8806
240	0.9424	0.9261	0.9104	0.8952	0.8805
270	0.9423	0.9260	0.9103	0.8951	0.8804
300	0.9423	0.9260	0.9103	0.8951	0.8804
330	0.9423	0.9260	0.9103	0.8950	0.8803
360	0.9423	0.9260	0.9102	0.8950	0.8803
MTBF	341.30	335.88	330.64	325.56	320.63

Table 3 Effect of failure rate of Steckel mill (α_3) on system availability

Time (days)	α_3				
	0.0006667	0.001	0.0013333	0.0016667	0.002
30	0.9667	0.9603	0.9540	0.9477	0.9414
60	0.9529	0.9440	0.9354	0.9268	0.9183
90	0.9470	0.9373	0.9278	0.9184	0.9092
120	0.9445	0.9345	0.9246	0.9149	0.9055
150	0.9434	0.9332	0.9232	0.9135	0.9039
180	0.9428	0.9326	0.9226	0.9128	0.9032
210	0.9426	0.9323	0.9223	0.9125	0.9029
240	0.9424	0.9322	0.9221	0.9123	0.9027
270	0.9423	0.9321	0.9221	0.9123	0.9027
300	0.9423	0.9320	0.9220	0.9122	0.9026
330	0.9423	0.9320	0.9220	0.9122	0.9026
360	0.9423	0.9320	0.9220	0.9122	0.9026
MTBF	341.30	337.92	334.62	331.60	328.19

Table 4 Effect of failure rate of down coiler (α_4) on system availability

Time (days)	α_4				
	0.0011111	0.0058333	0.0105556	0.0152778	0.02
30	0.9667	0.9612	0.9494	0.9327	0.9121
60	0.9529	0.9431	0.9231	0.8959	0.8641
90	0.9470	0.9356	0.9126	0.8819	0.8468
120	0.9445	0.9325	0.9085	0.8767	0.8406
150	0.9434	0.9312	0.9069	0.8748	0.8384
180	0.9428	0.9306	0.9062	0.8740	0.8376
210	0.9426	0.9304	0.9059	0.8737	0.8373
240	0.9424	0.9302	0.9058	0.8736	0.8371
270	0.9423	0.9302	0.9057	0.8735	0.8371
300	0.9423	0.9301	0.9057	0.8735	0.8371
330	0.9423	0.9301	0.9057	0.8735	0.8371
360	0.9423	0.9301	0.9057	0.8735	0.8371
MTBF	341.30	337.38	329.49	319	307.03

Table 5 Effect of failure rate of strapping machine (α_5) on system availability

Time (days)	α_5				
	0.0011765	0.0044538	0.0077311	0.0110084	0.0142857
30	0.9667	0.9630	0.9555	0.9448	0.9314
60	0.9529	0.9453	0.9308	0.9109	0.8871
90	0.9470	0.9375	0.9195	0.8954	0.8672
120	0.9445	0.9341	0.9146	0.8888	0.8589
150	0.9434	0.9326	0.9125	0.8860	0.8556
180	0.9428	0.9320	0.9116	0.8849	0.8543
210	0.9426	0.9317	0.9113	0.8846	0.8540
240	0.9424	0.9315	0.9113	0.8846	0.8540
270	0.9423	0.9315	0.9113	0.8846	0.8540
300	0.9423	0.9315	0.9113	0.8846	0.8540
330	0.9423	0.9315	0.9113	0.8846	0.8540
360	0.9423	0.9315	0.9113	0.8846	0.8540
MTBF	341.30	337.92	331.56	323.11	313.33

Table 6 Effect of repair rate of furnace (β_1) on system availability

Time (days)	β_1				
	0.0208333	0.078125	0.1354167	0.1927083	0.25
30	0.9667	0.9671	0.9672	0.9672	0.9672
60	0.9529	0.9541	0.9543	0.9543	0.9543
90	0.9470	0.9490	0.9492	0.9493	0.9493
120	0.9445	0.9471	0.9473	0.9473	0.9473
150	0.9434	0.9463	0.9465	0.9466	0.9466
180	0.9428	0.9460	0.9462	0.9463	0.9463
210	0.9426	0.9459	0.9461	0.9462	0.9462
240	0.9424	0.9459	0.9461	0.9461	0.9461
270	0.9423	0.9459	0.9460	0.9461	0.9461
300	0.9423	0.9459	0.9460	0.9461	0.9461
330	0.9423	0.9459	0.9460	0.9461	0.9461
360	0.9423	0.9459	0.9460	0.9461	0.9461
MTBF	341.30	342.25	342.31	342.33	342.33

Table 7 Effect of repair rate of roughing mill (β_2) on system availability

Time (days)	β_2				
	0.03125	0.0546875	0.078125	0.105625	0.125
30	0.9667	0.9713	0.9743	0.9768	0.9780
60	0.9529	0.9618	0.9665	0.9695	0.9709
90	0.9470	0.9581	0.9631	0.9662	0.9676
120	0.9445	0.9564	0.9614	0.9645	0.9659
150	0.9434	0.9556	0.9606	0.9637	0.9650
180	0.9428	0.9551	0.9601	0.9632	0.9646
210	0.9426	0.9549	0.9599	0.9630	0.9643
240	0.9424	0.9547	0.9598	0.9629	0.9642
270	0.9423	0.9547	0.9597	0.9628	0.9641
300	0.9423	0.9546	0.9596	0.9627	0.9641
330	0.9423	0.9546	0.9596	0.9627	0.9641
360	0.9423	0.9546	0.9596	0.9627	0.9641
MTBF	341.30	345.17	346.84	347.90	348.37

Table 8 Effect of repair rate of Steckel mill (β_3) on system availability

Time (days)	β_3				
	0.0285714	0.0714286	0.1142857	0.1571429	0.20
30	0.9667	0.9717	0.9742	0.9756	0.9765
60	0.9529	0.9622	0.9654	0.9669	0.9677
90	0.9470	0.9583	0.9616	0.9630	0.9639
120	0.9445	0.9566	0.9598	0.9613	0.9621
150	0.9434	0.9557	0.9589	0.9604	0.9612
180	0.9428	0.9553	0.9585	0.9599	0.9608
210	0.9426	0.9551	0.9582	0.9597	0.9605
240	0.9424	0.9549	0.9581	0.9595	0.9604
270	0.9423	0.9548	0.9580	0.9594	0.9603
300	0.9423	0.9548	0.9579	0.9594	0.9602
330	0.9423	0.9547	0.9579	0.9593	0.9602
360	0.9423	0.9547	0.9579	0.9593	0.9601
MTBF	341.30	345.27	346.33	346.84	347.14

Table 9 Effect of repair rate of down coiler (β_4) on system availability

Time (days)	β_4				
	0.0454545	0.1590909	0.2727273	0.3836364	0.50
30	0.9667	0.9669	0.9669	0.9669	0.9669
60	0.9529	0.9532	0.9533	0.9533	0.9533
90	0.9470	0.9475	0.9475	0.9475	0.9475
120	0.9445	0.9450	0.9450	0.9450	0.9450
150	0.9434	0.9438	0.9439	0.9439	0.9439
180	0.9428	0.9433	0.9433	0.9433	0.9433
210	0.9426	0.9430	0.9430	0.9430	0.9430
240	0.9424	0.9429	0.9429	0.9429	0.9429
270	0.9423	0.9428	0.9428	0.9428	0.9428
300	0.9423	0.9427	0.9428	0.9428	0.9428
330	0.9423	0.9427	0.9427	0.9427	0.9427
360	0.9423	0.9427	0.9427	0.9427	0.9427
MTBF	341.30	341.44	341.45	341.45	341.45

Table 10 Effect of repair rate of strapping machine (β_5) on system availability

Time (days)	β_5				
	0.0357143	0.0625	0.0892857	0.1160714	0.1428571
30	0.9667	0.9668	0.9669	0.9669	0.9669
60	0.9529	0.9532	0.9533	0.9534	0.9534
90	0.9470	0.9475	0.9477	0.9478	0.9478
120	0.9445	0.9451	0.9453	0.9453	0.9454
150	0.9434	0.9440	0.9442	0.9442	0.9443
180	0.9428	0.9435	0.9437	0.9437	0.9438
210	0.9426	0.9432	0.9434	0.9435	0.9435
240	0.9424	0.9431	0.9433	0.9434	0.9434
270	0.9423	0.9430	0.9432	0.9433	0.9433
300	0.9423	0.9430	0.9432	0.9433	0.9433
330	0.9423	0.9430	0.9432	0.9433	0.9433
360	0.9423	0.9430	0.9432	0.9433	0.9433
MTBF	341.30	341.50	341.56	341.58	341.59

which is further sent to shearing section for manufacturing sheets of required lengths. Figure 1 gives us the schematic diagram of sheet manufacturing system.

2.1 System Description

The sheet manufacturing system consists of following subsystems:

Conveyor. It consists of cylindrically shaped barrels used to transport slabs through the entire mill. It rarely fails.

Extractor. It is a hydraulically operated robotic arm having fingers like structure to hold the slab for inward and outward movement. This subsystem never fails.

Furnace (A). It employs walking beam mechanism and consists of heating and soaking zones. It has two units in parallel. Failure of single unit reduces the capacity of the system. Complete system fails when both units fail.

De-scaling unit. It removes oxide scale from the hot slab and consists of pump, hose pipe, and nozzle. It never fails.

Roughing Mill (B). It consists of four horizontal rolls. Out of these, two are intermediate rolls whereas the remaining two are called ‘backup roll’ and ‘work roll.’ This machine reduces the thickness of slab from 200 to 40 mm in five to seven passes. After this process, the slab is called ‘transfer bar.’ It is a single unit, failure of which results in complete failure of the system.

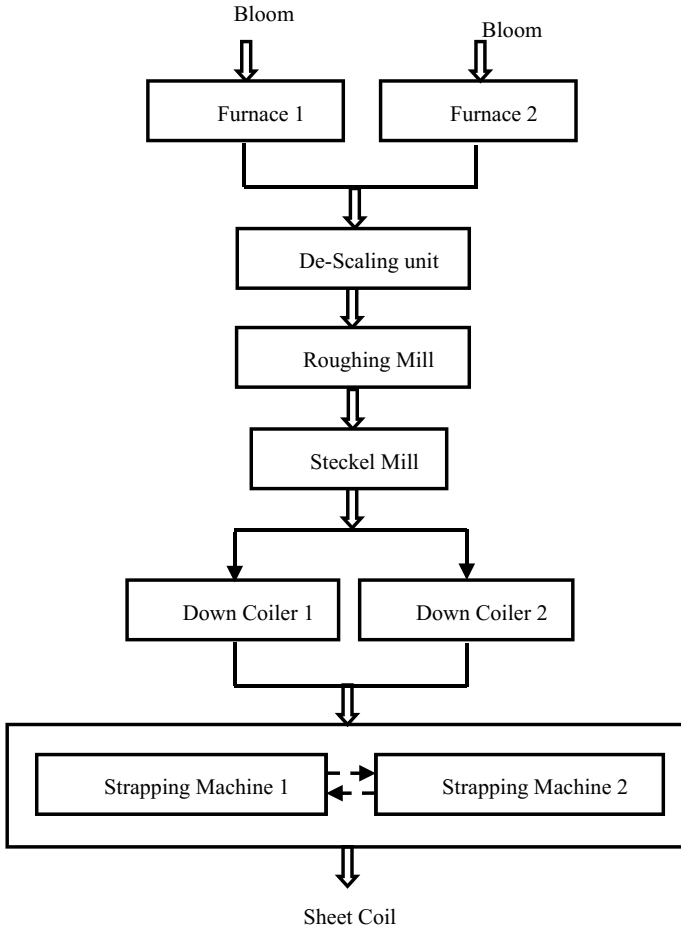


Fig. 1 Schematic diagram of sheet production system

Steckel Mill (C). This machine is meant for final thickness reduction and consists of two hot coilers; one at entry and the other at exit, two pinch rolls (one on each side) and a roughing stand in the middle. Pinch rolls retain the bar in tension and avoid loopy formation. Roughing stand consists of V-edger which cuts the extra material from the sides of the bar. Transfer bar is passed through pinch rolls and roughing stand five to seven times and is finally called ‘sheet.’ It is single unit whose failure shuts down the complete system.

Down Coiler (D). Its main function is winding of coil. It consists of a rotating mandrel on which coil is wound. After complete winding, the mandrel moves inside and the coil falls down on the platform. This coil is then carried away by the conveyors

and overhead crane. It consists of two units. If one unit fails, system still keeps working, though at reduced capacity. Failure of both units results in failure of the system.

Strapping Machine (E). Its function is to wind straps on the coil so that coil does not open up while being carried away. It also comprises of two units, one main and the other standby. System fails only when both units fail.

2.2 Notations

A, B, C, D, E	Indicate that respective subsystem is working at full capacity
a, b, c, d, e	Indicate that respective subsystem is in failed state
A', D'	Indicate that respective subsystem is working at reduced capacity
E _s	Indicate that one respective subsystem has failed
a_i ($i = 1-5$)	Indicate the failure rates of subsystems A, B, C, D, and E, respectively
β_i ($i = 1-5$)	Indicate the repair rates of subsystems A, B, C, D, and E, respectively
$P_0(t)$	Denotes the probability that at time 't', all the units are working
$P_i(x, t)$	Denotes the probability that at time 't', the system is in state i and having an elapsed repair time x

2.3 Assumptions

Present analysis is based on following assumptions:

- Failure and repair rates are constant and independent of each other and their unit is taken as per day.
- In case of assessment of availability using SVT, repair rates are considered variable and failure rates as constant.
- Performance wise, a repaired unit is as good as new.
- Sufficient service, repair/maintenance, and replacement facilities are available.
- There are no simultaneous failures.
- System may work at reduced capacity.
- Standby units are of the same nature and capacity as active units.

3 Mathematical Formulation of the System

To determine the reliability of sheet manufacturing system, Chapman–Kolmogorov differential equations are developed by applying SVT. Probability considerations, using mnemonic rule, give us the following set of differential equations associated with the transition diagram (Fig. 2) of the system at time $(t + \Delta t)$:

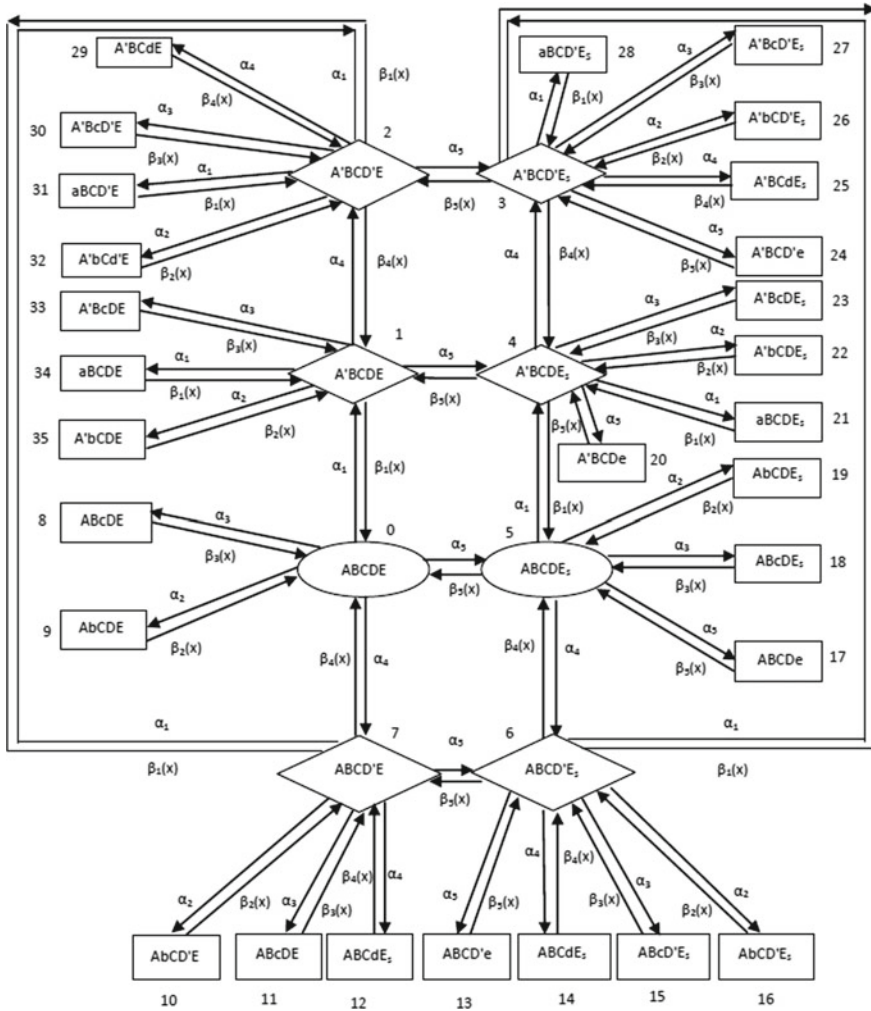


Fig. 2 Transition diagram of sheet production system

$$\begin{aligned}
 P_0(t + \Delta t) &= [1 - \alpha_1 \Delta t - \alpha_2 \Delta t - \alpha_3 \Delta t - \alpha_4 \Delta t - \alpha_5 \Delta t] P_0(t) \\
 &+ \int \beta_1(x) P_1(x, t) dx \Delta t + \int \beta_2(x) P_9(x, t) dx \Delta t \\
 &+ \int \beta_3(x) P_8(x, t) dx \Delta t + \int \beta_4(x) P_7(x, t) dx \Delta t \\
 &+ \int \beta_5(x) P_5(x, t) dx \Delta t
 \end{aligned}$$

$$\begin{aligned}
 P_0(t + \Delta t) - P_0(t) &= -[\alpha_1 \Delta t + \alpha_2 \Delta t + \alpha_3 \Delta t + \alpha_4 \Delta t + \alpha_5 \Delta t] P_0(t) \\
 &\quad + \int \beta_1(x) P_1(x, t) dx \Delta t + \int \beta_2(x) P_9(x, t) dx \Delta t \\
 &\quad + \int \beta_3(x) P_8(x, t) dx \Delta t \\
 &\quad + \int \beta_4(x) P_7(x, t) dx \Delta t + \int \beta_5(x) P_5(x, t) dx \Delta t \\
 \frac{P_0(t + \Delta t) - P_0(t)}{\Delta t} &= -[\alpha_1 + \alpha_2 + \alpha_3 + \alpha_4 + \alpha_5] P_0(t) + \int \beta_1(x) P_1(x, t) dx \\
 &\quad + \int \beta_2(x) P_9(x, t) dx + \int \beta_3(x) P_8(x, t) dx \\
 &\quad + \int \beta_4(x) P_7(x, t) dx + \int \beta_5(x) P_5(x, t) dx
 \end{aligned}$$

Dividing both sides by Δt , we get

$$\left[\frac{\partial}{\partial t} + L_0 \right] P_0(t) = M_0(t) \tag{1}$$

Similarly, we can write the differential equations for other states as

$$\left[\frac{\partial}{\partial t} + \frac{\partial}{\partial x} + L_1(x) \right] P_1(x, t) = M_1(x, t) \tag{2}$$

$$\left[\frac{\partial}{\partial t} + \frac{\partial}{\partial x} + L_2(x) \right] P_2(x, t) = M_2(x, t) \tag{3}$$

$$\left[\frac{\partial}{\partial t} + \frac{\partial}{\partial x} + L_3(x) \right] P_3(x, t) = M_3(x, t) \tag{4}$$

$$\left[\frac{\partial}{\partial t} + \frac{\partial}{\partial x} + L_4(x) \right] P_4(x, t) = M_4(x, t) \tag{5}$$

$$\left[\frac{\partial}{\partial t} + \frac{\partial}{\partial x} + L_5(x) \right] P_5(x, t) = M_5(x, t) \tag{6}$$

$$\left[\frac{\partial}{\partial t} + \frac{\partial}{\partial x} + L_6(x) \right] P_6(x, t) = M_6(x, t) \tag{7}$$

$$\left[\frac{\partial}{\partial t} + \frac{\partial}{\partial x} + L_7(x) \right] P_7(x, t) = M_7(x, t) \tag{8}$$

$$\left[\frac{\partial}{\partial t} + \frac{\partial}{\partial x} + \beta_1(x) \right] P_j(x, t) = 0; \quad j = 21, 28, 31, 34 \tag{9}$$

$$\left[\frac{\partial}{\partial t} + \frac{\partial}{\partial x} + \beta_2(x) \right] P_k(x, t) = 0; \quad k = 9, 10, 16, 19, 22, 26, 32, 35 \tag{10}$$

$$\left[\frac{\partial}{\partial t} + \frac{\partial}{\partial x} + \beta_3(x) \right] P_l(x, t) = 0; \quad l = 8, 11, 15, 18, 23, 27, 30, 33 \quad (11)$$

$$\left[\frac{\partial}{\partial t} + \frac{\partial}{\partial x} + \beta_4(x) \right] P_m(x, t) = 0; \quad m = 12, 14, 15, 29 \quad (12)$$

$$\left[\frac{\partial}{\partial t} + \frac{\partial}{\partial x} + \beta_5(x) \right] P_n(x, t) = 0; \quad n = 13, 17, 20, 24 \quad (13)$$

where

$$L_0 = \sum_{i=1}^5 \alpha_i$$

$$L_1(x) = \sum_{i=1}^5 \alpha_i + \beta_1(x)$$

$$L_2(x) = \sum_{i=1}^5 \alpha_i + \beta_1(x) + \beta_4(x)$$

$$L_3(x) = \sum_{i=1}^5 \alpha_i + \beta_1(x) + \beta_4(x) + \beta_5(x)$$

$$L_4(x) = \sum_{i=1}^5 \alpha_i + \beta_1(x) + \beta_5(x)$$

$$L_5(x) = \sum_{i=1}^5 \alpha_i + \beta_5(x)$$

$$L_6(x) = \sum_{i=1}^5 \alpha_i + \beta_4(x) + \beta_5(x)$$

$$L_7(x) = \sum_{i=1}^5 \alpha_i + \beta_4(x)$$

$$M_0(t) = \int \beta_1(x) P_1(x, t) dx + \int \beta_2(x) P_9(x, t) dx + \int \beta_3(x) P_8(x, t) dx \\ + \int \beta_4(x) P_7(x, t) dx + \int \beta_5(x) P_5(x, t) dx$$

$$M_1(x, t) = \alpha_1 P_0(t) + \int \beta_1(x) P_{34}(x, t) dx + \int \beta_2(x) P_{35}(x, t) dx \\ + \int \beta_3(x) P_{33}(x, t) dx + \int \beta_4(x) P_2(x, t) dx \\ + \int \beta_5(x) P_4(x, t) dx$$

$$\begin{aligned}
 M_2(x, t) &= \alpha_1 P_7(t) + \alpha_4 P_1(t) + \int \beta_1(x) P_{31}(x, t) dx + \int \beta_2(x) P_{32}(x, t) dx \\
 &+ \int \beta_3(x) P_{30}(x, t) dx + \int \beta_4(x) P_{29}(x, t) dx \\
 &+ \int \beta_5(x) P_3(x, t) dx
 \end{aligned}$$

$$\begin{aligned}
 M_3(x, t) &= \alpha_1 P_6(t) + \alpha_4 P_4(t) + \alpha_5 P_2(t) + \int \beta_1(x) P_{28}(x, t) dx \\
 &+ \int \beta_2(x) P_{26}(x, t) dx + \int \beta_3(x) P_{27}(x, t) dx \\
 &+ \int \beta_4(x) P_{25}(x, t) dx + \int \beta_5(x) P_{24}(x, t) dx
 \end{aligned}$$

$$\begin{aligned}
 M_4(x, t) &= \alpha_1 P_5(t) + \alpha_5 P_1(t) + \int \beta_1(x) P_{21}(x, t) dx + \int \beta_2(x) P_{22}(x, t) dx \\
 &+ \int \beta_3(x) P_{23}(x, t) dx + \int \beta_4(x) P_3(x, t) dx \\
 &+ \int \beta_5(x) P_{20}(x, t) dx
 \end{aligned}$$

$$\begin{aligned}
 M_5(x, t) &= \alpha_5 P_0(t) + \int \beta_1(x) P_4(x, t) dx + \int \beta_2(x) P_{19}(x, t) dx \\
 &+ \int \beta_3(x) P_{18}(x, t) dx + \int \beta_4(x) P_6(x, t) dx \\
 &+ \int \beta_5(x) P_{13}(x, t) dx
 \end{aligned}$$

$$\begin{aligned}
 M_6(x, t) &= \alpha_4 P_5(t) + \alpha_5 P_7(t) + \int \beta_1(x) P_3(x, t) dx + \int \beta_2(x) P_{16}(x, t) dx \\
 &+ \int \beta_3(x) P_{15}(x, t) dx + \int \beta_4(x) P_{14}(x, t) dx \\
 &+ \int \beta_5(x) P_{13}(x, t) dx
 \end{aligned}$$

$$\begin{aligned}
 M_7(x, t) &= \alpha_4 P_0(t) + \int \beta_1(x) P_2(x, t) dx + \int \beta_2(x) P_{10}(x, t) dx \\
 &+ \int \beta_3(x) P_{11}(x, t) dx + \int \beta_4(x) P_{12}(x, t) dx \\
 &+ \int \beta_5(x) P_6(x, t) dx
 \end{aligned}$$

Initial Conditions

$$P_0(0) = 1$$

$$P_i(x, 0) = 0, \quad \text{where, } i = 1, 2, 3 \dots 35$$

Boundary Conditions

$$P_1(0, t) = \alpha_1 P_0(t)$$

$$P_2(0, t) = \int \alpha_1 P_7(x, t) dx + \int \alpha_4 P_1(x, t) dx$$

$$P_3(0, t) = \int \alpha_1 P_6(x, t) dx + \int \alpha_4 P_4(x, t) dx + \int \alpha_5 P_2(x, t) dx$$

$$P_4(0, t) = \int \alpha_1 P_5(x, t) dx + \int \alpha_5 P_1(x, t) dx$$

$$P_5(0, t) = \alpha_5 P_0(t)$$

$$P_6(0, t) = \int \alpha_4 P_5(x, t) dx + \int \alpha_5 P_7(x, t) dx$$

$$P_7(0, t) = \alpha_4 P_0(t)$$

$$P_8(0, t) = \alpha_3 P_0(t)$$

$$P_9(0, t) = \alpha_2 P_0(t)$$

$$P_{10}(0, t) = \int \alpha_2 P_7(x, t) dx$$

$$P_{11}(0, t) = \int \alpha_3 P_7(x, t) dx$$

$$P_{12}(0, t) = \int \alpha_4 P_7(x, t) dx$$

$$P_{13}(0, t) = \int \alpha_5 P_6(x, t) dx$$

$$P_{14}(0, t) = \int \alpha_4 P_6(x, t) dx$$

$$P_{15}(0, t) = \int \alpha_3 P_6(x, t) dx$$

$$P_{16}(0, t) = \int \alpha_2 P_6(x, t) dx$$

$$P_{17}(0, t) = \int \alpha_5 P_5(x, t) dx$$

$$P_{18}(0, t) = \int \alpha_3 P_5(x, t) dx$$

$$P_{19}(0, t) = \int \alpha_2 P_5(x, t) dx$$

$$P_{20}(0, t) = \int \alpha_5 P_4(x, t) dx$$

$$P_{21}(0, t) = \int \alpha_1 P_4(x, t) dx$$

$$P_{22}(0, t) = \int \alpha_2 P_4(x, t) dx$$

$$P_{23}(0, t) = \int \alpha_3 P_4(x, t) dx$$

$$P_{24}(0, t) = \int \alpha_5 P_3(x, t) dx$$

$$P_{25}(0, t) = \int \alpha_4 P_3(x, t) dx$$

$$P_{26}(0, t) = \int \alpha_2 P_3(x, t) dx$$

$$P_{27}(0, t) = \int \alpha_3 P_3(x, t) dx$$

$$P_{28}(0, t) = \int \alpha_1 P_3(x, t) dx$$

$$P_{29}(0, t) = \int \alpha_4 P_2(x, t) dx$$

$$P_{30}(0, t) = \int \alpha_3 P_2(x, t) dx$$

$$P_{31}(0, t) = \int \alpha_1 P_2(x, t) dx$$

$$P_{32}(0, t) = \int \alpha_2 P_2(x, t) dx$$

$$P_{33}(0, t) = \int \alpha_3 P_1(x, t) dx$$

$$P_{34}(0, t) = \int \alpha_1 P_1(x, t) dx$$

$$P_{35}(0, t) = \int \alpha_2 P_1(x, t) dx$$

Unless otherwise mentioned, the limits of integration are from 0 to ∞ .

Set of differential equations from (1) to (13) along with initial conditions and boundary conditions is called Chapman–Kolmogorov differential-difference equations.

3.1 Availability of the System When Failure and Repair Rates are Constant

As has been observed above, solving the equations becomes a cumbersome task if either failure rate or repair rate is varied. Hence, in order to simplify the problem, failure and repair rates are considered constant. In this case, the system of Eqs. (1–13) can be represented as follows:

$$P_0(t) \left[\frac{\partial}{\partial t} + \sum_{i=1}^5 \alpha_i \right] = P_1(t)\beta_1 + P_9(t)\beta_2 + P_8(t)\beta_3 + P_7(t)\beta_4 + P_5(t)\beta_5 \quad (14)$$

$$P_1(t) \left[\frac{\partial}{\partial t} + \sum_{i=1}^5 \alpha_i + \beta_1 \right] = P_{34}(t)\beta_1 + P_{35}(t)\beta_2 + P_{33}(t)\beta_3 + P_2(t)\beta_4 + P_4(t)\beta_5 + P_0(t)\alpha_1 \quad (15)$$

$$P_2(t) \left[\frac{\partial}{\partial t} + \sum_{i=1}^5 \alpha_i + \beta_1 + \beta_4 \right] = P_{31}(t)\beta_1 + P_{32}(t)\beta_2 + P_{30}(t)\beta_3 + P_{29}(t)\beta_4 + P_3(t)\beta_5 + P_7(t)\alpha_1 + P_1(t)\alpha_4 \quad (16)$$

$$P_3(t) \left[\frac{\partial}{\partial t} + \sum_{i=1}^5 \alpha_i + \beta_1 + \beta_4 + \beta_5 \right] = P_{28}(t)\beta_1 + P_{26}(t)\beta_2 + P_{27}(t)\beta_3 + P_{25}(t)\beta_4 + P_{24}(t)\beta_5 + P_6(t)\alpha_1 + P_4(t)\alpha_4 + P_2(t)\alpha_5 \quad (17)$$

$$P_4(t) \left[\frac{\partial}{\partial t} + \sum_{i=1}^5 \alpha_i + \beta_1 + \beta_5 \right] = P_{21}(t)\beta_1 + P_{22}(t)\beta_2 + P_{23}(t)\beta_3 + P_3(t)\beta_4 + P_{20}(t)\beta_5 + P_5(t)\alpha_1 + P_1(t)\alpha_5 \quad (18)$$

$$P_5(t) \left[\frac{\partial}{\partial t} + \sum_{i=1}^5 \alpha_i + \beta_5 \right] = P_4(t)\beta_1 + P_{19}(t)\beta_2 + P_{18}(t)\beta_3 + P_6(t)\beta_4 + P_{13}(t)\beta_5 + P_0(t)\alpha_5 \quad (19)$$

$$P_6(t) \left[\frac{\partial}{\partial t} + \sum_{i=1}^5 \alpha_i + \beta_4 + \beta_5 \right] = P_3(t)\beta_1 + P_{16}(t)\beta_2 + P_{15}(t)\beta_3 + P_{14}(t)\beta_4 + P_{13}(t)\beta_5 + P_5(t)\alpha_4 + P_7(t)\alpha_5 \quad (20)$$

$$P_7(t) \left[\frac{\partial}{\partial t} + \sum_{i=1}^5 \alpha_i + \beta_4 \right] = P_2(t)\beta_1 + P_{10}(t)\beta_2 + P_{11}(t)\beta_3 + P_{12}(t)\beta_4 + P_6(t)\beta_5 + P_0(t)\alpha_4 \quad (21)$$

$$P_i(t) \left[\frac{\partial}{\partial t} + \beta_1 \right] = P_j(t) \alpha_1 \quad (22)$$

for $i = 21, j = 4; i = 28, j = 3; i = 31, j = 2; i = 34, j = 1$

$$P_i(t) \left[\frac{\partial}{\partial t} + \beta_2 \right] = P_j(t) \alpha_2 \quad (23)$$

for $i = 9, j = 0; i = 10, j = 7; i = 16, j = 6; i = 19, j = 5; i = 22, j = 4; i = 26, j = 3; i = 32, j = 2; i = 35, j = 1$

$$P_i(t) \left[\frac{\partial}{\partial t} + \beta_3 \right] = P_j(t) \alpha_3 \quad (24)$$

for $i = 8, j = 3; i = 11, j = 7; i = 15, j = 6; i = 18, j = 5; i = 23, j = 4; i = 27, j = 3; i = 30, j = 2; i = 33, j = 1$

$$P_i(t) \left[\frac{\partial}{\partial t} + \beta_4 \right] = P_j(t) \alpha_4 \quad (25)$$

for $i = 12, j = 7; i = 14, j = 6; i = 25, j = 3; i = 29, j = 2$

$$P_i(t) \left[\frac{\partial}{\partial t} + \beta_5 \right] = P_j(t) \alpha_5 \quad (26)$$

for $i = 13, j = 6; i = 17, j = 5; i = 20, j = 4; i = 24, j = 3$

Initial Conditions

$$\begin{aligned} P_i(t) &= 1 \quad \text{for } i = 0 \\ &= 0 \quad \text{for } i \neq 0 \end{aligned}$$

The system of differential Eqs. (14–26) with initial conditions has been solved numerically using Runge–Kutta fourth order method to examine the effect of failure and repair rates on availability in transient state. Analysis has been done for a period of one year (360 days) divided over an interval of 1 month (30 days) and the data has been tabulated in Tables 1, 2, 3, 4, 5, 6, 7, 8, 9, 10. These tables present the effect of failure and repair rates of various subsystems on the overall system reliability. MTBF, computed using Simpson's 3/8 rule, has been given in the last row of each table.

4 Results and Analysis

4.1 Effect of Failure Rate of Furnace (α_1) on System Availability

By taking failure rate α_1 as 0.0014286, 0.0073214, 0.0132143, 0.0191071, 0.025 and keeping $\alpha_2 = 0.001$, $\alpha_3 = 0.0006667$, $\alpha_4 = 0.0011111$, $\alpha_5 = 0.0011765$, $\beta_1 = 0.0208333$, $\beta_2 = 0.03125$, $\beta_3 = 0.0285714$, $\beta_4 = 0.0454545$ and $\beta_5 = 0.0357143$, the availability of the system has been computed and compiled in Table 1, which shows that availability and MTBF decrease by 35.78 and 31.88%, respectively. Also availability decreases by up to 26.51% with the increase in time from 30 to 360 days.

4.2 Effect of Failure Rate of Roughing Mill (α_2) on System Availability

As presented in Table 2, as failure rate α_2 increases from 0.001 to 0.0033333 and the values of α_1 , α_3 , α_4 , α_5 , β_1 , β_2 , β_3 , β_4 , and β_5 are kept at 0.0014286, 0.0006667, 0.0011111, 0.0011765, 0.0208333, 0.03125, 0.0285714, 0.0454545, and 0.0357143 respectively, availability and MTBF both decline by around 6%. However availability decreases by up to 4.42% as time increases from 30 to 360 days.

4.3 Effect of Failure Rate of Steckel Mill (α_3) on System Availability

Next, the effect of failure rate of Steckel mill on the system availability has been studied. The results shown in Table 3 indicate that by varying failure rate $\alpha_3 = 0.0006667$, 0.001, 0.0013333, 0.0016667, and 0.002 and taking $\alpha_1 = 0.0014286$, $\alpha_2 = 0.001$, $\alpha_4 = 0.0011111$, $\alpha_5 = 0.0011765$, $\beta_1 = 0.0208333$, $\beta_2 = 0.03125$, $\beta_3 = 0.0285714$, $\beta_4 = 0.0454545$, and $\beta_5 = 0.0357143$, availability decreases by 3.97%. It is also observed that there is a decrease of 3.88% in availability with the increase in time from 30 to 360 days. In this case, MTBF decreases by 3.84% with the increase in failure rate.

4.4 Effect of Failure Rate of Down Coiler (α_4) on System Availability

In this case, as failure rate α_4 increases from 0.0011111 to 0.02 and the values of $\alpha_1, \alpha_2, \alpha_3, \alpha_5, \beta_1, \beta_2, \beta_3, \beta_4,$ and β_5 are kept at 0.0014286, 0.001, 0.0006667, 0.0011765, 0.0208333, 0.03125, 0.0285714, 0.0454545, and 0.0357143, availability goes down by 10.53%. However, it decreases by up to 7.5% as time increases from 30 to 360 days. It is observed that MTBF also decreases by 10% as failure rate increases.

4.5 Effect of Failure Rate of Strapping Machine (α_5) on System Availability

Table 5 shows that as failure rate α_5 increases from 0.0011765 to 0.0142857 and the values of $\alpha_1, \alpha_2, \alpha_3, \alpha_4, \beta_1, \beta_2, \beta_3, \beta_4,$ and β_5 are kept at 0.0014286, 0.001, 0.0006667, 0.0011111, 0.0208333, 0.03125, 0.0285714, 0.0454545, and 0.0357143 respectively, availability shows a downward trend of maximum 8.86%. Availability also decreases by 7.74% as time increases from 30 to 360 days. MTBF decreases by 8.19% as failure rate increases.

4.6 Effect of Repair Rate of Furnace (β_1) on System Availability

The results presented in Table 6 indicate the availability of the system when repair rate β_1 of the furnace subsystem is varied from 0.0208333 to 0.25. Taking values of $\alpha_1 = 0.0014286, \alpha_2 = 0.001, \alpha_3 = 0.0006667, \alpha_4 = 0.0011111, \alpha_5 = 0.0011765, \beta_2 = 0.03125, \beta_3 = 0.0285714, \beta_4 = 0.0454545$ and $\beta_5 = 0.0357143$, availability increases by 0.38%. Whereas, there is a decrease of 2.12–2.44% in availability as number of days increases from 30 to 360. MTBF decreases by 0.3%.

4.7 Effect of Repair Rate of Roughing Mill (β_2) on System Availability

The effect of repair rate of roughing mill on the system availability has been studied and it is observed that as β_2 is varied from 0.03125 to 0.125 in five steps and the values of failure and repair rates of other subsystems, i.e., $\alpha_1, \alpha_2, \alpha_3, \alpha_4, \alpha_5, \beta_1, \beta_3, \beta_4,$ and β_5 are taken as 0.0014286, 0.001, 0.0006667, 0.0011111, 0.0011765, 0.0208333, 0.0285714, 0.0454545, and 0.0357143, respectively, availability of the system decreases by 1.39–2.44% with the increase in time from 30 to 360 days. But,

it increases by 2.18% as repair rate increases from 0.03333 to 0.125. Improvement in repair rate increases the MTBF by approximately 2% as shown in Table 7.

4.8 Effect of Repair Rate of Steckel Mill (β_3) on System Availability

Table 8 shows the effect of improvement of repair rate of Steckel mill on overall system availability. One can observe that as β_3 increases from 0.0285714 to 0.20 and the value of failure and repair rates of other subsystems is kept at $\alpha_1 = 0.0014286$, $\alpha_2 = 0.001$, $\alpha_3 = 0.0006667$, $\alpha_4 = 0.0011111$, $\alpha_5 = 0.0011765$, $\beta_1 = 0.0208333$, $\beta_2 = 0.03125$, $\beta_4 = 0.0454545$, and $\beta_5 = 0.0357143$, availability increases by 1.8%. But as the number of days increases from 30 to 360, availability decreases by 1.63–2.44%. MTBF increases by 1.68% with the increase in repair rate.

4.9 Effect of Repair Rate of Down Coiler (β_4) on System Availability

Next, the effect of improvement of repair rate of down coiler on the overall system availability has been computed as shown in Table 9. It is seen that as β_4 increases from 0.0454545 to 0.50 and the value of failure and repair rates of other subsystems is kept at $\alpha_1 = 0.0014286$, $\alpha_2 = 0.001$, $\alpha_3 = 0.0006667$, $\alpha_4 = 0.0011111$, $\alpha_5 = 0.0011765$, $\beta_1 = 0.0208333$, $\beta_2 = 0.03125$, $\beta_3 = 0.0285714$, and $\beta_5 = 0.0357143$, availability shows an increase of 0.05%. But as the number of days increases from 30 to 360, there is a decrease of around 2.42–2.44% in the value of availability. MTBF increases by 0.04% with the increase in repair rate.

4.10 Effect of Repair Rate of Strapping Machine (β_5) on System Availability

At last, the effect of improvement of repair rate of strapping machine on the overall system availability has been analyzed as shown in Table 10. It is observed that as β_5 increases from 0.0357143 to 0.1428571 and the value of failure and repair rates of other subsystems is kept at $\alpha_1 = 0.0014286$, $\alpha_2 = 0.001$, $\alpha_3 = 0.0006667$, $\alpha_4 = 0.0011111$, $\alpha_5 = 0.0011765$, $\beta_1 = 0.0208333$, $\beta_2 = 0.03125$, $\beta_3 = 0.0285714$, and $\beta_4 = 0.0454545$, availability increases by 0.10%. But as the number of days increases from 30 to 360, there is a decrease of around 2.36–2.44% in the value of availability. MTBF also increases by 0.08%.

5 Conclusions

By analyzing the results computed in Tables 1, 2, 3, 4, 5, 6, 7, 8, 9, 10, it reveals that:

- Improvement in repair rate of furnace, down coiler, and strapping machine subsystems do not have much effect on the system availability. Roughing mill and Steckel mill subsystems are almost equally effective toward the overall system availability.
- In case of increase in failure rate, it is observed that all the subsystems have substantial effect on the system availability. Furnace subsystem has maximum impact on the availability as well as on MTBF of the system. Second and third most important subsystems are down coiler and strapping machine, respectively. However, Steckel mill subsystem has minimum impact on the availability and MTBF of the system.
- Hence, it is suggested that more attention should be paid to the upkeep of furnace subsystem.
- As far as maintenance planning and scheduling of subsystems are concerned, it should be as given below:
 - (i) Furnace subsystem
 - (ii) Down coiler subsystem
 - (iii) Strapping machine subsystem
 - (iv) Roughing mill subsystem
 - (v) Steckel mill subsystem

References

1. Moustafa MS (1996) Transient analysis of reliability with and without repair for K-out-of-N: G systems with two failure modes. *Reliab Eng Syst Safe* 53:31–35. [https://doi.org/10.1016/0951-8320\(96\)00014-2](https://doi.org/10.1016/0951-8320(96)00014-2)
2. Limnios N (1997) Dependability analysis of semi-markov systems. *Reliab Eng Syst Safe* 55:203–207. [https://doi.org/10.1016/S0951-8320\(96\)00121-4](https://doi.org/10.1016/S0951-8320(96)00121-4)
3. Qamber IS (1999) Reliability study of two engineering models using LU decomposition. *Reliab Eng Syst Safe* 64:359–364. [https://doi.org/10.1016/S0951-8320\(98\)00082-9](https://doi.org/10.1016/S0951-8320(98)00082-9)
4. Biswas A, Sarkar J (2000) Availability of a system maintained through several imperfect repairs before a replacement or a perfect repair. *Stat Probab Lett* 50(2):105–114. [https://doi.org/10.1016/S0167-7152\(00\)00087-0](https://doi.org/10.1016/S0167-7152(00)00087-0)
5. Dai Y, Jia Y (2001) Reliability of a VMC and its improvement. *Reliab Eng Syst Safe* 72:99–102. [https://doi.org/10.1016/S0951-8320\(00\)00104-6](https://doi.org/10.1016/S0951-8320(00)00104-6)
6. Avontuur GC, Werff KV (2002) Systems reliability analysis of mechanical and hydraulic drive systems. *Reliab Eng Syst Safe* 77:121–130. [https://doi.org/10.1016/S0951-8320\(02\)00039-X](https://doi.org/10.1016/S0951-8320(02)00039-X)
7. Zou T, Mahadevan S, Mourelatos Z, Meernik P (2002) Reliability analysis of automotive body-door subsystem. *Reliab Eng Syst Safe* 78:315–324. [https://doi.org/10.1016/S0951-8320\(02\)00178-3](https://doi.org/10.1016/S0951-8320(02)00178-3)
8. Ebrahimi NB (2003) Indirect assessment of system reliability. *IEEE T Reliab* 52(1):58–62. <https://doi.org/10.1109/TR.2002.805779>

9. Rauzy A (2004) An experimental study on iterative methods to compute transient solutions of large Markov models. *Reliab Eng Syst Safe* 86:105–115. <https://doi.org/10.1016/j.res.2004.01.007>
10. Chen D, Trivedi KS (2005) Optimization for condition-based maintenance with semi-Markov decision process. *Reliab Eng Syst Safe* 90:25–29. <https://doi.org/10.1016/j.res.2004.11.001>
11. Samrout M, Yalaoui F, Châtelet E, Chebbo N (2005) New methods to minimize the preventive maintenance cost of series-parallel systems using ant colony optimization. *Reliab Eng Syst Safe* 89:346–354. <https://doi.org/10.1016/j.res.2004.09.005>
12. Hamada M, Martz HF, Berg EC, Koehler AJ (2006) Optimizing the product-based availability of a buffered industrial process. *Reliab Eng Syst Safe* 91:1039–1048. <https://doi.org/10.1016/j.res.2005.11.059>
13. Levitin G (2007) Block diagram method for analyzing multi-state systems with uncovered failures. *Reliab Eng Syst Safe* 92:727–734. <https://doi.org/10.1016/j.res.2006.02.009>
14. Dhillon BS, Shah AS (2007) Availability analysis of a generalized maintainable three-state device parallel system with human error and common-cause failures. *J Qual Maint Eng* 13(4):411–432. <https://doi.org/10.1108/13552510710829498>
15. Sachdeva A, Kumar P, Kumar D (2009) Behavioral and performance analysis of feeding system using stochastic reward nets. *Int J Adv Manuf Technol* 45(1–2):156–169. <https://doi.org/10.1007/s00170-009-1960-8>
16. Garg S, Singh J, Singh DV (2010) Availability analysis of crank-case manufacturing in a two-wheeler automobile industry. *Appl Math Model* 34:1672–1683. <https://doi.org/10.1016/j.apm.2009.09.016>
17. Rodriguez CEP, De Souza GFM (2010) Reliability concepts applied to cutting tool change time. *Reliab Eng Syst Safe* 95:866–873. <https://doi.org/10.1016/j.res.2010.03.005>
18. Sinha P (2011) Architectural design and reliability analysis of a fail-operational brake-by-wire system from ISO 26262 perspectives. *Reliab Eng Syst Safe* 96:1349–1359. <https://doi.org/10.1016/j.res.2011.03.013>
19. Levitin G, Xing L, Amari SV, Dai Y (2013) Reliability of non-repairable phased-mission systems with propagated failures. *Reliab Eng Syst Safe* 119:218–228. <https://doi.org/10.1016/j.res.2013.06.005>
20. Doostparast M, Kolahan F, Doostparast M (2014) A reliability-based approach to optimize preventive maintenance scheduling for coherent systems. *Reliab Eng Syst Safe* 126:98–106. <https://doi.org/10.1016/j.res.2014.01.010>
21. Liu Z, Tan C, Leng F (2015) A reliability-based design concept for lithium-ion battery pack in electric vehicles. *Reliab Eng Syst Safe* 134:169–177. <https://doi.org/10.1016/j.res.2014.10.010>
22. Amann C, Kadau K (2016) Numerically efficient modified Runge-Kutta solver for fatigue crack growth analysis. *Eng Fract Mech* 161:55–62. <https://doi.org/10.1016/j.engfractmech.2016.03.021>
23. Pakdaman M, Ahmadian A, Effati S, Salahshour S, Baleanu D (2017) Solving differential equations of fractional order using an optimization technique based on training artificial neural network. *Appl Math Comput* 293:81–95. <https://doi.org/10.1016/j.amc.2016.07.021>

Modeling the Metrics of MRB, TRB, and ORB in the Implementation of Green Agile Manufacturing Strategies: An ANP Approach



Bhupendra Prakash Sharma, K. Ranade, Ankit Singh, Umesh Kumar Vates and G. S. Rao

Abstract In this research work, an attempt has been made toward easy and fast adjustment to sudden change and improvements in the quality of products and customer services is known as “agility” in the manufacturing environment. Implementation of agile practices in any organization refers a tremendous commitment toward identifying and recognizing the critical barriers. Presently, certain barriers have been identified and further been categorized into management-related barriers (MRB), technology-related barriers (TRB), and operator-related barriers (ORB). The barriers affecting the implementation of agility due to the operators and their weak skills fall under ORB, the hindrances created due to the various technologies that are in use which restrict some of the work comes under TRB, and the problems occurring at the management level, due to the employees, are considered under MRB. The main purpose of this research is to suggest the measured effectiveness of MRB, TRB, and ORB, using an analytical network process (ANP) framework. This quantified value shall help the decision makers to derive suitable strategies to overcome identified category of barriers before the implementation of agile practices. The ANP framework development was carried out through identified categories of barriers with respect to certain determinants and dimensions for evaluating the impact of each category of identified barriers. Findings portray that the TRBs have maximum impact on implementation process followed by MRBs and ORBs.

Keywords Agile manufacturing · Operator-related barriers · Management-related barriers · Technology-related barriers · Analytical network process

1 Introduction

Taking into account the present scenario, to remain a recognized and valuable part in today’s competition, it is important to explore and adapt to an advancing manufacturing environment. After the successful implementation of lean manufacturing

B. P. Sharma (✉) · K. Ranade · A. Singh · U. K. Vates · G. S. Rao
Department of Mechanical Engineering, Amity University, Noida 201313, Uttar Pradesh, India
e-mail: bpsharma@amity.edu

techniques and methodologies, a new and advanced concept of manufacturing was sought after known as agile manufacturing. This concept is nearly related to lean: that is in which the aim of the company was to reduce wastes and cut all the costs not related to the products directly to increase their profits. Agility on the other hand adds another dimension to it that is meeting their customer demands effectively as well as rapidly. Agile manufacturing is an approach to manufacturing and is focused on prioritizing and meeting the demands and needs of the customers while in parallel, maintenance of high-quality standards, and overall expense control that are involved while producing a product [1]. This approach is directed toward companies which work in an environment that is highly competitive and where even the smallest variations in product delivery and performance can create a big difference to the company's survival and reputation among consumers over the long run. It has four main principles: valuing human knowledge and skills; being ready for change; forming virtual partnerships; and delivering value to the customers [2].

All this said, for implementing something new or bringing about a change in a certain way of working, many problems come in our direction, trying to deviate us from our goal. We meet many barriers and hindrances on our path to implementing agile manufacturing in the companies. These barriers can be many and may fall under various categories. In the current research paper, these barriers have been broadly classified into three main categories and have to be weighed out according to their impact on the company, using a multi-criteria selection tool, i.e., analytical network process (ANP).

2 Impact of AM Implementation: Literature Review

Due to the upsurge of the competition in today's manufacturing environment's scenario, industries strive to remain in the game. Their goal is to advance their company's manufacturing strategies and methodologies and meet their customers' demands more quickly and effectively. Nowadays, companies are familiarizing themselves with agile manufacturing methods and practices and are working their way to implement it. To gain agility, a company has to advance its way of working and manufacturing. Not only that, agility is concerned with adaptive capabilities of an industry as well, i.e., how easily and rapidly an industry is able to adapt and adjust to sudden changes (can be changed in customer demands or other requirements).

2.1 Agile Manufacturing

Agility of a company is notified as the ability of an organization to live up to the mark in the environment of continuous high competition, unexpected and uncalculated change and to respond efficiently and quickly to comply to rapidly changing markets, driven by valuing of products and services according to the customer [3]. It can

likewise be said that the idea of deftness alludes to specific strategies which makes an organization invulnerable to harm caused by unforeseen occasions and startling conditions. This is accomplished by the association having the capacity to respond and adjust rapidly [4].

2.2 *Evolution to Agile Manufacturing*

All the important measurements of agile manufacturing, for example, innovation, individuals, organization, administration, and so forth are however unique for various organizations.

For progressing to agile manufacturing, we have to:

- Examine and characterize the fundamental reasonable system on which the agile manufacturing undertakings must be assembled.
- Explore and comprehend the idea of large-scale manufacturing worldview and of the social and methodological troubles included, similar to the obstructions and the hindrances looked amid the change to agile manufacturing.
- Define a hindrance-free philosophy for outlining an assembling endeavor.

Amid the changing procedure, different methodological troubles are associated with the procedure. The troubles are the hindrances to fruitful execution of agile manufacturing.

To expel these hindrances, we initially need to learn about the squanders that prompt these boundaries. The squanders recognized are of eight sorts:

- **Overproduction:** Producing in overabundance or too early brings about poor stream of merchandise and data and causes abundance of stock.
- **Defects:** Frequent and various mistakes in printed material and quality issues in the item or material outcomes in scrap or revamp and corrupted conveyance execution.
- **Unnecessary stock:** Excessive capacity and deferral of data or items brings about surfeit stock and costs, which prompts poor client benefit.
- **Inappropriate processing:** Doing the work processes using wrong systems, procedures, or set of tools often, when a much simpler approach might turn out to be more effective.
- **Excessive transportation:** Extra movement of operators, goods, and information results in wastage of time and cost.
- **Waiting:** Long periods of inactivity of goods, operators, machines, and information results in poor flow and long lead times.
- **Unnecessary motion:** Poor space utilization or workplace organization results in poor ergonomics (e.g., frequently lost items and excessive stretching or bending).
- **Underutilization of employee:** Unused skills and creativity of employees to improve the processes and practices refer to wastage of available knowledge, experience, or skill of the workforce not using them in the proper department and

by not exploiting their skills usefully. This can be due to poor hiring techniques by the management [5].

Several barriers have been identified by performing a literature review of various research papers and discussions with the academia and experts in the industry.

- Sharing various resources and newer technologies among companies is mandatory and so one should think a little beyond just a single firm [6].
- Flexible Workforce: Flexibility of the workforce and multi-skilled personnel, implementation of the job rotation system, making workforce largely aware and trained, and demanding high capacity to innovate [6].
- Flexible Workplace: An eco- and worker friendly workplace should be maintained; also highly automated setups and their upgradation and retrofitting should be done from time to time, usage of collapsible setups, and usage of jigs fixtures. Well-equipped servicing centers help to build a flexible workplace [7].
- Supplier Involvement: One should keep a rather close contact with all the suppliers for various deliveries so that it is delivered in the right and specified qualities and quantities which will further help to reduce waste. So maintain a relationship with the supplier for spontaneous supply of raw material which would help in satisfying customer's flexible demand [8].
- Human Resource Management (HRM): Active involvement, cooperativeness, firm belief and dedication, and decision-making capability among the workers/employees are very important factors for setting up of Lean-Green-Agile Manufacturing System (LGAMS) [9].
- Customer Focus: Close contacts with the customer will help in having direct access on their given feedback on quality, cost, and delivery. Due to increase in awareness of environmental degradation, customers prefer environment friendly products. Specification of product life to customer should be provided, and encourage the customer to switch to new products [10].
- Customer Feedback System: The usage of a well-defined voice of customer (VOC), empowers and trains the employee to resolve customer-related problems. Welcome the suggestions made by the customer about the concept and develop such an environment so that the customer can give their feedback with ease. Incorporation of customer's feedback of products will lead to effective and efficient customer feedback and their contentment regarding the service [11].
- Information Technology Integration: The increase in communication between the departments will reduce wastage of time. Handling material flow and various other resources will help in managing the green supply chain quite efficiently. Eliminate paper work and replace it with applications of IT and adoption of multimedia technology for communication in LGA systems [12].
- Resource Optimization: Usage of advanced optimization techniques to reduce wastage of materials by maintaining minimum inventory. Also the usage of natural resources in a sustainable manner [13].
- Top Management Commitment (TMC): AM recommends and supports that as leader's reference to employees must be as associates and not commodities, leading them by examples, coaching, and mentoring.

- Transparent sharing of information, regularity in conducting management–employee meetings, and participative management are just some of the many attributes of AMS [14, 15].

The identified barriers are further divided into three categories namely, operator-related barriers, management-related barriers, and technology-related barriers. Now, investigation and prioritization of these barriers are done using the ANP method.

3 Analytical Network Process (ANP)

As said above, ANP approach is utilized to explore and organize the classes of these hindrances. The effect every classification of hindrances has on the organization is ascertained utilizing this approach. As of today, a considerably more broad type of the analytical hierarchical process has been proposed as a precise approach, which joins reliant connections and input among choices and choice characteristics for demonstrating the mind-boggling choice conditions. This method is known as the logical system process (ANP) [16]. ANP is a multi-criteria basic leadership apparatus. It permits the thought of interdependencies between and in addition among various property levels. ANP includes speaking to progressively the connections, yet does not take after an unbending various leveled structure as AHP does. The ANP approach permits more complex interrelationships among the properties and the choice levels. ANP structures out the issues of the frameworks in which the connections between the levels are not effectively spoken to as higher or lower since all are practically taken as similarly heightening (Fig. 1; Table 1).

Table 1 Abbreviation key

FWF	Flexible work force	SI	Supplier involvement
HRM	Human resource management	FWP	Flexible workplace
RO	Resource optimization	TMC	Top management commitment
ST	Sharing resources and technology	ORB	Operator-related barriers
ITI	Information technology integration	TRB	Technology-related barriers
CFS	Customer feedback system	MRB	Management-related barriers

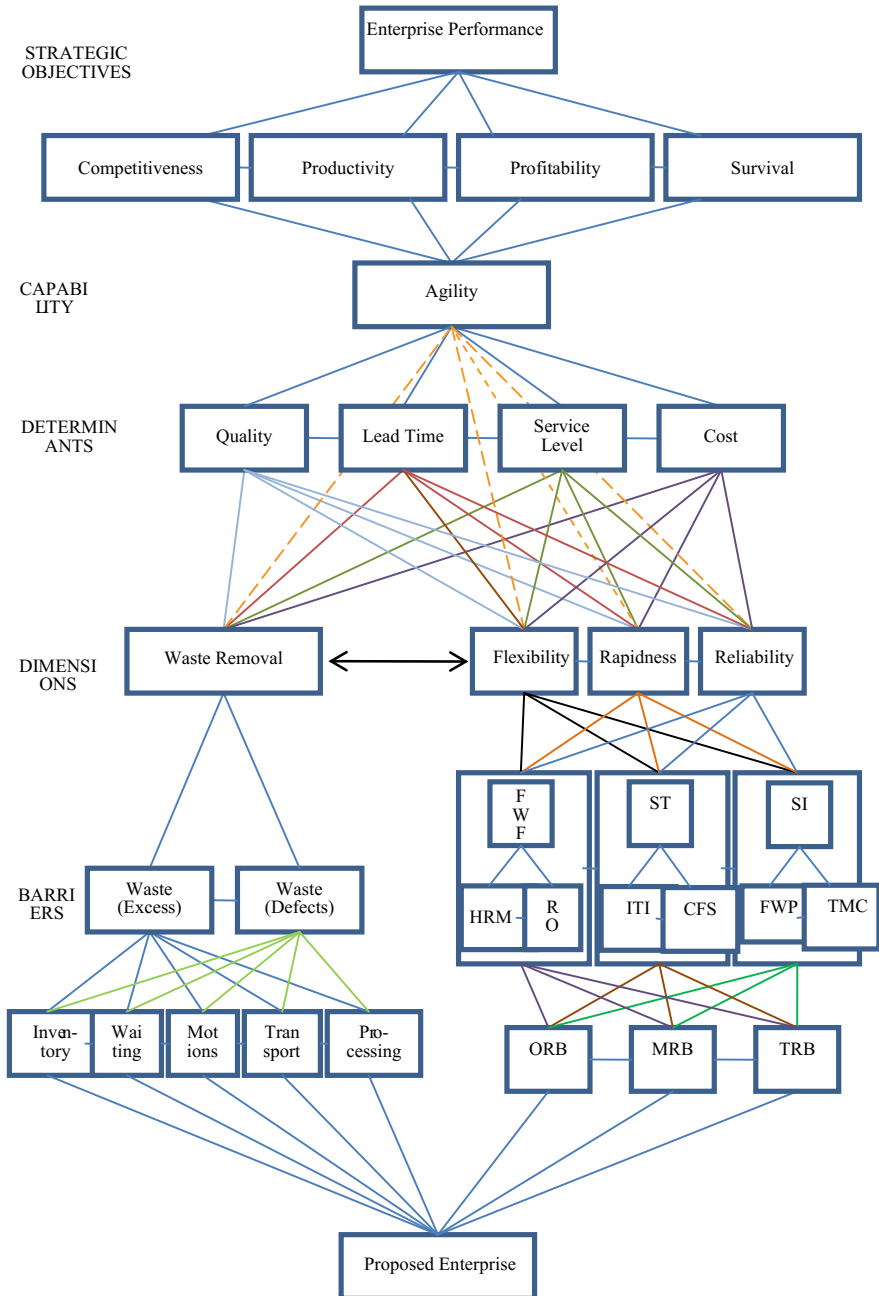


Fig. 1 Framework for ANP

4 Effectiveness Measurement of AM Barriers’s Paradigme

4.1 Pairwise Comparison and Consistency Check

In view of the match insightful examination, Prof. Saaty has proposed the ANP procedure as an apparatus for multi-criteria basic leadership. In light of audit, during writing of a typical classification, arranges has been created to combine savvy correlation and estimation of need as appeared in Table 2.

Consistency index (CI): where λ_{max} = maximum eigenvalue and n = the size of matrix of pairwise comparison.

Consistency ratio, (CR) = CI/RI [16] (Table 3).

4.2 Evaluation of the Framework Based on ANP

Structuring the metrics of ORB, MRB, and TRB to evaluate the impact with the help of the steps of ANP approach mentioned below (Tables 4, 5, 6 and 7).

Additionally, match astute examinations of all hindrances under all measurements concerning the sum total of what determinants have been computed. These computed estimations of every determinant have been transported into acquire super-matrices as in Table 8.

In the same way, three super matrices have been framed as for all determinants and converged at power of seventy-one as appeared in Table 9 (Table 10).

4.3 Desirability Index

This step assesses the estimations of “total desirability index” (TDI) of the option “i” as for determinant “a” for the estimation of the viability of choices (ORBs, TRBs, and MRBs). The estimation has been improved the situation add up to attractive quality records of all options as for determinant cost as appeared in Table 11. Meade and Sarkishas built up a relationship for the count of TDI as given:

$$D_{ia} = \sum_{j=1}^j \sum_{k=1}^{kja} P_{ja} A_{kja}^D A_{kja}^I S_{ikja} \text{ [17].}$$

Also, agile manufacturing barrier’s weighted index $AMBEWI_i = \sum_a D_{ia} C_a$ [17].

Similarly, steps were repeated for all the determinants and for the calculation of effectiveness through overall weighted index of ORBs, TRBs, and MRBs as given in Table 12.

Table 2 Matrix of pairwise comparison for the calculation of important weights and consistency [17]

Variables	Variable '1' (V_1)	Variable '2' (V_2)	Variable 'n' (V_n)	$M = \sqrt[n]{V_1 V_2 \dots V_n}$	Priority wts $W = \sum M$	$X = [A] \times [W]$	Eigen value $\lambda = \frac{[A] \times [W]}{W}$
V_1	1	r	r'	M_1	W_1	X_1	$\lambda_1 = X_1/W_1$
V_2	$1/r$	1	r''	M_2	W_1	X_2	$\lambda_2 = X_2/W_2$
V_n	$1/r'$	$1/r''$	1	M_n	W_n	X_n	$\lambda_n = X_n/W_n$
	Matrix of pair wise comparison [A]; Here, $1/9 < r, r', \dots, r'' < 9$ is based on a judgement			$\sum M = M_1 + M_2 + \dots + M_n$	Normalized matrix [W]		Maximum eigenvalue $\lambda_{\max} = \sum \lambda_i/n$

Table 3 RI values for matrices used after pairwise comparisons [16]

<i>n</i>	2.0	3.0	4.0	5.0	6.0	7.0	8.0	9.0	10.0	
RI	00	0.5245	0.8815	0.1086	0.2479	0.3417	0.4056	0.4499	0.4854	
<i>n</i>	11.0	12.0	13.0	14.0	15.0	16.0	17.0	18.0	19.0	
RI	0.5141	0.5365	0.5551	0.5713	0.5838	0.5978	0.6086	0.6181	0.6265	
<i>n</i>	20.0	21.0	22.0	23.0	24.0	25.0	26.0	27.0	28.0	29.0
RI	0.6341	0.6409	0.647	0.6526	0.6577	0.6624	0.6667	0.6706	0.6743	0.6777
<i>n</i>	30.0	31.0	32.0	33.0	34.0	35.0	36.0	37.0	38.0	39.0
RI	0.6809	0.6839	0.6867	0.6893	0.6917	0.694	0.6962	0.6982	0.7002	0.702

Table 4 Determinant’s pairwise comparison (CR = 0.0434)

	Cost	Lead time	Service level	Quality	<i>M</i>	<i>W</i>	<i>X</i>	λ
Cost	1	3	5	9	3.409	0.5622	2.347	4.174
LT time	0.333	1	3	9	1.732	0.2857	1.18	4.13
SL	0.2	0.333	1	3	0.669	0.1103	0.443	4.019
Quality	0.111	0.111	0.333	1	0.253	0.0418	0.173	4.135
	Pair-wise comparison matrix [A]				6.063	<i>C_a</i>		4.115

Bold characters are the main factors in pairwise comparisons and bold numbers are the main waight factors calculated for consideration in next iterations

Table 5 Dimensions w.r.t. cost (CR = 0.0645)

Cost	Waste removal	Flexibility	Rapidness	Reliability	<i>M</i>	<i>W</i>	<i>X</i>	Λ
WR	1	5	7	9	4.213	0.6545	2.755	4.21
Flexibility	0.2	1	3	5	1.316	0.2045	0.85	4.156
Rapidness	0.143	0.333	1	3	0.615	0.0955	0.394	4.124
Reliability	0.111	0.2	0.333	1	0.293	0.0456	0.191	4.191
	[A]				6.437	<i>P_{j cost}</i>		4.17

Bold characters are the main factors in pairwise comparisons and bold numbers are the main waight factors calculated for consideration in next iterations

5 Conclusion

In the present research, the adequacy of three classes of AM execution obstructions has been assessed by utilizing the ANP structure created. This system coordinates and depends on the different determinants, measurements, and obstructions and their connections. According to assessment, the technology-related boundaries have the most extreme impact on AM execution trailed by management-related and

Table 6 Comparison of the barriers under waste removal w.r.t. cost (CR = 0.08)

Cost/waste removal	Inventory	Processing	Waiting	<i>M</i>	<i>W</i>	<i>X</i>	Λ
Inventory	1	7	9	3.98	0.79	2.42	3.08
Processing	0.14	1.00	3.00	0.75	0.15	0.46	3.08
Waiting	0.11	0.33	1.00	0.33	0.07	0.20	3.08
	[A]			5.07			3.08

Bold characters are the main factors in pairwise comparisons and bold numbers are the main weight factors calculated for consideration in next iterations

Table 7 Matrix for comparison of barriers under waste removal w.r.t. inventory for cost (CI = 0)

Cost/inventory	Processing	Waiting	<i>M</i>	<i>W</i>	<i>X</i>	λ
Processing	1	3	1.732	0.75	1.5	2
Waiting	0.333	1	0.577	0.25	0.5	2
	[A]		2.309			2

Bold characters are the main factors in pairwise comparisons and bold numbers are the main weight factors calculated for consideration in next iterations

Table 8 Super-matrix of interdependency of barriers w.r.t. cost

Cost	Inventory	Processing	Waiting	FWF	FWP	HRM	RO	SI	ITI	CF	TMC	ST
Inventory	0.00	0.83	0.25									
Processing	0.75	0.00	0.75									
Waiting	0.25	0.17	0.00									
FWF				0.00	0.88	0.90						
FWP				0.83	0.00	0.10						
HRM				0.17	0.13	0.00						
RO							0.00	0.83	0.90			
SI							0.75	0.00	0.10			
ITI							0.25	0.17	0.00			
CF										0.00	0.25	0.75
TMC										0.17	0.00	0.25
ST										0.83	0.75	0.00

operator-related obstructions. The outcome demonstrates that the technology-related boundaries are the best obstruction to mind amid AM execution in the designing ventures. These discoveries likewise recommend that the enterprises can enhance their costs, service level, lead time, and quality through fruitful AM rehearses by dealing with these boundaries as per their effect. According to the outcome acquired by proposed ANP demonstrate, it has been watched that the TRBs have a maximum level of adequacy, i.e., 38.52% trailed by MRBs, i.e., 34.17%, and ORBs, i.e., 27.31% in the ventures. A value of CR for all pairwise comparisons differs from 0 to 0.08

Table 9 Super-matrix of interdependency of barriers with respect to cost after convergence

Cost	Inventory	Processing	Waiting	FWF	FWP	HRM	RO	SI	ITI	CF	TMC	ST
Inventory	0.4	0.4	0.4									
Processing	0.43	0.43	0.43									
Waiting	0.17	0.17	0.17									
FWF				0.62	0.62	0.62						
FWP				0.53	0.53	0.53						
HRM				0.17	0.17	0.17						
RO							0.46	0.46	0.46			
SI							0.36	0.36	0.36			
ITI							0.18	0.18	0.18			
CF										0.38	0.38	0.38
TMC										0.18	0.18	0.18
ST										0.45	0.45	0.45

Table 10 Matrix for impact of ORBs, TRBs, and MRBs on cost w.r.t. waste removal (CR = 0.06)

Cost/inventory	ORB	TRBs	MRBs	<i>M</i>	<i>W</i>	<i>X</i>	Δ
ORBs	1.00	0.14	0.20	0.31	0.07	0.22	3.06
TRBs	7.00	1.00	3.00	2.76	0.65	1.99	3.06
MRBs	5.00	0.33	1.00	1.19	0.28	0.85	3.06
	Pairwise comparison matrix [A]			4.25			3.06

Bold characters are the main factors in pairwise comparisons and bold numbers are the main weight factors calculated for consideration in next iterations

verdicts an affectability examination to watch the effect of variety in the supposition of experts. This demonstrates the rule for filling the vital choice of experts in the form of weight comparisons to accomplish the objectives of AM methodology. It likewise causes the building ventures to stay aggressive in competitive environment. Finding recommends that AM is a proper system for enhancing their costs, service level, lead time, and quality of the building ventures and thus to accomplish fitting efficiency by taking evaluated barrier category into account as per their impacts.

Table 11 TDI of alternatives w.r.t. cost

Dimensions	P_{ja}	Barriers	A_{kja}^D	A_{kja}^I	S_{ikja}			$P_{ja}A_{kja}^D A_{kja}^I S_{ikja}$		
					S_1 (ORBs)	S_2 (TRBs)	S_3 (MRBs)	ORBs	TRBs	MRBs
Waste removal	0.6545	Inventory	0.79	0.40	0.07	0.65	0.28	0.01447	0.134434	0.057910
	0.6545	Processing	0.15	0.43	0.06	0.27	0.67	0.00253	0.011398	0.028284
	0.6545	Waiting	0.07	0.17	0.75	0.07	0.18	0.00584	0.000545	0.001401
Flexibility	0.2045	SI	0.67	0.62	0.69	0.23	0.08	0.05861	0.019538	0.006795
	0.2045	CF	0.06	0.53	0.67	0.09	0.24	0.00435	0.000585	0.001560
	0.2045	RO	0.27	0.17	0.67	0.24	0.09	0.00628	0.002252	0.000844
Rapidness	0.0955	CFS	0.75	0.46	0.75	0.18	0.07	0.02471	0.005930	0.002306
	0.0955	FWF	0.18	0.36	0.69	0.08	0.23	0.00427	0.000495	0.001423
	0.0955	HRM	0.07	0.18	0.10	0.26	0.64	0.00012	0.000312	0.000770
Reliability	0.0456	ST	0.29	0.38	0.10	0.64	0.26	0.00050	0.003216	0.001306
	0.0456	ITI	0.66	0.18	0.06	0.27	0.67	0.00032	0.001462	0.003629
	0.0456	TMC	0.05	0.45	0.75	0.07	0.18	0.00077	0.000071	0.000184
TDI of choices for determinant cost $D_{iLDM} = \sum_{j=1}^i \sum_{k=1}^{kja} P_{ja}A_{kja}^D A_{kja}^I S_{ikja}$										
								0.1228	0.1802430	0.10641

Table 12 AMBEWI of ORBs, TRBs, and MRBs

Determinants	Cost	Service Level	Lead time	Quality	Intended weights of alternatives	
Weights (C_a)	0.5622	0.2857	0.1103	0.0418	AMBEWI _i	% Impact
Alternatives(D_{ia})					Normalized values	
ORBs	0.122811	0.117138	0.107811	0.124725	0.119616	0.273097
TRBs	0.180243	0.135375	0.160855	0.26226	0.168714	0.385194
MRBs	0.106418	0.199216	0.244591	0.142228	0.149668	0.341709
Total					0.437998	

Bold characters are the main factors in pairwise comparisons and bold numbers are the main weight factors calculated for consideration in next iterations

References

1. Stratton R, Warburton RDH (2003) The strategic integration of agile and lean supply. *Int J Prod Econ* 14(1):21–25
2. Goldman S, Nagel R, Preiss K (1995) *Agile competitors and virtual organizations*. Van Nostrand Reinhold, New York
3. Nagel R, Dove R (1991) *21st century manufacturing enterprise strategy: an industry led view of agile manufacturing*, vols I, II. Iococca Institute, Lehigh University
4. Gupta S, Herrmann JW, Lam G, Minis I (1997) Automated high level process planning to aid design for agile manufacturing. In: *IERC proceedings, 6th annual industrial engineering research conference*, Norcross, GA, USA, pp 1–19
5. Womack JP, Jones DT (2003) *Lean thinking: banish waste and create wealth in your corporation*, 2nd edn. Free Press, New York
6. Sindhvani R, Malhotra V (2016) Modelling the attributes affecting design and implementation of agile manufacturing system. *Int J Process Manag Benchmarking* 6(2):216–234
7. Sindhvani R, Malhotra V (2016) Modelling and analysis of agile manufacturing system by ISM and MICMAC analysis. *Int J Syst Assur Eng Manag* 8(2):253–263
8. Sindhvani R, Malhotra V (2013) Overview and drivers of agile manufacturing system: a review. *Int J Market Technol* 3(12):144–154
9. Mittal VK, Sangwan KS (2014) Prioritizing barriers to green manufacturing: environmental, social and economic perspectives. *Procedia CIRP* 17:559–564 Elsevier
10. Sangwan KS, Mittal VK (2015) A bibliometric analysis of green manufacturing and similar frameworks. *Manag Environ Qual Int J* 26(4):566–587
11. Singh MD, Shankar R, Narain R, Kumar A (2006) Survey of knowledge management practices in Indian manufacturing industries. *Int J Knowl Manag* 10(6):110–128
12. Saaty TL (2007) Time dependent decision-making; dynamic priorities in the AHP/ANP: generalizing from points to functions and from real to complex variables. *Math Comput Model* 46(7–8):860–891
13. Mittal VK, Sindhvani R, Kapur PK (2016) Two-way assessment of barriers to lean-green manufacturing system: insights from India. *Int J Syst Assur Eng Manag* 7(4):400–407
14. Singh MD, Kant R (2009) Selected knowledge management implementation issues: a sectorial analysis. *Int J Innov Learn* 6(5):550–567
15. Sharma BP, Singh MD (2014) Modeling the metrics of individual, organizational and technological knowledge sharing barriers: an analytical network process approach. *Int J Knowl Manag* 10(1):43–57
16. Alonso JA, Lamata MT (2006) Consistency in the analytic hierarchy process: a new approach. *Int J Uncertainty Fuzziness Knowl Based Syst* 14(4):445–459
17. Meade LM, Sarkis J (1999) Analyzing organizational project alternatives for agile manufacturing processes: an analytical network approach. *Int J Prod Res* 37:241–261

Agile System in Health Care: Literature Review



Rahul Sindhvani, Punj Lata Singh, Devendra Kumar Prajapati, Aamir Iqbal, Rakesh Kumar Phanden and Vasdev Malhotra

Abstract The goal of this exploratory paper is to focus on the present status of implementation of the agile system in health care. In this article, analysis emphasizes the definition of agile in health care, enablers cum characteristic, implementation procedure, and barriers. An inclusive research of the literature pertaining to the implementation of this system in health care was used to produce a technique to implement it. A system that is flexible in nature and enables to respond quickly to customer demand and market fluctuations while still optimizing costs and quality by adopting upgraded tools, processes, and trainings is termed as an agile system. The agile system in health care basically offers an efficient framework to organize and govern process improvement. It can be only accomplished if a systems approach is enforced together with a proper orientation. The common implementation steps suggest conduct agile training, start pilot projects, and executing improvements using interdisciplinary teams. Lack of instructors and advisors is one of the barriers and they can furnish support by sharing their knowledge and experience and illustrating with help of an example from real-life applications of agile in health care.

Keywords Health care · Agile · Enablers · Barriers · Factors · System · Implementation

R. Sindhvani (✉) · D. K. Prajapati · A. Iqbal · R. K. Phanden
Department of Mechanical Engineering, Amity School of Engineering
and Technology, Amity University Uttar Pradesh, Noida 201301, Uttar Pradesh, India
e-mail: rsindhvani@amity.edu

P. L. Singh
Civil Engineering Department, Amity School of Engineering and Technology,
Amity University Uttar Pradesh, Noida 201313, Uttar Pradesh, India

V. Malhotra
Department of Mechanical Engineering, YMCA University of Science & Technology,
Faridabad, Haryana, India

1 Introduction

In this globalization era, healthcare organization is facing difficulty to respond dynamic, uncertain demand of customer and to continuously varying environment. And this difficulty should be minimized because the necessity of healthcare services is arising day by day due to the changing environment and culture of society. But on another site, financial condition is not ameliorating of these organizations to offer this service which is easily accessible, affordable, and accurate. For this purpose, there is a requirement of the new and efficient way of facilitating healthcare service. Hence, it is a very challenging issue for both industry and academia that how to improve it? However, there is various resolutions that have been suggested such as networking, re-engineering, high-performance organization, employee empowerment, flexible manufacturing, and just in time (JIT) [1].

According to WHO, there are some following factors required to maintain a good healthcare system, which are sophisticated financing mechanism, trained and skilled workforce, trusted information on which to base decision and policies, and robust mechanism to deliver quality medicine and technologies. And these factors are influenced by the disparate player and they are patient stakeholders, non-governmental, commercial, academic as well as local, and regional political forces [2]. Recently, experts from industry and academia have been trying to manage these turbulences to provide effective and efficient healthcare.

Apart from this, there is also some internal complexity to deal with these complexities healthcare organizations, adopted process development strategies, and lean healthcare management to provide improved quality and safety to the patient [3]. Although lean thinking is beneficial to the organization, there are some limitations of applying a lean approach in healthcare due to the limited consideration of external effectiveness; hence, lean seems inadequate to deal with instability and complexity of external environment as well as dynamic demand [4]. To cope with this instability and complexity, it is essential to understand the requirements and constraints of the marketplace and need to adopt new strategies which ensure the needs of the supply chain and the end customer. To fulfill the higher variety of demand of customer in terms of services and products where the degree of uncertainty is high, the organization should be equipped with agile practice [5].

On the basis of the literature review, the goal of this paper is to update the reader regarding the implementation of the agile system in healthcare organization. In this article, analysis emphasizes the definition of agile in health care, and implementation procedures, factors, barriers, enablers, issue, and results of implementing the agile system in health care.

2 Methodology

The compilation of this review paper initiated through the comprehensive exploration of the various databases which include ScienceDirect, Interscience, Springer, Emerald, Elsevier, IEEE, etc. An attempt was also made in search of databases of medical journals; for example, BioMed, Telemedicine, and e-Health and journals from several areas such as quality management, operational management, health-care management, and business and economic. The search criteria include the papers from year 2000 to 2017, almost 200 papers was reviewed using key words such as “agile health care,” “agile healthcare organization,” “agile management in health care,” “agile software development in health care,” “barrier and challenges in health-care organization,” and “agile implementation in health care.” This spacious search strategy was required because the paper on agile health care has been published in a wide range of journals in many fields. On the basis of the above survey, nearly 60 most relevant papers related to agile health care are selected to write this review paper.

3 Literature Review

The reviewed paper is segregated into three parts, namely agile healthcare delivery, agile healthcare management, and agile healthcare software development which are shown in Table 1.

4 What Is Agile Health Care

The report nominated the twenty-first century Manufacturing Enterprise Strategy has originally presented the concept of “agile.” This report revealed the consideration of the chief representative of management principle from the US industry, government, and academia [6]. Agile strategy empowers the organizations to deliver efficient, customized, and standard quality service on time at an optimized cost. In health care, lean only focuses on process and eliminating waste within the organization but agile makes the healthcare organization flexible which considers the turbulence in the environment within and outside the organization [7]. In healthcare organization, the agile practice involves a group of parameter termed as agile characteristic listed in Table 2.

Table 1 Review of “Agile HealthCare System”

S. no.	Field	Sub-field	Paper reviewed
1.	Agile healthcare delivery	Patient flow and planning process	Towill and Christopher (2005): This paper helps to develop the healthcare pipeline, putting the patient in centered and considering the vision of NHS, using a suitable architecture which covers the great extent of patient demand [5] Rahimnia and Moghadasian (2010): It is the case study, conducted in hospital focuses on supply chain regarding health care using the concept of leagile strategy [13]
		Portable healthcare clinic	Robertson and DeHart (2010): Emphases are given on how to provide healthcare facility in the rural and remote area. Using artificial intelligence [14] Kai et al. (2014): This paper supports and strengthens the healthcare worker to identify non-communicable diseases in an inaccessible located area with the help of portable health clinic (PHC) [15]
		Medical product supply chain	Mehralianan et al. (2015): Supply chain model has been developed in this paper for the pharmaceutical industry and trying to show the most dominating factors using agile concept [16] Nabelsi and Gagnon (2016): In this paper, authors trying to show how supply chain management affect the cost involving in health care. Cost relating to SCM is more than 40% of hospital operating budget [17]
2.	Agile healthcare management	Organizational structural	Keating (2000): This paper provides the symptoms of weak organizational structure and advice to modify those focal areas so that organization can respond turbulence environment [18] Rust et al. (2013): This paper suggests a procedure to adopt an agile approach while a lean approach already used in healthcare organization [19] Tolf et al. (2015): To increase internal efficiency and external effectiveness, need to redesign the organizational structure in optimizing the way in the hospital using the concept of agile principles [20]

(continued)

Table 1 (continued)

S. no.	Field	Sub-field	Paper reviewed
		Managerial strategies	Kitzmilller et al. (2006): This paper proposes the implementation of agile technique into the traditional organization without obsoleting it [21] Patri et al. (2017): This paper suggests the manager of healthcare organization that organizational structure, management–employee cohesion, implementation of employee and patient’s suggestion etc are an important enabler and should be highly focused to achieve agility in the organization using TISM technique [11]
		Agile workplace management	Michael et al. (2003): To achieve agility in healthcare organization, we have to first make workplace agile [22] Moore et al. (2008): To scale agile practice at large extent in healthcare organization, it demands to build agile tribe using the power of information [23]
3.	Agile software development	Electronic health record	Lenz and Kuhn (2004): This paper provides documentation technique based on an application framework and rapid application development [24] Bamiah et al. (2012): This paper concludes that how an organization can use the cloud computing paradigm to make electronic health record [25] Ozcan (2013): This paper examined the feasibility electronic care report form (e-CRF) using open source software (OSS) [26]
		e-healthcare network	Chiu et al. (2007): In this paper, e-healthcare network is developed using medical informatics standard called health level 7 (HL7) [27] Bender and Sartipi (2013): To develop e-healthcare network it is necessary to make system interoperable [28]

5 Agile Implementation in Health Care

The literature review suggests that implementation patterns for agile health care are same as lean healthcare implementation pattern. To implement the agile strategy in healthcare, the following key measures are identified [1, 8].

- Conduct agile training
- Start pilot projects and
- Executing improvements

In the first step, management appoints an agile manager who states the basic agile principle, methods, and tools to the all employee and staff of that organization

Table 2 Overview of agile healthcare enabler cum characteristics

Agile characteristic	References	Description
Organization structure	[1, 21, 29, 30]	A flat and horizontal organization with less distinct authority having decentralized knowledge and effective influence should be preferred
IT integration	[8, 29, 31]	Through the adaptation of IT in a healthcare organization, information exchange takes place easily and quickly with help multimedia devices
Process design	[4, 29]	Process design ensures high level of safety and reliability to the patient and provides the scope of self-improvement to the organization
Employee empowerment	[1, 29]	Need to provide some authority to an employee to take self-decision without consulting higher officials in some cases
Customer feedback management	[31–33]	To make organization efficient and effective patient suggestion should be incorporated into the system, there should be the separate department to manage the customer feedback and its implementation
Training for the workforce	[29, 8]	To enhance the productivity and to adopt a new practice in organization training project should be initiated frequently for the workforce
Outsourcing	[34, 35]	Some resources could not be available in organization and purchasing may be more expensive then it is better to outsource from outside

followed by training [9]. This step creates the base for commencing practical work. A strong leadership is required, the person who has all concept of agile system and can lead the whole team, for this purpose because when changes occur in any organization, a certain degree of resistance is offered by the member of the organization. And this resistance can be reduced by creating interest and motivating them regarding agile system [10].

The second steps start with the concept of agile on the ground with the help of a pilot project. Initially, a pilot project was a segment of education program but now it is directly connected to the training program. The basic idea behind this project is to

let people know the idea of agile and also try it within the organization to get a fast result [4].

The third steps start with executing improvement in the organization with the help of fully involved employees. This step involves troubleshooting of problem using agile techniques and tools and incorporates those changes in the organization. And also find out the main reason behind the problem, and provide the optimum solution for that problem by analyzing it at various levels [4].

6 Barriers and Challenges to Agile Implementation

The major barrier need to overcome in agile implementation is followed.

- Adaptivity
- Convince staff
- Training
- Customer focus

The first barrier is adaptivity and it is the indicator of the ability to adopt a change in organizational structure, working pattern, etc. To implement agile practice in health-care organization, degree of adaptivity should be high [1]. It makes the organization professionally flexible and helps to learn new paradigms and responsibilities that enable the organization to respond rapidly [11].

The second barriers are to convince the staff. When a change takes place in the system, a certain level of resistance is offered by the employee against that change. Hence to implement agile system successfully in health care, organization need to convince staff by changing mindset to adopt new culture [1]. However, when training is offered, the staff gradually realize that this system makes our organization more efficient.

Training itself is a third challenging task because, in healthcare organization, there is a lack of people who have real-time exposure to agile practice having sound knowledge, principles methods, and tools of agile production. The instructor who is hired from manufacturing sector often uses manufacturing language which is difficult to understand for healthcare staff [8].

The fourth problem is customer focus and to implement the agile system in health-care organization; therefore, it is essential to understand the agile principle, the demand of the customer, and delightness. The word customer is not straightforward in health care, although patient is the primary customer in health care regarding the market economic perspective that patient is not a customer because customer generally does not pay directly for services [12].

7 Conclusion

This survey shows that agile is mostly used in health care as agile software development is still a great scope in the agile healthcare delivery system followed by agile healthcare management. Agile health care applied in the system to overcome the ineffectiveness of lean principles is due to constantly varying demand of the customer. Implementation in health care faces some vibrating challenges which are lack of training, inadequate infrastructure along with resistance offered by a staff member, and lack of customer focus. For successful implementation of the agile system in health care, it is essential to understand, what is the meaning of agile health care and at what degree it deviates from the agile system which is implemented in the industrial and manufacturing sector. This technique can be interpreted with help of academia and expert who has real-time experimenter of the agile system. While implementing agile in healthcare organization, health characteristic which is listed in this paper, play a very crucial role because these characteristics work as enablers and also helpful to find out agility in healthcare organization. Initially, in healthcare organization, agile technique is used to develop software to overcome the problem regarding documentation, but present demand is that agile approach should be thoroughly adopted by healthcare organization to meet the customer demands.

References

1. Sherehiy B, Karwowski W, Layer JK (2007) A review of enterprise agility: concepts, frameworks, and attributes. *Int J Ind Ergon* 37(5):445–460
2. Martínez-García M, Hernandez-Lemus E (2013) Health systems as complex systems. *Am J Oper Res* 3(1A):113–126
3. Poksinska B (2010) The current state of lean implementation in health care: literature review. *Qual Manag Healthc* 19(4):319–329
4. Radnor Z, Osborne SP (2013) Lean: a failed theory for public services? *Public Manag Rev* 15(2):265–287
5. Towill DR, Christopher M (2005) An evolutionary approach to the architecture of effective healthcare delivery systems. *J Health Organ Manag* 19(2):130–147
6. Goldman S, Nagel R, Preiss K (1995) *Agile competitors and virtual organizations strategies for enriching the customer*, 1st edn. International Thomson Publishing Inc., New York, NY
7. Jimmerson C, Weber D, Sobek D (2005) Reducing waste and errors: piloting lean principles at IHC. *J Qual Saf* 31(5):249–257
8. Aravind Raj S, Sudheer A, Vinodh S, Anand G (2013) A mathematical model to evaluate the role of agility enablers and criteria in a manufacturing environment. *Int J Prod Res* 51(19):5971–5984
9. Chen YP, Hsieh SH, Cheng PH, Chien TN, Chen HS, Luh JJ, Chen SJ et al (2010) An agile enterprise regulation architecture for health information security management. *Telemed e-Health* 16(7):807–817
10. van Hoek RI, Harrison A, Christopher M (2001) Measuring agile capabilities in the supply chain. *Int J Oper Prod Manag* 21(1/2):126–148
11. Patri R, Suresh M (2017) Modelling the enablers of agile performance in healthcare organization: a TISM approach. *Glob J Flex Syst Manag* 18(3):251–272

12. Sindhwani R, Malhotra V (2015) Lean and agile manufacturing system barriers. *Int J Adv Res Innov* 3(1):110–112
13. Rahimnia F, Moghadasian M (2010) Supply chain leagility in professional services: how to apply decoupling point concept in healthcare delivery system. *Supply Chain Manag Int J* 15(1):80–91
14. Robertson J, DeHart D (2010) An agile and accessible adaptation of Bayesian inference to medical diagnostics for rural health extension workers. In: AAAI spring symposium: artificial intelligence for development, Mar 2010
15. Kai E, Rebeiro-Hargrave A, Inoue S, Nohara Y, Maruf RI, Nakashima N, Ahmed A (2014) Empowering the healthcare worker using the portable health clinic. In: 2014 IEEE 28th international conference on advanced information networking and applications (AINA), IEEE, May 2014, pp 759–764
16. Mehralian G, Zarenezhad F, Ghatari AR (2015) Developing a model for an agile supply chain in pharmaceutical industry. *Int J Pharm Healthc Mark* 9(1):74–91
17. Nabelsi V, Gagnon S (2016) Information technology strategy for a patient-oriented, lean, and agile integration of hospital pharmacy and medical equipment supply chains. *Int J Prod Res.* <https://doi.org/10.1080/00207543.2016.1218082>
18. Keating CB (2000) A systems-based methodology for structural analysis of health care operations. *J Manag Med* 14(3/4):179–198
19. Rust T, Saeed K, Bar-On I, Pavlov O (2013) Dynamic analysis of healthcare service delivery: application of lean and agile concepts
20. Tolf S, Nyström ME, Tishelman C, Brommels M, Hansson J (2015) Agile, a guiding principle for health care improvement? *Int J Health Care Qual Assur* 28(5):468–493
21. Kitzmiller R, Hunt E, Sproat SB (2006) Adopting best practices: “Agility” moves from software development to healthcare project management. *CIN Comput Inform Nurs* 24(2):75–82
22. Joroff ML, Porter WL, Feinberg B, Kukla C (2003) The agile workplace. *J Corp Real Estate* 5(4):293–311
23. Moore E, Spens J (2008) Scaling agile: finding your agile tribe. In: Conference Agile, 2008. AGILE’08, IEEE, Aug 2008, pp 121–124
24. Lenz R, Kuhn KA (2004) Towards a continuous evolution and adaptation of information systems in healthcare. *Int J Med Inf* 73(1):75–89
25. Bamiah M, Brohi S, Chuprat S (2012) A study on significance of adopting cloud computing paradigm in healthcare sector. In: 2012 international conference on cloud computing technologies, applications and management (ICCTAM), IEEE, Dec 2012, pp 65–68
26. Özcan T, Kocak S, Brune P (2013) Agile software development with open source software in a hospital environment—case study of an eCRF-system for orthopaedical studies. In: International conference on web engineering. Springer, Berlin, Heidelberg, July 2013, pp 439–451
27. Chiu RK, Tsai KC, Chang CM, Koh SL, Lin KC (2007) The implementation of an agile information delivery system in building service-oriented e-healthcare network. *Int J Enterp Netw Manag* 1(3):283–298
28. Bender D, Sartipi K (2013) HL7 FHIR: an Agile and RESTful approach to healthcare information exchange. In: 2013 IEEE 26th international symposium on computer-based medical systems (CBMS), IEEE, June 2013, pp 326–331
29. Sindhwani R, Malhotra V (2017) Modelling and analysis of agile manufacturing system by ISM and MICMAC analysis. *Int J Syst Assur Eng Manag* 8(2):253–263
30. Sindhwani R, Malhotra V (2016) Barriers evaluation for agile manufacturing system with fuzzy performance importance index approach. *Int J Agile Syst Manag* 9(4):292–301
31. Vinodh S, Kumar VU, Girubha RJ (2012) Thirty-criteria based agility assessment: a case study in an Indian pump manufacturing organization. *Int J Adv Manuf Technol* 63(9):915–929
32. Sindhwani R, Malhotra V (2017) A framework to enhance agile manufacturing system: a total interpretive structural modelling (TISM) approach. *Benchmarking Int J* 24(4):467–487
33. Sindhwani R, Malhotra V (2016) Modelling the attributes affecting design and implementation of agile manufacturing system. *Int J Process Manag Benchmarking* 6(2):216–234

34. Mittal VK, Sindhvani R, Kapur PK (2016) Two-way assessment of barriers to lean-green manufacturing system: insights from India. *Int J Syst Assur Eng Manag* 7(4):400–407
35. Mittal VK, Sindhvani R, Kalsariya V, Salroo F, Sangwan KS, Singh PL (2017) Adoption of integrated lean-green-agile strategies for modern manufacturing systems. *Procedia CIRP* 61:463–468

Evaluation of Common Barriers to the Combined Lean-Green-Agile Manufacturing System by Two-Way Assessment Method



Punj Lata Singh, Rahul Sindhwani, Naresh Kumar Dua, Anbesh Jamwal, Ankur Aggarwal, Aamir Iqbal and Nishant Gautam

Abstract The rapid development in the industry and ever-increasing manufacturing competitiveness around the globe has diverted industries towards the adoption of new manufacturing systems. The industries have moved from a singular manufacturing system to a combination of two of them in order to cope with the expansion of market structure and customer requirements. In today's scenario, a need for a more sustainable manufacturing system has emerged, therefore a combination of lean, green and agile manufacturing systems can provide the required results. The adoption of a Lean-Green-Agile Manufacturing System (LGAMS) in the present market scenario would be influenced by a few barriers viz. lack of top management support and commitment, fear and resistance to organizational change, financial constraints/risk of business, etc. The barriers can be attributed to different perspectives depending on their field of influence like economic, technical and organizational perspective. An attempt has been made to prioritize the influencing nature of each barrier. Application of analytical hierarchy process (AHP) would yield the required prioritization of the LGAMS barriers. This multi-criteria decision method is prone to instability due to crisp inputs. A further extension of AHP, i.e. fuzzy AHP—AHP with fuzzy inputs has been utilized. Further, a cross-check has been performed for the above results by using two-way assessment method.

Keywords Lean manufacturing · Green manufacturing · Agile manufacturing · Barriers · Multi-criteria decision analysis · Analytical hierarchy process · Fuzzy AHP · Two-way assessment method

P. L. Singh (✉)

Department of Civil Engineering, Amity School of Engineering and Technology,
Amity University Uttar Pradesh, 201313 Noida, Uttar Pradesh, India
e-mail: plsingh@amity.edu

R. Sindhwani · A. Jamwal · A. Aggarwal · A. Iqbal · N. Gautam
Department of Mechanical Engineering, Amity School of Engineering
and Technology, Amity University Uttar Pradesh, 201301 Noida, India

N. K. Dua
Department of Mathematics, Satjinda Kalayana College, Kalanaur, Rohtak,
Haryana, India

1 Introduction

To sustain in the present economic scenario, a company has to gradually polish up its production. This will eventually lead to the advancement of technology as well as improvement in the quality of the product, which would perhaps increase the consumer demand and decrease the non-value added time. The adaptation of a new manufacturing system for a company is not at all an unconstrained task. The reformation of any company is only possible when some minor losses are incurred. The success of any implementation in the manufacturing practice depends upon the organizational characteristics but not the all organization can implement the same practice [1]. Thereby, it is suggested to implement new methods in a manufacturing system. This can be done by using three approaches: (1) lean approach (2) green approach (3) agile approach. The past methodologies of work have been a combination of any two approaches out of these three. In the LGAMS method, all of the three methods will be used at once. Lean approach, green approach, and agile approach which are explained below:

The lean thinking is originated from the shop floors of the Japanese manufacturers and the innovations in the Toyota motor corporation [2–4]. These innovations are the result of lack of resources, rapid market competition in the automobile industries. The word “Lean” may be defined as a set of techniques and the methods which can be implemented in an industry to optimize the time of manufacturing process and productivity for improving the service and quality level of product for the betterment of the customers [5]. The lean approach aims to reduce the undesirable waste that doesn’t provide any value to the final product and services of the product [6]. Lean manufacturing works on the principle of eliminating wastes from the processes and reducing the variability to processes [7]. Lean strongly focuses on the elimination or reducing wastes. Lean manufacturing reduces the manufacturing cost and helps the manufacturer to gain more profit [8]. The lean manufacturing is the systematic approach to identifying and elimination of waste from industries by the continuous improvement of product flow [9]. Manufacturers are quickly changing their manufacturing system from traditional to lean manufacturing because of high quality on the small quantities in manufacturing system [10]. Lean manufacturing systems are more responsive to customers and more flexible in the industry [11].

In the present scenario manufacturing organizations are facing the challenges in two directions: one is to maintain the market competition, as the newer manufacturing technologies are emerging and outdating the older one and another one is that the customer’s product choice is regularly changing to newer product [12, 13]. To complete the customer demands and act quickly to a new manufacturing system comes out to solve the problem termed as “Agile Manufacturing” [14–17]. Agile manufacturing is a term applied to an organization to react quickly customer demands and market changes and still controlling the quality and cost [17–20]. Agility is the new way to running companies for the new challenges that aim at changing the old ways of doing things that are no longer appropriate, there is the need of manufacturing system which is more flexible and more responsive in nature [21]. Agile manufacturing

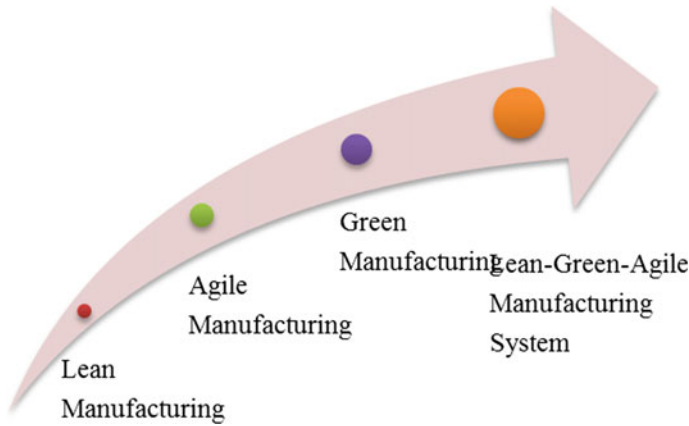


Fig. 1 Development of LGAMS system

is not about the continuous improvement on small scales, but it is an entirely different way of doing business [22, 23].

Green manufacturing reduces the waste which is averse to environmental impact [24]. Green manufacturing means to design, manufacture, delivery and disposal of the product at the minimum negative effect on the environment [25]. Green manufacturing aims to minimize environmental impact, and there is less to gain consumers and manufacturer directly [26]. The aim of green manufacturing is to designing and delivering that product which minimizes the negative effect on the environment during production and disposal [27].

Previous work has been done either on LG manufacturing system or either on LA manufacturing system but still, there was always lack of a manufacturing system which provides quality products at low cost with fulfilling customer needs and without minimum environmental impact so LGAMS introduced. In this research work, the detailed study of the literature review of LM, AM and GM is done. The literature on lean, green and agile manufacturing is used to identify the facilitators. The common facilitators among these three manufacturing systems are found, and these facilitators are analysed and validated with the two-way assessment approach. First of all, the analytical hierarchical process is used to obtain the weight of facilitators. Secondly, the questionnaire survey is done with the experts. This will help to find the impact of facilitators during the implementation of LGAMS (Fig. 1).

2 Literature Review

In the past, a lot of research has been done on the lean manufacturing [6, 8, 9, 10, 27, 28, 29], green manufacturing [25, 30, 31] and agile manufacturing [28, 32, 33, 34]. Lean manufacturing aims at reducing the waste from the manufacturing system and

thereby cost, green manufacturing aims at reducing the environmental degradation by the minimizing the environmental impact during production [35]. Manufacturers are changing their manufacturing system with the time from the traditional to lean manufacturing for the better quality of product and service. It allows producing high degree level of quality products in the small quantities [10]. There is less to gain customers in lean manufacturing, but it reduces the manufacturing costs by reducing the waste from the system, therefore gain more profits [8]. Diaz-Elsayed et al. describes lean manufacturing is the systematic approach to reducing the cost by elimination of waste with the continuous improvement [36]. He applied the VSM tool in the oilseed industry. After the questioner, he prepares the supply chain mapping and identified the waste and eliminates them by some modification which helps to improve productivity. Rehman and Shrivastava analysed thirteen barriers by literature review and suggestions from experts to energy saving in China [37]. Fullerton et al. suggested that on applying the lean and agile principle of pull system and value stream flow, the production rate of the lower frame may be increased [38]. The agile manufacturing should have the lower manufacturing costs, satisfy customer requirements, eliminate the non-value added activities from the system and introduced new products to the customer at the time [39]. The studies between the LM and GM shows positive results and till now few number of the scholarly studies have been investigated on the relationship between the lean manufacturing and green manufacturing [10]. Agile manufacturing is a concept that evolved from the lean manufacturing [40]. Cost reduction is most important in the lean manufacturing [13]. Agile manufacturing is the combination of lean manufacturing and flexible manufacturing system [41, 42]. During the recent years, many of the automobile companies act quickly on the customer requirements by quick designing of new models [12]. The adoption of the agile manufacturing maintained the market share of the industry by acting quickly and providing the better services to the customer [43]. The adoption of agile principles consumed the long time to attain agility in the organization because the majority of manufacturers are stringent about work culture and adopted production technology.

Environment, population and the resources are the major problems of the global world these days. Change in the climate can lead to the imbalance of the earth, so ISO has suggested a new system for the production. The main aim of this system is to minimize the effect of industries on the environment. The system termed as “Green manufacturing” [44]. The economic performance of any industry can be achieved by reducing the waste and emission at the source. This will also help to minimize the negative impact of production on the environment [45]. Green manufacturing is based on the manufacturing for reuse. GM can help to reduce the future cost of disposal and better worker protection, it will also help to improve the quality of better services at the lower cost with the better public image [46]. These days, better business strategies provide the good quality products to customers at the lower cost with the minimum environmental degradation during production [20, 47].

3 Methodology

Analytical hierarchy process has been widely used in the literature to analyse the barriers influencing manufacturing systems. It involves pairwise comparison of the barriers by expert's views. Further, an extension to the above process is used, i.e. fuzzy analytical hierarchy process. The stepwise methodology adopted for the research is listed below:

3.1 Identification of LGAMS Barriers

Identification of barriers to LGAMS through a review of literature and discussion with experts from industry and academia is shown in Table 1. Also, the three criteria chosen to establish the hierarchical structure of barriers are selected as shown in Table 2.

3.2 Establishment of Hierarchy

Establishment of the hierarchy of various barriers using three criteria in consultation with experts as discussed (Table 3).

3.3 Application of AHP

Application of AHP to get the overall weights of each barrier using pairwise comparison through inputs from industrial managers involved in operations management and decision-making. Before calculating the weights, the consistency of the pairwise comparison of criteria and barriers should be checked. The consistency of the pairwise comparison can be checked as follows:

- Calculate the largest Eigenvalue (λ_{\max}).
- Check the consistency ratio (CR).

The consistency of the comparison matrix can be determined by the CR, which is defined as [Eq. (1)]:

$$CR = CIRI = \frac{\lambda_{\max} - n}{n(n-1)} \quad (1)$$

As a rule, only if $CR \leq 0.10$, the consistency of the matrix is considered as acceptable, otherwise, the pairwise comparisons should be revised. The RI values for sizes 1, 2, 3, 4, 5, 6, 7, 8, 9 are taken as 0.00, 0.00, 0.58, 0.90, 1.12, 1.24, 1.32, 1.41,

Table 1 List of LGAMS barriers along with their description (self-compiled)

Barrier no.	Barrier name	Self-description
B1	Lack of management commitment	The unwillingness of management for a particular step or lack of commitment towards a goal
B2	Fear and resistance to change	Resilience among employees or workers to adapt to new technology or work structure
B3	Financial constraints	Lack of funds or loss of business to/on adopting a new manufacturing system
B4	Lack of training and education	Irregular and inappropriate training and guidance to employees/workers
B5	Lack of government support	Unsuitable government policies/laws and regulations
B6	Volatile customer demand	Irregular customer demand and preferences
B7	Technological constraints	Unavailability of the required technology or inability to harness it
B8	Market competition	Tough market and competitive atmosphere
B9	Improper communication	Lack of proper communication channels
B10	Lack of planning of strategies	Lack of intricate planning put into the strategies to adopt the new system
B11	Inadequate data collection	Inadequate data collection and performance management
B12	Poor layout and infrastructure	Poor industry layout and available infrastructure hinder progress
B13	Lack of mutual trust	Trust is the basis of a healthy work environment

Table 2 Criteria to establish structure

Criteria no.	Criteria name
C1	Economic criteria
C2	Technical criteria
C3	Organizational criteria

Table 3 Distribution of barriers among criteria

Barrier no.	Barrier name	Criteria no.	Criteria name
B1	Lack of top management support and commitment	C3	Organizational perspective
B2	Fear and resistance to organizational change	C3	Organizational perspective
B3	Financial constraints/risk of business	C1	Economic perspective
B4	Lack of training and education	C2	Technical perspective
B5	Lack of government support	C1	Economic perspective
B6	Volatile customer demand	C1	Economic perspective
B7	Technological constraints	C2	Technical perspective
B8	Market competition	C1	Economic perspective
B9	Improper communication	C3	Organizational perspective
B10	Lack of planning of improvement programs and strategies	C2	Technical perspective
B11	Data collection and performance measurement	C2	Technical perspective
B12	Industry layout and infrastructure	C2	Technical perspective
B13	Lack of trust among managers and employees	C3	Organizational perspective

Table 4 CR calculation for criteria

Criteria	C1	C2	C3	3rd root	Priority vector
C1	1.0000	3.0000	0.2000	0.8434	0.1884
C2	0.3333	1.0000	0.1429	0.3625	0.0810
C3	5.0000	7.0000	1.0000	3.2711	0.7306
				4.4770	
Sum	6.3333	11.0000	1.3429		
Sum*PV	1.1932	0.8906	0.9812		
λ_{max}	3.0649				
CI	0.0324				
CR	0.0559				

1.45, respectively. The raw inputs using Likert’s scale (1–5), the normalized inputs and the weights of the criteria and barriers to LGAMS are presented in Tables 4, 5, 6 and 7. The k max, CI and CR of each case is provided at the foot of each table.

Table 5 CR calculation for barriers under criteria C1

C1 criteria	B3	B5	B6	B8	3rd root	Priority vector
B3	1.0000	2.0000	4.0000	5.0000	2.5149	0.5065
B5	0.5000	1.0000	2.0000	3.0000	1.3161	0.2651
B6	0.2500	0.5000	1.0000	2.0000	0.7071	0.1424
B8	0.2000	0.3333	0.5000	1.0000	0.4273	0.0861
					4.9653	
Sum	1.9500	3.8333	7.5000	11.0000		
Sum*PV	0.9876	1.0160	1.0681	0.9466		
λ_{max}	4.0183					
CI	0.0061					
CR	0.0068					

Table 6 CR calculation for barriers under criteria 2

C2 criteria	B1	B2	B9	B13	3rd root	Priority vector
B1	1.0000	3.0000	5.0000	2.0000	2.3403	0.4829
B2	0.3333	1.0000	3.0000	2.0000	1.1892	0.2454
B9	0.2000	0.3333	1.0000	0.3333	0.3861	0.0797
B13	0.5000	0.5000	3.0000	1.0000	0.9306	0.1920
					4.8463	
Sum	2.0333	4.8333	12.0000	5.3333		
Sum*PV	0.9819	1.1860	0.9560	1.0241		
λ_{max}	4.1481					
CI	0.0494					
CR	0.0549					

Table 7 CR calculation for barriers under criteria C3

C3 criteria	B4	B7	B10	B11	B12	3rd root	Priority vector
B4	1.0000	2.0000	0.3333	5.0000	4.0000	1.6788	0.3020
B7	0.5000	1.0000	0.3333	2.0000	1.0000	0.8027	0.1444
B10	3.0000	3.0000	1.0000	0.3333	3.0000	1.5518	0.2792
B11	0.2000	0.5000	3.0000	1.0000	5.0000	1.0845	0.1951
B12	0.2500	1.0000	0.3333	0.2000	1.0000	0.4409	0.0793
						5.5587	
Sum	4.9500	7.5000	5.0000	8.5333	14.000		
Sum*PV	1.4949	1.0831	1.3959	1.6648	1.1105		
λ_{max}	6.7492						
CI	0.4373						
CR	0.0904						

Table 8 Scale of relative importance used in the pairwise comparison

Scale of relative importance (crisp number)	Triangular fuzzy number	Linguistic variable	Description
1	(1, 1, 1)	Equally important	Both challenges have equal impact
3	(2.5, 3, 3.5)	Weakly important	Experience and judgment favour one factor over another
5	(4.5, 5, 5.5)	Essentially important	Experience and judgment slightly favour one factor over another
7	(6.5, 7, 7.5)	Very strongly important	A factor is very strongly favoured and its dominance is demonstrated in practice
9	(9, 9, 9)	Absolutely important	The evidence favouring one challenge over another is of the highest possible order of affirmation

Note $X = 2, 4, 6, 8$ are intermediate scales

3.4 Conversion of Crisp Data to Triangular Fuzzy Numbers (TFN)

As all the above matrices are found consistent, we can proceed further. A triangular fuzzy number V is represented by (a, b, c) , and the membership function is defined as see Eq. (2)

$$\mu_V(x) = \begin{cases} \frac{x-a}{b-a}, & a \leq x \leq b \\ \frac{c-x}{c-b}, & b \leq x \leq c \\ 0, & \text{otherwise} \end{cases} \tag{2}$$

The crisp data collected from the decision-makers is transformed into fuzzy data by using the triangular fuzzy number. A 9-point scale [48] is frequently used to represent the pairwise comparison. In this study, triangular fuzzy numbers are used to represent subjective pairwise comparisons. The scale of the relative importance to measure comparison and the corresponding triangular fuzzy numbers are given in Table 8.

Table 9 TFN for criteria

C	C1			C2			C3		
	A	B	G	A	B	G	A	B	G
C1	1.00	1.00	1.00	2.50	3.00	3.50	0.18	0.20	0.22
C2	0.29	0.33	0.40	1.00	1.00	1.00	0.13	0.14	0.15
C3	4.50	5.00	5.50	6.50	7.00	7.50	1.00	1.00	1.00

Table 10 TFN for barriers under criteria C1

C1	B3			B5			B6			B8		
	A	B	G	A	B	G	A	B	G	A	B	G
B3	1.00	1.00	1.00	1.50	2.00	2.50	3.50	4.00	4.50	4.50	5.00	5.50
B5	0.40	0.50	0.67	1.00	1.00	1.00	1.50	2.00	2.50	2.50	3.00	3.50
B6	0.22	0.25	0.29	0.40	0.50	0.67	1.00	1.00	1.00	1.50	2.00	2.50
B8	0.18	0.20	0.22	0.29	0.33	0.40	0.40	0.50	0.67	1.00	1.00	1.00

Table 11 TFN for barriers under criteria C2

C2	B1			B2			B9			B13		
	A	B	G	A	B	G	A	B	G	A	B	G
B1	1.00	1.00	1.00	2.50	3.00	3.50	4.50	5.00	5.50	1.50	2.00	2.50
B2	0.29	0.33	0.40	1.00	1.00	1.00	2.50	3.00	3.50	1.50	2.00	2.50
B9	0.18	0.20	0.22	0.29	0.33	0.40	1.00	1.00	1.00	0.29	0.33	0.40
B13	0.40	0.50	0.67	0.40	0.50	0.67	2.50	3.00	3.50	1.00	1.00	1.00

The below formula [Eq. (3)] is used for converting the above crisp inputs into fuzzy numbers. The α -cut value of 0.5 is considered for converting the crisp inputs into fuzzy inputs. The α -cut values of zero are considered for upper and lower bound numbers [49].

$$A = \left(x - \frac{1}{2}, x, x + \frac{1}{2} \right) \tag{3}$$

Tables 9, 10, 11 and 12 represent the TFN for various parameters. Alpha, beta and gamma parts of TFN are represented by A, B, and G, respectively.

3.5 Weight Calculation

Based on the pairwise comparison matrix, the weights can be calculated as follows [Eqs. (4)–(10)]:

Table 12 TFN for barriers under criteria C3

C3	B4			B7			B10			B11			B12		
	A	B	G	A	B	G	A	B	G	A	B	G	A	B	G
B4	1.00	1.00	1.00	1.50	2.00	2.50	0.29	0.33	0.40	4.50	5.00	5.50	3.50	4.00	4.50
B7	0.40	0.50	0.67	1.00	1.00	1.00	0.29	0.33	0.40	1.50	2.00	2.50	1.00	1.00	1.00
B10	2.50	3.00	3.50	2.50	3.00	3.50	1.00	1.00	1.00	0.29	0.33	0.40	2.50	3.00	3.50
B11	0.18	0.20	0.22	0.40	0.50	0.67	2.50	3.00	3.50	1.00	1.00	1.00	4.50	5.00	5.50
B12	0.22	0.25	0.29	1.00	1.00	1.00	0.29	0.33	0.40	0.18	0.20	0.22	1.00	1.00	1.00

$$\alpha_j = \left[\prod_{j=1}^n l_{ij} \right]^{1/n} \tag{4}$$

$$\beta_j = \left[\prod_{j=1}^n m_{ij} \right]^{1/n} \tag{5}$$

$$\gamma_j = \left[\prod_{j=1}^n n_{ij} \right]^{1/n} \tag{6}$$

and

$$\alpha = \sum_{j=1}^n \alpha_j \tag{7}$$

$$\beta = \sum_{j=1}^n \beta_j \tag{8}$$

$$\gamma = \sum_{j=1}^n \gamma_j \tag{9}$$

Then fuzzy weight vector W is constructed as [Eq. (10)]:

$$\hat{w} = (\alpha_j \gamma^{-1}, \beta_j \beta^{-1}, \gamma_j \alpha^{-1}) \tag{10}$$

Tables 13, 14, 15 and 16 present the fuzzy weights and fuzzy weight vectors.

Table 13 Weight calculation for criteria

	A	B	G	Fuzzy weight vector		Local weights	Normalized local weights	*100
C1	0.7689	0.8434	0.9196	0.1612	0.1884	0.1898	0.1887	18.8684
C2	0.3365	0.3625	0.3948	0.0705	0.0810	0.0819	0.0815	8.1475
C3	3.0811	3.2711	3.4552	0.6460	0.7306	0.7340	0.7298	72.9841
Sum	4.1865	4.4770	4.7697			1.0057		

Table 14 Weight calculation for barriers under criteria C1

C1	A	B	G	Fuzzy weight vector		Local weights	Normalized local weights	*100
B3	2.2047	2.5149	2.8047	0.3880	0.5065	0.5158	0.5026	50.2585
B5	1.1067	1.3161	1.5541	0.1947	0.2651	0.2739	0.2669	26.6853
B6	0.6043	0.7071	0.8307	0.1063	0.1424	0.1474	0.1436	14.3604
B8	0.3797	0.4273	0.4934	0.0668	0.0861	0.0892	0.0870	8.6958
Sum	4.2953	4.9653	5.6828			1.0263		

Table 15 Weight calculation for barriers under criteria C2

C2	A	B	G	Fuzzy weight vector		Local weights	Normalized local weights	*100
B1	2.0268	2.3403	2.6339	0.3650	0.4829	0.4923	0.4795	47.9466
B2	1.0174	1.1892	1.3678	0.1832	0.2454	0.2517	0.2452	24.5184
B9	0.3490	0.3861	0.4342	0.0629	0.0797	0.0821	0.0799	7.9935
B13	0.7953	0.9306	1.1168	0.1432	0.1920	0.2006	0.1954	19.5415
Sum	4.1885	4.8463	5.5527			1.0267		

Table 16 Weight calculation for barriers under criteria C3

C3		A	B	G	Fuzzy weight vector			Local weights	Normalized local weights	*100
	B4	1.4651	1.6788	1.8998	0.2325	0.3020	0.3887	0.3078	0.3013	30.1252
	B7	0.7028	0.8027	0.9221	0.1115	0.1444	0.1887	0.1482	0.1451	14.5077
	B10	1.3488	1.5518	1.7654	0.2141	0.2792	0.3613	0.2848	0.2788	27.8808
	B11	0.9607	1.0845	1.2332	0.1525	0.1951	0.2523	0.2000	0.1957	19.5738
	B12	0.4097	0.4409	0.4797	0.0650	0.0793	0.0982	0.0808	0.0791	7.9125
	Sum	4.8870	5.5587	6.3002				1.0216		

Table 17 Relative global weights of barriers

Barriers	Weight
B1	0.0403
B2	0.0206
B3	0.0979
B4	0.2259
B5	0.0520
B6	0.0280
B7	0.1088
B8	0.0169
B9	0.0067
B10	0.2091
B11	0.1468
B12	0.0593
B13	0.0164
Sum	1.0287

Table 18 Normalized relative global weights of barriers

Barriers	Weight	*100
B1	0.0392	3.9208
B2	0.0200	2.0050
B3	0.0951	9.5143
B4	0.2196	21.9588
B5	0.0505	5.0517
B6	0.0272	2.7185
B7	0.1057	10.5750
B8	0.0165	1.6462
B9	0.0065	0.6537
B10	0.2032	20.3229
B11	0.1427	14.2677
B12	0.0577	5.7676
B13	0.0160	1.5980

3.6 Calculation of the Relative Weights

The de-fuzzified weights of the criteria are multiplied with their sub-criteria to find out their relative weights (Table 17). The weights are then normalized and represented in decreasing order in Tables 18 and 19, respectively. The highest weight shows most important sub-criteria, and the least weight shows the least important sub-criteria.

Table 19 Two-way assessment

Levels												
Barriers	Normalized global weights	5	4	3	2	1	Expected level weights				CTI	%
B1	3.9208	0	0	1	0	0	3				11.7624	3.92079216
B2	2.005	0	0	1	0	0	3				6.015	2.00499599
B3	9.5143	0	0	1	0	0	3				28.5429	9.51428097
B4	21.9588	0	0	1	0	0	3				65.8764	21.9587561
B5	5.0517	0	0	1	0	0	3				15.1551	5.0516899
B6	2.7185	0	0	1	0	0	3				8.1555	2.71849456
B7	10.575	0	0	1	0	0	3				31.725	10.5749789
B8	1.6462	0	0	1	0	0	3				4.9386	1.64619671
B9	0.6537	0	0	1	0	0	3				1.9611	0.65369869
B10	20.3229	0	0	1	0	0	3				60.9687	20.3228594
B11	14.2667	0	0	1	0	0	3				42.8031	14.2676715
B12	5.7676	0	0	1	0	0	3				17.3028	5.76758846
B13	1.598	0	0	1	0	0	3				4.794	1.5979968
											300.00	

Table 20 Normalized relative global weights of barriers (decreasing order)

Barriers	Weight	*100
B4	0.2196	21.9588
B10	0.2032	20.3229
B11	0.1427	14.2677
B7	0.1057	10.5750
B3	0.0951	9.5143
B12	0.0577	5.7676
B5	0.0505	5.0517
B1	0.0392	3.9208
B6	0.0272	2.7185
B2	0.0200	2.0050
B8	0.0165	1.6462
B13	0.0160	1.5980
B9	0.0065	0.6537

3.7 Two-Way Assessment

The two-way assessment of the impact of barriers through inputs from the academia and the middle management of industry and then the global weight is calculated by AHP which is calculated in the previous step.

3.8 Establishment of the Impact of Barriers

Finally, using the two-way assessment of actual, ideal, average and worst cases, the impact of barriers to LGMS is assessed (Table 20).

4 Results

Table 19 clearly orders the barriers into their decreasing impact on the application of LGAMS in a manufacturing industry. Barrier B4 (lack of training and education) with approximately a weight of 22% has the highest precedence among all the barriers and is the most influential to the application of a combined LGAMS in an industry. On the other hand, Barrier B9 (improper communication) with approximately a weight of 0.65% had the lowest weight and is least influential to the application of LGAMS in an industry. Other Barriers like B10 (lack of planning of improvement programs and strategies) and B11 (data collection and performance measurement) have high weight precedents and are influential. The barriers with high percentage must be

taken care of while initiating the application of the above system as they can hinder its progress.

References

- Galbraith JR (1977) *Organization design*. Addison Wesley Publishing Company
- Shingo S, Dillon AP (1989) *A study of the Toyota production system: from an industrial engineering viewpoint*. CRC Press
- Monden Y (1983) *Toyota production system. An integrated approach to just-in-time*
- Ohno T (1988) *Toyota production system: beyond large-scale production*. CRC Press
- Becker RM (1998) *Lean manufacturing and the Toyota production system*. Encyclopedia of world biography
- Jaiswal P, Kumar A (2016) Analyzing barriers of lean manufacturing adoption in Indian SMEs using an integrated approach of grey decision making trial and evaluation laboratory (DEMA-TEL). In: *World congress on engineering*, pp 688–691
- Anvari A, Ismail Y, Hojjati SMH (2011) A study on total quality management and lean manufacturing: through lean thinking approach. *World Appl Sci J* 12(9):1585–1596
- Kainuma Y, Tawara N (2006) A multiple attribute utility theory approach to lean and green supply chain management. *Int J Prod Econ* 101(1):99–108
- Bergmiller GG (2006) Lean manufacturers transcendence to green manufacturing: correlating the diffusion of lean and green manufacturing systems
- Singh BK, Bhar C, Pandurangan V (2011) Competitive advantage of lean manufacturing over traditional manufacturing. In: *Proceedings of the international conference on industrial engineering held at SVNIT, Surat, 17–19 Nov 2011*, pp 442–446
- Maskell B (2001) The age of agile manufacturing. *Int J Supply Chain Manage* 6(1):5–11
- Gunasekaran A (1999) Agile manufacturing: a framework for research and development. *Int J Prod Econ* 62(1–2):87–105
- Power DJ, Sohal AS, Rahman SU (2001) Critical success factors in agile supply chain management—an empirical study. *Int J Phys Distrib Logist Manage* 31(4):247–265
- Jin-Hai L, Anderson AR, Harrison RT (2003) The evolution of agile manufacturing. *Bus Process Manage J* 9(2):170–189
- Crocitto M, Youssef M (2003) The human side of organizational agility. *Ind Manage Data Syst* 103(6):388–397
- Sindhwani R, Malhotra V (2013) Overview and drivers of agile manufacturing system: a review. *Int J Mark Technol* 3(12):144
- Sindhwani R, Malhotra V (2016) Barriers evaluation for agile manufacturing system with fuzzy performance importance index approach. *Int J Agile Syst Manage* 9(4):292–301
- Routroy S, Shankar A (2015) Performance analysis of agile supply chain. *Int J Manuf Technol Manage* 29(3–4):180–210
- Meredith S, Francis D (2000) Journey towards agility: the agile wheel explored. *TQM Mag* 12(2):137–143
- Sindhwani R, Malhotra V (2016) Modelling the attributes affecting design and implementation of agile manufacturing system. *Int J Process Manage Benchmark* 6(2):216–234
- Dubey R, Gunasekaran A (2015) Agile manufacturing: framework and its empirical validation. *Int J Adv Manuf Technol* 76(9–12):2147–2157
- Mittal VK, Sindhwani R, Kapur PK (2016) Two-way assessment of barriers to lean–green manufacturing system: insights from India. *Int J Syst Assur Eng Manage* 7(4):400–407
- Sindhwani R, Malhotra V (2017) A framework to enhance agile manufacturing system: a total interpretive structural modelling (TISM) approach. *Benchmark Int J* 24(4):467–487
- Seth D, Seth N, Goel D (2008) Journal of manufacturing technology management, 19(4):529–550. <https://doi.org/10.1108/17410380810869950>

25. Wang BJ (2008) Analysis of efficiency of lean production implemented in multi-national optic enterprises. *Int J Technol Manage* 43(4):304–319
26. Sindhvani R, Malhotra V (2015) Lean and agile manufacturing system barriers. *Int J Adv Res Innov* 3(1):110–112
27. Gunasekaran A (1998) Agile manufacturing: enablers and an implementation framework. *Int J Prod Res* 36(5):1223–1247
28. Sarkis J (2001) Benchmarking for agility. *Benchmark Int J* 8(2):88–107
29. Vokurka RJ, Fliedner G (1998) The journey toward agility. *Ind Manage Data Syst* 98(4):165–171
30. Tan XC, Liu F, Cao HJ, Zhang H (2002) A decision-making framework model of cutting fluid selection for green manufacturing and a case study. *J Mater Process Technol* 129(1–3):467–470
31. Völkner P, Werners B (2000) A decision support system for business process planning. *Eur J Oper Res* 125(3):633–647
32. Gould P (1997) What is agility? *Manuf Eng* 76(1):28–31
33. Kidd PT (1996) Agile manufacturing: a strategy for the 21st century. 1–1
34. Sawhney R, Teeparakul P, Bagchi A, Li X (2007) En-lean: a framework to align lean and green manufacturing in the metal cutting supply chain. *Int J Enterp Netw Manage* 1(3):238–260
35. Mittal VK, Sangwan KS (2014) Prioritizing drivers for green manufacturing: environmental, social and economic perspectives. *Procedia CIRP* 15:135–140
36. Diaz-Elsayed N, Jondral A, Greinacher S, Dornfeld D, Lanza G (2013) Assessment of lean and green strategies by simulation of manufacturing systems in discrete production environments. *CIRP Ann Manuf Technol* 62(1):475–478
37. Rehman MAA, Shrivastava RL (2013) Green manufacturing (GM): past, present and future (a state of art review). *World Rev Sci Technol Sustain Develop* 10(1–2–3):17–55
38. Fullerton RR, Kennedy FA, Widener SK (2014) Lean manufacturing and firm performance: the incremental contribution of lean management accounting practices. *J Oper Manage* 32(7–8):414–428
39. Jabbour CJC, de Sousa Jabbour ABL, Govindan K, Teixeira AA, de Souza Freitas WR (2013) Environmental management and operational performance in automotive companies in Brazil: the role of human resource management and lean manufacturing. *J Clean Prod* 47:129–140
40. Sindhvani R, Malhotra V (2017) Modelling and analysis of agile manufacturing system by ISM and MICMAC analysis. *Int J Syst Assur Eng Manage* 8(2):253–263
41. Mittal VK, Sangwan KS (2014) Development of a model of barriers to environmentally conscious manufacturing implementation. *Int J Prod Res* 52(2):584–594
42. Mittal VK, Sindhvani R, Kalsariya V, Salroo F, Sangwan KS, Singh PL (2017) Adoption of integrated lean-green-agile strategies for modern manufacturing systems. *Procedia CIRP* 61:463–468
43. Sangwan KS, Mittal VK (2015) A bibliometric analysis of green manufacturing and similar frameworks. *Manage Environ Qual Int J* 26(4):566–587
44. Tseng ML, Chiu ASF, Lin YH, Chinag JH (2006) The relationship of continuous improvement and cleaner production on operational performance: an empirical study in electronic manufacturing firms, Taiwan China. *Int J Manage Sci Eng Manage* 1(1):71–80
45. Gutowski TG (2002) Environmentally benign manufacturing and eco materials; product induced material flows. *Mater Trans* 43(3):359–363
46. Atasu A, Sarvary M, Van Wassenhove LN (2008) Remanufacturing as a marketing strategy. *Manage Sci* 54(10):1731–1746
47. Kleindorfer PR, Singhal K, Wassenhove LN (2005) Sustainable operations management. *Prod Operat Manage* 14(4):482–492
48. Saaty TL (1990) Eigenvector and logarithmic least squares. *Eur J Oper Res* 48(1):156–160
49. Lee AH, Chen WC, Chang CJ (2008) A fuzzy AHP and BSC approach for evaluating performance of IT department in the manufacturing industry in Taiwan. *Expert Syst Appl* 34(1):96–107

Simulation for Effective Shop-Floor Decision Making: A Case Study



Durgesh Sharma

Abstract Shop-floor simulation has been recognized as a useful tool to analyze the effectiveness of any decision taken by shop-floor manager. The importance of simulation in shop-floor control decision making has further increased with globalization and complexity of operations. The work presents a case study of an SME unit supplying parts to a reputed automobile manufacturer in the National Capital Region. The study had been undertaken to analyze possibilities of increasing production capacity with minimum increase in infrastructure. The study was conducted under various production scenarios. Simulation software WITNESS was used for this purpose. The study identified relationships between specific investments under consideration and expected throughput.

Keywords Simulation · Production · Shop-floor control · Decision making · SMEs

1 Introduction

Globalization has posed both challenges and opportunities to industries all over world. Industries are looking for ways to improve their systems performance and increase their competitiveness in order to survive in the market place. Business opportunities need to be explored quickly and adapted to customers demand [1]. Numerous approaches, including mathematical modeling and shop-floor simulation, etc., have been used to assess and improve the shop-floor performance. However, the success of measuring and managing operational performance lies in simulating the desired shop-floor behavior [2]. Many researchers argue that simulation is one of the major tools to assist in the re-engineering process and improve the businesses effectiveness and performance [3–5]. Simulation technology enables organizations to analyze and re-engineer their processes effectively in the best possible way, using “what-if” scenarios [6]. It can identify bottlenecks; evaluate machine utilization,

D. Sharma (✉)
Raj Kumar Goel Institute of Technology, Ghaziabad, India
e-mail: durgeshrsharma@gmail.com

© Springer Nature Singapore Pte Ltd. 2019
K. Shanker et al. (eds.), *Advances in Industrial and Production Engineering*, Lecture Notes in Mechanical Engineering, https://doi.org/10.1007/978-981-13-6412-9_63

673

machine performance, impact of various scheduling strategies, etc., simulation helps in reducing cycle time, eliminating errors and defects, and improving productivity [7].

Many researchers and practitioners have used simulation to solve complex problems of industries. Williams and Zottolo [8] have used simulation to identify bottlenecks in material handling and to increasing utilization of a costly stamping press and quantified the relationships between specific capital investments under consideration and the throughput. Altuger and Chassapis [9] have used multi-criteria decision-making approach to select the preventive maintenance schedule that gives the best utility and performance values. Saeheaw et al. [7] presented the result of implementing a simulation model to design hard disk drive manufacturing process by applying line balancing to improve both productivity and quality of hard disk drive process.

The application of simulation methodologies in the SME sector is somewhat overlooked and most simulation studies tend to focus on larger organizations [1, 10]. This may be due to high cost of simulation tools and the expertise required in developing credible models [1]. However, there is a need for SMEs to improve their production and production processes and to apply simulation tools particularly at the operational aspects of their business. Simulation models can provide a unique insight into production issues, problems within the SME sector and models can help to identify opportunities for system improvements. In particular, production improvement in terms of production planning, scheduling, layout planning, and optimization of processes are key areas in which simulation can support operational decision making. Process design in SMEs in terms of process efficacy improvements and bottleneck analysis can also be modeled and analyzed using simulation methodology [1, 11].

The objective of the study was to analyze and evaluate the impact of management decisions on performance of the manufacturing system. Simulation software WITNESS was used for this purpose.

2 Case Study

A manufacturing unit located in the National Capital Region of Delhi has identified for this case study. The unit has capabilities to design and manufacture different types of automobile parts. The brief profile of the company is described in Table 1.

The flow chart below explains the typical process followed for machining of the component (Fig. 1).

The manufacturing unit had received new orders and wanted to increase its production capacity. To meet this additional demand, the management was considering the following decisions:

- Replacing all conventional machines with CNC machines
- Purchasing additional CNC machines
- Change the design of Pallet/Fixtures

Table 1 Company’s profile

a. Location:	NCR Delhi
b. Annual turnover:	Rs. 8 Crore
c. No. of employees:	62
d. No. of shifts	2
e. Product variety:	8
f. Inventory:	2–8 days
g. Monthly output	11,000 components (approx)

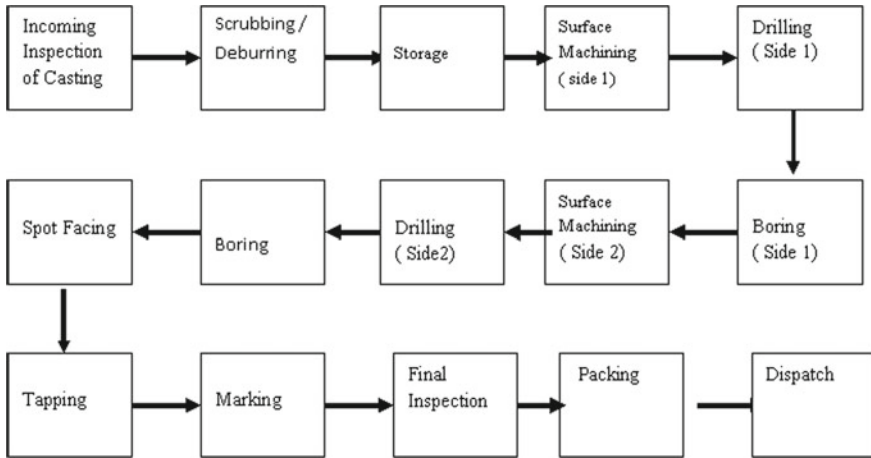


Fig. 1 Flow process chart of machining of component

However, within the organization, there was an element of uncertainty about how these changes would affect the system performance, and therefore, the simulation study was undertaken to gauge system performance, detect potential problems and to support overall manufacturing strategic decision making [1].

3 Methodology

A systematic procedure was used to study the effect of any management decision on performance of system using shop-floor simulation models. The process consisted of four phases. Phase 1 began a floor analysis, in which the shop-floor conditions were examined and useful data, such as machine cycle time, setup time, tool change time, customer demand, etc., were collected. In Phase 2, a base model was developed by incorporating the data collected in Phase 1. In Phase 3, the effects of alternative decisions were examined using shop-floor simulation. Finally, in Phase 4, the results obtained in Phase 3 were compared with base model to assess its suitability for recommendation to management for implementation.

3.1 Phase 1 Shop-Floor Analysis

Shop-floor analysis is the primary and essential step in the whole process of simulation. A detailed shop analysis has to be completed to gain a better understanding of the working environment before developing the simulation model. The collected data was applied in the simulation to emulate real-world operation processes without disrupting the system. Thus, the required data that should be collected from the shop floor include existing processes, machine cycle time, setup time, transportation time, customer demand, types of parts, and part routing, etc.

Following were the objectives:

- Throughput rate
- Machine utilization
- Processes and equipment alternatives
- Pallet/Fixture design alternatives

3.2 Phase 2 Base Model Developments

A model was developed by using WITNESS simulation software. The collected data was entered into software in order to build the model. Once the model was completely designed and developed, verification was conducted by comparing the simulation and theoretical outputs. Verification was necessary to determine whether the obtained simulated output results were within the acceptable range before proceeding to the next phase, which is experimental design.

To develop the simulation model following assumptions were made:

- The process flow for the simulation was assumed to be continuous.
- It was assumed that no breakdown occurred and no there was no product quality problem.
- Part mix was assumed to be fixed.
- Inter-arrival time was assumed to be fixed.
- The transportation time between workstations was assumed to be constant.
- The machine cycle times were assumed to be the same for both single-sided and double-sided parts.
- The production plant assumed to run six days a week with two shifts per day.
- Sequencing rule max balance processing time (Max BPT) and dispatching rule minimum in queue were used.
- All CNC machines were assumed to be highly flexible.

The study consisted of developing a model of the existing unit (the base model) together with a number of “what-if” models to test various scenarios [1]. For each model, developed a runtime of 80 h and a warm-up period 8 h was set in order to allow the model to reach a steady state condition [12]. For each model, statistics for the number of parts machined and machine utilization were collected. After the base

model was designed and developed, following experiments were conducted with this model to test various operational scenarios [1]:

- Base model of existing unit: Production rate and machine utilization were calculated based on the existing machines and process used by the manufacturing unit.
- Experiment 1: Replacing existing conventional machines with CNC machines
- Experiment 2: Adding more CNC machines:
- Experiment 3: Changing the fixture design

Performance Measures: Following two performance measures were considered in this model:

Machine Utilization: It measures the machine usage intensity and is computed as the percentage of busy hours that a machine runs to complete given tasks. The data can be acquired from the statistical report generated by WITNESS. Average machine utilization can be expressed as the sum of all the machine busy times divided by the total number of machines.

Throughput Rate: It is defined as the rate of production in a process over a specific amount of time. It is a measure of the number of parts completed per unit time.

3.3 Phase 3 Effects of Alternative Decisions

Experiment 1: Existing four drilling machines and two boring machines to be replaced by two CNC machines.

Model 1 represents the base model and Model 2 represents the model where existing four drilling machines and two boring machine machines were replaced by two CNC machines. Table 2 summarizes the details of experiment and the results obtained from simulation.

The result shows that there was a considerable improvement in both throughput rate and machine utilization. The increase of throughput rate and machine utilization may be due to saving in setup time and tool changing time and higher cutting speed of CNC machines.

Experiment 2, Adding CNC machines to the production system: Model 1 represents the base model; Model 2 represents the scenario of Experiment 1; Model 3 to

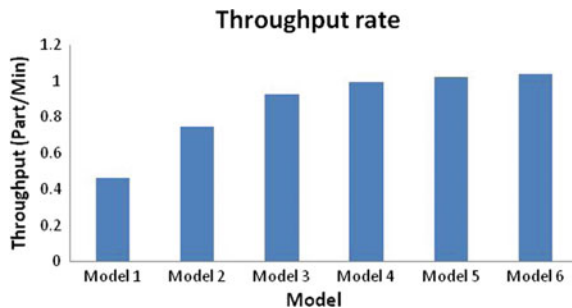
Table 2 Simulation results for replacing existing machines with CNC machines

	Model description	Throughput rate (Parts/Min)	Machine utilization (%)
Model 1	Base model	0.461	27.52
Model 2	Existing conventional machines replaced by two CNC machines	0.725	43.27

Table 3 Simulation results by adding machines to CNC system

	Model description	Throughput rate (Parts/Min)	Machine utilization
Model 1	Base model	0.461	27.52
Model 2	Existing conventional machines replaced by two CNC machines	0.745	43.27
Model 3	Existing conventional machines replaced by three CNC machines	0.926	45.72
Model 4	Existing conventional machines replaced by four CNC machines	0.995	47.12
Model 5	Existing conventional machines replaced by five CNC machines	1.042	47.82
Model 6	Existing conventional machines replaced by six CNC machines	1.038	47.97

Fig. 2 Effect of adding CNC machines on throughput



Model 6 represent the models, when one CNC machine was added from previous models. Table 3 summarizes the details of experiment and the results obtained from simulation.

Figures 2 and 3 show the effect of adding CNC machines on throughput time and machine utilization. The results demonstrate that there was a significant improvement in throughput rates and machine utilization until four additional machines were added to the system. Beyond this, there was no significant improvement in both throughput rate and machine utilization. This may be because adding machines, beyond four would create new bottlenecks.

Experiment 3: changing the design of fixture such that it can accommodate more number of parts at a time.

When the simulation studies were conducted, the manufacturing unit was using a fixture, where two parts can be mounted at a time. Model 2 represents the basic model for this experiment. Models 8–10, represent the models when two additional parts

Fig. 3 Effect of adding CNC machines on machine utilization

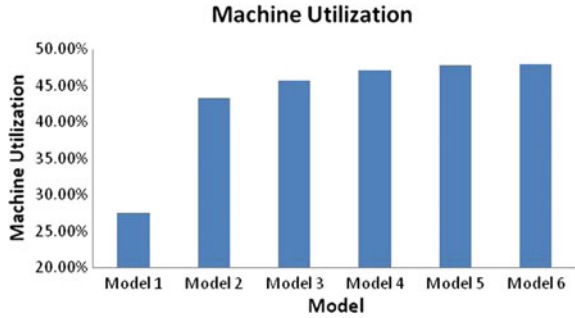
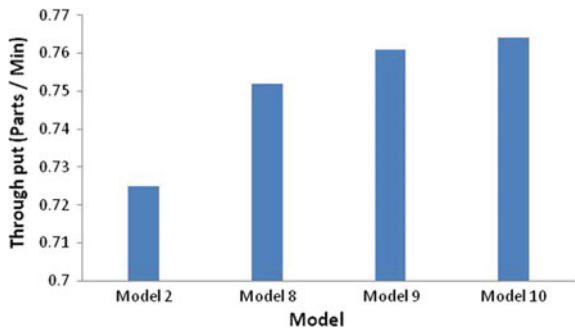


Table 4 Effect of changing the design of fixture

	No of parts mounted	Throughput rate (Parts/Min)	Machine utilization (%)
Model 2	2	0.725	43.27
Model 8	4	0.752	44.52
Model 9	6	0.761	44.55
Model 10	8	0.764	44.56

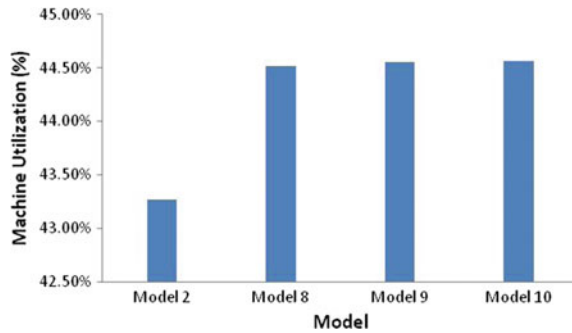
Fig. 4 Effect change in fixture design on throughput time



were mounted from previous models. Table 4 summarizes the details of experiment and the results obtained from simulation.

Figures 4 and 5 show the effect of change in design of fixture on throughput and machine utilization. The results demonstrate that there was improvement in throughput rates and machine utilization if the existing fixture design was changed to accommodate four parts at a time. Beyond this, the improvement in throughput time and machine utilization was marginal.

Fig. 5 Effect change in fixture design on machine utilization



4 Conclusions and Future Work

The simulation study has provided significant help and value to the automotive parts manufacturer in making right decisions about utilizing existing machines and purchasing new machines by confirming the throughput of the system under a variety of operating conditions. An automobile part manufacturing unit was examined for this case study. Simulation was used as tool to examine following management decisions:

- The first decision examined was to replace existing conventional machines with CNC machines. The study concluded that the decision would improve both throughput and machine utilization.
- Second decision examined was to increase the number of CNC machines. The study suggested adding four CNC machines, as it would significantly increase throughput rate and machine utilization.
- The third decision examined was to change the design of fixture. The study suggested change in the design of fixture to accommodate four parts at a time as this would result in significant improvement in shop-floor performance.

The study was limited to one case study involving three management decisions. The study may be extended to several management decisions. Additional studies can be carried out in other areas like quality control, production planning, layout planning, etc., to make effective decisions. To conclude, simulation is very powerful tool, which can assist in the effective management of operations and optimizing investments in upgrading the shop-floor technologies.

References

1. O'Kane J, Papadoukakis A, Hunter D (2007) Simulation usage in SMEs. *J Small Bus Enterp Dev* 14(3):514–527
2. Barnes D, Radnor Z (2008) Performance measurement and management: the operations management perspective. Palgrave Macmillan, London, UK

3. Greasley A, Barlow S (1998) Using simulation modelling for BPR: resource allocation in a police custody process. *Int J Oper Prod Manage* 18:978–988
4. Cheung Y, Bal J (1998) Process analysis techniques and tools for business improvements. *Bus Process Manage J* 4(4):274–290
5. Paul RJ, Hlupic V, Giaglis GM (1998) Simulation modeling of business processes. In: *Proceedings of 3rd UK academy for information systems conference, UK*, pp 311–320
6. Profozich D (1998) *Managing change with business process simulation*. Pearson
7. Saeheaw T, Charoenchai N, Chattinnawat W (2009) Line balancing in the hard disk drive process using simulation techniques. *Methodology* 3(12):660–664
8. Williams E, Zottolo M, Williams EJ (2003) Improvement of throughput and resource utilization in an automotive stamping plant. In: *1st international industrial simulation conference, Valencia*
9. Altuger G, Chassapis C (2009) Multi criteria preventive maintenance scheduling through Arena based simulation modeling. In: *Proceedings of 2009 Winter Simulation Conference, Austin*, pp 2123–2134
10. Robinson S, Brooks R, Kotiadis K, Zee DJV (2010) *Conceptual model of discrete event simulation*. Taylor & Francis
11. Velumani S, Tang H (2017) Operations status and bottleneck analysis and improvement of a batch process manufacturing line using discrete event simulation. In: *45th SME North American Manufacturing Research Conference, LA, USA*, pp 100–111
12. Law AM (2007) Statistical analysis of simulation output data: the practical state of art. In: *Proceedings of 2007 winter simulation conference, Washington DC*, pp 73–83

Modeling and Analysis of Factors Influencing Agility in Healthcare Organizations: An ISM Approach



Rahul Sindhwani, Punj Lata Singh, Aamir Iqbal,
Devender Kumar Prajapati and Varinder Kumar Mittal

Abstract Healthcare sector effectuates agile application to upgrade services level and competitive advantage. It states utilizing expertise ideas relating numerous managing methods in obtaining a correlation between variable. The paper begins with the idea of agility in the healthcare organization; secondly, it facilitates us in finding out the factors affecting the agility in the healthcare organization; thirdly, it explicates the interrelationship among them using Interpretive Structure Modelling (ISM) technique and MICMAC analysis. Agility being imperative for healthcare organization as it helps healthcare companies reconcile more rapidly to fluctuating customer needs, competitor feedback. This study helps in the ranking of factors influencing agility in healthcare, which finally help hospitals and healthcare organization in implementing agile system efficiently and effectively.

Keywords Agility · Healthcare · Interpretive structure modeling (ISM) · MICMAC · Factors · Implementation

1 Introduction

To survive in the current competition of advance era of globalization, every line of work of the company is working hard to develop the best quality management parameters, tools, and strategies. Every manufacturing organization now requires effective remote sensing and degree of automation in synchronizing with Web facilities platform. Moreover, an organization needs to amalgamate environmental management

R. Sindhwani (✉) · A. Iqbal · D. K. Prajapati
Department of Mechanical Engineering, Amity School of Engineering
and Technology, Amity University Uttar Pradesh, Noida 201301, Uttar Pradesh, India
e-mail: rsindhwani@amity.edu

P. L. Singh
Department of Civil Engineering, Amity School of Engineering and Technology, Amity
University Uttar Pradesh, Noida 201313, Uttar Pradesh, India

V. K. Mittal
Meridian Manufacturing Inc, Regina, Canada

© Springer Nature Singapore Pte Ltd. 2019
K. Shanker et al. (eds.), *Advances in Industrial and Production Engineering*, Lecture
Notes in Mechanical Engineering, https://doi.org/10.1007/978-981-13-6412-9_64

into their plan so as to achieve suppleness in an agile manufacturing system. The idea of agility long last from a century, with an organization from US military to Japanese manufactures. Healthcare organization nowadays being a great center of interest and are under severe pressure to improve. It is now a challenging sector, it comprises hospitals, nursing homes, clinics, and institutions with every level of patient care. As the time passes, the demand for health care is increasing day by day, but the financial condition is becoming more worsening. Hence, there is a need for the efficient way of facilitating health care services. In this era, customer requires affordable, accessible, safe, and cost-effective health care. So it is a challenging issue for both industries and academia to how to tackle this issue? However, there are many solutions to this issue such as networking, reengineering, and high-performance organization. Variation in customer demand has left the manufacturing industries bewildered. Today customers have ample of the option to choose, so to compete in the market manufacturing industries are compelled to fulfill the desires of the customer. So there is the need to implement agile techniques in the healthcare organization. Although, lean manufacturing is implemented in health care to eliminate unnecessary motion, wastage, inventory and defects for better flow of goods, information, patients [1]. Various studies show that lean technique is already implemented in hospitals showing better impact [2, 3]. But now there is a need to implement agile techniques in every organization. Implementing agility in health care would lead to remove the complication and will improve the efficiency of the healthcare organization. Agile manufacturing refers to all process, ideas, tools, and training which respond to customer's needs and market need maintaining cost and quality. Healthcare industry is basically divided into two parts: (a) Healthcare products manufacturing (b) Healthcare services. Healthcare product manufacturing includes health equipment manufacturers, drug manufacturers. Healthcare services include services such as consultation, exercise centers, medical software, and medical insurance. An organization can only fulfill the increasing, complex, unpredictable demand and variation in product design and services by applying agile techniques [4, 5]. The ultimate goal is to obtain development, upgradation, and refinement of the healthcare organization internationally so that quality service can be given to patients. Improving the quality with simultaneously reducing cost is a challenging task. As stated by Natarajan, that in last two decades, health care has improved a lot in the field of delivery of service, quality of care, in absentia health care (that is non-face-to-face communication) and among many others factors.

Hence, 10 factors have been recognized through various literature reviews, articles, and expertise views which are then analyzed by Interpretive Structure Modeling (ISM) technique and MICMAC analysis. ISM techniques are one of the ideal approaches to examine the interconnections between numerous factors [6–8]. With the help of ISM technique and MICMAC analysis linkage between numerous factors are obtained, the factors are then isolated as the driving factors (the main cause of others factors to occur) and dependence factors (depends on others). The segregation and examination of factors are done so that researchers can provide proper devotion and care and it also helps the managers while applying agility in their company.

The main aim behind writing this paperwork is:

- To detect and identify the factors or elements and make changes in healthcare organization switching from conventional to the agile system.
- With the help of ISM techniques, develop a relationship between factors.
- Using MICMAC analysis, determine the driving and dependence power of the factors affecting AMS in health care.
- To determine the best scope of these techniques.

The residue of this paperwork contains recognition of key factors with the help of reports and publications and expertise ideas are described in the Sects. 2 and 3. Section 4 contains a brief introduction of the ISM approach. Implementation of the ISM approach and MICMAC analysis is shown in Sect. 5. In the last, Sect. 6 has results, conclusions, and future scope.

2 Literature Review

While looking into various literatures and papers, we found numerous obstacles faced by healthcare organization during agile practices. This shows that there are various factors which affect the agility in health care or decides the upbringings and downfall of agile projects in health care. First of all, we should know what agile companies are? According to Christopher and Jultner, agility is a reply to the high level of intricacy and uncertainty in the advanced market. Naylor et al. [9] stated that “agility implies applying market understanding and utilizing chances for fast-changing market”. Agility and flexibility are inter-related to each other as discussed in the literature [10, 11]. Roots of agility lie in the flexible manufacturing system [12]. The main aim of the agile endeavor is to fulfill customer and employees satisfaction. In a competitive market where the demand of customer fluctuates rapidly, Agility is believed as the winning scheme or plan of action. According to a case study of a public health care organization in Europe by Helena Santos-Rodrigues, Joao Faria, and Desiree Cranfield focuses on finding the effect of intellectual capital on healthcare organization. On the basis of this, 68 questionnaires data were used in research which were filled by hospital managers and leaders between July and August 2011. Researchers show that there is a direct relationship between human capital and innovation. Katzenbach and Smith [13] cited that Team-based management is a highly active facilitator of organizational agility. Kidd [14] stated that improved agility requires the amalgamation of human capital, ideas and advanced technology. Various activity and effort to execute agility in an organization are sharing information among the different group, giving the power to take the decision to employees integrating technologies, design specification, product planning [15].

3 Identification of Factors Affecting Agility in Healthcare Organization

Now a day's disease growing in the society must be considered as a priority to be dealt at every level. Evolution from a traditional or conventional approach to agile techniques is not an easy deal it requires identifying and analyzing the factors that could facilitate faster implementation of agility in healthcare organization [16]. So this paper identifies 10 crucial factors through literature and experts views from academia and industry. These factors are as follows (Table 1).

4 An Introduction of ISM Approach

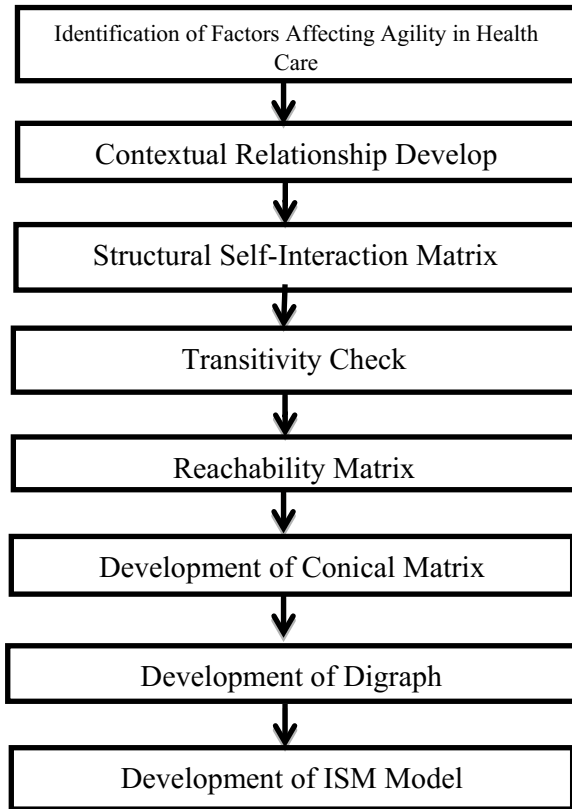
Due to the availability of a large number of elements and connectivity among these elements researchers faced ample of the problem which required to be solved for obtaining an optimal solution [29]. So to solve these type of complex structures various methodology have been tested, among them ISM is the ideal and advance one. ISM was first proposed by Warfield in 1973 to solve complexly structured modeling [30]. ISM is a computer-aided forming method which enables us in joining three methodologies, i.e., words, graphics, and mathematics. It is a methodology to solve complex cases and models [31]. As stated by Attri et al. [32], ISM converts an ambiguous and complex problem to structure a well-defined problem and provides the impact of variables on decision objects. ISM is defined as a procedure which helps in supporting the user to realize what they believe and examine clearly what they don't know [33, 34]. It is a method which converts unsystematic and unarranged models of the system into well-arranged models [32]. ISM methodology facilitates us to use expert's ideas, knowledge to divide complex situation models into various factors or subfactors and provides a multi-level structural model. It is a structural analysis tool which helps in defining variables according to the extent they influence other factors.

In the ISM approach, first identification of factors which affect the system and the factors that are related to each other are identified [35]. After the factors being recognized, relationship is developed between the factors which are aligned into matrix named structure self-interaction matrix (SSIM). After obtaining the SSIM matrix, reachability matrix (RM) is obtained with the help of SSIM and is checked for transitivity. After that reachability matrix is converted into conical matrix. With the help of relationship developed by reachability matrix, digraph is drawn. The digraph is now converted into ISM model [29, 30, 33, 36]. The steps are illustrated via diagram as shown in Fig. 1.

Table 1 Factors affecting agility in the healthcare organization

Factors	Description	References
Organizational structure	With flatter and team-managed organization leads to eradicate disputes and causes less failure and loss in health care organization and avoid wasting time on non-value added work	[17, 18]
Leadership	Leadership is the prime requirement in any health care as it imparts confidence to the team and other members	[19]
Patient assumption and hospital discernment	The distinction between patient belief and hospital discernment has a greater impact on quality parameters	[20]
Chain management in hospitals	It improves the quality of healthcare management by joint work between the different members	[20, 21]
Implementing clinical governance	Emphasize on integrating human resources and information technology	[14, 22]
Technology upgrade	With the advancement of technology in every aspect so there is also a need for advancement in medical and healthcare organization	[23, 24]
Market awareness	Prior to implementing agility in healthcare organization, we must have a clear knowledge of the market condition and virtual corporation	[25, 26]
Outsourcing	Agile promotes outsourcing as supply chain management are adopted in health care; outsourcing is a boom nowadays in health care as an advanced tech is available and practiced more frequently abroad	[27]
Supporting customers mentally	Supportive ideas are created for customer comfort and care. It creates satisfaction in others group of the patient like family members	[20, 25]
Multi-skill and Multi-knowledgeable employees	Employees must be provided with the best training program so that everyone has multi-skill and knowledge and flexibility to rapidly switch to new task if required	[20, 28]

Fig. 1 Flow diagram for ISM methodology



5 Modeling of AMS Factors with ISM Approach and MICMAC Analysis

For model making, several steps which are to be followed are:

Step 1 Determining relevant key factors influencing health care

The factors influencing agility healthcare organization are determined via literature survey and brainstorming with knowledgeable from academia and health care.

Step 2 Preparation of structural self-interactive matrix (SSIM)

In SSIM, four notation are shown to indicate inter-connection factors (i and j)

- V indicates that factor j will be helped by factor i .
- A indicates that factor i will be helped by factor j .
- X indicates i and j will influence each other.
- O indicates both are not related to each other.

Table 2 Structural self-interactive matrix (SSIM)

	10	9	8	7	6	5	4	3	2
1	<i>O</i>	<i>V</i>	<i>O</i>	<i>O</i>	<i>O</i>	<i>V</i>	<i>O</i>	<i>V</i>	<i>A</i>
2	<i>A</i>	<i>O</i>	<i>O</i>	<i>O</i>	<i>O</i>	<i>V</i>	<i>O</i>	<i>O</i>	
3	<i>A</i>	<i>V</i>	<i>O</i>	<i>A</i>	<i>O</i>	<i>A</i>	<i>A</i>		
4	<i>O</i>	<i>V</i>	<i>O</i>	<i>X</i>	<i>O</i>	<i>O</i>			
5	<i>A</i>	<i>V</i>	<i>O</i>	<i>O</i>	<i>O</i>				
6	<i>A</i>	<i>V</i>	<i>O</i>	<i>O</i>					
7	<i>A</i>	<i>O</i>	<i>V</i>						
8	<i>O</i>	<i>V</i>							
9	<i>A</i>								

The relationship between the factors has been determined and then SSIM has been developed. This SSIM is then discussed by expertise as depicted in Table 2. The symbols *V*, *A*, *X*, *O* denote the relationship between the factors (*i* and *j*) [37]

- Notation *V* is used for cell (1, 9) because of factor 1 effect factor 12.
- Notation *A* is used for cell (2, 10) because of factor 10 effect factors 2.
- Notation *X* is used for cell (4, 7) because factor 4 and 7 affect each factor.
- Notation *O* is used for cell (1, 8) because factor 1 and 8 are unrelated.

Step 3 Establishing reachability matrixes

After obtaining the SSIM matrix, a reachability matrix is created. In this, SSIM is transformed into a binary matrix by replacing *V*, *A*, *X*, *O* by 1, 0 as per case. The rules for substituting 1 and 0 are as follows:

- If *V* is used in place of (*i*, *j*) in Table 2, then the (*i*, *j*) will have 1 and (*j*, *i*) will have 0.
- If *A* is used in place of (*i*, *j*) in Table 2, then the (*i*, *j*) will have 0 and (*j*, *i*) will have 1.
- If *X* is used in place of (*i*, *j*) in Table 2, then the (*i*, *j*) will have 1 and (*j*, *i*) will also have 1.
- If *O* is used in place of (*i*, *j*) in Table 2, then the (*i*, *j*) will have 0 and (*j*, *i*) will have 0.
- *V* is used for (1, 9), thus reachability matrix will have 1 for (*i*, *j*) and 0 for (*j*, *i*).
- *A* is used for (2, 10), thus reachability matrix will have 0 for (*i*, *j*) and 1 for (*j*, *i*).
- *X* is used for (4, 7), thus reachability matrix will have 1 for both (*i*, *j*) and (*j*, *i*).
- *O* is used for (1, 7), thus reachability matrix will have 0 for both (*i*, *j*) and (*j*, *i*).

Final reachability matrix is calculated by integrating transitivity. Transitivity is a connection between three elements such that if a relationship holds for *A* and *B* and also the relation occurs between *B* and *C* then *A* and *C* itself comes in a relation. Table 3 depicts Final reachability matrix and 1* stands for transitivity.

Table 3 Initial and final reachability matrix

	1	2	3	4	5	6	7	8	9	10
1	1	0	1	0	1	0	0	0	1	0
2	1	1	1*	0	1	0	0	0	1*	0
3	0	0	1	0	0	0	0	0	1	0
4	0	0	1	1	0	0	1	1*	1	0
5	0	0	1	0	1	0	0	0	1	0
6	0	0	0	0	0	1	0	0	1	0
7	0	0	1	1	0	0	1	1	1*	0
8	0	0	0	0	0	0	0	1	1	0
9	0	0	0	0	0	0	0	0	1	0
10	1*	1	1	1*	1	1	1	1*	1	1

Step 4 Partition of reachability matrix into different levels

Final reachability matrix possesses reachability and antecedent set. The horizontal factors come under reachability set and antecedent set comprises vertical factors. After that common value is obtained [38]. The factors having the same value for reachability and intersection set occurs in the first position. The first level is then eliminated from the table, and then this process repeats for the next level of a hierarchy. This process repeats until each element got its position in the pecking order. This order enables us in the modeling of the digraph. Ten factors along with the reachability set, antecedent set, intersection set, and the levels are shown in Table 4.

Step 5 Making of conical matrix

Conical matrix is obtained by arranging the factors according to highness of hierarchy from top to bottom. By summing a total number of ones in the rows, we get drive power and by adding in a column we get dependence power. Now, the drive

Table 4 Iteration (1–7)

Factors	Reachability set	Antecedent set	Intersection set	Level
1	1	1, 2, 10	1	5th
2	2	2, 10	2	6th
3	3	1, 2, 3, 4, 5, 7, 10	3	3rd
4	4	4	4	4th
5	5	1, 2, 5, 10	5	4th
6	6	6, 10	6	3rd
7	4,7	4, 7, 10	4,7	3rd
8	8	4, 7, 8, 10	8	2nd
9	9	1, 2, 3, 4, 5, 6, 7, 8, 9, 10	9	1st
10	10	10	10	7th

power and dependence power are ranked by checking maximum no of ones in rows and column, respectively, as depicted in Table 5.

Step 6 Development of digraph

In the making of the digraph, the top-level factors are located at the topmost place of the digraph and then the second level is indicated in the second level of the digraph and rest follow the same till we get bottom level in the last position.

Step 7 Drafting ISM model

Now after obtaining digraph, an ISM model is created by exchanging nodes with their respective factors as displayed in Fig. 3. ISM model represents that multi-skill and multi-knowledgeable employees and leadership in the healthcare organization have high driving power. The employees must be provided with the best training program so that everyone has multi-skill and knowledge and flexibility to rapidly switch to a new task if required. For better agility in healthcare, proper leadership must be there as a good leader has a great impact on the worker by their personality leadership is the foundation and basic requirement in any healthcare as it imparts confidence to the team. Unlike traditional management style of control and command leadership, trust and confidence should be there. ISM model shows that factors having high driving factors as organization structure play a vital role in the execution of agile manufacturing system. They also need more attention and care as they have high driving and low dependency. Patient assumption and hospital discernment and chain management in hospitals also play a vital role in AMS. After those factors like a patient assumption and hospital discernment, technology upgrade and market awareness come in the hierarchy level after that, hence, these factors have the average drive and dependency powers. Outsourcing and supporting customers mentally have high dependency and less driving powers. These required less care as it would not have much effect.

Table 5 Conical matrix

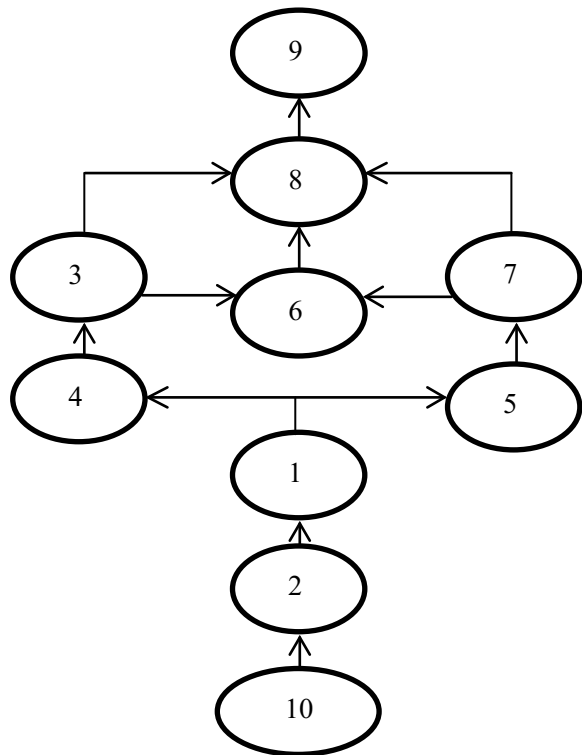
	9	8	3	6	7	4	5	1	2	10	Drive factor
9	1	0	0	0	0	0	0	0	0	0	1
8	1	1	0	0	0	0	0	0	0	0	2
3	1	0	1	0	0	0	0	0	0	0	2
6	1	0	0	1	0	0	0	0	0	0	2
7	1	1	1	0	1	1	0	0	0	0	5
4	1	1	1	0	1	1	0	0	0	0	5
5	1	0	1	0	0	0	1	0	0	0	3
1	1	0	1	0	0	0	1	1	0	0	4
2	1	0	1	0	0	0	1	1	1	0	5
10	1	1	1	1	1	1	1	1	1	1	10
Dependence power	10	4	7	2	3	3	4	3	2	1	39/39

Step 8 MICMAC analysis

The main idea behind the MICMAC technique is to get the driving and dependency powers of the above factors. Now these factors have been divided into four groups as described in Fig. 4.

- Group 1: Autonomous factors;
 - Group 2: Dependent factors;
 - Group 3: Linkage factors;
 - Group 4: Driving factors.
- Group 1: Autonomous factors—weak driving power and weak dependency is the characteristic of this group. In this group, we have four factors, i.e., organizational structure, Implementing clinical governance, technology upgrade, and outsourcing (Factors 1, 5, 6 and 8), respectively.
- Group 2: Dependence factors—this group shows weak drive power but strong dependence. In this group, two factors have been identified, i.e., patient assumption and hospital discernment and supporting customers mentally (Factors 3 and 9), respectively.

Fig. 2 Digraph for AMS factor



- Group 3: Linkage factors—No factors have been identified in this group. These groups possess both driving and dependency power strong.
- Group 4: Driving factors—weak dependence and strong driving power is the characteristic of this group. In this group, we have four identified factors, i.e., leadership, Chain management in hospitals, market awareness, multi-skill and multi-knowledgeable employees (Factors, 2, 4, 7, and 10) respectively (Fig. 2).

6 Results and Conclusion

This paper has identified 10 factors affecting agility in healthcare organization by reviewing several kinds of literature, research papers, and experts’ ideas. ISM analysis and MICMAC analysis have been applied to those factors to develop the contextual relationship between them. The result of above is shown in Figs. 3 and 4. The factors play a crucial role in the upliftment of healthcare services; these models show a hierarchy that which factors have a greater influence on a healthcare organization. This approach can be helpful for medical colleges, nursing homes, super specialty hospital, healthcare practitioners, and decision makers. The factors which have been identified are very recent and useful for the growth of hospitals. The Indian health care is still facing problems due to practicing traditional approach in spite of using new agile techniques. The rapid changes in the market and customer demands variation requires agile manufacturing techniques to be implemented [23].

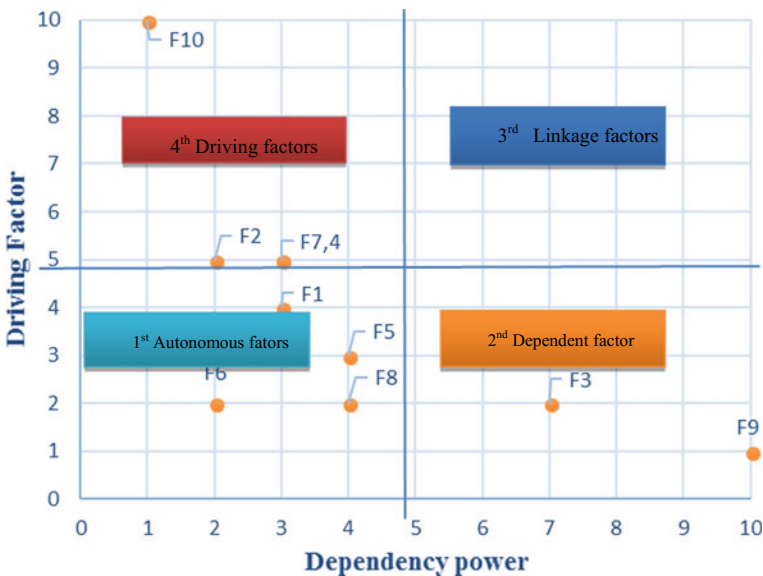


Fig. 3 MICMAC analysis

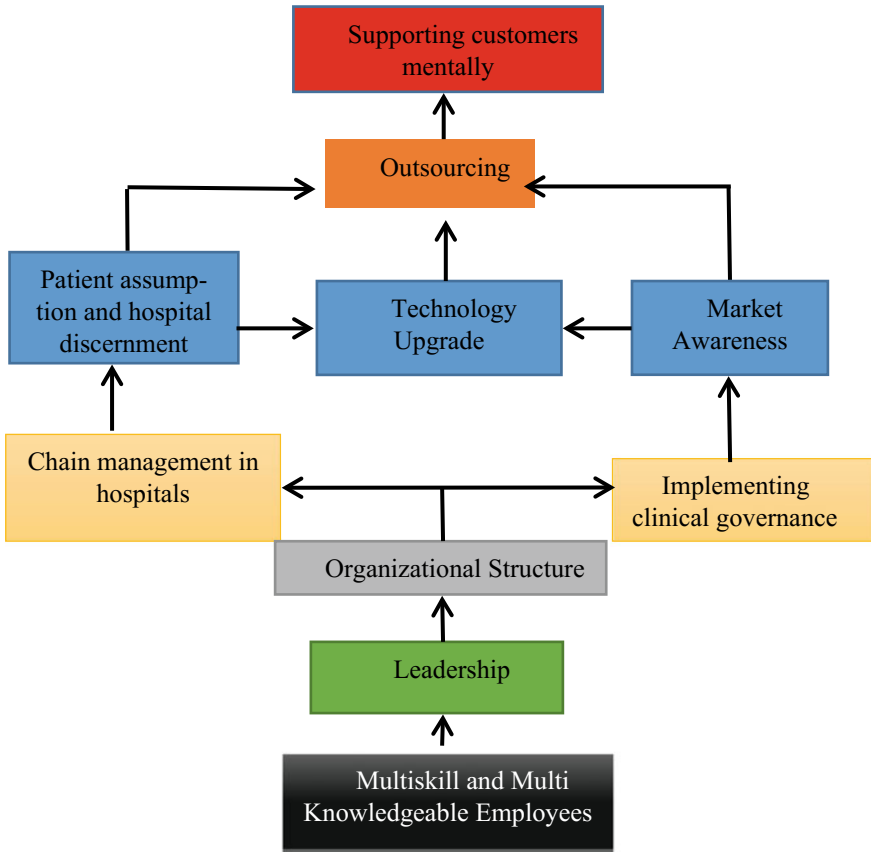


Fig. 4 ISM model for AMS in healthcare

New optimized healthcare models are required for sustainable development in healthcare organization and for that we have to choose the correct path for applying input resources.

Based on the result obtained in this paper, the following points are noted as:

- This research paper uses ISM and MICMAC approach for determining key factors that should be implemented in a healthcare organization.
- This approach also lets us know the relationship between the factors and type extent of influence of one factor on another factor.
- Factors like multi-skill and multi-knowledgeable employees, leadership, organization structure have high driving factor, i.e., if these factors severely affect others factors, hence, these key factors require pure devotion and care on the priority basis.

- This research also shows a path for an organization which still run on traditional techniques to rapidly switch over implementing new agile techniques to their organization.

The health care now is a wide sector and requires huge attention and researches to be done so that new and more innovative ideas can be implements in this sector for economic growth of the country.

References

1. Brandao de Souza L (2009) Trends and approaches in lean healthcare. *Leadership Health Serv* 22(2):121–139
2. Radnor Z, Osborne SP (2013) Lean: a failed theory for public services? *Public Manage Rev* 15(2):265–287
3. Sindhwani R, Malhotra V (2013) Overview and drivers of agile manufacturing system: a review. *Int J Mark Technol* 3(12):144
4. Towill D, Christopher M (2002) The supply chain strategy conundrum: to be lean or agile or to be lean and agile? *Int J Logist* 5(3):299–309
5. Sindhwani R, Malhotra V (2015) Lean and agile manufacturing system barriers. *Int J Adv Res Innov* 3(1):110–112
6. Kumar S, Sharma RK (2015) An ISM based framework for structural relationship among various manufacturing flexibility dimensions. *Int J Syst Assur Eng Manage* 6(4):511–521
7. Jain V, Raj T (2015) Modeling and analysis of FMS flexibility factors by TISM and fuzzy MICMAC. *Int J Syst Assur Eng Manage* 6(3):350–371
8. Attri R, Dev N, Sharma V (2013) Interpretive structural modelling (ISM) approach: an overview. *Res J Manage Sci* 2(2):3–8
9. Naylor JB, Naim MM, Berry D (1999) Leagility: integrating the lean and agile manufacturing paradigms in the total supply chain. *Int J Prod Econ* 62(1–2):107–118
10. Christopher M (2000) The agile supply chain: competing in volatile markets. *Ind Mark Manage* 29(1):37–44
11. Swafford PM, Ghosh S, Murthy NN (2006) A framework for assessing value chain agility. *Int J Oper Prod Manage* 26(2):118–140
12. Gosling J, Purvis L, Naim MM (2010) Supply chain flexibility as a determinant of supplier selection. *Int J Prod Econ* 128(1):11–21
13. Katzenbach JR, Smith DK (1993) *The wisdom of teams: creating the high-performance organization*. Harvard Business Press, Boston
14. Kidd PT (1995) *Agile manufacturing: forging new frontiers*. Addison-Wesley Longman Publishing Co., Inc, London
15. Gehani RR (1995) Time-based management of technology: a taxonomic integration of tactical and strategic roles. *Int J Oper Prod Manage* 15(2):19–35
16. Sindhwani R, Malhotra V (2016) Modelling the attributes affecting design and implementation of agile manufacturing system. *Int J Process Manage Benchmarking* 6(2):216–234
17. <https://www.beckershospitalreview.com/human-capital-and-risk/agile-management-can-benefit-healthcare-process-improvement-projects.html>, last accessed 2018/12/24
18. Powell L (2002) Shedding a tier: flattening organisational structures and employee empowerment. *Int J Educ Manage* 16(1):54–59
19. <https://www.linkedin.com/pulse/20140915033433-34529931-leadership-impact-on-healthcare-organizational-behavior>, last accessed 2018/12/24
20. Talib F, Rahman Z (2015) An interpretive structural modelling for sustainable healthcare quality dimensions in hospital services. *Int J Qual Res Serv* 2(1):28–46

21. Vanu SC (2004) Clinical governance: a fresh look at its definition. *Clin Governance Int J* 9(2):87–90
22. Thomson R (1998) Quality to the fore in health policy at last. *Br Med J* 317(7151):95–96
23. Mittal VK, Sindhwani R, Kalsariya V, Salroo F, Sangwan KS, Singh PL (2017) Adoption of integrated Lean-Green-Agile strategies for modern manufacturing systems. *Proc CIRP* 61:463–468
24. Feeney AR, Zairi M (1994) Best practice quality management in pathology: results of a benchmarking study. *Benchmarking Qual Manage Technol* 1(2):64–80
25. Christopher M, Towill D (2001) An integrated model for the design of agile supply chains. *Int J Phys Distrib Logist Manage*, 31(4):235–246
26. Tolf S, Nyström ME, Tishelman C, Brommels M, Hansson J (2015) Agile, a guiding principle for health care improvement? *Int J Health Care Qual Assur* 28(5):468–493
27. Guimarães CM, de Carvalho JC (2011) Outsourcing in the healthcare sector—a state-of-the-art review. *Supply Chain Forum Int J* 12(2):140–148
28. Sharp JM, Irani Z, Desai S (1999) Working towards agile manufacturing in the UK industry. *Int J Prod Econ* 62(1–2):155–169
29. Jayant A, Azhar M, Singh P (2015) Interpretive structural modelling (ISM) approach: a state of the art literature review. *Int J Res Mech Eng Technol* 5(1):15–21
30. Malhotra V (2014) Modelling the barriers affecting design and implementation of reconfigurable manufacturing system. *Int J Logist Syst Manage* 17(2):200–2017
31. Janes FR (1988) Interpretive structural modelling: a methodology for structuring complex issues. *Trans Instrum Meas Control* 10(3):145–154
32. Attri R, Grover S, Dev N, Kumar D (2013) An ISM approach for modelling the enablers in the implementation of total productive maintenance (TPM). *Int J Syst Assur Eng Manage* 4(4):313–326
33. Raj T, Shankar R, Suhaib M (2008) An ISM approach for modelling the enablers of flexible manufacturing system: the case for India. *Int J Prod Res* 46(24):6883–6912
34. Sindhwani R, Malhotra V (2017) Modelling and analysis of agile manufacturing system by ISM and MICMAC analysis. *Int J Syst Assur Eng Manage* 8(2):253–263
35. Mittal VK, Sangwan KS (2011) Development of an interpretive structural model of obstacles to environmentally conscious technology adoption in Indian industry. In: *Globalized solutions for sustainability in manufacturing*. Springer, Berlin, pp 383–388
36. Talib F, Rahman Z, Qureshi MN (2011) An interpretive structural modelling approach for modelling the practices of total quality management in service sector. *Int J Model Oper Manage* 1(3):223–250
37. Sindhwani R, Malhotra V (2016) Barriers evaluation for agile manufacturing system with fuzzy performance importance index approach. *Int J Agile Syst Manag* 9(4):292–301
38. Sindhwani R, Malhotra V (2017) A framework to enhance agile manufacturing system: a total interpretive structural modelling (TISM) approach. *Benchmarking Int J* 24(4):467–487

An Empirical Study of Performance Improvement in Product Delivery System Through Six Sigma DMAIC Approach



Rajak Anup Kumar , Kumar Nilesh, Nayak Yogesh Kumar and Peesapati V. V. Rajagopal

Abstract The paper presents key features, obstacles and shortcoming of Six Sigma method which allows an organization simply a means of measurement of quality that strives for near perfection. In industry, on the globe due to the competitive market and customer pressure struggles to sustain. Focusing on DMAIC processes with great impact on business performance, the methodology involves the static analysis of quality and quantity common variance which can be reduced by the Six Sigma team. Six Sigma application in product resulted in performance improvement of 48.66%, quality improvement of 67.47%, delivery time is improved 36.63%, cost reduction is 72.02% and the marginal reduction in procurement and inventory carrying cost. Overall improvement in customer satisfaction is registered by a margin of 8%. This case study on Six Sigma principle and practices will succeed by refining the organizational culture continuously.

Keywords DMAIC · Defects per million opportunities (DPMO) · Delivery system

R. Anup Kumar (✉)

Department of Mechanical Engineering,
Chaibasa Engineering College, Chaibasa 831001, Jharkhand, India
e-mail: anuprajak14@gmail.com

K. Nilesh

Department of Electrical Engineering,
Jabalpur Engineering College, Jabalpur 482011, Madhya Pradesh, India

N. Yogesh Kumar

Department of Electrical Engineering,
Rewa Engineering College, Rewa 486001, Madhya Pradesh, India

P. V. V. Rajagopal

Department of Electrical Engineering, Raghu Engineering College,
Visakhapatnam 531162, Andhra Pradesh, India

© Springer Nature Singapore Pte Ltd. 2019

K. Shanker et al. (eds.), *Advances in Industrial and Production Engineering*, Lecture Notes in Mechanical Engineering, https://doi.org/10.1007/978-981-13-6412-9_65

1 Introduction

In 1987, Motorola's Six Sigma Quality Program was created by Devane [1]. The concepts of Six Sigma are developed as a way to improve the reliability and quality of products [2–4]. The main goal of this approach is reaching levels of quality and reliability that will satisfy and even exceed demand and expectations of today's demanding customer [5]. The objective of this study is to develop a model for implementation of Six Sigma in Indian organizations. Considering specific need of Indian companies to implement Six Sigma effectively, this section is for studies the problem.

The main objectives of the research are as follows:

- To understand the need of Six Sigma in an organization,
- To reduce the scraped materials and reaching levels of quality and reliability that will satisfy and even exceed demand and expectations of today's demanding customer and
- To improve the performance of system by improving the delivery system of the company.

2 Case Study on Product

Six Sigma has two key methodologies DMAIC and DMADV where DMAIC is used to improve an existing business process while DMADV is used to create a new product design or process design in such a way that it yields in a more predictable nature and defects free performance. A heuristic model is present for company XYZ. Six Sigma has been considered as an effective business process improvement strategy [2, 6].

2.1 Phase 1: Define

The first step is to identify the problem areas of the business, by using a tool called “business case” where the business problems are summarized in terms of the situation and estimate the potential value of improvement efforts. Figure 1 shows the deployment flow of current study.

2.2 Phase 2: Measurement

At the critical point in selection process probably have a number of voices sharing and demanding attention: the voice of the customer (VOC), the voice of the process

Table 1 Complaints of customers

S. No.	Complaints	Frequency
1	Wrong order	10
2	Late delivery	28
3	Product return-not prepared properly	12
4	Incorrect bill	6
5	Wrong address	10
6	Features not available according to need	30
7	Miscellaneous	4
Total		100

(VOP) and the voice of the business (VOB). Sampling of 100 customer complaints in the past 6 months in Tables 1 and 2 shows the business-customer process scorecard.

It has been decided that making product is the place to start improvement efforts. **“There is a problem with the number of features is not available in the products.”**

Solution In the last six months, 5% of the products had to be scrapped prior to boxing due to unfinished. The boxer had no procedures for sending products back for an additional manufacturing time. In addition, 2% of products delivered to customers were unprepared or rough, resulting in 125 customer complaints. Product scraping costs the company Rs. 117,750 during last six months in addition to a loss of customers.

The goal is to reduce the cancelation of product orders due to features unavailability from 5% to less than 0.05% by six months (January 1, 2017 to June 30, 2017). In addition, we also wish to reduce the number of unfinished products that reach customers from 2 to 0 by the same date. It will lead to restore the image as a quality product, and subsequently, it will save the company as much as Rs. 2,500,000 annually.

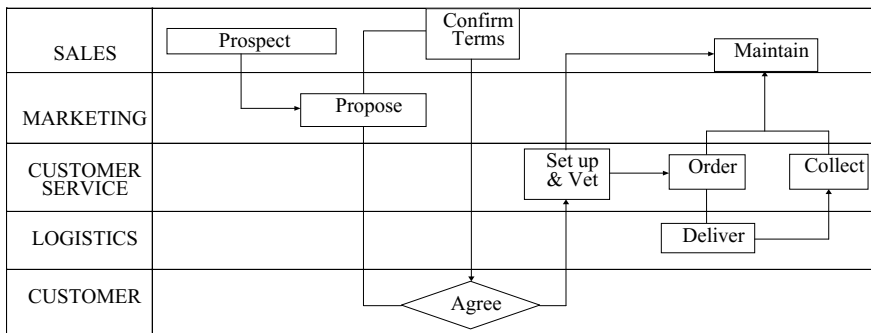


Fig. 1 Deployment flows or swim lane process map

Table 2 Business-customer scorecard

S. No.	Name of process	Impact on customer needs internal/external (VOC)	Improvement or amount (VOP)	Importance to meeting business goal and objectives (VOB)	Overall ranking (VOC × VOP × VOB)
1	Inventory management	2	2	4	16 (5)
2	Staffing and training	3	3	2	18 (4)
3	Phone in order	4	3	3	36 (3)
4	Manufacturing product	5	4	4	80 (1)
5	Delivering product	5	2	5	50 (2)

Note impact rating: 1 = little; 2 = somewhat; 3 = moderate; 4 = High; 5 = extreme

Prioritizing and aligning projects with business-customer process scorecards product delivery were the second-ranked problem area.

A company gives a guarantee of delivery within thirty days from the time of accepting an order was considered where in the event of failure of delivery in time, the customer receives a 100% refund.

2.3 Phase 3: Analysis

We seek to establish the capability of the current product or process in statistical terms (i.e., what is the current sigma quality level) in this stage. Then we seek to develop an appropriate transfer function that relates the inputs to the outputs, so that realistic delivery dates can be determined and on-time delivery can be ensured.

Defects per Million Opportunities (DPMO)

DPMO is a measure of process performance in process improvement efforts. It stands for defects per million opportunities. A defect is defined as a nonconformance of a quality characteristic to its specification. DPMO is stated in opportunities per million units for convenience: Processes that are considered highly capable (e.g., processes of Six Sigma quality) are those that experience only a handful of defects per million units produced (or services provided).

$$\text{Defects} = 100$$

$$\text{Unit} = 37,625 \text{ (Jan–June 2017—6 months)}$$

$$\text{DPMO} = \frac{\text{total defects}}{\text{total opportunity}} \times 1,000,000 \tag{1}$$

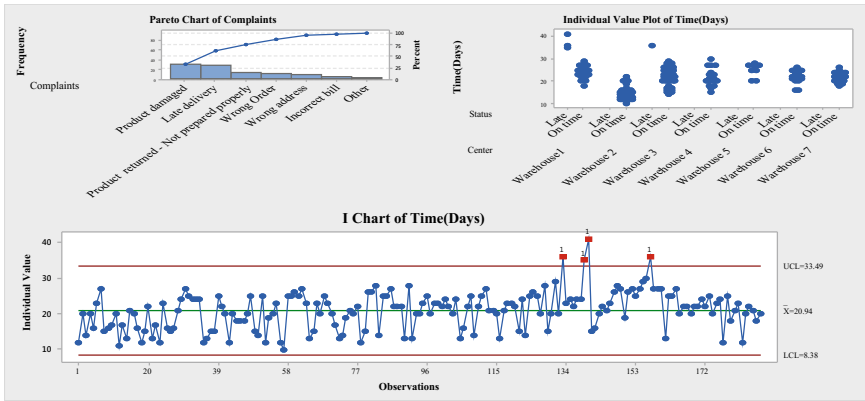


Fig. 2 Pareto charts of complaint and individual value plot

$$\text{Defects (\%)} = \frac{\text{Total defects}}{\text{Total opportunity}} \times 100 \tag{2}$$

$$\text{Yield (\%)} = 100 - (\text{Defects percentage}) \tag{3}$$

$$\text{Process sigma} = \text{NORMSINV} \left(1 - \left(\frac{\text{Total defects}}{\text{Total opportunity}} \right) \right) + 1.5 \tag{4}$$

$$\text{Process sigma} = 0.8406 + \sqrt{(29.37 - 2.221 \times \log_n \text{ DPMO})} \tag{5}$$

Most of the companies produce at an average of ± 3 sigma quality level (99.73% good product), which generates 2700 defects per million parts, but for most real-world situations, this is a level of defects that is excessively high whereas the optimum quality level is usually not as tight as ± 6 sigma. A realistic goal is to make a product that satisfies the customer and minimizes supplier losses to the point that it is not cost effective to pursue tighter quality.

Pareto charts

Here, a leading automobile company is considered to derive a case study on the delivery of products into the warehouse by the suppliers. MINITAB software is used to evaluate the potential of suppliers (Fig. 2).

2.4 Phase 4: Analysis

The improvement phases focus on amplifying hypothesis to take away principle causes of variation, examination and standardizing those solutions. Improvement is more than just planning or redesigning. It involves implementing the new process with an implementation plan for redesign.

Table 3 Identification of problem causes

S. No.	Factor	Cause
1	Time error	(a) Is there delayed when ordered by both internet and phone?
		(b) Is the material not available on time?
2	Process error	(a) Is something wrong with the equipment or procedure?
		(b) Manufacturing staff, delaying the product finishing
		(c) Identifies the delivery person takes longer?
		(d) Delivery person transportation is not quick, is it traffic issue or vehicle issue?
3	Human resource error	(a) Delivery person is not good at locating addresses, is it a specific area that is hard to locate or he/she had not enough training?

Root cause analysis

The root cause analysis is an iterative question answer technique used to explore the cause and effect relationships underlying a particular problem. After the identification of problem causes, improvements to enhance the performance of the analysis process have been proposed through Table 3.

2.5 Phase 5: Control

The next step is to place the necessary control to ensure that improvements are maintained for the long term. This involves monitoring and publicizing the key process metrics to promote continuous improvement and to guard against regression.

Following are the recommendations for easily delivery of product.

- a. Handling: The products are to be handled carefully without any unscheduled stops.
- b. Delivering products: Product delivery boy must know the rout of his area in detail as well as carry enough money to make a change.
- c. Advertisement: Offering combo deals, coupons and give a better product at a lower price for the customers. Create a VIP club or a punch card system. Use online marketing and other online recourses can be tapped to advertise special deals or events and targeting the specific persons.

3 Results and Discussions

Data generated/collected during case study is reproduced, and cost analysis was carried out by applying the recommendation of different phases is presented in Tables 4,

Table 4 Cost analysis on the basis of operating costs (Rs. in Lakhs)

	2011	2012	2013	2014	2015	2016	(Jan–June 2017)
Revenues	75	108.67	150.5	203.5	252.52	283.64	230.45
<i>Operating costs</i>							
Salaries	23.92	24.51	25.13	33.63	34.48	34.48	18.11
Owner Comp.	0	10	25	32.5	50	62.5	31.25
Ingredients	26.25	37.66	50.4	67.52	83.49	92.43	89.35
Marketing	0.12	0.25	0.3	0.3	0.325	0.325	0.4
Supplies	1.875	2.625	3.64	4.81	6.063	6.585	9.41
Rent	5	5.125	5.25	5.375	5.5	5.625	2.875
Mileage	1.5	3.15	4.2	5.55	9.1	10.13	16.932
Vehicle maintenance	0.2	0.28	0.32	0.5	0.575	0.625	2.625
Utilities/janitorial maintenance	2	2	2	2	2	2	1
Insurance	0.5	0.5	0.5	0.5	0.5	0.5	0.288
Refunds	0.075	0.163	0.301	0.306	0.404	0.568	0.618
Total cost	61.445	86.325	117.04	153.06	192.49	216.7	172.866
Operating income	13.555	22.395	33.458	50.445	60.035	66.9545	57.588
% profit margin	18.07	20.61	22.23	24.79	23.77	23.61	24.99

Note

Cost of goods sold (primary ingredients) was historically 35% of the average Rs. 500 retail product price

Supply costs historically averaged 12.52 per product (cardboard boxes, plastic utensils, napkins and office supplies)

Drivers are paid Rs. 10 per mile for deliveries. Mileage has historically been 3 miles per delivery

Late deliveries have historically averaged Rs. 8.5 of total product. Customers are refunded in full for late deliveries

5 and 6. Equations (1)–(5), the value of DPMO, defects and process sigma are as follows:

DPMO = 2658;

Defects (%) = 0.27;

Yield (%) = 99.73;

Process Sigma = 5.50;

Figure 3a, b is showing a cost analysis in terms of performance improvement and profit margin and defect reduction and time reduction, respectively. Comparing the initial data with the data gathered after implementation of improvements based on the study of 6 months onward June 30, 2017.

Table 5 Cost analysis on the basis of labor cost (Rs. in Lakhs)

Labor	2011	2012	2013	2014	2015	2016	(Jan–June 2017)
Chef (currently 650 per hour)	10.4	10.6	10.9	12.48	12.8	13.1	6.7
Receptionist/cashier (Rs. 457.5 per hour)	7.8	7.99	8.19	8.84	9.06	9.28	4.76
Driver (Rs. 319/- per hour)	5.7	5.86	6	6.16	6.31	6.47	3.31
Driver (Rs. 319/- per hour)	0	0	0	6.16	6.31	6.47	3.31
Total salaries	23.9	24.5	25.13	33.64	34.48	35.34	18.11

Table 6 Cost analysis on the basis of quantity of selling products

Key matrix	2011	2012	2013	2014	2015	2016	(Jan–June 2017)
Product per year	15,000	21,000	28,000	37,000	45,500	50,650	37,650
Product per week	288	404	538	712	875	974	1447
Product per day	41	58	77	102	125	139	207
Avg. price per product	500	517.5	537.5	550	555	560	562.5
Incremental product	–	6000	7000	9000	8500	5150	24,600
% growth in products	–	40	33	32	23	11	49

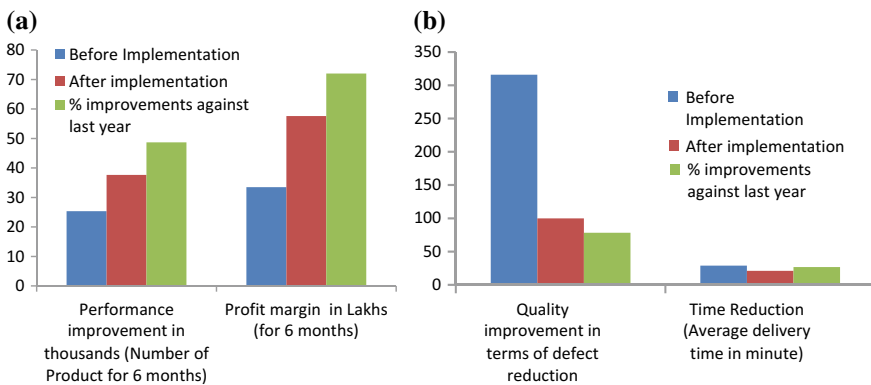


Fig. 3 a, b Integrated performance analysis

Focusing on those processes with a great impact on business performance, the methodology involves this statistical analysis to improve the quality and quantity of common variants. A customer's delight is paramount, and the means to exceed customer expectations must be put into an organization.

Some of the salient conclusions emerged out from the present study, which is typical and interesting, are given below:

- Impact on performance improvement, quality improvement, time and cost reduction as well as customer satisfaction,
- The Six Sigma application in Product Emporium resulted in performance improvement of 48.66%, quality improvement of 67.47%, time delivery improvements of 36.63% and reduction in cost of 72.02% and
- Marginal reduction in procurement and inventory carrying cost. Overall improvement in customer satisfaction is registered by a margin of 8%.

References

1. Devane T (2004) Integrating lean six sigma and high performance organizations. Pfeiffer/A Wiley Imprint, San Francisco
2. Abreu P, Sousa S, Lopes I (2012) Using six-sigma to improve complaints handling. In: Proceedings of the world congress on engineering (IAENG). ISSN: 2078-0966, 3
3. Harry M, Schroeder R (2000) Six Sigma. Doubleday, New York
4. Kumar RK, Sambhe U (2012) Six-sigma practice for poor quality improvement—a case study of indian auto ancillary unit. IOSR J Mech Civ Eng 4(4):26–42
5. Sokovic M, Pavletic D, Krilcic E (2006) Six-sigma process improvements in automotive parts production. J Achiev Mater Manuf Eng 19(1):96–102
6. Antony J, Snee R, Hoerl R (2017) Lean six sigma: yesterday, today and tomorrow. Int J Qual Reliab Manage 34(7):1074–1093. <https://doi.org/10.1108/IJQRM-03-2016-0035>

A Critical Review on Friction Stir Welding of Dissimilar Aluminium Alloys



Munna Singh Dahiya, Vikas Kumar and Shubham Verma

Abstract Friction stir welding (FSW) is a solid-state joining process having capability of joining materials which differ in chemical composition, properties, etc., and where fusion can lead to harmful reactions. Nowadays, the arena of aerospace, railway, ship building industries, etc., are moving towards the use of this technique as compared to fusion welding process for the fabrication of structural parts. It is energy-efficient, eco-friendly and versatile process of joining. In the current study, an attempt has been made to study the effect of process parameters, i.e. rotational speed, welding speed, tool tilt angle, dwell time, etc., on the weld characteristics of dissimilar aluminium alloys. Moreover, difficulties and other issues related to FSW of dissimilar metals are addressed to provide guidelines to research community to carry out extensive research in this field.

Keywords FSW · Dissimilar alloys · Weld characteristics

1 Introduction

Recently, manufacturing industries are moving towards the use of aluminium and its alloys owing to its unique features, i.e. high strength-to-weight ratio, corrosion resistance, good formability, etc. The conventional welding of these alloys are problematic and occurrence of various defects such as voids, hot cracking, distortion, precipitate dissolution, loss of work hardening, and hot cracking. To overcome the problems of fusion welding of low metal alloys, The Welding Institute (TWI, UK) invented a new welding technique, i.e. friction stir welding (FSW), in 1991. The schematic diagram of process principle for FSW is shown in Fig. 1. It consists of non-consumable tool with specially design pin and shoulder. The pin plunges between the faying surfaces of the plates [1]. The shoulder is in direct contact with the workpiece surface, and

M. S. Dahiya (✉) · V. Kumar · S. Verma
National Institute of Technology, Kurukshetra, India
e-mail: munna.dahiya93@gmail.com

S. Verma
e-mail: shubham6140005@gmail.com

© Springer Nature Singapore Pte Ltd. 2019
K. Shanker et al. (eds.), *Advances in Industrial and Production Engineering*, Lecture Notes in Mechanical Engineering, https://doi.org/10.1007/978-981-13-6412-9_66

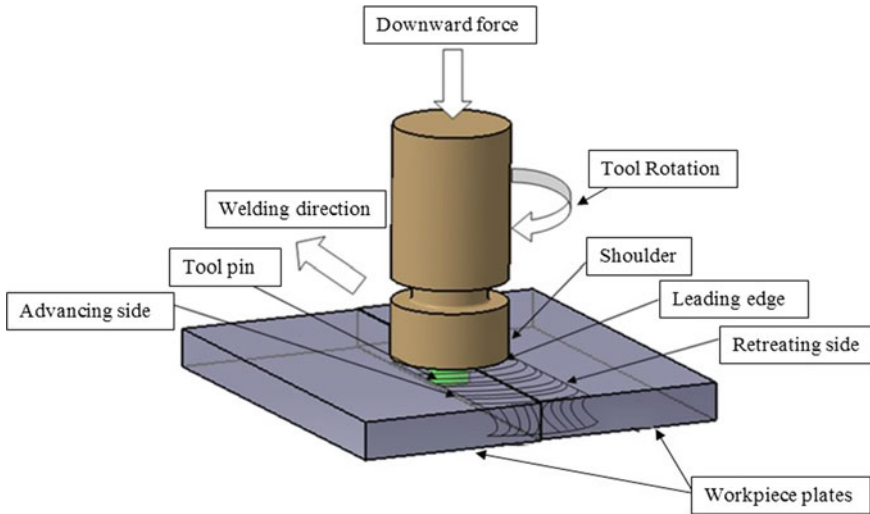


Fig. 1 Principle of friction stir welding (Verma and Misra [2])

due to its rotational movement on the workpiece, friction heat is generated which results in softening of the faying surface material. Due to the translation and rotational movements of tool, solid-state joint is produced. In the current study, an attempt has been made to explain the effect of process parameters on the weld characteristics of dissimilar aluminium alloys.

2 Process Parameters

In friction stir welding, the process parameters are mainly classified into three groups:

Tooling-related parameters: shoulder and pin material, pin profile, pin and shoulder diameter, pin length, shoulder shape, feature geometry, thread pitch, etc.

Machine-related parameters: traverse speed, plunge force or depth, spindle speed, tool tilt angle, etc.

Other parameters: anvil material, anvil size, workpiece size, workpiece properties, etc. The effected process parameters are exemplified using a cause–effect diagram in Fig. 2.

3 Literature Review

FSW process has capability of joining similar and dissimilar aluminium alloys. Owing to this, manufacturing industries are moving towards the use of this

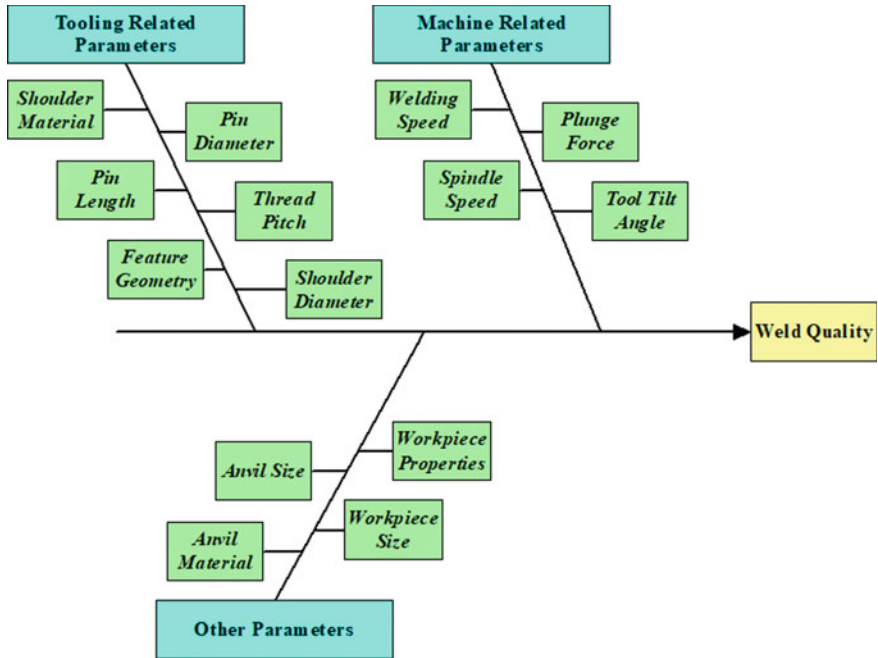
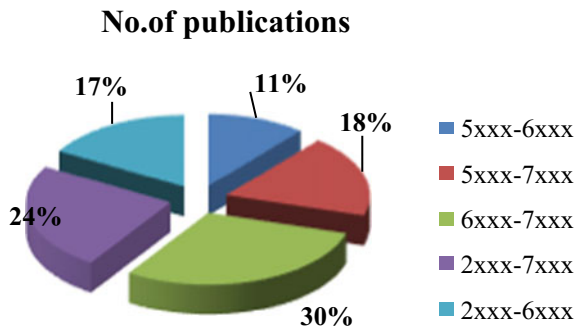


Fig. 2 Cause-effect diagram [2]

technology. A comparative study of published research work on FSW of dissimilar aluminium series is shown in Fig. 3.

It is clear from the figure that maximum work has been done on 6xxx-7xxx series of aluminium alloys and minimum work is done on 5xxx-6xxx series. In this chapter, an attempt has been made to summarize the work already carried out and to provide a guideline for future research work on joining of dissimilar aluminium alloys. The literature review is classified into three different groups as shown in Fig. 4 (Tables 1, 2 and 3).

Fig. 3 Previous work on FSW of dissimilar aluminium series



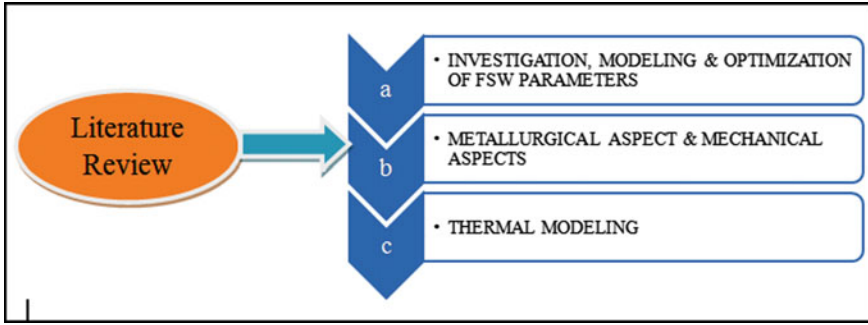


Fig. 4 Classification of the literature survey

Table 1 Optimization of FSW parameters

Researchers	Workpiece	Tool	Conclusion
Ataya et al. [3]	AA7075 AA5083	H13	<ul style="list-style-type: none"> • They concluded that welding speed has no significant effect on weld characteristics
Kundu and Singh [4]	AA5083 AA5086	H13	<ul style="list-style-type: none"> • The entire fabricated joints have less joint efficiency than the parent metal owing to dynamic recrystallization • The maximum tensile strength is obtained at a rotational speed of 1000 rpm, a tilt angle of 2 degree and a minimum value of feed rate
Ravikumar et al. [5]	AA6061 AA7075	H13	<ul style="list-style-type: none"> • Better weld characteristics are obtained at a rotational speed of 900 rpm and a feed rate of 100 mm/min
Gupta and Singh [6]	AA3003 AA5052	H13	<ul style="list-style-type: none"> • They employed Taguchi method for designing the experiment of FSW of AA3003 and AA5052 plates

(continued)

Table 1 (continued)

Researchers	Workpiece	Tool	Conclusion
Bozkurt [7]	AA2024 AA5754	H13	<ul style="list-style-type: none"> • Taguchi's L9 orthogonal array are used for conducting the experiments • The contributions of each parameters are 53.66% of rotational speed, 23.74% of tool tilt angle, 12.54% of tool plunge depth and 5.45% of dwell time
Gungor et al. [8]	AA5083 AA6082	H13	<ul style="list-style-type: none"> • The joint efficient is found to be 38% less than that of the similar fabricated joint • Desirable weld characteristics are obtained at 1250 rpm tool rotation, 64 mm/min feed rate and 2° tool tilt angle
Elanchezhian et al. [9]	AA6062 AA8011	H13	<ul style="list-style-type: none"> • Taguchi L9 orthogonal array are used optimizing the process parameters of FSW process. The maximum UTS of 153 MPa is obtained
Koilraj et al. [10]	AA2219 AA5083	H13	<ul style="list-style-type: none"> • They observed 66% contribution of D/d ratio on the FSW process
Giraud et al. [11]	AA7020 AA6060	H13	<ul style="list-style-type: none"> • Most efficient result is obtained at rotational speed from 1000 to 2000 rpm and feed rate from 300 to 1100 mm/min
Shojaeefard et al. [12]	AA7075 AA5083	H13	<ul style="list-style-type: none"> • Defect-free friction stir welds have been produced for the dissimilar alloy system AA5083 and AA7075 • A sound weld is obtained at a rpm of 1400 rpm and feed of 20 mm/min

(continued)

Table 1 (continued)

Researchers	Workpiece	Tool	Conclusion
Singh and Dhuria [13]	AA2014 AA7075	H13	<ul style="list-style-type: none"> They employed Taguchi method for experimentation and optimizing the process parameters for FSW. It is concluded that tool material has significant effect on the joint efficiency
Hema et al. [14]	AA6061 AA2014	H13	<ul style="list-style-type: none"> RSM is used for designing the experiments. The maximum tensile strength of 133 MPa is obtained at optimum values of 2000 rpm, 37 mm/min of feed rate and 75 kN of axial force
Sadeesh et al. [15]	AA2024 AA6061	AISI H13	<ul style="list-style-type: none"> Five different tool pin profiles are used for fabricating the joint by FSW. It is observed that square pin profile produces sound weld as compared to other pin profile The fabricated joint efficiency is maximum at a rotational speed of 1000 rpm and a welding speed of 40 mm/min with square pin profile
da Silva et al. [16]	AA2024 AA7075	H13	<ul style="list-style-type: none"> They used threaded and unthreaded pin profiles tool for fabricating the joint and observed that threaded tool pin profile tools produce sound weld. This is due to the proper mixing of materials due to thread on the pin

Table 2 Metallurgical aspect and mechanical aspects

Researchers	Workpiece	Tool	Conclusion
Ilangovan et al. [17]	AA6061 AA5086	HSS	<ul style="list-style-type: none"> Defect-free joint is obtained with a tensile strength of 140 MPa and micro-hardness of 115HV The joint efficient is found to be 30% less than that of the similar fabricated joint. This is attributed towards difference in heat generation during the process
Giraud et al. [11]	AA7020 AA6060	HSS	<ul style="list-style-type: none"> They employed FSW for joining of dissimilar metal alloys. The joint efficient is found to be satisfactory
Vinayak and Bhatwadekar [18]	AA1100 AA6101	H13	<ul style="list-style-type: none"> The fabricated joint is defect free with a joint efficient less than that of the parent metals
Hariharan and Golden Renjith Nimal [19]	AA6061 AA7075	Hchr	<ul style="list-style-type: none"> The grain size of 100 microns is observed in the nugget zone owing to dynamic recrystallization
Cavaliere et al. [20]	AA2024 AA7075	H13	<ul style="list-style-type: none"> They employed FSW for joining AA2024 and AA7075 plates and measured the fatigue properties of the weld
Palanivel et al. [21]	AA6351 AA5083	HCHCr	<ul style="list-style-type: none"> They observed that square pin profile produces higher tensile strength than the other pin profile owing to pulsating moment of the pin
Infante et al. [22]	AA5754 AA6082	H13	<ul style="list-style-type: none"> They employed FSW for joint to the weld of AA6082 with AA7075 and measured the fatigue properties of the joint
Rodriguez et al. [23]	AA6061 AA7050	H13	<ul style="list-style-type: none"> The rotational speed has significant effect on tensile strength

(continued)

Table 2 (continued)

Researchers	Workpiece	Tool	Conclusion
Steuwer et al. [24]	AA5083 AA6082	H13	<ul style="list-style-type: none"> • Rotational speed has more significant effect on the residual stresses than the welding speed
Robe et al. [25]	AA2024 AA2198	H13	<ul style="list-style-type: none"> • They observed minimum micro-hardness in the transition zone
Avinash et al. [26]	AA2024 AA7075	H13	<ul style="list-style-type: none"> • Mixing of material in the stir zone is uniform in nature for both materials. The tensile failure occurred in the nugget zone for all fabricated joints
RajKumar et al. [27]	AA5052 AA6061	H13	<ul style="list-style-type: none"> • It is concluded that micro-structural properties are correlated with mechanical properties of the joint
Moradi et al. [28]	AA2024 AA6061	H13	<ul style="list-style-type: none"> • They employed FSW for joining dissimilar alloys, i.e. AA2046 and AA6061, and observed that efficiency of joint is satisfactory • It is concluded that advancing side texture intensity decreased, whereas retreating side intensity increased than the initial sheets
Moradi et al. [29]	AA2024 AA6061	H13	<ul style="list-style-type: none"> • They observed surface defects on FSW joint of AA2024 and AA6061 • The joint efficiency is found to be satisfactory
Park et al. [30]	AA6111 AA5023	H13	<ul style="list-style-type: none"> • Shoulder diameter has significant effect on the mechanical and metallurgical properties of the joint. This is attributed towards the change in heat input due to change in diameter of the tool shoulder

(continued)

Table 2 (continued)

Researchers	Workpiece	Tool	Conclusion
Paik [31]	AA5083 AA5383	H13	<ul style="list-style-type: none"> • The objective of the present study has been to obtain test database on mechanical properties of friction stir welded aluminium alloys with the focus on 5083 and 5383 alloys • The test database developed in the present study will be very useful for the design and building of aluminium ship structures fabricated by friction stir welding

Table 3 Thermal modelling

Researchers	Workpiece	Tool	Conclusion
Bayazid et al. [32]	6063-T6 7075-T6	H13	<ul style="list-style-type: none"> • The weld characteristics depend upon the heat generation during the process
Kumbhar et al. [33]	AA5052 AA6061	HSS	<ul style="list-style-type: none"> • Improper mixing of material takes place in the nugget zone
Palanive et al. [34]	AA6351 AA5083	HCHCr	<ul style="list-style-type: none"> • They concluded that feed rate has significant effect on mixing of material in the nugget zone
Hamed [35]	AA7075 AA5086	H13	<ul style="list-style-type: none"> • Heat generation depends upon the thermal diffusivity, tool geometry and process parameters of FSW. AA5086 side grains are coarse in nature than the AA7075 side
Ilangovan et al. [36]	AA5086 AA6061	HSS	<ul style="list-style-type: none"> • They concluded that threaded pin profile produces higher strength than the taper pin profiled owing to proper mixing of material • Onion rings are observed on the macrostructure of the threaded pin profile joint weld

(continued)

Table 3 (continued)

Researchers	Workpiece	Tool	Conclusion
Aval [37]	AA7075 AA6082	H13	<ul style="list-style-type: none"> • Heat generation has significant effect on tensile residual stress • The grain size on the AA7075 side is fine as compared to AA6082
Khodir and Shibayanagi [38]	AA2024 AA7075	SKD61	<ul style="list-style-type: none"> • Enhancement in welding speed caused in the formation of kissing bond and pores in the weld joint. This is mainly due to improper mixing of material in the nugget zone
Shen et al. [39]	AA6022 AA7075	H13	<ul style="list-style-type: none"> • Tool plunge depth has significant effect on the void formation in the nugget zone
Khan et al. [40]	AA2219 AA 7475	HCS	<ul style="list-style-type: none"> • They observed fine equiaxed grain in the stir zone. This is attributed towards dynamic recrystallization in the stir zone. A maximum hardness of 162 HV is obtained in the stir zone of dissimilar alloys
Pabandi et al. [41]	AA2024 AA6061	H13	<ul style="list-style-type: none"> • The joint efficient is found to be 26% less than that of the similar fabricated joint • It is observed that heat treatment enhanced the mechanical and metallurgical properties of dissimilar aluminium alloys as compared to simple FSW
Kumar et al. [42]	AA2014 AA6061	H13	<ul style="list-style-type: none"> • The nugget zone has fine equiaxed grain as compared to base metal due to dynamic recrystallization • It is concluded that with increase in rotational speed the hardness of nugget zone decreases due to dislocation of strengthening particles with increase in temperature

(continued)

Table 3 (continued)

Researchers	Workpiece	Tool	Conclusion
Kumar [43]	AA3003 AA6082	H13	<ul style="list-style-type: none"> It is observed that weld speed enhances the tensile strength, whereas rotational speed decreases the tensile strength. This is attributed towards the heat generation during the process
Barbini et al. [44]	AA2024 AA7050	H13	<ul style="list-style-type: none"> The SZ size is considered an important parameter to qualitatively define the value of the weldments

4 Conclusion

In the current study, an attempt has been made on different aspects of FSW of dissimilar aluminium alloys. The major findings related to FSW of dissimilar aluminium alloys are listed below:

It is evident that FSW process parameters—tool rotation rate, traverse speed, spindle tilt angle—influence the mechanical and metallurgical behaviour of joints and hence are crucial to produce sound- and defect-free weld.

According to the available literature, most of the research work is focused on friction stir welding of aluminium, copper and magnesium and their alloys. Friction stir welding of dissimilar aluminium alloys, dissimilar metals and composites, etc., is having huge scope for future research.

The tribological, corrosional and surface topographical behaviour of FS welded dissimilar aluminium alloys is not elaborately discussed in the literature.

No proper guideline in terms of mathematical/theoretical model of process performance parameters of FSW is available for selecting input parameters to obtain the desired output.

Thermal modelling of FSW of dissimilar alloys is also not elaborately discussed in the literature.

References

1. Verma S, Gupta M, Misra JP (2016) Friction stir welding of aerospace materials: a state of art review, pp 135–150
2. Verma S, Misra JP (2015) A critical review of friction stir welding process, pp 249–266
3. Ahmed MMZ, Ataya S, El-Sayed Seleman MM, Ammar HR, Ahmed E (2017) Friction stir welding of similar and dissimilar AA7075 and AA5083. *J Mater Process Technol* 242:77–91
4. Kundu J, Singh H (2016) Friction stir welding of dissimilar Al alloys: effect of process parameters on mechanical properties. *Eng Solid Mech* 4:125–132

5. Ravikumar S, Seshagiri Rao V, Pranesh RV (2014) Effect of process parameters on mechanical properties of friction stir welded dissimilar materials between AA6061-T651 and AA7075-T651 alloys. *Int J Adv Mech Eng* 4(1):101–114
6. Gupta D, Singh G (2017) Effect of friction stir welding parameters on tensile strength of Al 3003 and Al 5052. *Int J Curr Eng Technol* 7(3):1019–1021
7. Bozkurt Y (2011) Dissimilar friction stir welded joints between AA2124/SiC-T4 MMC and AA3003-H24 alloy, pp 17–20, Aug 2011
8. Gungor B, Kaluc E, Taban E, Sik A (2014) Mechanical, fatigue and microstructural properties of friction stir welded 5083-H111 and 6082-T651 aluminum alloys. *Mater Des* 56:84–90
9. Elanchezhian C et al (2014) Parameter optimization of friction stir welding of AA8011-6062 using mathematical method. *Procedia Eng* 97:775–782
10. Koilraj M, Sundareswaran V, Vijayan S, Koteswara Rao SR (2012) Friction stir welding of dissimilar aluminum alloys AA2219 to AA5083—optimization of process parameters using Taguchi technique. *Mater Des* 42:1–7
11. Giraud L, Robe H, Claudin C, Desrayaud C, Bocher P, Feulvarch E (2016) Investigation into the dissimilar friction stir welding of AA7020-T651 and AA6060-T6. *J Mater Process Technol* 235:220–230
12. Shojaefard MH, Behnagh RA, Akbari M, Givi MKB, Farhani F (2013) Modelling and pareto optimization of mechanical properties of friction stir welded AA7075/AA5083 butt joints using neural network and particle swarm algorithm. *Mater Des* 44:190–198
13. Singh S, Dhuria G (2017) Investigation of post weld cryogenic treatment on weld strength in friction stir welded dissimilar aluminium alloys AA2014-T651 and AA7075-T651. *Mater Today Proc* 4(8):8866–8873
14. Hema P, Sai Kumar Naik K, Ravindranath K (2017) Prediction of effect of process parameters on friction stir welded joints of dissimilar aluminium alloy AA2014 & AA6061 using taper pin profile. *Mater Today Proc* 4(2):L2174–2183
15. Sadeesh P et al (2014) Studies on friction stir welding of aa 2024 and aa 6061 dissimilar metals. *Procedia Eng* 75:145–149
16. da Silva AAM, Arruti E, Janeiro G, Aldanondo E, Alvarez P, Echeverria A (2011) Material flow and mechanical behaviour of dissimilar AA2024-T3 and AA7075-T6 aluminium alloys friction stir welds. *Mater Des* 32(4):2021–2027
17. Ilangovan M, Rajendra Boopathy S, Balasubramanian V (2015) Effect of tool pin profile on microstructure and tensile properties of friction stir welded dissimilar AA6061–AA5086 aluminium alloy joints. *Def Technol* 11(2):174–184
18. Yadhav VD, Bhatwadekar SG (2015) Friction stir welding of dissimilar aluminium alloys AA1100 to AA6101-T6. *Int J Res Aeronaut Mech Eng* 3(1):1–6
19. Hariharan R, Golden Renjith Nimal RJ (2014) Friction stir welding of dissimilar aluminium alloys (6061 & 7075) by using computerized numerical control machine. *Middle East J Sci Res* 20(5):601–605
20. Cavaliere P, Nobile R, Panella FW, Squillace A (2006) Mechanical and microstructural behaviour of 2024-7075 aluminium alloy sheets joined by friction stir welding. *Int J Mach Tools Manuf* 46(6):588–594
21. Palanivel R, Koshy Mathews P, Murugan N, Dinaharan I (2012) Effect of tool rotational speed and pin profile on microstructure and tensile strength of dissimilar friction stir welded AA5083-H111 and AA6351-T6 aluminum alloys. *Mater Des* 40:7–16
22. Infante V, Braga DFO, Duarte F, Moreira PMG, De Freitas M, De Castro PMST (2016) Study of the fatigue behaviour of dissimilar aluminium joints produced by friction stir welding. *Int J Fatigue* 82:310–316
23. Rodriguez RI, Jordon JB, Allison PG, Rushing T, Garcia L (2015) Microstructure and mechanical properties of dissimilar friction stir welding of 6061-to-7050 aluminum alloys. *Mater Des* 83:60–65
24. Steuwer A, Peel MJ, Withers PJ (2006) Dissimilar friction stir welds in AA5083-AA6082: the effect of process parameters on residual stress. *Mater Sci Eng A* 441(1–2):187–196

25. Robe H, Zedan Y, Chen J, Monajati H, Feulvarch E, Bocher P (2015) Microstructural and mechanical characterization of a dissimilar friction stir welded butt joint made of AA2024-T3 and AA2198-T3. *Mater Charact* 110:242–251
26. Avinash P, Manikandan M, Arivazhagan N, Devendranath RK, Narayanan S (2014) Friction stir welded butt joints of AA2024 T3 and AA7075 T6 aluminum alloys. *Procedia Eng* 75:98–102
27. RajKumar V, VenkateshKannan M, Sadeesh P, Arivazhagan N, Devendranath Ramkumar K (2014) Studies on effect of tool design and welding parameters on the friction stir welding of dissimilar aluminium alloys AA 5052–AA 6061. *Procedia Eng* 75:93–97
28. Moradi MM, Jamshidi Aval H, Jamaati R, Amirkhanlou S, Ji S (2018) Microstructure and texture evolution of friction stir welded dissimilar aluminum alloys: AA2024 and AA6061. *J Manuf Process* 32:1–10
29. Moradi MM, Jamshidi Aval H, Jamaati R (2017) Effect of pre and post welding heat treatment in SiC-fortified dissimilar AA6061-AA2024 FSW butt joint. *J Manuf Process* 30:97–105
30. Park SW, Yoon TJ, Kang CY (2017) Effects of the shoulder diameter and weld pitch on the tensile shear load in friction-stir welding of AA6111/AA5023 aluminum alloys. *J Mater Process Technol* 241:112–119
31. Paik JK (2009) Mechanical properties of friction stir welded aluminum alloys 5083 and 5383. *Int J Nav Archit Ocean Eng* 1(1):39–49
32. Bayazid SM, Farhangi H, Ghahramani A (2015) Investigation of friction stir welding parameters of 6063-7075 aluminum alloys by Taguchi method. *Procedia Mater Sci* 11(2010):6–11
33. Kumbhar NT, Bhanumurthy K (2012) Friction stir welding of Al 5052 with Al 6061 alloys. *J Metall* 2012:1–7
34. Palanivel R, Koshy Mathews P, Dinaharan I, Murugan N (2014) Mechanical and metallurgical properties of dissimilar friction stir welded AA5083-H111 and AA6351-T6 aluminum alloys. *Trans Nonferrous Met Soc China (English Ed)* 24(1):58–65
35. Hamed JA (2017) Effect of welding heat input and post-weld aging time on microstructure and mechanical properties in dissimilar friction stir welded AA7075–AA5086. *Trans Nonferrous Met Soc China (English Ed.)* 27(8):1707–1715
36. Ilangovan M, Boopathy SR, Balasubramanian V (2015) Microstructure and tensile properties of friction stir welded dissimilar AA6061-AA5086 aluminium alloy joints. *Trans Nonferrous Met Soc China (English Ed.)* 25(4):1080–1090 (2015)
37. Aval HJ, Serajzadeh S, Kokabi AH (2011) Evolution of microstructures and mechanical properties in similar and dissimilar friction stir welding of AA5086 and AA6061. *Mater Sci Eng A* 528(28):8071–8083
38. Khodir SA, Shibayanagi T (2008) Friction stir welding of dissimilar AA2024 and AA7075 aluminum alloys. *Mater Sci Eng B Solid-State Mater Adv Technol* 148(1–3):82–87
39. Shen Z, Ding Y, Gopkalo O, Diak B, Gerlich AP (2018) Effects of tool design on the microstructure and mechanical properties of refill friction stir spot welding of dissimilar Al alloys. *J Mater Process Technol* 252:751–759
40. Khan NZ, Siddiquee AN, Khan ZA, Mukhopadhyay AK (2017) Mechanical and microstructural behavior of friction stir welded similar and dissimilar sheets of AA2219 and AA7475 aluminium alloys. *J Alloys Compd* 695:2902–2908
41. Pabandi HK, Jashnani HR, Paidar M (2018) Effect of precipitation hardening heat treatment on mechanical and microstructure features of dissimilar friction stir welded AA2024-T6 and AA6061-T6 alloys. *J Manuf Process* 31:214–220
42. Kumar M, Kumar P, Singh B (2013) Evaluation of mechanical properties of FSW Al 1040 T4 & Al 6061 T6 alloys. *Asian Rev Mech Eng* 2(2):1–5
43. Kumar TV (2013) Evaluation of microstructure and mechanical properties of Al3003-H18, Al6082-H30 and commercial grade aluminum under friction stir, pp 18–23, Jan 2015
44. Barbini A, Carstensen J, dos Santos JF (2017) Influence of a non-rotating shoulder on heat generation, microstructure and mechanical properties of dissimilar AA2024/AA7050 FSW joints. *J Mater Sci Technol* 34(1):119–127

Microstructure, Economic, and Emission Evaluation of Castings Produced from Biodiesel-fired Self-designed Rotary Furnace



Purshottam Kumar and Rohit Sharma

Abstract In this research work, various types of furnace systems, i.e., coke-less cupola, coke-fired cupola, and biodiesel-fired self-designed rotary furnace have been utilized for the economic analysis of the produced castings. In the comparison of other furnaces, the results of regressive experimentation on the self-designed and fabricated rotary furnace found the saving of around 5.8% in the cost of the casting. The microstructure and mechanical properties analysis was also performed to check the quality of the produced castings with the self-designed rotary furnace. In addition, the emission levels were found to be within the specified limits given by CPCB norms.

Keywords Rotary furnace · Pollution · Microstructure · Economic analysis · SG iron · Gray CI

1 Introduction

The foundry industry plays a vital part in the industrial growth of India. India is the third largest producer of foundry products, which are not only used in the domestic markets but also exported worldwide. This industry has developed in volumes over several years and is expected to develop further in future. The foundry industry is an export-oriented industry because of the enormous demand in the international market. The foundry is facing problems, viz, the supply of raw material, power requirements, funds, limitations by the central pollution control board (CPCB), energy utilization and hard competition by liberalization, globalization, and privatization.

There are different types of conventional furnaces for producing these materials, and the rotary furnace is one of the newest modern developed technologies for producing structural materials. It has been found out that recuperating systems increase

P. Kumar (✉)
DEI, Agra, India
e-mail: purshottam.agra@gmail.com

R. Sharma
Amity University, Noida, Uttar Pradesh, India
e-mail: r25sharma@gmail.com

the efficiency of the rotary furnace by the collection of hot flue gases by preheating the air and fuel help reducing time in processing [1]. There has been a 10% loss in the carbon through utilization of rotary furnace [2]. Some metals such as aluminum prefer butane gas instead of diesel fuel for viable solution during the casting process [3]. The rotary furnace has excellent heat transfer capability and reaches flame temperature maximum at 2800 °C with high thermal exchange and higher degrees of radiation [4]. NO_x emission was also reduced through the utilization of the rotary reactors containing flue gases [5]. Operability analysis enables the production engineers to reduce the emission effect through utilization of coal in an industrial rotary kiln [6]. The rotary furnace has been found to be the best effective method for the thermal treatment of medical waste in hospitals [7]. To reduce the fugitive dust in foundry kilns; water sprinkling, tree plantation, and daily cleaning are some measures to be taken by industries [8]. The pollutant found in the rotary furnace can be checked by using electrostatic separator [9]. The relative amount of flushing agents and better mixing of charge metallurgical materials can be assessed through rotary furnaces [10]. Ferritic-pearlite ductile iron was produced through utilization of rotary furnace as explain [11].

The cupola is being utilized as a primary melting unit in iron foundries for the last several decades and still holds the position despite strong competition. Prior, the energy and ecological esteems were optional. Nowadays, nonetheless, the ecological issues have been brought into the center. The Honorable Supreme Court of India gave certain mandates, which apply to the Taj trapezium zone (TTZ), Agra, intending to saving Taj Mahal. Subsequently, most of the foundries have been shut.

Therefore, as a solution to the society, the rotary furnace has designed on which experimental trials were performed to optimize the execution parameters of the furnace. The self-designed and developed rotary furnace performed better when contrasted with different furnaces while working with optimal air preheat temperature and percentage of excess air for standardized rotational speed. The experimental trials were performed to optimize the carbon loss in the melt.

Therefore, in this paper, the comparative cost analysis of castings produced on coke-less, coke-fired cupola, and the self-designed biodiesel-fired rotary furnace was done. The microstructure and mechanical properties analysis was also performed to check the quality of the produced castings with the self-designed rotary furnace. In addition, the pollutant level was checked with the CPCB norms.

2 Economic Analysis of Coke-Less, Coke-Fired Cupola, and Rotary Furnace

The economics of any melting unit is very crucial, and a number of factors need to be taken into account. The capital cost has a major importance, and the environmental control equipment has a large effect on the overall capital cost. A large amount

of money requires to melting with a conventional coke-fired cupola to satisfy the environmental norms.

2.1 Technical Details

The capacity of cupola may vary from 1 to 20 ton/hr for MT/hr, the details are as follows:

Electricity consumption/MT of molten iron (including superheater and auxiliary services) = 130.89 kWh.

The feedstock is steel scrap = 15%; pig iron = 50%; return scrap = 35% (ceramic balls consumption is 1.5% using duplex superheater); iron temperature = 1380 °C; % CO in flue gasses = Nil; tapping temperature = 1520 °C; gray CI grades = 15, 20, 25; and SG base iron 1, 2 are very easily cast (Tables 1, 2, 3, 4).

Table 5 shows the comparative evaluation cost of the coke-fired cupola, coke-less cupola (LDO-fired), coke-less cupola (gas-fired), and biodiesel-fired rotary furnace and found a saving of 5.8% by utilizing biodiesel-fired rotary furnace.

3 Microstructural Analysis

To ensure the quality and the cost of the product, a detailed microstructures study of different samples of gray cast iron and SG iron castings produced from the rotary furnace has been done using “Biovis Materials Plus” image analysis software. The software has primarily four materials module panels, viz, main, analysis, configuration, and result. The main panel gives options for selecting the technique to be used for analysis. The analysis panel gives choices for identifying the features for analysis. The resulting panel illustrates the result of the analysis. For the majority of the modules, we can automatically run the analysis for the several images, and for the group run, we can set up a succession of processes with analysis to run on these images.

3.1 Phase/Volume Fraction

In this module, the images of microstructures are analyzed and assessed the volume fractions of identifiable phases or elements. Several images were analyzed to enhance the accuracy of measurements. Results for each field were shown in the form of result summary. The report that conforms to ASTM E 562 was then produced for the analysis.

Table 1 Economic analysis of coke-less cupola (light-diesel-oil-fired)

S. no.	Item	Quantity	Rate (Rs.)	Total cost (Rs.)
<i>Operating cost</i>				
1.	Fuel cost (LDO)	70.00 l	25.00/l	1750.00
2.	Energy consumption			
	(a) Blower	0.75 kWh		
	(b) Carburization of fuel	75.00 kWh	6.00/kWh	459.00
	(c) Cooling	0.75 kWh		
		76.50 kWh		
3.	Limestone addition	50.00 kg	2.50/kg	125.00
4.	Refractory consumption	30.00 kg	10.00/kg	300.00
5.	Water consumption	1.50 m ³	1.00/m ³	1.50
6.	Ceramic spheres	15.00 kg	200.00/kg	3000.00
7.	Carburizing material	20.00 kg	8.00/kg	160.00
8.	Ramming mass	0.50 kg	2.50/kg	1.25
9.	Ferrosilicon	5.00 kg	100.00/kg	500.00
10.	Labor cost	Contract	500.00/MT	500.00
11.	Maintenance and repair		600.00/MT	600.00
	Total operating cost			Rs. 7396.75
<i>Material cost</i>				
1.	Pig iron	500.00 kg	20.00/kg	10,000.00
2.	Cast iron (CI) scrap	350.00 kg	18.00/kg	6300.00
3.	Mild steel (MS) scrap	150.00 kg	17.00/kg	2550.50
	Total material cost			Rs. 18,850.50
<i>Total cost</i>				
Total cost = Total [Operating + Material] cost				
= Rs. 7396.75 + Rs. 18,850.50 = Rs. 26,247.25				
Adding rejection 1% (Max.) = Rs. 262.46				
Total cost/MT of molten metal = Rs. 26,509.71				

Table 2 Economic analysis of coke-less cupola (gas-fired)

S. no.	Item	Quantity	Rate (Rs.)	Total cost (Rs.)
<i>Operating cost</i>				
1.	Fuel cost (natural gas)			
	(a) Preheating	15.00 m ³		
	(b) Melting	85.00 m ³	22.00/m ³	2200.00
		100.00 m ³		
2.	Miscellaneous energy			
	(a) Blower	0.75 kWh		
	(b) Carburization of fuel	75.00 kWh	6.00/kWh	459.00
	(c) Cooling	0.75 kWh		
		76.50 kWh		
3.	Limestone addition	50.00 kg	2.50/kg	125.00
4.	Refractory consumption	30.00 kg	10.00/kg	300.00
5.	Water consumption	2.00 m ³	1.00/m ³	2.00
6.	Ceramic spheres	12.00 kg	200.00/kg	2400.00
7.	Carburizing material	15.00 kg	8.00/kg	120.00
8.	Ramming mass	1.00 kg	2.50/kg	2.50
9.	Ferrosilicon	5.00 kg	100.00/kg	500.00
10.	Labor cost	Contract	600.00/MT	600.00
11.	Maintenance and repair		600.00/MT	600.00
	Total operating cost			Rs. 7308.50
<i>Material cost</i>				
1.	Pig iron	500.00 kg	20.00/kg	10000.00
2.	Cast iron (CI) scrap	350.00 kg	18.00/kg	6300.00
3.	Mild steel (MS) scrap	150.00 kg	17.00/kg	2550.50
	Total material cost			Rs. 18,850.00
<i>Total cost</i>				
Total cost = Total operating cost + Total material cost				
= Rs. 7308.50 + Rs. 18,850.50 = Rs. 26,158.50				
Grand total				
Total cost = Rs. 26,158.50				
Adding rejection 1% (Max.) = Rs. 261.58				
Total cost/MT of molten metal = Rs. 26,420.08				

Table 3 Economic analysis of coke-fired cupola

S. no.	Item	Quantity	Rate (Rs.)	Total cost (Rs.)
<i>Operating cost</i>				
1.	Coke with 12 ± 2% Ash	60.00 kg		
	(a) Apreheat	200.00 kg	15.00/kg	3900.00
	(b) Meltin	260.00 kg		
2.	Miscellaneous energy			
	(a) Blower	10.00 kWh		
	(b) Dust extraction	15.00 kWh		
	(c) Desulfurization	12.00 kWh	5.00/kWh	235.00
	(d) Bleeding fuel	10.00 kWh		
		47.00 kWh		
3.	Limestone addition	60.00 kg	2.50/kg	150.00
4.	Refractory consumption			
	(a) Preheat zone	10.50 kg		
	(b) Melting zone	60.00 kg	10.00/kg	857.00
	(c) Outlet zone	15.20 kg		
		85.70 kg		
5.	Ramming mass	2.00 kg	2.50/kg	5.00
6.	Ferrosilicon	5.00 kg	90.00/kg	450.00
7.	Carburizing material	12.00 kg	35.00/kg	420.00
8.	Labor cost	Contract	500.00/MT	500.00
9.	Maintenance and repair		900.00/MT	900.00
	Total operating cost			Rs. 7417.00
<i>Material cost</i>				
1.	Pig iron	500.00 kg	20.00/kg	10,000.00
2.	Cast iron (CI) scrap	400.00 kg	18.00/kg	7200.00
3.	Mild steel (MS) scrap	100.00 kg	17.00/kg	1700.00
	Total material cost			Rs. 18,900.00
<i>Total cost</i>				
Total cost = Total operating cost + Total material cost				
= Rs. 7417.00 + Rs. 18,900.00 = Rs. 26,317.00				
<i>Grand total</i>				
Total cost = Rs. 26,317.00				
Adding rejection 4% (Max.) = Rs. 1052.68				
Total cost/MT of molten metal = Rs. 27,369.68				

Table 4 Economic analysis of biodiesel-fired rotary furnace

S. no.	Item	Quantity	Rate (Rs.)	Total cost (Rs.)
<i>Operating cost</i>				
1.	Fuel cost (biodiesel)	160.00 l	40.00/l	6400.00
2.	Energy consumption			
	(a) One hp motor for furnace rotation	$(0.746 \times 1 \times 3) = 2.238$ kWh	4.50/kWh	85.60
	(b) 7.5 hp motor for air compressor	$(0.746 \times 7.5 \times 3) = 16.785$ kWh		
		19.023 kWh		
3.	Water consumption	0.60 m ³	0.50/m ³	0.30
4.	Relining	9.00 kg	10.00/kg	90.00
5.	Labor cost	Contract	100.00/MT	100.00
6.	Maintenance and repair		300.00/MT	300.00
	Total operating cost			Rs. 6975.90
<i>Material cost</i>				
1.	Pig iron	350.00 kg	20.00/kg	7000.00
2.	Cast iron (CI) scrap	500.00 kg	18.00/kg	9000.00
3.	Mild steel (MS) scrap	150.00 kg	17.00/kg	2550.00
	Total material cost			Rs. 18,550.00
<i>Total cost</i>				
Total cost = Total operating cost + Total material cost				
= Rs. 6975.90 + Rs. 18,550.00 = Rs. 25,525.90				
<i>Grand total</i>				
Total cost = Rs. 25,525.90				
Adding rejection 1% (Max.) = Rs. 255.25				
Total cost/MT of molten metal = Rs. 25,781.16				

Table 5 Comparative evaluation of cost

Furnace Cost and saving	Coke-fired cupola	Coke-less cupola (LDO-fired)	Coke-less cupola (Gas-fired)	Biodiesel-fired rotary furnace
Cost/MT of molten metal	Rs. 27,369.68	Rs. 26,509.21	Rs. 26,420.08	Rs. 25,781.16
Saving		3.14%	3.46%	5.80%

3.2 Measurement of Grain Size

The role of grain-size module is to find the mean grain-size measurement and distribution of grain diameters, areas, etc. from images of grain structures. The grain-size measurement module includes the test approaches suggested in the ASTM E 930 Standards (for ALA grain-size measurement), ASTM E 112, ASTM E 1382 (for average grain-size measurement), and ASTM E 1181 (for duplex grain-size measurement). It provides automatic as well as a semi-automatic interactive technique for analyzing the images of grain structures (Tables 6, 7, 8, 9).

Table 6 Phase analysis (ASTM E 562)

% Flakes area	Maximum length (μm)		
	Pearlite	Ferrite	Graphite
SG iron	62.703	12.978	20.341
	62.302	14.152	19.127
	61.712	20.034	16.003
Gray CI	45.124	19.713	35.130
	50.015	18.012	31.071
	50.230	18.813	33.713

Table 7 Nodularity measurement (ASTM A 247) and graphite flakes of SG iron

% Flake area	Nodule count	Nodule area	Nodules (mm ²)	Minimum size (μm)	Maximum size (μm)	Nodularity (%)	Mean
2.000	86	7.72	266.125	0	64.72	86.00	37.40
3.980	83	8.34	259.930	0	58.01	81.41	59.20
1.812	108	12.36	335.250	0	68.92	87.60	36.50
0.665	116	9.10	382.700	0	58.75	69.82	30.20
0.956	98	9.88	308.650	0	49.60	67.21	27.20
2.480	112	11.88	308.880	0	68.76	88.30	26.42
3.900	84	11.92	286.760	0	57.70	71.90	25.52
3.620	92	8.67	314.873	0	49.10	79.60	24.01
2.182	93	9.62	301.820	0	56.30	83.21	46.72
2.300	81	8.93	280.770	0	56.41	85.10	50.24

Table 8 Representation of graphite flake area and maximum length of gray CI

% Flakes Area	Maximum length (μm)								
	Size 1	Size 2	Size 3	Size 4	Size 5	Size 6	Size 7	Size 8	
18.16	1017.3	-	1.96	3.19	2.98	3.79	3.70	1.86	1.27
18.37	1096.7	-	3.78	2.48	4.35	3.18	3.13	2.60	1.39
9.91	817.7	-	-	1.41	1.87	2.76	2.57	1.13	0.28
17.08	1583.1	-	4.28	4.98	2.20	2.10	0.86	0.85	0.31

Table 9 Inclusions (ASTM E 1122 JK)

Severity level	A (Thin)	A (Thick)	B (Thin)	B (Thick)	C (Thin)	C (Thick)	D (Thin)	D (Thick)
0.5	0	0	0	0	1	0	0	0
1.0	0	0	1	0	0	0	0	0
1.5	0	0	0	0	0	0	0	0
2.0	0	0	0	0	0	0	0	1
2.5	0	0	0	0	0	0	1	0
3.0	0	0	0	0	0	0	0	0
3.5	0	0	0	0	0	0	0	0
4.0	0	0	0	0	0	0	0	0
4.5	0	0	1	0	0	0	0	0
5.0	0	0	0	0	0	0	0	0

3.3 Measurement of Nodularity

This module helps to investigate the images of microstructures and to identify and measure graphite nodules. The factors that can be measured here are nodularity, nodule density, nodule count, etc. Here, the nodules are categorized according to their sizes. The intensity or the gray level in the image is used to identify the graphite particles. The user sets the range to detect the particles as nodules. A number of images were analyzed to enhance the accuracy of measurements. The results of each field are then shown. A summary of results was generated as per ASTM A 247 for analysis.

3.4 Measurement of Graphite Flakes

This module helps to identify the microstructures of the images and measured graphite flakes. The analysis also includes the measurement of graphite percentage and sorting of flakes by size. Graphite particles were identified by their intensity or gray level in the image. The length is measured for each graphite flake. Size and shape factors were set to identify the particles as graphite flakes. Numerous images were analyzed for enhancing the accuracy of measurements. A summary of results was generated after the analysis of multiple fields. A report that conforms to ASTM A 247 was produced for analyzing the flake sizes and graphite measurement.

Figures 1a, b, c, and d show the microstructures obtained during gray cast iron casting, and Fig. 1d shows the weaker nodular graphite flakes, and Fig. 1b shows the strongest nodular graphite flakes. The microstructural image obtained in Fig. 1b is of highest strength and high impact resistance.

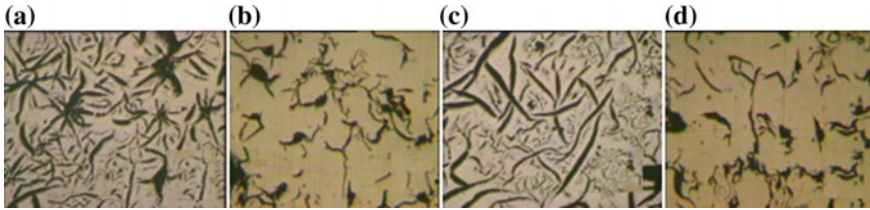


Fig. 1 a–d Snapshots of microstructures of gray CI castings for analysis—graphite flake analysis

3.5 Inclusion Analysis

It incorporates procedures based on ASTM E 45 and ASTM E 1122. The role of this module is to analyze the sulfide and oxide inclusions resulting from the deoxidization and precipitation of sulfides during the solidification process. The inclusions used are categorized only by gray shade, morphology, reflectivity, length, thickness, and number. The inclusion types A, B, C, and D are distinguished on the following basis:

Sulfides (type A)—all sulfides are higher in reflectivity than oxides. Type A inclusions are continuous stringers and pretty similar to type C inclusions.

Oxides (type B, C, D)—all oxides are lower in light reflectivity than sulfides, i.e., oxides appear darker as compared to sulfides.

Once separated the oxides are distinguished further by the morphology as follows:

type B—discontinuous stringers

type C—continuous stringers

type D—non-stringer globular oxide particles with an aspect ratio < 5

4 Mechanical Property Analysis of Castings

Samples of gray CI and SG iron from the rotary furnace were obtained with the standardized parameters. In addition, mechanical strength, ductility, and hardness were measured for different compositions of carbon. Results are shown in Tables 10 and 11, respectively.

5 Ambient Air Quality

Table 12 shows the quality of air and the permissible limits of air pollution defined by the Central Pollution Control Board (CPCB). Table 13 shows the comparison of pollution level between LDO and biofuel used in the rotary furnace. Moreover, the results show that the pollution level using 50% biodiesel was under CPCB norms

Table 10 Mechanical properties of the gray CI specimen

Specimen	σ_t	BHN	%C	%Si	%Mn	%P	%S	%Cr	%Mo	%Ni
1.	142	160	3.80	2.14	0.741	0.090	0.062	0.0186	<0.0020	0.0113
2.	146	155	3.50	2.90	0.684	0.099	0.058	0.0244	<0.0013	0.0113
3.	152	164	3.68	2.30	0.692	0.109	0.068	0.0176	<0.0019	0.0113
4.	165	156	3.48	2.29	0.801	0.092	0.064	0.0194	<0.0021	0.0113
5.	175	160	3.24	2.32	0.691	0.085	0.066	0.0193	<0.0013	0.0113
6.	188	152	3.42	2.32	0.742	0.099	0.062	0.0189	<0.0019	0.0113
7.	164	162	3.64	2.31	0.769	0.098	0.064	0.0162	<0.0012	0.0113
8.	185	160	3.58	2.31	0.697	0.102	0.057	0.0193	<0.0014	0.0113
9.	192	164	3.58	2.32	0.680	0.087	0.058	0.0191	<0.0017	0.0113
10.	204	160	3.80	2.34	0.721	0.097	0.061	0.0186	<0.0017	0.0113

Table 11 Mechanical properties of SG iron specimen

S. no.	UTS	%Elongation	BHN	%C	%Si	%Mg	%Mn	%S	%Mo
1.	398	14.7	189	3.81	3.17	0.041	0.40	0.019	Negligible
2.	405	15.2	190	3.76	3.31	0.042	0.41	0.020	Negligible
3.	394	14.9	194	3.81	3.26	0.039	0.34	0.014	Negligible
4.	391	15.3	186	3.86	3.31	0.044	0.35	0.017	Negligible
5.	512	10.2	201	3.83	2.96	0.052	0.54	0.021	Negligible
6.	503	10.3	196	3.82	3.11	0.062	0.56	0.019	Negligible
7.	496	9.98	199	3.79	3.04	0.059	0.62	0.015	Negligible
8.	498	10.2	204	3.77	3.07	0.045	0.52	0.018	Negligible
9.	604	3.06	269	3.41	2.83		0.80	0.021	0.30
10.	607	3.09	276	3.36	2.81		0.74	0.020	0.28

comparatively to LDO. Therefore, it has been found that the rotary furnace with biofuel is safe for the environment.

6 Conclusion

In this paper, the economic analysis of different furnaces and microstructure analysis of the castings produced by the rotary furnace are completed. The findings show the sovereignty of rotary furnace over the others.

1. The economic analysis of the four furnaces illustrates that the cost of molten metal per metric ton is minimum in the case of the rotary furnace in comparison with other furnaces. The comparative evaluation shows that a cost of about 5.8%

Table 12 Pollutants and permissible concentrations in ambient air

Pollutants	Permissible concentrations in ambient air (mg/m ³)		
	Industrial areas	Residential, rural, and other areas	Sensitive areas
Sulfur dioxide (SO ₂)	80	60	15
Oxides of nitrogen as (NO _x)	80	60	15
Suspended particulate matter (SPM)	360	140	70
Respirable suspended particulate matter (RSPM)	120	60	50
Carbon monoxide (CO)	5000	2000	1000

Table 13 Comparison of pollution levels of light diesel oil (LDO) and biofuel (Jatropha 50% Biodiesel)

Pollution levels using light diesel oil (LDO)					Pollution levels using 50% biodiesel			
S. no.	SO ₂ level (mg/m ³)	SPM level (mg/m ³)	CO (mg/m ³)	NO _x (mg/m ³)	SO ₂ level (mg/m ³)	SPM Level (mg/m ³)	NO _x (mg/m ³)	CO (mg/m ³)
1	120	50	280	73	58	43	75	260
2	90	58	300	80	52	42	70	245
3	90	45	310	78	55	47	72	240
4	89	95	290	82	48	45	71	250
5	92	85	300	78	51	40	72	265
6	89	65	320	70	48	68	69	245
7	89	55	300	81	49	49	72	265
8	89	85	290	78	50	48	71	270
9	96	65	295	80	51	43	76	225
10	106	85	290	78	55	49	73	245

is saved in the rotary furnace over the others. The level of pollutants also satisfies the pollution level set by CPCB to the biggest conceivable degree.

- The results of the microstructural analysis of the castings produced shown in Figs. 1 and 2, respectively, indicate maximum flake area, more amount of graphite and well-distributed graphite flakes which have excellent machinability, easy grinding, high thermal conductivity, high damping, and high production of the castings.
- Investigation of castings for strength and other related factors shows that the samples produced from the rotary furnace are having excellent tensile strength, hardness, and the meager percentage of sulfur, molybdenum, nickel, and phosphorus, with a good percentage of carbon as shown in Tables 10 and 11.

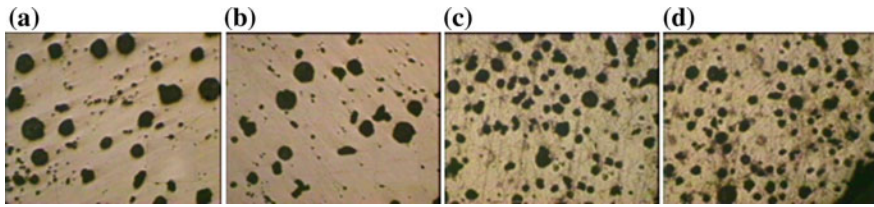


Fig. 2 a–d Snapshots of microstructures of SG iron castings for analysis—graphite flake analysis

In Agra foundries, the produced castings are very hard, and their machining is complicated. The microstructural analysis results of the current research work give some extremely eager outcomes concerning this issue. It provides an understanding that a thorough microstructural examination of rotary furnace castings can most likely be the harbinger of the challenges looked by the foundry industries of Agra.

Given the present-day stringent pollution control requirements, it is imperative that the melting technique used should satisfy the environmentalists and the economy of the process should not be affected. The biodiesel-fired rotary furnace scores well on all counts and ought to be utilized rather than conventional coke-less and coke-fired cupolas, and gas-fired cupola furnaces.

References

1. Omole SO, Oluyori RT (2014) Optimization of recuperative system in rotary furnace for minimization of elemental loss during melting. *J Miner Mater Charact Eng* 2:579–585
2. Omole SO, Oluyori RT (2015) Study of carbon and silicon loss through oxidation in cast iron base metal using rotary furnace for melting. *Leonardo Electr J Pract Technol* 26:59–64
3. Akhaze MN (2012) Comparison of diesel with butane gas in firing crucible furnace for melting aluminium. *Int J Eng Res Technol* 1
4. <http://www.sogemieng.it/en/prod/rotary-oxy-combustion-melting-furnace-for-cast-ron.aspx>
5. Cheng X, Zhang X, Zhang M, Sun P, Wang Z, Ma C (2017) A simulated rotary reactor for NO_x reduction by carbon monoxide over Fe/ZSM-5 catalysts. *Chem Eng J* 307:24–40
6. Baikadi A, Runkana V, Subramaian S (2016) Operability analysis of direct reduction of iron ore by coal in an industrial rotary kiln. *IFAC* 49:468–473
7. Bujak J (2015) Thermal treatment of medical waste in a rotary kiln. *J Environ Manage* 162:139–147
8. Allaban MA, Qudais HA (2011) Impact assessment of ambient air quality by cement industry: a case study in Jordan. *Aerosol Air Qual Res* 11:802–810
9. Subashini LM (2016) Mitigation of air pollution in sponge iron industries. *J Chem Pharm Sci* 9:229–231
10. Locating and estimating air emissions from sources of polycyclic organic matter United States July 1998 Agency Research Triangle NC 27711. A Report EPA-454/R-98-014
11. Akinlabi O, Omole SO (2011) Evaluation of ductile iron produced using rotary furnace with variable compositions of magnesium addition 9:276–282

Study of Sliding Wear Behavior of Alumina Oxide Filled Fiber Composite Using Design of Experiment



Bhanu Pratap, R. K. Gupta and Bhuvnesh Bhardwaj

Abstract The carbon fiber reinforced polymer composites are extensively used in different manufacturing applications due to their superior strength to weight, high thermal stability, and excellent corrosion resistance. The main objective of present research work is to optimize the sliding wear conditions (applied load, sliding velocity, and %wt Al_2O_3 particulates) for minimum wear volume of Al_2O_3 filled carbon reinforcement fiber composites against EN-32 steel. Taguchi-based L_9 orthogonal array and ANOVA are used to find the optimum parameters for minimum wear. The sliding velocity has been found the most significant parameter that affects the sliding wear followed by filler loading and normal load. On the other hand, it has been found that sliding wear rate continuously decreases with increase in filler loading and increases with increase in applied normal load and sliding velocity.

Keywords Carbon fiber · Alumina oxide particulates · EN-32 steel · Sliding wear

1 Introduction

In the present scenario, more emphasis is given on the quality of the products. Therefore, recently developed advanced materials like composites, high-performance steels, and ceramics are replacing the general metallic materials to increase the quality of the products. Among these materials, fiber composites are extensively used for many applications due to their unique properties and advantages over other materials [1].

Among the entire fiber reinforced polymer composites, the carbon fiber reinforced polymer composites are widely used in different manufacturing applications due to their better strength to weight and excellent corrosion resistance [2].

B. Pratap (✉) · R. K. Gupta

Department of Mechanical Engineering, Manipal University Jaipur, Jaipur, Rajasthan, India
e-mail: bhanu132@yahoo.com

B. Bhardwaj

Department of Mechanical Engineering, Jaipur Engineering College & Research Centre, Jaipur, Rajasthan, India

© Springer Nature Singapore Pte Ltd. 2019

K. Shanker et al. (eds.), *Advances in Industrial and Production Engineering*, Lecture Notes in Mechanical Engineering, https://doi.org/10.1007/978-981-13-6412-9_68

735

The polymer composites with Al_2O_3 as filler exhibited better erosion resistance as compared to the polymer composites with SiC and fly ash as filler material [3]. Al_2O_3 is also used as reinforcement material in metal matrix composites as well as in polymer matrix composites. The addition of Al_2O_3 , increases the mechanical properties as well as high wear resistance [4, 5]. Nowadays, improved wear resistance against hardened steel is one of the prime concerns among researchers. Adhikari et al. [6] fabricated jute fiber reinforced epoxy polymer composite using simple hand layup method. The zirconia and alumina particles in 5, 10, 15, and 20 %wt have been used as filler material. The maximum microhardness has been achieved with 20% filler material. It has also been revealed that jute fiber reinforced epoxy polymer composite with ZrO_2 exhibited better thermal stability, degradation temperature, and fire-resistant property as compared to jute fiber reinforced epoxy polymer composite with Al_2O_3 .

Agrawal et al. [7] investigated friction and wear characteristics of glass fiber reinforced epoxy polymer composite with three different sliding atmospheres against EN31 steel. The sliding speed and load have been considered as sliding conditions. The maximum coefficient of friction has been achieved with inert gas (argon) followed by dry and oil-lubricated environment.

Österle et al. [8] characterized surface features and nanostructure of tribofilms using advanced microscopic techniques. The wear tests have been conducted using pin-on-disk apparatus with material against 100Cr6 steel. The scanning electron microscopy, light optical microscopy, and energy-dispersive X-ray spectroscopy have also been carried out to examine wear scars on disk surface. The nano-structured silica with at least 10 vol.% exhibited minimum wear and friction coefficient.

Karthik and Senthilkumar [9] investigated tribological and mechanical properties of ceramic particles reinforced carbon-epoxy composites. Then, aluminum oxide and silicon carbide particles have been used as reinforcement. The composites have been fabricated using vacuum bag molding technique. The composite with 10% SiC and 5% Al_2O_3 exhibited superior mechanical properties as well as wear resistance among all the fabricated composites.

Shivakumar et al. [10] fabricated ZA-27-based composites with nano-sized Al_2O_3 particles as reinforcement to investigate the effect of %wt of nano-sized Al_2O_3 particles in composites on wear volume. It has been revealed that as the %wt of Al_2O_3 reinforcement increases, the wear volume loss of the fabricated composite decreases.

Annappa and Basavarajappa [11] investigated the effect of sliding wear conditions on wear rate of functionally graded glass-epoxy composite with graphite. The composites have been fabricated using hand layup technique. The applied normal load, sliding velocity, and sliding distance have been considered as wear conditions. It has been revealed that specific wear rate increases with increase in load, sliding velocity, and sliding distance.

Anjum et al. [12] studied mechanical tribological properties of glass-epoxy composites with SiO_2 filler in different wt%. The composites have been fabricated using hand layup technique followed by compression molding technique. Taguchi methodology based on L_9 orthogonal array has been applied to investigate the effect of normal

load, sliding velocity, and sliding distance on wear rate. It has been revealed that wear volume increases with increase in applied load, sliding distance, and velocity.

Dass et al. [13] investigated the mechanical and tribological properties of orthocresol novolac epoxy filled with aluminum oxide and micro-size silicon carbide composites. For the wear analysis, the load and sliding velocity have been considered as wear parameters. It has been revealed that composites with filler particles exhibited excellent mechanical and tribological properties as compared to unfilled composites.

Andrich et al. [14] investigated the tribological behavior of polypropylene composites fabricated using resin transfer molding technique. The developed composites have been coated with diamond-like carbon. The remarkable decrease in specific wear rate of composite against uncoated and coated steel 100Cr6 has been obtained.

Alsharif et al. [15] studied dental resin composites (DRCs) cured with LED light using monomer along with 40–60 wt% Al_2O_3 particles as filler. The fracture toughness, apparent porosity, and bulk density have been evaluated. The significant influence of Al_2O_3 particles on the mechanical properties of DRCs has been observed.

Basavarajappa and Ellangovan [16] studied dry sliding wear characteristics of glass–epoxy (G-E) composites reinforced with graphite and silicon carbide. The applied load, sliding velocity, and sliding distance have been considered as wear parameters. The excellent wear resistance has been observed. The applied load has been found the most significant parameter that affects the wear rate.

Rout and Satapathy [17] studied erosion wear behavior and mechanical properties of glass fiber–epoxy composite with unfilled and filled rice husk particles. Taguchi optimization technique has been employed to optimize the wear parameters for minimum wear rate. The impact velocity, erodent size, filler content, and impingent angle have been found significant parameters that affect the wear rate. The maximum wear resistance has been obtained for composite with 15 wt% rice husk. It has also been found that addition of filler content reduces the flexural strength and strength, while it increases the tensile modulus, impact energy, and hardness.

Sahu et al. [18] experimentally investigated the mechanical properties of composite having polyester resin along with glass fiber and 0, 5, 10, and 15 wt% alumina particles as reinforcement. It has been revealed that these fillers significantly influence the mechanical properties of developed composites.

El-Tayeb and Gadelrab [19] studied friction and wear characteristics of E-glass fiber reinforced epoxy composite. The normal load, sliding velocities, and surface conditions have been considered as process parameters. The minimum wear has been obtained against wet and clean surfaces.

The aim of the present research is to investigate the effect of wear conditions (applied load, sliding velocity, and %wt Al_2O_3 particulates) on wear rate. An attempt has also been made to optimize the sliding wear conditions for minimum wear rate.

2 Methods

2.1 Specimen Preparation

The low-temperature carbon fiber (locally supplied) was reinforced with epoxy resin (Araldite LY 556) with aluminum oxide particles as filler. The composite has been fabricated using conventional hand layup method [20]. The hardener (HY951) is mixed in a ratio of 10:1 by weight.

Aluminum oxide (Al_2O_3) is a chemical compound of aluminum and oxygen and is atmospheric in nature. It is commonly known as alumina and is 15% of the earth's crust. The key properties of alumina particles are high mechanical strength, high temperature resistance, high corrosion resistance, and high wear resistance.

2.2 Dry Sliding Wear Test Apparatus

The wear specimens of the composites were prepared as per ASTM G-99. All wear tests have been conducted on pin-on-disk test rig (TR-20 LE, supplied by DUCOM). The counter disk is prepared of hardened ground steel (EN-32) having hardness of 72 HRC and surface roughness of 0.6 μ m. The test specimens are kept stationary and the disk is rotated during which a normal force is applied through a lever mechanism. A number of experimental tests were conducted according to L_9 orthogonal array-based Taguchi design. Table 1 represents the wear conditions and levels of conditions according to Taguchi methodology, while Table 2 shows the design matrix for experimentation. A precision electronic balance (Denver Instruments Germany, TB-2150) is used to measure the material loss of the test specimens examined. The specific wear rate as the output parameter of the test specimens is determined by the following equation.

$$W_s = \frac{\Delta m}{\rho \cdot t \cdot V_s \cdot F_n} \quad (1)$$

Table 1 Levels of wear conditions

Level	Factors		
	Sliding velocity	Fiber loading	Normal load
	(m/s)	(%)	(N)
1	1.5	5	10
2	2.5	10	20
3	3.5	15	30

where W_s is the specific wear rate in mm^3/Nm , Δm is the mass loss during specified test in grams, ρ is the density of the composites in g/mm^3 , t is the test duration in s, V_s is the sliding velocity in m/s, and F_n is the average normal load applied in N.

3 Results and Discussions

Table 2 shows the design matrix for experimentation along with the measured values of wear rate. Table 3 shows the ANOVA analysis for the mean values of wear rate.

In the present work, the analysis of variance test (ANOVA) is carried out for a significance level of $\alpha = 0.05$, i.e., for a confidence level of 95%. The ANOVA for wear is summarized in Table 3.

Table 3 shows that “Prob. > F ” values for sliding velocity, filler loading, and load are less than 0.05, which implies that these are the significant parameters that affect the wear. The R^2 value and adjusted R^2 value are equal to 0.997 and 0.989,

Table 2 Standard orthogonal L_9 array with output results

Experiment no	Sliding velocity	Fiber loading	Normal load	W_s
	(m/s)	(%)	(N)	$10^{-6} \times (\text{mm}^3/\text{Nm})$
1	1.5	5	10	2.98
2	1.5	10	20	2.51
3	1.5	15	30	2.13
4	2.5	5	20	4.76
5	2.5	10	30	4.43
6	2.5	15	10	2.54
7	3.5	5	30	6.24
8	3.5	10	10	4.43
9	3.5	15	20	3.48

Table 3 ANOVA table for sliding wear

Process parameters	DOF	Seq SS	Adj. SS	Adj. MS	F -value	P value
Sliding velocity (m/s)	2	7.2655	7.2655	3.63275	189.2057	0.005
Fiber loading (%wt)	2	5.6855	5.6855	2.84275	148.0599	0.007
Normal load (N)	2	1.4406	1.4406	0.7203	37.51563	0.026
Error	2	0.0384	0.0384	0.0192		
Total	8	14.43				
R -square		0.997		Adj. R -square		0.989

respectively. The result shows that the adjusted R^2 value is very close to the ordinary R^2 value, which indicates that the wear parameters have a strong effect on wear.

Table 4 presents the difference between the maximum and the minimum value of the wear parameters for sliding wear values and rank of wear condition.

The most effective factor affecting performance characteristics is obtained by comparing these values. This comparison gives the level of importance of controllable factors. The most effective controllable factor corresponds to the maximum of these values. Thus, the sliding velocity has been found most significant parameter that affects the wear followed by filler loading and load.

To investigate the influence of each parameter on wear, graph between the wear parameters and wear has been plotted as shown in Fig. 1.

From the figure, it has been revealed that wear rate increases with increase in sliding velocity from 1.5 to 3.5 m/s. The minimum wear is achieved at the first level of sliding speed that is 1.5 m/s. Figure 1 also shows the variation of wear with respect to filler loading. From the figure, it is clear that wear continuously decreased with

Table 4 Response table for wear

Wear conditions	Levels			Max.–Min. (Δ)	Rank
	1	2	3		
Sliding velocity (m/s)	2.54	3.91	4.717	2.177	1
Fiber loading (%wt)	4.66	3.79	2.717	1.943	2
Normal load (N)	3.317	3.583	4.267	0.95	3

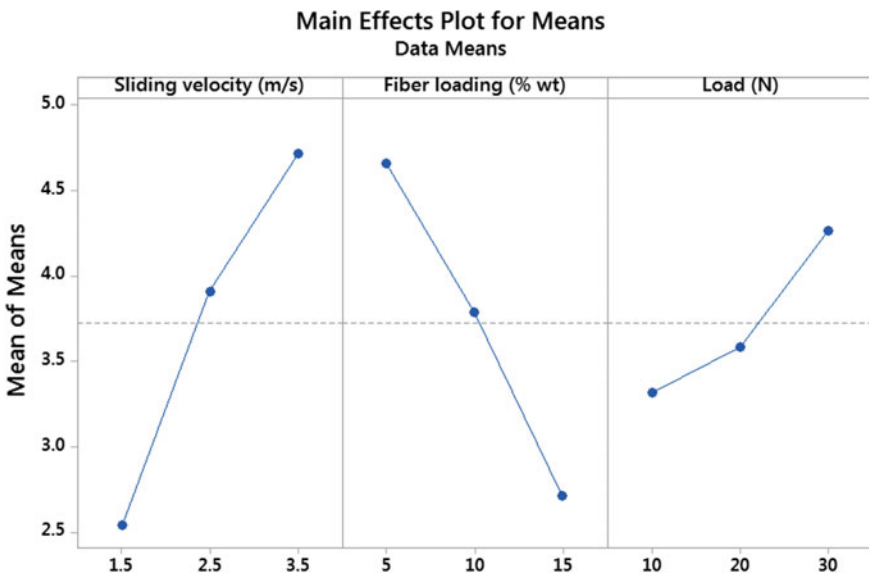


Fig. 1 Operating parameters versus main effect plot

increase in filler loading from 5 to 15 %wt. The minimum wear has been obtained with 15 %wt filler loading. The influence of normal load on wear is also presented in Fig. 1. From the figure, it is clear that wear volume increases with increase in applied load from 10 to 30 N. The minimum wear is achieved at first level of load that is 10 N.

Analyzing Fig. 1, it has been revealed that minimum wear volume is obtained with 15 %wt Al_2O_3 filled carbon fiber reinforcement composites, at 10 N applied load and at sliding velocity of 1.5 m/s, i.e., third level of filler loading, first level of applied load, and first level of sliding velocity give minimum wear volume for the composite.

4 Conclusion

Polymeric composite usage is increasing at rapid pace for tribological applications, and hence, it is necessary to study the behavior of these composite materials under different operating conditions. The present investigation has been carried out to optimize the sliding wear conditions (applied load, sliding velocity, and %wt Al_2O_3 particulates) for minimum wear volume of Al_2O_3 filled carbon reinforcement fiber composites against EN-32 steel. In this investigation, the following conclusions are drawn on the basis of the results obtained from the investigations.

1. Results of sliding wear tests depict that sliding wear rate decreases continuously with the increase in the filler loading.
2. Wear rate of Al_2O_3 filled carbon reinforcement fiber composites increases with increase in applied normal load and sliding velocity.
3. Sliding velocity has been found the most significant parameter that affects the sliding wear followed by filler loading and applied load.
4. The minimum wear volume is obtained with 15 %wt Al_2O_3 filled carbon fiber reinforcement composites, at 10 N applied load and at 1.5 m/s.

References

1. Suresha B, Ramesh BN, Subbaya KM, Chandramohan BKG (2010) Parametric optimisation of three-body abrasive wear behaviour of long and short carbon fibre reinforced epoxy composites. *Mater Des* 31:1833–1841
2. Argon A, Cohen R (2003) Toughenability of polymers. *Polymer* 44:6013–6032
3. Biswas S, Satapathy A (2009) Erosion wear behavior of polymer composites: a review. *J Reinf Plast Compos* 29:2898–2924
4. Kumar NGS, Shankar GSS, Basavarajappa S (2015) A study on dry sliding wear behaviour of hybrid metal matrix composites at room temperature. *Appl Mech Mater* 25:766–767
5. Rajesh AM, Kaleemulla M (2016) Experimental investigations on mechanical behavior of aluminium metal matrix composites. *IOP Conf Ser Mater Sci Eng* 149:012121

6. Adhikari J, Biswas B, Chabri S, Bandyapadhyay NR, Sawai P, Mitra BC, Sinha A (2017) Effect of functionalized metal oxides addition on the mechanical, thermal and swelling behaviour of polyester/jute composites. *Eng Sci Technol Int J* 20:760–774
7. Agrawal S, Singh KK, Sarkar PK (2016) A comparative study of wear and friction characteristics of glass fibre reinforced epoxy resin, sliding under dry, oil-lubricated and inert gas environments. *Tribol Int* 96:217–224
8. Österle W, Dmitriev AI, Wetzel B, Zhang G, Häusler I, Jim BC (2016) The role of carbon fibers and silica nanoparticles on friction and wear reduction of an advanced polymer matrix composite. *Materials* 93:474–484
9. Karthik K, Senthilkumar P (2015) Tribological characteristics of carbon-epoxy with ceramic particles composites for centrifugal pump bearing application. *Int J ChemTech Res* 8:612–620
10. Shivakumar N, Vasu V, Narasaiah N, Subodh K (2015) Synthesis and characterization of nano-sized Al_2O_3 particle reinforced ZA-27 metal matrix composites. *Procedia Mater Sci* 10:159–167
11. Annappa AR, Basavarajappa S (2014) Studies on dry sliding wear behaviour of functionally graded graphite particle-filled glass-epoxy composites. *Compos Interfaces* 21:395–414
12. Anjum N, Prasad SLA, Chauhan SR (2013) Role of silicon dioxide filler on mechanical and dry sliding wear behaviour of glass-epoxy composites. *Adv Tribol* 2013:324952 9
13. Dass K, Chauhan SR, Gaur B (2013) Mechanical and dry sliding wear characterization of microsize silicon carbide and aluminum oxide-filled ortho cresol novalac epoxy composites. *J Compos Mater* 48:2747–2759
14. Andrich M, Hufenbach W, Kunze K, Scheibe H-J (2013) Characterisation of the friction and wear behaviour of textile reinforced polymer composites in contact with diamond-like carbon layers. *Tribol Int* 62:29–36
15. Alsharif SO, Akil HBM, El-Aziz NAA, Ahma ZAB (2013) Influence of Al_2O_3 as filler loading on the fracture toughness of light-cured dental resin composites. *Adv Mater Res* 816:227–231
16. Basavarajappa S, Ellangovan S (2012) Dry sliding wear characteristics of glass-epoxy composite filled with silicon carbide and graphite particles. *Wear* 296:491–496
17. Rout AK, Satapathy A (2012) Study on mechanical and tribo-performance of rice-husk filled glass-epoxy hybrid composites. *Mater Des* 41:131–141
18. Sahu H, Rout A, Kumar A (2012) Development and characterization of particulate filled glass fibre reinforced hybrid composite. *Int J Mech Ind Eng (IJMIE)* 2
19. El-Tayeb NS, Gadelrab RM (1996) Friction and wear properties of E-glass fiber reinforced epoxy composites under different sliding contact conditions. *Wear* 192:112–117
20. Gangil B, Patnaik A, Kumar A (2013) Evaluation of thermo-mechanical and wear behavior of short carbon fibre vinyl-ester. *Int Polym Process* 28:207–220

Role of Acoustic Softening Effects in Ultrasonic Spot Welded Dissimilar Materials



Mantra Prasad Satpathy, Susanta Kumar Sahoo and Diptikanta Das

Abstract Ultrasonic spot welding (USW) is a rapid solid-state welding process in which thin sheets are joined under the influence of high-frequency ultrasonic vibration and pressure. USW has several advantages over conventional fusion welding processes such as less energy consumption, no use of flux or filler material and generation of temperature below the melting point of parent materials. Experimental results have confirmed that USW is a combination of both thermal and acoustic softening effects. These two facts are essential for plastic deformation and bond formation during the welding process. In the present work, an attempt has been made to develop a novel thermomechanical model to characterize thermal and acoustic softening in AA1100 sheets. Experimental temperatures and increment in a width of the sheet are considered to quantify the amount of acoustic softening for different surface conditions. Acoustic softening confers a maximum reduction of 93.98% in yield strength of AA1100 sheets. This model provides a new approach to understand this complex bonding process in a very effective way.

Keywords Ultrasonic welding · Acoustic softening · Thermomechanical model · Plastic deformation · Frictional heat

1 Introduction

Ultrasonic metal welding (USMW) is one of the clean, innovative and novel solid-state welding processes which utilize high-frequency vibration of 20 kHz to produce a joint between similar or dissimilar metal sheets within a fraction of seconds. Thus, it finds its widespread applications in the automotive sector and microelectronic

M. P. Satpathy (✉) · D. Das

School of Mechanical Engineering, Kalinga Institute of Industrial Technology (Deemed to be University), Bhubaneswar 751024, Odisha, India

e-mail: mantraofficial@gmail.com

S. K. Sahoo

Department of Mechanical Engineering, National Institute of Technology Rourkela, Rourkela 769008, Odisha, India

© Springer Nature Singapore Pte Ltd. 2019

K. Shanker et al. (eds.), *Advances in Industrial and Production Engineering*, Lecture Notes in Mechanical Engineering, https://doi.org/10.1007/978-981-13-6412-9_69

743

industries. This technique is mainly used for joining of highly conductive materials such as aluminum, copper, gold and silver [1]. During USMW process, the ultrasonic vibration with normal force disperses oxide layer and other contaminants on the surfaces ensuring pure metal to metal contact. The relative motion between the sheets produces heat due to the friction and it causes severe plastic deformation in the welding zone. This phenomenon depends on the various weld conditions. The yield strength of most metal is sensitive toward the noticeable rise in the interface temperature. It reduces significantly with the growth in temperature resulting in the flow of materials. As there is a contact of horn with the top workpiece, the amount of plastic deformation and yielding is more than the bottom workpiece. These happenings also depend on the process parameters as well as specimen-related properties [2–4].

Acoustic softening is the second source of material softening during USMW. It was first identified by Blaha and Langenecker [5]. It was observed that at a sufficient level of ultrasonic energy, the yield stress of the material reduced. Kirchner et al. [6] also performed several experiments on aluminum alloys, and from the quasi-static compression test, a similar type of reduction in the yield stress value under the presence of ultrasonic energy over a broad range of frequencies was found. Izumi et al. [7] also revealed acoustic softening during the ultrasonic irradiation of copper, aluminum, steel, silver and lead in compression. Acoustic softening of a material depends on the acoustic impedance, melting point, Young's modulus and hardenability. Doumanidis and Gao [8] explored a finite element model to investigate the plastic deformation and stress fields during the ultrasonic welding and used the results to find the optimum process conditions. Their study concluded that the plastic deformation was a relevant feature in the bonding process. Zhang and Li [9] employed thermomechanical modeling to study the mechanics of ultrasonic consolidation. It was reported that severe plastic deformation in the bonding region caused a formation of joint during ultrasonic consolidation.

Plastic deformation and material softening are the two important parts of ultrasonic welding process since they bring metal to metal surface so close that bond formation happens. Both thermal softening and acoustic softening play a crucial role to achieve a high temperature which was the sole reason for plastic deformation. But very few kinds of literature are available related to this study. The objectives of the present study are to quantify acoustic softening in USMW process and compare it with the experimental results.

2 Experimental Procedure

The USMW equipment utilized in this study is a spot welder provided by Telsonic® Ultrasonics. It has a D2 steel sonotrode tip of 11 mm × 9 mm with serrations. This spot welder has the maximum power of 3 kW with a preset frequency of 20 kHz. Figure 1 depicts the schematic diagram ultrasonic welding setup with the positions of thermocouples. The quality of the weld is controlled by changing the three process

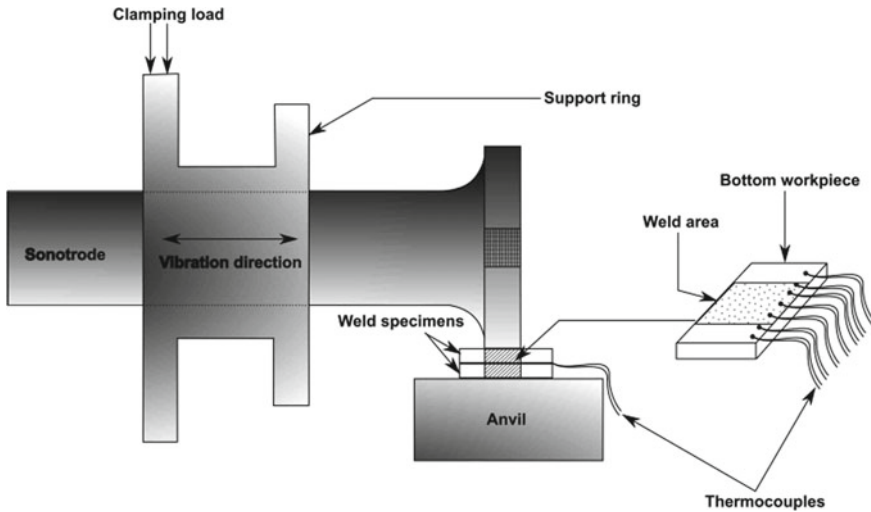


Fig. 1 Schematic diagram of ultrasonic welding setup with thermocouples

parameters. The vibration amplitude varies from 47 to 68 μm , clamping force ranging from 0.34 to 0.42 MPa and weld time changes from 0.5 to 0.9 s. However, the experiments in this study have been conducted at 68 μm of vibration amplitude, 0.9 s of weld time and 0.38 MPa of weld pressure. This setting is preferred on the basis of generation of maximum interface temperature, and it is also believed that the plastic deformation is maximum at the weld spot. The two dissimilar materials employed in this study are 0.7 mm AA1100 aluminum sheet and 0.4 mm UNS C10100 copper sheet. Between these sheets, aluminum has low yield strength than the copper sheet. Thus, it is expected that much plastic deformation will occur in the aluminum sheet, and the finite element modeling process is more simplified by considering it.

Another reason for choosing the AA1100 material as the top workpiece is that its yield strength has been already well established over a broad range of temperatures given by various authors [10, 11]. Optical stereo microscope made by Radical Instrument[®] with 25 \times magnification has been utilized to observe the weld area, and the grabbed image is processed by Image J[®] software. Meanwhile, the interface temperature has been measured by 0.15-mm sacrificial K-type thermocouples. It provides the root cause of plastic deformation and acoustic softening during the welding process.

3 Finite Element Model Development

Acoustic softening is the second reason for material softening in which the static stress of the material is significantly reduced under the influence of ultrasonic energy. It was first observed by Langenecker [12]. It is different from material to material and mainly depends on acoustic impedance, melting point, Young's modulus and hardenability of the material. Without the knowledge of acoustic softening effect, the accurate stress field and plastic deformation cannot be modeled.

3.1 Material Model

In the experiments, AA1100 aluminum alloy is used as one of the weld materials and it was placed on the top during the welding process. Hence, a material model is necessary to find the relationship between acoustic softening, thermal softening and strain hardening. Hockett [13] observed the strain hardening behavior of AA1100 material with respect to the thermal softening. He presented the stress–strain relationship at a particular temperature in the plastic region by using the power law equation. In the present analysis, the power law model given by Hockett is slightly modified by adding an acoustic softening parameter (β). The range of this newly added term varies from zero to one. If $\beta = 1$, then it is believed that the acoustic softening has no impact on the material deformation and the material is deformed normally. But when the $\beta = 0$, then it implies that the ultrasonic energy deforms the material sufficiently. The following shows the power law equation with an acoustic softening parameter.

$$\sigma_y = \beta \times K_s \times \varepsilon_p^n \quad (1)$$

It is assumed that the effect of parameter “ n ” on the yield strength of the material is negligible and K_s is the important term which mostly affects the yield strength (σ_y) of the material. Thus, the acoustic softening parameter linearly affects the K_s term.

3.2 Thermomechanical Finite Element Model

For numerical analysis, a 3D finite element model has been considered and analyzed by the explicit dynamics solver of ANSYS® 15.0. Figure 2 depicts the boundary conditions of the numerical model used for acoustic softening analysis. In this model, hexahedral type of meshing is selected for sonotrode and work materials along with tetrahedral meshing for an anvil are selected for the improvement in computational efficiency. The boundary conditions for surfaces of the top and bottom work materials

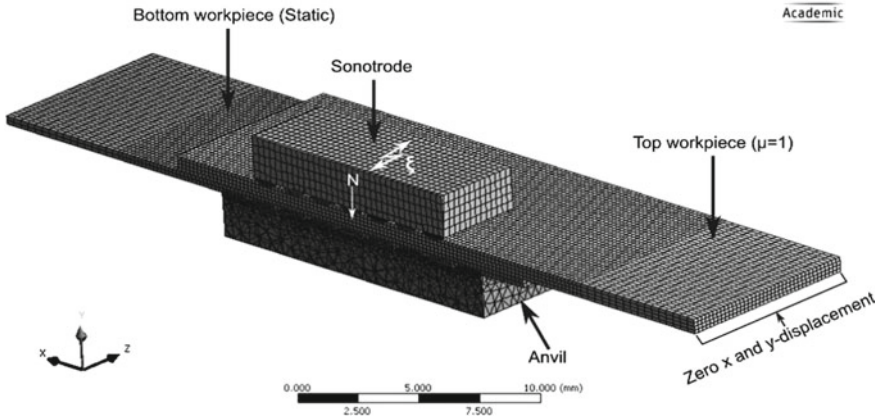


Fig. 2 Boundary conditions of the numerical model used for acoustic softening analysis

are defined by using penalty contact method. Meanwhile, the contact between sonotrode and the top part is determined by penalty friction method with a coefficient of friction of 1. It means the relative motion between the top sheet and sonotrode is restricted. Similar penalty friction method is applied to the bottom sheet and anvil. The coefficient of friction between the two sheets is applied according to the surface conditions. A zero X- and Y-displacement is assigned to one of the edges of the top sheet to constrain the displacement of sheet in that direction. To increase the computational efficiency, this thermomechanical model is executed only for 0.001 s. This time period is selected after simulating the model and observing the time period at which adequate plastic deformation has taken place.

Meantime, to quantify the acoustic softening in the sheets during USMW process, the β is decreased from one to zero until the error between modeling result (i.e., increase in sheet width) and experimental result is minimized. For clear understanding, a contour plot of modeled sheet deformation is demonstrated in Fig. 3.

4 Results and Discussion

4.1 Experimental Results

An optical image of each welded sample produced with different surface conditions has been selected to measure the average width increase near to the weld spot. Figure 4 displays a sample image used to calculate average width after welding. It was noticed that although original width (W_0) of the specimen was 20 mm, after welding, the width ($W_0 + \Delta W$) became 20.8 mm.

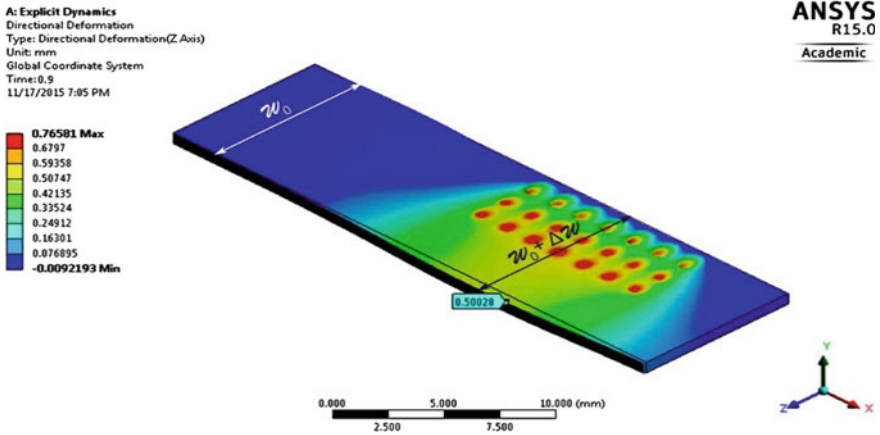
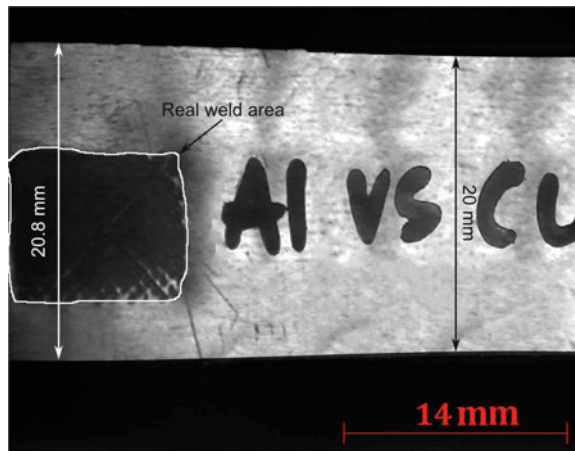


Fig. 3 Contour plot of sheet with initial sheet width and deformed sheet dimension

Fig. 4 Sample image used to calculate average width after welding in Image J



4.2 Model Validation Results

In this section, the effect of acoustic softening parameter using Eq. (1) is described by using thermomechanical model. Thus, to validate it, steady-state temperature (T) and $\Delta W/W_0$ are calculated for the 0.7Al–0.4Cu sheets. Meantime, for establishing the acoustic softening parameter, it is necessary to convert the vibration amplitude and weld pressure to a dimensionless form. Firstly, the dimensionless vibration amplitude (ψ) can be found out by dividing the amplitude (ξ) with initial foil thickness (t). Mathematically, it can be expressed as:

$$\psi = \frac{\xi}{t} = \frac{68 \times 10^{-3}}{0.7} = 0.9 \tag{2}$$

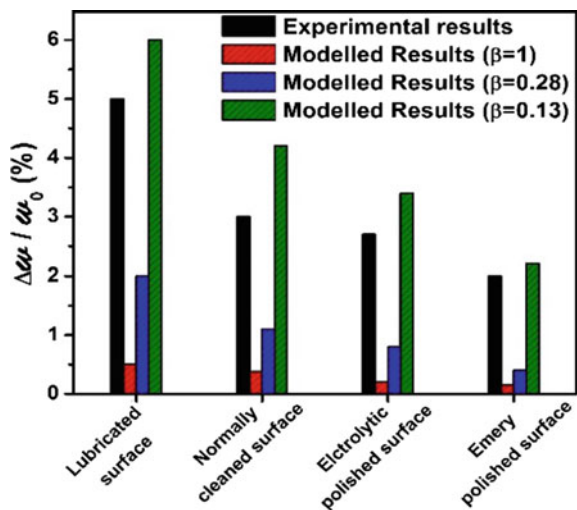
Likewise, the dimensionless weld pressure (P) can be written as the division between weld pressure (WP) and yield strength (σ_y) of the material ($\sigma_y = 34$ MPa at room temperature). Therefore, the mathematical expression is:

$$P = \frac{WP}{\sigma_y} = \frac{0.38}{34} = 0.01 \tag{3}$$

The coefficient of friction values those described previously are used in this section, and acoustic softening parameter (β) is solved by decreasing the β value incrementally. This will be carried out until the predicted $\Delta W/W_0$ and experimental $\Delta W/W_0$ are a good match. Thus, to enlighten the effect of acoustic softening, Fig. 5 represents the experimental as well as predicted $\Delta W/W_0$ with three β values for different surface conditions.

For all the surface conditions, ψ is 0.09 and P is 0.01. Thus, the model with $\beta = 1$ severely underpredicts the sheet width increase as compared to $\beta = 0.13$. As it is previously described that when $\beta = 1$, there is no acoustic softening happened. Meanwhile, if this value is decreased, the acoustic softening will play a vital role. It clearly perceives from the figure that majority of the material softening and reduction in yield strength happened due to acoustic softening effect. To test the model results of different surface conditions, it is important to compare the modeled decrease in the thickness of the top sheet and the experimentally measured sheet thickness. This checking has been done after fixing the β value for minimization of error between the modeled and experimental $\Delta W/W_0$ results. This comparison is displayed in Fig. 6 for 0.7Al–0.4Cu sheets. Table 1 compares the effects of thermal and acoustic softening on strength coefficient (K_s) which is provided in Eq. (1). It can be noticed that in the case of lubricating condition, there is a significant acoustic softening (53.73%) in AA1100 aluminum sheet at 375.37 °C as compared to room temperature (20 °C)

Fig. 5 Comparison of $\Delta W/W_0$ between modeled and experimental results β values



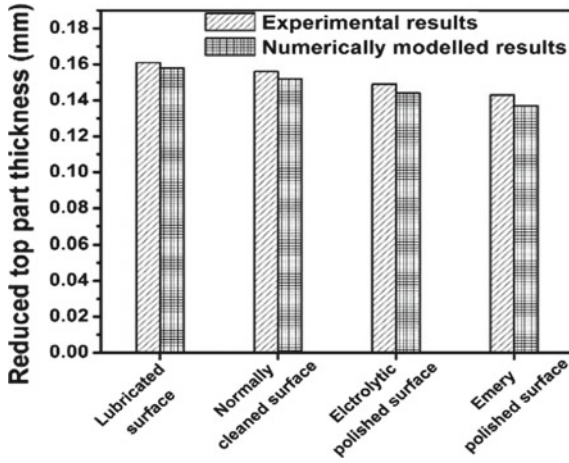


Fig. 6 Comparison results of reduced top part thickness values for various surface conditions

Table 1 Effect of acoustic softening parameter (β) on strength coefficient (K_s)

Temperature (T_s) ($^{\circ}$ C)	Acoustic softening parameter (β)	Strength coefficient (K_s) (MPa)	% K_s reduction from room condition
20	1	157.8	0
375.37	1	73	53.73
350.35	1	85.6	45.75
319.09	1	98.2	37.76
295.08	1	110.8	29.78
20	0.13	20.51	87
375.37	0.13	9.49	93.98
350.35	0.13	11.12	92.95
319.09	0.13	12.76	91.91
295.08	0.13	14.40	90.87

properties. Likewise, in the case of normally polished, electrolytic polished and emery polished surface conditions, acoustic softening effects of 45.75, 37.76 and 29.78% are observed. But when the $\beta = 0.13$, there is a considerable reduction in the yield strength of the material for different surface condition values, and these are 87, 93.98, 92.95, 91.91 and 90.87% while doing a comparison study with the normal temperature properties.

5 Conclusions

The acoustic softening analysis is applied for accurate prediction of stress field, plastic deformation and yield stress of the material. It shows that in the case of lubricating condition, there is a significant acoustic softening (53.73%) in AA1100 aluminum sheet at 375.37 °C as compared to room temperature (20 °C) properties. Likewise, in the case of normally polished, electrolytic polished and emery polished surface conditions, acoustic softening effects of 45.75, 37.76 and 29.78% are observed. But when the acoustic softening parameter ($\beta = 0.13$) is introduced, there is a considerable reduction in the yield strength of the material for different surface condition values, and these are 87, 93.98, 92.95, 91.91 and 90.87% while doing a comparison study with the standard temperature properties. Thus, it clearly signifies that majority of the material softening and reduction in yield strength happened due to acoustic softening effect.

References

1. Society AW (1950) *Welding handbook*. American Welding Society
2. Bloss MC (2008) *Ultrasonic metal welding: the weldability of stainless steel, titanium, and nickel-based superalloys*
3. De Vries E (2004) *Mechanics and mechanisms of ultrasonic metal welding*
4. Derks P (1984) *The design of ultrasonic resonators with wide output cross-sections*. Thesis, Technische Hogeschool Eindhoven, Eindhoven, 154 p
5. Blaha F, Langenecker B (1955) Tensile deformation of zinc crystal under ultrasonic vibration. *Naturwissenschaften* 42:1–10
6. Kirchner HOK, Kromp WK, Prinz FB, Trimmel P (1985) Plastic deformation under simultaneous cyclic and unidirectional loading at low and ultrasonic frequencies. *Mater Sci Eng* 68:197–206
7. Izumi O, Oyama K, Suzuki Y (1966) Effects of superimposed ultrasonic vibration on compressive deformation of metals. *Trans Japan Inst Met* 7:162–167
8. Dومانidis C, Gao Y (2004) Mechanical modeling of ultrasonic welding. *Weld J* 83:140–146
9. Zhang C, Li L (2008) A friction-based finite element analysis of ultrasonic consolidation. *Weld J* 87:187
10. Pao YH, Gilat A (1989) Modeling 1100-0 aluminum over a wide range of temperatures and strain rates. *Int J Plast* 5:183–196
11. Puchi ES, Staia MH, Villalobos C (1997) On the mechanical behavior of commercial-purity aluminum deformed under axisymmetric compression conditions. *Int J Plast* 13:723–742
12. Langenecker B (1966) Effects of ultrasound on deformation characteristics of metals. *IEEE Trans Sonics Ultrason* 13:1–8
13. Hockett JE (1966) On relating the flow stress of aluminum to strain, strain rate, and temperature

Agility Evaluation in the Rolling Industry: A Case Study



Rahul Sindhvani, Punj Lata Singh, Raj Chopra, Karan Sharma, Apratim Basu, Devendra Kumar Prajapati and Vasdev Malhotra

Abstract In the contemporary marketplace, the rate of competition is high both at local and global levels. Rolling industries are used for manufacturing materials which are used further for developing various finished products. The products developed are in accordance with a volatile market keeping in mind the cost and productivity. Thus, the manufacturing system, i.e., integrated lean-agile manufacturing system (LAMS) can be adopted. However, the implementation of the integrated form of manufacturing can be difficult to accomplish. Some attributes and sub-attributes are there which besides having an impact on the implementation process. This paper's main objective is the identification and analysis of the attributes. These attributes have been determined with the help of literature review, and then the rating is implemented using the questionnaire survey and fuzzy agility evaluation (FAE) approach has been utilized for the analysis of the agility level of the rolling industry.

R. Sindhvani (✉) · R. Chopra · K. Sharma · A. Basu · D. K. Prajapati
Department of Mechanical Engineering, Amity School of Engineering and Technology, Amity University Uttar Pradesh, Noida 201301, Uttar Pradesh, India
e-mail: rsindhvani@amity.edu

R. Chopra
e-mail: rajchopra19.rc@gmail.com

K. Sharma
e-mail: sharma.karan26@yahoo.com

A. Basu
e-mail: apratim58@gmail.com

D. K. Prajapati
e-mail: prjptdk@rediffmail.com

P. L. Singh
Civil Engineering Department, Amity School of Engineering and Technology,
Amity University Uttar Pradesh, Noida 201313, Uttar Pradesh, India
e-mail: plsingh@amity.edu

V. Malhotra
Department of Mechanical Engineering, YMCA University of Science & Technology,
Faridabad, Haryana, India
e-mail: vaslymca@yahoo.co.in

Keywords Rolling industry · Fuzzy agility evaluation · Lean manufacturing · Agile manufacturing · Productivity first section

1 Introduction

There have been continuous efforts to enhance and amend the manufacturing processes since last few decades. Some of the strategies that have been formulated in order to achieve the above include total quality management (TQM); just in time (JIT); computerized planning systems incorporating: materials requirement planning, manufacturing resource planning, and enterprise resource planning [1]. There were certain shortcomings with these techniques as they could not cope well with the instabilities within the marketplace. Newer strategies like lean and agile manufacturing systems were introduced during the late 1990s and the early twenty-first century.

Lean manufacturing is a strategy wherein the term “lean” focuses on using less of the resources required as inputs in order to gain a higher degree of production quality as well as minimized waste elimination. This strategy helps in the production of vivid components in addition to providing services in variable volumes. In the contemporary world, the customers not only require the variety with the high quality of finish for lower prices, they also need newer variations in accordance with diverse tastes [2]. Many manufacturing firms nowadays are implementing the lean strategy in order to achieve an extra competitive edge over other manufacturing firms.

There is a presence of a scenario globally where some of the manufacturing firms are finding ways to react to the demands of the customers which are dynamic in nature and competitive in the competitive marketplace. On the other hand, there are certain manufacturing firms that are just able to sustain or are gradually fading from the marketplace competition. Hence, it is required for the manufacturing firms to adhere to some newer flexible strategies.

Agile manufacturing particularly deals with coexistent superiority over a distinct set of driving parameters, which include being able to market prior to others amidst provision of solutions which are able to outshine the customer belief alongside putting competitors’ strategies under distress, delivered at the cost of mass production [3]. It helps manufacturing firms to have a strong position in an environment where the changes occur continuously and in an unanticipated manner [4]. In other words, it provides strategies which help in responding to the dynamism and turbulence which is present in the marketplace [5].

A comprehensive approach has been applied to combine the factors of both lean and agile manufacturing systems through modeling. The common factors or attributes have further been divided into sub-attributes. These attributes are identified using literature, questionnaire-based survey, and through interaction with experts from the industrial field as well as the academia. A questionnaire-based survey has been carried out in order to record the opinions of the top management pertaining to the attributes. The survey has been utilized to weigh the attributes as well. Further, the

analysis has been carried out using the fuzzy agility evaluation (FAE) technique. The FAE technique proves to be among the best techniques for finding the relationship established between various attributes. This differentiation and the analysis will help the researchers and also the managers to understand and overcome the issues accordingly.

Desired objectives of the paper are as follows:

- To evaluate fuzzy agility index using FAE approach
- To analyze interrelation within attributes using FAE technique.

Section 2 deals with the determination of the attributes using literature, questionnaire survey, and interactions with professionals. An overview of the FAE technique is provided in Sect. 3. Then, Sect. 4 deals with the application of FAE technique in the modeling of different attributes and sub-attributes. Finally, conclusion, limitations, and future scope of research have been discussed in Sect. 5.

2 Literature Review

In this section, the literature on lean manufacturing, agile manufacturing, and integrated lean and agile manufacturing has been discussed. This section also highlights the factors for implementation of a lean-agile manufacturing system in rolling industry.

2.1 *Lean Manufacturing*

Lean manufacturing was initially identified with the Toyota Production System and was established by Taiichi Ohno after World War 2 [6, 7]. It is devised to eradicate activities and operations that produce waste and create non-value in production. The success of LM in the automotive industry and Japanese industry has led to its implementation in non-Japanese industries and non-automotive industries. Its success has led it to be implementation extended from manufacturing industries to supply chain managements [8].

LM can be adapted successfully to a strategic and orderly procedure [9]. Consequently, the execution and determination of the suitable LM methods must be established on knowledge and experience [10]. At present, there are a lot of lean manufacturing methods available and being undertaken by many organizations and firms [11]. The organizations and firms ought to prioritize and determine what method to begin initially [12]. Generally, large organizations have little or no obstacles and constraints when LM methods are implemented and may implement all of the lean manufacturing methods probably in contrast to small organizations and firms [1]. Therefore, small organizations and firms are advised to begin with the achievable lean methods such as 5S, multifunction, continuous improvement and reduction in

setup time [12, 13]. These methods are considered basic, low risk, minimum investment and are possible to be overseen internally.

Organizations and firms can utilize the methods of lean manufacturing to methodically increase their efficiency and productivity into order to meet challenges like high cost and competition in the market [14]. Primary tools of lean manufacturing are directed on steadying specific individual procedures and consequently establishing the foundations for making products [15]. Lean manufacturing is able to decrease the level of inventory between different production shops; the outcome of this technique is a short lead time of products and accordingly increases the chance to respond to fluctuations [16].

Value stream mapping (VSM) is one of the most powerful tools employed in lean manufacturing to identify and remove waste occurring in production. It is a graphical representation method which maps the value addition cycle of the product. The processes are divided into two groups: value adding (VA) and non-value adding (NVA). VSM permits to identify the location in the production chain where excess inventory is accumulating and the inactive time a product is consuming. It helps in following the decision-making for subsequent process improvement in the organization. VSM is also capable to be utilized in future state visualization [17].

Andrade et al. used VSM in an automotive company to increase the utilization of unexploited production shops, distribute the workload evenly to every operator, and reduce the total production time [18]. Lacerda et al. used VSM and associated lean tools in an OEM producer for an automotive company in reducing waste in production, improve the financial performance of the firm, and change the social structure of the firm by engaging workers in solution making so that new ways of working can be implemented [19]. Chauhan et al. implemented VSM in a conveyor pulley manufacturer to reduce idle time between process operations, decrease the material travel distance, and reduce the labor cost and hence the total production cost [20].

Other tools such as generic algorithm (GA) which is used to improve scheduling along with VSM were used Saleeshya et al. to reduce product lead time and increased productivity by further improving resource utilization and effectiveness of resource used in processes [21]. Lean information management system was used by Bevilacqua et al. to improve the customer service and reducing the chances of not meeting the delivery time by exploiting the full potential of information systems and associated software to eliminate the main waste, lack of information flow inside the company [22].

2.2 Agile Manufacturing

Agile manufacturing was initially formulated in 1991 as a new philosophy of manufacturing which consisted of integrated management that can rapidly adapt to changing market conditions. It was formulated in a forum organized by the US Department of Defense which consisted of senior leaders from important US organization for

improving competitiveness [23]. Numerous point of views about agile manufacturing were also devised in this forum such as highly customized products for every order, long-term relationship with customers, multidisciplinary teams for simultaneous development, knowledge of new technologies, modular production, inter- and intra-company information flow and strategic partnerships with customer satisfaction [24].

Vázquez-Bustelo and Avella suggest that flexibility, speed, quality, service, and efficiency be the key factors in providing agility in manufacturing operation by integration with highly qualified human resources and organization who can adapt accordingly with modern technology and methods [25].

The difference between agile manufacturing and other philosophy of manufacturing can be seen as the capability to reorganize and adapt to volatile market conditions. These volatile conditions are very dynamic and constitute fast and perpetual variations in the structure: surrounding workspace atmosphere, choices or property of those engaged in markets [5]. The agile manufacturing has evolved into a fundamental situation to endure inside such a workspace described as volatile by Goldman et al. and is indeed acknowledged as absolutely important and applicable route to initiate in a market requiring an immediate solution to quickly occurring changes [26, 27].

The strategy of inclusion of additional value for customer satisfaction in highly customized products with a significant increase in quality is the main principle behind agile manufacturing. These demands for flexible processes, expedited feedback from the suppliers, the shortened time span of such processes, work collaboration inside supply chain, utilization of modern technology, and highly proficient human resources. Agile considers it as necessary principles for internal as well as external collaboration alongside the sphere of development and unpredictability [3, 5].

The company has to specify its approach to competition to find the position it desires. Porter classified the competitive strategy adopted by businesses as cost, management, diversification, and focus [28]. After the completion of the competitive approach and the methodology of operations, the assessment of operational performance is conducted. Potdar and Routroy defined the critical domain of AM for performance assessment such as

- Manufacturing performance which refers to the time taken to respond to new orders, production lead time, product variation, and degree of customization.
- Financial performance for monitoring the financial sustainability of the organization, profit margin, and profit prediction.
- Marketing performance which is tasked to enhance organization profile in the market, boost share in the market, and reach out to new customers.
- Development performance refers to design, development, and testing of the product along the management of process and procedure undertaken in development.
- Customer satisfaction performance concerns to the customer approval of the product, its design, its performance, and the customer retention.

- Bottom line performance is concerned regarding manufacturing operations. It assesses the operational efficiency, performance, and sustainability.
- The top-level performance consists of decision-making at the strategic level consisting of overall performance, knowledge, culture, and competitive advantage.
- Supply chain performance includes upstream and downstream segments of the supply chain and the synchronization between them [29].

For the evaluation of agile operation performance, a technical survey is carried out with the assistance of an appropriate questionnaire from which quantitative analysis can be conducted. Gunasekaran conducted the research in an aerospace company. Their work was related to evaluating the agility in the production of pumping systems and control systems used in the aerospace industry [30]. Routroy et al. employed a questionnaire survey for the collection of data expectation about agile manufacturing enablers in past, present, and future scenarios [31]. Bargshady et al. utilized this method to investigate the relationship between integrated information systems and agile supply chain in the power generation industry [32].

Fuzzy logic and multi-grade fuzzy approaches have been applied to the operational performance of agile manufacturing of businesses.

Vinodh and Aravindraj used fuzzy logic and multi-grade fuzzy approaches for assessing the agility of the manufacturing strategy of an Indian pump manufacturer and found the industrial implication of the strategy. The limitation of the study was the requirement of more studies to be conducted because of the comparison of the results of two agility assessments done using two different methods [33].

Sindhwani and Malhotra used fuzzy agility evaluation for assessing the effect of attributes during the transition to an agile manufacturing system and the manufacturing implication in the strategy of the company [34].

Singh et al. utilized a fuzzy agility index for the evaluation of agile enablers in the agile supply chain. By applying fuzzy mathematical logic, it has been found that the supply chain was very agile but not very agile. It was found out that it was due to the presence of unknown barriers which had an impact on agility levels [35].

2.3 Identification of Attributes for Implementation in LAMS

Implementing LAMS into a traditional manufacturing system is difficult in comparison with the implementation of either lean manufacturing or agile manufacturing separately. During the process of implementation, the balance between lean attributes and agile attributes need to be kept in mind. The purpose of the paper is to identify those factors which ensure that the company is able to make its manufacturing operations efficient with low inventory levels while remaining flexible enough to respond to customer requirements and fluctuation. The attributes influencing the implantation of LAMS have been explained in Table 1.

Table 1 Attributes for implementation in LAMS

Sr. no.	Attributes	Reference	Description
1.	Voice of customer	[9, 36, 37, 57, 63]	The products should be made according to customer-specific requirements. The involvement of customer in quality and design programs along with the use of JIT (Just in Time) guarantees customer satisfaction
2.	Design	[30, 38, 39]	The product design needs to be concurrent and has customer involvement and also requires the heavy involvement of suppliers in the product design and development process
3.	After sales service	[37, 40]	The producer should provide maximum customer service for the product before, during functionality of the product
4.	Quality conformance	[1, 5, 9, 41]	The product design and manufacturing should be following the accepted quality standards and methods to make the product free from manufacturing defects and variation in operational parameters
5.	Leadership	[40, 42–44, 58]	The company’s top management should provide leadership during the implementation of LAMS
6.	Decision-making	[5, 43, 45]	The company needs to include “enterprise-wide” decision-making tools which help in digesting information quickly
7.	Providing resource	[37, 45, 46]	Resources should be distributed at production sites in accordance with the order processed by the sites

(continued)

Table 1 (continued)

Sr. no.	Attributes	Reference	Description
8.	Technical and business knowledge	[1, 3, 48]	The managers need to have a sound knowledge of process and procedure of the production to make better decisions about where modifications are required. Managers are required to have sufficient knowledge in this regard to lead the project
9.	Workplace awareness	[1, 40, 49, 50]	The management must have knowledge of all workers in the company to provide proper guidance and conflict resolving between workers
10.	Adaptable work force	[37, 49, 51, 52, 59]	The workforce is required to be adaptable to learn and integrate and new skill and methods which are required in the new system. The workers must be able to do a variety of tasks assigned to them
11.	Communication skills	[37, 52, 53, 60]	The workers must have good communication skills so that information can flow smoothly between different workstation to avoid confusion and save time in the production line
12.	Creativity	[39, 44, 51]	The workforce of the company needs to be innovative to make frequent changes in production processes and services to address dynamic market conditions
13.	Standardization	[37, 39, 47, 61]	Standardizing operation contributes to reducing costs and improving the efficiency of product design and manufacturing. Standardizing reduces part and product cost since the cost of the product is decided during the planning and development stages

(continued)

Table 1 (continued)

Sr. no.	Attributes	Reference	Description
14.	Changes in machine set-up	[3, 39, 54, 62]	Changes in machine setup after every product order helps the producer to prepare for next order. Flexible tooling permits tool change by a tool-feeder to machine different variation of parts to conform to specific requirements
15.	Specialization in technology	[3, 36, 63]	Non-dedicated specialized equipment offers the most flexibility in its ability to switch to different types of part production without loss of efficiency

3 Methodology of FAE

FAE approach was implemented to analyze the agility level of rolling industry (Fig. 1).

3.1 Step 1

The semantic scale is determined to estimate the important weights and performance ratings of agility potential. Fuzzy logic is used to criticize the linguistic terms and corresponding membership functions. A large variety of semantic terms and their relatable membership functions were formulated for semantic assessment [55, 56]. Generally, semantic levels should be limited to 9 levels, which are basically used to depict absolute human discrimination. Following linguistic notations are implemented to represent the ratings and weight of different attributes and sub-attributes (Table 2).

3.2 Step 2

In this step, questionnaire and linguistic terms are used to estimate the significance and performance of the attributes. The linguistic terms must be relatable to the policy, strategy customs, and business execution practices of the enterprise. Linguistic terms mentioned above are used to specify the degree of agility potential, and the experts and specialist can easily use these linguistic terms to compute the performance ratings.

3.3 Step 3

Further, we convert the linguistic variables into numerical values. This is done according to a scale and the scale should be selected cautiously because the outcome depends on this scale. Fuzzy triangular values of these variables are represented in Tables 3 and 4. Triangular values for FAE are represented in Table 5.



Fig. 1 Research methodology

Table 2 Linguistic variables notations for performance rating and weight

S. no	Linguistic variable performance rating	Notation used	Linguistic variable for weightage	Notation used
1	Excellent	E	Very high	VH
2	Very good	VG	High	H
3	Good	G	Fairly high	FH
4	Fare	F	Medium	M
5	Poor	P	Fairly low	FL
6	Very poor	VP	Low	L
7	Worst	W	Very low	VL

Table 3 Fuzzy triangular values of linguistic variables for a performance rating

Performance rating (R)			
Linguistic variables	Fuzzy triangular values		
Worst (W)	0	0.5	1.5
Very poor (VP)	1	2	3
Poor (P)	2	3.5	5
Fair (F)	3	5	7
Good (G)	5	6.5	8
Very good (VG)	7	8	9
Excellent (E)	8.5	9.5	10

Table 4 Fuzzy triangular values of linguistic variables for importance weighting

Importance weighting (W)			
Linguistic variables	Fuzzy triangular values		
Very low (VL)	0	0.5	0.15
Low (L)	0.1	0.2	0.3
Fairly low (FL)	0.2	0.35	0.5
Medium (M)	0.3	0.5	0.7
Fairly high (FH)	0.5	0.65	0.8
High (H)	0.7	0.8	0.9
Very high (VH)	0.85	0.95	1.00

Table 5 Fuzzy triangular values of linguistic variables for FAE

Fuzzy agility index (FAE)			
Linguistic variables	Fuzzy triangular values		
Slowly (S)	0	1.5	3
Fairly (F)	1.5	3	4.5
Agile (A)	3.5	5	6.5
Very agile (VA)	5.5	7	8.5
Extremely agile (EA)	7	8.5	10

3.4 Step 4

FAE shows complete agility level of industry. As FAE increases, this level also increases. In order to determine the agility level, we use the member functions of FAE. Weighted average definition of the fuzzy matrix can be used in order to find out agility capability AC_{ij} which can be further calculated as:

$$R_{ij} = \frac{\sum_{k=1}^n (W_{ijk} * R_{ijk})}{\sum_{k=1}^n W_{ijk}}$$

Here W_{ijk} and R_{ijk} represent the fuzzy importance weight and rating of performance, respectively.

Agility index is calculated with the help of following formula, where R_i and W_i denote the rating and weightage, respectively.

$$AGILITY_{INDEX} = \sum_{i=1}^n (W_i * R_i)$$

3.5 Step 5

After the estimation of FAE, the level of agility is determined, and then FAE is compared with linguistic functions having similar membership functions which can be related to the natural set of FAE agility. Then successive approximation is implemented as follows.

4 Demonstration of Attributes Using FAE Technique

The different steps, to accomplish model, have been discussed as follows:

Step 1: Attributes which affect the system.

The attributes of the LAMS system have been deduced after a thorough study of literature and advice from experts, and they have been illustrated in Table 2.

Step 2: Establish suitable linguistic scales to estimate importance weight and performance ratings of the selected attributes.

Step 3: Evaluation of importance weight and a performance rating of the agility potential are done with the help of linguistic variables. In this stage, evaluation based on the questionnaire is carried by the professionals of distinct departments. Essentially, specialists will survey the rating and weightage of various distinctive traits and their sub-attributes.

Table 6 Linguistic variables for performance rating, importance weighting, and FAE

Performance rating (R)	Importance weighting (W)	Fuzzy agility index (FAE)
Worst (W)	Very low (VL)	Slowly (S)
Very poor (VP)	Low (L)	Fairly (F)
Poor (P)	Fairly low (FL)	Agile (A)
Fair (F)	Medium (M)	Very agile (VA)
Good (G)	Fairly high (FH)	Extremely agile (EA)
Very good (VG)	High (H)	
Excellent (E)	Very high (VH)	

Step 4: Fuzzy numbers are used for the estimation of linguistic terms. In this progression, the transformation of semantic variables into numerical values is done in order to compute calculations as illustrated in Tables 3 and 6.

Step 5: Fuzzy weights and fuzzy ratings are aggregated in order to obtain the overall agility level of the industry. FAE is the representation of enterprise agility. As FAE increases, the agility level also increases. Further, agility level is identified using FAE membership functions. Using triangular technique, the agility index AC_{ij} can be measured as:

$$R_{ij} = \frac{\sum_{k=1}^n (W_{ij} * R_{ij})}{\sum_{k=1}^n W_{ij}}$$

In the above equation, R_{ij} and W_{ij} represent the performance rating and importance weight of the attributes (Table 7).

$$R_1 = \frac{\{(8.5 - 9.5 - 10) * (0.85 - 0.95 - 1)\} + \{(8.5 - 9.5 - 10) * (0.7 - 0.8 - 0.9)\} + \{(7 - 8 - 9) * (0.5 - 0.65 - 0.8)\} + \{(8.5 - 9.5 - 10) * (0.7 - 0.8 - 0.9)\}}{[(0.85 - 0.95 - 1.0) + (0.7 - 0.8 - 0.9) + (0.5 - 0.65 - 0.8) + (0.7 - 0.8 - 0.9)]}$$

$$R_1 = \frac{[(7.225 - 9.025 - 10) + (5.95 - 7.6 - 9) + (3.5 - 5.2 - 7.2) + (5.95 - 7.6 - 9)]}{[(2.75 - 3.2 - 3.6)]}$$

$$R_1 = (22.625 - 29.425 - 35.2) / (2.75 - 3.2 - 3.6)$$

$$R_1 = [8.22 - 9.19 - 9.77]$$

$$R_2 = \frac{[(5.95 - 7.6 - 9) + (5.95 - 7.6 - 9) + (2.5 - 4.22 - 6.4) + (7.22 - 9.02 - 10) + (4.9 - 6.4 - 8.1)]}{[(3.6 - 3.15 - 4.6)]}$$

$$R_2 = [(26.52 - 34.85 - 42.5) / (3.6 - 3.15 - 4.6)]$$

Table 7 Measurement of performance rating (R) and importance weighting (W) in terms of linguistic variables

AC_i	AC_{ij}	R_{ij}	W_{ij}	W_i
AC ₁	AC ₁₁	(8.5–9.5–10)	(0.85–0.95–1)	(0.85–0.95–1)
	AC ₁₂	(8.5–9.5–10)	(0.7–0.8–0.9)	
	AC ₁₃	(7–8–9)	(0.5–0.65–0.8)	
	AC ₁₄	(8.5–9.5–10)	(0.7–0.8–0.9)	
AC ₂	AC ₂₁	(7–8–9)	(0.85–0.95–1)	(0.5–0.65–0.8)
	AC ₂₂	(8.5–9.5–10)	(0.7–0.8–0.9)	
	AC ₂₃	(5–6.5–8)	(0.5–0.65–0.8)	
	AC ₂₄	(8.5–9.5–10)	(0.85–0.95–1)	
	AC ₂₅	(7–8–9)	(0.7–0.8–0.9)	
AC ₃	AC ₃₁	(5–6.5–8)	(0.3–0.5–0.7)	(0.7–0.8–0.9)
	AC ₃₂	(7–8–9)	(0.3–0.5–0.7)	
	AC ₃₃	(8.5–9.5–10)	(0.7–0.8–0.9)	
	AC ₃₄	(7–8–9)	(0.5–0.65–0.8)	
AC ₄	AC ₄₁	(5–6.5–8)	(0.7–0.8–0.9)	(0.7–0.8–0.9)
	AC ₄₂	(3–5–7)	(0.3–0.5–0.7)	
	AC ₄₃	(5–6.5–8)	(0.5–0.65–0.8)	

$$R_2 = [7.36–8.39–9.23]$$

$$R_3 = [(1.5–3.25 – 5.6) + (2.1–4 – 6.3) + (5.95–7.6–9) + (3.5–5.2–7.2)] / [(1.8–2.45–3.1)]$$

$$R_3 = [(13.05–20.05–28.1) / (1.8–2.45–3.1)]$$

$$R_3 = [7.25–8.18–9.06]$$

$$R_4 = [(3.5–5.2–7.2) + (0.9–2.5–4.96) + (2.5–4.22–6.4)] / [(1.5–1.95–2.4)]$$

$$R_4 = [(6.9–11.92–18.5) / (1.5–1.95–2.4)]$$

$$R_4 = [4.6–6.11–7.70]$$

If W_i and R_i signify the weight and performance rating of each agility. Potential then agility index can be calculated as:

Fig. 2 Linguistic level to match fuzzy agility index

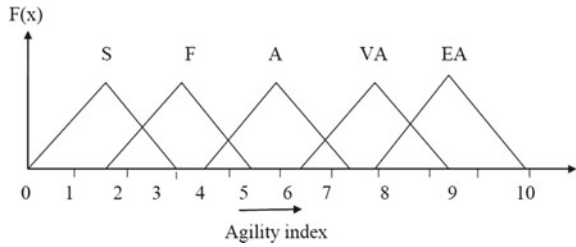
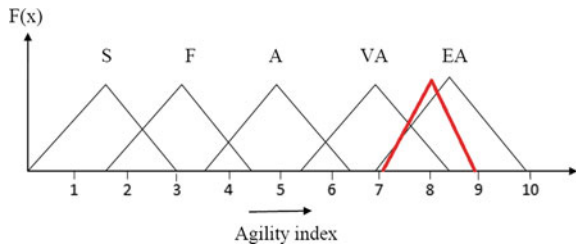


Fig. 3 Agility evaluation of the industry



$$AGILITY_{INDEX} = \sum_{k=1}^n (W_i * R_i) / W_i$$

$$AGILITY_{INDEX} = \{ \{ (8.22 - 9.19 - 9.77) * (0.85 - 0.95 - 1) \} + \{ (7.36 - 8.39 - 9.23) * (0.5 - 0.65 - 0.8) \} + \{ (7.25 - 8.18 - 9.06) * (0.7 - 0.8 - 0.9) \} + \{ (4.6 - 6.11 - 7.70) * (0.7 - 0.8 - 0.9) \} \} / \{ (0.85 - 0.95 - 1) + (0.5 - 0.65 - 0.8) + (0.7 - 0.8 - 0.9) + (0.7 - 0.8 - 0.9) \}$$

$$AGILITY_{INDEX} = \{ (18.95 - 25.6 - 32.23) \} / \{ (2.7 - 3.2 - 3.6) \}$$

$$AGILITY_{INDEX} = \{ (7.01 - 8 - 8.9) \}$$

Step 6: Comparing FAE with suitable levels.

After identifying agility level using FAE, FAE is compared with different linguistic levels as depicted in Fig. 2. Agility index of the enterprise is determined as “extremely agile” (Fig. 3).

5 Discussions and Conclusion

The identification of essential attributes which affect the functioning of the manufacturing firm through integrated lean-agile manufacturing system has been accomplished. The identification of these attributes is important as they have a strong effect

on the better functioning and operation of the firm. The value of the agility index has been determined by the use of FAE approach. This paper presents the FAE approach with the help of which a desirable strategy has been developed for implementing the LAMS keeping in focus each attribute's effect. The agility index value is of great importance for the managers of the manufacturing firm in order to carry out appropriate improvements. In the paper, the agility index value of the firm has been determined through the FAE approach. There is a possibility of change in the rankings or reversing the order of alternatives upon introduction of a new alternative. A large number of attributes have been considered which may lead to poor or inconsistent outcomes. There is a lack of accuracy in decision-making due to differences in judgments of decision makers. There is a future scope for improvements to make the implementation unchallenging. The following proposition has been made for the above-mentioned purpose: Comparing the various manufacturing paradigms for more efficient functioning and analyzing the different approaches may lead to developing more flexible processes and strategies.

References

1. Shah R, Ward PT (2003) Lean manufacturing: context, practice bundles, and performance. *J Oper Manag* 21(2):129–149
2. Carvalho H, Duarte S, Cruz Machado V (2011) Lean, agile, resilient and green: divergencies and synergies. *Int J Lean Six Sigma* 2(2):151–179
3. Gunasekaran A (1999) Agile manufacturing: a framework for research and development. *Int J Prod Econ* 62(1–2):87–105
4. Sarkis J (2001) Benchmarking for agility. *Benchmarking Int J* 8(2):88–107
5. Vazquez-Bustelo D, Avella L, Fernández E (2007) Agility drivers, enablers and outcomes: an empirical test of an integrated agile manufacturing model. *Int J Oper Prod Manag* 27(12):1303–1332
6. Womack JP, Jones DT, Roos D (1990) *Machine that changed the world*. Simon and Schuster, New York
7. Womack JP, Jones DT (2003) *Lean thinking: banish waste and create wealth in your corporation*, 2nd edn. Free Press, New York
8. Lamming R (1996) Squaring lean supply with supply chain management. *Int J Oper Prod Manag* 16(2):183–196
9. Nordin N, Deros BM, Wahab DA (2010) A survey on lean manufacturing implementation in Malaysian automotive industry. *Int J Innov Manag Technol* 1(4):374
10. Rose ANM, Deros BM, Rahman MNA (2013) Lean manufacturing practices implementation in Malaysian's SME automotive component industry. *Appl Mech Mater* 315:686–690
11. Pavaskar SJ, Gershenson JK, Jambekar AB (2003) Classification scheme for lean manufacturing tools. *Int J Prod Res* 41(13):3075–3090
12. Rose AMN, Deros BM, Rahman MA, Nordin N (2011) Lean manufacturing best practices in SMEs. In: *Proceedings of the 2011 international conference on industrial engineering and operations management*, vol 2, no 5, Jan 2011, pp 872–877
13. Kumar M, Antony J (2008) Comparing the quality management practices in UK SMEs. *Ind Manage Data Syst* 108(9):1153–1166
14. Helleno AL, de Moraes AJI, Simon AT (2017) Integrating sustainability indicators and lean manufacturing to assess manufacturing processes: application case studies in Brazilian industry. *J Clean Prod* 153:405–416

15. Alvarez K, Aldas D, Reyes J (2017) Towards lean manufacturing from theory of constraints: a case study in footwear industry. In: 2017 International conference on industrial engineering, management science and application (ICIMSA). IEEE, Seoul, pp 1–8
16. Metternich J, Bechtloff S, Seifermann S (2014) Efficiency and economic evaluation of cellular manufacturing to enable lean machining. In: Cunha PF (ed) Forty sixth CIRP conference on manufacturing systems 2013, vol 7. Curran, New York, pp 592–597
17. Rohac T, Januska M (2015) Value stream mapping demonstration on real case study. In: Katalinic B (ed) 25th DAAAM international symposium on intelligent manufacturing and automation 2014, vol 100. Curran, New York, pp 520–529
18. Andrade PF, Pereira VG, Del Conte EG (2016) Value stream mapping and lean simulation: a case study in automotive company. *Int J Adv Manuf Technol* 85(1–4):547–555
19. Lacerda AP, Xambre AR, Alvelos HM (2016) Applying value stream mapping to eliminate waste: a case study of an original equipment manufacturer for the automotive industry. *Int J Prod Res* 54(6):1708–1720
20. Chauhan P, Rangrej S, Samvatsar K, Sheth S (2015) Application of lean manufacturing principles for process time reduction—a case of conveyor pulley manufacturing. In: Proceedings of 5th national conference on recent advances in manufacturing (RAM-2015), pp 423–428
21. Saleeshya PG, Sneha A, Karthikeyan C, Sreenu C, Rohith AK (2015) Lean practices in machinery manufacturing industries—a case study. *Int J Logist Syst Manag* 20(4):536–554
22. Bevilacqua M, Ciarapica FE, Paciaroni C (2015) Implementing lean information management: the case study of an automotive company. *Prod Plan Control* 26(10):753–768
23. Nagel RN, Dove R (1991) 21st-century manufacturing enterprise strategy: an industry-led view, 1st edn. Diane Publishing, Pennsylvania
24. Leite M, Braz V (2016) Agile manufacturing practices for new product development: industrial case studies. *J Manuf Technol Manage* 27(4):560–576
25. Vázquez-Bustelo D, Avella L (2006) Agile manufacturing: industrial case studies in Spain. *Technovation* 26(10):1147–1161
26. Goldman SL, Nagel RN, Preiss K (1995) Agile competition and virtual organisations. Van Nostrand Reinhold, New York, NY
27. Bottani E (2010) Profile and enablers of agile companies: an empirical investigation. *Int J Prod Econ* 125(2):251–261
28. Porter ME (2008) *Competitive strategy: techniques for analyzing industries and competitors*. Simon and Schuster, New York, NY
29. Potdar PK, Routroy S (2017) Performance analysis of agile manufacturing: a case study on an Indian auto component manufacturer. *Meas Bus Excellence* 21(2):117–135
30. Gunasekaran A, Tirtiroglu E, Wolstencroft V (2002) An investigation into the application of agile manufacturing in an aerospace company. *Technovation* 22(7):405–415
31. Routroy S, Potdar PK, Shankar A (2015) Measurement of manufacturing agility: a case study. *Meas Bus Excellence* 19(2):1–22
32. Bargshady G, Zahraee SM, Ahmadi M, Parto A (2016) The effect of information technology on the agility of the supply chain in the Iranian power plant industry. *J Manuf Technol Manage* 27(3):427–442
33. Vinodh S, Aravindraj S (2015) Benchmarking agility assessment approaches: a case study. *Benchmarking Int J* 22(1):2–17
34. Sindhwani R, Malhotra V (2016) Modelling the attributes affecting design and implementation of agile manufacturing system. *Int J Proc Manage Benchmarking* 6(2):216–234
35. Singh Patel B, Samuel C, Sharma SK (2017) Evaluation of agility in supply chains: a case study of an Indian manufacturing organization. *J Manuf Technol Manage* 28(2):212–231
36. Abdulmalek FA, Rajgopal J, Needy KL (2006) A classification scheme for the process industry to guide the implementation of lean. *Eng Manage J* 18(2):15–25
37. Elmoselhy SA (2013) Hybrid lean–agile manufacturing system technical facet, in automotive sector. *J Manuf Syst* 32(4):598–619
38. Abdullah FM (2003) *Lean manufacturing tools and techniques in the process industry with a focus on steel*. University of Pittsburgh

39. Sanchez LM, Nagi R (2001) A review of agile manufacturing systems. *Int J Prod Res* 39(16):3561–3600
40. Gopalakrishnan K, Yusuf YY, Musa A, Abubakar T, Ambursa HM (2012) Sustainable supply chain management: a case study of British Aerospace (BAe) Systems. *Int J Prod Econ* 140(1):193–203
41. Adeleye EO, Yusuf YY (2006) Towards agile manufacturing: models of competition and performance outcomes. *Int J Agile Syst Manag* 1(1):93–110
42. Achanga P, Shehab E, Roy R, Nelder G (2006) Critical success factors for lean implementation within SMEs. *J Manuf Technol Manage* 17(4):460–471
43. Berlec T, Kleindienst M, Rabitsch C, Ramsauer C (2017) Methodology to facilitate successful lean implementation. *Stroj Vestn J Mech Eng* 63(7–8):457–465
44. McCarthy I, Tsinopoulos C (2003) Strategies for agility: an evolutionary and configurational approach. *Integr Manuf Syst* 14(2):103–113
45. Gunasekaran A, Lai KH, Cheng TE (2008) Responsive supply chain: a competitive strategy in a networked economy. *Omega* 36(4):549–564
46. Crute V, Ward Y, Brown S, Graves A (2003) Implementing lean in aerospace—challenging the assumptions and understanding the challenges. *Technovation* 23(12):917–928
47. Sundar R, Balaji AN, Kumar RS (2015) A review on lean manufacturing implementation techniques. In: Xavier AM, Prasad KD VY (eds) 12th global congress on manufacturing and management, GCMM 2014, vol 97. Curran, New York, NY, pp 1875–1885
48. Singh B, Garg SK, Sharma SK, Grewal C (2010) Lean implementation and its benefits to production industry. *Int J Lean Six Sigma* 1(2):157–168
49. Jin-Hai L, Anderson AR, Harrison RT (2003) The evolution of agile manufacturing. *Bus Proc Manage J* 9(2):170–189
50. Singh B, Garg SK, Sharma SK (2010) Scope for lean implementation: a survey of 127 Indian industries. *Int J Rapid Manuf* 1(3):323–333
51. Bessant J, Caffyn S (1997) High-involvement innovation through continuous improvement. *Int J Technol Manage* 14(1):7–28
52. Gunasekaran A, Yusuf YY (2002) Agile manufacturing: a taxonomy of strategic and technological imperatives. *Int J Prod Res* 40(6):1357–1385
53. Fahmi S, Abdelwahab T (2014) Case study: improving production planning in steel industry in light of lean principles. In: Proceedings of the 2012 international conference on industrial engineering and operations management
54. Elkins DA, Huang N, Alden JM (2004) Agile manufacturing systems in the automotive industry. *Int J Prod Econ* 91(3):201–214
55. Karwowski W, Mital A (1986) Applications of approximate reasoning in risk analysis. *Adv Hum Fact/Ergon Elsevier* 6:227–243
56. Chen SJ, Hwang CL (1992) Fuzzy multiple attribute decision making methods. In: *Fuzzy multiple attribute decision making*. Springer, Berlin, Heidelberg, pp 289–486
57. Sindhwani R, Malhotra V (2013) Overview and drivers of agile manufacturing system: a review. *Int J Market Technol* 3(12):144
58. Sindhwani R, Malhotra V (2015) Lean and agile manufacturing system barriers. *Int J Adv Res Innov* 3(1):110–112
59. Sindhwani R, Malhotra V (2017) Modelling and analysis of agile manufacturing system by ISM and MICMAC analysis. *Int J Syst Assur Eng Manag* 8(2):253–263
60. Sindhwani R, Malhotra V (2016) Barriers evaluation for agile manufacturing system with fuzzy performance importance index approach. *Int J Agile Syst Manag* 9(4):292–301
61. Sindhwani R, Malhotra V (2017) A framework to enhance agile manufacturing system: a total interpretive structural modelling (TISM) approach. *Benchmarking Int J* 24(4):467–487
62. Mittal VK, Sindhwani R, Kalsariya V, Salroo F, Sangwan KS, Singh PL (2017) Adoption of integrated lean-green-agile strategies for modern manufacturing systems. *Procedia CIRP* 61:463–468
63. Mittal VK, Sindhwani R, Kapur PK (2016) Two-way assessment of barriers to lean-green manufacturing system: insights from India. *Int J Syst Assur Eng Manag* 7(4):400–407

Weld Strength Analysis of Ultrasonic Polymer Welding Using Adaptive Neuro-Fuzzy Inference System



T. Chinnadurai , S. Saravanan , M. Karthigai Pandian ,
N. Prabakaran  and J. Dhanaselvam 

Abstract Polymers are widely used in automotive and aerospace industries for its better strength and easy to design the expected shape and size of parts. To join the two plastic parts, ultrasonic welding is an effective way because of fast and clean process. The present study intends to investigate the weld strength of Ultrasonic Welding (USW) for PC/ABS blend using adaptive neuro-fuzzy inference system (ANFIS). The ANFIS models are utilized for the formulation of mathematical model of USW. All the input parameters are expected to have a significant impact on the weld strength but the most influencing input parameters are pressure, weld time and amplitude are prepared for this study. By comparing the real-time experimental results with the ANFIS predicted results, it is observed that the predicted and experimental models are in accordance with each other. This novel ANFIS model could be further employed for identifying the tensile strength of USW joints in various joining applications. Finally, the SEM images are analyzed to predict the nature of the weld condition.

Keywords Ultrasonic welding · PC/ABS · ANFIS · SEM

1 Introduction

Polymers are used in many applications like day-to-day packaging, automotive industry, aerospace and various other industries. Further improving the polymer usage in industry, two separate polymers are blended together to attain a new blend with the required strength for specific applications. These blended polymers are playing a significant role in interior and exterior parts of vehicles, their body and structural components [1]. Polycarbonate (PC) and acrylonitrile–butadiene–styrene (ABS) polymers

T. Chinnadurai (✉) · M. Karthigai Pandian · J. Dhanaselvam
Department of ICE, Sri Krishna College of Technology, Coimbatore, India
e-mail: jeevadurai07@gmail.com

S. Saravanan
Department of EEE, Sri Krishna College of Technology, Coimbatore, India

N. Prabakaran
Department of EEE, SASTRA Deemed University, Thanjavur, Tamil Nadu 613401, India

© Springer Nature Singapore Pte Ltd. 2019

K. Shanker et al. (eds.), *Advances in Industrial and Production Engineering*, Lecture Notes in Mechanical Engineering, https://doi.org/10.1007/978-981-13-6412-9_71

are blended together for their great practical significance. PC is a ductile thermoplastic polymer and ABS is classified as strengthened thermoplastic with wide range of industrial applications. Some industrial components are expected to have high strength as well as elastic nature to withstand heavy loads. ABS will reduce the ductile nature of PC when its get blended with it and produces a lot of complementary properties. PC/ABS blended polymer has acquired considerable interest in engineering applications that require a high degree of toughness, as seen in the automotive industry.

Ultrasonic Welding (USW) method is the most effective method of joining individual and blended polymers. The PC/ABS blended polymers are joined by applying high-frequency vibrations (the range between 20 and 70 kHz) under pressure. When the high-frequency vibrations are applied perpendicular to the weld between the parts, it provides localized heating; this will cause the joining of the materials [2]. In USW, the weld strength mainly depends on the material properties and welding parameters. Most important process parameters in a welding process include weld pressure, welding time, holding time, holding pressure and amplitude etc. Among these parameters amplitude, weld time and pressure are the most influencing ones on the weld strength of materials [3] and also the energy director (ED) design (shape and size) will also contribute toward the weld strength [4].

ANFIS is an adaptive neuro-fuzzy inference system, which is a combination of artificial neural network (ANN) and fuzzy logic control (FLC). ANFIS is an effective and powerful tool for non-linear-based systems. NN is used to map the uncertain condition from the system and output is decided by FLC using correct fuzzy rules. Because of the combined operation of NN and FLC, the ANFIS-based controller is very accurate in supervisory part of the system [5–7]. In this study, the ANFIS model is used to forecast the weld strength for resistance spot welding. It discusses about employing AI techniques of ANFIS to predict the quality of weld strength in ultrasonically welded PC/ABS blends. Simulation results are validated by comparing them with the mechanical experimental results.

2 Experimental Setup

PC and ABS granules are mixed in 60–40% ratio and mold preparation using injection molding equipment are used for this investigation. Mold specimens used in the study are prepared as two different sets. Energy director is engaged in preparing one mold specimen set while the other is prepared without employing it. The injection time required for the sample and the holding time for the process is fixed to be 5 s. Injection pressure is 207 kPa and holding pressures are kept at 167 kPa for the molding process. The cooling time for the process is maintained at 30 s. Injection temperatures from 170 to 185 °C are chosen as one of the major attributes to find the impact made by varying temperatures on the polymer properties. A Dukane i220 USW equipment that is available in a range of 20 kHz with its power levels ranging from 1200 to

Table 1 PC and ABS material mechanical and thermal properties

S.No	Physical	PP	PC
1	Density (g/cm ³)	0.904	1.2
	<i>Mechanical</i>		
2	Tensile strength (psi)	3625	9500
3	Flexural strength (psi)	17,000	15,000
4	Compressive strength (psi)	8000	12,000
	<i>Thermal</i>		
5	Heat Deflection temperature (°C)	160	132
6	Glass transition temperature (°C)	110	145
7	Max operating temperature (°C)	125	151
8	Thermal conductivity (°C)	2.8	6.9

2400 W. The properties of PP and PC and ABS are described in Tables 1 and 2 described the total number of trails carried out for the experiment.

2.1 ANFIS

The neural network is designed to have five layers as shown in Fig. 1. In layer 1, each input node has an adaptive node with a parameter triggering function. The outcome of this node is the evaluation of membership that executes the crisp fuzzy value. Each membership function (MF) is denoted and adjusted using various parameters in the learning process. The membership function is given by

$$\mu_a(x) = \frac{1}{1 + \left| \frac{x - C_i}{A_i} \right|^{2B}} \tag{1}$$

Fig. 1 Ultrasonically welded PC/ABS blends

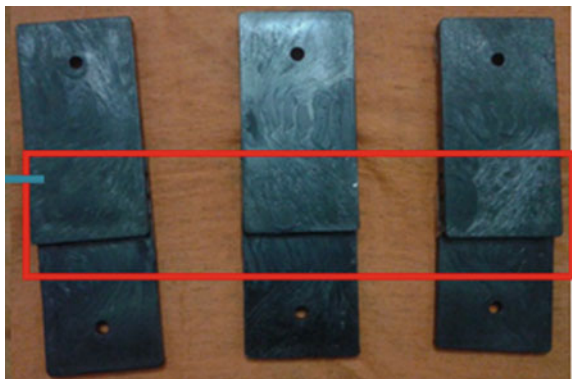


Table 2 Welding input parameters with tensile strength

Sl. No	Welding pressure (bar)	Welding time (ms)	Amplitude (μm)	Strength (N)
1	3	400	100	570.29
2	3.5	500	100	791.68
3	3.5	500	100	803.84
4	3.5	500	100	819.33
5	3.5	500	100	826.58
6	3.5	500	100	798.97
7	4	500	100	798.34
8	4	500	100	785.83
9	4	550	100	792.50
10	4	550	100	813.68
11	4	550	100	858.48
12	4	550	100	833.89
13	6	600	100	916.82
14	4.5	600	100	811.84
15	4.5	600	100	807.99
16	4.5	600	100	797.26
17	5	650	100	835.34
18	5	650	100	789.65
19	5	650	100	839.23
20	5	650	100	878.73
21	5	650	100	862.12
22	5.5	700	100	827.76
23	5.5	700	100	815.90
24	6	750	100	847.24
25	6	750	100	840.93
26	6	750	100	826.43

where A_i, B, C_i are the parameter set and value of $\mu_a(x)$ is between 0 and 1. If the parameter varies, the bell-shaped functions change accordingly and it reflects in different forms of membership functions.

In layer 2, each node is a stable node and the product of the input signals is obtained as the output. All nodes denote the strength of the rule represented in Eq. 2.

$$O_{2,i} = \omega = \mu_a(x) \cdot \mu_b(x) \tag{2}$$

where $O_{2,i}$ represents the output layer 2.

In layer 3, the nodes are fixed nodes that compute the ratio of the i th rules strength. Eq. 3 gives the normalized firing strength as an output.

$$O_{3,i} = (\omega_1 \times \varpi) / (\omega_1 + \omega_2) \quad (3)$$

In layer 4, every node is an adaptive node. The connection between the input and output layer can be represented by Eq. 4.

$$O_{4,i} = \varpi_i f_i = \varpi_i (P_i x + Q_i y + R_i) \quad (4)$$

In layer 5, the nodes are fixed node with the addition of all input signals as total output which is specified in Eq. 5.

$$O_{5,i} = \sum \varpi_i f_i = \frac{\sum_i \omega_i f_i}{\sum_i \omega_i} \quad (5)$$

The ANFIS recognizes the rules automatically and adjusts the membership function parameters. The main focus of the training algorithm is to adjust the above parameter sets to create the ANFIS output matches with the trained data as shown in Fig. 2.

3 Results and Discussion

3.1 Tensile Strength Analysis

The true stress–strain curves of PC/ABS alloy measured from different specimens are plotted and shown in Fig. 3. It is seen that there is no obvious strain softening for the PC/ABS alloy. In the molded part, the strain rate is high compared with the welded specimen. The welded specimen's stress–strain curve is obtained at different levels. The curve shows very little changes with varying levels. From the result, it is evident that the welded parts have noticeable change in materials properties while still retaining the majority of original properties. The welding of these materials reveals good thermal properties and performance (Fig. 4).

The fact that the process parameters have an influence over the tensile strength of ultrasonic welding process has been proved via experimental validation. It is necessary to find a solution that is able to precisely calculate the tensile strength for a given set of USW process parameters [8, 9]. For this purpose, adaptive neuro-fuzzy inference system (ANFIS) is a good choice to predict tensile strength as a function of three input variables. The simulations and experimental results are compared in Fig. 5. It shows the accurate prediction between the measured and simulated results. The measured values are closely matching with predicted values. This reveals that the chosen input parameters are more effective and influence parameters to the weld

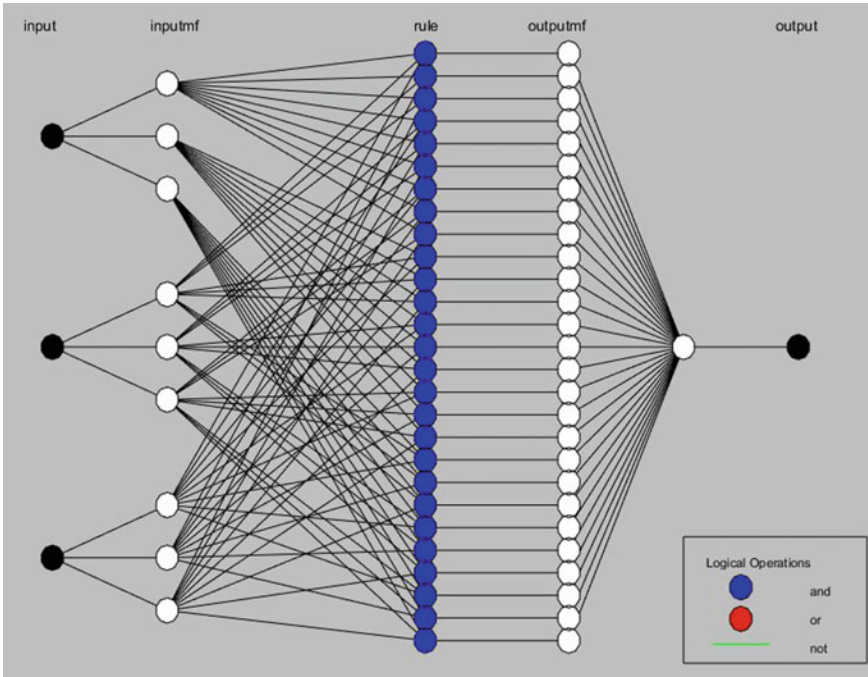


Fig. 2 ANFIS model for predicting the weld strength

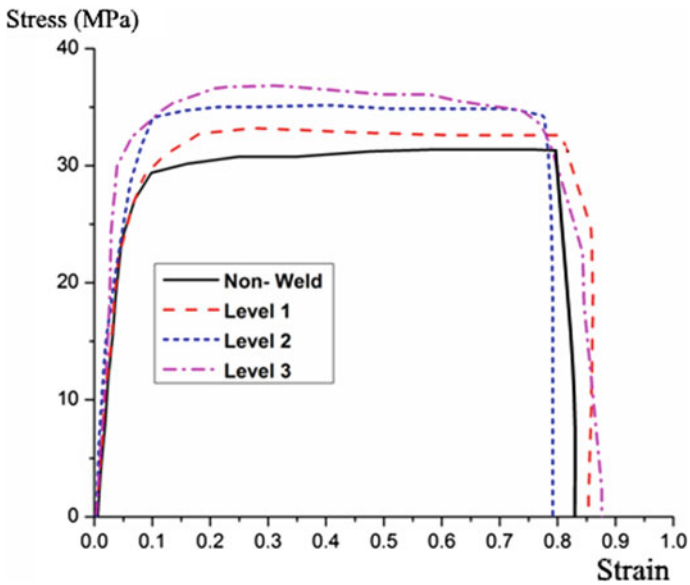


Fig. 3 Stress-strain curve for PC/ABS material

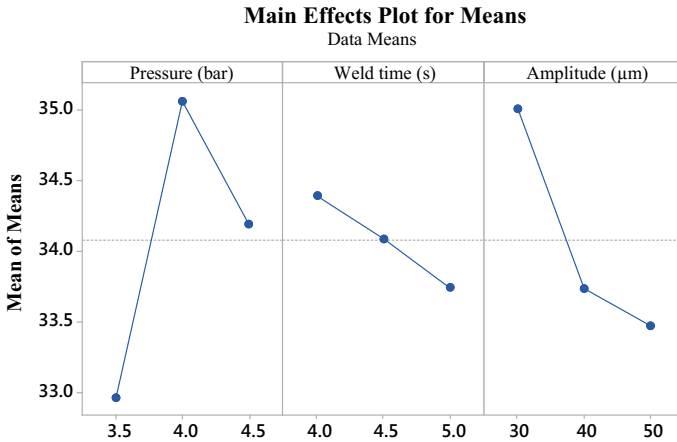


Fig. 4 Main effect plot for weld strength experimental

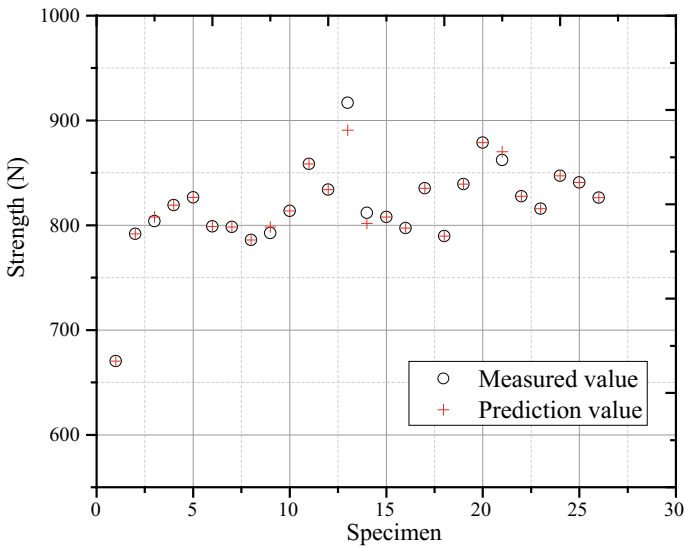


Fig. 5 Comparison between the measured and predicted variables

strength. The variations in weld strength are minimal deviation appear in predicted and measured values.

For an unconditional direct variable, a mains effect plot is used to understand the means for each group of data. Process parameters employed in the welding process are actually interdependent on each other, and the mains effect of these parameters has to be studied to understand their characteristics. It is actually calculated by subtracting the overall mean for the factor from the mean for each level. Figure 4

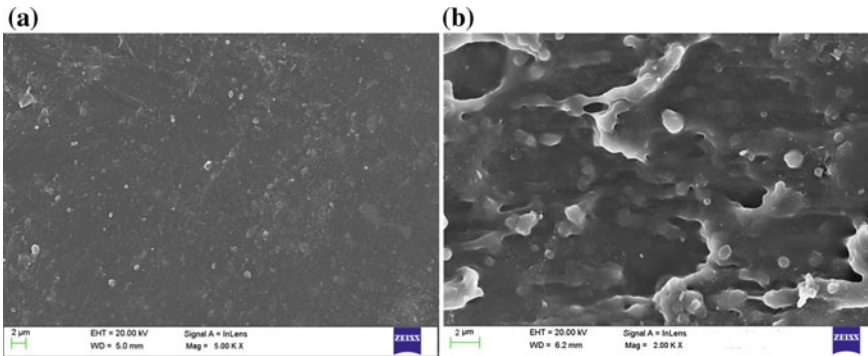


Fig. 6 SEM analysis for predicted sample **a** Before **b** After welding condition

shows the positions of the main effects for input process parameters used in the ultrasonic welding and weld strength, respectively. Every level corresponding to pressure, amplitude and weld time has an impact on the response differently. Each factor at their high-level results in higher mean responses in comparison with those at the lower level. Accordingly, from the results, pressure has a greater effect on the responses.

4 SEM Analysis

When a polymer is subjected to welding, it is mandatory to study the deformation in the morphology of its welded interface. The process parameters are expected to directly influence their number and the welding depth. If the process welding time is less, it results in a very little depth of interpenetration across the interface, further leading to reduction in the strength and the energy at the welded interface. Figure 6 shows SEM micrographs of PC/ABS samples for different blend input combinations. Energy directors are found to be widely dispersed in both phases of the polymer, which are indicated by the high peaks representing the fact that proper melting has occurred in the interface. The ABS-rich blends have conventional blend morphology with PC domains dispersed in ABS.

5 Conclusion

The performance prediction model is analyzed for each single data using ANFIS. Both the ANFIS and experimental models were found to be accurate in predicting the tensile strength based on the input parameters of USW.

In the experimental results, the tensile strength is 912 N achieved at the higher value of input parameter setting. But the nominal weld strength is achieved in 783 N at mid weld parameter settings. The ANFIS results also indicate that the best weld strength range is around 738.36 N. Comparing both the predicted and measured weld strength, they are found to be complementing each other.

SEM analysis reveals that greater voids are caused by high-frequency vibrations, when compared to small and medium frequency vibrations. However, the weld strength also appears to be high for medium frequency vibrations, emphasizing that the lap joint interface strength has high implications due to the presence of voids.

References

1. Ahmed AN, Mohd Noor CW, Allawi MF, El-Shafie A (2016) RBF-NN-based model for prediction of weld bead geometry in shielded metal arc welding (SMAW). *Neural Comput App* 1–11. <https://doi.org/10.1007/s00521-016-2496-0>
2. Grewell DA, Benatar A, Park JB (2003) *Plastics and composites welding handbook*, vol. 10
3. Suresh KS, Rani MR, Prakasan K, Rudramoorthy R (2007) Modeling of temperature distribution in ultrasonic welding of thermoplastics for various joint designs. *J Mater Process Technol* 186 (1):138–146. <https://doi.org/10.1016/j.jmatprotec.2006.12.028>
4. Das CK, Malas A, Pal P, Friedrich S, Gehde M (2013) Ultrasonic welding of amorphous and semi crystalline materials. *Adv Mater Res* 271–275. <https://doi.org/10.4028/www.scientific.net/AMR.716.271>
5. Zaharuddin MFA, Kim D, Rhee S (2017) An ANFIS based approach for predicting the weld strength of resistance spot welding in artificial intelligence development. *J Mech Sci and Tech* 31(11):5467–5476. <https://doi.org/10.1007/s12206-017-1041-0>
6. Rezaei E, Karami A, Yousefi T, Mahmoudinezhad S (2012) Modeling the free convection heat transfer in a partitioned cavity using ANFIS. *Int Commun Heat Mass Transfer* 39(3):470–475. <https://doi.org/10.1016/j.icheatmasstransfer.2011.12.006>
7. Hayati M, Rashidi AM, Rezaei A (2011) Prediction of grain size of nanocrystalline nickel coatings using adaptive neuro-fuzzy inference system. *Solid State Sci* 13(1):163–167. <https://doi.org/10.1016/j.solidstatesciences.2010.11.007>
8. Diedrich G, Kempe B (1980) Welding of pipes and fittings made from different grades of HDPE. *Kunststoffe-German Plast* 70(2):87–89
9. Abram J, Clegg DW, Quayle DV (1982) The strength of welds in uPVC. *Plast Rubber Int* 7(2):58–60

Mechanical Properties of Flax Fiber Reinforced Composites Manufactured Using Hand Layup and Compression Molding—A Comparison



Vishnu Prasad, C. V. Muhammed Hunize, R. I. Abhiraj, M. A. Josph, K. Sekar and Mubarak Ali

Abstract The focus of the researchers has been shifted toward natural fiber reinforced composites due to their biodegradability and environmental compatibility. These composites can be made by traditional hand layup process or can be manufactured with the help of machines, out of which compression molding is a versatile and efficient method. In this paper, hand layup method and compression molding method are compared to find out the optimal process for fabrication. For optimizing the fabrication parameters, tensile strength under various fabrication conditions was found. The compression pressure was varied from 2 to 10 MPa, and the optimum result was found for 4 MPa. On the other hand, 100 °C resulted in ideal properties, when the specimen was fabricated under different temperatures. Three different volume fractions of fiber were also evaluated and 0.27% volume fraction exhibited the optimal performance. Further, the effect of post-curing on tensile and thermal properties was studied. The influence of various parameters in compression molding was also investigated.

Keywords Flax fiber · Natural fiber composite material · Hand layup · Compression molding · Fabrication parameters · Curing

1 Introduction

Since industrial revolution, the increased strength requirements in various industries lead to the invention of composite materials. Fiber reinforced composites are a class of composites that are having high strength to weight ratio which made them the most suitable option for various sectors like aerospace, automobile and construction sectors. These composite materials consisting of high strength fibers such as carbon, glass and aramid, and low strength polymeric matrix, have various advantages such as high specific strength, high corrosion resistance and high specific stiffness [1].

V. Prasad (✉) · C. V. Muhammed Hunize · R. I. Abhiraj · M. A. Josph · K. Sekar · M. Ali
Department of Mechanical Engineering, National Institute of Technology,
Calicut 673601, Kerala, India
e-mail: vishnuprasad193@gmail.com

Unfortunately, these fibers have serious drawbacks such as (i) non-renewable, (ii) non-recyclable, (iii) high energy consumption for production and (iv) health risks when inhaled. Most importantly, majority of these composites being made of synthetic fibers pose a serious threat to the environment, since they are non-biodegradable in nature. The use of natural fiber reinforced composites is the solution to this problem. Natural fibers are fibers that are derived from natural sources. They may be either directly extracted from plants or animals, or produced as a result of some geological processes. Plant fibers such as jute, flax, coir, sisal and animal fibers such as silk, wool, feather are examples of natural fibers. Although the strength of natural fibers is usually far less than that of synthetic fibers, the recent studies and experiments prove that their strength can be made comparable to or even higher than that of natural fibers by suitable treatments [2].

Different manufacturing processes such as hand layup and compression molding techniques were studied. Although hand layup process has different advantages such as low cost and versatility in operation [3], it suffers from numerous limitations such as higher production time and lower mechanical properties as compared to techniques such as compression molding [4]. Various studies have done in the preparation of composites reinforced with natural fibers like flax [5] and kenaf [6]. Application of green composites in automobile body panels seems to be feasible since green composites can match the mechanical performance of synthetic ones [7]. The use of natural fiber reinforced composites in automobile parts was discussed in detail by various literatures [8]. Composites made from fibers such as flax, sisal and hemp are widely used in door cladding, floor panels and seatback linings, cotton fiber based composites in well sound insulation and coconut fiber composites in seat bottoms and back cushions [9]. The natural fiber reinforced composites can be a promising solution in bioengineering and biomedical applications such as dental implants and substitute for bone [10]. The effect of various treatments like alkali and silane treatments were also investigated by numerous literatures [11]. A study made to find out the effect of different treatments on the mechanical properties of kenaf fibers shows that the tensile properties of silane treated kenaf fibers were enhanced as compared to untreated fibers. The study further says that the tensile properties were increased due to alkali treatment also. Influences of volume fraction of fibers on the mechanical properties of epoxy composites were also investigated and concluded that volume fraction between 24 and 27% will result in best properties [12].

2 Experimental

2.1 Materials Used

High quality flax fibers imported from B Comp Pvt., Switzerland was opted as the reinforcement material. The fiber mats used were a special satin weave type of arrangement. Epofine 556 was used as the epoxy along with Finehard-1926 hardener.

Moreover, Finelube SI 01 was used as the releasing agent. Epoxy, hardener and releasing agent were procured from Fine finish organics Pvt. Ltd, Maharashtra, India.

2.2 Composite Preparation

Composite material was initially fabricated using hand layup method. Hand layup was done to find out the optimal volume fraction of fibers. Three different volume fractions for fibers were used (0.24, 0.27 and 0.30), and corresponding volumes of epoxy and hardener were taken. The epoxy to hardener ratio selected was 100:60 in volume as recommended by the supplier. Composite lamina was fabricated in between the glass plates and loading them with a dead weight for 24 h in room temperature. Four layers of flax fibers were uniformly coated with epoxy resin and placed over one by one. Glass plates were initially coated with releasing agent for easy removal of lamina after fabrication. After completing of hand layup procedure, the samples were subjected to two-stage curing recommended by the epoxy supplier. The curing cycles were 80 °C for 4 h and 120 °C for 2 h. Then tensile tests were conducted on the samples having different volume fractions, and based on the results 0.27 volume fraction was selected. Cured and non-cured samples were also prepared to find the influence of curing on mechanical and thermal properties. To evaluate the influence of fabrication procedure of composite materials, the tensile properties were studied and compared by considering samples fabricated by hand layup and compression molding technique. Samples prepared by compression molding technique were developed by placing uniformly coated flax fibers with epoxy resin in the mold. The mold was then placed in between the plates of compression molding machine at a certain pressure and temperature. Pressure and temperature parameters were varied to find out the optimum condition.

2.3 Characterization

Tensile test (ASTM D3039)

The equipment used for tensile test was Shimadzu AG-X plus UTM machine. Six samples of each case were prepared according to ASTM D3039 standard [13], and the average value was concluded as the result. The samples were 250 mm long, 25 mm wide and 30 mm thick in dimensions. Figure 1 shows the photograph of the equipment used in tensile testing. The head displacement was set at 0.5 mm/min for all the samples.

Scanning electron microscopy (SEM)

Scanning electron microscopy was performed to study the interaction between the fiber and the matrix, in view of the fact that interfacial bonding is a critical factor which decides the mechanical strength of the composite material. Initially, the



Fig. 1 Tensile testing according to ASTM D3039

fractured surfaces of the samples were cut and gold coated uniformly for testing. SEM was conducted with SU 6600 Field Emission Scanning Electron Microscopy (FESEM) with emission current of 58 μA and acceleration voltage of 5.0 kV.

Thermogravimetric analysis (TGA)

The thermal properties of cured and non-cured composites fabricated using hand layup were evaluated by performing thermogravimetric analysis (TGA). Thermogravimetric analysis quantifies the extent and percentage of weight loss of a material by keeping temperature or time as a function in a controlled atmosphere. The atmosphere selected here is nitrogen and heating range from 25 to 700 $^{\circ}\text{C}$ with a heating rate of 10 $^{\circ}\text{C}$ per min. TGA was conducted in Hitachi Thermal Analysis System Model STA7200 following ASTM E1868 standard with a specimen weight of 10 mg. The test is conducted to evaluate the composition of materials and gauge the thermal stability of the sample.

3 Results and Discussion

3.1 Tensile Test

The tensile test was taken as the reference for optimizing various parameters used during fabrication, in view of the fact that it is the basic parameter to analyze the mechanical properties of a material. Initially, for determining the optimal volume fraction of fibers, a range of volume fraction is selected according to various literatures. Accordingly, three volume fractions were selected (24, 27 and 30%), and samples were prepared taking the number of layers as four. The compression molding temperature was taken as 100 °C as a inference from visual inspection (a good flow of the epoxy is observed at this temperature). The compression molding pressure was taken as 4 MPa as a random value. Tensile test was conducted on the samples, and the results showed a tensile strength of 53.90 MPa corresponding to a volume fraction of 27%, which is the highest as compared to 49.56 MPa for 24% volume fraction and 48.19 MPa for 30% volume fraction. Hence, 27% volume of fibers was selected for further experiments (refer Fig. 2).

The traditional hand layup method has several disadvantages like more time consumption due to the fact that it is cured in room temperature. Furthermore, many researchers indicated lower performance of samples fabricated by hand layup as compared to other processes such as compression molding. Hence, samples were fabricated through compression molding and tensile test was conducted, taking the number of layers as four and volume fraction as 27%. The compression temperature was taken as 100 °C, and samples were subjected to four different compression pressures (2, 4, 6 and 8 MPa). The results showed a tensile strength of 65.07 MPa corresponding to 4 MPa pressure as the highest, compared to 60.53 MPa for the sample applied with 2 MPa pressure, 57.93 MPa for 6 MPa pressure and 53.40 MPa for 8 MPa pressure. Thus, 4 MPa compression pressure was selected as the optimum. This will be due to the fact that very high pressures squeeze out the epoxy out of the composite which will eventually result in the lower performance. Figure 3 describes

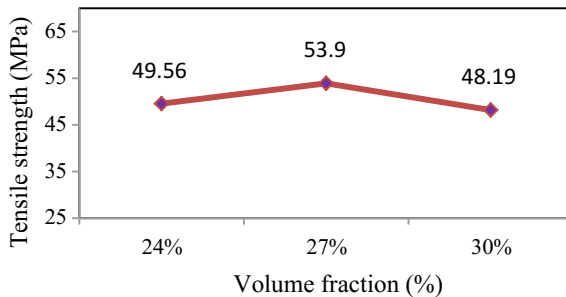


Fig. 2 Tensile strength values with various volume fraction levels

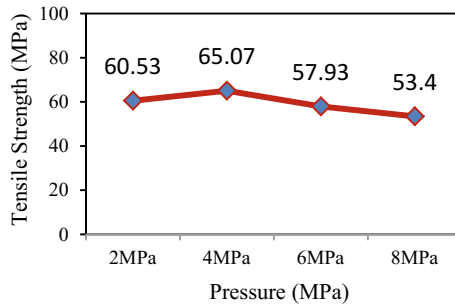


Fig. 3 Tensile strength values with varying pressure values

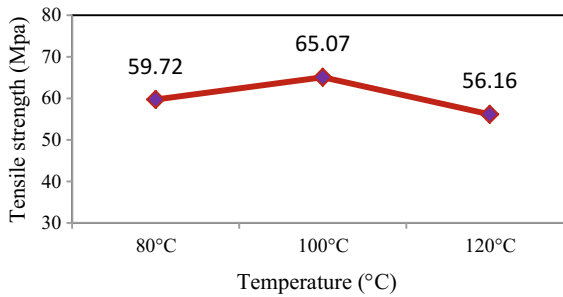


Fig. 4 Tensile strength with varying temperature values

the variation in tensile strength values across few levels of compression molding pressure parameter.

To find the effect of compression temperature, samples were fabricated under three different temperatures. The temperatures selected were 80, 100 and 120 °C, in view of the fact that at higher temperatures the viscosity of the epoxy reduces resulting in the reduction of epoxy by leakage. The compression pressure was taken as 4 MPa. The results indicated 59.72 MPa tensile strength for a temperature of 80 °C, 65.07 MPa for 100 °C and 56.16 MPa for 120 °C. Figure 4 shows the variation in tensile strength values across different compression molding temperature values.

3.2 Scanning Electron Microscopy (SEM)

From the tensile test results, it is noted that the manufacturing process has influence in tensile strength values. Samples prepared by compression molding technique had a god improvement in the tensile properties. Evidence from the SEM image shows that improvement in the tensile strength values was due to better fiber matrix interactions. Using compression molding for composite fabrication with optimum pressure and temperature provides better fiber and matrix interface bonding thereby improving

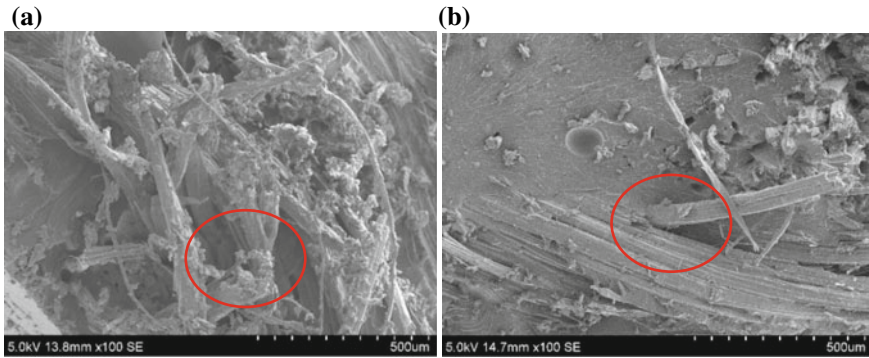


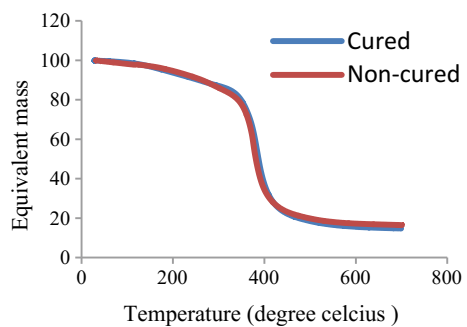
Fig. 5 SEM images of composite samples fabricates using **a** hand layup **b** compression molding

the mechanical properties. Figure 5a and b explains about the superior bonding in case of composite samples fabricated using compression molding techniques.

3.3 Thermogravimetric Analysis

Thermal analyses were conducted on the samples to study the composition and thermal stability. Cured and uncured samples prepared using hand layup were studied. The samples were cured after fabrication recommended by the epoxy manufacturer. Two-stage curing was conducted on the samples 80 °C for 4 h and then 120 °C for 2 h. From Fig. 6, it is clear that the initial mass loss will indicate the amount of moisture content in the sample. The major mass loss is indicated in the slope with temperature starting from 100 to 490 °C. Though the curves show a similar track, it can be inferred that the mass loss is dominant at temperature 380 °C, where the weight loss for cured sample is 53.61% and for uncured sample is 61%. This shows the curing of composites samples has a positive effect on thermal stability.

Fig. 6 Weight loss percentage versus temperature curve from TGA analysis



4 Conclusions

It can be concluded that the fabrication procedure has a great influence on the mechanical strength of the composites, and volume fraction contributes to the final strength of the composite. Proper optimization of these influencing factors needs to be studied for developing a composite with better mechanical strength. The results conclude that 42% volume fraction of fibers in composite with 4 layers of fiber has shown better tensile strength value. The flax fiber reinforced composite samples prepared by compression molding showed better results in tensile and hardness test.

The work has various future scopes such as exploring other types of fabrication processes such as injection molding and vacuum bag method to find out the best method for fabrication of natural fiber reinforced composites. Also, other parameters such as curing time and temperature have to be further optimized for getting a finest range of properties.

Acknowledgements The authors wish to express thanks to National Institute of Technology, Calicut, India for facilitating to conduct the preparation and testing of composite samples, also TEQIP-II for funding the project work. Authors wish to express our sincere thanks to Dr. Soney Varghese, Associate Professor, School of Nano-Science & Technology, NIT Calicut for his support and advices during the project.

References

1. Ali M, Joshi SC, Sultan MTH (2017) Palliatives for low velocity impact damage in composite laminates. *Adv Mater Sci Eng*
2. Asim M, Jawaid M, Abdan K, Ishak MR (2016) Effect of alkali and silane treatments on mechanical and fibre-matrix bond strength of kenaf and pineapple leaf fibres. *J Bionic Eng* 13:426–435
3. Graupner N, Ziegmann G, Wilde F, Beckmann F, Müssig J (2016) Procedural influences on compression and injection moulded cellulose fibre-reinforced polylactide (PLA) composites: influence of fibre loading, fibre length, fibre orientation and voids. *Composites Part A* (81):158–171
4. Sreekumar PA, Joseph K, Unnikrishnan G, Thomas S (2007) A comparative study on mechanical properties of sisal-leaf fibre-reinforced polyester composites prepared by resin transfer and compression moulding techniques. *Compos Sci Technol* (67):453–461
5. Omrani F, Wang P, Soulat D, Ferreira M (2017) Mechanical properties of flax-fibre-reinforced preforms and composites: influence of the type of yarns on multi-scale characterisations. *Composites Part A* (93):72–81
6. Ochi S (2008) Mechanical properties of kenaf fibers and kenaf/PLA composites. *Mech Mater* 40:446–452
7. Koronis G, Silva A, Fontul M (2013) Green composites: a review of adequate materials for automotive applications. *Composites Part B* (44):120–127
8. Alves C, Ferrão PMC, Silva AJ, Reis LG, Freitas M, Rodrigues LB, Alves DE (2010) Eco design of automotive components making use of natural jute fiber components. *J Clean Prod* (18):313–327
9. Al-Oqla MF, Sapuan SM (2014) Natural fiber reinforced polymer composites in industrial applications: feasibility of date palm fibers for sustainable automotive industry. *J Clean Prod* (66):347–354

10. Cheung H, Ho M, Lau K, Cardona F, Hui D (2009) Natural fibre-reinforced composites for bioengineering and environmental engineering applications. *Composites Part B* (40):655–663
11. Downey MA, Drzal LT (2016) Toughening of carbon fiber-reinforced epoxy polymer composites utilizing fiber surface treatment and sizing. *Composites Part A* (90):687–698
12. Murugan R, Ramesh R, Padmanabhan K (2014) Investigation on static and dynamic mechanical properties of epoxy based woven fabric glass/carbon hybrid composite laminates. *Procedia Eng* 97:459–468
13. Fragassa C, Pavlovic A, Santulli C (2017) Mechanical and impact characterization of flax and basalt fibre vinylester composites and their hybrids. *Composites Part B*

Design and Development of an Online Process Measurement System for Zero Defect Production



Joseph John Valiaveetil, Saurabh Singh, Akshat Jain, AkshayUpadhyaya and Sumit Gupta

Abstract The objective of this paper is to fabricate a system for press line that allows for real-time sorting of parts with defects caused by process variation. Despite high investment and advanced technology, defects like thinning, cracks and wrinkles are still common in products in the sheet metal forming industries. Variation of the process parameter is an unavoidable reality resulting in heavy investment in process control technologies like adaptive control and closed-loop systems. The limitations of a control system mandate an inspection line post-production. With this scheme, the dependence of product quality on the effectiveness of the inspection line can be reduced. The project that was undertaken herein mainly focuses on design and fabrication of online inspection measurement system which is used to monitor the process parameters-alignment, uneven force distribution and non-uniform pneumatic pressure. Comparison of real-time values is done with ideal value of process parameters to check variation of values in the press line. The readings on GUI of MATLAB show the exact parameters of the system at particular instants through which estimation of the reason for defect and an exact number of defective pieces can be found. The experiments affirmed the importance of process parameters in the consistency of quality through the feedback from sensors. The scheme can successfully reduce both producer and consumer risk. Savings in space, time, manpower and capital in inspection system can also be achieved.

Keywords Zero defect · Manufacturing · Online inspection · MATLAB · Press line · Productivity

1 Introduction

Growth in the automotive market will increase demand for metal forming equipment. The use of novel sheet materials and new technologies in press equipment requires

J. J. Valiaveetil · S. Singh · A. Jain · AkshayUpadhyaya · S. Gupta (✉)
Department of Mechanical Engineering, Amity School of Engineering & Technology, Amity University, 201313 Noida, Uttar Pradesh, India
e-mail: sumitgupta2007@gmail.com

continuous automation. Today, several press builders are trying to improve product quality, efficiency and productivity through various schemes. One such is dying try-out which is a procedure to adjust tools design and process variables. Other is closed-loop machine control strategy to control blank holder force (BHF) in order to follow determined reference trajectory. The main aim is to exchange information between people and processes to generate new sophisticated and advanced practices. The scheme is different from a closed-loop control system as it reduces closed-loop variability, acts as an alarming system in line as well as act as feedback in a closed-loop control system.

It means the measurement and monitoring of parameters that cause major defects in the product, which is an inline inspection. The scheme can be designed to eliminate inspection time invested products by sorting them on the feedback of process parameters, to improve productivity. It's applicable to press lines, forging operations, injection moulding, extrusion processes. The system is capable of removing defective products from the press line without their inspection at the end of production. The need is to have good quality with less investment, reduces cycle time, less asset and manpower requirement. The advantages of this scheme are the optimum utilization of time in the production line, the option to update product variety is easy, money can be saved by not investing in the inspection department. The final product as circular pan lid is manufactured from the scheme with a hole at the centre for provision of the hook by the shallow drawing of the pure aluminium sheet.

2 Literature Review

During the drawing process, the cause of defects and effects of geometrical parameters are observed. Punch defects, die profile radius and radial clearance were some of the reasons for defective manufacturing. Zaid was concluded that with the increase of die profile radius results in a decrease of maximum drawing force and due to an increase of the die profile radius it increases [1]. Except die and punch clearances, there are still many factors which affect the burr formation [2]. With CAD/CAM software, it's an easy task to maintain a proper clearance accordingly. It also includes the best selection materials and methods for machine selection, press tools, tool design review [3]. Made use of orthogonal experiment method through LS-DYNA software to test the box specimen by finite element simulation. The results conclude that the four punch fillet are subjected to biaxial tensile stress and create a serious change in thickness. It was concluded to choose the suitable blank holder force and die entrance radius [4]. Main focus was on the reduction of human interaction with the machine by using industrial monitoring robots to measure the process parameter. A special ZIG-BEE protocol to control room is designed using MATLAB GUI model. MATLAB GUI displays all the parameter like temperature, light intensity in a graphical manner in the form of graphs showing a continuous change in the parameter which allows detecting the error and defect in the machine to a greater extent [5]. Concluded for few structural faults were made in the formed body components.

Thinning is major failure parameter in the forming industry. Edge cracking is another significant failure mode in many forming processes in the advancement of high strength steels. Opportunity for online measurements of parameters is offered by inline measurements with the help of Non-Destructive Technique (micro-magnetic) and electromagnetic. The most critical process parameters causing defects like thinning in blanks was done. The main parameters are like blank holder force (BHF), Punch Radii, friction between the punch and blank and die and many more [6]. The relevance of the thesis is through this publication. With the help of process control for sheet metal stamping, it can lead to a greater reduction in a defect in deep and shallow drawn parts which saves material and reduces scrap. [7] found changes associated with construction of a machine to be used in the die and die-less sheet metal forming was made. The selected future directions of development in new technologies and machines for sheet metal forming takes into account modern blank holding systems in the process of deep drawing. Two sensing methods to create a tooling-integrated sensing system: mutual inductance-based displacement measurement for sheet draw-in, and distributed contact pressure measurement at the tool-workpiece interface was revealed [8]. The integrated sensing technique provides insight into the stamping process by quantifying process variations and providing a reference base for process control to reduce product disparities.

3 Materials and Methods

The prototype for the demonstration of the scheme consists of a pneumatic plunger system with pneumatic input for reciprocating motion of ram. The system consists of the upper die and lower die apparatus. The setup of the pneumatic press was designed and fabricated according to the requirement of the experiment, the frame of the press machine was made by the mild steel C shape beam as it provides good structural strength due to its high strength, stiffness, toughness properties and lightweight. The vertical movement to the plunger was provided by the double actuating pneumatic cylinder. The pneumatic system was equipped with FRL unit along with the pneumatic cylinder from the compressor. The die and punch are made from high-carbon, high-chromium tool steel. The dimensions of dies have been set as per analytical calculations for force and pressure with particular d/h ratio for dies. An aluminium sheet (6061) was used as a blank material for drawing operation to produce a lid shape by calculations of working stress and yield stress applied by a punch on the sheet.

4 Analytical Calculations

Die dimensions

Lower die => inner diameter = 84 mm, outer diameter = 104.5 mm

Upper die => inner diameter = 83 mm, outer diameter (d/D_p) = 102.7 mm

Depth of cup in lower die (h) = 10 mm

Blank diameter (D/D_0) = 112 mm

Corner radius of punch (r) = 10 mm

If $h/d < 0.75$, **Draws = 1**

Clearance = 1.07–1.09 (as per theory)

Clearance between die and punch = 0.9 mm

Thickness of sheet = 36 gauge

Yield Strength of sheet = 55 MPa

Force required for drawing = 1.721 kN

Pressure required in the pneumatic plunger = 6.14 bar

Shear stress = 26.14 MPa

Yield stress = 55 MPa (Data from standard values for the sheet)

The material for the sheet is **6061 Aluminium alloy** which has this value of yield stress which can bear shear stress at this value. Die material is D2 (High carbon high chromium steel). Shear stress is less than yield stress, so blank doesn't shear according to stress-strain diagram theory. Frame material required to sustain and support this force is Mild steel.

To detect the presence of punch, velocity and time of punch at different interval of distances, inductive proximity sensor are used at a different location, one at the beginning of travel of punch, another at end of travel of punch and another at the middle of the punch travel; each at a distance of 90 mm from each other. These sensors have a sensing region of 1–15 mm and diameter of the sensor is 30 mm. To check the non-uniform pressure at the different places at the lower die, force sensors are fixed on the base plate. To collect and process the data from the sensors an Arduino at mega microprocessor is used which communicate with sensors and MATLAB software. By the extracting data from sensors and microprocessor, live data points can be plotted in the form of pictorial representation as run charts over a large interval of time (Figs. 1 and 2).

Few components like a punch, die, base plate and frame of the press machine were fabricated in the metal cutting workshop. For the making of punch and die, the raw material of High Carbon High Chromium Steel (D2) was used. Lathe Machine was used for the manufacturing of punch and die. For die polishing sandpapers, abrasive stones and die polishing paste was used. For base plate making again lathe machine was used. C-shaped channel also known as (PFC) is used for frame making. The raw material used for the frame is made of mild steel. Total six C-shaped channel of different dimension was used for fabricating the frame. Power hacksaw machine was used for cutting the C-shaped channel into six parts of the required dimension. Radial drilling machine was used for drilling holes in the C-shaped channel. Nut and bolt were used to fasten the C-shaped channels for the frame making (Figs. 3 and 4).

Frame, punch and die, base plate, pneumatic cylinder, filter regulator lubricator, 5/2 valve, gauge pipes, force resistive sensor, inductive proximity sensor are the components used for assembly of the press machine. Before bolting the base plate to the frame, two force resistive were fixed at the desired position between them. Then

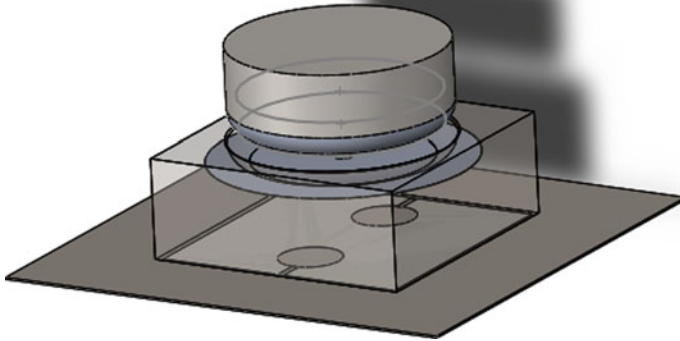


Fig. 1 CAD model of punch and lower die

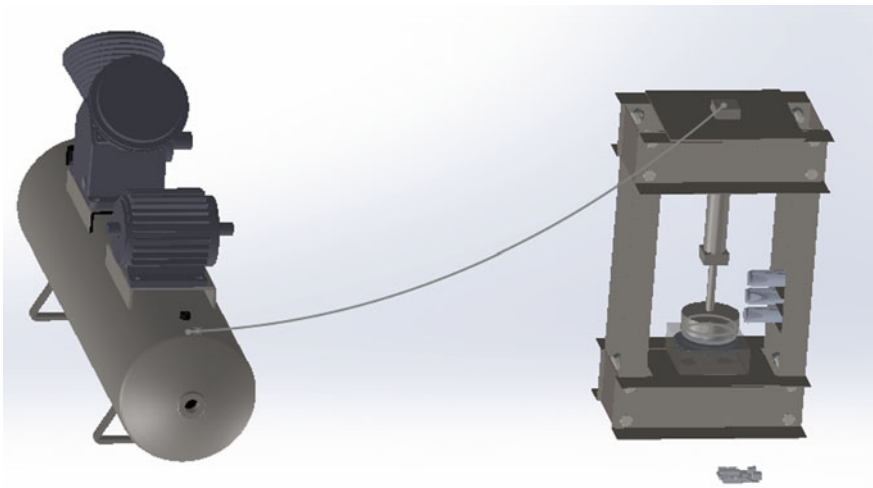


Fig. 2 CAD model of the whole scheme

pneumatic cylinder with upper die was fixed to the mild steel plate with help of nuts and bolts. Then filter regulator lubricator and 5/2 valve was bolted to the wooden block. After that, gauge pipe was attached from the filter regulator lubricator then to 5/2 valve and from the pneumatic cylinder to the 5/2 valve. Then aluminium plate was fixed to one the required C-shaped channel with nuts and bolts. Then finally inductive proximity sensors were attached to the aluminium plate.

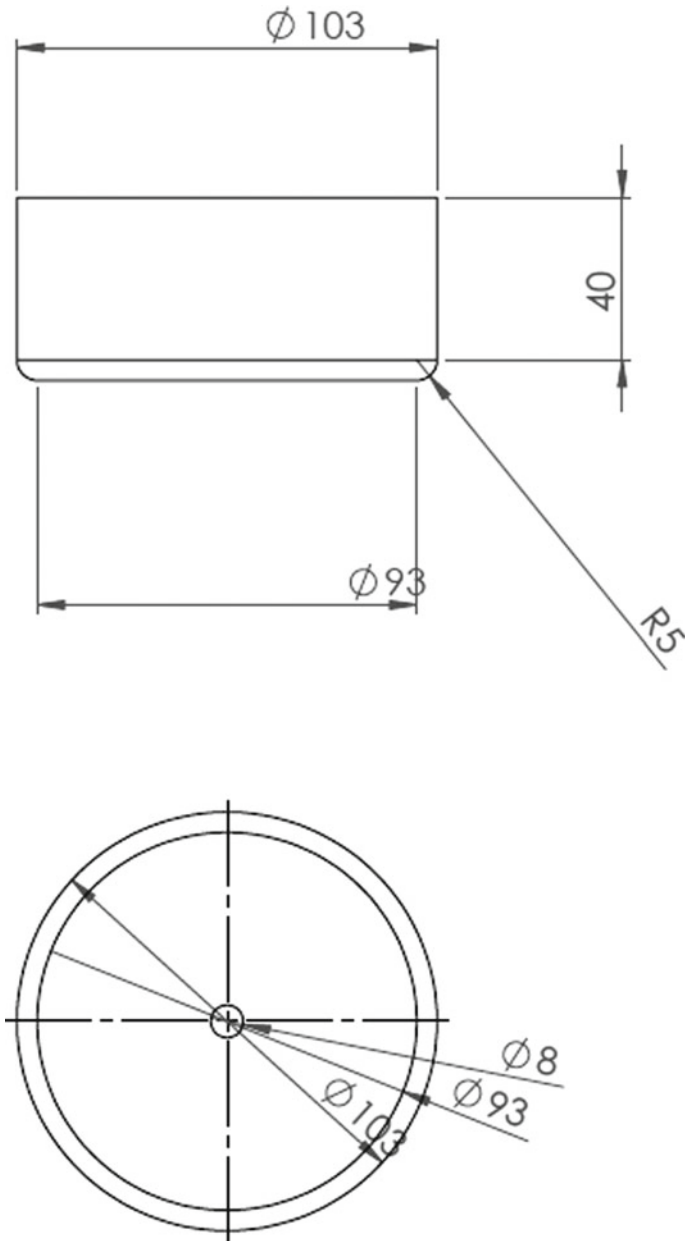
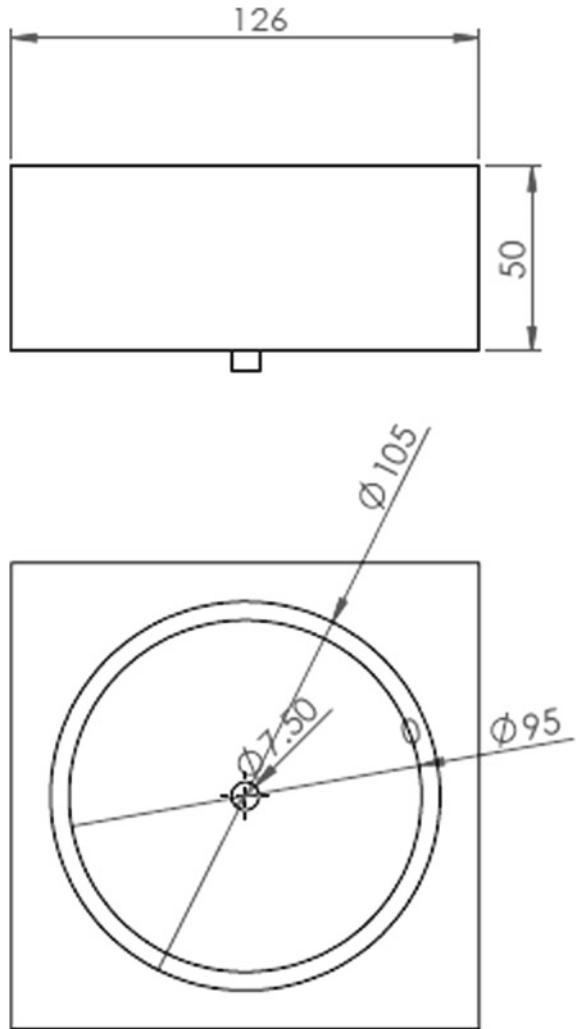


Fig. 3 Drafted sketch of lower die

Fig. 4 Drafted sketch of the upper die



5 Testing and Results

According to calculations and referred literature, the ideal values of the parameters monitored are: Force = 1.7 kN. Velocity = 900 mm/s. Velocity was calculated using three equally spaced inductive proximity sensors placed 90 mm apart from each other. Force was monitored by force resistor sensors measuring the force dispersed to the frame from lower die. Voltage readings were directly compared during force monitoring. Required pressure to obtain 1.7 kN of force was calculated as 85 psi. After numerous experimental trials, the values of force sensor voltage at best product.



Fig. 5 Fabricated scheme

The combined average value of voltage readings corresponding to the value of force was 2700–2800 mV; this value was used as ideal in graphs.

The program on the Arduino Board and MATLAB is used to transmit/receive live data. Calculations are done for each part for values from sensors. The values are handled in the form of a matrix whose format is in h/min/s for the three inductive sensors. Two values of velocity are calculated between each pair of inductive sensors. The velocity between the second and third sensors is more important as it is closer to the value of velocity during forming. The microprocessor stores ideal values and sets it as a reference through MATLAB GUI. The force sensor values are used to plot the average on the third plot, compared with the reference. The experiments on the prototype prove that the scheme can be used to identify possible defectives and separate them on the basis of process parameters. The defects and variations of the experiments are largely exaggerated and animated. The investments made to achieve better control of the same are a testimony to its importance. The relevance to the scheme to not just the sheet metal industry but any manufacturing unit is thus established. Use of hydraulic system to power the punch and use of load cell to monitor force will provide a better representation of the scheme (Figs. 5, 6 and Table 1).

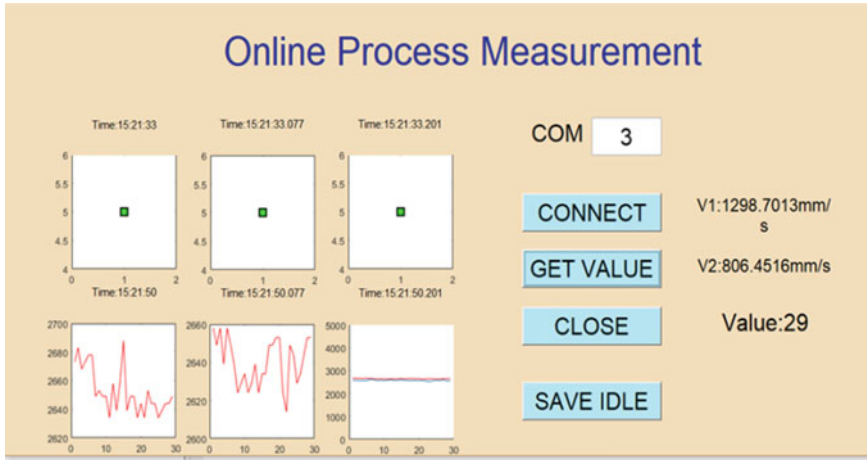


Fig. 6 Output screen from the process performed at 82 psi

Table 1 Observation from various parameter trials

S. no.	Sheet thickness (Gauge)	Sheet diameter (mm)	Pressure (psi)	Velocity (m/s)	Average voltage (V)	Defect	Reason
1	36	112	85	0.8	2.7	None	Ideal process parameters
2	36	112	88	0.9	2.6	None	Ideal process parameters
3	36	112	82	0.8	2.6	None	Ideal process parameters
4	32	112	90	0.76	3.1	Half drawn product	Incomplete punch
5	36	112	97	1.2	3.3	Crack	High force velocity
6	36	112	65	5.2	2.3	Wrinkles	Low velocity
7	36	114	90	0.8	3.2	Wrinkles	Incomplete punch movement

6 Conclusion

“Zero defect production—A step towards perfect manufacturing”. Zero defect coined by Philip Crosby meant production that yields no defects making inspection obsolete. He believed in the need to achieve process control to the extent that there would be no need to have an inspection line. Automation is largely aimed at achieving this by lowering variations.

The main objective of this scheme was to eliminate the cost of inspecting products after production, which can be reduced by this model of sorting parts after it machining. Ideally manufactured products move to the lot. Whereas parts with possible defectives, i.e. parts with process parameters beyond tolerance range are moved to be inspected and reworked if needed.

This scheme reduces the probability of defective products reaching the final lot allowing many industries to shift from 100% inspection to acceptance sampling with low risk. Further rework will be done on the defective products. The scheme can thus successfully reduce both producer and consumer risk; create savings in the form of floor space, time, manpower and capital in inspection system can also be achieved. The use of feedback in most manufacturing units it can be integrated with the closed-loop or adaptive control system, use their feedback to provide a low investment installation of the scheme. Its universal application in all manufacturing units remains its biggest advantage. The scheme can be considered “A path towards perfect manufacturing”.

References

1. Zaid AIO (2016) Deep drawing mechanism, parameters, defects, and recent results: state of the art. In: IOP conference series: materials science and engineering, IOP Publishing Ltd
2. Rai PK, Mohammad A, Jafri HZ (2013) Causes & prevention of defects (burrs) in sheet metal component. *Int J Eng Res Appl* 3(4):511–515
3. Tian L (2015) Optimization of process parameters in deep drawing process based on orthogonal experiment method. In: International conference on mechanical engineering and intelligent system, Tianjin, pp 117–121
4. Vijaya KK, Surender S (2016) Industry monitoring robot using Arduino Uno with Matlab interface. *Adv Robot Autom* 5–150
5. Zoesch A, Wiener T, Kuhl M (2015) Zero defect manufacturing: detection of cracks and thinning of material during deep drawing processes. *Procedia CIRP* 33:179–184
6. Shah K, Bhatt D, Panchal T, Panchal D, Dogra B (2014) Influence of the process parameters in deep drawing. *Int J Emerg Res Manage Technol* 3(11)
7. Trzepiecinski T (2012) Advances in sheet metal forming technologies. *Mechanika—Sci Lett Rzeszow Univ Technol* 59–70
8. Mahayotsanum N, Sah S, Cao J, Peshkin M, Gao R, Wang CT (2009) Tooling-integrated sensing systems for stamping process monitoring. *Int J Mach Tools Manuf* 49:634–644

Performance Study of Gas-Assisted Electric Discharge Machining on Carbon–Chromium Die Steel



Nishant K. Singh, Rakesh Prasad, Dilip Johari and Yashvir Singh

Abstract The present study focuses on studying the effect of liquid cum gas as dielectric during Electric Discharge Machining (EDM) of carbon chromium die steel. In this work, a hybrid process of EDM employing both liquid (commercial kerosene oil) and gas (compressed helium gas) as dielectrics in die-sinking EDM has been explored. Experimentation has been done to the study effect of process factors like discharge current, pulse on time, duty cycle, tool rotation and discharge gas pressure on material removal rate (MRR), electrode wear ratio (EWR) and surface roughness (SR). Further, a comparative study of conventional EDM with liquid dielectric and hybrid EDM with liquid cum gaseous dielectric has been performed. It has been found that high MRR, low EWR and low SR are obtained when liquid cum gaseous dielectric was used as compared to conventional EDM with liquid dielectric. Analysis of surface morphology reveals that the formation of recast layer and surface cracks is less on specimen machined with liquid cum gaseous dielectric with respect to specimen machined with conventional liquid dielectric. The results show that the use of compressed helium gas has a positive impact on the machining performance. Superior surface finish and higher MRR reveal the possible implementation of the process in modern machining.

Keywords MRR · EDM · EWR · Helium

1 Introduction

Electric Discharge Machining (EDM) is non-conventional machining process that remains as one of the most versatile processes for machining of metals having high level of hardness and which are hard to machine using conventional machining techniques [1]. The most commonly used dielectric fluid in EDM operation is kerosene.

N. K. Singh (✉) · R. Prasad · D. Johari
Department of Mechanical Engineering, HCST, Mathura, India
e-mail: nishant.singh78@gmail.com

Y. Singh
Department of Mechanical Engineering, Sir Padampat Singhania University, Udaipur, India

© Springer Nature Singapore Pte Ltd. 2019
K. Shanker et al. (eds.), *Advances in Industrial and Production Engineering*, Lecture Notes in Mechanical Engineering, https://doi.org/10.1007/978-981-13-6412-9_74

The tool is generally made of a conducting material such as brass, copper and graphite. [2].

However, EDM has numerous advantages over other conventional and non-conventional machining processes, but it has limitation of low material removal rate (MRR). Various researchers have used different techniques and approaches to overcome this limitation.

Ramani and Cassidenti [3] used argon and helium gases as dielectrics in dry electrical discharge drilling. They showed that this method resulted in a low tool wear rate (TWR) and comparatively better surface finish than oil-based EDM process. However, MRR by this process was found to be lower than conventional EDM process. Kunieda et al. [4], Kunieda and Yoshida [5] showed that high-velocity gas flows through tool electrode reduced debris reattachment after a spark and thus considered it as effective in flushing. The debris reattachment was much lower for a thin-walled tube and this increased the MRR. It was also shown that the tool wear rate (TWR) was negligible in dry EDM. MRR was found to increase when oxygen gas was used. The results suggested that the heat generated by oxidation was responsible for the increased MRR. Yu et al. [6] performed groove milling and three-dimensional milling by using dry EDM process. They employed high-velocity oxygen gas through rotary tubular tool electrode. Further, they compared the performance of dry EDM process with conventional EDM and conventional EDM milling. They found that dry EDM milling resulted in better electrode wear ratio in comparison with other two processes considered. Further, comparative analysis shows that the machining performance of dry EDM was better than conventional EDM process. However, the machining performance of dry EDM was lower than conventional EDM process. Soni et al. [7] observed an interesting phenomenon when rotary motion was provided to tool electrode. The same was verified by Mohan et al. [8] in their experimentation. They observed that the whirl condition due to rotary action helped to remove the evaporated materials from inter-electrode gap which consequently improved the flushing efficiency as well as MRR. Kuppan et al. [9] explored the effect of electrode rotation while EDM drilling of Inconel 718. Their findings revealed that MRR was notably affected by non-electrical parameters like tool rotation and electrical parameters, i.e., discharge current and duty cycle. They observed that surface finish improved with an increase in pulse on time.

Koyano et al. [10] studied effect of gas bubbles by varying the hydrostatic pressure on EDM performance. The results indicated that formation of gas bubbles enhanced the flushing performance of EDM. Aliakbari and Baseri [11] investigated the rotary EDM and studied effect of prominent electrical parameters on process output, viz. EWR, MRR and SR. Their observations depicted that EWR, MRR and SR were notably affected by electrode rotation, pulse duration, discharge current and tool electrode geometry. They stated that the improvement in process output (EWR, MRR and SR) was attributed due to use of multiple hole rotary tool electrodes. Recently, Plaza et al. [12] investigated the effect of helical-shaped electrode on EDM performance during deep hole machining of Ti6Al4V. Their findings suggested that the use of helical-shaped electrode enhanced the flushing action resulting in an improvement in MRR, EWR and machining time. Further, they showed that as compared to

conventional solid electrode the use of helical electrode significantly reduced machining time. Singh and Pandey [13] studied the effect of air-assisted multi-hole tool electrodes during machinability of EDM process. They concluded that the application of air-assisted multi-hole tool improved the MRR and reduced the EWR with respect to solid rotary tool electrodes under same machining conditions. Yoshida et al. [14] studied the effect of supply of oxygen gas in dielectric liquid in EDM operation. They observed that when oxygen is dissolved in dielectric liquid and supplied in electrode gap, machining performance improves significantly.

Having gone through these existent processes available, it was observed that MRR in dry EDM with air as dielectric was poor than oil-based EDM. However, tool wear and surface finish were found to be better than conventional EDM. Hence, in order to extract the benefits of oil EDM as well as dry EDM, the present work aims to develop a hybrid process of EDM employing both liquid (kerosene) and gas (compressed helium gas) as dielectrics during die-sinking EDM process. Helium is used as gas to prevent the oxidation reaction during machining. Also, helium having high-heat capacity found to be more effective in precision of the cut and may provide better surface finish due to its inert nature. In this experimental exploration, compressed gas was supplied through an eccentric-three hole tool, to study the effect of both liquid and gas as dielectrics on EDM performance. The effect of various process factors such as discharge current, pulse duration, duty cycle, tool rotation and discharge gas pressure has been used to study behavior of MRR, EWR and SR. A comparative analysis of conventional EDM with liquid dielectric and EDM with liquid cum gaseous dielectric has also been performed in the following sections.

2 Methodology

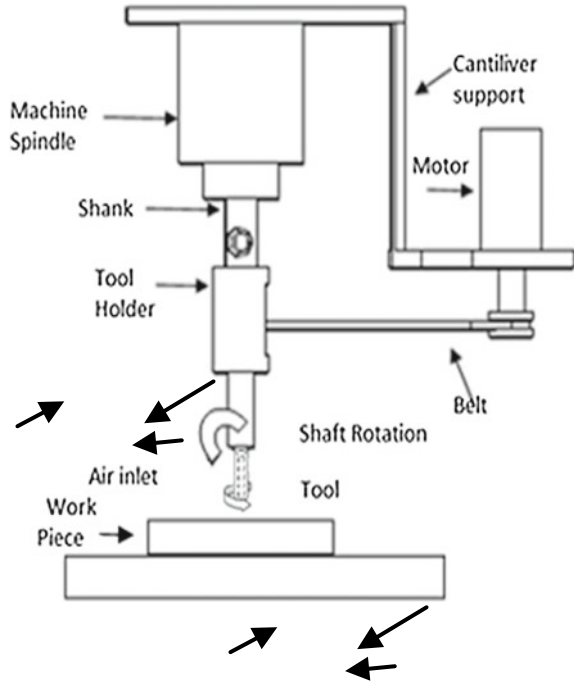
The experimentation was carried out on carbon chromium die steel having dimension of $15 \times 15 \times 10$ mm. The workpiece, considered for the study, had a hardness of 45HRC. Table 1 shows chemical composition of selected specimen.

In order to ensure effective transfer of heat from tool tip, a tool of diameter of 8 and 70 mm length was chosen. Figure 1 shows the schematic setup mounted on EDM machine. The pictorial view of tool and machined workpiece is shown in Fig. 2a, b.

Table 1 Chemical composition of specimen

C	Si	Cr	Mn	Fe
1.35	0.70	0.90	0.30	Rest

Fig. 1 Schematic of the experimental setup



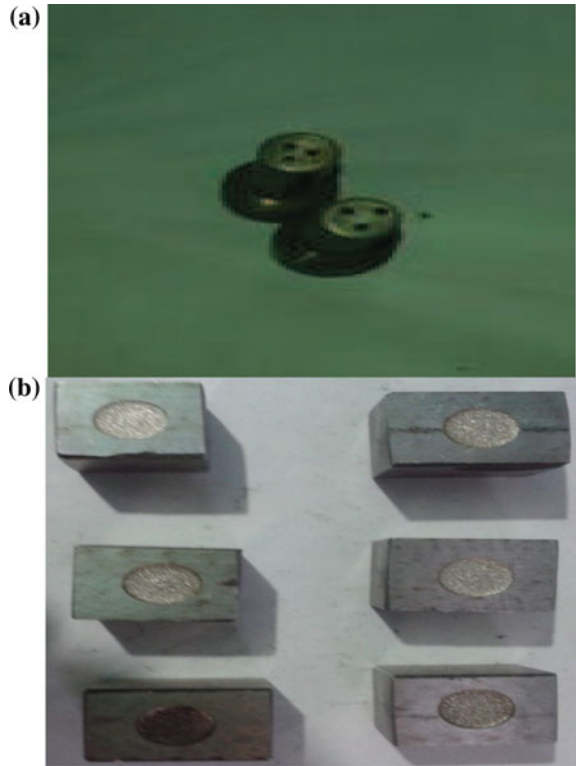
3 Experimentation

The gas-assisted die-sinking EDM with an eccentric-hole tool was performed on EDM machine. The machining time was fixed to be 15 min during experiments. Hydrocarbon-based oil (Kerosene) was employed as dielectric medium. For the experimental work, four controllable process factors, viz. discharge current, pulse on time, duty cycle and tool rotation speed, were selected. The values of these factors were selected based on trial experimentation and the capability of machine. Table 2 shows machining parameters range used during present work. For experimentation, open circuit voltage was kept at 60 V [13].

Table 2 Process factors used in present work

Machining parameter	Range
Discharge current (I_p) (A)	3–7
Pulse on time (T_{on}) (μs)	100–500
Duty cycle (DC)	0.52–0.76
Tool rotation speed (rpm)	100–900
Discharge gas pressure (mm Hg)	3–15

Fig. 2 a Pictorial view of tool **b** Pictorial view of workpiece after machining



The electrode wear ratio was evaluated as proportion of wear weight of tool to wear weight of specimen,

$$\text{Electrode wear rate} = \frac{\text{Wear weight of tool}}{\text{Wear weight of specimen}} \times 100 \tag{1}$$

The material removal rate was evaluated as proportion of wear weight of specimen to machining time [15],

$$\text{Material removal rate (mg/min)} = \frac{\text{Wear weight of the specimen}}{\text{Machining time}} \tag{2}$$

Specimens and tool electrodes were cleaned in acetone bath after each experiment before taking measurement of its weight loss. Electronic weighing machining (least count 0.1 mg) was put into service to measure weight loss of specimens and tool electrodes. A portable SR tester Mitutoyo (Model: SJ 201P) was used to quantify the SR of the machined workpiece.

Analysis of variance (ANOVA) has been performed based on experimental outcome of the test. The percentage contribution of each factor and error on response

determined by value of variance of error (v_e) and sum of squares for regression as obtained from ANOVA table.

$$\Delta Y = t_{\alpha/2}, \quad DF\sqrt{V_e} \quad (3)$$

where ΔY stands for the error in response, and t is value of horizontal coordinate with respect to designate degree of freedom (DF). The level of confidence interval is denoted by α , and its value is taken as 0.05. The variance of error of the anticipated process responses is denoted by V_e . The calculated error has been indicated in the following figures by employing the errors bars.

3.1 Effect of Process Factors on MRR

The influence of discharge current, pulse on time, duty cycle and tool rotational speed on MRR has been presented below.

Figure 3a depicts effect of discharge current on MRR for EDM process with liquid dielectric as well as liquid cum gaseous dielectric. It can be inferred that for both processes, MRR improves with an enhancement in discharge current. This can be reasoned because of a rise in discharge energy in machining zone which resulted in greater extent of melting and evaporation of workpiece [13]. It can be deduced that MRR is more with liquid cum gaseous dielectric than the conventional liquid dielectric only. It may be due to gas-assisted eccentric-hole tool with rotation improves flushing efficiency of molten material from machining gap, and hence, molten metal is removed from the inter-electrode gap more effectively.

Figure 3b shows effect of pulse on time on MRR for EDM process with liquid dielectric as well as liquid cum gaseous dielectric. It can be deduced from plot that MRR decreased with rise in the pulse duration. Due to tool rotation, the width of plasma channel is expanded at longer pulse on time value. Hence, magnitude of energy is decreased. So less melting and evaporation of specimen occurred, and reduced MRR is produced at longer pulse on time [8, 16]. Further, it can be deduced from the figure that MRR is high with liquid cum gaseous dielectric than the conventional liquid dielectric only.

Figure 3c presents effect of duty cycle on MRR with liquid dielectric as well as liquid cum gaseous dielectric. It can be deduced that MRR improves with an increase in duty cycle. This can be reasoned that magnitude of spark energy increases with a rise in duty cycle which results in more melting and vaporization of workpiece [13]. From plot, it can be seen that MRR is high with liquid cum gaseous dielectric than conventional liquid dielectric. It is probably due to the injection of compressed gas through rotary eccentric-hole tool which results in a faster removal of the eroded particles. This results in effective flushing of debris from inter-electrode gap.

From Fig. 3d, it can be seen that MRR increases with a rise in tool rpm and then decreases. This is due to the reason that immensity of centrifugal force rises with

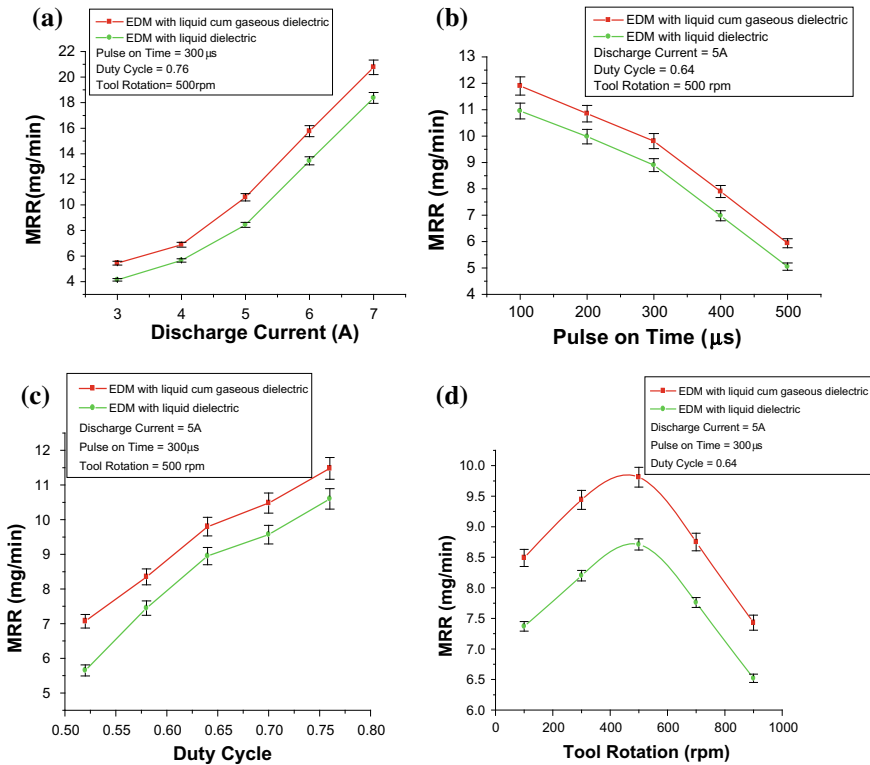


Fig. 3 Influence of a discharge current, b pulse on time, c duty cycle, d tool rotation on MRR

a rise in tool rpm which results in better evacuation of debris from inter-electrode gap, and hence, MRR is increased [13, 14]. Further, an increase in tool speed stirred up the plasma channel resulting in a decrease in the energy density. This results in reduced MRR.

3.2 Effect of Process Factors on EWR

Figure 4a depicts the effect of discharge current on EWR for EDM process with liquid dielectric as well as liquid cum gaseous dielectric. In both processes, EWR increases with a rise in discharge current. This is probably due to reason that magnitude of discharge energy increases with a rise in current resulting in more melting and evaporation of electrode [17, 18]. Moreover, it can be observed from Fig. 4a that EWR is less with liquid cum gaseous dielectric than the conventional liquid dielectric. This was probably due to reason that when compressed helium gas passes through rotary

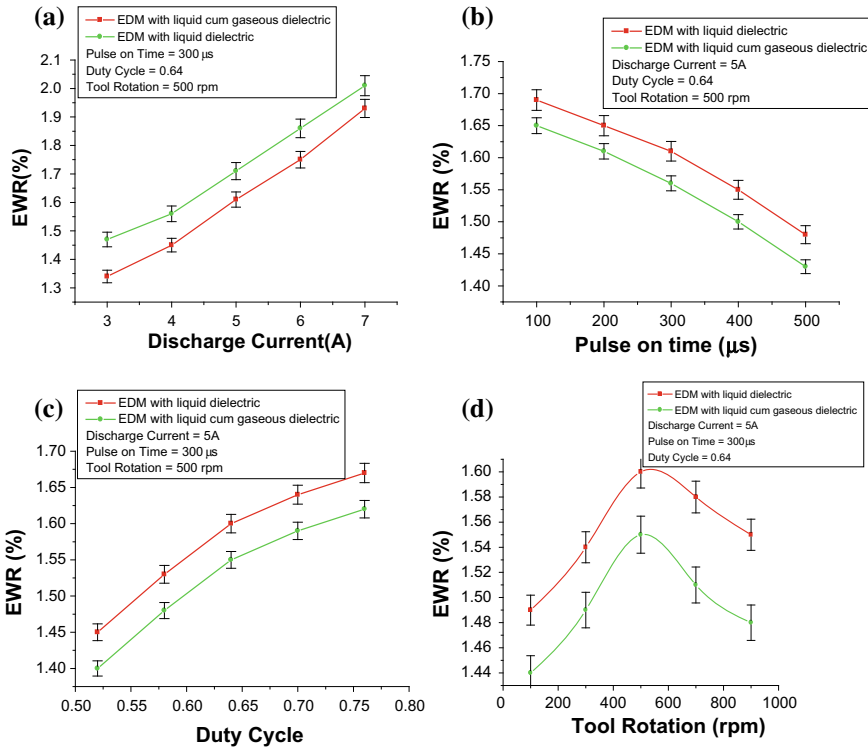


Fig. 4 Influence of **a** discharge current, **b** pulse on time, **c** duty cycle, **d** tool rotation on EWR

eccentric-hole electrode, it reduces the tool tip temperature significantly. This results in formation of smaller crater on tool surface; hence, EWR is reduced.

Figure 4b presents influence of pulse on time on EWR for EDM process with liquid dielectric as well as liquid cum gaseous dielectric. The tool wears decrease with an increase in pulse duration. This is probably because at longer pulse duration, carbon as a result of breakdown of hydrocarbon (dielectric) is deposited on tool surface. This deposited layer increased tool wear resistance [15]. Further, it can be observed from the figure that EWR is less with liquid cum gaseous dielectric than conventional liquid dielectric. It is probably because when compressed gas passes through the tool, it cools surface of the tool which results in lesser melting of the tool, and hence, EWR is reduced.

From Fig. 4c, it can be deduced that EWR rises with a rise in duty cycle. The magnitude of energy increases with an increase in duty cycle, and this results in an increased EWR [18]. Further, it can be seen that EWR is less in case of EDM process with liquid cum gaseous dielectric than EDM with conventional liquid dielectric. It is due to the use of eccentric-hole rotary tool in case of EDM process with liquid

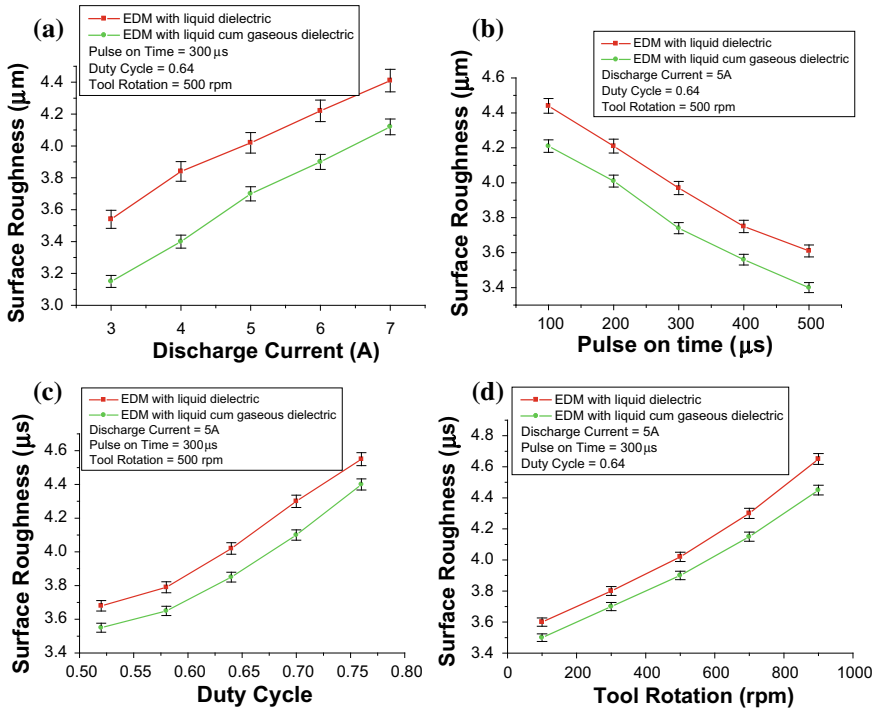


Fig. 5 Influence of a discharge current, b pulse on time, c duty cycle, d tool rotation on SR

cum gaseous dielectric enhances flushing efficiency which effectively carries away the eroded particles and heat.

Figure 5d reveals that EWR increases with a rise in tool rotation for both processes. Due to the increase in tool rotation, magnitude of centrifugal force is increased. Under the influence of increased centrifugal forces, the deposited black carbon is removed from tool surface [15]. This resulted in an increased EWR.

3.3 Effect of Process Factors on SR

Figure 5a shows influence of discharge current on SR during EDM process with liquid and liquid cum gaseous dielectric. It can be seen that for both processes, SR increases with a rise in discharge current. The spark densities of discharge increased with arise in current which causes a deeper crater and resulted in an increased surface roughness.

Further, it can be deduced from the figure that SR is less in case of EDM process with liquid cum gaseous dielectric than EDM with conventional liquid dielectric. Figure 5b presents influence of pulse on time on SR during EDM process with liquid

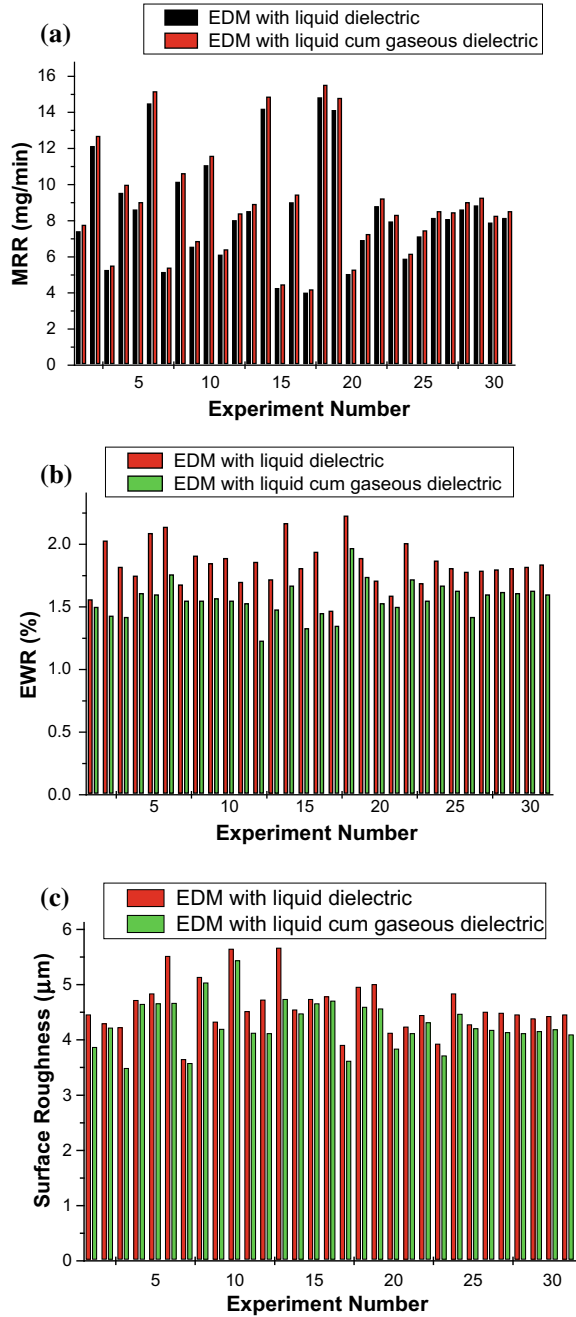
and liquid cum gaseous dielectric. From plot, it can be deduced that SR decreases with arise in pulse duration. It was probably due to expansion plasma channel which resulted in formation of shallow craters. Hence, surface roughness decreased with a rise in pulse on time. Further, it can be deduced from the figure that SR is less in case of EDM process with liquid cum gaseous dielectric than EDM with conventional liquid dielectric. Similar observation has been found by Chatopadhyay et al. [16] and Wang et al. [19] during their experimental investigation of rotary EDM process. Figure 5c shows influence of duty cycle on SR during EDM process with liquid and liquid cum gaseous dielectric. It can be seen that SR rises with a rise in duty cycle. The increase in duty cycle results in higher spark energy, and this resulted in enhanced surface roughness. Besides this, SR is less in case of EDM process with liquid cum gaseous dielectric than EDM with conventional liquid dielectric. Figure 5d presents the influence of tool speed on SR during EDM process with liquid and liquid cum gaseous dielectric. It can be inferred that SR starts decreasing with a rise in tool speed. It was probably due to increase in tool speed which improved the flushing of debris and resulted in less deposition of re-melted material; hence, high-surface roughness is obtained. Further, it can be observed from plot that SR is less in case of EDM process with liquid cum gaseous dielectric than EDM with conventional liquid dielectric. The decrease in surface roughness was probably due to high heat carrying capacity of argon with effective heat reaching the work surface is to a smaller extent. This caused small sized crater resulting in least surface roughness among the two processes.

The comparison of MRR for EDM machining with liquid dielectric and machining with liquid cum gaseous dielectric is shown in Fig. 6a. Under same combinations of process factors, MRR is found higher in EDM machining with liquid cum gaseous dielectric in comparison with EDM machining with conventional liquid dielectric. The use of compressed gas causes an enhancement in material vaporization due to reduction in temperature. This generates better removal of molten material and led to less molten material to be deposited on machined surface, resulting in a rise in MRR [20]. The use of liquid cum gaseous dielectric with eccentric-hole rotating electrode led to increase in MRR. Based on the results obtained, the use of liquid cum gaseous dielectric led to more than 65% increase in MRR for the same machining conditions.

Figure 6b reveals the comparison of EWR for EDM machining with conventional liquid dielectric and machining with liquid cum gaseous dielectric. For the same set of process parameters, EWR is found to be comparatively less in EDM machining with liquid cum gaseous dielectric in comparison of EDM machining with conventional liquid dielectric. This was probably because temperature of electrode tip reduced by compressed argon gas which minimized the melting and vaporization of the tool electrode thereby reducing its wear. The use of liquid cum gaseous dielectric with eccentric-hole rotating electrode leads to a reduction of EWR. Based on the results obtained, the use of liquid cum gaseous dielectric led to more than 27% reduction in EWR for the same combinations of process factors.

The comparison of SR for EDM machining with liquid dielectric and machining with liquid cum gaseous dielectric is shown in Fig. 6c. For the same set of process parameters, SR is found less in EDM machining with liquid cum gaseous dielectric in

Fig. 6 Comparative analysis of **a** MRR, **b** EWR, **c** SR of two processes



comparison with EDM machining with conventional liquid dielectric. Argon having high heat carrying capacity the effective heat reaching the work surface is less. This caused small sized crater resulting in less surface roughness while machining with liquid cum gaseous dielectric. The use of liquid cum gaseous dielectric with eccentric-hole rotating electrode led to reduction in SR. Based on the result obtained, the use of liquid cum gaseous dielectric led to more than 12% reduction in SR.

4 Surface Morphology of Specimen Machined Using Liquid and Liquid Cum Gaseous Dielectric in EDM Process

Surface crack formation can be observed by SEM image (refer Fig. 7). It is seen that formation of cracks on machined specimens using liquid cum gaseous dielectric is less in comparison with workpiece machined using conventional liquid dielectric.

This was probably due to cooling provided by compressed gas reduces the temperature of plasma channel and dielectric in tool tip region. As a consequence, the temperature of the crater drops significantly. This caused a reduction in residual stress [20] underneath of machined surface and propagates less surface cracks. Further, analysis of SEM images reveals that formation of recast layers per unit area relatively found less on surface of specimens machined with liquid cum gaseous dielectric in comparison of specimens machined with conventional liquid dielectric. The critical analysis of surface morphology reveals that surface integrity of specimens machined with liquid cum gaseous dielectric found to be better than specimens machined with conventional liquid dielectric under the same processing conditions.

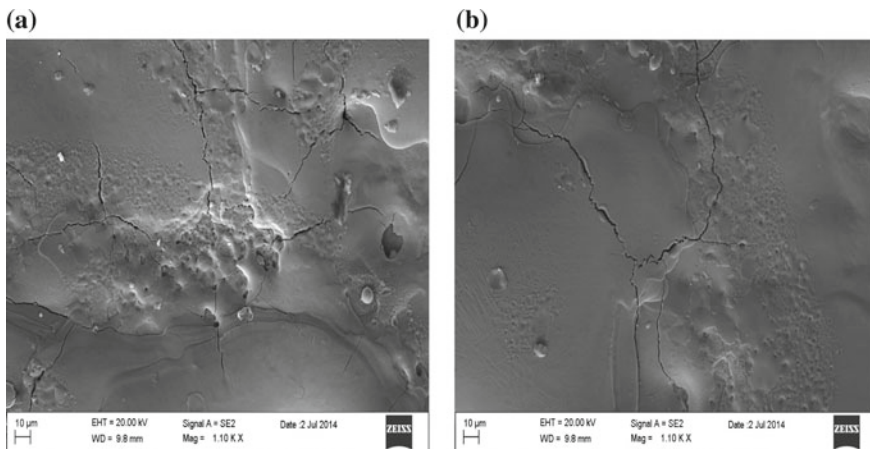


Fig. 7 Surface characteristic of workpiece machined by EDM using **a** liquid dielectric, **b** liquid cum gaseous dielectric

5 Conclusions

In present study, a hybrid process of EDM employing both liquid (commercial kerosene oil) and gas (compressed helium gas) as dielectrics has been developed successfully to machine the die steel specimens.

Parametric analysis of data revealed high MRR, low EWR and low SR when liquid cum gaseous dielectric was used as compared to EDM with conventional liquid dielectric, under same processing conditions.

Based on the result obtained, the use of liquid cum gaseous dielectric led to more than 65% rise in MRR, 27 and 12% reduction in EWR and SR, respectively, in comparison with conventional EDM with liquid dielectric.

The examination of machined surface revealed that the formation of recast layers and surface cracks decreased in EDM with liquid cum gaseous dielectric as compared to EDM with conventional liquid dielectric.

The critical analysis of surface morphology reveals that surface integrity of specimens machined with liquid cum gaseous dielectric found to be better than specimens machined with conventional liquid dielectric under the same processing conditions.

References

1. Ho KH, Newman ST (2003) State of the art electrical discharge machining (EDM). *Inter J Mach Tools Manuf* 43:1287–1300
2. Singh NK, Pandey PM, Singh KK, Sharma MK (2016) Steps towards green manufacturing through EDM process: a review. *Cogent Eng* 3:1272662
3. Ramani M, Cassidenti ML (1985) Inert gas electrical discharge machining. NASA Technol NPO 15660
4. Kunieda M et al (1991) Improvement of EDM efficiency by supplying oxygen gas into gap. *CIRP Ann Manuf Technol* 40:215–218
5. Kunieda M, Yoshida M (1997) Electrical discharge machining in gas. *Ann CIRP* 46(1):143–156
6. Yu Z, Jun T, Kunieda M (2004) Dry electrical discharge machining of cemented carbide. *J Matter Process Technol* 149(1–3):353–357
7. Soni et al (1994) Microanalysis of debris formed during EDM of titanium alloy and die steel. *Wear* 177(1):71–79
8. Mohan B, Rajadurai A, Satyanarayana KG (2002) Effect of SiC and rotation of electrode on electric discharge machining of Al-SiC composite. *J Mater Process Technol* 124:297–3042
9. Kuppan P, Rajadurai A, Narayanan S (2008) Influence of EDM process parameters in deep hole drilling of Inconel 718. *Inter J Adv Manuf Technol* 38:74–84
10. Koyano T, Suzuki S, Hosokawa A, Furumoto T (2016) Study on the effect of external hydrostatic pressure on electrical discharge machining. In: 18th CIRP conference on electro physical and chemical machining (ISEM XVIII), *Procedia CIRP*, vol 42, pp 46–50
11. Aliakabari E, Baseri H (2012) Optimization of machining parameters in rotary EDM process by using the Taguchi method. *Inter J Adv Manuf Technol* 62(9–12):1041–1053
12. Plaza S, Sanchez J, Perez E, Gill R, Izquierdo B, Ortega N, Pombo I (2014) Experimental study on micro EDM-drilling of Ti6Al4V using helical electrode. *J Precis Engg* 38(4):821–827
13. Singh NK, Pandey PM, Singh KK (2016) EDM with air assisted multi-hole rotating tool. *Mater Manuf Process* 31(14):1872–1878

14. Yoshida M, Ishii Y, Ueda T (2017) Study on electrical discharge machining for cemented carbide with non-flammable dielectric liquid: Influence of form of oxygen supplied to dielectric liquid on machining Proc IMechE Part B: J Eng Manuf. <https://doi.org/10.1177/0954405417706995>
15. Teimouri R, Baseri H (2012) Effects of magnetic field and rotary tool on EDM performance. J Manuf Process 14(3):316–322
16. Chattopadhyaya KD, Verma S, Satsangi PC, Sharma PC (2009) Development of empirical model for different process parameters during rotary electrical discharge machining of copper–steel (EN-8) system. J Mater Process Technol 209(3):1454–1465
17. Koshy P, Jain VK, Lal K (1993) Experimental investigation into electrical discharge machining with rotating disk electrode. J Prec Eng 15:6–15
18. Srivastava V, Pandey PM (2012) Experimental investigation on electrical discharge machining process with ultrasonic-assisted cryogenically cooled electrode. Proc IMechE Part B: J Eng Manuf 227(2):301–314
19. Wang CC, Yan BH (2000) Feasibility study of rotary electrical discharge machining with ball burnishing for Al₂O₃/6061Al composite. Int J Mach Tools Manuf 40:1403–1421
20. Srivastava V, Pandey PM (2012) Performance evaluation of electrical discharge machining (EDM) process using cryogenically cooled electrode. Mater Manuf Process 27(6):683–688

Effects of Welding Parameters in Friction Stir Welding of Stainless Steel and Aluminum



Pankul Goel, A. W. Mohd, Nidhi Sharma, A. N. Siddiquee
and Zahid A. Khan

Abstract Joining of dissimilar materials (DMs) is the growing demand of various industries to attain distinct features of individual material. In this regard, friction stir welding (FSW) has emerged as a unique joining method to weld DMs among various joining techniques. FSW is a solid-state welding process used to join similar and dissimilar materials (DMs). In this study, DMs AA7475-T761 aluminum alloy (AA) and AISI 304 stainless steel (SS) are joined using FSW. These DMs are widely lap welded in industries such as space shuttles and aerospace. Friction stir welded (FSWed) half-lap joints are obtained and analyzed under three different tool rotation speeds: 450, 560, and 710 rpm. The joint quality is analyzed by tensile strength and microstructure. The improper heat generation at different tool rotation speeds affected joint quality considerably. The defects such as tunneling and void were observed which resulted in poor efficiency of joints. The joint efficiency was obtained maximum 62.83% of the base material (BM) AA 7475 at rotational speed 560 rpm with 6.89% elongation.

Keywords Friction stir welding · AA7475 · AISI 304 · Microstructure · Tensile strength

P. Goel (✉) · A. W. Mohd · N. Sharma · A. N. Siddiquee · Z. A. Khan
Department of Mechanical Engineering, Jamia Millia Islamia, New Delhi, India
e-mail: pankul.goel@gmail.com

A. W. Mohd
e-mail: wahidatif89@gmail.com

N. Sharma
e-mail: nid.sharma83@gmail.com

A. N. Siddiquee
e-mail: arshadnsiddiqui@gmail.com

Z. A. Khan
e-mail: zakhan@jmi.ac.in

1 Introduction

Recently, the manufacturing industries are using DMs to produce the products of lightweight with high strength and high corrosion resistance, etc. Moreover, another criterion is to derive the best combination of mechanical properties of DMs to improvise the functioning of product with cost reduction. In this context, several industries have adopted DMs for manufacturing of the large number of products for the sectors such as aerospace, automotive, and shipbuilding [1, 2]. AA is a low-temperature material (LTM) and finds a wide application in aerospace, railcars, automobile, and shipbuilding sectors, etc., being enriched with features such as low absorbing energy, anti-corrosive, good forming, and high strength-to-weight ratio [3]. SS is a high-temperature material (HTM) and finds extensive applications in outer panels, engine parts, fuel tanks, and exhaust parts of various industries [4]. The extensive applications and several features of both AA and SS put emphasis to join these DMs using an appropriate technology. A new green technology, friction stir welding (FSW), was invented by “The Welding Institute” (TWI), UK in 1991 [5]. FSW was initially employed on LTM, but its inherited features have developed and matured this process to weld HTM as well as DMs [6, 7]. FSW is a solid-state welding process, due to which it overcomes the various quality issues associated with fusion welding processes such as occurrence of solidification cracks, distortion, porosity, and significant change in microstructure. To perform the FSW, both BMs are firmly clamped in a competent fixture. A non-consumable tool (with rotary motion) with the suitable profile is plunged into the faying surfaces of the fixed plates. The frictional force generated between tool shoulder and plates produces the significant amount of heat causing softening of materials. Tool pin stirs this soften materials for mixing of DMs [8]. During traversing of the tool, tool pin executes severe plastic deformation between the faying surfaces (along the joint line) to produce good quality of weld in solid-state condition as shown in Fig. 1 [9].

Limited literatures are observed on the joining of DMs using FSW. Inertia friction welding on 6061-T6 AA and AISI 1018 steel was conducted by Taban et al. [10] for different welding parameters. They obtained tensile strength in the range

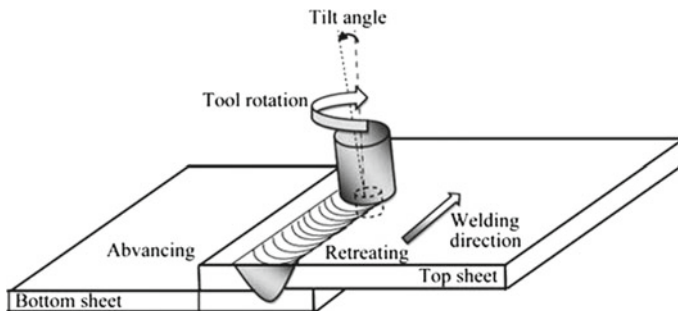


Fig. 1 Schematic diagram of friction stir welding

of 170–250 MPa and noticed intermetallic compound (IMC) layer consisting two phases of FeAl and Fe₂Al₅. Dehghani et al. [11] investigated the effects of welding parameters and tool geometry on FSWed joint of AA 3003-H18 and mild steel. They observed large steel fragments and platelets of small sizes in the weld nugget region. The effects of FSW parameters on dissimilar 5050 AA–304 SS were scrutinized by Habibina et al. [12]. They found sound quality of joint by decreasing the tool rotational speed coupled with increasing the traverse speed. Consequently, tensile strength was attained maximum 175 MPa at tool offset 1.5 mm due to decreasing defects in the weld nugget region. Yazdipour et al. [13] conducted the FSW on AA 5083-H321 and 316L SS, at the tool rotational speed of 280 rpm, and scrutinized the effects of FSW parameters on tensile strength and microstructure at different regions. They found maximum tensile strength of 238 MPa as compared to 320 MPa of BM AA5083. Chen [14] optimized friction stir welding parameters for joining of AA6061 to SS400. He obtained optimized strength at tool rotational speed of 550 rpm and transverse speed of 0.9 mm/s. The reported literature shows that majority of portion for AA and SS is on AA5xxx, 6xxx series. However, limited studies are reported on 3xxx for dissimilar joining with steel. The high strength AA7xxx alloys which are extensively preferred in aero and aerospace applications alongside Ti and SS alloys are very poorly reported. Due to large potential, the scarceness of literature put impetus that understanding the maturity of science and technology regarding joining of this potential dissimilar pair is very crucial. Hence, an attempt is made in this study to join Al 7475–AISI 304 SS for half-lap joint configuration using FSW. The metallurgical characteristics and tensile strength of joints were analyzed and presented.

2 Experimental Method

In all experiments, the plates of BMs were used for length 150 mm and width 50 mm. However, the thickness of AA and SS plates was 1.5 and 1 mm, respectively. The chemical composition of DMs AA 7475 and AISI 304 SS is shown in Tables 1 and 2, respectively. Mechanical and thermal properties of the BMs are shown in Table 3.

Table 1 Chemical composition of AA7475 (wt%)

Material	Al	Zn	Mg	Cu	Cr	Si	Ti	Fe	Mn
AA7475	Base	5.26	2.22	1.64	0.20	0.05	0.02	0.10	0.01

Table 2 Chemical composition of AISI 304 (wt%)

Material	Fe	Cr	Mn	Mg	Cu	Si	Ni	N	C
AISI 304	Base	12.87	9.43	2.22	1.34	0.34	0.31	0.15	0.08

Table 3 Mechanical and thermal properties of AA7475 and AISI 304

Material	UTS (MPa)	Yield strength (MPa)	Elongation (%)	Melting point (°C)	Thermal conductivity (W/mK)
AA7475	452	419	13	477–635	163
AISI 304	505	215	70	1400–1450	16.2

The HTM AISI 304 SS was kept lower on the advancing side being associated with high temperature. However, LTM AA 7475 was kept over SS on retreating side of the joint line as associated with low temperature. A non-consumable tungsten carbide tool consisting shoulder diameter of 20 mm with the cylindrical tapered pin of length 1.7 mm, root diameter 6.5 mm with semi-cone of angle 20° was used to conduct FSW. In all three experiments, parameters such as tool traversing speed 31.5 mm/min, plunge depth 2.2 mm, the thickness ratio of AA to SS sheet 1.5:1 and tool to workpiece tilt angle 1.5° were kept fixed. The tool rotation speed was varied to obtain half-lap joint configuration of AA 7475 to AISI 304 as shown in Fig. 2. These tensile test samples were prepared in accordance with the ASTM: E8M standard.

FSW was conducted by mounting and fixing of dissimilar plates in a robust fixture. Subsequently, three runs were performed (experimental plan shown in Table 4), on retrofitted robust vertical milling machine (Make: Bharat Fritz Werner, India) as shown in Fig. 3. Joint quality was analyzed through tensile strength and microstructure. Tensile test coupons were prepared according to ASTM: E8 M, and tensile strength were evaluated using a computer interfaced tensometer. The experimental plan and tensile strength of each experiment are shown in Table 4. To analyze microstructure analysis, samples were polished using standard procedure, and subsequently, AA and SS were etched separately, using different reagents. AA 7475 was etched with Keller's reagent (HF 2 ml + HCl 3 ml + HNO₃ 5 ml + H₂O 190 ml), and AISI 304 was etched by reagent consisting of ferric chloride 45 gm + copper ammonium chloride 9 gm + HCl 150 ml + H₂O 75 ml. The microstructure analysis was conducted using stereo zoom microscope.

**Fig. 2** Joint configuration in tensile test coupon

Table 4 Experimental plan, tensile strength, and joint efficiency

Experiment no.	Tool rotational speed (rpm)	Tensile strength (MPa)	Joint efficiency (%)
1	450	159	35.18
2	560	284	62.83
3	710	195	43.14

**Fig. 3** FSW machine

3 Results and Discussion

3.1 Tensile Strength Analysis

In this study, the effect of tool rotation speed is evaluated on the joint quality of DMs. The joint quality is analyzed by tensile strength and microstructure. The tensile strength and joint efficiency of all experiments are shown in Table 4. Welded sample of experiment 1 was found with lowest ultimate tensile strength of 159 MPa. This is on account of low heat generation at low tool rotation speed (450 rpm) which could not soften AISI 304 being HTM and tool resulted inadequate stirring of steel. Due to this, the pin could not shear off the HTM and inadequate material movement resulted in insufficient mixing of DMs. However, welded sample of experiment 3 was attained with little better tensile strength of 195 MPa. This joint was produced at highest tool rotation speed (710 rpm), but again quality of joint was deteriorated

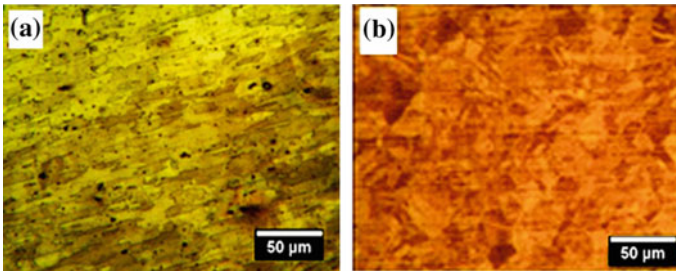


Fig. 4 Microstructure of BM **a** AA 7475, **b** AISI 304

because of excessive heat generation. This results in excessive plastic deformation of LTM at stir zone (SZ) and leads to turbulent flow of material causing voids which resulted in poor strength of joint. However, highest tensile strength 284 MPa was obtained at tool rotation speed (560 rpm) in experiment 2. The joint efficiency was observed with 62.83% of BM AA 7475 (strength 452 MPa) with percent elongation of 6.98.

3.2 Microstructural Analysis

The microstructure of the BM of AA 7475 and AISI 304 is shown in Fig. 4a, b, respectively.

Further, the investigations are well supported by microstructure correlation. For sample 2, microstructures of heat-affected zone (HAZ), TMAZ, and SZ are shown in Fig. 5a–c. In HAZ, coarse grains are observed similar to the BM as this area is affected only by the thermal cycles developed during the process [15]. In TMAZ on AA side, the aluminum grains got elongated and surrounded over SS as shown in Fig. 5b. This might be due to partial recrystallization. Subsequently, grains are refined in SZ in comparison with both TMAZ/HAZ due to intense plastic deformation caused by tool stirring [15] as shown in Fig. 5c. In the present study, tool rotational speed 560 rpm coupled with traverse speed 31.5 mm/min produced optimum heat generation which has resulted in dynamic recrystallization [16]. As an effect, the refined grain structure with better mechanical properties is obtained. The mixing of AA 7475 is observed in SZ (SS side) as shown in Fig. 6.

Fractograph was performed and analyzed on all fractured tensile test samples as shown in Fig. 7a–c. The defects tunnel and voids were observed in FSWed samples 1 and 3, respectively. These defects were appeared due to insufficient mixing of DMs and causes for imminent failure. However, DMs were well segregated in sample 2 around the SZ. Apart from the topography of the fractured surface, an elemental profile was also spectrographed around the region from where the fractograph was taken (sample 2). The elemental topographic surface scanned through the electron

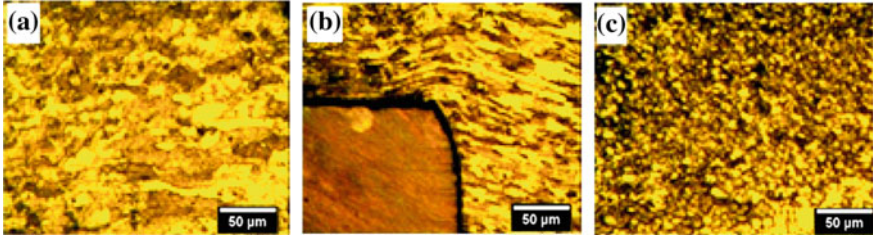


Fig. 5 Microstructure of AA 7475 a HAZ, b TMAZ, c SZ

Fig. 6 Microstructure: mixing of AA 7475 on SS SZ side

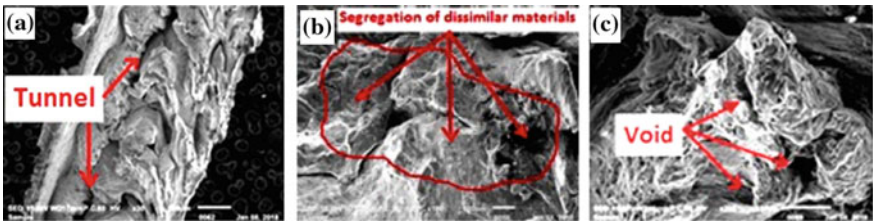
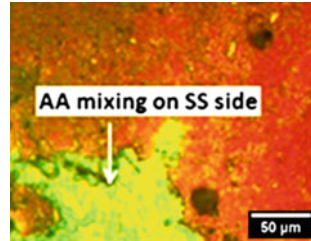


Fig. 7 Fractograph of the fractured surface of tensile specimens a sample 1, b sample 2, c sample 3

dispersive spectroscopy (EDS) is shown in Fig. 8. This confirms that HTM is well distributed on LTM AA side. Similarly, the LTM is also showing good mixing on HTM SS side. This reflects that both DMs are well distributed around SZ and pin has steered the soften materials and consolidated the DMs from both the sides. It is interesting to note that the elemental data obtained from the EDS (as shown in Fig. 9) confirm the presence of constituents of both DMs.

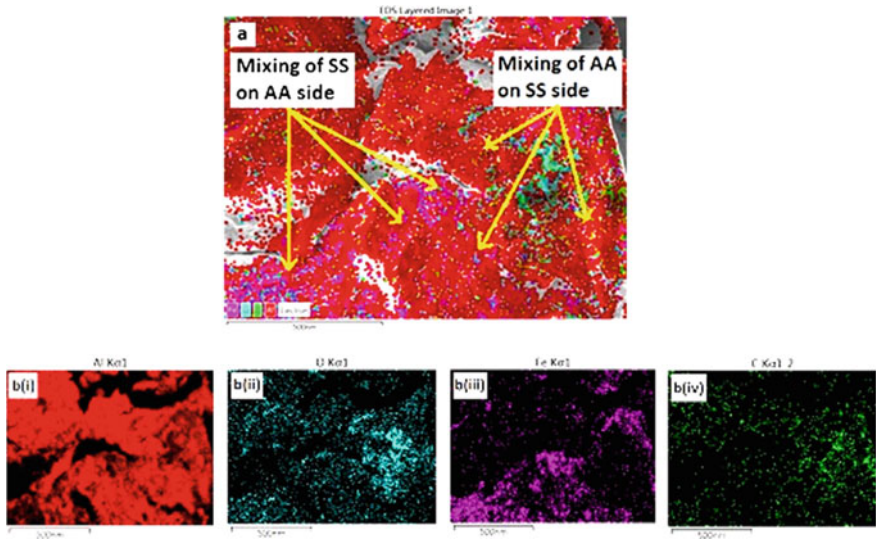
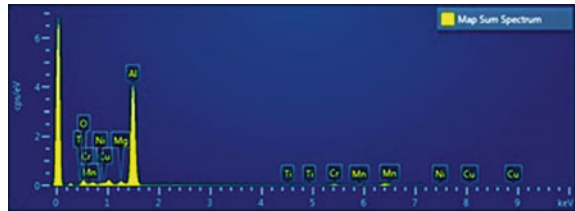


Fig. 8 Elemental surface topography on the fractured surface of sample 2

Fig. 9 EDX spectra for the fractured surface of sample 2



4 Conclusion

DMs AA7475-T761 and AISI 304 were successfully joined for half-lap joint configuration using FSW at tool rotational speed 560 rpm. The following conclusions are drawn from the analysis of the results of the present study:

- The tensile test of the FSWed joint was measured with ultimate tensile strength (UTS) of 284 MPa with joint efficiency of 62.83% against BM (AA) strength of 452 MPa with a percent elongation of 6.98.
- Joints were observed with poor strength at low rotational speed (450 rpm) due to the formation of tunneling defect, and the poor strength was attained at high rotational speed (710 rpm) due to formation of voids.
- In sample 2, the SZ and TMAZ confirm significant grain refinement which contributed to the strength of the joint.
- The optimum rotational speed of tool (560rpm) plays a significant role to attain joints with high quality.

- The optimum rotational speed of the tool steers the DMs significantly which can enhance the microstructure and properties of the SZ and resulted heat generation neither worsens the mechanical properties of HAZ and TMAZ and neither cause defects in SZ.

References

1. Barnes T, Pashby I (2000) Joining techniques for aluminium spaceframes used in automobiles. *J Mater Process Technol* 99(1–3):62–71
2. Hirsch J (2014) Recent development in aluminum for automotive applications. *Trans Nonferrous Met Soc China* 24(7):1995–2002
3. Goel P, Siddiquee AN, Khan NZ (2018) Investigation on the effect of tool pin profiles on mechanical and microstructural properties of friction stir butt and scarf welded aluminium alloy 6063. *Metals* 8(1):74
4. Uzun H, Donne CD, Argagnotto A, Ghidini T, Gambaro C (2005) Friction stir welding of dissimilar Al 6013-T4 To X5CrNi18-10 stainless steel. *Mater Des* 26(1):41–46
5. Thomas WM, Nicholas ED, Needham JC, Murch MG, Temple-Smith P, Dawes CJ (1991) Friction stir butt welding international patent application no. PCT/GB92/02203 and great britain patent application no. 9125978.8
6. Haghshenas M, Gerlich AP (2018) Joining of automotive sheet materials by friction-based welding methods: a review. *Eng Sci Technol Int J* 21(1):130–148
7. Rafiei R, Ostovari Moghaddam A, Hatami MR, Khodabakhshi F, Abdolazadeh A, Shokuhfar A (2017) Microstructural characteristics and mechanical properties of the dissimilar friction-stir butt welds between an Al–Mg alloy and A316L stainless steel. *Int J Adv Manuf Technol* 90(9–12):2785–2801
8. Sharma N, Siddiquee AN, Khan ZA, Mohsin T (2017) Material stirring during FSW of Al–Cu: effect of pin profile. *Mater Manuf Process* 33(7):786–794
9. Gharavi F, Matori KA, Yunus R, Othman NK, Fadaeifard F (2016) Corrosion evaluation of friction stir welded lap joints of AA6061-T6 aluminum alloy. *Trans Nonferrous Met Soc China* 26(3):684–696
10. Taban E, Gould JE, Lippold JC (2010) Dissimilar friction welding of 6061-T6 aluminum and AISI 1018 steel: Properties and microstructural characterization. *Mater Des* 31(5):2305–2311
11. Dehghani M, Mousavi SA, Amadeh A (2013) Effects of welding parameters and tool geometry on properties of 3003-H18 aluminum alloy to mild steel friction stir weld. *Trans Nonferrous Met Soc China* 23(7):1957–1965
12. Habibnia M, Shakeri M, Nourouzi S, Givi MKB (2015) Microstructural and mechanical properties of friction stir welded 5050 Al alloy and 304 stainless steel plates. *Int J Adv Manuf Technol* 76(5–8):819–829
13. Yazdipour A, Heidarzadeh A (2016) Effect of friction stir welding on microstructure and mechanical properties of dissimilar Al 5083-H321 and 316L stainless steel alloy joints. *J. Alloys Compd* 680:595–603
14. Chen T (2009) Process parameters study on FSW joint of dissimilar metals for aluminum–steel. *J Mater Sci* 44:2573–2580
15. Wahid MA, Khan ZA, Siddiquee AN (2018) Review on underwater friction stir welding: a variant of friction stir welding with great potential of improving joint properties. *Nonferrous Met Soc China* 28(1):193–219
16. Mostafapour A, Jamalian HM, Bolghari AJ, Chamanara A (2017) Comprehensive investigation into the dissimilar friction stir welding of Al 2024 to St37. *Int J Adv Manuf Technol* 93(9–12):3599–3613

Case Study of Critical Success Factors Affecting Knowledge Management in Small- and Medium-Sized Enterprises in Developing State: Steel Sector



Agrawal Animesh and Suraj Kumar Mukti

Abstract The small- and medium-sized enterprises (SMEs) need to compete with many other established organizations. Knowledge management (KM) may be the appropriate strategic tool for businesses to compete with the other established organizations. So there is a need of the adopting the knowledge management in SMEs to compete the competitors and satisfying the customer. But in this stage, adoption of KM is a very tedious task for an organization. The objective of this study to present a better way by implementing the KM in an organization and do something better for the organization for the improvement of customer satisfaction and increase competitive level as well. In this study, the present scenario of SMEs in Chhattisgarh state is taken under consideration. In this study, the factors affecting the knowledge management for SMEs, mainly in steel sector organizations have been focused and decided a critical success factor affecting the industries from previous literatures. After the identification of the critical success factors from the previous literature, some factors which affect the steel sector most are considered. To test the reliability of the questionnaire, Cronbach's alpha has been used by SPSS software.

Keywords Knowledge management · Success factors · SMEs · Steel sectors

1 Introduction

Knowledge management (KM) plays a vital role in an organization, whether the organization is small sized or a very reputed and settled one. Although this fact that the KM implementation is a very tedious task for implementing in any organization due to its initial settling cost or lacking organizational support. KM involves a high risk in implementation in the organization. In the implementation of KM, the community of practice (COP) plays an important role. The COP is a group formed by the internal workers in which everybody is free to share ideas in the form of tacit

A. Animesh (✉) · S. K. Mukti
Department of Mechanical Engineering, National Institute of Technology,
492001 Raipur, India
e-mail: animeshgrw@gmail.com

or implicit knowledge. In that group, a supervisor is also appointed to monitor the whole activity of the group. If the idea shared by the group members is appropriate for company's success, the company provides them some platforms to implement those ideas after successful examination of the ideas [1]. For the implementation of KM, the company will take the responsibilities of risk factor. KM can be subdivided into two categories which are firstly the tacit knowledge management and secondly the implicit knowledge management [2].

Tacit knowledge management involves the management of ideas present in the mind but cannot be represented in the hard copy. It is difficult to transfer the tacit knowledge to another person by writing, notes, and lectures. Only the tacit to tacit knowledge can be transferred e.g. if anybody knows how to ride the bicycle, so this knowledge cannot be transferred by giving notes of any kind of written material to another person [3].

Implicit knowledge management involves the management of ideas which can be transferred from one person to another one by giving some written materials or by giving notes. A good example of implicit knowledge is to tell the worker how to work in any organization [4].

2 Literature Review

Many of the researchers have studied the knowledge management philosophy for the improvement of organizational goal. Some of the researchers have discussed the knowledge sharing and application, and some others have suggested some critical factors affecting knowledge management. The publication related knowledge sharing and application of knowledge management is described below.

Sanchez and Mahoney discussed the interrelationships of item outline, association configuration, forms for learning and overseeing knowledge, and aggressive system. This paper utilized the standards of almost decomposable frameworks to research the capacity of institutionalized interfaces between segments in an item configuration to implant coordination of item improvement forms [5]. Muthuveloo et al. have proposed to investigate and decide whether associations have procedures for unsaid knowledge management which is relied upon to impact their hierarchical execution both tangibly and intangibly [6]. Ruggles has discussed the organization using the knowledge management and what firm is doing to manage the knowledge. In this literature, barrier for applying knowledge management is also discussed and focused on the intranet using [7].

Lugo-Mata et al. have performed a non-exploratory, cross-sectional, and expository investigation with an accommodation test utilizing an organized study to quantify the level of knowledge about blood vessel hypertension. Recurrence figurings and multivariate investigation were performed to decide the relationship between a few components with the level of knowledge, which is considered factually huge at $p < 0.05$ [8]. Pillania [9–11] distributed a progression reports of papers about KM related

issues in SMEs. This paper investigated the information utilization for car production in India and concentrated on a few parts of KM in SMEs in India.

3 Research Methodology

In this paper, the statistical approaches with grounded theory have been adopted that aims to test the reliability of the factors affecting in the SMEs.

3.1 Identification of Critical Success Factor

The factors have been selected from the previous literature. Some of the literatures have discussed different affecting factors for knowledge management for different kinds of industries. So in this research, the factors are first taken by the previous literatures and then the selections of some factors have been done by interview of the management persons.

Miklosik and Zak researched knowledge management execution in Slovak Companies, in an examination that intended to explore and introduce a structure for the viable evacuation of obstructions to knowledge management. The creator explored the seven basic knowledge management requirements.

- Business and technology strategy
- Organizational control
- Information sharing culture
- Knowledge representation
- Organizational structure
- Managerial command and control
- Economic return [12].

3.2 Hypothesis Formation

To identify the critical success factors, some hypothesizes have been made and tested. List of hypothesis related to the critical success factors of knowledge management in SMEs is given below.

H1: There is an association between the business and technology strategy of the business and the way firm deals with KM issues.

Business and technology have a very significant role in the organization for better implementation of knowledge management which involves a systematic approach. It involves a process for adoption of knowledge management; these systems can be

termed under technology strategy. The implementation of knowledge management is a very long-term job. For example, aiming to achieve the certain level is the process of three to four years of the plan [12].

H2: There is an association between the organizational control of the business and the way firm dealing with KM issues.

Without the support of top management along with the board members, it is impossible to motivate the team members in an organization for the enhancement of the organization. These people have some vision and mission strategies for moving forward and will be able to compete with others. Strong leadership is a very essential parameter for an organization. No systematic leadership will be implemented without the organizational control.

H3: There is an association between the information sharing culture of the business and the way firm deals with KM issues.

The rich form of information can be termed as knowledge which is equally important to the organization for its growth rate. For improving the productivity rate of an organization, top-level management persons need to understand the factors affecting knowledge management, which can improve the quality of the organization to compete with others. Many of the literatures have noticed that there is no motivation in most of the organization to share his information. The study also says that the people are afraid of sharing their knowledge with others due to lack of the communication, language, and responsibilities. It is very important to take initiative to the manager-level person to give some platform for sharing others' knowledge without hesitation [13].

H4: There is an association between the knowledge representation of the business and the way firms deal with KM issues.

As far as the knowledge representation is concerned, one needs to be advised and motivated to convert the tacit knowledge to implicit knowledge. This is done for the purpose of preservation of the knowledge so that the junior-level (unskilled) person can use the knowledge whenever it will be needed. As Solik discussed the use of electronic gadgets for instant use of the knowledge, by the use of electronic media, it can transform the culture, values, and relationship [14, 15].

H5: There is an association between the organizational structures of the business dealing with KM issues.

To distinguish the highlights of authoritative structure that helps or encourages the advancement of knowledge management process. This will enable workers to take the better-preferred standpoint of their individual capacities, to create association schedules and to expand the estimation of their commitments on account of the opportunity of activity they are given. The first aim of any firm should involve the knowledge creation and transmission. The generation of knowledge can be termed as a strategic resource of an organization [16].

H6: There is an association between the managerial command and control of business dealing with KM issues.

The top-down principle is used in managerial command and control. Only the upper-level persons have the authority/power to implement an idea and solution, and lower-level persons do not have the power. Financial and non-financial effect of KM is untouched by most of the companies. Only a few of the company has incorporated already.

H7: There is an association between the economic return of business dealing with KM issues.

To measure the financial impact is a very tedious task for an organization. It is essential to have the support of board members and owner of the company. Non-financial to financial targets are very necessary. Certain things have to define like how the satisfaction of the employees can be improved for the contribution of the income, how can the quality of product be improved by financial effect, and how market opportunity can be discovered in terms of financial assets.

3.3 Sample Selection Method

The population can be defined as the total number of units in any investigation, and sample can be taken as part of the population that can represent the view of the population. The sample can be selected as per the different criteria like the experience of the people, age, and post. For this research purpose, a sample size of 150 people has been taken from different small and medium enterprises according to the experiences. In this sample, managerial-level person and shift incharges were involved to fill the questionnaire. Minimum experience of the person is more or equal than 10 years. The data have been analyzed using the SPSS software version 20.

3.4 Data Analysis

Cronbach's alpha technique has been adopted for the validation of hypotheses. Cronbach's alpha is a measure of internal consistency if the value of α is greater than 0.9 than it shows the excellency and between 0.8 to 0.9 shows the good value. The value of alpha (α) less than 0.7 is questionable. Thus, the reliability is confirmed in this research.

The overall reliability of the questionnaire is presented in Table 1. Table 2 gives the reliability for every set of the questionnaire (Table 3).

Table 1 Reliability statistics

Cronbach's alpha	Cronbach's alpha based on standardized items	No. of items
0.899	0.898	14

Table 2 Item-total statistics

	Scale mean if item deleted	Scale variance if item deleted	Corrected item-total correlation	Cronbach's alpha if item deleted
Q-1	43.67	83.174	0.443	0.898
Q-2	43.95	80.300	0.577	0.893
Q-3	44.24	81.029	0.576	0.893
Q-4	44.07	77.432	0.734	0.886
Q-5	43.93	81.700	0.600	0.892
Q-6	43.77	79.465	0.534	0.895
Q-7	43.85	78.032	0.645	0.890
Q-8	43.99	78.638	0.644	0.890
Q-9	44.04	75.368	0.752	0.884
Q-10	43.87	83.870	0.411	0.899
Q-11	43.67	83.174	0.443	0.898
Q-12	43.95	80.300	0.577	0.893
Q-13	44.24	81.029	0.576	0.893
Q-14	44.07	77.432	0.734	0.886

Table 3 Scale statistics

Mean	Variance	Standard deviation	No. of items
47.33	92.143	9.599	14

4 Result and Discussion

On the basis of data collection and data analysis, conclusion was made that all the factors discussed above are important for the success of SMEs.

The top-level management and the experienced person (experience more than or equal to 10 years) from different branches were involved to fill the questionnaire. The research focuses mainly on the SMEs situated in Chhattisgarh region. Here, different companies have been taken as a population and 150 people involved as a sample size for the research. In this research first, the factors have identified and the questionnaire has prepared according to that identified factors.

5 Conclusion

This research initiates the factors affecting knowledge management in small and medium enterprises. The focus of the research was concentrated on SMEs in Chhattisgarh state. By this research, it is very clear that KM plays a very important role in the stable development of any organization. It indicates that factors affecting SMEs like business and technology strategy, organizational control, information sharing culture, knowledge representation, organizational structure, managerial command and control and economic return are very important for the SMEs to compete with the other companies. It can be noticed that many of the companies are focusing toward personnel benefits, but this research shows that knowledge management is more important than others.

References

1. Palincsar AS, Magnusson SJ, Marano N, Ford D, Brown N (1998) Designing a community of practice: principles and practices of the GIsML community. *Teach Teach Educ* 14(1):5–19
2. De Jong T, Ferguson-Hessler MGM (1996) Types and qualities of knowledge. *Educ Psychol* 31(2):105–113
3. Smith EA (2001) The role of tacit and explicit knowledge in the workplace. *J Knowl Manage* 5(4):311–321
4. Frappaolo C (2008) Implicit knowledge. *Knowl Manage Res Pract* 6(1):23–25
5. Sanchez R, Mahoney JT (1996) Modularity, flexibility, and knowledge management in product and organization design. *Strateg Manage J* 17(S2):63–76
6. Muthuveloo R, Shanmugam N, Teoh AP (2017) The impact of tacit knowledge management on organizational performance: evidence from Malaysia. *Asia Pac Manage Rev* 22(4):192–201
7. Ruggles R (2014) The state of the notion : knowledge management in practice 40(3):80–89
8. Lugo-Mata AR, Urich-Landeta AS, Andrades-Pérez AL, León-Dugarte MJ, Marcano-Acevedo LA, Jofreed López Guillen MH (2018) Factors associated with the level of knowledge about hypertension in primary care patients. *Med Univ*
9. Pillania RK (2005) Leveraging knowledge: Indian industry's expectations and shortcomings. *Glob Bus Rev* 6(2):231–249
10. Pillania RK (2006) State of organizational culture for knowledge management in Indian industry. *Glob Bus Rev* 7(1):119–135
11. Pillania RK (2008) Strategic issues in knowledge management in small and medium enterprises. *Knowl Manage Res Pract* 6(4):334–338
12. Miklosik A, Zak S (2015) Framework for effective removal of knowledge management implementation barriers. *Procedia Econ Financ* 30(15):513–521
13. Wang S, Noe RA (2010) Knowledge sharing: a review and directions for future research. *Hum Resour Manage Rev* 20(2):115–131
14. Solík M, Višňovský J, Láluňová J (2013) Media as a tool for fostering values in the contemporary society. *Eur J Sci Theol* 9(6):71–77
15. Brachman R, Levesque H (2004) Knowledge representation and reasoning, vol. 1
16. Claver-Cortés E, Zaragoza-Sáez P, Pertusa-Ortega E (2007) Organizational structure features supporting knowledge management processes. *J Knowl Manage* 11(4):45–57

Optimization of FSW Process Parameters During Joining of Al to Cu Using Taguchi-Based GA



Nidhi Sharma, Pankul Goel, M. A. Wahid, Zahid. A. Khan
and Arshad Noor Siddiquee

Abstract Friction stir welding (FSW) is a new and effective solid-state joining process and getting evolved to join the dissimilar materials such as aluminum (Al) and copper (Cu). FSW tool design, geometry, and FSW process parameters possess a considerable impact on the material movement and stirring during joining and govern the microstructure and mechanical properties of the joints. In the present study, the effect of the combination of different process parameters, i.e., shoulder diameter (A), welding speed (B), and rotational speed (C) on the ultimate tensile strength (UTS) during joining of Al-6101, and pure copper has been studied. The joining is performed using the cylindrical tool pin, and the Taguchi's L_9 standard orthogonal array for three process parameters each at three levels are chosen to perform the experimentation. The optimal combination of the FSW parameters yielding maximum UTS is determined using the ANOM (Analysis of Mean), and the significance of each parameter on the UTS is ascertained through ANOVA (Analysis of Variance). It is observed that the UTS of the FSWed joints varied significantly within the selected process parameter range. Further, the observed results were verified by applying genetic algorithm (GA) using the MATLAB software.

Keywords Aluminum · Copper · Friction stir welding · Genetic algorithm · Optimization · Taguchi

N. Sharma (✉) · P. Goel · M. A. Wahid · Zahid. A. Khan · A. Noor Siddiquee
Department of Mechanical Engineering, Jamia Millia Islamia,
New Delhi, India
e-mail: nid.sharma83@gmail.com

P. Goel
e-mail: pankul.goel@gmail.com

M. A. Wahid
e-mail: wahidatif89@gmail.com

Zahid. A. Khan
e-mail: zakhan@jmi.ac.in

A. Noor Siddiquee
e-mail: arshadnsiddiqui@gmail.com

1 Introduction

Friction stir welding (FSW) process is able to effectively join various similar and dissimilar materials in the solid state [1–3]. However, dissimilar joining is a very difficult and challenging task owing to the vast difference in the properties of the materials required to be joined. Conventionally, the fusion welding processes are used to join the nonferrous similar or dissimilar materials. During FSW, the materials required to join has to sustain the melting and solidification phenomenon at the joint location; therefore, the joint properties differ considerably from the base materials. Also the fusion welding process creates a large number of welding defects such as porosity, cavity, slag inclusion, etc. [3]. The formation of intermetallic compounds (IMCs) is also higher during joining of dissimilar materials using fusion welding process due to higher affinity of the materials at higher temperatures [4, 5]. FSW occurs in solid state and joining occurs without the base material's melting; therefore, the joints are usually free from the various defects which occur in fusion welding [6]. FSW is also a green process due to the absence of harmful radiation and gases. FSW has been effectively used by many researchers to dissimilar joining of materials such as Al to Cu and observed the elimination of the inherent limitations of fusion joining processes [7–10]. The main element required to join the materials using FSW is the FSW tool, which is divided into two segments, shoulder and pin. Tool shoulder and pin usually consist of different profiles, shapes, and sizes, and their selection is on the basis of base materials properties required to join the materials. To perform the FSW, a rotating and traversing FSW is first FSW plunged inside the butting surfaces and further allowed to traverse along the weld direction. The movement of the FSW tool inside the butting surface creates a large frictional heat, sufficient enough to join the materials in solid state [1, 11]. The materials movement and stirring also occur by the rotating action of the pin and forms the mixed material zone and welding occurs without the use of any additional filler material. This technique has been successfully used by many researchers to join Al alloys and copper. Copper is a highly conductive material; therefore, it is widely used material as the conducting element in the electrical industries. The conducting component made by using copper is generally heavier and costly due to the higher density and cost of the copper. Some Al grades are reasonably conductive and cheaper which may be used partial replace the copper so the lighter, economical, and competitive conducting element can be formed [12, 13]. The available literature on FSW of Al to Cu suggests that the FSW joint quality depends upon the various FSW process parameters, i.e., rotational speed, travel speed, pin offset, shoulder diameter, tilt angle, base plates positioning and placement [14, 15]. The literature pertaining to the FSW of the electrical grade Al with Cu is not sufficiently available [16, 17]. Keeping this in view, the present study is aimed to successfully join electrical grade Al-6101 with pure Cu using FSW and to explore the influence of different FSW process parameters on UTS of the fabricated joints. FSW is performed using three FSW process parameters each at three levels using a cylindrical tool pin profile. The experimentation is performed according to Taguchi's L_9 orthogonal array, and the data for UTS and μH of the fabricated

joint is collected. The collected data is statistically analyzed using signal-to-noise (S/N) ratio, ANOM, and ANOVA to obtain the optimal FSW process parameter combination which maximizes both UTS of the welded joint. Further the ANOVA results were confirmed using the genetic algorithm optimization using the MATLAB tool.

2 Materials and Methods

The Al-6101 alloy and pure Cu of the thickness of 2.8 mm, length of 195 mm, and width of 37 mm were butt welded using FSW. FSW tool materials used were H13 hot die steel due to its high strength, wear resistance, and stability at the higher temperature. The chemical composition of the base materials and tool material is given in Table 1.

FSW is performed on a robust vertical milling machine consisting of specially designed tool adapter and a work fixture to securely hold and clamp the tool and work-pieces, respectively, during joining. FSW tool of 5 mm pin diameter and 2.5 mm pin length was used during joining. As per the literature recommendation, the Cu was placed on the advancing side (AS) and Al was placed on retreating side (RS), respectively, and 20 tilt angle was selected during joining [18–20]. Three FSW process parameters, i.e., tool shoulder diameter, welding speed, and rotational speed each at three levels are varied during joining. The range of FSW process parameters used during experimentation is shown in Table 2.

Taguchi's L_9 orthogonal design is considered for performing the nine experiments as shown in Table 3. UTS and S/N ratio of the joints are shown in Table 3.

3 Results and Discussion

The following sections describe the analysis of the results for optimization of FSW parameters for UTS. Also, genetic algorithm optimization is performed to validate the results obtained by the ANOVA technique. Macrostructure and microstructure of the joints obtained at optimal combinations of the FSW process parameters are presented and discussed.

3.1 Analysis of UTS

The test specimens for UTS were cut using wire EDM machine as per the ASTM E8 standards (shown in Fig. 1). The UTS of the joints was measured on a computer controlled tensiometer (Kudale, Pune).

Table 1 Chemical composition (wt%) of Al-6101, pure Cu, tool material and their mechanical and physical properties

Chemical composition of Al-6101 alloy (wt%)										
B	Cr	Cu	Fe	Mg	Mn	Si	Zn	Al		
0.05	0.009	0.038	0.260	0.68	0.029	0.404	0.054	Balance		
Chemical composition of pure Cu (wt%)										
Sn	Fe	P	Ni	Co	Ag	Zn	Pb	Others	Cu	
0.04	0.001	0.043	0.24	0.001	0.018	0.012	0.003	<0.001	99.65	
Composition of H13 hot die steel tool (wt%)										
C	Mn	Si	Cr	Ni	Mo	V	Cu	P	S	Iron
0.32–0.45	0.20–0.50	0.80–1.20	4.75–5.50	0.3	1.10–1.75	0.80–1.20	0.25	0.03	0.03	Balance

Table 2 FSW parameters and their levels

Parameter	Designation	Unit	Level 1	Level 2	Level 3
Shoulder diameter	A	mm	14	16	18
Welding speed	B	mm	63	80	100
Rotational speed	C	mm/min	540	710	900

Table 3 FSW parameters and their levels

Exp No.	Shoulder diameter (A)	Welding speed (B)	Rotational speed (C)	UTS	S/N ratio
1	1	1	1	181	45.1536
2	1	2	2	192	45.6660
3	1	3	3	178	45.0084
4	2	1	2	192	45.6660
5	2	2	3	197	45.8893
6	2	3	1	173	44.7609
7	3	1	3	203	46.1499
8	3	2	1	190	45.5751
9	3	3	2	184	45.2964

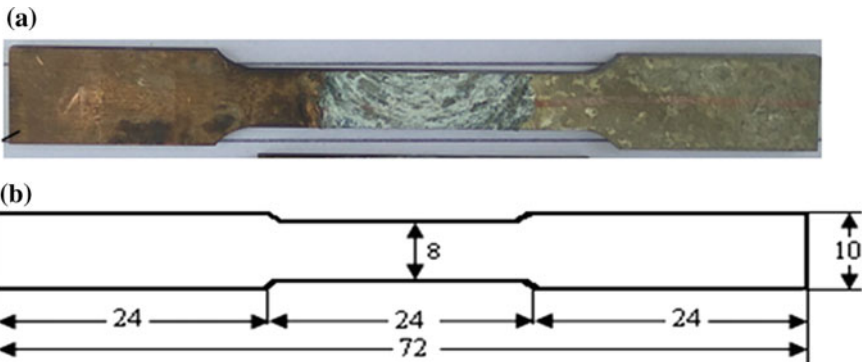


Fig. 1 a Tensile specimen, b Tensile specimen dimensions

The effect of process parameters on UTS is analyzed using *S/N* ratio and ANOVA techniques. *S/N* ratio for UTS is calculated by considering the higher-the-better characteristic for UTS as the objective is to maximize UTS. The values of *S/N* ratio for UTS are shown in Table 3. The mean *S/N* ratio of UTS at different levels of the FSW process parameters is shown in Table 4.

Table 4 also shows the rank of each process parameter which defines the extent of sensitiveness of UTS for the process parameters. It can be seen from Table 4 that the UTS is highly sensitive to the welding speed and sequentially followed by rotational speed and shoulder diameter. Process parameter’s optimum combination is obtained

Table 4 Response table of mean *S/N* ratio for UTS

Symbol	Process parameter	Mean <i>S/N</i> ratio			Max-min	Rank
		Level 1	Level 2	Level 3		
A	Shoulder diameter	45.28	45.44	45.67	0.40	3
B	Welding speed	45.66	45.71	45.02	0.69	1
C	Rotational speed	45.16	45.54	45.68	0.52	2

Table 5 ANOVA table for UTS

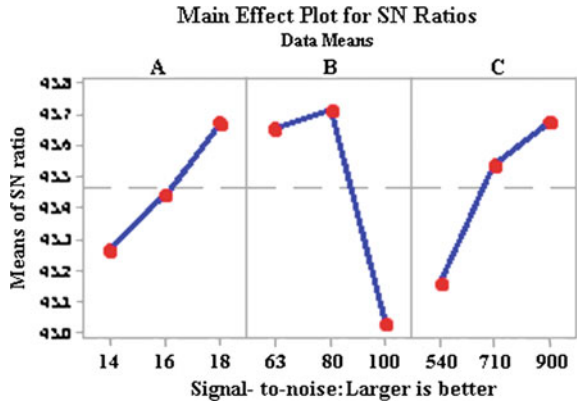
Source	DF	SS	MS	F	P
A	2	0.23996	0.119980	12.58	0.074
B	2	0.87929	0.439647	46.09	0.021
C	2	0.43337	0.216685	22.72	0.042
Error	2	0.01908			
Total	8	1.57170			

by considering maximum value of the *S/N* ratio. Thus, Table 4 reveals that the optimum combination of the process parameters for maximizing the UTS is $A_3B_2C_3$, i.e., shoulder diameter at level 3 (18 mm), welding speed at level 2 (80 mm/min), and the rotational speed at level 3 (900 rpm). The statistical significance of process parameters on the UTS is obtained through ANOVA technique and the results of ANOVA are shown in Table 5. The regression equation showing the relationship between the process parameters and the UTS is given in the Eq. 1.

$$\begin{aligned}
 \text{UTS} = & -1.090 - 4.312 A + 4.709 B + 0.06798 C \\
 & + 0.1667 A * A - 0.02552 B * B - 0.000113 C * C \\
 & - 0.05276 A * B + 0.007560 A * C
 \end{aligned}
 \tag{1}$$

R^2 value is also determined to see the fitness of the data with the regression Eq. 1, and it is 98.88% which shows a close agreement between the data and the regression equation. Thus, the prediction of the UTS based on the Eq. 1 is quite acceptable. To find the significant process parameter, the *F* value given in Table 5 is compared with the critical *F* value for each process parameter for 5% level of significance ($\alpha = 0.05$). The process parameters which have higher values than their critical value are considered as significant process parameters. Further, the *P* value is also observed, and the process parameters are categorized as most significant, significant, and insignificant based on their *P* value as lesser than 0.05, 0.05–0.10, and greater than 0.10, respectively. From Table 5, it is interpreted that the welding (*B*), and rotational speed (*C*) all are the most significant and shoulder diameter (*A*) is the significant process parameter. The main effects plot depicting the optimal parameter combination for the UTS is shown in Fig. 2.

Fig. 2 Main effect plots for S/N ratio (UTS)



The melting point of the Al-6101 and Cu is 533 and 1083 °C, respectively, which shows the considerable difference in their values; therefore, the plastic deformation temperature also differs. From Fig. 2, it is evident that the UTS increase with the increment of the shoulder diameter (A). FSW tool diameter strongly influences the frictional heat and materials entrapment in the weld zone during the joining process and, thus its diameter affects the UTS of the welded joint. The larger shoulder diameter increases the frictional heating, and therefore, the higher strength Cu which also possesses higher thermal conductivity could not dissipate maximum portion of the formed frictional heat instantaneously, and therefore, Cu deforms sufficiently to mix in Al matrix and provides good quality joints. From Fig. 2, it is clear that the UTS first increases with increment of the welding speed (B) from level 1 to level 2 and further decreases with its increment from level 2 to level 3. The lower welding speed creates a hotter weld zone therefore the precipitates strengthening, grain coarsening, and IMCs formation increases which decrease the UTS and the increment in the welding speed increases the UTS till a certain level. However, the further increment of welding speed after attaining the level 2, decreases the UTS, which may be attributed to the lesser frictional heat, therefore, the insufficient material movement, stirring, and mixing. From Fig. 2, it is clear that the UTS increase with increment of the rotational speed (C). The lower rotational speed creates the insufficiently heated weld zone which creates difficulty in the material mixing; therefore, the homogeneously mixed weld zones are difficult to obtain. So the extremely lower rotational speed creates the lesser UTS. The increment in the rotational speed increases the UTS by providing the sufficient frictional heat for homogeneous mixing.

3.2 Confirmation Test for UTS

The optimal process parameters combination for maximum UTS is $A_3B_2C_3$. An experiment was run on this optimal condition, and UTS at the weld section was

measured. UTS obtained at this run is 198 MPa, and the value of S/N ratio for UTS is 45.9333 dB. The predicted value of the UTS at the optimal combination is 202.444 MPa, and the value of S/N ratio for optimal UTS is 46.1408 dB. The average and predicted UTS and S/N ratio values show a very close agreement, and thus, it may be concluded that the derived optimal combination is acceptable.

3.3 Analysis for UTS Using Genetic Algorithm

The present study aims to determine the optimum values of the FSW process parameters in order to achieve higher UTS. Genetic algorithm (GA) is an effective optimization technique, and it is used to find the best combination of process parameters for UTS. GA is based on the genetics and natural selection. GA is basically a biological simulation process which is based on Darwin's theory of survival of the fittest. GA solves the optimization problem by randomly selecting a set of potential. Further the new set of solution is derived through crossover and mutation technique. The potential solutions are evaluated based on the fitness criteria and the best one is kept. This process repeats until the potential solution has achieved the best fitness, and this solution is known as the optimal solution of the problem. Expression for the optimization problem is given below:

Optimization of UTS: Find (A, B, C)

Minimize: UTS (A, B, C) using the second order regression equation of UTS given in Eq. 1.

Process parameters range: $14 < A < 18$; $63 < B < 100$; $540 < C < 900$

GA parameters; Population size = 40; Mutation Rate = 1.0; Crossover rate = 0.8; Number of generation = 1000

The optimum values of the process parameters obtained by GA are 17.72813, 63.04427, and 769.475511. Therefore, the optimum combination from near level obtained by GA is $A_3B_1C_3$. This combination of the process parameters is indeed experiment number 7 with the UTS value of 203 MPa which is highest among all the performed experiments. The UTS obtained at the GA-based optimum combination is even higher than the ANOVA-based optimal combination and prediction.

4 Conclusions

It is observed from the present study that FSW is an effective technique to join the dissimilar materials. This study provides a systematic approach to study the effect of different FSW process parameters combination over the joint integrity. The limitation in conducting the total number of experiments shortens the range of process parameters used in the study. However, this approach can be utilized similarly for the various materials using different possible ranges of FSW process parameters. The variation in mechanical properties joints made by using FSW is a

function of FSW process parameters. In this study, the optimal combination of the FSW process parameters for maximum UTS is obtained by Taguchi-based ANOVA and GA. Conclusions drawn from the present study are mention below:

FSW is an effective process for dissimilar joining of Al to Cu.

UTS increases with the increment of shoulder diameter and rotational speed.

UTS increases with the increment of welding speed up to a maximum possible level and further decreases.

The optimum combination of the FSW process parameters obtained through ANOVA is $A_3B_2C_3$, i.e., shoulder diameter 18 mm, welding speed 80 mm/min, and rotational speed 900 rpm which gives maximum UTS within the investigated range of process parameters.

UTS is highly sensitive to the welding speed and sequentially followed by rotational speed and shoulder diameter.

The optimum combination of the process parameters obtained through GA is $A_3B_1C_3$, i.e., shoulder diameter 18 mm, welding speed 63 mm/min, and rotational speed 900 rpm which provides the UTS more than Taguchi-based optimization.

GA has resulted in a fairly better FSW parameters combination for maximizing the UTS.

References

1. Sharma N, Khan ZA, Siddiquee AN (2017) Friction stir welding of aluminum to copper—an overview. *Trans Nonferrous Met Soc China* 27:2113–2136
2. Wahid M, Siddiquee AN, Khan ZA, Sharma N (2018) Analysis of cooling media effects on microstructure and mechanical properties during FSW/UFSW of AA 6082-T6. *Mater Res Express* 5(4)
3. Braunovic M, Aleksandrov N (1993) Effect of electrical current on the morphology and kinetics of formation of intermetallic phases in bimetallic aluminium-copper joints. In: *Proceedings of thirty-ninth IEEE Holm conference*, IEEE, 261–268
4. Çevik B, Özçatalbaş Y, Güleç B (2016) Friction stir welding of 7075-T651 aluminium alloy. *Pract Metallography* 53(1):6–23
5. Wahid MA, Khan ZA, Siddiquee AN (2018) Review on underwater friction stir welding: a variant of friction stir welding with great potential of improving joint properties. *Trans Nonferrous Met Soc China* 2:193–219
6. Sharma N, Siddiquee AN, Khan ZA, Mohsin T (2017) Material stirring during FSW of Al-Cu: effect of pin profile. *Mater Manuf Process* 33(7):786–794
7. Bergmann JP, Petzoldt F, Schürer R, Schneider S (2013) Solid-state welding of aluminum to copper—case studies. *Weld World* 57:541–550
8. Okamura H, Aota K (2004) Joining of dissimilar materials with friction stir welding. *Weld Int* 18:852–860
9. Sharma N, Khan ZA, Siddiquee AN, Shihab SK, Wahid MA (2018) Effect of process parameters on microstructure and electrical conductivity during FSW of Al-6101 and pure copper. *Mater Res Express* 5(4)
10. Bhattacharya TK, Das H, Jana SS, Pal TK (2017) Numerical and experimental investigation of thermal history, material flow and mechanical properties of friction stir welded aluminium alloy to DHP copper dissimilar joint. *Int J Adv Manuf Technol* 88(1–4):847–861
11. Sharma N, Siddiquee AN, Khan ZA (2017) Friction stir welding defects in aluminum to copper joining—an overview. *J Manuf Technol Res* 9(1–2):1–11

12. Singh H, Arora HS (2010) Friction stir welding-technology and future. *Natl Conf Adv Future Trends Mech Mater Eng* 32–38
13. Sahin M (2010) Joining of aluminium and copper materials with friction welding. *Int J Adv Manuf Technol* 49(5):527–534
14. Wahid MA, Siddiquee AN, Khan ZA, Asjad M (2016) Friction stir welds of Al alloy-Cu: an investigation on effect of plunge depth. *Arch Mech Eng* 63:619–634
15. Saeid T, Abdollah-zadeh A, Sazgari B (2010) Weldability and mechanical properties of dissimilar aluminum—copper lap joints made by friction stir welding. *J Alloys Compd* 490:652–655
16. Mehta KP, Badheka VJ (2015) Influence of tool design and process parameters on dissimilar friction stir welding of copper to AA 6061-T651 joints. *Int J Adv Manuf Technol* 80(9–12):2073–2082
17. DebRoy T, Bhadeshia H (2010) Friction stir welding of dissimilar alloys—a perspective. *Sci Technol Weld Joining* 15(4):266–270
18. Xue P, Ni D, Wang D, Xiao B, Ma Z (2011) Effect of friction stir welding parameters on the microstructure and mechanical properties of the dissimilar al–cu joints. *Mater Sci Eng, A* 528(13):4683–4689
19. Xue P, Xiao B, Ni D, Ma Z (2010) Enhanced mechanical properties of friction stir welded dissimilar Al–Cu joint by intermetallic compounds. *Mater Sci Eng, A* 527:5723–5727
20. Galvao I, Oliveira J, Loureiro A, Rodrigues D (2011) Formation and distribution of brittle structures in friction stir welding of aluminium and copper: influence of process parameters. *Sci Technol Weld Joining* 16:681–689

Analyzing Success Factors of Small and Medium Enterprises (SMEs): A Study in Indian Context



Sachin Meshram and A. M. Rawani

Abstract The importance of small and medium enterprises (SMEs) is recognized in the academic and policy literature. Entrepreneurship and SMEs are integral to economic and social development and regeneration. It is recognized that, SMEs are the engine of economic growth through employment generation, contribution to GDP, technological innovations, and other aspects of economic and social development. With this in consideration, the objective of this research is to identify the success factors (SFs) for small and medium enterprises in Chhattisgarh, India. Based on the literature review, 28 factors have been identified and subsequently categorized into three groups, namely entrepreneurial and enterprise factors, motivational factors, and managerial and environmental factors. Analyzing identified success factors in the present study shows that need for achievement under motivational factor, education level and financial resources under entrepreneur and enterprise factor, managerial capability, and government support under managerial and environmental factors are the important success factors (SFs) for the development of entrepreneurship through SMEs in Chhattisgarh region of India.

Keywords Entrepreneurship · Success factors · Small and medium-sized enterprises (SMEs)

1 Introduction

The term “Entrepreneurship” refers to the development and growth of new enterprises [1]. Entrepreneurship is the establishment and operation of a business, taking greater risk than normal by mobilizing resources to satisfy the needs of society, create jobs, and realize profits for the owner of the business [2]. The literature confirm that entrepreneurs play an important role especially in establishing small and medium enterprises (SMEs) which lead to high employment [3]. SMEs are considered to be a

S. Meshram (✉)

Department of Mechanical Engineering, National Institute of Technology Raipur, Raipur, India
e-mail: meshram.sa10@gmail.com

A. M. Rawani

National Institute of Technology Raipur, Raipur, India

© Springer Nature Singapore Pte Ltd. 2019

K. Shanker et al. (eds.), *Advances in Industrial and Production Engineering*, Lecture Notes in Mechanical Engineering, https://doi.org/10.1007/978-981-13-6412-9_78

843

most efficient tool to achieve economic and social development to attain significant progress and development as they offer useful services to consumers, and provide much needed employment [4]. It is ingrained reality that there is a positive connection between business and economic development [3, 4].

In present situation, entrepreneurship creating employment opportunities for mass unemployed particularly jobless graduates is one of the real worries of Indian government and policy makers. Therefore, “entrepreneurship development” through SMEs could be the solution to these problems [5, 6]. Development of entrepreneurship through SMEs is difficult and requires attention from various research studies [7]. One of the most important steps in the development of entrepreneurship and SMEs is to identify the success factors (SFs) of entrepreneurs in small- and medium-sized enterprises (SMEs). Recognition and assessment of these success factors (SFs) can be used as a guide to investigate and evaluate their relationship (if any) with entrepreneurial and SMEs success in Chhattisgarh. Accordingly, this paper aim to achieve the following objectives.

1. To identify success factors (SFs) to entrepreneurship in small and medium enterprises success in Chhattisgarh.
2. To evaluate and rank based on important index of those identified success factors (SFs) into groups.

The rest of the paper is organized as follows. Section 2 presents the literature on factors of entrepreneurial and SMEs success. In Sect. 3, the definition/criteria of Indian SMEs have been reviewed. Further, the research methodology has been discussed in Sect. 4. Section 5 presents the findings and conclusions of the study.

2 Literature Review

The objective of every enterprise is to be successful and success has got different criteria. In entrepreneurship literature, the concept of success remains a topic of debate [8]. There is no universally accepted definition of success and therefore business success has been interpreted in many ways [9]. Various researchers concentrate on use of financial measures while others considered non-financial measures of success [10]. The most common measures of success are profitability [11–13]. All businesses must be financially viable on some level in order to continue to survive [11]. The longer the business survives and prevent involuntary exit, the more success it has [14]. In smaller entrepreneurial and independent firms, measures of success may have more complex dimensions than just financial performance [15]. Non-financial measures of success used by business owners, such as autonomy, job satisfaction or the ability to balance work and family responsibilities, customer satisfaction, and customer retention are not only subjective but also difficult to quantify [11, 15, 16].

The findings of previous research revealed that, the factors which affect success of SMEs can be categorized into characteristics of an entrepreneur [17], enterprise or firm characteristics, management and know-how [18] customers and markets

[19] resources and finance, and external environment [20]. According to Philip, the entrepreneurs' profile has a constructive effect on the success of SMEs [21]. It is universally accepted that efficient management is crucial for the success of any type of organization. Even though a number of studies have uncovered poor management is the main cause of business failure [22, 23].

From a marketing point of view, Makura & Nyoni [24], emphasize the use of social media marketing while others, recommend the use of neuro-marketing as a way of grabbing a huge customer base on the market [25, 26]. Many researchers confirm the significance of marketing in the success of SMEs [19]. Furthermore, Hinson and Mahmoud conclude that the higher the level of market orientation, the greater the level of performance of Ghanaian small and medium enterprises [27].

In regard to the business experience, Hussain and Yaqub found that organizations that were controlled by business visionaries with past entrepreneurial involvement in comparative endeavors scored altogether higher achievement levels than those without such experience. The entrepreneur characteristics covered age, education, managerial competence, and experience. Charney and Libecap found that entrepreneurship education produces self-sufficient successful enterprising individuals [28]. Besides, the investigation found that business enterprise education improves the probability of SMEs achievement. In a comparative report by Sinha, the effect of educational background on enterprise success was analyzed and the study found that 72% of the successful entrepreneurs had a minimum level of technical qualification [29].

From firm characteristics point of view, factors influencing success of SMEs are—business operation time, size of the enterprise, sector and source of capital [30]. Kristiansen et al. [17], found that time spend in operating the business has significant effect on enterprise success. McMahan express that business experience on the part of the owner or manager had a huge commitment on success of small- and medium-sized enterprises [31]. Further in respect to size of the enterprise, McMahan found that size of an enterprise had a significant effect on success of small and medium enterprises [31].

Having established the fact that success factors for SMEs vary with the type of enterprise and region they operate in and having identified the Indian SMEs especially Chhattisgarh region as a severely understudied area, a very clear and well-defined gap in literature is established. This study attempts to address this gap; therefore, its primary aim is to identify the success factors (SFs) for SMEs and to evaluate and rank those identified factors in groups in Chhattisgarh, India.

3 Criteria of Small and Medium Enterprises (SMEs) in India

The definitions of SMEs vary from country to country and industry to industry [32]. There is no global agreed definition of an SME [33], even in a single jurisdiction;

SMEs can have several definitions depending on the industry they operate in. According to the provision of Micro, Small and Medium Enterprises Development (MSMED) Act, 2006, Indian small and medium enterprises (SMEs) are classified as below [34].

4 Research Methodology

This study was conducted with the intention to identify success factors which affect the entrepreneurial and SMEs success in Chhattisgarh region, India. To identify success factors, an extensive literature review was carried out. In order to extract relevant factors, a brainstorming session was also arranged, comprising a team of five research scholars, four post graduate students, and three academicians of management studies. Based on brainstorming and literature review, list of 15 motivational factors of entrepreneurial success and 13 managerial and environmental factors of SMEs success are identified. These success factors are grouped in three groups derived from literature review and expert opinion as: “Entrepreneurial and Enterprise Factors,” “Motivational Factors,” and “Managerial and Environmental Factors.” A complete list of these success factors are as shown in Table 1.

To understand the importance of these factors toward entrepreneurial and SMEs success, questionnaires survey was carried out. SMEs entrepreneurs in Chhattisgarh region were requested to rate the importance of these factors on a five point likert scale: 1 (Not Important) to 5 (Absolutely Essential). Total 70 copies of questionnaires were distributed and out of which 66 entrepreneurs answered the survey questions, thus the final sample contained 66 SMEs. Care is taken to cover manufacturing as well as service enterprises after very nearly 45 days of putting a great deal of endeavors. Due to deficiencies in data entry, three questionnaires were rejected and at the end 63 questionnaires were compiled which is totally 0.84 of all distributed questionnaires. The “Important Index” is used to analyze the data and rank the factors considered in this study. The important index is calculated based on the following equation:

$$\text{Important Index} = \frac{5n5 + 4n4 + 3n3 + 2n2 + n1}{5(n1 + n2 + n3 + n4 + n5)} \times 100$$

Table 1 Classifications of enterprises

Classification	Investment ceiling (excluding land and building)	
	Manufacturing (in Rs.)	Service (in Rs.)
Small	‘Between 25 Lakhs to 5 Crores’	‘Between 10 Lakhs to 2 Crores’
Medium	‘Between 5 Crores to 10 Crores’	‘Between 2 Crores to 5 Crores’

In which n_1 is the amount of subjects picked “Not Important” option, alternative, n_2 is the amount of subjects picked “Marginally Important” option, n_3 is the amount of subjects picked “Moderately Important” option, n_4 is the amount of subjects chosen “Very Important,” and n_5 is the amount of subjects picked “Absolutely Essential” option. Once the “Importance index” ascertained for all parameters, the Important Index for each group is obtained by calculating the average of group (Table 2).

Table 2 Success factors to Entrepreneurial and SMEs Success

No.	Factor group	Factors
1.	Entrepreneurial and enterprise factor	Age
		Gender
		Education level
		Personality
		Size of company
		Business networks
		Financial resources
		Human capital
		Market and product development
2.	Motivational factor	Need for achievement
		Independence
		Intrinsic
		Job security
		Previous experience
		Self-employment
		Innovative ideas
		Financial ability
		Support factors
3.	Managerial and environmental factor	Managerial capability
		Decision making
		Market support factors
		Customer satisfaction
		Business environmental
		Government support
		Socio-cultural factors
		Political factors
		Support of families and friends
Demand for supply		

5 Result and Discussion

In the present study, Chhattisgarh region's SMEs and entrepreneurial success factors (SFs) were classified based on their importance. These success factors were categorized in three main groups. With help of expert opinions, the importance index of each main factor group was calculated. Next the Importance index of each group were obtained through calculating the average score of each group. Among the known factors, the entrepreneurial and enterprise factors were in the first group. As Table 3 shows, the group includes nine sub-factors. As it is seen, education level is the most important entrepreneurial and enterprise factor and obtains the highest importance index. Table 3 shows the importance index of entrepreneurial and enterprise factor.

Table 4 shows the importance index for nine motivational factors. The importance index in the group was obtained 69.06 which ranked as first among the three groups. Also "Need for achievement" sub-factor got the highest score with the important index of 79.67 and was introduced as the main motivational factor. The second highest score in this group was "Self-employment" which is very important.

The third and the last group includes most important is managerial and environmental factor. There are ten sub-factors in main factor group (Table 5). The results also show that "Managerial Capability" and "Socio-cultural factors" first and last rank in this group respectively.

Table 3 Importance index and rank of each entrepreneurial and enterprise factors

Main factor group	Importance index	Factors	Importance index	Rank in group
Entrepreneurial and enterprise factor	67.37	Age	78.75	2
		Gender	72.32	3
		Education level	79.36	1
		Personality	54.17	9
		size of company	67.20	5
		Business networks	61.39	7
		Financial resources	69.23	4
		Human capital	65.14	6
		Market and product development	58.78	8

Table 4 Importance index and rank of each motivational factors

Main factor group	Importance index	Factors	Importance index	Rank in group
Motivational factor	69.06	Need for achievement	79.67	1
		Independence	75.32	4
		Intrinsic	77.65	3
		Job security	68.27	6
		Previous experience	54.78	9
		Self-employment	78.45	2
		Innovative ideas	56.78	8
		Financial ability	72.40	5
		Support factors	58.24	7

Table 5 Importance index and rank of each managerial and environmental factors

Main factor group	Importance index	Factors	Importance index	Rank in group
Managerial and environmental factors	68.74	Managerial capability	79.12	1
		Decision making	75.56	4
		Market support factors	76.25	3
		Customer satisfaction	77.54	2
		Business environmental	57.00	9
		Government support	72.54	5
		Socio-cultural factors	54.22	10
		Political factors	59.87	8
		Support family and friend	69.85	6
		Demand for supply	65.45	7

6 Conclusion

The purpose of this study is to identify the success factors (SFs) of entrepreneurship in small and medium enterprises in Chhattisgarh region, India. This paper prioritized the success factors (SFs) of entrepreneurship through SMEs in Chhattisgarh region, India using the important index. The result shows that the motivation factors are very important among the groups of success factors. Also “Need for achievement,” “Education Level of entrepreneurs,” “Managerial Capability,” “Age,” and “Self-employment motivation” ranked top five success factors, respectively.

The finding of this study has implications for entrepreneurs as well as the policy makers who work for the improvement of entrepreneurship. This can be said that factors associated with motivation, success, and challenges will appear differently in different regions. These differences reveal due to regional political systems and the economic policies [35].

References

1. Bennett A (2006) A shrinking staff propels a newspaper's transformation. *Nieman Rep* 60(1):48
2. Khosa RM, Kalitanyi V (2014) Challenges in operating micro-enterprises by African foreign entrepreneurs in Cape Town, South Africa. *Mediterr J Soc Sci* 5(10):205
3. Hashemi MS, Hashemi S, Naseri R, Houshmandi S (2014) The relationship between cultural, social, economic and public policy with entrepreneurial intentions. Case study city university graduates Kouhdasht
4. Ahmadpoor Daryani M, Erfanian A (2007) The role and place of entrepreneurship in reaching economic growth and development. *Econ Mag Mon Rev Econ Policy Issues Off Econ Aff Minist Econ Aff Assets* 7(69):1–19
5. Benzing C, Chu HM, Kara O (2009) Entrepreneurs in Turkey: a factor analysis of motivations, success factors, and problems. *J Small Bus Manag* 47(1):58–91
6. Valliere D, Peterson R (2009) Entrepreneurship and economic growth: evidence from emerging and developed countries. *Entrep Reg Dev* 21(5–6):459–480
7. Belás J, Sopková G (2016) Significant determinants of the competitive environment for SMEs in the context of financial and credit risks. *J Int Stud*
8. Gorgievski MJ, Ascalon ME, Stephan U (2011) Small business owners' success criteria, a values approach to personal differences. *J Small Bus Manag* 49(2):207–232
9. Ibrahim AB, Goodwin JR (1986) Perceived causes of success in small business. *Am J Small Bus* 11(2):41–50
10. Garengo P, Biazzo S, Bititci US (2005) Performance measurement systems in SMEs: a review for a research agenda. *Int J Manag Rev* 7(1):25–47
11. Walker E, Brown A (2004) What success factors are important to small business owners? *Int Small Bus J* 22(6):577–594
12. Luk TK (1996) Success in Hong Kong: factors self-reported by successful small business owners. *J Small Bus Manag* 34(3):68
13. Kalleberg AL, Leicht KT (1991) Gender and organizational performance: determinants of small business survival and success. *Acad Manag J* 34(1):136–161
14. Van Praag CM (2003) Business survival and success of young small business owners. *Small Bus Econ* 21(1):1–17
15. Mohan-Neill S (2009) The influence of education and technology use in the success of US small businesses. *J Manag Syst* 21(1)

16. Montagno RV, Kuratko DF, Scarcella JH (1985) Perception of entrepreneurial success characteristics. *Am J Small Bus* 10(3):25–32
17. Kristiansen S, Furuholt B, Wahid F (2003) Internet cafe entrepreneurs: pioneers in information dissemination in Indonesia. *Int J Entrep Innov* 4(4):251–263
18. Swierczek FW, Ha TT (2003) Entrepreneurial orientation, uncertainty avoidance and firm performance: an analysis of Thai and Vietnamese SMEs. *Int J Entrep Innov* 4(1):46–58
19. Ganyaupfu EM (2013) Entrepreneur and firm characteristics affecting success of small and medium enterprises (SMEs) in Gauteng Province
20. Chittithaworn C, Islam MA, Keawchana T, Yusuf DHM (2011) Factors affecting business success of small & medium enterprises (SMEs) in Thailand. *Asian Soc Sci* 7(5):180
21. Philip M (2011) Factors affecting business success of small & medium enterprises (SMEs). *Amity Glob Bus Rev* 6(1):118–136
22. Adnan Z, Abdullah HS, Ahmad J (2011) Direct influence of human resource management practices on financial performance in Malaysian R&D companies. *World Rev Bus Res* 1(3):61–77
23. Islam MZ, Siengthai S (2010) Human resource management practices and firm performance improvement in Dhaka Export Processing Zone (DEPZ). *Res Pract Hum Resour Manag* 18(1):60–77
24. Nyoni T, Bonga WG (2018) Anatomy of the small & medium enterprises (SMEs) critical success factors (CSFs) in Zimbabwe: introducing the 3E model
25. Tichafa M, Nyoni T (2017) The impact of social media marketing in the telecommunication industry: a case of Netone Plc. Ltd., Zimbabwe
26. Keh HT, Nguyen TTM, Ng HP (2007) The effects of entrepreneurial orientation and marketing information on the performance of SMEs. *J Bus Ventur* 22(4):592–611
27. Hinson RE, Mahmoud MA (2011) Qualitative insights into market orientation in small Ghanaian businesses. *Int J Mark Stud* 3(1):35
28. Charney A, Libecap G (2000) The impact of entrepreneurship education: an evaluation of the Berger Entrepreneurship Program at the University of Arizona, 1985–1999
29. Sinha TN (1996) Human factors in entrepreneurship effectiveness. *J Entrep* 5(1):23–39
30. Smallbone D, Leig R, North D (1995) The characteristics and strategies of high growth SMEs. *Int J Entrep Behav Res* 1(3):44–62
31. McMahon RGP (2001) Business growth and performance and the financial reporting practices of Australian manufacturing SMEs. *J Small Bus Manag* 39(2):152–164
32. Nyathi KA, Nyoni T, Nyoni M, Bonga WG (2018) The role of accounting information in the success of small & medium enterprises (SMEs) in Zimbabwe: a case of Harare
33. Quartey P (2003) Financing small and medium enterprises (SMEs) in Ghana. *J Afr Bus* 4(1):37–55
34. Jain MKC, Gandhi SKP (2016) Defining Indian SMEs: a critical analysis. *Int J Arts Humanit Manag Stud*
35. Zimmerman MA, Chu HM (2013) Motivation, success, and problems of entrepreneurs in Venezuela. *J Manag Policy Pract* 14(2):76

A Brief Review on Different Lubricants Used in MQL Process During Hard Turning



Hemant Tiwari, Ramanuj Kumar, Amlana Panda, Ashok Kumar Sahoo and Soumikh Roy

Abstract Heat generation during hard turning exhibits delamination of cutting tool edge rapidly, as a result the quality of finished job got deteriorate. However, nowadays, various alternative cooling techniques/different cutting fluids are utilized to minimize the cutting heat during machining action. Some severe diverse effects of use of coolants in machining create the challenges for researchers to choose environment-friendly coolant. Quality as well as economic concerns is also very important for the selection of cooling technique as well as cutting fluid. In recent years, minimum quality lubrication (MQL) technique provides very impressive cooling during hard machining. The MQL approach leads toward manufacturing sustainability and green manufacturing for enhancing cooling as well as the lubrication system. In MQL, a mixture of cutting fluid and compressed air is sprayed into the cutting zone which minimizes the heat during machining. MQL attribute lower fluid consumption with flow rate may vary from 5 ml/h to 100 ml/h. However, MQL machining is under the category of near-to-dry machining. In literatures, various categories of coolant like vegetable oil, castor oil, and oil with suspension of nanoparticles were found. However, with proper selection of cutting parameters along with lubricant through MQL can attribute enhanced machinability.

Keywords Lubricants · MQL · Hard turning

1 Introduction

The purpose of answering the growing demand of machining sector and the requirement to improve productivity, surface quality are influential for thoroughly review of the characteristics and requirements of the hard turning process for technological development. With the fast expansion of manufacturing scenario, for example, coating technology, tool materials, and CNC machine, it is likely to directly machine

H. Tiwari · R. Kumar (✉) · A. Panda · A. K. Sahoo · S. Roy
School of Mechanical Engineering, Kalinga Institute of Industrial
Technology Deemed to Be University, Bhubaneswar, Odisha, India
e-mail: ramanujkumar22@gmail.com

materials with hardness level more than 45 HRC, which is termed as hard turning [1]. Cutting liquids are used in order to reduce the machining temperature by lessening the rubbing between workpiece and tool, thus enhancing tool life, diminishing tool wear along with these lines decreasing tooling cost, expanding speed, and removing chip from cutting zone. Cutting liquids cause a few issues, for example, contamination, operational demerits and when they interact with oil from machining operations or because of bacterial development [2, 3]. Under these conditions, researchers have tried different aspects with cryogenic cooling, minimum quantity lubricant (MQL), and solid lubricants. Among these, MQL is an important process that can be utilized as here less quantity of cutting liquid is applied machining zone. In MQL, the cutting liquid is divided into very small drops with its size conversely relative to the pressure of infusion and ideal change in the apparatus workpiece and device chip cooperation [4, 5]. Different lubricants used during turning operation are presented in Table 1.

Chinchanikar et al. found that using coconut oil as machining fluid in MQL environment performed better machining and produce superior surface quality when compared to dry condition [6]. Mahadi et al. enhanced the performance of machining fluid by the use of a boric acid powder with palm kernel oil. It was found that the major facets that affected the surface quality were the type of coolant and depth of cut and feed rate. In addition, experiment results revealed that machining performance of boric acid lubricant surpassed conventional lubricant [7].

2 Effect of Lubricants on Different Parameters

Different lubricants were used by different researchers in finding its effect on different machinability behaviors such as cutting force, cutting temperature, surface temperature, surface finish, tool flank wear, and the coefficient of friction.

2.1 Cutting Forces

Cutting forces are important parameters in machining to acquire better dimensional accuracy, stability, and high productivity. As friction between cutting tool increases, the cutting force also increases. An et al. conducted an experiment and found that cutting force increases with increase in depth of cut, but by using MQL (cutting fluid was vegetable oil-based lubrication oil), the cutting force reduces by 60% approximately [8]. Similarly, Gupta and Sood determined that by using Balmerol-make soluble cutting oil and found out that cutting force reduces [9]. Rahim et al. also determined that as the feed rate was increased the cutting force also increased, but by the use of MQL (synthetic ester as a cutting fluid) it was noted that the cutting force decreases by 5–28% and the cutting process becomes easier [10]. Similar observations were observed by Padmini et al. [11], Pejryd et al. [12], Su et al. [13]. Elmunafi et al. found that the performance of MQL during turning operation of stainless steel

Table 1 Different lubricants used for different workpieces and cutting tool materials

Author (s)/references	Workpiece material	Machining tool	Lubricant used
An et al. [8]	AISI 1215 steel	TiAlN-coated carbide	Vegetable oil-based lubrication oil
Gupta and Sood [9]	Inconel-800 and titanium alloy	Cubic boron nitride inserts	Balmerol-make soluble cutting oil
Rahim et al. [10]	AISI 1045 steel	Uncoated carbide insert	Synthetic ester
Padmini et al. [11]	AISI 1040 steel	Coated carbide insert	Vegetable oil-based cutting fluids
Pejryd et al. [12]	Inconel 718 and Waspaloy, titanium alloy and Cr steel	Uncoated cemented carbide	Ester (Accu-Lube LB2000) and fatty alcohol (Shell Garia SL501)
Su et al. [13]	AISI 1045	Uncoated carbide insert	Vegetable oil-based oil and ester oil
Ji et al. [18]	AISI 4130 alloy steel	Carbide tool insert with PDV coating	The air-oil mixture (Coolube 2210)
Amrita et al. [19]	AISI 1040 steel	Cemented carbide cutting tool insert	Nanographite fluid
Padmini et al. [20]	AISI 1040 steel	Coated carbide inserts	Coconut oil and sesame oil
Krishna et al. [24]	AISI 1040 steel	Cemented carbide insert	Graphite and boric acid solid lubricant
Leppert [25]	AISI 316L steel	Carbide Insert with PDV TiAlN coating	Accu-Lube LB 8000 oil
Noordin et al. [26]	AISI 420 stainless steel	Coated carbide tool with PVD TiAlN coating	Castor oil
Khan and Dhar [31]	AISI 1060 steel	Uncoated carbide insert	Food grade vegetable oil

(heat treated) using castor oil was better as compared to dry machining. The tool life, quality of turned surface have significantly improved due to the decrease in machining temperature at the machining zone [14].

2.2 Cutting Temperature

Cutting temperature plays a key role in hard turning process. At acceptable wear rate, the cutting tool needs to sustain higher temperature that limits the machining rate. This provides the development of modern cutting tool materials. Work hardness, ductility, work hardening, and thermal characteristics affect the temperature [15].

Machining conditions such as cutting speed, feed rate and depth of cut and tool geometry majorly influence the temperature of the cutting zone. In a similar manner, these cutting conditions depend upon workpiece material properties and physical properties. There are various scientific and experimental outcomes with respect to the impact of the cutting conditions on the temperature of the cutting tool, workpiece, or chip. The temperature rises because the high quantity of heat is generated or hypothetically is compacted in a very small region and/or little amount of heat is being circulated. Because of this, the impact of the cutting conditions will develop the temperature. Also, more effects are due to the tool geometry, the workpiece and cutting tool material, and the cutting fluid [16]. Krishna et al. experimentally observed that specific heat generation decreases with increase in the nanoboric acid concentration in machining oil. Machining performance of coconut oil was found better than SAE-40-based lubricant [17]. Rahim et al. used FLIR thermal imager to find out the cutting temperature and found that in MQL, (cutting fluid was synthetic ester) the machining temperature was reduced by 10–30% as related to dry conditions. Consequently, drop of cutting temperature increases lifespan of tool contributing to enduring tool life [10]. Ji et al. used a thermocouple and thermal camera; he too found that the cutting temperature reduces in case of MQL as compared to dry condition but not as much as in case of the flooded condition. Most probably because as the cutting temperature decreases with increase in flow rate an in case of a flooded condition the flow rate is more [18]. Same observations were performed by Amrita et al. [19], Padmini et al. [20].

2.3 Surface Roughness/Finish

The surface quality is swayed by the operating parameters, machine tool condition, cutting tool geometry, and the machining operations. Surface roughness is principally influenced by feed rate and cutting force. One of the fundamental variables adding to surface roughness is the built-up edge. Therefore, larger the built-up edge, the rougher would be the surface generated, and factors having a tendency to diminish chip-tool friction [21]. Das compared the machining performance of steel under both MQL and dry environments. Using MQL technique during turning operation resulted in the superior surface finish as compared to dry condition and machining speed was the most predominant factor affecting flank wear [22]. Singh noticed that by using solid lubricant during machining of bearing steel with mixed ceramic shows a considerable increase in surface finish. Using solid lubricants resulted in a decrease in surface roughness from 8 to 15% as compared to that of dry machining [23]. Krishna et al. found that under dry machining conditions the surface morphology disintegration because of high pressure and over the top plastic distortion attributable for the substantial rubbing, while in MQL smooth surface was established because of great grease impact due to small-scale beads at the contact interface of the workpiece and the tool [24]. An et al. concluded that at low feed rates and cutting speeds the application of MQL managed to lessen the surface roughness (1.34–1.50 mm) as

compared to those of dry turning (1.54–1.82 mm) and emulsion (1.68–2.26 mm) [8]. Similarly, Lepper observed that surface finish was most affected by the feed rate with the contribution of 40.46% for dry, 52.40% for wet, and 41.04% for MQL machining and the MQL cooling contribute in the improvement of the surface quality [25]. Noordin et al. found out that MQL produces slightly less surface roughness than dry machining; this might be because of reduced cutting temperature in the cutting zone. It was also perceived that the surface finish decreases with a reduce in cutting speed and feed rate [26].

2.4 Tool Wear

In hard turning, tool wear affect the properties of the surface and machining efficiency. Tool wear is dominant at nose corner, which in turn subsequently affects surface quality adversely. Due to tool wear cutting forces and cutting temperature decreases resulting in the decrease of tool lifespan, surface quality, and accuracy of the product. Further, tool wear can be classified into two categories, namely flank wear and crater wear. Flank wear occurs on the flank surface due to friction between the machined surface of workpiece and tool flank. Crater wear arises on the rake surface of the tool as a result of chip sliding against the surface [27]. Gunjal and Patil experimentally found that using synthetic oil at high machining speed resulted in greater tool life of around three times than that of canola oil. On the other hand, canola oil displayed better results in terms of tool wear than that of coconut oil and soybean oil [28]. Stephenson et al. compared the machining performance of supercritical CO₂-based MQL with water-based flooded cooling. Machining under supercritical CO₂-based MQL resulted in an increase in tool life, greater material removal rate and lower wear of the tool [29]. Khalil et al. investigated on wear mechanism during turning of mild steel with Al₂O₃ nanolubricant using MQL. By utilizing Al₂O₃ nanolubricant resulted in a reduction in tool wear and increase in tool life [30], Khan and Dhar experimented with AISI-1060 steel as the workpiece and uncoated carbide, TSS, SNMM 120408 as the cutting tool material and found out that initially the flank wear starts with a very fast rate but by using MQL (vegetable oil) the growth rate of flank wear decreases. Thus, it provided better surface finish and tool life as in case of the dry condition [31]. Noordin et al. determined that with an increase in feed rate and cutting speed the tool wear increases thus decreasing the tool life. It was concluded that the MQL performance was far better than those of dry condition. In case of MQL, the cutting force decreases, as a result, the temperature decreases theirs by decreasing the tool wear and increasing the tool life [26].

2.5 Chip Formation

Chip formation is a fundamental phenomenon considering the benefits in hard turning process. Rahim et al. experimented with AISI 1045 steel as workpiece material and uncoated carbide as the cutting tool material. It was determined that the chip thickness is majorly influenced by the feed rate. It was found by using MQL (synthetic ester) thinner chip was produced because the cutting temperature decreases and thus reducing friction and adhesion between tool and workpiece, and hence the chip thickness reduced. It was determined that under MQL condition the chip thickness reduced by 3–9% than that of the dry condition and also the contact length of tool chip under MQL condition declined by 12% [10]. Similar observations were performed by Gupta et al. used titanium and Inconel alloys as a workpiece material. It was concluded that the chip formed in case of dry and wet condition was unbroken and long but in case of MQL, the chip formed was small helical and washer type [9]. Gajrani et al. proposed that the use of eco-friendly vegetable oil lubrication is better over the use of conventional petroleum-based machining fluid. Vegetable oil lubricants were found eco-friendly, highly biodegradable, and it has the ability to withstand high temperature and high pressure [32].

3 Conclusion

In this paper, a comprehensive review of literatures on various lubricants used in MQL processes was presented which will be more effective in new direction for scientific research during hard turning technology. The machining efficiency and productivity of hard-turned components is predominantly limited by cutting tool wear, which reduces surface quality of the workpiece. Implementation of MQL in hard turning reduced the cutting forces and cutting temperature drastically, however, the surface finish as well as tool life was increased. Furthermore, solid lubricants under MQL condition are more effective than that of normal liquid lubricants. The subsequent research gap has been observed and that could provide an important research direction for future work.

- Various categories of coolant like vegetable oil, castor oil, and oil with suspension of nanoparticles were generally used in literatures. However, MQL with different types of oil tremendously affect the performance of cutting tool which needs to be further explored.
- Limited analysis has been reported so far for white layer formation, variation in residual stress, effect of coating thickness in different lubricants used in MQL-assisted hard turning.
- Implementation of finite element analysis for proper identification of temperature distribution, cutting force analysis and chip morphology may be useful for future investigation.

- The sway of nanofluid lubricants through MQL approach on surface finish, cutting temperature, chip reduction coefficient, tool wear, and environmental point of view are less discussed.
- Very less literatures are available describing economical and performance analysis during dry, MQL, and nanofluid lubrication for feasibility of cutting insert during hard turning. Therefore, an extensive analysis considering the prescribed parameters should be performed.

References

1. Bartarya G, Choudhury SK (2012) State of the art in hard turning. *Int J Mach Tools Manuf* 53(1):1–14
2. Weinert K, Inasaki I, Sutherland JW, Wakabayashi T (2004) Dry Mach Minim Quant Lubr 53(2):511–537
3. Kasim MS, Haron CHC, Ghani JA, Hadi MA, Izamshah R, Anand TJS, Mohamed SB (2016) Cost evaluation on the performance of a PVD coated cutting tool during end-milling of Inconel 718 under MQL conditions. *Int J Surface Eng Coat IMF* 94(4):175–181
4. Cica D, Sredanovic B, Globocki GL, Kramar D (2013) Modeling of the cutting forces in turning process using various methods of cooling and lubricating: an artificial intelligence approach. *Adv Mech Eng*. <http://dx.doi.org/10.1155/2013/798597>
5. Joshi KK, Kumar R, Anurag (2018) An experimental investigations in turning of Incoloy 800 in dry, MQL and flood cooling condition. *Proc Manuf* 20:350–357
6. Chinchankar S, Salve AV, Netake P, More A, Kumar R (2014) Comparative evaluation of surface roughness during hard turning under dry and with water-based and vegetable oil-based cutting fluid. *Proc Mater Sci* 5:1966–1975
7. Mahadi MA, Choudhury IA, Azuddin M, Nukman Y (2017) Use of boric acid powder aided vegetable oil lubricant in turning AISI 431 Steel. *Proc Eng* 184:128–136
8. An Q, Liu Z, Jiang L, Chen M (2014) Experimental and numerical research on the effects of minimum quantity lubrication in thread turning of free-cutting steel AISI 1215. *Proc IMechE Part B J Eng Manuf* 1–8
9. Gupta MK, Sood PK (2017) Machining comparison of aerospace materials considering minimum quantity cutting fluid: a clean and green approach. *Proc IMechE Part C J Mech Eng Sci* 231(8):1445–1464
10. Rahim EA, Ibrahim MR, Rahim AA, Aziz S, Mohid Z (2015) Experimental investigation of minimum quantity lubrication (MQL) as a sustainable cooling technique. *Proc CIRP* 26:351–354
11. Padmini R, Krishna PV, Rao GKM (2014) Performance assessment of micro and nano solid lubricant suspensions in vegetable oils during machining. *Proc IMechE Part B J Eng Manuf* 1–9
12. Pejryd L, Beno T, Isaksson M (2010) Machining aerospace materials with room-temperature and cooled minimal-quantity cutting fluids. *Proc IMechE Part B J Eng Manuf* 225
13. Su Y, Gong L, Li B, Liu Z, Chen D (2016) Performance evaluation of nano fluid MQL with vegetable-based oil and ester oil as base fluids in turning. *Int J Adv Manuf Technol* 83:2083–2089
14. Elmunafi MHS, Kurniawan D, Noordin MY (2015) Use of castor oil as cutting fluid in machining of hardened stainless steel with minimum quantity of lubricant. *Proc CIRP* 26:408–411
15. Silva MBD, Walibank J (1999) Cutting temperature: prediction and measurement methods—a review. *J Mater Process Technol* 88:195–202
16. Patole PB, Kulkarni VV, Meng W (2017) Experimental investigation and optimization of cutting parameters with multi-response characteristics in MQL turning of AISI 4340 using nanofluid. *Cong Eng* 4:1–24

17. Krishna PV, Srikant RR, Rao DN (2010) Experimental investigation on the performance of nanoboric acid suspension in SAE-40 and coconut oil during turning of AISI 1040 steel. *Int J Mach Tool Manuf* 50:911–916
18. Ji X, Li B, Zhang X, Liang SY (2014) The effects of minimum quantity lubrication (MQL) on machining force, temperature, and residual stress. *Int J Proc Eng Manuf* 15(11):2443–2451
19. Amrita M, Srikant RR, Sitaramaraju AV, Prashad MMS, Krishna PV (2013) Experimental investigations on the influence of mist cooling using nanofluids on machining parameters in turning AISI 1040 steel. *Proc IMechE Part J J Eng Tribo* 227(12):1334–1346
20. Padmini R, Krishna PV, Rao GKM (2015) Experimental evaluation of nano-molybdenum disulfide and nano-boric acid suspensions in vegetable oils as prospective cutting fluids during turning of AISI 1040 steel. *Proc IMechE Part J J Eng Tribo* 1–13
21. Gaitonde VN, Karnik SR, Davim JP (2012) Optimal MQL and cutting conditions determination for desired surface roughness in turning of brass using a genetic algorithm. *Int J Mach Sci Technol* 16(2)
22. Das RK, Sahoo AK, Mishra PC, Kumar R, Panda A (2018) Comparative machinability performance of heat treated 4340 steel under dry and minimum quality lubrication surroundings. *Proc Manuf* 20:377–385
23. Singh D, Paruchuri VR (2007) Performance improvement of hard turning with a solid lubricant. *Int J Adv Manuf Technol*. <https://doi.org/10.1007/s00170-007-1079-8>
24. Krishna PV, Shrikant RR, Rao DN (2010) An experimental investigation to study the performance of solid lubricants in turning of AISI 1040 steel. *Proc IMechE Parts J J Eng Trib* 224:1273–1281
25. Leppert T (2014) Surface layer properties of AISI 316L steel when turning under dry and with minimum quantity lubrication conditions. *Proc IMechE226 Part B J Eng Manuf* 617–613
26. Elmunafi MHS, Kurniawan D, Noordin MY (2015) Use of castor oil as cutting fluid in machining of hardened stainless steel with minimum quantity of lubricant. *Proc CIRP* 26:408–411
27. Attanasio A, Gelfi M, Giardini C, Remioni C (2006) Minimal quantity lubrication in turning: effect on tool wear. *Wear* 260:333–338
28. Gunjal SU, Patil NG (2018) Experimental investigation into turning of Hardened AISI 4340 steel using vegetable based cutting fluid under minimum quantity lubrication. *Proc Manuf* 20:18–23
29. Stephenson DA, Skerlos SJ, King AS, Supekar SD (2014) Rough turning Inconel 750 with supercritical CO₂-based minimum quantity lubrication. *J Mater Process Technol* 214:673–680
30. Khalila ANM, Alib MAM, Azmi AI (2015) Effect of Al₂O₃ nanolubricant with SDBS on tool wear during turning process of AISI 1050 with minimal quantity lubricant. *Proc Manuf* 2:130–134
31. Khan MMA, Dhar NR (2006) Performance evaluation of minimum quantity lubrication by vegetable oil in terms of cutting force, cutting zone temperature, tool wear, job dimension and surface finish in turning AISI-1060 steel. *J Zhejiang Univ Sci A* 7(11):1790–1799
32. Gajrani KK, Sankar MR (2017) Past and current status of eco-friendly vegetable oil based metal cutting fluids. *Mater Today Proc* 4:3786–3795

Applicability of Lean Six Sigma in Hospitals



Vimal Kumar Deshmukh , Suraj Kumar Mukti and Animesh Agrawal 

Abstract Most of previous researches on Lean Six Sigma focused on various perspective of Six Sigma, lean philosophy then role of Lean Six Sigma in sustainability but never paid much attention in field of health service sector, e.g., hospital. This article concentrates on checking feasibility of Six Sigma in hospitals. Defects and loopholes in hospital and healthcare industries can sentence a difference between a life and death. Since to mitigate mishaps and increase patient experiences during the visit of hospitals, this research is an extreme effort to reduce variation in service quality using quality management tool Lean Six Sigma (LSS) in registration counter at hospitals. Data-driven methodology approach and applicability of LSS in service sector encompass not only the people but information and resource utilization. This is a mainstream pillar to be used as a methodology for research. DMAIC tool was found useful to enhance service quality during the study. Improvisation of outcomes is comparatively discussed in a chronological sense for ease of understanding. This research work will contribute to academia as well as service sectors like hospitals, restaurants, banks etc.

Keywords Lean Six Sigma · Quality management · Service sector · Hospital · DMAIC tool

1 Introduction

The Modern era of competition challenges the health service providers to survive in markets. For the hospital, the patient satisfaction reflects the outcomes and extent of service quality being served. Improving the patient satisfaction and happiness always remains ideal. Since the health service providers continuously rely on increasing patient satisfaction and it starts with the patient entrance into hospitals [1]. Particularly in hospitals, it is mandatory for a patient to make registration and prepare a

V. K. Deshmukh (✉) · S. K. Mukti · A. Agrawal
Department of Mechanical Engineering, National Institute of Technology,
Raipur 492001, India
e-mail: deshmukh.vimal1920@gmail.com

© Springer Nature Singapore Pte Ltd. 2019
K. Shanker et al. (eds.), *Advances in Industrial and Production Engineering*, Lecture Notes in Mechanical Engineering, https://doi.org/10.1007/978-981-13-6412-9_80

861

slip or file before going for checkups to the doctors. Employees in hospitals registration and admitting departments smoothens the patient care and patient flow in the hospital. For a patient, time is very crucial since management plays a vital role to minimize the time associated with these processes. From patient's perspective, at the registration desk, the patient's behavior and understanding reflect the difficulties faced in filling the registration form. The terminologies used sometimes are out of the domain of the patient's knowledge. This does not show only patient's incapability but also lack of management and working knowledge of emergency preparedness procedures which is an essential element. It results that time taken by the patient is much higher than standard time. Waiting in a queue shows a systematic structure but it has no value if a patient dies due to unavailability of medical services at right time. We have various quality management and an industrial tool to reduce unnecessary time. Hospitals have already various criterion and standard time but practical they are not self-constraint. There are a few research articles focusing on patient problem at various stages hospitals. This research article encompasses the problem of patient at registration or reception desk.

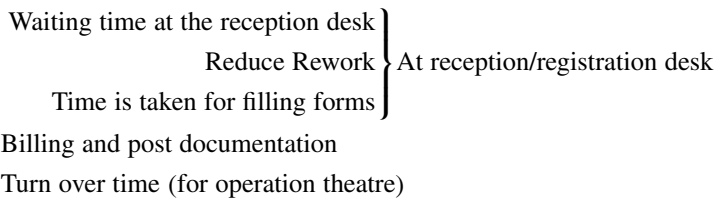
1.1 Six Sigma and Lean Philosophy

Most of the time, management issues are identifiable and can be eliminated by management tools. The Six Sigma has proven its significance in this area. It is not only a systematic data-driven approach but also can be used as a cost-effective tool. The purpose of management is to develop a complete cycle process of hospital operational system that will eliminate medical errors entirely [2]. Since 1985 and onwards, Motorola took advantage and made working cycle smooth. 34 defects per ten million are the extent to which Six Sigma serves or deliver services. Theoretically, we can say, If the six sigma is applied in healthcare services particularly at the reception desk at the hospital it shows that 9,999,966 out of 1,000,000 patients will be satisfied [3–5] these expected outcomes encourage the management and hospital administration to implement Six Sigma in hospitals. Also, unnecessary process and movement of hospital staff can be seen which are of no value. To mitigate these, lean philosophy may become an opportunity. It believes that errors can be eliminated by cutout in-efficient processes. Taiichi Ohno and associates architected the lean philosophy at Toyota Production System to stay in the scenario of the competition of resources and capital, which were consequences of the Second World War. The Toyota production system is additionally credited with being the origination of just in time (JIT) production strategies, an embedded component of lean philosophy, and hence the Toyota production system remains a model of brilliance for an advocate of lean philosophy. Lean philosophy assumed that defects are produced due to irrelevant process or unnecessary activity. Whereas Six Sigma emphasizes on incapability of the process. The idea of Lean ended up plainly prominent through Womack and Jones (1990) book 'The Machine That Changed the World' [6, 7]. Implementation of Lean Six Sigma basically brings processes within Six Sigma control limit and lean

management cutout irrelevant processes. Six Sigma and lean philosophy are used parallelly since last twenty years and together called Lean Six Sigma (LSS).

1.2 The Flow of Patient in Hospital

The cycle of patient flow in the hospital starts from the ambulance arrived at the reception counter; the patient has to wait for registration. The receptionist appoints a time slot and refers to doctors from which treatment of patient starts. The doctor examines and investigates by various diagnosis methods. It depends upon the patient’s condition that patient would refer either to general ward or to the operation theater. Here the patient also has to wait for the preparation for operation if referred but time associated with operation can’t be manipulated because of the risk of failure of the operation. Time taken by doctors for diagnosis and medical tests cannot be a focus for management to reduce it. After treatment, the patient again goes to reception to clear pending bills and medicine charges. The waiting time at the various stage is the main focus in throughout movement of the patient in the hospital. The potential subject in terms of time identified from field survey is



2 Methodology

For this research, the subject is restricted to first four only, which take place at the reception desk or front desk in hospital. It includes people and process (registration form). The strategy for this research is divided into two phases in first phase root cause will be identified, and in the second phase, an attempt will be done to solve the problem using Six Sigma tools, i.e., DMAIC or DMADV based on data and information gathered. Since the second phase includes analysis and problem-solving techniques. Both the tools are equally useful and essential. But DMAIC is used more frequently over DMADV because it uses existing resources to give a solution. DMADV is used where some new methods are adopted to resolve the problem. Despite first three steps are same in both the technique and last two processes for the outcomes are totally different (Table 1).

Table 1 Steps involved in DMAIC and DMADV

DMAIC	DMADV
D—Define Includes identification and determination of problem to conduct business process to define we can use a cause-effect diagram, interview and survey and method study. This is a Foremost critical step	
M—Measure Suitable measurement should be taken to identify the culprit and compare different processes. Stopwatch and work measurement method can be used for measurement	
A—Analysis Includes critically examine the steps involved in each process from demand’s perspective to approach the goal	
I—Improve Include attempt to make changes for reducing error and improve existing process. Change management is a management tool to improve an existing process	D—Design Includes adaptation of a new process or idea to achieve a goal and eliminate error or defects. Brainstorming and BPR can be an effective tool
C—Control If the improved process works properly and satisfied then Next step is to maintain it	V—Verify Includes testing of new process or idea and verify it up to enormity

2.1 Identification and Determination of Problem (Define)

For the first phase, we have to understand the functions and responsibilities performed by the receptionist and carefully analyze registration form and find loopholes and find that why unnecessary time is taking place. The function to be performed by receptionists at the front desk in hospital includes

- Listening to patient comfort and communicating in an affirmative, friendly manner and act with confidence with patients at the front desk and over the phone too. Setting up appointments and schedule meetings at the truthful time and with the exact doctor.
- Tackle invoicing and manage errors, human interruption and detailing patient’s documents. Provide different modes for collecting fee to ease of payment for patients and ensure a profit.
- Listen to patient’s complaints at first and take suitable action and verify the health insurance grievances and complete related legal procedures with it.

Generally, the staff employed at reception do not focus on the patient. This makes incapable him/her to rectify the actual problem of the patient and this may lead to refer the patient to wrong doctors. Not addressing the actual problem can result in a lot of rework and unnecessary travel of patient and precious time of doctor, since the patient has to go to the right doctor. The reason behind this may be lack of training of staff. The flow of patient should be smooth in hospitals. Training of hospital staff plays a vital role in this perspective. Also, the hospitals should have a number of employees to accomplish tasks and responsibilities. In EHR (Electronic

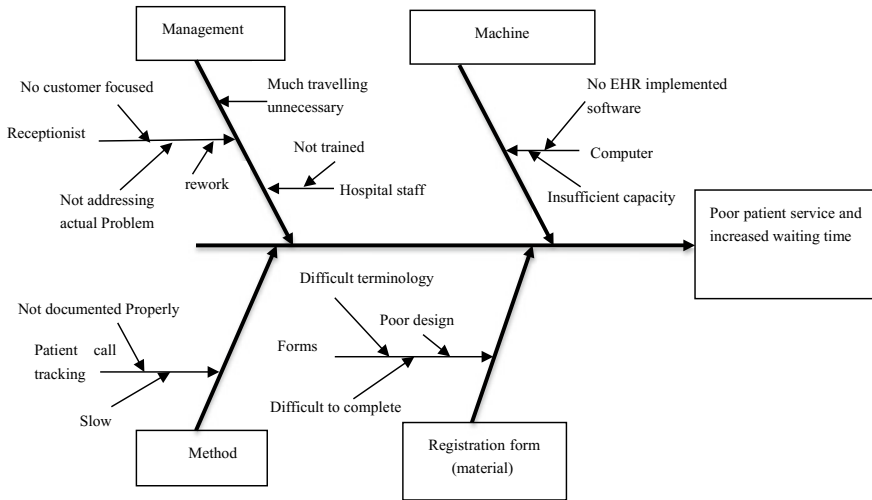


Fig. 1 Cause effect diagram to identify and define problem and after effect

Health Record) implemented hospitals, the receptionist asks the patient a series of question which includes name, age, gender, health insurance, reference and health problems. An automatic system generates a digital report for patients and receptionist refers him to a right doctor. The reports automatically send to doctors too by various management software here, the waiting time in the queue depends on skills of the computer operator since training of operator may reduce this time. In conventional type, receptionist gives a registration form and patient himself/herself has to fill the form. In conventional type, the patient fills general information quickly but feels uncomfortable while completing legal procedure and writing brief detail about the medical condition and problem due to lack of knowledge of medical terminology asked in the registration form. Since each patient takes their own time which defers from patient to patient. Rework is the main culprit for waiting time. Most of the staff at reception are busy to complete the health insurance formalities and arrange and prepare documents of patients when the case file of the patient is referred again by health insurance company. They search for various information of past and this process takes a huge time. The frequency of these type rework is also large. Since the patient needs to suffer due to an overload of staff work and lack of management. Figure 1 shows main and sub-causes and their final due to which the waiting time increases and the patient suffer poor service.

Table 2 Average time taken by various processes

S. No.	Processes	Average time taken for a patient	
1	Waiting time in queue (min)	3.41	
2	Time Taken by receptionist or patient to fill reception form	For conventional type 17.20 min (if filled by the patient)	For computer generated slips 4.2 min
3	Rework (if documented) (min)	13.66	7.4
4	Delay due to overload and pre-consultation (min)	2.4	1.33
5	Due to software lag, insufficient capacity and another computer-related issue if occurs (min)	–	9.4
Total time spent at the reception desk		For conventional type window system = 36.67 min	For digital type window = 25.74 min

2.2 Measurement of Processes at the Reception Desk

Measurement parameter selection is a critical situation and may lead to chaos. A measurement parameter should also capable to measure all procedure in a single scale. In this Research ‘Time’ is associated at all stages. Since it is used as measuring parameter here. Stopwatch method is used to evaluate the process and waiting time. Table 2 shows time taken at hospital reception. Time taken are an average of 10 reading at each hospital and it included 5 local government hospital reception counters in Drug district, Chhattisgarh, India.

2.3 Analysis of Processes at the Registration Desk

Analysis phase includes critically examine the processes involved and identify loop-holes. It is seen that waiting time in the queue cannot be reduced alone without changing other processes. Without reducing waiting time, management can increase the patient satisfaction by implementing a token system but this idea adds additional cost and space which diminishing its value. The process should not only cost-effective but also goal approached. The time taken to fill registration form depends upon:

Length of pages in the form.

The terminology used in a form for a medical condition. It defers person to person depends upon knowledge and understanding.

The specially categorized section should not mix with general patient information health insurance related question and eligibility criteria for a medical condition.

Patient's domain of knowledge is a behavior constraint and management cannot deal with it because it is different for each patient. But management can simplify medical terms used and categorize the patient information. Also, to save time, paper and money, management should use a different form for the different patient based on their medical condition. The form should be in the different color code for ease of patient. The patient takes much time to overview all the section in the form and spend unnecessary time. The receptionist should mark a cross sign and guide patient to fill the mandatory information. If the patient is waiting for his previous records, waiting time depends on skills of the receptionist in the way that how he/she manage documentation of patient and for how long time they store it. Storing a documented medical history of patient consists of a variety of clinical observation, diagnostic test results, pre- & post-operative reports, previous surgery or operation records, references, routine improvement report of patient and surgical notes of operation it also includes a list of medicines prescribed by doctors in past. It does not sound good but it is true that management knows the importance and value of patient record keeping but feels paralyzed when coming to implementation. In Indian scenario, the condition is in a promising step. However, customized software like EHR (electronic health record) refrain this situation up to gratifying level. Hospital administration should keep multiple windows at reception to cope up difficulty faced due to terminology and legal processes by the patient.

2.4 Improvisation or Alternation of Processes

To improve certain processes, management does not change the process but make some small changes in it to achieve the goal with less time and money. The economy of change is also a very important factor. The improvised model shows that motion of general patient will be smooth entirely if management starts a multi-window token system and provides a healthy environment to a patient in waiting hall. Magazine, newspaper and book of clinical safety and benefits of cleanness, etc. should be there to entertain patient in unoccupied time. Patient need not submit same information if he/she is a regular patient of same doctor or hospital. There must be a dedicated window for previous or frequent patient to collect their reports or file. There should be sufficient staff to tackle phones and help desk if the patient feels uncomfortable during filling form. For emergency case, receptionist should follow emergency response preparedness protocol (ERPP). The objective of ERPP is to take action in initial minutes to save patients life. Paperwork is done either parallel or later by the person associated with the patient. Hospitals and doctors are not responsible for a sentence of death of patient according to this protocol. So, it does not require that much paperwork, unlike general patients. For EHR or such customized software implemented hospital, the time is taken for registration entirely depends on skills

of the receptionist. To reduce this time, there are two ways. First, improve the staff for dedicated work at reception by giving proper training and second make software customized such that it asked general but essential information precisely. With the advancement of AI (artificial intelligence), it would be great if the system would suggest right doctors available in hospital in sight of the receptionist. And the same information should send to the referred doctor. Online appointment is a good solution to refrain from waiting in the queue.

2.5 Control and Verification of Implemented Model of DMAIC or DMADV

The last step is to control the implemented model and maintain its efficiency. It is the sole responsibility of hospital administration to maintain the process effectiveness and collect feedback from the patient from time to time. There should be discussion with the patient about service and satisfaction in Likert scale for simplicity. Likert scale is a scale used to represent people's opinion and quantify it. Likert scale can be used on parameter from 1 to 5 where 1 stands for extremely dissatisfied and 5 stands for very satisfied. Needs always changes itself with time since feedback is necessary to be ready in position to meet patient's demand. A periodic audit is conducted to assess the model and make all the process within Six Sigma control limits. Sustainability of model depends on flexibility, timeliness, fast responsiveness and corrective measurements of the model.

3 Results and Discussion

Reduction in total time spent at reception desk enables receptionist to serve a number of the patient which shows well-structured and determined system and enhance patient satisfaction. After comparing the time taken with the super specialty hospital which already implemented EHR and use an electronic medium to save time, the time saved came out was about 32% of previous, i.e., 15.32 min patient spent time at reception in EHR enabled front desk. Although LSS did not change drastically the whole processes but made some small potential changes (Fig. 2).

An inverse relationship between waiting time in queue and patient's satisfaction was observed by previous researchers. Since health service providers always try to give their best and make their customer happy [8]. Training of clinical staff should be such that patient should feel comfortable while conversation. Staff will aware of their role and importance in health service industries. Organizational culture may be affected while changes take place but people's positive attitude and willingness to serve clients enthusiastically can overcome this problem. LSS makes a strategy to optimize things and make more control over the flow of processes. Results show

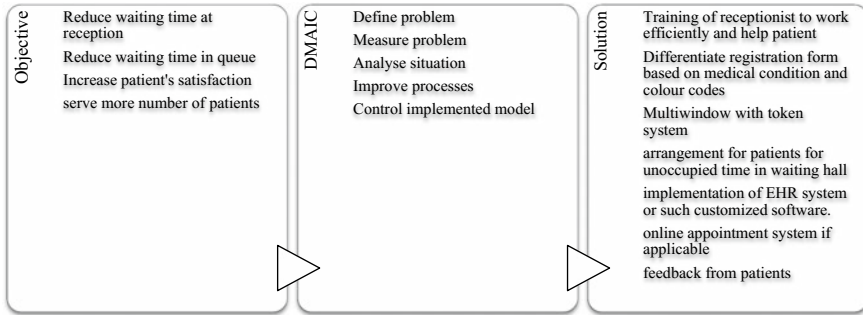


Fig. 2 Continuous process diagram of improvised model of processes at registration desk

that implementing such changes in hospitals, the total time can be reduced by near about 32% as compared to the non-implemented hospital which satisfies its economic value. Now a number of patients served will also increase because reception desk can handle more patients. DMAIC is preferred over DMADV due to economic variance and time-saving characteristic. However, big changes need DMADV, which also satisfy its cost-effectiveness.

4 Conclusion

The objective of management tools is not only to refrain from errors or defect but for enhancement of safety of patient and employee. In the hospital, management took errors as the absence of standardization and work to eliminate it completely. Service and patient satisfaction are the barterings, in which healthcare service provider provides services and expect satisfaction from the patient. LSS proved its potentiality and emerges an effective quality management tool. Hospital with conventional type registration desk is not in situation handle a large number of the patient but most of the patient arrives with general diseases at the reception desk. Since LSS has a lot of opportunities to eliminate this problematic scenario. Reduction of time from 25.74 to 15.32 min even both hospital use electronic medium shows having customized MIS software and computers are not enough. Utilization of resources and optimization of techniques is the key to every problem in the domain of LSS. For conventional paperwork-based registration desk, LSS minimizes the use of paper, time to fill the registration form and prove its utility here too. Since all these evidences conclude that it is feasible to implement Six Sigma at hospital which has sufficient fund. This research article opened a new perspective to standardize processes at the various stations from the patient entrance to exit from the hospital.

References

1. Moreno RP, Rhodes A, Donchin Y (2009) Patient safety in intensive care medicine: the declaration of Vienna. *Intensive Care Med* 35(10):1667–1672
2. Deshmukh VK, Mukti SK (2018) Impact of lean six sigma implementation success factor on growth-rate of e-service based organisation. *Int J Mech Eng Technol* 9(1):852–865
3. Pyzdek T, Keller P (2010) *The six sigma handbook*
4. Cherrafi A, Elfezazi S, Chiarini A, Mokhlis A, Benhida K (2016) The integration of lean manufacturing, six sigma and sustainability: a literature review and future research directions for developing a specific model. *J Clean Prod* 139:828–846
5. Cherrafi A, Elfezazi S, Govindan K, Garza-Reyes JA, Benhida K, Mokhlis A (2017) A framework for the integration of green and lean six sigma for superior sustainability performance. *Int J Prod Res* 55(15):4481–4515
6. Kurdve M, Zackrisson M, Wiktorsson M, Harlin U (2014) Lean and green integration into production system models—experiences from Swedish industry. *J Clean Prod* 85:180–190
7. Manufacturing JIT, Production L, Standard C, Davis D, Haven W (2001) Pull systems: implementation experience in american manufacturing pull systems: implementation experience in american manufacturing introduction. *Prod Oper Manage*
8. Hassali MA et al (2014) Assessment of general public satisfaction with public healthcare services. *Aust Med J* 7(1):35–44